

STRUCTURES ANALYSIS MANUAL

SAM

VOLUME II
Revision 2

10.43

GENERAL DYNAMICS SPACE SYSTEMS DIVISION

STRUCTURAL ANALYSIS MANUAL
GENERAL DYNAMICS/CONVAIR AND SPACE SYSTEMS DIVISION

PREFACE

This Structures Manual has been prepared by Convair and Space Systems Division Structures Analysis Groups as a reference source of data and procedures for use in the analysis and design of aerospace and ground handling structures. The manual has been compiled largely from material presented in the General Dynamics Fort Worth Structures Manual, Vol. 1. These data have been updated and expanded to cover current materials and construction methods.

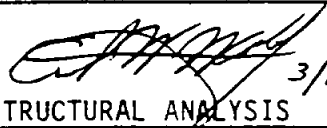
In general, the source data reference numbers within the individual sections of the manual have been retained. This will enable the reader to easily locate any additional material that may be required from the original data source.

Comments and suggestions are welcome, and should be addressed to the Structural Analysis Group.

PREFACE - FORT WORTH DIVISION

The Fort Worth Division Structures Technology department endorses the Convair and Space System Division Structures Analysis Manual as a reference source of data and procedures for structural analysis at the Fort Worth Division. The data and procedures contained in Volumes I and II are recommended for use at the Fort Worth Division at the discretion of each structural analysis group Engineering Chief considering individual program guidelines. Use of all data and procedures including those contained herein and from other sources must be approved by the structural analysis group Engineering Chief and documented sufficiently to support customer approval.

A. L. Stratton
Engineering Manager for Structures Technology
General Dynamics/Fort Worth Division

GENERAL DYNAMICS Space Systems Division STRUCTURES ANALYSIS MANUAL - NO. 10.43 DEPARTMENTAL INSTRUCTION	DATE 3/1/88 ISSUE 1 PAGE 1 of 1
REVISION RECORD	APPROVED  E.W. WOLF MANAGER STRUCTURAL ANALYSIS 3/1/88

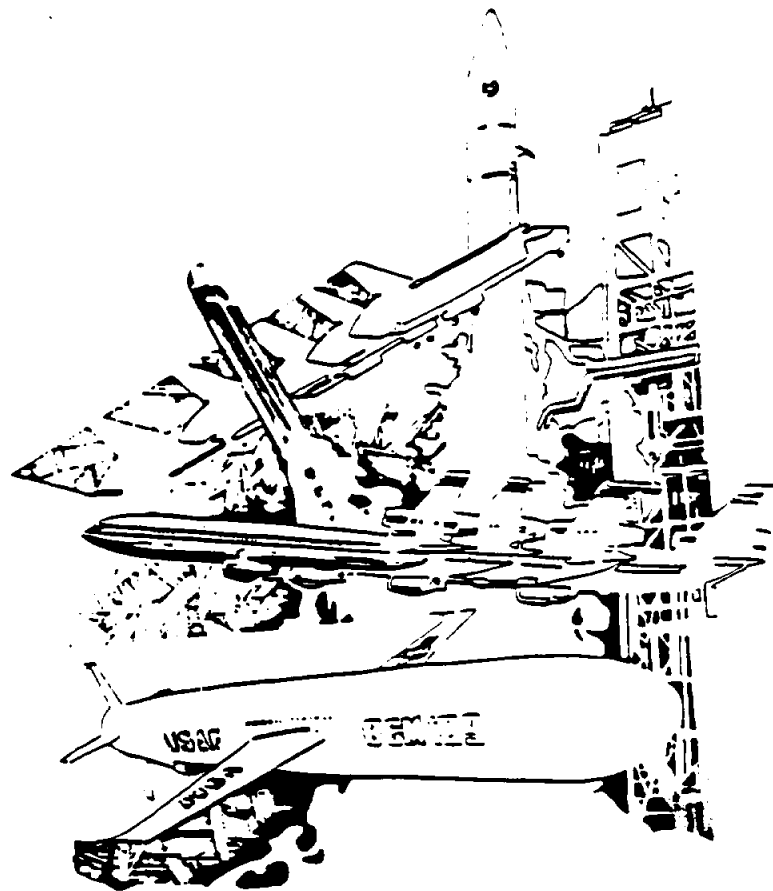
REVISION RECORD

CHAPTER - ISSUE	REVISION DESCRIPTION	DATE
All - 1	Original Issue	3/88
As noted -2	Deleted: Pages 14.9.2, 14.9.3, 14.9.4, 14.9.5, 20.0.1, [REDACTED] Added: [REDACTED] [REDACTED] Pages 4.8.21 4.8.22, 20.1.1 Revised: Pages 1.1.6 Vol. 1 & 2, 1.3.4 Vol. 1 & 2, 2.1.4, 2.7.1, 4.1.3, 4.9.1, 4.9.2, 4.9.3, 6.4.7, 6.4.15, 7.1.2, 7.1.3, 7.1.4, 7.1.5, 8.11.1, 8.11.3, 10.0.1, 10.1.1, 10.2.1, 10.5.2, 10.7.1, 10.8.2, 11.2.4, 14.1.4, 14.1.5, 14.1.24, 14.1.54, 14.9.1, 17.4.5, 17.5.27, 17.6.10, 17.6.17, 17.6.18, 17.6.19, 27.1.17	10/89

*AlS
GDR*

GENERAL DYNAMICS
Convair Division and Space Systems Division

STRUCTURES ANALYSIS MANUAL VOLUME 2 OF 2 (Revision 2)



**GENERAL DYNAMICS
PROPRIETARY DATA RESTRICTIONS**

This document contains proprietary information of General Dynamics, including trade secrets and/or privileged or sensitive commercial or financial information. Distribution within General Dynamics shall be restricted to those having an actual need for the information and no copies shall be sent outside of General Dynamics without management approval.

Copyright, General Dynamics, 1988

STRUCTURAL ANALYSIS MANUAL
GENERAL DYNAMICS/CONVAIR AND SPACE SYSTEMS DIVISION

VOLUME 1
TABLE OF CONTENTS

	<u>SECTION</u>
PREFACE	1.0
TABLE OF CONTENTS	1.1
SYMBOLS AND ABBREVIATIONS	1.2
REFERENCES	1.3
SECTION PROPERTIES	2.0
GEOMETRICAL SHAPES	2.1
CIRCLES	2.2
90° BENDS	2.3
ANGLES	2.4
CENTROID OF TRAPEZOID	2.5
SHEAR CENTER	2.6
MOMENT OF INERTIA SAMPLE CALCULATION	2.7
MATERIAL PROPERTY DEFINITIONS	3.0
STRESS-STRAIN CURVE DEFINITIONS	3.1
MATERIAL PROPERTIES: DUCTILE-BRITTLE BEHAVIOR	3.2
CREEP: STRAIN RATE AND IMPACT	3.3
"A" AND "B" MATERIAL PROPERTY VALUES	3.4
PLASTIC STRESS-STRAIN CURVES	3.5
SURFACE ROUGHNESS	3.6
NON-DIMENSIONAL STRESS-STRAIN CURVES	3.7
RAMBERG-OSGOOD CONSTANTS	3.8
BEAMS	4.0
BEAM TABLES	4.1
VARIABLE CROSS SECTION	4.2
CONTINUOUS BEAMS	4.3
MOMENT DISTRIBUTION METHOD	4.4
CURVED BEAMS	4.5
LATERAL STABILITY	4.6
SHEAR STRESSES	4.7
TENSION FIELD WEBS	4.8
CUT-OUTS	4.9
SLOTTED BEAM	4.10
ELASTIC FOUNDATION	4.11

STRUCTURAL ANALYSIS MANUAL
GENERAL DYNAMICS/CONVAIR AND SPACE SYSTEMS DIVISION

VOLUME 1
TABLE OF CONTENTS (CONTINUED)

	<u>SECTION</u>
COLUMNS	5.0
THEORY	5.1
CONSTANT CROSS SECTION COLUMNS	5.2
VARIABLE CROSS SECTION COLUMNS	5.3
CRIPPLING OF SECTIONS	5.4
BEAM COLUMNS	5.5
CONTINUOUS BEAM COLUMNS	5.6
TORSIONAL INSTABILITY	5.7
COLUMN ALLOWABLES	5.8
PLATES	6.0
IN-PLANE STABILITY LOADING, RECTANGULAR	6.1
IN-PLANE STABILITY LOADING, PARALLELOGRAM	6.2
CURVED PLATES	6.3
NORMAL LOADING	6.4
MEMBRANES	6.5
STIFFENED PLATES	7.0
BUCKLING IN AXIAL COMPRESSION	7.1
ANALYTICAL METHODS	7.2
EFFECTIVE SKIN WIDTHS	7.2.4
ISOGRID STRUCTURES	7.3
SANDWICH CONSTRUCTION	8.0
GENERAL	8.1
MATERIALS	8.2
METHODS OF ANALYSIS	8.3
FACE WRINKLING	8.4
FACE DIMPLING	8.5
EDGEWISE COMPRESSION	8.6
EDGEWISE SHEAR	8.7
NORMAL LOADING	8.8
CYLINDER TORSION	8.9
CYLINDER AXIAL COMPRESSION	8.10
CYLINDER EXTERNAL PRESSURE	8.11
BEAMS	8.12
ATTACHMENT DETAILS	8.13
ANALYSIS METHOD REFERENCES	8.14
PRESSURE VESSELS AND PIPES	9.0
STRESSES AND DEFLECTIONS	9.1
TANK GEOMETRY	9.2
PIPING SYSTEMS (ELBOWS, BELLWS, DUCTS)	9.3
DISCONTINUITY ANALYSIS OF SHELLS	9.4

STRUCTURAL ANALYSIS MANUAL
GENERAL DYNAMICS/CONVAIR AND SPACE SYSTEMS DIVISION

VOLUME 1
TABLE OF CONTENTS (CONTINUED)

	<u>SECTION</u>
CYLINDER AND SHELL STABILITY	10.0
UNPRESSURIZED	10.1
INTERNALLY PRESSURIZED	10.2
EXTERNALLY PRESSURIZED	10.3
TRUNCATED CONES	10.4
DOUBLY CURVED SHELLS	10.5
IMPERFECTIONS	10.6
POST-BUCKLING	10.7
LOCAL LOADING ON SHELLS	10.8
LANGLEY SOLUTION	10.9
 TORSION	 11.0
TORSION OF SOLID SECTIONS	11.1
TORSION OF THIN-WALLED CLOSED SECTIONS	11.2
TORSION OF THIN-WALLED OPEN SECTIONS	11.3
MULTI-CELL CLOSED BEAMS IN TORSION	11.4
PLASTIC TORSION	11.5
ALLOWABLE STRESSES	11.6
RESTRAINED TORSION	11.7
 SPRINGS	 12.0
COMPRESSION SPRINGS	12.1
EXTENSION SPRINGS	12.2
TORSION SPRINGS	12.3
CONSTANT FORCE SPRINGS	12.4
FLAT SPRINGS	12.5
CONED DISC (BELLEVILLE) SPRINGS	12.6
WORKING STRESSES	12.7

STRUCTURAL ANALYSIS MANUAL
GENERAL DYNAMICS/CONVAIR AND SPACE SYSTEMS DIVISION

VOLUME 2
TABLE OF CONTENTS

	<u>SECTION</u>
PREFACE	1.0
TABLE OF CONTENTS	1.1
SYMBOLS AND ABBREVIATIONS	1.2
REFERENCES	1.3
STRESS CONCENTRATION FACTORS	13.0
STATIC LOADING	13.1
REPEATED LOADING	13.2
GEOMETRIC EFFECTS	13.3
JOINTS AND FITTINGS	14.0
LUG ANALYSIS	14.1
MULTIPLE FASTENER PATTERNS	14.2
BEAM IN A SOCKET	14.3
INTERFERENCE FIT BUSHINGS	14.4
TENSION CLIPS AND TEES	14.5
BOLT STRENGTH	14.6
BATHTUB TYPE TENSION FITTINGS	14.7
WELD JOINTS	14.8
WELD-ON BRACKETS	14.9
BONDED JOINTS	14.10
JOINT FLEXIBILITY	14.11
PRELOADED BOLTS AND SCREWS	14.12
BOLT TORQUE EFFECTS	14.13
EFFICIENCY OF PLATES IN TENSION JOINTS	14.14
ACOUSTICS, VIBRATION, FLUTTER	15.0
LINEAR SYSTEMS	15.1
FORCED VIBRATION	15.2
METHODS OF CALCULATIONS	15.3
SONIC FATIGUE	15.4
FLUTTER	15.5
ACOUSTICS AND VIBRATION	15.6
EXPERIMENTAL STRESS ANALYSIS	16.0
STRAIN GAGES	16.1
PLASTIC ANALYSIS	17.0
BENDING STRENGTH IN PLASTIC RANGE	17.1
SIMPLE BENDING	17.2
COMPLEX BENDING	17.3
INTERACTION	17.4
PLASTIC BENDING MATERIAL PROPERTIES	17.5

STRUCTURAL ANALYSIS MANUAL
GENERAL DYNAMICS/CONVAIR AND SPACE SYSTEMS DIVISION

VOLUME 2
TABLE OF CONTENTS (CONTINUED)

	<u>SECTION</u>
BENDING MODULUS SYMMETRICAL SECTIONS	17.6
MINIMUM PLASTIC BENDING CURVES	17.7
ELASTIC-PLASTIC THEORY	17.8
BENDING NEAR LIMIT LOAD	17.9
BENDING MODULUS FOR ROUND TUBES	17.10
SHEAR STRESS IN ROUND TUBES	17.11
 RINGS, FRAMES AND ARCHES	 18.0
RIGID RINGS	18.1
BENTS AND SEMI-CIRCULAR ARCHES	18.2
RIGID AND FLEXIBLE RINGS	18.3
REDUNDANT FRAMES	18.4
 THERMAL EFFECTS	 19.0
GENERAL	19.1
BEAMS AND COLUMNS	19.2
FLAT PLATES	19.3
BOX BEAMS	19.4
BOLTED JOINTS	19.5
THERMAL BUCKLING	19.6
THERMAL STRUCTURAL ANALYSIS WITH MSC NASTRAN	19.7
 STATISTICAL ANALYSIS	 20.0
INTRODUCTION	20.1
DEFINITIONS	20.2
DISCUSSION	20.3
SAMPLE PROBLEMS	20.4
TABLES OF STATISTICAL VALUES	20.5
 MECHANISMS	 21.0
BEARINGS	21.1
GEARS	21.2
ACTUATORS	21.3
 COMPOSITE MATERIALS	 22.0
FIBERGLASS LAMINATES, POLYESTER RESINS	22.1
FIBERGLASS LAMINATES, PHENOLIC OR EPOXY RESINS	22.2
KEVLAR EPOXY DESIGN ALLOWABLES	22.3
 FRACTURE MECHANICS	 23.0
GENERAL	23.1
STRESS INTENSITY FACTORS	23.2
FLAW GROWTH	23.3
APPLICATION OF TECHNOLOGY	23.4
DAMAGE TOLERANCE	23.5

STRUCTURAL ANALYSIS MANUAL
GENERAL DYNAMICS/CONVAIR AND SPACE SYSTEMS DIVISION

VOLUME 2
TABLE OF CONTENTS (CONTINUED)

	<u>SECTION</u>
COMPUTERIZED METHODS	24.0
OPTIMIZATION DESIGN	25.0
MISCELLANEOUS TABLES AND CHARTS	26.0
TEMPERATURE CONVERSION	26.1
SI UNITS AND PREFIXES	26.1
METRIC CONVERSION FACTORS	26.2
HARDNESS CONVERSION	26.3
STANDARD ATMOSPHERE	26.4
TEMPERATURE VS. ALTITUDE	26.5
COEFFICIENTS OF STATIC AND SLIDING FRICTION	26.6
REPORT FORMAT	27.0
STRESS ANALYSIS REPORT STANDARDS	27.1

STRUCTURAL ANALYSIS MANUAL

GENERAL DYNAMICS/CONVAIR AND SPACE SYSTEMS DIVISION

List of Standard Symbols and Abbreviations

A.... Ratio of stress amplitude and mean stress; area of cross section	k.... Stiffness factor; spring constant; radius of gyration
a.... Length of panel edge: for compressive or bending loads, "a" is length not loaded; for shear loads, "a" is the longer edge of panel.	L.... Length, longitudinal grain direction; edgewise shear stiffness for sandwich
B.... Flexural rigidity of a beam	l.... (Not used, to avoid confusion with numeral 1)
b.... Length of panel edge: for compressive or bending loads, "b" is the length of the loaded edge; for shear loads, "b" is the shorter edge of the panel. Width of sections; stiffener spacings.	M.... Bending moment or couple
C.... Circumference; damping coefficient; spring constant	m.... Mass; half width of corrugation; bending moment; number of half waves
C_{cr} ... Critical damping coefficient	N.... Load per inch of edge; sample size
c.... Fixity coefficient for columns; distance from neutral axis to extreme fiber	n.... Load factor; number of half waves;
c_r ... Rivet factor	P.... Applied load or force (total, not unit load)
D.... Diameter; bending stiffness; distribution factor; flexural rigidity parameter	p.... Pressure
d.... Depth, height, or thickness; distance between centroids of facings	Q.... Static moment of a cross section
E.... Modulus of elasticity in tension	q.... Shear flow; dynamic pressure
e.... Elongation in percent; total deformation; eccentricity; the minimum distance from a hole center to the edge of a sheet	R.... Stress ratio
F.... Allowable stress; force	r.... Radius
G.... Modulus of rigidity	S.... Shear force; surface area
g.... Acceleration due to gravity	s.... Core cell size
H.... Extensional stiffness of sandwich	T.... Applied torsional moment; torque; transverse grain direction; temperature
h.... Height or depth; distance between centroids of facings	t.... Thickness; time
I.... Moment of inertia	U.... Factor of utilization; gust velocity; transverse shear stiffness for sandwich; strain energy
I_{xy} ... Product of inertia	V.... Shear force; velocity; volume; flexibility parameter for sandwich panels
J.... Polar moment of inertia	W.... Total weight; length of cell wall in sandwich construction
j.... Coefficient of critical shear for orthotropic sandwich panels	w.... Distributed load
K.... A constant, generally empirical	x.... Axis; distance along elastic curve of beam
	y.... Axis; deflection; distance from neutral axis to given fiber
	\bar{y} Distance to centroid of section
	Z.... Section modulus
	z.... Axis normal to surface of panel

STRUCTURAL ANALYSIS MANUAL

GENERAL DYNAMICS/CONVAIR AND SPACE SYSTEMS DIVISION

α (Alpha)	Coefficient of thermal expansion; angle of attack; angle of diagonal tension; constant	θ (Theta)	An angle with respect to a reference line
β (Beta)	Stiffener angle; constant	λ (Lambda)	One minus the product of two Poisson's ratios ($1 - \mu^2$)
γ (Gamma)	Unit shear strain	Λ (Lambda)	Constant
δ (Delta)	Deflection; relative retardation	μ (Mu)	Poisson's ratio
ϵ (Epsilon)	Compression or expansion Strain; rotational restraint coefficient	π (Pi)	A constant
η (Eta)	Plasticity coefficient	ρ (Rho)	Density; radius of curvature
		σ (Sigma)	Normal stress
		τ (Tau)	Shear stress
		ϕ (Phi)	Constant
		ψ (Psi)	Angular displacement

Subscripts

1 ...	Denotes facing of sandwich	n ...	Normal; natural
2 ...	Denotes facing of sandwich	o ...	Denoting corrugation sheet
a ...	Allowable	p ...	Proportional limit; polar
b ...	Bending	r ...	Effective; reduced
br ...	Bearing	s ...	Secant
c ...	Core, compression	si ...	Denoting shear instability
cr ...	Critical	t ...	Tangent
E ...	Elastic limit	u ...	Ultimate
e ...	Endurance; eccentricity; Euler's equation	w ...	Wrinkling
f ...	Face	x ...	Parallel to x axis
i ...	Denotes final segment; intercellular	y ...	Yield; parallel to y axis
m ...	Moment	z ...	Parallel to z axis

STRUCTURAL ANALYSIS MANUAL

GENERAL DYNAMICS/CONVAIR AND SPACE SYSTEMS DIVISION

Abbreviations

average	avg	inch-pound	in-lb
British thermal unit	Btu	inches per second	ips
coefficient	coef	inside diameter	ID
cosine	cos	Inspection Minor Rework Order	IMRO
cotangent	cot	Inspection Rejection	IR
ombic	cu	logarithm (common)	log
cubic foot	cu ft	logarithm (natural)	log _e or ln
cubic inch	cu in	Material Review Board	MRB
decibal	db	maximum	max
degree	deg or °	minimum	min
degree Centigrade	C	minute	min
degree Fahrenheit	F	outside diameter	OD
diameter	diam	pound	lb or #
Division Standard Practice	D.S.P.	pounds per cubic foot	lbs per cu ft
Engineering Department Instructions	E.D.I.	pounds per square foot	psf
feet per minute	fpm	pounds per square inch	psi
feet per second	fps	pounds per square inch absolute	psia
figure	fig	revolutions per minute	rpm
foot	ft	root mean square	rms
foot-pound	ft-lb	secant	sec
horsepower	hp	second	sec
hour	hr	size	sin
hyperbolic cosine	cosh	standard	std
hyperbolic sin	sinh	tangent	tan
hyperbolic tangent	tanh	temperature	temp
inch	in	weight	wt

NOTE: With very few exceptions, the abbreviations and letter symbols conform with those approved by the American Standards Association, ANC #5, ANC #23 (Revised), and GD/FW Standard Practices.

Data Source, Section 1.3 Reference |

STRUCTURAL ANALYSIS MANUAL
GENERAL DYNAMICS/CONVAIR AND SPACE SYSTEMS DIVISION

SECTION 1.3

REFERENCES:

IN ADDITION TO REFERENCES CONTAINED IN INDIVIDUAL SECTIONS OF THE REPORT, DATA SOURCES LISTED BELOW HAVE ALSO BEEN USED.

1. GD FORT WORTH STRUCTURES
MANUAL VOL 1 1963
2. CONVAIR/ASTRONAUTICS
STRUCTURES MANUAL 4.15.60
3. BELL STRUCTURE DESIGN
MANUAL
4. BOEING STRESS MANUAL
APRIL 1970
5. NASA ASTRONAUTICS STRUCTURES
MANUAL 7.1.69
6. LOCKHEED STRESS MEMO MANUAL 4.18.66
7. BRUHN, ANALYSIS & DESIGN OF FLIGHT
VEHICLE STRUCTURES JAN. 1965
8. NACA TN 3784
9. NACA TN 3785
10. NASA CR-124075
11. NASA CR-1457
12. HEXEL TSB 123, DESIGN HANDBOOK
FOR HONEYCOMB SANDWICH STRUCTURES
OCT. 1967
13. ROARK, FORMULAS FOR STRESS AND
STRAIN, 3RD ED. 1954
14. CONVAIR, ZP-7-022 TN,
ANALYSIS OF MISSILE TANK
GEOMETRIES, 2-14-56

STRUCTURAL ANALYSIS MANUAL
GENERAL DYNAMICS/CONVAIR AND SPACE SYSTEMS DIVISION

15. NASA SP-8007
16. NASA SP-8019
17. NASA SP-8032
18. BRUSH AND ALMROTH, BUCKLING OF BARS,
PLATES AND SHELLS.
19. GENERAL DYNAMICS/ASTRONAUTICS
GD/A-DDG 64-024A, POST-BUCKLING
STRENGTH OF A PRESSURIZED CYLINDER 1964
20. GENERAL DYNAMICS CONVAIR,
GDC-DDG-67-006. VOL VI
21. MIL-STD-29A, SPRINGS MECHANICAL;
DRAWING REQUIREMENTS FOR 3.1.62
22. CONSOLIDATED VULTEE, ZS-202,
FATIGUE DATA BOOK PART IV STRESS
CONCENTRATIONS, 1.12.54
23. AFFDL-TR-69-42, STRESS ANALYSIS
MANUAL, 4.30.69
24. MCDONNELL DOUGLAS DC-10
STRESS MANUAL, 4-1-68.
25. GENERAL DYNAMICS, GDSS-TC-87-010
26. LAUGHNER AND HARGAN, HANDBOOK
OF FASTENING AND JOINING OF METAL
PARTS.
27. AFFDL-TR-67-140, DESIGN CRITERIA
FOR THE PREDICTION AND PREVENTION
OF PANEL FLUTTER JAN. 1968
28. MIL-HDBK-5E, METALLIC MATERIALS
AND ELEMENTS FOR AEROSPACE VEHICLE
STRUCTURES. 9.15.76
29. PERRY, ADHESIVE BONDING OF
REINFORCED PLASTICS, 1959

STRUCTURAL ANALYSIS MANUAL
GENERAL DYNAMICS/CONVAIR AND SPACE SYSTEMS DIVISION

30. GENERAL DYNAMICS CONVAIR, GDC-BTD65-168, DESIGN ALLOWABLES FOR CENTAUR STRUCTURAL MATERIALS, 2/1/66.
31. GENERAL DYNAMICS ASTRONAUTICS, ZS-7-002, STRESS ANALYSIS REPORT STANDARDS, 8/14/63.
32. GENERAL DYNAMICS, CASD-SSO-76-021, ANALYSIS OF BLADE STIFFENED INTEGRALLY MACHINED PANELS, SPACE SHUTTLE ORBITER MID-FUSELAGE, 10/5/76.
33. GENERAL DYNAMICS CASD-SSO-76-007, ANALYSIS OF T-STIFFENED INTEGRALLY MACHINED PANELS, SPACE SHUTTLE ORBITER MID-FUSELAGE, 2/5/76.
34. GENERAL DYNAMICS CASD-SSO-76-016, "HONEYCOMB SANDWICH PANEL ANALYSIS METHOD, SPACE SHUTTLE ORBITER MID-FUSELAGE", W. S. BUSSEY JR., 22 JULY 1976.
35. E. F. BRUHN, J. I. ORLANDO, J. F. MEYERS, "ANALYSIS AND DESIGN OF MISSILE STRUCTURE", TRI-STATE OFFSET COMPANY, CINCINNATI, OHIO.
36. STRESS ANALYSIS MANUAL, AIR FORCE FLIGHT DYNAMICS LABORATORY, WRIGHT-PATTERSON AIR FORCE BASE, 1969.
37. GERALD, G. AND BECKER, H., HANDBOOK OF STRUCTURAL STABILITY, PART I- BUCKLING OF FLAT PLATES, NACA TN 3781, 1957.
38. BECKER, H., HANDBOOK OF STRUCTURAL STABILITY, PART II- BUCKLING OF COMPOSITE ELEMENTS, NACA TN 3782, 1957.
39. SMITH, G. W., ANALYSIS OF MULTIPLE DISCONTINUITIES IN SHELLS, REPORT NO. AE61-0179, 1 MARCH 1961.

STRUCTURAL ANALYSIS MANUAL
GENERAL DYNAMICS/CONVAIR AND SPACE SYSTEMS DIVISION

- 40. MIL-HDBK-17A MILITARY HANDBOOK, PLASTICS FOR AEROSPACE VEHICLES.
- 41. GDSS MEMO NUMBER 883-0-86-099, 30 OCTOBER 1986.

STRUCTURAL ANALYSIS MANUAL
GENERAL DYNAMICS/CONVAIR AND SPACE SYSTEMS DIVISION

SECTION 13.0

STRESS CONCENTRATION FACTORS.

DESIGN CONSIDERATIONS TOGETHER WITH CHARTS FOR STRESS CONCENTRATION FACTORS ARE PRESENTED IN THIS SECTION.

	PAGE
13.1 STATIC LOADING	13.1.1
13.2 REPEATED LOADING	13.2.1
13.3 GEOMETRIC EFFECTS	13.3.1

STRUCTURAL ANALYSIS MANUAL

GENERAL DYNAMICS/CONVAIR AND SPACE SYSTEMS DIVISION

Data Source, Section 1.3 Reference 1

Stress Concentration Factors

The distribution of stress across the section of a member may be nominally uniform or may vary in some regular manner, as illustrated by the linear distribution of stress in flexure. When the variation is abrupt, so that within a very short distance the intensity of stress increases greatly, the condition is described as a stress concentration. It is usually due to local irregularities such as holes, screw threads, notches, nicks, keyways, scratches, etc.

Static Loading

If an axially loaded member has an abrupt change in section as shown in Fig. 10.5.1-1, the maximum elastic stress that occurs in each cross

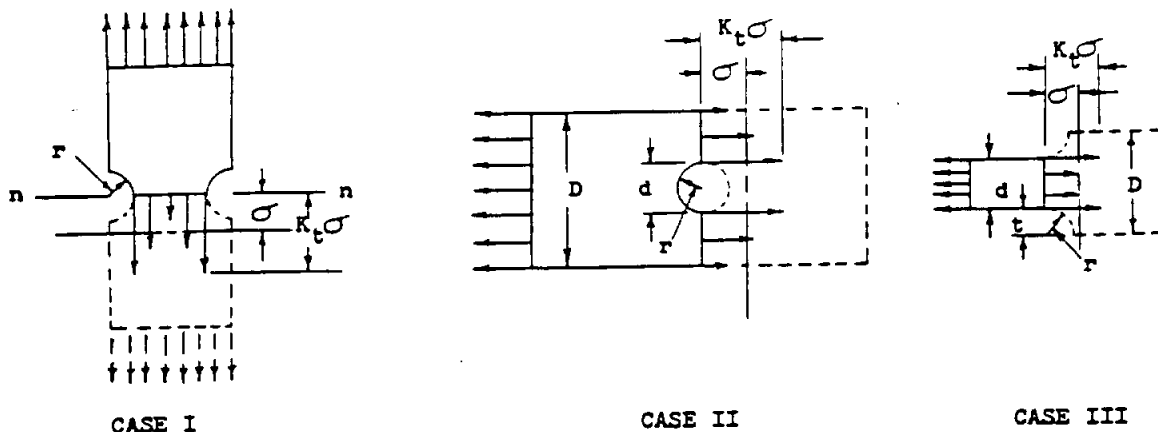


Fig. 10.5.1-1

section is greater than the average stress (P/a) where (a) is the area of the net or small portion of the section at the abrupt change of section. The maximum stress at such changes in section usually is called a stress concentration and the factor by which (P/a) must be multiplied to obtain the value of the maximum stress for axially loaded members is called an ideal, theoretical, or elastic-stress-concentration factor and is denoted by (k_t). Thus,

$$\sigma_{\max} = k_t P/a \quad \therefore \quad k_t = \frac{\sigma_{\max}}{P/a} \quad (1)$$

The value (k_t) depends on the geometry of the member: that is, on the relative values of the dimensions of the member in the neighborhood of the stress concentration.

Values of (k_t) for various types of abrupt changes of section are given in Figs. #10.5.2.1 ; #10.5.2.2 ; etc. The maximum stresses for axial, torsional, and flexural loads are given by:

$$\sigma = k_t P/A \quad , \quad \sigma = k_t \frac{Tr}{J} \quad , \quad \sigma = k_t \frac{Mc}{I} \quad (2)$$

STRUCTURAL ANALYSIS MANUAL
GENERAL DYNAMICS/CONVAIR AND SPACE SYSTEMS DIVISION

Data Source, Section 1.3 Reference 1

For members made of ductile metal and subjected to static loads and to essentially unidirectional stress, stress concentrations, are usually relatively unimportant.

Repeated Loading

A repeated load is a force that is applied many times to a member, causing stresses in the material that continually vary, usually through some definite range.

Stress concentrations are very important for both brittle and ductile materials under repeated stresses. Members with stress concentrations usually fail under repeated loads which are considerably smaller than similar static loads which were required to cause failure.

In calculating the significant (localized) stress in a member that contains some form of an abrupt change in section, the formulas developed previously can be used. The stress distribution at an abrupt change in section in a tension and a flexural member is shown in Fig. 10.5.2-1.

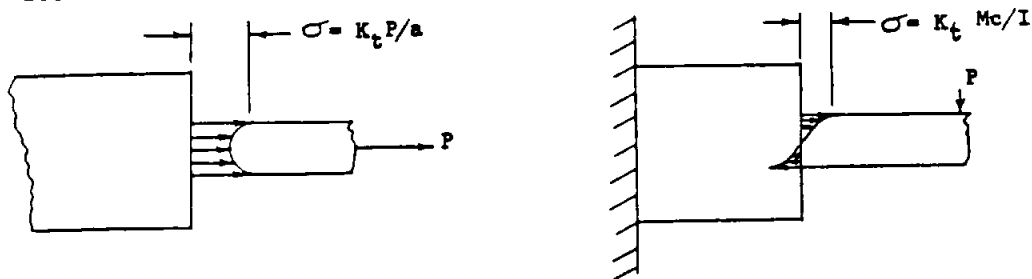


Fig. 10.5.2-1

In order to make intelligent use of the foregoing equations, we must know the following two quantities:

- (1) The maximum value of the repeated stress that the material can resist without being structurally damaged.
- (2) The value of the stress-concentration factor, (k_t) .

The values of the stress concentration factors depends mainly on two conditions: namely, (1) the form of the member or nature of the discontinuities that give rise to the stress concentrations, and (2) the properties of the material that modify the damaging influence of the stress concentrations. The stress-concentration factor resulting from the first condition only is called the theoretical factor and is denoted as (k_t) ; and that resulting from both conditions jointly is frequently called the effective stress concentration factor and is denoted as (k_f) .

The values of (k_t) are usually found either by mathematical analysis, photoelastic analysis, or direct strain measurements. Values of (k_f) are found by use of tests of the actual material.

The values of (k_f) are functions of the material, geometry of the stress concentration, heat treat, number of cycles, stress level, test temperature, grain size, surface finish, etc. In most cases (k_t) is

STRUCTURAL ANALYSIS MANUAL
GENERAL DYNAMICS/CONVAIR AND SPACE SYSTEMS DIVISION

acceptable as this factor can be theoretically obtained and will produce only slightly conservative results. If more accurate results are required, values of (k_f) can be obtained from S-N curves of unnotched and notched specimens.

$$k_f = \frac{\text{Fatigue Strength of Unnotched Specimens at N Cycles}}{\text{Fatigue Strength of Notched Specimens at N Cycles}}$$

The specimen, test temperature, stress level, geometry of the stress concentration, etc. should represent actual conditions as closely as possible.

The ratio $q = \frac{k_f - 1}{k_t - 1}$ is often referred to as "notch sensitivity" of a material. It is a measure of the susceptibility of the material to stress concentrations. Values of (k_f) and (q) for four types of steel are given in Fig. #10.5.2.15. These curves were obtained from tests of grooved specimens. Additional tests show that these results can also be used for stress concentrations caused by fillets or holes. Some of the relative values of notch sensitivity are given in Fig. #10.5.2.16, #10.5.2.17, etc. These values were obtained from room temperature tests. In general, they will be only slightly conservative for application at elevated temperatures.

If $(q = 0)$, $(k_f = 1)$ and the material is insensitive to the effects of the stress concentration. If $(q = 1)$, $(k_f = k_t)$ and the material is fully sensitive to the effects of the stress concentration.

Some of the ways to overcome the damaging effects of localized stresses are listed as follows:

1. Reducing the abruptness of the change in cross-section of the member by use of fillets, etc.,
2. Reducing the value of the stress concentration by making the portion of the member in the neighborhood of the stress concentration less stiff; this sometimes may be done by substituting a member made of material with a lower modulus of elasticity, such as replacing a steel nut on a steel bolt by a bronze nut for reducing the stress concentration at the threads of the steel bolt.
3. Increasing the fatigue strength of the material by cold-working the portions of the members where the stress concentrations occur: For example, by the cold rolling of fillets and of bearing surfaces on axles, by the shot blasting or shot peening of surfaces of machine parts.
4. Increasing the fatigue strength of the material by alloying or heat treating. Heat treating to a certain point will increase the fatigue strength. Heat treating beyond this point might actually reduce the fatigue strength.

It may be necessary to design for the increase in stress by using a lower allowable.

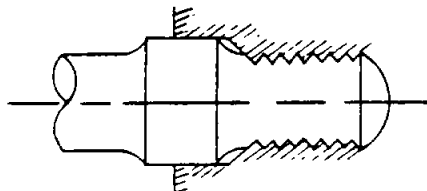
5. Some additional methods of decreasing stress concentration are shown on the following pages.

STRUCTURAL ANALYSIS MANUAL

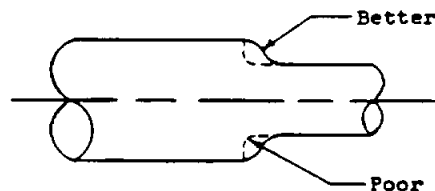
GENERAL DYNAMICS/CONVAIR AND SPACE SYSTEMS DIVISION

METHODS OF AVOIDING OR DECREASING STRESS CONCENTRATIONS

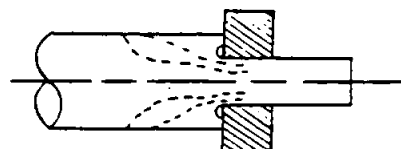
1. The number stamp should be called out on the unstressed or the low stressed portion of the part, or raised bosses should be provided. Other types of marking are available and should be used if possible.
2. Highly stressed members should have smooth surfaces.
3. Locate all oil holes in regions of low stress.
4. Use a thread relief by undercutting below the threads.



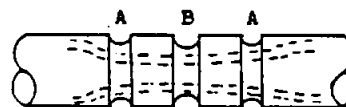
5. Grain direction should be parallel to the load imposed on the part whenever possible. Low endurance limits are typical of specimens tested normal to the grain.
6. Avoid sharp bends and internal corners. Internal machined corners should not be dimensioned as $R = .XXX_{max}$. Such a dimension is interpreted to mean anything from zero to the dimension given. Radii should always be dimensioned with permissible tolerances.
7. Avoid spot facing into stressed fillet.
8. Avoid abrupt changes in sections. Use generous fillet or faired lines.



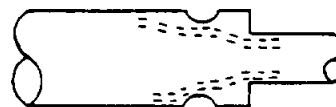
9. When a sharp corner is necessary to accommodate a part which has a small radius, a stress relieving groove can be used effectively.



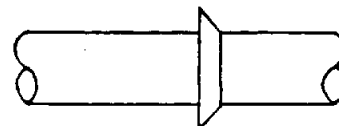
10. Additional well placed grooves at "A" help to relieve the stress concentrations caused by "B".



11. A relieving groove can be used to reduce the notch effect.



12. Avoid the use of large collars. Small collars do not disrupt the stress flow appreciably.

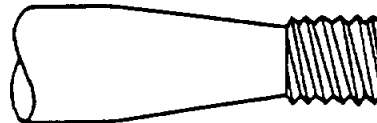


STRUCTURAL ANALYSIS MANUAL

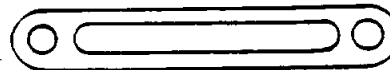
GENERAL DYNAMICS/CONVAIR AND SPACE SYSTEMS DIVISION

METHODS OF AVOIDING OR DECREASING STRESS CONCENTRATIONS (CONT'D)

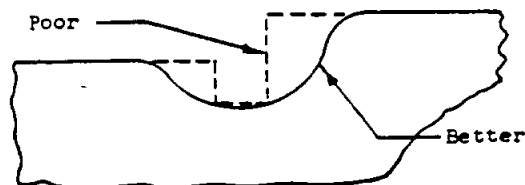
13. Threads placed outside of effective material reduce the stress concentrations.



14. A stress relieving hole lightens the shackle and may increase the allowable stress.



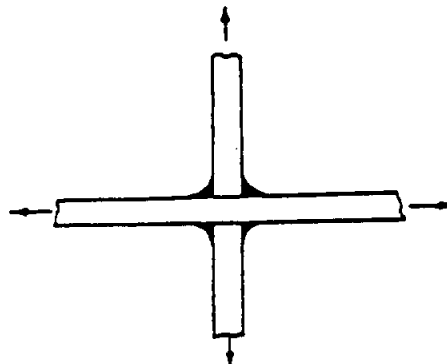
15. Never use sharp re-entrant angles or notches in a part subjected to repeated loading. Use a faired line as shown.



16. Heat treating will raise the static strength of the part but it will not necessarily increase its fatigue strength.

17. Avoid carrying loads around "corners" of angles, zeos, etc., as much as possible.

18. Avoid welded parts such as that in the figure. The part will fail at a rather low repeated stress around the weld regardless of which member is loaded.



19. Patch weld members fail at low stresses under repeated loads.



20. Where members are under repeated loads avoid all welds which induce abrupt changes in cross section. Low endurance limits are typical for such specimens.



Undesirable



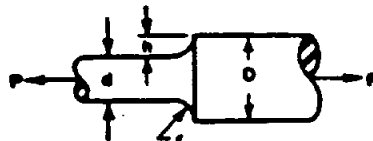
Preferred

STRUCTURAL ANALYSIS MANUAL
GENERAL DYNAMICS/CONVAIR AND SPACE SYSTEMS DIVISION

Data Source, Section 1.3 Reference 22

GEOMETRIC STRESS CONCENTRATION FACTORS

SOLID CIRCULAR SHAFT
Circular Fillet
Tension



$$\sigma_{nom} = \frac{4P}{\pi d^2}$$

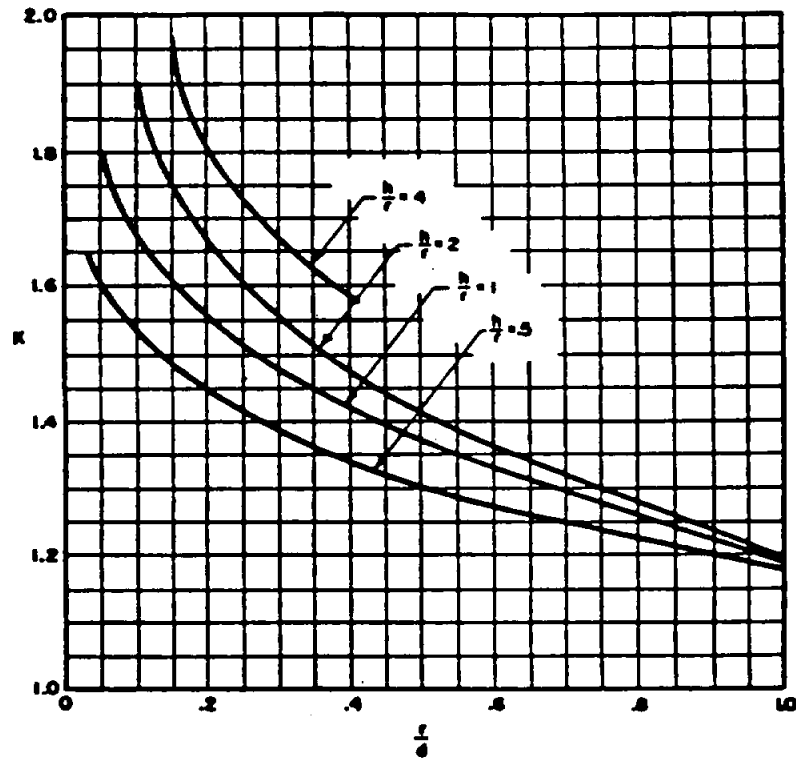
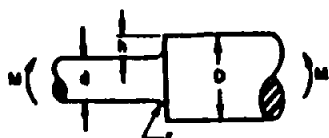


CHART 1

GEOMETRIC STRESS CONCENTRATION FACTORS

SOLID CIRCULAR SHAFT
Circular Fillet
Bending



$$S_{nom} = \frac{32M}{\pi d^3}$$

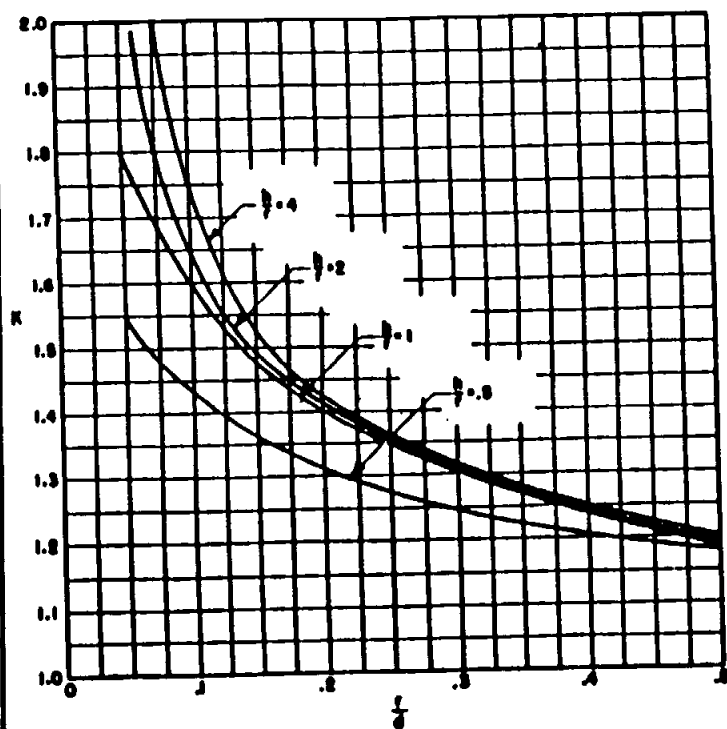
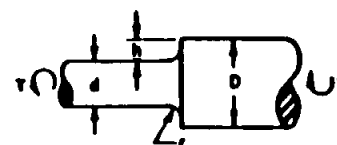


CHART 2

GEOMETRIC STRESS CONCENTRATION FACTORS

SOLID CIRCULAR SHAFT
Circular Fillet
Torsion



$$S_{nom} = \frac{16T}{\pi d^3}$$

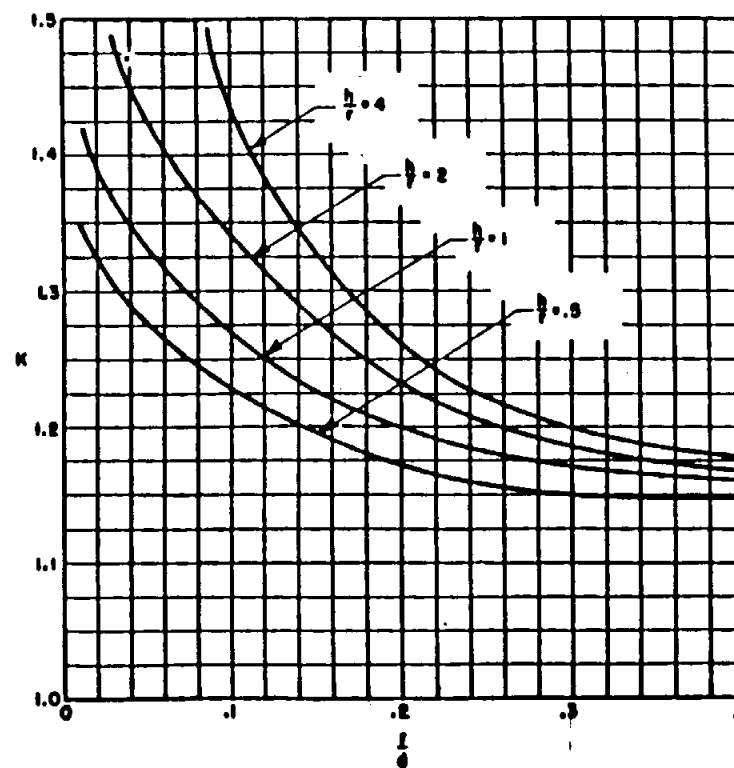


CHART 3

GEOMETRIC STRESS CONCENTRATION FACTORS

SOLID CIRCULAR SHAFT
 Circular Groove
 Tension

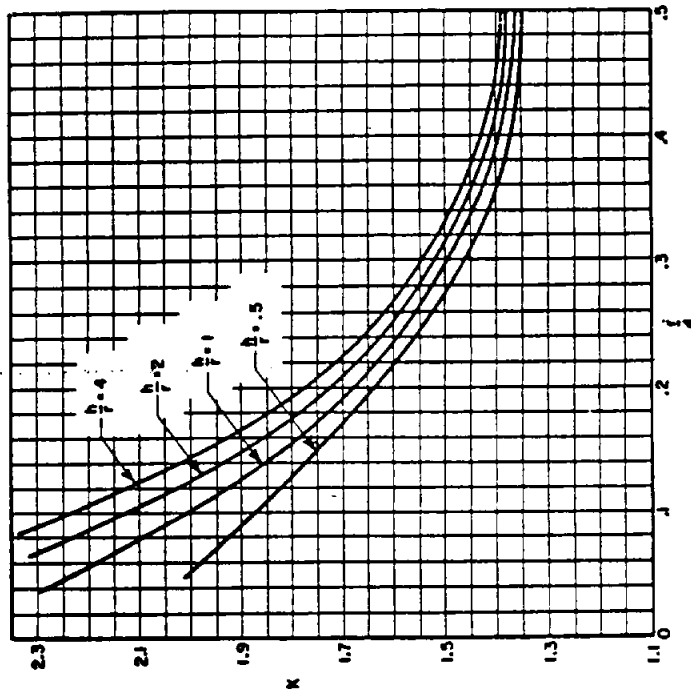
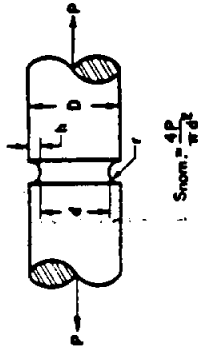


CHART 5

GEOMETRIC STRESS CONCENTRATION FACTORS

SOLID CIRCULAR SHAFT
 Elliptical Fillet
 Bending

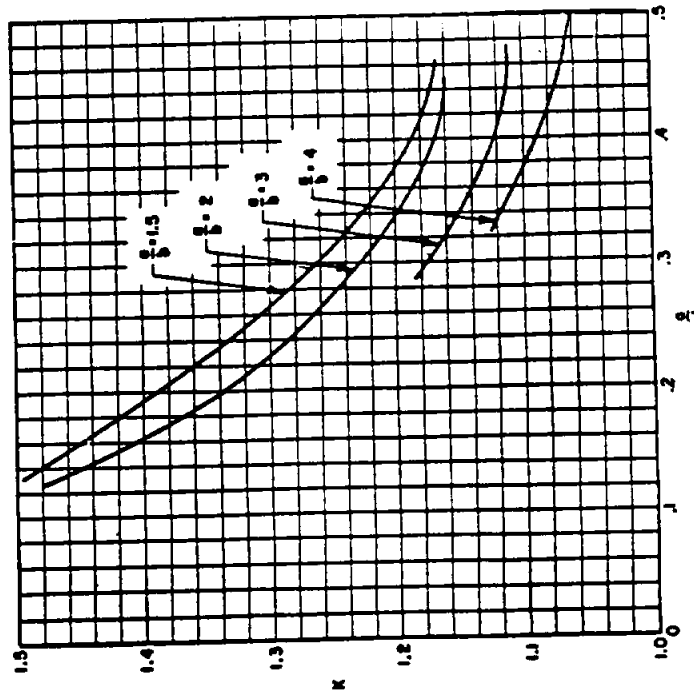
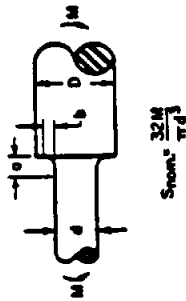
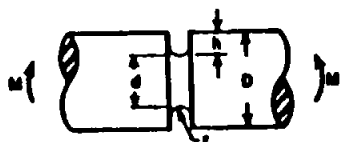


CHART 4

GEOMETRIC STRESS CONCENTRATION FACTORS

SOLID CIRCULAR SHAFT
Circular Groove
Bending



$$\sigma_{nom} = \frac{32M}{\pi d^3}$$

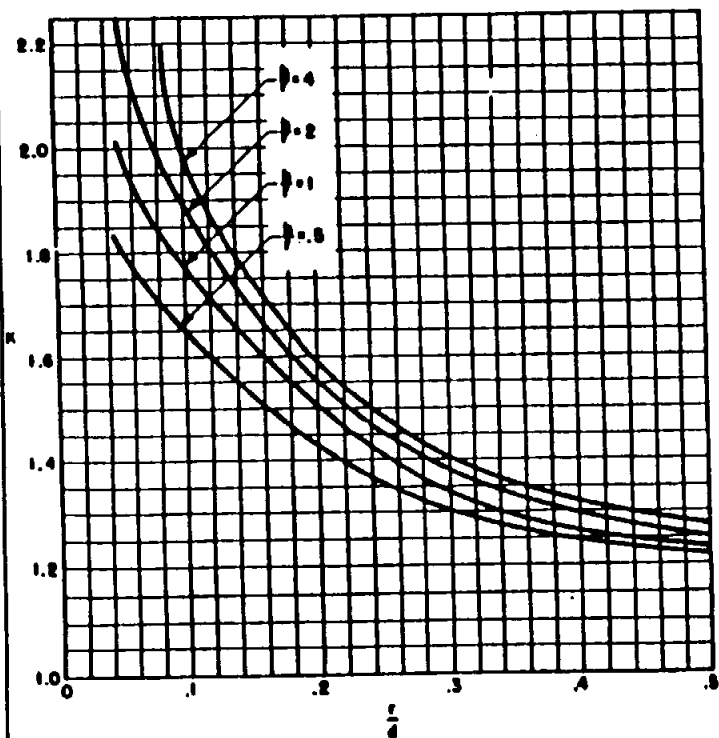
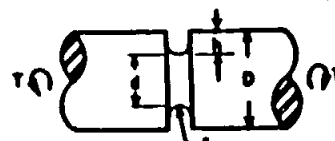


CHART 6

GEOMETRIC STRESS CONCENTRATION FACTORS

SOLID CIRCULAR SHAFT
Circular Groove
Torsion



$$\tau_{nom} = \frac{MT}{\pi d^3}$$

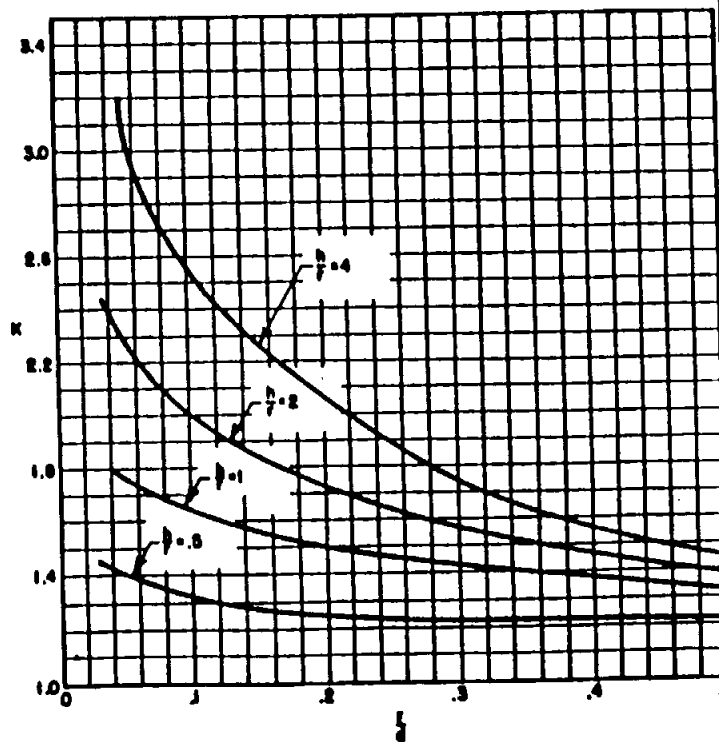


CHART 7

GEOMETRIC STRESS CONCENTRATION FACTORS

SOLID CIRCULAR SHAFT
Transverse Hole
Tension



$$S_{nom} = \frac{4P}{D^2(\pi - 4\frac{d}{D})}$$

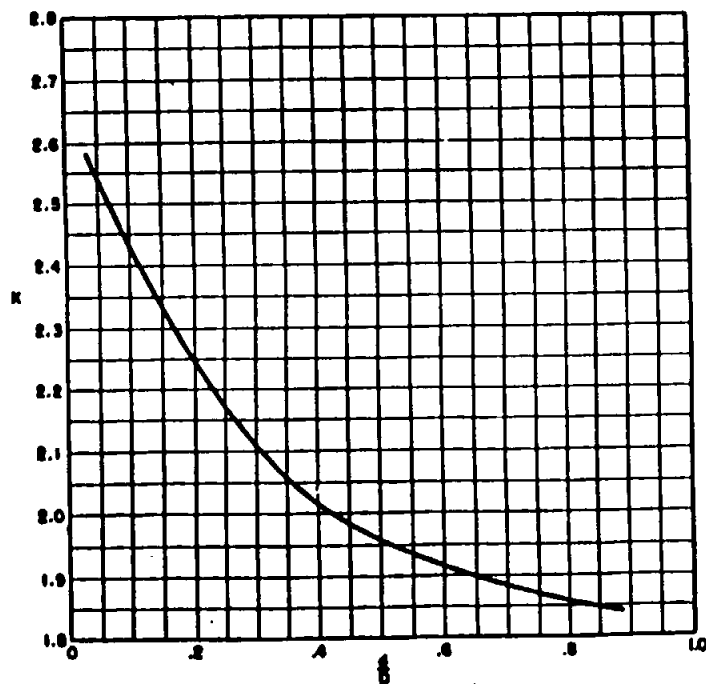
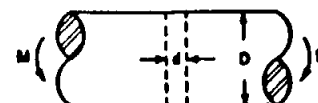


CHART 10

GEOMETRIC STRESS CONCENTRATION FACTORS

SOLID CIRCULAR SHAFT
Transverse Hole
Bending



$$S_{nom} = \frac{96M}{D^3(1.3\pi - 1.6\frac{d}{D})}$$

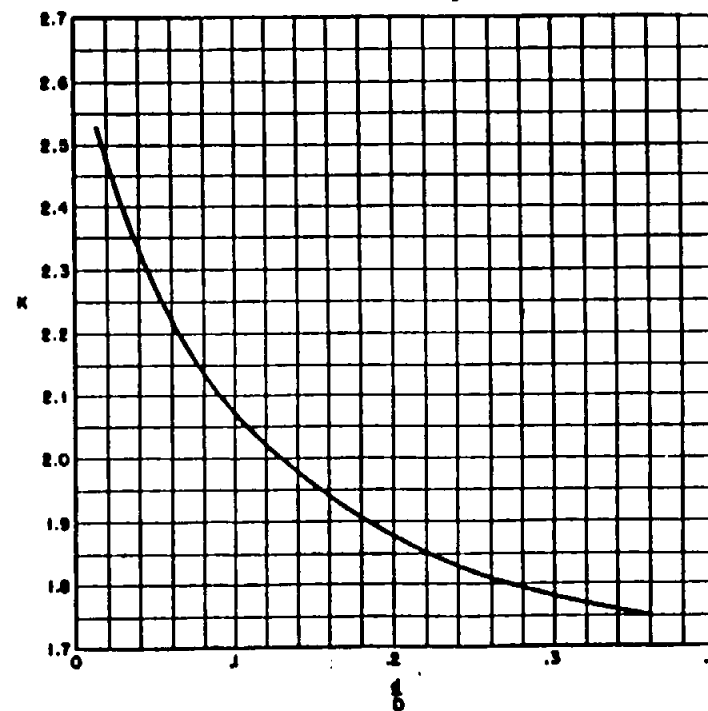
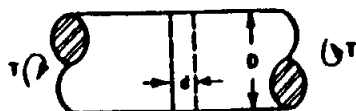


CHART 11

GEOMETRIC STRESS CONCENTRATION FACTORS

SOLID CIRCULAR SHAFT
Transverse Hole
Torsion



$$S_{nom} = \frac{16T}{\pi D^3}$$

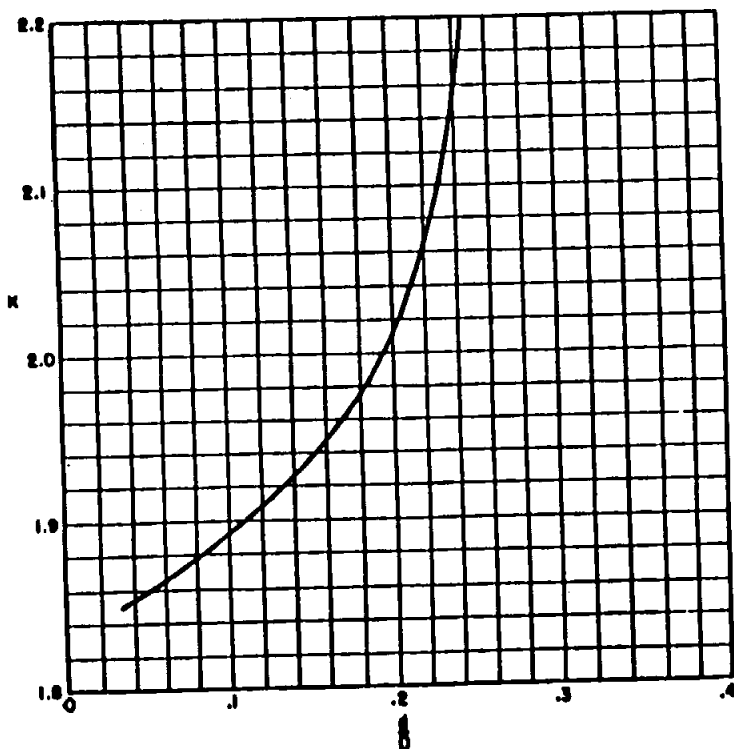
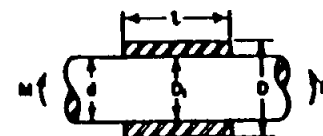


CHART 12

GEOMETRIC STRESS CONCENTRATION FACTORS

SOLID CIRCULAR SHAFT
Plain Press Fit
Bending



$$P = \frac{E M (D - d) D^2 - d^3}{2 d D^3}$$

P = RADIAL PRESSURE, PSI
E = MODULUS OF ELASTICITY, PSI
D = INTERNAL DIA. COLLAR, IN.

$$S_{nom} = \frac{32M}{\pi d^3}$$

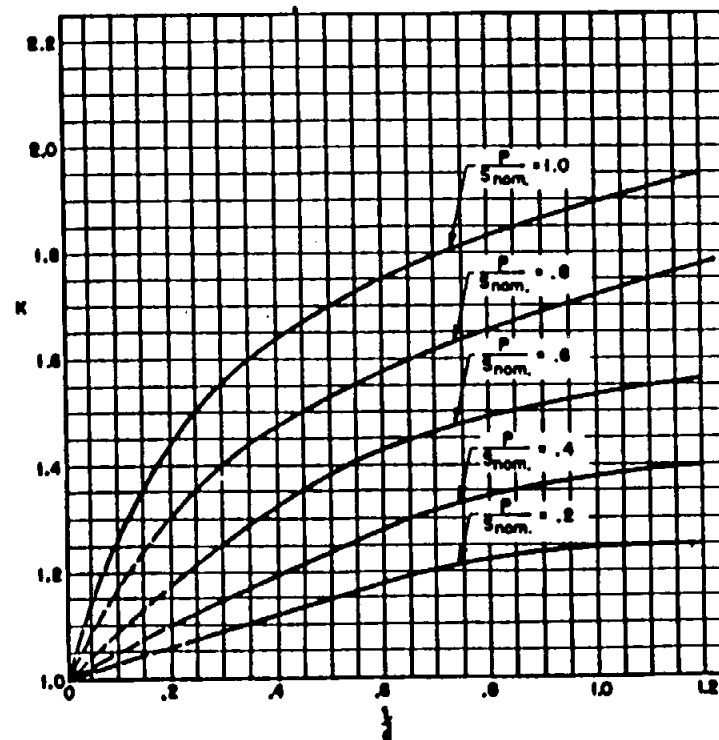


CHART 13

GEOMETRIC STRESS CONCENTRATION FACTORS

HOLLOW CIRCULAR SHAFT
External Circular Groove
Tension



$$S_{nom} = \frac{P}{\pi(R^2 - C^2)}$$

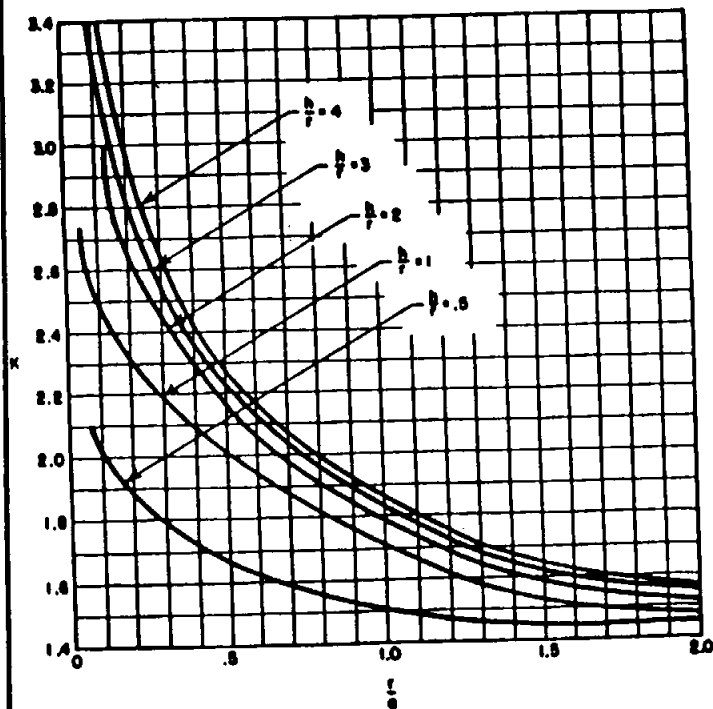
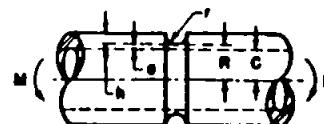


CHART 14

GEOMETRIC STRESS CONCENTRATION FACTORS

HOLLOW CIRCULAR SHAFT
External Circular Groove
Bending



$$S_{nom} = \frac{4MR}{\pi(R^4 - C^4)}$$

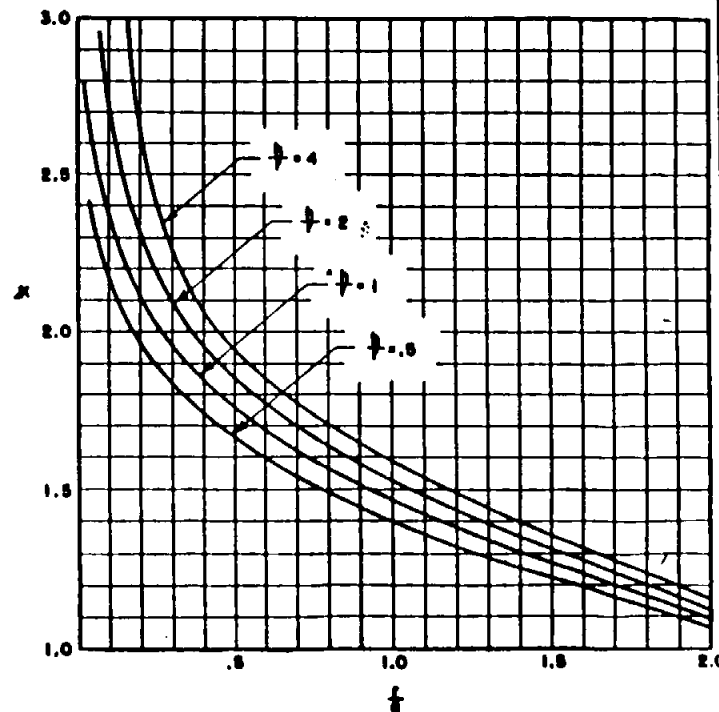


CHART 15

GEOMETRIC STRESS CONCENTRATION FACTORS

HOLLOW CIRCULAR SHAFT
External Circular Groove
Torsion



$$S_{nom} = \frac{RT}{\pi(R^3 - C^3)}$$

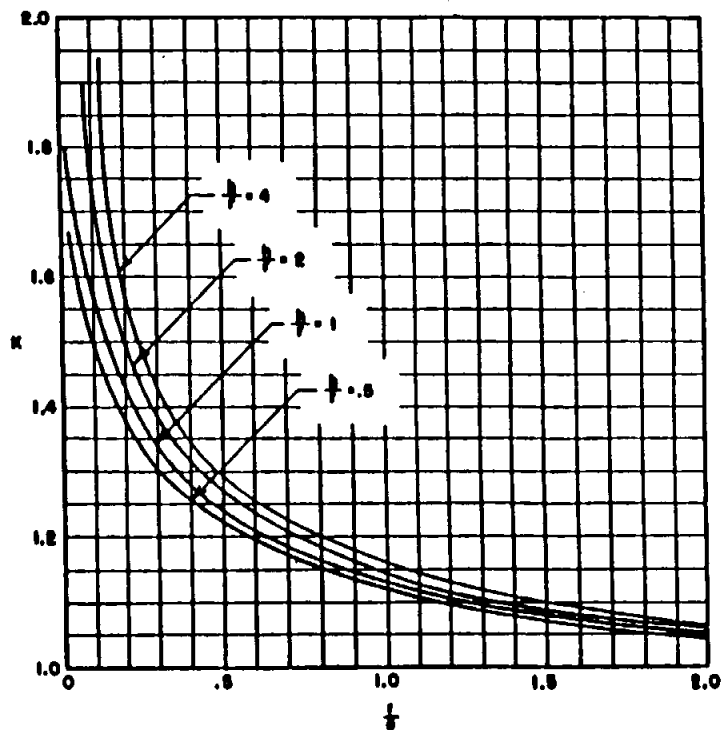
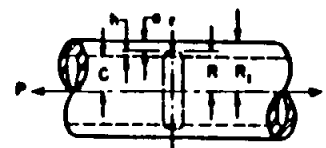


CHART 16

GEOMETRIC STRESS CONCENTRATION FACTORS

HOLLOW CIRCULAR SHAFT
Internal Circular Groove
Tension



$$S_{nom} = \frac{P}{\pi(R^2 - C^2)}$$

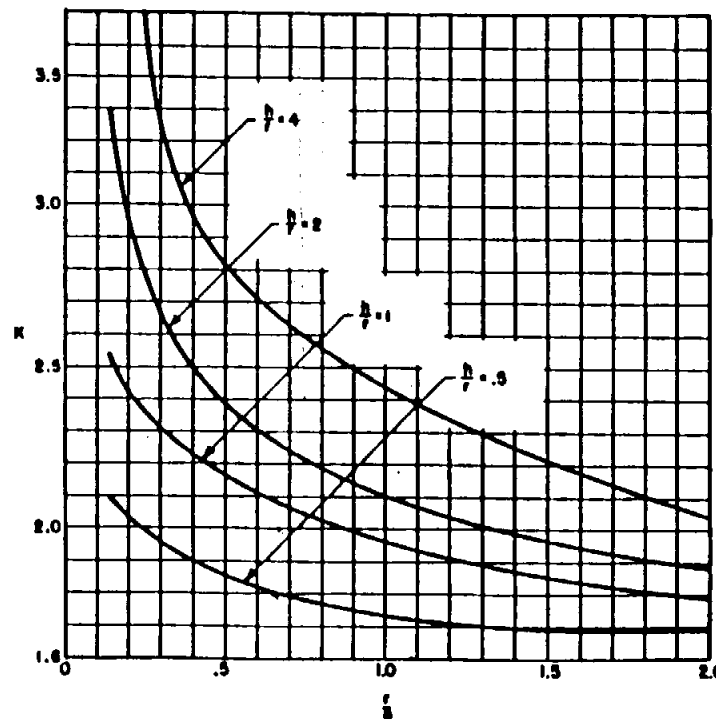


CHART 17

GEOMETRIC STRESS CONCENTRATION FACTORS

HOLLOW CIRCULAR SHAFT
Internal Circular Groove
Bending



$$S_{nom} = \frac{4MR}{\pi(R_1^4 - R^4)}$$

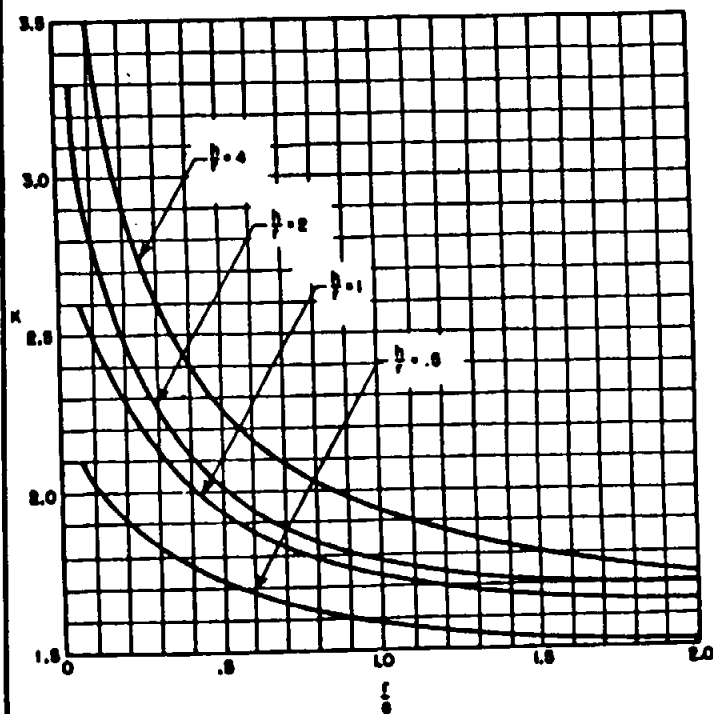
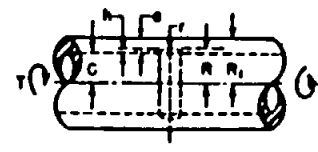


CHART 18

GEOMETRIC STRESS CONCENTRATION FACTORS

HOLLOW CIRCULAR SHAFT
Internal Circular Groove
Torsion



$$S_{nom} = \frac{2TR}{\pi(R_1^4 - R^4)}$$

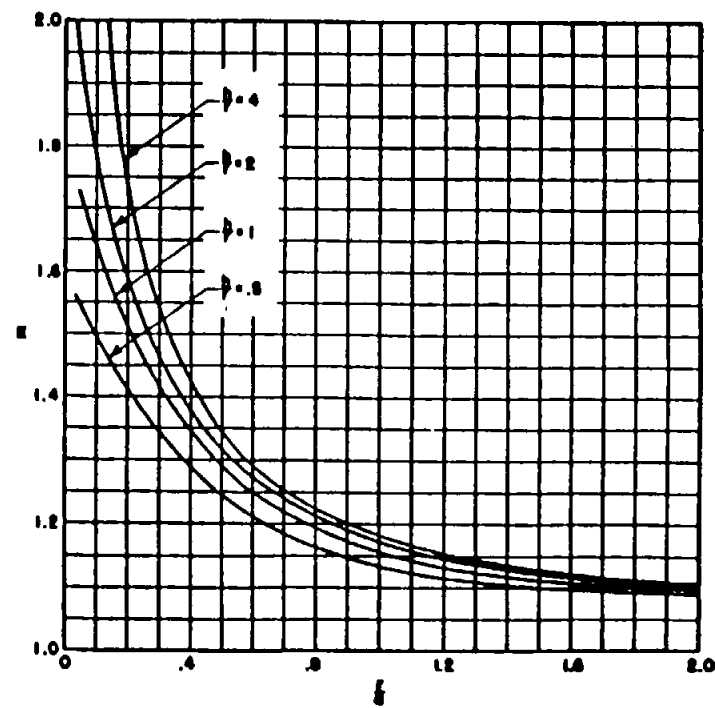
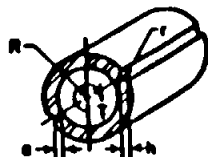


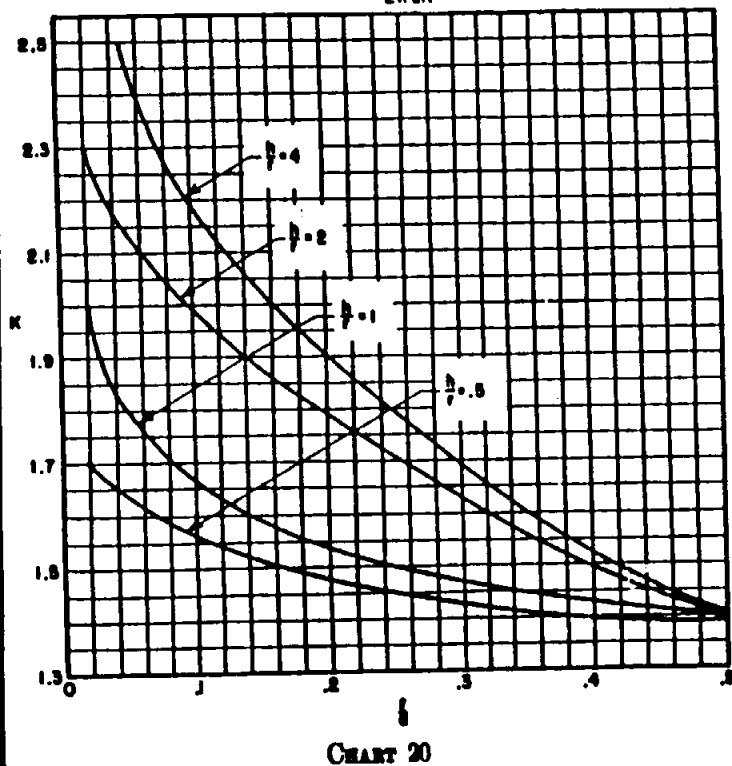
CHART 19

GEOMETRIC STRESS CONCENTRATION FACTORS

HOLLOW CIRCULAR SHAFT
Longitudinal Circular Groove
Torsion

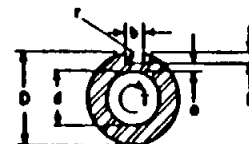


$$S_{nom} = \frac{T}{2\pi R^2}$$

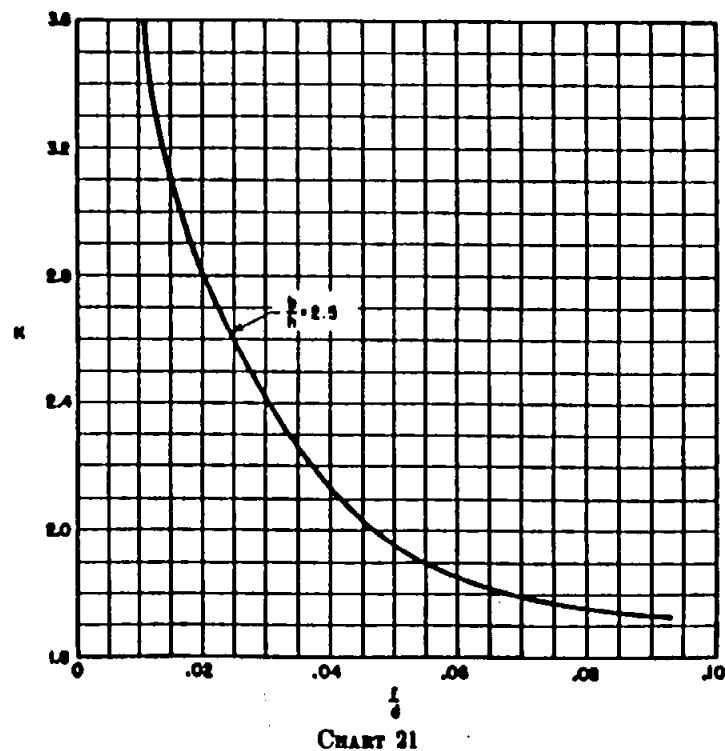


GEOMETRIC STRESS CONCENTRATION FACTORS

HOLLOW CIRCULAR SHAFT
Keyway
Torsion



$$S_{nom} = \frac{2T}{\pi R^3}$$

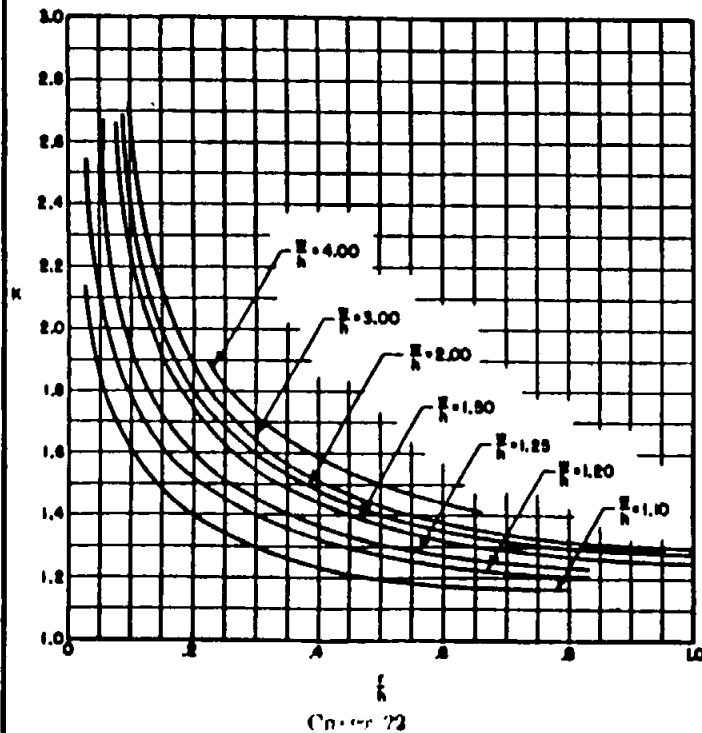


GEOMETRIC STRESS CONCENTRATION FACTORS

FLAT PLATES
Circular Fillets
Tension

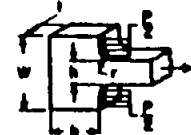


$$s_{nom} = \frac{P}{At}$$

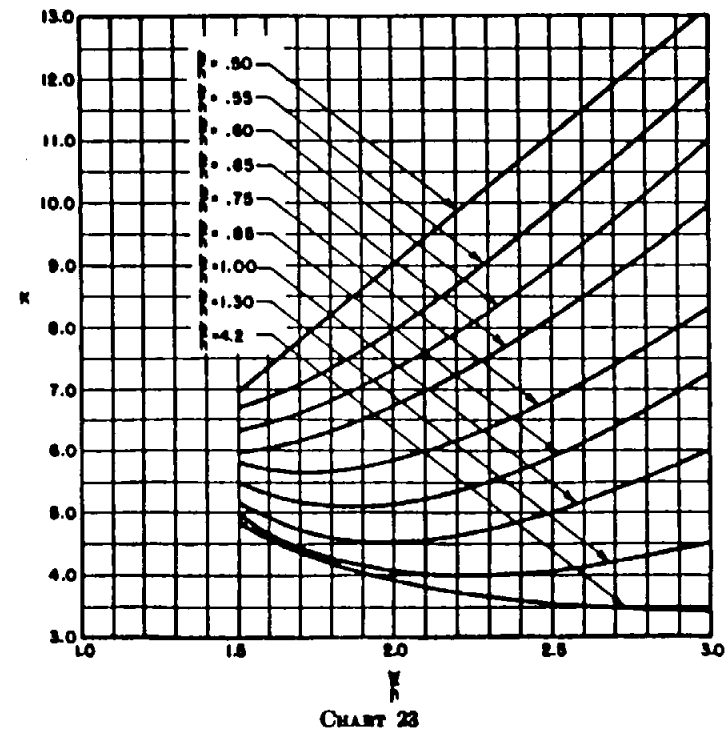


GEOMETRIC STRESS CONCENTRATION FACTORS

FLAT PLATES
Circular Fillets
Tension with Uniformly Distributed Reaction on Flanges

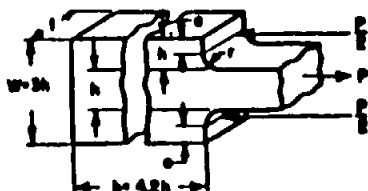


$$s_{nom} = \frac{P}{bt}$$



GEOMETRIC STRESS CONCENTRATION FACTORS

FLAT PLATES
Circular Fillets
Tension with Concentrated Reaction on Flanges



$$S_{nom} = \frac{P}{h}$$

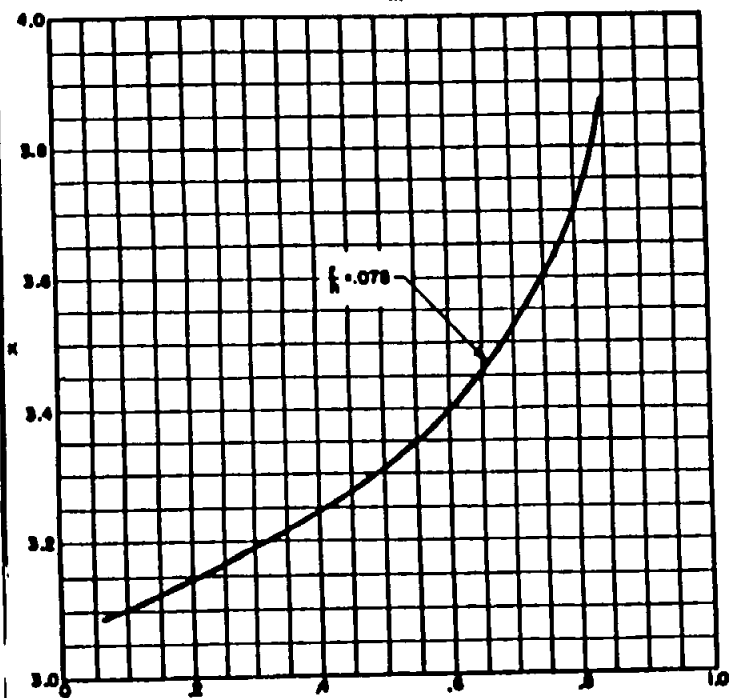
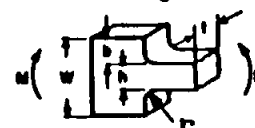


CHART 24

GEOMETRIC STRESS CONCENTRATION FACTORS

FLAT PLATES
Circular Fillets
Bending



$$S_{nom} = \frac{6M}{h^2}$$

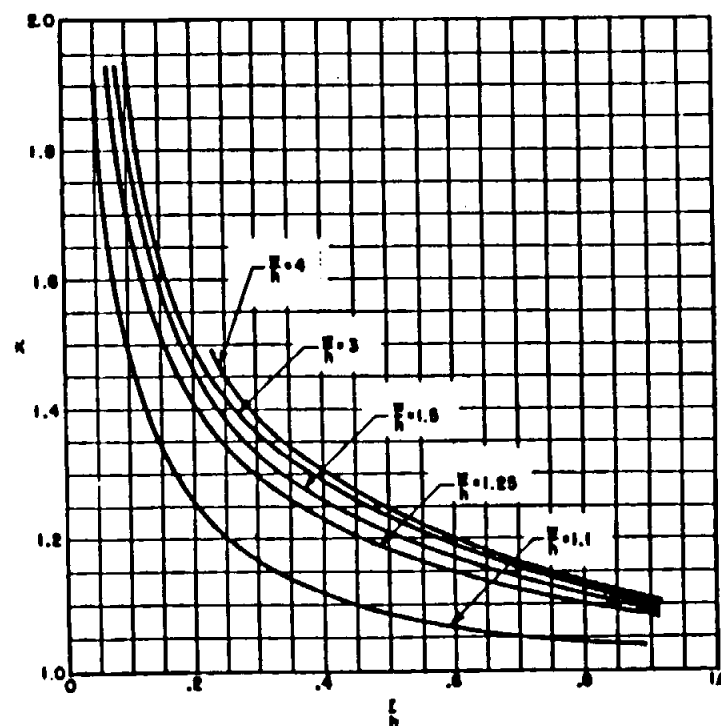
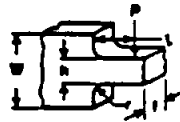


CHART 25

STRUCTURAL ANALYSIS MANUAL
GENERAL DYNAMICS/CONVAIR AND SPACE SYSTEMS DIVISION

GEOMETRIC STRESS CONCENTRATION FACTORS

FLAT PLATES
 Circular Fillets
 Bending—Concentrated Load



$$S_{max} = \frac{6Pl}{Wt^2}$$

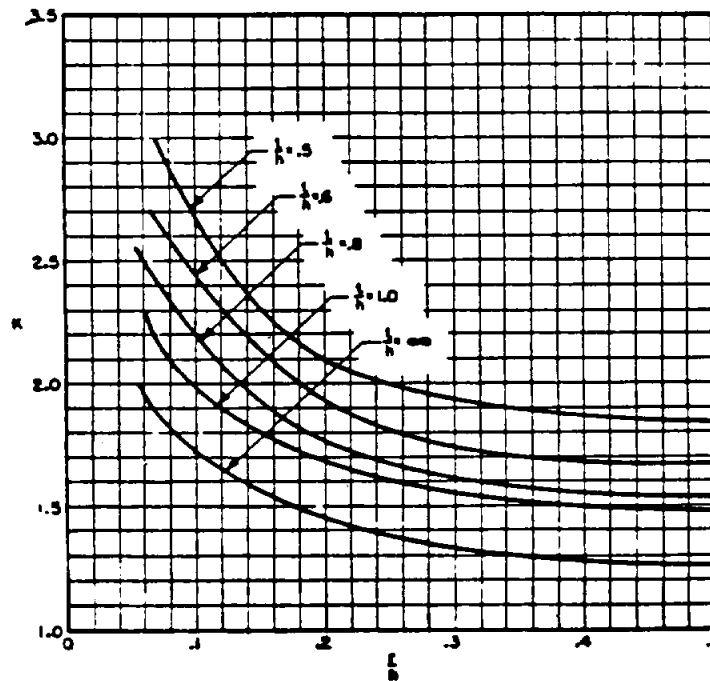
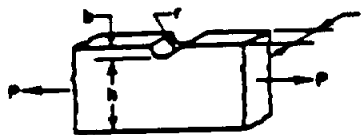


CHART 26

STRUCTURAL ANALYSIS MANUAL
GENERAL DYNAMICS/CONVAIR AND SPACE SYSTEMS DIVISION

GEOMETRIC STRESS CONCENTRATION FACTORS

FLAT PLATES
 Hyperbolic Groove on One Edge
 Tension



$$S_{max} = \frac{P}{th}$$

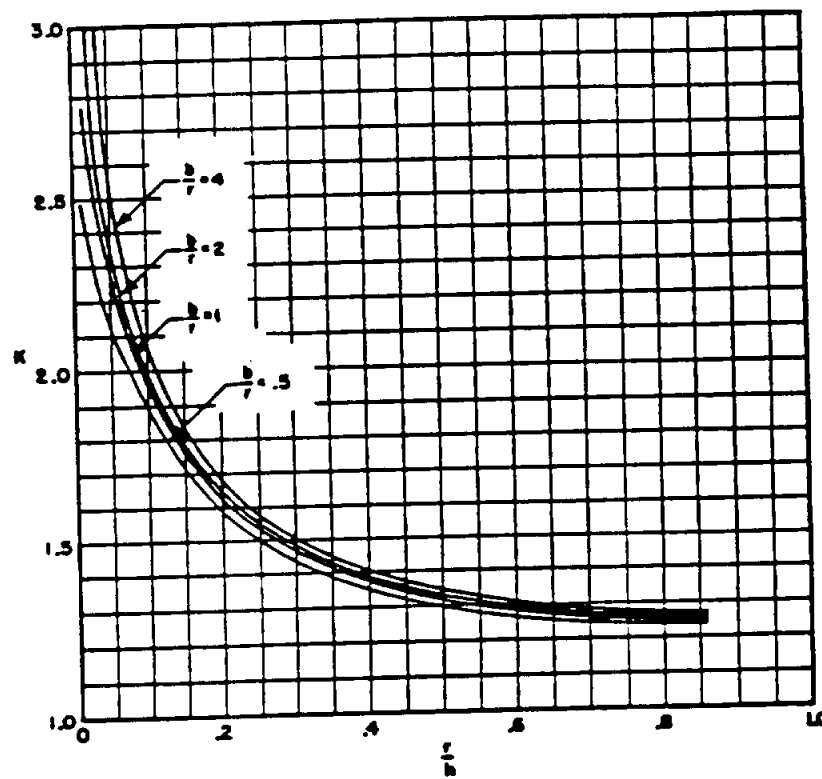


CHART 33

GEOMETRIC STRESS CONCENTRATION FACTORS

FLAT PLATES
 Hyperbolic Groove on One Edge
 Bending



$$S_{nom} = \frac{M}{I} \cdot \frac{W}{t}$$

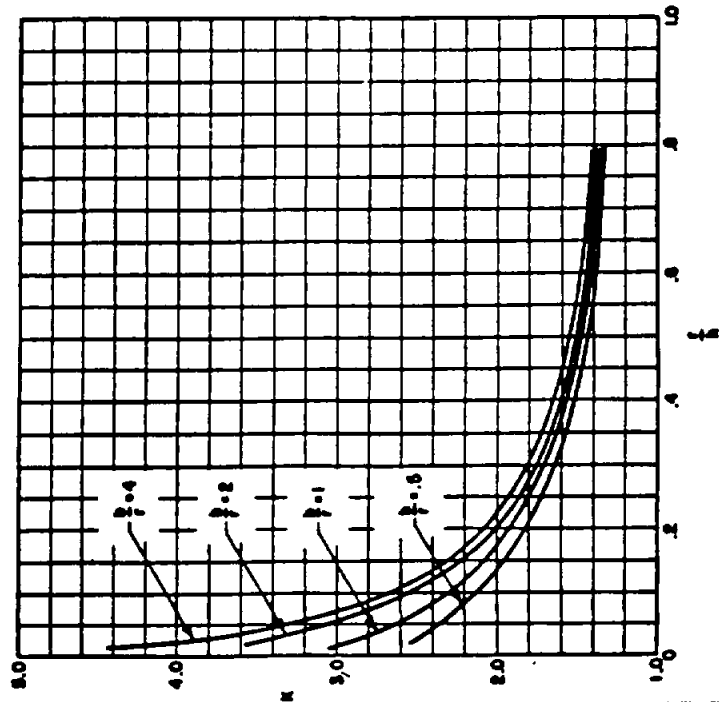
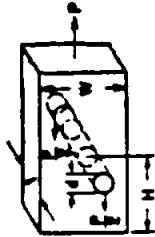


CHART 34

GEOMETRIC STRESS CONCENTRATION FACTORS

FLAT PLATES
 Pin in Transverse Hole at Center



$$S_{nom} = \frac{P}{(W-d)t}$$

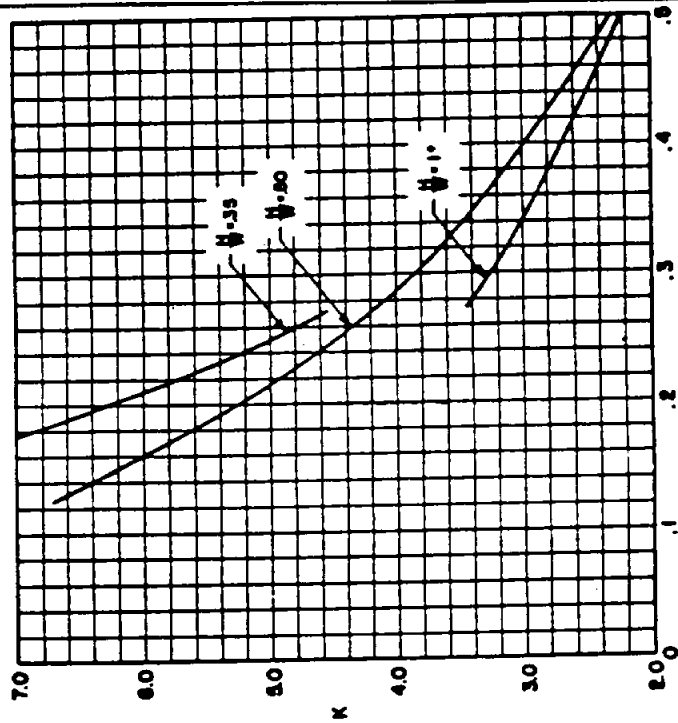


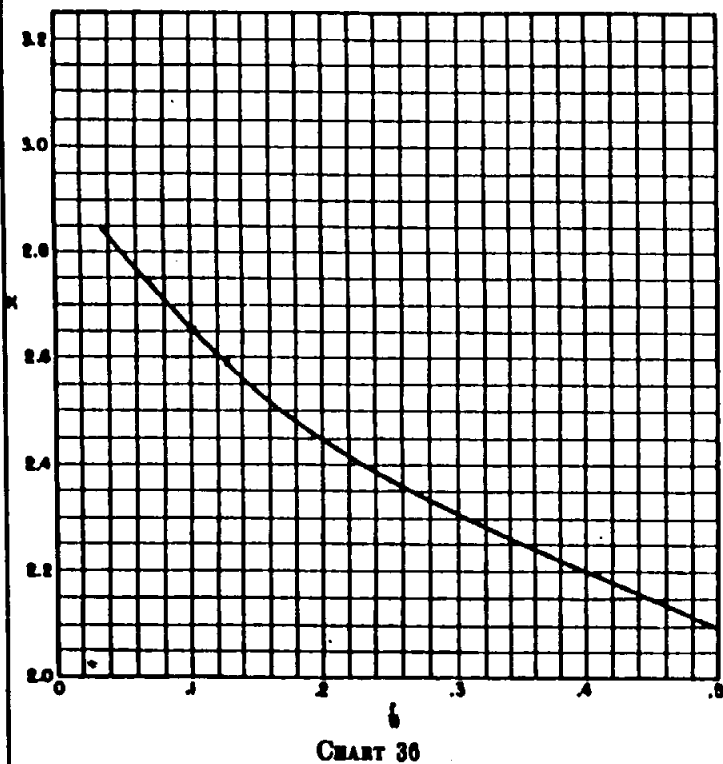
CHART 35

GEOMETRIC STRESS CONCENTRATION FACTORS

FLAT PLATES
Transverse Hole at Center
Tension

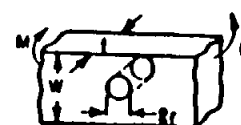


$$S_{nom} = \frac{P}{(W-2r)t}$$

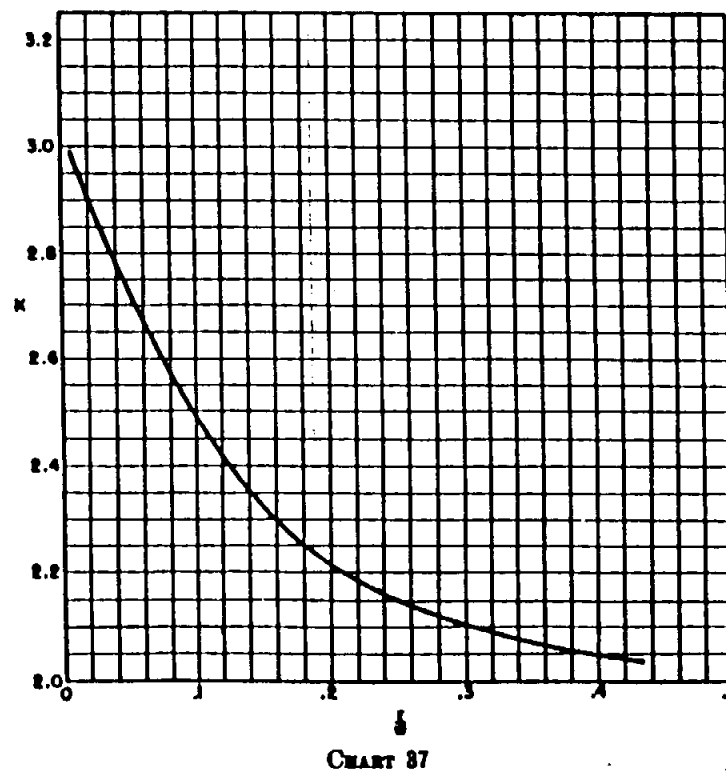


GEOMETRIC STRESS CONCENTRATION FACTORS

FLAT PLATES
Transverse Hole At Center
Transverse Bending



$$S_{nom} = \frac{6M}{(W-2r)t^2}$$



GEOMETRIC STRESS CONCENTRATION FACTORS

FLAT PLATES
Transverse Hole Near Edge
Tension



$$S_{nom} = \frac{P}{(W-d)t}$$

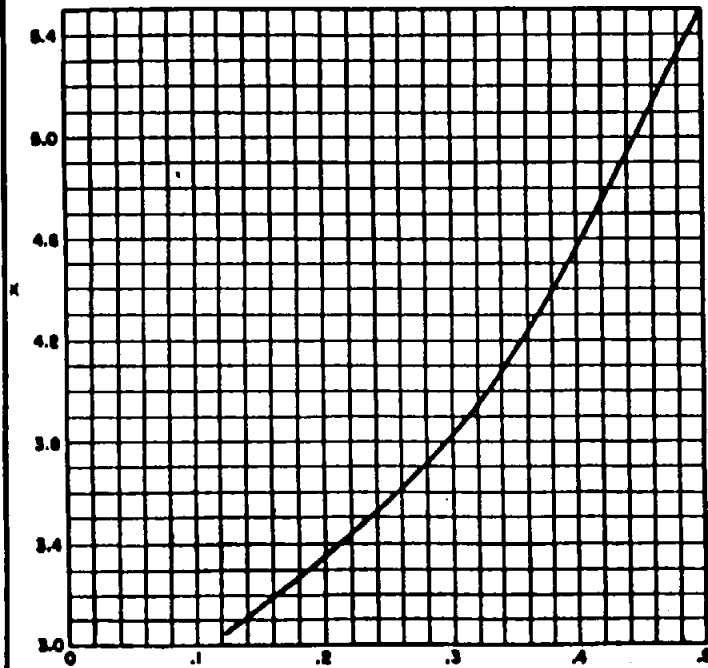


CHART 28

GEOMETRIC STRESS CONCENTRATION FACTORS

FLAT PLATES
Transverse Hole Near Edge
Bending



$$S_{Anom} = \frac{6M(2h+d)}{(W-d)^2t}$$

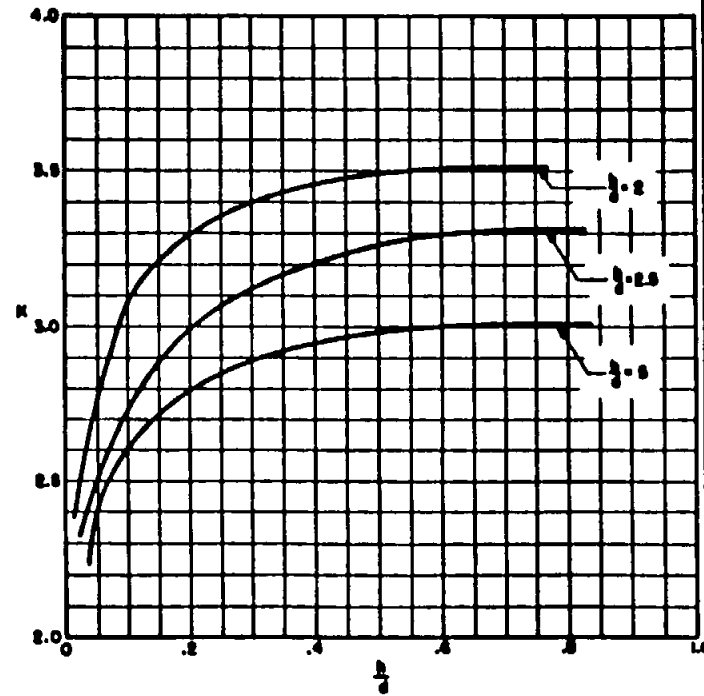
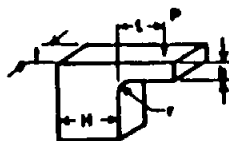


CHART 29

GEOMETRIC STRESS CONCENTRATION FACTORS

FLAT PLATES
Angle-shaped Section
Bending



$$S_{nom} = \frac{bH^2}{12t}$$

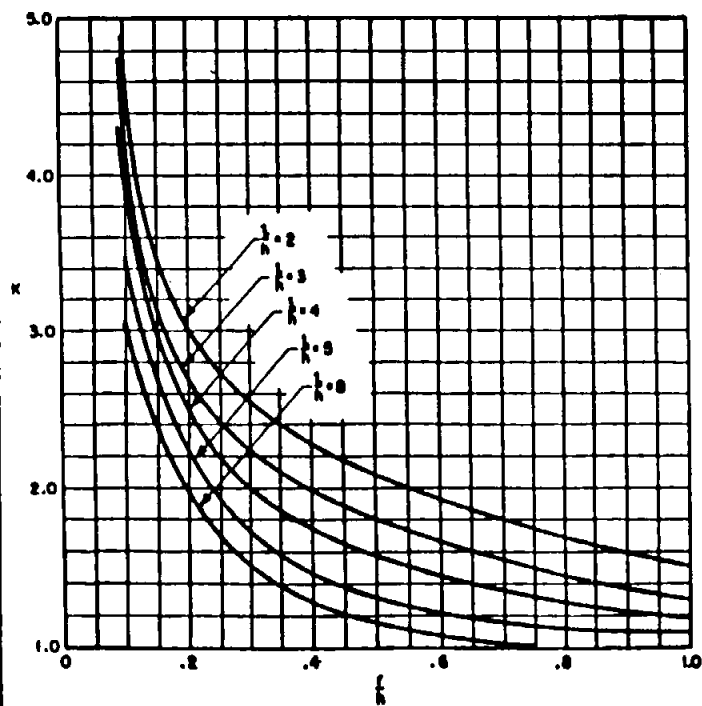


CHART 42

GEOMETRIC STRESS CONCENTRATION FACTORS

FLAT PLATES
Flange
Bending



$$S_{nom} = \frac{bH^2}{12t}$$

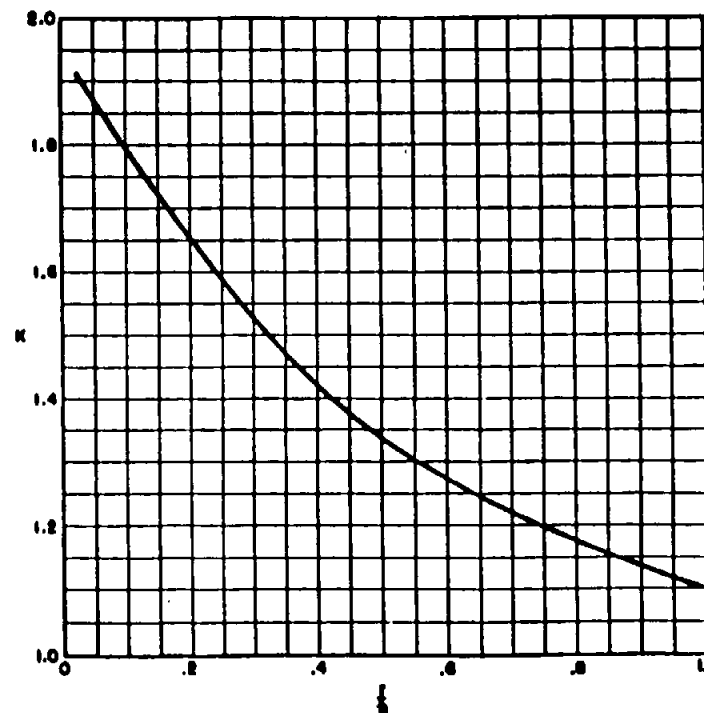


CHART 43

GEOMETRIC STRESS CONCENTRATION FACTORS

FLAT PLATES
Circular Transverse Hole at Center
Biaxial Stress

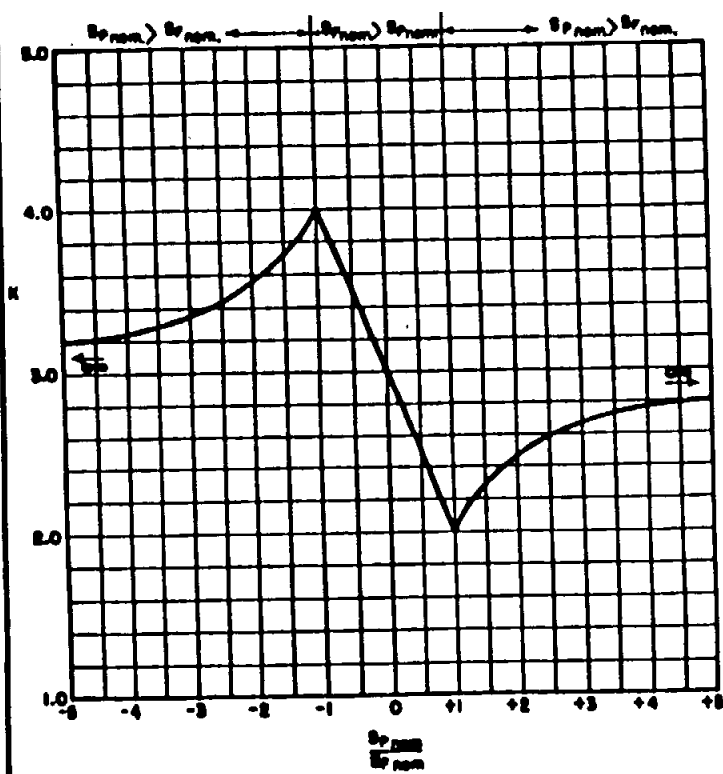
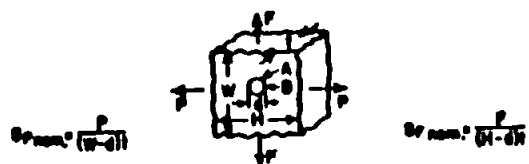


CHART 44

GEOMETRIC STRESS CONCENTRATION FACTORS

FLAT PLATES
Elliptical Transverse Hole at Center
Biaxial Stress

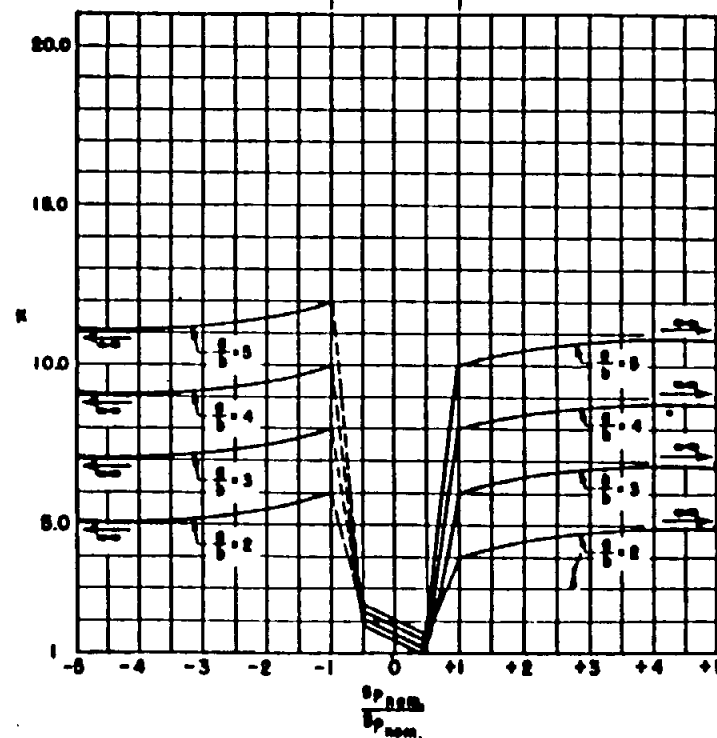
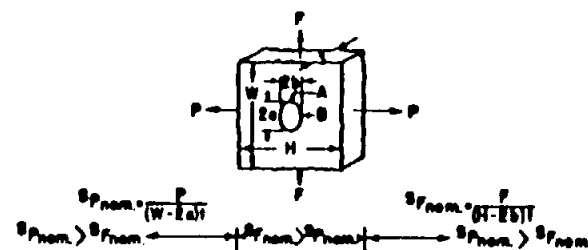


CHART 45

**FATIGUE STRESS CONCENTRATION FACTORS
FOR ANNEALED STEELS**

**SOLID CIRCULAR SHAFT
Threads
Tension and Bending**

U.S. STANDARD



	BENDING OR TENSION	
	ROLLED	CUT
K_f	2.2	2.8

WHITWORTH



	BENDING OR TENSION	
	ROLLED	CUT
K_f	1.4	1.8

DARDALET



	BENDING OR TENSION	
	ROLLED	CUT
K_f	1.8	2.3

AERO STUD



	BENDING OR TENSION	
	ROLLED	CUT
K_f	1.2	1.5

CHART 60

STRUCTURAL ANALYSIS MANUAL
GENERAL DYNAMICS/CONVAIR AND SPACE SYSTEMS DIVISION

**FATIGUE STRESS CONCENTRATION FACTORS
FOR QUENCHED AND DRAWN STEELS**

SOLID CIRCULAR SHAFT
Threads
Tension and Bending

U.S. STANDARD



	BENDING OR TENSION	
	ROLLED	CUT
K_f	3.0	3.8

WHITWORTH



	BENDING OR TENSION	
	ROLLED	CUT
K_f	2.6	3.3

DARDALET



	BENDING OR TENSION	
	ROLLED	CUT
K_f	2.6	3.3

AERO STUD

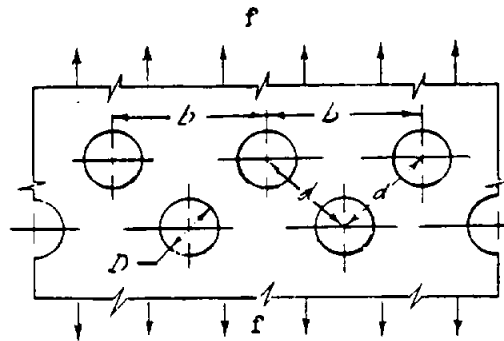


	BENDING OR TENSION	
	ROLLED	CUT
K_f	2.3	2.8

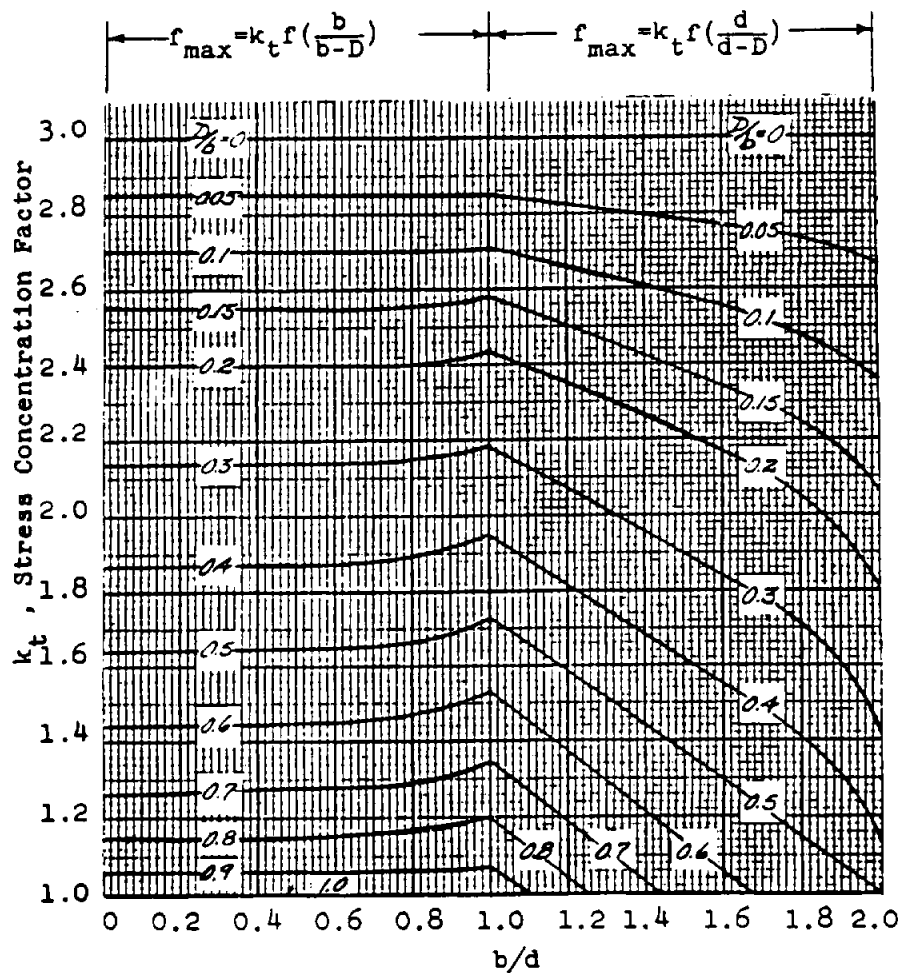
CHART 107

STRUCTURAL ANALYSIS MANUAL
GENERAL DYNAMICS/CONVAIR AND SPACE SYSTEMS DIVISION

Data Source, Section 1.3 Reference |



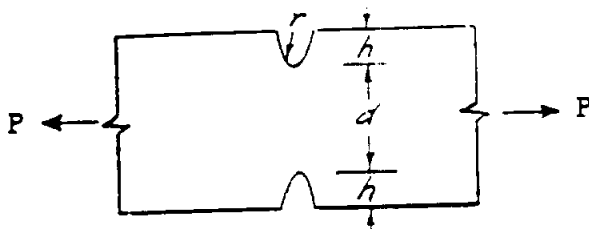
NOTE:
 f = ave. stress on cross section



Stress Concentration Factors for a Wide Sheet With a Double Row of Holes Perpendicular to the Load

Fig. 10.5.2.9

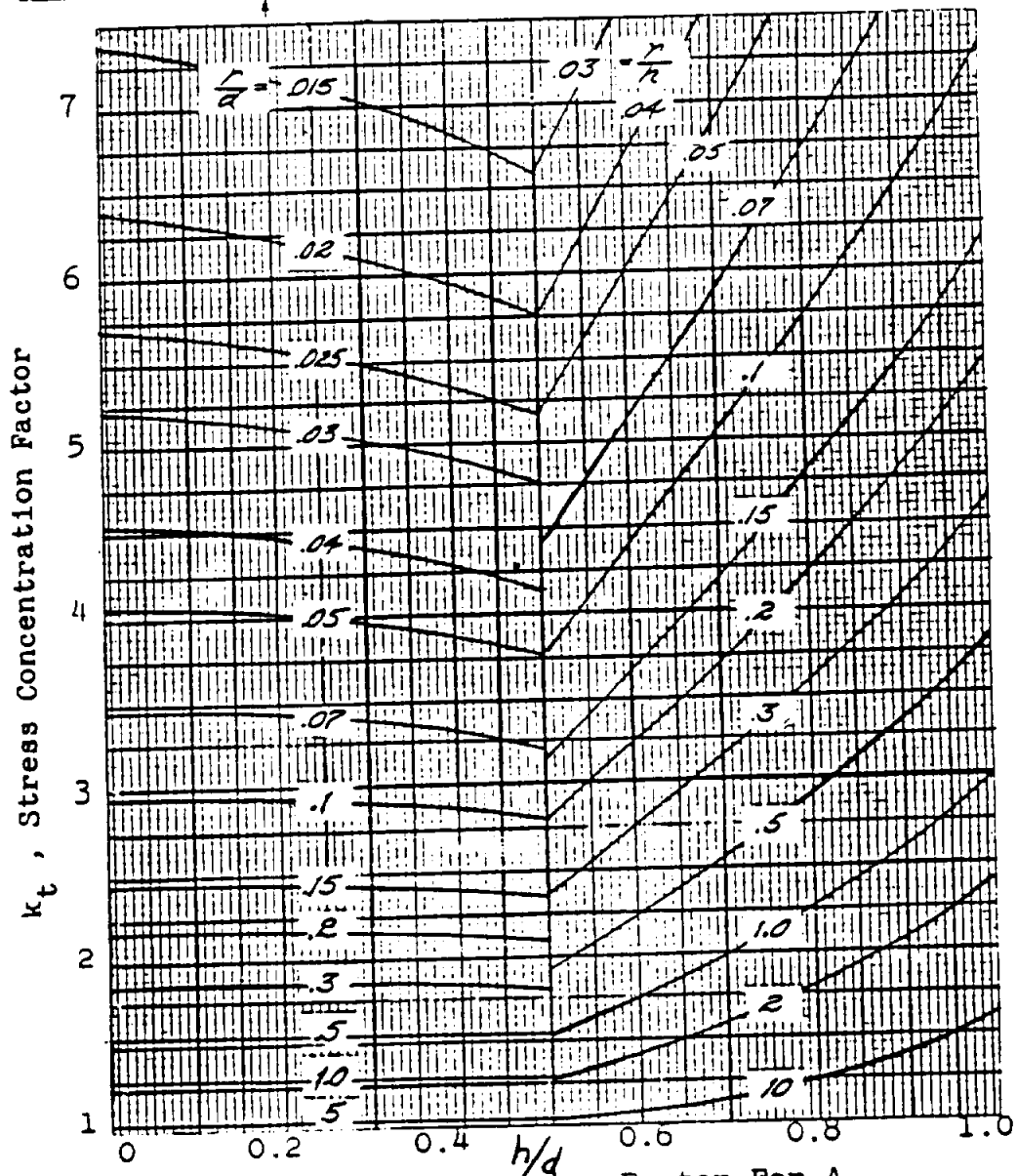
STRUCTURAL ANALYSIS MANUAL
GENERAL DYNAMICS/CONVAIR AND SPACE SYSTEMS DIVISION



$$f_{\max} = k_t f_{\text{ave}}$$

$$f_{\text{ave}} = \frac{P}{dt}$$

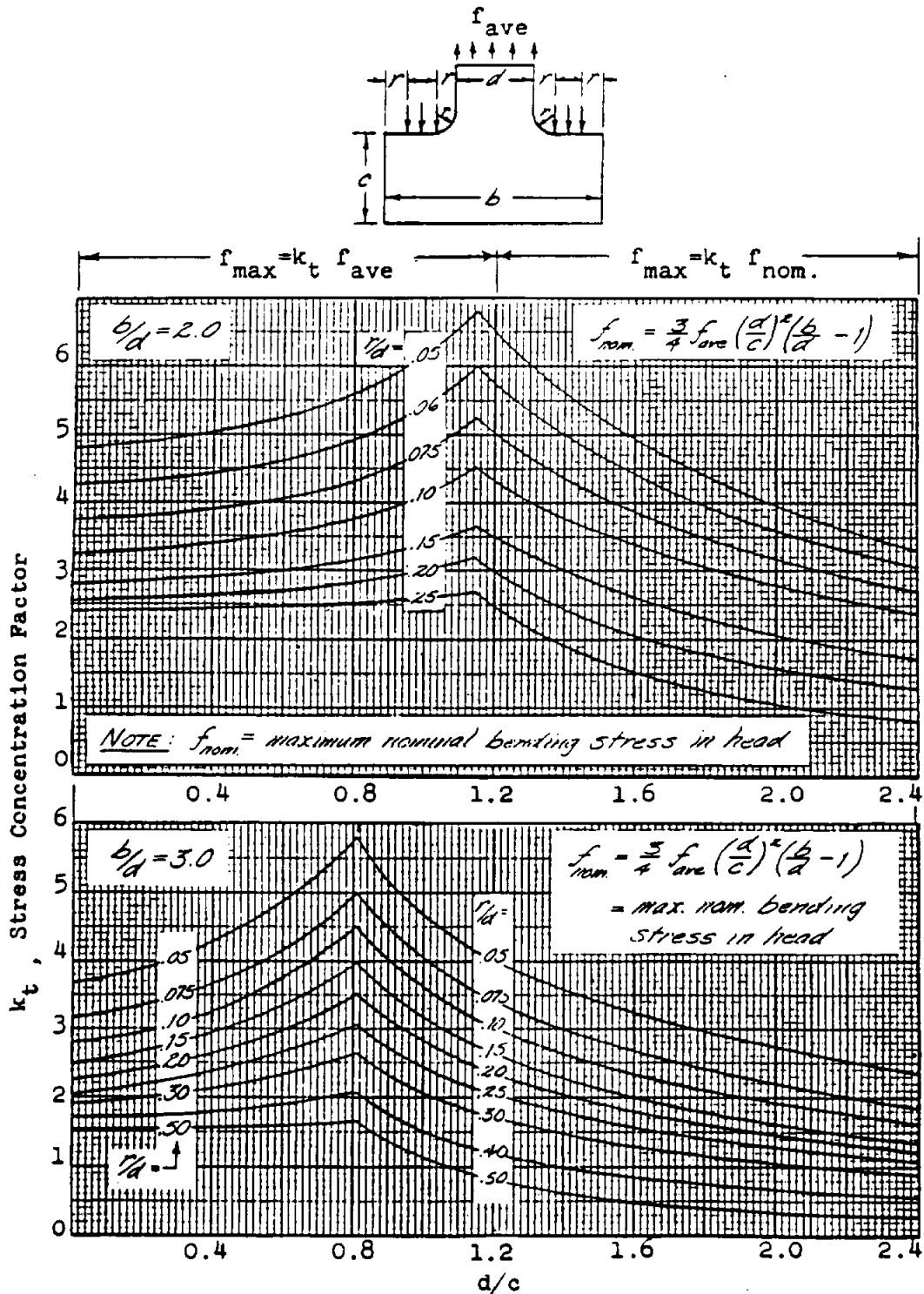
t = plate thickness



Stress Concentration Factor For A
 Notched Flat Plate Under Axial Load

Fig. 10.5.2.10

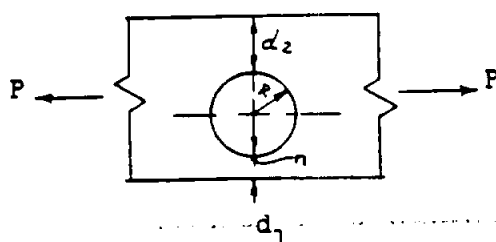
STRUCTURAL ANALYSIS MANUAL
GENERAL DYNAMICS/CONVAIR AND SPACE SYSTEMS DIVISION



Stress Concentration Factors

Fig. 10.5.2.11

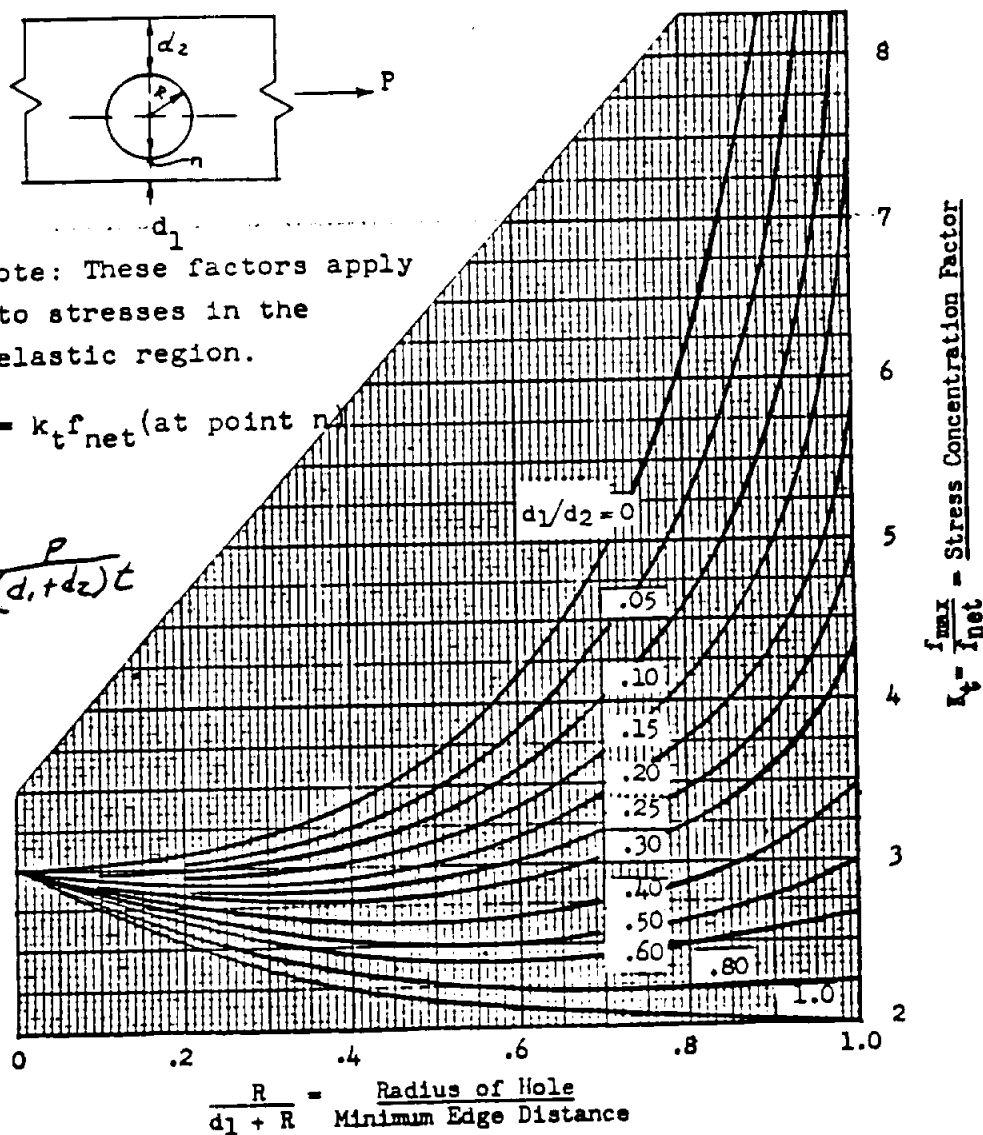
STRUCTURAL ANALYSIS MANUAL
GENERAL DYNAMICS/CONVAIR AND SPACE SYSTEMS DIVISION



Note: These factors apply to stresses in the elastic region.

$$f_{\max} = k_t f_{\text{net}} \text{ (at point n)}$$

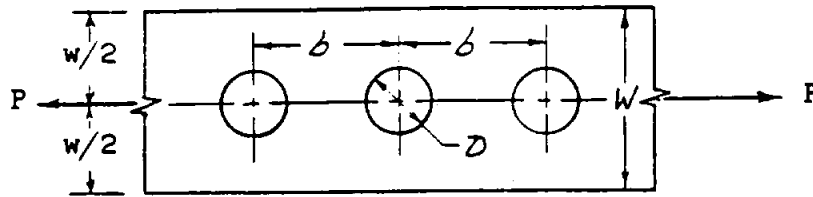
$$f_{\text{net}} = \frac{P}{(d_1 + d_2)t}$$



Stress Concentration Factors for an Axially
 Loaded Plate with an Eccentric Circular Hole

Fig. 10.5.2.12

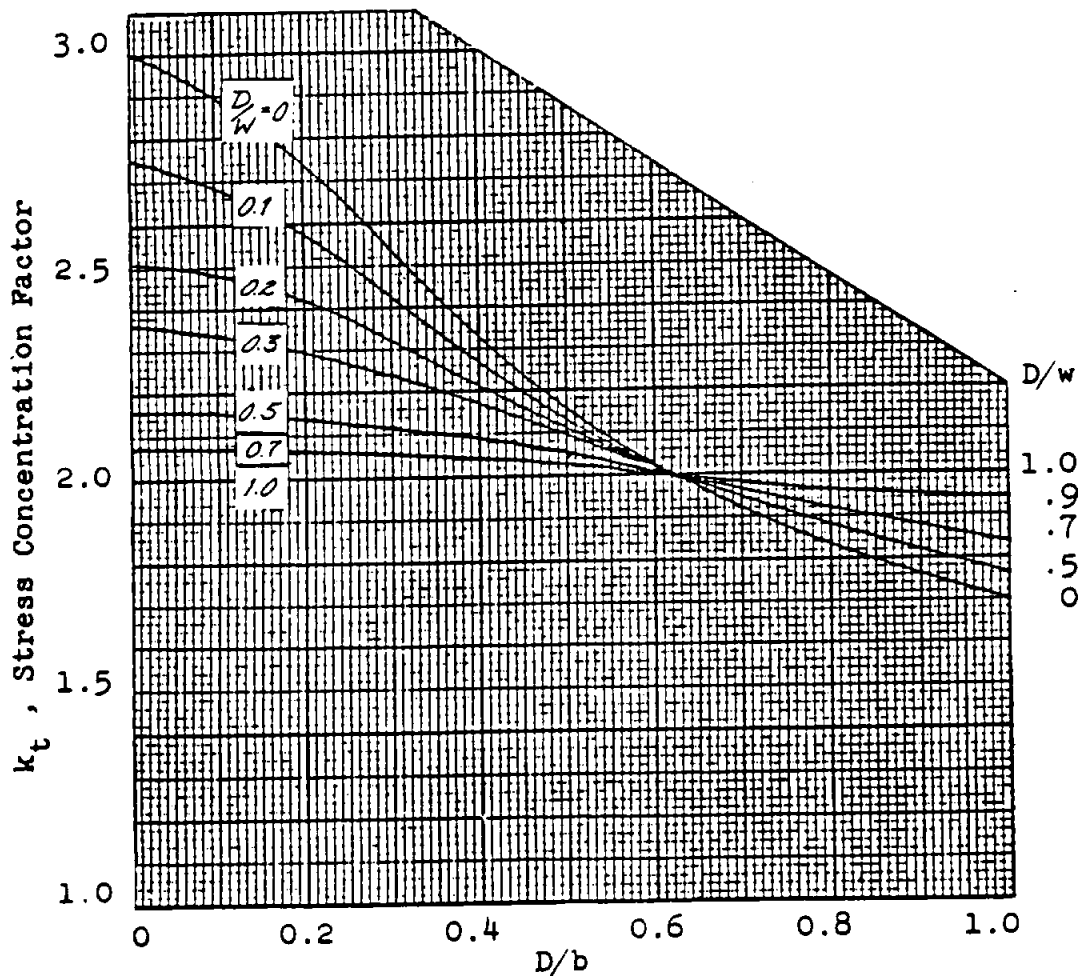
STRUCTURAL ANALYSIS MANUAL
GENERAL DYNAMICS/CONVAIR AND SPACE SYSTEMS DIVISION



$$f_{\max.} = k_t f_{\text{nom.}} \text{ (at edge of holes)}$$

$$f_{\text{nom.}} = \frac{P}{(w-D)t} \text{ (nominal stress in net section)}$$

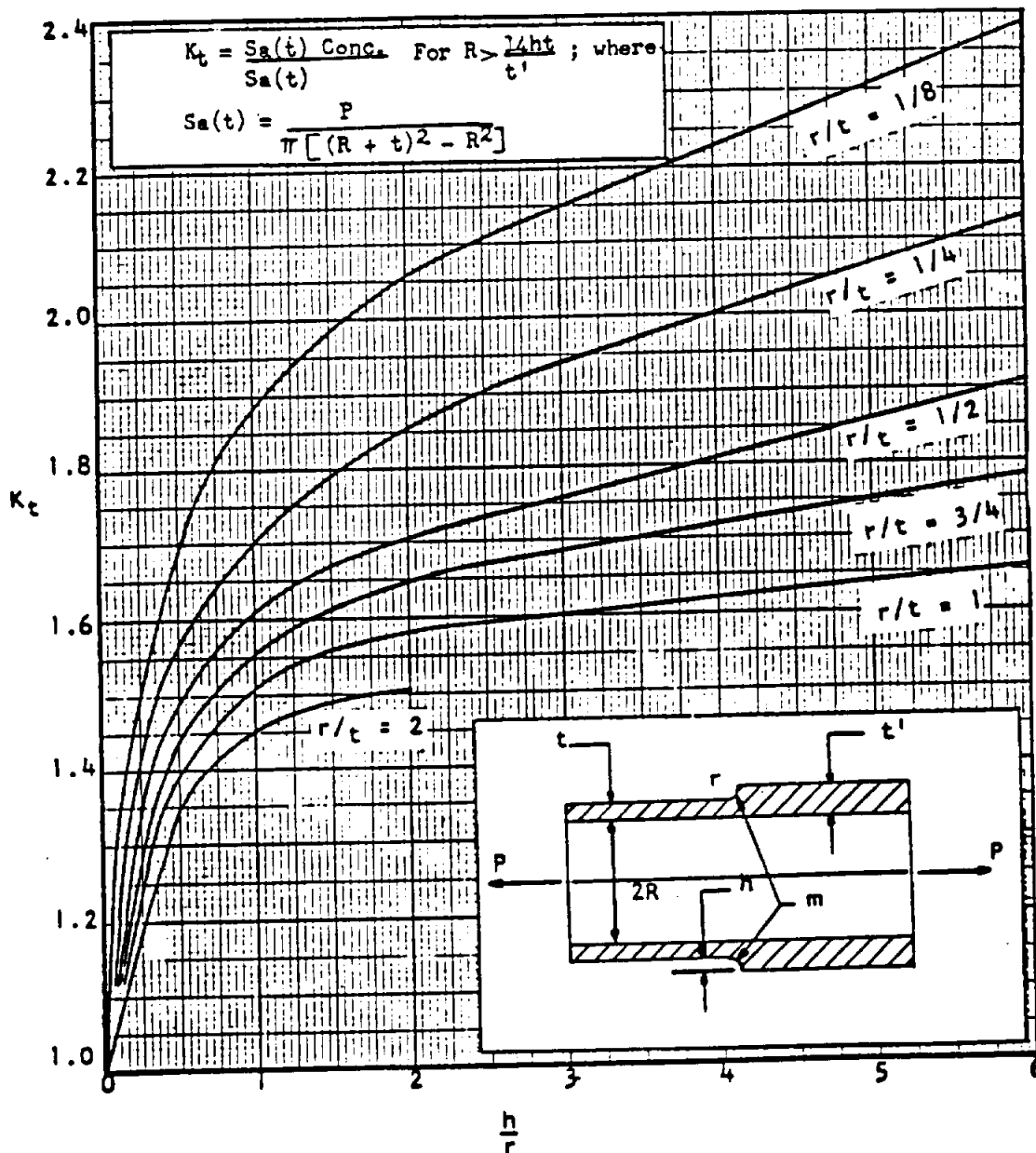
t = plate thickness



Stress Concentration Factors

Fig. 10.5.2.13

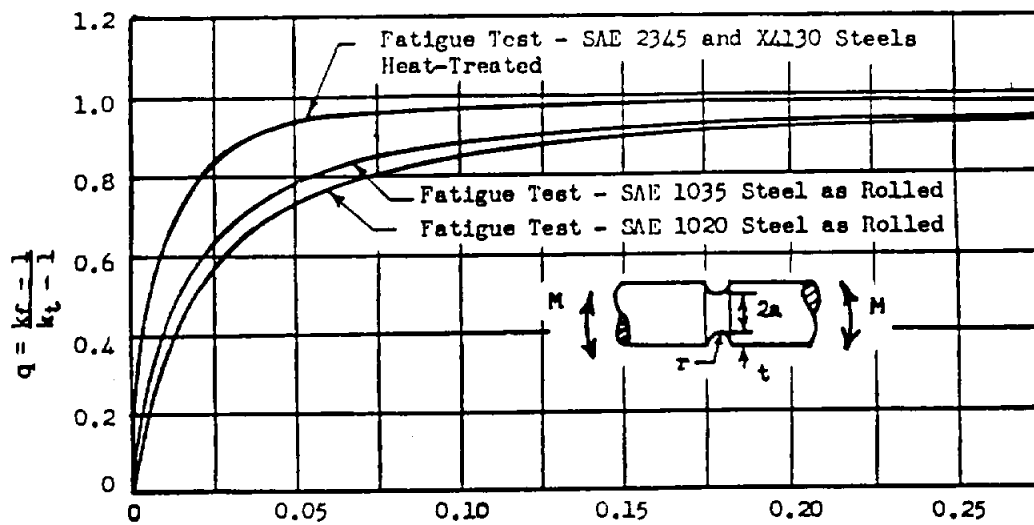
STRUCTURAL ANALYSIS MANUAL
GENERAL DYNAMICS/CONVAIR AND SPACE SYSTEMS DIVISION



Stress Concentration Factors for Circular Fillets
in Stepped Wall Cylinders Subjected to Axial Tension

Fig. 10.5.2.14

STRUCTURAL ANALYSIS MANUAL
GENERAL DYNAMICS/CONVAIR AND SPACE SYSTEMS DIVISION



Radius of Groove, r, in.
Influence of Radius of Groove on Notch Sensitivity Index.
Fig. 10.5.2.15

STRUCTURAL ANALYSIS MANUAL
GENERAL DYNAMICS/CONVAIR AND SPACE SYSTEMS DIVISION

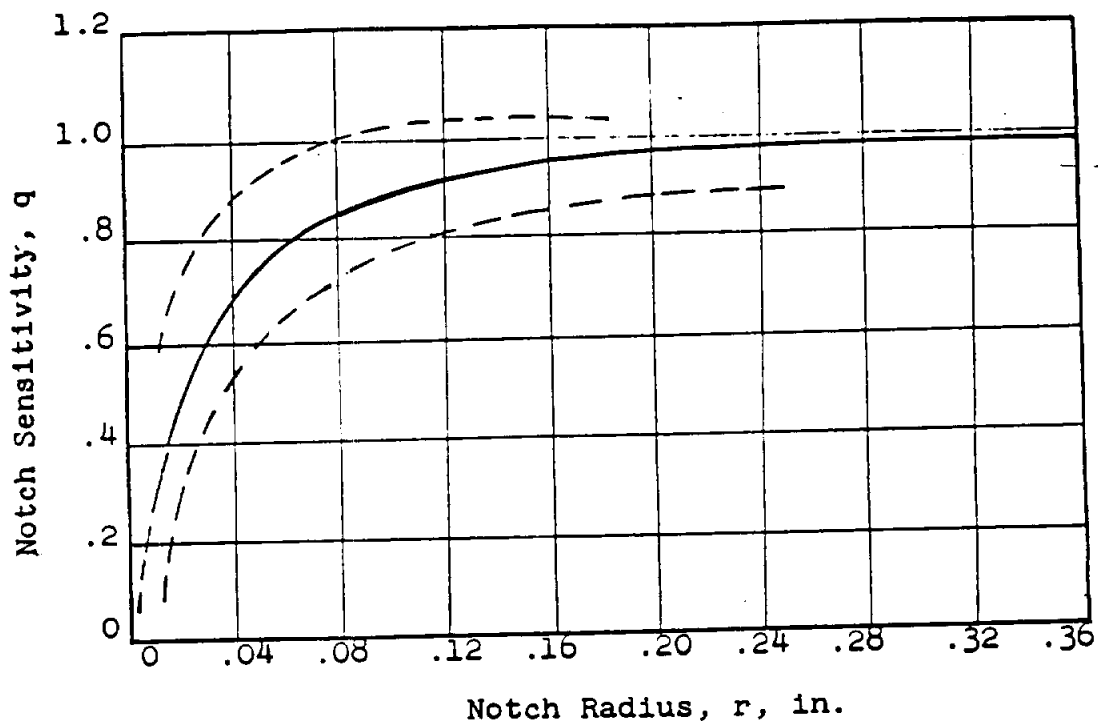


Fig. 10.5.2.16 Notch-Sensitivity of Normalized-Steel Rotating Beam Specimens

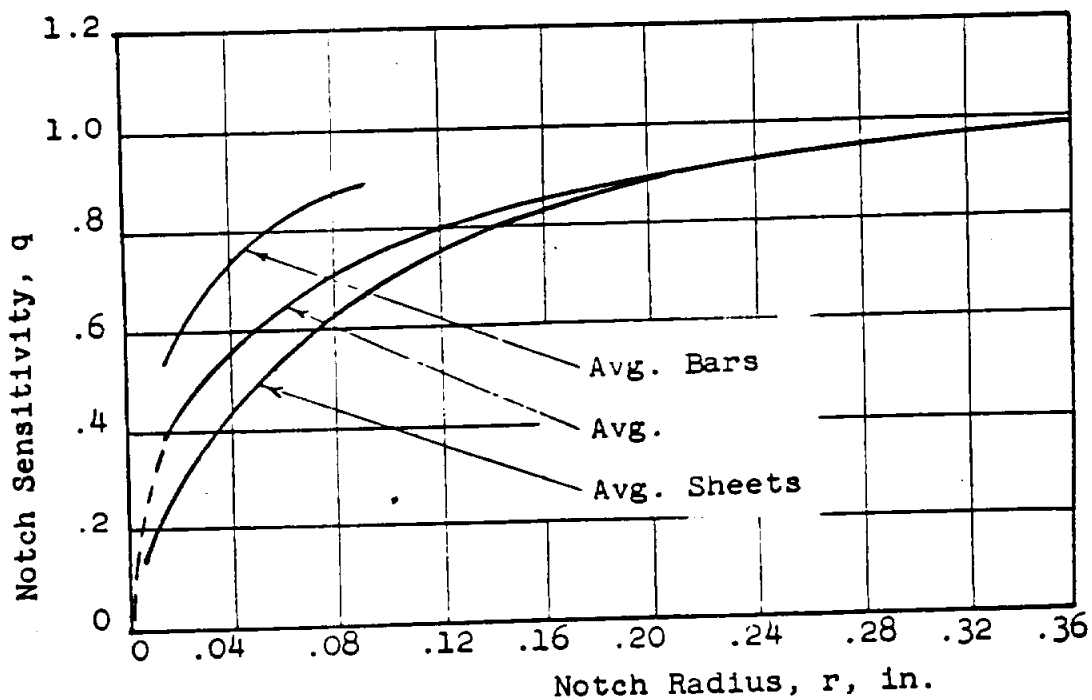


Fig. 10.5.2.17 Notch-Sensitivity of 24S-T Aluminum Alloy, Axial Loading (Completely Reversed)

STRUCTURAL ANALYSIS MANUAL
GENERAL DYNAMICS/CONVAIR AND SPACE SYSTEMS DIVISION

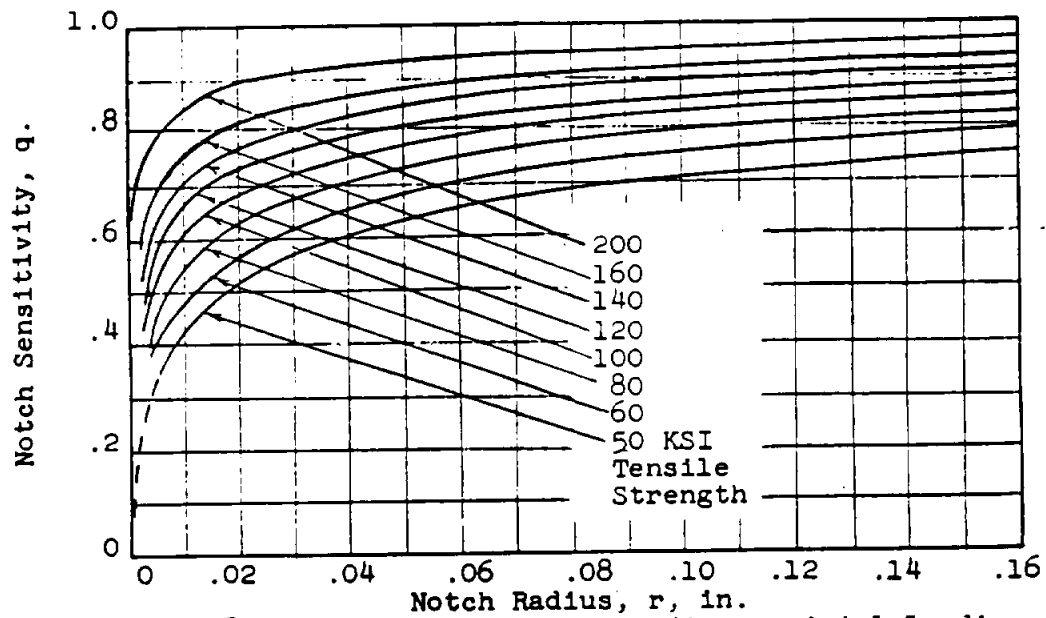


Fig. 10.5.2.18 Curves for Steel, Bending or Axial Loading.

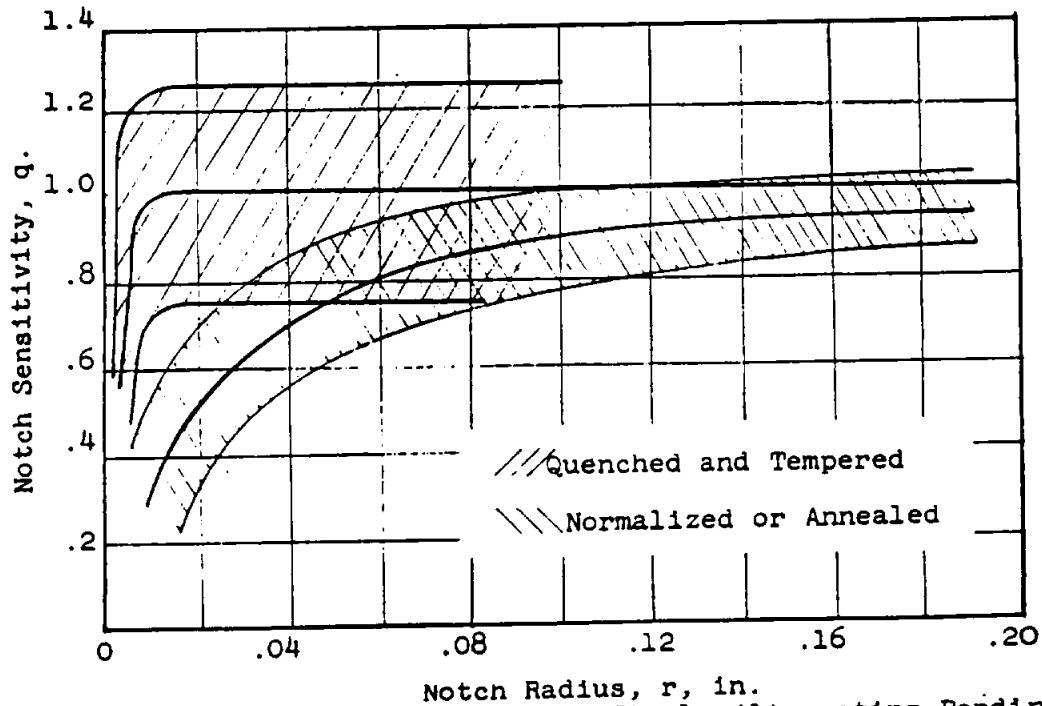


Fig. 10.5.2.19 Scatter Bands for Steel, Alternating Bending.

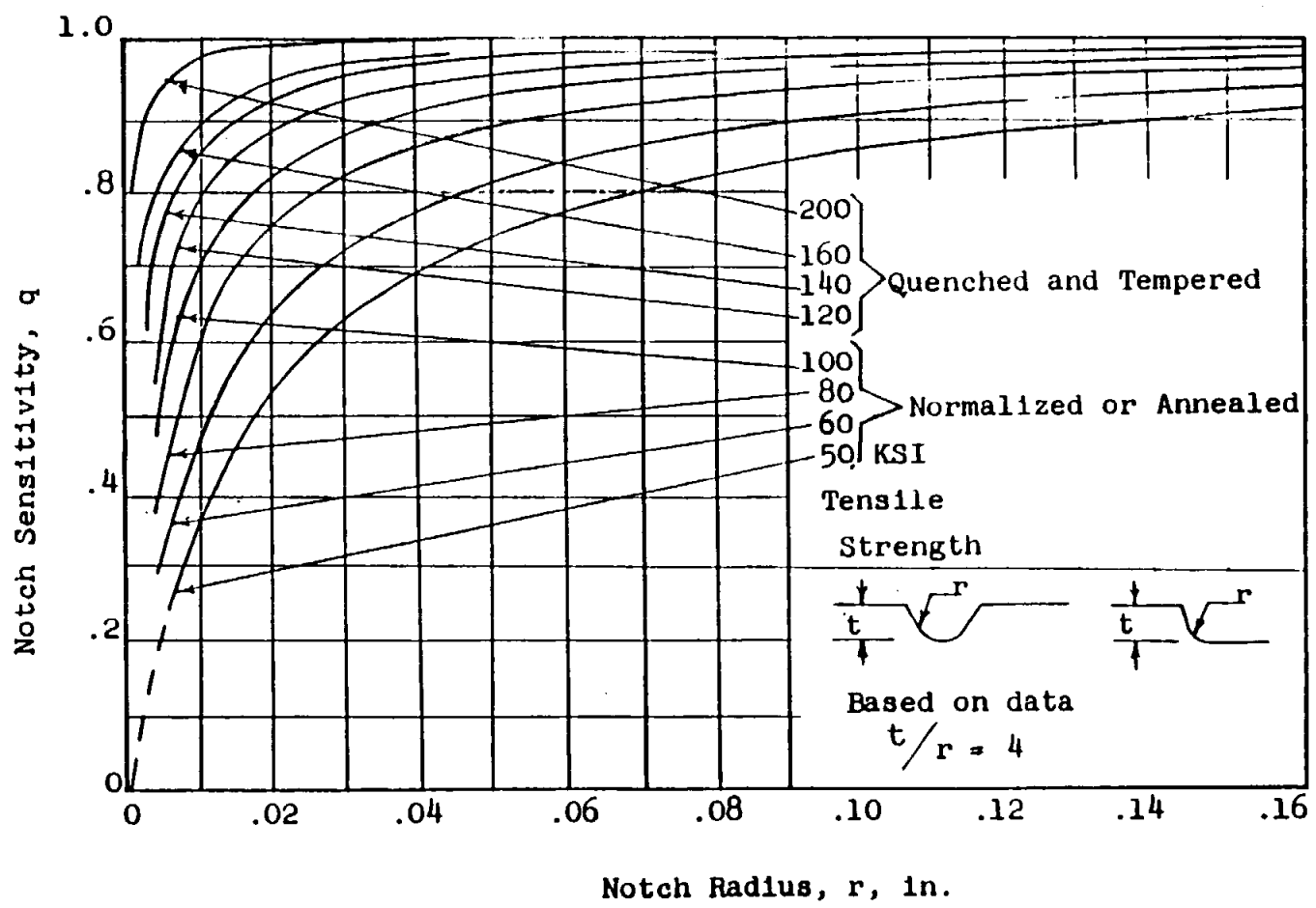


Fig. 10.5.2.20 Curves for Steel Bending or Axial Loading

8856

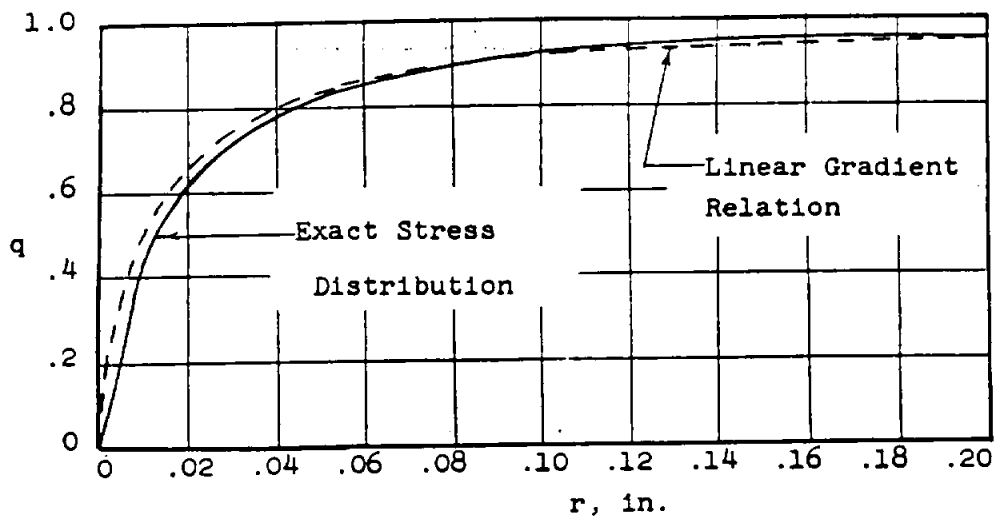


Fig. 10.5.2.21 Compression of q vs. r curves, using exact stress distribution at an elliptical hole and linear stress gradient

STRUCTURAL ANALYSIS MANUAL
GENERAL DYNAMICS/CONVAIR AND SPACE SYSTEMS DIVISION

REFERENCES

- 10.5.0 Stress Concentration Factors
Hayes, J. E., SRQ-26, Fatigue as a Problem in Aircraft Structure Design, 1956.
Peterson, R. E., Stress Concentration Design Factors, J. Wiley and Sons, 1953
Sines, G. and Waisman, J. L., Metal Fatigue, McGraw-Hill, 1959

STRUCTURAL ANALYSIS MANUAL
GENERAL DYNAMICS/CONVAIR AND SPACE SYSTEMS DIVISION

SECTION 14.0

JOINTS & FITTINGS

ANALYSIS METHODS FOR A VARIETY OF JOINTS AND FITTINGS IS PRESENTED IN THIS SECTION.

	PAGE
14.1 LUG ANALYSIS	14.1.1
14.2 MULTIPLE FASTENER PATTERNS	14.2.1
14.3 BEAM IN SOCKET	14.3.1
14.4 INTERFERENCE FIT BUSHINGS	14.4.1
14.5 TENSION CLIPS AND TEES	14.5.1
14.6 BOLT STRENGTH	14.6.1
14.7 BATH TUB TYPE TENSION FITTINGS	14.7.1
14.8 WELD JOINTS	14.8.1
14.9 WELD-ON BRACKETS	14.9.1
14.10 BONDED JOINTS	14.10.1
14.11 JOINT FLEXIBILITY	14.11.1
14.12 PRELOADED BOLTS AND SCREWS	14.12.1
14.13 BOLT TORQUE EFFECTS	14.13.1
14.14 EFFICIENCY OF PLATES IN TENSION JOINTS	14.14.1

STRUCTURAL ANALYSIS MANUAL

GENERAL DYNAMICS/CONVAIR AND SPACE SYSTEMS DIVISION

Data Source, Section 1.3 Reference 23

9. LUG ANALYSIS

9.1 Introduction to Lug Analysis

Lugs are connector-type elements widely used as structural supports for pin connections. In the past, the lug strength was overdesigned since weight and size requirements were for the most part unrestricted. However, the refinement of these requirements have necessitated conservative methods of design.

This section presents static strength analysis procedures for uniformly loaded lugs and bushings, for double shear joints, and for single shear joints, subjected to axial, transverse, or oblique loading. Also listed is a section which applies to lugs made from materials having ultimate elongations of at least 5% in any direction in the plane of the lug. Modifications for lugs with less than 5% elongation are also presented. In addition, a short section on the stresses due to press fit bushings is presented.

9.2 Lug Analysis Nomenclature

F_{brL}	= Lug ultimate bearing stress
F_{brY}	= Lug yield bearing stress
F_{tL}	= Cross grain tensile ultimate stress of lug material
F_{tY}	= Cross grain tensile yield stress of lug material
F_{br}	= Allowable ultimate bearing stress, MHB 5
F_{brY}	= Allowable yield bearing stress, MHB 5
F_{tL}	= Ultimate tensile stress
F_{tL}	= Allowable lug net-section tensile ultimate stress
F_{tY}	= Allowable lug net-section tensile yield stress
F_{brY}	= Allowable bearing yield stress for bushings
F_{cY}	= Bushing compressive yield stress
F_{brY}	= Allowable bearing ultimate stress for bushings
F_{sL}	= Ultimate shear stress of the pin material
F_{tL}	= Pin ultimate tensile stress
F_{tL}	= Allowable ultimate tang stress
$F_{br max}$	= Maximum lug bearing stress
$F_{br max}$	= Maximum bushing bearing stress
$F_{s max}$	= Maximum pin shear stress
$F_{b max}$	= Maximum pin bending stress
P_{brL}	= Allowable lug ultimate bearing load
P_{brL}	= Allowable lug net-section ultimate load
P_{br}	= Allowable bushing ultimate load
P_{br}	= Allowable design ultimate load
P_{sL}	= Allowable lug-bushing ultimate load
P_{sL}	= Pin ultimate shear load
P_{bL}	= Pin ultimate bending load

STRUCTURAL ANALYSIS MANUAL
GENERAL DYNAMICS/CONVAIR AND SPACE SYSTEMS DIVISION

$P_{b, \text{bal}}$	= "Balanced design" pin ultimate bending load
P_{all}	= Allowable joint ultimate load
P_t	= Lug tang strength
$P_{t, \text{lug}}$	= Allowable lug transverse ultimate load
$P_{t, \text{bush}}$	= Allowable bushing transverse ultimate load
K_n	= Net-tension stress coefficient
$K_{b, p}$	= Plastic bending coefficient for pin
$K_{b, t}$	= Plastic bending coefficient for tang
$K_{b, l}$	= Plastic bearing coefficient for lug
$K_{b, l}$	= Plastic bending coefficient for lug
$K_{t, \text{lug}}$	= Transverse ultimate load coefficient
$K_{t, \text{lug}}$	= Transverse yield load coefficient
M_{max}	= Maximum pin bending moment
M_{ult}	= Ultimate pin failing moment
A	= Area, in. ²
a	= Distance from edge of hole to edge of lug, inches
B	= Ductility factor for lugs with less than 5% elongation
b	= Effective bearing width, inches
D	= Hole diameter of pin diameter, inches
E	= Modulus of elasticity, psi
e	= Edge distance, inches
f	= Stress, psi
f_n	= Cyclic stress amplitude on net section of given lug, lbs/in. ²
f_m	= Mean cyclic stress on net section of given lug, lbs/in. ²
f_{max}	= Maximum cyclic stress on net section of given lug, lbs/in. ²
f_{min}	= Minimum cyclic stress on net section of given lug, lbs/in. ²
g	= Gap between lugs, inches
h_1, h_4	= Edge distances in transversely loaded lug, inches
h_e	= Effective edge distance in transversely loaded lug
K	= Allowable stress (or load) coefficient
k_1, k_2, k_3	= Fatigue parameters
M	= Bending moment, in.-lbs.
N	= Fatigue life, number of cycles
P	= Load, lbs.
R	= Stress ratio, $f_{\text{min}}/f_{\text{max}}$
t_b	= Bushing wall thickness, inches
t	= Lug thickness, inches
w	= Lug width, inches
α	= Angle of load to axial direction, degrees
ϵ	= Strain, inches/inch
ρ	= Density, lbs/in. ³

STRUCTURAL ANALYSIS MANUAL

GENERAL DYNAMICS/CONVAIR AND SPACE SYSTEMS DIVISION

Subscripts

all	= Allowable	opt	= Optimum
ax	= Axial	p	= Pin
b	= Bushing	s	= Shear
b	= Bending	t	= Tang
br	= Bearing	t	= Tensile
c	= Compression	tr	= Transverse
l	= Lug	u	= Ultimate
max	= Maximum	z	= Cross grain
n	= Net tensile	y	= Yield
o	= Oblique	1, 2	= Female and male lugs

9.3 Lug and Bushing Strength Under Uniform Axial Load

Axially loaded lugs in tension must be checked for bearing strength and for net-section strength. The bearing strength of a lug loaded in tension, as shown in Figure 9-1, depends largely on the interaction between bearing, shear-out, and hoop-tension stresses in the part of the lug ahead of the pin. The net-section of the lug through the pin must be checked against net-tension failure. In addition, the lug and bushing must be checked to ensure that the deformations at design yield load are not excessive.

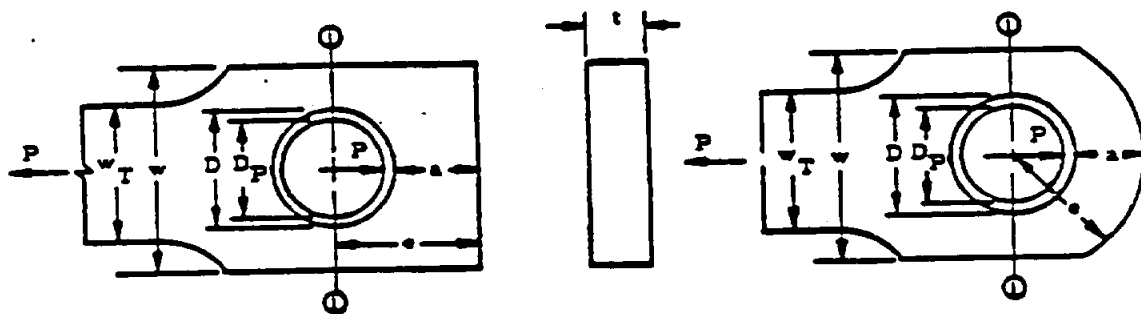


Figure 9-1. Schematics of Lugs Loaded in Tension

9.3.1 Lug Bearing Strength Under Uniform Axial Load

The bearing stresses and loads for lug failure involving bearing, shear-tearout, or hoop tension in the region forward of the net-section in Figure 9-1 are determined from the equations below, with an allowable load coefficient (K) determined from Figures 9-2 and 9-3. For values of e/D less than 1.5, lug failures are likely to involve shear-out or hoop-tension; and for values of e/D greater than 1.5, the bearing is likely to be critical. Actual lug failures may involve more than one failure mode, but

STRUCTURAL ANALYSIS MANUAL **GENERAL DYNAMICS/CONVAIR AND SPACE SYSTEMS DIVISION**

such interaction effects are accounted for in the values of K. The lug ultimate bearing stress (F_{bru_L}) is

$$F_{bru_L} = K \frac{a}{D} F_{tux}, (e/D < 1.5) \quad (9-1a)$$

$$F_{bru_L} = K F_{tux}, (e/D \geq 1.5) \quad (9-1b)$$

The lug yield bearing stress (F_{bry_L}) is

$$F_{bry_L} = K \frac{a}{D} F_{tyx}, (e/D < 1.5) \quad (9-2a)$$

$$F_{bry_L} = K F_{tyx}, (e/D \geq 1.5) \quad (9-2b)$$

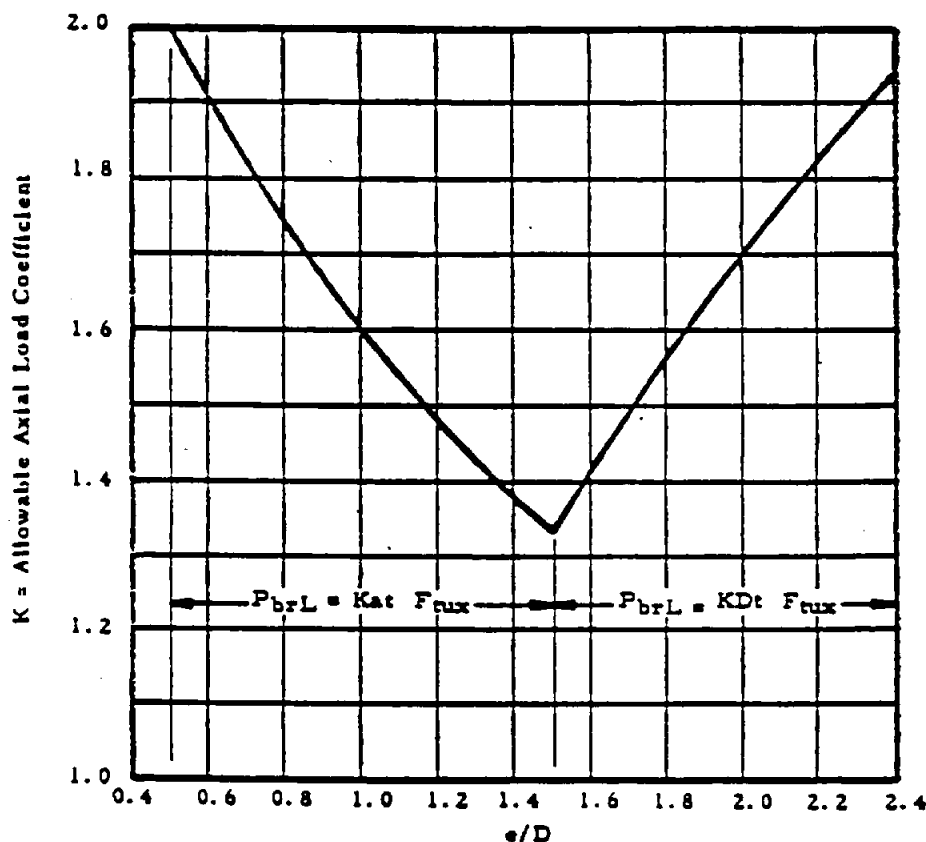


Figure 9-2. Allowable Uniform Axial Load Coefficient

The graph in Figure 9-2 applies only to cases where D/t is 5 or less, which covers most of the cases. If D/t is greater than 5, there is a reduction in strength which can be approximated by the curves and equations on Figure 9-3.

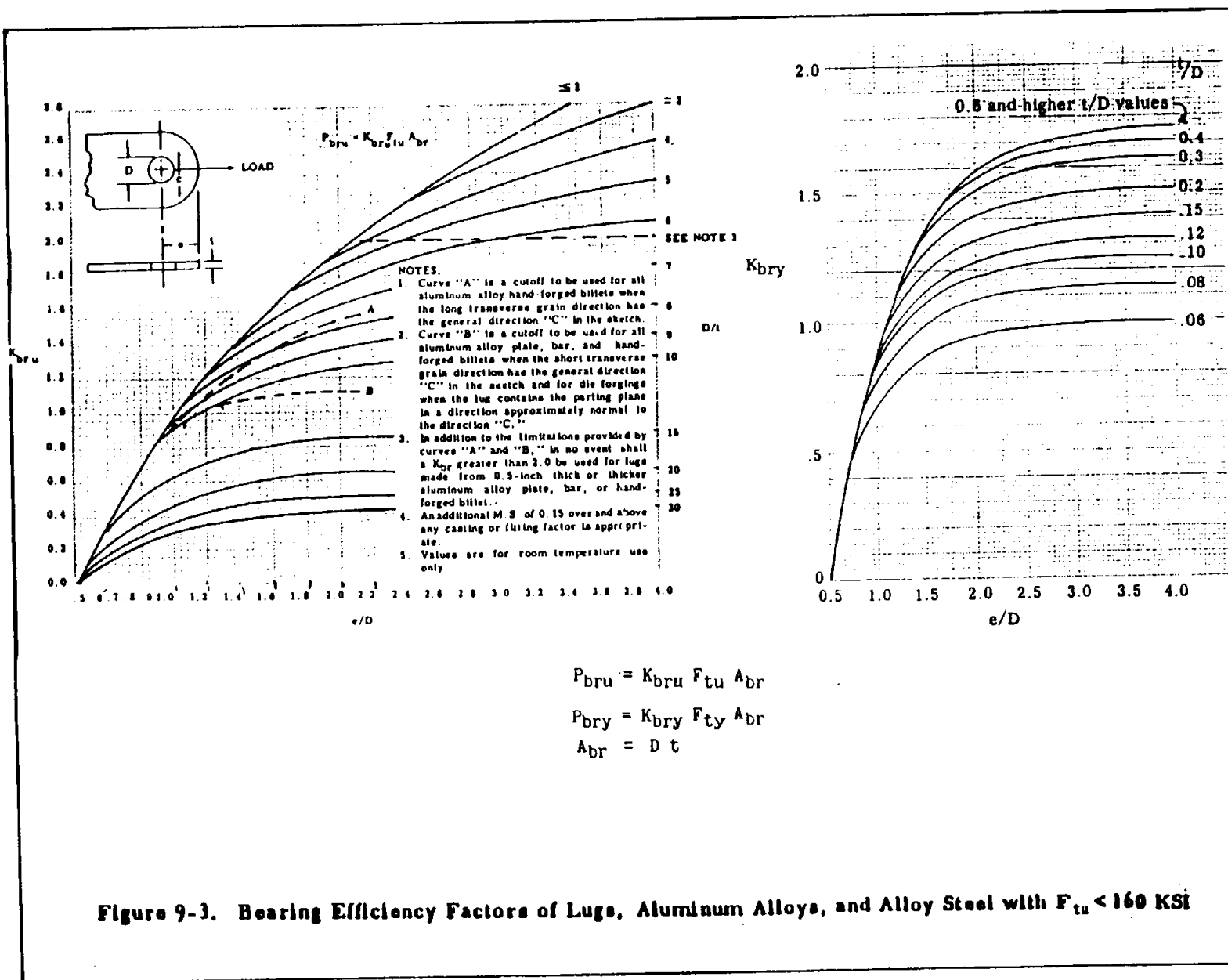


Figure 9-3. Bearing Efficiency Factors of Lugs, Aluminum Alloys, and Alloy Steel with $F_{tu} < 160$ KSI

STRUCTURAL ANALYSIS MANUAL
GENERAL DYNAMICS/CONVAIR AND SPACE SYSTEMS DIVISION

The allowable lug ultimate bearing load (P_{brl}) for lug failure in bearing, shear-out, or hoop tension is

$$P_{brl} = F_{brl} Dt, \text{ (if } F_{111} \leq 1.304 F_{171} \text{)} \quad (9-3a)$$

$$P_{brl} = 1.304 F_{171} Dt, \text{ (if } F_{111} > 1.304 F_{171} \text{)} \quad (9-3b)$$

P_{brl}/Dt should not exceed either F_{brl} or $1.304 F_{171}$, where F_{brl} and F_{171} are the allowable ultimate and yield bearing stresses for the lug material for $e/D = 2.0$, as given in MIL-HDBK-5 or other applicable specification.

Equations (9-3a) and (9-3b) apply only if the load is uniformly distributed across the lug thickness. If the pin is too flexible and bends excessively, the load on the lug will tend to peak up near the shear faces and possibly cause premature failure of the lug.

A procedure to check the pin bending strength in order to prevent premature lug failure is given in Section 9.4 entitled "Double Shear Joint Strength Under Uniform Axial Load."

9.3.2 Lug Net-Section Strength Under Uniform Axial Load

The allowable lug net-section tensile ultimate stress (F_{111}) on Section 1-1 in Figure 9-4a is affected by the ability of the lug material to yield and thereby relieve the stress concentration at the edge of the hole.

$$F_{111} = K_n F_{111} \quad (9-4)$$

K_n , the net-tension stress coefficient, is obtained from the graphs shown in Figure 9-4 as a function of the ultimate and yield stress and strains of the lug material in the direction of the applied load. The ultimate strain (ϵ_u) can be obtained from MIL-HDBK-5.

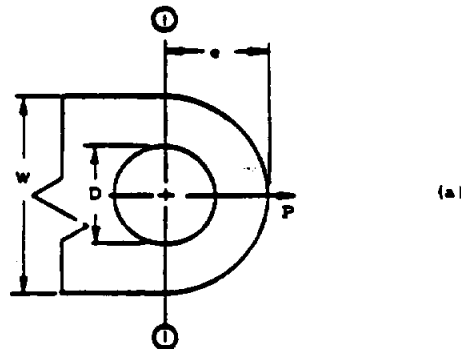


Figure 9-4. Net Tension Stress Coefficient

STRUCTURAL ANALYSIS MANUAL
GENERAL DYNAMICS/CONVAIR AND SPACE SYSTEMS DIVISION

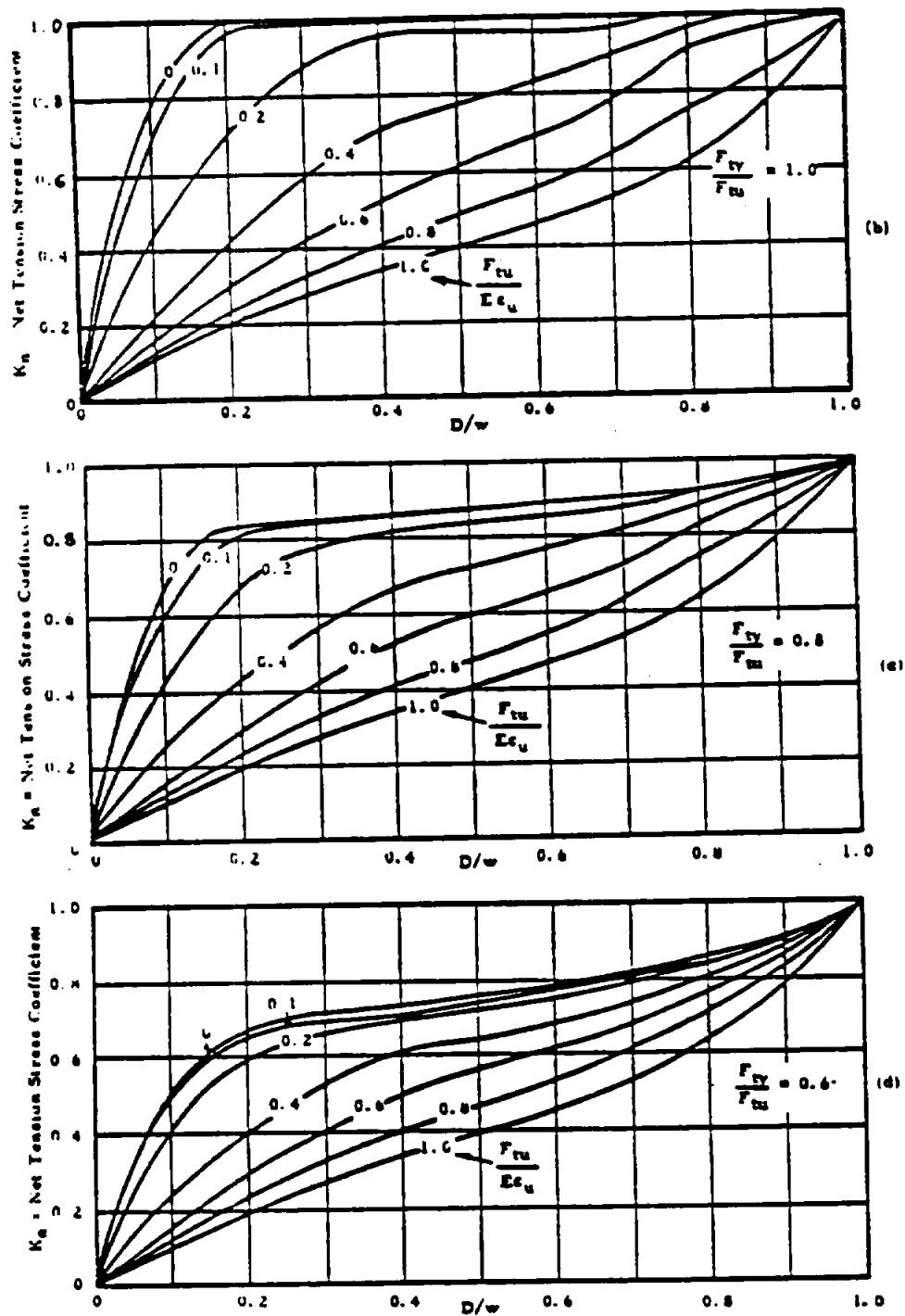


Figure 9-4. Net Tension Stress Coefficient (concluded)

STRUCTURAL ANALYSIS MANUAL
GENERAL DYNAMICS/CONVAIR AND SPACE SYSTEMS DIVISION

The allowable lug net-section tensile yield stress (F_{sy}) is

$$F_{sy} = K_s F_{ty} \quad (9-5)$$

The allowable lug net-section ultimate load (P_{su}) is

$$P_{su} = F_{su} (w-D)t, \text{ (if } F_{ty} \leq 1.304 F_{ty} \text{)} \quad (9-6a)$$

$$P_{su} = 1.304 F_{sy} (w-D)t, \text{ (if } F_{ty} > 1.304 F_{ty} \text{)} \quad (9-6b)$$

9.3.3 Lug Design Strength Under Uniform Axial Load

The allowable design ultimate load for the lug (P_u) is the lower of the values obtained from Equations (9-3) and (9-6).

$$P_u \leq P_{su} \text{ (Equations (9-3a) and (9-3b), or } P_{su} \text{ (Equations (9-6a) and (9-6b))} \quad (9-7)$$

9.3.4 Bushing Bearing Strength Under Uniform Axial Load

The allowable bearing yield stress for bushings (F_{by}) is restricted to the compressive yield stress (F_{cy}) of the bushing material, unless higher values are substantiated by tests.

The allowable bearing ultimate stress for bushings (F_{bu}) is

$$F_{bu} = 1.304 F_{cy} \quad (9-8)$$

The allowable bushing ultimate load (P_u) is

$$P_u = 1.304 F_{cy} D_b t \quad (9-9)$$

This assumes that the bushing extends through the full thickness of the lug.

9.3.5 Combined Lug-Bushing Design Strength Under Uniform Axial Load

The allowable lug-bushing ultimate load ($P_{u,b}$) is the lower of the loads obtained from Equations (9-7) and (9-9).

$$P_{u,b} \leq P_u \text{ (Equation (9-7), or } P_u \text{ (Equation (9-9))} \quad (9-10)$$

9.4 Double Shear Joint Strength Under Uniform Axial Load

The strength of a joint such as the one shown in Figure 9-5 depends on the lug-bushing ultimate strength ($P_{u,b}$) and on the pin shear and pin bending strengths.

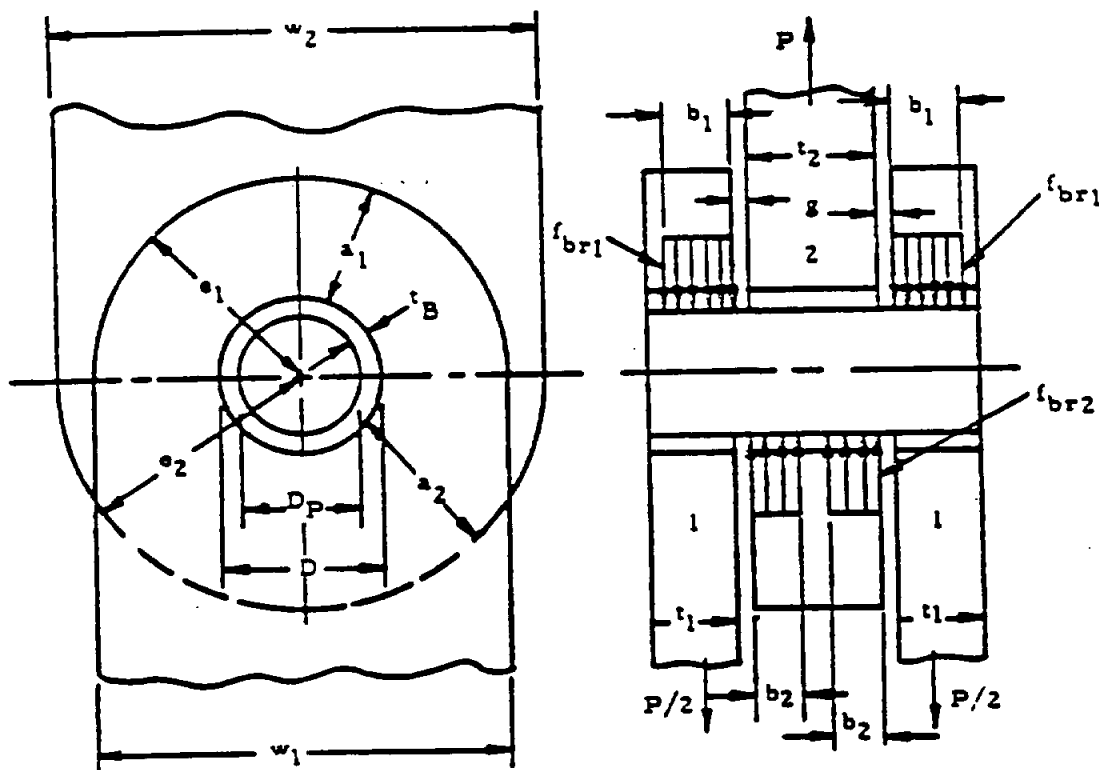


Figure 9-5. Double Shear Lug Joint

9.4.1 Lug-Bushing Design Strength for Double Shear Joints Under Uniform Axial Load

The allowable lug-bushing ultimate load (P_{t_0}) for the joint is computed, using Equation (9-10). For the symmetrical joint shown in the figure, Equation (9-10) is used to calculate the ultimate load for the outer lugs and bushings ($2P_{t_{01}}$) and the ultimate load for the inner lug and bushing ($P_{t_{02}}$). The allowable value of P_{t_0} for the joint is the lower of these two values.

$$P_{t_0} \leq 2P_{t_{01}} \text{ (Equation (9-10)), or } P_{t_{02}} \text{ (Equation (9-10))} \quad (9-11)$$

STRUCTURAL ANALYSIS MANUAL
GENERAL DYNAMICS/CONVAIR AND SPACE SYSTEMS DIVISION

9.4.2 Pin Shear Strength for Double Shear Joints Under Uniform Axial Load

The pin ultimate shear load (P_{su}) for the symmetrical joint shown in Figure 9-5 is the double shear strength of the pin:

$$P_{su} = 1.571 D_p^2 F_{su} \quad (9-12)$$

where F_{su} is the ultimate shear stress of the pin material.

9.4.3 Pin Bending Strength for Double Shear Joints Under Uniform Axial Load

Although actual pin bending failures are infrequent, excessive pin deflections can cause the load in the lugs to peak up near the shear planes instead of being uniformly distributed across the lug thickness, thereby leading to premature lug or bushing failures at loads less than those predicted by Equation (9-11). At the same time, however, the concentration of load near the lug shear planes reduces the bending arm and, therefore, the bending moment in the pin, making the pin less critical in bending. The following procedure is used in determining the pin ultimate bending load.

Assume that the load in each lug is uniformly distributed across the lug thickness ($b_1 = t_1$, and $2b_2 = t_2$). For the symmetrical joint shown in Figure 9-5, the resulting maximum pin bending moment is

$$M_{max} = \frac{P}{2} \left(\frac{t_1}{2} + \frac{t_2}{4} + g \right) \quad (9-13)$$

The ultimate failing moment for the pin is

$$M_u = 0.0982 k_b D_p^3 F_{tu} \quad (9-14)$$

where k_b is the plastic bending coefficient for the pin. The value of k_b varies from 1.0 for a perfectly elastic pin to 1.7 for a perfectly plastic pin, with a value of 1.56 for pins made from reasonably ductile materials (more than 5% elongation).

The pin ultimate bending load (P_{bu}) is, therefore,

$$P_{bu} = \frac{0.1963 k_b D_p^3 F_{tu}}{\left(\frac{1}{2} + \frac{t_2}{4} + g \right)} \quad (9-15)$$

STRUCTURAL ANALYSIS MANUAL
GENERAL DYNAMICS/CONVAIR AND SPACE SYSTEMS DIVISION

If P_{ub} is equal to or greater than either P_{u1} (Equation (9-11)) or P_{u2} (Equation (9-12)), then the pin is a relatively strong pin that is not critical in bending, and no further pin bending calculations are required. The allowable load for the joint (P_{all}) can be determined by going directly to Equation (9-19a).

If P_{ub} (Equation (9-15)) is less than both P_{u1} (Equation (9-11)) and P_{u2} (Equation (9-12)), the pin is considered a relatively weak pin, critical in bending. However, such a pin may deflect sufficiently under load to shift the c. g. of the bearing loads toward the shear faces of the lugs, resulting in a decreased pin bending moment and an increased value of P_{ub} . These shifted loads are assumed to be uniformly distributed over widths b_1 and $2b_2$, which are less than t_1 and t_2 , respectively, as shown in Figure 9-5. The portions of the lugs and bushings not included in b_1 and $2b_2$ are considered ineffective. The new increased value of pin ultimate bending load is

$$P_{ub} = \frac{0.1963 k_b D^3 F_{ub}}{\left(\frac{b_1}{2} + \frac{b_2}{2} + g\right)} \quad (9-15a)$$

The maximum allowable value of P_{ub} is reached when b_1 and b_2 are sufficiently reduced so that P_{ub} (Equation (9-15a)) is equal to P_{u1} (Equation (9-11)), provided that b_1 and $2b_2$ are substituted for t_1 and t_2 , respectively. At this point we have a balanced design where the joint is equally critical in pin-bending failure or lug-bushing failure.

The following equations give the "balanced design" pin ultimate bending load ($P_{ub, max}$) and effective bearing widths ($b_{1, max}$ and $2b_{2, max}$):

$$P_{ub, max} = 2C \sqrt{\frac{P_{u1} P_{u2}}{C} \left(\frac{t_1}{2} + \frac{t_2}{4} + g\right) + g^2 - 2Cg} \quad (9-16)$$

where

$$C = \frac{P_{u1} P_{u2}}{P_{u1} t_2 + P_{u2} t_1}$$

The value of P_{ub} on the right hand side of Equation (9-16) and the values of P_{u1} and P_{u2} in the expression for C are based on the assumption that the full thicknesses of the lugs are effective and have already been calculated. (Equations (9-10) and (9-15)).

STRUCTURAL ANALYSIS MANUAL
GENERAL DYNAMICS/CONVAIR AND SPACE SYSTEMS DIVISION

If the inner lug strength is equal to the total strength of the two outer lugs ($P_{u,2} = 2P_{u,1}$), and if $g = 0$, then

$$P_{u, \text{max}} = \sqrt{P_u, P_{u,2}} \quad (9-17)$$

The "balanced design" effective bearing widths are

$$b_{1 \text{ eff}} = \frac{P_{u, \text{max}} t_1}{2P_{u,1}} \quad (9-18a)$$

$$2b_{2 \text{ eff}} = \frac{P_{u, \text{max}} t_2}{P_{u,2}} \quad (9-18b)$$

where $P_{u, \text{max}}$ is obtained from Equation (9-16) and $P_{u,1}$ and $P_{u,2}$ are the previously calculated values based on the full thicknesses of the lugs. Since any lug thicknesses greater than $b_{1 \text{ eff}}$ or $b_{2 \text{ eff}}$ are not considered effective, an efficient static strength design would have $t_1 = b_{1 \text{ eff}}$ and $t_2 = 2b_{2 \text{ eff}}$.

The allowable joint ultimate load (P_{u1}) for the double-shear joint is obtained as follows:

If $P_{u,1}$ (Equation (9-15)) is greater than either $P_{u,1}$ (Equation (9-11)) or $P_{u,2}$ (Equation (9-12)), then P_{u1} is the lower of the values of $P_{u,1}$ or $P_{u,2}$.

$$P_{u1} \leq P_{u,1} \text{ (Equation (9-11)) or } P_{u,2} \text{ (Equation (9-12))} \quad (9-19a)$$

If $P_{u,1}$ (Equation (9-15)) is less than both $P_{u,1}$ and $P_{u,2}$, then P_{u1} is the lower of the values of $P_{u,1}$ and $P_{u,2}$.

$$P_{u1} \leq P_{u,1} \text{ (Equation (9-12)) or } P_{u,2} \text{ (Equation (9-16))} \quad (9-19b)$$

9.4.4 Lug Tang Strength for Double Shear Joints Under Uniform Axial Load

If Equation (9-19a) has been used to determine the joint allowable load, then we have a condition where the load in the lugs and tangs is assumed uniformly distributed. The allowable stress in the tangs is F_{uT} . The lug tang

STRUCTURAL ANALYSIS MANUAL
GENERAL DYNAMICS/CONVAIR AND SPACE SYSTEMS DIVISION

strength (P_r) is the lower of the following values.

$$P_r = 2F_{t_{r1}} w_{r1} t_1 \quad (9-20a)$$

$$P_r = F_{t_{r2}} w_{r2} t_2 \quad (9-20b)$$

If Equation (9-19b) was used to determine the joint allowable load, the tangs of the outer lugs should be checked for the combined axial and bending stresses resulting from the eccentric application of the bearing loads. Assuming that the lug thickness remains constant beyond the pin, a load ($P/2$) applied over the width b_1 in each outer lug will produce the following bending moment in the tangs:

$$M_1 = \frac{P}{2} \left(\frac{t_1 - b_1}{2} \right)$$

A simple, but generally conservative, approximation to the maximum combined stress in the outer lug tangs is

$$F_{t_{r1}} = \frac{P}{2w_{r1} t_1} + \frac{6M_1}{k_{b_r} w_{r1} t_1^2} \quad (9-21)$$

where k_{b_r} , the plastic bending coefficient for a lug tang of rectangular cross-section, varies from 1.0 for a perfectly elastic tang to 1.5 for a perfectly plastic tang, with a value of 1.4 representative of rectangular cross sections with materials of reasonable ductility (more than 5% elongation). The allowable value of $F_{t_{r1}}$ is $F_{t_{r1}}$. The lug tang strength is the lower of the following values:

$$P_r = \frac{2F_{t_{r1}} w_{r1} t_1}{1 + \frac{3}{k_{b_r}} \left(1 - \frac{b_{1_{max}}}{t_1} \right)} \quad (9-22a)$$

$$P_r = F_{t_{r2}} w_{r2} t_2 \quad (9-22b)$$

where $b_{1_{max}}$ is given by Equation (9-18a)

9.5 Single-Shear Joint Strength Under Uniform Axial Load

In single-shear joints, lug and pin bending are more critical than in double-shear joints. The amount of bending can be significantly affected by bolt clamping. In the cases considered in Figure 9-6, no bolt clamping is assumed, and the bending moment in the pin is resisted by socket action in the lugs.

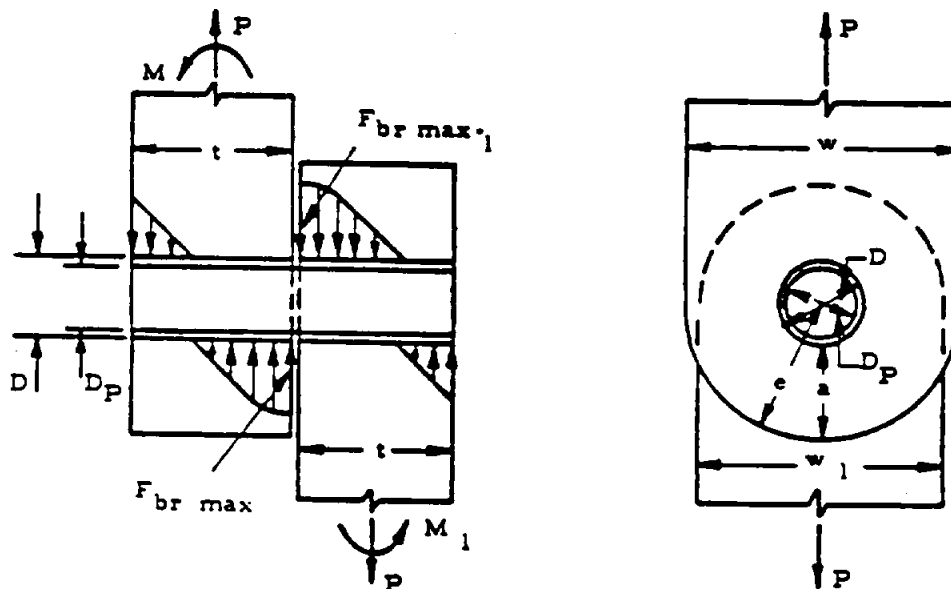


Figure 9-6. Single Shear Lug Joint

In Figure 9-6 a representative single-shear joint is shown, with centrally applied loads (P) in each lug, and bending moments (M and M_1) that keep the system in equilibrium. (Assuming that there is no gap between the lugs, $M + M_1 = P(t + t_1)/2$). The individual values of M and M_1 are determined from the loading of the lugs as modified by the deflection, if any, of the lugs, according to the principles of mechanics.

The strength analysis procedure outlined below applies to either lug. The joint strength is determined by the lowest of the margins of safety calculated for the different failure modes defined by Equations (9-23) through (9-27).

9.5.1 Lug Bearing Strength for Single Shear Joints Under Uniform Axial Loads

The bearing stress distribution between lug and bushing is assumed to be similar to the stress distribution that would be obtained in a rectangular cross section of width (D) and depth (t), subjected to a load (P) and moment (M). At ultimate load the maximum lug bearing stress ($F_{br \max}$) is approximated by

$$F_{br \max} = \frac{P}{Dt} + \frac{6M}{k_{br} Dt^2} \quad (9-23)$$

where k_{br} is a plastic bearing coefficient for the lug material, and is assumed to be the same as the plastic bending coefficient (k_b) for a rectangular section.

STRUCTURAL ANALYSIS MANUAL
GENERAL DYNAMICS/CONVAIR AND SPACE SYSTEMS DIVISION

The allowable ultimate value of $F_{br, max}$ is either $F_{br, y}$ (Equations (9-1a) (9-1b)) or $1.304 F_{br, y}$ (Equations (9-2a) (9-2b)), whichever is lower.

9.5.2 Lug Net-Section Strength for Single Shear Joints Under Uniform Axial Load

At ultimate load the nominal value of the outer fiber tensile stress in the lug net-section is approximated by

$$F_t, max = \frac{P}{(w-D)t} + \frac{6M}{k_{br} (w-D)t^2} \quad (9-24)$$

where k_{br} is the plastic bending coefficient for the lug net-section.

The allowable ultimate value of F_t, max is $F_{br, y}$ (Equation (9-4)) or $1.304 F_{br, y}$ (Equation (9-5)), whichever is lower.

9.5.3 Bushing Strength for Single Shear Joints Under Uniform Axial Load

The bearing stress distribution between bushing and pin is assumed to be similar to that between the lug and bushing. At ultimate bushing load the maximum bushing bearing stress is approximated by

$$F_{br, max} = \frac{P}{D_b t} + \frac{6M}{k_{br} D_b t^2} \quad (9-25)$$

where k_{br} , the plastic bearing coefficient, is assumed the same as the plastic bending coefficient (k_{br}) for a rectangular section.

The allowable ultimate value of $F_{br, max}$ is $1.304 F_{br, y}$, where $F_{br, y}$ is the bushing material compressive yield strength.

9.5.4 Pin Shear Strength for Single Shear Joints Under Uniform Axial Load

The maximum value of pin shear can occur either within the lug or at the common shear face of the two lugs, depending upon the value of M/Pt . At the lug ultimate load the maximum pin shear stress (F_s, max) is approximated by

$$F_s, max = \frac{1.273 P}{D_b^2}, \text{ (if } \frac{M}{Pt} \leq 2/3 \text{)} \quad (9-26a)$$

$$F_s, max = \frac{1.273 P}{D_b^2} \frac{\left(\sqrt{\left(\frac{2M}{Pt} \right)^2 + 1} - 1 \right)}{\left(\frac{2M}{Pt} + 1 - \sqrt{\left(\frac{2M}{Pt} \right)^2 + 1} \right)}, \text{ (if } \frac{M}{Pt} > 2/3 \text{)} \quad (9-26b)$$

STRUCTURAL ANALYSIS MANUAL
GENERAL DYNAMICS/CONVAIR AND SPACE SYSTEMS DIVISION

Equation (9-26a) defines the case where the maximum pin shear is obtained at the common shear face of the lugs, and Equation (9-26b) defines the case where the maximum pin shear occurs away from the shear face.

The allowable ultimate value of $F_{b, \max}$ is F_{ts} , the ultimate shear stress of the pin material.

9.5.5 Pin Bending Strength for Single Shear Joints Under Uniform Axial Load

The maximum pin bending moment can occur within the lug or at the common shear faces of the two lugs, depending on the value of M/Pt . At the lug ultimate load the maximum pin bending stress ($F_{b, \max}$) is approximated by

$$F_{b, \max} = \frac{10.19M}{k_{bp} D_p^3} \left(\frac{Pt}{2M} - 1 \right), \text{ (if } \frac{M}{Pt} \leq 3/8 \text{)} \quad (9-27a)$$

$$F_{b, \max} = \frac{10.19M}{k_{bp} D_p^3} \frac{\left(\sqrt{\left(\frac{2M}{Pt} \right)^2 + 1} - 1 \right)}{\frac{2M}{Pt}}, \quad (9-27b)$$

(if $\frac{M}{Pt} > 3/8$)

where k_{bp} is the plastic bending coefficient for the pin.

Equation (9-27a) defines the case where the maximum pin bending moment is obtained at the common shear face of the lugs, and Equation (9-27b) defines the case where the maximum pin bending moment occurs away from the shear face, where the pin shear is zero.

The allowable ultimate value of $F_{b, \max}$ is F_{ts} , the ultimate tensile stress of the pin material.

9.6 Example of Uniform Axially Loaded Lug Analysis

Determine the static strength of an axially loaded, double shear joint, such as shown in Section 9.4. with dimensions and material properties given in Table 9-1.

STRUCTURAL ANALYSIS MANUAL
GENERAL DYNAMICS/CONVAIR AND SPACE SYSTEMS DIVISION

Table 9-1. Dimensions and Properties

	Female Lugs, 1	Male Lug, 2	Bushings, 1 and 2	Pin
Material	2024-T351 Plate	7075-T651 Plate	Al. Bronze	4130 Steel
F_{tu}	64000 psi (X-grain)	77000 psi (X-grain)	110,000 psi	125,000 psi
F_{ty}	40000 psi (X-grain)	66000 psi (X-grain)	60,000 psi	103,000 psi
F_{ey}			60,000 psi	
F_{su}				82,000 psi
E	10.5×10^6 psi	10.3×10^6		29×10^6 psi
ϵ_s	0.12	0.06		
D or D_s	D = 1.00 in.	D = 1.00 in.	$D_b = 0.75$ in., D = 1.00 in.	$D_p = 0.75$ in.
e	1.25 in.	1.50 in.		
a	0.75 in.	1.00 in.		
w w_1	2.50 in.	3.00 in.		
t	0.50 in.	0.75 in.	0.50 and 0.75 in.	
g	0.10 in.			

(1) Female Lugs and Bushings

$$F_{tu} = 64,000 \text{ psi}; 1.304 F_{ty} = 1.304 \times 40000 = 52160 \text{ psi.}$$

a) Lug Bearing Strength (Equations (9-2a) and (9-3b))

$$\frac{e_1}{D} = \frac{1.25}{1.00} = 1.25; \text{ therefore } K_1 = 1.46 \text{ (from Figure 9-2)}$$

$$P_{br_{l_1}} = 1.304 \times 1.46 \times 0.75 \times 40000 \times 1.00 \times 0.50 = 28600 \text{ lbs.}$$

b) Lug Net-Section Tension Strength (Equations (9-5) and (9-6b))

$$\frac{D}{w_1} = \frac{1.00}{2.50} = 0.40; \frac{F_{ty}}{F_{tu}} = \frac{40000}{64000} = 0.625;$$

$$\frac{F_{tu}}{E\epsilon_s} = \frac{64000}{10.5 \times 10^6 \times 0.12} = 0.051; \text{ therefore, } k_{s_1} = 0.74$$

(by interpolation from Figure 9-4)

$$P_{nt} = 2 \times 1.304 \times 0.74 \times 4000 \times (2.5 - 1.0) \times .5 = 57,898 \text{ lbs.}$$

STRUCTURAL ANALYSIS MANUAL
GENERAL DYNAMICS/CONVAIR AND SPACE SYSTEMS DIVISION

- c) Lug Design Strength (Equation (9-7))

$$P_{t_1} = P_{brt_1} = 28600 \text{ lbs.}$$

- d) Bushing Bearing Strength (Equation (9-9))

$$P_{b_1} = 1.304 \times 60000 \times 0.75 \times 0.50 = 29300 \text{ lbs.}$$

- e) Combined Lug-Bushing Design Strength (Equation (9-10))

$$P_{t,b_1} = P_{t_1} = 28600 \text{ lbs.}$$

- (2) Male Lug and Bushing

$$F_{ty} = 77000 \text{ psi}; 1.304 F_{ty} = 1.304 \times 66000 = 86100 \text{ psi.}$$

- a) Lug Bearing Strength (Equations (9-1b) and (9-3a))

$$\frac{e_2}{D} = \frac{1.50}{1.00} = 1.50; \text{ therefore, } K_2 = 1.33 \text{ (from Figure 9-7)}$$

$$P_{brt_2} = 1.33 \times 77000 \times 1.00 \times 0.75 = 77000 \text{ lbs.}$$

- b) Lug Net-Section Tension Strength (Equations (9-4) and (9-6a))

$$\frac{D}{w_2} = \frac{1.00}{3.00} = 0.333; \frac{F_{ty}}{F_{ts}} = \frac{66000}{77000} = 0.857;$$

$$\frac{F_{tu}}{E\epsilon_s} = \frac{77000}{10.3 \times 10^6 \times 0.06} = 0.125; \text{ therefore } K_{t_2} = 0.87$$

(by interpolation from Figure 9-4)

$$P_{nt} = 1.304 \times 87 \times 66000 \times (3.0 - 1.0) \times 0.75 = 112,313 \text{ lbs.}$$

- c) Lug Design Strength (Equation (9-7))

$$P_{t_2} = P_{brt_2} = 77000 \text{ lbs.}$$

- d) Bushing Bearing Strength (Equation (9-9))

$$P_{b_2} = 1.304 \times 60000 \times 0.75 \times 0.75 = 44000 \text{ lbs.}$$

- e) Combined Lug-Bushing Design Strength (Equation (9-10))

$$P_{t,b_2} = P_{b_2} = 44000 \text{ lbs.}$$

STRUCTURAL ANALYSIS MANUAL
GENERAL DYNAMICS/CONVAIR AND SPACE SYSTEMS DIVISION

(3) Joint Analysis

a) Lug-Bushing Strength (Equation (9-11))

$$P_{t_1} = P_{t_2} = 44000 \text{ lbs.}$$

b) Pin Shear Strength (Equation (9-12))

$$P_{vs} = 1.571 \times (0.75)^2 \times 82000 = 72400 \text{ lbs.}$$

c) Pin Bending Strength (Equation (9-15))

The pin ultimate bending load, assuming uniform bearing across the lugs, is

$$P_{vb} = \frac{0.1963 \times 1.56 \times (0.75)^3 \times 125000}{0.25 + 0.1875 + 0.10} = 30100 \text{ lbs.}$$

Since P_{vb} is less than both P_{t_1} and P_{vs} , the pin is a relatively weak pin which deflects sufficiently under load to shift the bearing loads toward the shear faces of the lugs. The new value of pin bending strength is, then,

$$P_{vb \text{ max}} = 2C \times \left(\sqrt{\frac{30100}{C} \times (0.25 + 0.1875 + 0.10) + (0.10)^2} - 0.10 \right),$$

(from Equation (9-16)) where $C = \frac{28600 \times 44000}{286 \times 0.75 + 44000 \times 0.050}$
 $= 29000 \text{ lbs/in.}$

$$\text{Therefore, } P_{vb \text{ max}} = 2 \times 29000 \times (0.754 - 0.10) = 37900 \text{ lbs.}$$

The "balanced design" effective bearing widths are

$$b_{1 \text{ max}} = \frac{37900 \times 0.50}{2 \times 28600} = 0.331 \text{ in. (from Equation (9-18a))}$$

$$b_{2 \text{ max}} = \frac{37900 \times 0.75}{44000} = 0.646 \text{ in. (from Equation (9-18b))}$$

Therefore, the same value of $P_{vb \text{ max}}$ would be obtained if the thickness of each female lug was reduced to 0.331 inches and the thickness of the male lug reduced to 0.646 inches.

d) Joint Strength (Equation (9-19b))

The final allowable load for the joint, exclusive of the lug tangs, is

STRUCTURAL ANALYSIS MANUAL
GENERAL DYNAMICS/CONVAIR AND SPACE SYSTEMS DIVISION

$$P_{all} = P_{ult, max} = 37900 \text{ lbs.}$$

(4) Lug Tang Analysis

$$P_r = \frac{2 \times 64000 \times 2.50 \times 0.50}{1 + \frac{3}{1.4} \times \left(1 - \frac{0.331}{0.500}\right)} = 92700 \text{ lbs. (from Equation (9-22a))}$$

or

$$P_r = 77000 \times 3.00 \times 0.75 = 173300 \text{ lbs. (from Equation (9-22b))}$$

Therefore, the lug tangs are not critical and the allowable joint load remains at 37900 pounds.

9.7 Lug and Bushing Strength Under Transverse Load

Transversely loaded lugs and bushings are checked in the same general manner as axially loaded lugs. The transversely loaded lug, however, is a more redundant structure than an axially loaded lug, and it has a more complicated failure mode. Figure 9-7 illustrates the different lug dimensions that are critical in determining the lug strength.

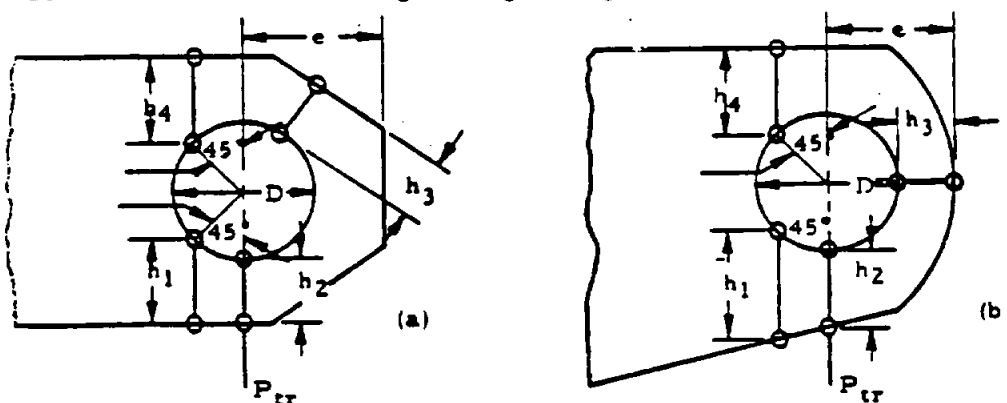


Figure 9-7. Schematic of Lugs Under Transverse Loads

9.7.1 Lug Strength Under Transverse Load

The lug ultimate bearing stress (F_{bru}) is

$$F_{bru} = K_{tr} F_{tu} \quad (9-28)$$

where K_{tr} , the transverse ultimate load coefficient, is obtained from Figure 9-8 as a function of the "effective" edge distance (h_{e*}):

$$h_{e*} = \frac{6}{3/h_1 + 1/h_2 + 1/h_3 + 1/h_4}$$

STRUCTURAL ANALYSIS MANUAL
GENERAL DYNAMICS/CONVAIR AND SPACE SYSTEMS DIVISION

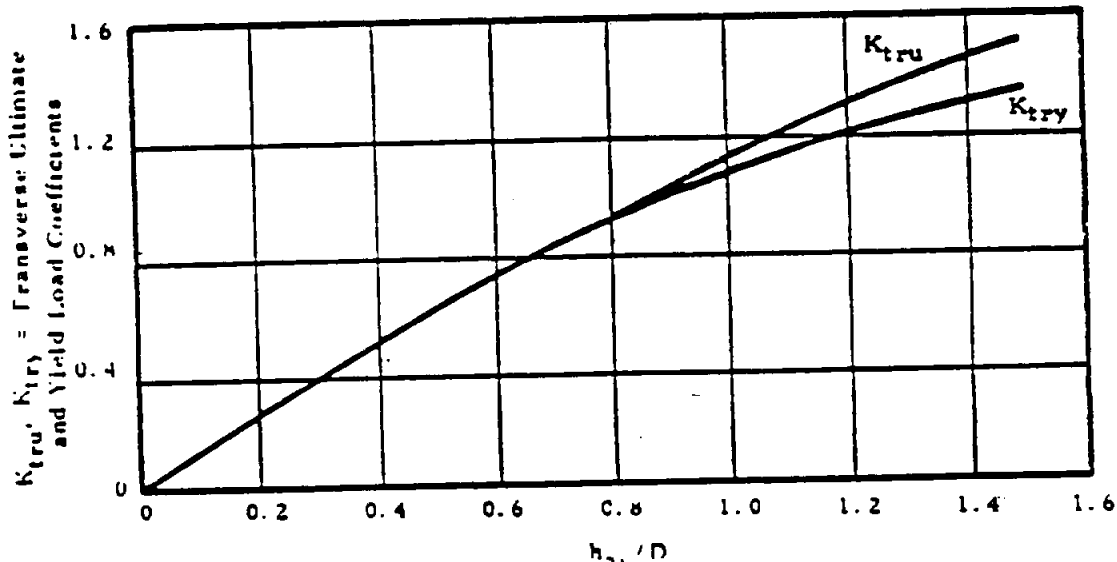


Figure 9-8

The effective edge distance can be found by using the nomograph in Figure 9-9. The nomograph is used by first connecting the h_1 and h_2 lines at the appropriate value of h_1 and h_2 . The intersection with line A is noted. Next connect the h_3 and h_4 lines similarly, and note the B line intersection. Connecting the A and B line intersection gives the value of $h_{e,e}$ to be read at the intersection with the $h_{e,e}$ line. The different edge distances (h_1 , h_2 , h_3 , h_4) indicate different critical regions in the lug, h_1 being the most critical. The distance h_3 is the smallest distance from the hole to the edge of the lug. If the lug is a concentric lug with parallel sides, $h_{e,e}/D$ can be obtained directly from Figure 9-10 for any value of e/D . In concentric lugs, $h_1 = h_4$ and $h_2 = h_3$.

The lug yield bearing stress (F_{byl}) is

$$F_{byl} = K_{try} F_{ty} \quad (9-29)$$

where K_{try} , the transverse yield load coefficient, is obtained from Figure 9-9.

The allowable lug transverse ultimate load ($P_{t,ul}$) is

$$P_{t,ul} = F_{byl} D t \quad (\text{if } F_{t,uz} \leq 1.304 F_{ty}) \quad (9-30a)$$

$$P_{t,ul} = 1.304 F_{byl} D t \quad (\text{if } F_{t,uz} > 1.304 F_{ty}) \quad (9-30b)$$

where $F_{t,uz}$ and F_{byl} are obtained from Equations (9-28) and (9-29).

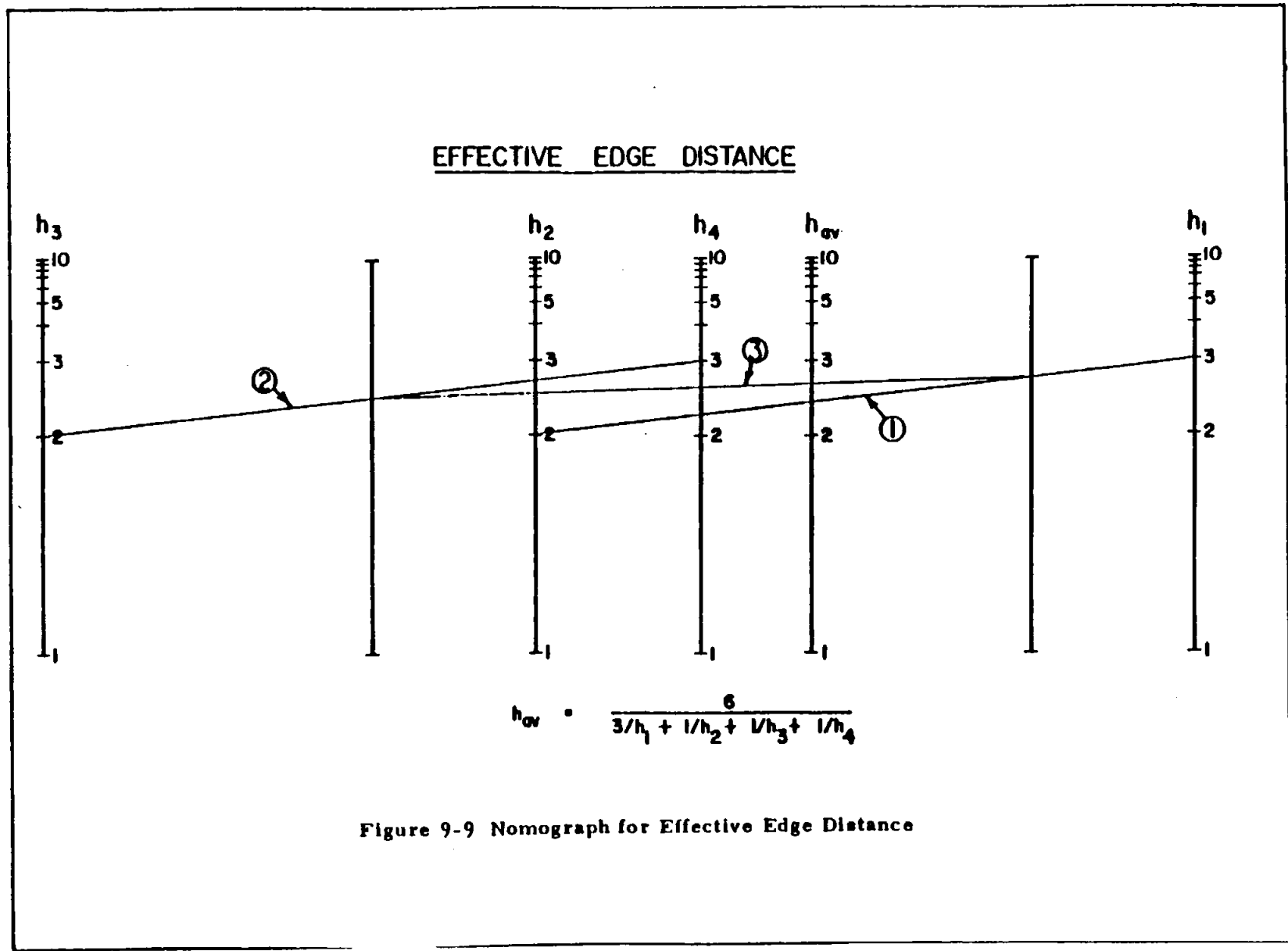


Figure 9-9 Nomograph for Effective Edge Distance

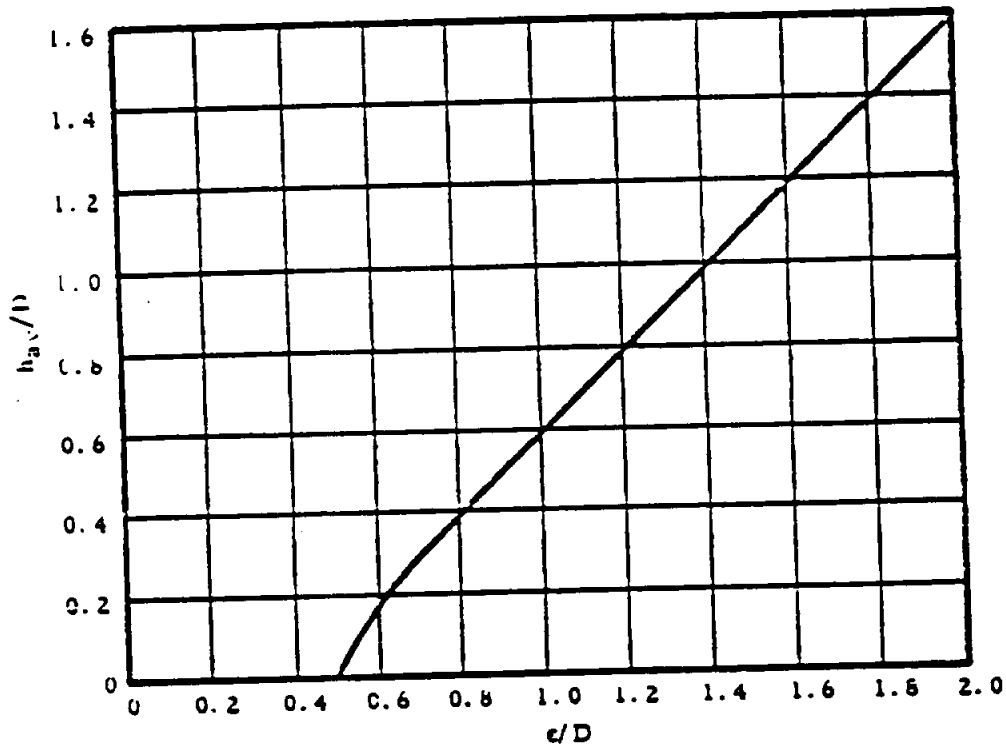


Figure 9-10. Effective Edge Distance

If the lug is not of constant thickness, then A_{av}/A_{br} is substituted for h_{av}/D on the horizontal scale of the graph in Figure 9-8, where A_{br} is the lug bearing area, and

$$A_{av} = \frac{6}{3/A_1 + 1/A_2 + 1/A_3 + 1/A_4}$$

A_1 , A_2 , A_3 , and A_4 are the areas of the sections defined by h_1 , h_2 , h_3 , and h_4 , respectively.

The values of $K_{t,br}$ and $K_{t,rv}$ corresponding to A_{av}/A_{br} are then obtained from the graph in Figure 9-8 and the allowable bearing stresses are obtained as before from Equations (9-28) and (9-29)).

9.7.2 Bushing Strength Under Transverse Load

The allowable bearing stress on the bushing is the same as that for the bushing in an axially loaded lug and is given by Equation (9-8). The allowable bushing ultimate load ($P_{t,rv}$) is equal to P_{br} (Equation (9-9)).

STRUCTURAL ANALYSIS MANUAL

GENERAL DYNAMICS/CONVAIR AND SPACE SYSTEMS DIVISION

9.8 Double Shear Joints Under Transverse Load

The strength calculations needed for double shear joint strength analysis are basically the same as those needed for axially loaded. Equations (9-11) through (9-19) can be used; however, the maximum lug bearing stresses at ultimate and yield loads must not exceed those given by Equations (9-28) and (9-29).

9.9 Single Shear Joints Under Transverse Load

The previous discussion on double shear joint applies to single shear joint strength analysis except the equations to be used are now Equations (9-23) through (9-27).

9.10 Lug and Bushing Strength Under Oblique Load

The analysis procedures used to check the strength of axially loaded lugs and of transversely loaded lugs are combined to analyze obliquely loaded lugs such as the one shown in Figure 9-11. These procedures apply only if α does not exceed 90° .

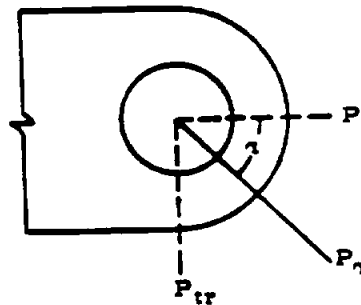


Figure 9-11. Obliquely Loaded Lug

9.10.1 Lug Strength Under Oblique Load

The obliquely applied load (P_α) is resolved into an axial component ($P = P_\alpha \cos \alpha$) and a transverse component ($P_{tr} = P_\alpha \sin \alpha$). The allowable ultimate value of P_α is $P_{\alpha l}$ and its axial and transverse components satisfy the following equation:

$$\left(\frac{P}{P_{ul}} \right)^{1.6} + \left(\frac{P_{tr}}{P_{tru_l}} \right)^{1.6} = 1 \quad (9-31)$$

where P_{ul} is the strength of an axially loaded lug (Equation (9-7)) and P_{tru_l} is the strength of a transversely loaded lug (Equations (9-30a), (9-30b)). The allowable load curve defined by Equation (9-31) is plotted on the graph in Figure 9-12.

$$MS = \frac{1}{\left[\left(\frac{P}{P_{ul}} \right)^{1.6} + \left(\frac{P_{tr}}{P_{tru_l}} \right)^{1.6} \right]^{0.625}} - 1.0$$

STRUCTURAL ANALYSIS MANUAL
GENERAL DYNAMICS/CONVAIR AND SPACE SYSTEMS DIVISION

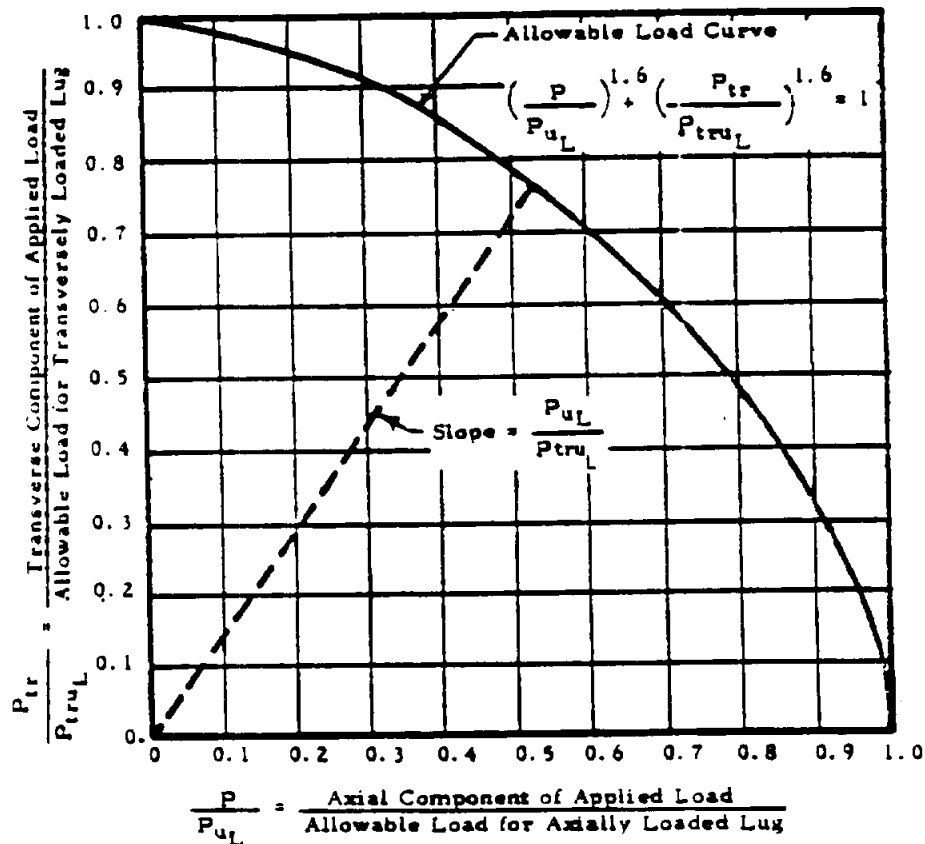


Figure 9-12. Allowable Load Curve

For any given value of α the allowable load (P_{uL}) for a lug can be determined from the graph shown in Figure 9-12 by drawing a line from the origin with a slope equal to (P_{uL}/P_{truL}) . The intersection of this line with the allowable load curve (point 1 on the graph) indicates the allowable values of P/P_{uL} and P_{tr}/P_{truL} , from which the axial and transverse components, P and P_{tr} , of the allowable load can be readily obtained.

9.10.2 Bushing Strength Under Oblique Load

The bushing strength calculations are identical to those for axial loading (Equations (9-8) and (9-9)).

9.11 Double Shear Joints Under Oblique Load

The strength calculations are basically the same as those for an axially loaded joint except that the maximum lug bearing stress at ultimate load must

STRUCTURAL ANALYSIS MANUAL
GENERAL DYNAMICS/CONVAIR AND SPACE SYSTEMS DIVISION

not exceed P_{α} / Dt , where P_{α} is defined by Equation (9-31). Use Equations (9-11) through (9-19)).

9.12 Single Shear Joints Under Oblique Load

The previous discussion on double shear joints applies to single shear joint strength analysis except the equations to be used are now Equations (9-23) through (9-27).

9.13 Multiple Shear and Single Shear Connections

Lug-pin combinations having the geometry indicated in Figure 9-13 should be analyzed according to the following criteria:

- (1) The load carried by each lug should be determined by distributing the total applied load P among the lugs as indicated in Figure 9-13, b being obtained in Table 9-2. This distribution is based on the assumption of plastic behavior (at ultimate load) of the lugs and elastic bending of the pin, and gives approximately zero bending deflection of the pin.
- (2) The maximum shear load on the pin is given in Table 9-2.
- (3) The maximum bending moment in the pin is given by the formulae

$$M = \frac{P_1 b}{2} \quad \text{where } b \text{ is given in Table 9-2.}$$

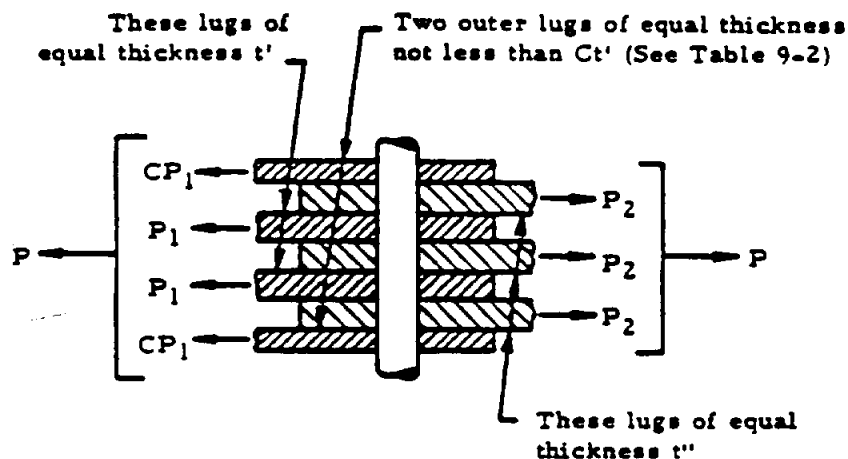


Figure 9-13. Schematic of Multiple Shear Joint in Tension

STRUCTURAL ANALYSIS MANUAL
GENERAL DYNAMICS/CONVAIR AND SPACE SYSTEMS DIVISION

Total number of lugs including both sides	C	Pin Shear	b
5	.35	.50 P_1	.28 $\frac{t' + t''}{2}$
7	.40	.53 P_1	.33 $\frac{t' + t''}{2}$
9	.43	.54 P_1	.37 $\frac{t' + t''}{2}$
11	.44	.54 P_1	.39 $\frac{t' + t''}{2}$
∞	.50	.50 P_1	.50 $\frac{t' + t''}{2}$

9.14 Axially Loaded Lug Design

This section presents procedures for the optimized design of lugs, bushings and pin in a symmetrical, double-shear joint, such as shown in Figure 9-5, subjected to a static axial load (P). One design procedure applies to the case where the pin is critical in shear, the other to the case where the pin is critical in bending. A method is given to help determine which mode of pin failure is more likely, so that the appropriate design procedure will be used.

Portions of the design procedures may be useful in obtaining efficient designs for joints other than symmetrical, double-shear joints.

9.14.1 Axial Lug Design for Pin Failure

An indication of whether the pin in an optimized joint design is more likely to fail in shear or in bending can be obtained from the value of R (Equation (9-32)). If R is less than 1.0, the pin is likely to fail in shear and the design procedure for joints with pins critical in shear should be used to get an optimized design. If R is greater than 1.0, the pin is likely to be critical in bending and the design procedures for joints with pins critical in bending should be used.

$$R = \frac{\pi F_{su}}{k_p F_{tu}} \left(\frac{F_{su}}{F_{w all 1}} + \frac{F_{su}}{F_{w all 2}} \right) \quad (9-32)$$

where F_{su} and F_{tu} are the ultimate shear and ultimate tension stresses for the pin material, k_p is the plastic bending coefficient for the pin, and $F_{w all 1}$

STRUCTURAL ANALYSIS MANUAL
GENERAL DYNAMICS/CONVAIR AND SPACE SYSTEMS DIVISION

and $F_{br all 2}$ are allowable bearing stresses in the female and male lugs. The value of $F_{br all 1}$ can be approximated by the lowest of the following three values:

$$K F_{tuz 1} \frac{D}{D_p} ; 1.304 K F_{tyz 1} \frac{D}{D_p} ; 1.304 F_{cy 1}$$

where $F_{tuz 1}$ and $F_{tyz 1}$ are the cross-grain tensile ultimate and tensile yield stress for female lugs, $F_{cy 1}$ is the compressive yield stress of the bushings in the female lugs, and K is obtained from Figure 9-14. Assume $D = D_p$ if a better estimate cannot be made. $F_{br all 2}$ is approximated in a similar manner.

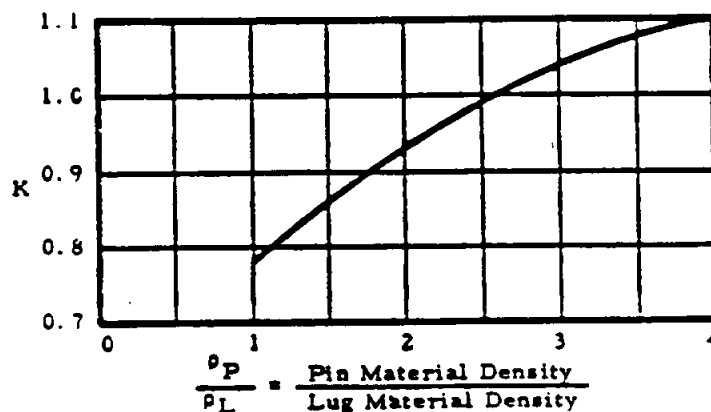


Figure 9-14. Allowable Bearing Coefficient

9.14.1.1 Axial Lug Design for Pin Failure in the Shearing Mode

Pin and Bushing Diameter

The minimum allowable diameter for a pin in double shear is

$$D_p = 0.798 \sqrt{\frac{P}{F_{cy}}} \quad (9-33)$$

The outside diameter of the bushing is $D = D_p + 2t_b$, where t_b is the bushing wall thickness.

Edge Distance Ratio (e/D)

The value of e/D that will minimize the combined lug and pin weight is obtained from Figure (9-15)(a) for the case where lug bearing failure and pin shear failure occur simultaneously. The lug is assumed not critical in net tension, and the bushing is assumed not critical in bearing.

STRUCTURAL ANALYSIS MANUAL
GENERAL DYNAMICS/CONVAIR AND SPACE SYSTEMS DIVISION

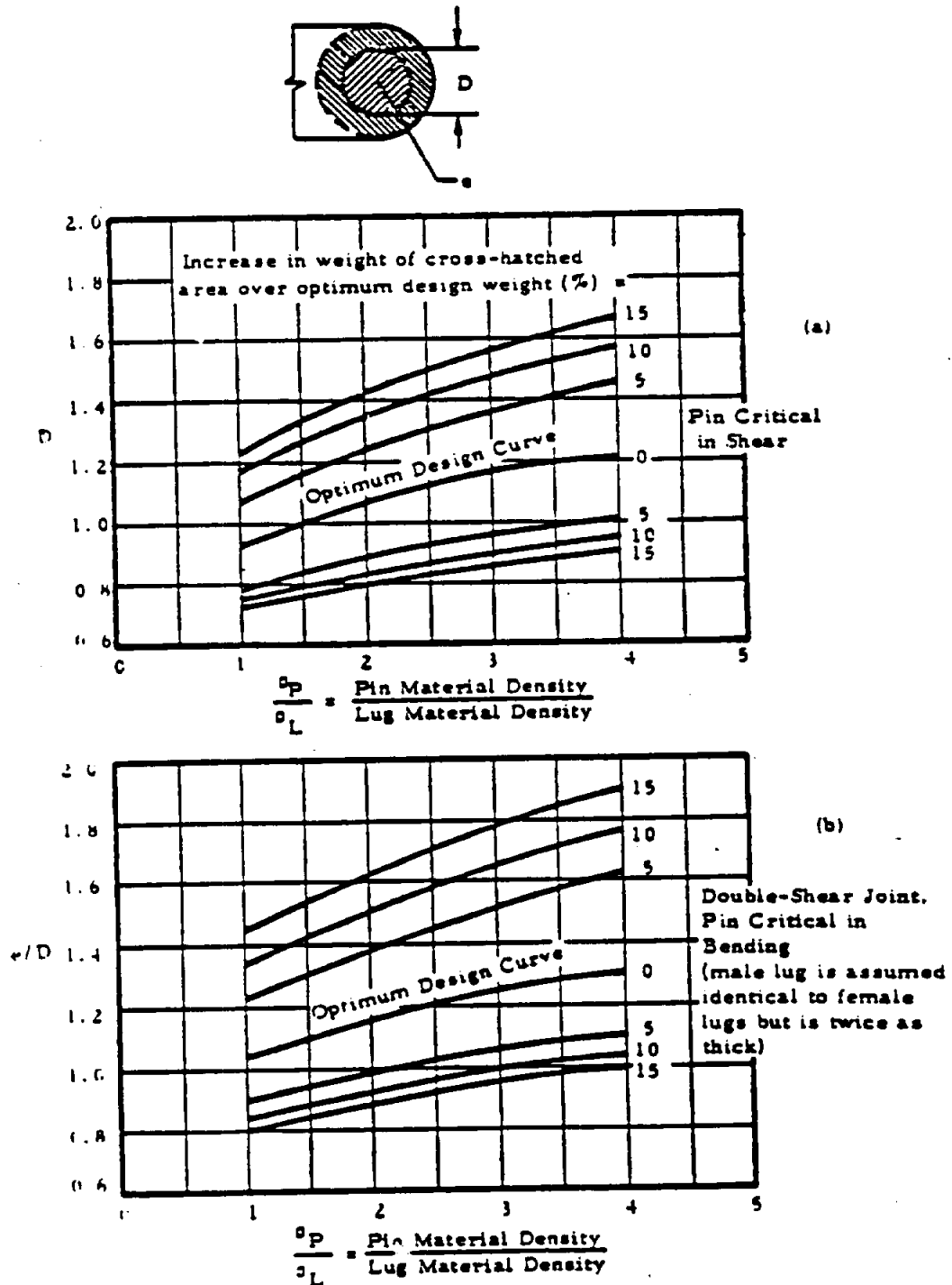


Figure 9-15. Edge Distance Ratio

STRUCTURAL ANALYSIS MANUAL
GENERAL DYNAMICS/CONVAIR AND SPACE SYSTEMS DIVISION

The curves in Figure 9-15 apply specifically to concentric lugs ($a = e - D/2$, and $w = 2e$), but they can be used for reasonably similar lugs.

Allowable Loads

The allowable loads for the different failure modes (lug bearing failure, lug net-tension failure, and bushing failure) are determined from Equations (9-3), (9-6), and (9-9) in terms of the (unknown) lug thickness. The lowest of these loads is critical.

Lug Thicknesses

The required male and female lug thicknesses are determined by equating the applied load in each lug to the critical failure load for the lug.

Pin Bending

To prevent bending failure of the pin before lug or bushing failure occurs in a uniformly loaded symmetrical double-shear joint, the required pin diameter is

$$D_p = \sqrt[3]{\frac{2.55 P}{k_p F_{tu}} \left(t_1 + \frac{t_2}{2} + 2g \right)} \quad (9-34)$$

where k_p is the plastic bending coefficient for the pin. If the value of D_p from Equation (9-34) is greater than that from Equation (9-33), the joint must be redesigned because the pin is critical in bending.

Reduced Edge Distance

If the allowable bushing load (Equation (9-9)) is less than the allowable lug load (Equation (9-3)), a reduced value of e , obtained by using the curve shown in Figure 9-16 for optimum e/D , will give a lighter joint in which lug bearing failure and bushing bearing failure will occur simultaneously. The previously calculated pin diameter and lug thicknesses are unchanged.

Reduced Lug Width

If the lug net-tension strength (Equation (9-6)) exceeds the bearing strength (Equation (9-3)), the net-section width can be reduced by the ratio of the bearing strength to the net-tension strength.

9.14.1.2 Axial Lug Design for Pin Failure in the Bending Mode

Pin and Bushing Diameters (First Approximation)

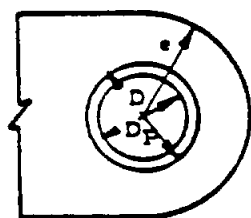
A first approximation to the optimum pin diameter is shown in Equation (9-35).

STRUCTURAL ANALYSIS MANUAL
GENERAL DYNAMICS/CONVAIR AND SPACE SYSTEMS DIVISION.

$$D_p = \sqrt[4]{\frac{1.273}{k_{b_0}} \left(\frac{P}{F_{t_{u_0}}} \right)^2 \left(\frac{F_{t_{u_1}}}{F_{t_{all1}}} + \frac{F_{t_{u_2}}}{F_{t_{all2}}} \right)} \quad (9-35)$$

where $F_{t_{all1}}$ is either $F_{t_{u1}}$ or $1.304 F_{t_{u1}}$, whichever is smaller; and $F_{t_{all2}}$ is either $F_{t_{u2}}$ or $1.304 F_{t_{u2}}$, whichever is smaller. This approximation becomes more accurate when there are no bushings and when there is no gap between lugs.

The first approximation to the outside diameter of the bushing is $D = D_p + 2t_b$.



F_{brB} = Allowable bushing ultimate bearing stress

F_{tux} = Lug material cross-grain ultimate tensile stress

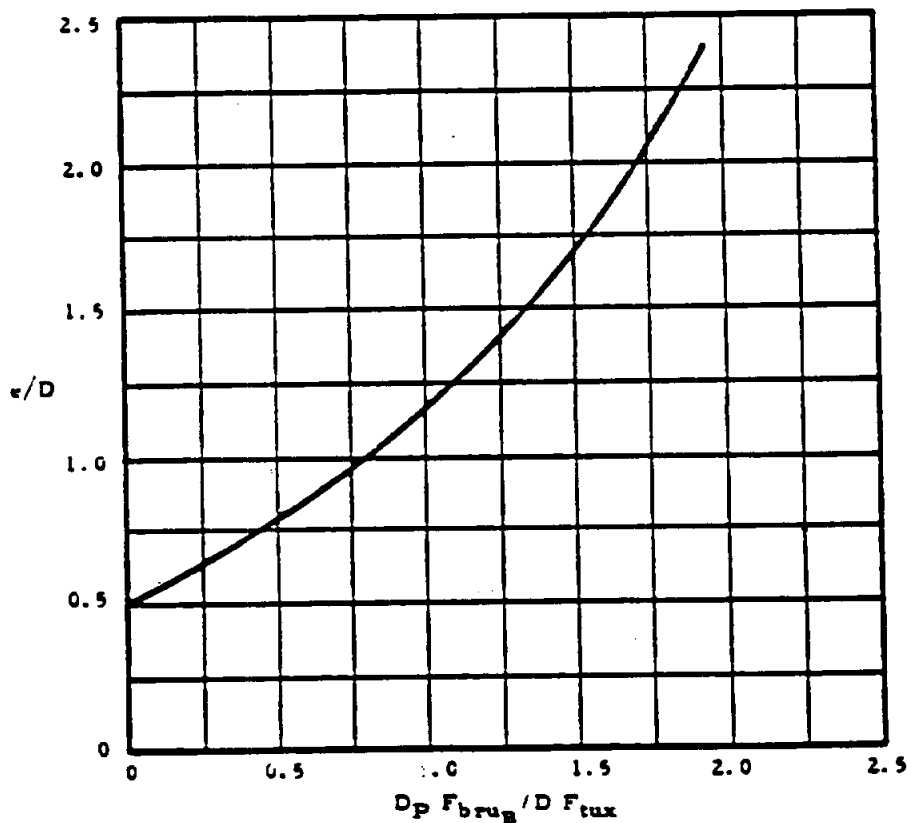


Figure 9-16. Edge Distance Ratio

STRUCTURAL ANALYSIS MANUAL
GENERAL DYNAMICS/CONVAIR AND SPACE SYSTEMS DIVISION

Edge Distance Ratio (e/D)

The value of e/D that will minimize the combined lug and pin weight is obtained from Figure (9-15)(b) for the case of symmetrical double-shear joints in which lug bearing failure and pin bending failure occur simultaneously. The lug is assumed not critical in tension and the bushing is assumed not critical in bearing.

The curves apply specifically to concentric lugs ($a = e - D/2$, and $w = 2e$), but can be used for reasonably similar lugs.

Allowable Loads (First Approximation)

The allowable loads for the different failure modes (lug bearing failure, lug net-tension failure, and bushing failure) are determined from Equations (9-3), (9-6), and (9-9), in terms of the (unknown) lug thickness. The lowest of these loads is critical.

Lug Thicknesses (First Approximation)

The first approximation to the required male and female lug thicknesses are determined by equating the applied load in each lug to the lowest allowable load for the lug.

Pin Diameter (Second Approximation)

The second approximation to the pin diameter is obtained by substituting the first approximation lug thicknesses into Equation (9-34).

Final Pin and Bushing Diameters and Lug Thicknesses

The final optimum pin diameter is very closely approximated by

$$D_{opt} = 1/3 D, \text{ (Equation (9-35))} + 2/3 D, \text{ (Equation (9-34))} \quad (9-36)$$

An average value, however, is generally sufficient. If the final optimum value is not a standard pin diameter, choose the next larger standard pin and bushing.

The final lug thicknesses corresponding to the standard pin and bushing are then determined.

Pin Shear

The pin is checked for shear strength (Equation (9-33)).

STRUCTURAL ANALYSIS MANUAL
GENERAL DYNAMICS/CONVAIR AND SPACE SYSTEMS DIVISION

Reduced Edge Distance

If the bushing bearing strength (Equation (9-9)) is less than the lug bearing strength (Equation (9-3)), a reduced value of e/D , obtained from the curve in Figure 9-16, will give a lighter joint. The pin diameter and lug thicknesses are unchanged.

Reduced Lug Width

If the lug net-tension strength (Equation (9-6)) exceeds the lug bearing strength (Equation (9-3)), the net-section width can be reduced by the ratio of the bearing strength to the net-tension strength.

9.14.1.3 Example of Axially Loaded Lug Design

Using the same materials for the lug, bushing and pin as mentioned in Section 9.6, and assuming the same allowable static load of 37900 pounds, a symmetrical double-shear joint will be designed to carry this load. A 0.10-inch gap is again assumed between the lugs. The bushing wall thickness is assumed to be 1/8 inch.

The lug will first be assumed to be concentric ($a = e = D/2$, and $w = 2e$) but the final minimum weight design will not necessarily be concentric.

Pin Failure Mode (Equation (9-32))

The pin is first checked to determine whether it will be critical in shear or bending, using Equation (9-32). Assuming $D = D_0$ as a first approximation, determine $F_{br \ 111}$ and $F_{br \ 112}$, using the graph in Figure 9-14 to determine K.

$$\begin{aligned} KF_{br \ 1} &= 1.02 \times 64000 = 65300 \text{ psi}; 1.304 KF_{br \ 1} \\ &= 1.304 \times 1.02 \times 40000 = 53100 \text{ psi}; \end{aligned}$$

$$1.304 F_{br \ 1} = 1.304 \times 60000 = 78200 \text{ psi}; \text{ therefore, } F_{br \ 111} = 53100 \text{ psi}$$

$$\begin{aligned} KF_{br \ 2} &= 1.02 \times 77000 = 78500 \text{ psi}; 1.304 KF_{br \ 2} \\ &= 1.304 \times 1.02 \times 66000 = 87900 \text{ psi} \end{aligned}$$

$$1.304 F_{br \ 2} = 1.304 \times 60000 = 78200 \text{ psi}; \text{ therefore } F_{br \ 112} = 78200 \text{ psi}$$

Therefore,

STRUCTURAL ANALYSIS MANUAL
GENERAL DYNAMICS/CONVAIR AND SPACE SYSTEMS DIVISION

$$R = \frac{\pi \times 82000}{1.56 \times 125000} \times \left(\frac{82000}{53100} + \frac{82000}{78200} \right) = 3.4 \text{ (Equation (9-32))}$$

Therefore, the design procedure for pins critical in bending applies.

Pin and Bushing Diameters - First Approximation (Equation (9-35))

$$D_p = \sqrt[4]{\frac{1.273}{1.56} \times \left(\frac{37900}{125000} \right)^2 \times \left(\frac{125000}{52160} + \frac{125000}{77000} \right)} = 0.741 \text{ in.}$$

$$D = 0.741 + 2 \times 0.125 = 0.991 \text{ in.}$$

Edge Distance Ratio (e/D)

The optimum value of e/D for both male and female lugs is 1.24 (Figure 9-15 (b)). Therefore a/D is 0.74 and w/D is 2.48 for a concentric lug (therefore, w = 2.46 in.).

Allowable Loads - Female Lugs and Bushings (First Approximation)

(a) Lug Bearing Strength (Equations (9-2a) and (9-36))

$$P_{br,1} = 1.304 \times 1.46 \times 0.74 \times 40000 \times 0.991 t_1 = 55900 t_1 \text{ lbs.}$$

where K = 1.46 is obtained from Figure 9-2 for e/D = 1.24

(b) Lug Net-Section Tension Strength (Equations (9-5) and (9-6b))

$K_{s,1} = 0.74$ (obtained by interpolation from the graphs shown in Figure 9-9-4) for

$$\frac{D}{w} = 0.403; \quad \frac{F_{t7}}{F_{t9}} = 0.625; \quad \frac{F_{t9}}{E \epsilon_s} = 0.051$$

$$P_{st,1} = 1.304 \times 40000 \times (2.46 - 0.991) t_1 = 56600 t_1 \text{ lbs.}$$

(c) Bushing Bearing Strength (Equation (9-9))

$$P_{b,1} = 1.304 \times 60000 \times 0.741 t_1 = 58000 t_1 \text{ lbs.}$$

Allowable Loads - Male Lug and Bushing (First Approximation)

(a) Lug Bearing Strength (Equations (9-1a) and (9-3a))

STRUCTURAL ANALYSIS MANUAL
GENERAL DYNAMICS/CONVAIR AND SPACE SYSTEMS DIVISION

$$P_{b_{m_2}} = 1.46 \times 0.74 \times 77000 \times 0.991 t_2 = 82500 t_2 \text{ lbs.}$$

(b) Lug Net-Section Tension Strength (Equations (9-4) and (9-6a))

$K_{a_2} = 0.88$ (obtained by interpolation from graphs shown in Figure 9-4) for.

$$\frac{D}{w_2} = 0.403; \frac{F_{t_2}}{F_{u_2}} = 0.857; \frac{F_{u_2}}{E t_2} = 0.125$$

$$P_{a_2} = 0.88 \times 77000 \times (2.46 - 0.991) t_2 = 99500 t_2 \text{ lbs.}$$

(c) Bushing Bearing Strength (Equation (9-9))

$$P_{b_2} = 1.304 \times 60000 \times 0.741 t_2 = 58000 t_2 \text{ lbs.}$$

Lug Thicknesses (First Approximation)

$$t_1 = \frac{37900}{2 \times 55900} = 0.339 \text{ in.}; t_2 = \frac{37900}{58000} = 0.654 \text{ in.}$$

Pin Diameter - Second Approximation (Equation (9-34))

$$D_p = \sqrt[3]{\frac{2.55 \times 37900}{1.56 \times 125000} (0.339 + 0.327 + 0.200)} = 0.755 \text{ in.}$$

$$D = 0.755 + 2 \times 0.125 = 1.0005 \text{ in.}$$

Final Pin and Bushing Diameter (Equation (9-36))

$$D_{b_{opt}} = \frac{0.741}{2} + \frac{0.755}{2} = 0.748 \text{ in. (Use 0.750 inch pin)}$$

$$D = 0.750 + 2 \times 0.125 = 1.000 \text{ in.}$$

Pin Shear (Equation (9-33))

$$D_s = 0.798 \sqrt{\frac{37900}{82000}} = 0.541 \text{ in.}$$

Therefore, the pin is not critical in shear.

Final Lug Thicknesses

$$t_1 = 0.339 \times \frac{0.991}{1.000} = 0.336 \text{ in.}$$

STRUCTURAL ANALYSIS MANUAL
GENERAL DYNAMICS/CONVAIR AND SPACE SYSTEMS DIVISION

$$t_2 = 0.654 \times \frac{0.741}{0.750} = 0.646 \text{ in.}$$

Reduced Edge Distance

The lug tension strength (Equation (9-3)) exceeds the bushing strength (Equation (9-9)) for the male lug. Therefore, a reduced e/D can be obtained for the male lug shown in Figure 9-16.

$$\frac{D_p}{D} \frac{F_{brg}}{F_{tug}} = \frac{0.750}{1.000} \times \frac{1.304 \times 60000}{77000} = 0.762$$

Therefore, $e/D = 0.97$ (male lug)

Reduced Lug Width

The lug net-section tension strength (Equation (9-6)) exceeds the bearing strength (Equation (9-3)) for both the male and female lugs. Therefore, the widths can be reduced as follows:

$$w_1 = 1.00 + (2.48 - 1.00) \left(\frac{55900 t_1}{56600 t_1} \right) = 2.46 \text{ in.}$$

$$w_2 = 1.00 + (2.48 - 1.00) \left(\frac{82500 t_2}{99500 t_2} \right) = 2.23 \text{ in.}$$

Final Dimensions

$$D_p = 0.750 \text{ in.}; D = 1.000 \text{ in.}$$

$$t_1 = 0.336 \text{ in.}; e_1 = 1.24 \text{ in.}; w_1 = 2.46 \text{ in.}$$

$$t_2 = 0.646 \text{ in.}; e_2 = 0.97 \text{ in.}; w_2 = 2.23 \text{ in.}$$

Since w_2 is larger than $2e_2$, the final male lug is not concentric.

9.15 Analysis of Lugs with Less Than 5 PCT Elongation

The procedures given through Section 9-14 for determining the static strength of lugs apply to lugs made from materials which have ultimate elongations, ϵ_u , of at least 5% in all directions in the plane of the lug. This section describes procedures for calculating reductions in strength for lugs made from materials which do not meet the elongation requirement. In addition to using these procedures, special consideration must be given to possible further loss in strength resulting from material defects when the short transverse grain direction of the lug material is in the plane of the lug.

STRUCTURAL ANALYSIS MANUAL
GENERAL DYNAMICS/CONVAIR AND SPACE SYSTEMS DIVISION

The analysis procedures for lugs made from materials without defects but with less than 5% elongation are as follows:

9.15.1 Bearing Strength of Axially Loaded Lugs with Less Than 5 PCT Elongation

- (1) Determine F_{ty}/F_{tu} and ϵ_y/ϵ_u using values of F_{ty} , F_{tu} , ϵ_y , and ϵ_u that correspond to the minimum value of ϵ_y in the plane of the lug.
- (2) Determine the value of B, the ductility factor, from the graph shown in Figure 9-17.
- (3) Determine a second value of B (denoted by $B_{.05}$) for the same values of F_{ty} , F_{tu} , and ϵ_y as before, but with $\epsilon_u = 0.05$.
- (4) Multiply the bearing stress and bearing load allowables given by Equations (9-1a) through (9-3b) by $B/B_{.05}$ to obtain the corrected allowables.

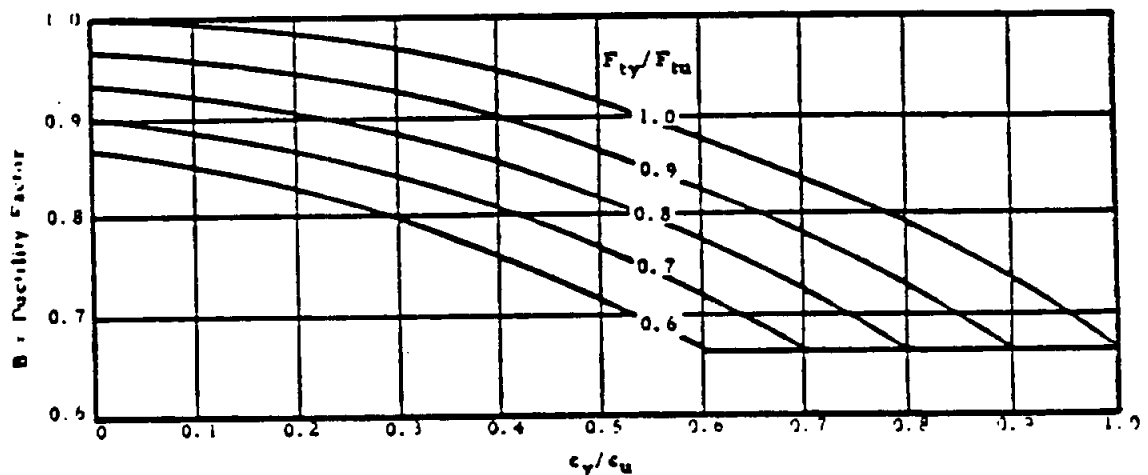


Figure 9-17. Ductility Factor

9.15.2 Net-Section Strength of Axially Loaded Lugs with Less Than 5 PCT Elongation

The procedure for determining net-section allowables is the same for all values of ϵ_y . The graphs in Figure 9-4 are used to obtain a value of K_t which is substituted in Equations (9-4) and (9-5). If the grain direction of the material is known, the values of F_{ty} , F_{tu} , and ϵ_y used in entering the graphs should correspond to the grain direction parallel to the load. Otherwise, use values corresponding to the minimum value of ϵ_y in the plane of the lug.

STRUCTURAL ANALYSIS MANUAL
GENERAL DYNAMICS/CONVAIR AND SPACE SYSTEMS DIVISION

9.15.3 Strength of Lug Tangs in Axially Loaded Lugs with Less Than 5 PCT Elongation

The plastic bending coefficient for a rectangular cross section can be approximated by $k_{pl} = 1.5B$, where B is obtained from Figure 9-17, in which y and u are the yield and ultimate strains of the lug tang material in the direction of loading. The maximum allowable value of k_{pl} for a rectangle is 1.4.

9.15.4 Lug-Bushing Strength in Axially-Loaded Single-Shear Joint with Less Than 5 PCT Elongation

The values of k_{pl} and k_{pt} for rectangular cross sections are approximated by $1.5B$, where B is determined from the graph as described in Figure 9-17. The maximum allowable values of k_{pl} and k_{pt} are 1.4.

9.15.5 Bearing Strength of Transversely Loaded Lugs with Less Than 5% Elongation (Equations (9-28) through (9-30b) in Section 9.7.1

The same procedure as that for the bearing strength of axially loaded lugs is used.

- (1) Determine B and $B_{0.5}$ as described for axially loaded lugs, where B corresponds to the minimum value of ϵ_u in the plane of the lug.
- (2) Multiply the bearing stress and bearing load allowables given by Equations (9-28) through (9-30b) by $B/B_{0.5}$ to obtain the corrected allowables.

9.16 Stresses Due to Press Fit Bushings

Pressure between a lug and bushing assembly having negative clearance can be determined from consideration of the radial displacements. After assembly, the increase in inner radius of the ring (lug) plus the decrease in outer radius of the bushing equals the difference between the radii of the bushing and ring before assembly:

$$\delta = u_{\text{ring}} - u_{\text{bushing}} \quad (9-36)$$

where

δ = Difference between outer radius of bushing and inner radius of the ring.

u = Radial displacement, positive away from the axis of ring or bushing.

STRUCTURAL ANALYSIS MANUAL
GENERAL DYNAMICS/CONVAIR AND SPACE SYSTEMS DIVISION

Radial displacement at the inner surface of a ring subjected to internal pressure p is

$$u = \frac{D}{E_{\text{ring}}} \left[\frac{C^2 + D^2}{C^2 - D^2} + \mu_{\text{ring}} \right] \quad (9-37)$$

Radial displacement at the outer surface of a bushing subjected to external pressure p is

$$u = - \frac{B}{E_{\text{bush.}}} \left[\frac{B^2 + A^2}{B^2 - A^2} - \mu_{\text{bush.}} \right] \quad (9-38)$$

where

A = Inner radius of bushing	D = Inner radius of ring (lug)
B = Outer radius of bushing	E = Modulus of elasticity
C = Outer radius of ring (lug)	μ = Poisson's ratio

Substitute Equations (9-37) and (9-38) into Equation (9-36) and solve for p :

$$p = \frac{\delta}{\frac{D}{E_{\text{ring}}} \left(\frac{C^2 + D^2}{C^2 - D^2} + \mu_{\text{ring}} \right) + \frac{B}{E_{\text{bush.}}} \left(\frac{B^2 + A^2}{B^2 - A^2} - \mu_{\text{bush.}} \right)}$$

Maximum radial and tangential stresses for a ring subjected to internal pressure occur at the inner surface of the ring (lug).

$$F_r = -p \quad F_t = p \left[\frac{C^2 + D^2}{C^2 - D^2} \right]$$

Positive sign indicates tension. The maximum shear stress at this point is

$$F_s = \frac{F_t - F_r}{2}$$

The maximum radial stress for a bushing subjected to external pressure occurs at the outer surface of the bushing is

$$F_r = -p$$

The maximum tangential stress for a bushing subjected to external pressure occurs at the inner surface of the bushing is

$$F_t = - \frac{2p^2}{B^2 - A^2}$$

STRUCTURAL ANALYSIS MANUAL
GENERAL DYNAMICS/CONVAIR AND SPACE SYSTEMS DIVISION

The allowable press fit stress may be based on:

- (1) Stress Corrosion. The maximum allowable press fit stress in magnesium alloys should not exceed 8000 psi. For all aluminum alloys the maximum press fit stress should not exceed $0.50 F_{17}$.
- (2) Static Fatigue. Static fatigue is the brittle fracture of metals under sustained loading, and in steel may result from several different phenomena, the most familiar of which is hydrogen embrittlement. Steel parts heat treated above 200 ksi, which by nature of their function or other considerations are exposed to hydrogen embrittlement, should be designed to an allowable press fit stress of $25\% F_{17}$.
- (3) Ultimate Strength. Ultimate strength cannot be exceeded, but is not usually critical in a press fit application.
- (4) Fatigue Life. The hoop tension stresses resulting from the press fit of a bushing in a lug will reduce the stress range for oscillating loads, thereby improving fatigue life.

The presence of hard brittle coatings in holes that contain a press fit bushing or bearing can cause premature failure by cracking of the coating or by high press fit stresses caused by build-up of coating. Therefore, Hardcoat or HAE coatings should not be used in holes that will subsequently contain a press fit bushing or bearing.

Figures 9-18 and 9-19 permit determining the tangential stress, F_{17} , for bushings pressed into aluminum rings. Figure 9-18 presents data for general steel bushings, and Figure 9-19 presents data for the NAS 75 class bushings. Figure 9-20 gives limits for maximum interference fits for steel bushings in magnesium alloy rings.

9.17 Lug Fatigue Analysis

A method for determining the fatigue strength of 2024-T3 and 7075-T6 aluminum alloy lugs under axial loading is presented.

Figures 9-21 and 9-22 show the lug and the range of lug geometries covered by the fatigue strength prediction method. Fatigue lives for lugs having dimensional ratios falling outside the region shown should be corroborated by tests.

In this method the important fatigue parameters are k_1 , k_2 , and k_3 (see Figure 9-23).

STRUCTURAL ANALYSIS MANUAL
GENERAL DYNAMICS/CONVAIR AND SPACE SYSTEMS DIVISION

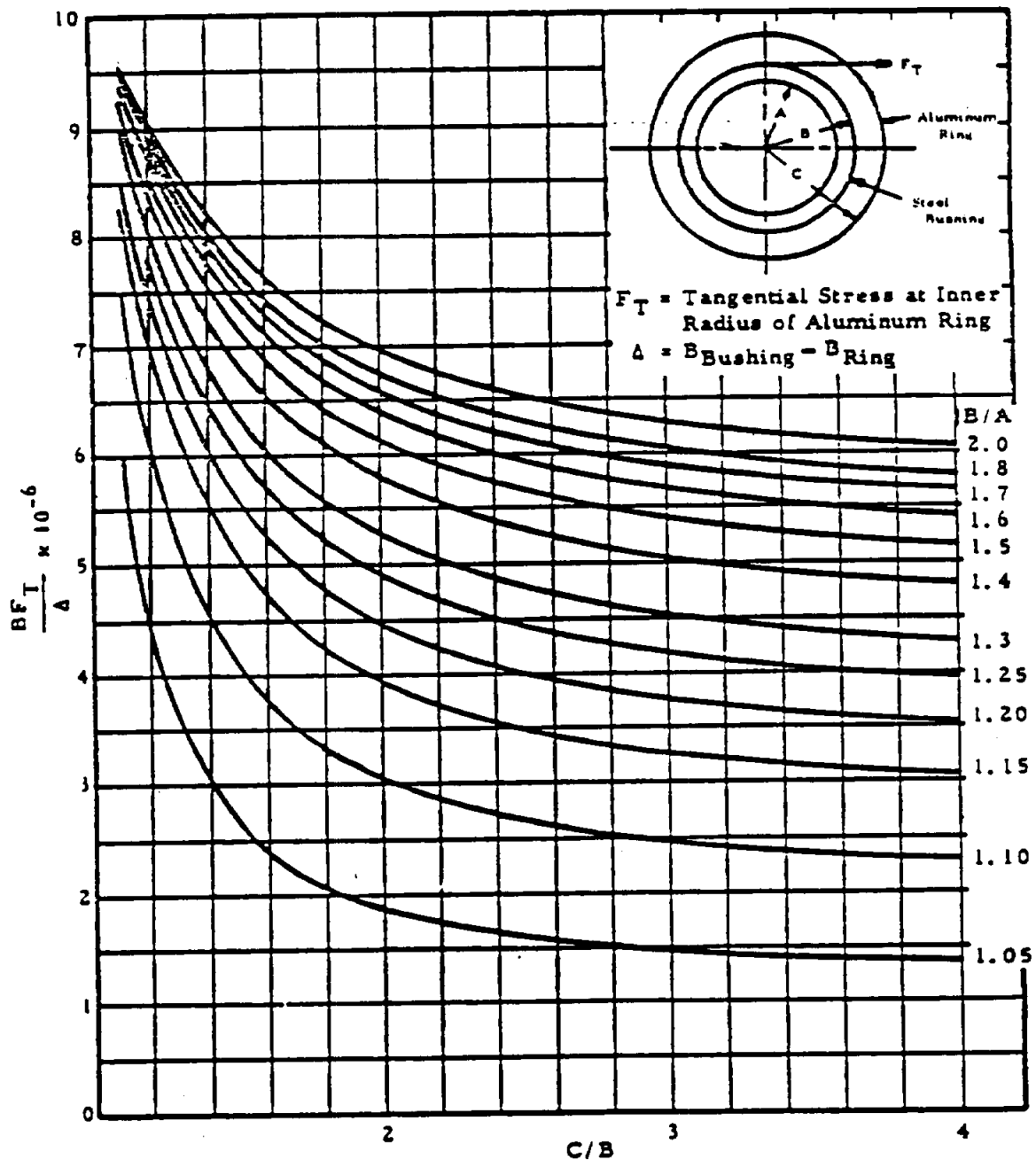


Figure 9-18. Tangential Stresses for Pressed Steel Bushings in Aluminum Rings

STRUCTURAL ANALYSIS MANUAL
GENERAL DYNAMICS/CONVAIR AND SPACE SYSTEMS DIVISION

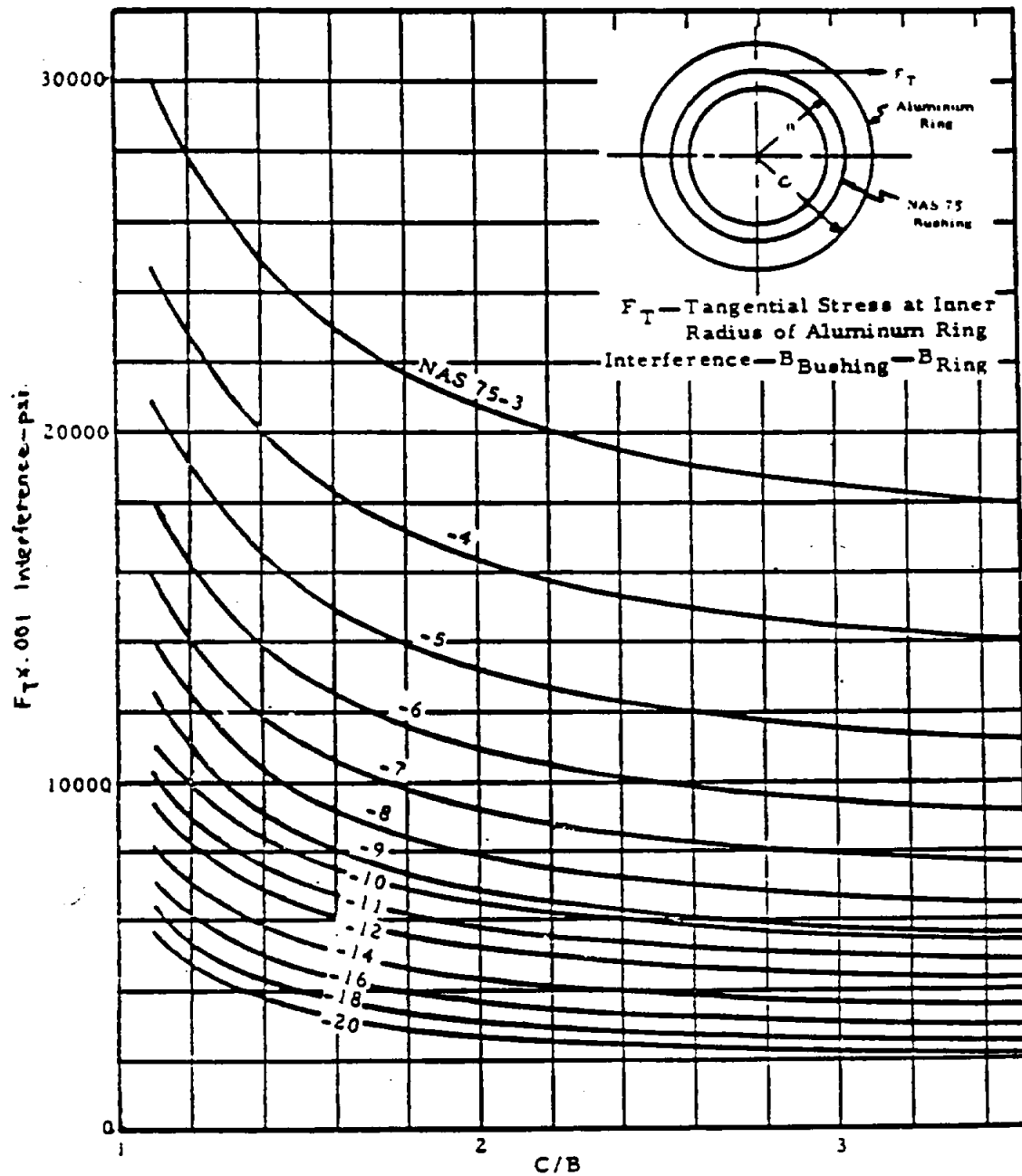
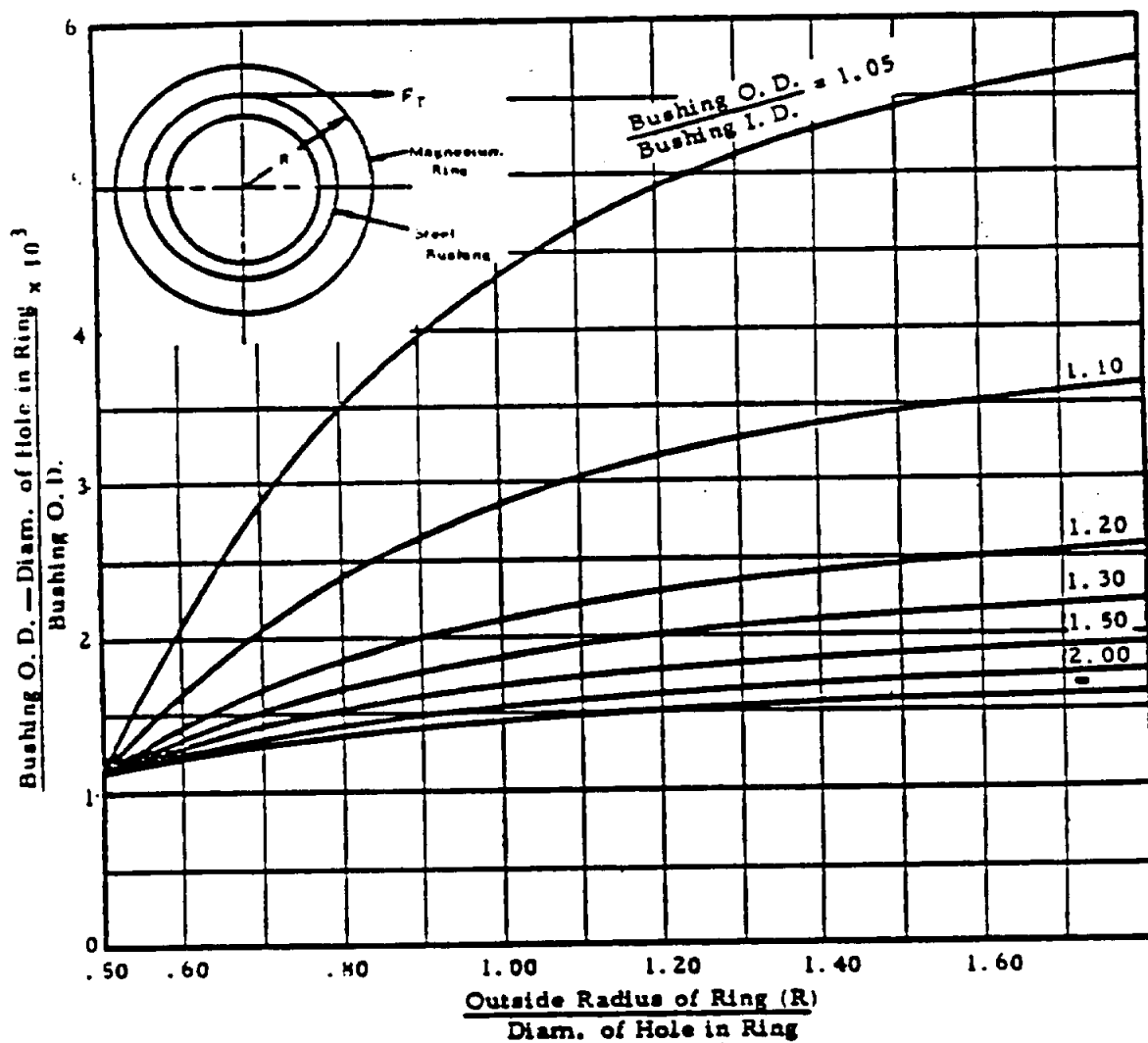


Figure 9-19. Tangential Stresses for Pressed NAS 75 Bushings

STRUCTURAL ANALYSIS MANUAL
GENERAL DYNAMICS/CONVAIR AND SPACE SYSTEMS DIVISION



O. D. of the bushing is the after-plating diameter of the bushing.

The curves are based upon a maximum allowable interference tangential stress of 8000 psi.

Figure 9-20. Maximum Interference Fits of Steel Bushings in Magnesium Alloy Rings

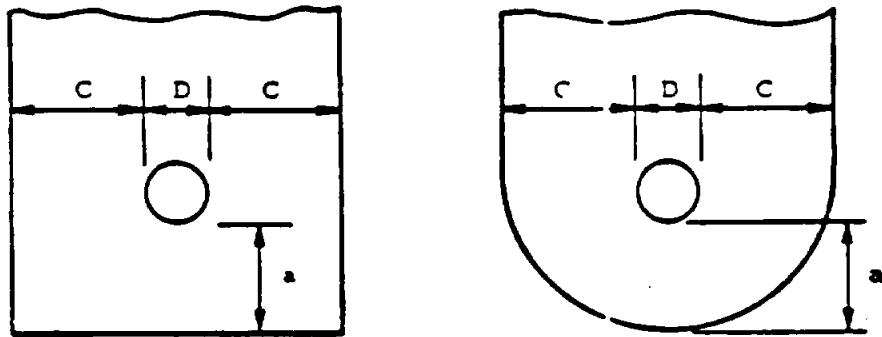


Figure 9-21. Lug Geometry for Fatigue Analysis

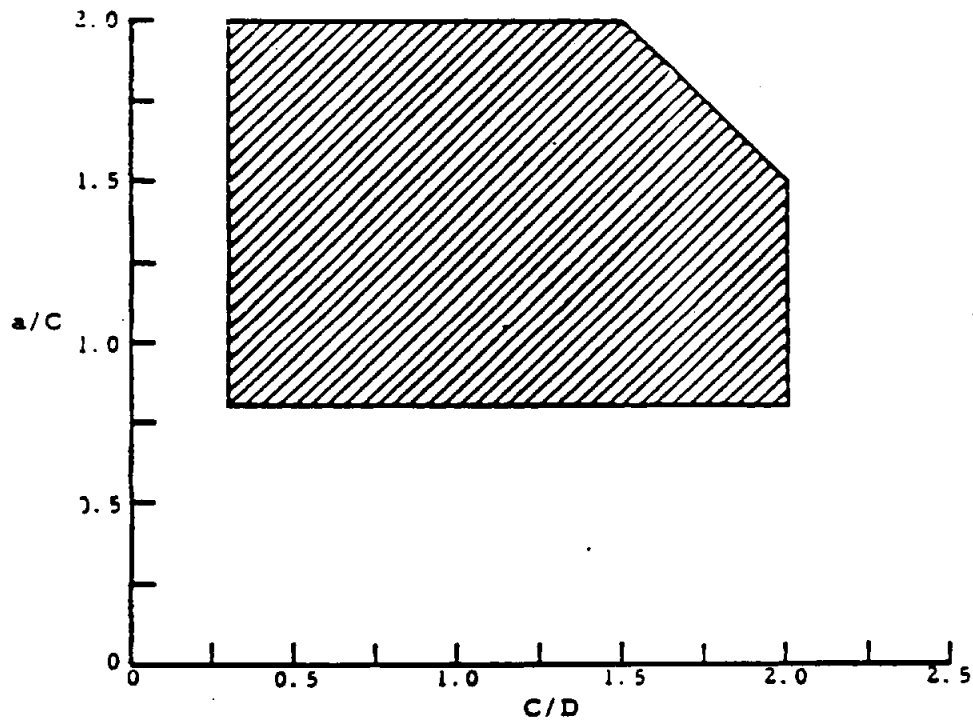


Figure 9-22. Region of Lug Geometries Covered by Fatigue Prediction Method

STRUCTURAL ANALYSIS MANUAL
GENERAL DYNAMICS/CONVAIR AND SPACE SYSTEMS DIVISION

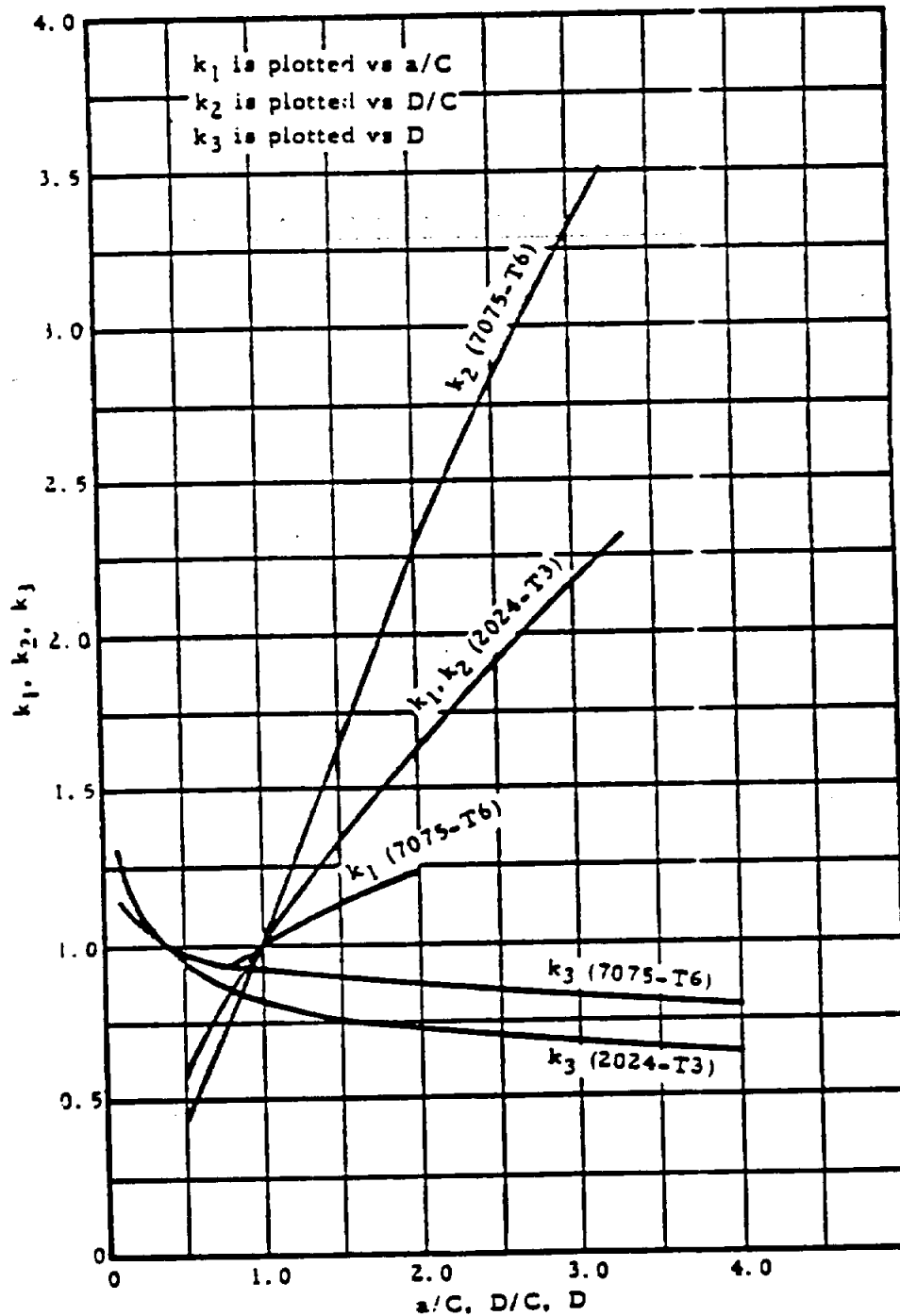


Figure 9-23. Parameters To Be Used in Figure 9-24 or Lug Fatigue Analysis

STRUCTURAL ANALYSIS MANUAL
GENERAL DYNAMICS/CONVAIR AND SPACE SYSTEMS DIVISION

To find the allowable life knowing the applied stresses and lug dimensions, or to find the allowable stresses knowing the life, R value ($R = f_{alt}/f_{max}$) and, lug dimensions, use the following procedure:

- (1) Enter Figure 9-22 to check that the lug dimensional ratios fall within the region covered by the method. Enter Figure 9-23 and read k_1 , k_2 , and k_3 ; calculate the product $k_1 k_2 k_3$.
- (2) Calculate the allowable net-tension static stress for the lug, F_{su} , according to the method described in Section 9.3.2.
- (3) Determine the value $0.4 F_{su}$. This is the alternating stress corresponding to a maximum stress value of $0.8 F_{su}$ when $f_{alt} = 0$. $0.8 F_{su}$ was chosen as an average yield stress value for 2024 and 7075 aluminum alloy lugs.
- (4) Using the value $0.4 F_{su}$ as an alternating stress, draw a straight line between the intersection of this value and the appropriate $k_1 k_2 k_3$ curve on Figures 9-24 or 9-25, and the point $0.5 F_{su}$ at 1 cycle. This extends the $k_1 k_2 k_3$ curve to cover the entire life range to static failure.
- (5) Enter Figure 9-24 or 9-25 (lug fatigue curves for the case where $R = 0$) with $k_1 k_2 k_3$. For values of life, $N = 10^3$, 3×10^3 , 10^4 , etc., or any other convenient values, determine the corresponding values of f_a , the stress amplitude causing fatigue failure when $R = 0$.
- (6) Plot the values of f_a found in Step 5 along the $R = 0$ line in a Goodman diagram such as shown in Figure 9-26 ($f_a = 0$ when $R = 0$). The Goodman diagram shown in Figure 9-27 applies to a particular 7075-T6 lug for which $k_1 k_2 k_3 = 1.32$ (see example problem 1), but is typical of all such diagrams.
- (7) Plot the allowable net-tension static stress found in Step 2 as f_u at the point ($f_a, 0$) of the Goodman diagram ($f_a = f_{su}$ when $f_a = 0$). For the case considered in Figure 9-26, this point is plotted as ($f_a = 70,000$ psi, $f_u = 0$).
- (8) Connect the point plotted in Step 7 with each of the points plotted in Step 6 by straight lines. These are the constant life lines for the particular lug being analyzed. The Goodman diagram is now complete and may be used to determine a life for any given applied stresses, or to determine allowable stresses knowing the life and R value.

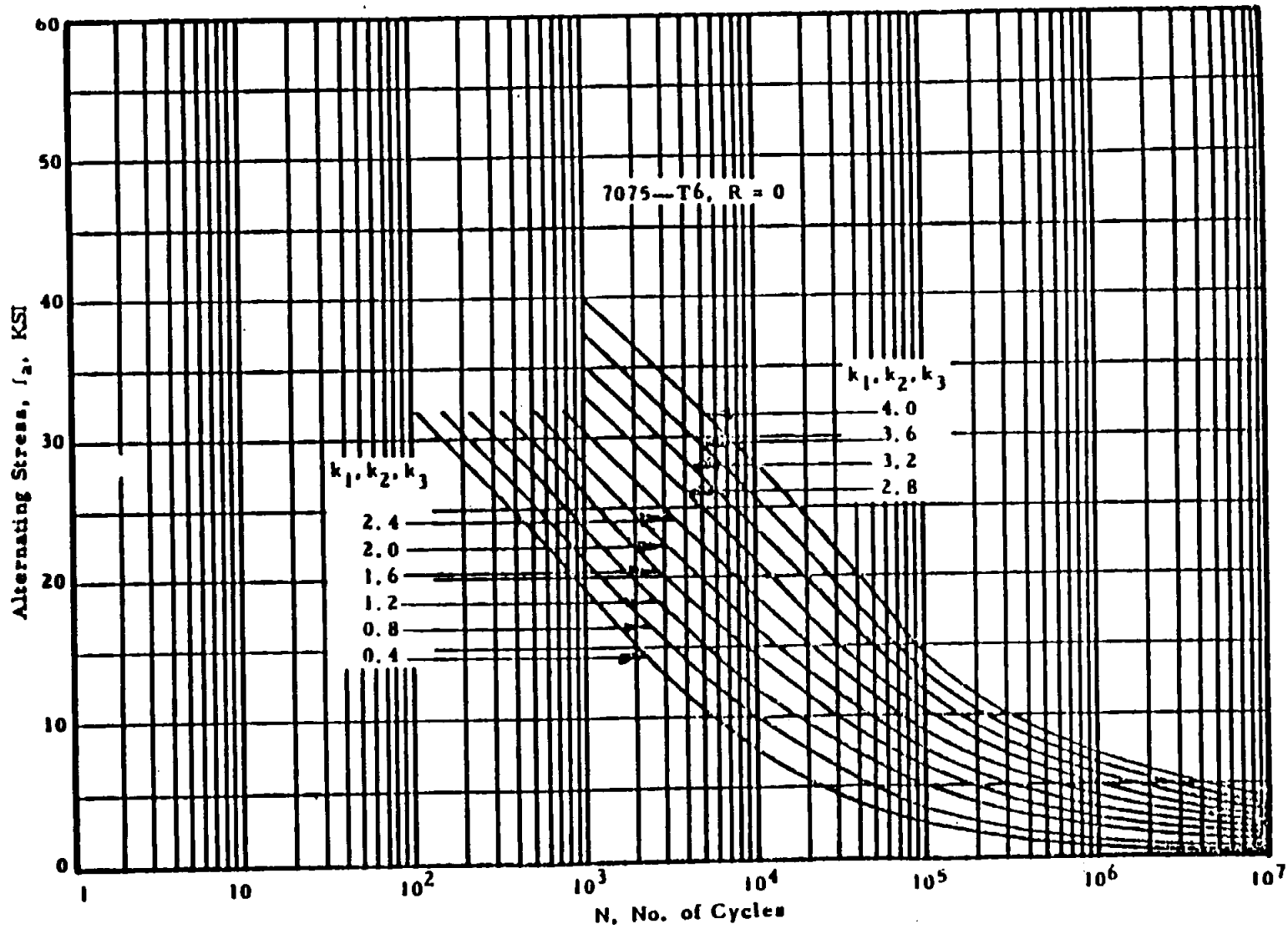


Figure 9-24. Fatigue Life Curves for Constant k_1, k_2, k_3 Values; 7075-T6, R = 0

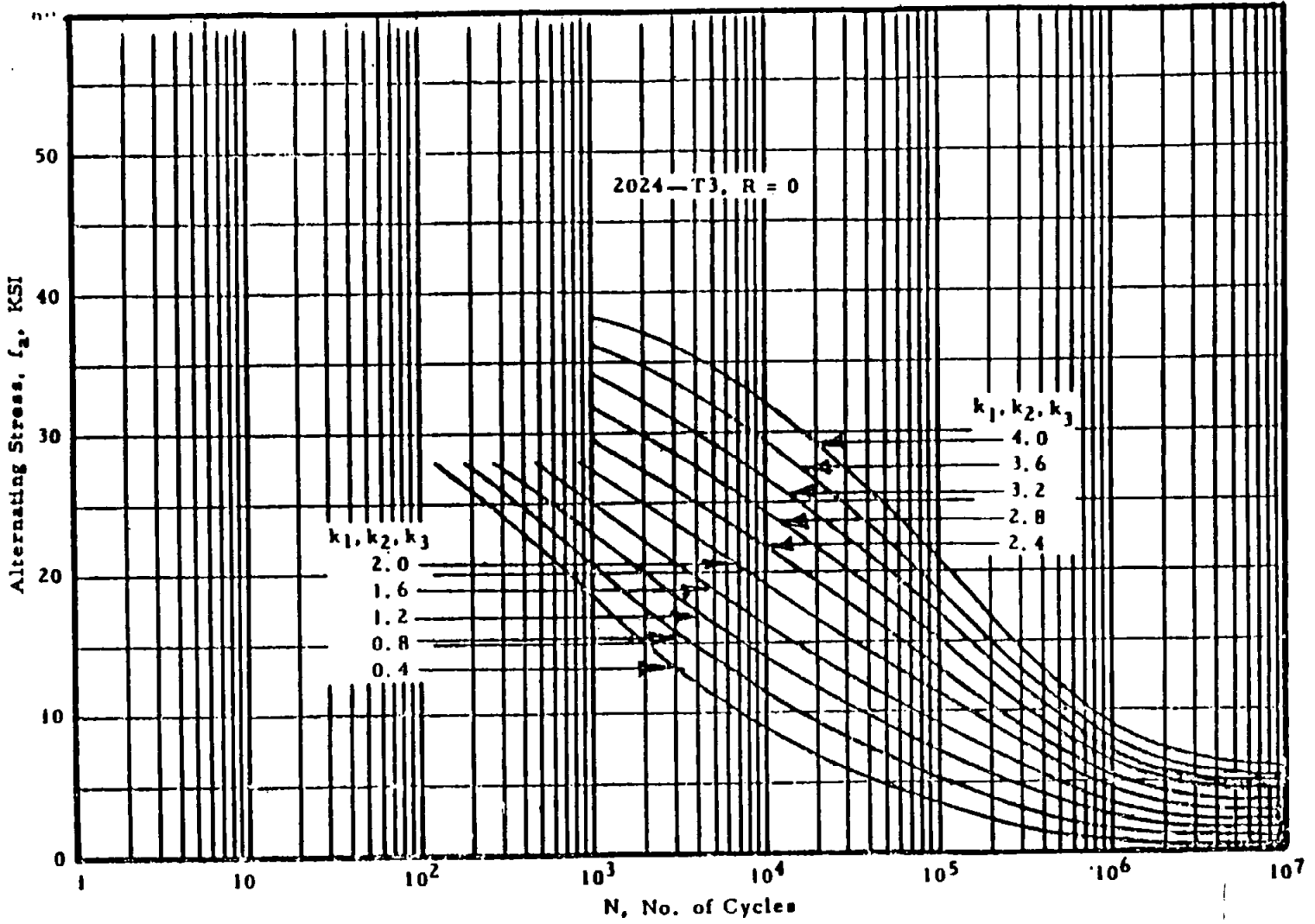


Figure 9-25. Fatigue Life Curves for Constant k_1, k_2, k_3 Values; 2024-T3, R = 0

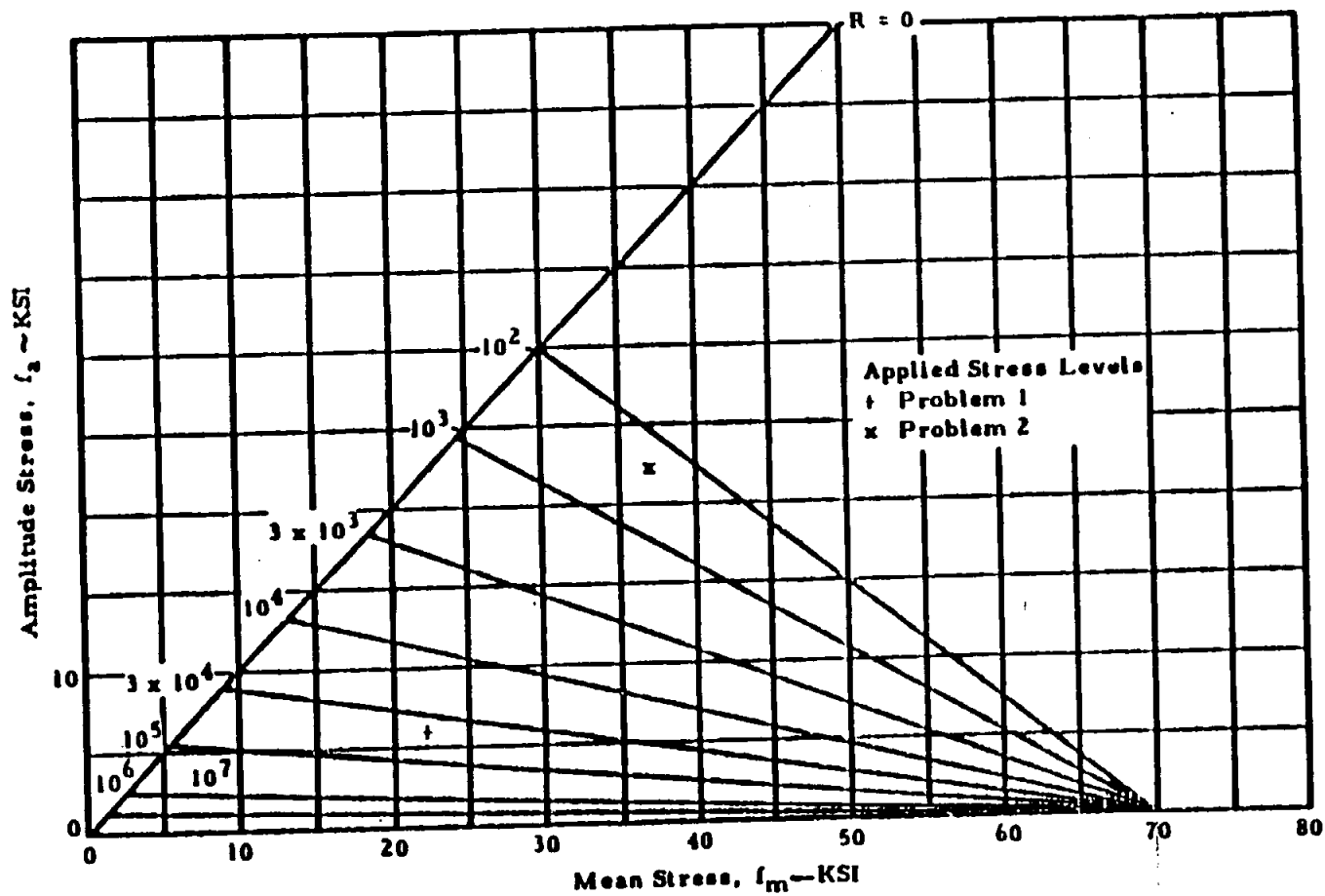


Figure 9-26. Goodman Diagram for Example Problems

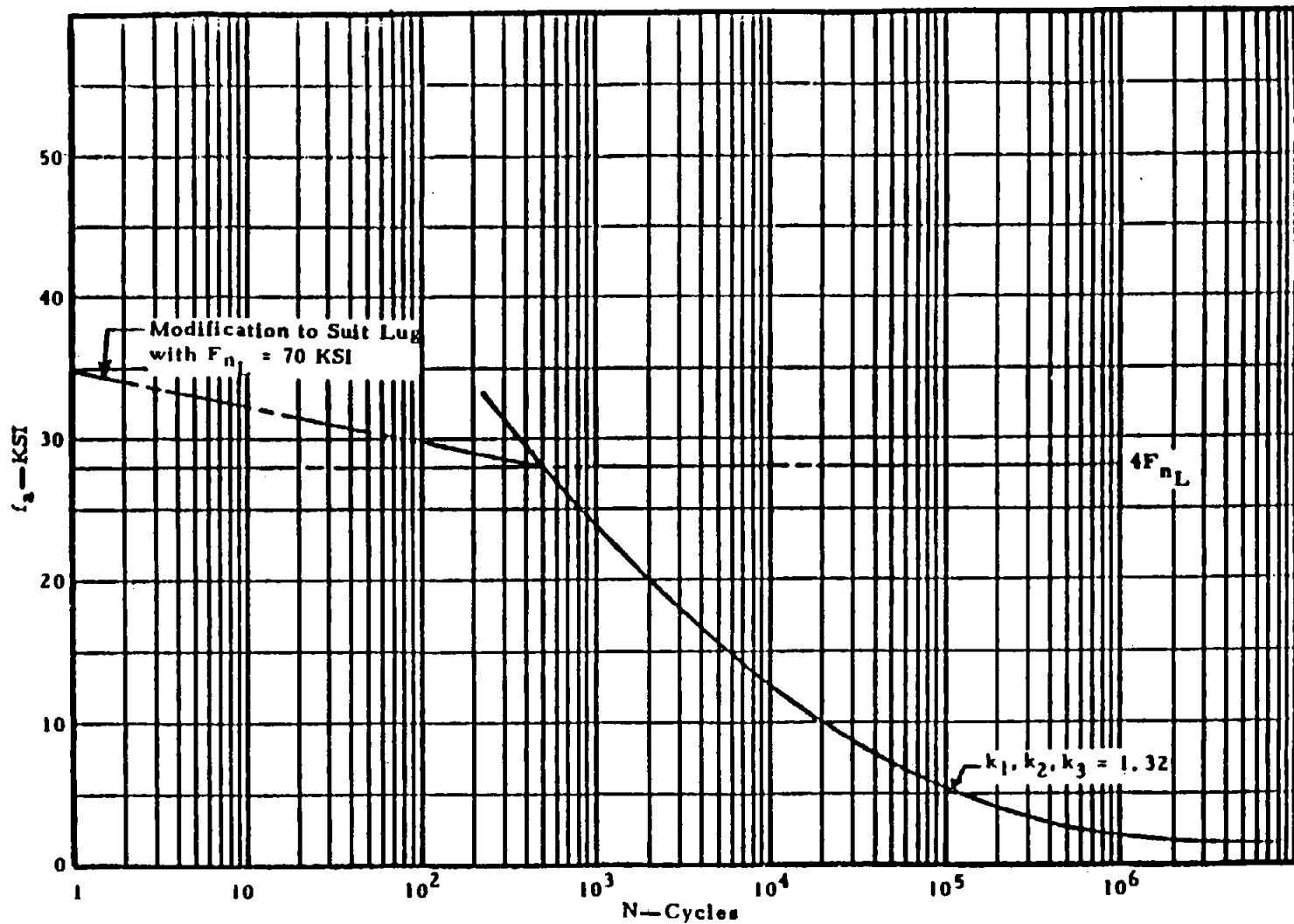


Figure 9-27. Modification to Curve $k_1, k_2, k_3 = 1.32$

STRUCTURAL ANALYSIS MANUAL
GENERAL DYNAMICS/CONVAIR AND SPACE SYSTEMS DIVISION

9.18 Example Problem of Lug Fatigue Analysis

Given a concentric 7075-T6 aluminum lug as shown in Figure 9-21, with the following dimensions: $a = 0.344$ in, $c = 0.3444$ in, and $D = 0.437$ in. If the lug is subjected to a cycle axial load such that the maximum net-section stress is 27,000 psi and the minimum net section stress is 18,470 psi, find the fatigue life.

From the lug dimensions,

$$a/c = 1.0 \quad c/D = 0.787 \quad (D/c = 1.27)$$

- (1) Figure 9-22 indicates that the lug may be analyzed using this method. From Figure 9-23,

$$k_1 = 1.0; k_2 = 1.33; k_3 = 0.99; k_1 k_2 k_3 = 1.32$$

- (2) Calculate the allowable net-section tensile ultimate stress, F_{su} , for Equation (9-4) in Section 9.3.2. For the given lug, $F_{su} = 70,000$ psi.

(3) $0.4 F_{su} = 0.4 \times 70,000 = 28,000$ psi.

- (4) Draw a light pencil line on Figure 9-24 from the point ($f_u = 28,000$ psi on $k_1 k_2 k_3 = 1.32$) to the point ($f_u = 35,000$, $N = 1$ cycle) (This is illustrated, for clarity, on Figure 9-27).

- (5) Enter Figure 9-24 and read values of f_u for various numbers of life cycles, using the line $k_1 k_2 k_3 = 1.32$. These numbers are as follows:

N	10^2	10^3	3×10^3	10^4	3×10^4	10^5	10^6	10^7
f_u	30KSI	24.5	18.8	13.5	8.88	5.70	2.34	1.30

- (6) Plot the values of f_u along the $R = 0$ line of the Goodman diagram. (Refer to Figure 9-26.)
- (7) Plot $F_{su} = 70,000$ psi, as f_u at the point ($f_u, 0$) of the Goodman diagram. (Refer to Figure 9-26.)
- (8) Connect the points plotted in Step 6 with the point plotted in Step 7 by straight lines. The Goodman diagram is now complete.

STRUCTURAL ANALYSIS MANUAL
GENERAL DYNAMICS/CONVAIR AND SPACE SYSTEMS DIVISION

- (9) Enter the Goodman diagram with values of $f_a = \frac{27,700 - 18,470}{2} = 4,615$ psi and $f_m = \frac{27,700 + 18,470}{2} = 23,085$ psi, and read the fatigue life, $N = 8 \times 10^4$ cycles, by interpolation (test results show $N = 8.6 \times 10^4$ cycles).

If the known quantities are life and R value, e. g., $N = 10^4$ cycles and $R = 0$, the allowable stresses can be obtained by using the same Goodman diagram. Enter the completed Goodman diagram at $R = 0$ and $N = 10^4$ cycles and read the amplitude and mean stresses (in this case $f_a = f_m = 13,500$ psi).

Only if the lug dimensions are changed, must a new Goodman diagram be drawn.

STRUCTURAL ANALYSIS MANUAL
GENERAL DYNAMICS/CONVAIR AND SPACE SYSTEMS DIVISION

Data Source, Section 1.3 Reference 2

LUGS

A Method of checking lugs is presented on page 4-8 of ANC-5 (Dec. 1942 Revision). This method may also be applied to holes in sheet and other structural parts.

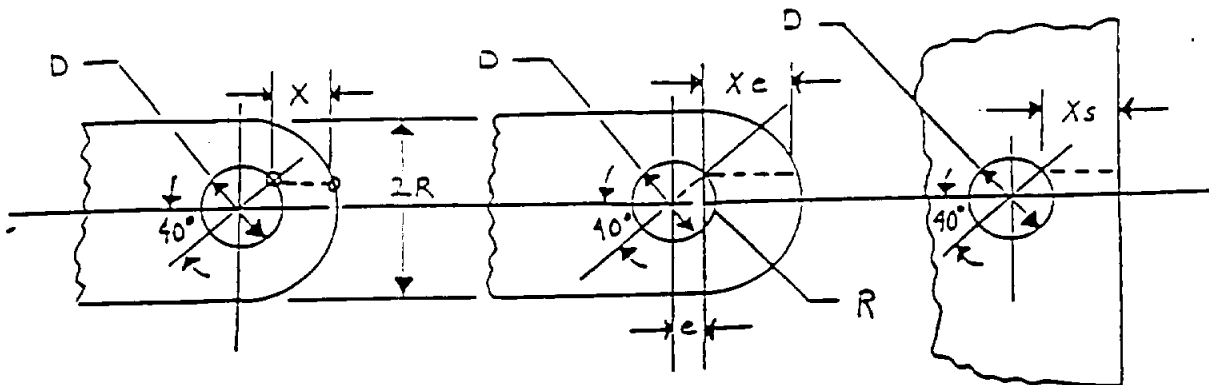


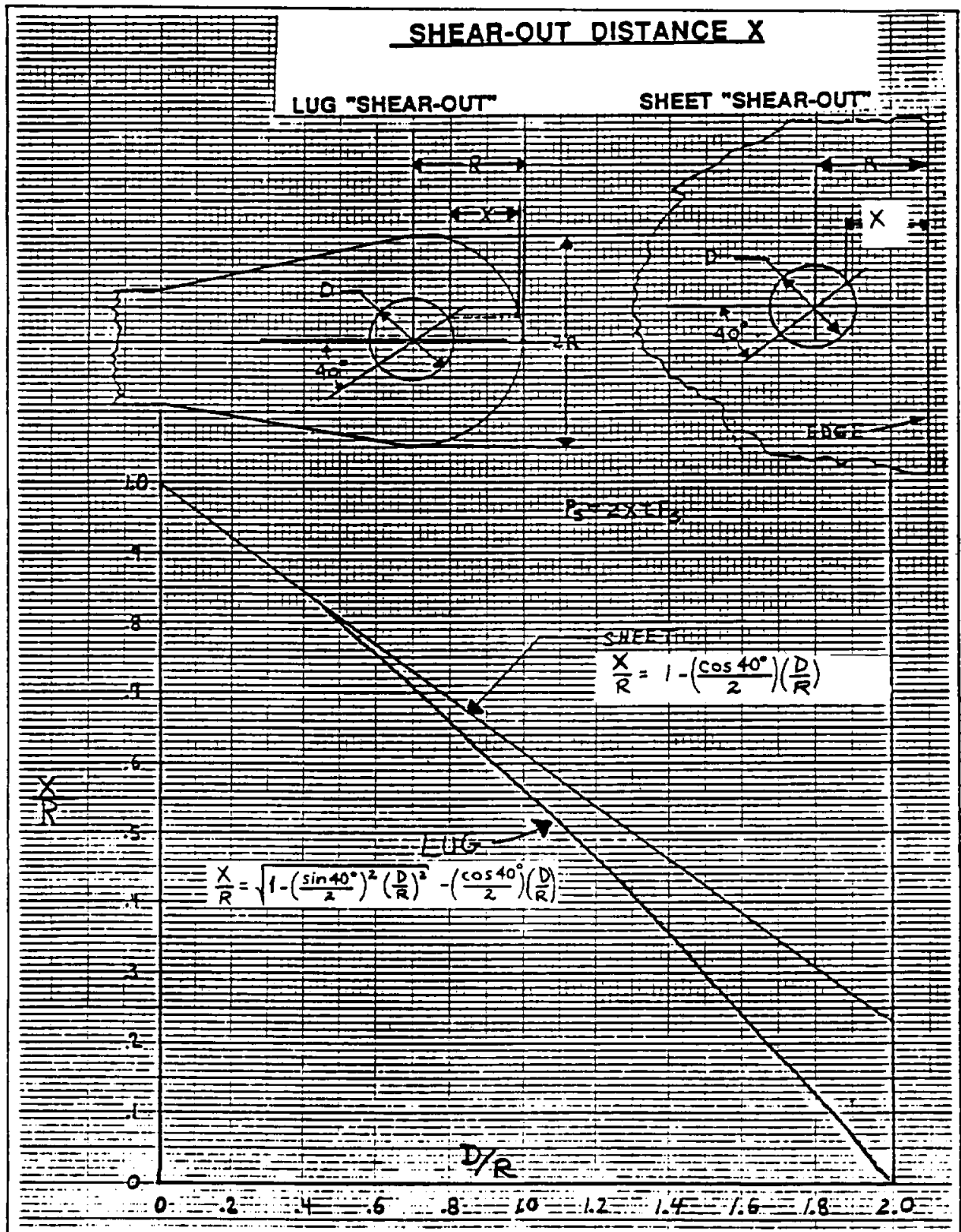
FIGURE 8-b

FIGURE 8-c

FIGURE 8-d

Use the ANC-5 method mentioned above for cases simulating Figures 8-b, 8-c and 8d using X , X_e and X_s in the Allowable shear strength formula ($P_s = 2XtF_s$)

STRUCTURAL ANALYSIS MANUAL
GENERAL DYNAMICS/CONVAIR AND SPACE SYSTEMS DIVISION



STRUCTURAL ANALYSIS MANUAL

GENERAL DYNAMICS/CONVAIR AND SPACE SYSTEMS DIVISION

Data Source, Section 1.3 Reference 24

KNUCKLE OR CLEVIS TYPE JOINTS - ROD ENDS

- a = Inner diameter of bushing, in.
- b = Outer diameter of bushing, in.
- d = Variable diameter pertaining to lug, in.
- D_1 = Inner diameter of lug, in.
- D_o = Outer diameter of lug, in.
- $D = d/D_1$
- D_n = Elastic-plastic boundary diameter, in.
- E_1 = Young's modulus of elasticity of lug material, ksi
- E_2 = Young's modulus of elasticity of bushing material, ksi
- e = Edge distance from center of hole, in.
- f_t = Tangential or hoop stress in lug, ksi
- F_{ty} = Allowable yield shear stress of lug material, ksi
- F_{ty} = Allowable yield stress in tension of lug material, ksi
- m = D_{ty}/D_1 Diameter ratio
- n = D_o/D_1 Diameter ratio
- P = Lug-bushing inter-surface pressure, ksi
- a = Strain-hardening parameter
- δ = Force-fit interference in terms of diameter
- γ = Poisson's ratio (0.3)

Subscripts

- i = Inner notation
- o = Outer notation
- sy = Shear yield
- t = Tangential
- ty = Tensile yield
- n = Arbitrary boundary notation
- 1 = Pertaining to lug
- 2 = Pertaining to bushing

13-4.8 References

1. Anon: *Structures Manual*, NASA. (Section 82.)
2. Melcok, M. A. and Hoblit, F. N.: *Developments in the Analysis of Method for Determining the Strength of Lugs Loaded Obliquely or Transversely*, Product Engineering, June 1963
3. Cozzone, F. P., Melcok, M. A., and Hoblit, F. N.: *Analysis of Lugs and Shear Pins Made of Aluminum or Steel Alloys*, Product Engineering, May 1960
4. Anon: *Metallic Materials and Elements for Aerospace Vehicle Structures*, MIL-HDBK-5A, Department of Defense, 8 February 1968
5. Anon: *Analysis of Lugs and Shear Pins and Comparison to Tests*, DACO Report S. M. 22913, 12 September, 1967
6. Anon: McDonnell Aircraft Corp. Report 339.

13-8 KNUCKLE OR CLEVIS TYPE JOINTS - ROD ENDS

13-8.1 General

Knuckle joints are used in aerospace vehicles to connect control rods. They can be readily disconnected for adjustments or repairs. The ends of each of the rods are formed by upsetting the rod and machining to form an eye on one end and a clevis (fork or yoke) on the other (Figure 13-83).

Each fork of the clevis and the eye are forms of lugs and are analyzed by the methods discussed in paragraph 13-4 except as discussed in following paragraphs.

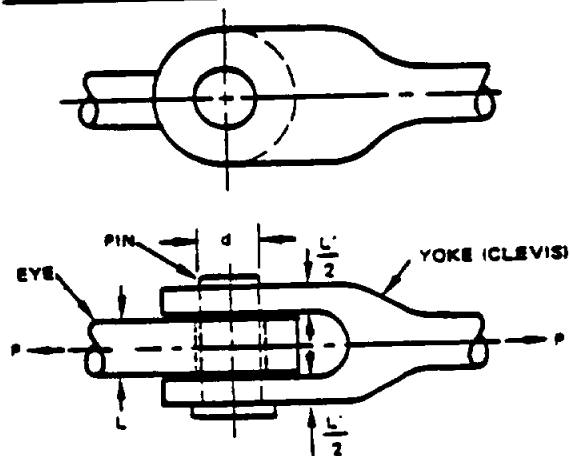


Figure 13-83. Knuckle Joint

Necked Lugs — Rod Ends

13-5.2 Necked Lugs — Rod Ends

Sharply necked rod ends differ from lugs previously discussed. The rim material between the pin and outer surface is usually thinner and more susceptible to in-plane bending (Figure 13-94). (Reference 3)

Sharply necked rod ends, such as shown in Figure 13-95 (A) should also be checked for bending at the juncture of the shank and rim; this juncture is designated section 3 by the following procedure. All angles are in degrees.

- a. Compute I and A for section 1, Figure 13-95A
- b. Compute $L = \pi r [(90 + \beta)/180^\circ]$
- c. Compute $K = (LI)/(Ar^3)$
- d. Enter graph (Figure 13-96) with K and β , then find α and γ where:
 $\gamma = \beta - \alpha$

- e. Compute pure hoop tension at section 2, (B), Figure 13-95.

from:

$$T_2 = P/(2 \cos \alpha)$$

- f. Compute loads at section 3, (B) Figure 13-95.

from:

$$T_3 = T_2 \cos \gamma$$

$$S_3 = T_2 \sin \gamma$$

$$M_3 = T_2 r (1 - \cos \gamma)$$

This procedure has been derived theoretically, assuming a rigid pin and assuming that the increase in length around the rim is given by a tension load T_2 acting upon a member of length L . Within the elastic range, this procedure gives results in close agreement with tests; for example, in checking stresses resulting from fatigue loading against fatigue allowable.

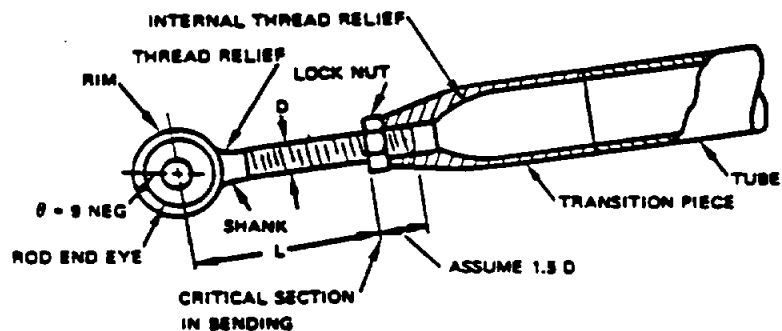


Figure 13-94. Rod End with Anti-Friction Bearing

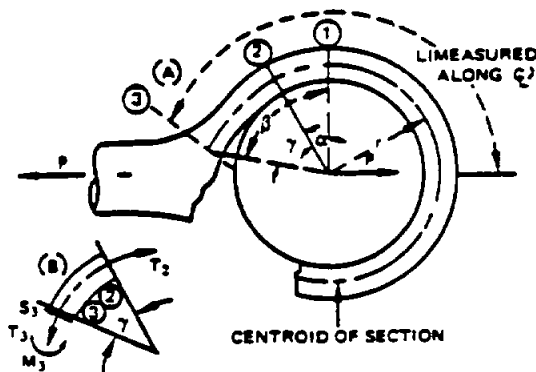


Figure 13-95. Loads in Necked Rod End

STRUCTURAL ANALYSIS MANUAL
GENERAL DYNAMICS/CONVAIR AND SPACE SYSTEMS DIVISION

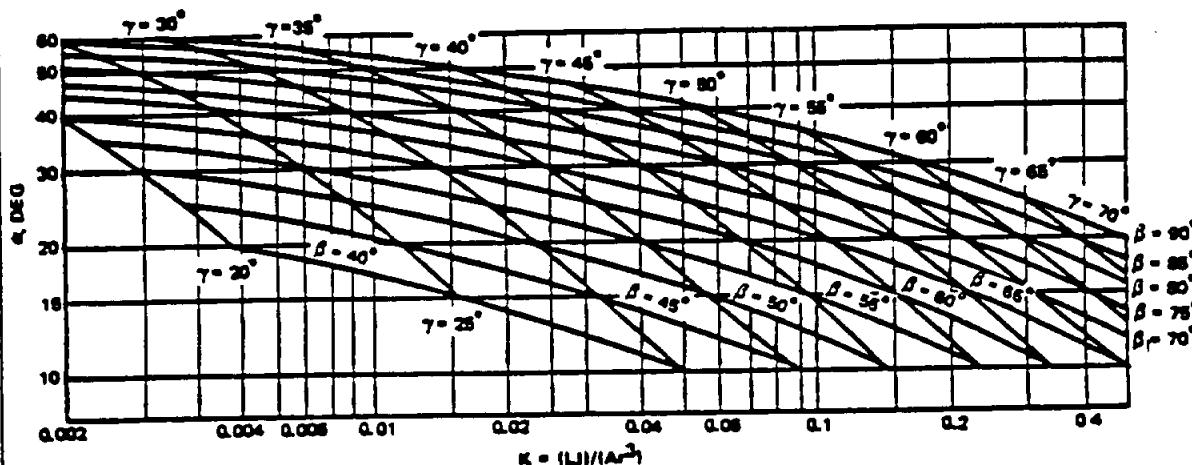


Figure 13-86. Values of α and γ

At ultimate load, this procedure can still be used, but will be conservative, where:

$$R_b = [M_2 / (I/y)_2] / F_{bu}$$

$$R_t = (T_2 / A_2) / F_{tu}$$

$$R_s = (S_2 / A_2) / F_{su}$$

This procedure should be used in conjunction with the following interaction equation:

$$(R_b + R_t)^2 + R_s^2 = 1$$

whence:

$$MS = \frac{1}{\sqrt{(R_b + R_t)^2 + R_s^2}} - 1$$

In addition to an analysis at section 3, if the minimum section of the ring is less than the area of section 3, the minimum section should be checked for pure hoop tension stress with the applied hoop tension load taken equal to T_2 as obtained from step e in the foregoing procedure.

13-8.3 References

1. *Pin Joint Design*, M. Korkut, Machine Design, 28 Sept. 1961.
2. *Effective Design of Knuckle Joints*, S. Warren Kays, Design News, 11 May 1959.
3. *Structural Analysis of Control Rods*, F. M. Hoblit, Lockheed Aircraft Co., Product Engineering, Oct. 1952.

STRUCTURAL ANALYSIS MANUAL
GENERAL DYNAMICS/CONVAIR AND SPACE SYSTEMS DIVISION

Data Source, Section 1.3 Reference 2

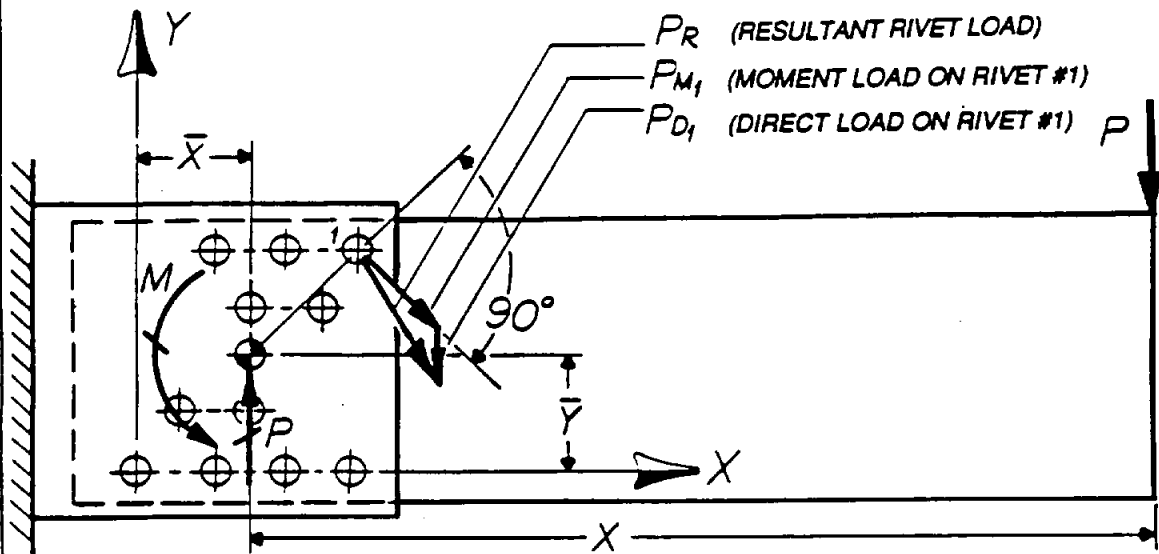
Data Source, Section 1.3 Reference 2

JOINTS

When bolted or riveted joints are loaded as indicated in figure 8A, the patterns may be analyzed as indicated in the following two cases:

FIGURE 8A

⊙ is the center-of-gravity (C.G.) of the rivet pattern.



Case #1: Where rivets are of the same size and critical in either bearing or shear:

$$P_{m_1} = \text{moment load on rivet \#1}$$

$$= (M \times d_1) / \sum d^2$$

Where: M = the moment of external loads about the C.G. of the rivet pattern = PX
 d = distance of rivet from C.G. of the rivet pattern

STRUCTURAL ANALYSIS MANUAL
GENERAL DYNAMICS/CONVAIR AND SPACE SYSTEMS DIVISION

The center of gravity of the rivet pattern is determined by inspection for a simple rivet pattern. Where the pattern is too complex to determine the C. G. by inspection, the C. G. location may be determined by summing up moments about reference axes:

$$\bar{x} = \frac{\sum x}{n}$$

$$\bar{y} = \frac{\sum y}{n}$$

Where X & Y = the distance of the rivet from the reference axes

n = number of rivets in the pattern

The direct rivet load for this case is determined by dividing the load "P" by the number of rivets in the pattern

$$P_d = \frac{P}{n}$$

P_d has the same direction as P

P_R = the resultant rivet load and is equal to the vector sum of $P_m + P_d$ obtained as indicated for rivet #1 in Figure 8A

119

STRUCTURAL ANALYSIS MANUAL
GENERAL DYNAMICS/CONVAIR AND SPACE SYSTEMS DIVISION

Data Source, Section 1.3 Reference **6**

SUBJECT: Beam in a Socket

1. Depending upon the fit of the beam in the socket and the relative rigidity of the beam and the socket, several cases of bearing load distribution arise as illustrated in the figures below.

**EQUAL FLEXIBILITY
CLOSE FIT**

**RELATIVELY RIGID SUPPORT
CLOSE FIT**

**POSITIVE CLEARANCE
PRACTICAL FIT**

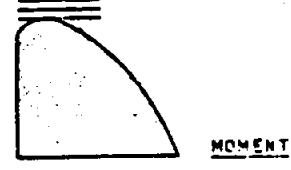
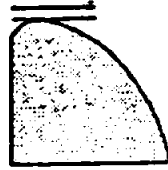
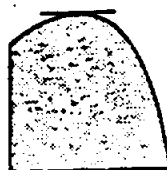
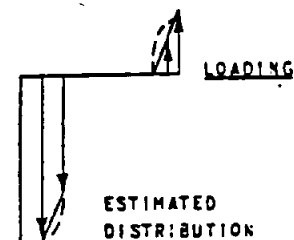
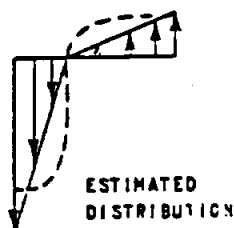
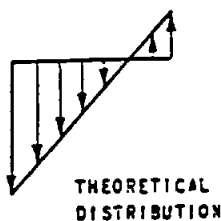
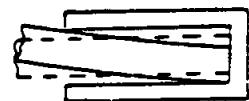
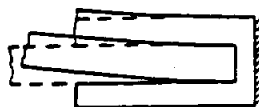
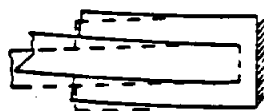


FIG. 1

FIG. 2

FIG. 3

STRUCTURAL ANALYSIS MANUAL
GENERAL DYNAMICS/CONVAIR AND SPACE SYSTEMS DIVISION

The maximum bearing load per inch corresponding to the load distribution of Fig. 1 and solved for graphically in Figs. 5 and 6 may be used for other conditions such as those shown in Fig. 2 and Fig. 3, since under the latter conditions the loading peaks are rounded off, as indicated by the dotted lines, due to local plastic deformations. Hence bearing loads conforming with the distribution of Fig. 1 should be used in practically every case.

The maximum moment obtained from the load distribution of Fig. 1 (see Figs. 5 and 6 at end of memo) tends to be conservative for the load distribution of Figs. 2 and 3 (Ref. 1). The maximum shear corresponding to the load distribution of Fig. 1 tends to be conservative for the distribution of Fig. 3 (Ref. 1).

STRUCTURAL ANALYSIS MANUAL
GENERAL DYNAMICS/CONVAIR AND SPACE SYSTEMS DIVISION

2. Raised bearing surfaces on pins, such as a piston in a shock strut, should be used in preference to a uniform cylindrical section for the following reasons:
- a. Ease of assembly.
 - b. The distribution of moment load is accurately known since it is taken out as a couple load on the bearing surfaces.

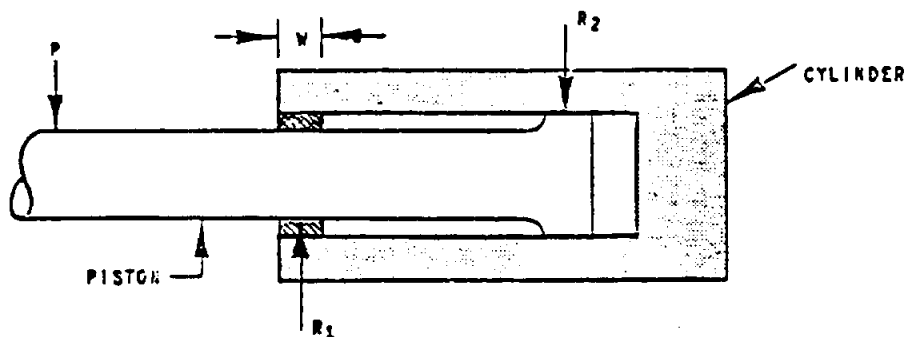


FIG. 4

The dimension " w " is determined by the packing requirements for cylinder leakage or bearing area.

STRUCTURAL ANALYSIS MANUAL
GENERAL DYNAMICS/CONVAIR AND SPACE SYSTEMS DIVISION

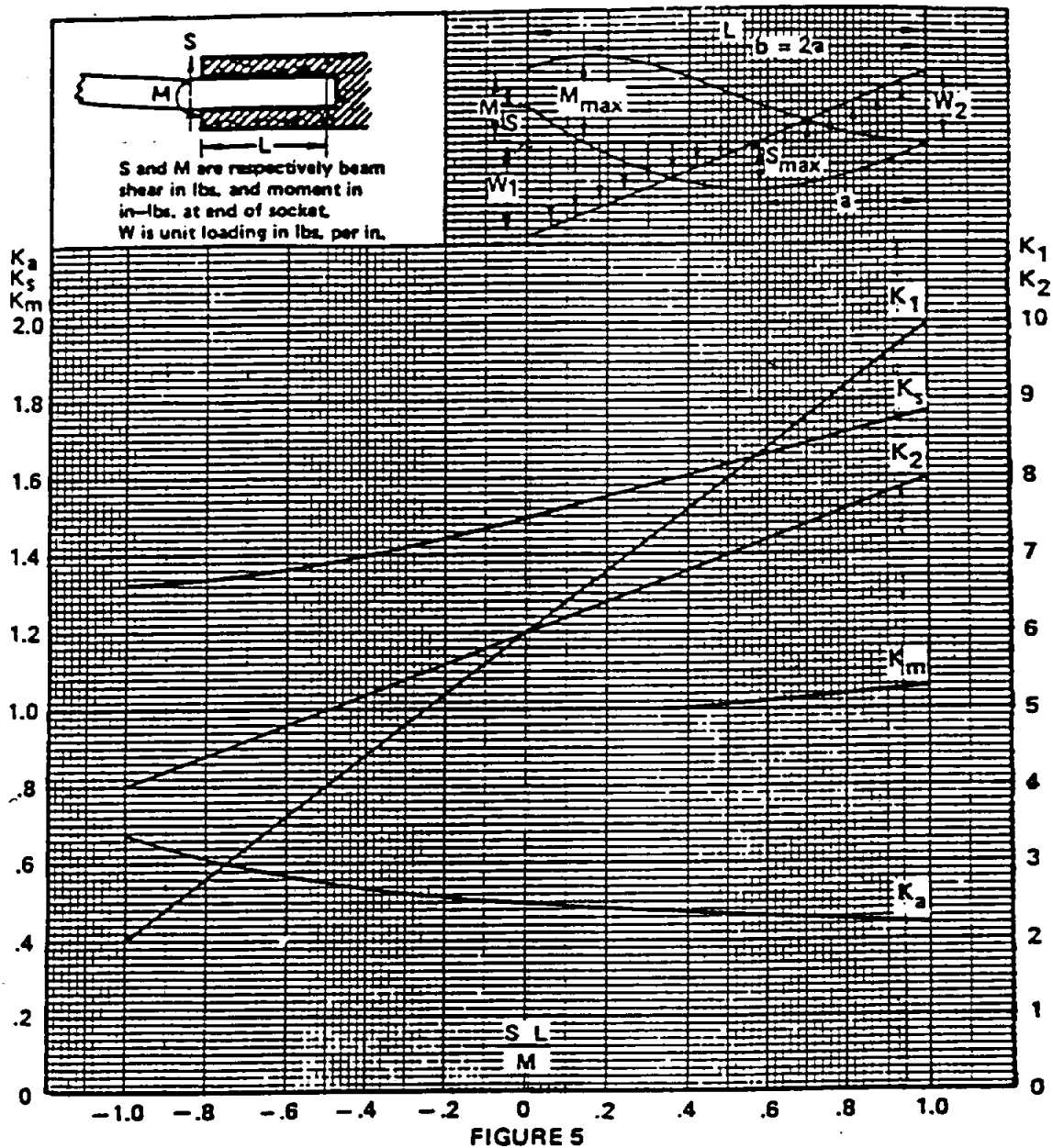


TABLE I. Use with Fig. 5 when $\left| \frac{SL}{M} \right| \leq 1$

To Obtain	w_1	w_2	a	S_{max}	M_{max}
Compute	$\frac{K_1 M}{L^2}$	$\frac{K_2 M}{L^2}$	$K_a L$	$-\frac{K_s M}{L}$	$K_m M$

THE VALUES OF S_{max} AND M_{max} GIVEN BY THE CURVES AND TABLES OF FIGS. 5 AND 6 ARE INTERNAL MAXIMA. THE EXTERNAL MAXIMA ARE M AND S. IF A K VALUE IS NOT SHOWN, THE CORRESPONDING INTERNAL MAXIMUM DOES NOT EXIST.

STRUCTURAL ANALYSIS MANUAL
GENERAL DYNAMICS/CONVAIR AND SPACE SYSTEMS DIVISION

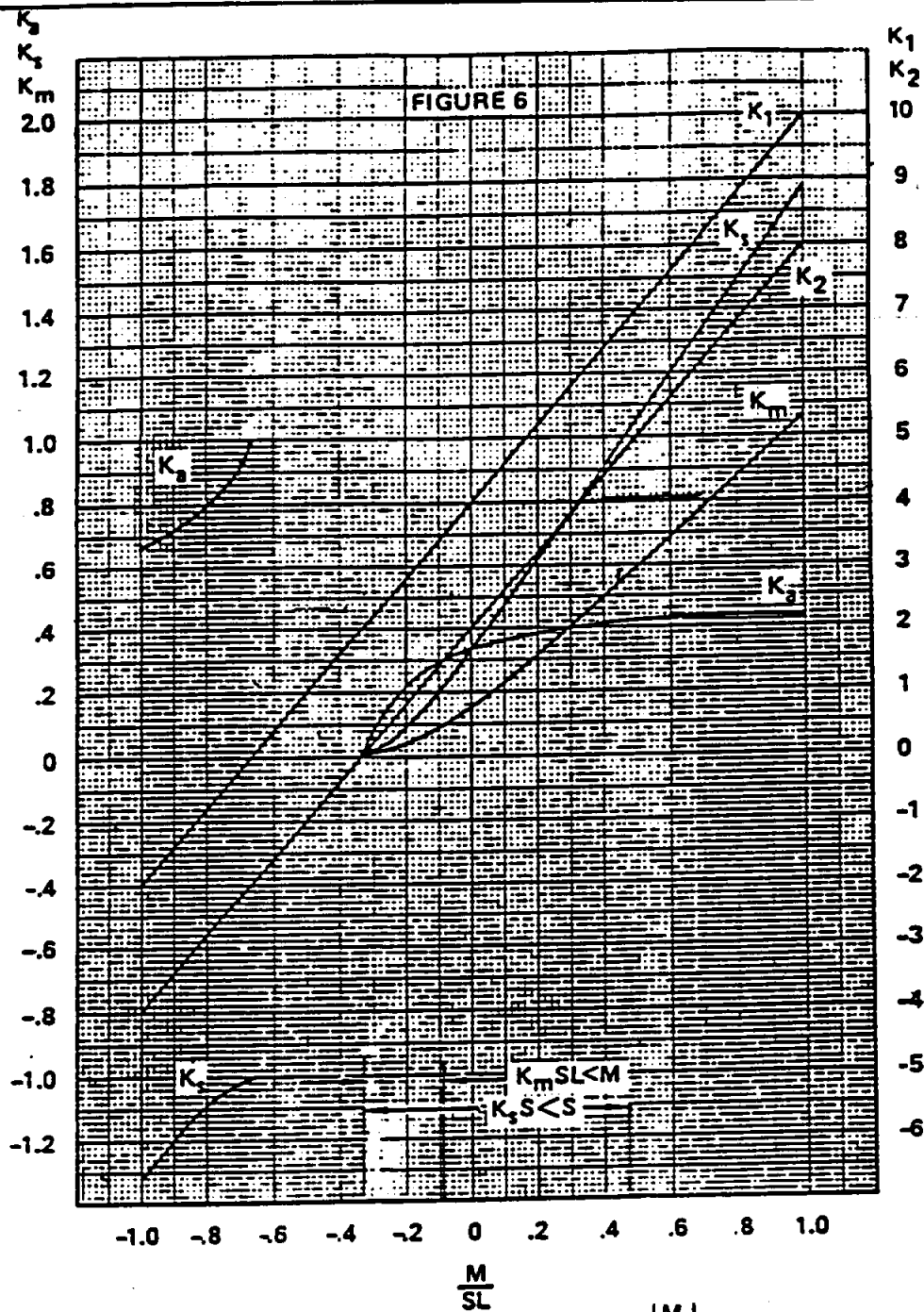


TABLE II. USE WITH FIG. 6 WHEN $\left| \frac{M}{SL} \right| \leq 1$

TO OBTAIN	w_1	w_2	a	S_{max}	M_{max}
COMPUTE	$\frac{K_1 S}{L}$	$\frac{K_2 S}{L}$	$K_s L$	$-K_s S$	$K_m SL$

STRUCTURAL ANALYSIS MANUAL
GENERAL DYNAMICS/CONVAIR AND SPACE SYSTEMS DIVISION

Data Source, Section 1.3 Reference 24

12.41 STRESSES DUE TO PRESS FIT BUSHINGS*

Pressure between a lug and bushing assembly having negative clearance can be determined from consideration of the radial displacements. After assembly, the increase in inner radius of the ring (lug) plus the decrease in outer radius of the bushing equals the difference between the radii of the bushing and ring before assembly.

$$\delta = u_{\text{ring}} - u_{\text{bushing}} \quad (1)$$

δ - Difference between outer radius of bushing and inner radius of the ring.
 u - Radial displacement, positive away from the axis of ring or bushing.
Radial displacement at the inner surface of a ring subjected to internal pressure p is

$$u = \frac{Dp}{E_{\text{ring}}} \left[\frac{C^2 + D^2}{C^2 - D^2} + \nu_{\text{ring}} \right] \quad (2)$$

Radial displacement at the outer surface of a bushing subjected to external pressure p is

$$u = - \frac{Bp}{E_{\text{bush.}}} \left[\frac{B^2 + A^2}{B^2 - A^2} - \nu_{\text{bush.}} \right] \quad (3)$$

A - Inner radius of bushing
 B - Outer radius of bushing
 C - Outer radius of ring (lug)

D - Inner radius of ring (lug)
 E - Modulus of elasticity
 ν - Poisson's ratio

Substitute equations (2) and (3) into equation (1) and solve for p ;

$$p = \frac{\delta}{\frac{D}{E_{\text{ring}}} \left(\frac{C^2 + D^2}{C^2 - D^2} + \nu_{\text{ring}} \right) + \frac{B}{E_{\text{bush.}}} \left(\frac{B^2 + A^2}{B^2 - A^2} - \nu_{\text{bush.}} \right)}$$

Maximum radial and tangential stresses for a ring subjected to internal pressure occur at the inner surface of the ring (lug).

$$f_r = -p \quad f_t = p \left[\frac{C^2 + D^2}{C^2 - D^2} \right]$$

Positive sign indicates tension. The maximum shear stress at this point is

$$f_s = \frac{f_t - f_r}{2}$$

Maximum radial stress for a bushing subjected to external pressure occurs at the outer surface of the bushing.

$$f_r = -p$$

Maximum tangential stress for a bushing subjected to external pressure occurs at the inner surface of the bushing.

$$f_t = - \frac{2pB^2}{B^2 - A^2}$$

* Timoshenko, Strength of Materials, Volume 2, 1941, Page 241.

STRUCTURAL ANALYSIS MANUAL
GENERAL DYNAMICS/CONVAIR AND SPACE SYSTEMS DIVISION

The allowable press fit stress may be based on:

- (1) Stress Corrosion. The maximum allowable press fit stress in magnesium alloys should not exceed 8000 psi. For all aluminum alloys the maximum press fit stress should not exceed $0.60 F_{ty}$.
- (2) Static Fatigue. Static fatigue is the brittle fracture of metals under sustained loading, and in steel may result from several different phenomena, the most familiar of which is hydrogen embrittlement. Steel parts heat treated above 200 ksi, which by nature of their function or other considerations are exposed to hydrogen embrittlement, should be designed to an allowable press fit stress of 25% F_{u} .
- (3) Ultimate Strength. Ultimate strength cannot be exceeded, but is not usually critical in a press fit application.
- (4) Fatigue Life. The hoop tension stresses resulting from the press fit of a bushing in a lug will reduce the stress range for oscillating loads, thereby improving fatigue life.

The presence of hard brittle coatings in holes that contain a press fit bushing or bearing can cause premature failure by cracking of the coating or by high press fit stresses caused by build-up of coating. Therefore, Hardcoat or HAE coatings should not be used in holes that will subsequently contain a press fit bushing or bearing.

Reference AFEDL-TR-65-42 AIR-FORCE MANUAL

STRUCTURAL ANALYSIS MANUAL
GENERAL DYNAMICS/CONVAIR AND SPACE SYSTEMS DIVISION

Data Source, Section 1.3 Reference 3

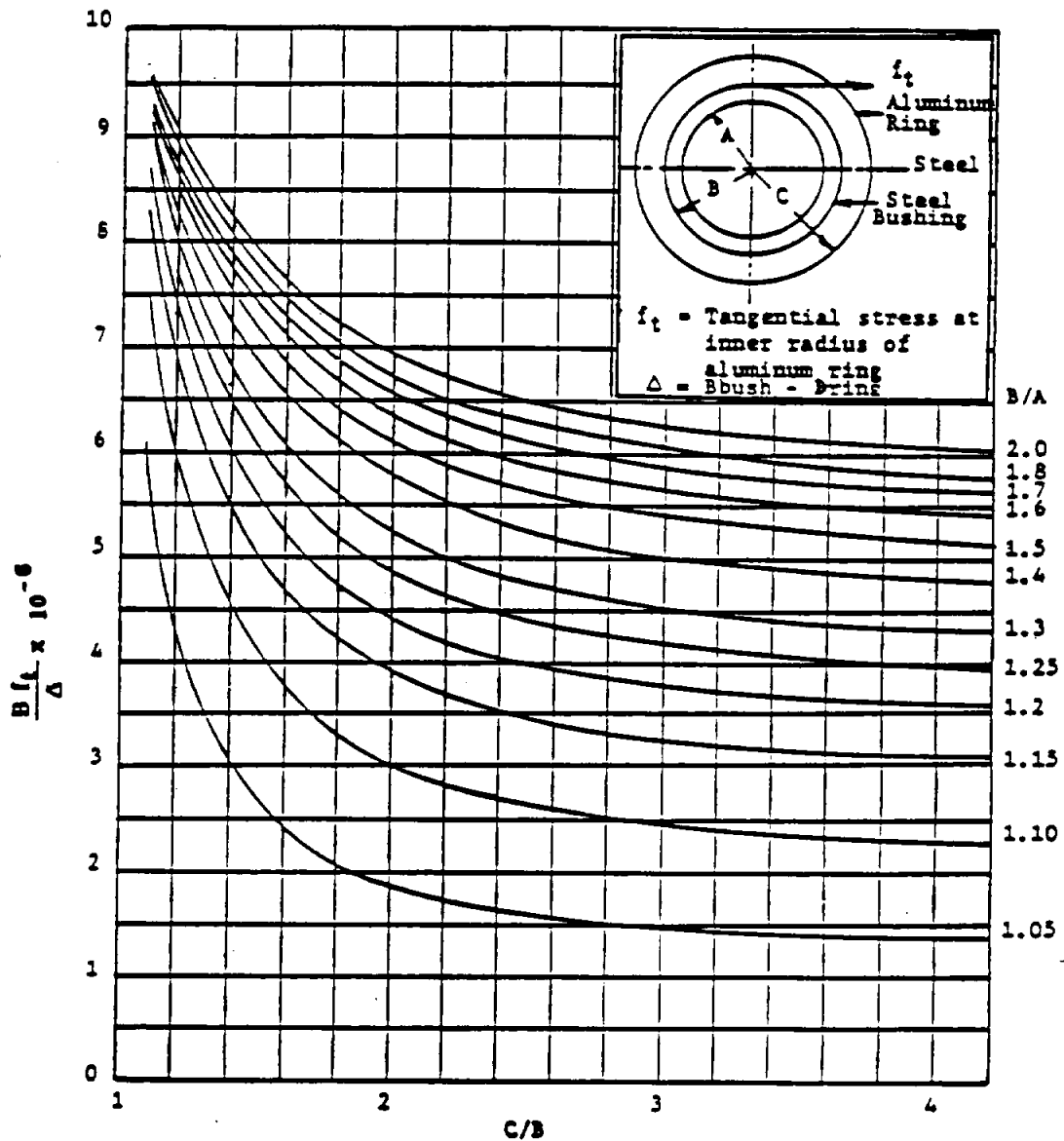


FIGURE 6.40 - TANGENTIAL STRESSES FOR PRESSED STEEL BUSHINGS IN ALUMINUM RINGS

STRUCTURAL ANALYSIS MANUAL
GENERAL DYNAMICS/CONVAIR AND SPACE SYSTEMS DIVISION

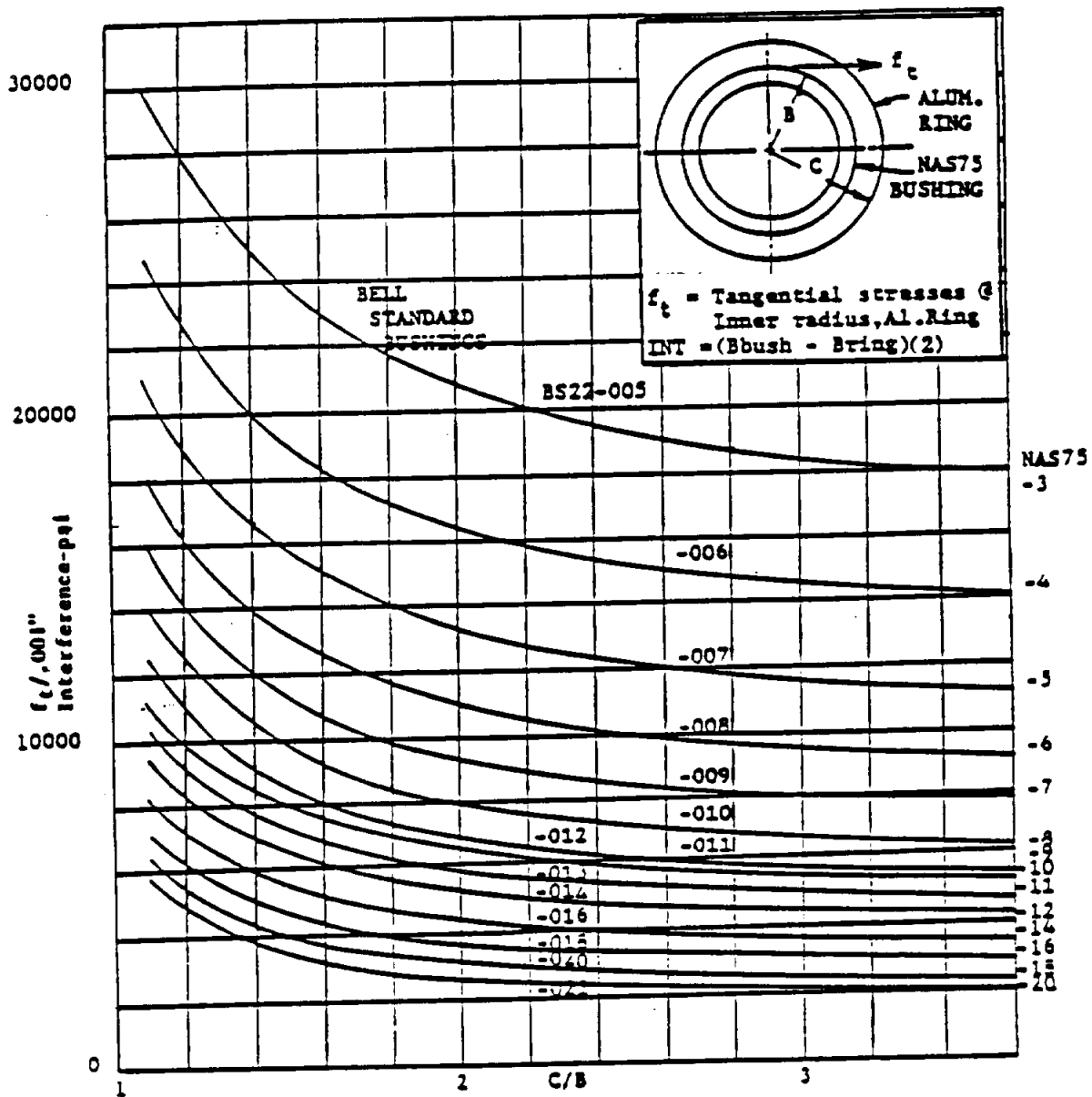


FIGURE 6.41 TANGENTIAL STRESSES FOR PRESSED NAS75 BUSHINGS

STRUCTURAL ANALYSIS MANUAL
GENERAL DYNAMICS/CONVAIR AND SPACE SYSTEMS DIVISION

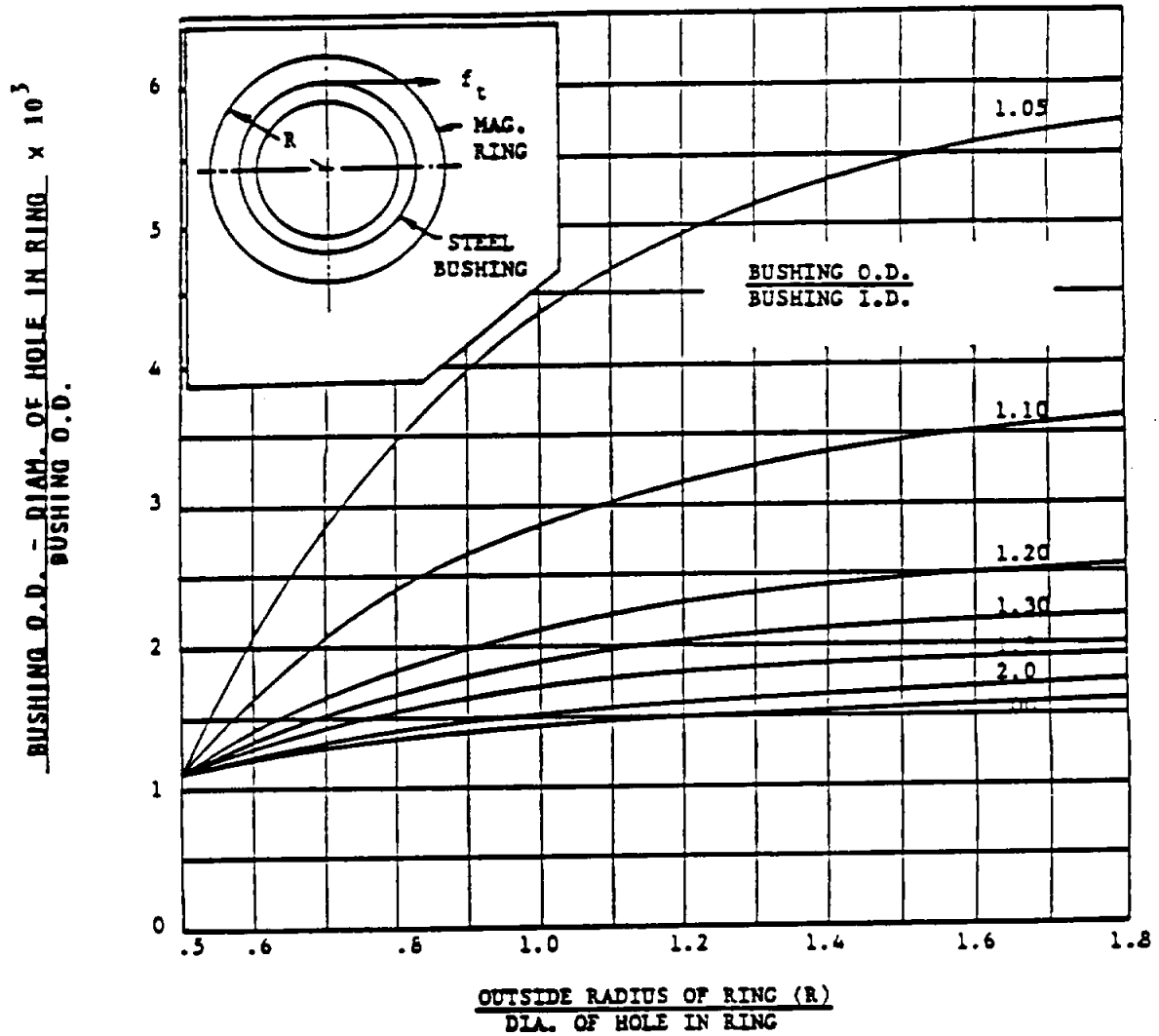


FIGURE 6.42 MAXIMUM INTERFERENCE FITS OF STEEL BUSHINGS IN MAGNESIUM ALLOY RINGS

STRUCTURAL ANALYSIS MANUAL
GENERAL DYNAMICS/CONVAIR AND SPACE SYSTEMS DIVISION

Data Source, Section 1.3 Reference **G**

SUBJECT: Flange Bending Strength of Angles

INTRODUCTION

When a tension load is applied normal to the outstanding leg of an angle, tension, bending, and shear stresses occur. If the outstanding leg is not rigidly supported, the allowable load is usually limited by considerations of permissible deflection and permanent set. If the attachment points through which the load is transmitted to the angle are not spaced sufficiently close, the full strength of the angle is not developed since local deformation at the attachment points becomes the limiting factor.

This Stress Memo presents design considerations and allowable loads for aluminum alloy extruded and formed sheet metal angles subjected to flange bending loads.

I. DESIGN CONSIDERATIONS

- A. In vital tension joints wherein part of the structure is continuous across the joint and a part discontinuous, angles loaded normal to the outstanding legs shall not be used to join the discontinuous members.
- B. Generous corner fillets on extruded angles and minimum bend radii on formed sheet metal angles shall be used in all cases where applied loads tend to "open" or "close" the angle.
- C. For maximum strength, the bolt or rivet head should be adjacent to the point of tangency of the fillet or bend radius.
- D. High local stresses and large deflections in angle joints prohibit their use in applications subject to repeated or alternating loads.

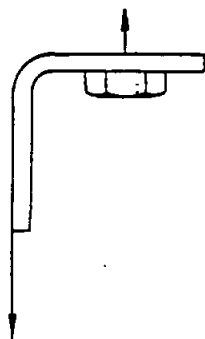
II. METHODS OF ATTACHMENT

Three (3) methods of attachment in their order of preference are illustrated below.

STRUCTURAL ANALYSIS MANUAL
GENERAL DYNAMICS/CONVAIR AND SPACE SYSTEMS DIVISION

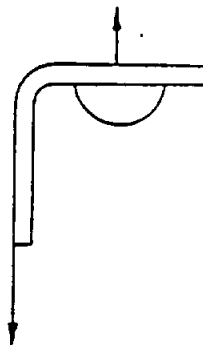
II. METHODS OF ATTACHMENT (Contd.)

A. Bolts



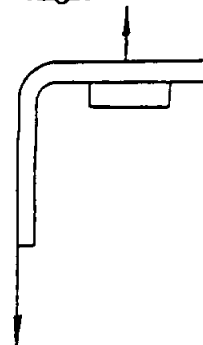
Preferable to "B" or "C"

B. Rivets - Manufactured Heads Inside Angle



Preferable to "C"

C. Rivets - Formed Heads Inside Angle



Least Preferable

III. ALLOWABLES

A. Single Angles

1. Figures 1 and 2 give the ultimate allowable loads for various gages of 2024-T3 alclad formed sheet metal and 2024-T4 extruded angles respectively.
2. Ultimate allowable loads for aluminum alloy angles other than 2024-T4 extrusion and 2024-T3 alclad formed sheet metal may be derived from the values obtained from Figures 1 and 2 by direct proportionality with the transverse yield strengths.

$$\text{i.e., } P_{(\text{allowable})} = \frac{P(\text{from figures}) \times F_{tyT}}{K}$$

where:

K = 42,000 for extruded angle
= 40,000 for formed sheet metal angle

B. Double Angles and Tees

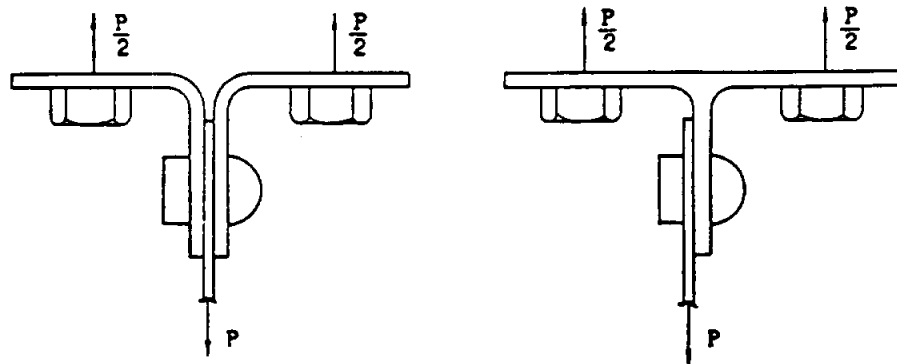
1. When two (2) angles are used back to back and loaded symmetrically in both outstanding flanges, the allowables obtained from Figures 1 and 2 may be multiplied by two and one-half (2.5).

STRUCTURAL ANALYSIS MANUAL
GENERAL DYNAMICS/CONVAIR AND SPACE SYSTEMS DIVISION

III. ALLOWABLES (Contd.)

B. Double Angles and Tees (Contd.)

2. When tees are loaded symmetrically in both outstanding flanges, the allowables obtained from Figure 2 may be multiplied by three (3).

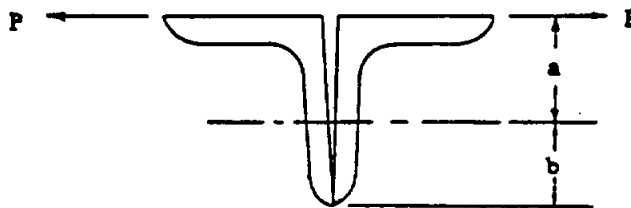


C. Loads on Connectors

When heavy angles are used as a tension joint, the tension load on the connector shall be calculated as follows:

$$\text{Load on Connector} = P \times \frac{a+b}{b}$$

If the mating surfaces undergo excessive separation, bending of the bolt may become a critical factor.

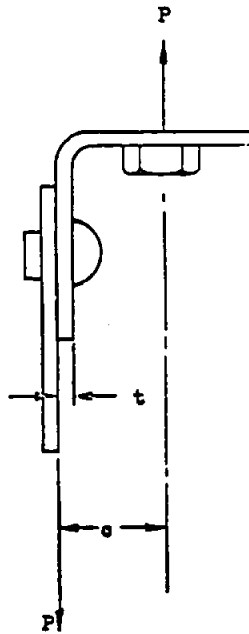


STRUCTURAL ANALYSIS MANUAL
GENERAL DYNAMICS/CONVAIR AND SPACE SYSTEMS DIVISION

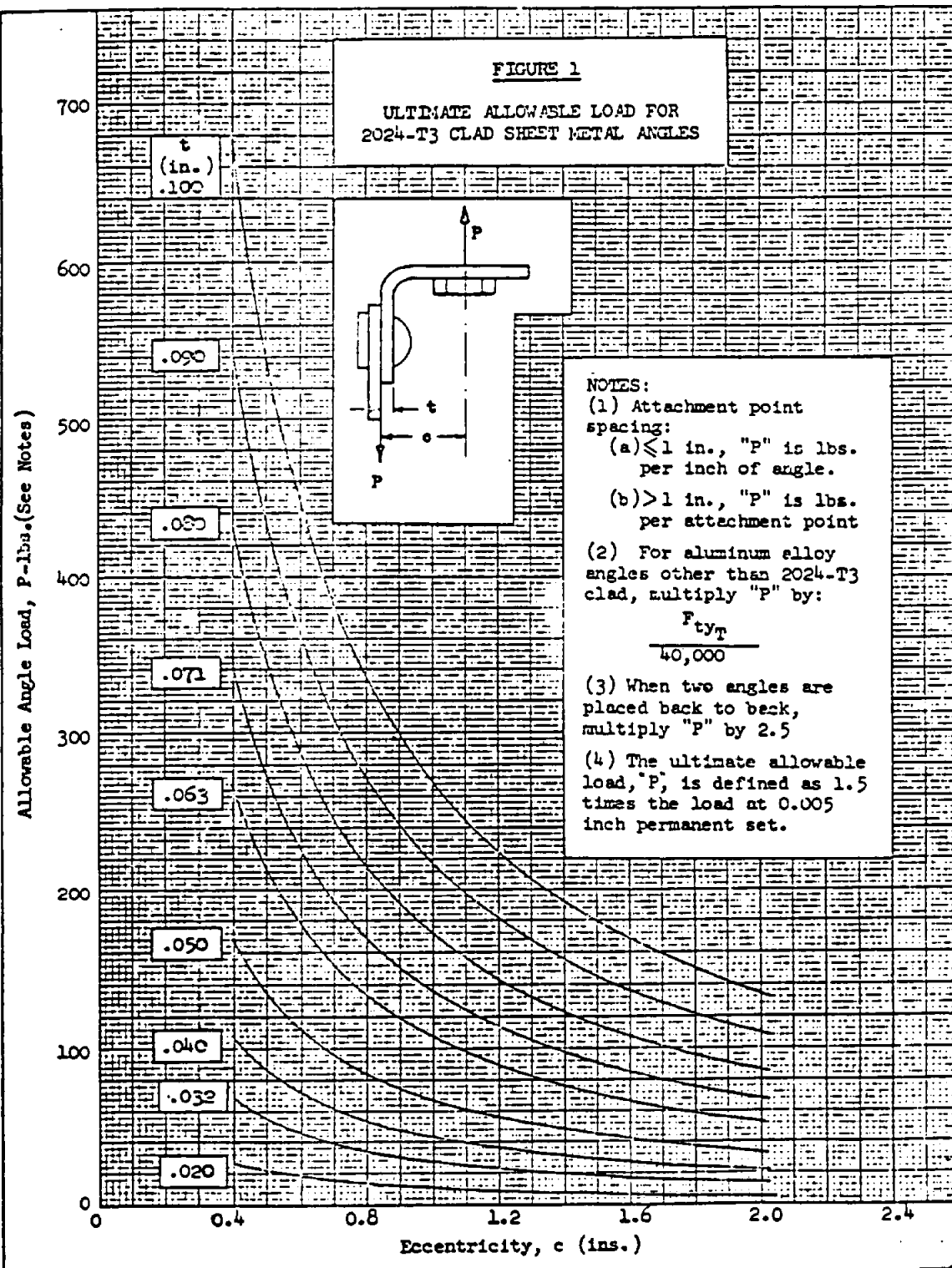
V. DEFLECTION

The following formula will yield conservative values of deflection at the connectors:

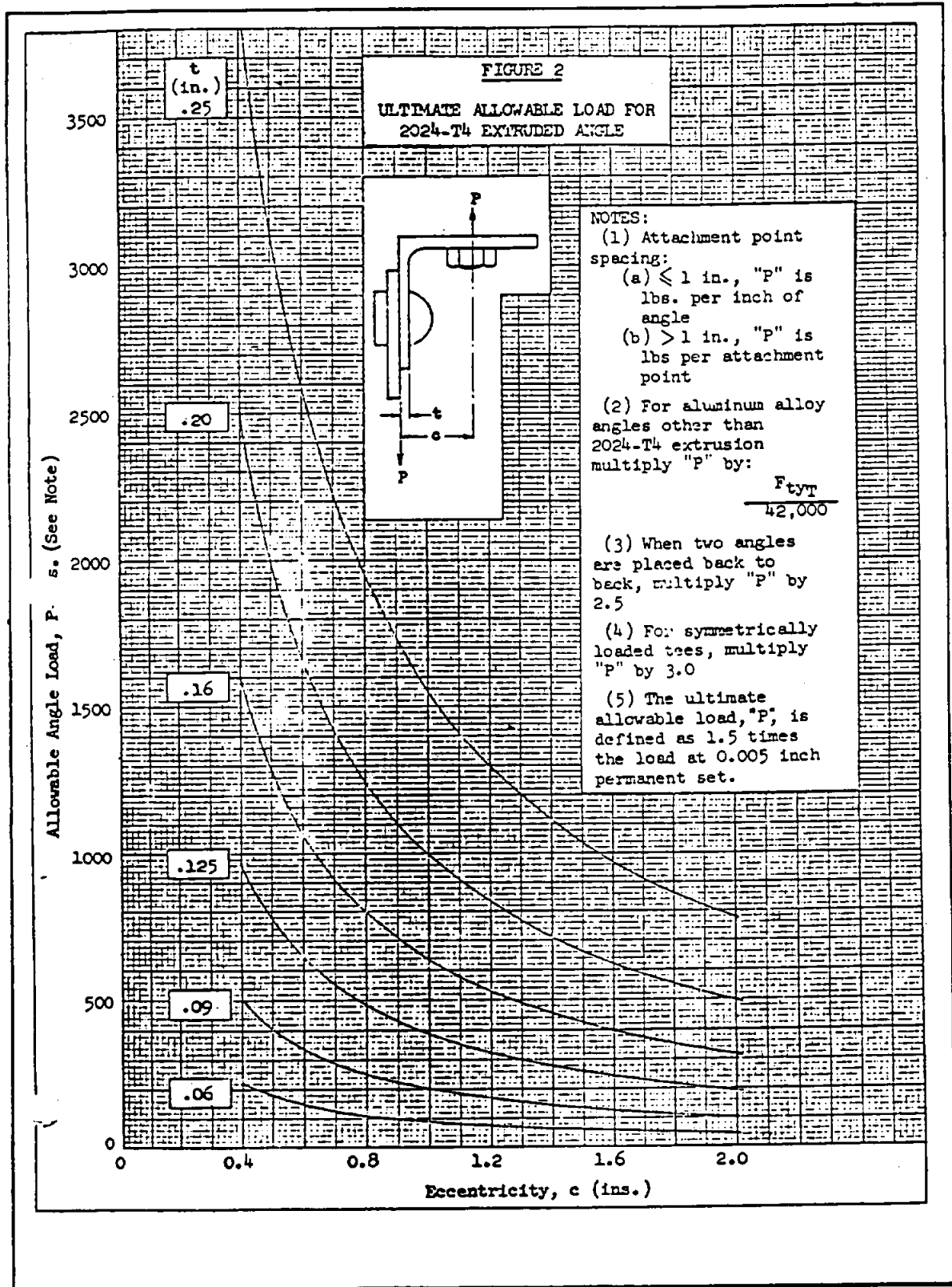
$$\delta = \frac{4 P c^3}{E t^3}$$



STRUCTURAL ANALYSIS MANUAL
GENERAL DYNAMICS/CONVAIR AND SPACE SYSTEMS DIVISION



STRUCTURAL ANALYSIS MANUAL
GENERAL DYNAMICS/CONVAIR AND SPACE SYSTEMS DIVISION



D1.8 - THREADED FASTENERS

D1.83.02

D1.83.02 - STEEL BOLT STRENGTH DATA - SINGLE SHEAR, TENSION & BENDING MOMENT ALLOWABLES (Lb.)

		BOLT NUMBER	3	4	5	6	7	8	9	10	12	14	16	18	20	22	24
		FULL DIAMETER	.1900	.2500	.3125	.3750	.4375	.5000	.5625	.6250	.7500	.8750	1.000	1.1250	1.250	1.3750	1.5000
		ROOT DIAMETER (FINE THREAD)	.1494	.2036	.2584	.3209	.3725	.4375	.4903	.5528	.6688	.7822	.9072	1.0167	1.1417	1.2667	1.3917
125 HT	125,000 HT ATTACHMENTS	FULL DIA. SHEAR	2,126	3,682	5,750	8,290	11,270	14,730	18,640	23,010	33,130	45,100	58,900	74,600	92,000	111,400	132,500
	EXAMPLE: AN 3-70, 23-36	FULL DIA. B.M.	130	314	614	1,061	1,684	2,516	3,581	4,914	8,490	13,485	20,123	28,655	39,308	—	—
	502, 509; NAS 221-227	ROOT DIA. TENSION (2)	2,254	4,170	6,710	10,300	13,890	18,908	23,990	30,440	44,500	60,900	79,100	102,700	129,300	159,000	191,800
160 HT	ALL 160,000 HT ATTACHMENTS	FULL DIA. SHEAR	2,694	4,660	7,290	10,490	14,200	18,650	23,610	29,150	42,000	57,100	74,600	94,400	116,600	141,100	167,900
	ALL 160,000 HT ATTACHMENTS	FULL DIA. B.M.	181	411	803	1,388	2,202	3,288	4,681	6,471	11,095	17,618	26,299	37,445	51,366	68,368	88,762
	ALL 160 HT ATTACHMENTS (1)	ROOT DIA. TENSION (3)	2,892	5,340	8,590	13,100	17,700	24,190	30,700	38,960	57,000	77,900	101,300	131,500	165,600	203,600	245,500
	ALL 160 HT ATTACHMENTS (1)	ROOT DIA. TENSION (2)	2,259	4,170	6,710	10,300	13,890	18,908	23,990	30,440	44,500	60,900	79,100	102,700	129,300	159,000	191,800
180 HT	180,000 HT ATTACHMENTS	FULL DIA. SHEAR	3,062	5,300	8,280	11,930	16,240	21,210	26,840	33,130	47,700	64,900	84,800	107,400	137,500	166,400	190,800
	EXTERNAL WRENCHING BOLTS	FULL DIA. B.M.	—	450	896	1,546	2,456	3,667	5,220	7,160	12,373	19,647	29,320	41,757	57,281	76,241	98,984
	(NAS 624-644)	ROOT DIA. TENSION (3)	—	6,810	9,660	14,830	20,810	27,210	34,540	43,800	64,100	87,700	114,000	147,900	186,200	229,000	276,200

NOTES: (1) Example: MS 70004 - MS 70024; NAS 333-340, 503-590, 1103-1120, 1203-1207, 1303-1320, 1403-1406, 1503-1510, 664.

(2) Reduce tension allowables to 25% of tabulated values when using AN 320 or NAS 1022 ALUMINUM shear nuts.

Reduce tension allowables to 50% of tabulated values when using AN 320 or NAS 1022 STEEL shear nuts or other ALUMINUM nuts where nominal diameter > 1/2".

(3) Tension values apply when using H-20, 82FW or NAS 577 nuts.

Reference: D-2

STRUCTURAL ANALYSIS MANUAL
GENERAL DYNAMICS/CONVAIR AND SPACE SYSTEMS DIVISION

Data Source, Section 1.3 Reference 6

SUBJECT: TENSION TYPE FITTINGS

INTRODUCTION

This memo contains methods of analysis applicable to certain common types of tension fittings. The methods have a rational basis and give loads agreeing well with available test data.

GENERAL

Pertinent fitting and casting factors shall always be used in the analysis. If in any application both a fitting and a casting factor are applicable, they shall not be multiplied, but only the larger shall be used.

In addition to the factors above, the analysis shall show a minimum margin of safety of 0.20. This shall be demonstrated for both yield and ultimate strength. This requirement may be relaxed upon the approval of the Project Structures Engineer.

Bolts highly loaded in tension should be assembled with a washer under both the head and nut.

Eccentricities in fitting attachment should be kept to a minimum. Unavoidable eccentricities shall be considered in the analysis.

Fitting attachment edge distances shall conform to design handbook requirements to prevent premature tension failures in the fitting wall.

The methods of analysis of tension fittings in this memo are shown on an ultimate basis. For yield analysis, the same procedure is followed except that yield loads, moments and multiplying factors are substituted for the ultimate values wherever necessary.

STRUCTURAL ANALYSIS MANUAL
GENERAL DYNAMICS/CONVAIR AND SPACE SYSTEMS DIVISION

I. Bathtub Fitting

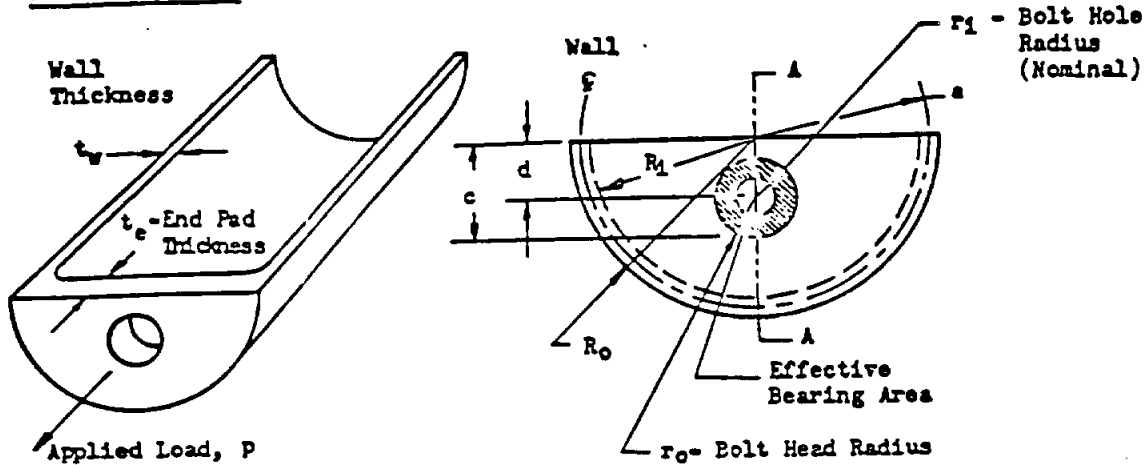


Fig. 1

A. Wall Analysis

1. Tension in Wall

- a. Determine the maximum tension stress, f_{tu_w} , in the fitting wall due to the ultimate load, P_u , from

$$f_{tu_w} = \frac{P_u}{A_g}$$

where, A_g = gross area = $\frac{\pi}{2} (R_o^2 - R_i^2)$

- b. Obtain the basic tension efficiency, η , of the wall from Stress Memo No. 56, considering the wall as one sheet in a tension joint between sheets.

- c. Determine the wall tension stress ratio from

$$R_{tu_w} = \frac{j_{mu} f_{tu_w}}{\eta F_{tu}}$$

where j_{mu} is an additional (multiplying) factor of safety, if any; otherwise use $j_{mu} = 1$

2. Bending in Wall

- a. Compute the centroid and I about the centroidal axis for one-half of a hollow cylinder, respectively, by:

STRUCTURAL ANALYSIS MANUAL
GENERAL DYNAMICS/CONVAIR AND SPACE SYSTEMS DIVISION

I. Bathtub Fitting (Cont'd)

A. Wall Analysis (Cont'd)

2. Bending in Wall (Cont'd)

a. (Cont'd)

$$c = \frac{4}{3\pi} \frac{R_o^2 + R_o R_1 + R_1^2}{R_o + R_1}$$

$$I = .1098(R_o^4 - R_1^4) - \frac{.283(R_o^2 R_1^2)(R_o - R_1)}{R_o + R_1}$$

b. Determine the applied ultimate bending moment, M_u , from

$$M_u = P_u (c - d)$$

c. Obtain the allowable $\frac{M_u}{I}$ bending stress, F_{bu} , from S.M. 53, assuming $k = 1.70$ and calculate the allowable bending moment from

$$M_u = F_{bu} \frac{I}{c}$$

d. Determine the wall bending ratio from

$$R_{buw} = \frac{M_u j_{wu}}{M_u}$$

3. Interaction - Bending and Tension

Obtain the ultimate margin of safety using the interaction equation $R_b + R_t^n = 1$, assuming a solid round section for the determination of n . (See paragraphs VIII-D to VIII-G of S.M.53.)

B. End Pad Analysis

1. Bending

a. Compute: $\frac{R_1}{a}$, $\frac{a-d}{R_o}$, and $\frac{t_o}{t_w}$

b. Obtain K_1 from Fig. 6.

c. Obtain K_2 from Fig. 7.

d. Determine the bending stress, f_{bu} , on section A-A of Fig. 1 from

$$f_{bu} = \frac{P_u}{t_o} K_1 K_2$$

STRUCTURAL ANALYSIS MANUAL
GENERAL DYNAMICS/CONVAIR AND SPACE SYSTEMS DIVISION

I. Bathtub Fitting (Cont'd)

B. End Pad Analysis (Cont'd)

1. Bending (Cont'd)

e. Obtain the allowable $\frac{no}{I}$ bending stress, F_{bu} , assuming a rectangular section ($k = 1.5$), from SECT. 17.0

f. The margin of safety for bending on section A-A of Fig. 1 is given by

$$M.S._u = \frac{F_{bu}}{J_{mu} f_{buo}} - 1$$

2. Shear of End Pad

a. Determine shear stress, f_{su_o} , on end pad by

$$f_{su_o} = \frac{P_u}{2\pi r_o t_o}$$

b. Obtain allowable shear stress, F_{su} .

c. The margin of safety for shear is given by

$$M.S._u = \frac{F_{su}}{J_{mu} f_{su_o}} - 1$$

II. Channel Type Fittings

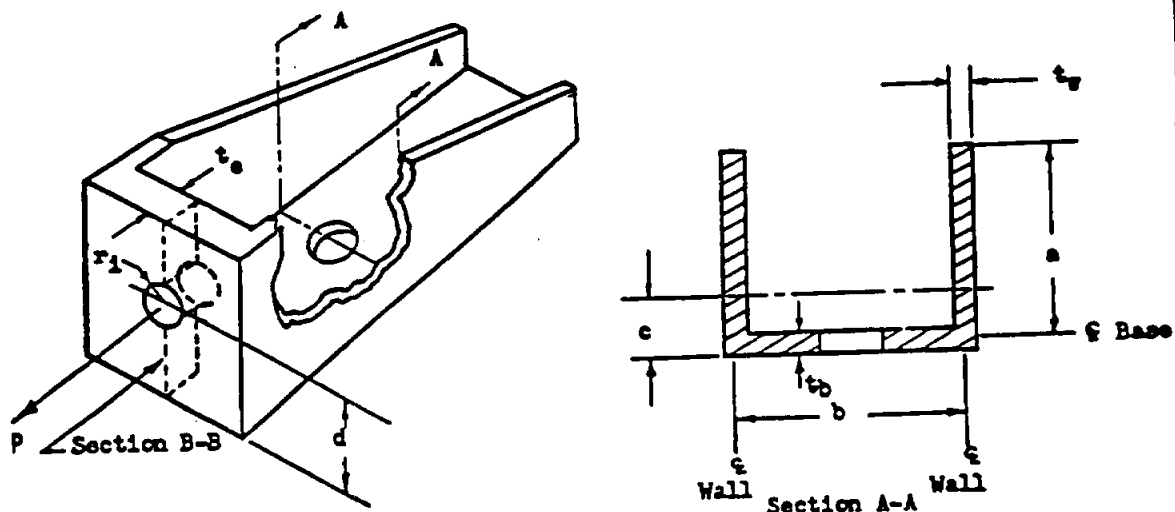


Fig. 2

STRUCTURAL ANALYSIS MANUAL
GENERAL DYNAMICS/CONVAIR AND SPACE SYSTEMS DIVISION

II. Channel Type Fittings (Cont'd)

A. Wall Analysis

1. Tension in the wall may be analyzed by the method as shown in section I-A with the exception that A_g is defined as,

$$A_g = 2at_w + bt_b$$

and if $t_b = t_w$ then,

$$A_g = t_w(2a + b)$$

2. Bending in Wall

- a. Compute c for section A-A of Fig. 2 by,

$$c = \frac{\frac{t_b^2}{2} \left(b - \frac{t_w}{2} \right) + at_w (a + t_b)}{2at_w + bt_b}$$

and if $t_b = t_w$ then,

$$c = \frac{\frac{t_w}{2} \left(b - \frac{t_w}{2} \right) + a(a + t_w)}{2a + b}$$

- b. Determine the applied ultimate bending moment, M_u , from

$$M_u = P_u (d - c)$$

- c. Determine the allowable bending moment, M_u , of an unsymmetrical section per pg. 17.2.3

- d. Determine the wall bending ratio from

$$R_{buw} = \frac{M_u J_{mu}}{M_u}$$

3. Interaction - Bending and Tension

Obtain the ultimate margin of safety using the interaction equation $R_b + R_t = 1$ for the values of R_{tw} and R_{buw} as determined in par. A-1 and A-2-d above. (See pg. 17.4.3)

B. End Pad Analysis

1. Bending

- a. Compute $\frac{r_1}{a}$ and $\frac{b}{a}$.

- b. Obtain K_3 from Fig. 8.

STRUCTURAL ANALYSIS MANUAL
GENERAL DYNAMICS/CONVAIR AND SPACE SYSTEMS DIVISION

II. Channel Type Fittings (Cont'd)

B. End Pad Analysis (Cont'd)

1. Bending (Cont'd)

- c. Determine the bending stress, f_{bu} , on section B-B of Fig. 2 from

$$f_{bu} = \frac{P_u (2d - t_b) I_x}{t_e^2 a}$$

- d. Obtain the allowable $\frac{MC}{I}$ bending stress, F_{bu} , assuming a rectangular section ($k = 1.5$), from **SECT. 17.0**

- e. The margin of safety for bending on section B-B of Fig. 2 is given by

$$M.S._u = \frac{F_{bu}}{f_{bu}} - 1$$

2. Shear of End Pad

Check shear of end pad as shown in section I-B-2.

III. Angle Type Fittings

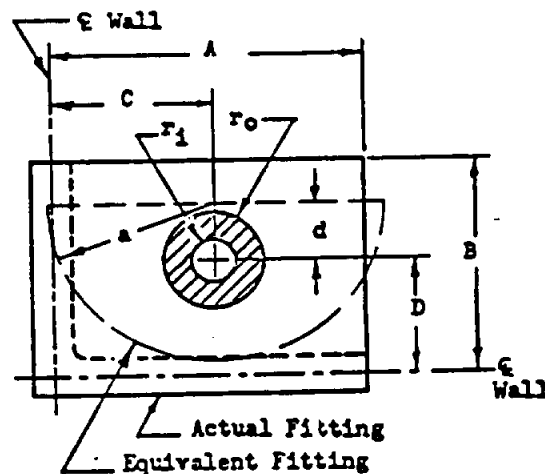
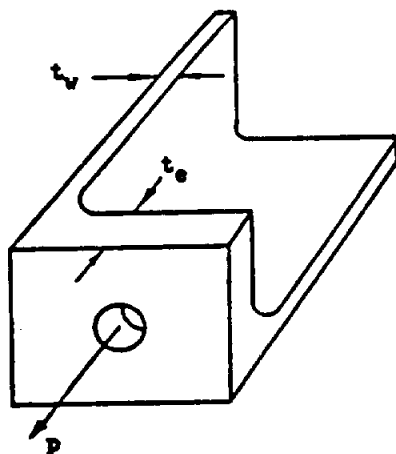


Fig. 3

STRUCTURAL ANALYSIS MANUAL
GENERAL DYNAMICS/CONVAIR AND SPACE SYSTEMS DIVISION

III. Angle Type Fittings (Cont'd)

Angle type fittings may be analysed as bathtub fittings by the methods of section I provided that the ratio, A/B , as defined in Fig. 3 is not larger than 2. The effective values of a and d for the equivalent bathtub fitting used in the analysis are given by

$$a = \frac{A+B}{2}$$

$$d = a - \left(\frac{C+D}{2} \right)$$

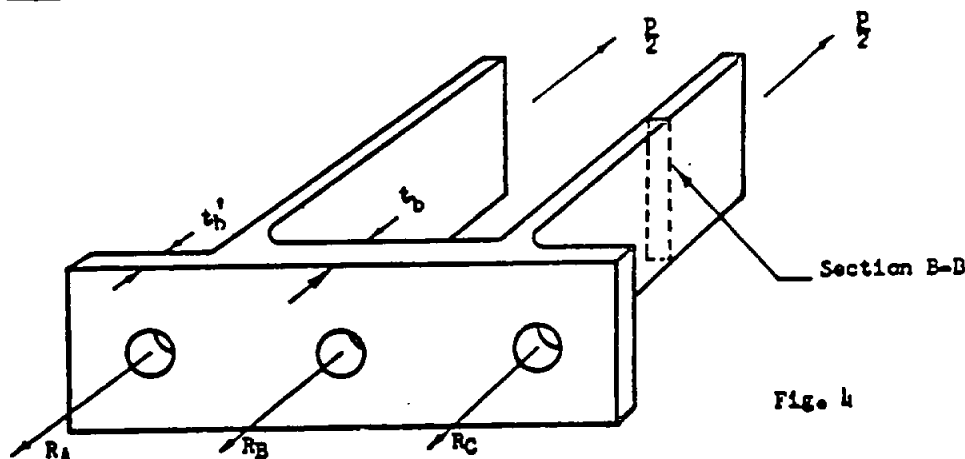
The section properties of the equivalent section are obtained from:

$$A_g = \pi a t_w$$

$$e = .637a$$

$$I = .298a^3 t_w$$

IV. "PI" Type Fittings



A. Tension in Wall

1. Determine the maximum tension stress, f_{tuw} , in the fitting wall due to the ultimate fitting load, P_u , from

$$f_{tuw} = \frac{P_u}{2 A_g}$$

where A_g is the gross area of section B-B in Fig. 4.

2. Obtain the basic tension efficiency, η , of the wall from SECT. 14.14 considering the wall as one sheet in a tension joint between sheets.

STRUCTURAL ANALYSIS MANUAL
GENERAL DYNAMICS/CONVAIR AND SPACE SYSTEMS DIVISION

IV. "PI" Type Fittings (Cont'd)

A. Tension in Wall (Cont'd)

3. The margin of safety for tension in the wall is given by

$$M.S._u = \frac{\eta F_{tu}}{\sum_{i=1}^n F_{tu_i}} - 1$$

B. End Pad Bending

1. Determine the fixed end moment for a beam continuous over three supports assuming all loads as concentrated.

2. Assume 50% of the above values as end moments and determine bolt loads (concentrated).

Analyze the end bolts for the combined loading (moment plus tension) and the center bolt for direct tension.

3. To determine the bending moment curve, assume the center bolt load computed in (2) is uniformly distributed over the bolt head flat.

4. The above steps are graphically represented in Fig. 5.

5. Obtain the allowable $\frac{M_u}{I}$ bending stress, F_{bu} , from Sect. 17.0, assuming a rectangular section ($k = 1.5$) and calculate the allowable bending moment from

$$M_u = F_{bu} \frac{I}{k}$$

6. The margin of safety for bending is given by

$$M.S._u = \frac{M_u}{\sum_{i=1}^n M_{u_i}} - 1$$

Note: A check of several sections may be necessary to determine the critical section in the end pad.

STRUCTURAL ANALYSIS MANUAL
GENERAL DYNAMICS/CONVAIR AND SPACE SYSTEMS DIVISION

IV. "PI" Type Fittings (Cont'd)

B. End Pad Bending (Cont'd)

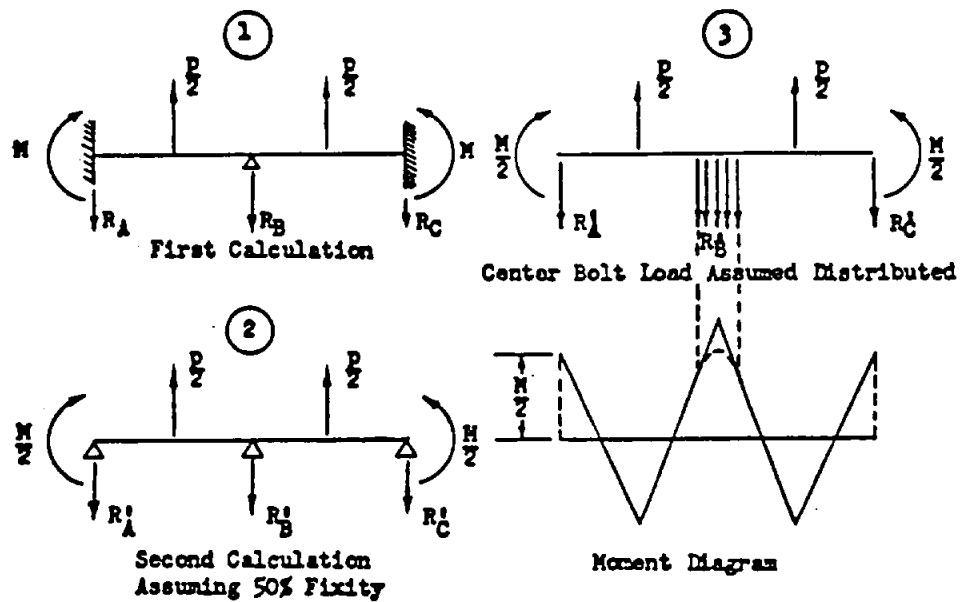
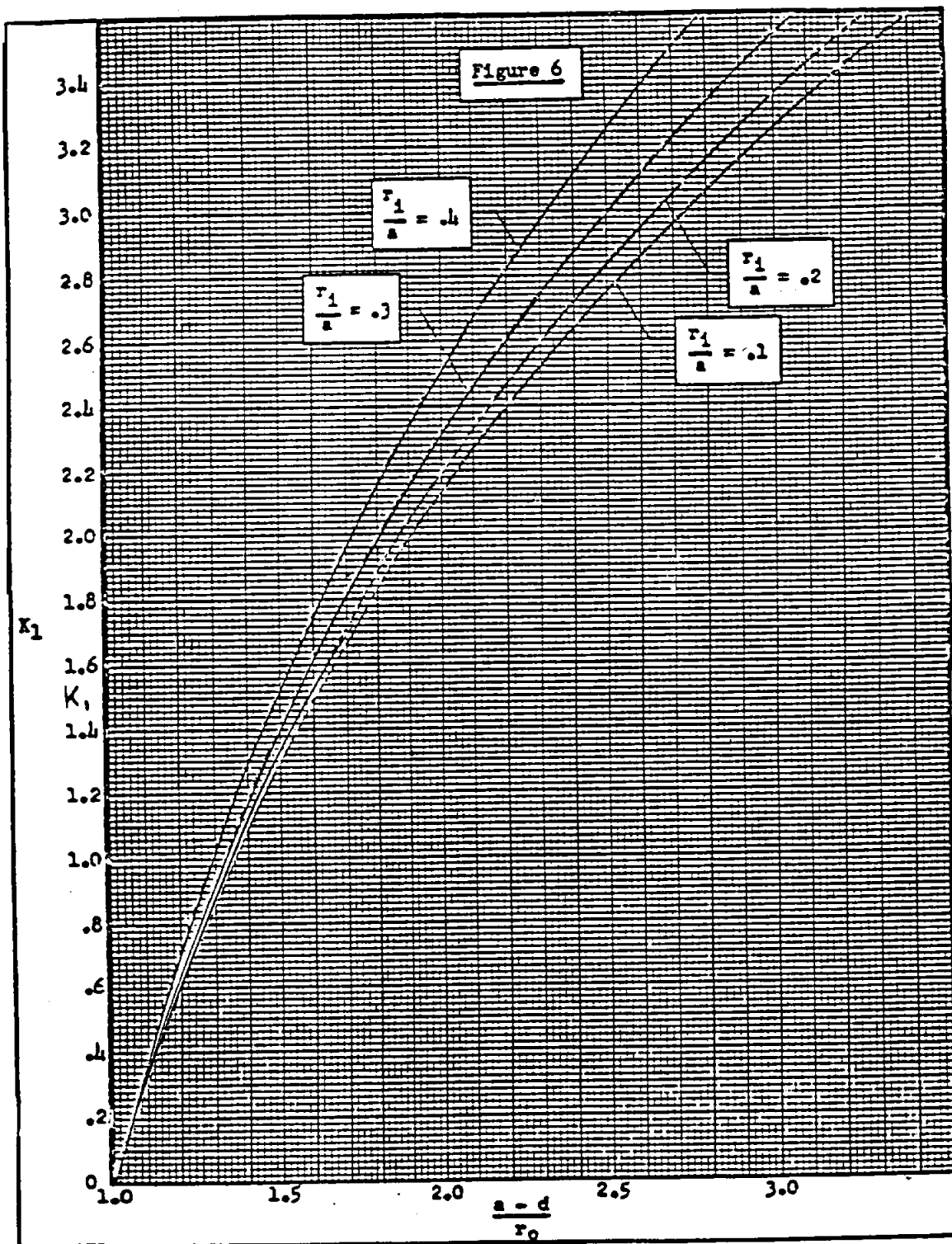


Fig. 5

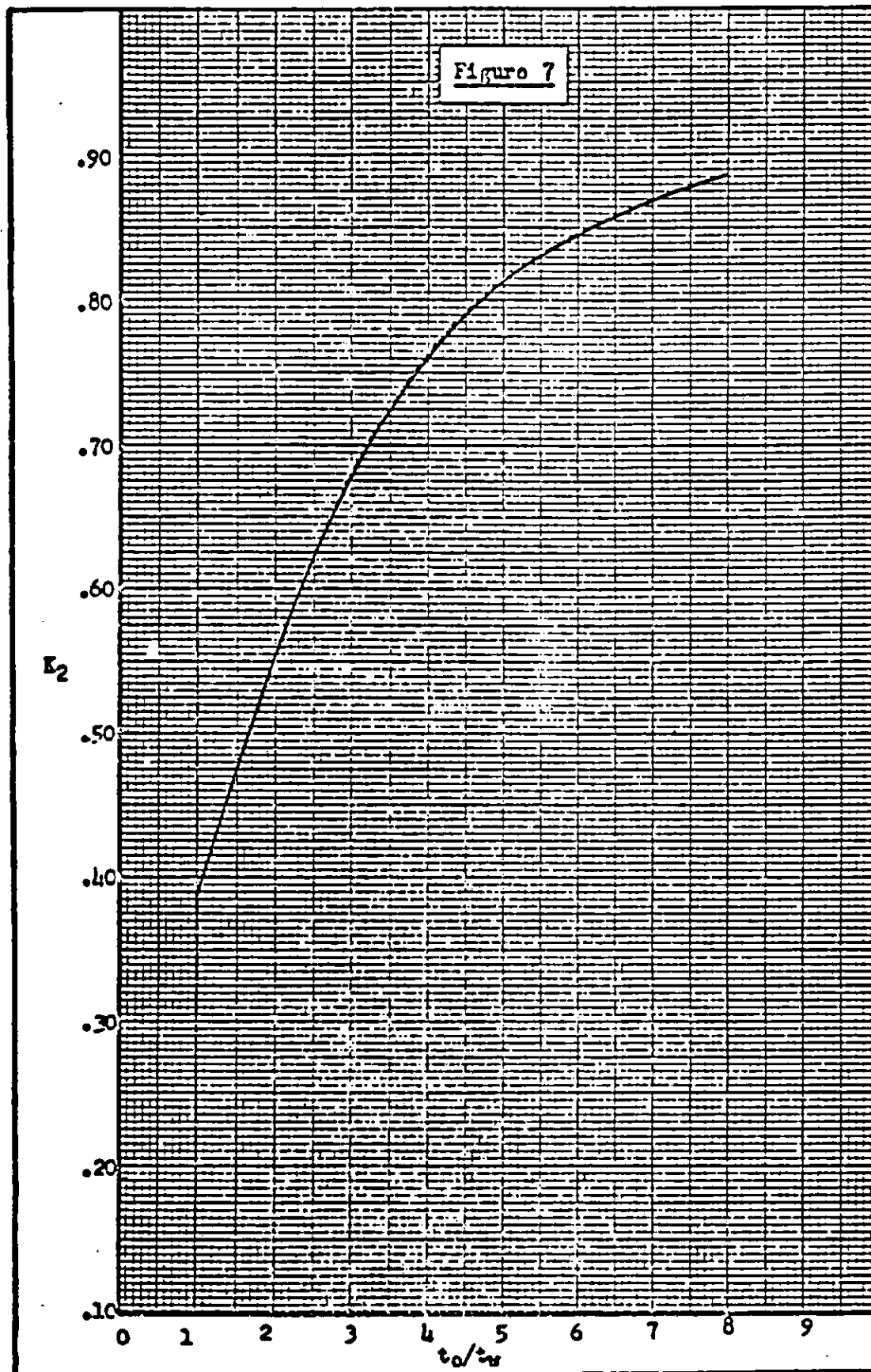
C. Shear of End Pad

Check shear of end pad as shown in section I-B-2.

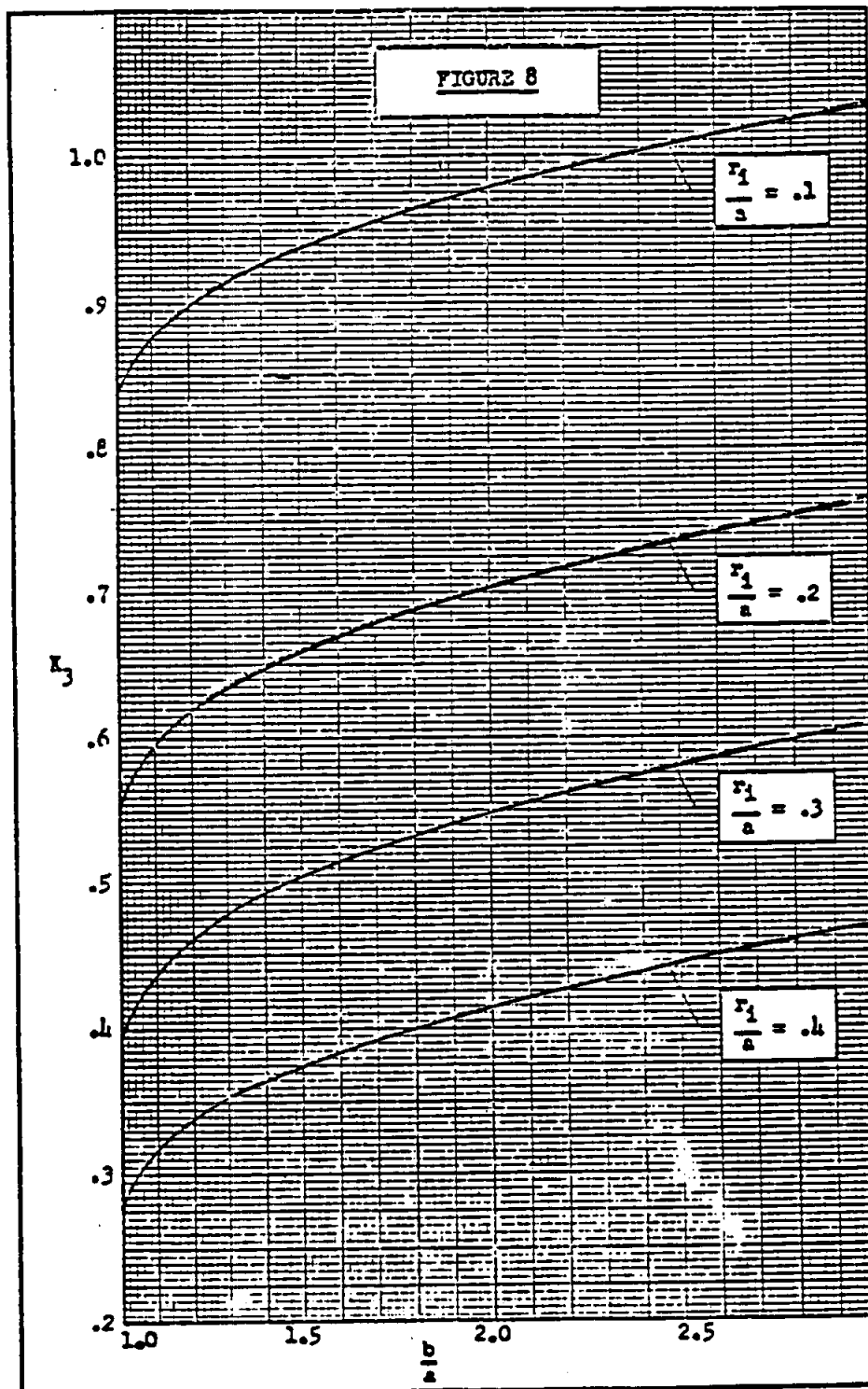
STRUCTURAL ANALYSIS MANUAL
GENERAL DYNAMICS/CONVAIR AND SPACE SYSTEMS DIVISION



STRUCTURAL ANALYSIS MANUAL
GENERAL DYNAMICS/CONVAIR AND SPACE SYSTEMS DIVISION












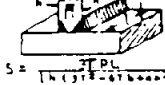



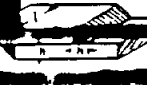
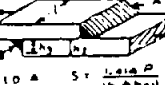
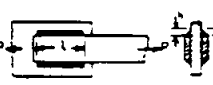
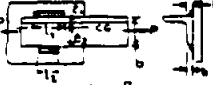







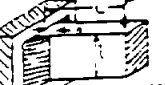




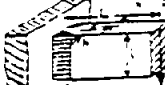


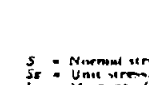
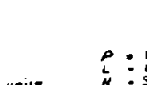

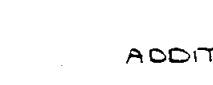
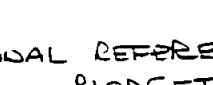
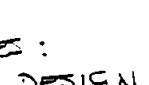
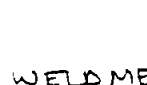

STRUCTURAL ANALYSIS MANUAL
GENERAL DYNAMICS/CONVAIR AND SPACE SYSTEMS DIVISION



STRUCTURAL ANALYSIS MANUAL

GENERAL DYNAMICS/CONVAIR AND SPACE SYSTEMS DIVISION

TABLE 2-L WELD STRESS FORMULAS

 $S = \frac{P}{hL}$	 $S = \frac{P}{(h_1 + h_2)L}$	 $S = \frac{P}{hL}$	 $S = \frac{6M}{hL^2}$	 $S_t = \frac{6PL}{hL^2} \quad S_m = \frac{P}{hL}$
 $S = \frac{6M}{hL^2}$	 $S = \frac{3TM}{[h(3T^2 - 6Th + 3h^2)]}$	 $S = \frac{P}{(h_1 + h_2)L}$	 $S = \frac{3TM}{[h(3T^2 - 6Th + 3h^2)]}$	 $S = \frac{3TDL}{[h(3T^2 - 6Th + 3h^2)]} \quad S_m = \frac{P}{2hL}$
 $S = \frac{.707P}{hL}$	 STRESS IN WELD A = EQUALS STRESS IN WELD B $S = \frac{.707P}{(h_1 + h_2)L}$	 $S = \frac{.707P}{hL}$	 $S = \frac{.707P}{hL}$	 WELD A: $S = \frac{.707P}{h_1L}$ WELD B: $S = \frac{.707P}{h_2L}$
 $S = \frac{.354P}{hL}$	 $S = \frac{.707P}{hL}$ OR $S = \frac{.707P}{hL}$	 $S = \frac{.707P}{hL}$	 $S = \frac{.707P}{hL}$	 $S = \frac{.707P}{hL}$
 $S = \frac{.707P}{hL}$	 $S = \frac{.707P}{hL}$	 $S = \frac{.707P}{hL}$	 $S = \frac{.707P}{hL}$	 $S = \frac{.707P}{hL}$
 $S = \frac{.707P}{hL}$	 $S = \frac{.707P}{hL}$	 $S = \frac{.707P}{hL}$	 $S = \frac{.707P}{hL}$	 $S = \frac{.707P}{hL}$
 $S = \frac{.707P}{hL}$	 $S = \frac{.707P}{hL}$	 $S = \frac{.707P}{hL}$	 $S = \frac{.707P}{hL}$	 $S = \frac{.707P}{hL}$
 $S = \frac{.707P}{hL}$	 $S = \frac{.707P}{hL}$	 $S = \frac{.707P}{hL}$	 $S = \frac{.707P}{hL}$	 $S = \frac{.707P}{hL}$

ADDITIONAL REFERENCES:

BLODGETT, DESIGN OF WELDMENTS.

BLODGETT, DESIGN OF WELDED STRUCTURES.

Data Source,

GENERAL DYNAMICS | ASTRONAUTICS DESIGN MANUAL

STRUCTURAL ANALYSIS MANUAL
GENERAL DYNAMICS/CONVAIR AND SPACE SYSTEMS DIVISION

SECTION 14.9

WELD-ON BRACKETS

A SIMPLE ANALYSIS FOR A TYPICAL BRACKET WELDED TO A PRESSURIZED
PROPELLANT TANK IS SHOWN ON THE PAGES FOLLOWING.

THIS ANALYSIS

PAGES 14.9.2 THRU' 14.9.5 HAVE BEEN DELETED.

ALJ GPFW

STRUCTURAL ANALYSIS MANUAL
GENERAL DYNAMICS/CONVAIR AND SPACE SYSTEMS DIVISION

SECTION 14.10

BONDED JOINTS

THIS SECTION WILL BE ADDED WHEN AVAILABLE

STRUCTURAL ANALYSIS MANUAL

GENERAL DYNAMICS/CONVAIR AND SPACE SYSTEMS DIVISION

Data Source, Section 1.3 Reference 3

6.4.3 Attachment Flexibility

The flexibility of an attachment/sheet combination should be determined experimentally. If load-deflection curves for a particular fastener/sheet combination are available, the flexibility is the slope of the curve at the estimated load level.

If load-deflection test data is not available for the exact fastener/sheet combination, two methods can be used to determine a spring rate.

6.4.3.1 Method I - Generalized Test Data

Some test data is available to develop generalized stiffness curves. Figure 6.27 shows a curve of t/D versus K for a single shear joint with a steel fastener. The procedure for determining joint stiffness is as follows:

DIA	1/8	5/32	3/16	1/4	5/16	3/8	7/16	1/2	9/16	5/8
	SRx10 ⁻⁶									
ALUM	.163	.203	.244	.325	.406	.497	.563	.650	.732	.813
STEEL	3.62	4.53	5.44	7.25	9.06	10.9	12.6	14.5	15.5	18.1
TITAN	1.93	2.42	2.90	3.87	4.83	5.81	6.72	7.73	8.27	9.65
OTHER	(Eother/Esteel)xSRsteel									
SHEET SPRING RATE = K x SR										
JOINT SPRING RATE = 1/(1/SRu + 1/SRl)										

TABLE 6.9 - BASIC SPRING RATES

1. Calculate t/D for upper sheet
2. Calculate t/D for lower sheet
3. From Figure 6.27 determine K for upper sheet
4. From Figure 6.27 determine K for lower sheet

STRUCTURAL ANALYSIS MANUAL
GENERAL DYNAMICS/CONVAIR AND SPACE SYSTEMS DIVISION

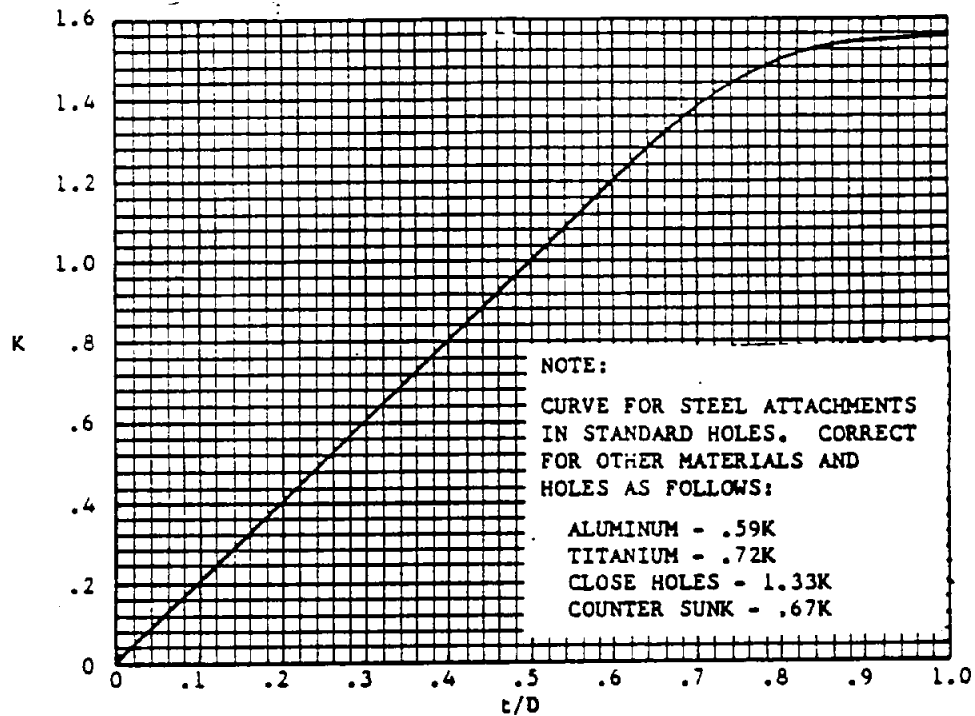


FIGURE 6.27 - EFFECTIVE SPRING RATES FOR STEEL
PINS IN SINGLE SHEAR

STRUCTURAL ANALYSIS MANUAL
GENERAL DYNAMICS/CONVAIR AND SPACE SYSTEMS DIVISION

5. If the fastener is steel and in a hole drilled to normal tolerance proceed to step 6. Modify the K factors of step A by the following factors

Aluminum Fastener, K x .59
Titanium Fastener, K x .72
Close Tolerance Hole, K x 1.33
Countersunk Hole, K x .67

Example:

Titanium fastener in close tolerance hole.
From step 4: K
Correct K: .72 x 1.33 x K

6. Determine SR from Table 6.9. Calculate spring rate for each sheet by

$$k_n = K_n \times SR$$

where:

k_n = spring rate of sheet
 K_n = constant from step 4 or 5
SR = value from Table 6.9

7. Calculate joint spring rate

$$k_{\text{joint}} = \frac{1}{1/k_u + 1/k_l}$$

6.4.3.2 Method II - Bearing Criteria

If load deflection data is not available, the limit bearing load criteria of Reference 1 may be used to obtain an estimate of the attachment-hole flexibility. These criteria result in an overestimate of the attachment-hole flexibility and an underestimate of the maximum attachment load at load levels below yield.

As an example of the way the criteria of MIL-HDBK-5B (Reference 1) may be used to determine the attachment-hole flexibility factor, consider a joint in which the bolt diameter is 0.25 inch, the upper sheet is 0.125 inch titanium and the lower sheet is 0.25 inch aluminum. Assuming that the aluminum is 2024-T6 and the titanium is 6 Al-4V, the respective bearing yield stress allowables from Reference 1 are 78,000 psi and 198,000 psi. The yield loads are then calculated to be

$$P_{al} = 78,000(.250)(.250) = 4875 \text{ lbs}$$

$$P_{\text{titanium}} = 198,000(.125)(.250) = 62,000 \text{ lbs}$$

STRUCTURAL ANALYSIS MANUAL
GENERAL DYNAMICS/CONVAIR AND SPACE SYSTEMS DIVISION

The average load is then

$$P_{avg} = (6200 + 4875)/2 = 5590 \text{ lbs.}$$

The flexibility is calculated for a deformation of 2 percent of the hole diameter per Section 1.3 Reference 2B.

$$f_{avg} = \Delta/P_{avg} = (.02)(.250)/5590 \approx 900(10^{-9}) \text{ in./lb}$$

STRUCTURAL ANALYSIS MANUAL
GENERAL DYNAMICS/CONVAIR AND SPACE SYSTEMS DIVISION

4.1 FASTENER ELASTIC STIFFNESS EQUATION

Reference: ASTM STP 486 and Swift, T., AIAA San Diego Section
 1979 Education Lecture Series, 14 March 1979

$$S = \frac{P}{ED} \left(A + C \left(\frac{D}{t_1} + \frac{D}{t_2} \right) \right)$$

S = Fastener Displacement

D = Fastener Diameter

P = Load

E = Plate Modulus

t_i = Plate Thickness

Fastener Material

	Aluminum	Titanium	Steel
A	5.000	3.947	1.666
C	0.80	0.82	0.86

The Titanium fastener values were interpolated based on Young's Moduli.
 The equation was rearranged with some guesses, to give

$$K_i = \frac{1.0}{\frac{A}{ED} + C \left(\frac{1}{E_1 t_1} + \frac{1}{E_2 t_2} \right)}$$

where $E^1 = 0.5 / \left(\frac{1}{E_1} + \frac{1}{E_2} \right)$

K_i = Fastener Spring Rate

STRUCTURAL ANALYSIS MANUAL
GENERAL DYNAMICS/CONVAIR AND SPACE SYSTEMS DIVISION

Data Source, Section 1.3 Reference 6

SUBJECT: Preloaded Bolts and Screws

Introduction

This Memo contains:

- (1) Methods for computing the loads in bolts and screws subjected to combined preload and applied tension loads,
- (2) Methods for computing the optimum preload for a repeated applied load,
- (3) Methods for computing the wrench torque required to produce a given preload, and
- (4) Restrictions on preloaded bolts and screws.

In the body of this Memo, reference is usually made to bolts, but the information is equally applicable to screws.

STRUCTURAL ANALYSIS MANUAL

GENERAL DYNAMICS/CONVAIR AND SPACE SYSTEMS DIVISION

II. Strength Requirements for Preloaded Bolts

The applied ultimate tension load on the bolt, including the effects of preload, shall not exceed the ultimate tension strength of the bolt.

The applied yield tension load on the bolt, including the effects of preload, shall not produce a stress, based on the thread root area, greater than the yield stress of the bolt material. Thread root areas may be obtained from Table I.

When the fitting faces are in contact, shear loads shall be combined with only the external tension load in the analysis of the bolt. When the fitting faces are not in contact, shear loads shall be combined with the total tension load in the bolt (ref. Fig. 2 and 3).

III. Total Load in Bolt

The total load in a bolt that is subjected to both an initial tension preload and an external load is given by the larger of:

$$P_b = P_{bi} + W \left[\frac{\frac{C}{L}}{1 + \frac{A_m E_m}{A_b E_b}} \right]$$

$$P_b = W$$

Where

- P_b = Total load in bolt, lbs.
- P_{bi} = Preload in bolt due to tightening, lbs.
- W = Applied (external) tension load, lbs.
- C = (See Fig. 1).
- L = Distance between bolt head and nut, in.
- E_b = Young's modulus for bolt, psi.
- E_m = Young's modulus for material in compression, psi.
- A_b = Shank area of bolt, sq. in.
- A_m = Area of material in compression, sq. in.
- = $\frac{\pi}{4} (B^2 - D^2)$, approximately, where
- B = Distance between flats of hex head or diameter of round head bolts, in.
- D = Diameter of bolt shank, in.

STRUCTURAL ANALYSIS MANUAL
GENERAL DYNAMICS/CONVAIR AND SPACE SYSTEMS DIVISION

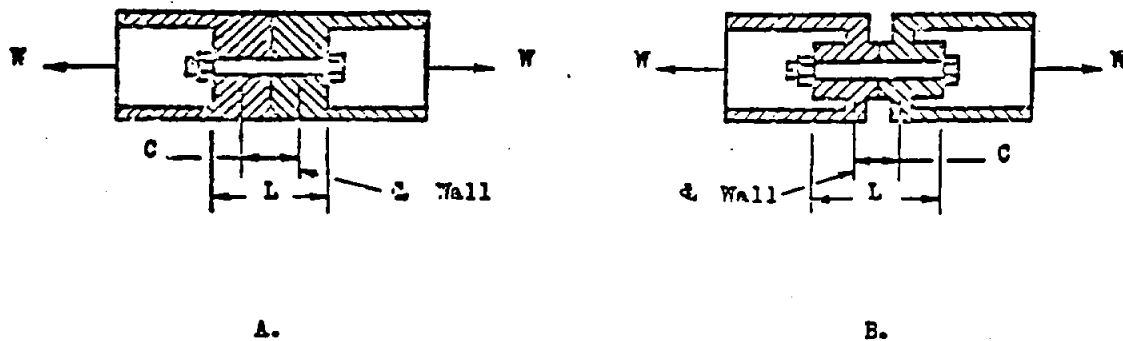


Fig. 1.

The distance C is measured between the centerlines of the walls adjacent to the area A_n . Thus, in Fig. 1 A, $C/L = .5$.

The relationship between the applied load, the initial preload, and the total bolt load is shown in Fig. 2.

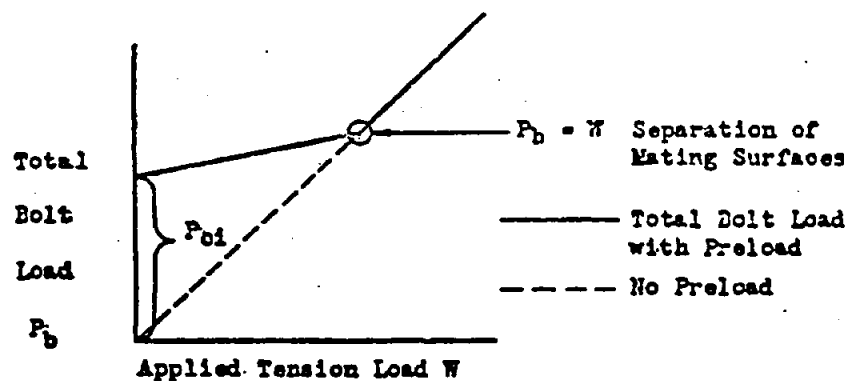


Fig. 2.

STRUCTURAL ANALYSIS MANUAL
GENERAL DYNAMICS/CONVAIR AND SPACE SYSTEMS DIVISION

IV. Preloaded Bolts under Repeated Loading

The optimum preload for repeated loading is obtained when the mating surfaces are just on the point of separating under the applied load; that is, the point $P_b = W$ in Fig. 2 (refs. 2 and 3). This will occur when the ratio of bolt preload P_{bi} to applied load W is given by:

$$\frac{P_{bi}}{W} = 1 - \frac{C}{L} \left[\frac{1}{1 + \frac{A_m E_m}{A_b E_b}} \right]$$

Both increasing and decreasing the preload from this value will result in a decreased number of loading cycles to produce fatigue failure. The decrease is less for preloads above this value than for preloads correspondingly below this value.

Values of P_{bi}/W for standard bolts and screws in common materials are given in Fig. 5.

V. Wrench Torque for a Given Preload

The average wrench torque applied to the nut to produce a specified preload or stress on the root area is given by

$$T = \frac{E P_{bi}}{A_r}$$

Where

- T = Wrench Torque, in.-lb.
- E = Wrench torque ratio (from Table II).
- P_{bi} = Preload in bolt due to tightening, lbs.
- A_r = Root area of bolt, sq. in. (See Table I).

Because of the variation of frictional resistance, the torque required on individual nuts to produce a given preload may vary by $\pm 30\%$ for dry nuts and by $\pm 15\%$ for lubricated nuts.

VI. Special Considerations

A. Aluminum and Magnesium Fittings

The additive effect of the initial preload to the applied load is largest when the material under compression has a low value of E as compared to the E of the bolt material. Special attention should therefore be given to steel bolts through aluminum or magnesium fittings.

STRUCTURAL ANALYSIS MANUAL
GENERAL DYNAMICS/CONVAIR AND SPACE SYSTEMS DIVISION

VI. Special Considerations (Continued)

B. Mating Surfaces Not in Contact.

When the mating surfaces of the fitting are not in contact, the initial preload and the applied tension load may add directly. A typical structure with a gap between mating surfaces is illustrated in Fig. 3, and a corresponding bolt loading is shown in Fig. 4. The corresponding bolt loading when the mating surfaces are in contact is shown in Fig. 2.

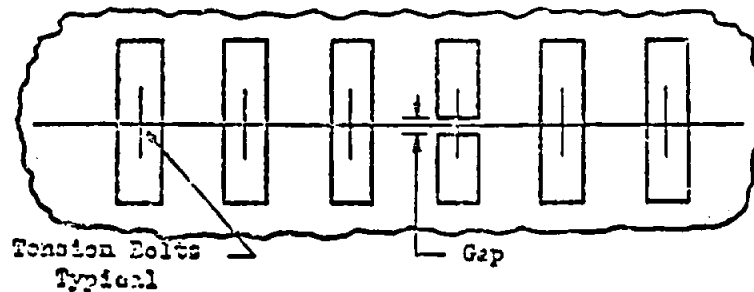


Fig. 3

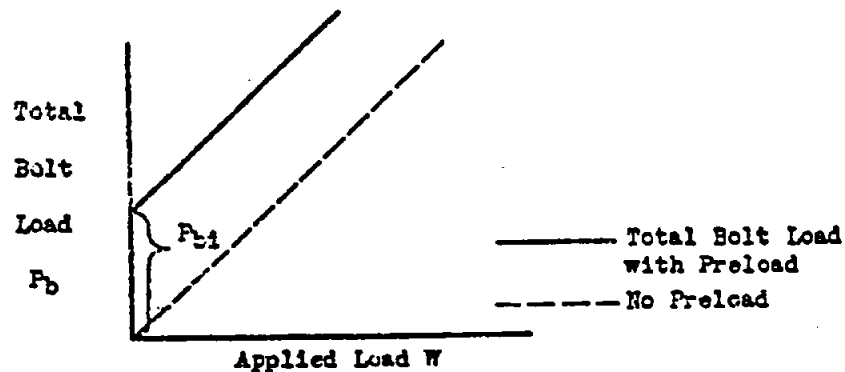


Fig. 4

STRUCTURAL ANALYSIS MANUAL
GENERAL DYNAMICS/CONVAIR AND SPACE SYSTEMS DIVISION

TABLE I
STANDARD STEEL BOLT PRELOADS

Bolt Size	Root Area Sq. In. (1)	P_{b1} - Lbs. (2)	
		Tension Nut	Shear Nut
10-32	.018074	720	430
1/4-28	.033394	1,340	800
5/16-24	.053666	2,150	1,290
3/8-24	.082397	3,300	1,950
7/16-20	.11115	4,450	2,670
1/2-20	.15116	6,050	3,630
9/16-18	.19190	7,680	4,600
5/8-18	.24349	9,740	5,840
3/4-16	.35605	14,200	8,520
7/8-14	.48595	19,500	11,700
1-14	.65382	26,200	15,700
1-12	.63307	25,300	15,200
1-1/8-12	.82162	32,900	19,700
1-1/4-12	1.0347	41,400	24,800

NOTE: (1) Based on MIL-S-7742 thread

(2) $P_{b1} = \begin{cases} 40,000 \times \text{Root Area} - \text{Tension nut} \\ 24,000 \times \text{Root Area} - \text{Shear nut} \end{cases}$

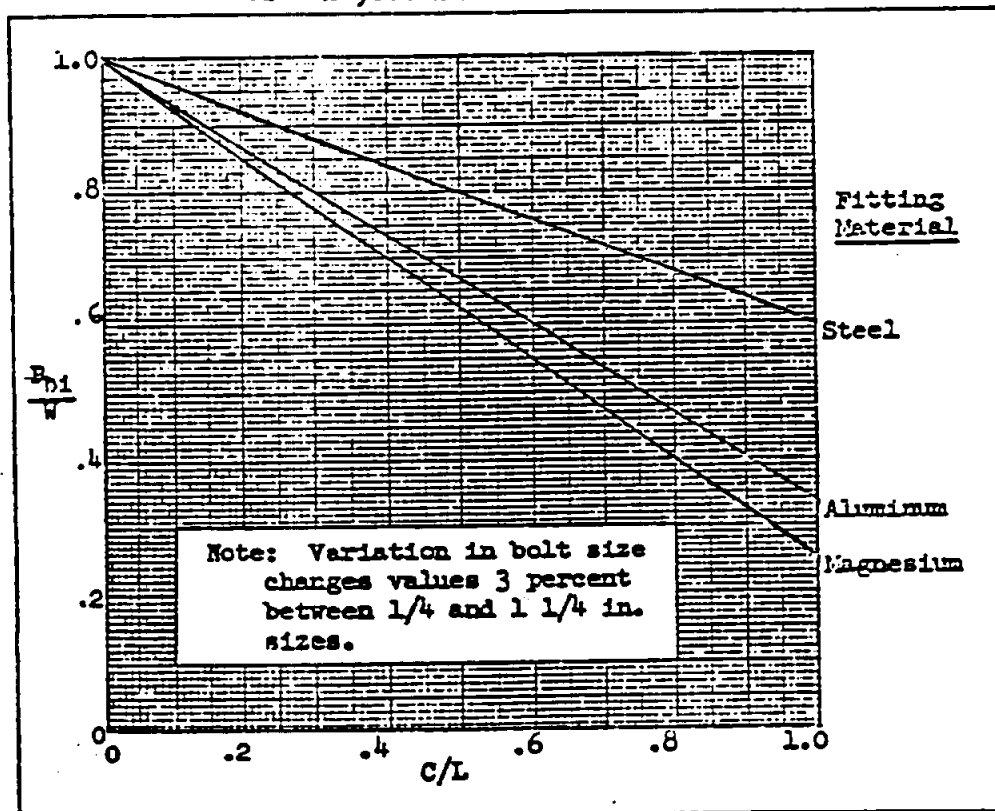


Figure 5. Values of optimum preload ratio P_{b1}/W for standard steel bolts and screws in common materials.

TABLE II

WRENCH TORQUE RATIOS R FOR STEEL BOLTS

Thread Size	Bolt and Nut ^{2,3}				Bolt and Tapped Plate ^{2,4} (Set Screw)			
	Nut Turning On Steel Fitting ⁵		Nut Turning On Aluminum Fitting ⁵		Flat-Ended Bolt Turning on Steel Plate		Round-Ended Bolt Turning on Steel Plate	
	Dry	Lubricated	Dry	Lubricated	Dry	Lubricated	Dry	Lubricated
10-32	.001038	.000767	.000865	.000546	.000639	.000319	.000470	.000149
1/4-28	.00246	.00167	.001966	.00119	.00153	.000757	.001113	.000333
5/16-24	.00509	.00350	.00408	.00249	.00305	.00151	.00224	.000659
3/8-24	.00829	.00533	.00675	.00379	.00588	.00272	.00408	.00126
7/16-20	.0127	.00806	.01039	.00575	.00890	.00429	.00642	.00179
1/2-20	.0203	.01174	.01648	.00915	.01386	.00665	.00993	.00262
9/16-18	.0293	.0191	.0238	.0134	.0197	.00917	.01412	.00374
5/8-18	.0421	.0282	.0340	.0192	.0278	.0150	.01992	.00503
3/4-16	.0713	.0453	.0579	.0318	.0489	.0227	.0348	.00866
7/8-14	.1138	.0720	.0922	.0507	.0779	.0382	.0653	.01568
1-14	.1742	.1098	.1412	.0753	.1192	.0548	.0845	.0201
1-1/8-12	.246	.1553	.1995	.1088	.1681	.0774	.1192	.0286
1-1/4-12	.333	.2175	.2610	.1522	.2375	.1064	.1578	.0392

Notes: 1. Torque (in.-lb.) = $R \times$ initial tension stress on root area (psi).

2. All bolts and nuts or tapped plates are steel, cadmium plated.

3. Values for bolt and nut combination are based on holding bolt fixed and turning nut.

4. Values for bolt and tapped plate (set screw) combination are based on head of bolt not in contact with tapped plate.

5. Where washers are used under the nut, the fitting material shall be taken as the material of the washer.

STRUCTURAL ANALYSIS MANUAL

GENERAL DYNAMICS/CONVAIR AND SPACE SYSTEMS DIVISION

Data Source, Section 1.3 Reference 26

Table 4.2 LOADS AND STRESSES PER UNIT TORQUE FOR NUMBERED SIZE THREADS

Size No.	Major diam. in.	No. of threads per in.		Basic area of section at root of threads, sq in.	Max combined tensile stress, psi, in screw with torque of 1 in-lb on nut	Max axial load, lb on screw with torque of 1 in-lb on nut
		Coarse	Fine			
0	0.060		80	0.0015	72,600	74
1	0.073	64	72	0.0022	43,900	63
2	0.086	56	64	0.0031	38,100	66
3	0.099	48	56	0.0041	26,200	55
4	0.112	40	48	0.0055	23,400	56
5	0.125	40	44	0.0072	18,200	50
6	0.138	32	40	0.0097	16,100	51
8	0.164	32	36	0.0120	12,600	42
10	0.190	24	32	0.0145	10,700	43
12	0.216	24	28	0.0175	7,890	36
				0.0206	7,190	37
				0.0226	6,810	34
					5,620	35
					3,560	30
					3,270	30
					2,660	26
					2,100	27
					1,600	23
					1,410	23

Table 4.3 LOADS AND STRESSES PER UNIT TORQUE FOR FRACTIONAL SIZE THREADS

Size, in.	No. of threads per in.			Basic area of section at root of threads, sq in.	Max combined tensile stress, psi, in screw with torque of 1 in-lb on nut	Max axial load, lb on screw with torque of 1 in-lb on nut
	Coarse	Fine	Extra fine			
1/16	20			0.0249	1,115	20.6
		28		0.0326	876	21.2
			32	0.0352	807	21.7
1/8	18			0.0454	512	16.6
		24		0.0524	432	17.3
			32	0.0590	377	17.6
3/16	16			0.0678	292	14.3
		24		0.0809	261	14.9
			32	0.0890	213	12.3
1/4	14			0.0933	179	12.2
		20		0.1090	150	12.6
			28	0.1217	132	13.0
5/16	13			0.1257	118	10.9
		20		0.1486	97.1	11.4
			28	0.1634	86.3	11.7
3/8	12			0.1620	82.3	9.9
		18		0.1358	64.3	10.3
			24	0.2054	63.3	10.5
7/16	11			0.2018	59.3	8.72
		18		0.2400	48.2	9.24
			24	0.2386	44.3	9.33
1/2	10			0.3020	32.1	7.34
		16		0.3513	27.0	7.64
			20	0.3725	23.3	7.68
5/8	9			0.4193	20.4	6.52
		14		0.4805	17.6	6.78
			20	0.5200	16.1	6.92
3/4	8			0.5310	13.6	5.73
		14		0.6464	11.4	5.99
			20	0.6921	10.6	6.09
7/8	7			0.6931	9.61	5.08
		12		0.8118	8.06	5.32
			18	0.8772	7.43	5.43
1 1/8	7			0.8898	6.71	4.62
		12		1.0238	5.73	4.80
			18	1.0969	5.33	4.90
1 1/4	6			1.0341	5.17	4.18
		12		1.2602	4.34	4.40
1 3/8	6			1.2938	3.84	3.86
		12		1.5212	3.31	4.16
			18	1.6101	3.17	4.32

STRUCTURAL ANALYSIS MANUAL
GENERAL DYNAMICS/CONVAIR AND SPACE SYSTEMS DIVISION

Data Source, Section 1.3 Reference 6

SUBJECT: Efficiency of Plates in Tension Joints

I. Introduction

This memo contains an empirical method of determining sheet efficiencies of lap and butt plate joints when the joints are made with rivets, bolts and/or screws. It is applicable to all metals commonly used in aircraft structures. The method does not determine the load on any of the connectors, or the load carried by doublers. These loads must be determined by other means.

STRUCTURAL ANALYSIS MANUAL
GENERAL DYNAMICS/CONVAIR AND SPACE SYSTEMS DIVISION

Notation

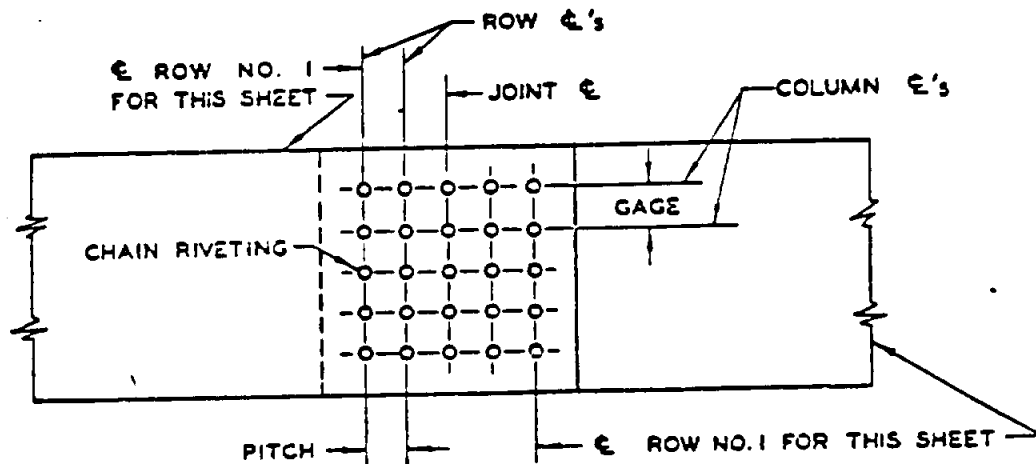


Fig. 1
Chain Spacing

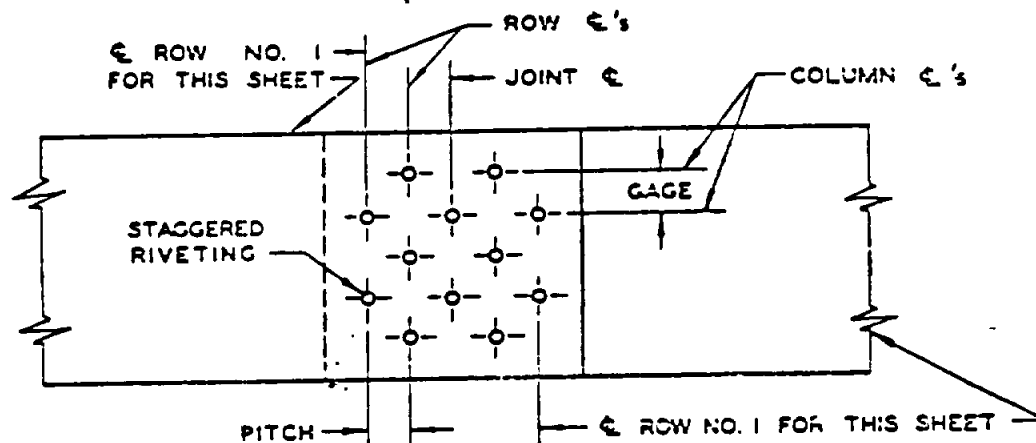


Fig. 2
Staggered Spacing

- Rows = Lines of connectors parallel to the joint centerline, the first row in any sheet being the row farthest away from the edge of the sheet.
- Columns = Lines of connectors normal to the joint centerline.

STRUCTURAL ANALYSIS MANUAL
GENERAL DYNAMICS/CONVAIR AND SPACE SYSTEMS DIVISION

II. (Continued)

- Pitch = Distance between rows (or, spacing normal to the joint centerline).
- Gage = Distance between columns (or, spacing parallel to the joint centerline).
- p = Pitch between the first and second rows.
- D_{1L} = Effective diameter of the largest hole in the first row.
- A_g = Gross cross-sectional area of the plate (area without holes).
- R_{1L} = Reduction in cross-sectional area due to the largest hole in the first row.
- ΣR_1 = Total reduction in cross-sectional area due to all the holes in the first row.
- ΣR_p = Total reduction in cross-sectional area due to all connectors within a pitch of SD_{1L} of the first row (including holes in first row) when projected upon a cross-section parallel to the joint centerline (see Fig. 3).
- t = Sheet thickness.

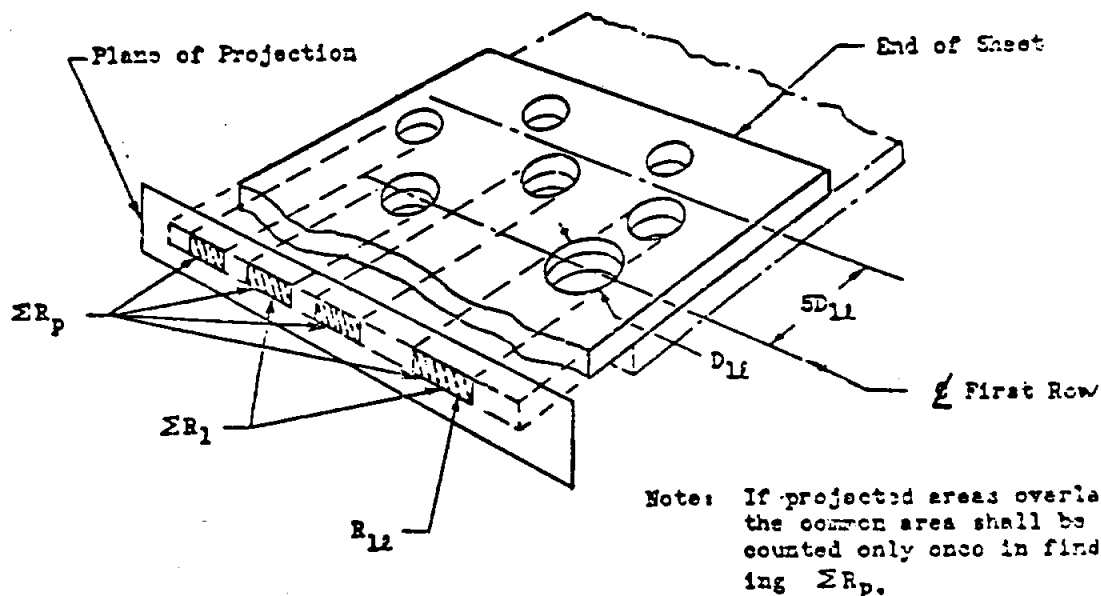


Fig. 3

STRUCTURAL ANALYSIS MANUAL
GENERAL DYNAMICS/CONVAIR AND SPACE SYSTEMS DIVISION

II. General

- A. Chain spacing should be used in preference to staggered spacing whenever possible. This practice eliminates the possibility of overlooking the weakest section and reduces the possibility of premature failure in the first row of connectors.
- B. Chain spaced joints in which the first row has a fewer number of connectors than the succeeding rows do not necessarily give higher efficiencies than those using ordinary chain spacing. In addition, as with staggered spacing, this spacing gives the possibility of premature failure in the first row of connectors.
- C. Staggered spacing may become necessary in such applications as cap splices, where the length and width available for the joint do not permit a sufficient number of chain-spaced connectors to transmit the applied load. In such cases, the rivets should be in straight lines parallel to the length of the member.
- D. Staggered spacing may become necessary to maintain pressure-tight joints. In such cases, a minimum gage of 2 diameters should be used, together with a pitch such that there is a minimum distance of 3 diameters between connectors.
- E. If a combination of members gives different efficiencies (e.g., a skin and corrugation combination fastened to a splice plate), the smallest of the efficiencies should be applied to all members in the combination.
- F. Highest plate efficiencies are obtained by using the maximum number of columns consistent with a value of R_e/λ_g equal to or less than .17.
- G. When the stress varies across the width of the joint, or when the hole pattern is not constant, the maximum stress for the critical representative width should be used with the efficiency as determined below for the critical width.
- H. This method provides for stress concentration effects at ultimate load, insofar as the connector holes are concerned, and no additional factor is necessary to provide for that phenomenon.

IV. Tension Efficiency

- A. Obtain p
- B. Obtain R_{12} as follows:
 - 1. For bolts, non-countersunk screws, and plain and dimpled rivets, use sheet thickness times actual hole diameter, if known; otherwise use sheet thickness times 1.05 times the nominal shank diameter.
 - 2. For 100° flush head fasteners, refer to Table I.

STRUCTURAL ANALYSIS MANUAL
GENERAL DYNAMICS/CONVAIR AND SPACE SYSTEMS DIVISION

IV. (Continued)

C. Obtain $D_{12} = \frac{R_{12}}{t}$

D. Obtain A_g , $\sum R_1$, and $\sum R_p$, considering the entire width of the joint. Use of a lesser width will result in too conservative efficiencies.

E. Obtain the effective reduction in area R_e from

$$R_e = \sum R_p - \frac{P}{5012} \left[\sum R_p - \sum R_1 \right]$$

or from the lower portion of Fig. 4.

F. The tension efficiency η of the plate based on gross area is given by

$$\eta = \left[1 - \left(\frac{R_e}{A_g} \right)^2 \right] \left[.88 - \frac{.18 R_{12}}{\sum R_p} \right]$$

$$\eta = \left[1 - \frac{R_e}{A_g} \right]$$

whichever is smaller, or from the upper portion of Fig. 4.

V. Margins of Safety

A. Tension Only

The margin of safety under an applied tension load (load normal to the joint centerline) is given by

$$M.S. = \frac{\eta F_{tu}}{P_t/A_g} - 1$$

$$= \frac{\eta F_{tu}}{f_t} - 1$$

where $f_t = P_t/A_g$ is the tension stress on the gross area.

STRUCTURAL ANALYSIS MANUAL
GENERAL DYNAMICS/CONVAIR AND SPACE SYSTEMS DIVISION

V. (Continued)

B. Shear Only

The margin of safety under an applied shear load (load parallel to the joint centerline) is given by

$$\begin{aligned} \text{M.S.} &= \frac{\eta F_{su}}{P_s/A_g} - 1 \\ &= \frac{\eta F_{su}}{f_s} - 1 \end{aligned}$$

where $f_s = P_s/A_g$ is the shear stress on the gross area.

C. Combined Tension and Shear

1. Obtain the tension stress ratio R_t and the shear stress ratio R_s from

$$\begin{aligned} R_t &= \frac{f_t}{\eta F_{tu}} \\ R_s &= \frac{f_s}{\eta F_{su}} \end{aligned}$$

2. The margin of safety of the plate at the joint in combined tension and shear is given by

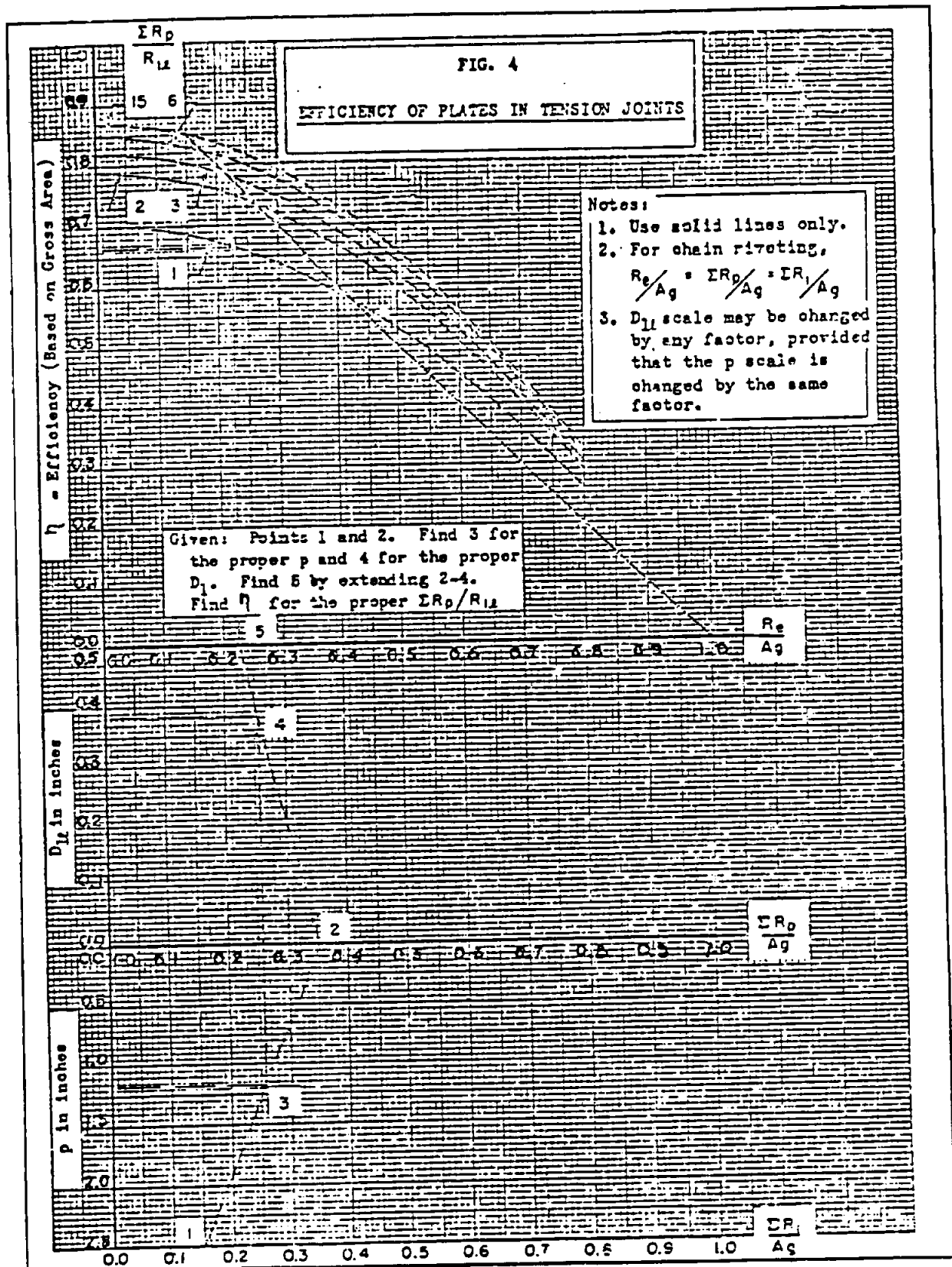
$$\text{M.S.} = \frac{1}{\sqrt{R_s^2 + R_t^2}} - 1$$

TABLE I

AREA REMOVED DUE TO DRILLING AND COUNTERSINKING FOR
100° FLUSH HEAD FASTENERS. (SQ. IN. PER FASTENER)

Fastener Head Style	Nominal Shank Dia. (Inches)	Sheet Thickness (Inches)											
		.025	.032	.040	.050	.063	.071	.080	.090	.100	.125	.160	.190
MS20426 (AN426) Rivet	1/16	.00213	.00260	.00314	.00381	.00468	.00522	.00582	.00649	.00716	.00883	.01118	.01319
	3/32	.00373	.00451	.00529	.00625	.00750	.00826	.00913	.01009	.01105	.01345	.01681	.01969
	1/8	.00563	.00694	.00829	.00977	.01146	.01248	.01364	.01493	.01621	.01942	.02392	.02778
	5/32	.00640	.00793	.00953	.01132	.01340	.01467	.01610	.01769	.01928	.02325	.02882	.03359
	3/16	.00808	.01008	.01221	.01467	.01751	.01907	.02079	.02270	.02461	.02938	.03607	.04180
	1/4	.01116	.01401	.01713	.02082	.02526	.02779	.03045	.03319	.03576	.04218	.05118	.05889
NAS517 Screw	#10 (.190)	.00678	.01097	.01333	.01607	.01927	.02104	.02286	.02479	.02673	.03156	.03834	.04414
	1/4	.01183	.01488	.01821	.02217	.02696	.02971	.03261	.03562	.03838	.04471	.05353	.06109
	5/16	.01501	.01894	.02329	.02852	.03496	.03872	.04277	.04705	.05108	.06013	.07124	.08072
	3/8	.01818	.02300	.02837	.03487	.04296	.04774	.05293	.05848	.06378	.07600	.09061	.10192
	7/16	.02316	.02707	.03345	.04122	.05056	.05676	.06309	.06991	.07648	.09188	.11093	.12495
Shear Type Lockbolt or Hi-Lok	3/16	.00687	.00853	.01028	.01226	.01472	.01624	.01794	.01984	.02173	.02647	.03310	.03879
	1/4	.00923	.01154	.01405	.01697	.02040	.02240	.02464	.02714	.02963	.03587	.04460	.05209
	5/16	.01122	.01410	.01724	.02096	.02543	.02798	.03079	.03391	.03703	.04483	.05575	.06511
	3/8	.01341	.01690	.02074	.02533	.03094	.03439	.03767	.04141	.04516	.05452	.06763	.07886

STRUCTURAL ANALYSIS MANUAL
GENERAL DYNAMICS/CONVAIR AND SPACE SYSTEMS DIVISION



STRUCTURAL ANALYSIS MANUAL
GENERAL DYNAMICS/CONVAIR AND SPACE SYSTEMS DIVISION

SECTION 15.0

ACOUSTICS, VIBRATION , FLUTTER

AN OVERVIEW OF ELEMENTARY STRUCTURAL DYNAMICS ANALYSIS METHODS IS PRESENTED IN THIS SECTION.

MORE COMPREHENSIVE DATA AND METHODS ARE CONTAINED IN THE STRUCTURAL DYNAMICS MANUAL

FOR SPECIFIC INFORMATION, CONSULT THE STRUCTURAL DYNAMICS GROUP.

		PAGE
15.1	LINEAR SYSTEMS	15.1.1
15.2	FORCED VIBRATION	15.2.1
15.3	METHODS OF CALCULATIONS	15.3.1
15.4	SONIC FATIGUE	15.4.1
15.5	FLUTTER	15.5.1
15.6	ACOUSTICS AND VIBRATION	15.6.1

STRUCTURAL ANALYSIS MANUAL

GENERAL DYNAMICS/CONVAIR AND SPACE SYSTEMS DIVISION

Data Source, Section 1.3 Reference 1

Acoustics and Vibrations

Practically all periodic waves, however complicated the form, may be considered as being composed of, or representing the sum of, two or more sine waves. Most waves may be analyzed into simple harmonic or sine wave components and these components generally form a harmonic series; i.e., they have frequencies which are integral multiples of the lowest frequency. The lowest frequency is called the fundamental, and the higher ones are called harmonics.

Frequency

The frequency of a vibrating body is the number of complete cycles of motion in a unit time.

Period

The period of a wave is the time elapsed while the motion repeats itself. It is simply the reciprocal of its frequency.

Amplitude

The amplitude of a wave is the maximum distance the vibrating particles of the medium in the path of the wave are displaced from their position of equilibrium.

Wavelength

The wavelength of a wave is the shortest distance between two particles along the wave which differ in phase by one cycle.

The Linear System With One Degree of Freedom

The number of independent coordinates necessary to describe the motion of a system is called degrees of freedom. Examples of systems possessing one, two, and many degrees of freedom are shown in Fig. 10.7.1-1.

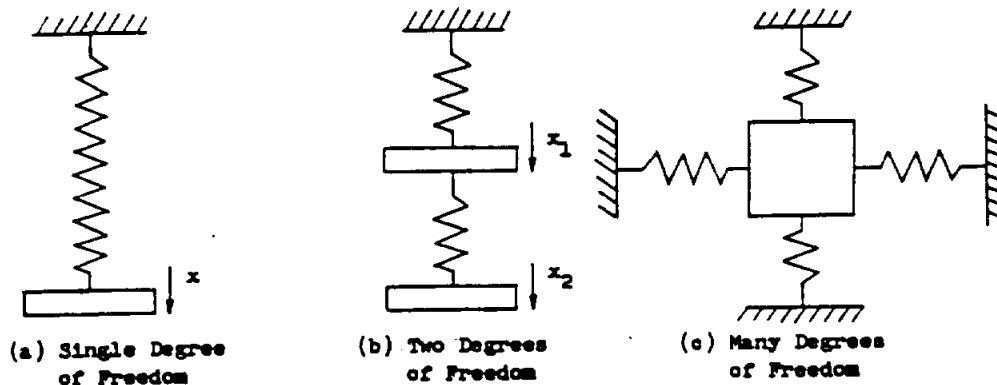


Fig. 10.7.1-1

The ideal vibratory system of one degree of freedom is represented in Fig. 10.7.1-2.

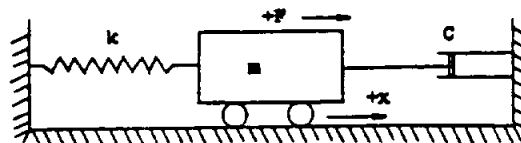


Fig. 10.7.1-2. Linear Vibratory System of One Degree of Freedom

STRUCTURAL ANALYSIS MANUAL
GENERAL DYNAMICS/CONVAIR AND SPACE SYSTEMS DIVISION

It consists of a mass "m" supported on frictionless and massless rollers attached to a spring and a dashpot. If a force "F" which is a function of time "t" acts on the mass, the differential equation,

$$m \frac{d^2 x}{dt^2} + C \frac{dx}{dt} + kx = F(t), \dots \dots \dots (1)$$

must be satisfied at all times,

where

- C is the coefficient of viscous damping,
- k is the spring constant,
- x is the displacement from rest, and
- F(t) is the external force varying with time.

If, after an initial disturbance of the system shown in Fig. 10.7.1-2, the external force ceases to act, the equation becomes

$$m \frac{d^2 x}{dt^2} + C \frac{dx}{dt} + kx = 0 \dots \dots \dots (2)$$

If $C^2/4m^2 > k/m$, the mass "m" will not oscillate but will gradually return to its rest position. If $C^2/4m^2 < k/m$, there will result a decaying oscillation of circular frequency,

$$\omega_n = \sqrt{k/m - C^2/4m^2} \text{ radians/sec., } \dots \dots (3)$$

for which the corresponding linear frequency will be

$$f_n = \frac{1}{2\pi} \sqrt{k/m - C^2/4m^2} \text{ cycles/sec., } \dots \dots (4)$$

where

"n" denotes natural frequency with damping,

and

$$\omega_n = 2\pi f_n \dots \dots \dots (5)$$

If $C^2/4m^2 = k/m$, this is the limiting case for no oscillation, and the system is said to be critically damped. This particular value of C is designated C_{cr} where

$$C_{cr} = 2m \sqrt{k/m} = 2 \sqrt{mk} = 2m\omega_n = 2k/\omega_n \dots \dots (6)$$

The solution of equation (2) for less than critical damping is

$$x = e^{-\frac{Ct}{2m}} (A \sin \omega_n t + B \cos \omega_n t) \dots \dots \dots (7)$$

where A and B are arbitrary constants depending on the initial conditions.

STRUCTURAL ANALYSIS MANUAL

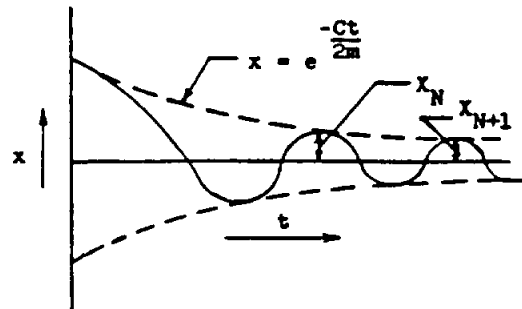
GENERAL DYNAMICS/CONVAIR AND SPACE SYSTEMS DIVISION

Data Source, Section 1.3 Reference 1

Fig. 10.7.1-3 shows x as a function of t for this case.

The amplitude decreases by a definite percentage with each cycle, and the natural logarithm of the ratio of two successive amplitudes is called the logarithmic decrement,

$$\delta = \log_e \frac{x_N}{x_{N+1}} ; \dots (8)$$



or, for an interval of ' q ' cycles

Fig. 10.7.1-3

separating the two measured amplitudes x_N and x_{N+q} .

$$\delta = \frac{1}{q} \log_e \frac{x_N}{x_{N+q}} \dots (9)$$

Also,

$$\delta = \frac{c}{m\omega_n} = \frac{2\pi c/c_{cr}}{\sqrt{1-(c/c_{cr})^2}} \dots (10)$$

For small damping

$$\delta \approx 2\pi(c/c_{cr}) \dots (11)$$

If there is no damping, $C = 0$, and the natural circular frequency is

$$\omega_n = \sqrt{k/m} = 2\pi f_n \dots (12)$$

Forced Vibration

If the driving force is sinusoidal

$[P(t) = P_0 \sin \omega t]$, Equation 10.7.1-(1) becomes

$$m \frac{d^2x}{dt^2} + c \frac{dx}{dt} + kx = P_0 \sin \omega t \dots (1)$$

where

P_0 is the maximum value of the sinusoidal force, and ω is the forced frequency.

The general solution to this equation is

$$x = e^{\frac{-Ct}{2m}} (A \sin \omega_n t + B \cos \omega_n t) + \frac{P_0 \sin (\omega t - \phi)}{(c\omega)^2 + (k - m\omega^2)^2} \dots (2)$$

STRUCTURAL ANALYSIS MANUAL

GENERAL DYNAMICS/CONVAIR AND SPACE SYSTEMS DIVISION

Data Source, Section 1.3 Reference 1

where

ϕ is the phase angle, and A and B are arbitrary constants depending on the initial conditions.

As before

$$\omega_n = \sqrt{k/m - \frac{c^2}{4m^2}} \quad \dots \dots \dots (3)$$

Also,

$$\phi = \tan^{-1} \frac{c\omega}{k - m\omega^2} \quad \dots \dots \dots (4)$$

The first term on the right hand side of equation (2) vanishes in time owing to the fact that the term, $e^{-Ct/2m}$, constantly diminishes and is called the transient term. The second term gives the amplitude of the forced vibration in terms of the system constants and driving force and is called the steady state term.

The amplitude of the steady-state vibration is

$$X = \frac{F_0}{\sqrt{(c\omega)^2 + (k - m\omega^2)^2}} \quad \dots \dots \dots (5)$$

This is also expressed in the convenient form,

$$X = \frac{F_0/k}{\sqrt{\left[1 - \left(\frac{\omega}{\omega_n}\right)^2\right]^2 + \left[2 \frac{c}{c_{cr}} \frac{\omega}{\omega_n}\right]^2}} \quad \dots \dots (6)$$

where

F_0/k is the displacement that would be produced by a static force, F_0 .

Basic Methods of Calculations

NOTE: The equations following are based on the simple beam theory and are accurate only for beams having a length to depth ratio of the order of 10 or more. The effects of rotary inertia and shear deflection are neglected.

Uniform Bar With Free Ends

The equations for finding the deflection for different mode patterns is as follows:

$$y = \frac{1}{2.04} \left[-\sin \alpha_n x + 1.02 \cos \alpha_n x - \sinh \alpha_n x + 1.02 \cosh \alpha_n x \right], \dots (1)$$

where α_n is the characteristic number for the n^{th} mode and is the root of the equation $\cos \alpha_n \cosh \alpha_n = 1$. The characteristic numbers for the first three modes of this beam are: 4.73, 7.853, and 10.996.

μ = mass per unit length

STRUCTURAL ANALYSIS MANUAL
GENERAL DYNAMICS/CONVAIR AND SPACE SYSTEMS DIVISION

Frequencies of higher modes for this beam are as follows:

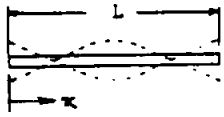
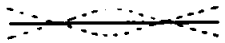
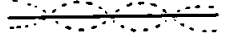
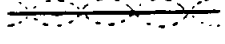
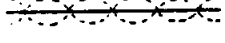
	Amplitude Profile	Mode	Natural Circular Frequency
		2 Nodes	$\omega_1 = \frac{22.4}{L} \sqrt{\frac{EI}{\mu}}$ (A)
		3 Nodes	$2.77 \omega_1$ (B)
		4 Nodes	$5.44 \omega_1$ (C)
		5 Nodes	$9.00 \omega_1$ (D)

Fig. 10.7.3-1

Uniform Bar With Simple Support at Ends

The equations of deflection for the fundamental mode is

$$y = \sin \frac{\pi x}{L} \dots \dots \dots (2)$$

if the amplitude is taken as unity at the center.

Frequencies of higher modes for this beam are as follows:

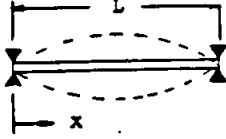
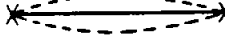
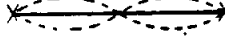
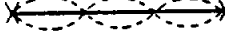
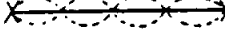
	Amplitude Profile	Mode	Natural Circular Frequency
		2 Nodes	$\omega_1 = \frac{\pi}{L^2} \sqrt{\frac{EI}{\mu}}$ (A)
		3 Nodes	$4 \omega_1$ (B)
		4 Nodes	$9 \omega_1$ (C)
		5 Nodes	$16 \omega_1$ (D)

Fig. 10.7.3-2

STRUCTURAL ANALYSIS MANUAL
GENERAL DYNAMICS/CONVAIR AND SPACE SYSTEMS DIVISION

Uniform Cantilever Beam

Frequencies of higher modes for this beam are as follows:

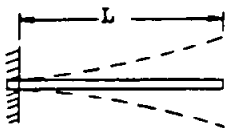
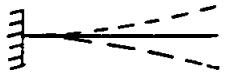
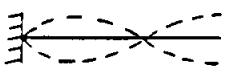
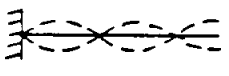
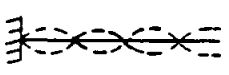
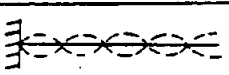
	Amplitude Profile	Mode	Natural Circular Frequency
		1 Nodes	$\omega_1 = \frac{.367\pi^2}{L^2} \sqrt{\frac{EI}{\mu}}$ (A)
		2 Nodes	$6.27 \omega_1$ (B)
		3 Nodes	$17.6 \omega_1$ (C)
		4 Nodes	$34.4 \omega_1$ (D)
		5 Nodes	$56.8 \omega_1$ (E)

Fig. 10.7.3-3

Uniform Beam With Clamped Ends

Frequencies of higher modes for this beam are as follows:

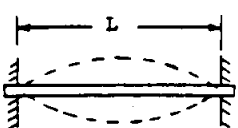
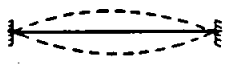
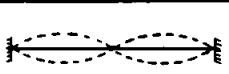
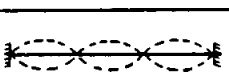
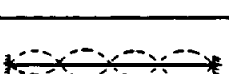
	Amplitude Profile	Mode	Natural Circular Frequency
		2 Nodes	$\omega_1 = \frac{22.4}{L^2} \sqrt{\frac{EI}{\mu}}$ (A)
		3 Nodes	$2.77 \omega_1$ (B)
		4 Nodes	$5.44 \omega_1$ (C)
		5 Nodes	$9.00 \omega_1$ (D)

Fig. 10.7.3-4

STRUCTURAL ANALYSIS MANUAL

GENERAL DYNAMICS/CONVAIR AND SPACE SYSTEMS DIVISION

Hinged Fixed Uniform Beam

Frequencies of higher modes for this beam are as follows:

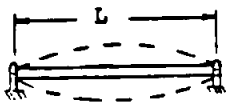
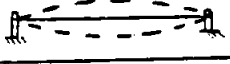
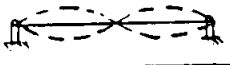
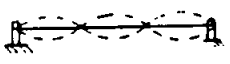
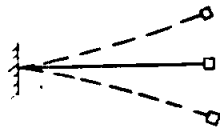
	Amplitude Profile	Mode	Natural Circular Frequency
		2 Nodes	$\omega_1 = \frac{15.4}{L^2} \sqrt{\frac{EI}{\mu}} \quad (A)$
		3 Nodes	$3.24 \omega_1 \quad (B)$
		4 Nodes	$6.76 \omega_1 \quad (C)$

Fig. 10.7.3-5

Uniform Cantilever Beam With Mass at the End



$$\omega_1 = 0.56\pi \sqrt{\frac{EI}{(m + \frac{33}{140}\mu L) L^3}} \quad (3)$$

Fig. 10.7.3-6

Uniform Beam With Simple Support at Ends and Concentrated Mass in the Center

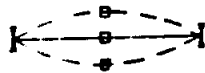


Fig. 10.7.3-7

$$\omega_1 = 2.2\pi \sqrt{\frac{EI}{(m + \frac{17}{35}\mu L) L^3}} \quad (4)$$

Rectangular Plates

A. Simple Support at Edges

$$\omega_1 = \pi^2 h \left(\frac{1}{a^2} + \frac{1}{b^2} \right) \sqrt{\frac{GE}{12(1-\mu^2)}} \quad (5)$$

The general formula is as follows:

$$\omega = \pi^2 h \left(\frac{M^2}{a^2} + \frac{N^2}{b^2} \right) \sqrt{\frac{GE}{12(1-\mu^2)}} \quad (6)$$

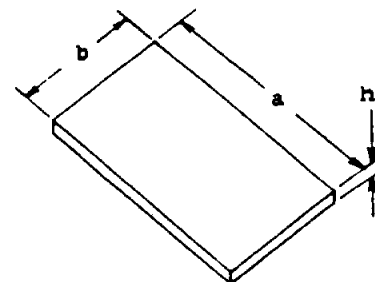


Fig. 10.7.3-8

STRUCTURAL ANALYSIS MANUAL

GENERAL DYNAMICS/CONVAIR AND SPACE SYSTEMS DIVISION

where M and N are integers depending on number of nodal lines.

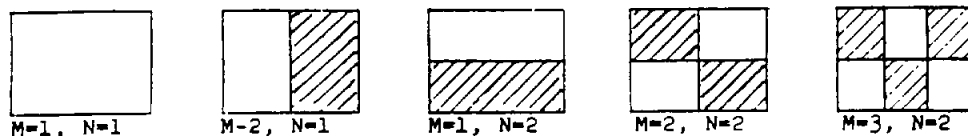


Fig. 10.7.3-9

(Normal Modes of Rectangular Membrane)

NOTE: Light areas are 180° out of time phase with shaded areas.

B. Clamped Edges

$$\omega_{1\text{steel}} = 164,000 \frac{\pi h}{ab} \sqrt{7\left(\frac{a^2}{b^2} + \frac{b^2}{a^2}\right) + 4} \dots (7)$$

Longitudinal or Axial Vibration of Uniform Beams or Shafts

A. Free Ends

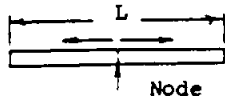


Fig. 10.7.3-10

The fundamental mode has a node in the middle. Higher modes are related by series of 1, 2, 3, etc.

$$\omega_1 = \frac{61.6}{L} \sqrt{E/\rho} \dots (8)$$

B. Both Ends Fixed

Same as above.

Columns - Effect of Axial Load on Natural Frequency

$$\omega_1 = \omega_0 \sqrt{1 - p/p_{cr}} \dots (9)$$

where p is the axial load,

p_{cr} is the Euler buckling load ($p_{cr} = \frac{\pi^2 EI}{L^2}$), and

ω_0 is the natural frequency for zero axial load.

For the pin-ended column ω_0 is given by ω_1 for a uniform bar with simple support at ends. For the fixed-end column ω_0 is given by ω_1 for a uniform beam with clamped ends.

STRUCTURAL ANALYSIS MANUAL

GENERAL DYNAMICS/CONVAIR AND SPACE SYSTEMS DIVISION

Stress and Strain in Vibrating Rectangular Plate

- Assume: 1. Perfectly elastic
 2. Homogeneous
 3. Isotropic
 4. Uniform thickness small compared to its other dimensions
 5. Deflections small compared to thickness
 6. No stretching of middle plane

Strain in thin layer of element indicated by shaded area and z distance from middle of plane is given by following equations:

$$\epsilon_{xx} = z/R_1 = -z \frac{\partial^2 \delta}{\partial x^2} \quad \dots \quad (10)$$

$$\epsilon_{yy} = z/R_2 = -z \frac{\partial^2 \delta}{\partial y^2} \quad \dots \quad (11)$$

$$\gamma_{xy} = -2z \frac{\partial^2 \delta}{\partial x \partial y} \quad \dots \quad (12)$$

ϵ_{xx} , ϵ_{yy} are unit elongations
 in the x and y directions.
 γ_{xy} is shear deformation in the xy plane.
 δ is deflection of the plate.

$1/R_1$, $1/R_2$ are curvatures in the xz and yz plane.

h = thickness of plate

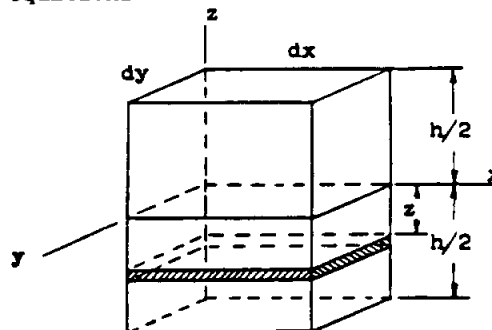


Fig. 10.7.3-11

The corresponding stress is then obtained from the following equations:

$$\sigma_x = E/(1-\mu^2) (\epsilon_{xx} + \mu \epsilon_{yy}) = \frac{-Ez}{1-\mu^2} \frac{\partial^2 \delta}{\partial x^2} + \mu \frac{\partial^2 \delta}{\partial y^2} \quad \dots \quad (13)$$

$$\sigma_y = E/(1-\mu^2) (\epsilon_{yy} + \mu \epsilon_{xx}) = \frac{-Ez}{1-\mu^2} \frac{\partial^2 \delta}{\partial y^2} + \mu \frac{\partial^2 \delta}{\partial x^2} \quad \dots \quad (14)$$

$$\tau = G \epsilon_{xy} = \left[\frac{-Ez}{(1+\mu)} \right] \frac{\partial^2 \delta}{\partial x \partial y} \quad \dots \quad (15)$$

where μ is Poisson's ratio.

STRUCTURAL ANALYSIS MANUAL

GENERAL DYNAMICS/CONVAIR AND SPACE SYSTEMS DIVISION

Data Source, Section 1.3 Reference 1

Factors Involved in the Design of Sonic Fatigue Resistant Structures

Although sonic fatigue life cannot be predicted with a great deal of accuracy, sonic testing of structures has revealed information which is of importance to the design engineer. It is possible to design sonic fatigue resistant structure.

Panel Size

Large unsupported panels should be avoided whenever possible. To accomplish this, stiffeners and ribs can be used effectively. From the standpoint of edge stress, a square section is much more effective than a rectangular shaped panel. The sonic fatigue life of a panel is a direct function of the stiffness and an inverse function of the vibrating mass. Therefore, any beef-up for this type of stress must increase the stiffness without significantly increasing the mass.

Plate Stringer

The boundaries of this type construction should be investigated critically. Any discontinuity irritates the fatigue problems. Attachment of ribs and stiffeners should be by means of symmetrical sections.

Chem-Milled Skin (Waffle Construction)

As previously stated, the boundaries should be critically investigated. The small ribs do offer stiffness but not enough to eliminate the use of intermediate supports. Care must be taken to make the radii of the reentrant corners of each cell as large as possible to reduce the concentration of stress.

Bonded Beaded Inner Skin

The edges must be critically investigated to insure proper tie-ins. Beads are frequently used over fairly large expanses of unsupported structure. These beads, however, are characterized by poor terminations. If large areas are unsupported, the panel will vibrate as one large diaphragm. This will cause cracks to form very rapidly because of the heavy working at the ends of the beads. The addition of a doubler at the end of each bead or a double ended bead could increase the life 50 to 100% more over that of the standard construction.

Honeycomb Construction

This is the best weight-wise structural approach to very high intensity sound. Again, the boundaries must be investigated to insure an adequate service life. This type of construction is fatigue resistant because of the large amount of structural damping.

Clips

All clips should be designed to provide continuity for all possible load paths. The gage of the clips should preferably be thicker than the lightest gage being connected and well riveted. It is advisable to reduce the bending stress in a clip or member being joined whenever possible.

STRUCTURAL ANALYSIS MANUAL
GENERAL DYNAMICS/CONVAIR AND SPACE SYSTEMS DIVISION

Stiffeners

All stiffeners should be designed using the rule of thumb that symmetrical attachments will prolong service life. Tests tend to indicate that the minimum gage of an aluminum stiffener should be .040 for intense sound pressure levels. Thicker gages will probably be necessary for each special case. One of the most critical regions of a stiffened panel is the change in stiffness at the end of a stiffener. This transition must be as gradual as possible with relatively low stresses in the fastener.

Curved Panels

The stresses in curved panels are much lower than in flat plates, if the plate width is more than a small percentage of the radius of curvature. This results from the pressure loads being carried as membrane stresses (like hoop tension) instead of by bending. Tests have indicated that the fatigue life due to curving a panel may be increased as much as 3,000 per cent.

Stress Concentrations

Anything that might possibly produce a stress raiser should be avoided. A majority of the failures due to sonic excitation can be attributed to stress concentrations at rivet holes, small bend radii, raw edges, reentrant corners, rough machine surfaces, etc. .

STRUCTURAL ANALYSIS MANUAL
GENERAL DYNAMICS/CONVAIR AND SPACE SYSTEMS DIVISION

REFERENCES

Acoustics and Vibrations

Goldbrick, R. T., A Vibration Manual for Engineers, Department of Commerce, 1957.

Myklestad, N. O., Vibration Analysis, McGraw-Hill, 1944.

STRUCTURAL ANALYSIS MANUAL
GENERAL DYNAMICS/CONVAIR AND SPACE SYSTEMS DIVISION

Data Source, Section 1.3 Reference 27

SYNOPSIS

Panel flutter is a self-excited, aeroelastic instability that may occur when a panel is exposed to a supersonic airstream. During flutter the panel oscillates in a direction normal to its plane and the amplitude of motion usually increases until limited by inplane stresses. The consequences of panel flutter cannot be reliably predicted, but the serious effects that have been encountered include very high noise levels within occupied compartments as well as panel failure due to fatigue.

A considerable amount of work, both experimental and theoretical, has been done during the last two decades not only to obtain insight into the phenomenon but to develop procedures for the prediction and prevention of panel flutter. This report presents the results of an extensive investigation to determine the state of the art in panel flutter, and from that basis, to formulate a comprehensive set of design criteria. The investigation consisted not only of literature review but also of personal consultation with individuals who have made significant contributions in the field. The report further brings together data from wind tunnel test, flight test, vibration test and theoretical investigation, and presents methods that have been developed to provide procedures, criteria, and guidelines for designing panels.

STRUCTURAL ANALYSIS MANUAL
GENERAL DYNAMICS/CONVAIR AND SPACE SYSTEMS DIVISION

Data Source, Section 1.3 Reference 4

ACOUSTICS AND VIBRATION

The development of structure adequate to sustain high acoustic loads is important to the basic airframe design. Although considerable engineering effort and investigation through testing have been devoted to the solution of the problem for individual aircraft, no rational, economical design method has appeared. General guidelines based on comparative test and service experience have been established and are presented along with a general discussion of sonic fatigue.

20.1 SONIC FATIGUE

To understand the problems created by sonic fatigue, it is necessary to be familiar with some of the fundamental acoustics concepts and the structure responses to sound. A sound is essentially a fluctuating pressure in air or some other medium. The intensity of a sound is determined by the amplitude of the pressure waves and is commonly expressed in decibels. The decibel rating or sound level is 10 times the logarithmic ratio of the intensity of the sound to a reference intensity, intensity being measured as power. For most purposes, the reference intensity has arbitrarily been set at 10^{-16} watts/cm², which is approximately the threshold of hearing. Expressed mathematically,

$$dB = 10 \log \frac{I_1}{I_0}$$

where:

I_1 = intensity of the sound

I_0 = reference sound intensity (threshold of hearing
= 10^{-16} watts/cm²)

The decibel level of a sound may be determined by its pressure fluctuation as follows:

$$dB = 20 \log \frac{P_1}{P_0}$$

where:

P_1 = the rms pressure fluctuation of sound in question

P_0 = the rms pressure fluctuation at the threshold of hearing (0.000204 dynes/cm²)

The pressure associated with a given decibel level is shown in Fig. 20.1-1. The peak-to-peak value of the alternating sound pressure is shown as well as the rms values. With the jet engines presently in use (145-170 dB), the airplanes are experiencing sonic fatigue failures as the pressures at these decibel levels are capable of exciting the structure well beyond the fatigue endurance limit of the material.

20.1.1 Sound Distribution Over Structure

Generally, the magnitude of the sonic noise is referred to in terms of sound pressure levels in decibels. The Acoustics unit normally provides estimates of sound pressure levels, in and around the aircraft structures, that are used in initial design of new structures. As powerplant information is firmed up, better design sound pressure levels are published; final confirmation is added during the early ground runs of the engines on the first aircraft. The design data usually takes the form of contour plots of the sound pressure levels. An example of the sound pressure levels on the lower extreme surface of the B-52 wing is shown in Fig. 20.1.1-1.

20.1.2 Response of Structures to Sonic Loading

When a structure is subjected to sonic loading, its vibrating frequency and amplitude are dependent on the structure and the intensity and frequency of the sound. The modern jet engine is a powerful source of random noise and produces essentially all frequencies within a range from 20 to 20,000 Hz. To analyze noise from jet engines, it is common practice to record the noise levels in the octave bands and thereby obtain a picture of the correspondence of frequencies and noise levels. Today, engines seem to distribute more noise energy in a frequency range of 150 to 600 Hz than in the higher or lower frequency ranges. A typical plot of the noise levels in the different octave bands and the total overall noise level is given in Fig. 20.1.2-1.

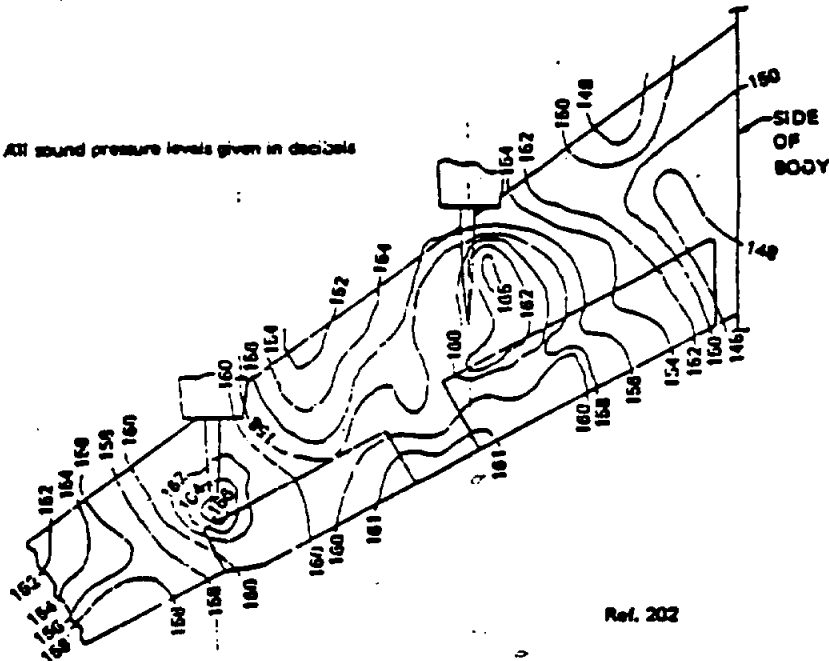
The response of a panel to random noise is somewhat unpredictable, but a typical response might be a resonant frequency vibration. The amplitude of this

STRUCTURAL ANALYSIS MANUAL

GENERAL DYNAMICS/CONVAIR AND SPACE SYSTEMS DIVISION

SOUND-LEVEL CONTOURS, B-52 LOWER WING EXTERIOR SURFACE (J57-P1 WET ENGINE)

NOTE: All sound pressure levels given in decibels

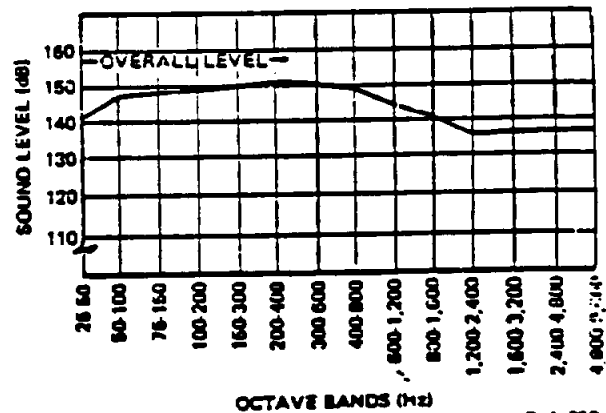


Ref. 202

FIGURE 20.1.1-1

vibration would be severely modulated, and there would be no repetition or pattern to the response. Although considerable engineering effort and testing expense have been devoted to determining the fatigue life of individual aircraft components, no rational, economical design method has appeared. Some attempts have been made to approximate a service life by considering the structural component as a simple damped-mass spring oscillator. A simple oscillator may be characterized by its resonant frequency ω_0 of the relative damping δ and the elastic response y_0 to some reference forcing input F_0 . The evaluation of δ , ω_0 , and y_0/F_0 along with a statistical description of the forcing function will provide a time history stress spectrum that can be summed by Miner's methods of accumulative damage to give a fatigue life (see Refs. 182 and 183). The Royal Aeronautical Society Engineering Sciences Data sheets also present an approximate analysis of sonic life for flat rectangular panels (Ref. 205).

SPECTRUM OF JET ENGINE NOISE AT MILITARY POWER



Ref. 207

FIGURE 20.1.2-1

STRUCTURAL ANALYSIS MANUAL

GENERAL DYNAMICS/CONVAIR AND SPACE SYSTEMS DIVISION

20.1.3 Sonic Testing

At the present time, the best design data has been compiled through extensive tests. The testing has taken three definite forms: testing of high-speed components for buffeting and flutter, behind and within a jet blast; testing of simulated panels behind a jet engine in a test cell; and testing of simulated panels in a sound chamber with a controlled sound source. The testing program, coupled with extensive service life experiences, has provided some design guidelines. Generally, the test results provide relative life data for variations in design details in riveted sheet structure up through fully bonded sandwich construction in metals as well as some plastics. Some of the early comparative test results are shown in Fig. 20.1.3-1.

20.2 GENERAL DESIGN RECOMMENDATIONS

The service experience and test programs from the B-52, KC-135, and commercial fleets have provided information that can be accepted as appropriate guidelines for structure in sonic areas. The following design charts may be used where sonic resistance is required. The sonic designs are not exact; however, their use should prevent gross errors. Boeing's design objective is minimum weight consistent with required life; this can be obtained only through close attention to details and optimistic design criteria to the extent that some failures are expected that may require redesign.

20.2.1 Bonded Honeycomb Panels

The design curves shown in Figs. 20.2.1-1, 20.2.1-2 and 20.2.1-3 give the maximum allowable sound pressure level to which the described panel can be subjected for a 300-hr serviceable life period. The service experience of present jet aircraft have shown that a panel, designed for 300 hr of maximum engine output noise, provides a total service life adequate for today's requirements. The curves are all plotted for square panels; the correction factors for rectangular panels are given in Fig. 20.2.1-4.

20.2.2 Stiffener-Supported Web and Skin Panels

The design curves shown in Fig. 20.2.2-2 for the panels described in Fig. 20.2.2-1, give the maximum

allowable sound pressure level to which the panel can be subjected for a 300-hr serviceable life period. The service experience of present jet aircraft has shown that a panel, designed for 300 hr of maximum engine output noise provides a total service life adequate for today's requirements. The curves are plotted for square panels; the correction factors for rectangular panels are given in Fig. 20.2-7.

20.2.3 General Design Tips

Applicable to the Design Charts

- All the design curves for aluminum material represent 2024-T3; 7075-T6 may be used if the panels are overdesigned by 2 dB.
- The edges of all webs and cutouts are assumed to be machined, except (1) edges may be sheared in "O" condition prior to heat treat or (2) edges may be sheared in heat-treated condition provided the area is overdesigned by 6 dB.
- Countersinks with knife edges are allowed only when the area is overdesigned by 6 dB. Laminated sheet may have a knife edge at the internal laying surface with no penalty in decibel level.
- When dimpling is used, an overdesign of 8 dB is required.
- When spotwelds are used, an overdesign of 14 dB is required.
- Holes in webs with diameters under 0.25b are allowed if the hole is reinforced with a doubler or the area is overdesigned by 3 dB. Overdesign by only 1 dB is required if the hole is flanged. Small holes filled with tight rivets do not require any reinforcement or overdesign.
- Holes or cutouts in webs with diameters over 0.25b require the addition of stiffeners on each side of the hole or an overdesign by 6 dB; only 4 dB overdesign is necessary if the hole is flanged.
- When using bead-type stiffeners, curves for design B (see Figs. 20.2.2-1 and 20.2.2-2) are applicable with the addition of a 4-dB overdesign; however, the addition of beads to a particular design will have an improvement limited to 5 dB above the same design without beads.

STRUCTURAL ANALYSIS MANUAL
GENERAL DYNAMICS/CONVAIR AND SPACE SYSTEMS DIVISION

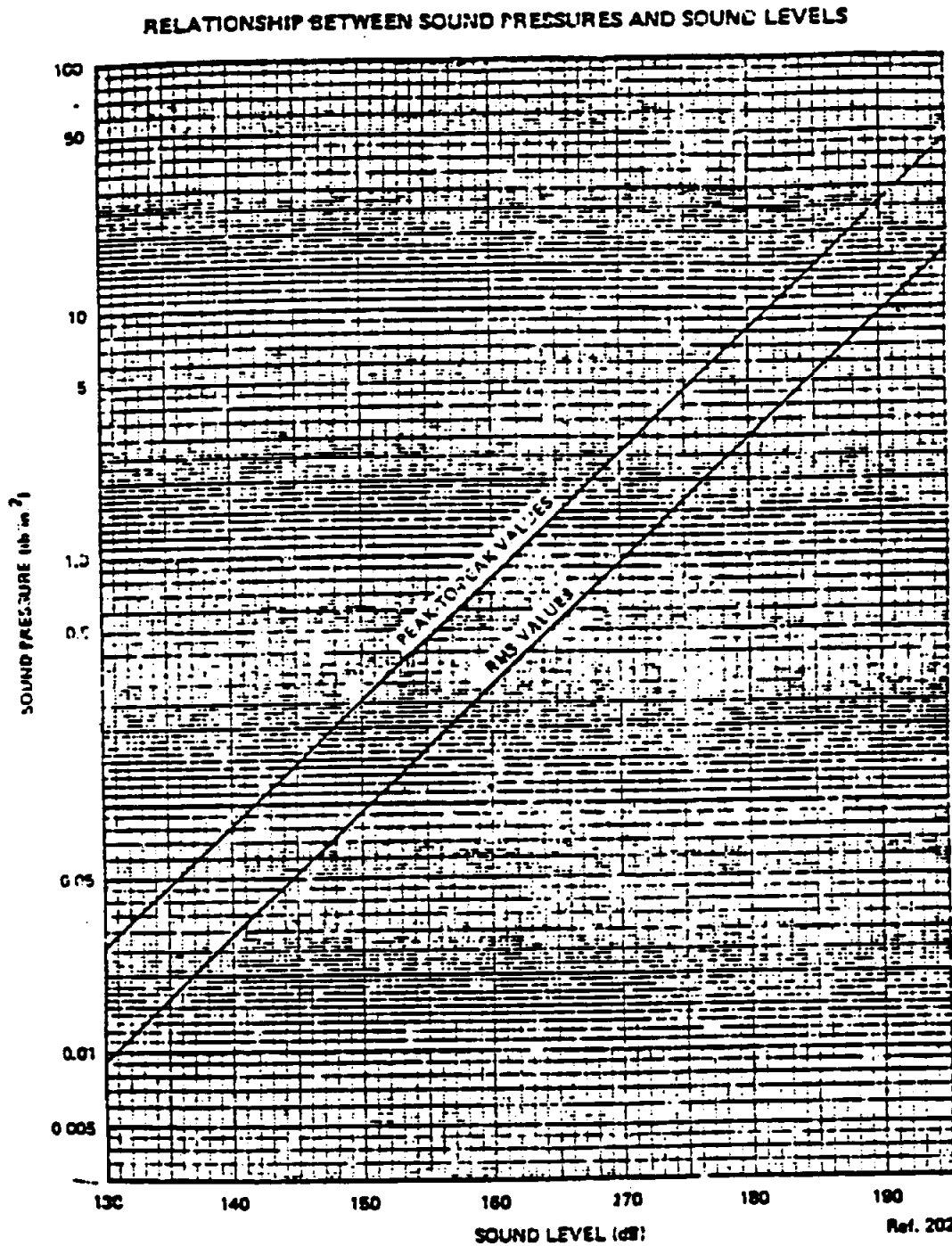
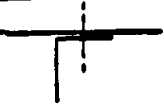






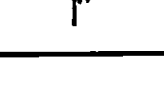


FIGURE 20.1-1

STRUCTURAL ANALYSIS MANUAL
GENERAL DYNAMICS/CONVAIR AND SPACE SYSTEMS DIVISION

LIFE OF B-52 FLAP SONIC TEST PANELS

Configuration	Attachment	Test Time at Various dB Levels					Failure
		150 dB	160 dB	163 dB	167 dB	170 dB	
	0.04 skin and pressed rib; 5/32 CSK rivets	53 sec	17 sec	-	-	-	Skin crack
	0.04 skin doubler & pressed rib; Metalbonded doubler; 5/32 CSK rivets	3 min 54 sec	3 min 7 sec	-	-	-	Skin & rib crack
	0.04 skin doubler, pressed rib & angle; Metalbonded doubler; 5/32 CSK rivets	-	25 min 5 sec	-	-	-	Rib crack
	0.04 skin, doubler & pressed rib; Metalbonded doubler & rib; 5/32 CSK rivets	-	8 min 10 sec	-	-	-	Skin crack
	0.04 skin, doubler, pressed rib & angle; Metalbonded doubler, rib & angle; 5/32 rivets	-	< 50 min	1 min 3 sec	35 sec	23 sec	Skin crack
	0.04 skin, doubler, pressed rib & angle; Shell 422 bond doubler, rib & angle; 5/32 rivets	-	> 50 min.	-	-	-	None
	0.02 skins; 0.04 doubler pressed angles & webs; Metalbonded skin laminate doubler & angle; 5/32 rivets	-	-	-	-	1 min 30 sec	Skin crack
	0.02 skins; 0.04 doubler, pressed angles & webs; Shell 422 bonded skin laminate doubler & angle; 5/32 rivets	-	-	-	-	15 sec	Skin crack

Metalbond is BMS 5-18
Shell 422 is BMS 5-17
Above test times are averages of several specimens

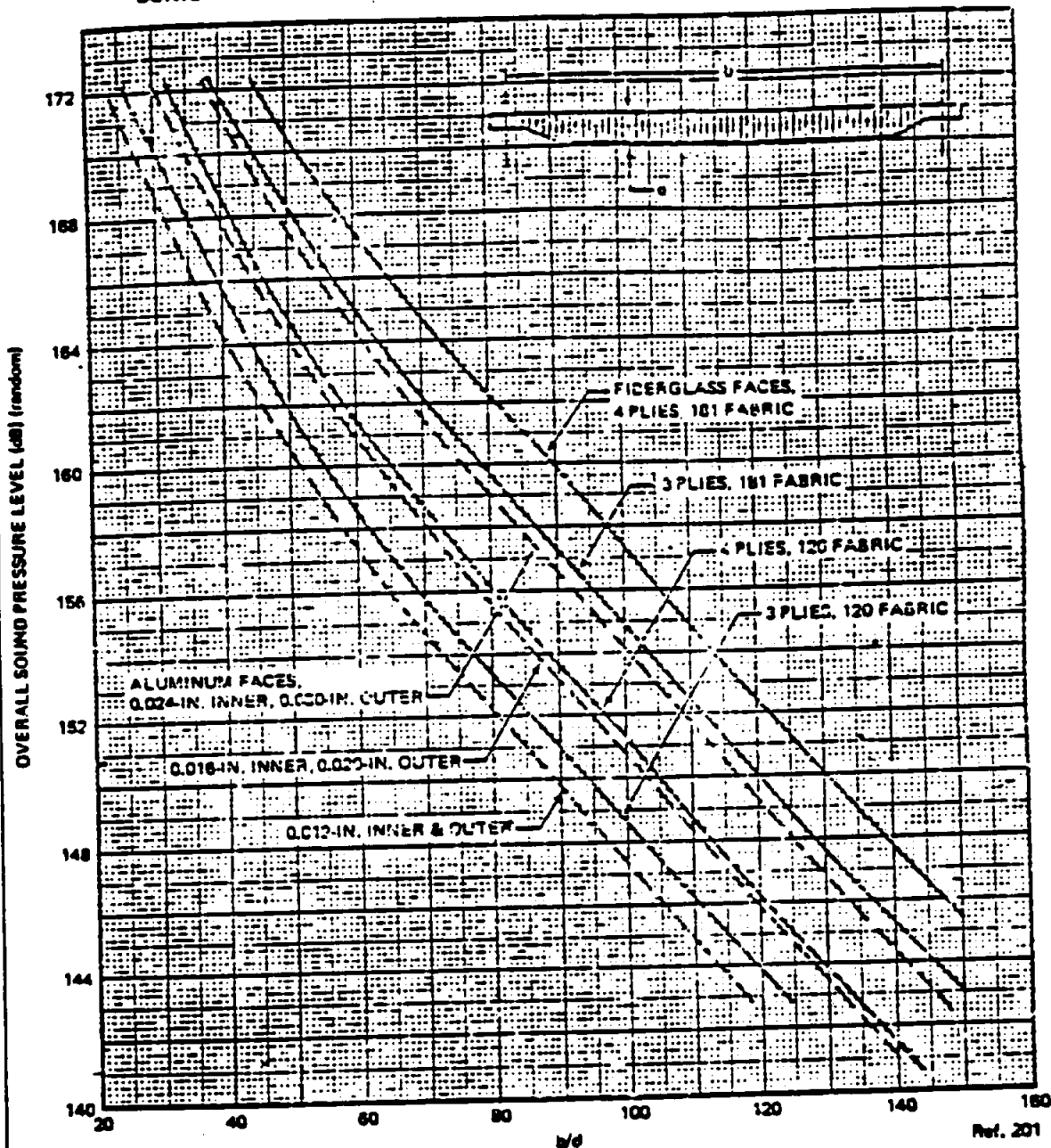
Ref. 202

FIGURE 20.1.3-1

195

STRUCTURAL ANALYSIS MANUAL
GENERAL DYNAMICS/CONVAIR AND SPACE SYSTEMS DIVISION

SONIC FATIGUE DESIGN CRITERIA FOR BONDED HONEYCOMB PANELS

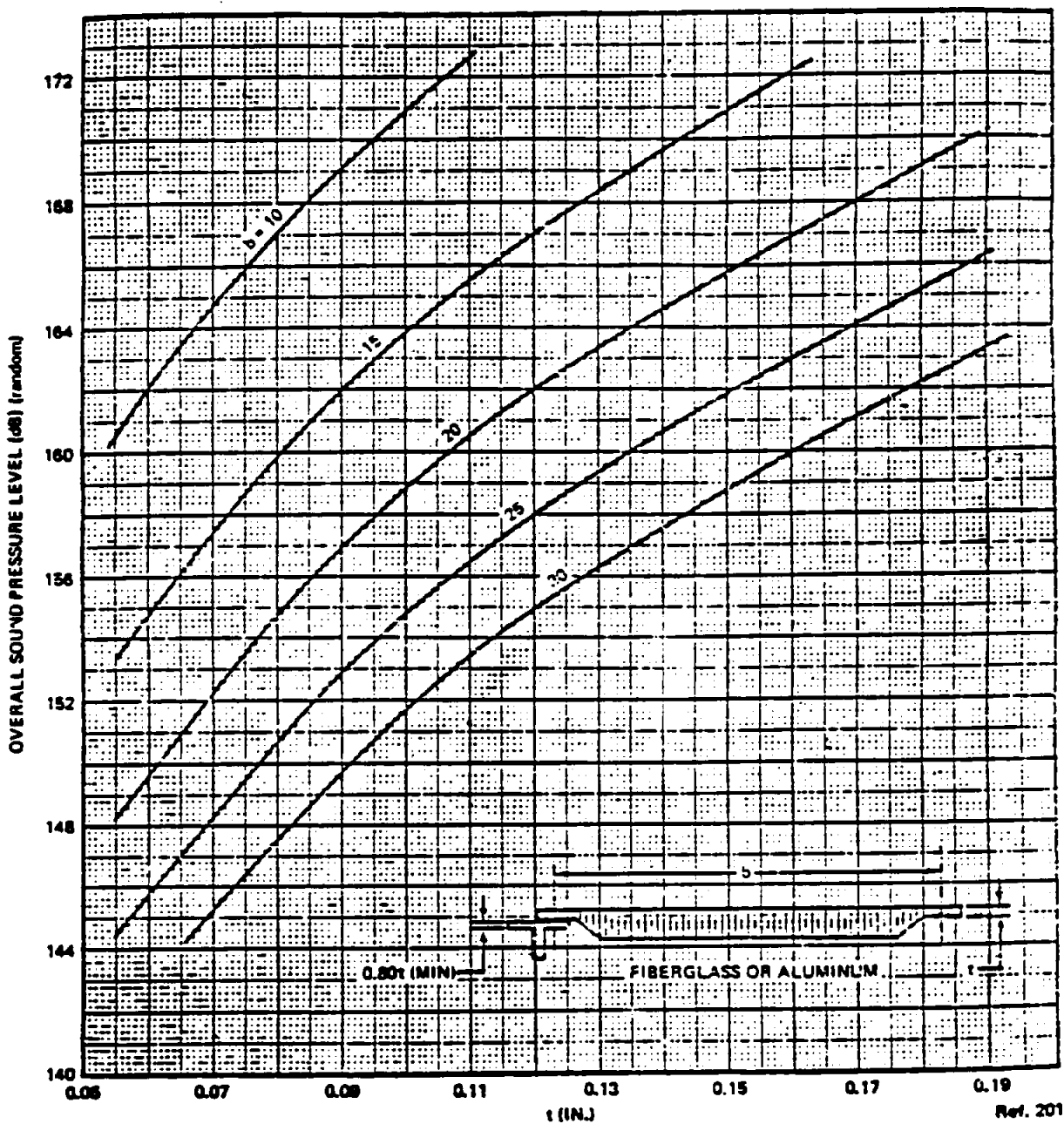


NOTE: Curves are for square panels; see Fig. 20.2.1-4 for corrections with rectangular panels.

FIGURE 20.2.1-1

STRUCTURAL ANALYSIS MANUAL
GENERAL DYNAMICS/CONVAIR AND SPACE SYSTEMS DIVISION

SONIC FATIGUE DESIGN CRITERIA FOR BONDED HONEYCOMB PANEL EDGE

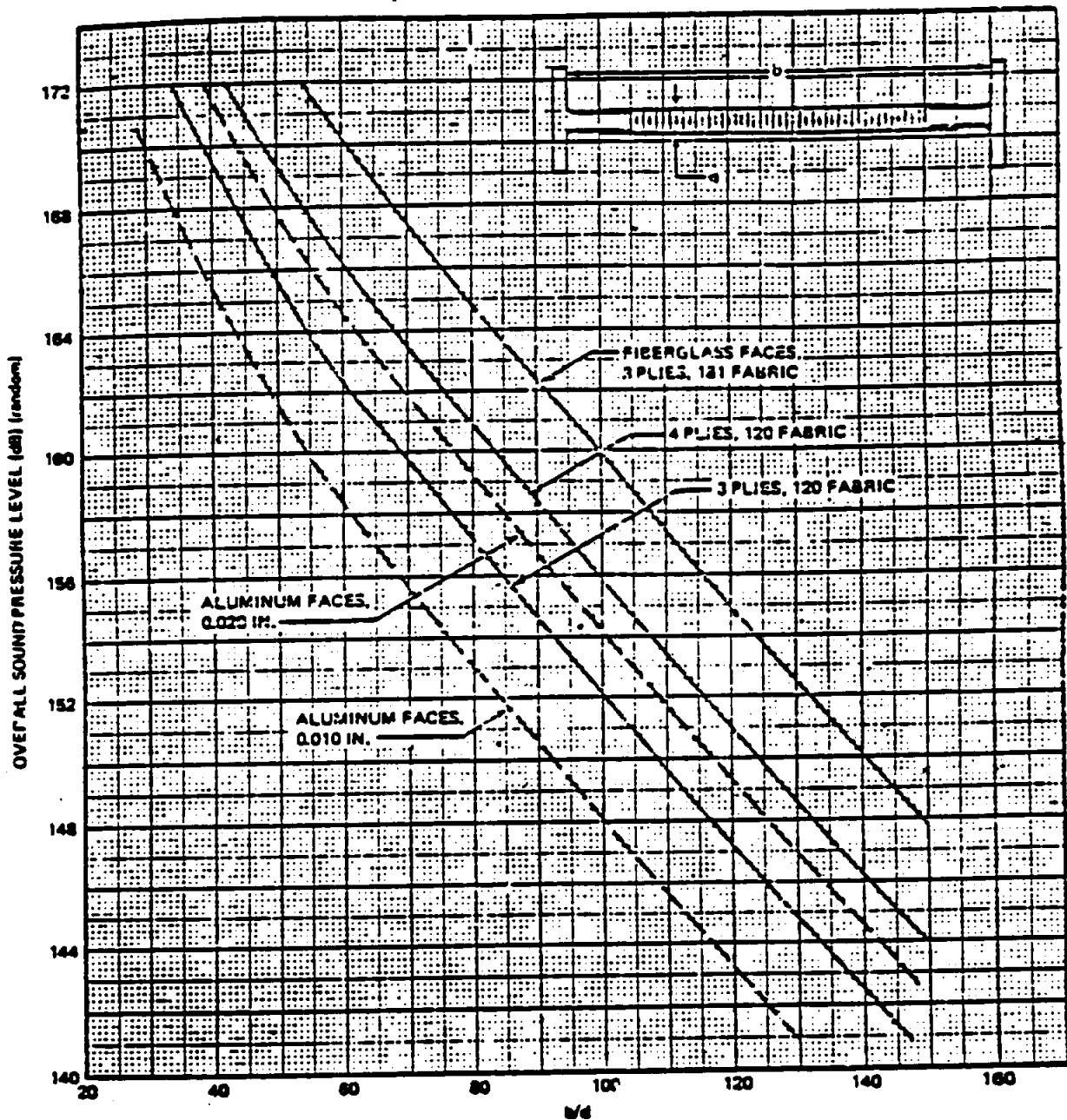


NOTE: Curves are for square panels; see Fig. 20.2.1-4 for corrections with rectangular panels.

FIGURE 20.2.1-2

STRUCTURAL ANALYSIS MANUAL
GENERAL DYNAMICS/CONVAIR AND SPACE SYSTEMS DIVISION

SONIC FATIGUE DESIGN CRITERIA FOR BONDED HONEYCOMB WEBS

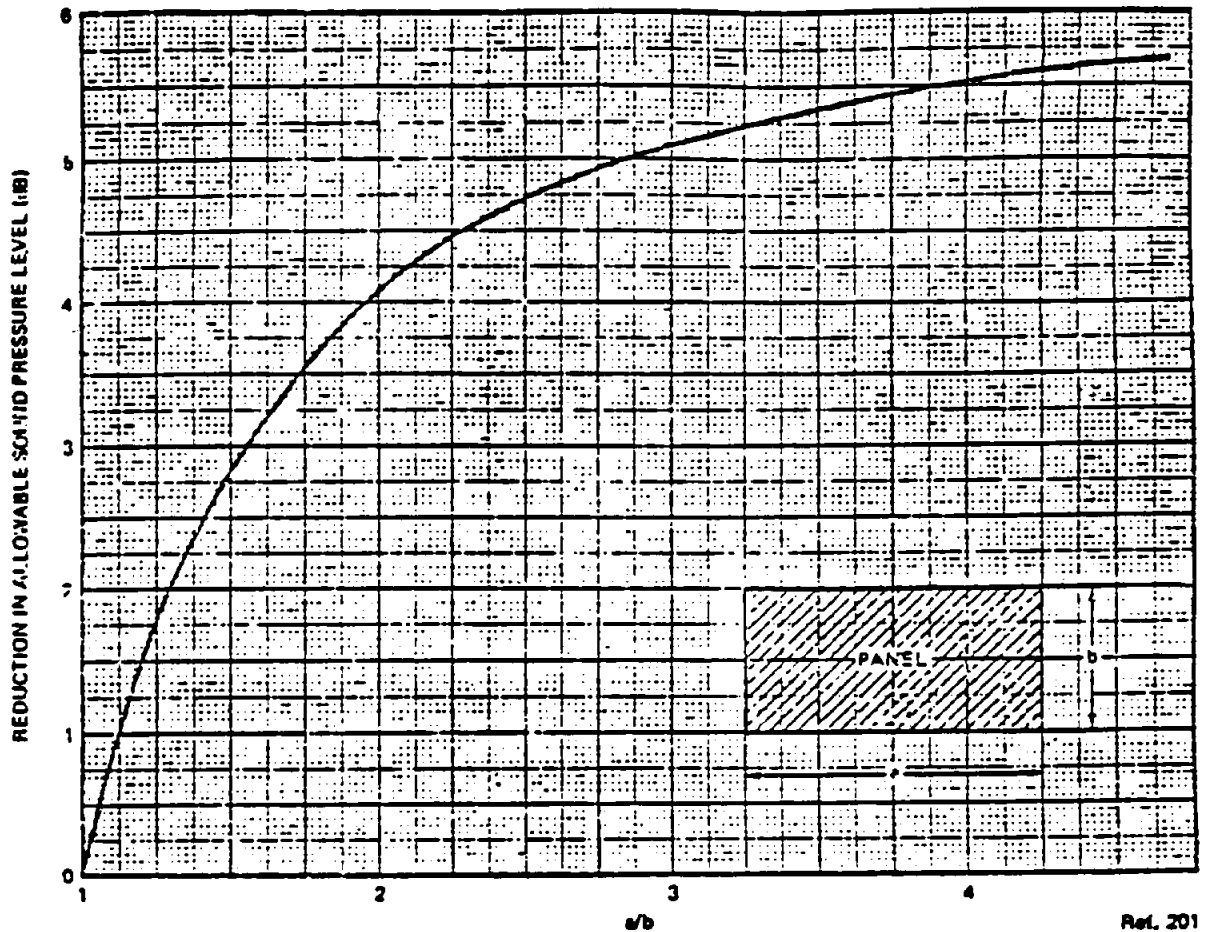


NOTE: Curves are for square panels; see Fig. 20.2.1-4 for corrections with rectangular panels.

FIGURE 20.2.1-3

STRUCTURAL ANALYSIS MANUAL
GENERAL DYNAMICS/CONVAIR AND SPACE SYSTEMS DIVISION

CORRECTION FACTOR FOR RECTANGULAR PANELS

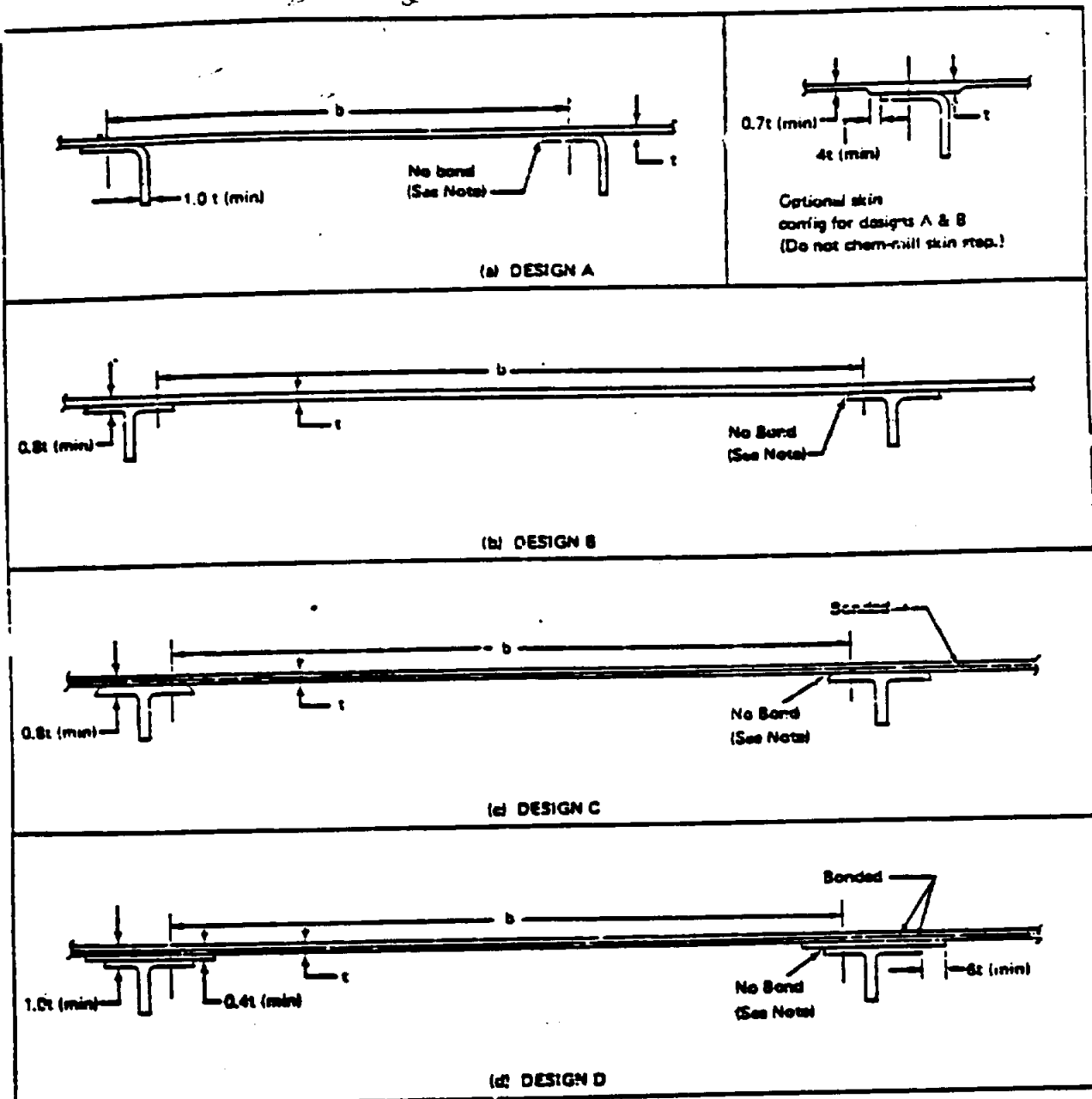


NOTE: Use this curve to correct results from Figs. 20.2.2-1, 20.2.2-2, and 20.2.2-3 when panels are not square.

FIGURE 20.2.1-4

STRUCTURAL ANALYSIS MANUAL **GENERAL DYNAMICS/CONVAIR AND SPACE SYSTEMS DIVISION**

SONIC FATIGUE DESIGN CRITERIA FOR STIFFENER-SUPPORTED WEB AND SKIN PANELS



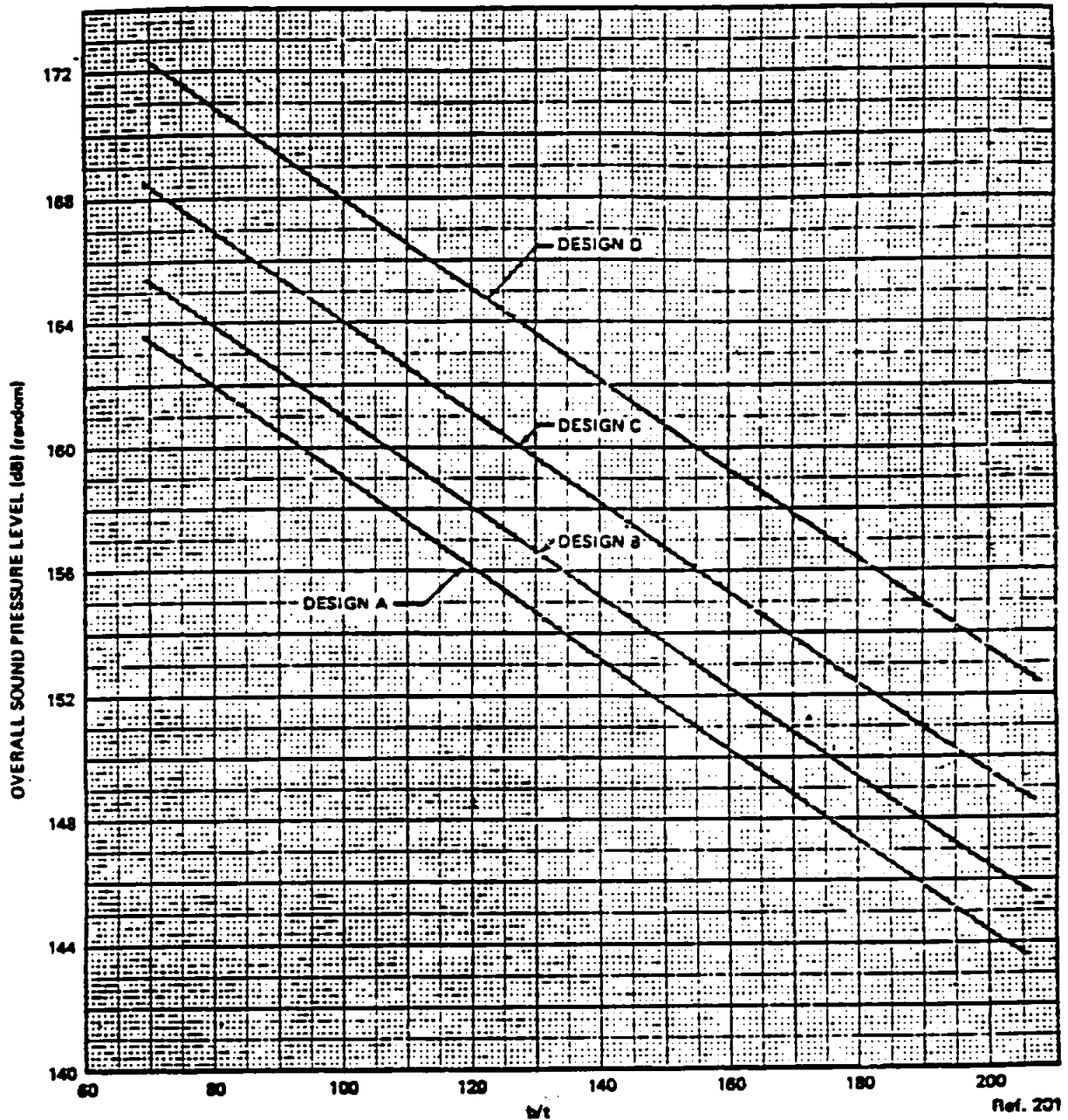
NOTE: Curves are for no bond; if bonded in addition to fasteners, increase allowable 2 dB

Ref. 2C1

FIGURE 20.2.2-1

STRUCTURAL ANALYSIS MANUAL
GENERAL DYNAMICS/CONVAIR AND SPACE SYSTEMS DIVISION

SONIC FATIGUE DESIGN CRITERIA—STIFFENER-SUPPORTED SKIN AND WEB PANELS

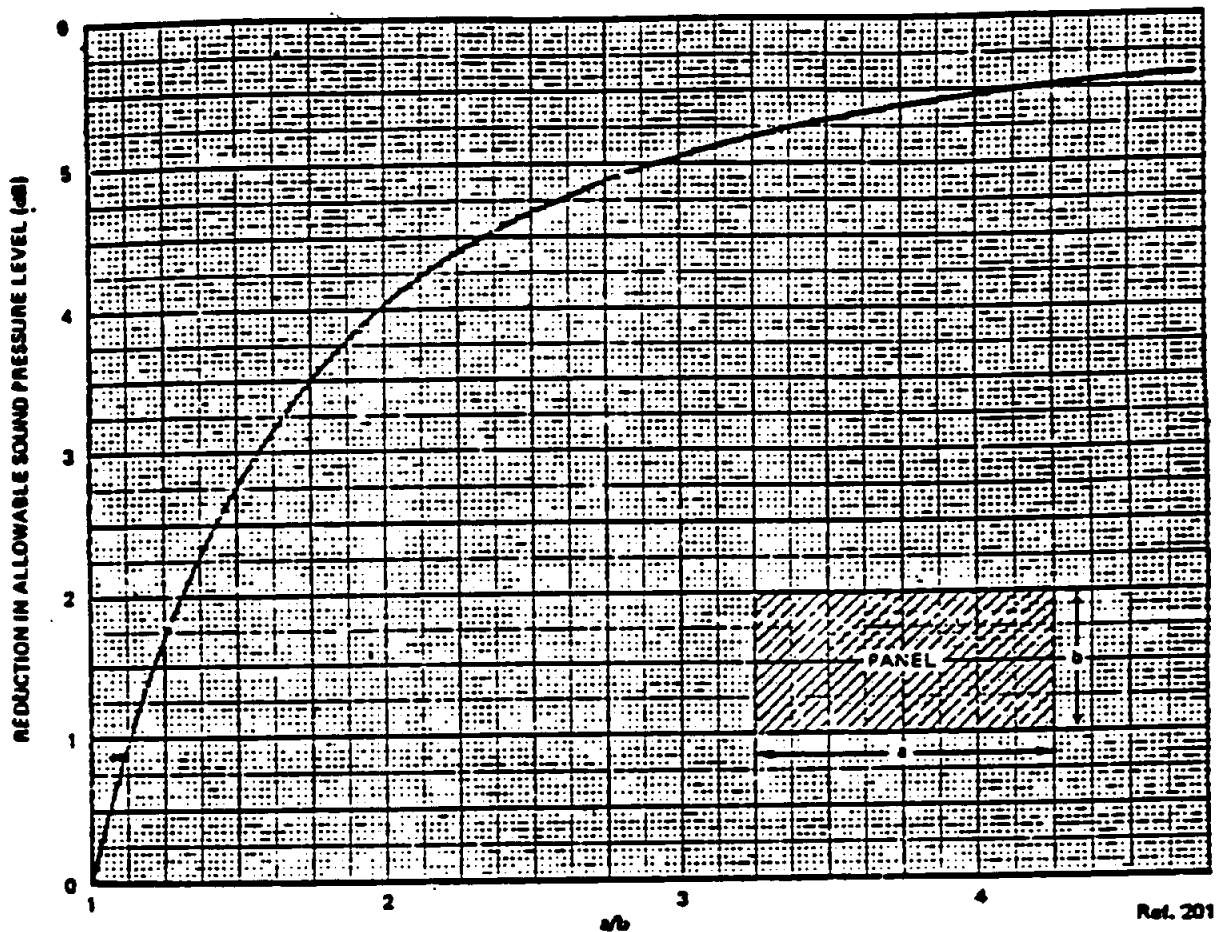


NOTE: Curves are for square panels; corrections for rectangular panels are shown in Fig. 20.2.2-1.

FIGURE 20.2.2-2

STRUCTURAL ANALYSIS MANUAL
GENERAL DYNAMICS/CONVAIR AND SPACE SYSTEMS DIVISION

CORRECTION FACTOR FOR RECTANGULAR PANELS



NOTE: Use this curve to correct results from Fig. 20.2.2-2 when panels are not square.

FIGURE 20.2.3

STRUCTURAL ANALYSIS MANUAL
GENERAL DYNAMICS/CONVAIR AND SPACE SYSTEMS DIVISION

SECTION 16.0

EXPERIMENTAL STRESS ANALYSIS

EXPERIMENTAL METHODS OF DETERMINING STRESSES IN A STRUCTURE
ARE PRESENTED IN THIS SECTION

	PAGE
16.1 STRAIN GAGE	16.1.1

STRUCTURAL ANALYSIS MANUAL

GENERAL DYNAMICS/CONVAIR AND SPACE SYSTEMS DIVISION

Data Source, Section 1.3 Reference 1

Stress Determination From Strain Measurements

The object of experimental stress analysis is to determine the stress distribution in a structure from strain measurement. If the directions of the principal stresses are known, only two strain measurements are required. It can be shown by Hooke's law that if the directions are known, the stresses can be obtained by making use of the following formulas:

$$\sigma_1 = \frac{E}{1-\mu^2} (\epsilon_1 + \mu \epsilon_2) \dots \dots \dots (1)$$

$$\sigma_2 = \frac{E}{1-\mu^2} (\epsilon_2 + \mu \epsilon_1) \dots \dots \dots (2)$$

where μ = Poisson's Ratio

σ_1 = Principal stress in one direction

σ_2 = Principal stress at right angles to σ_1

ϵ_1 = Strain in the direction of σ_1

ϵ_2 = Strain in the direction of σ_2

E = Modulus of elasticity

The maximum shearing stress will occur at 45° to the principal stresses and is found as follows:

$$\tau_{\max.} = \frac{E}{2(1+\mu)} (\epsilon_1 - \epsilon_2) \dots \dots \dots (3)$$

τ = Shear Stress

If the direction of the principal stresses are unknown, the problem is somewhat more complicated. Consider the axes shown in Fig. 10.9.3-8.

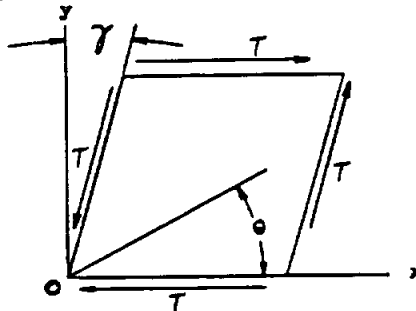


Fig. 10.9.3-8

The general equation for strain at angle θ with the results from a 45° rosette is as follows:

$$\epsilon_\theta = \frac{\epsilon_x + \epsilon_y}{2} + \frac{\epsilon_x - \epsilon_y}{2} \cos 2\theta + \frac{\gamma_{xy}}{2} \sin 2\theta \dots (4)$$

where γ_{xy} = the shearing strain.

204

STRUCTURAL ANALYSIS MANUAL
GENERAL DYNAMICS/CONVAIR AND SPACE SYSTEMS DIVISION

In Fig. 10.9.3-9, the strains measured along the (A), (B), and (C) axes can be used to calculate the principal stresses which act along axes (1) and (2). When a 45° rosette is used, the strain along (B) is measured on an axis at an angle of 45° to the (A) and (C) axes. The angles (AOB) and (BOC) are 45°. Axis (2) is at an angle of 90° to axis (1). The strains along axes (A), (B), and (C) will have the following relationships with the (x) and (y) axes of Fig. 10.9.3-8

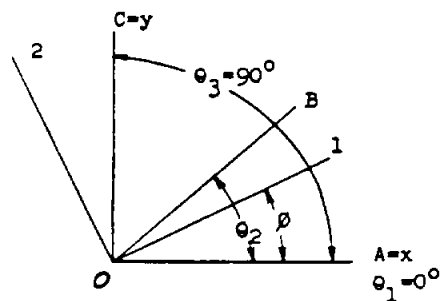


Fig. 10.9.3-9

$$\epsilon_A = \frac{\epsilon_x + \epsilon_y}{2} + \frac{\epsilon_x - \epsilon_y}{2} = \epsilon_x \quad \dots \quad (5)$$

$$\epsilon_B = \frac{\epsilon_x + \epsilon_y}{2} + \frac{\gamma_{xy}}{2} \quad \dots \quad (6)$$

$$\epsilon_C = \frac{\epsilon_x + \epsilon_y}{2} - \frac{\epsilon_x - \epsilon_y}{2} = \epsilon_y \quad \dots \quad (7)$$

or,

$$\epsilon_x = \epsilon_A \quad \dots \quad (8)$$

$$\epsilon_y = \epsilon_C \quad \dots \quad (9)$$

$$\gamma_{xy} = 2\epsilon_B - (\epsilon_A + \epsilon_C) \quad \dots \quad (10)$$

By using the equation for maximum shear and Hooke's law, the principal stresses can be obtained from the following formulas.

$$\sigma_1 = \frac{E}{2} \left[\frac{\epsilon_A + \epsilon_C}{1 - \mu} + \frac{1}{1 + \mu} \sqrt{2(\epsilon_A - \epsilon_B)^2 + 2(\epsilon_B - \epsilon_C)^2} \right] \quad \dots \quad (11)$$

$$\sigma_2 = \frac{E}{2} \left[\frac{\epsilon_A + \epsilon_C}{1 - \mu} - \frac{1}{1 + \mu} \sqrt{2(\epsilon_A - \epsilon_B)^2 + 2(\epsilon_B - \epsilon_C)^2} \right] \quad \dots \quad (12)$$

$$\tau_{max} = \sigma \sqrt{2(\epsilon_A - \epsilon_B)^2 + 2(\epsilon_B - \epsilon_C)^2} \quad \dots \quad (13)$$

$$\theta = \frac{1}{2} \tan^{-1} \left[\frac{\pm 2(\epsilon_B - \epsilon_A - \epsilon_C)}{\pm (\epsilon_A - \epsilon_C)} \right] \quad \dots \quad (14)$$

With the fundamental equations and the solution of the 45° rosette, expressions for other angles may be obtained.

Mohr's Circle

The use of Mohr's circle is very helpful in the reduction of strain gage data. It is a convenient graphical solution, especially if the strain is measured at angles of 45°.

STRUCTURAL ANALYSIS MANUAL

GENERAL DYNAMICS/CONVAIR AND SPACE SYSTEMS DIVISION

The 45° or Rectangular Strain Rosette

Mohr's circle is constructed so that the vertical axis represents shear strain and the horizontal axis represents the axial strains. The axial strains measured by the 45° rosette are plotted on the horizontal axis. The center "C" will always be midway between ϵ_a and ϵ_c . (Ref. Fig. 10.9.3-10)

$$OC = \frac{\epsilon_a + \epsilon_c}{2} \dots \dots \dots (15)$$

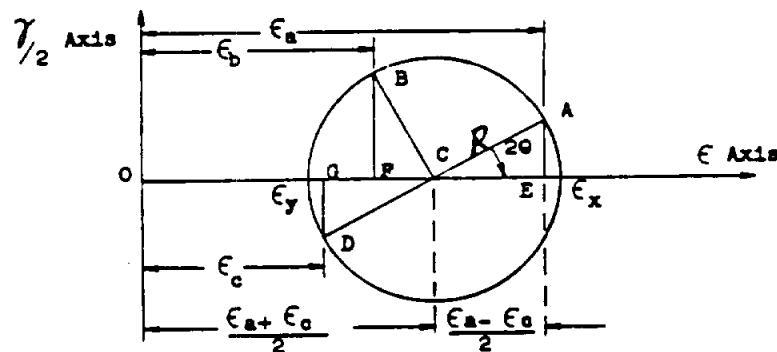


Fig. 10.9.3-10

Point "A" can then be located since triangles CBP and CAE are congruent and $AE = CP$. Since ϵ_a , ϵ_b , and ϵ_c are 45° apart, the radii CA, CB, and CD will be 90° apart. The radius, R, can be obtained as follows:

$$R = \sqrt{(CE)^2 + (AE)^2} \dots \dots \dots (16)$$

where

$$CE = \frac{\epsilon_a - \epsilon_c}{2} \dots \dots \dots (17)$$

$$AE = \frac{\epsilon_a + \epsilon_c}{2} - \epsilon_b \dots \dots \dots (18)$$

From the geometry of the circle,

$$AE = OC - \epsilon_b, \dots \dots \dots (19)$$

$$\left. \begin{aligned} \epsilon_x &= OC + R, \\ \epsilon_y &= OC - R, \end{aligned} \right\} \text{Principal Strains} \dots \dots \dots (20)$$

$$\dots \dots \dots (21)$$

and

$$2\theta = \tan^{-1} \frac{AE}{CE} \dots \dots \dots (22)$$

2060

STRUCTURAL ANALYSIS MANUAL
GENERAL DYNAMICS/CONVAIR AND SPACE SYSTEMS DIVISION

EXAMPLE: Assume that the three strains from a 45° rosette are

$$\epsilon_a = 700 \text{ at } 0^\circ, \quad \epsilon_b = 400 \text{ at } 45^\circ, \text{ and } \quad \epsilon_c = 300 \text{ at } 90^\circ,$$

expressed in micro-inches per inch. Find the principal strains and principal axes of strain and compute the principal stresses if

$$E = 30 \times 10^6 \text{ psi and } \mu = 0.3.$$

First, locate the center of the circle, which is at a distance

$$OC = \frac{\epsilon_a + \epsilon_c}{2} = \frac{700 + 300}{2} = 500 \quad \text{to the right of the origin. Compute the}$$

radius, R , from the right triangle whose sides are

$$CE = \frac{\epsilon_a - \epsilon_c}{2} = \frac{700 - 300}{2} = 200 \quad \text{and}$$

$$AE = OC - \epsilon_b = 500 - 400 = 100. \quad \text{Therefore,}$$

$$R = \sqrt{(200)^2 + (100)^2} = 224$$

and

$$2\theta = \tan^{-1} \frac{AE}{CE} = \frac{100}{200} = 26.6^\circ.$$

The direction of the maximum principal strain, ϵ_x , is $\theta = 13.3^\circ$ clockwise with respect to the direction of ϵ_a .

$$\text{The principal strains are } \epsilon_x = OC + R = 500 + 224 = 724$$

$$\text{and } \epsilon_y = OC - R = 500 - 224 = 276.$$

From Eq. (1) and Eq. (2), the principal stresses are

$$\sigma_x = \frac{E(\epsilon_x + \mu\epsilon_y)}{1 - \mu^2} = \frac{(30 \times 10^6)(724 + 0.3 \times 276)10^{-6}}{1 - (0.3)^2} = 26,600 \text{ psi}$$

and

$$\sigma_y = \frac{E(\epsilon_y + \mu\epsilon_x)}{1 - \mu^2} = \frac{(30 \times 10^6)(276 + 0.3 \times 724)10^{-6}}{1 - (0.3)^2} = 16,200 \text{ psi}$$

NOTE: A positive strain signifies tension. Positive and negative strains are to be added algebraically.

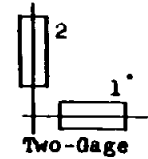
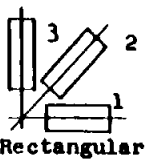
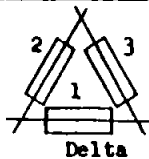
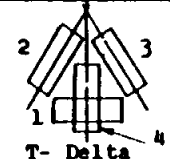
Rosette Types Required Solution	 Two-Gage	 Rectangular	 Delta	 T- Delta
Max. Normal Stress $\sigma_{max.}$	$\frac{E}{1-\mu^2} (\epsilon_1 + \mu \epsilon_2)$	$\frac{E}{2} \left[\frac{\epsilon_1 + \epsilon_3}{1-\mu} + \frac{1}{1+\mu} \sqrt{(\epsilon_1 - \epsilon_3)^2 + [2\epsilon_2 - (\epsilon_1 + \epsilon_3)]^2} \right]$	$E \left[\frac{\epsilon_1 + \epsilon_2 + \epsilon_3}{3(1-\mu)} + \frac{1}{1+\mu} \sqrt{\left(\epsilon_1 - \frac{\epsilon_1 + \epsilon_2 + \epsilon_3}{3} \right)^2 + \left(\frac{\epsilon_2 - \epsilon_3}{\sqrt{3}} \right)^2} \right]$	$\frac{E}{2} \left[\frac{\epsilon_1 + \epsilon_4}{1-\mu} + \frac{1}{1+\mu} \sqrt{(\epsilon_1 - \epsilon_4)^2 + \frac{4}{3}(\epsilon_2 - \epsilon_3)^2} \right]$
Min. Normal Stress $\sigma_{min.}$	$\frac{E}{1-\mu^2} (\epsilon_2 + \mu \epsilon_1)$	$\frac{E}{2} \left[\frac{\epsilon_1 + \epsilon_3}{1-\mu} - \frac{1}{1+\mu} \sqrt{(\epsilon_1 - \epsilon_3)^2 + [2\epsilon_2 - (\epsilon_1 + \epsilon_3)]^2} \right]$	$E \left[\frac{\epsilon_1 + \epsilon_2 + \epsilon_3}{3(1-\mu)} - \frac{1}{1+\mu} \sqrt{\left(\epsilon_1 - \frac{\epsilon_1 + \epsilon_2 + \epsilon_3}{3} \right)^2 + \left(\frac{\epsilon_2 - \epsilon_3}{\sqrt{3}} \right)^2} \right]$	$\frac{E}{2} \left[\frac{\epsilon_1 + \epsilon_4}{1-\mu} - \frac{1}{1+\mu} \sqrt{(\epsilon_1 - \epsilon_4)^2 + \frac{4}{3}(\epsilon_2 - \epsilon_3)^2} \right]$
Max. Shearing Stress $\tau_{max.}$	$\frac{E}{2(1+\mu)} (\epsilon_1 - \epsilon_2)$	$\frac{E}{2(1+\mu)} \sqrt{(\epsilon_1 - \epsilon_3)^2 + [2\epsilon_2 - (\epsilon_1 + \epsilon_3)]^2}$	$\frac{E}{1+\mu} \sqrt{\left(\epsilon_1 - \frac{\epsilon_1 + \epsilon_2 + \epsilon_3}{3} \right)^2 + \left(\frac{\epsilon_2 - \epsilon_3}{\sqrt{3}} \right)^2}$	$\frac{E}{2(1+\mu)} \sqrt{(\epsilon_1 - \epsilon_4)^2 + \frac{4}{3}(\epsilon_2 - \epsilon_3)^2}$
Angle From Gage 1 Axis To Max. Normal Stress Axis, θ_p	0	$\frac{1}{2} \tan^{-1} \left[\frac{2\epsilon_2 - (\epsilon_1 + \epsilon_3)}{\epsilon_1 - \epsilon_3} \right]$	$\frac{1}{2} \tan^{-1} \left[\frac{\frac{1}{\sqrt{3}}(\epsilon_2 - \epsilon_3)}{\epsilon_1 - \frac{\epsilon_1 + \epsilon_2 + \epsilon_3}{3}} \right]$	$\frac{1}{2} \tan^{-1} \frac{2(\epsilon_2 - \epsilon_3)}{3(\epsilon_1 - \epsilon_4)}$

TABLE 10.9.3.1
Relations Between Strain Rosette Readings
and Principal Stresses

STRUCTURAL ANALYSIS MANUAL
GENERAL DYNAMICS/CONVAIR AND SPACE SYSTEMS DIVISION

REFERENCES

Experimental Stress Analysis

- 10.9.1 Sweet, H. J., SRG-35, An Introduction to the Photoelastic Coating Technique Called Photostress, 1959.
- 10.9.2 Perry, C. C. and Lissner, H. R., The Strain Gage Primer, McGraw-Hill, 1955.
- Kelly, P. L., SRG-33, Introduction to Electric Strain Gages, 1958
- Murray, W. M., and Stein, P. K., Strain Gage Techniques, M.I.T. Press, 1959.
- Alexander, M. M., Interpretation of Rosette Strain Gage Data



STRUCTURAL ANALYSIS MANUAL
GENERAL DYNAMICS/CONVAIR AND SPACE SYSTEMS DIVISION

SECTION 17.0

PLASTIC ANALYSIS

ANALYTICAL METHODS, FOR DETERMINING STRESS IN A STRUCTURE BEYOND THE ELASTIC RANGE, ARE PRESENTED IN THIS SECTION.

	PAGE
17.1 BENDING STRENGTH IN PLASTIC RANGE.....	17.1.1
17.2 SIMPLE BENDING.....	17.2.1
17.3 COMPLEX BENDING.....	17.3.1
17.4 INTERACTION.....	17.4.1
17.5 PLASTIC BENDING MATERIAL PROPERTIES.....	17.5.1
17.6 BENDING MODULUS, SYMMETRICAL SECTIONS.....	17.6.1
17.7 MINIMUM PLASTIC BENDING CURVES.....	17.7.1
17.8 ELASTIC-PLASTIC THEORY.....	17.8.1
17.9 BENDING NEAR LIMIT LOAD.....	17.9.1
17.10 BENDING MODULUS FOR ROUND TUBES.....	17.10.1
17.11 SHEAR STRESS IN ROUND TUBE.....	17.11.1



212

STRUCTURAL ANALYSIS MANUAL
GENERAL DYNAMICS/CONVAIR AND SPACE SYSTEMS DIVISION

Data Source, Section 1.3 Reference **6**

INTRODUCTION

The conventional beam theory (based on the assumption that a plane section before bending remains plane after bending) gives a linear distribution of strain and stress in the elastic range (i.e., up to the proportional limit). In the plastic range, however, although the strain distribution is assumed to remain linear, the stress distribution corresponds with the stress-strain relationship for the material. An approximation of this distribution has been obtained, which enables the prediction of the effects of the shape and material properties on bending in the plastic range.

The methods outlined in this memo are also applicable to the calculation of the static bending strength of notched beams (beams with stress raisers) of ductile material provided the geometric properties are based on net area at the notch. For instance, when holes for fasteners are present in either or both tension and compression flanges of an "I" beam, the methods described are applicable provided the section properties are based on the net section through the holes.

This Stress Memo shall not be used for round tubes. Round tubes shall be analyzed in accordance with Section 17.10.1

SUMMARY

- I Simple Bending - Symmetrical Sections
- II Simple Bending - Unsymmetrical Sections
- III-A Shear Flow - Simple Bending - Symmetrical Sections
- III-B Shear Flow - Simple Bending - Unsymmetrical Sections
- IV Local Crippling - Simple Bending
- V Complex Bending - Symmetrical and Unsymmetrical Sections
- VI Shear Flow - Complex Bending
- VII Interaction - Bending (Simple or Complex) and Shear - Ultimate
- VIII Interaction - Bending (Simple or Complex) and Tension - Ultimate
- IX Interaction - Bending (Simple or Complex), Tension and Shear - Ultimate
- X Interaction - Bending (Simple or Complex) and Compression - Ultimate
- XI Interaction - Bending (Simple or Complex), Compression and Shear - Ultimate
- XII Interaction - Bending (Simple or Complex), Axial Load, and Shear - Yield



-

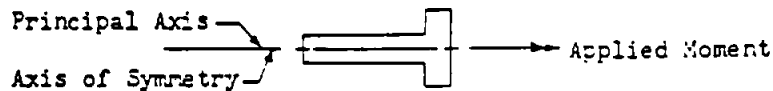
STRUCTURAL ANALYSIS MANUAL

GENERAL DYNAMICS/CONVAIR AND SPACE SYSTEMS DIVISION

Data Source, Section 1.3 Reference 6

SIMPLE BENDING - SYMMETRICAL SECTIONS

I Use following method when resultant applied moment vector is parallel to a principal axis which is also an axis of symmetry.



A. Determine the "section factor"

$$k = \frac{2 Q_m}{I/c}$$

(if $k > 2.0$, use $k = 2.0$)

Q_m is the static (first) moment, about the principal axis, of the area between the principal axis and the extreme fiber.

I is the moment of inertia of the whole section about the principal axis and c is the distance from the principal axis to the extreme fiber.

Note: When section being checked contains holes, Q_m and I are to be calculated using the net section.

Figure 1 below gives k values for various types of sections

Flanges only	I, C, or box	Hour glass	Rect-angle	Thin tube	Thick tube	Solid round	Diamond
$k=1$	$k=1$ to 1.5	$k=1.333$	$k=1.5$	$k=1.273$	$k=1.711$	$k=1.698$	$k=2$

Figure 1

B. BENDING STRESS at the extreme fiber due to any applied moment, m .

1. Determine mc/I

2. Enter the graph (plastic bending) with mc/I and obtain the maximum stress, f_m , at the extreme fiber, for the proper "section factor" k .

C. BENDING STRESS at an intermediate fiber due to any applied moment, m .

1. Obtain the stress at the extreme fiber from Section I-B above.

2. Enter the stress-strain curve with this stress and obtain the maximum strain e_m at the extreme fiber.

3. At the proper proportional strain e_y of the intermediate fiber which is at a distance y from the principal axis, read the corresponding stress.

$$e_y = \frac{y}{c} e_m$$

STRUCTURAL ANALYSIS MANUAL
GENERAL DYNAMICS/CONVAIR AND SPACE SYSTEMS DIVISION

I. SIMPLE BENDING - SYMMETRICAL Sections. (Cont'd)

D. MARGINS OF SAFETY in pure bending. The margins must be determined from the bending moments since stress is no longer proportional to moment.

1. Enter the graph (plastic bending) with the allowable ultimate tensile stress F_{tu} to obtain an mc/I value for the proper "section factor" k .

Note: Figure 5 has been included for convenience in order to avoid interpolation between k curves on the plastic bending graphs but may be used only to determine ultimate (or yield) mc/I values for symmetrical sections.

2. Multiply this value by I/c to obtain the allowable ultimate moment M_u .
3. Repeat (1) using the allowable yield stress F_{ty} to obtain the allowable yield moment M_y .
4. The margin of safety on an ultimate basis:

$$(M.S.)_u = \frac{M_u}{J_{mu} m_u} - 1$$

J_{mu} is an additional (multiplying) factor of safety, if any; otherwise use $J_{mu} = 1$

m_u is the applied ultimate moment.

5. The margin of safety on a yield basis:

$$(M.S.)_y = \frac{M_y}{J_{my} m_y} - 1$$

J_{my} is an additional (multiplying) factor of safety, if any; otherwise use $J_{my} = 1.0$.

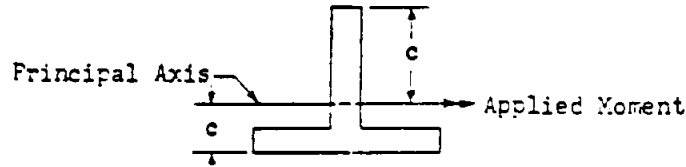
m_y is the applied yield moment.

This method of determining bending allowables has been substantiated by tests on aluminum alloy castings and forgings, and on magnesium forgings of relatively thick-walled sections only.

STRUCTURAL ANALYSIS MANUAL
GENERAL DYNAMICS/CONVAIR AND SPACE SYSTEMS DIVISION

II SIMPLE BENDING - UNSYMMETRICAL SECTIONS

Use following method when resultant applied moment vector is parallel to a principal axis which is not an axis of symmetry.



- A. Break the section down into the two parts on either side of the principal axis. For each part, compute Q_m , I , and I/c about the principal axis of the original complete section. Compute $k = \frac{Q_m}{I/c}$ for each part.

In utilizing Figure 1, the k value for each part computed as above will be the same as for a symmetrical section composed of the given part and its reflection about the principal axis of the original section.

Note: When section being checked contains holes, Q_m and I are to be calculated using the net section.

- B. MARGINS OF SAFETY in pure bending.

1. Enter the graph with the allowable ultimate tensile stress F_{tu} and the k value of the part with the larger c to obtain an mc/I value for this part.
2. Obtain the allowable maximum strain (e_s) in the part having the smaller c :

$$e_s = \frac{\text{smaller } c}{\text{larger } c} e_u$$

Enter the graph with this strain e_s and obtain the corresponding stress from the stress-strain curve. For this value of stress and with the k value for the part with the smaller c , obtain an mc/I value for this part.

3. Multiply the mc/I value for each part by I/c of each part and add the two to obtain total allowable ultimate moment M_u .
4. Repeat 1 - 3 using allowable yield stress F_{ty} and yield strain e_y to obtain the allowable yield moment M_y .
5. Obtain ultimate and yield margins of safety as explained on pg. 17.2.2

- C. BENDING STRESS due to any applied moment, m . This can be obtained only by trial and error. Select several values of strain for extreme fiber of part having larger c , and for each value of strain compute corresponding moment, as explained above. Plot total moment against strain; the strain corresponding to the given applied moment is then the actual strain at the extreme fiber, and the stress at any point in the section can be found therefrom by obtaining the proportionate strain at the point in question and reading the corresponding stress from the stress-strain curve.

STRUCTURAL ANALYSIS MANUAL

GENERAL DYNAMICS/CONVAIR AND SPACE SYSTEMS DIVISION

III SHEAR FLOW - SIMPLE BENDING

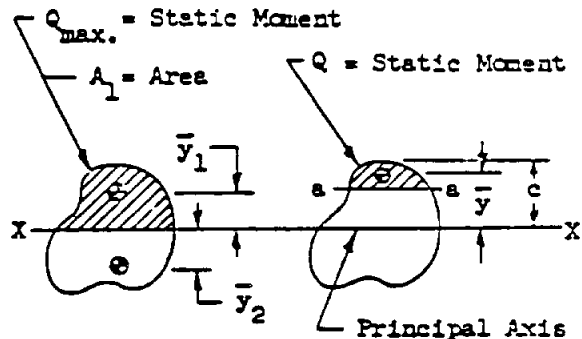
The methods outlined below show how the classical formula SQ/I may be modified to approximate the shear flow at any fiber when the material has been stressed in bending beyond the proportional limit. The formulas are applicable when bending is about a principal axis and the shear load is perpendicular to this axis.

A. SYMMETRICAL SECTION - Principal axis about which bending occurs is an axis of symmetry.

1. Determine:

$$\frac{mc}{I}, k, \text{ and } \theta = \frac{c}{\bar{y} k}$$

If $\theta < 1$, use $\theta = 1$. I , c , and k are defined in Section I-A and \bar{y} is the distance from the principal axis to the centroid of the area between the section at which the shear flow is being determined and the extreme fiber.



2. Enter the graph (plastic bending) with mc/I , and for the proper k and θ values, determine R .

3. Shear flow:

$$q = R \frac{SQ}{I}$$

B. UNSYMMETRICAL SECTION - Principal axis about which bending occurs is not an axis of symmetry.

1. Break the section down into the two parts on either side of the principal axis and compute $k = \frac{Q_m}{I/c}$ for each part as outlined in Section II-A.
2. By the method of Section II-C, determine the strain produced in the extreme fiber by the applied moment. Use the extreme fiber on the same side of the principal axis as the section for which the shear flow is being determined.
3. For this value of strain of the extreme fiber, and the k value for the corresponding part, determine the mc/I value from the curves.
4. Compute $\theta = \frac{I}{A_1 (\bar{y}_1 + \bar{y}_2) \bar{y}}$ (if $\theta < 1$, use $\theta = 1$). (Ref. Sketch in III-A above).
5. Enter the graph (plastic bending) with the mc/I value determined in step 3 above, and for the k and θ value of the corresponding part, determine
6. Shear flow, $q = R \frac{SQ}{I}$ (I is the moment of inertia of the entire section about the principal axis.)
7. When the shear flow is being determined at the principal axis, compute values using both parts of the section and use the larger.

STRUCTURAL ANALYSIS MANUAL
GENERAL DYNAMICS/CONVAIR AND SPACE SYSTEMS DIVISION

IV LOCAL CRIPPLING - SIMPLE BENDING

- A. Assume critical portion of section is developing its crippling stress.
- B. Enter the stress-strain curve with this crippling stress and determine the strain of the critical portion e_y .
- C. Determine the proportionate strains of the extreme fibers e_s and e_l .

$$e_s = \frac{c_s}{y} e_y \quad , \quad e_l = \frac{c_l}{y} e_y$$

(For a symmetrical section $e_s = e_l$)

D. SYMMETRICAL SECTIONS

1. Enter the graph (plastic bending) with the strain determined in C and determine the corresponding stress from the stress-strain curve.
2. For this value of stress and the k value as determined from Section I-A, obtain the mc/I value.
3. Multiply this mc/I value by I/c (I and c defined in Section I-A) to obtain the allowable moment M which will subject the critical fiber to its crippling stress.

E. UNSYMMETRICAL SECTIONS

1. Enter the graph (plastic bending) with the strains determined in C and determine the corresponding stresses from the stress-strain curve.
2. For these values of stress and the corresponding k values as determined from Section II-A, obtain the mc/I values.
3. Multiply each of the two mc/I values by the corresponding I/c (I and c defined in Section II-A) and add the two resulting moments to obtain the allowable moment, M , which will subject the critical fiber to its crippling stress.



STRUCTURAL ANALYSIS MANUAL
GENERAL DYNAMICS/CONVAIR AND SPACE SYSTEMS DIVISION

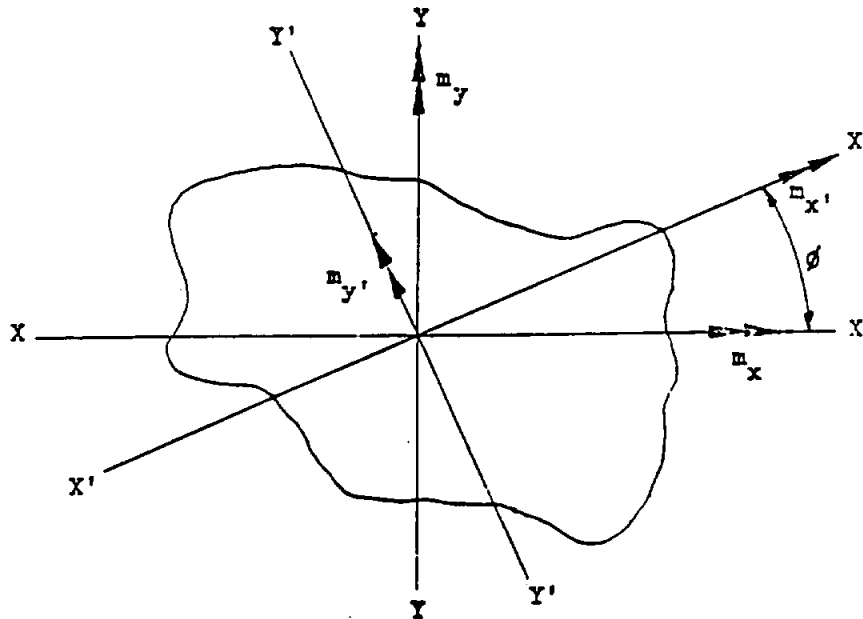
Data Source, Section 1.3 Reference 4

V COMPLEX BENDING - Symmetrical and Unsymmetrical Sections

This condition occurs when the resultant applied moment vector is not parallel to a principal axis.

Let X and Y represent two mutually perpendicular centroidal axes.

Let X' and Y' represent the principal axes.



Moment vectors are designated by double headed arrows and are to be interpreted by the left hand rule (i.e., point left thumb in direction of vector and natural curl of fingers will designate the direction of moment).

m_x = the applied moment about the X axis, the moment being positive when it tends to put compression in the "upper" fibers.

m_y = the applied moment about the Y axis, the moment being positive when it tends to put compression in the "left" fibers.

ϕ = The angle the X' principal axis makes with the original X axis, the angle being positive when measured in a counter-clockwise direction.

Any case of complex bending may be resolved into two cases of simple bending about the principal axes of the section. The principal axes are defined as mutually perpendicular centroidal axes, about which the moments of inertia are a maximum and minimum respectively and about which the product of inertia is zero.

STRUCTURAL ANALYSIS MANUAL
GENERAL DYNAMICS/CONVAIR AND SPACE SYSTEMS DIVISION

V COMPLEX BENDING - Symmetrical and Unsymmetrical Sections (Cont'd)

- A. Determine the principal axes X' and Y' . If they cannot be determined by inspection, obtain I_x , I_y , and I_{xy} about any arbitrary pair of centroidal axes. Then

$$\tan 2 \phi = \frac{2I_{xy}}{I_y - I_x}$$

- B. Using the X' axis as a reference, determine allowable moment $M_{x'}$ as described under simple bending. (Sections I and II)
- C. Using the Y' axis as a reference, determine allowable moment $M_{y'}$ as described under simple bending. (Sections I and II)
- D. Determine applied moments about the principal axes.

$$\begin{aligned} m_{x'} &= m_x \cos \phi + m_y \sin \phi \\ m_{y'} &= -m_x \sin \phi + m_y \cos \phi \end{aligned}$$

- E. Determine moment ratios.

$$R_{bx'} = \frac{m_{x'}}{M_{x'}}$$

and

$$R_{by'} = \frac{m_{y'}}{M_{y'}}$$

- F. The margin of safety, in pure bending, is given by:

$$M.S. = \frac{1}{j_m (R_{bx'} + R_{by'})} - 1$$

where j_m is the proper additional factor of safety depending on whether a yield or ultimate margin of safety is involved.

NOTE: Computing M.S. in this manner is always conservative and for certain shapes of section may be very conservative. A more precise method has not been developed.

STRUCTURAL ANALYSIS MANUAL
GENERAL DYNAMICS/CONVAIR AND SPACE SYSTEMS DIVISION

V. SHEAR FLOW - COMPLEX BENDING

- A. Resolve the applied shear force into components parallel to the principal axes. Denote the component parallel to the Y' axis by $S_{y'}$, and the component parallel to the X' axis by $S_{x'}$.
- B. Obtain $\theta_{x'}$ and $\theta_{y'}$, as explained in Sections III-A-1 and III-B-4, where subscripts 'x' and 'y' denote the axes to be used in computing θ .
- C. Determine the degree of plasticity, α . If no axial load is acting, α is obtained as follows:

Assuming elastic (M_y/I) stress distributions (about both principal axes), obtain the greatest total stress in the section due to the applied ultimate loads. Denoting this stress by f_{total} , obtain

$$\delta = R_b \frac{f_{tp}}{f_{total}} \quad \text{where } R_b = R_{bx'} + R_{by'} \quad (\text{Section V-2})$$

Then, $\alpha = \frac{R_b - \delta}{1 - \delta}$ If $\alpha < 0$, take $\alpha = 0$

- D. Obtain shear stress correction ratios, R:

$$R_{x'} = 1 + \alpha (\theta_{x'} - 1)$$

$$R_{y'} = 1 + \alpha (\theta_{y'} - 1)$$

- E. Obtain shear flows $q_{x'}$ and $q_{y'}$:

$$q_{x'} = R_{y'} \frac{S_{x'} q_{y'}}{I_{y'}}$$

$$q_{y'} = R_{x'} \frac{S_{y'} q_{x'}}{I_{x'}}$$



22~~4~~.

STRUCTURAL ANALYSIS MANUAL

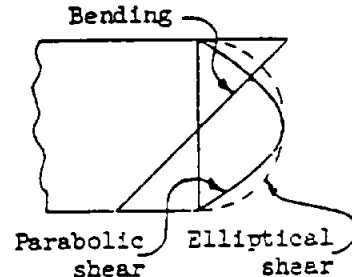
GENERAL DYNAMICS/CONVAIR AND SPACE SYSTEMS DIVISION

Data Source, Section 1.3 Reference 6

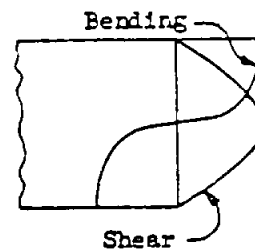
VII. INTERACTION - BENDING (Simple or Complex) and SHEAR - Ultimate

The maximum shear stress in a beam usually occurs at the principal axis, where the bending stress is zero. The maximum bending stress occurs at an extreme fiber, where usually the shear stress is zero.

In the elastic range, the distribution of shear and bending stress is usually such that the most critical point in the section is at either the principal axis or the extreme fiber. This is true on a rectangular section since the shear distribution across the section is parabolic and the bending distribution is linear. If the shear distribution had been elliptical every point in the cross section would be equally critical in combined stress based on circular interaction.



In the plastic range however, the distribution of the shear stress as well as the bending stress differs from that in the elastic range. This results in intermediate points which frequently become more critical in combined stress than either the shear stress at the principal axis or the bending stress at the extreme fiber.



To find the most critical point would require calculation of combined stresses at a series of points across the section. This procedure would be not only laborious but also probably incorrect (conservative) since there would undoubtedly be some redistribution of stress away from the most critical point, although the exact nature of this redistribution appears to be extremely difficult to determine.

Therefore the following procedure shall be used.

- A. Obtain $R_b = \frac{m_u}{M_u}$, where m_u and M_u are determined as explained in Sections I-D and II-B

For complex bending, $R_b = R_{bx} + R_{by}$, where R_{bx} and R_{by} are obtained from Section V-E.

- B. Obtain $R_s = \frac{f_s}{F_{su}}$, where f_s is the maximum shear stress based on shear

flows obtained according to Section III. (The maximum shear stress does not always occur at the principal axis.)

For complex bending, R_s is determined as follows:

- (1) Obtain maximum shear stresses f_{sx} and f_{sy} , based on shear flows determined in Section VI.

$$(2) R_{sx} = \frac{f_{sx}}{F_{su}} \text{ and } R_{sy} = \frac{f_{sy}}{F_{su}}$$

$$(3) R_s = \sqrt{R_{sx}^2 + R_{sy}^2}$$

STRUCTURAL ANALYSIS MANUAL
GENERAL DYNAMICS/CONVAIR AND SPACE SYSTEMS DIVISION

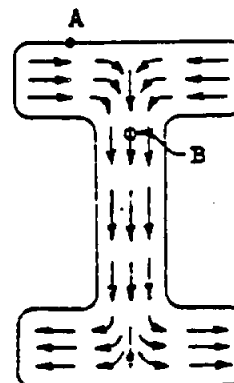
VII INTERACTION - BENDING (Simple or Complex) and SHEAR - Ultimate (Cont'd)

- C. **OBTAIN MARGIN OF SAFETY** from the interaction curve of Figure 2. Note: The margin thus obtained is not a "true" margin of safety, since its variation with applied load is non-linear; but if the calculated margin is positive the true margin is positive, and if the calculated margin is negative the true margin is negative. The margin of safety as computed above shall be used for formal stress analysis.

If the "true" margin of safety is desired, it may be obtained by a trial and error procedure in which the loading is varied (all loads varied in same proportion) until the loading is found for which the margin of safety as determined above is zero. This loading becomes the allowable, and the true margin of safety is given by:

$$\frac{\text{Allowable Load}}{\text{Applied Load}} - 1$$

- D. **THE MARGIN OF SAFETY**, obtained in Section C above does not include possible local interaction of shear and bending stresses at points such as A in the adjoining sketch, at which a substantial shear stress necessarily occurs in combination with the maximum bending stress. Such points must be checked separately, although judgment will have to be used in borderline cases as to whether this situation exists. Ordinarily points such as B in the sketch, even though highly stressed in both shear and bending, are protected by possible redistribution, hence are adequately covered by the interaction of Section C above, and should not be checked locally.



To check a point for local interaction, obtain true shear stress according to Section III and true bending stress according to Sections I-B and II-C, compute $R_t = \frac{f_b \text{ true}}{F_{tu}}$ and $R_s = \frac{f_s \text{ true}}{F_{su}}$, and obtain the margin of safety on the basis of a circular interaction curve:

$$\text{M.S.} = \frac{1}{\sqrt{R_t^2 + R_s^2}} - 1$$

This is not a true margin of safety - refer to discussion in Section C above.

For complex bending, the same problem may exist and should be investigated in a comparable manner.

STRUCTURAL ANALYSIS MANUAL
GENERAL DYNAMICS/CONVAIR AND SPACE SYSTEMS DIVISION

V. INTERACTION - BENDING (Simple or Complex) and TENSION - Ultimate

- A. Obtain $R_b = \frac{M_u}{M_u}$, where M_u and M_u are determined as explained in Sections I-D and II-B.

For complex bending, $R_b = R_{bx'} + R_{by'}$, where $R_{bx'}$ and $R_{by'}$ are determined from Section V-E.

- B. Obtain $R_t = \frac{P}{A F_{tu}}$, where P is the applied axial tension load and A is the cross sectional area.

- C. Obtain $\frac{Ac}{2Q_m}$. If the section is unsymmetrical, take c for the side for which axial and bending stresses are of opposite sign.

For complex bending, obtain both $(\frac{Ac}{2Q_m})_{x'}$ and $(\frac{Ac}{2Q_m})_{y'}$. In obtaining $(\frac{Ac}{2Q_m})_{x'}$, if the section is unsymmetrical about the x' axis, take $c_{x'}$ for the side for which axial stress and stress due to $m_{x'}$ are of opposite sign. Obtain $(\frac{Ac}{2Q_m})_{y'}$ analogously.

- D. Obtain γ from the Table I. γ is a material plasticity factor equal to zero for a perfectly elastic (brittle) material and equal to 1.00 for a perfectly plastic material (rectangular stress strain diagram).

- E. Obtain n from Figure 3.

For complex bending, obtain both $n_{x'}$ and $n_{y'}$ from Figure 3

$$n = \frac{n_{x'} R_{bx'} + n_{y'} R_{by'}}{R_b}$$

- F. Plot R_t , R_b on Figure 4 as point A. Draw OA and extend to its intersection B with the appropriate curve according to the value of n obtained in Section E. Determine coordinates of Point B and designate them as R_t' and R_b' .

- G. Margin of Safety for combined bending and tension is given by:

$$M.S. = \frac{R_b'}{R_b} - 1 \quad \text{or} \quad M.S. = \frac{R_t'}{R_t} - 1$$

INTERACTION - BENDING (Simple or Complex), TENSION, and SHEAR - Ultimate

When shear acts in addition to bending and tension, the calculation of shear flow as explained in Sections III and VI and the interaction of shear and bending (Ref. Section VII) must be modified.

- A. Follow the procedure required in Sections VIII-A through VIII-F.

STRUCTURAL ANALYSIS MANUAL
GENERAL DYNAMICS/CONVAIR AND SPACE SYSTEMS DIVISION

IX. INTERACTION - BENDING (Simple or Complex), TENSION, and SHEAR - Ultimate (Cont'd)

- B. Assuming elastic stress distributions (stresses given by P/A and My/I) obtain the greatest total fiber stress in the section due to the applied loads. Denoting this stress by f_{total} , obtain:

$$R_{t_D} = R_t \frac{F_{tp}}{f_{total}} \quad \text{and} \quad R_{b_D} = R_b \frac{F_{tp}}{f_{total}}$$

Plot these values of R_{t_D} , R_{b_D} as point D in Figure 4 (D will lie on the straight line OAB).

- C. Obtain $a = \overline{OA}$, $b = \overline{OB}$, and $d = \overline{OD}$ in Figure 4. For convenience, it is permissible to take a , b , and d as the projections of \overline{OA} , \overline{OB} , and \overline{OD} , respectively, on the R_t or R_b axis.
- D. Obtain the degree of plasticity, α

$$\alpha = \frac{a - d}{b - d}$$

If $\alpha < 0$, take $\alpha = 0$

- E. Obtain θ as explained in Sections III-A-1 and III-B-4

For complex bending, obtain θ_x , and θ_y , as explained in Section VI-B.

- F. Compute $R = 1 + \alpha(\theta - 1)$. Note: R will have a value between 1.00 (bending-tension in elastic range) and θ (bending-tension fully plastic).

For complex bending, obtain both

$$\begin{aligned} R_{x'} &= 1 + \alpha(\theta_{x'} - 1) \\ R_{y'} &= 1 + \alpha(\theta_{y'} - 1) \end{aligned}$$

- G. Compute maximum shear stress, f_s , obtaining shear flow from:

$$q = R \frac{SQ}{I}$$

where R is determined in step F above. (The maximum shear stress does not always occur at the principal axis.)

For complex bending, obtain maximum shear stresses in both direction, f_{sx} , and f_{sy} , based on the shear flows:

$$\begin{aligned} q_{x'} &= R_{y'} \frac{S_{x'} Q_{y'}}{I_{y'}} \\ q_{y'} &= R_{x'} \frac{S_{y'} Q_{x'}}{I_{x'}} \end{aligned}$$

STRUCTURAL ANALYSIS MANUAL
GENERAL DYNAMICS/CONVAIR AND SPACE SYSTEMS DIVISION

IX INTERACTION - BENDING (Simple or Complex), TENSION, and SHEAR - Ultimate (Cont'd)

where the R values are determined in step F above and S_x and S_y are the shear forces parallel to the x' and y' axes respectively.

E. Obtain
$$R_s = \frac{f_s}{F_{su}}$$

For complex bending,

$$R_s = \sqrt{R_{sx'}^2 + R_{sy'}^2}$$

where $R_{sx'} = \frac{f_{sx'}}{F_{su}}$ and $R_{sy'} = \frac{f_{sy'}}{F_{su}}$

- I. Obtain the bending-tension utilization factor, $U_{bt} = \frac{a}{b}$, where a and b were found in step C above.
- J. OBTAIN MARGIN OF SAFETY from the interaction curve of Figure 2, entering with R_s and U_{bt} . Note: This is not a true margin of safety - Refer to discussion in Section VII-C.
- K. Consider at least qualitatively the possibility of substantial shear stress occurring at the same point as maximum fiber stress, as in the I section sketched in Section VII-D.

INTERACTION - BENDING (Simple or Complex) and COMPRESSION - Ultimate

A. Obtain $R_b = \frac{m_u}{M_u}$ where m_u and M_u are determined by Sections I-D and II-B.

m_u must take account of secondary bending.

For complex bending $R_b = R_{bx'} + R_{by'}$, where $R_{bx'}$ and $R_{by'}$ are determined from Section V-E and must take account of secondary bending.

- B. Obtain $R_c = \frac{P}{P_c}$ where P = applied axial load and P_c is the axial load at which the member would fail in compression.

- C. Margin of Safety

$$M.S. = \frac{1}{R_b + R_c} - 1$$

STRUCTURAL ANALYSIS MANUAL
GENERAL DYNAMICS/CONVAIR AND SPACE SYSTEMS DIVISION

XI INTERACTION - BENDING (Simple or Complex), COMPRESSION, and SHEAR - Ultimate

- A. Follow procedure required in Sections X-A and X-B.
- B. Plot R_c , R_b on Figure 4 as point A. Draw OA and extend to its intersection B with the curve $n = 1$.
- C. Follow procedure of Section IX-B through IX-K replacing R_t with R_c and other tension subscripts with compression subscripts.

XII INTERACTION - Bending (Simple or Complex), Axial Load, and Shear - YIELD

The yield margin of safety of a beam under combined loading shall be obtained by means of S.M. 70, Section II, except that ordinarily only the point of maximum fiber stress and the point of maximum shear stress shall be checked. Whenever shear stresses are present, however, at points of maximum fiber stress (such as point A in the I section shown in Section VII-D) the shear stress and bending stress shall be combined at such points.

XIII Yielding of Compact Structure

To investigate yielding of a compact structure (crippling or buckling not pertinent), under the action of two dimensional combined stress, interaction curves should not be used. Instead, a maximum "equivalent" stress ratio \bar{R} is computed and a margin of safety obtained therefrom:

$$MS = \frac{1}{\bar{R}} - 1$$

\bar{R} is given by the following formula (which is based upon the "maximum distortion strain energy" criterion for yielding):

$$\bar{R} = \sqrt{R_{n1}^2 + R_{n2}^2 - R_{n1} R_{n2} + R_s^2}$$

R_n is a normal stress ratio due to combining direct stress and bending stress and is given by:

$$R_n = R_t + R_b \quad \text{or} \quad R_n = R_c + R_b$$

Stress ratios due to direct or bending stress are positive for tension and negative for compression; care must be taken that signs are correct. Subscripts 1 and 2 indicate directions which are mutually perpendicular.

In evaluating R_t or R_c , F_{ty} or F_{cy} should be chosen as the allowable according to whether the applied stress is tension or compression. If it is

STRUCTURAL ANALYSIS MANUAL
GENERAL DYNAMICS/CONVAIR AND SPACE SYSTEMS DIVISION

Yielding of Compact Structure (Cont'd)

desired to take account of the difference in yield allowable between with-grain and cross-grain directions, rather than to assume conservatively that the allowable is always the smaller of the two, then the "1" and "2" directions should be chosen to coincide with the grain directions and R_{t1} or R_{o1} and R_{t2} or R_{o2} each evaluated using its appropriate yield allowable.

R_s is a shear stress ratio due to combining simple shear and torsional shear and is given by:

$$R_s = R_{ss} + R_{st}$$

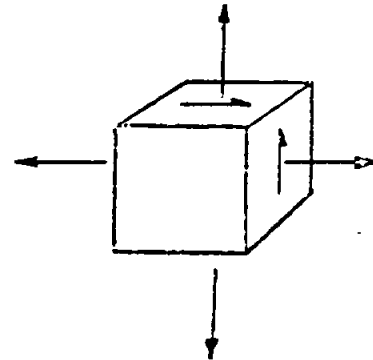
where R_{ss} and R_{st} are stress ratios for simple shear and torsional shear. R_{ss} and R_{st} may be combined to give R_s only when f_{ss} and f_{st} act in the same or opposite directions; and they must be oriented with respect to the normal stresses as shown in the adjacent sketch (for otherwise the stress condition is no longer two dimensional). The same sign convention must be used for both R_{ss} and R_{st} .

F_{sy} should be taken as $.577 F_{ty \text{ cross-grain}}$

F_{sty} may be approximated as:

$$F_{sty} = F_{sy} + \frac{F_{ty} - F_{ty}}{F_{tu} - F_{tu}} (F_{stu} - F_{su})$$

All R 's are evaluated for the same point in the structure. Several points may have to be checked to find the most critical one.



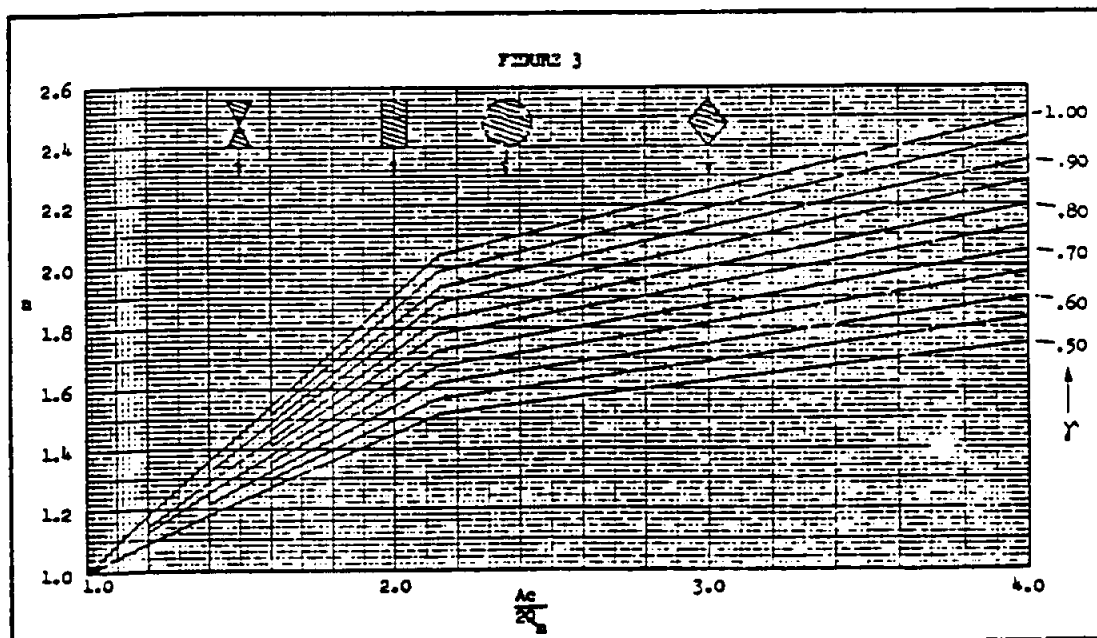
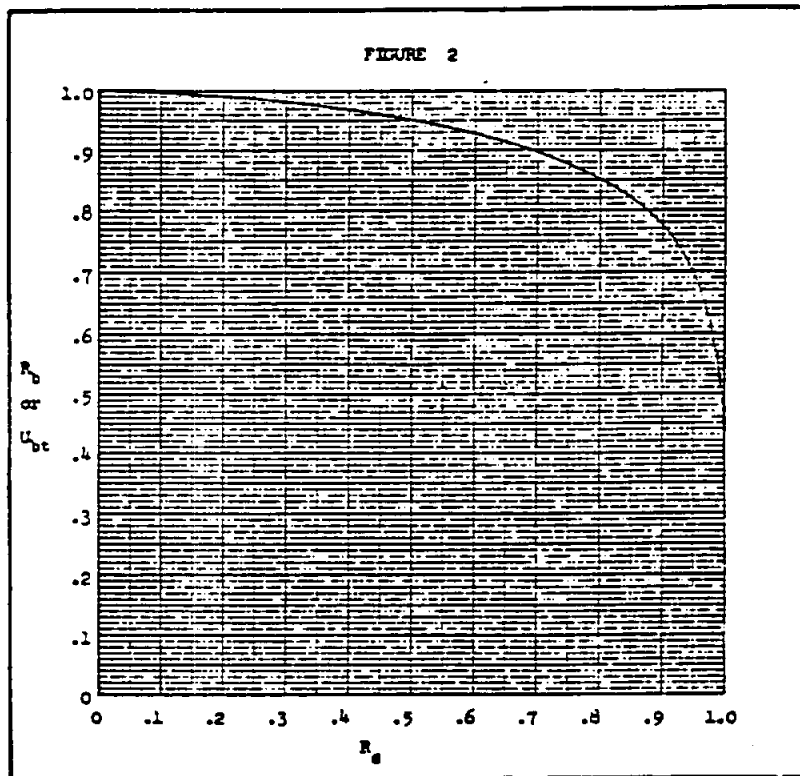


Data Source, Section 1.3 Reference 6

MATERIAL	R	Figure
ALUMINUM ALLOYS		
2014-T6 Die Forging (L)91	6
2024-T4 Extrusion $t < .250$ (L)88	7
.250 $\leq t < 3.00$ (L)88	8
7075-T6 Extrusion $t < .250$ (L)93	9
7075-T6 & -T651X Extrusion .250 $\leq t < 3.000$ (L)93	10
7075-T6 Die Forging $t \leq 2.00$ (L)92	11
356-T6 Sand Casting.75	12
MAGNESIUM ALLOYS		
ZK60A-T5 Extrusion (L)83	13
AZ63A-T6 Sand and Permanent Mold Casting54	14
AZ91C-T6 Sand and Permanent Mold Casting54	14
ALLOY STEEL		
Condition N $t \leq .187$91	15
Condition N $t > .187$91	16
H.T. 125 ksi93	17
H.T. 150 ksi95	18
H.T. 180 ksi96	19
H.T. 190 ksi95	20
H.T. 200 ksi94	21
H.T. 260 ksi (L)91	22
H.T. 260 ksi (T)97	23
TITANIUM ALLOYS		
5Al-2.5Sn Bar & Forging - Annealed98	24
6Al-4V Bar & Forging - Annealed96	25
- STA $t \leq 1.0$95	26
- STA $1.0 < t \leq 2.0$95	27
- STA $2.0 < t \leq 3.0$95	28
6Al-6V-2Sn Bar & Forging - STA $1.0 < t \leq 2.0$95	29
- STA $2.0 < t \leq 3.0$95	30
- STA $3.0 < t \leq 4.0$95	31
8Al-1Mo-1V Plate - Duplex Annealed $t \leq 2.00$96	32
13V-11Cr-3Al Plate - Annealed $t \leq .250$97	33
- STA $t \leq .250$89	34

page 17.5.1

STRUCTURAL ANALYSIS MANUAL
GENERAL DYNAMICS/CONVAIR AND SPACE SYSTEMS DIVISION



STRUCTURAL ANALYSIS MANUAL
GENERAL DYNAMICS/CONVAIR AND SPACE SYSTEMS DIVISION

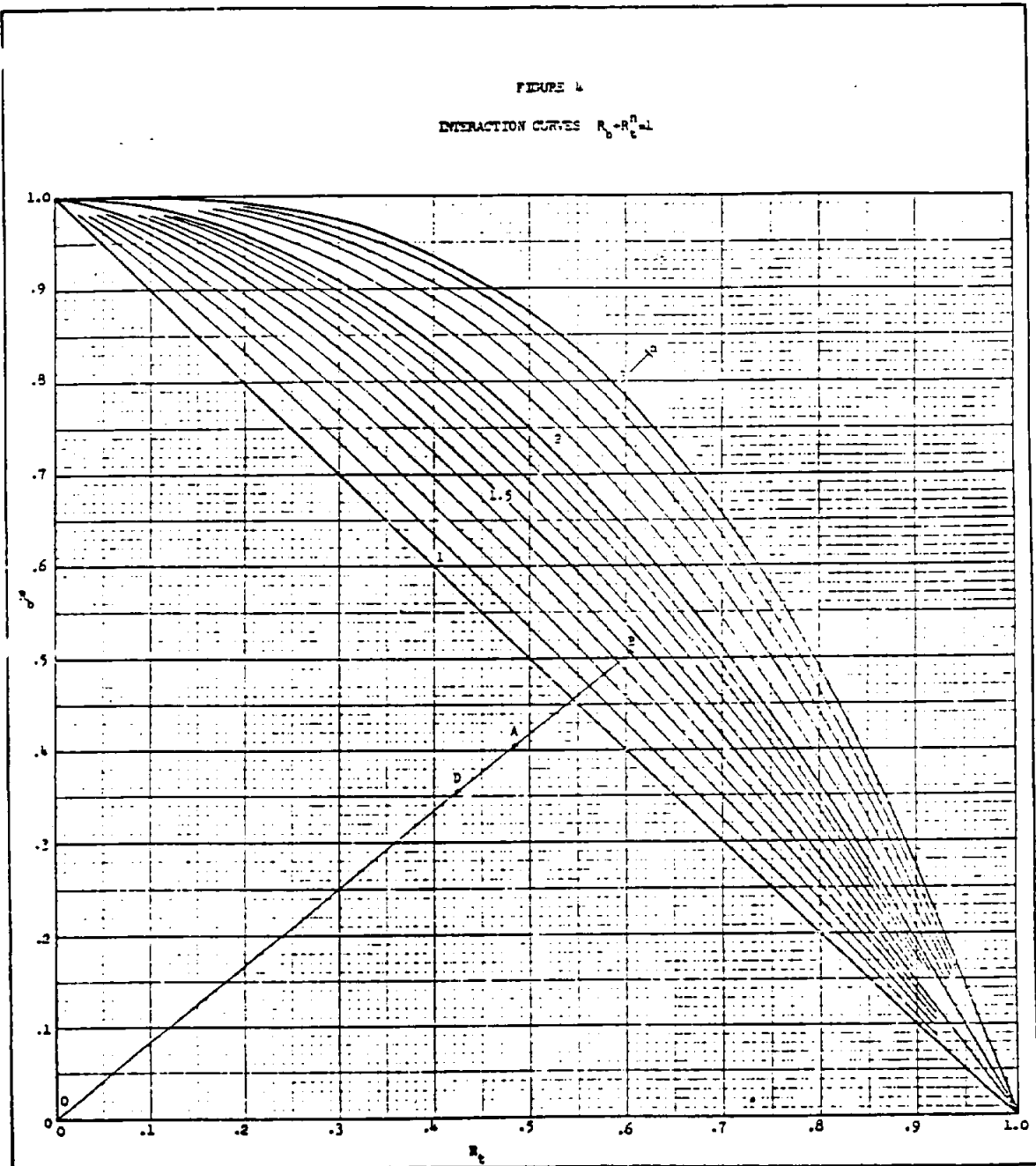


FIGURE 5a
Ultimate and Yield Values of $\frac{M_u}{T}$ for Symmetrical Sections
Aluminum and Magnesium Alloy
Room Temperature

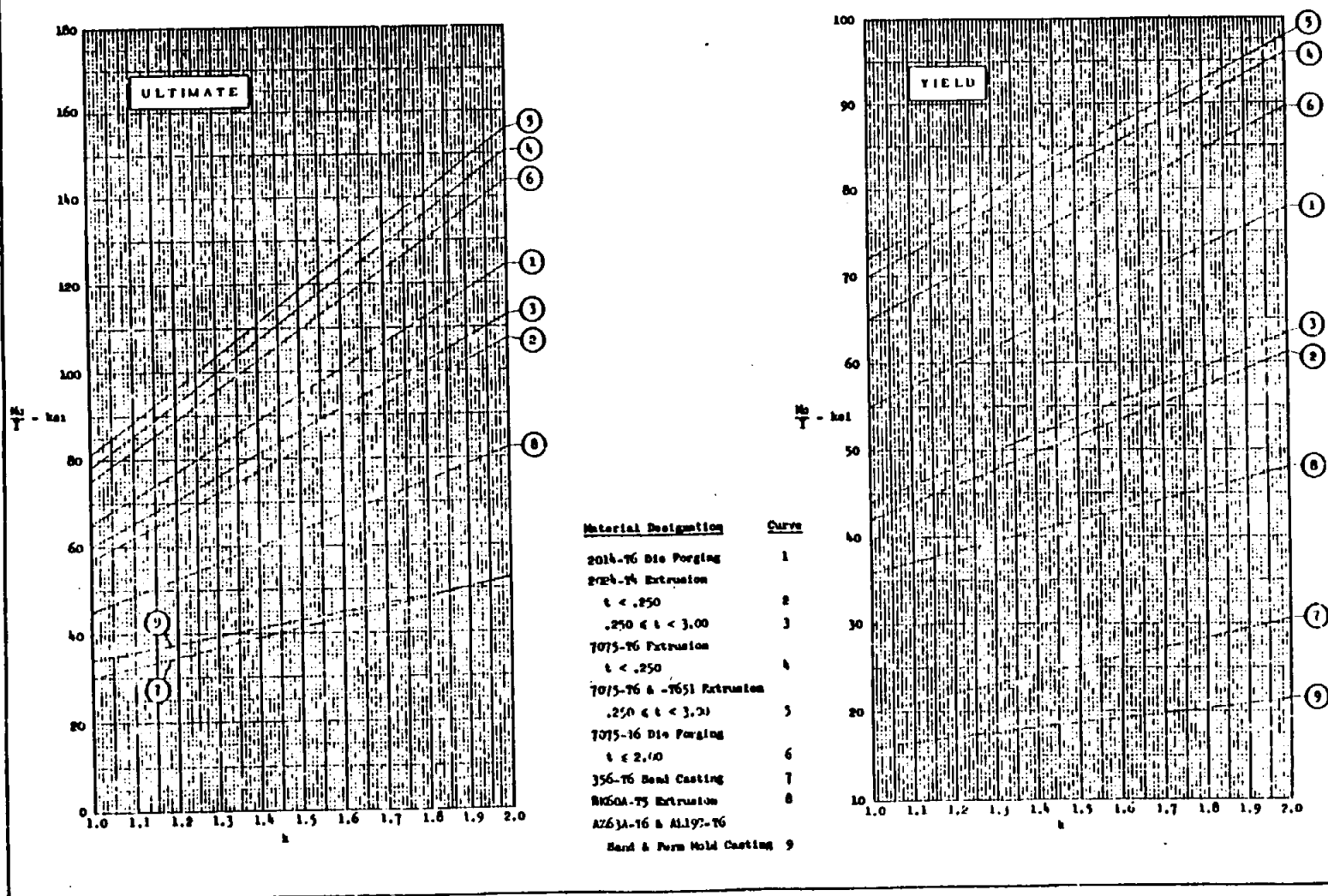


FIGURE 5b
Ultimate and Yield Values of $\frac{F_y}{F_u}$ for Symmetrical Sections
Alloy Steel
Room Temperature

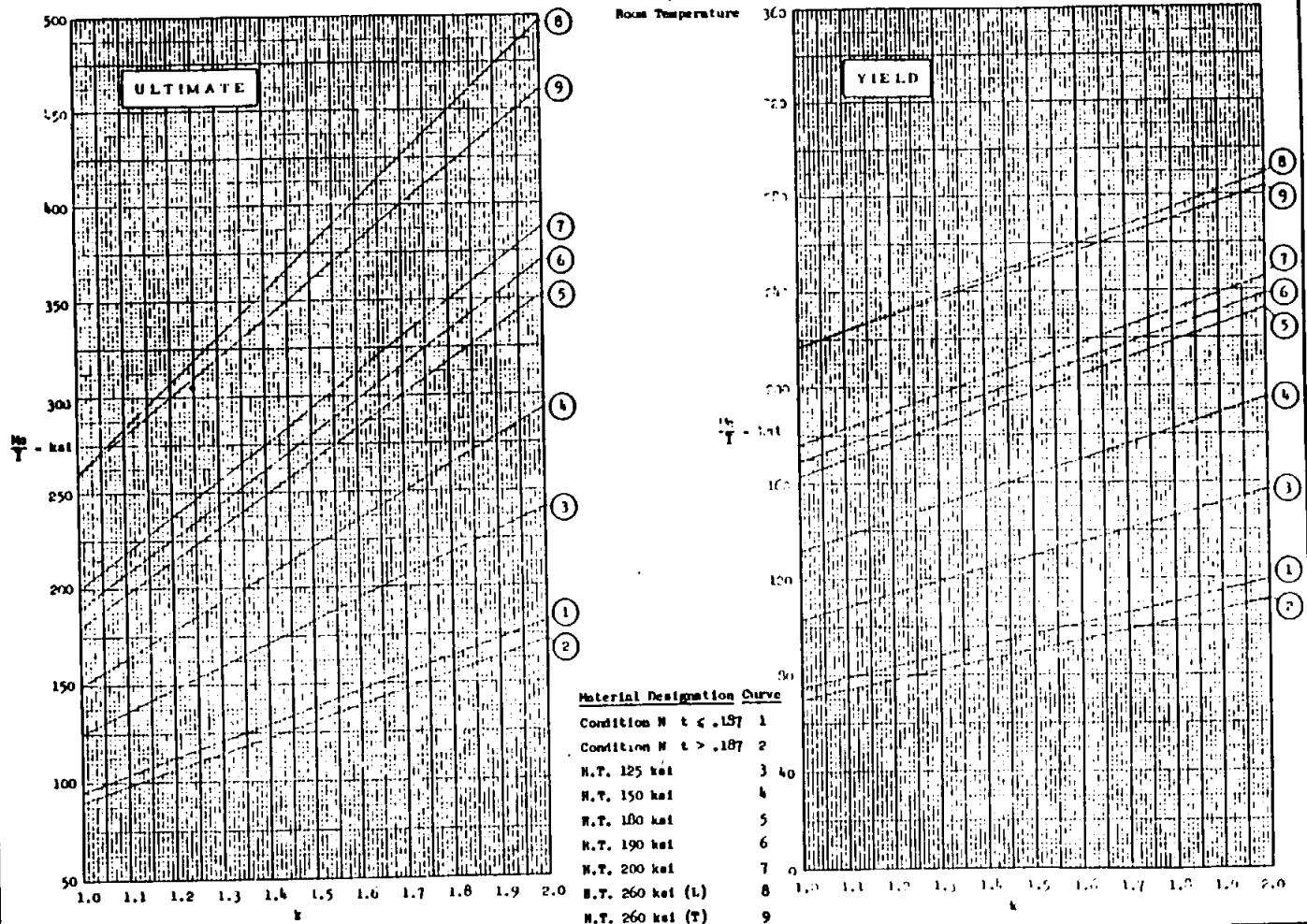


FIGURE 5a
Ultimate and Yield Values of $\frac{M_u}{Y}$ for Symmetrical Sections
Titanium Alloy
Room Temperature

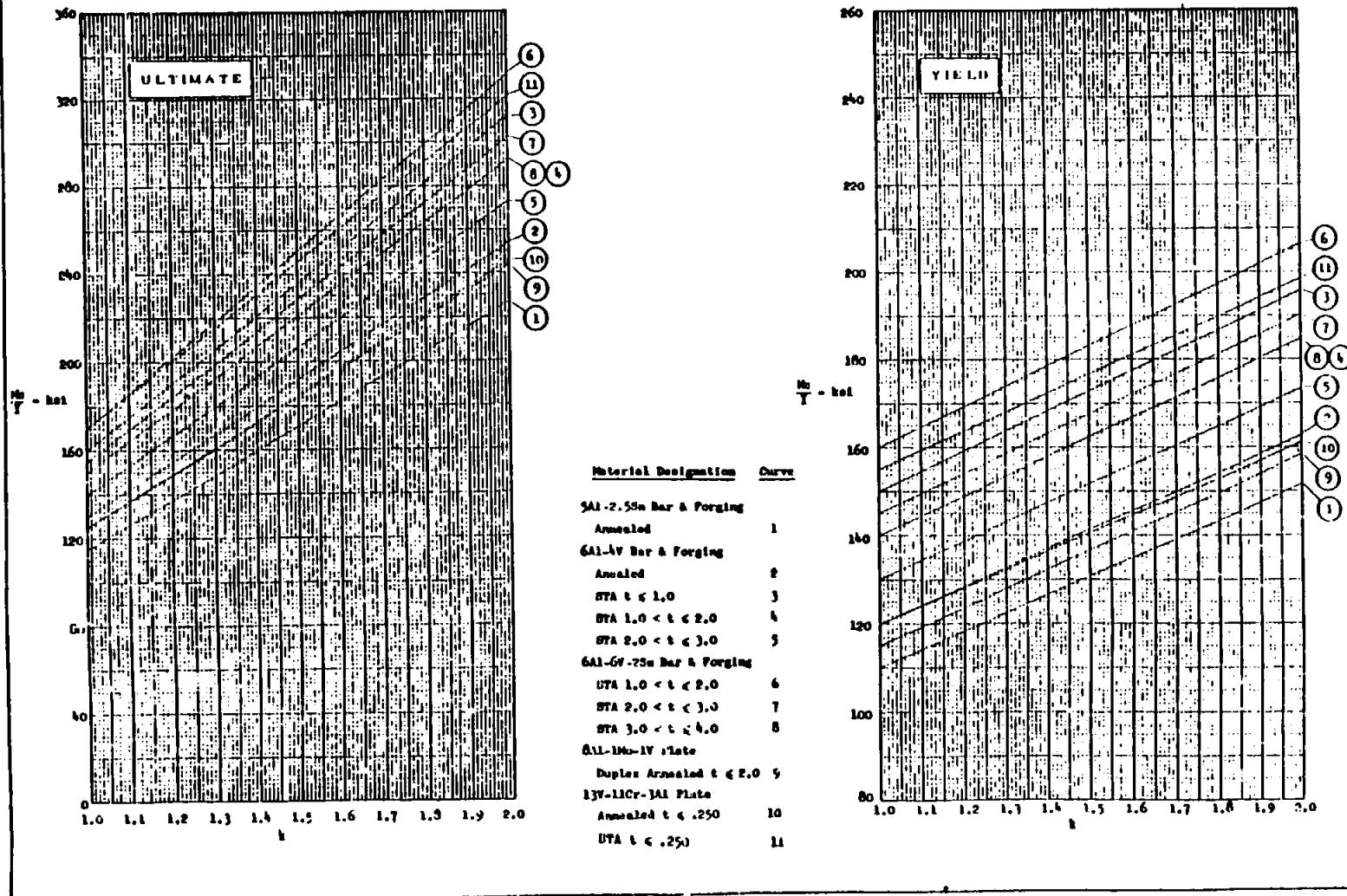
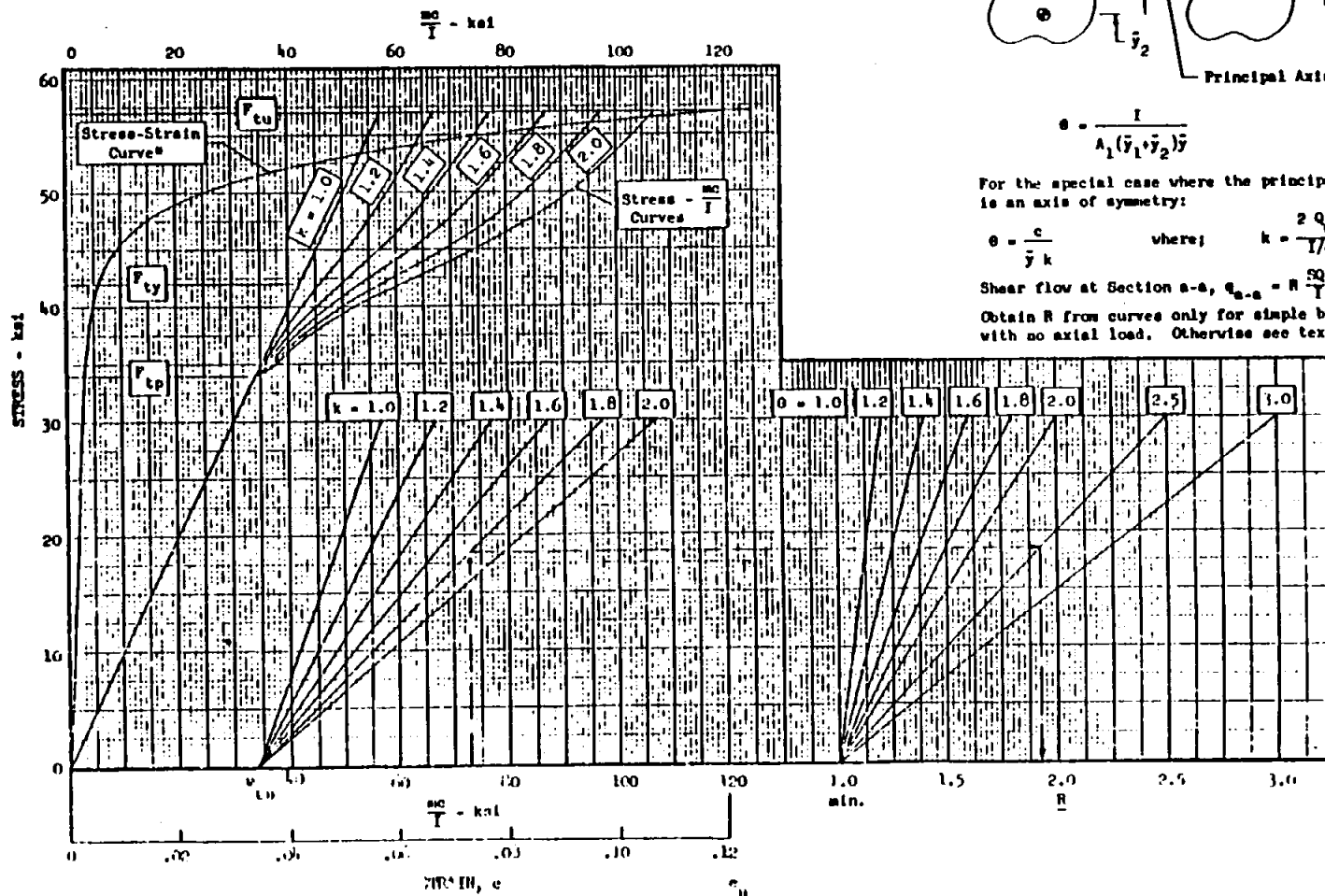


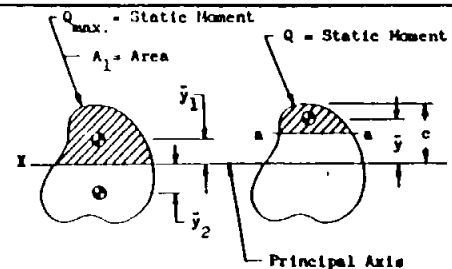


FIGURE 7
BENDING IN THE PLASTIC RANGE
2024-T4 Aluminum Alloy Extrusion $t \leq .250$
(Longitudinal)
Room Temperature



* Based on Minimum Guaranteed Values

FIGURE 11
BENDING IN THE PLASTIC RANGE
2024-T4 Aluminum Alloy Extrusion .250 ≤ t ≤ 3.00
(Longitudinal)
Room Temperature



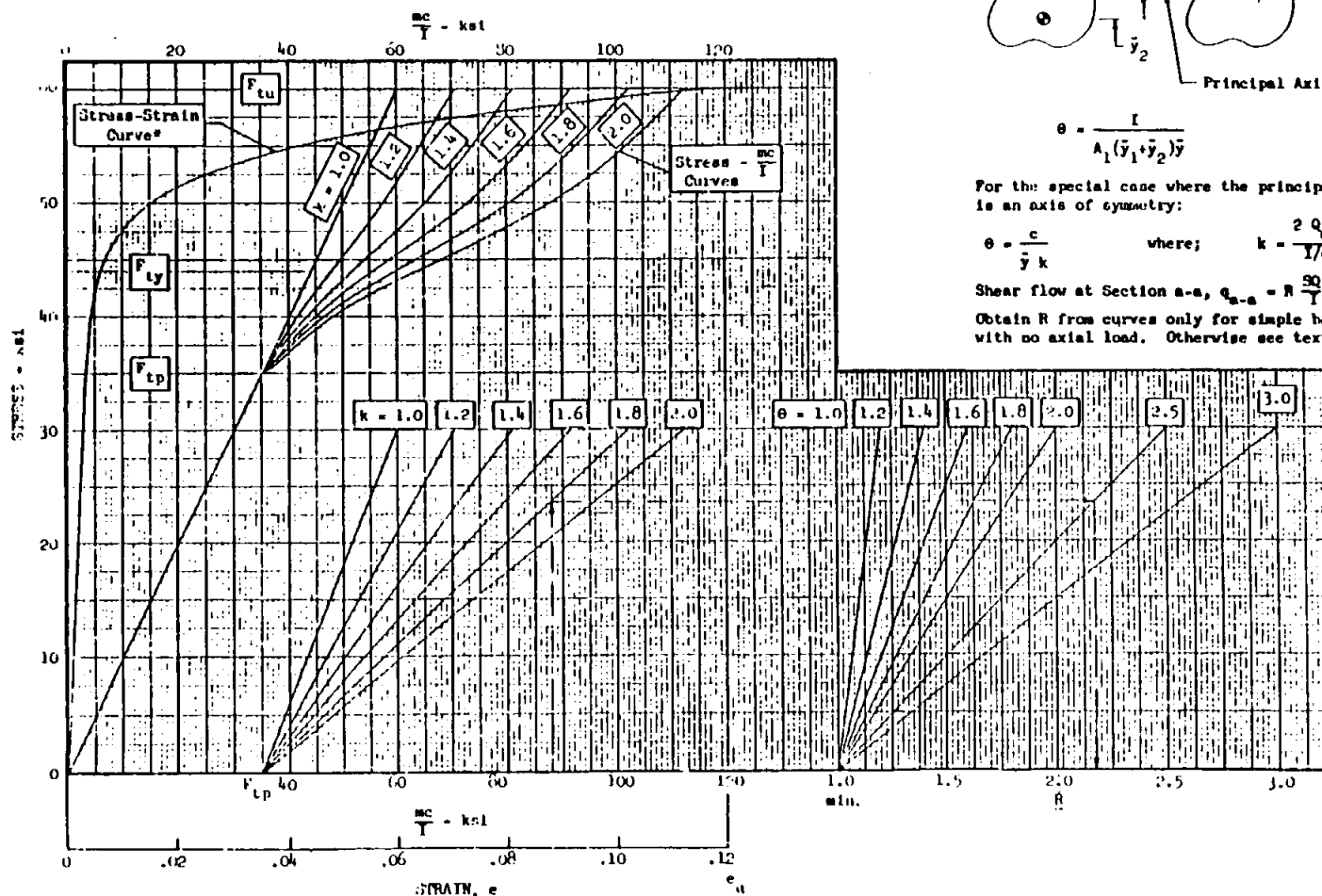
$$\theta = \frac{I}{A_1 (\bar{y}_1 + \bar{y}_2) \bar{y}}$$

For the special case where the principal axis is an axis of symmetry:

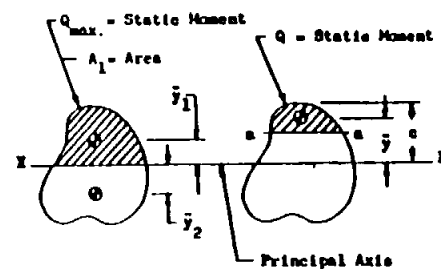
$$\theta = \frac{c}{\bar{y} k} \quad \text{where; } k = \frac{2 Q_{\max}}{I/c}$$

Shear flow at Section a-a, $q_{a-a} = R \frac{Q}{I}$

Obtain R from curves only for simple bending with no axial load. Otherwise see text.



* Based on Hinn: Unstressed Values



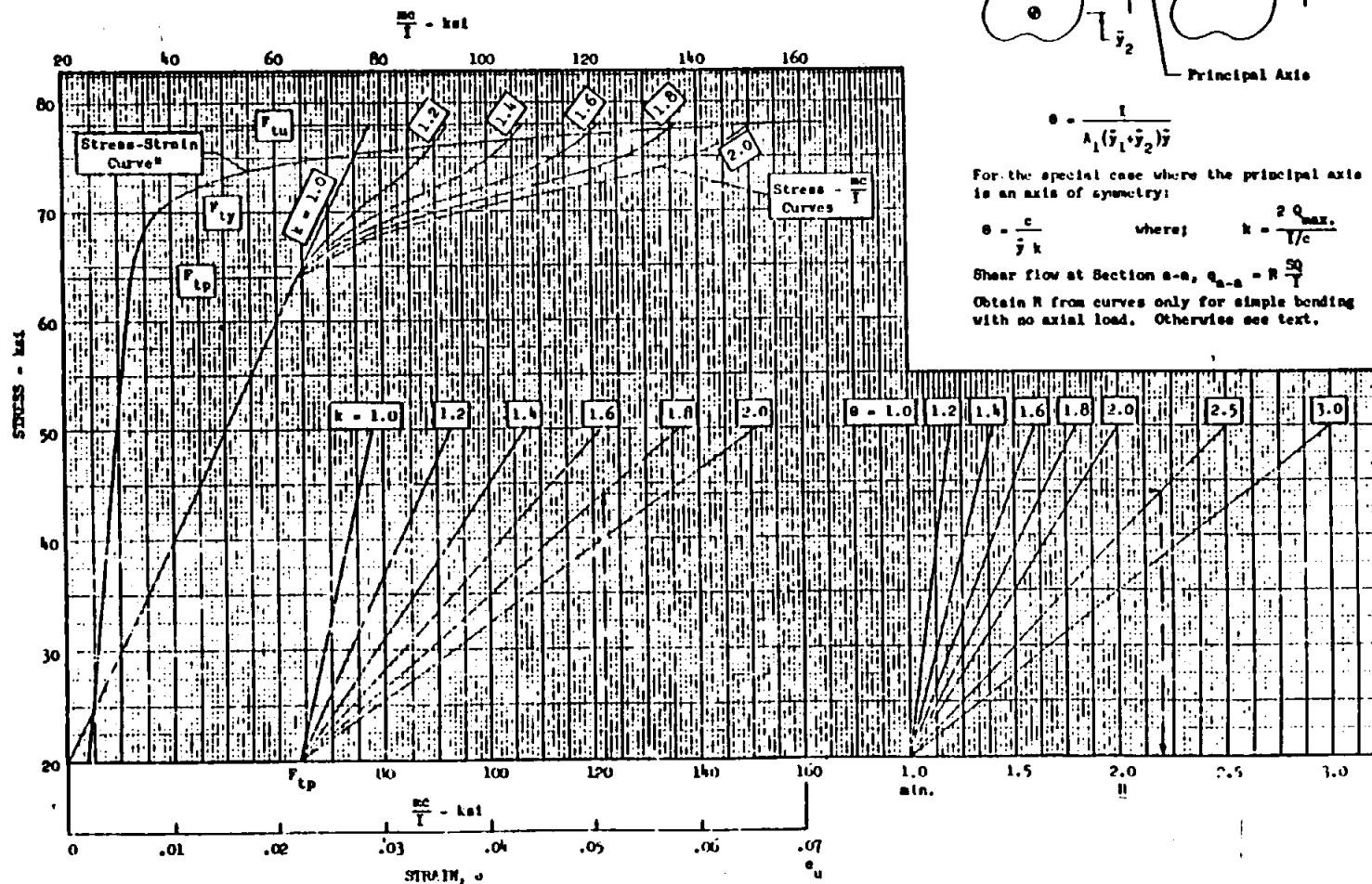
$$\theta = \frac{1}{\lambda_1 (\bar{y}_1 + \bar{y}_2) \bar{y}}$$

For the special case where the principal axis
is an axis of symmetry:

$$\theta = \frac{c}{\bar{y} k} \quad \text{where; } k = \frac{2 Q_{\max.}}{V/c}$$

Shear flow at Section a-a, $q_{a-a} = R \frac{SQ}{Y}$

Obtain R from curves only for simple bending with no axial load. Otherwise see text.

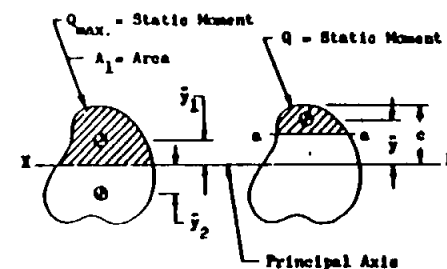


* Based on Minimum Guaranteed Values

242



FIGURE 11
BENDING IN THE PLASTIC RANGE
7075-T6 Aluminum Alloy Die Forging $t \leq 2.00$
(Longitudinal)
Room Temperature



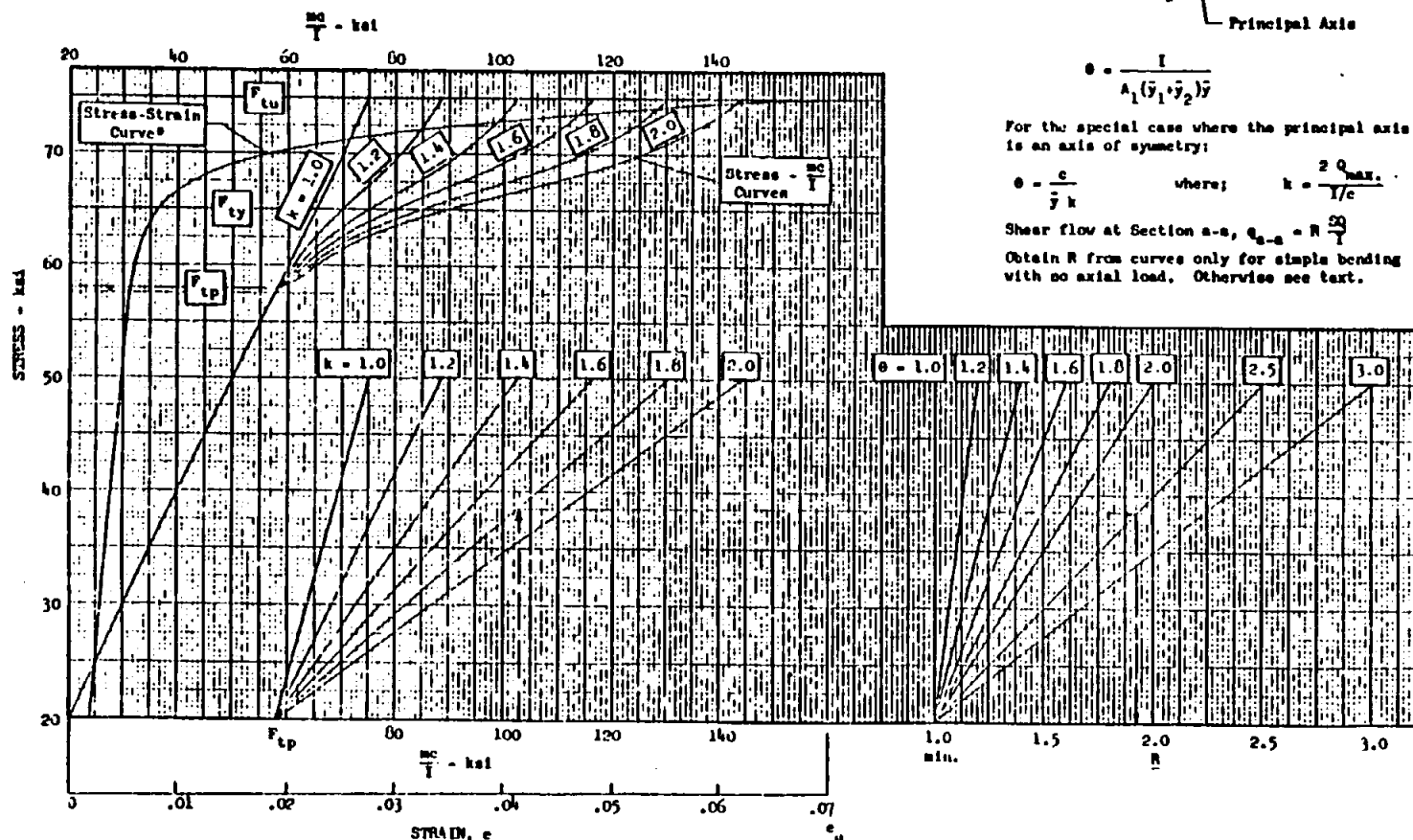
$$e = \frac{I}{A_1(\bar{y}_1 + \bar{y}_2)\bar{y}}$$

For the special case where the principal axis is an axis of symmetry:

$$e = \frac{c}{\bar{y}} k \quad \text{where; } k = \frac{2 Q_{max}}{I/c}$$

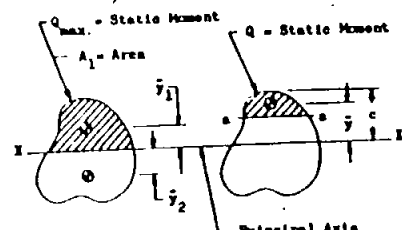
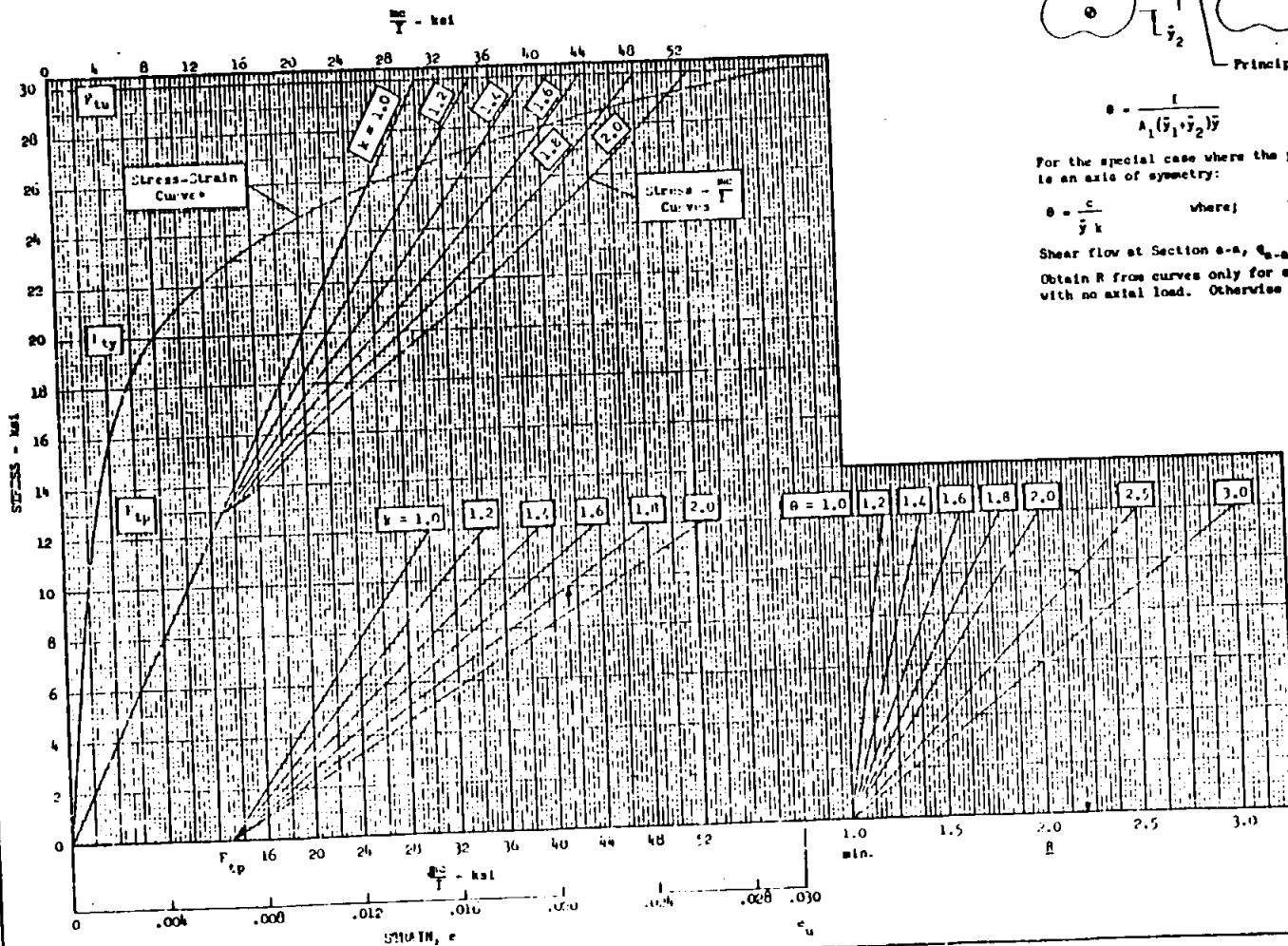
Shear flow at Section a-a, $q_{a-a} = R \frac{Q}{I}$

Obtain R from curves only for simple bending with no axial load. Otherwise see text.



* Based on Minimum Guaranteed Values

FIGURE 12
BENDING IN THE PLASTIC RANGE
356-T6 Aluminum Alloy Sand Casting
Room Temperature



$$Q = \frac{I}{A_1(\bar{y}_1 + \bar{y}_2)}$$

For the special case where the principal axis is an axis of symmetry:

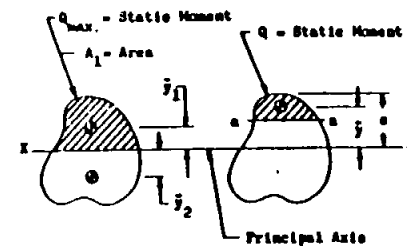
$$Q = \frac{c}{\bar{y}} k \quad \text{where:} \quad k = \frac{2 Q_{max}}{I/c}$$

Shear flow at Section a-a, $Q_{a-a} = R \frac{SQ}{I}$

Obtain R from curves only for simple bending with no axial load. Otherwise see text.

* Based on Minimum Guaranteed Values

FIGURE 13
BENDING IN THE PLASTIC RANGE
ENSOA-75 Magnesium Alloy Extrusion
(Longitudinal)
Room Temperature

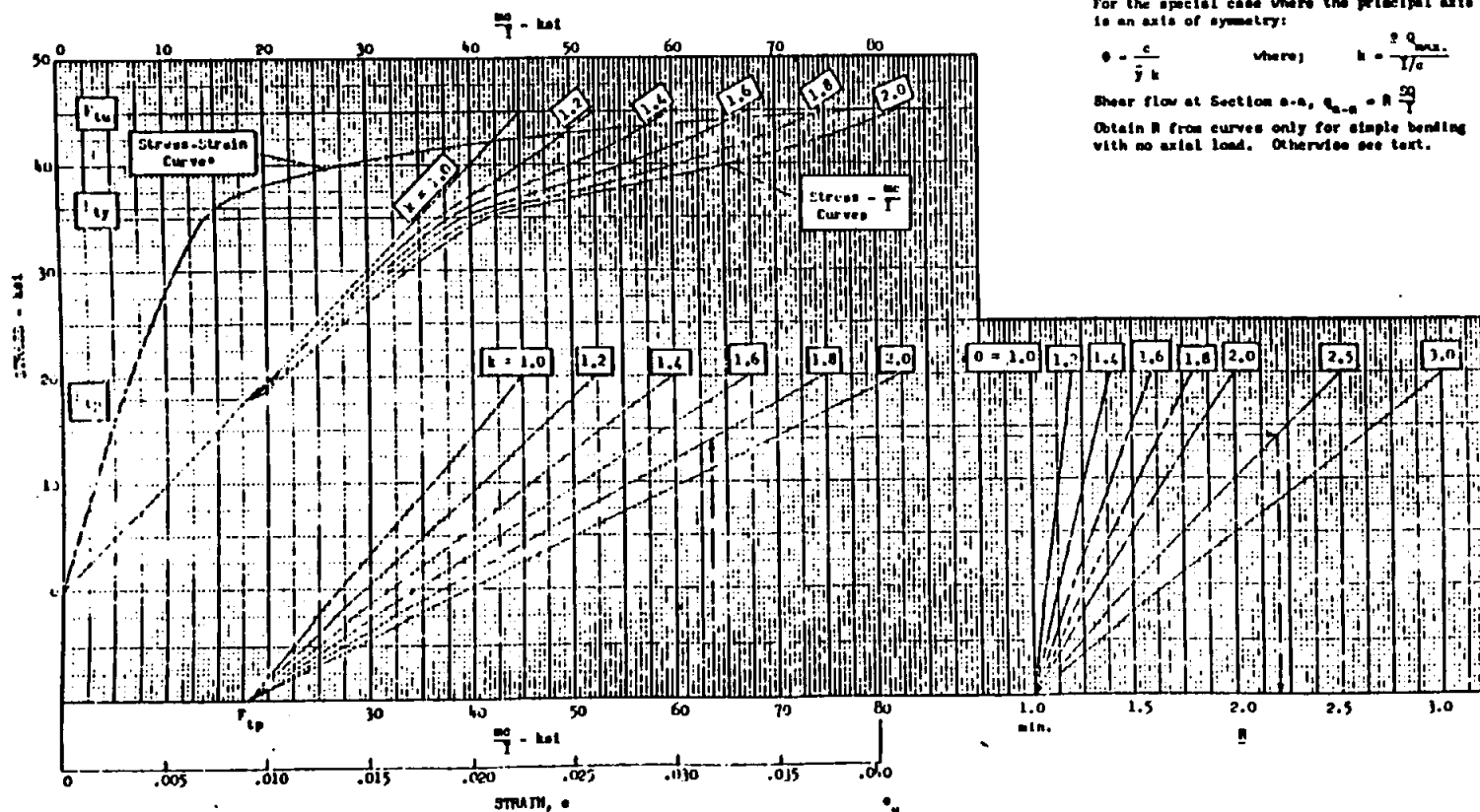


$$e = \frac{1}{A_1(\bar{y}_1 + \bar{y}_2)\bar{y}}$$

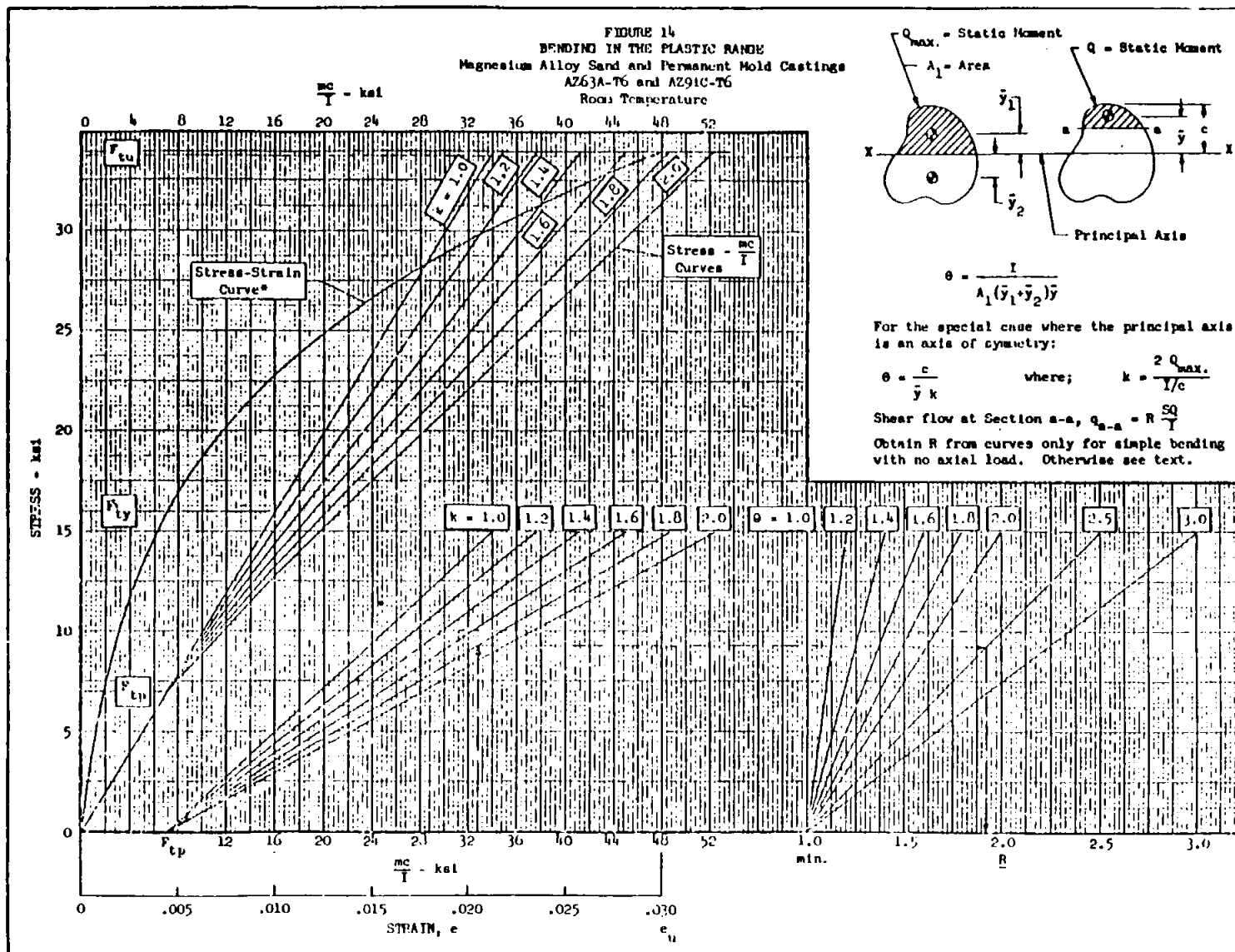
For the special case where the principal axis is an axis of symmetry:

$$e = \frac{c}{\bar{y}k} \quad \text{where;} \quad k = \frac{2Q_{max}}{I/a}$$

Shear flow at Section a-a, $q_{a-a} = R \frac{Q}{I}$
Obtain R from curves only for simple bending with no axial load. Otherwise see text.

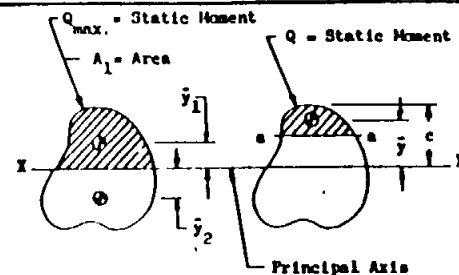


* Based on Minimum Guaranteed Values



* Based on MII. Guaranteed Values

FIGURE 15
BENDING IN THE PLASTIC RANGE
Alloy Steel Cold R & T ≤ .107
Room Temperature

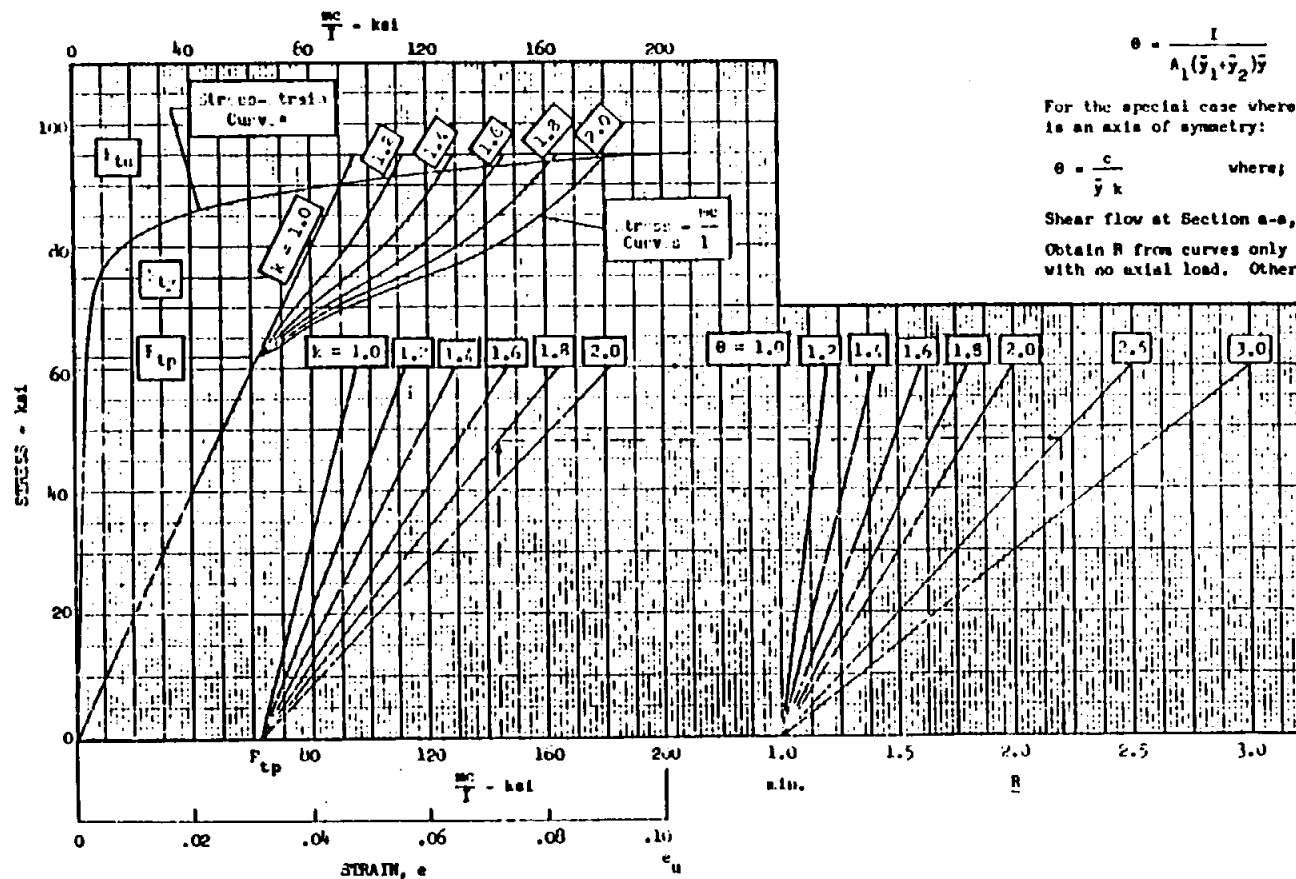


$$\theta = \frac{I}{A_1 (\bar{y}_1 + \bar{y}_2) \bar{y}}$$

For the special case where the principal axis is an axis of symmetry:

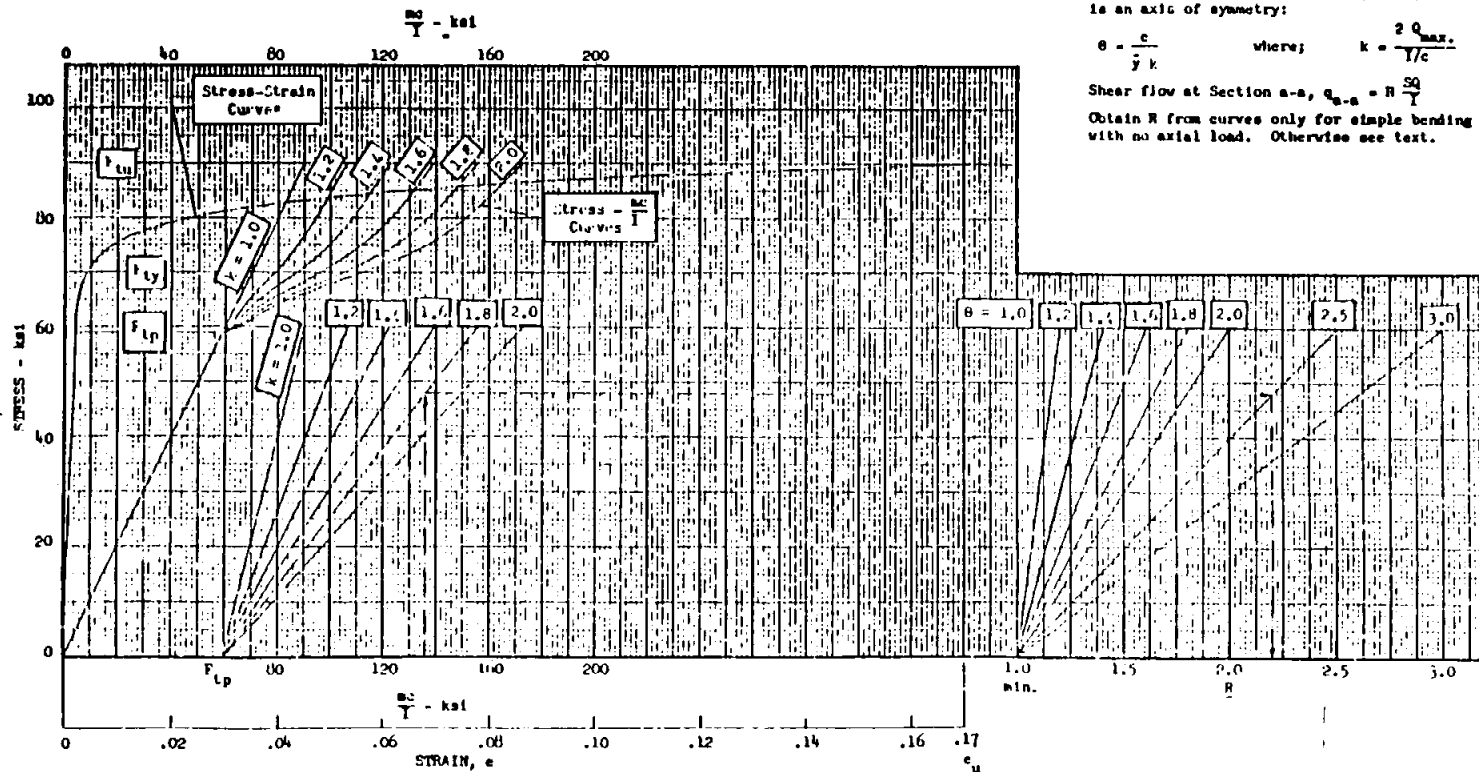
$$\theta = \frac{c}{\bar{y} k} \quad \text{where; } k = \frac{2 Q_{max}}{I/c}$$

Shear flow at Section a-a, $Q_{a-a} = R \frac{SQ}{I}$
Obtain R from curves only for simple bending with no axial load. Otherwise see text.



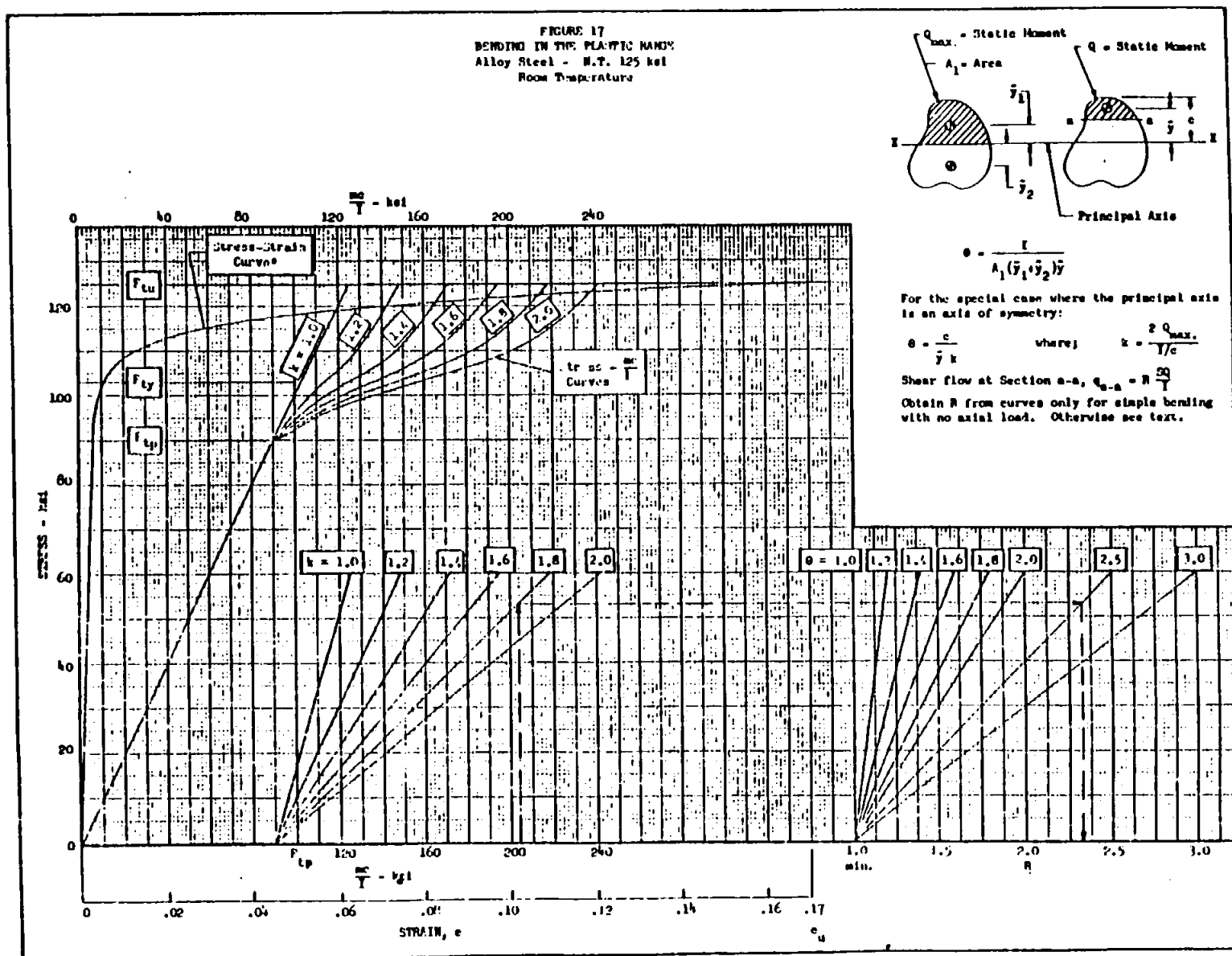
* Based on Minimum Guaranteed Values

FIGURE 16
BENDING IN THE PLASTIC RANGE
Alloy Steel Cond W t > .187
Room Temperature



* Based on Minimum Guaranteed Values

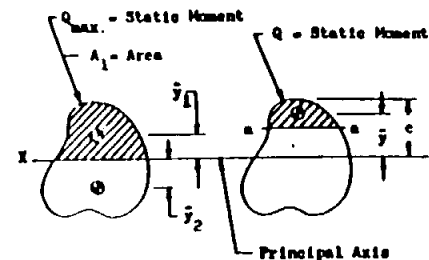
FIGURE 17
BENDING IN THE PLASTIC RANGE
Alloy Steel - M.T. 125 ksi
Room Temperature



* Based on Minimum Guaranteed Values



FIGURE 19
BENDING IN THE PLASTIC RANGE
Alloy Steel - R.T. 180 ksi
Room Temperature

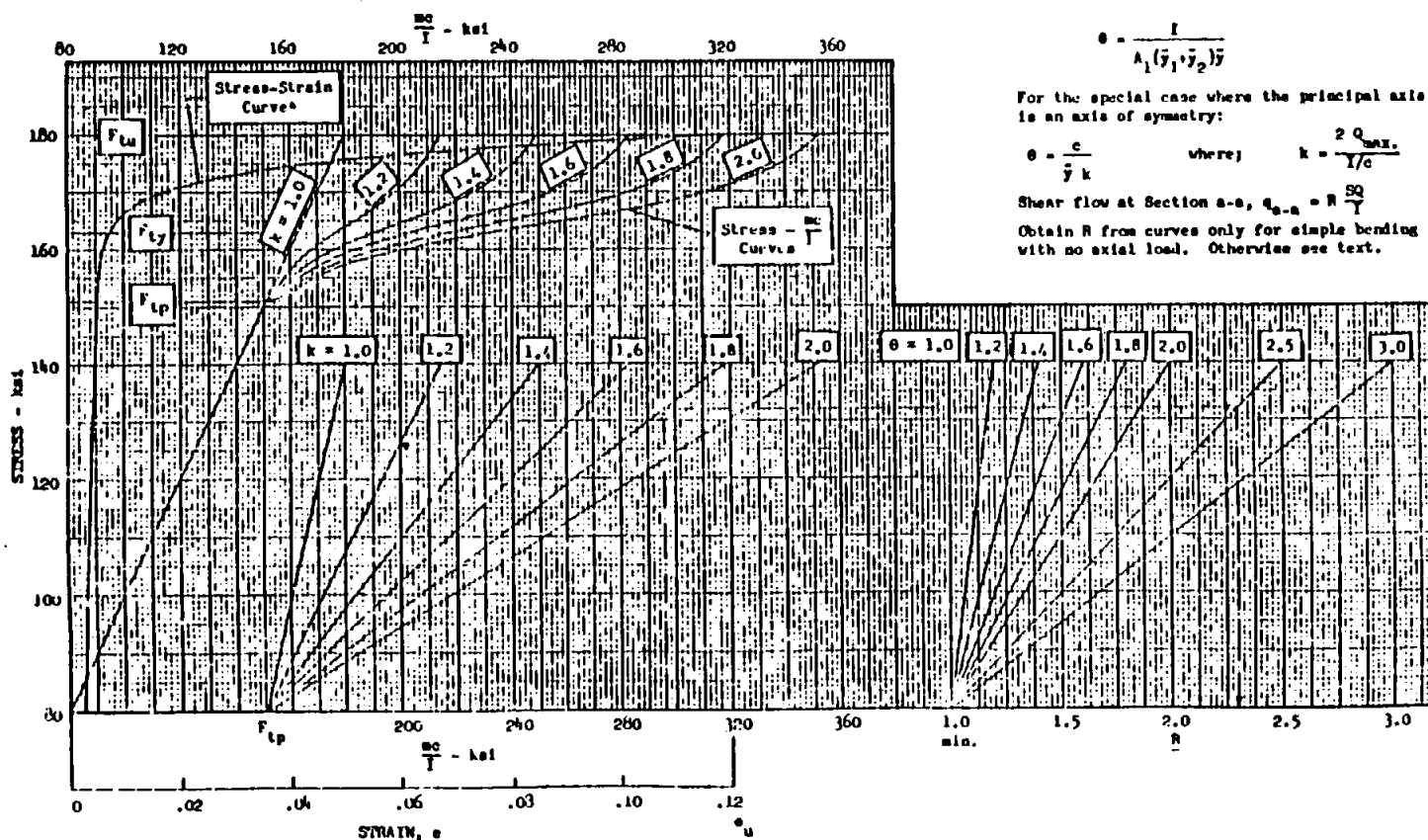


$$\theta = \frac{I}{A_1 (\bar{y}_1 + \bar{y}_2) \bar{y}}$$

For the special case where the principal axis is an axis of symmetry:

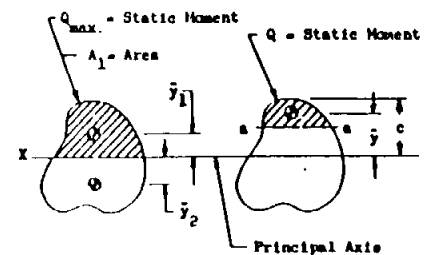
$$\theta = \frac{c}{\bar{y} k} \quad \text{where } k = \frac{2 Q_{max}}{Y/c}$$

Shear flow at Section a-a, $Q_{a-a} = R \frac{SQ}{Y}$
Obtain R from curves only for simple bending with no axial load. Otherwise see text.



* Based on Minimum Guaranteed Values

FIGURE 20
BENDING IN THE PLASTIC RANGE
Alloy Steel - H.T. 190 ksi
Room Temperature

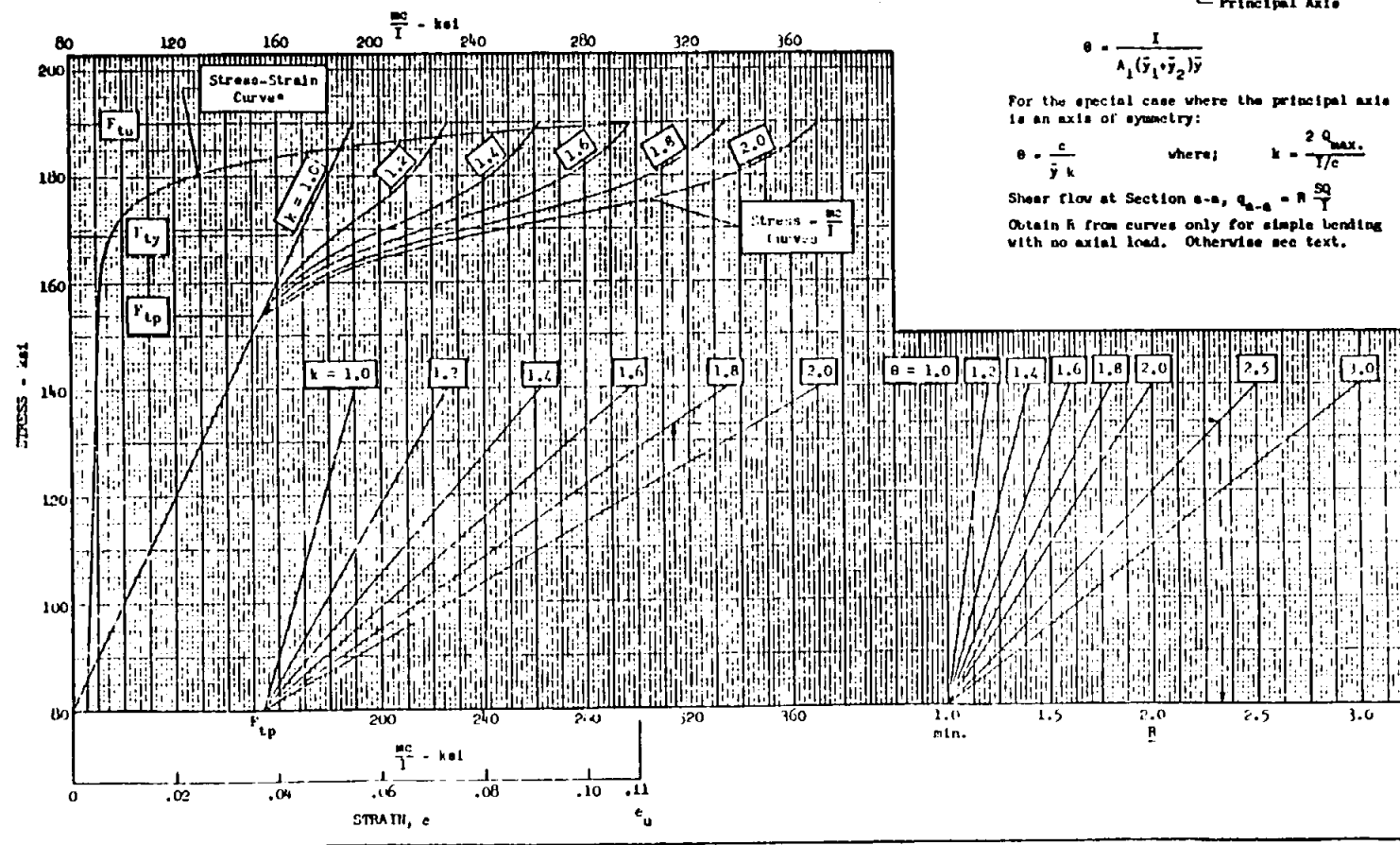


$$\theta = \frac{I}{A_1 (\bar{y}_1 + \bar{y}_2) \bar{y}}$$

For the special case where the principal axis is an axis of symmetry:

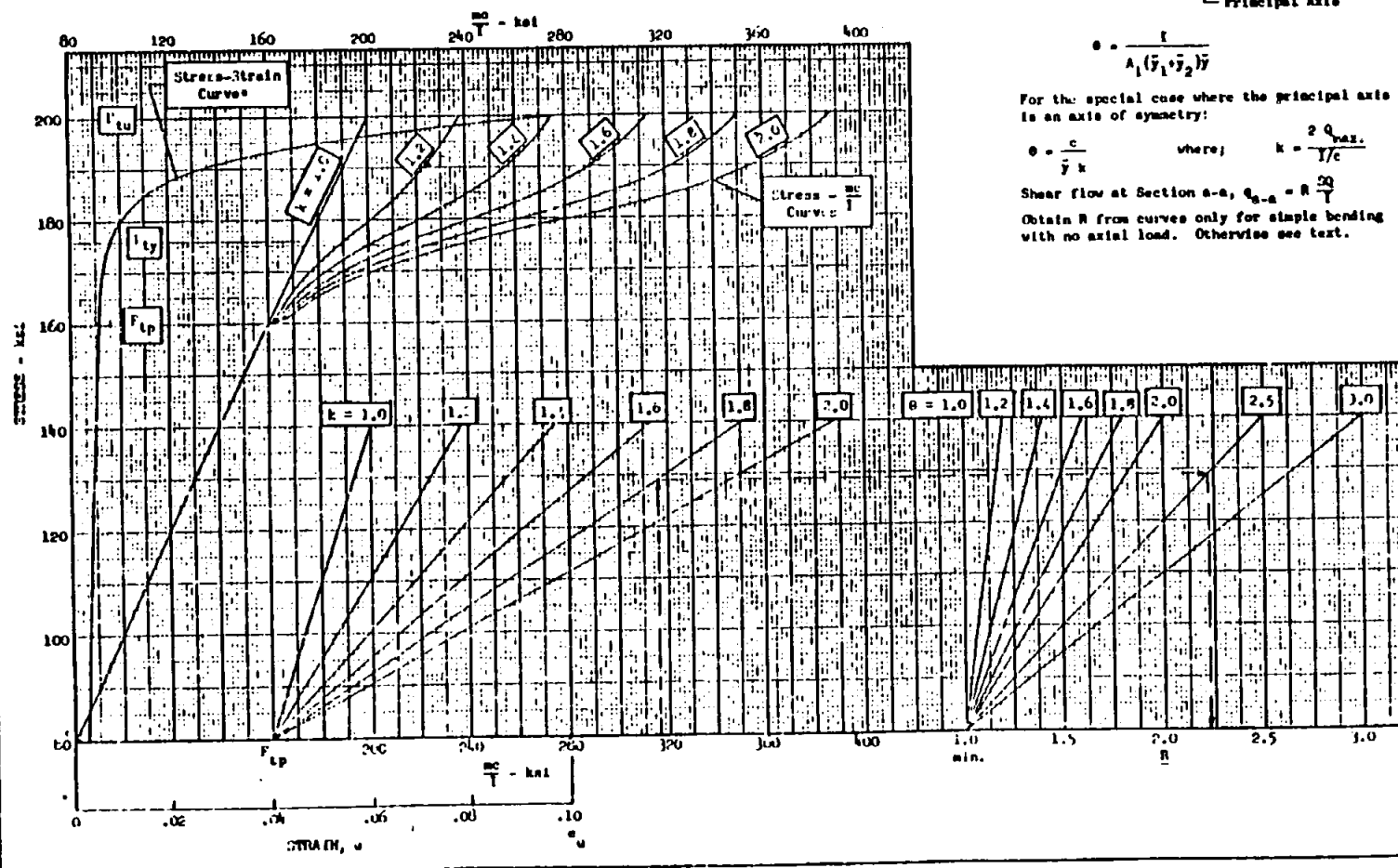
$$\theta = \frac{c}{\bar{y} k} \quad \text{where; } k = \frac{2 Q_{max}}{I/c}$$

Shear flow at Section a-a, $Q_{a-a} = R \frac{SQ}{Y}$
Obtain R from curves only for simple bending with no axial load. Otherwise see text.



* Based on Minimum Guaranteed Values

FIGURE 21
BENDING IN THE PLASTIC RANGE
Alloy Steel - H.T. 200 ksi
Room Temperature



* Based on Minimum Guaranteed Values

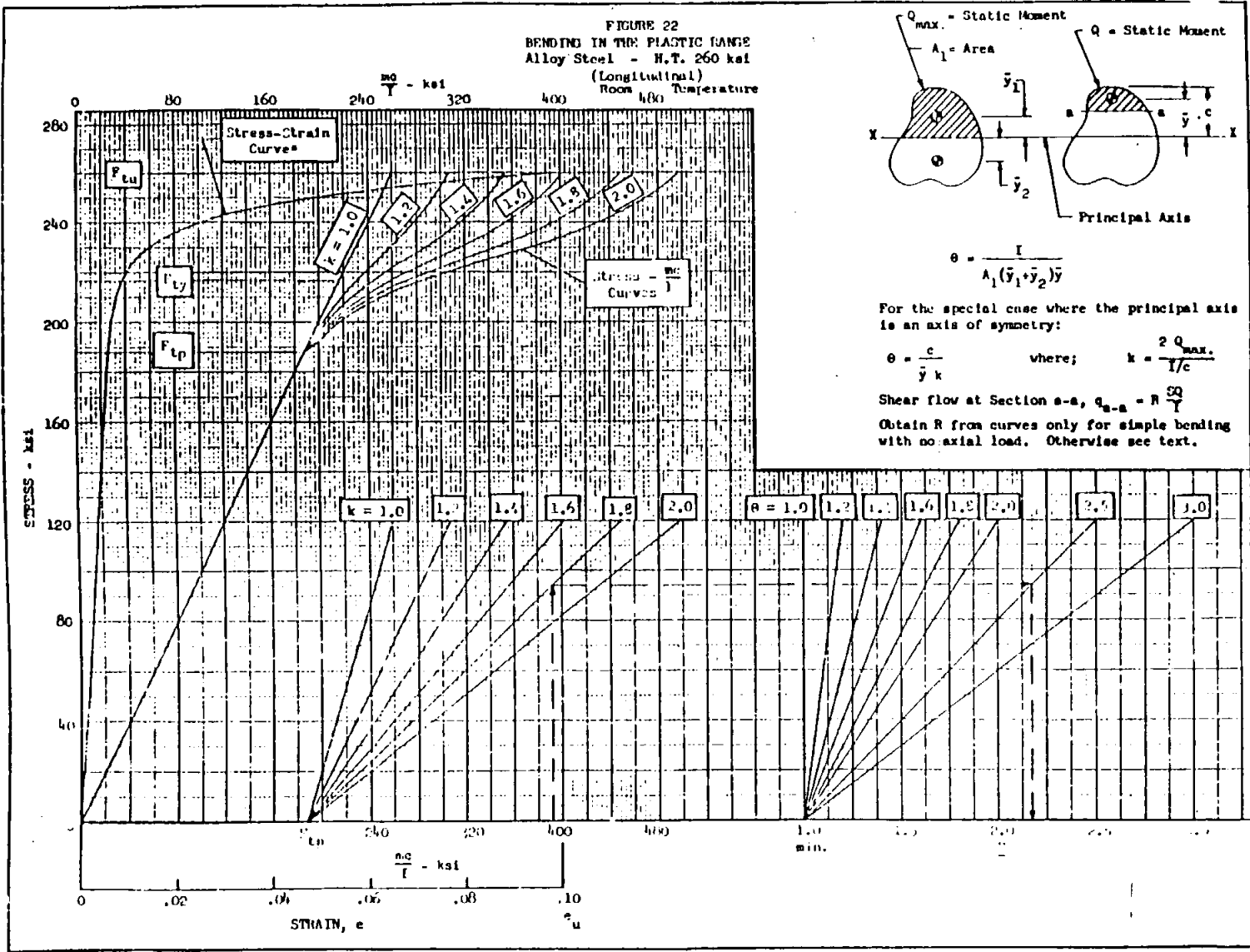
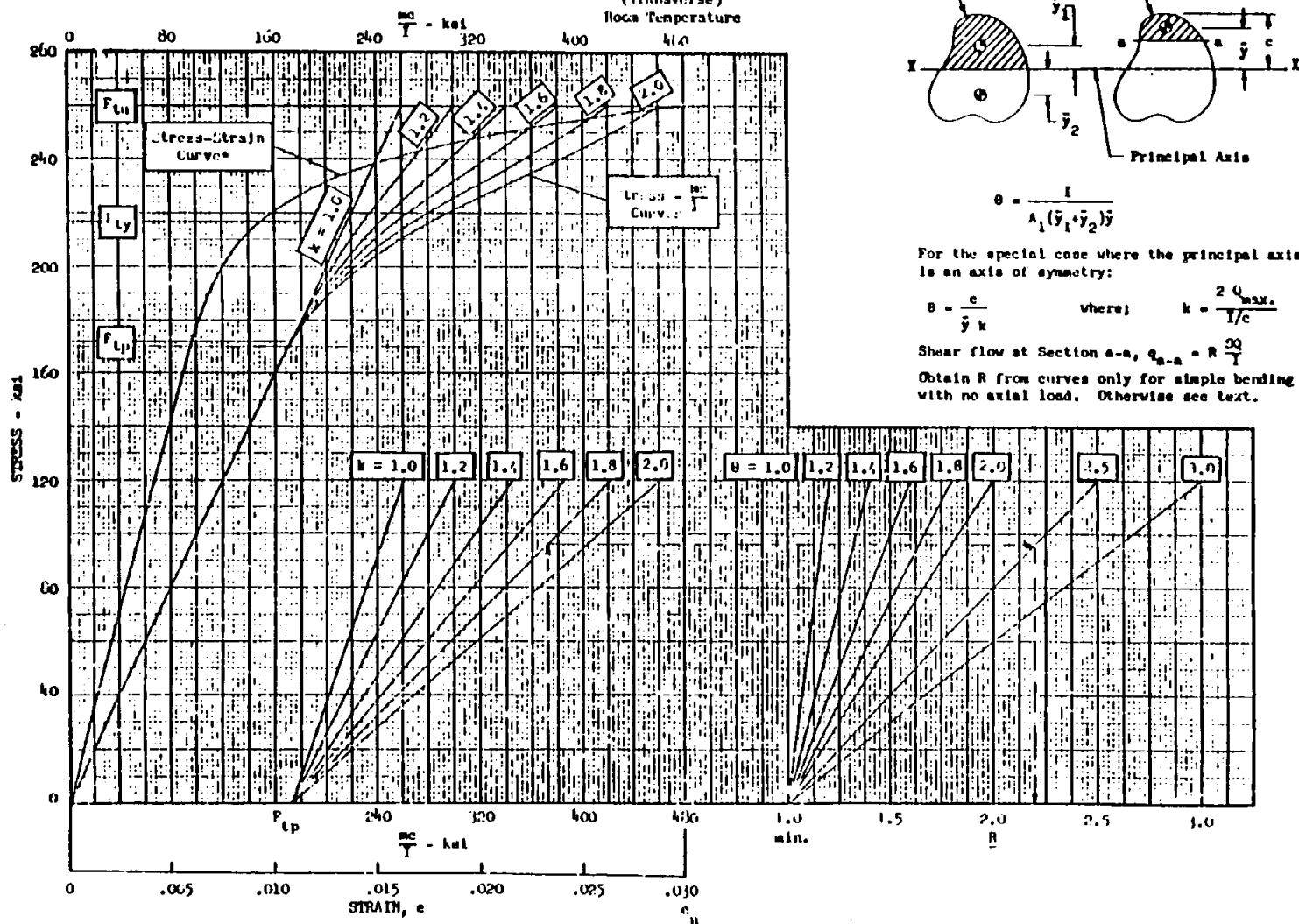
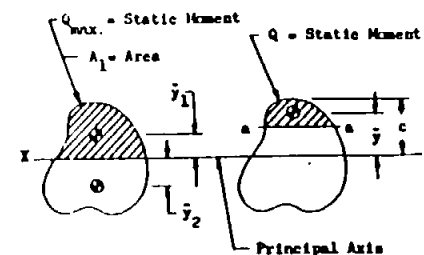


FIGURE 23
BENDING IN THE PLASTIC RANGE
Alloy Steel - H.T. 260 ksi
(Transverse)
Room Temperature



* Based on Minimum Guaranteed Values

FIGURE 24
BENDING IN THE PLASTIC RANGE
SA1-2.5Sn Titanium Alloy Bar and Forging
Annealed
Room Temperature

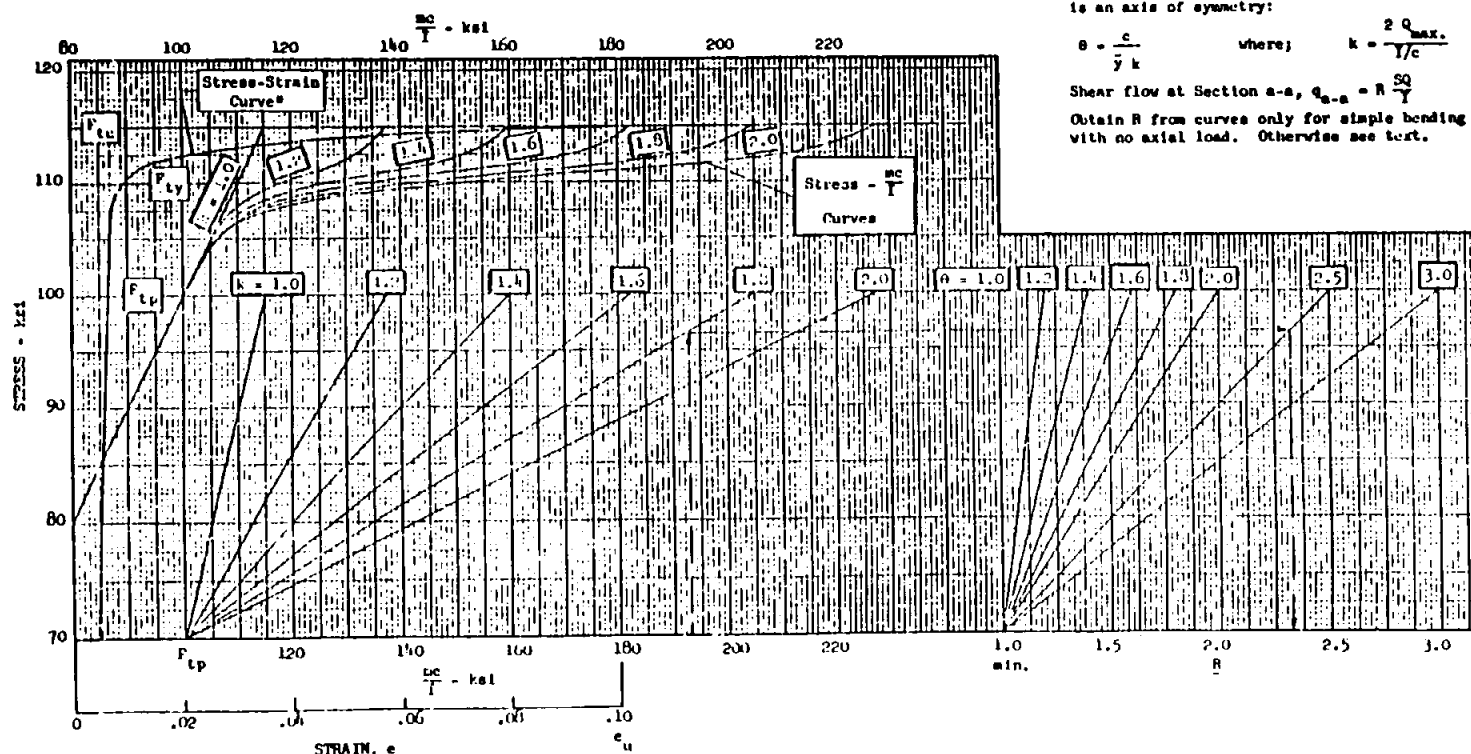


$$\theta = \frac{I}{A_1 (\bar{y}_1 + \bar{y}_2) \bar{y}}$$

For the special case where the principal axis is an axis of symmetry:

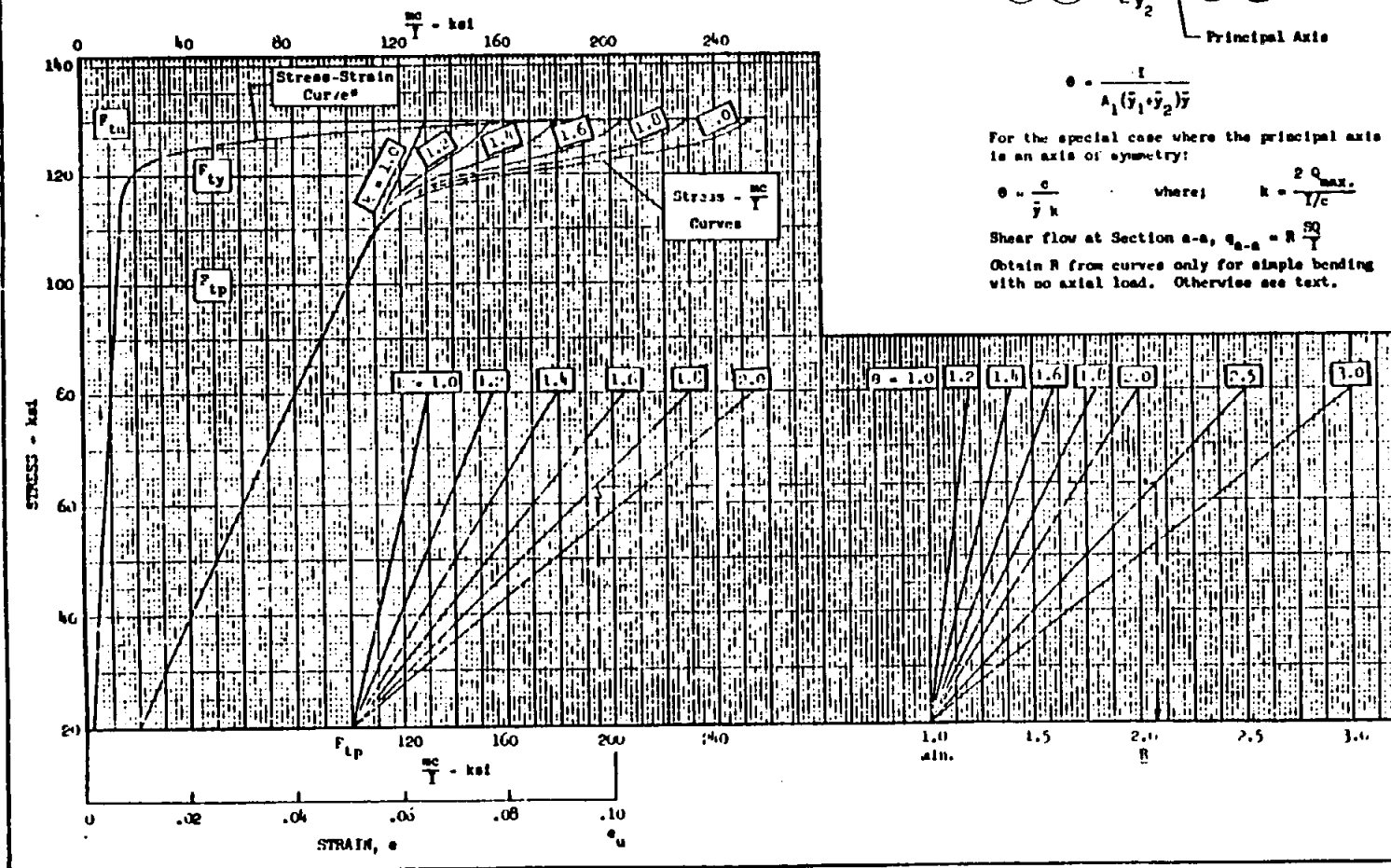
$$\theta = \frac{c}{\bar{y} k} \quad \text{where;} \quad k = \frac{2 Q_{\max}}{I/c}$$

Shear flow at Section a-a, $Q_{a-a} = R \frac{SQ}{Y}$
Obtain R from curves only for simple bending with no axial load. Otherwise see text.



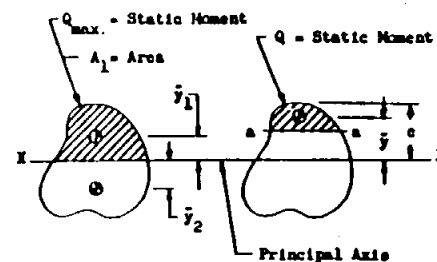
* Based on Minimum Guaranteed Values

FIGURE 25
BENDING IN THE PLASTIC RANGE
6Al-4V Titanium Alloy Bar and Forging
Annealed
Room Temperature



* Based on Minimum Guaranteed Values

FIGURE 26
BENDING IN THE PLASTIC RANGE
6AL-4V Titanium Alloy Bar and Forging $t \leq 1.0$
Solution Treated and Aged
Room Temperature



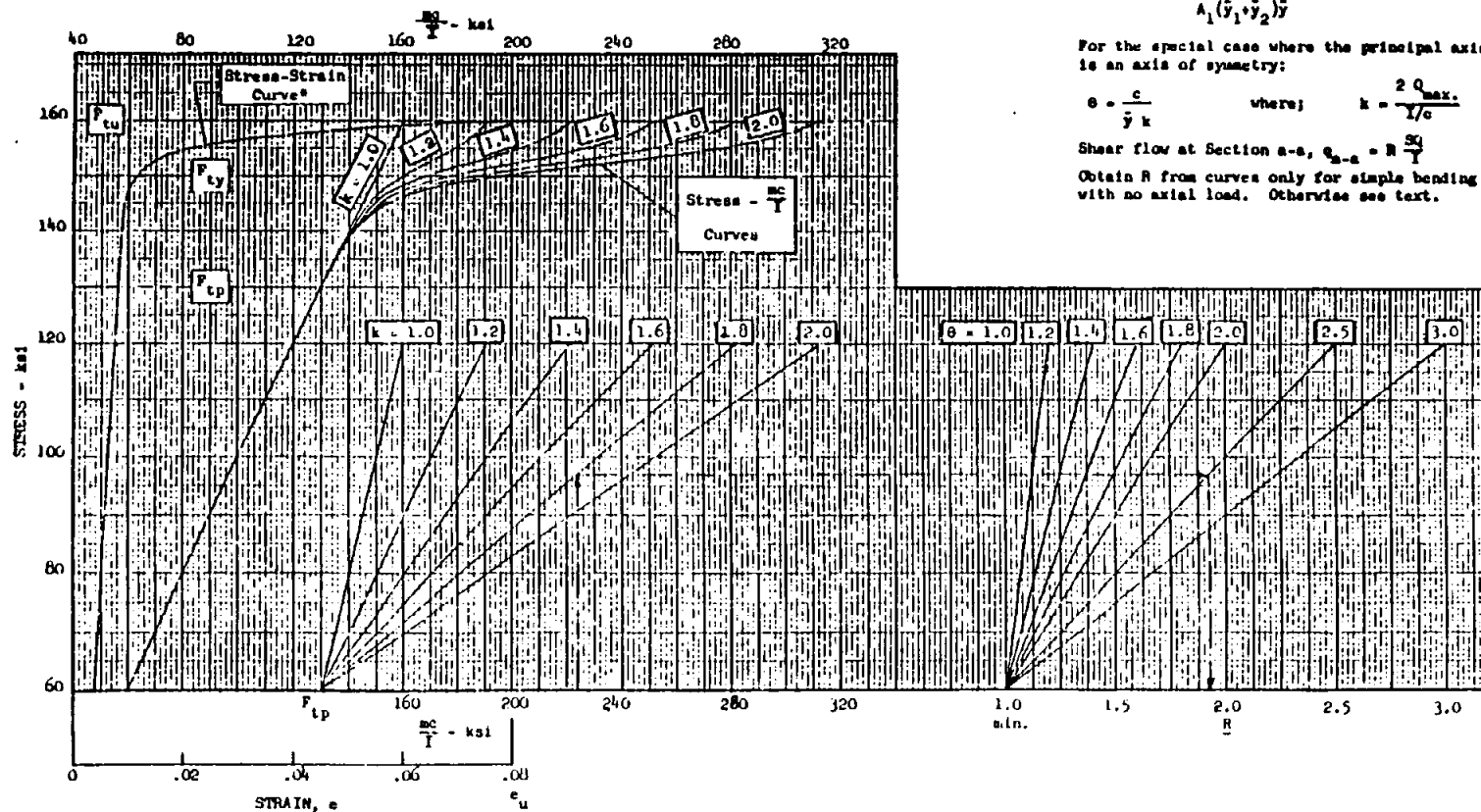
$$Q = \frac{I}{A_1(\bar{y}_1 + \bar{y}_2)\bar{y}}$$

For the special case where the principal axis is an axis of symmetry:

$$Q = \frac{c}{\bar{y}k} \quad \text{where;} \quad k = \frac{2Q_{max}}{I/c}$$

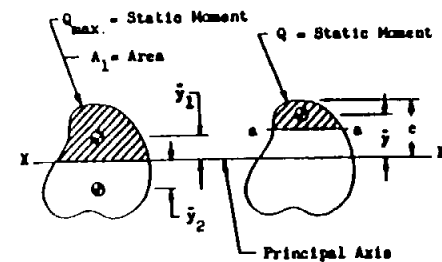
Shear flow at Section a-a, $Q_{a-a} = R \frac{SQ}{I}$

Obtain R from curves only for simple bending with no axial load. Otherwise see text.



* Based on Minimum Guaranteed Values

FIGURE 27
BENDING IN THE PLASTIC RANGE
6Al-4V Titanium Alloy Bar and Forging 1.0 < t ≤ 2.0
Solution Treated and Aged
Room Temperature

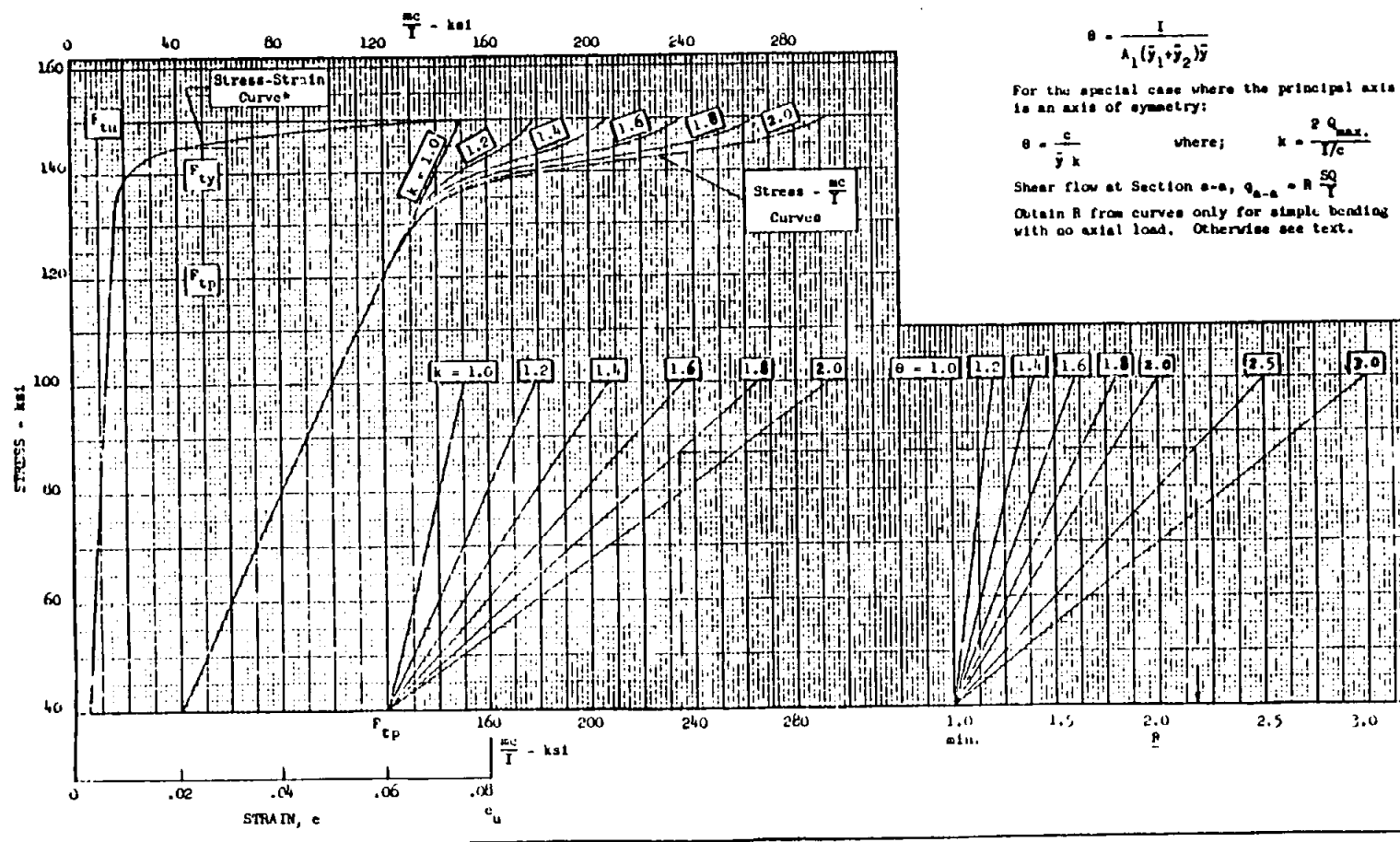


$$\theta = \frac{I}{A_1 (\bar{y}_1 + \bar{y}_2) \bar{y}}$$

For the special case where the principal axis is an axis of symmetry:

$$\theta = \frac{c}{\bar{y} k} \quad \text{where; } k = \frac{2 Q_{max}}{I/c}$$

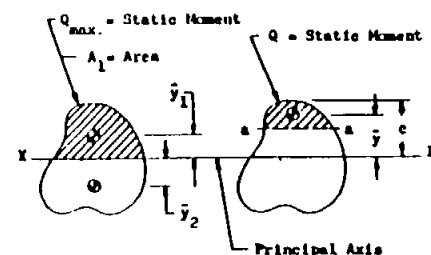
Shear flow at Section a-a, $Q_{a-a} = R \frac{SQ}{I}$
Obtain R from curves only for simple bending with no axial load. Otherwise see text.



* Based on Minimum Guaranteed Values

260

FIGURE 26
BENDING IN THE PLASTIC RANGE
6AL-4V Titanium Alloy Bar and Forging $2.0 < l \leq 3.0$
Solution Treated and Aged
Room Temperature

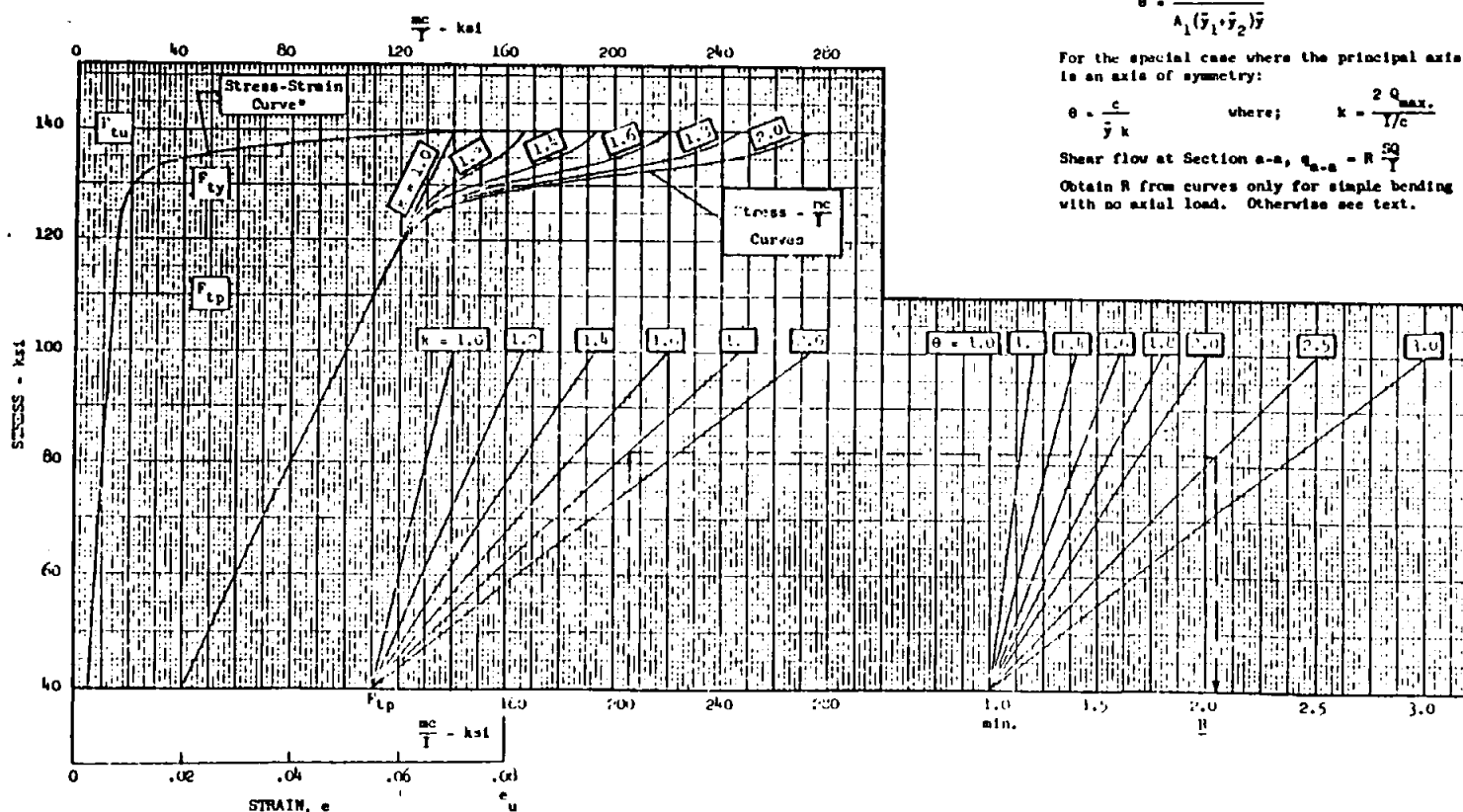


$$\theta = \frac{l}{A_1 (\bar{y}_1 + \bar{y}_2) \bar{y}}$$

For the special case where the principal axis is an axis of symmetry:

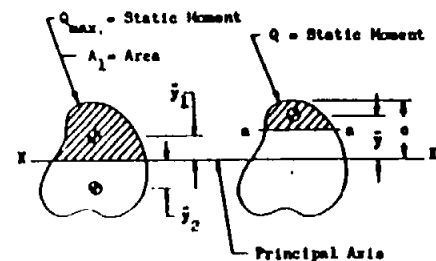
$$\theta = \frac{c}{\bar{y} k} \quad \text{where; } k = \frac{2 Q_{max}}{Y/c}$$

Shear flow at Section a-a, $q_{a-a} = R \frac{SQ}{I}$
Obtain R from curves only for simple bending with no axial load. Otherwise see text.



* Based on Minimum Guaranteed Values

FIGURE 29
BENDING IN THE PLASTIC RANGE
6AL-6V-2Sn Titanium Alloy Bar and Forging 1.0 < t ≤ 2.0
Solution Treated and Aged
Room Temperature

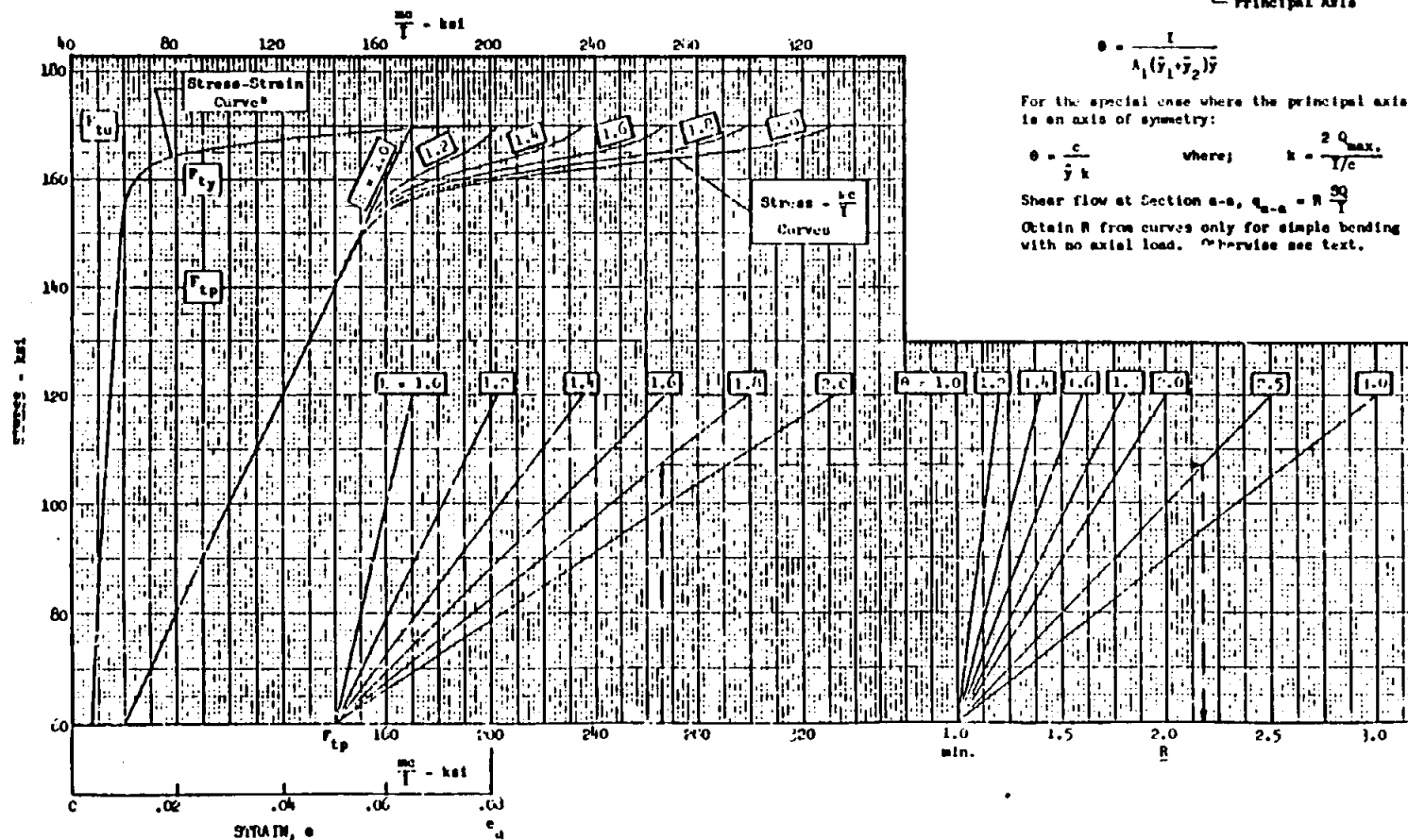


$$\theta = \frac{I}{A_1(\bar{y}_1 + \bar{y}_2)\bar{y}}$$

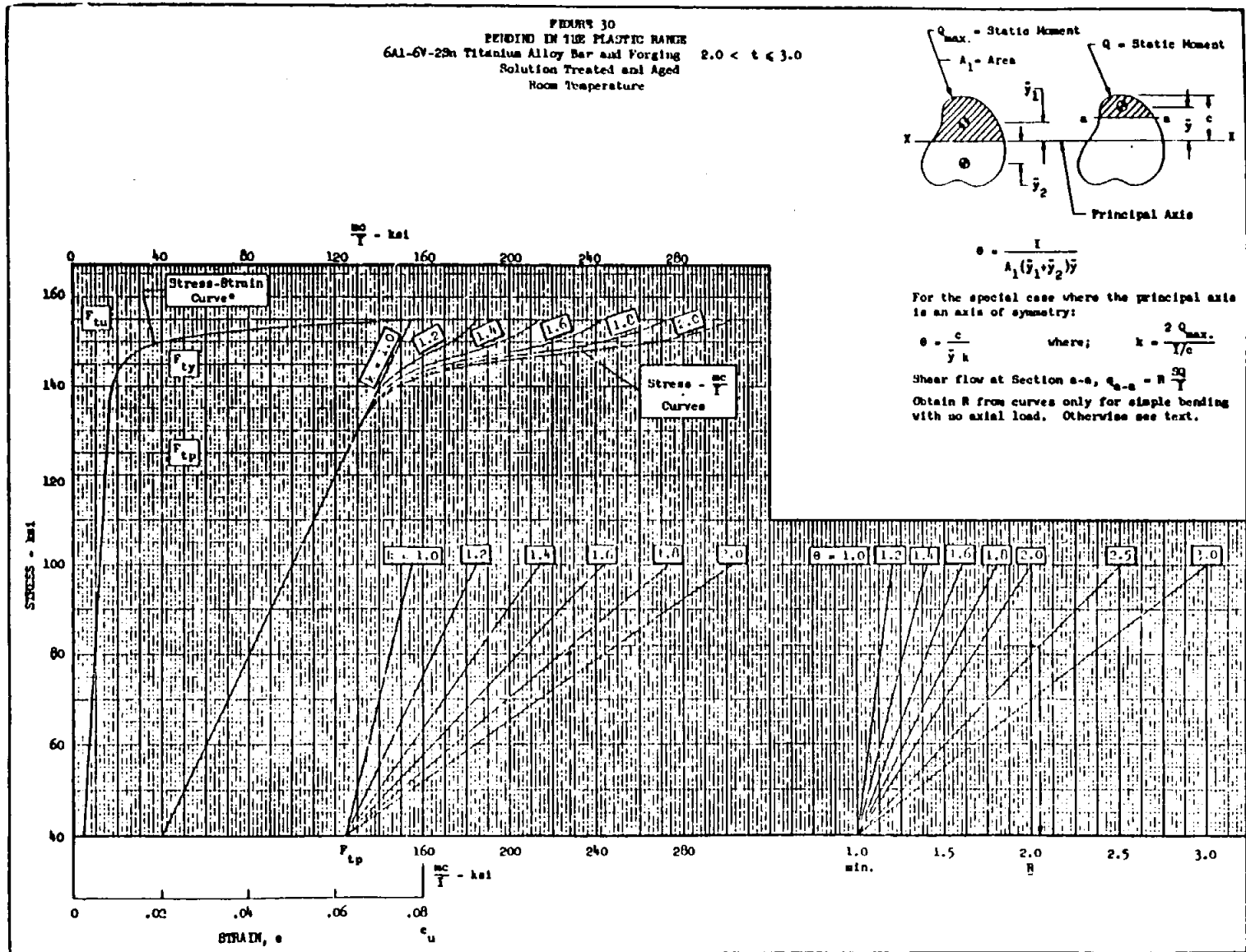
For the special case where the principal axis is an axis of symmetry:

$$\theta = \frac{c}{\bar{y}k} \quad \text{where; } k = \frac{2Q_{max}}{I/c}$$

Shear flow at Section a-a, $q_{a-a} = R \frac{Q}{I}$
Obtain R from curves only for simple bending with no axial load. Otherwise see text.

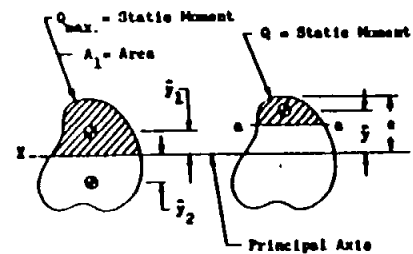


^a Based on Minimum Guaranteed Values



* Based on Minimum Guaranteed Values

FIGURE 31
BENDING IN THE PLASTIC RANGE
6Al-6V-2Sn Titanium Alloy Bar and Forging $3.0 < k \leq 4.0$
Solution Treated and Aged
Room Temperature

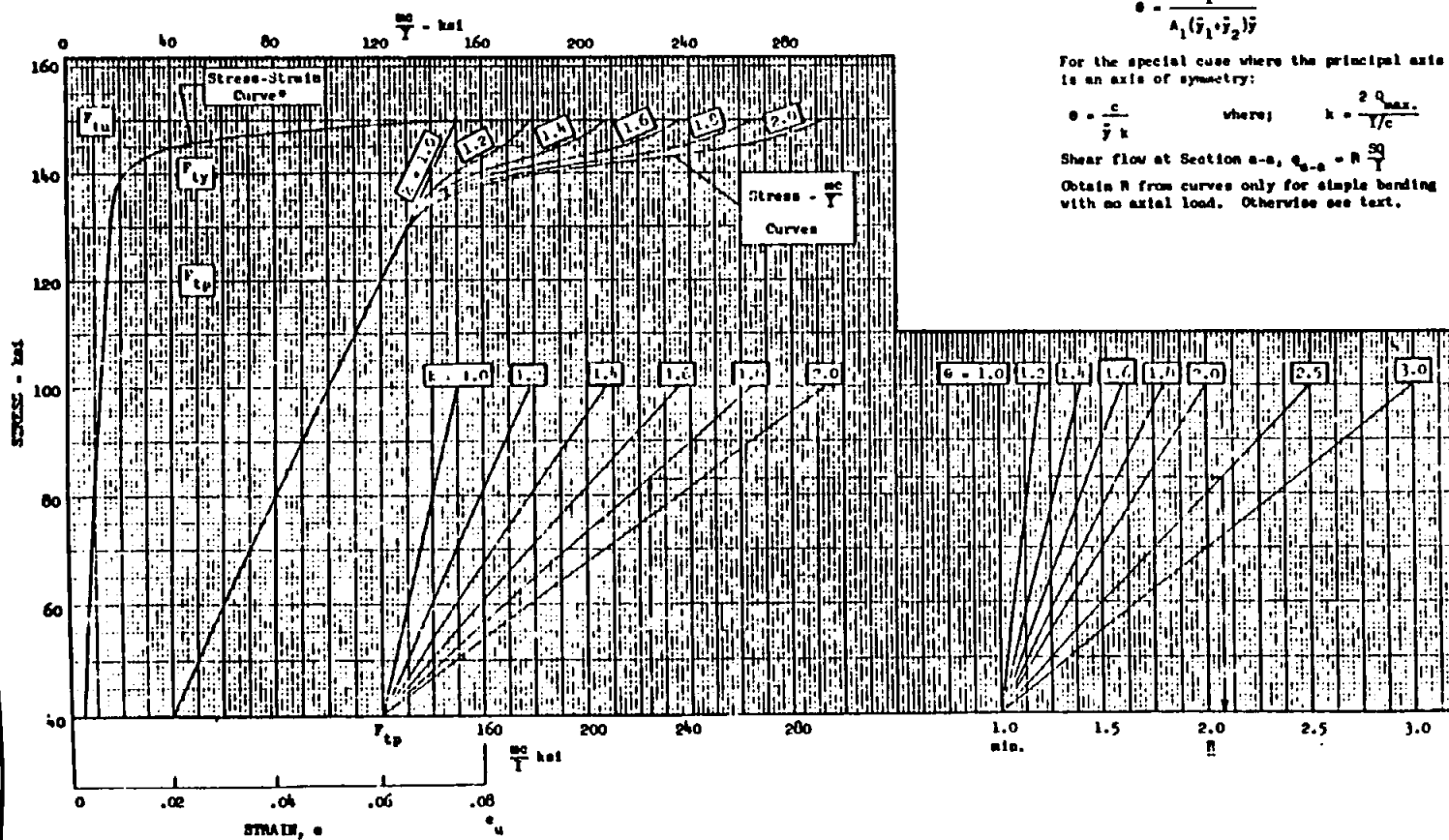


$$e = \frac{I}{A_1(\bar{y}_1 + \bar{y}_2)\bar{y}}$$

For the special case where the principal axis is an axis of symmetry:

$$e = \frac{c}{\bar{y}} k \quad \text{where; } k = \frac{2 Q_{max}}{Y/c}$$

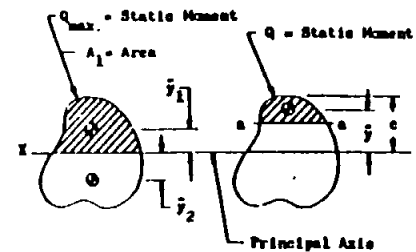
Shear flow at Section a-a, $q_{a-a} = R \frac{SQ}{Y}$
Obtain R from curves only for simple bending with no axial load. Otherwise see text.



* Based on Minimum Guaranteed Values



FIGURE 33
BENDING IN THE PLASTIC RANGE
13V-11Cr-3Al Titanium Alloy Plate $t \leq .250$
Annealed
Room Temperature

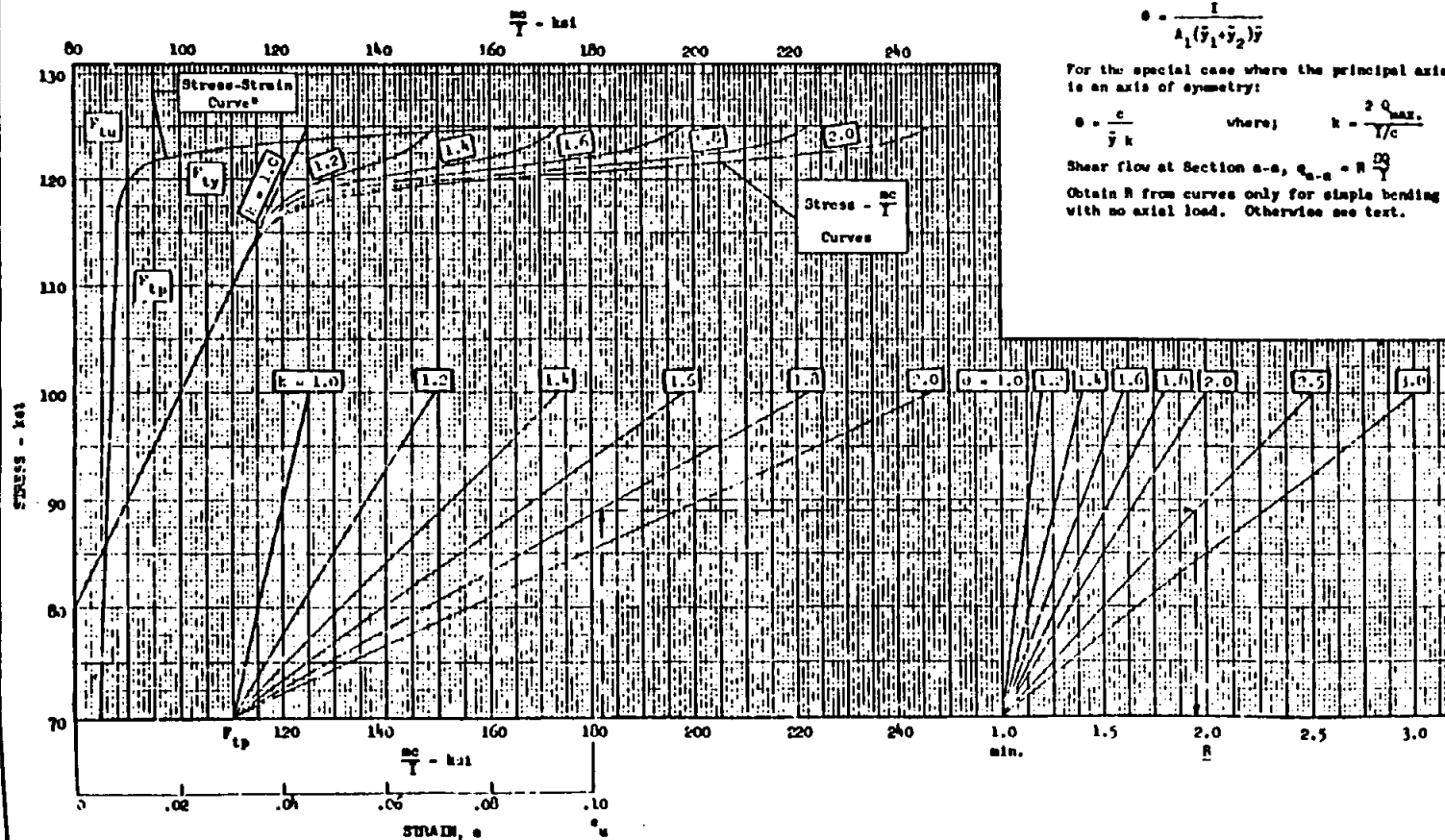


$$Q = \frac{I}{A_1(\bar{y}_1 + \bar{y}_2)\bar{y}}$$

For the special case where the principal axis is an axis of symmetry:

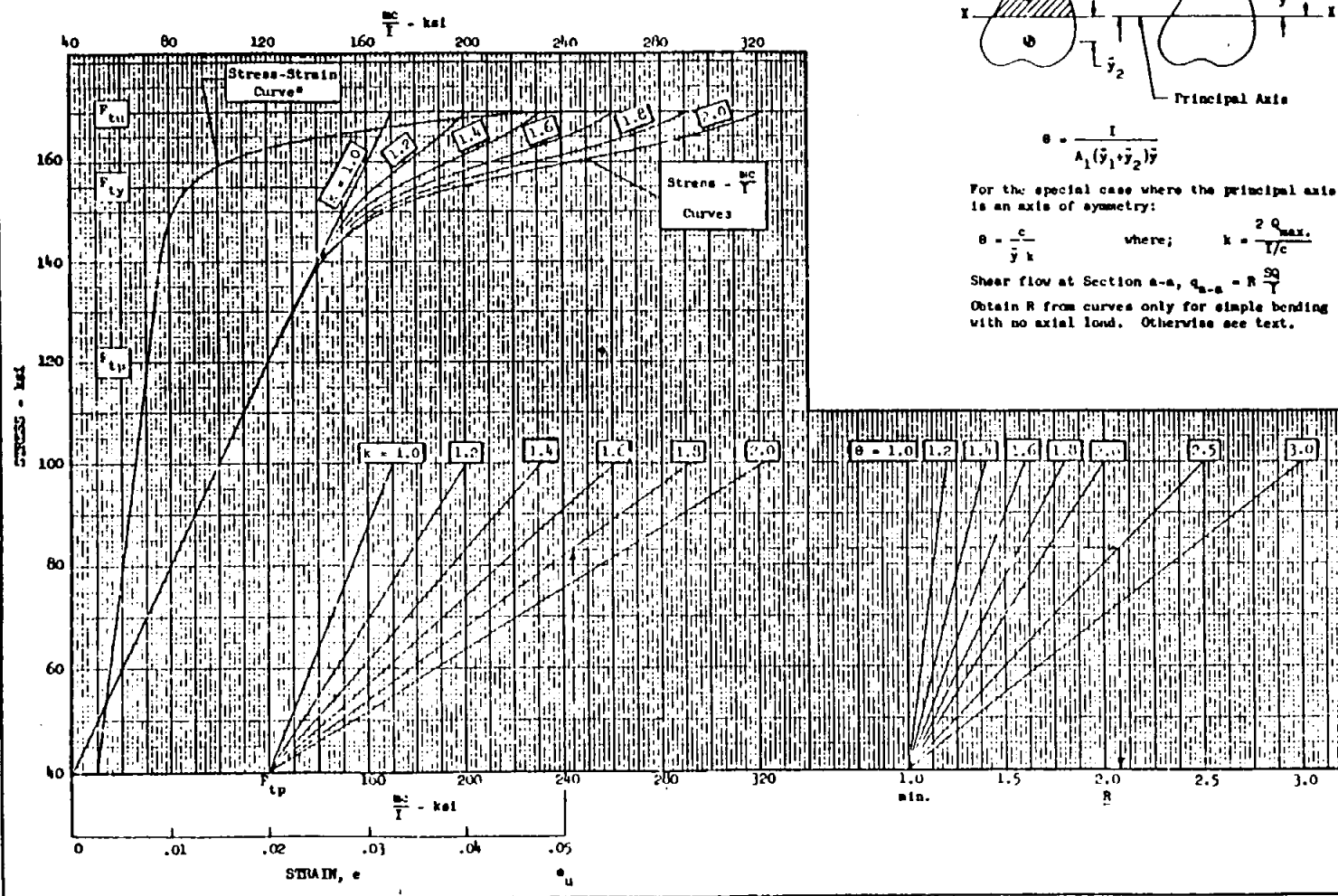
$$Q = \frac{c}{\bar{y}k} \quad \text{where;} \quad k = \frac{2Q_{max}}{I/c}$$

Shear flow at Section a-a, $Q_{a-a} = R \frac{dQ}{dy}$
Obtain R from curves only for simple bending with no axial load. Otherwise see text.



* See 1.4.4 Minimum Guaranteed Values

FIGURE 3b
BENDING IN THE PLASTIC RANGE
13V-11Cr-3Al Titanium Alloy Plate $t \leq .250$
Solution Treated and Aged
Room Temperature



* Based on Minimum Guaranteed Values

STRUCTURAL ANALYSIS MANUAL
GENERAL DYNAMICS/CONVAIR AND SPACE SYSTEMS DIVISION

Data Source, Section 1.3 Reference 2

17.6 TABLE OF CONTENTS FOR BENDING MODULUS OF RUPTURE CURVES FOR SYMMETRICAL SECTIONS

These curves provide yield and ultimate modulus of rupture values for symmetrical sections only. For materials with significantly different tension and compression stress-strain curves, the necessary corrections for shifting of the neutral axis are already included. In the case of work hardened stainless steels in longitudinal bending with all fibers in tension (as in pressurized cylinders), the transverse Modulus of Rupture Curves are applicable.

It is recommended that Reference [△]28 or other official sources be used for allowable material properties. Where these values correspond directly to the values called out on the graphs of this section, the modulus of rupture values are applicable as shown.

Where material allowables vary with thickness, cross-sectional area, etc., only one or two Modulus of Rupture Curves are presented. Therefore, for material properties slightly higher or lower than those used in the given curve, the modulus values may be ratioed up or down (provided the % elongations are practically the same).



Section 1.3

STRUCTURAL ANALYSIS MANUAL
GENERAL DYNAMICS/CONVAIR AND SPACE SYSTEMS DIVISION

SECTION 17.6

PLASTIC BENDING

MINIMUM BENDING MODULUS OF RUPTURE FOR SYMMETRICAL SECTIONS.

STEELS

	PAGE
CARBON STEEL AISI 1023-1025	17.6.4
AISI ALLOY STEEL Δ	17.6.5
A-286	17.6.7
AISI 301	17.6.8
AISI 321	17.6.11
PH 15-7 Mo	17.6.12
17-4 PH	17.6.13
17-7 PH	17.6.14
19-9 DL AND 19-9 DX	17.6.15

ALUMINUM

2014	17.6.16
2024	17.6.17
6061	17.6.20
7075	17.6.21
7079	17.6.24

Δ AISI ALLOY STEELS INCLUDE AISI 4130, 4140, 4340, 8630, 8735,
8740 AND 9840.

STRUCTURAL ANALYSIS MANUAL
GENERAL DYNAMICS/CONVAIR AND SPACE SYSTEMS DIVISION

TITANIUM

	PAGE
COMMERCIALLY PURE	17.6.27
Ti - 8 Mn	17.6.27
Ti - 6 AL-4V	17.6.28
Ti - 4 Mn-4AL	17.6.28

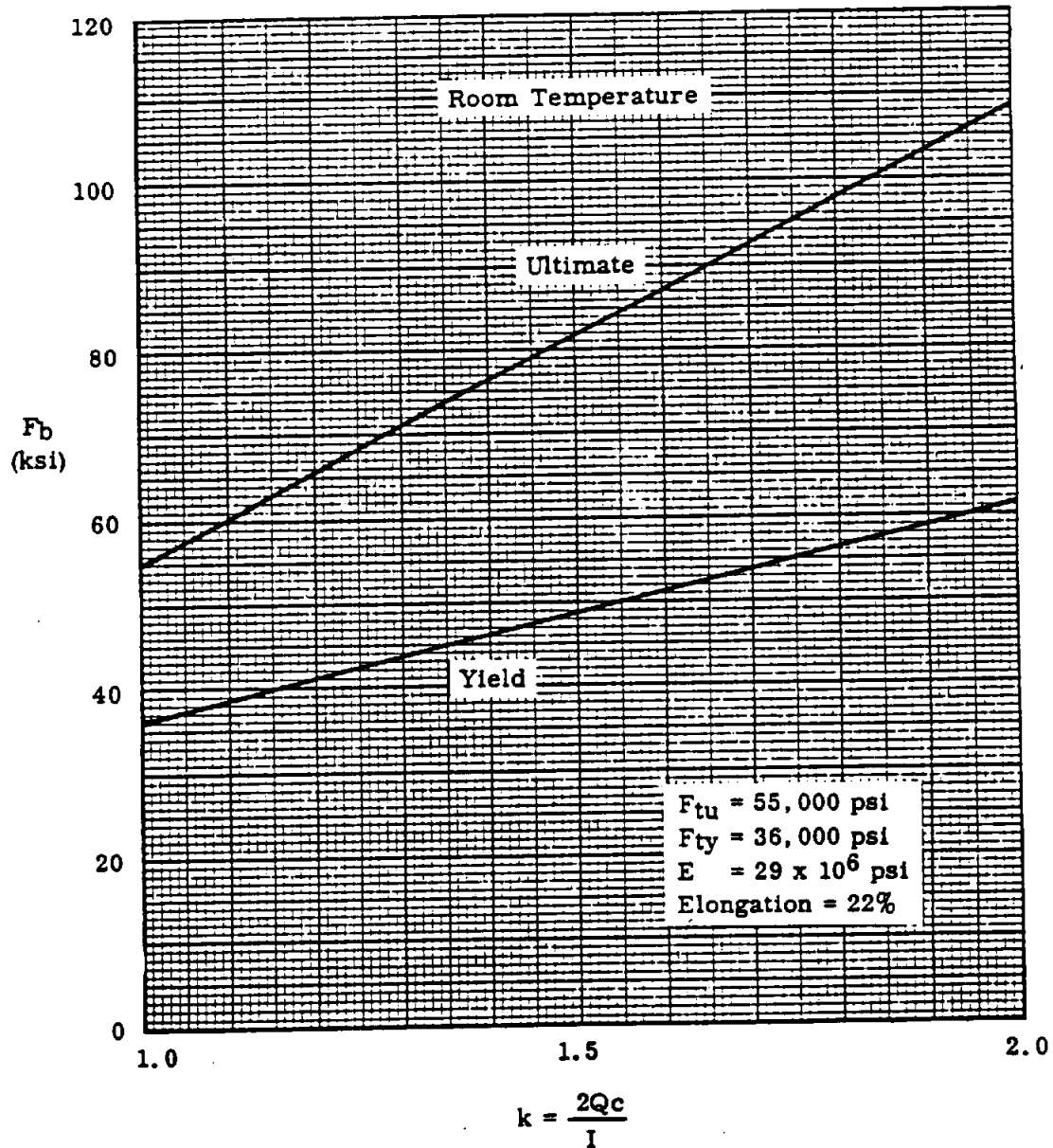
MONEL

K-MONEL	17.6.29
MONEL ALLOY	17.6.29

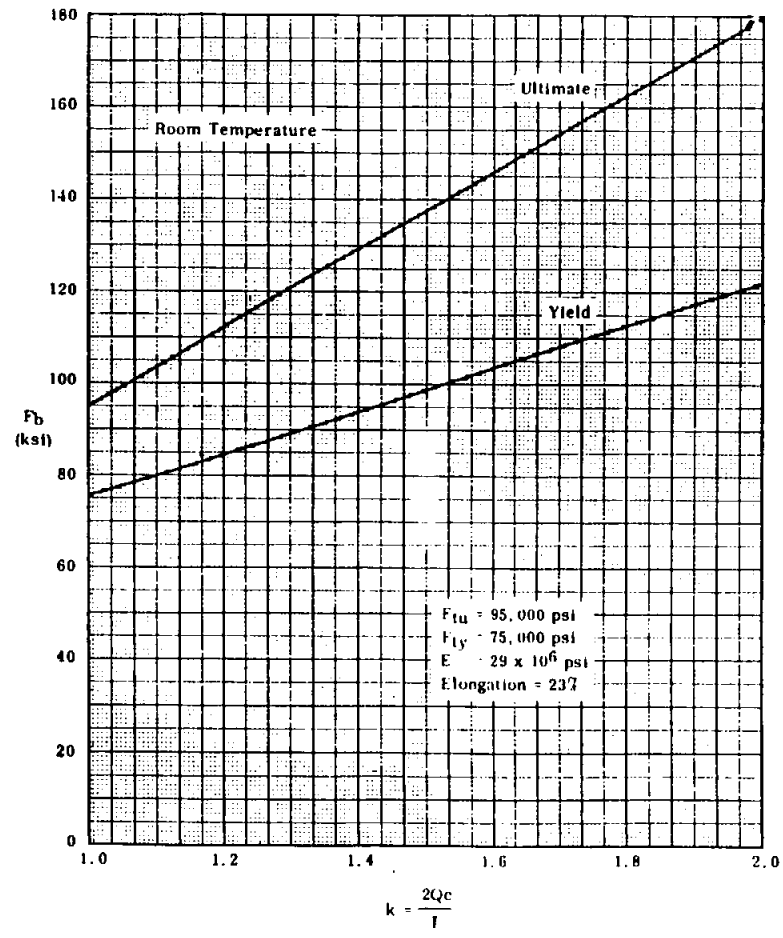
STRUCTURAL ANALYSIS MANUAL
GENERAL DYNAMICS/CONVAIR AND SPACE SYSTEMS DIVISION

STRUCTURES MANUAL

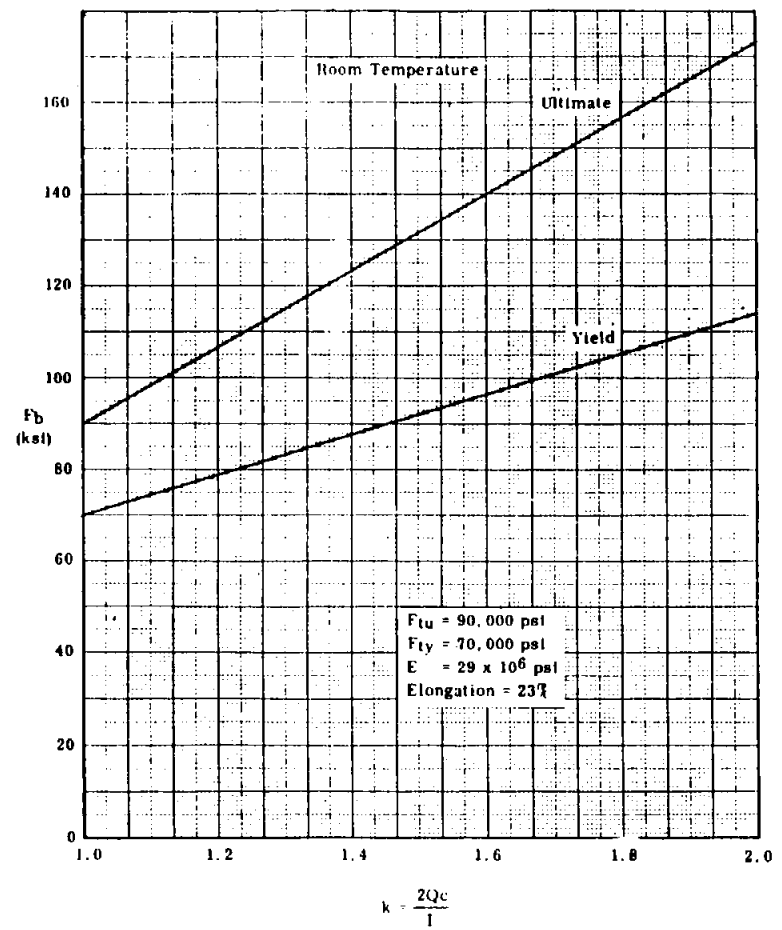
Minimum Bending Modulus of Rupture Curves for Symmetrical Sections
Carbon Steel AISI 1023-1025



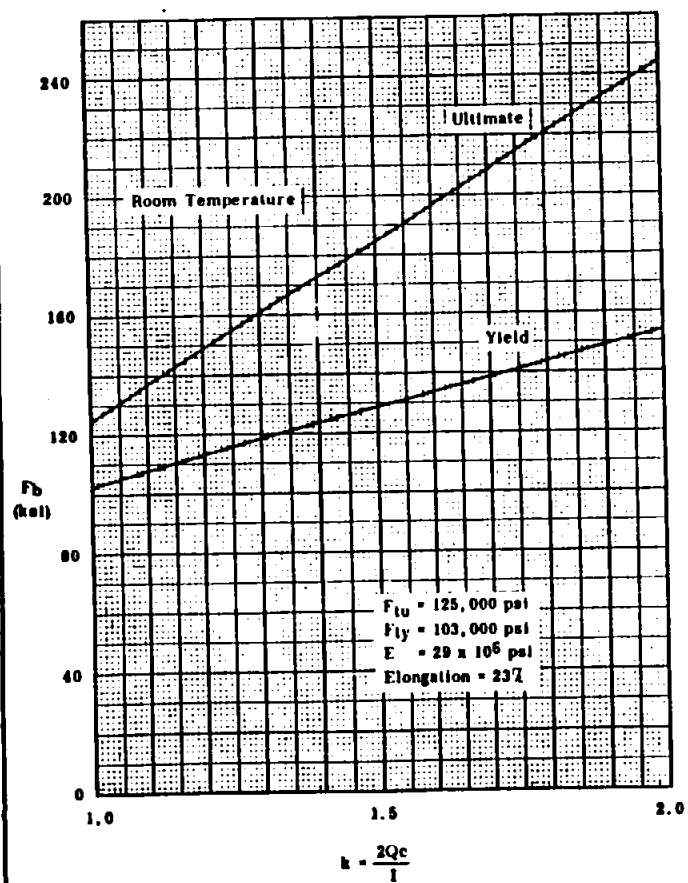
Minimum Bending Modulus of Rupture Curves for Symmetrical Sections
AISI Alloy Steel, Normalized, ≤ 0.188 Thick



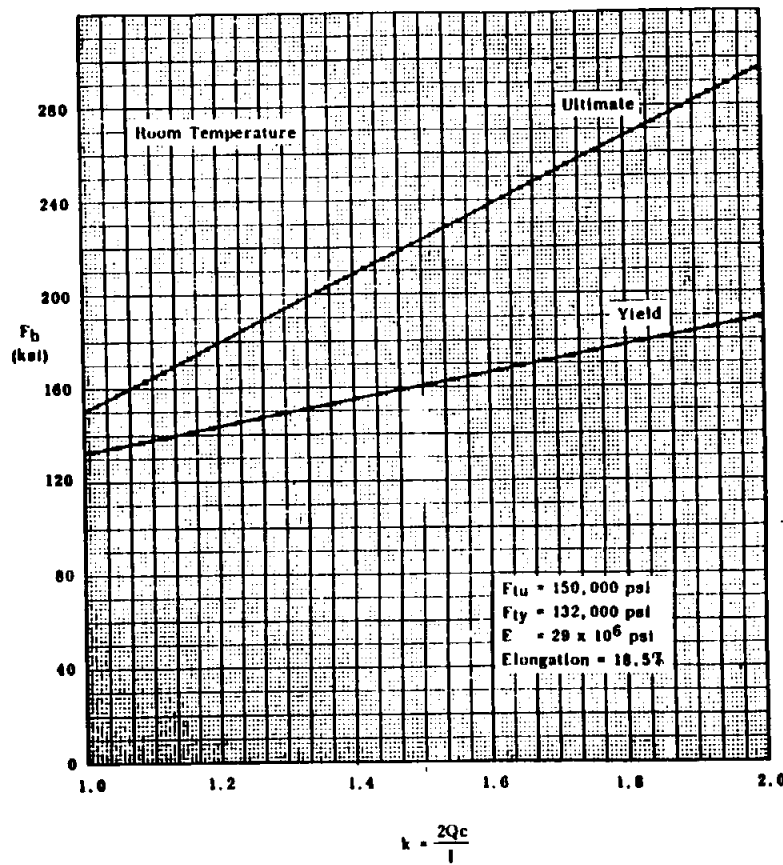
Minimum Bending Modulus of Rupture Curves for Symmetrical Sections
AISI Alloy Steel, Normalized, > 0.188 Thick



Minimum Bending Modulus of Rupture Curves for Symmetrical Sections
AISI Alloy Steel, Heat Treated

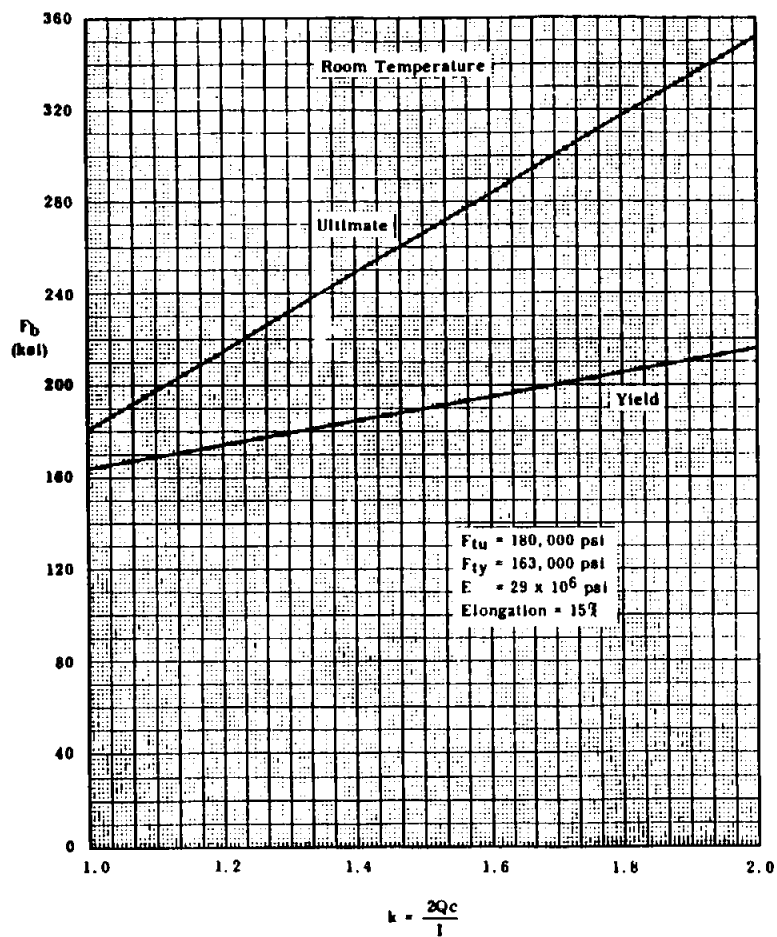


Minimum Bending Modulus of Rupture Curves for Symmetrical Sections
AISI Alloy Steel, Heat Treated

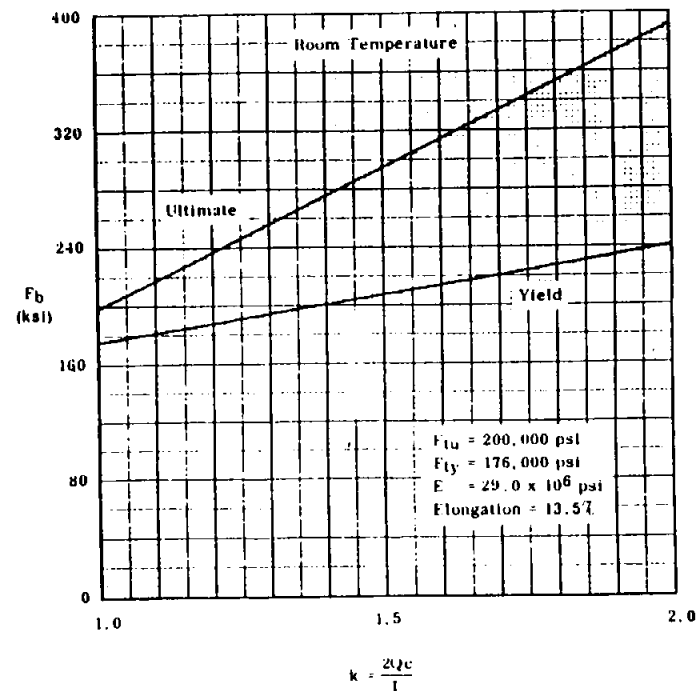


226

Minimum Bending Modulus of Rupture Curves for Symmetrical Sections
AISI Alloy Steel, Heat Treated

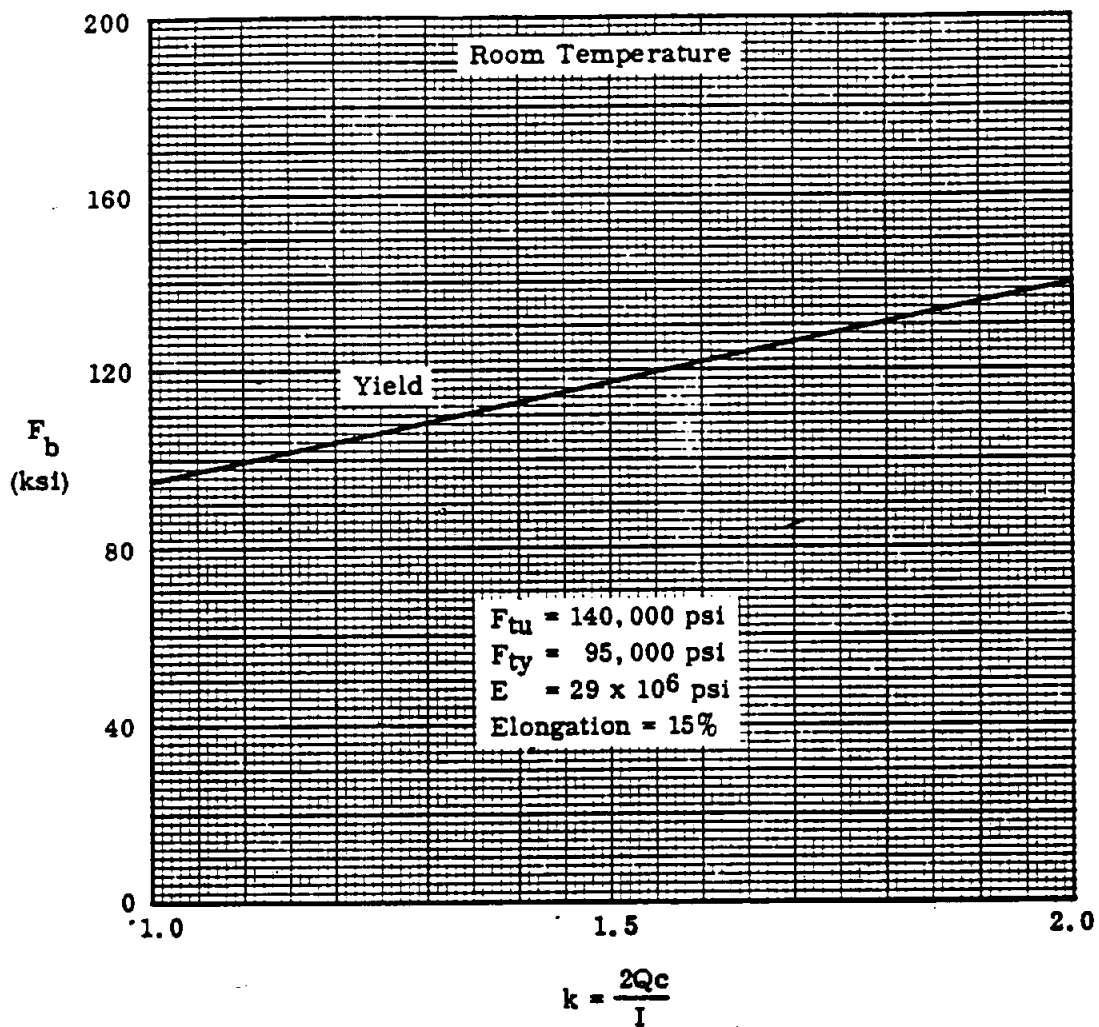


Minimum Bending Modulus of Rupture Curves for Symmetrical Sections
AISI Alloy Steel, Heat Treated



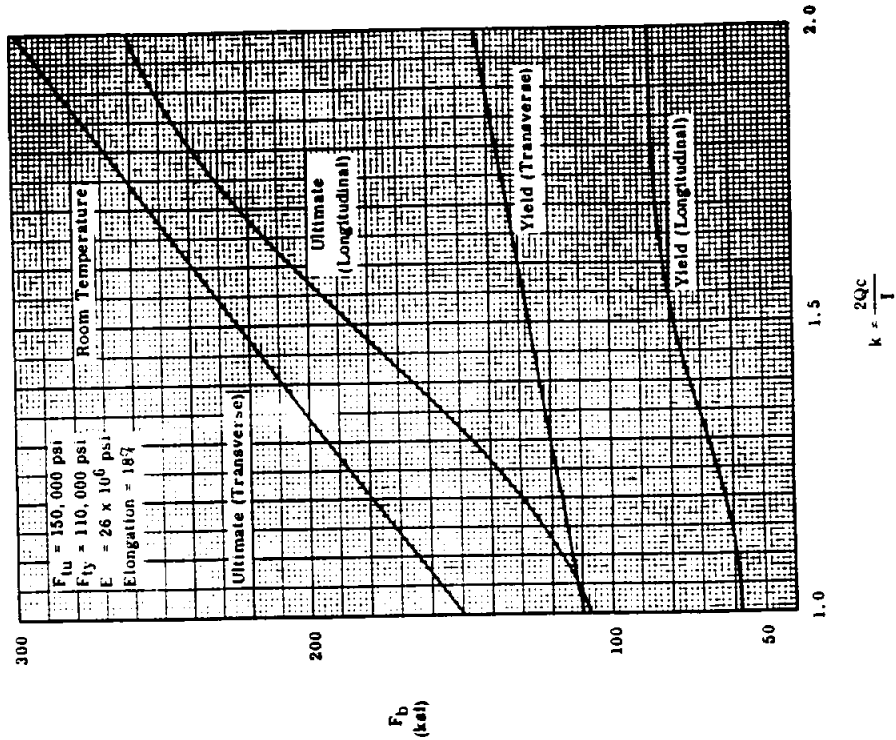
STRUCTURAL ANALYSIS MANUAL
GENERAL DYNAMICS/CONVAIR AND SPACE SYSTEMS DIVISION

Minimum Bending Modulus of Rupture Curves for Symmetrical Sections
A-286 Alloy, Heat Treated

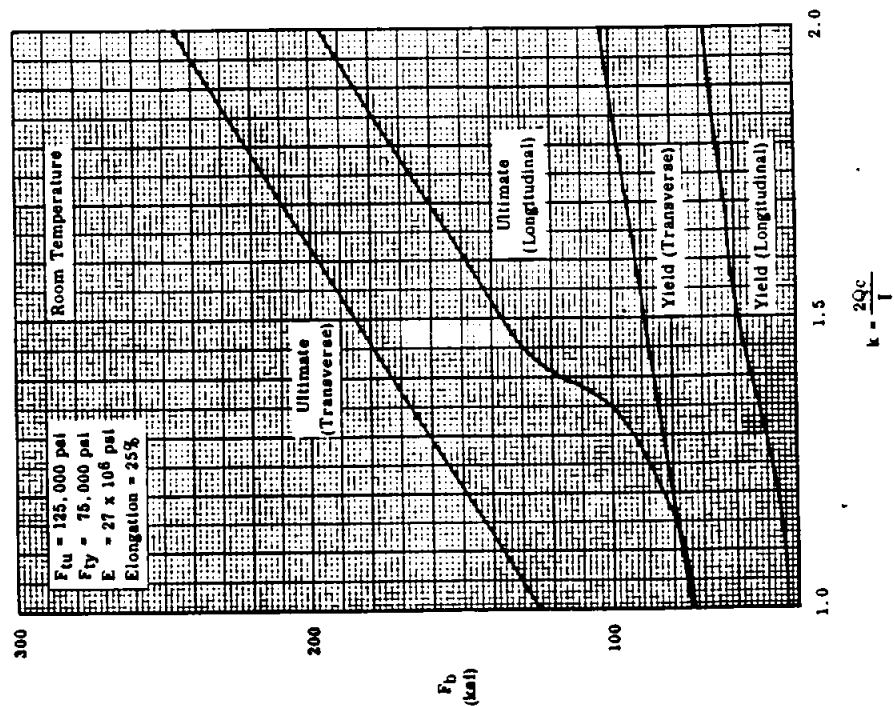


STRUCTURAL ANALYSIS MANUAL **GENERAL DYNAMICS/CONVAIR AND SPACE SYSTEMS DIVISION**

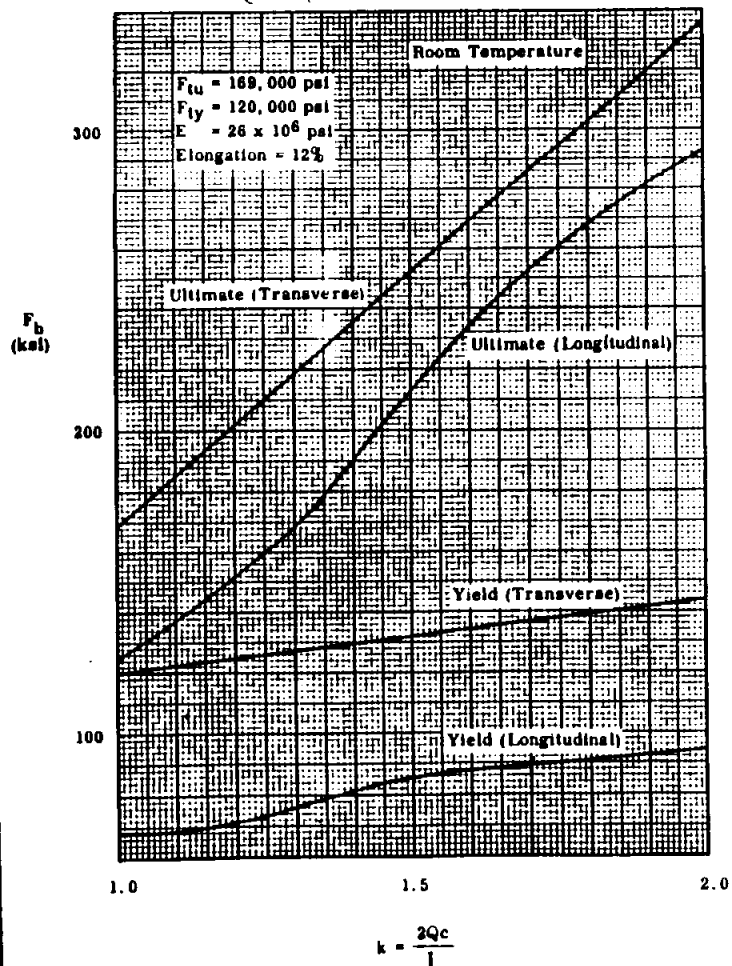
Minimum Bending Modulus of Rupture Curves for Symmetrical Sections
1/2 Hard AISI 301 Stainless Steel Sheet



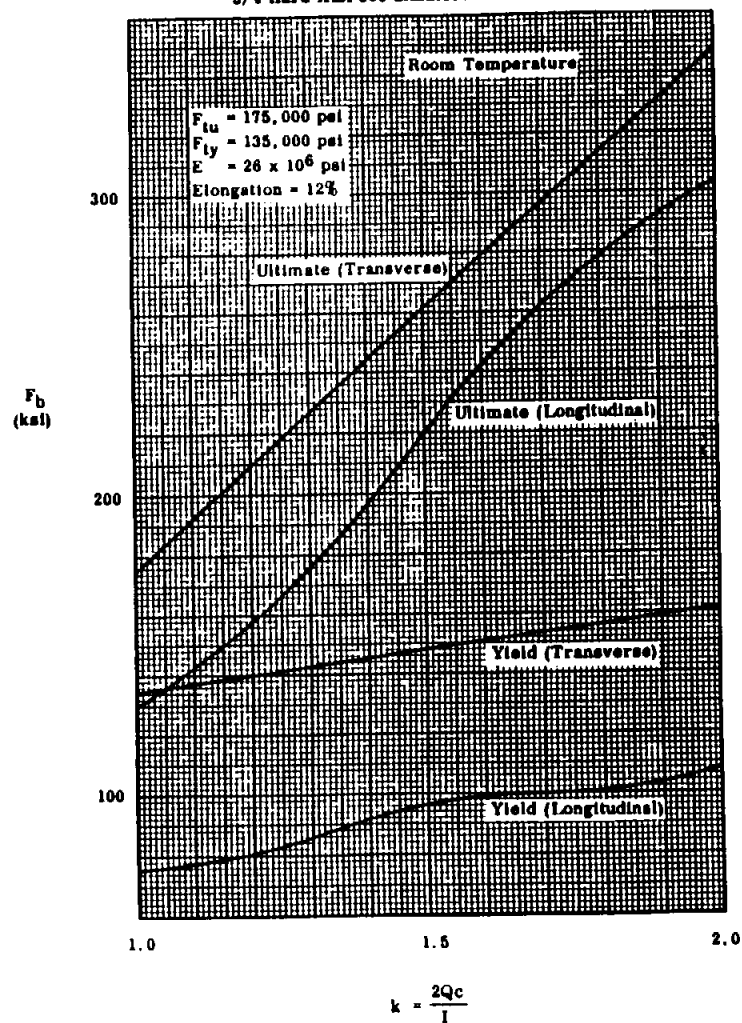
Minimum Bending Modulus of Rupture Curves for Symmetrical Sections
1/4 Hard AISI 301 Stainless Steel Sheet



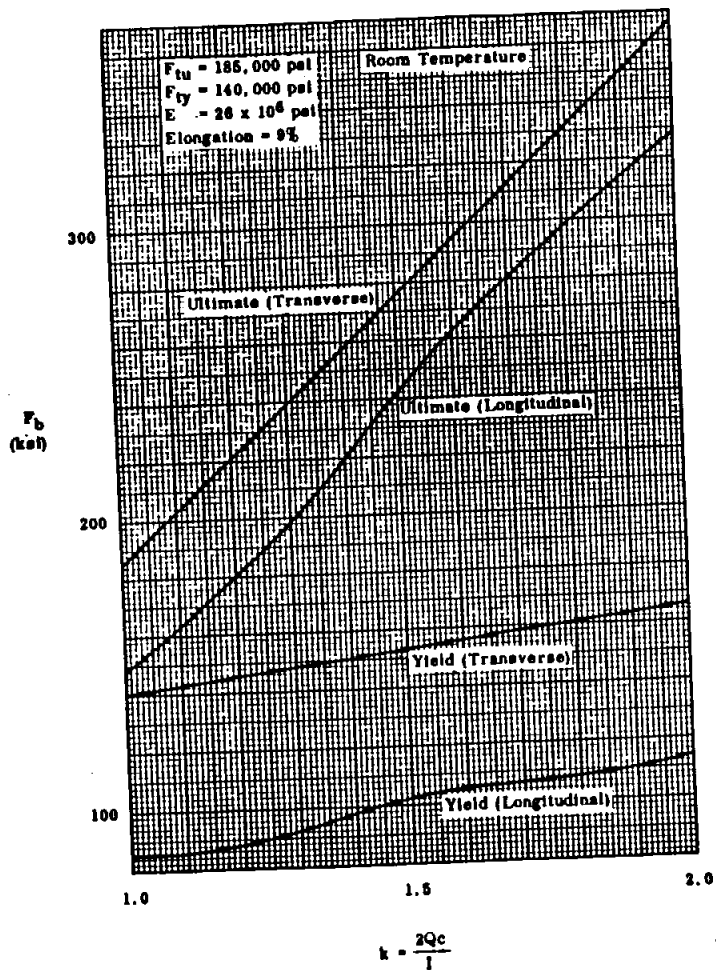
Minimum Bending Modulus of Rupture Curves for Symmetrical Sections
Convair Astronautics Special 3/4 Hard AISI 301 Stainless Steel Sheet
(SPEC. 0-71005)



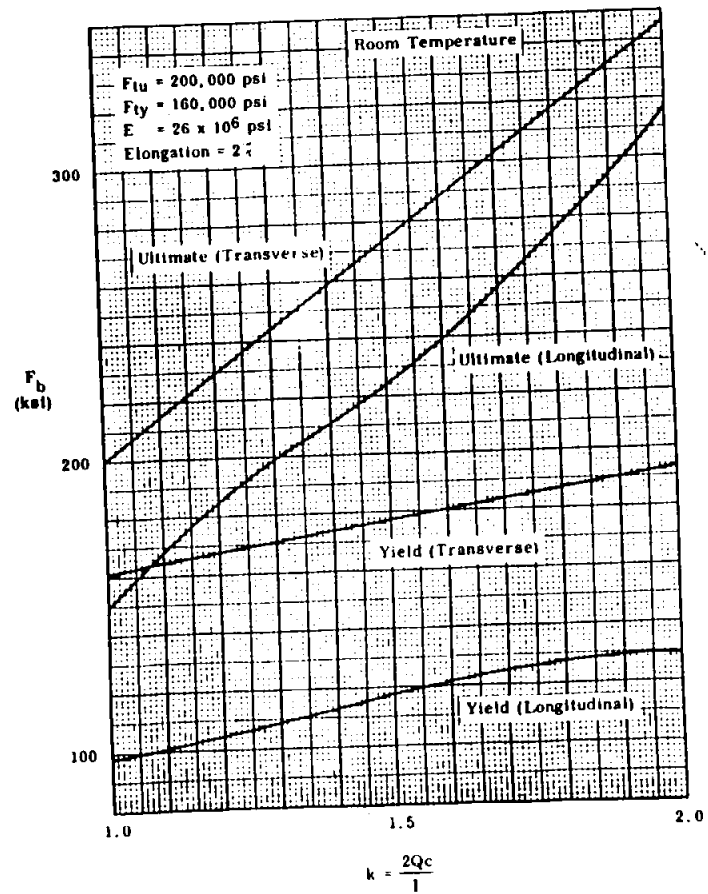
(SPEC. MIL-S-5059)
Minimum Bending Modulus of Rupture Curves for Symmetrical Sections
3/4 Hard AISI 301 Stainless Steel Sheet



Minimum Bending Modulus of Rupture Curves for Symmetrical Sections
Full Hard AISI 301 Stainless Steel Sheet

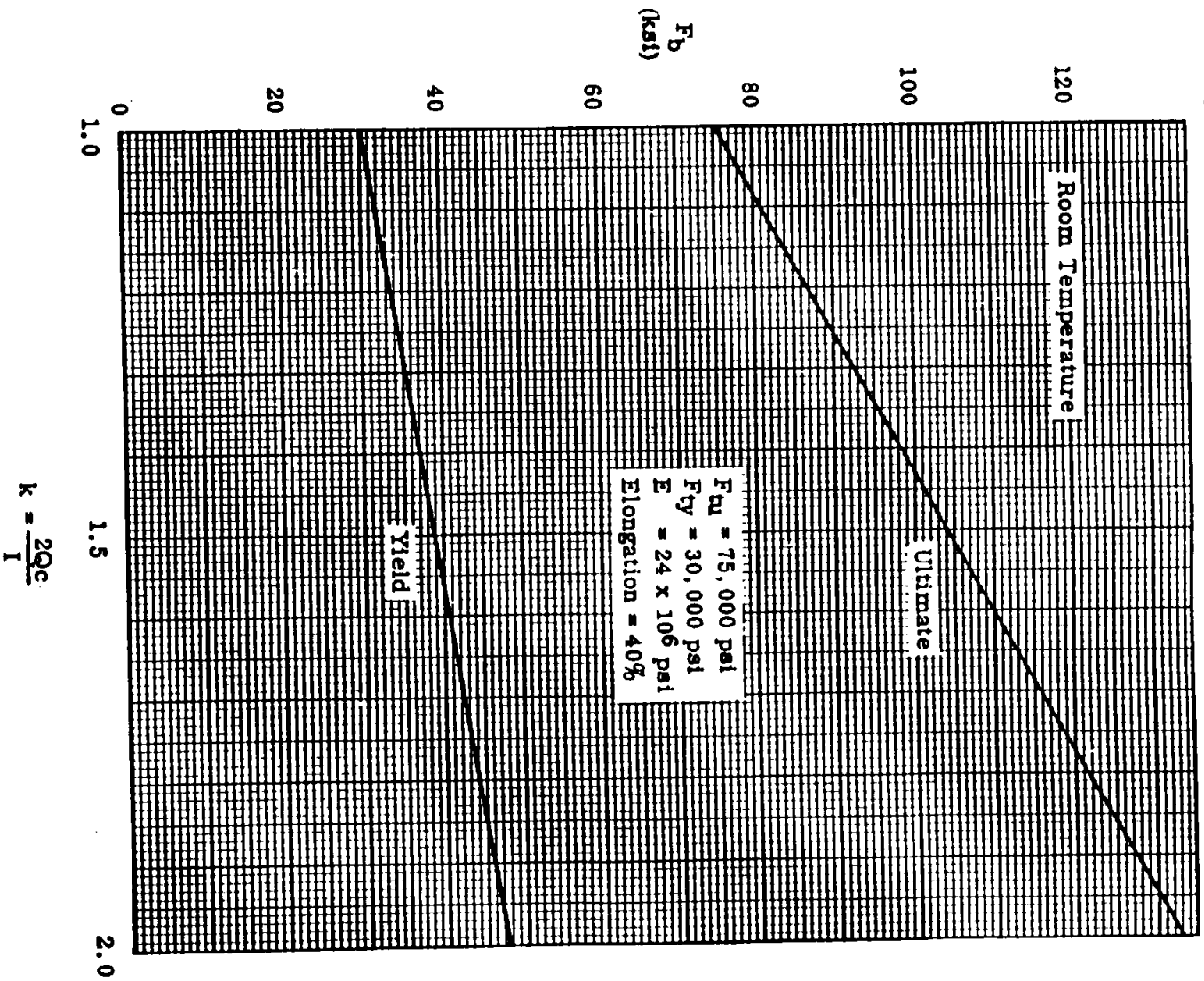


Minimum Bending Modulus of Rupture Curves for Symmetrical Sections
Extra Hard AISI 301 Stainless Steel Sheet

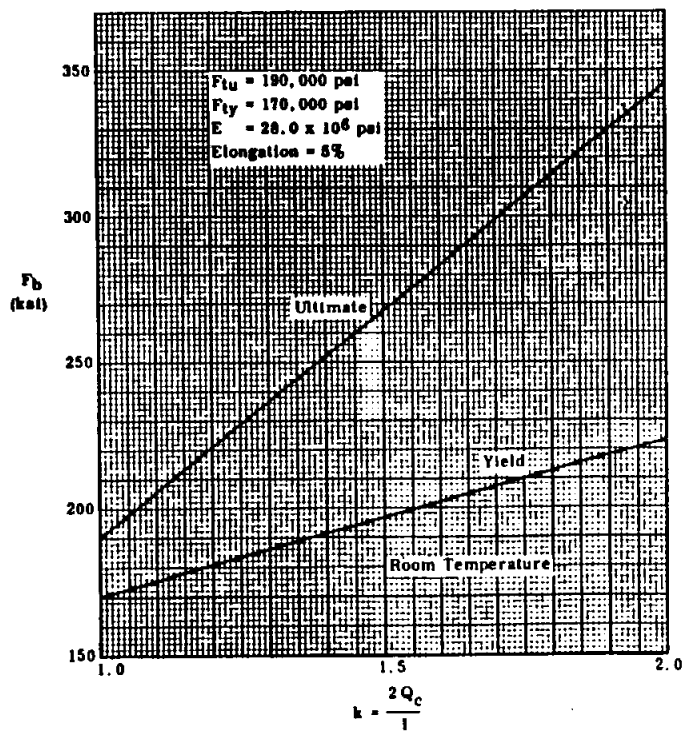


STRUCTURAL ANALYSIS MANUAL
GENERAL DYNAMICS/CONVAIR AND SPACE SYSTEMS DIVISION

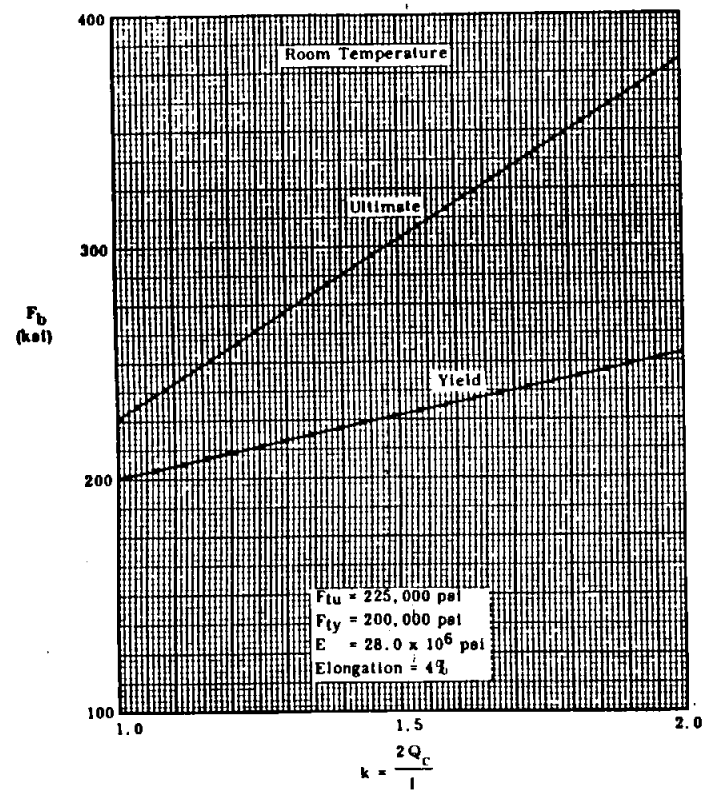
Minimum Bending Modulus of Rupture Curves for Symmetrical Sections
Annealed AISI 321 Stainless Steel Sheet



Minimum Bending Modulus of Rupture Curves for Symmetrical Sections
PH 15-7 Mo (TH 1050) Stainless Steel Sheet & Strip
Thickness 0.020 to 0.185 inches

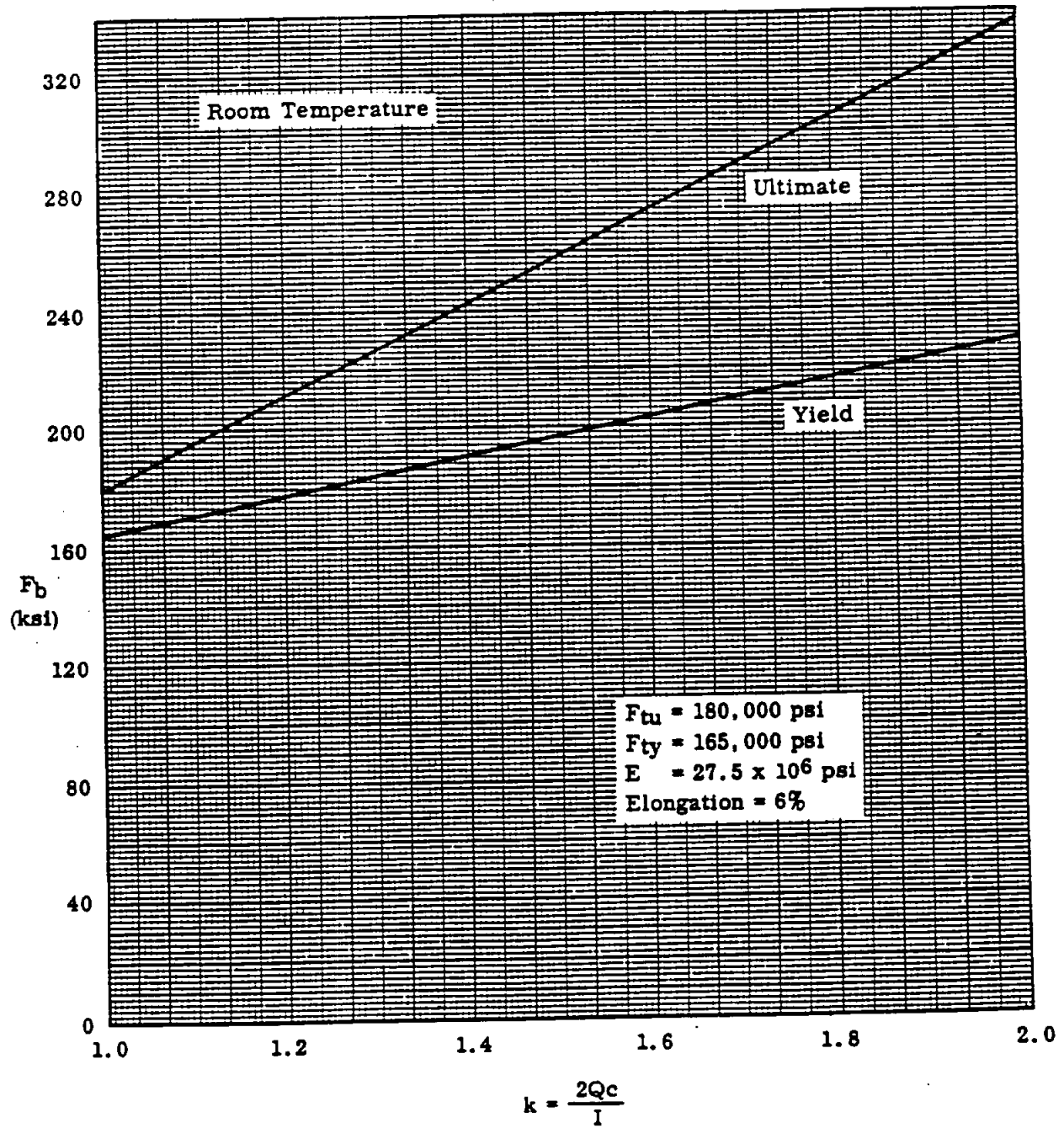


Minimum Bending Modulus of Rupture Curves for Symmetrical Sections
PH 15-7 Mo (RH 950) Stainless Steel Sheet & Strip
Thickness 0.020 to 0.187 inches

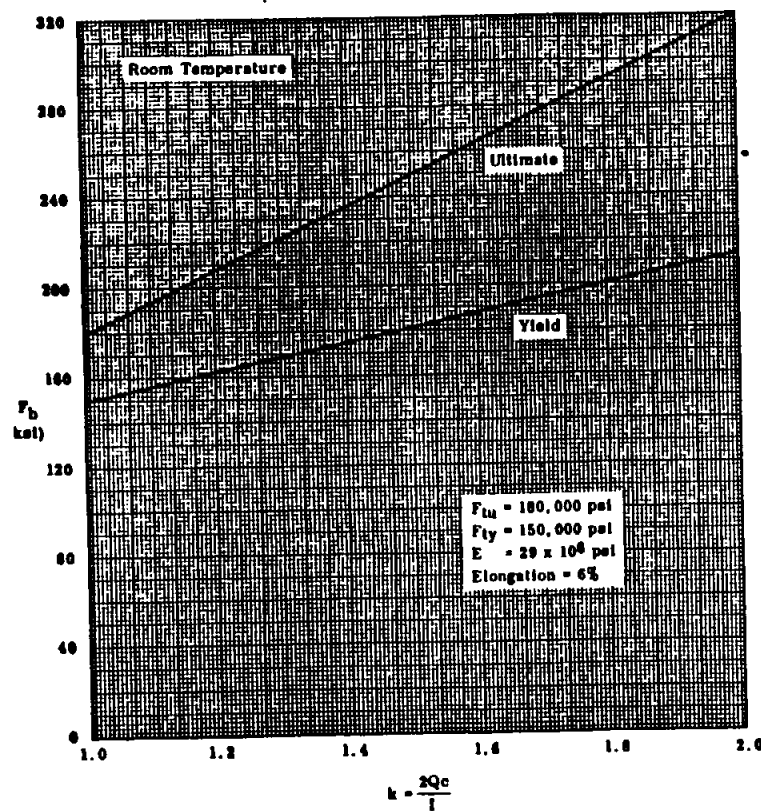


STRUCTURAL ANALYSIS MANUAL
GENERAL DYNAMICS/CONVAIR AND SPACE SYSTEMS DIVISION

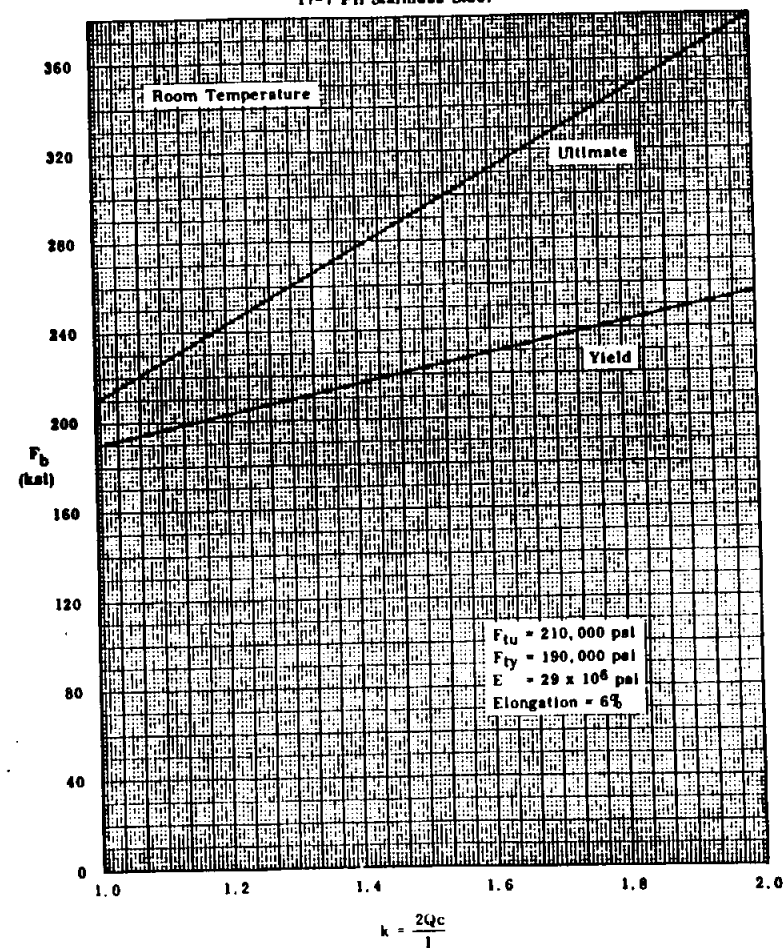
Minimum Bending Modulus of Rupture Curves for Symmetrical Sections
17-4 PH Stainless Steel - Heat Treated - Bars and Forgings



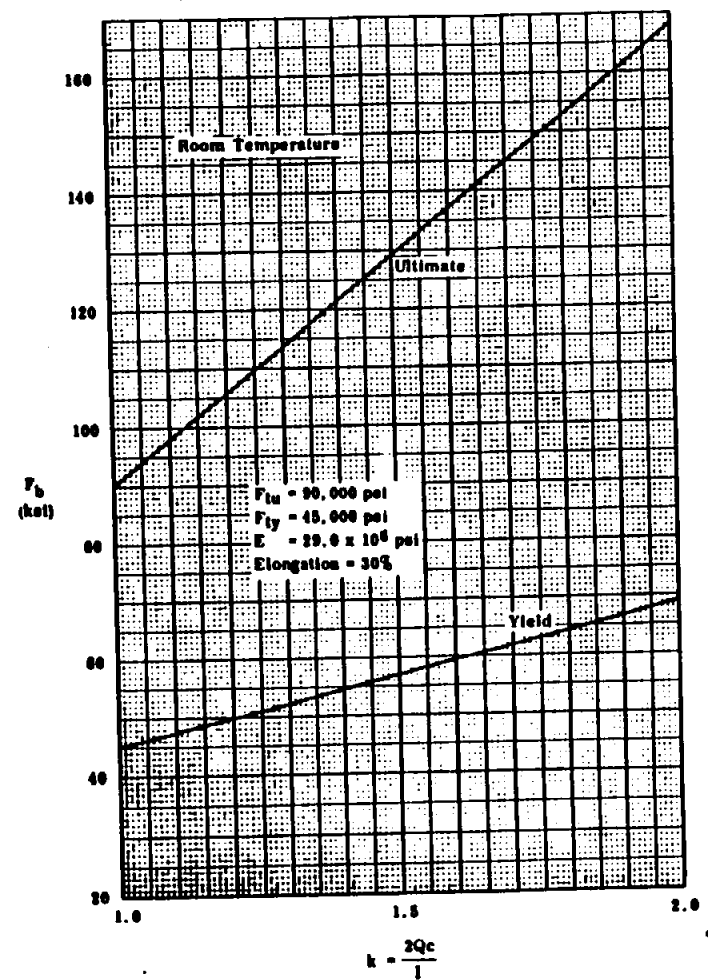
Minimum Bending Modulus of Rupture Curves for Symmetrical Sections
17-7 PH Stainless Steel



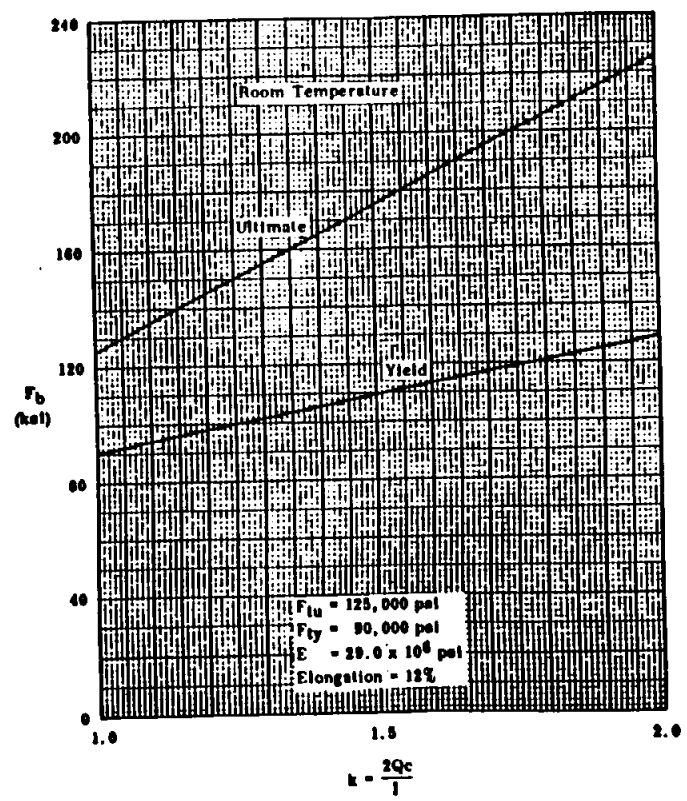
Minimum Bending Modulus of Rupture Curves for Symmetrical Sections
17-7 PH Stainless Steel



Minimum Bending Modulus of Rupture Curves for Symmetrical Sections
10-9 DL (AMS 5526) & 10-9 DX (AMS 5539) Stainless Steel



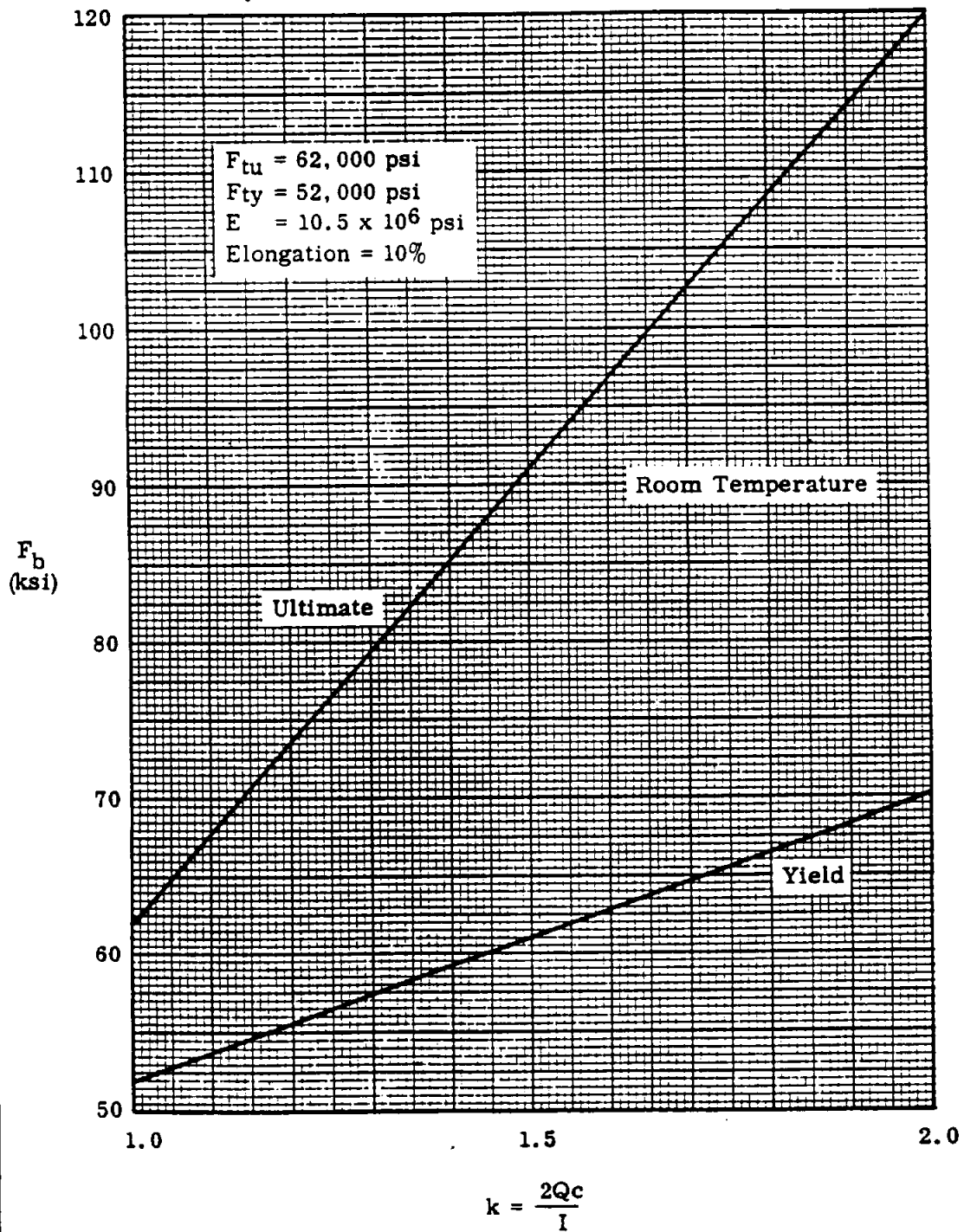
Minimum Bending Modulus of Rupture Curves for Symmetrical Sections
10-9DL (AMS 5527) & 10-9 DX (AMS 5539) Stainless Steel



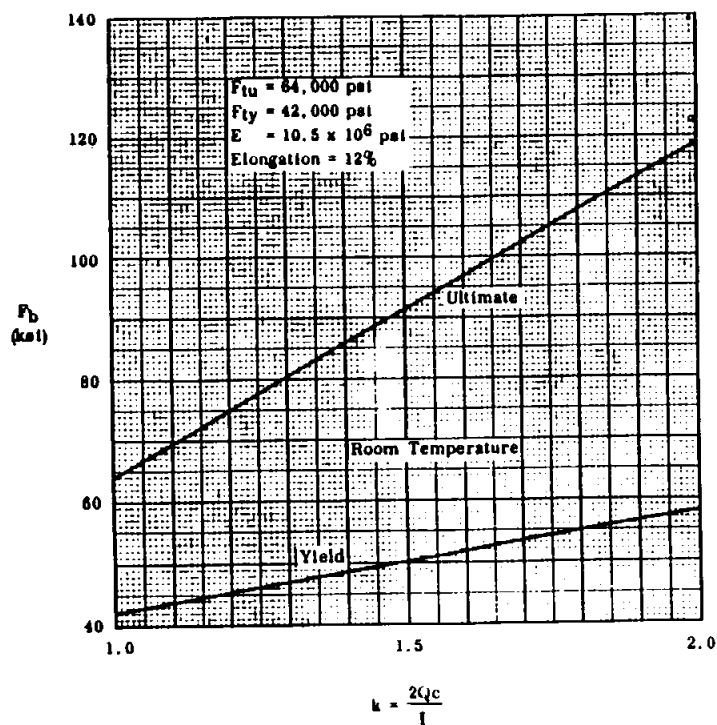
284

STRUCTURAL ANALYSIS MANUAL
 GENERAL DYNAMICS/CONVAIR AND SPACE SYSTEMS DIVISION

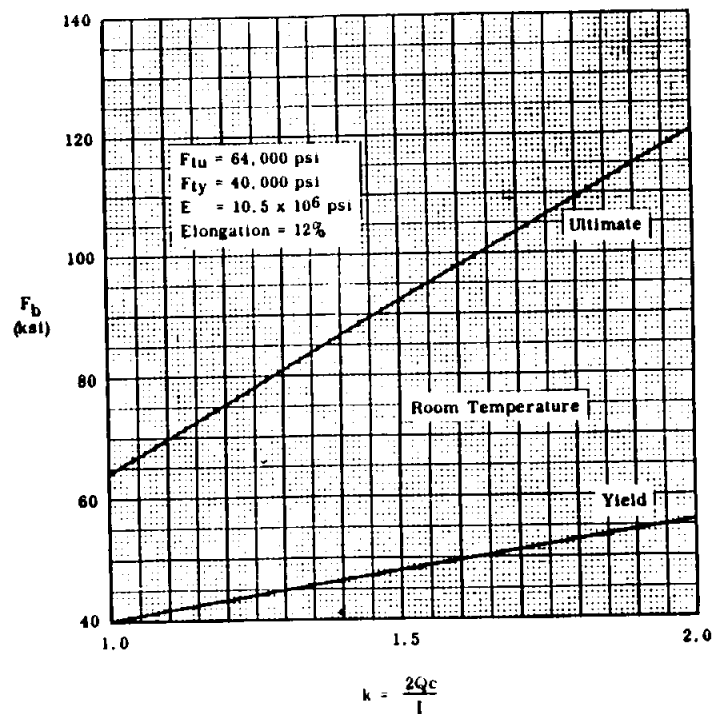
Minimum Bending Modulus of Rupture Curves for Symmetrical Sections
 2014-T6 Aluminum Alloy Forgings, (Transverse) Thickness ≤ 4 in.
 (SPEC. MIL-A-22771 AND QQ-A-367)



Minimum Bending Modulus of Rupture Curves for Symmetrical Sections
2024-T3 Aluminum Alloy Sheet & Plate - Heat Treated. Thickness ≤ 0.250 in.
(SPEC. QQ-A-250/4)

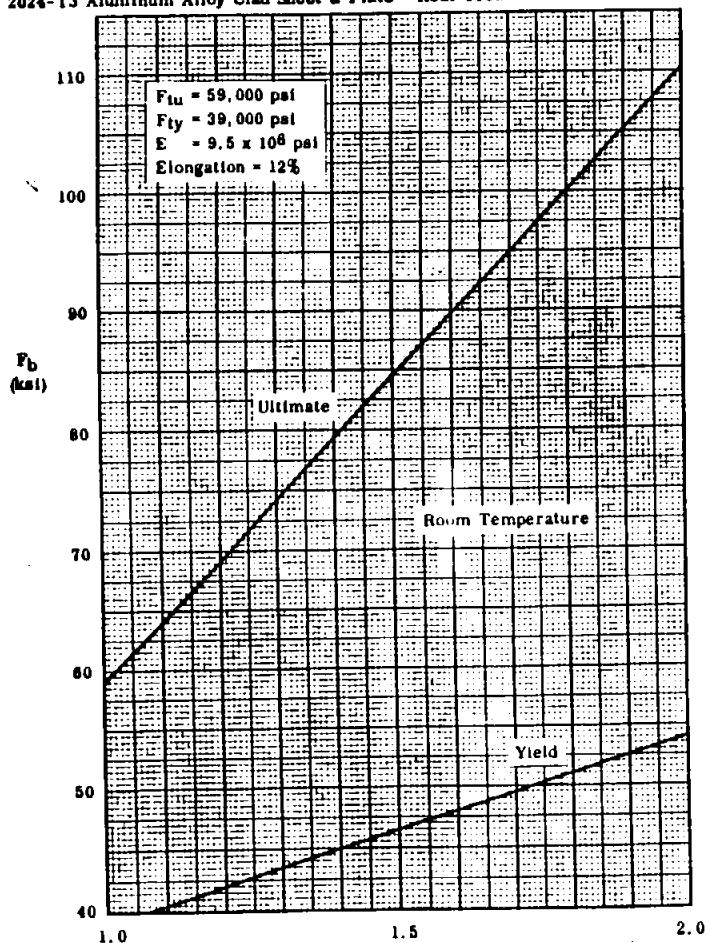


Minimum Bending Modulus of Rupture Curves for Symmetrical Sections
2024-T3 & T4 Aluminum Alloy Sheet & Plate - Heat Treated. Thickness ≤ 0.50 in.
(SPEC. QQ-A-250/4)



(SPEC. QQ-A-250/5)

Minimum Bending Modulus of Rupture Curves for Symmetrical Sections
2024-T3 Aluminum Alloy Clad Sheet & Plate - Heat Treated. Thickness 0.010 to 0.062 in.

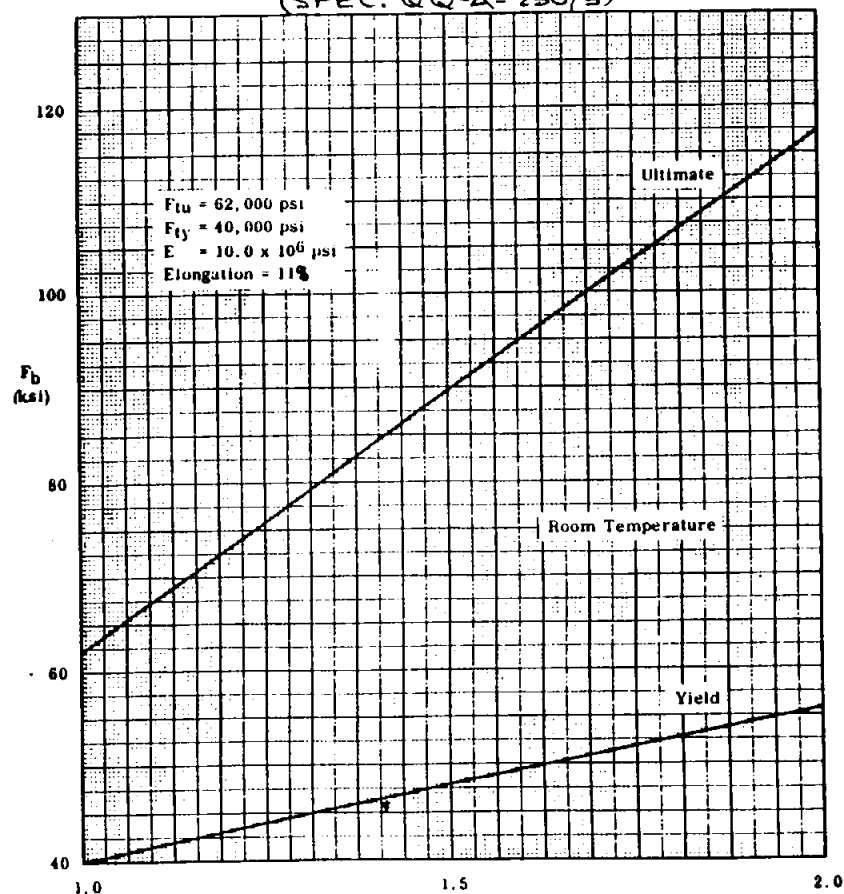


$$k = \frac{2Qc}{I}$$

2

Minimum Bending Modulus of Rupture Curves for Symmetrical Sections
2024-T4 Aluminum Alloy Clad Sheet & Plate - Heat Treated. Thickness 0.25 to 0.50 in.

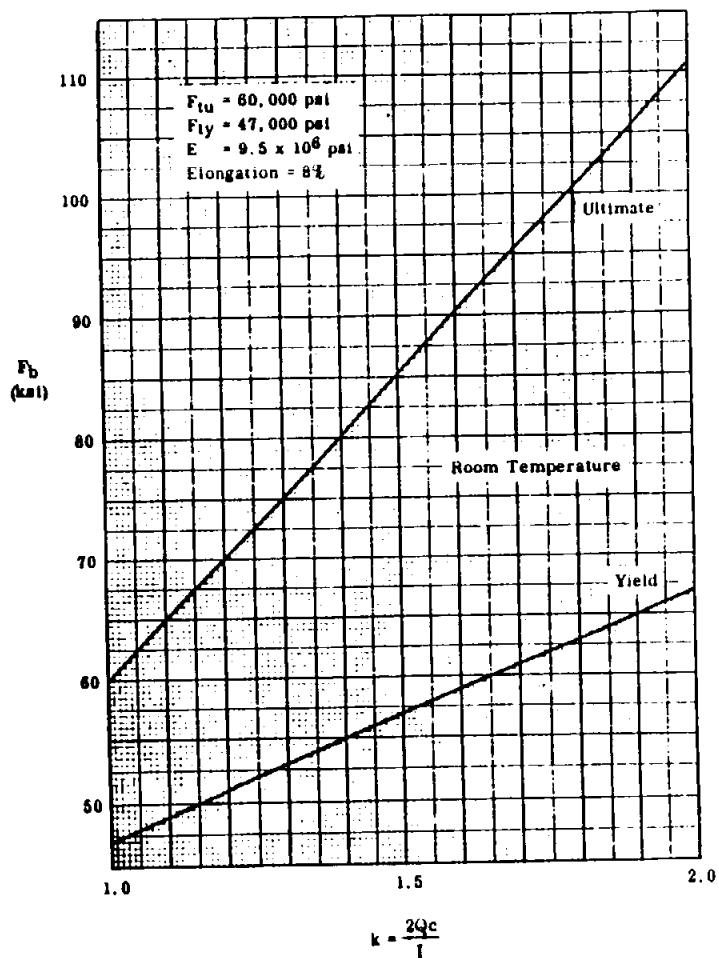
(SPEC. QQ-A-250/5)



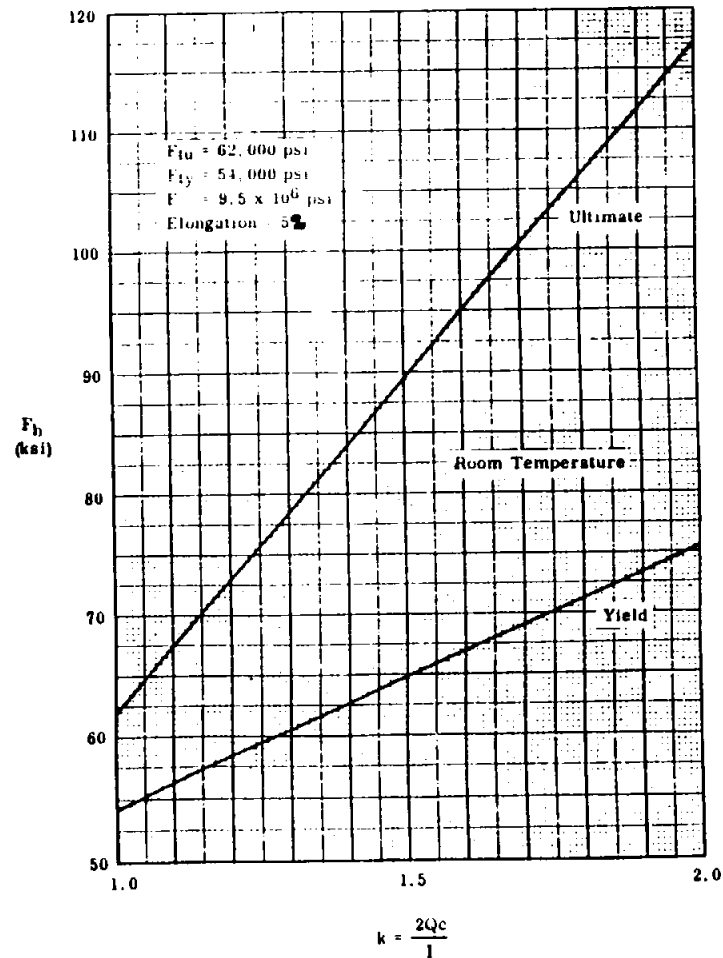
$$k = \frac{2Qc}{I}$$

2

Minimum Bending Modulus of Rupture Curves for Symmetrical Sections
2024-T6 Aluminum Alloy Clad Sheet - Heat Treated & Aged. Thickness < 0.064 in.

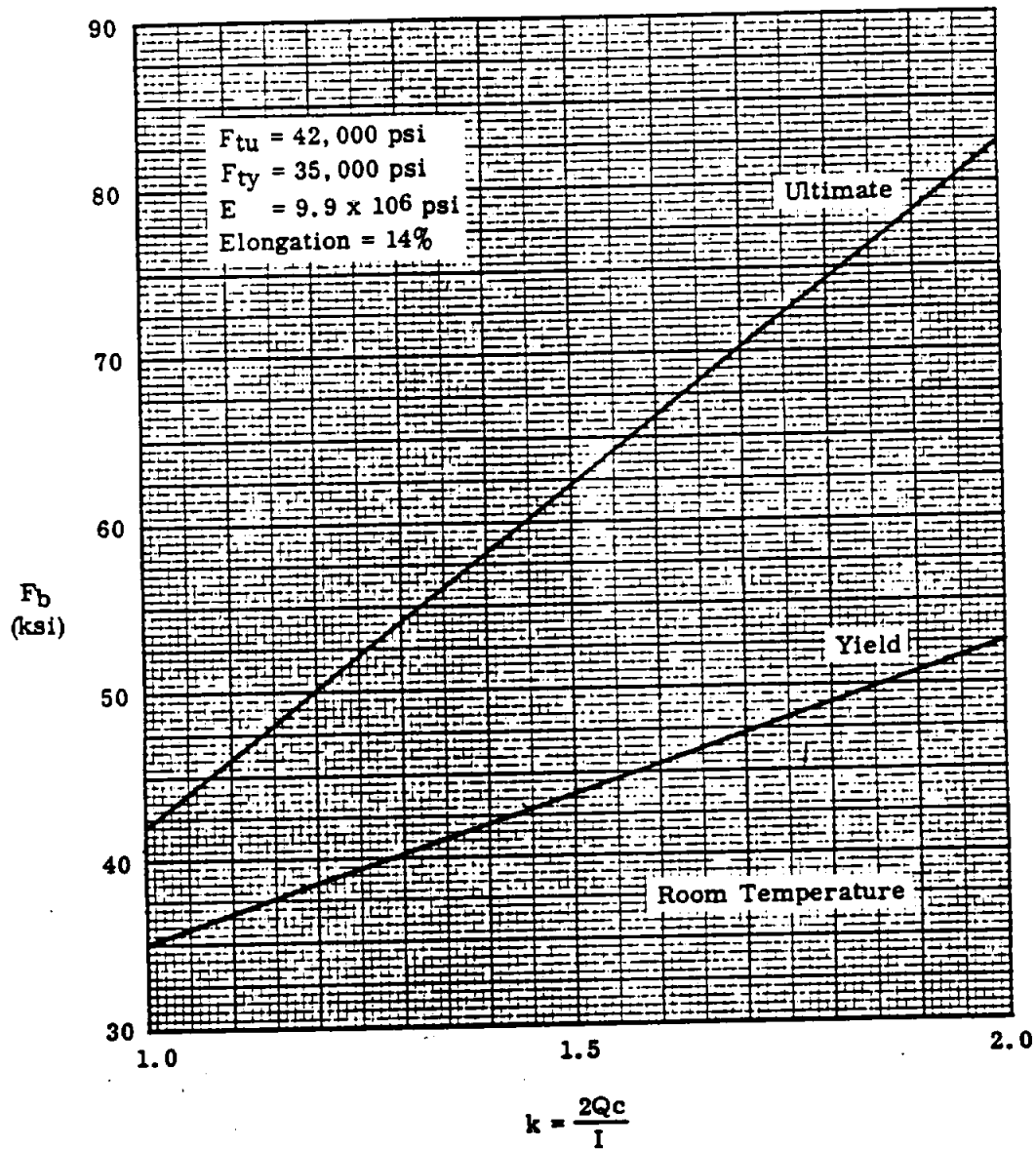


Minimum Bending Modulus of Rupture Curves for Symmetrical Sections
2024-T61 Aluminum Alloy Clad Sheet - Heat Treated, Cold Worked & Aged
Thickness < 0.064 in.

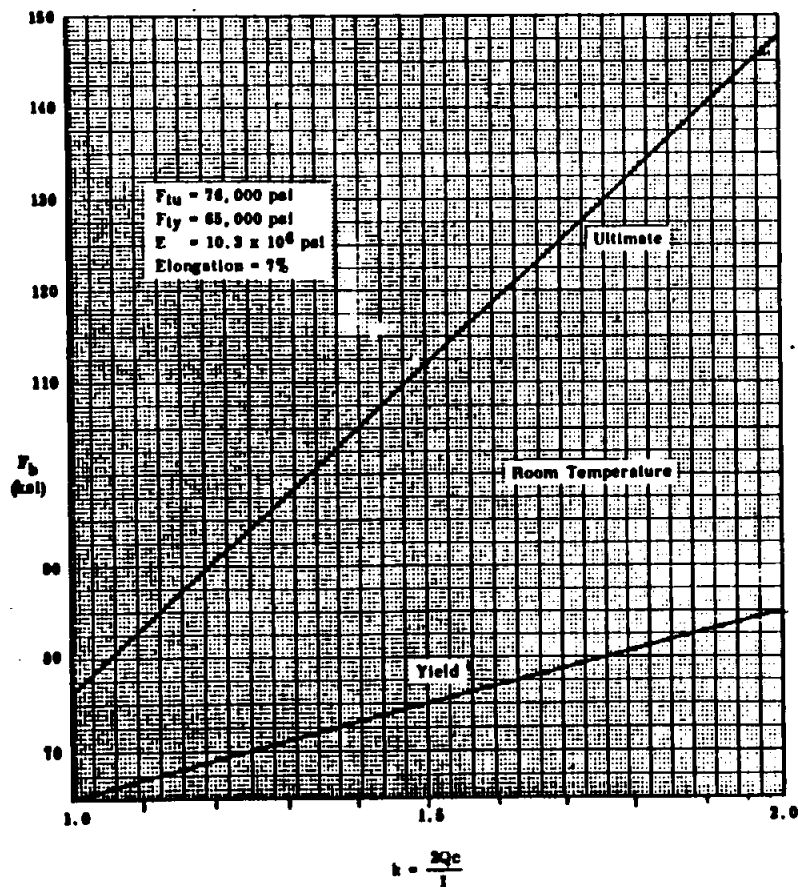


STRUCTURAL ANALYSIS MANUAL
GENERAL DYNAMICS/CONVAIR AND SPACE SYSTEMS DIVISION

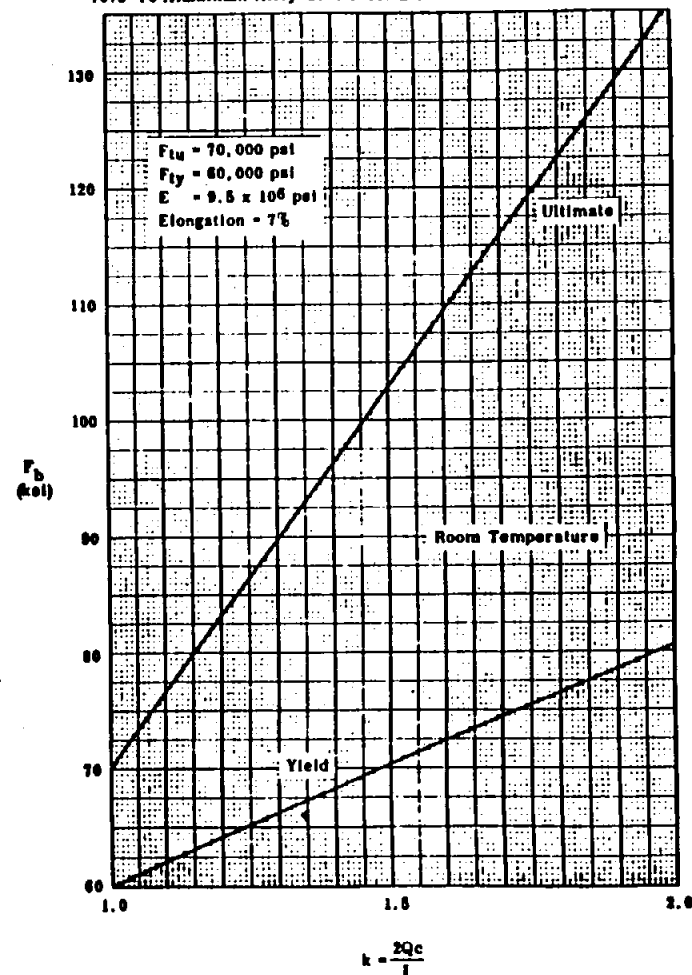
Minimum Bending Modulus of Rupture Curves for Symmetrical Sections
6061-T6 Aluminum Alloy Sheet - Heat Treated & Aged. Thickness ≥ 0.020 in.



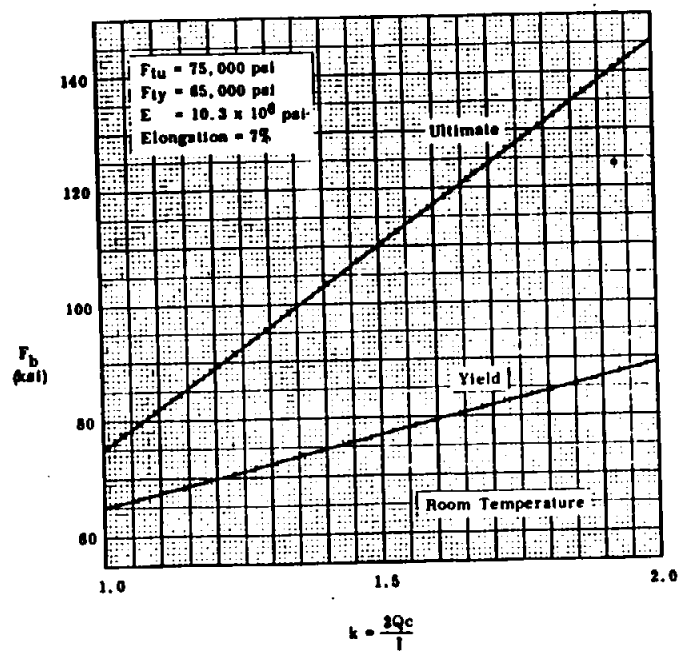
Minimum Bending Modulus of Rupture Curves for Symmetrical Sections
7075-T6 Aluminum Alloy Bare Sheet & Plate. Thickness $\leq .039$ in.



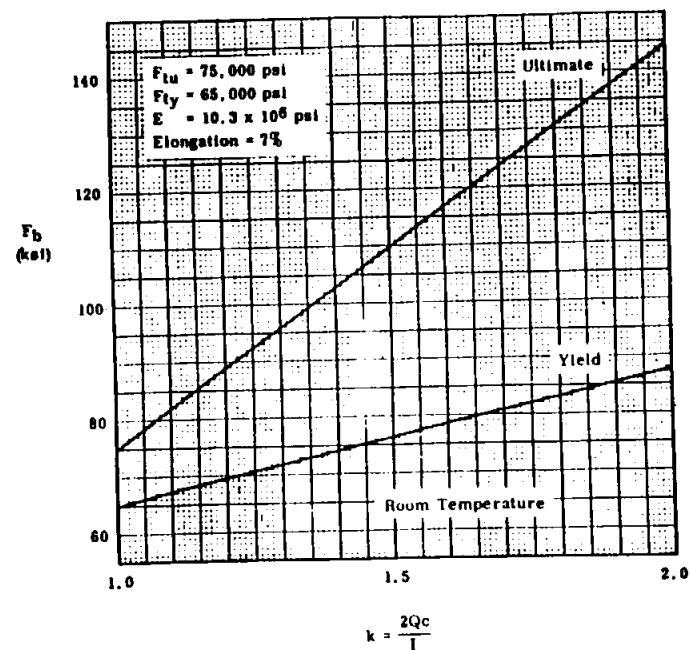
Minimum Bending Modulus of Rupture Curves for Symmetrical Sections
7075-T6 Aluminum Alloy Clad Sheet & Plate. Thickness $\leq .039$ in.



Minimum Bending Modulus of Rupture Curves for Symmetrical Sections
7075-T6 Aluminum Alloy Extrusions. Thickness ≤ 0.25 in.

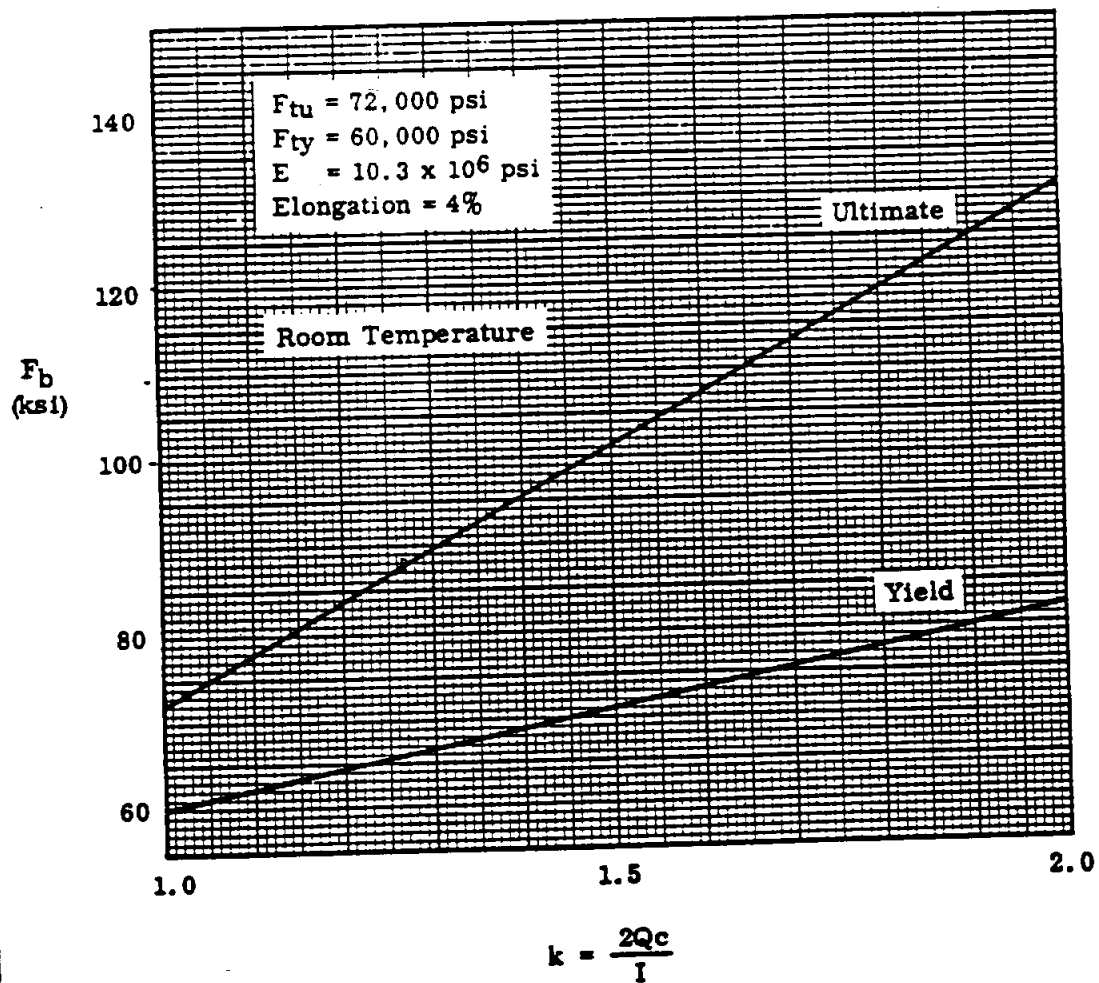


Minimum Bending Modulus of Rupture Curves for Symmetrical Sections
7075-T6 Aluminum Alloy Die Forgings. Thickness ≤ 3 in.

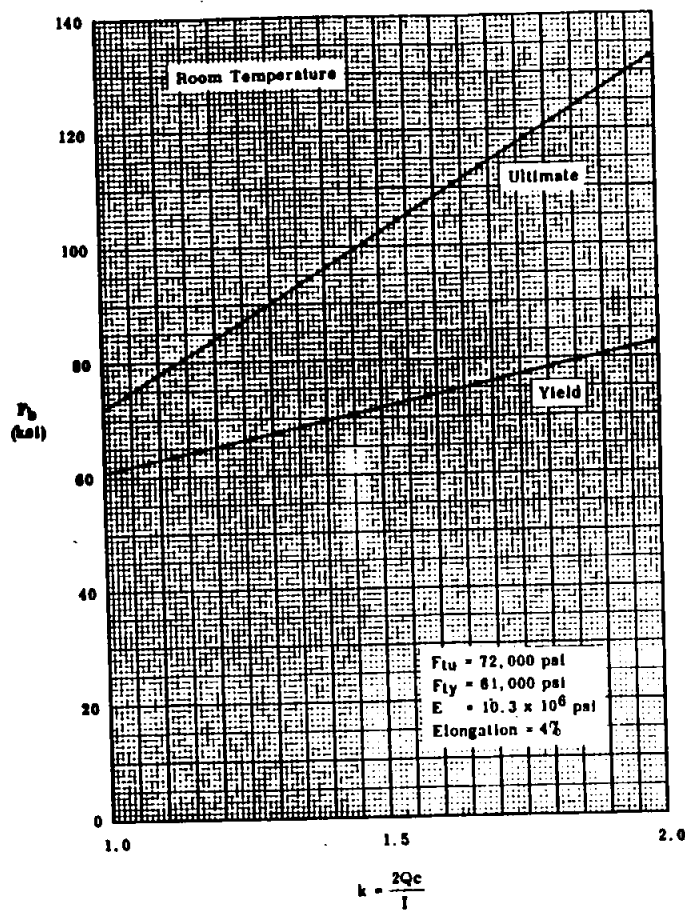


STRUCTURAL ANALYSIS MANUAL
GENERAL DYNAMICS/CONVAIR AND SPACE SYSTEMS DIVISION

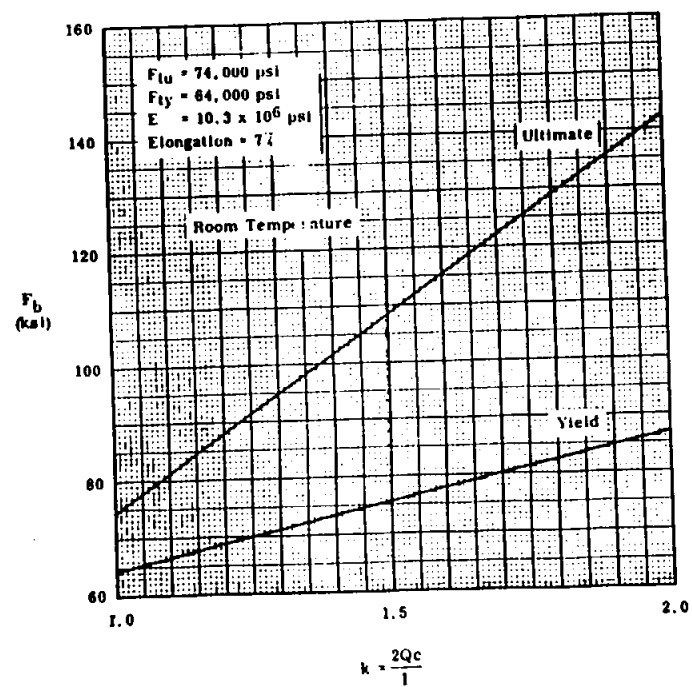
Minimum Bending Modulus of Rupture Curves for Symmetrical Sections
7075-T6 Aluminum Alloy Hand Forgings Area $\leq 16 \text{ in}^2$



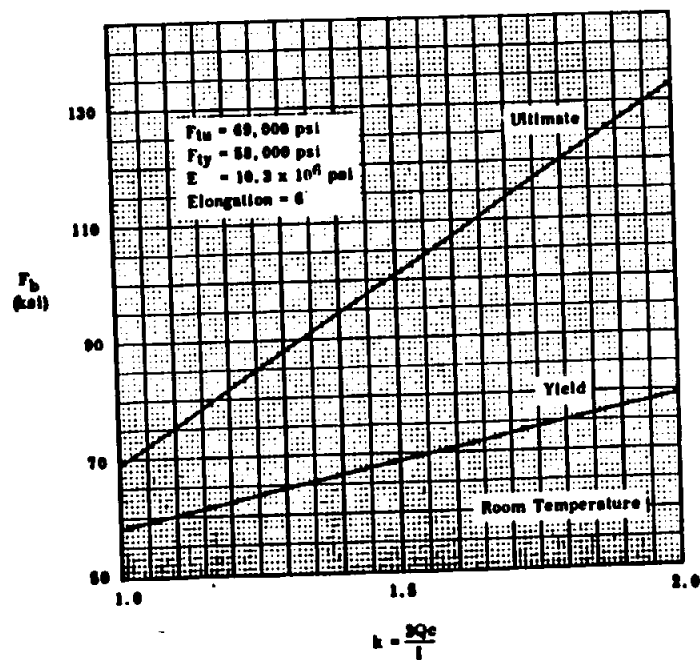
Minimum Bending Modulus of Rupture Curves for Symmetrical Sections
7079-T6 Aluminum Alloy Die Forgings (Transverse). Thickness ≤ 6.0 in.



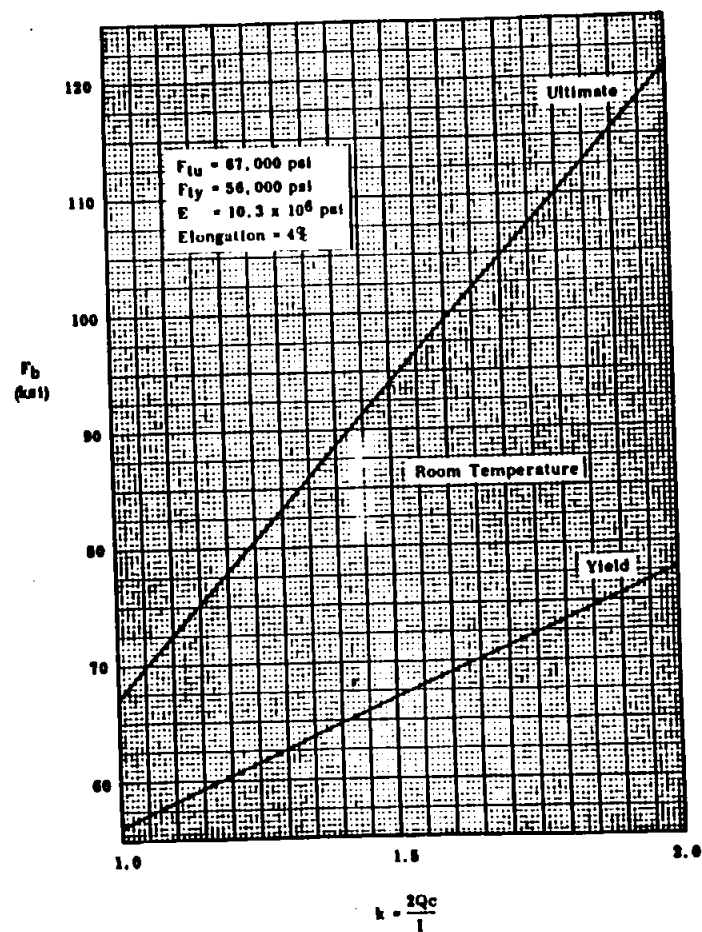
Minimum Bending Modulus of Rupture Curves for Symmetrical Sections
7079-T6 Aluminum Alloy Die Forgings (Longitudinal) Thickness ≤ 6.0 in.



Minimum Bending Modulus of Rupture Curves for Symmetrical Sections
7070-T6 Aluminum Alloy Hand Forgings - (Long Transverse) Thickness ≤ 6 in.

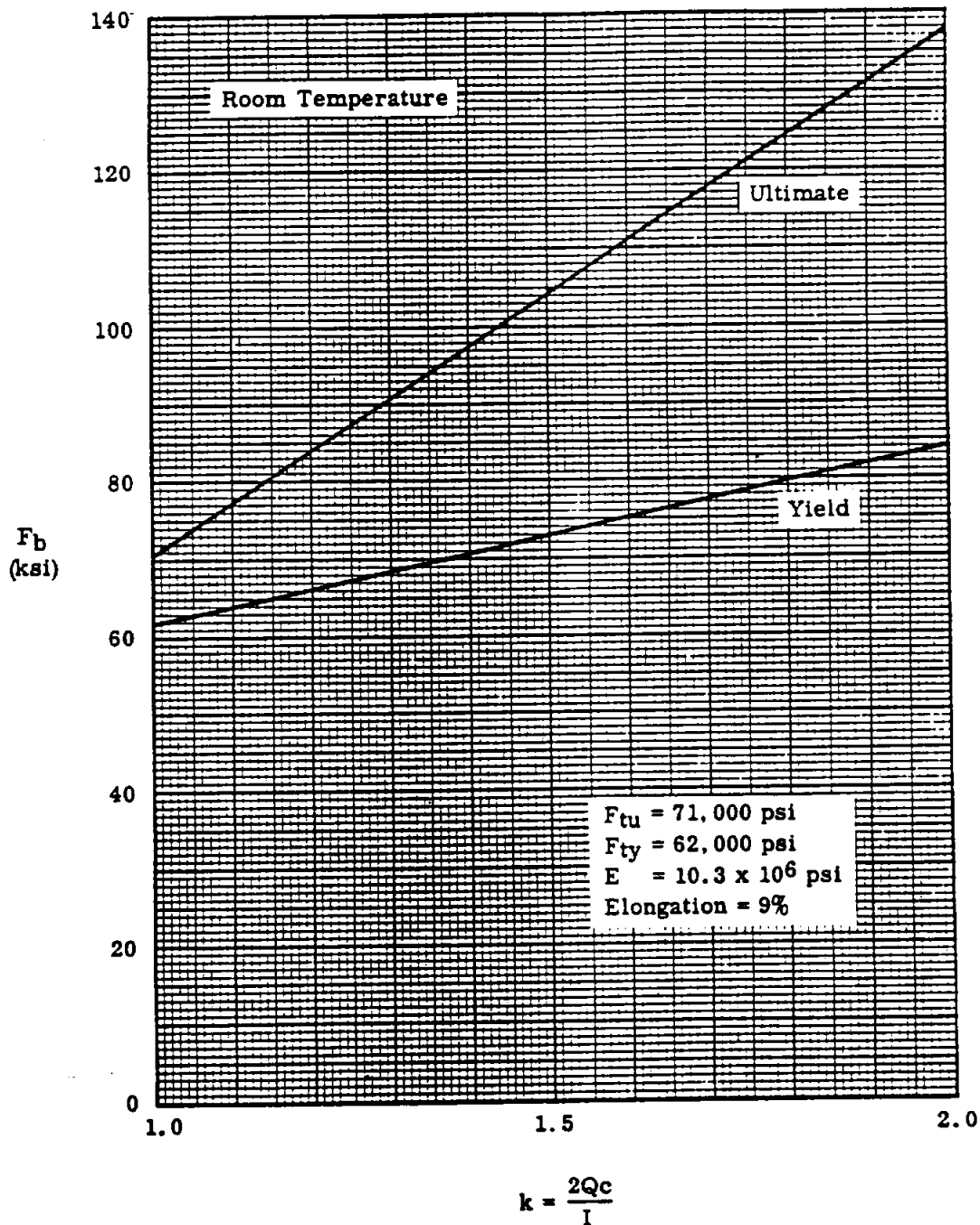


Minimum Bending Modulus of Rupture Curves for Symmetrical Sections
7070-T6 Aluminum Alloy Hand Forgings (Short Transverse) Thickness ≤ 6.9 in.

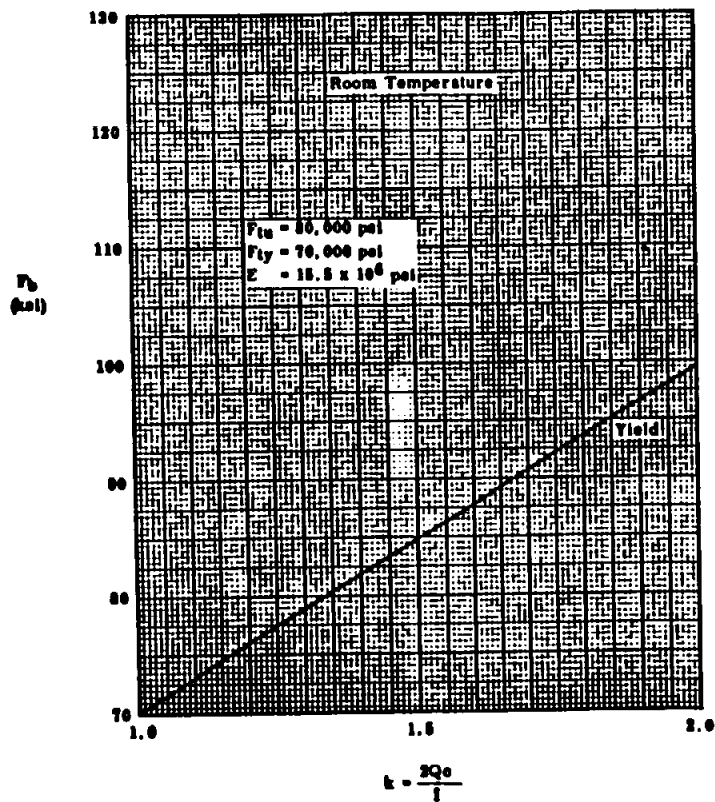


STRUCTURAL ANALYSIS MANUAL
GENERAL DYNAMICS/CONVAIR AND SPACE SYSTEMS DIVISION

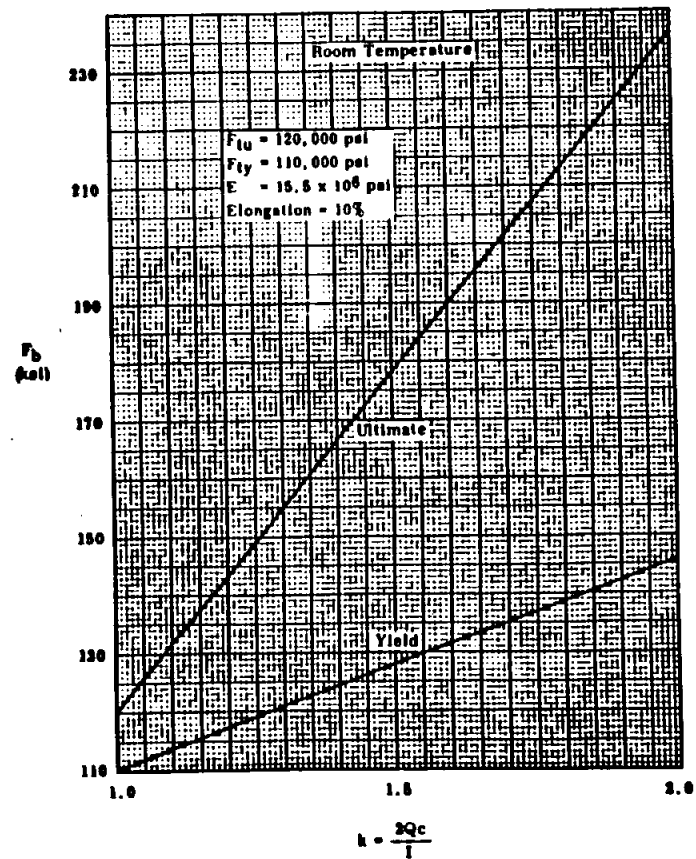
Minimum Bending Modulus of Rupture Curves for Symmetrical Sections
7079-T6 Aluminum Alloy Hand Forgings - (Longitudinal). Thickness ≤ 6 in.



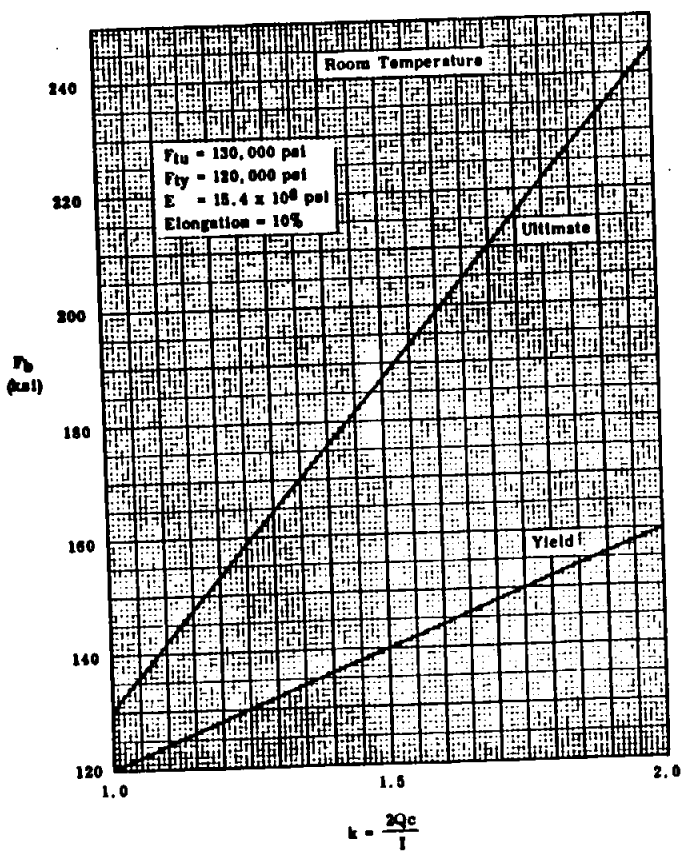
Minimum Bending Modulus of Rupture Curves for Symmetrical Sections
Commercially Pure Annealed Titanium



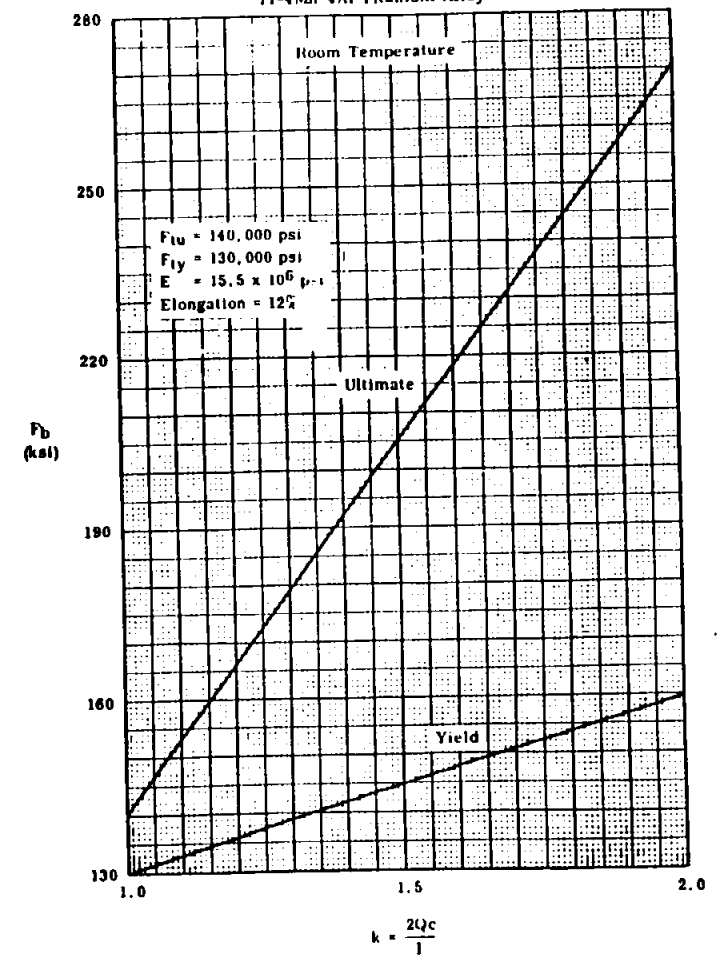
Minimum Bending Modulus of Rupture Curves for Symmetrical Sections
Ti-8Mn Titanium Alloy



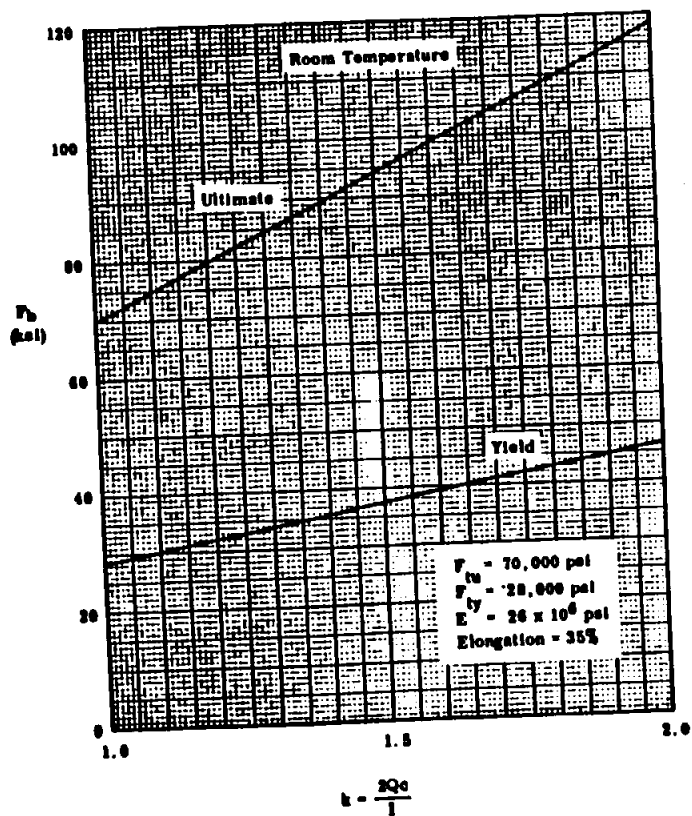
Minimum Bending Modulus of Rupture Curves for Symmetrical Sections
Ti-6Al-4V Titanium Alloy



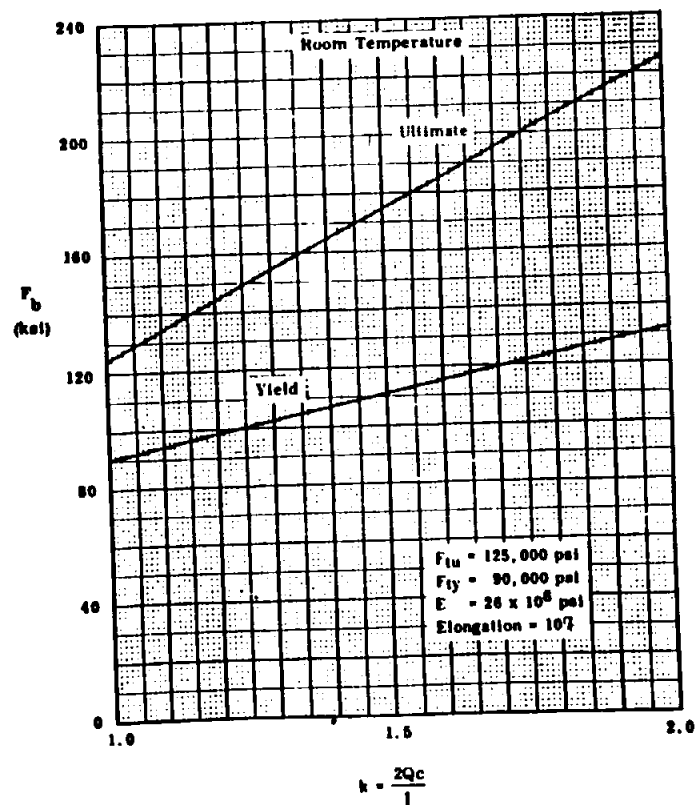
Minimum Bending Modulus of Rupture Curves for Symmetrical Sections
Ti-4Mn-4Al Titanium Alloy



Minimum Bending Modulus of Rupture Curves for Symmetrical Sections
Monel Alloy—Cold Rolled, Annealed Sheet



Minimum Bending Modulus of Rupture Curves for Symmetrical Sections
Age Hardened, K-Monel Alloy Sheet



STRUCTURAL ANALYSIS MANUAL
GENERAL DYNAMICS/CONVAIR AND SPACE SYSTEMS DIVISION


Data Source, Section 1.3 Reference 2

SECTION 17.7

PLASTIC BENDING

MINIMUM PLASTIC BENDING CURVES

STEELS

	PAGE
CARBON STEEL AISI 1023 - 1025	17.7.3
AISI ALLOY STEEL 	17.7.4
A-286	17.7.9
AISI 301	17.7.10
AISI 321	17.7.24
PH 15-7 Mo	17.7.25
17-4 PH	17.7.26
17-7 PH	17.7.27
19-9 DL AND 19-9 DX	17.7.30

ALUMINUM

2014	17.7.32
2024	17.7.34
6061	17.7.40
7075	17.7.41
7079	17.7.46

 AISI ALLOY STEELS INCLUDE AISI 4130, 4140, 4340, 8630, 8735, 8740, AND 9840.

STRUCTURAL ANALYSIS MANUAL
GENERAL DYNAMICS/CONVAIR AND SPACE SYSTEMS DIVISION

TITANIUM

	PAGE
Ti - 8 Mn	17.7.51
Ti - 6 AL-4V	17.7.52
Ti - 4 Mn-4AL	17.7.53

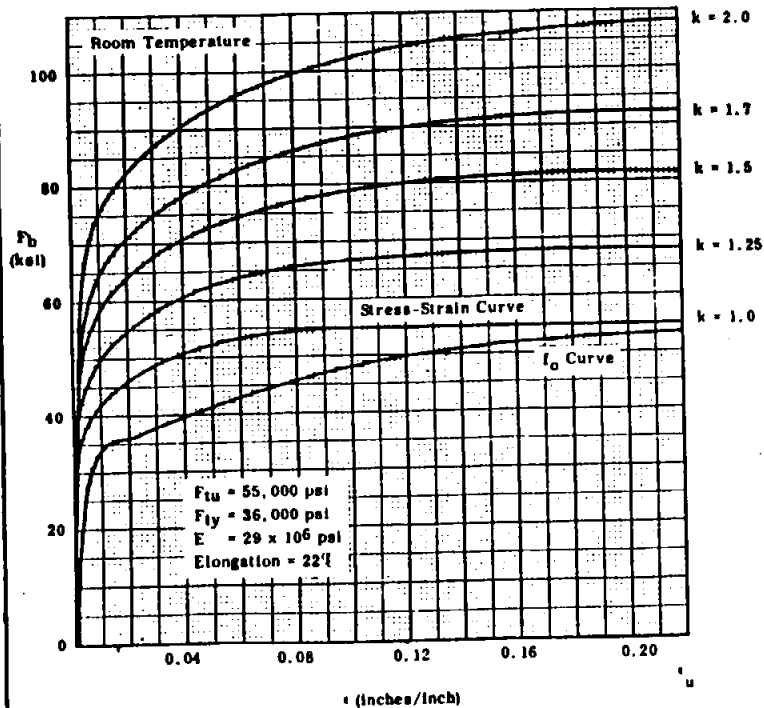
MONEL

K-MONEL	17.7.54
MONEL ALLOY	17.7.55

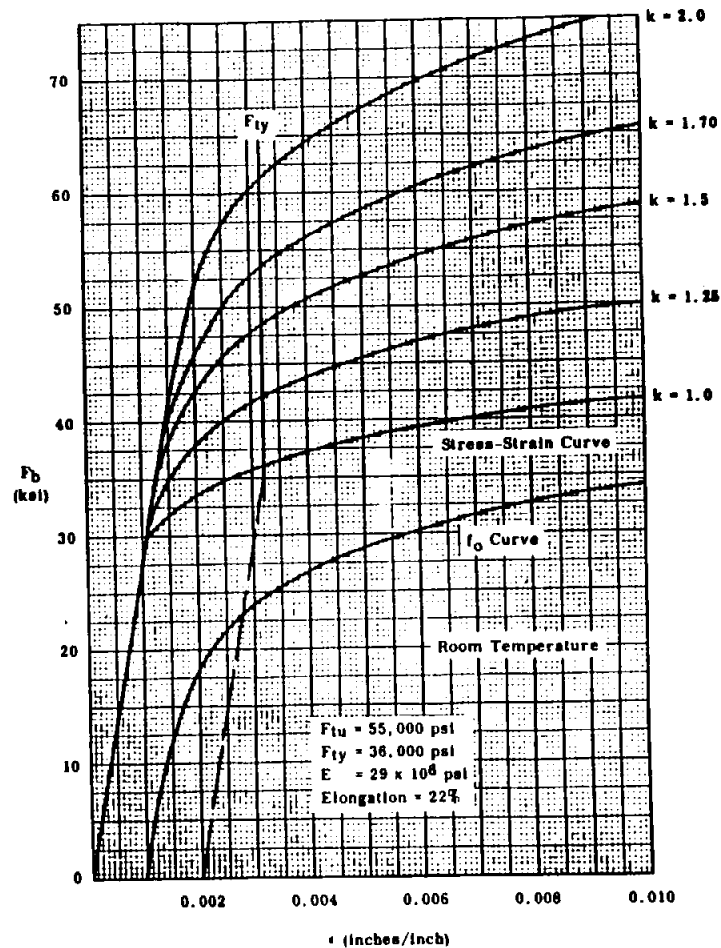
MAGNESIUM

AZ 61A	17.7.56
HK 31A-0	17.7.58
ZK 60A	17.7.60

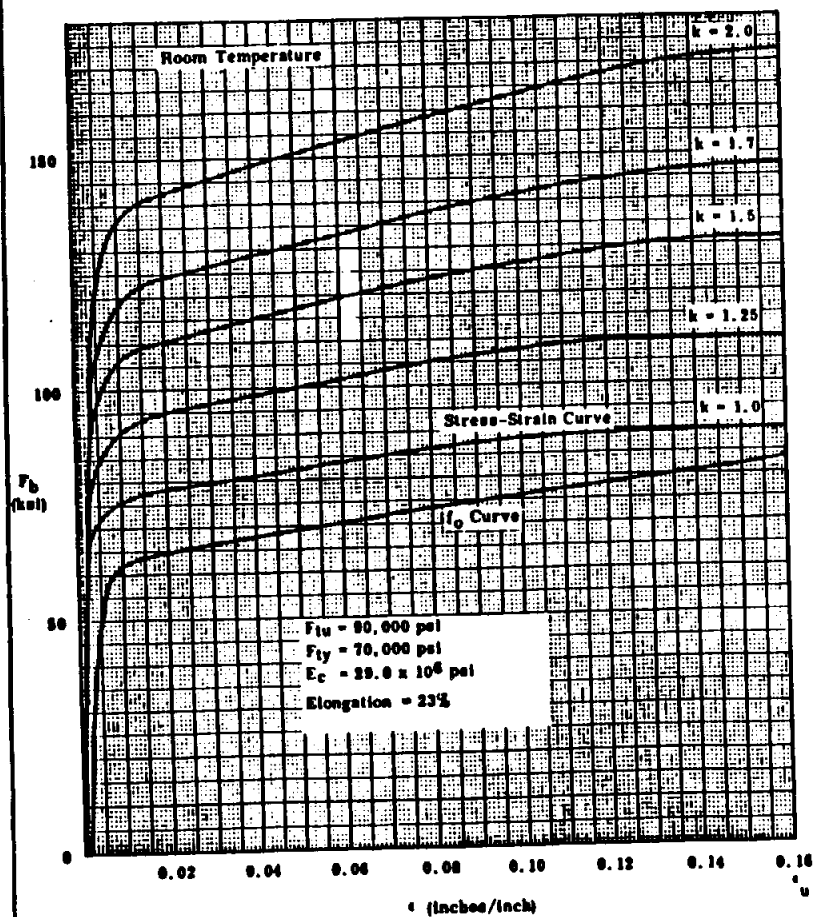
Minimum Plastic Bending Curves
Carbon Steel AISI 1023-1025



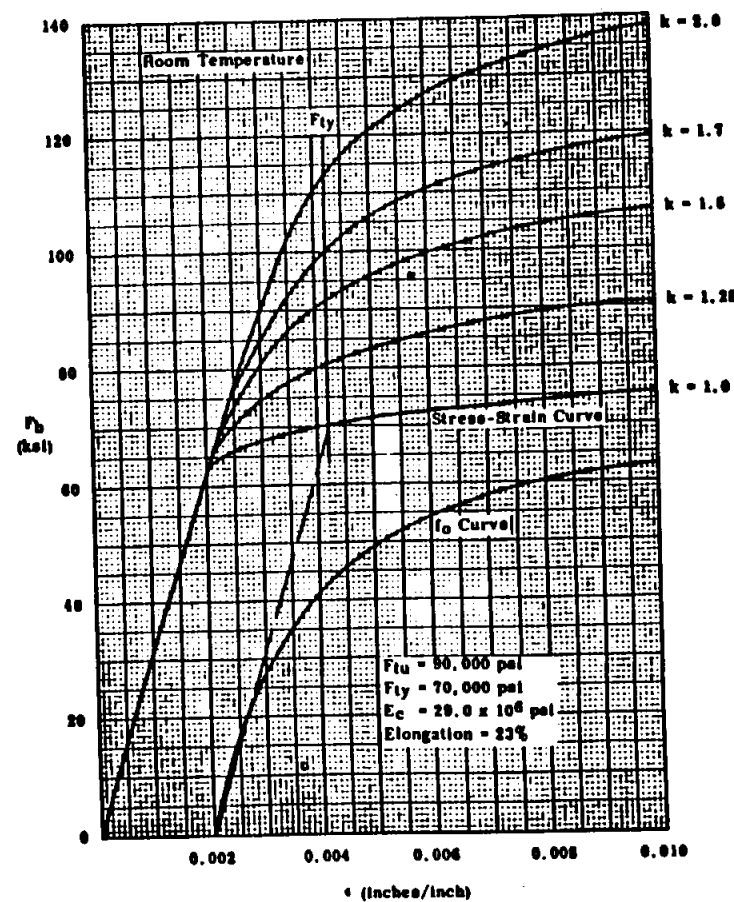
Minimum Plastic Bending Curves
Carbon Steel AISI 1023-1025



Minimum Plastic Bending Curves
AISI Alloy Steel, Normalized, Thickness > 0.100 in.

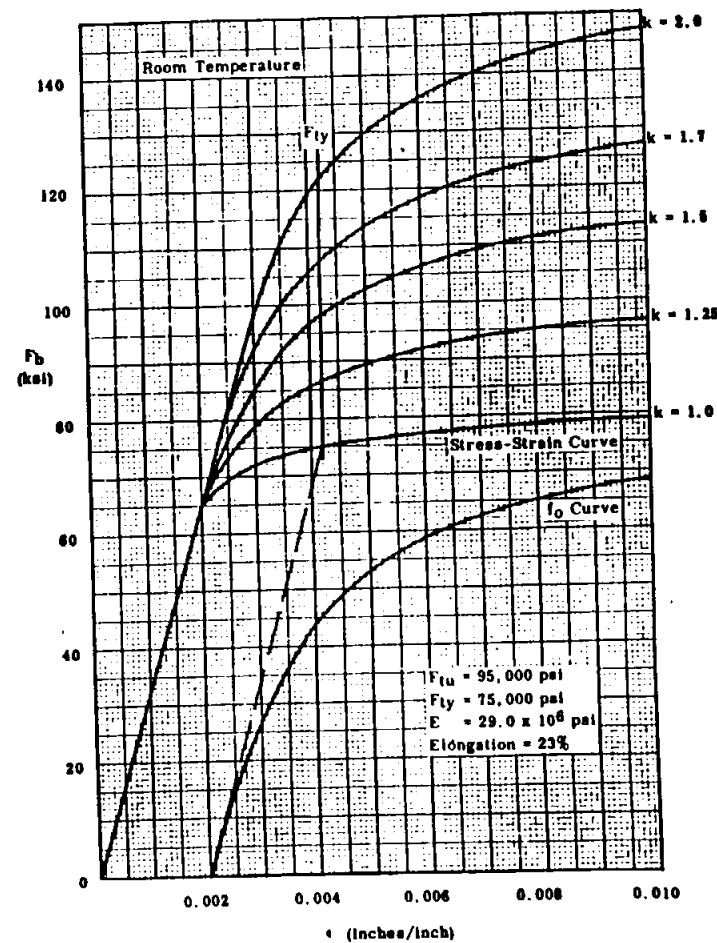


Minimum Plastic Bending Curves
AISI Alloy Steel, Normalized, > 0.100 in. Thick

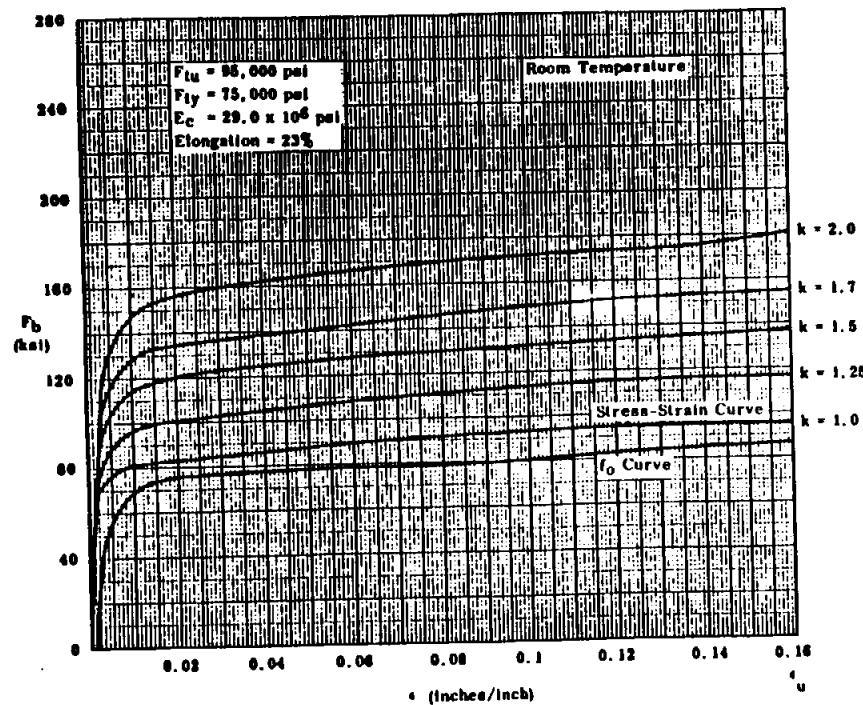


402

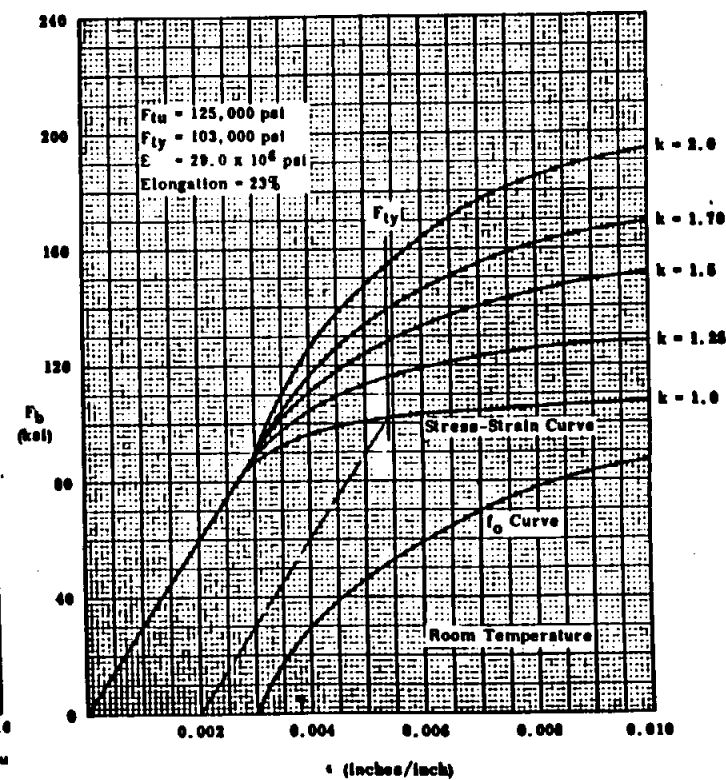
Minimum Plastic Bending Curves
AISI Alloy Steel, Normalized, Thickness ≤ 0.188 in.



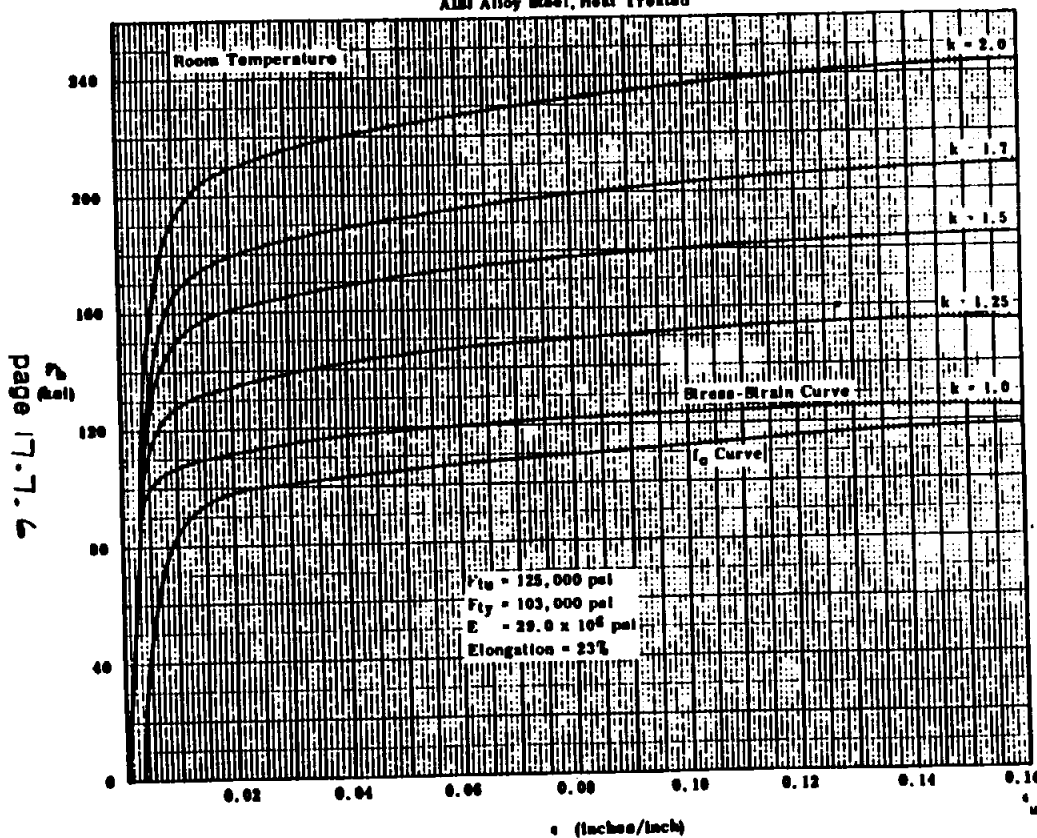
Minimum Plastic Bending Curves
AISI Alloy Steel, Normalized, Thickness ≤ 0.188 in.



Minimum Plastic Bending Curves
AISI Alloy Steel, Heat Treated



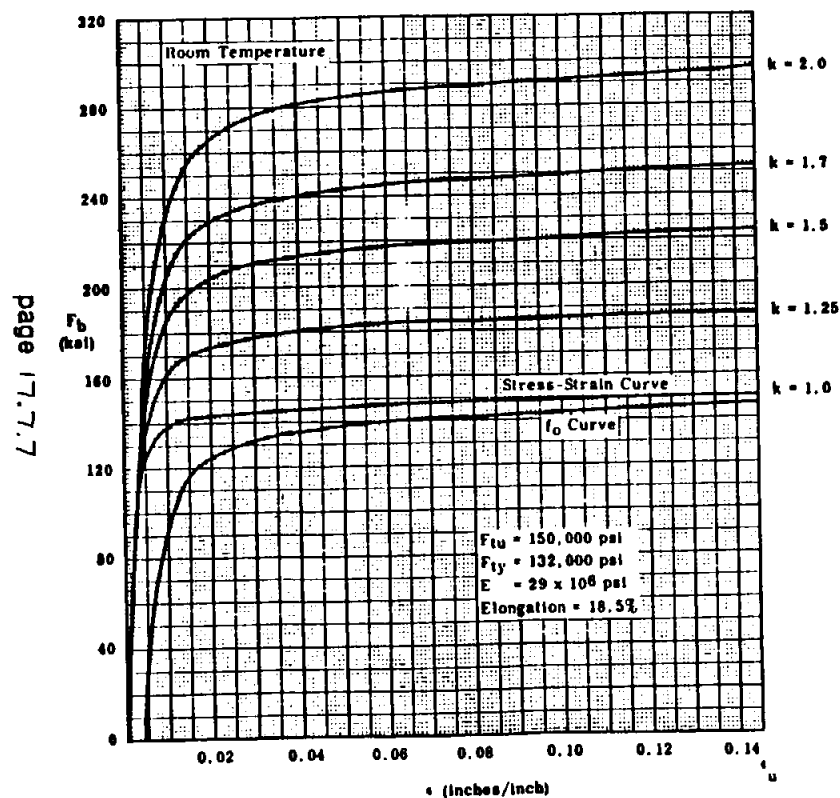
Minimum Plastic Bending Curves
AISI Alloy Steel, Heat Treated



page 17.7.6

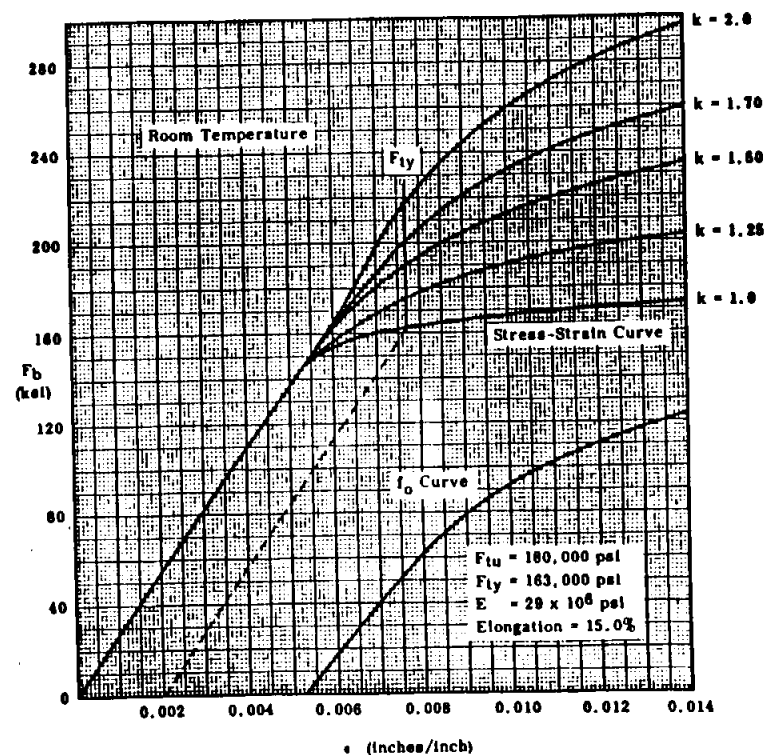
304

Minimum Plastic Bending Curves
AISI Alloy Steel, Heat Treated

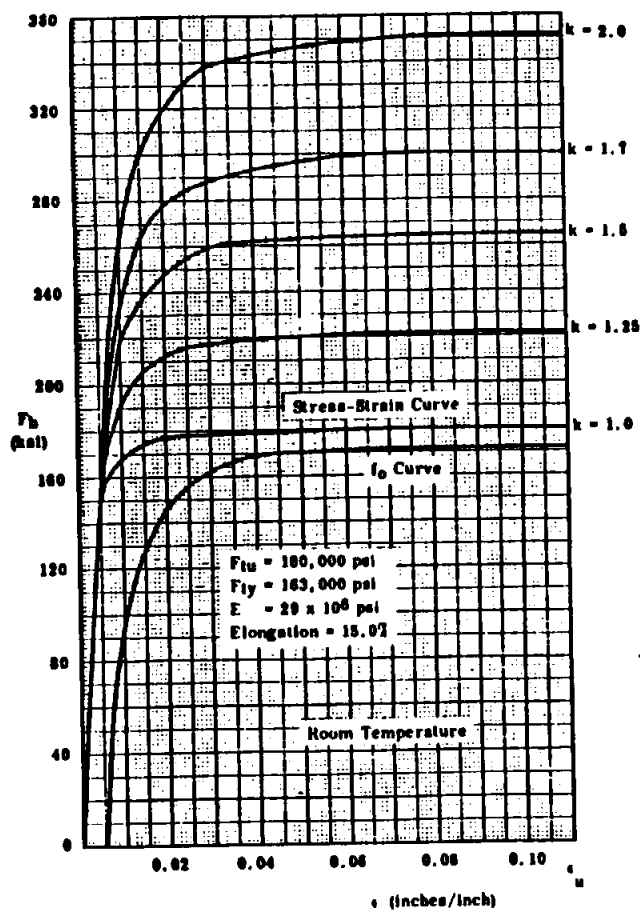


page 17.7.7

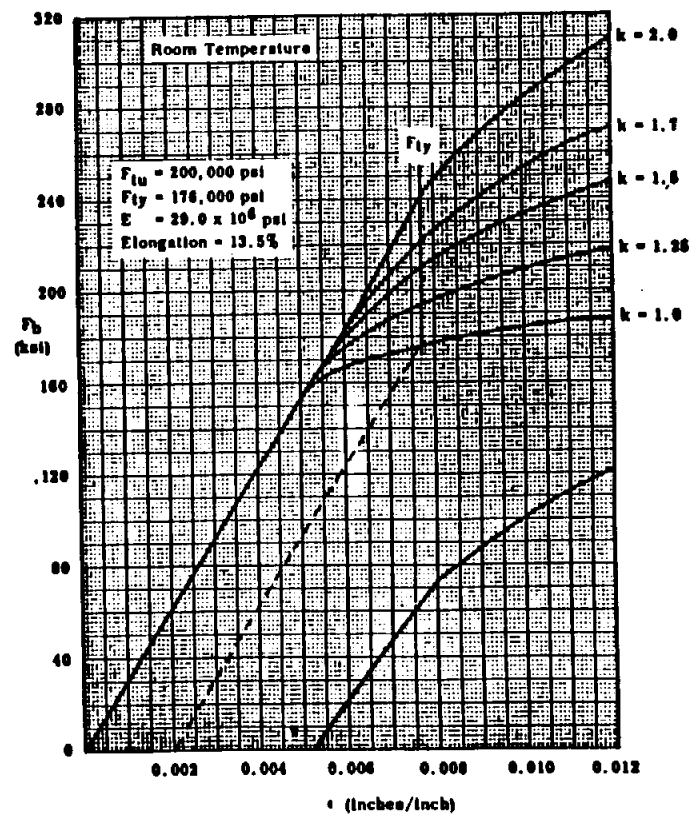
Minimum Plastic Bending Curves
AISI Alloy Steel, Heat Treated



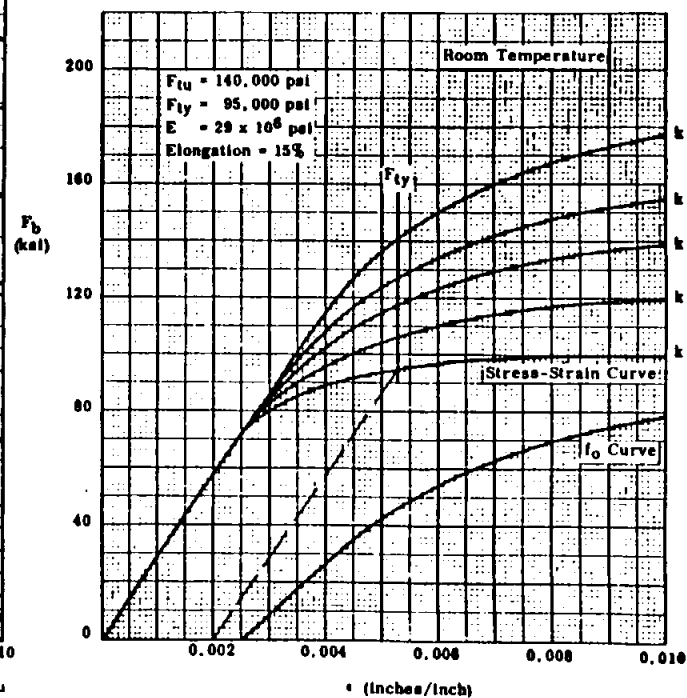
Minimum Plastic Bending Curves
AISI Alloy Steels, Heat Treated



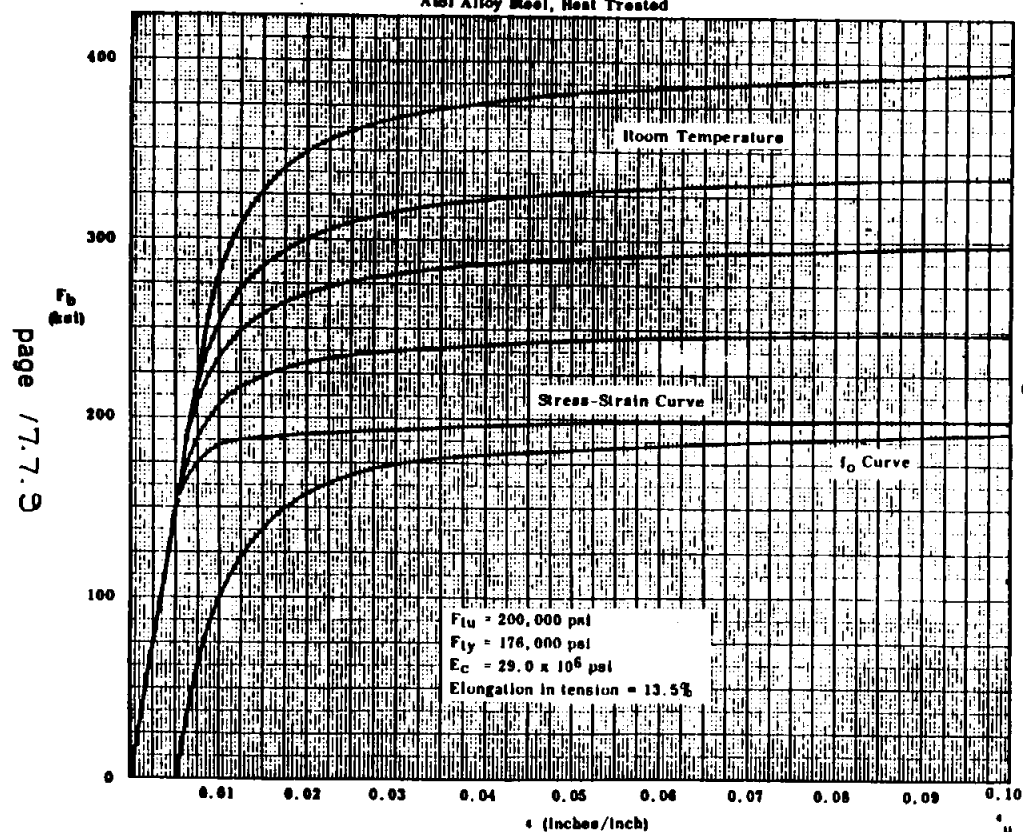
Minimum Plastic Bending Curves
AISI Alloy Steel, Heat Treated



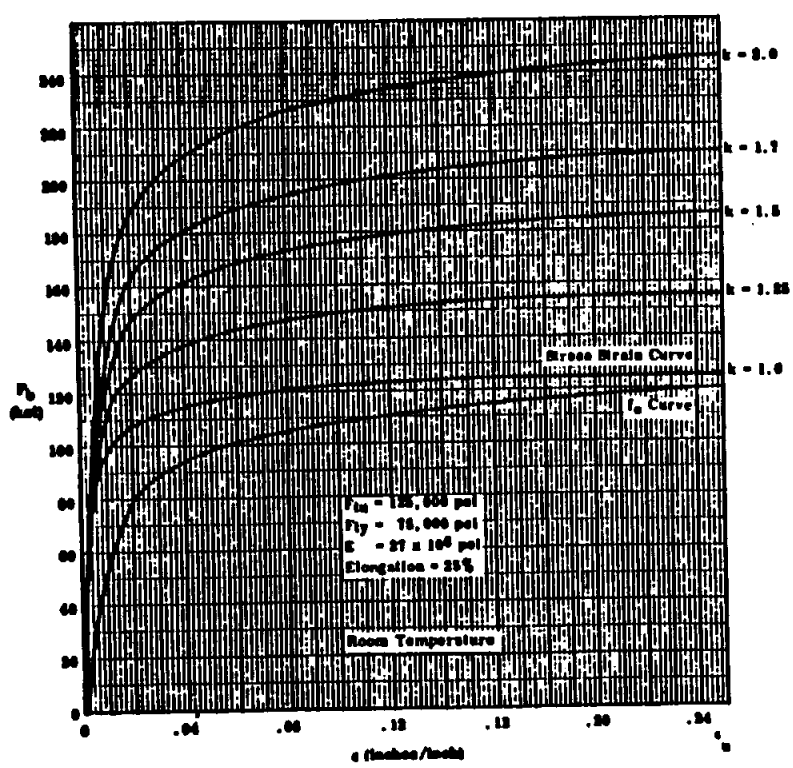
Minimum Plastic Bending Curves
A-286 Alloy, Heat Treated



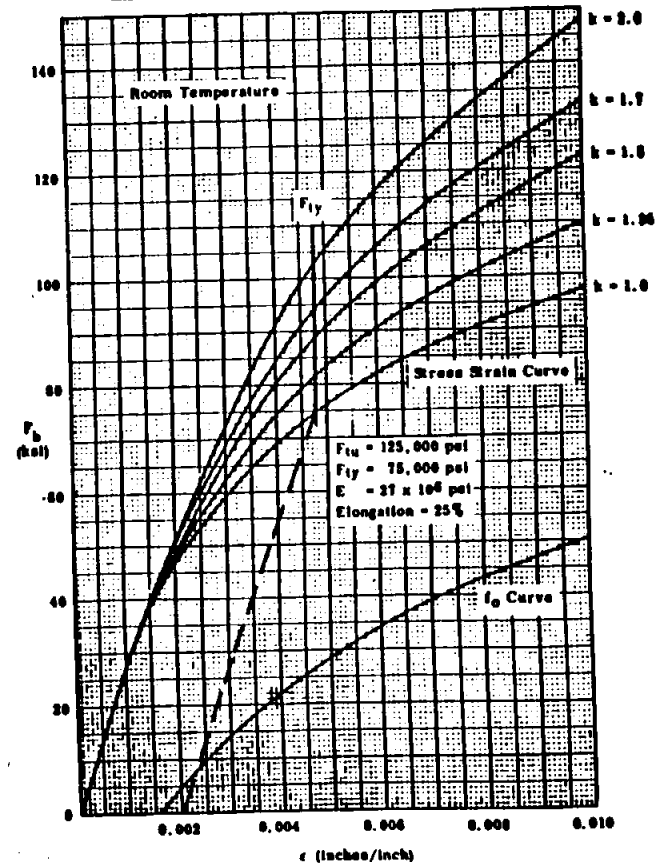
Minimum Plastic Bending Curves
AISI Alloy Steel, Heat Treated



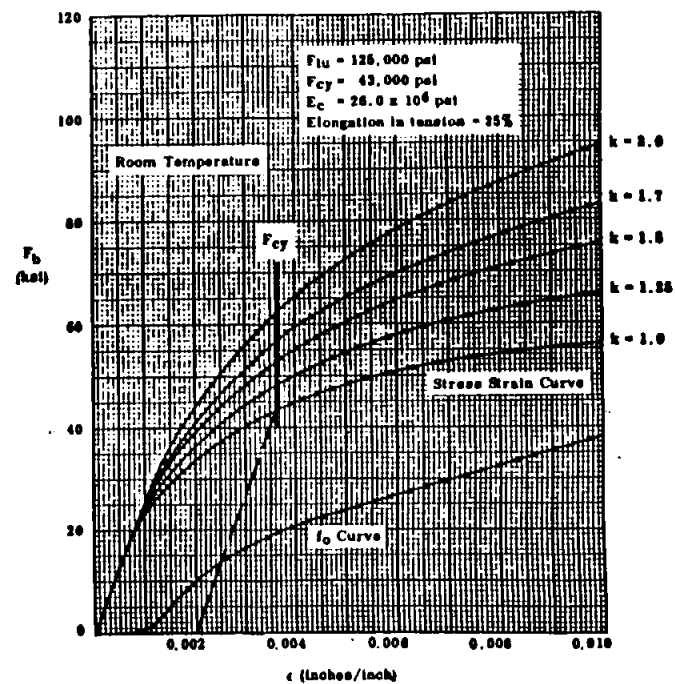
Minimum Plastic Bending Curves
1/4 Hard AISI 301 Stainless Steel Sheet-for Tension or Transverse Compression
and Stress Relieved Material-for Tension or Compression



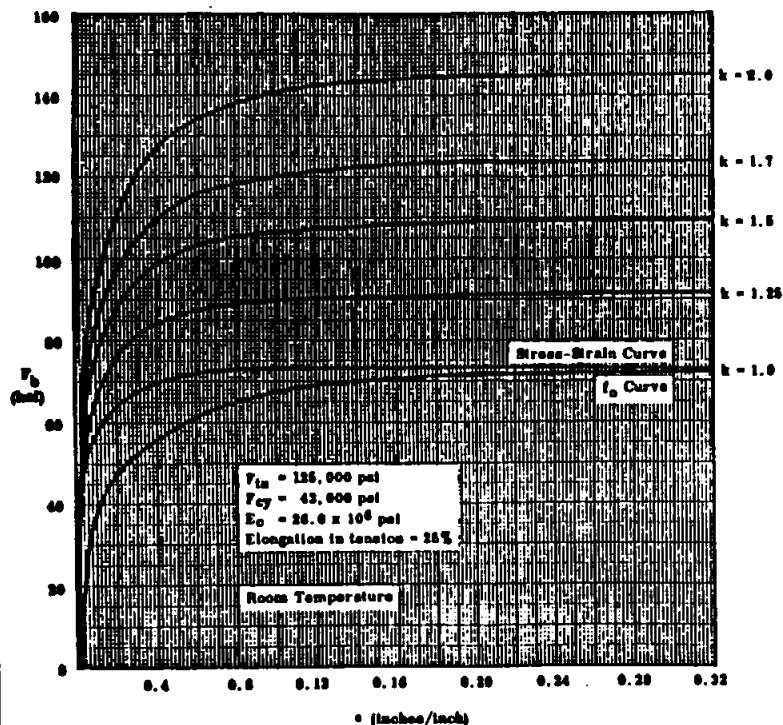
Minimum Plastic Bending Curves
1/4 Hard AISI 301 Stainless Steel Sheet-for Tension or Transverse Compression
and Stress Relieved Material-for Tension or Compression



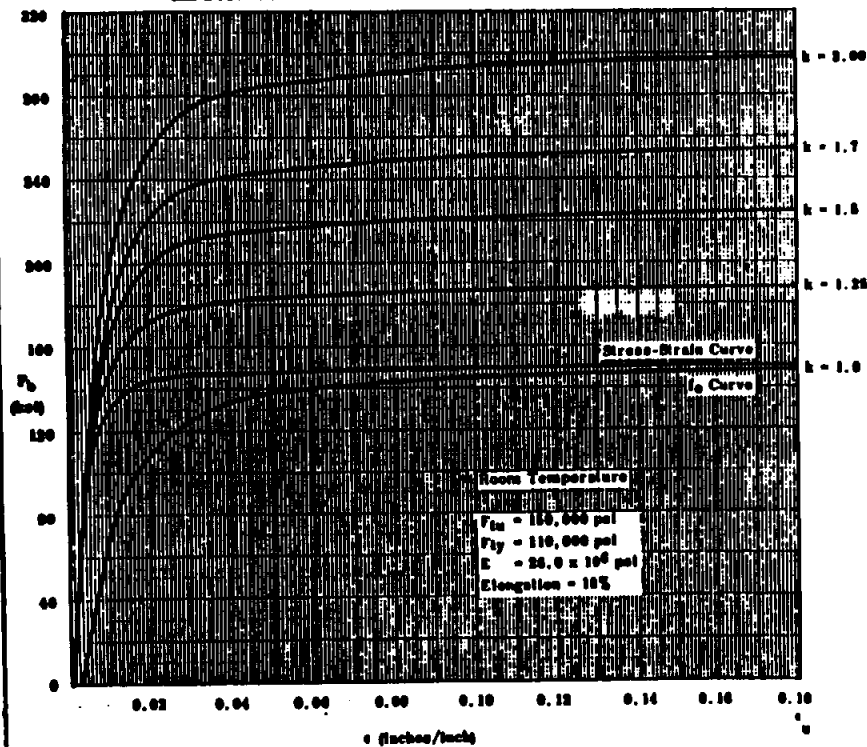
Minimum Plastic Bending Curves
1/4 Hard AISI 301 Stainless Steel Sheet - for Longitudinal Compression



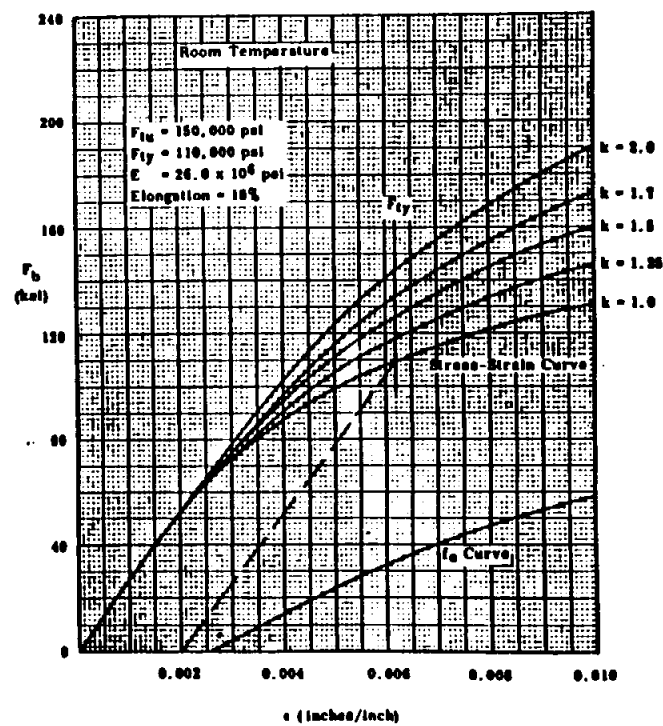
Minimum Plastic Bending Curves
1/4 Hard AISI 301 Stainless Steel Sheet - for Longitudinal Compression



Minimum Plastic Bending Curves
1/2 Hard AISI 301 Stainless Steel Sheet-for Tension or Transverse Compression
and Stress Relieved Material-for Tension or Transverse Compression



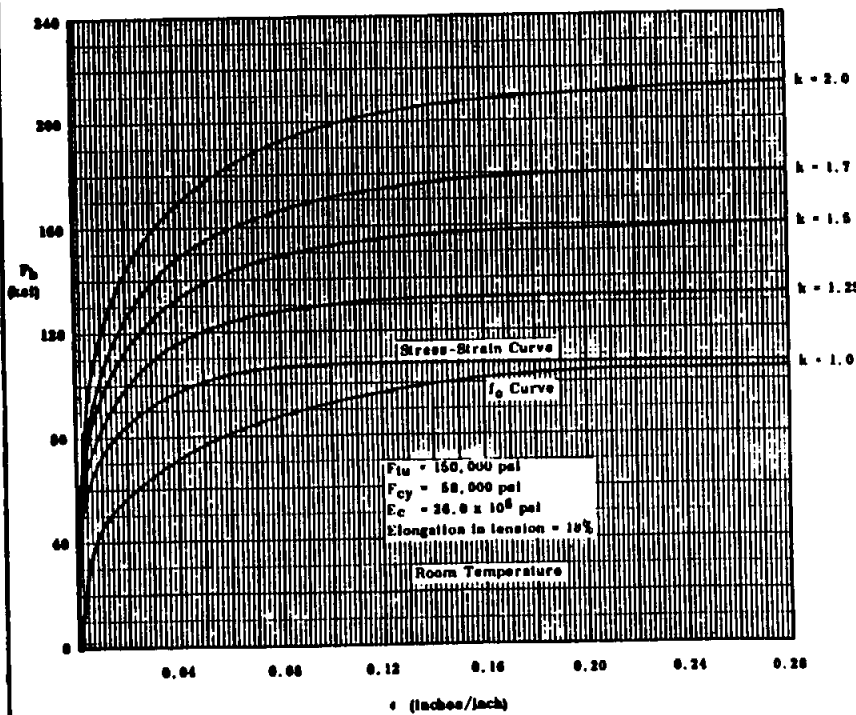
Minimum Plastic Bending Curves
1/2 Hard AISI 301 Stainless Steel Sheet-for Tension or Transverse Compression
and Stress Relieved Material-for Tension or Transverse Compression



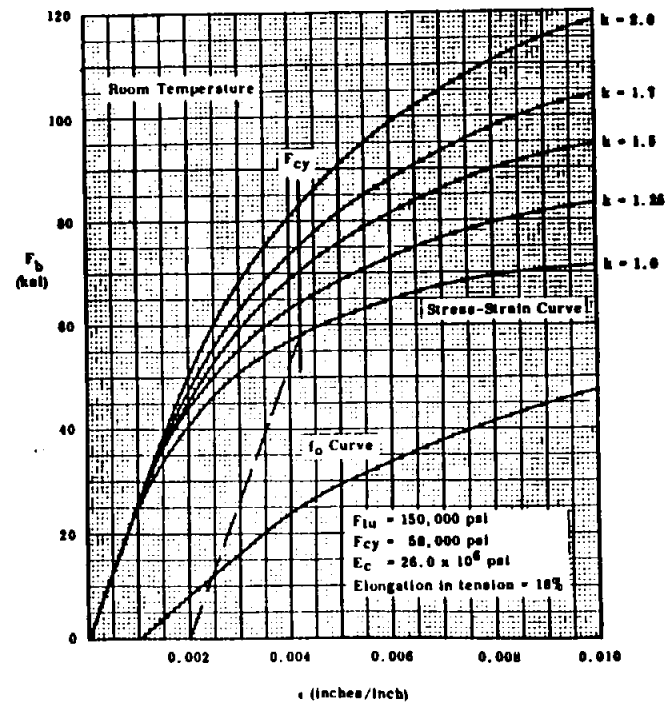
311

page 17.7.13

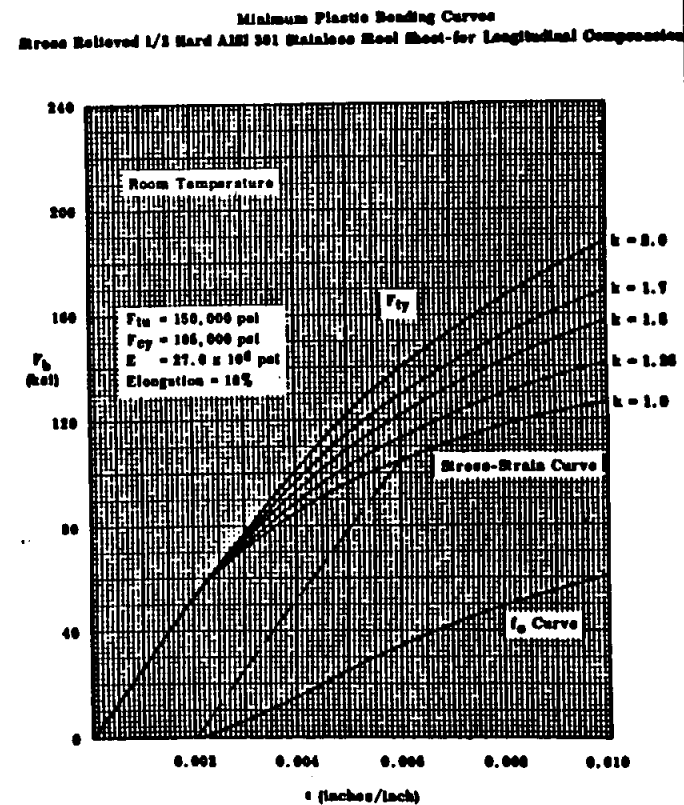
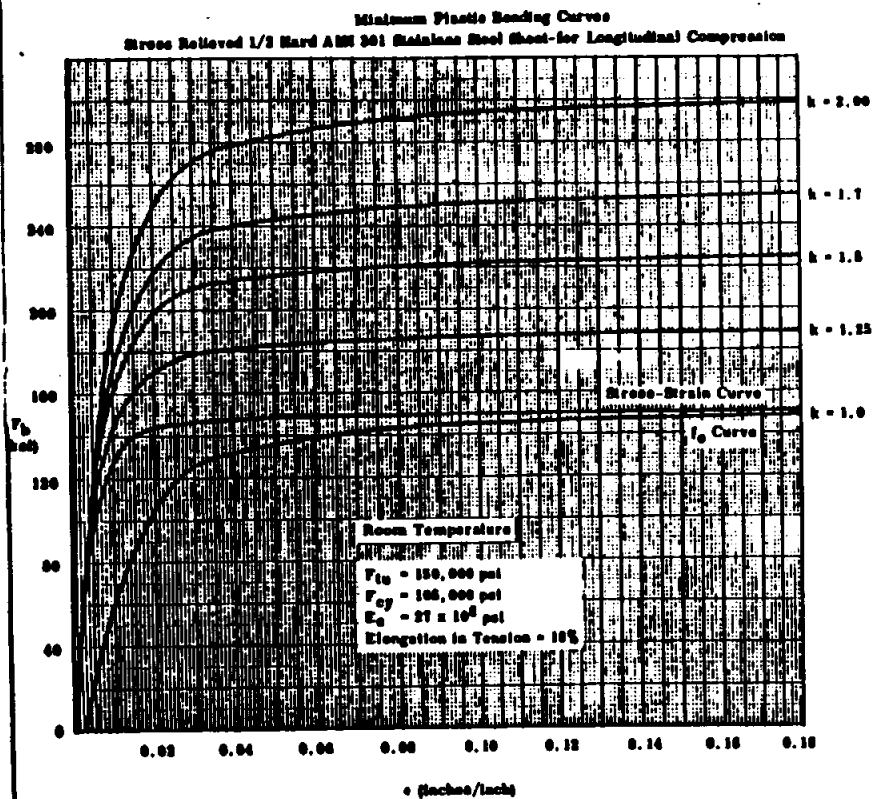
Minimum Plastic Bending Curves
1/2 Hard AHS 301 Stainless Steel Sheet - for Longitudinal Compression



Minimum Plastic Bending Curves
1/2 Hard AHS 301 Stainless Steel Sheet - for Longitudinal Compression

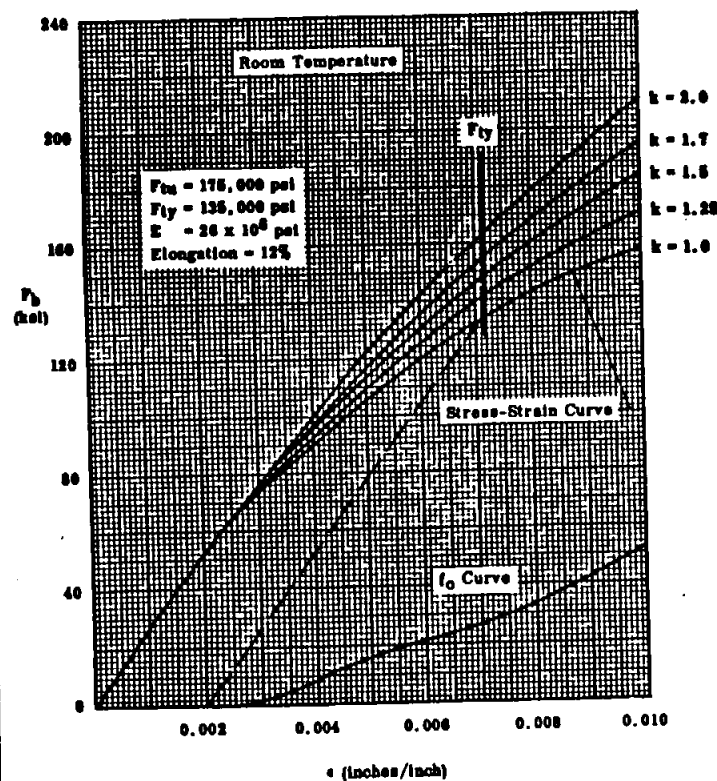


page 17.17.14

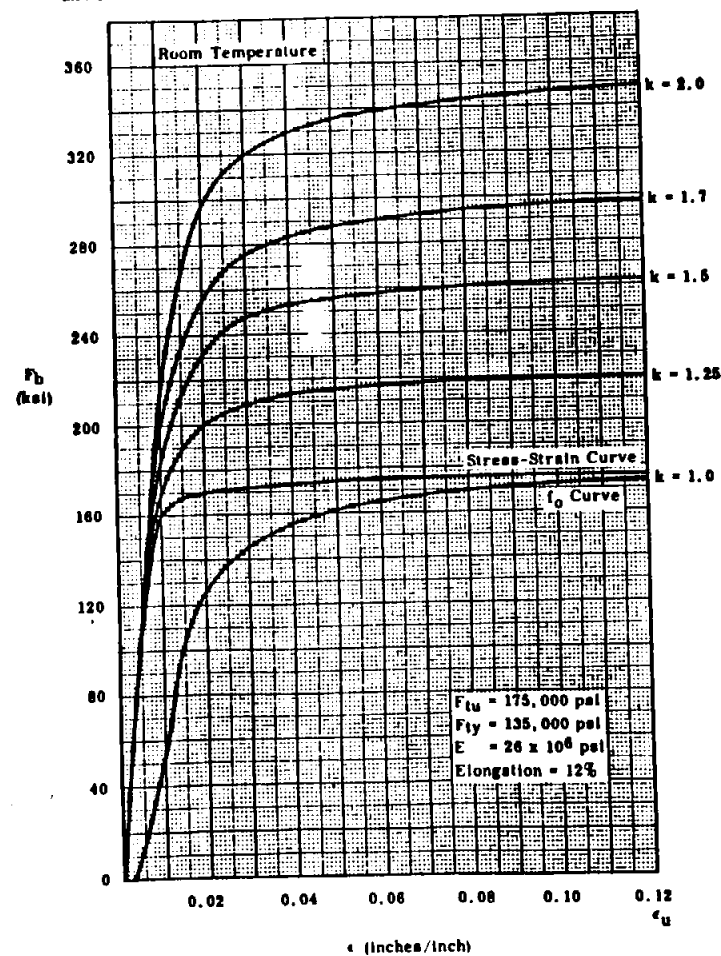


312

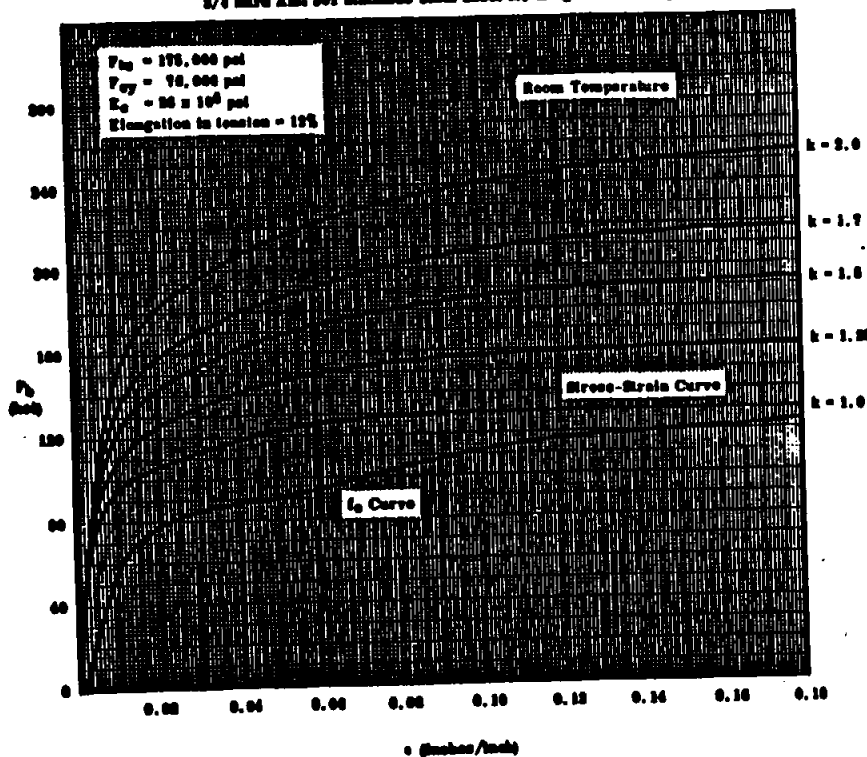
Minimum Plastic Bending Curves
3/4 Hard AISI 301 Stainless Steel Sheet - for Tension or Transverse Compression
and Stress Relieved Material - for Tension or Transverse Compression



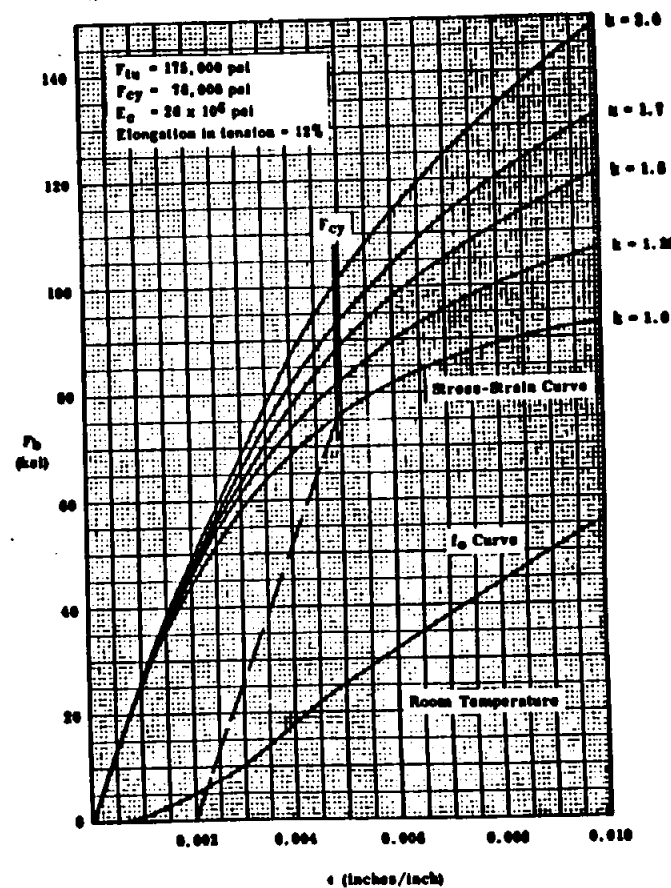
Minimum Plastic Bending Curves
3/4 Hard AISI 301 Stainless Steel Sheet - for Tension or Transverse Compression
and Stress Relieved Material - for Tension or Transverse Compression



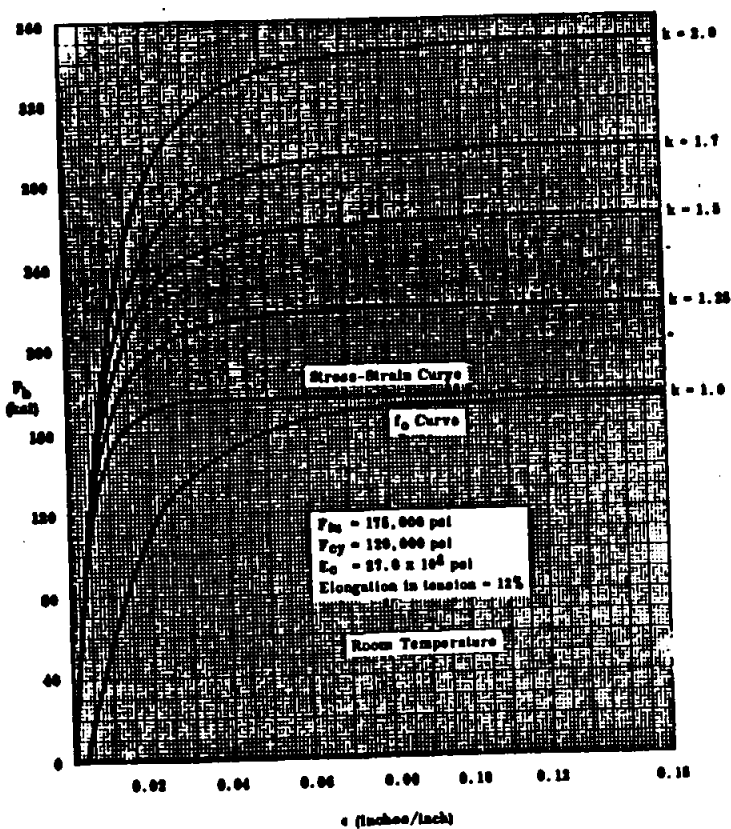
Minimum Plastic Bending Curves
3/4 Hard AHH 301 Stainless Steel Sheet for Longitudinal Compression



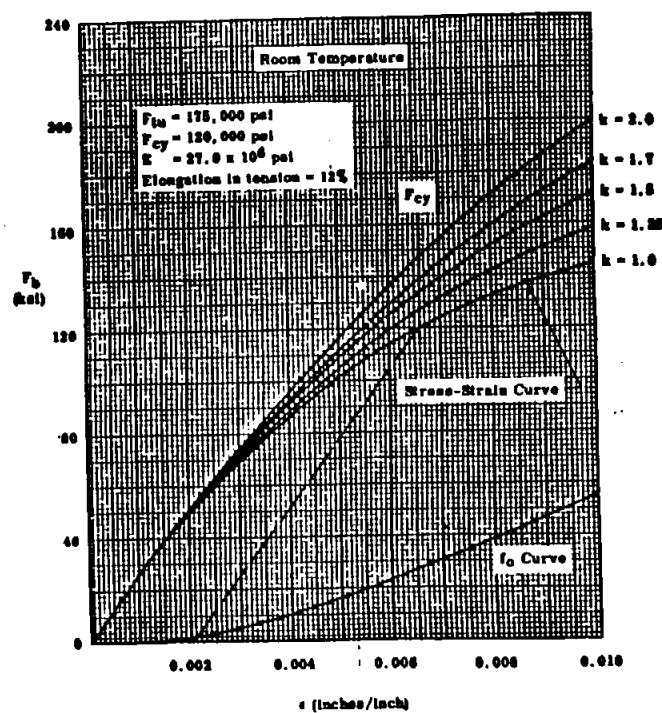
Minimum Plastic Bending Curves
3/4 Hard AHH 301 Stainless Steel Sheet for Longitudinal Compression



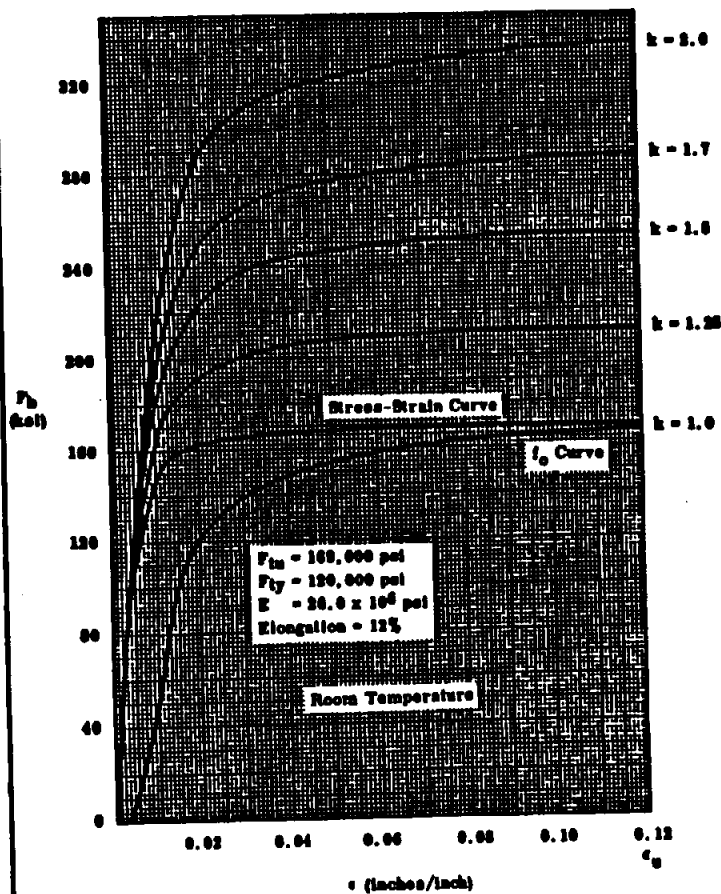
Minimum Plastic Bending Curves
Stress Relieved 3/4 Hard A31 301 Stainless Steel Sheet for Longitudinal Compression



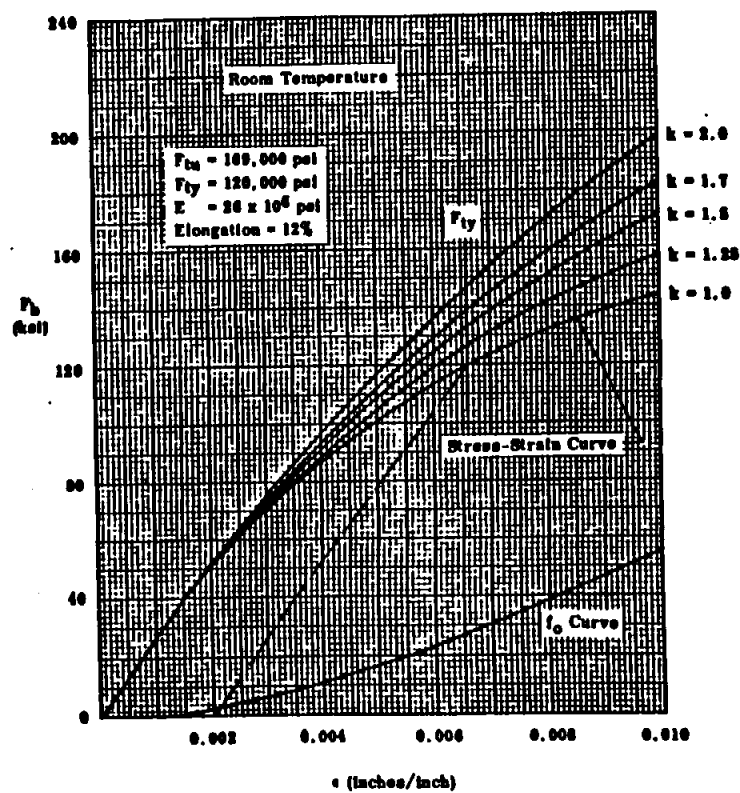
Minimum Plastic Bending Curves
Stress Relieved 3/4 Hard A31 301 Stainless Steel Sheet for Longitudinal Compression



Minimum Plastic Bending Curves
Convair Astronautics Special 3/4 Hard AISI 301 Stainless Steel Sheet
for Tension or Transverse Compression

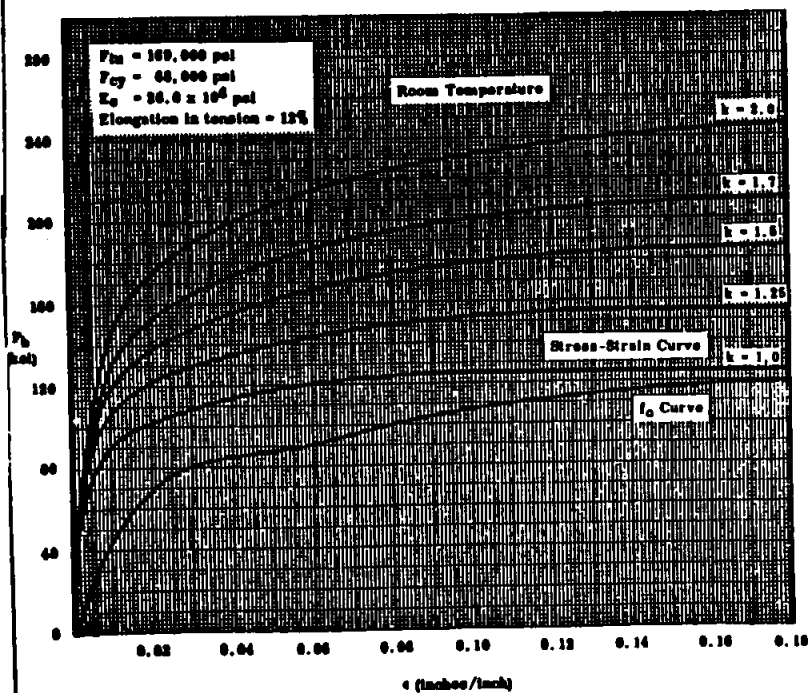


Minimum Plastic Bending Curves
Convair Astronautics Special 3/4 Hard AISI 301 Stainless Steel Sheet
for Tension or Transverse Compression

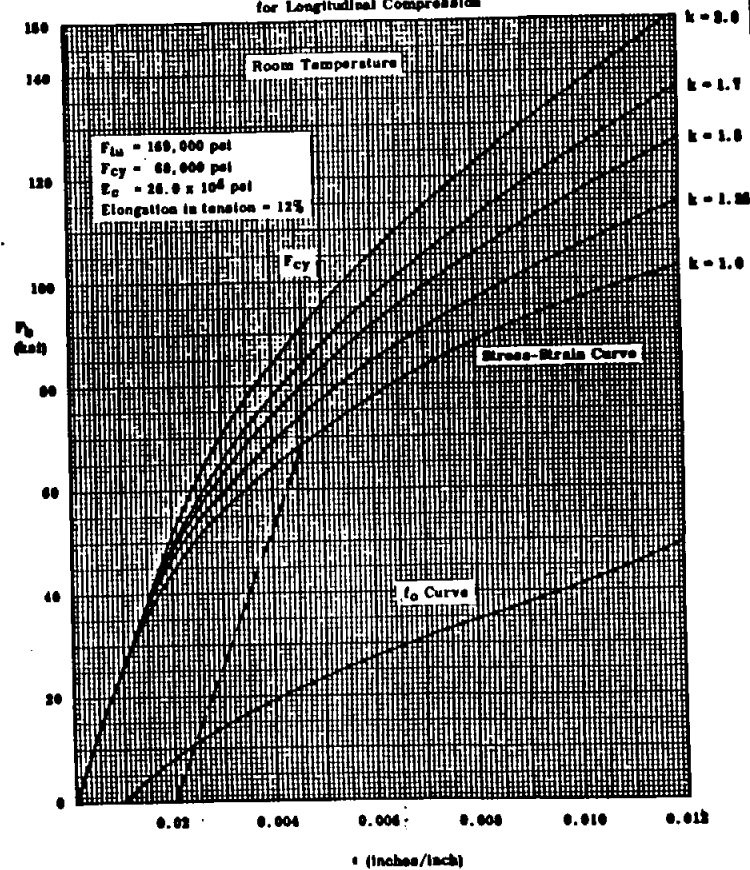


3/9

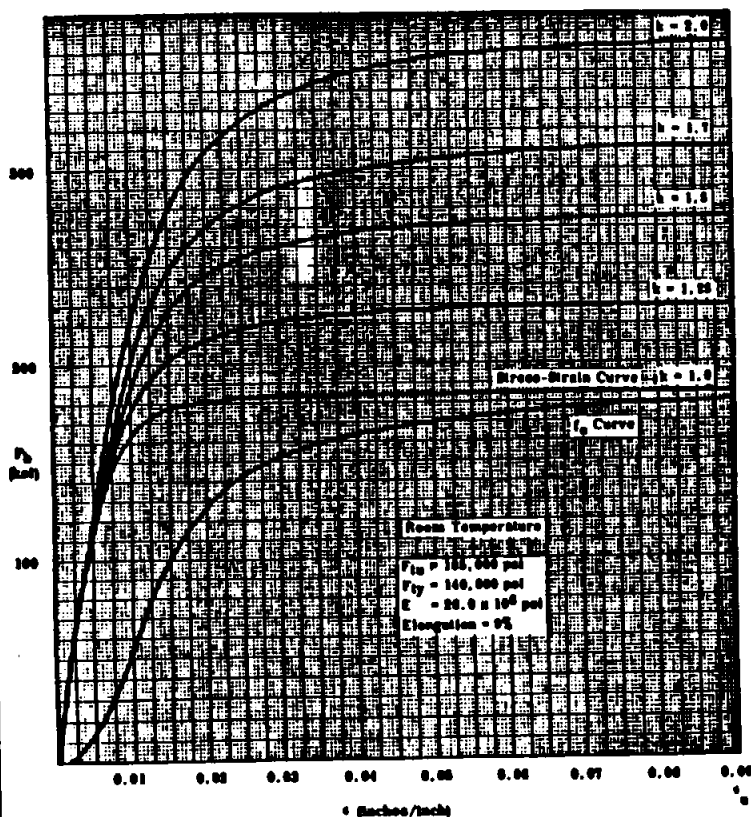
Minimum Plastic Bending Curves
Convairst Aerospace Special 3/4 Hard AISI 301 Stainless Steel Sheet
for Longitudinal Compression



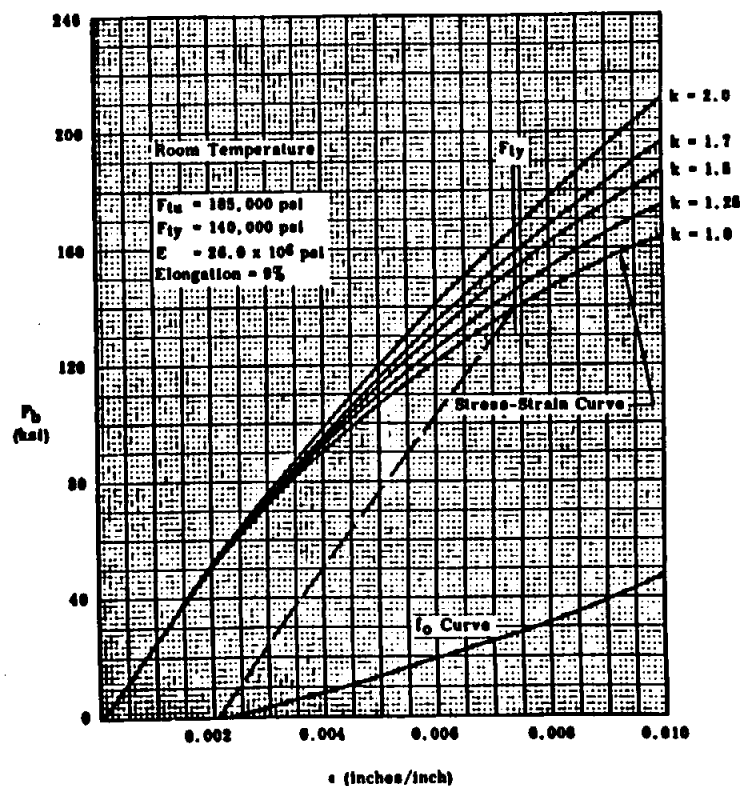
Minimum Plastic Bending Curves
Convairst Aerospace Special 3/4 Hard AISI 301 Stainless Steel Sheet
for Longitudinal Compression



Minimum Plastic Bending Curves
Full Hard AISI 301 Stainless Steel Sheet - for Tension or Transverse Compression
and Stress Relieved Material - for Tension or Compression

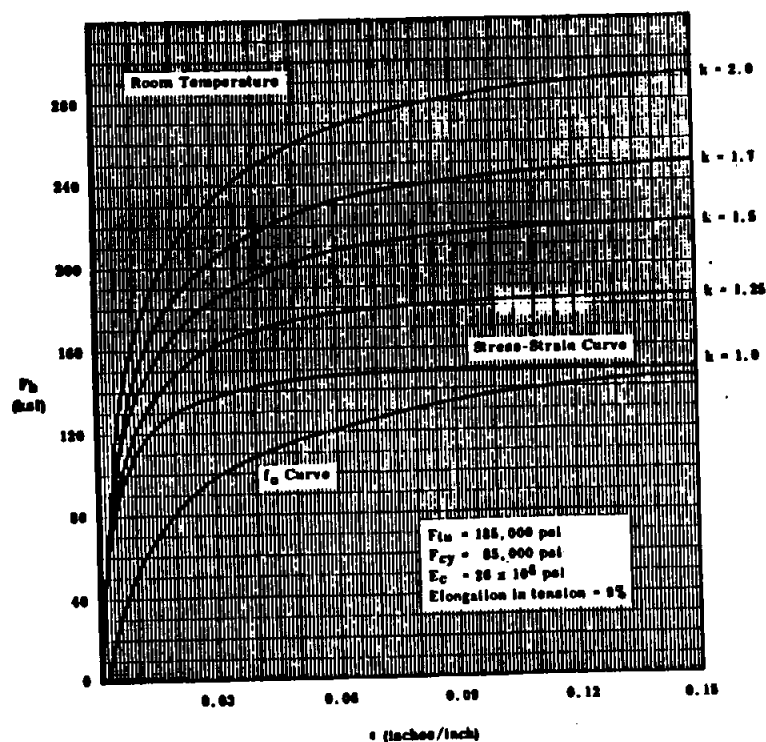


Minimum Plastic Bending Curves
Full Hard AISI 301 Stainless Steel Sheet - for Tension or Transverse Compression
and Stress Relieved Material - for Tension or Compression

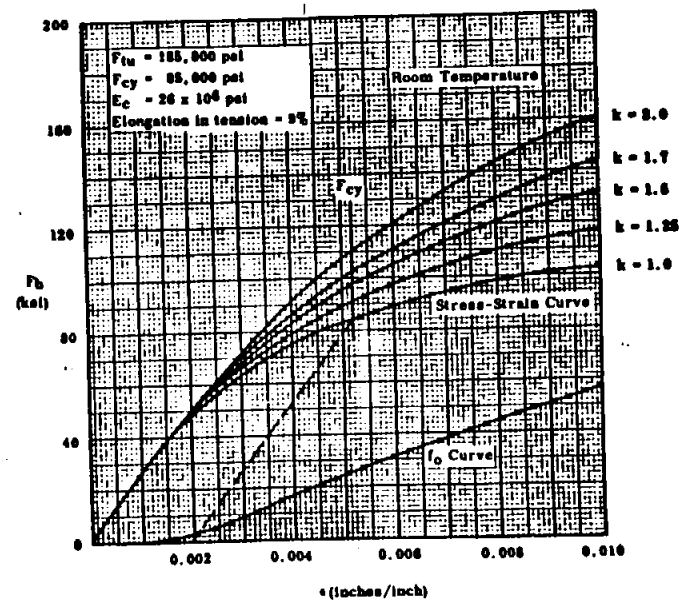


319

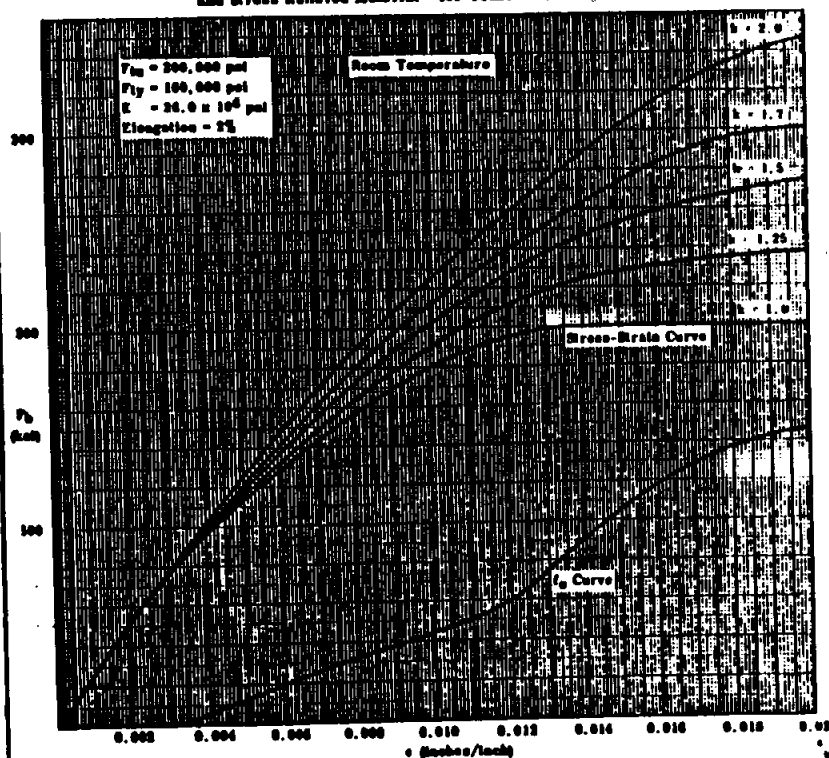
Minimum Plastic Bending Curves
Full Hard A301 Stainless Steel Sheet for Longitudinal Compression



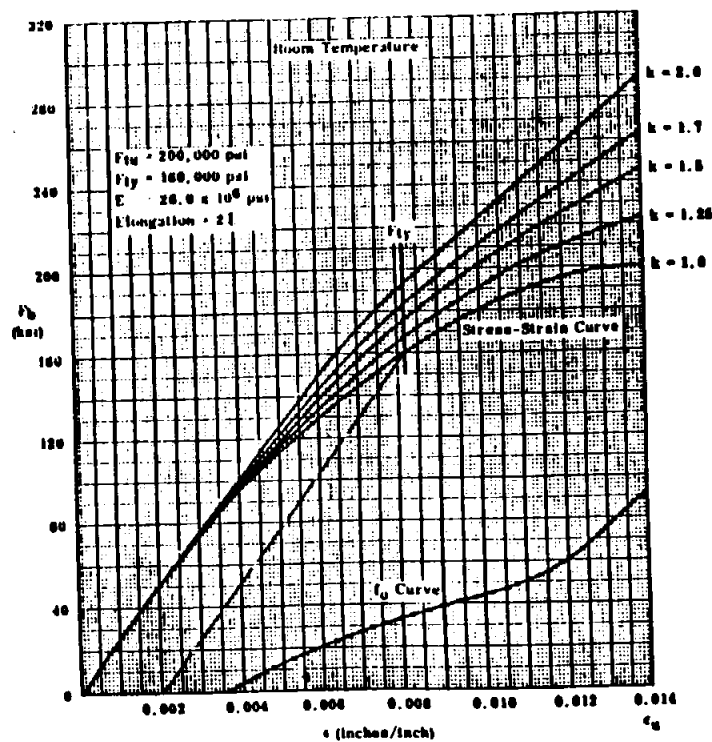
Minimum Plastic Bending Curves
Full Hard A301 Stainless Steel Sheet for Longitudinal Compression



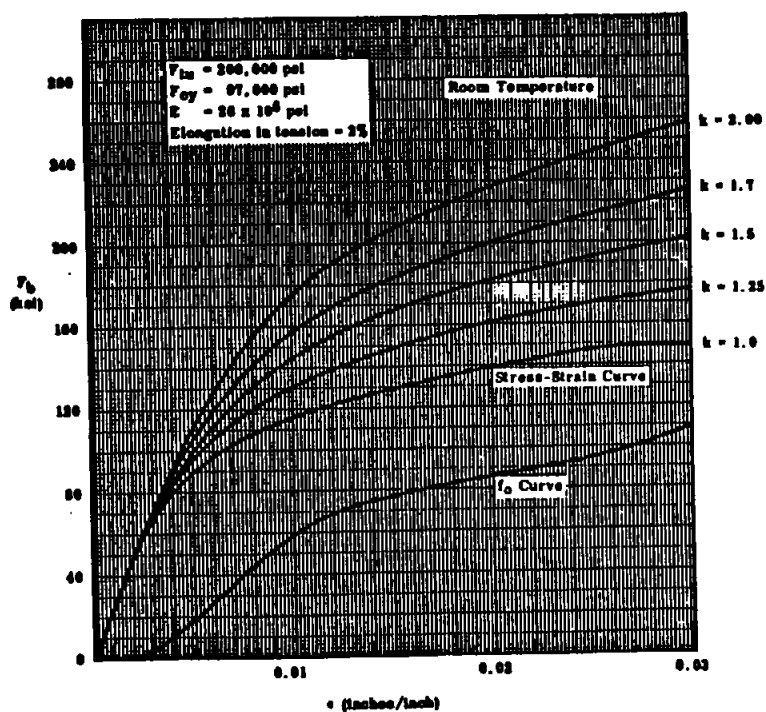
Minimum Plastic Bending Curves
Extra Hard AMS 301 Stainless Steel Sheet-for Tension or Transverse Compression
and Stress Relieved Material - for Tension or Compression



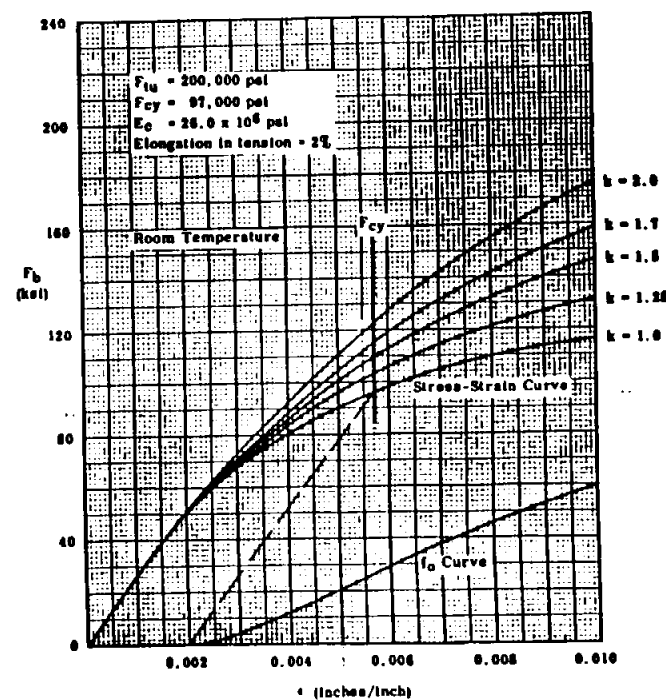
Minimum Plastic Bending Curves
Extra Hard AMS 301 Stainless Steel Sheet-for Tension or Transverse Compression
and Stress Relieved Material - for Tension or Compression



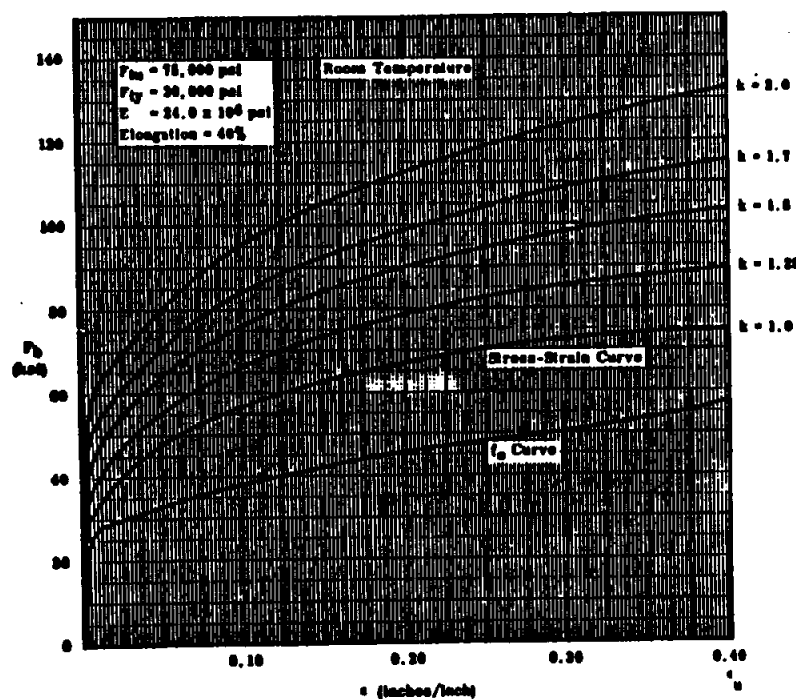
Minimum Plastic Bending Curves
Extra Hard A31 Stainless Steel Sheet-for Longitudinal Compression



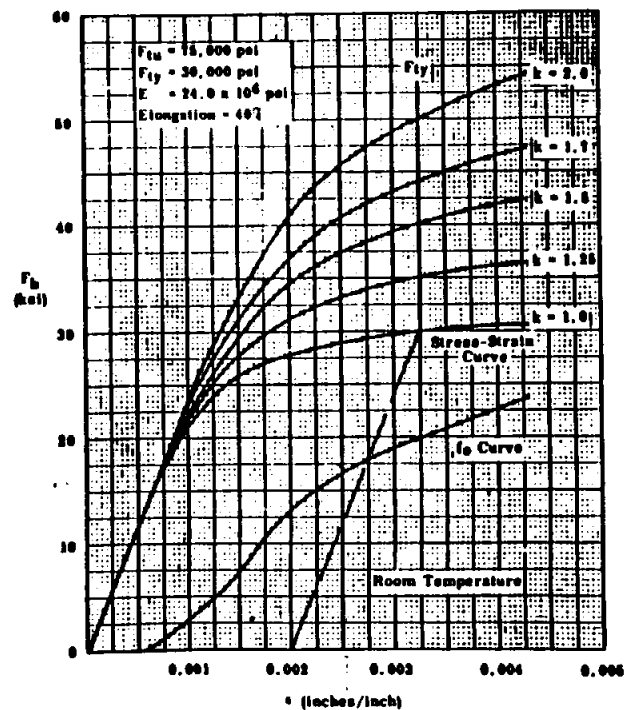
Minimum Plastic Bending Curves
Extra Hard A31 Stainless Steel Sheet-for Longitudinal Compression



Minimum Plastic Bending Curves
Annealed AISI 321 Stainless Steel Sheet

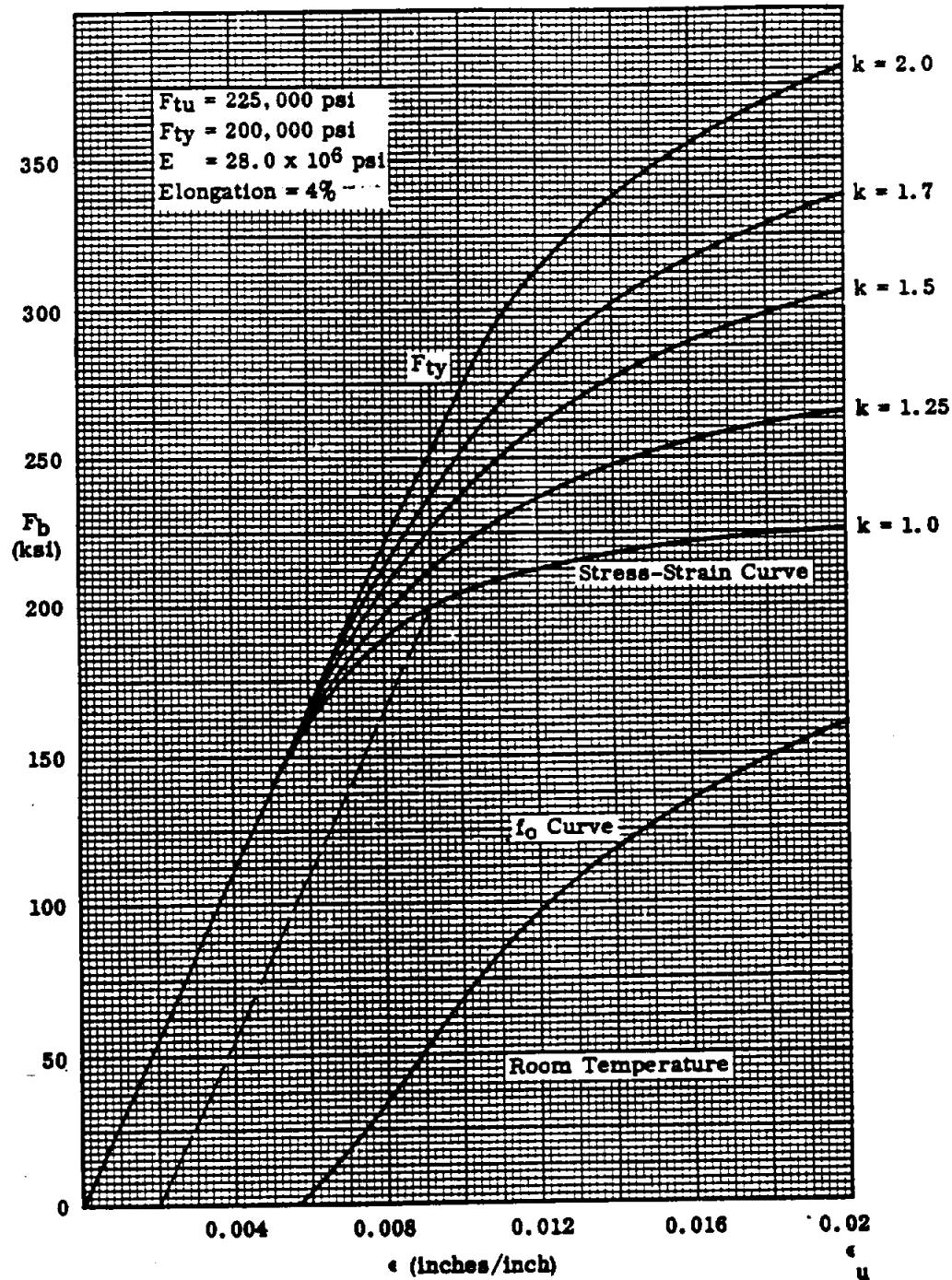


Minimum Plastic Bending Curves
Annealed AISI 321 Stainless Steel Sheet

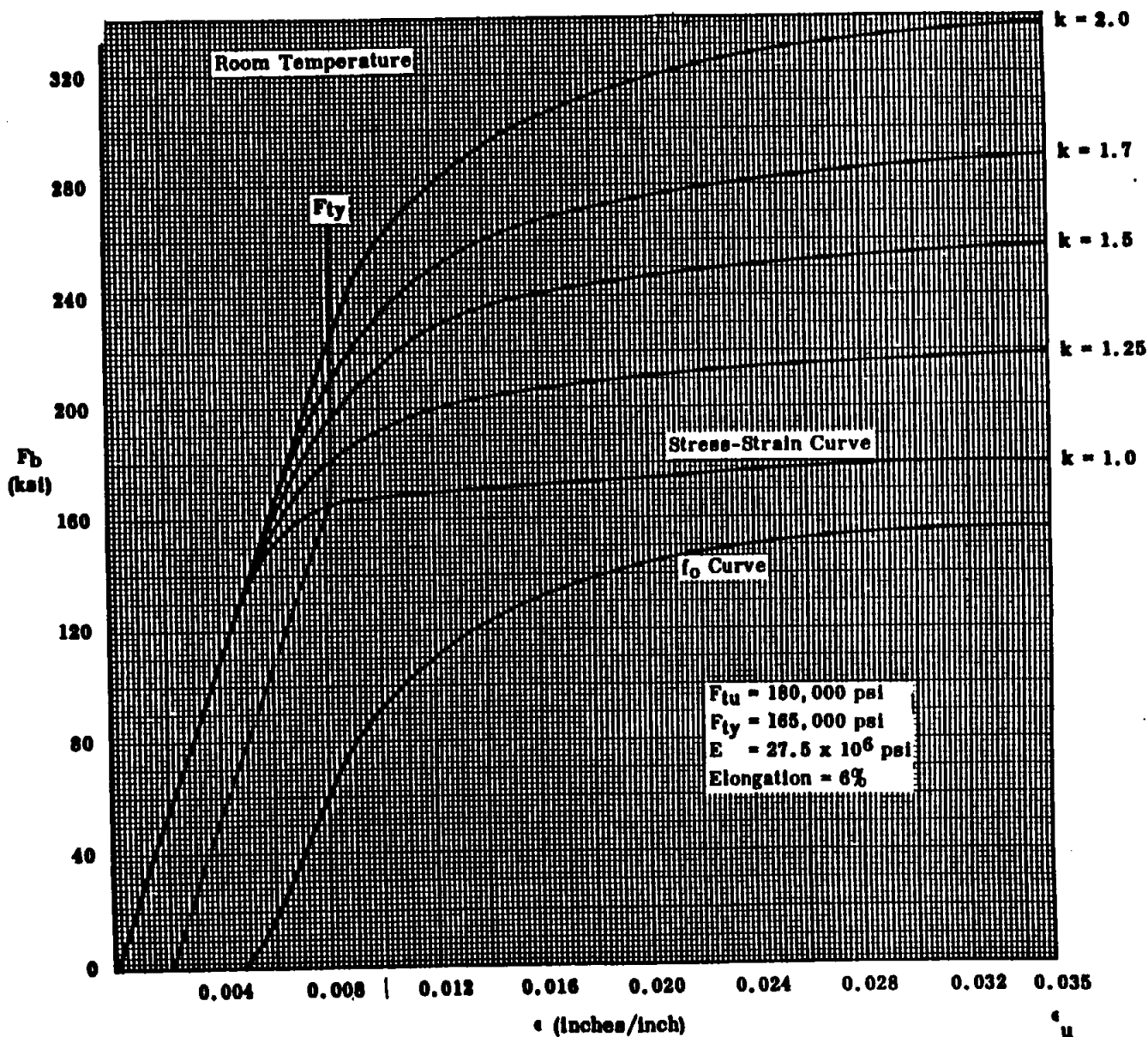


STRUCTURAL ANALYSIS MANUAL
GENERAL DYNAMICS/CONVAIR AND SPACE SYSTEMS DIVISION

Minimum Plastic Bending Curves
for PH 15-7 Mo (RH 950) Stainless Steel Sheet & Strip
Thickness 0.020 to 0.187 Inches

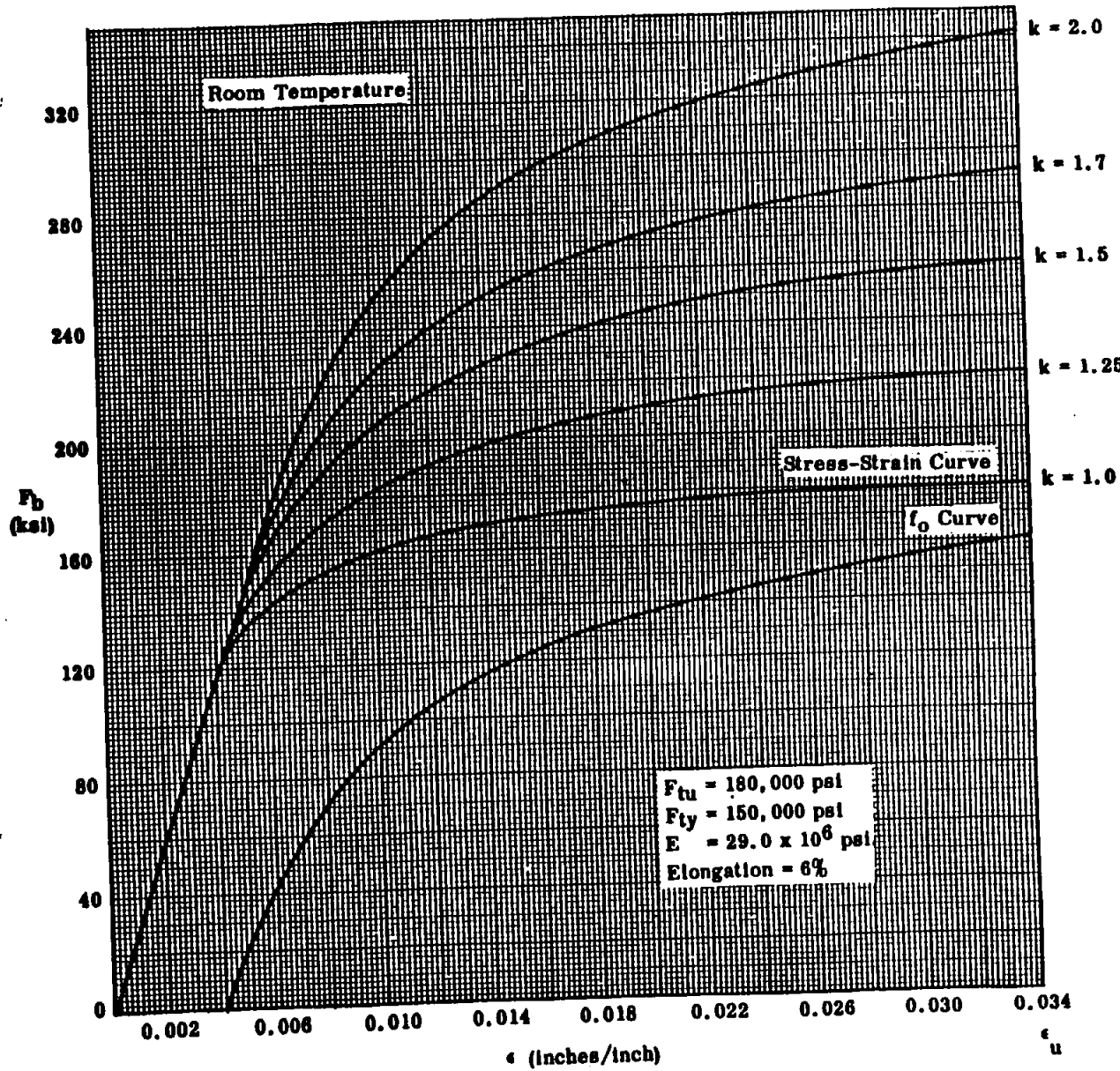


Minimum Plastic Bending Curves
17-4 PH Stainless Steel Heat Treated Bars and Forgings

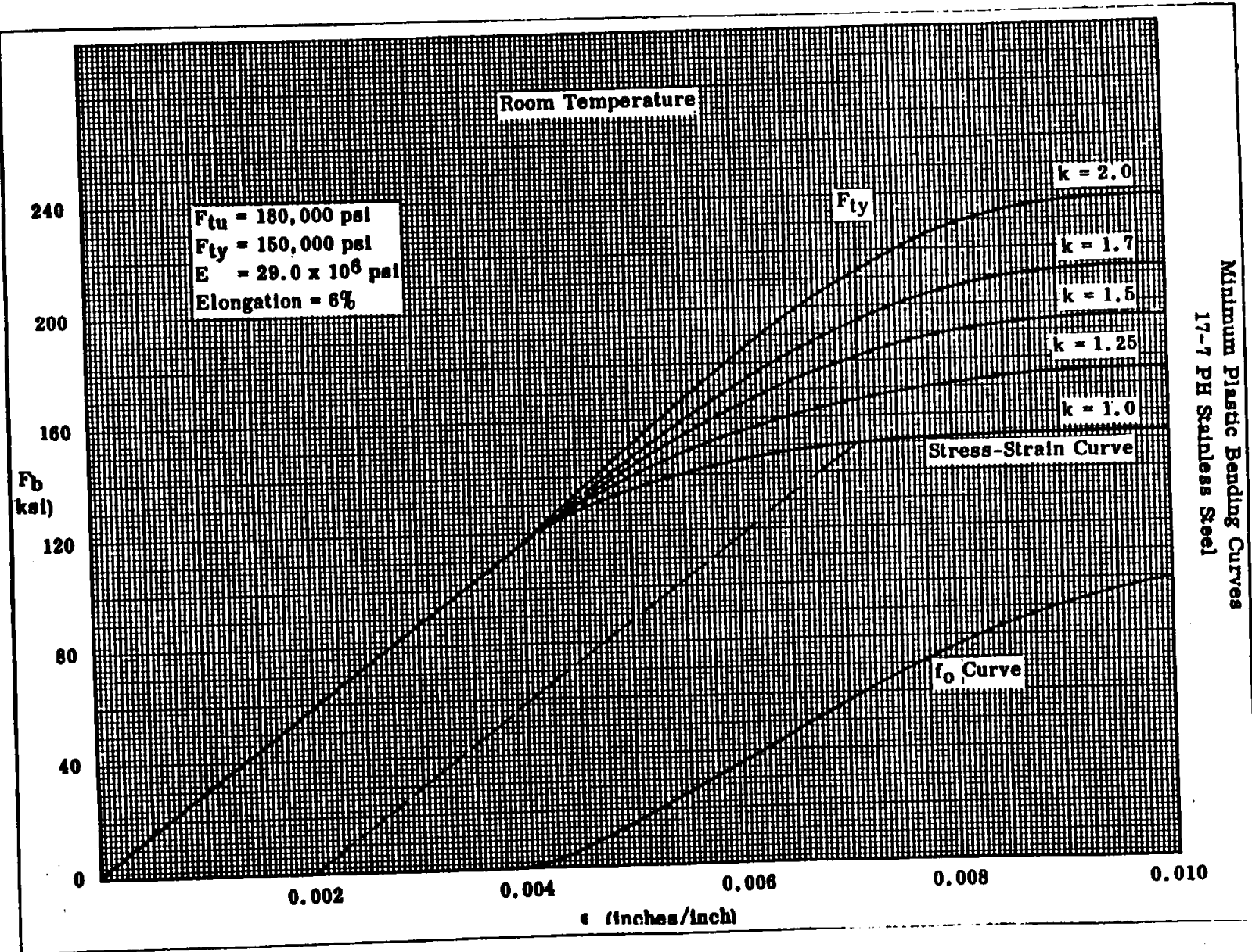


328

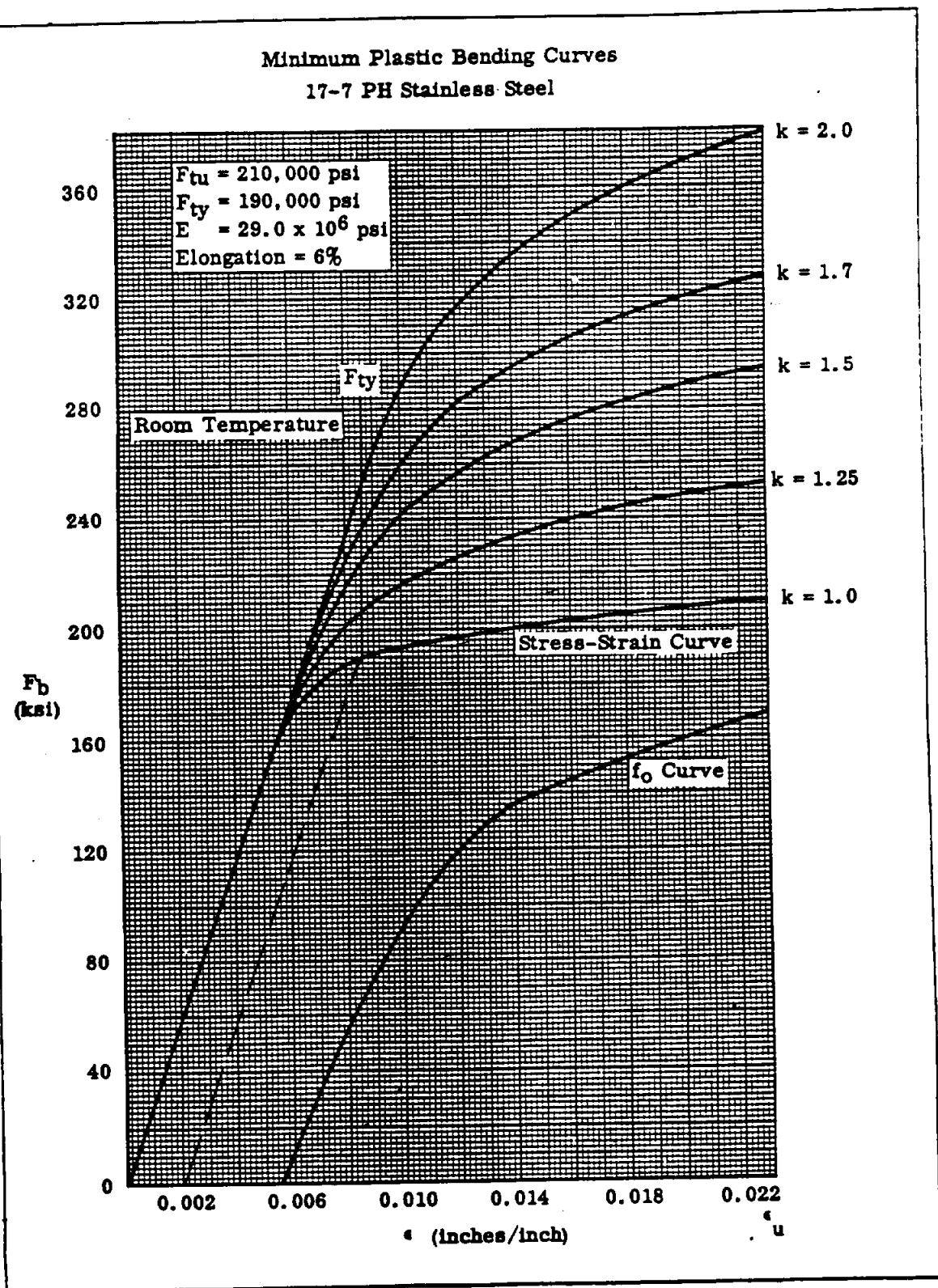
Minimum Plastic Bending Curves
17-7 PH Stainless Steel



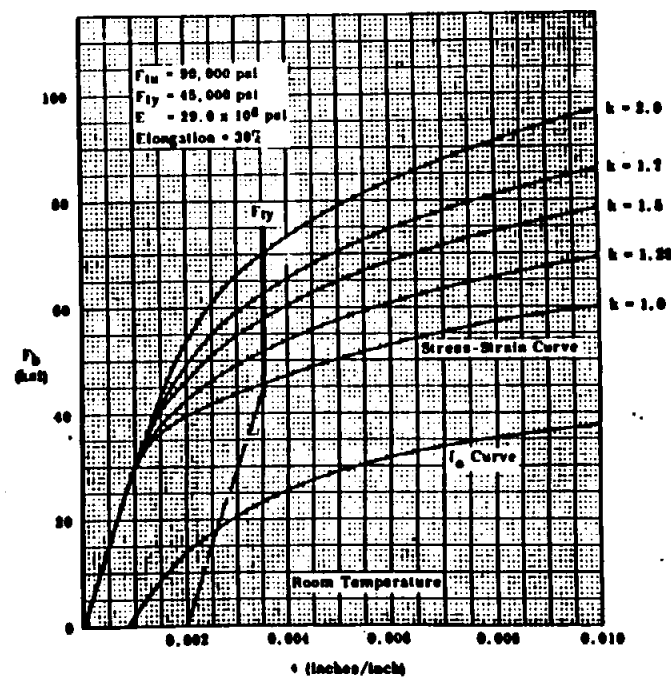
Minimum Plastic Bending Curves
17-7 PH Stainless Steel



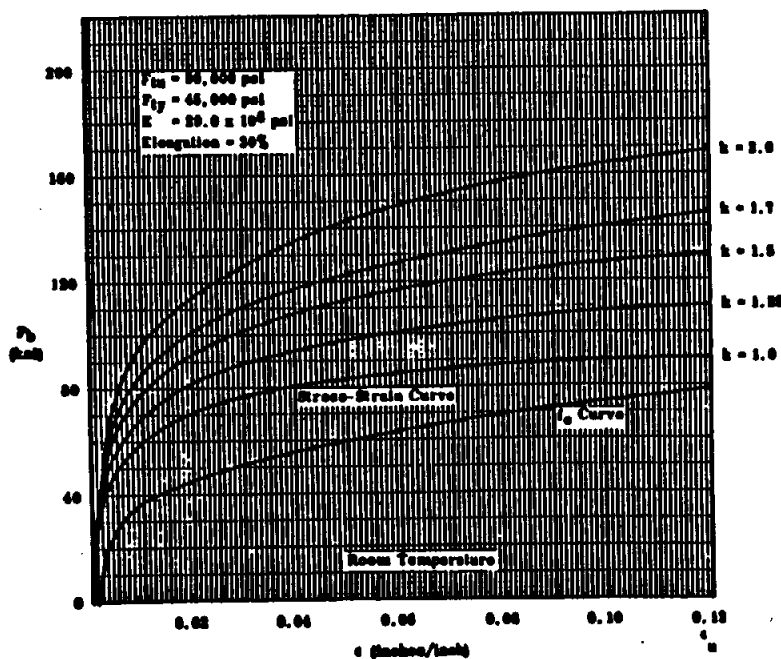
STRUCTURAL ANALYSIS MANUAL
GENERAL DYNAMICS/CONVAIR AND SPACE SYSTEMS DIVISION



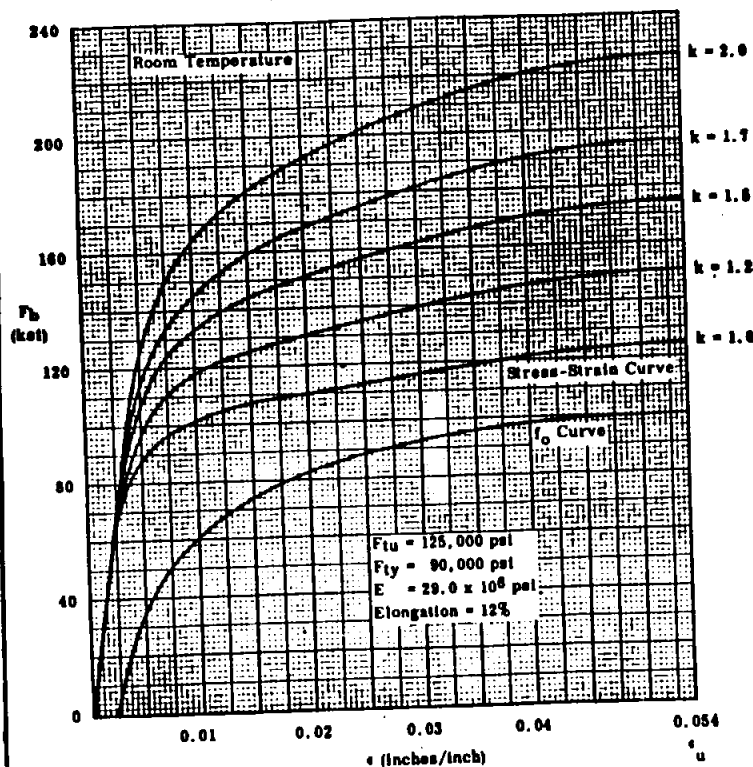
Minimum Plastic Bending Curves for
19-9DL (AMS 5530) & 19-9DX (AMS 5530) Stainless Steel



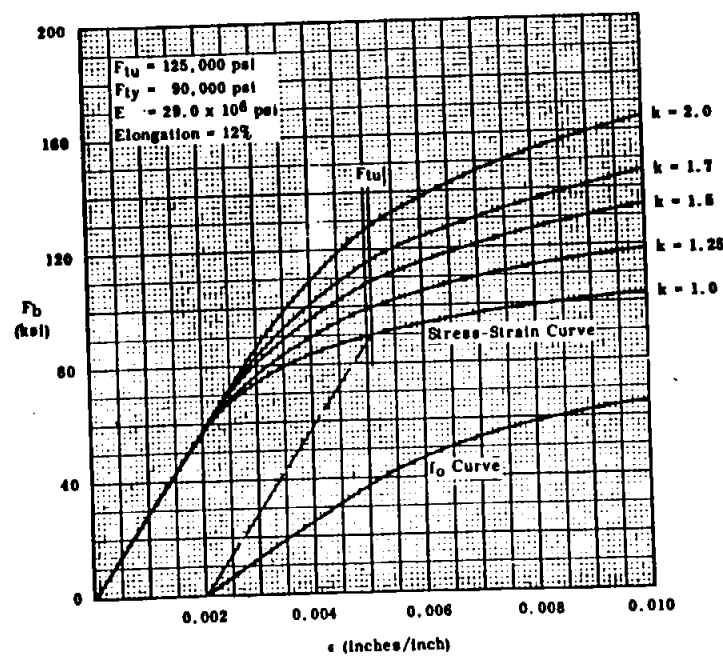
Minimum Plastic Bending Curves
19-9DL (AMS 5530) & 19-9DX (AMS 5530) Stainless Steel



Minimum Plastic Bending Curves
19-9DL (AMS 5527) & 19-9DX (AMS 5539) Stainless Steel

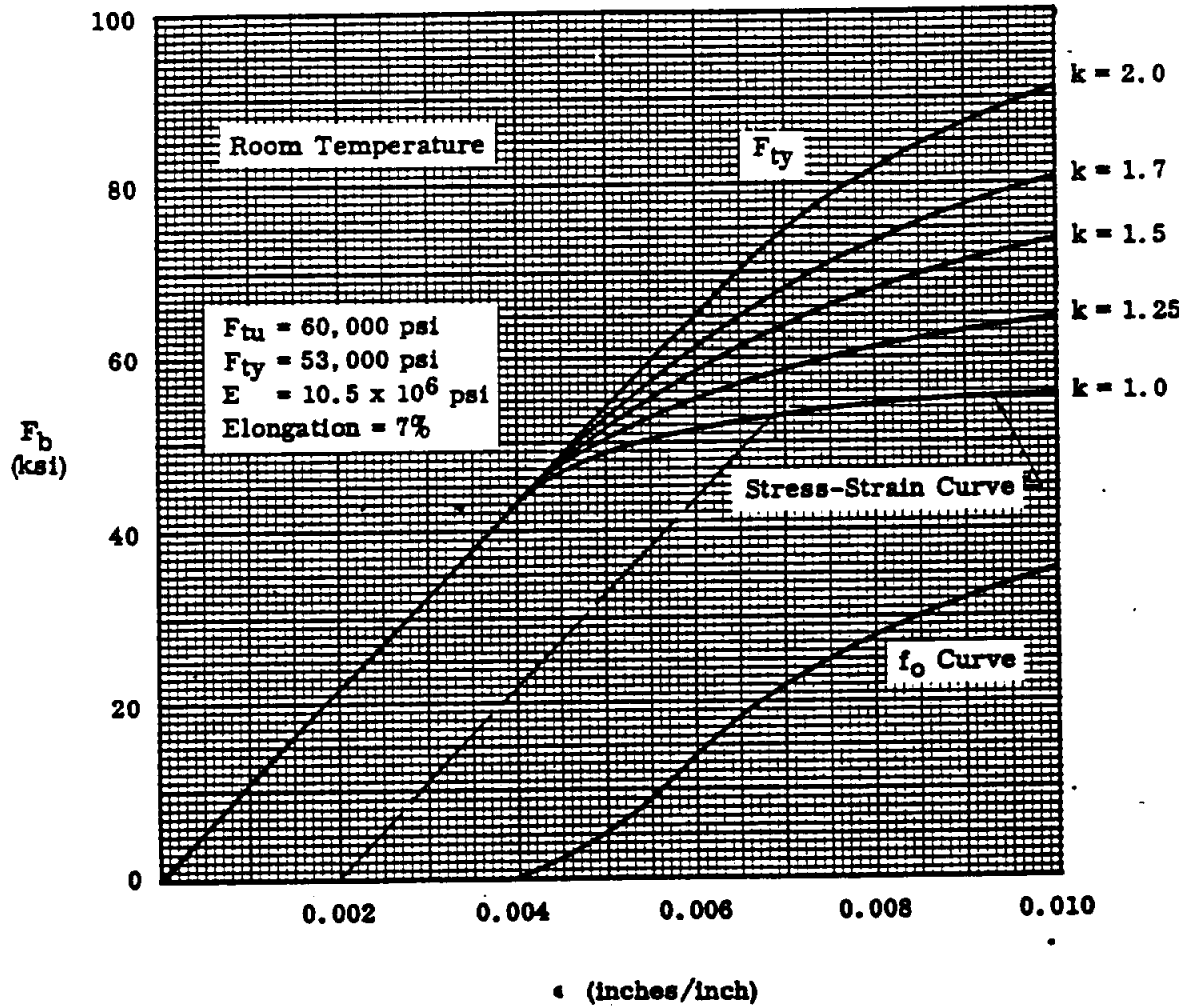


Minimum Plastic Bending Curves
19-9DL (AMS 5527) & 19-9DX (AMS 5539) Stainless Steel

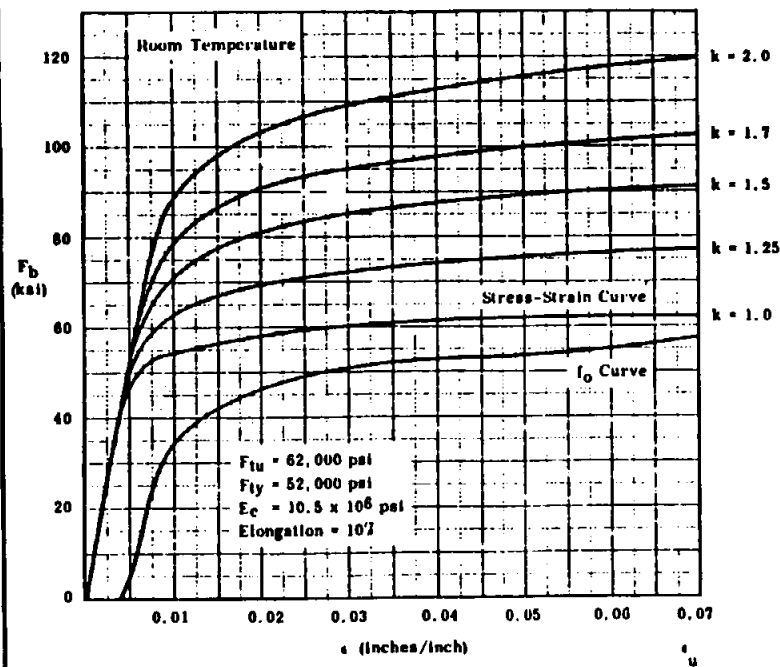


STRUCTURAL ANALYSIS MANUAL
GENERAL DYNAMICS/CONVAIR AND SPACE SYSTEMS DIVISION

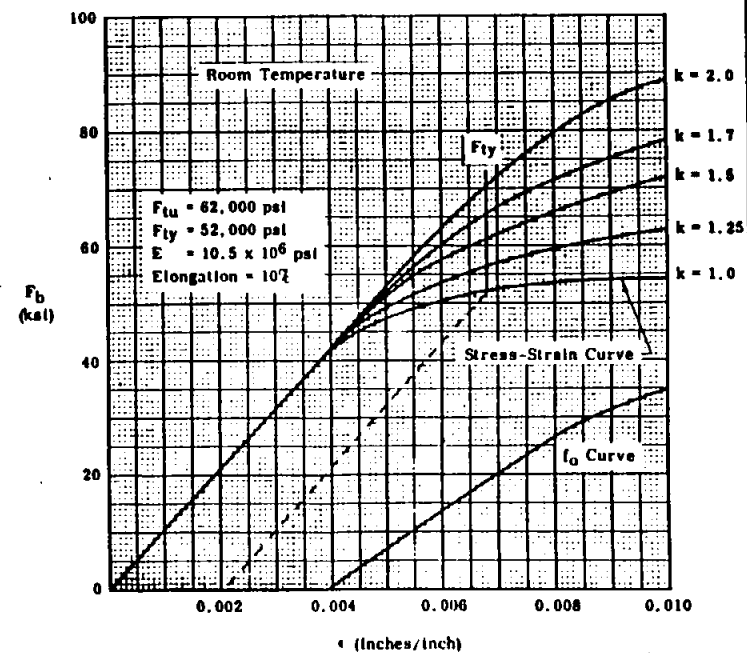
Minimum Plastic Bending Curves
2014-T6 Aluminum Alloy Extrusions. Thickness $\leq .499$ in.



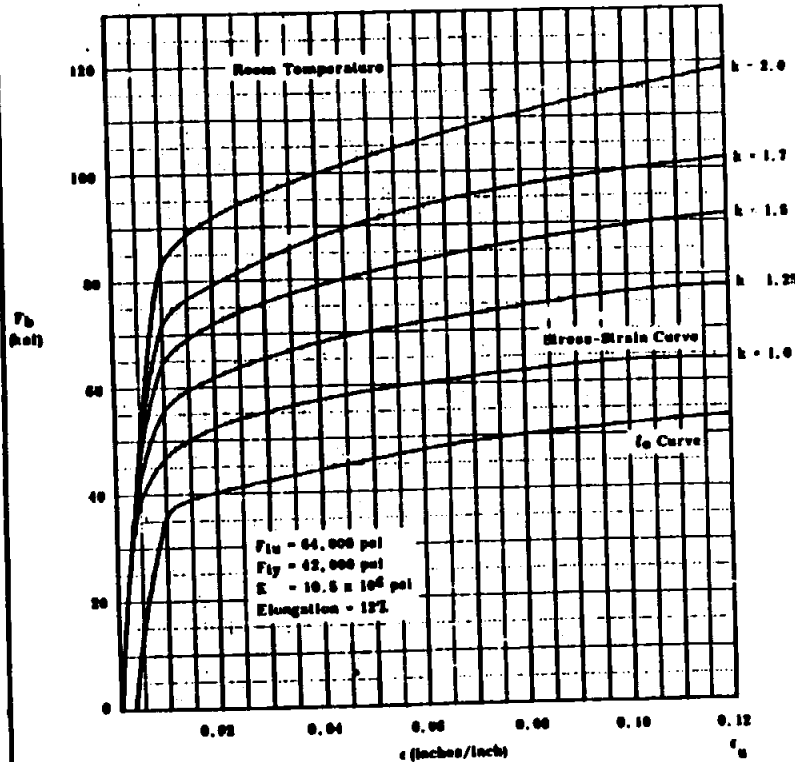
Minimum Plastic Bending Curves
2014-T6 Aluminum Alloy Die Forgings. Thickness ≤ 4 in.



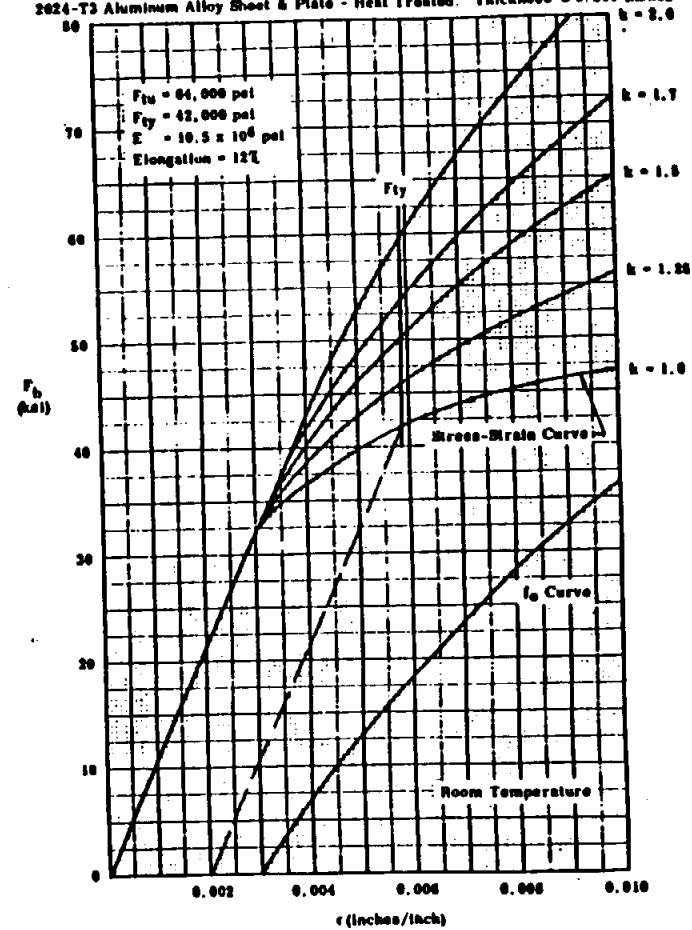
Minimum Plastic Bending Curves
2014-T6 Aluminum Alloy Die Forgings. Thickness ≤ 4 in.



Minimum Plastic Bending Curves
2024-T3 Aluminum Alloy Sheet and Plate - Heat Treated. Thickness ≤ 0.250 inches



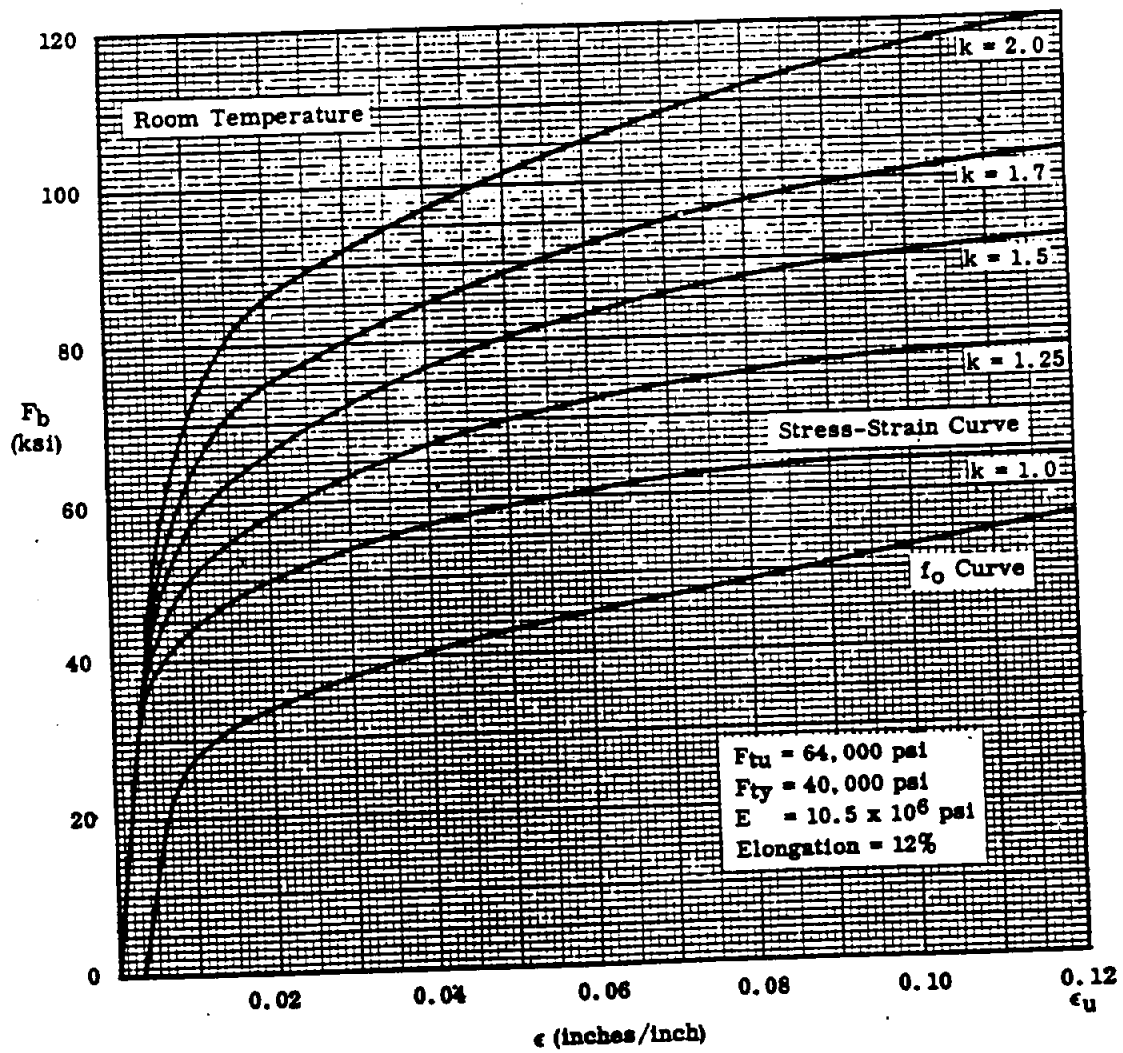
Minimum Plastic Bending Curves
2024-T3 Aluminum Alloy Sheet & Plate - Heat Treated. Thickness ≤ 0.250 inches



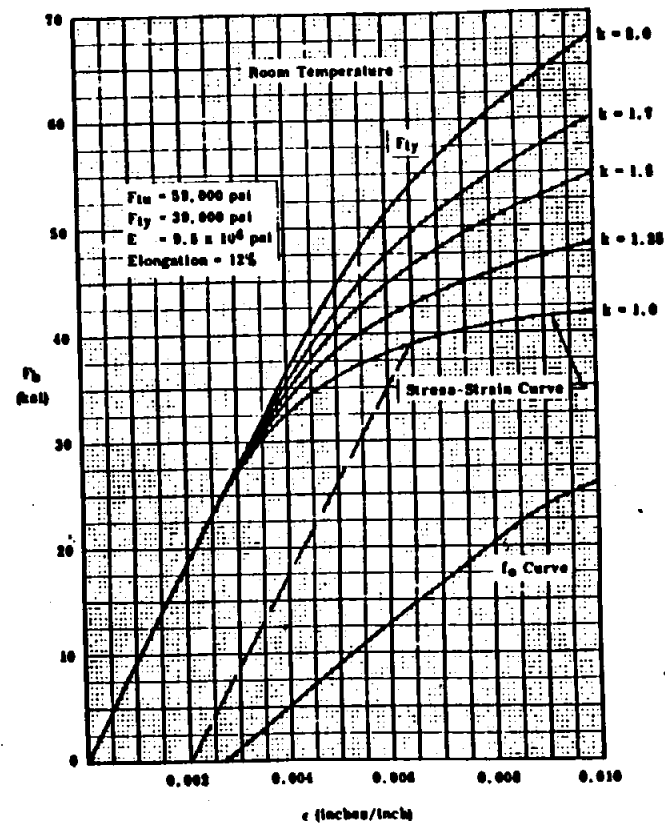
STRUCTURAL ANALYSIS MANUAL

GENERAL DYNAMICS/CONVAIR AND SPACE SYSTEMS DIVISION

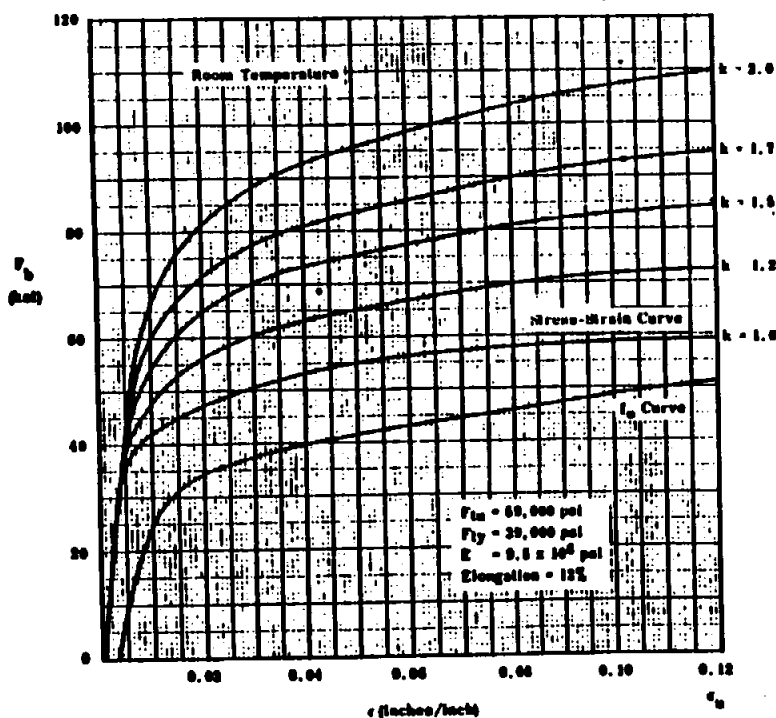
Minimum Plastic Bending Curves
for 2024-T3 & T4 Aluminum Alloy - Heat Treated - Sheet & Plate. Thickness ≤ 0.50 Inches



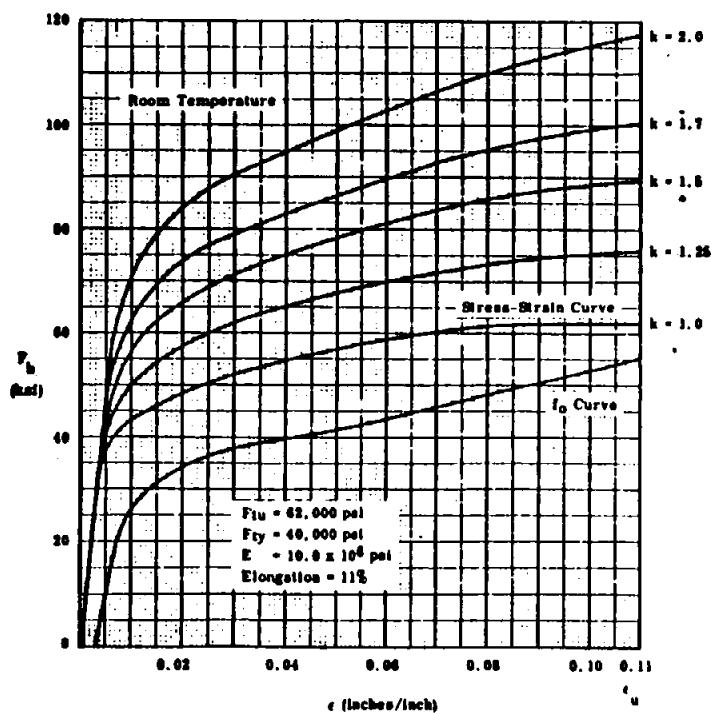
Minimum Plastic Bending Curves
2024-T3 Aluminum Alloy Clad Sheet & Plate - Heat Treated.
Thickness 0.010 to 0.063 in.



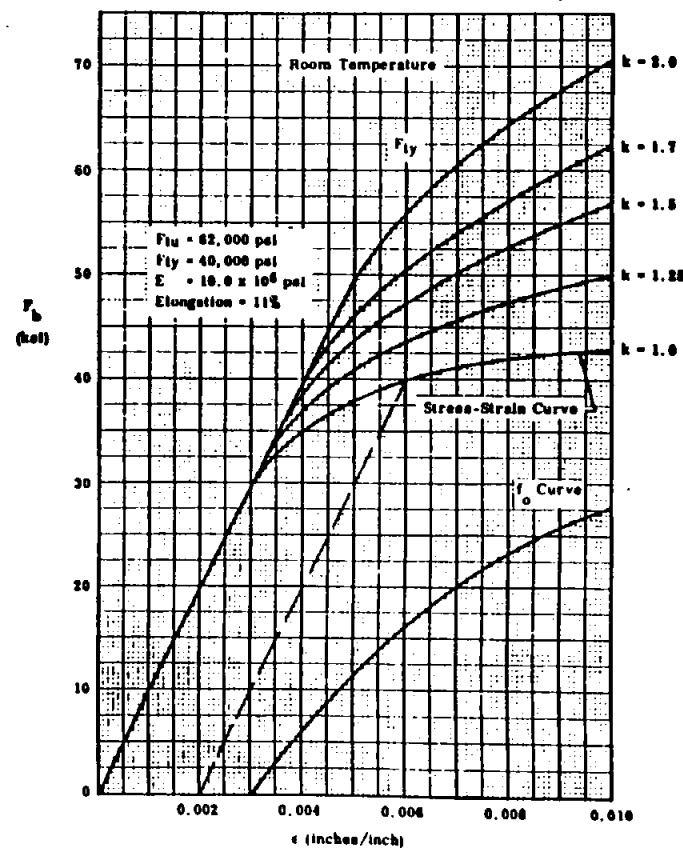
Minimum Plastic Bending Curves
2024-T3 Aluminum Alloy Clad Sheet and Plate-Heat Treated.
Thickness 0.010 to 0.063 in.



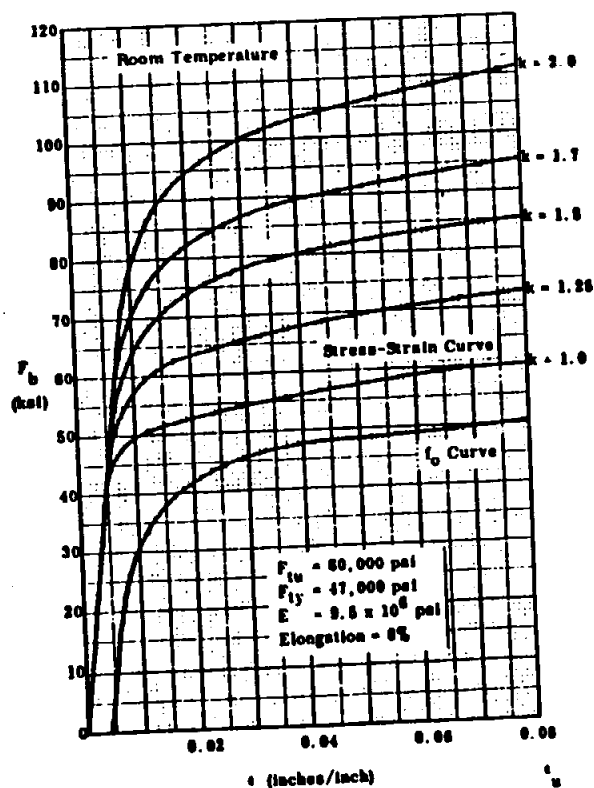
Minimum Plastic Bending Curves
2024-T4 Aluminum Alloy Clad Sheet and Plate-Heat Treated
Thickness 0.25 to 0.50 in.



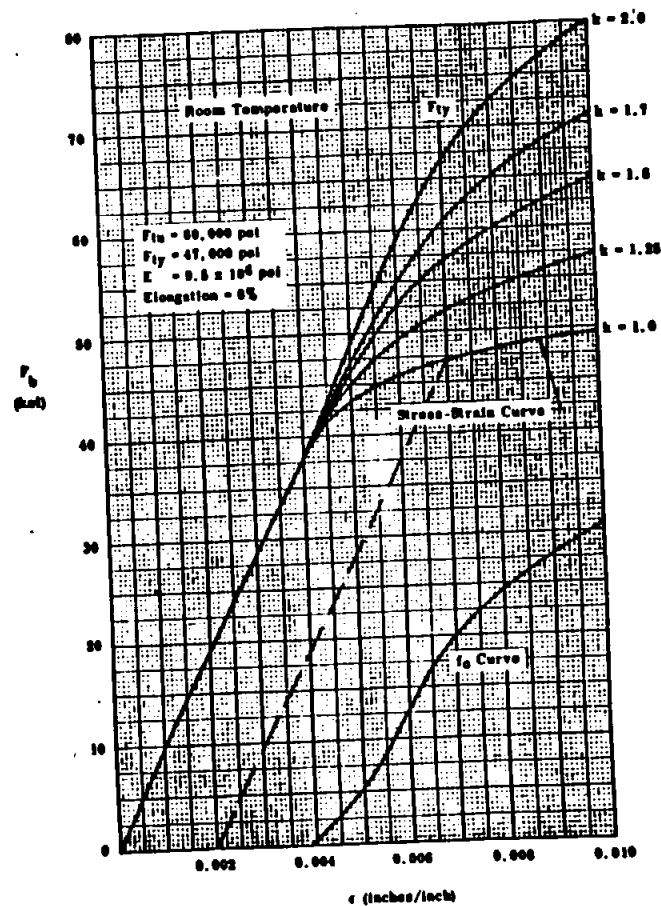
Minimum Plastic Bending Curve
2024-T4 Aluminum Alloy Clad Sheet & Plate - Heat Treated
Thickness 0.25 to 0.50 in.



Minimum Plastic Bending Curves
2024-T6 Aluminum Alloy Clad Sheet - Heat Treated and Aged
Thickness < 0.064 in.

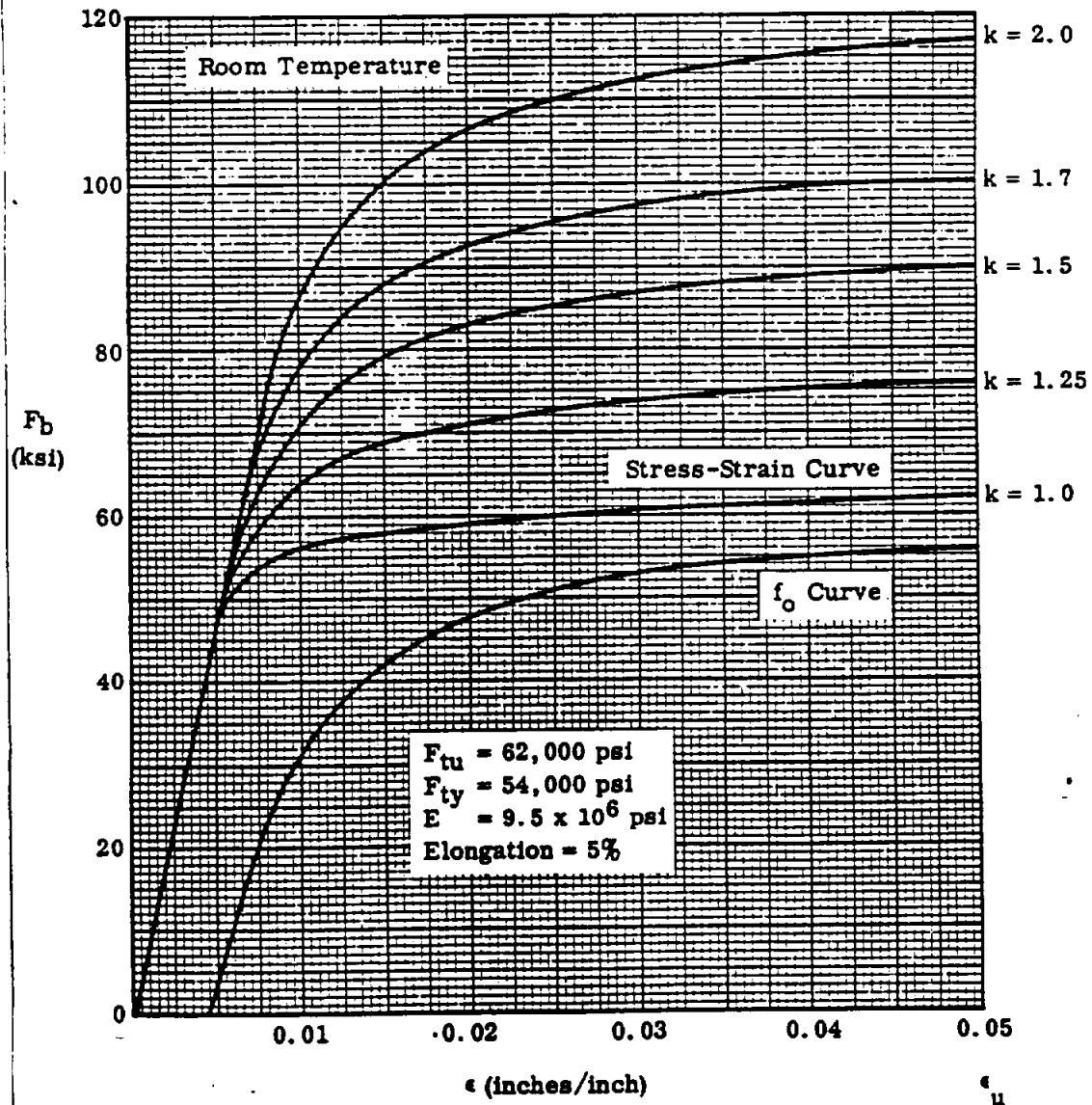


Minimum Plastic Bending Curves
2024-T6 Aluminum Alloy Clad Sheet - Heat Treated & Aged. Thickness < 0.064 inches

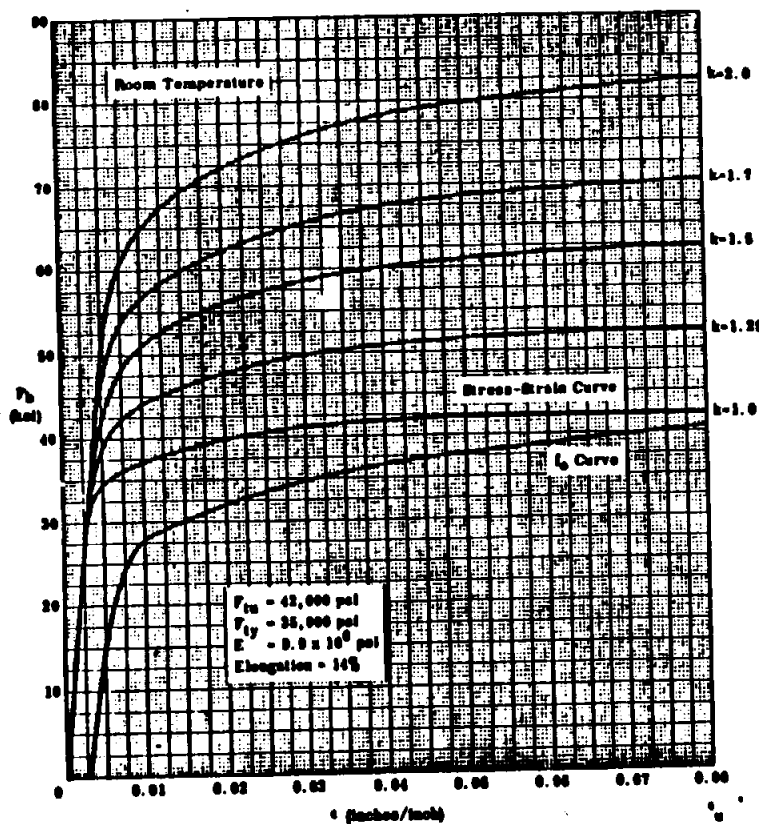


STRUCTURAL ANALYSIS MANUAL
GENERAL DYNAMICS/CONVAIR AND SPACE SYSTEMS DIVISION

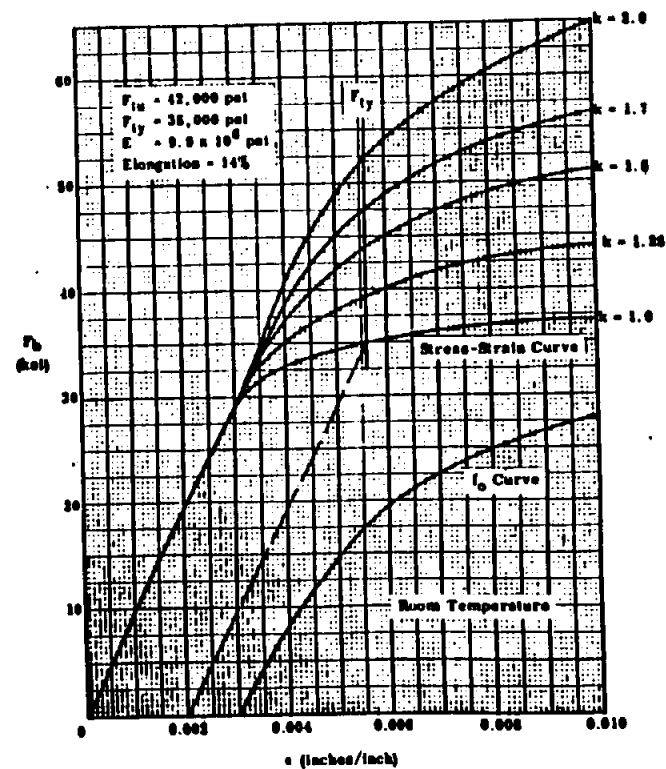
Minimum Plastic Bending Curves
2024-T81 Aluminum Alloy Clad Sheet - Heat Treat, Cold Worked and Aged
Thickness < 0.064 in.



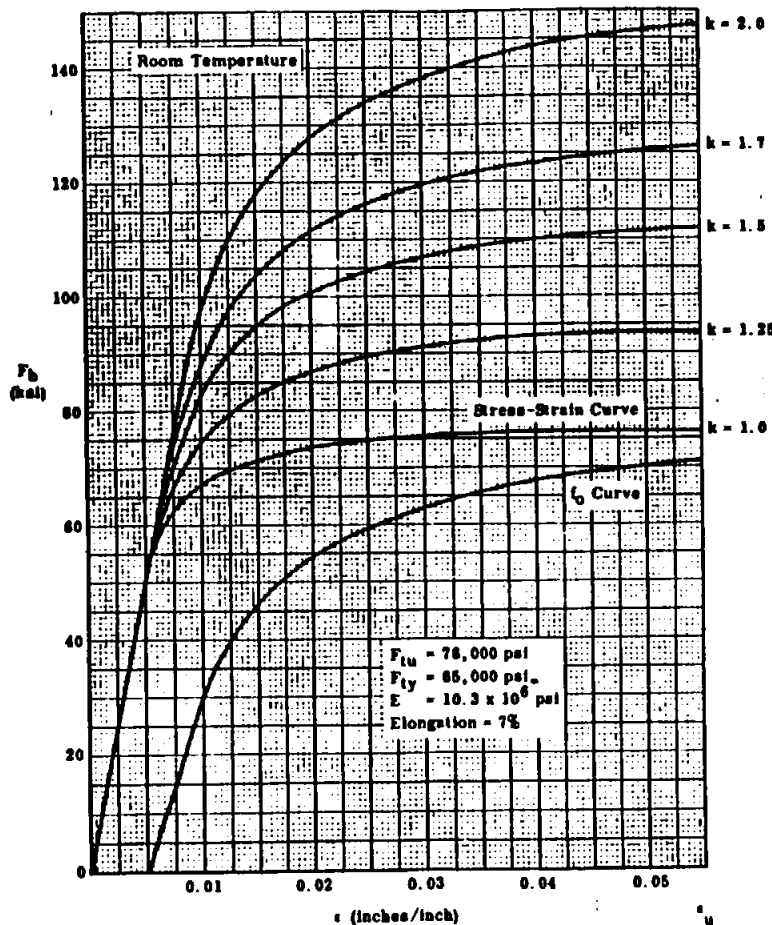
Minimum Plastic Bending Curves
6061-T6 Aluminum Alloy Sheet - Heat Treated & Aged
Thickness ± 0.030 in.



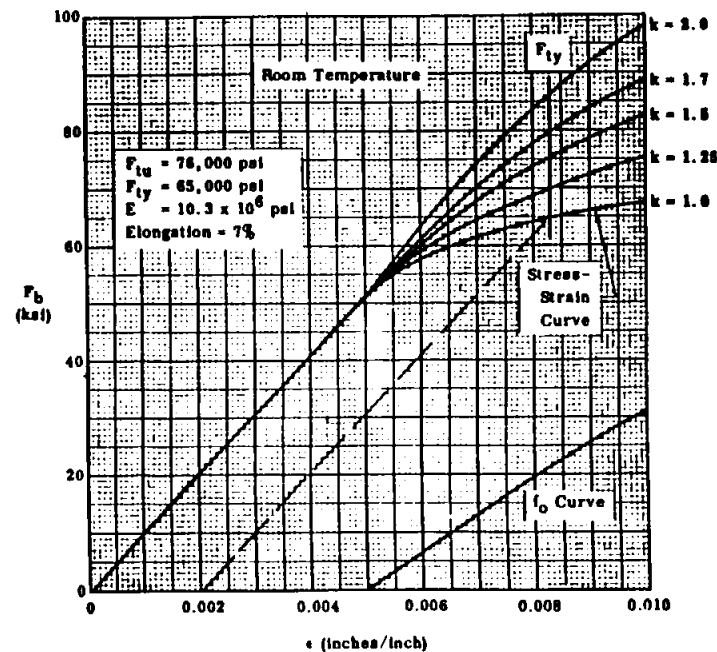
Minimum Plastic Bending Curves
6061-T6 Aluminum Alloy Sheet Heat Treated & Aged. Thickness ± 0.030 in.



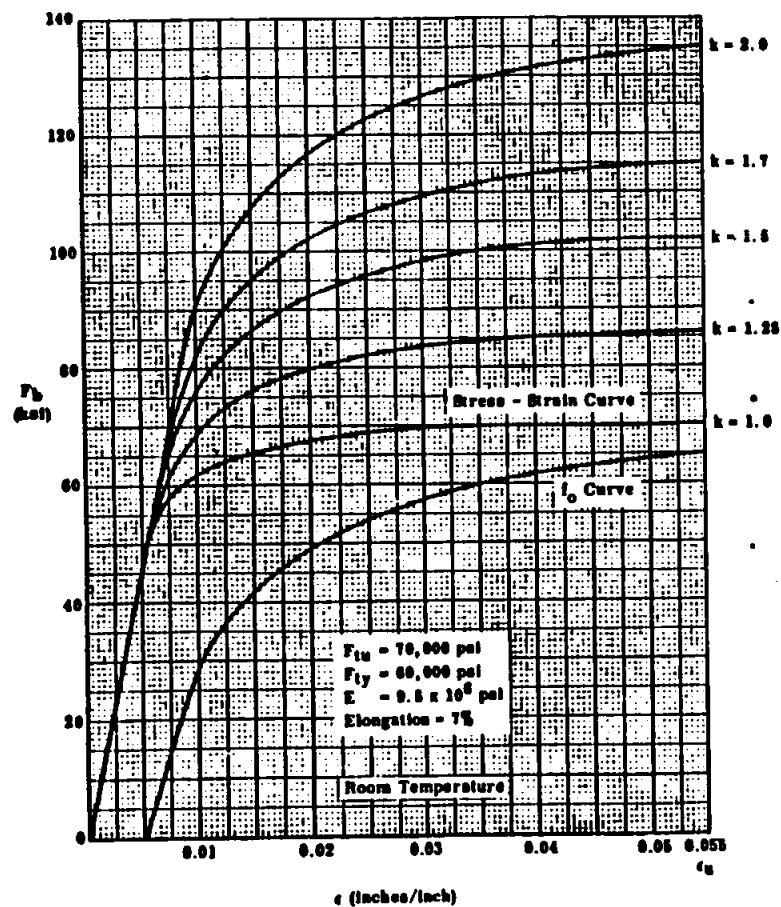
Minimum Plastic Bending Curves
7075-T6 Aluminum Alloy Bare Sheet & Plate
Thickness $\leq .039$ in.



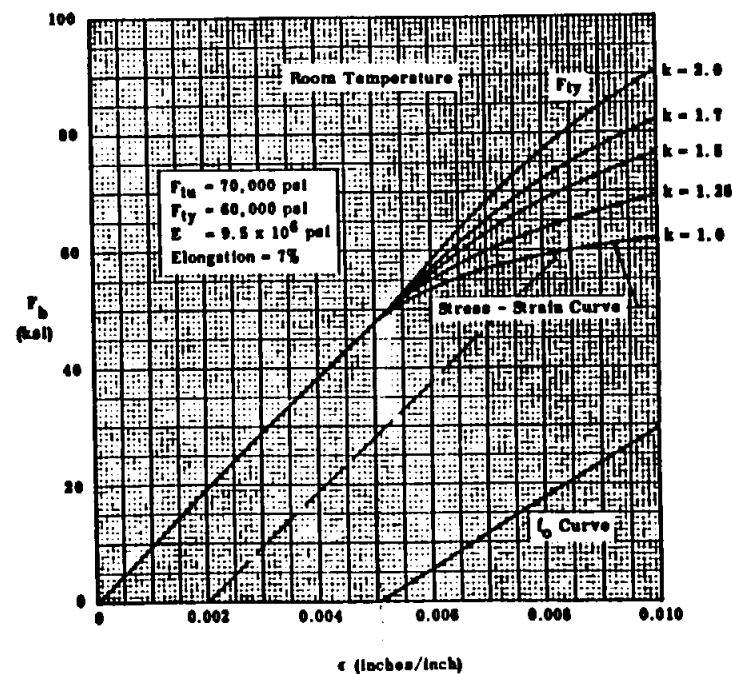
Minimum Plastic Bending Curves
7075-T6 Aluminum Alloy Bare Sheet & Plate. Thickness $\leq .039$ in.



Minimum Plastic Bending Curves
7075-T6 Aluminum Alloy Clad Sheet & Plate
Thickness ≤ 0.20 in.

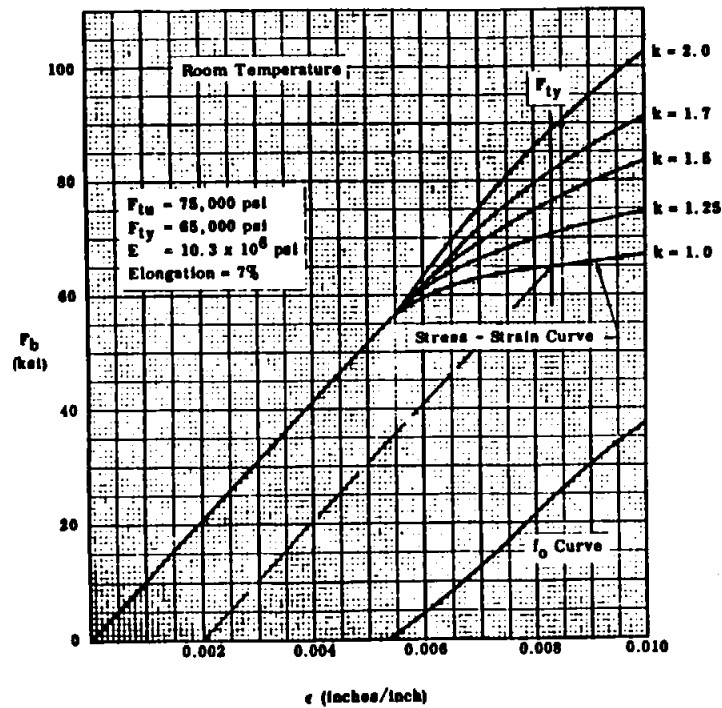


Minimum Plastic Bending Curves
7075-T6 Aluminum Alloy Clad Sheet & Plate, Thickness ≤ 0.030 in.



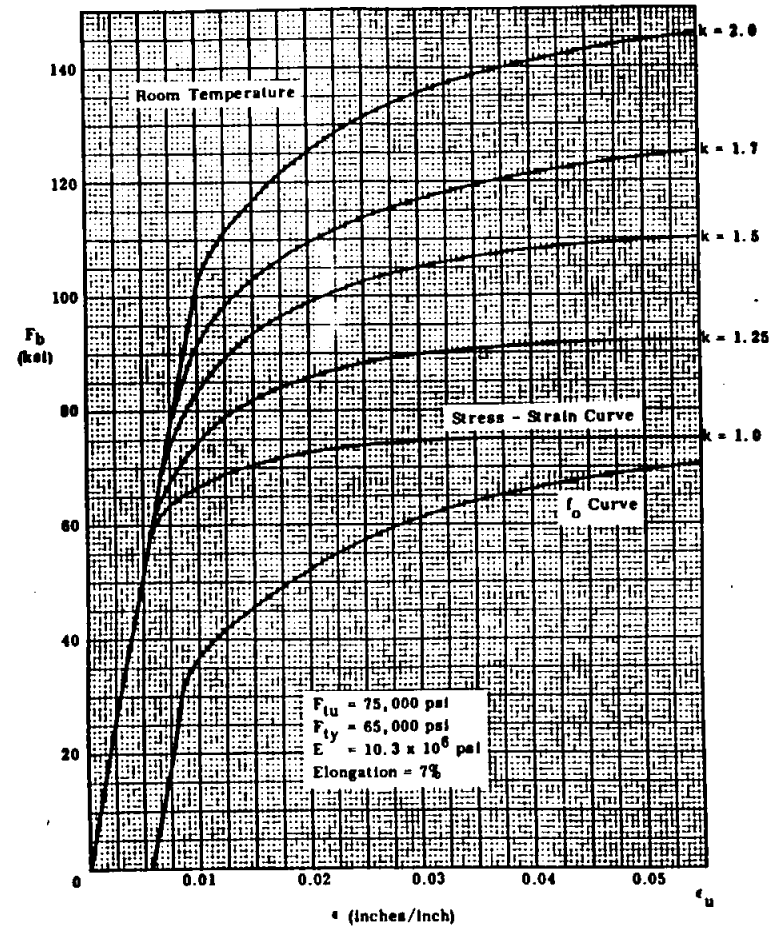
341

Minimum Plastic Bending Curves
7075-T6 Aluminum Alloy Extrusions. Thickness ≤ 0.25 in.



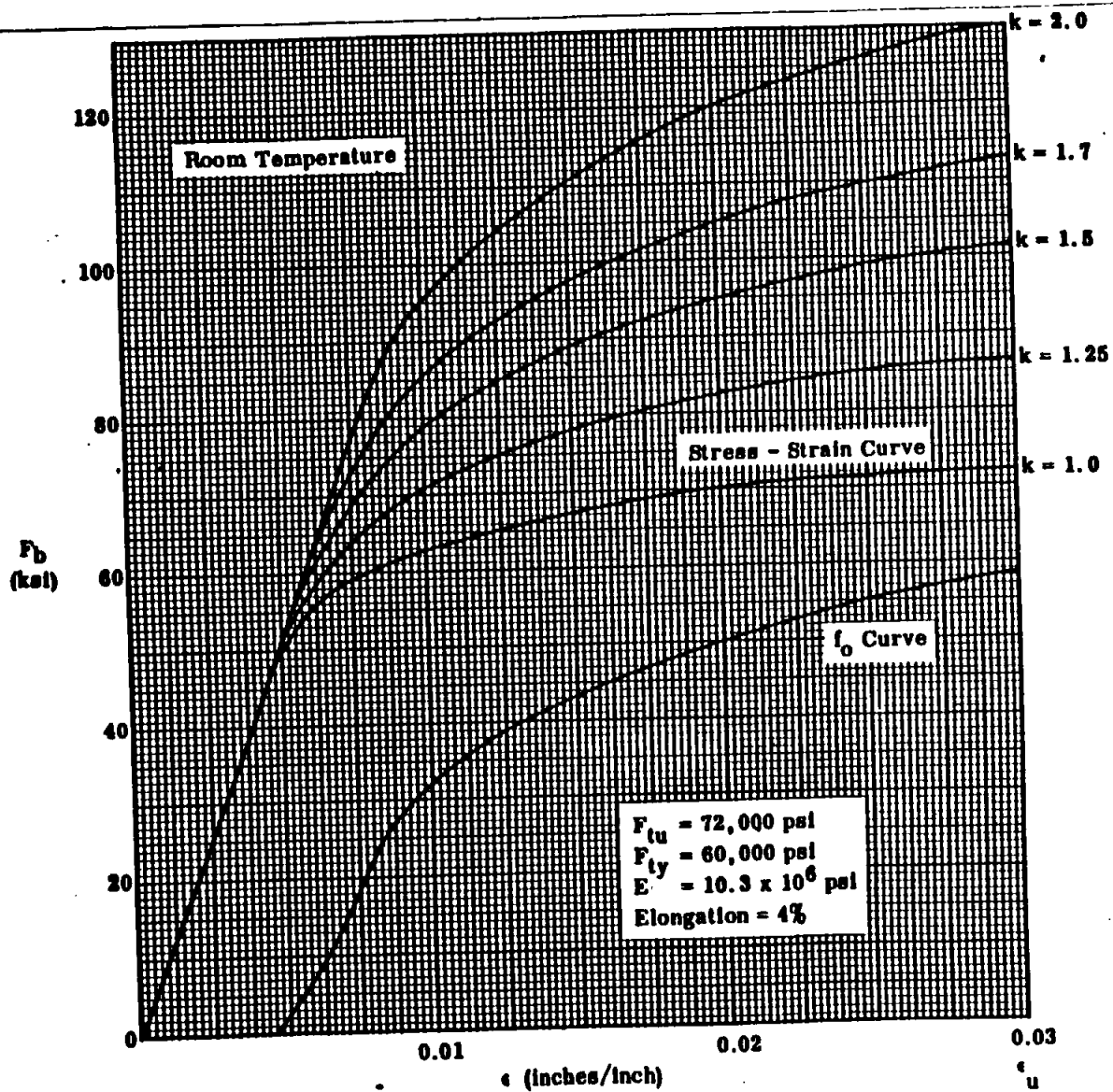
page 17.7.43

Minimum Plastic Bending Curves
7075-T6 Aluminum Alloy Extrusions. Thickness ≤ 0.25 in.



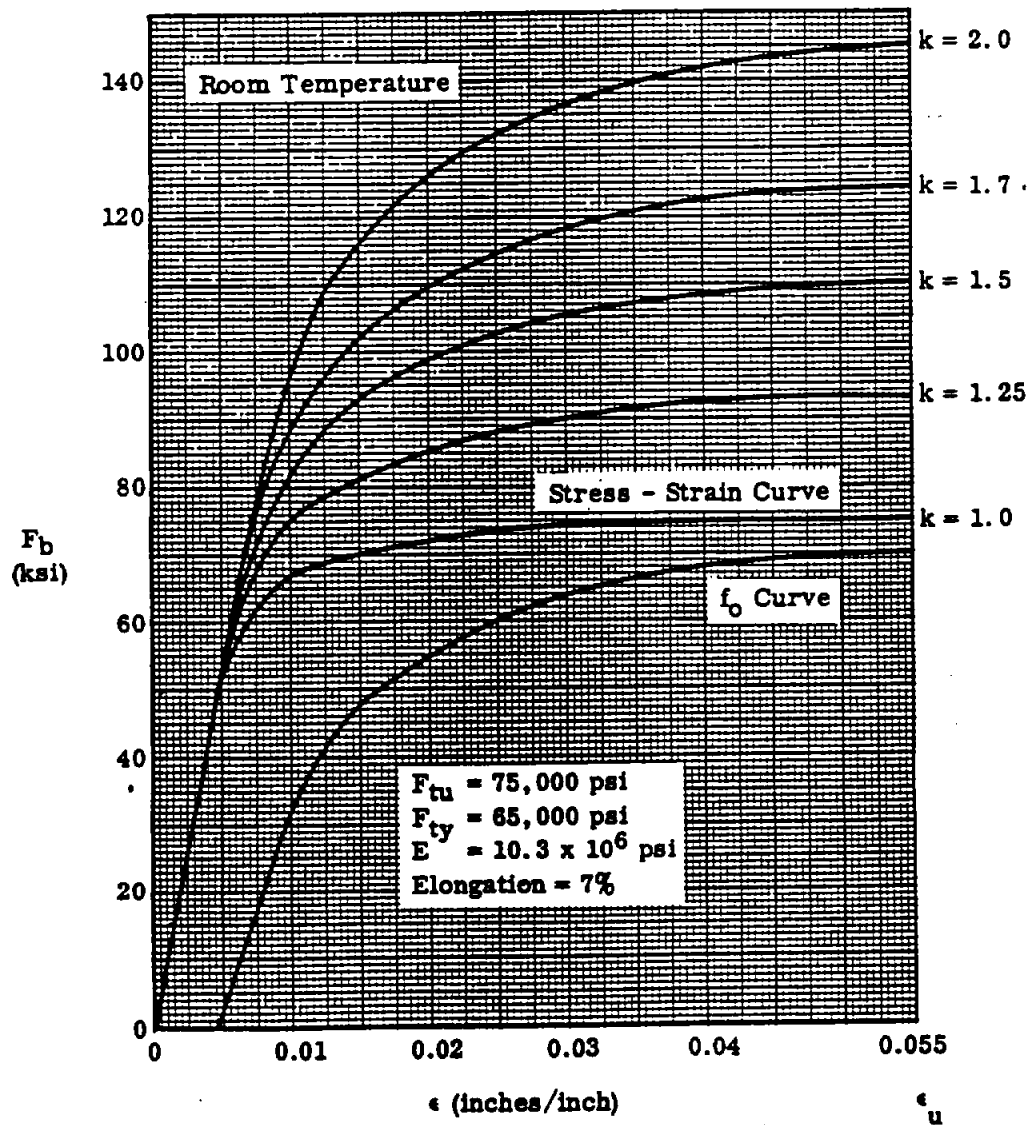
STRUCTURAL ANALYSIS MANUAL
GENERAL DYNAMICS/CONVAIR AND SPACE SYSTEMS DIVISION

Minimum Plastic Bending Curves
7075-T6 Aluminum Alloy Hand Forgings Area $\leq 16 \text{ in.}^2$



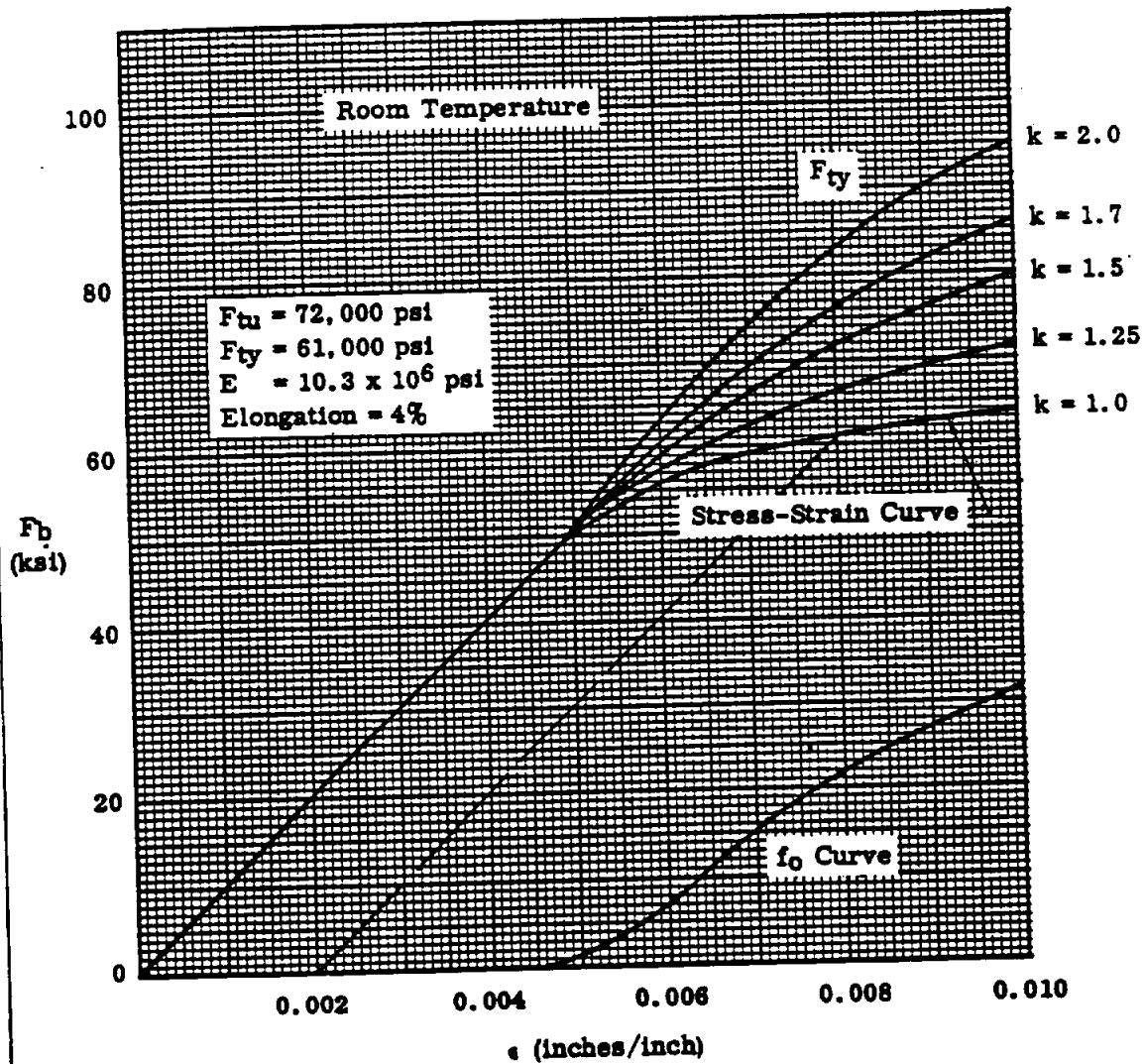
STRUCTURAL ANALYSIS MANUAL
GENERAL DYNAMICS/CONVAIR AND SPACE SYSTEMS DIVISION

Minimum Plastic Bending Curves
7075-T6 Aluminum Alloy Die Forgings. Thickness ≤ 2 in.

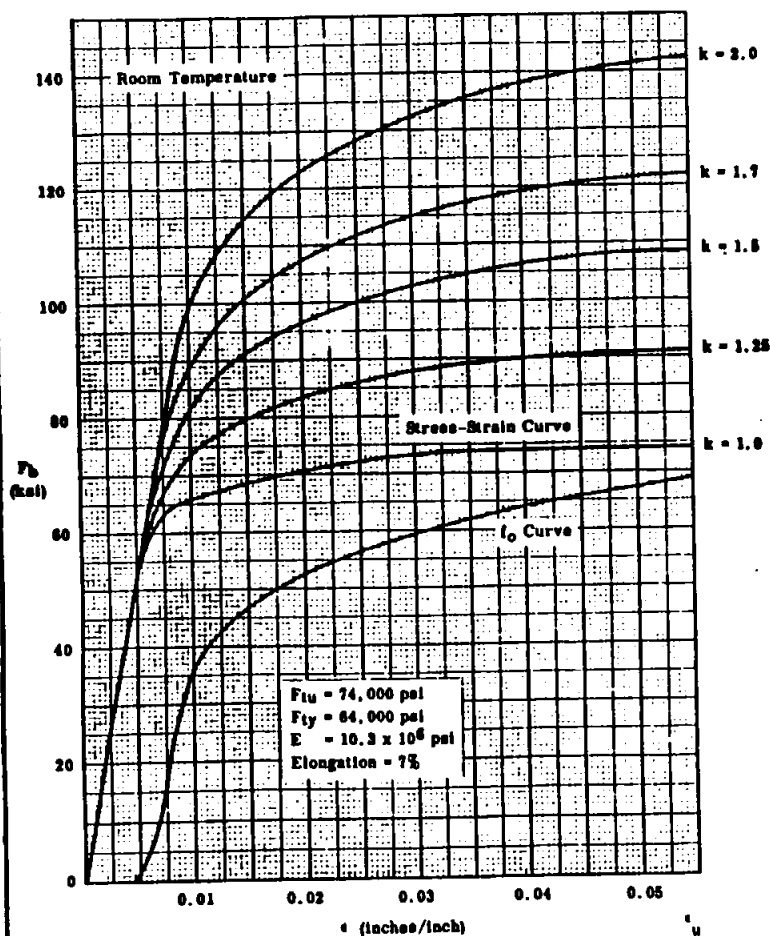


STRUCTURAL ANALYSIS MANUAL
GENERAL DYNAMICS/CONVAIR AND SPACE SYSTEMS DIVISION

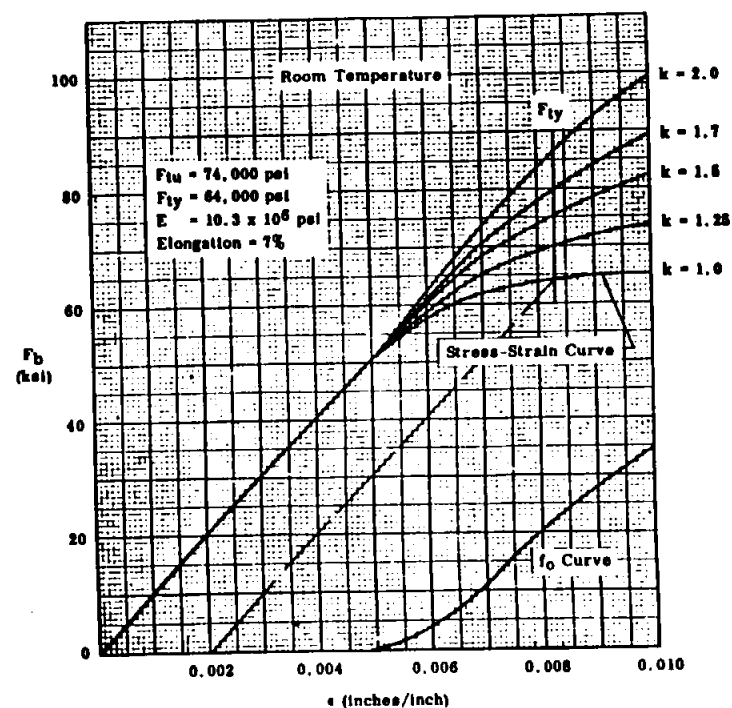
Minimum Plastic Bending Curves
7079-T6 Aluminum Alloy Die Forgings. (Transverse)
Thickness ≤ 6.0 in.



Minimum Plastic Bending Curves
7079-T6 Aluminum Alloy Die Forgings (Longitudinal)
Thickness ≤ 6.0 in.

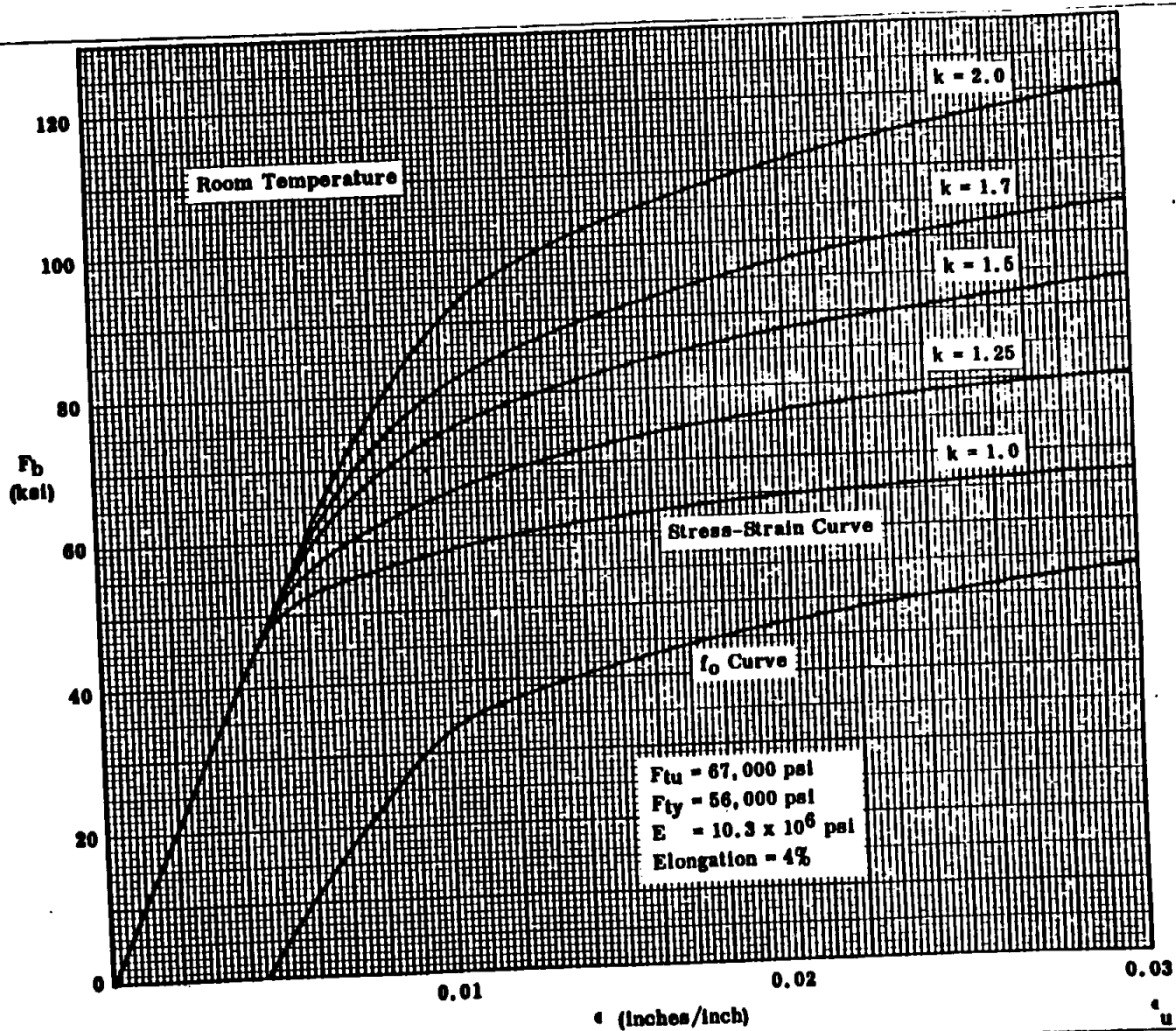


Minimum Plastic Bending Curves
7079-T6 Aluminum Alloy Die Forgings (Longitudinal)
Thickness ≤ 6.0 in.

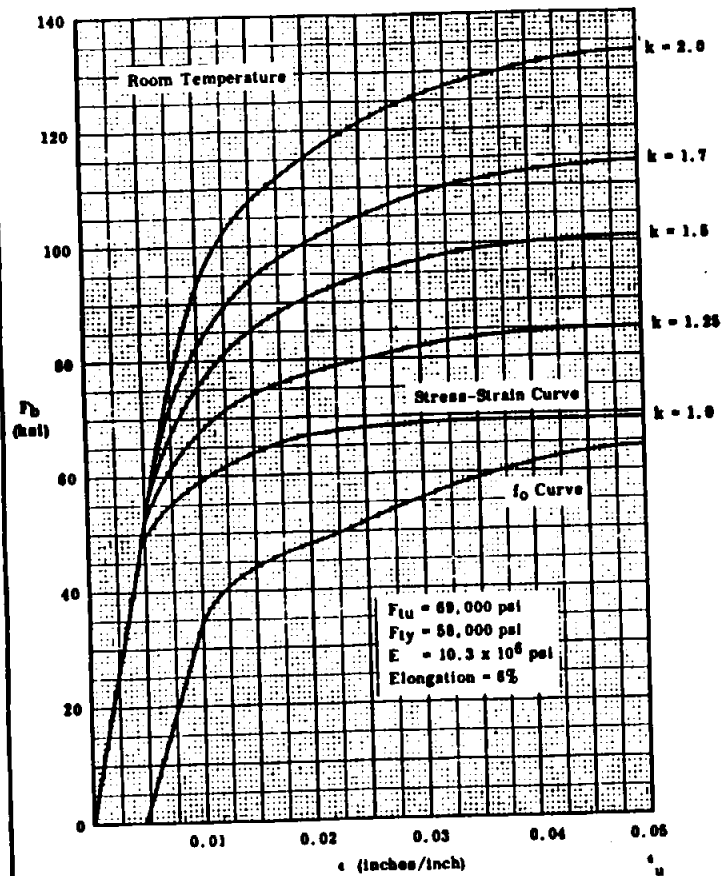


STRUCTURAL ANALYSIS MANUAL
GENERAL DYNAMICS/CONVAIR AND SPACE SYSTEMS DIVISION

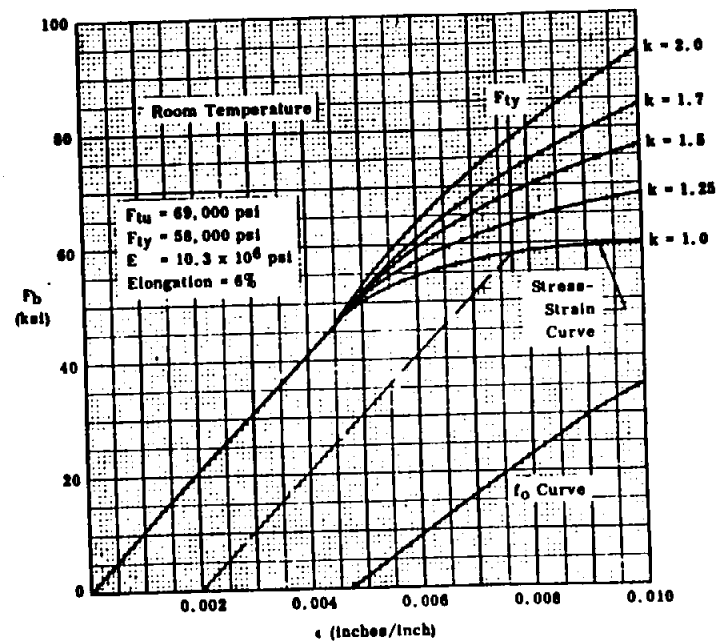
Minimum Plastic Bending Curves
7079-T6 Aluminum Alloy Hand Forgings (Short Transverse)
Thickness ≤ 6.0 in.



Minimum Plastic Bending Curves
7079-T6 Aluminum Alloy Hand Forgings (Long Transverse)
Thickness ≤ 6 in.

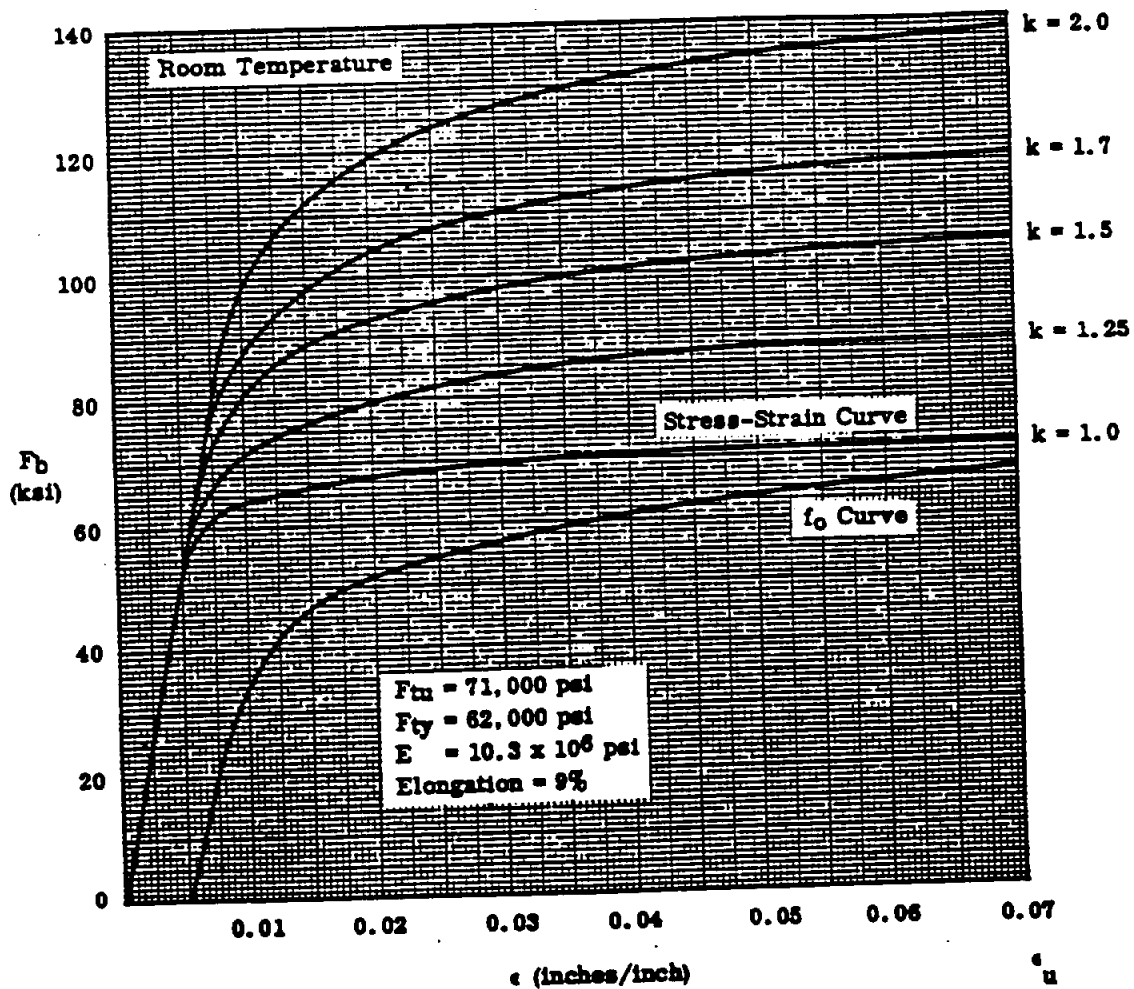


Minimum Plastic Bending Curves
7079-T6 Aluminum Alloy Hand Forgings (Long Transverse)
Thickness ≤ 6 in.

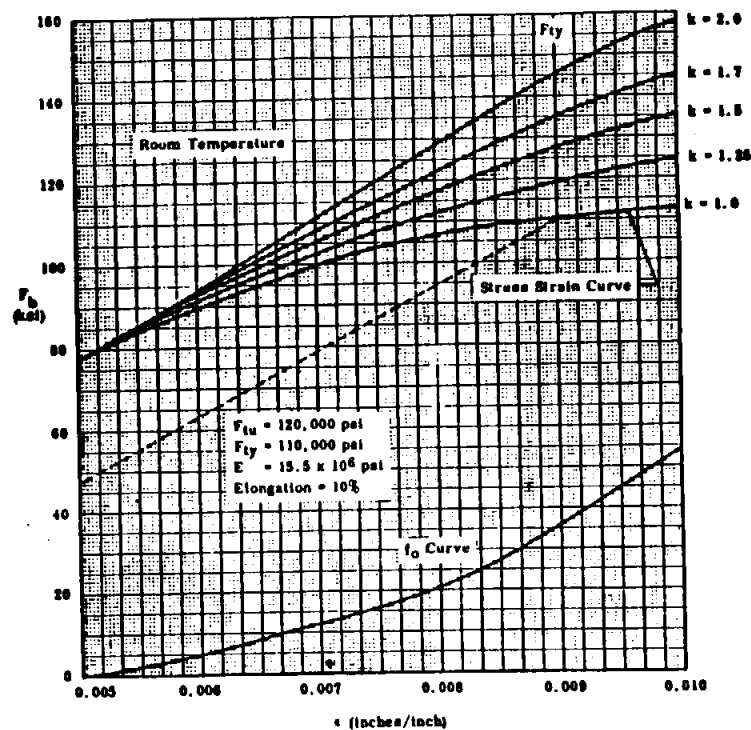


STRUCTURAL ANALYSIS MANUAL
GENERAL DYNAMICS/CONVAIR AND SPACE SYSTEMS DIVISION

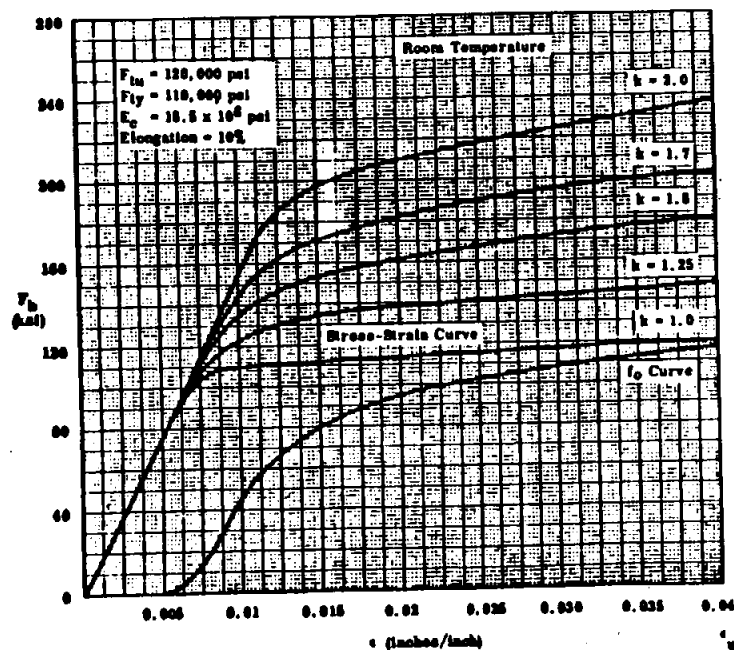
Minimum Plastic Bending Curves
7079-T6 Aluminum Alloy Hand Forgings (Longitudinal)
Thickness ≤ 6.0 in.



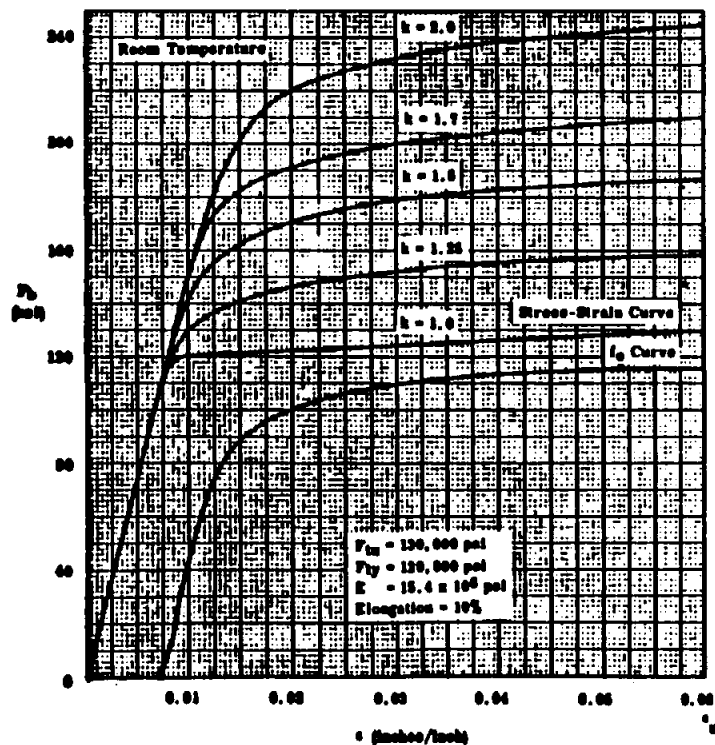
Minimum Plastic Bending Curves
for Ti-6Al Titanium Alloy



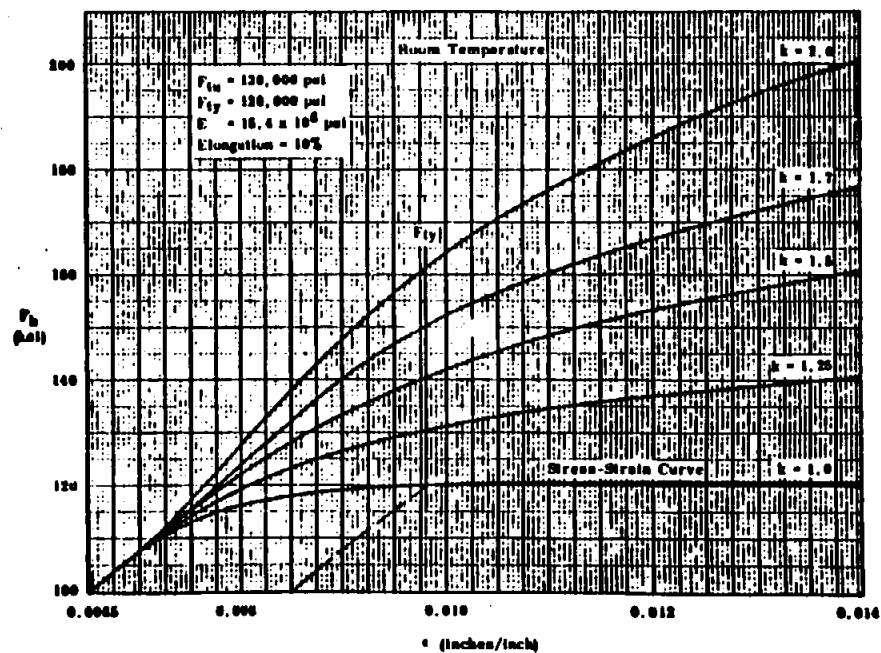
Minimum Plastic Bending Curves
Ti-6Al Titanium Alloy



Minimum Plastic Bending Curves
Ti-6Al-4V Titanium Alloy

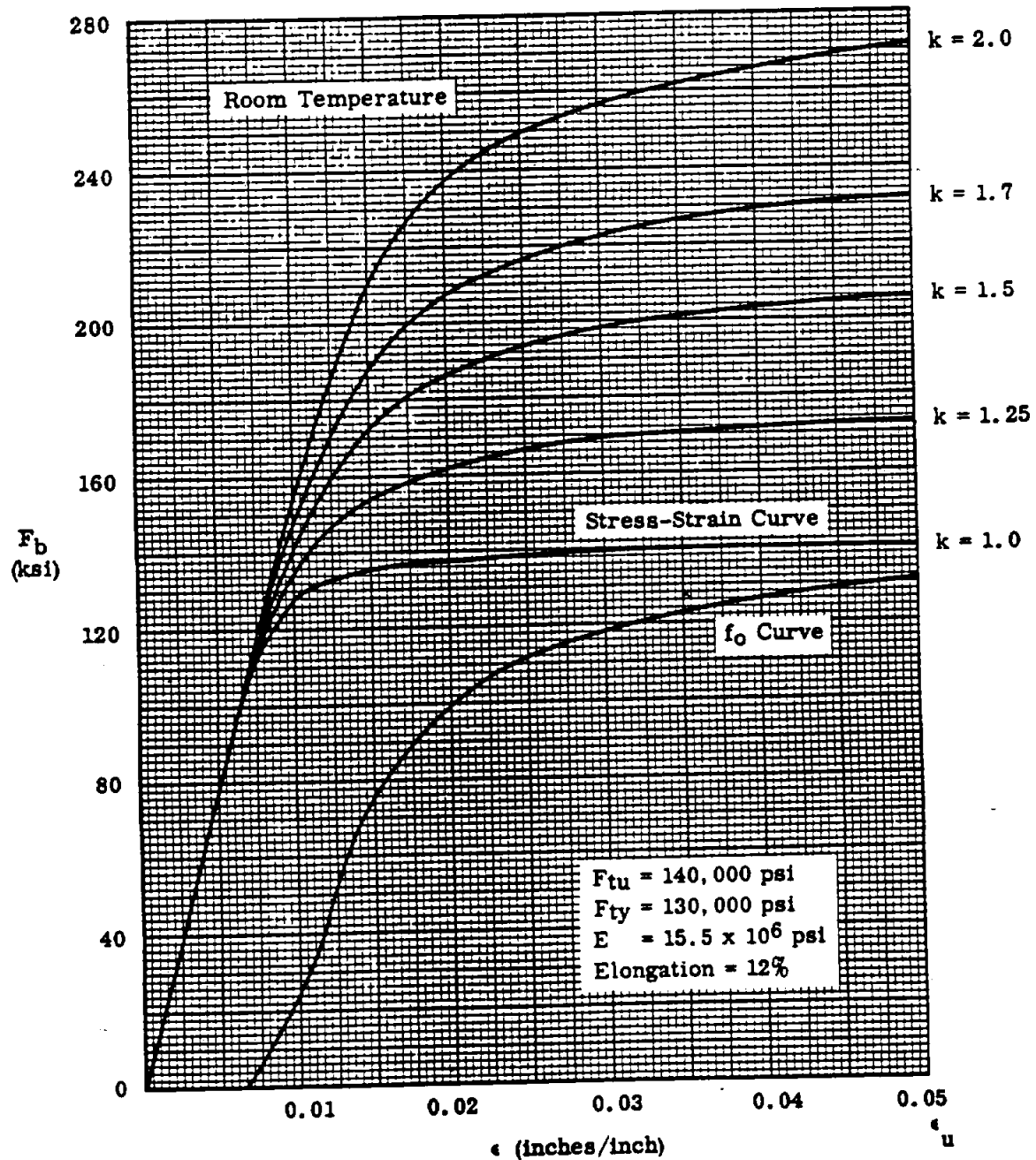


Minimum Plastic Bending Curves
for Ti-6Al-4V Titanium Alloy



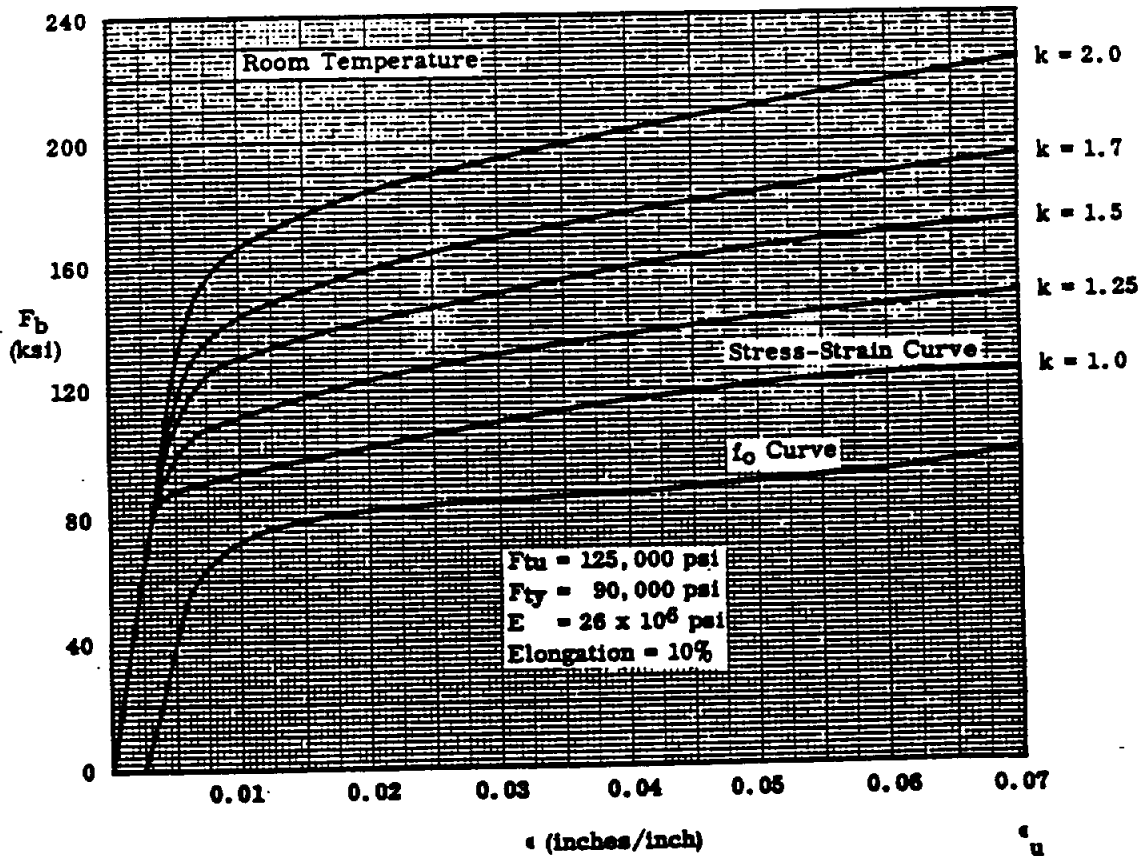
STRUCTURAL ANALYSIS MANUAL
GENERAL DYNAMICS/CONVAIR AND SPACE SYSTEMS DIVISION

Minimum Plastic Bending Curves
for Ti-4Mn-4Al Titanium Alloy

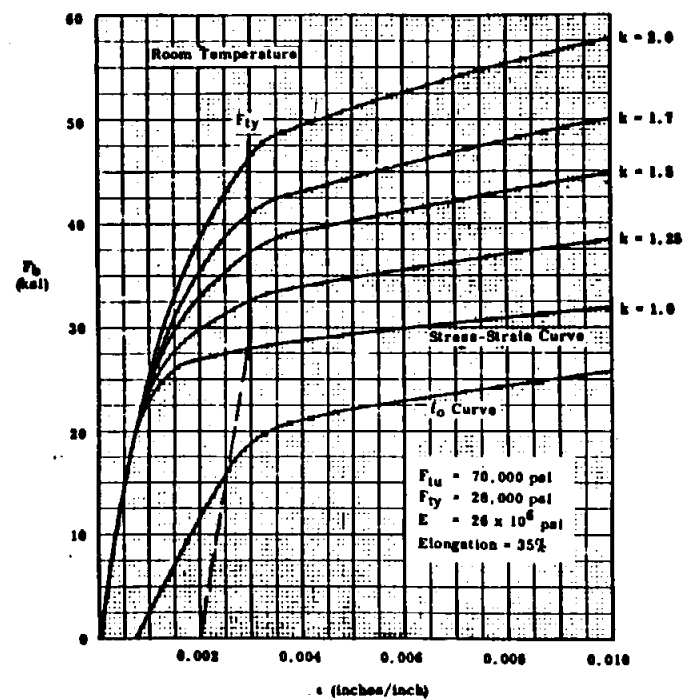


STRUCTURAL ANALYSIS MANUAL
GENERAL DYNAMICS/CONVAIR AND SPACE SYSTEMS DIVISION

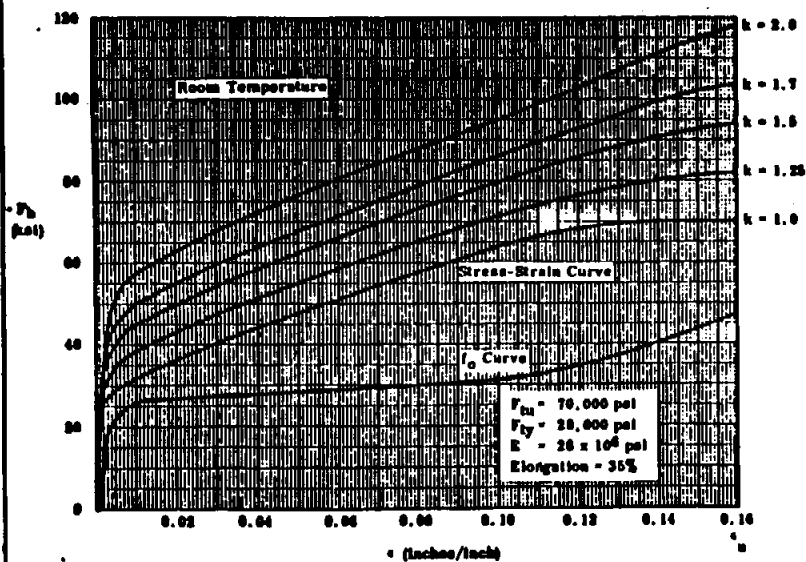
**Minimum Plastic Bending Curves
for Age Hardened K-Monel Alloy Sheet**



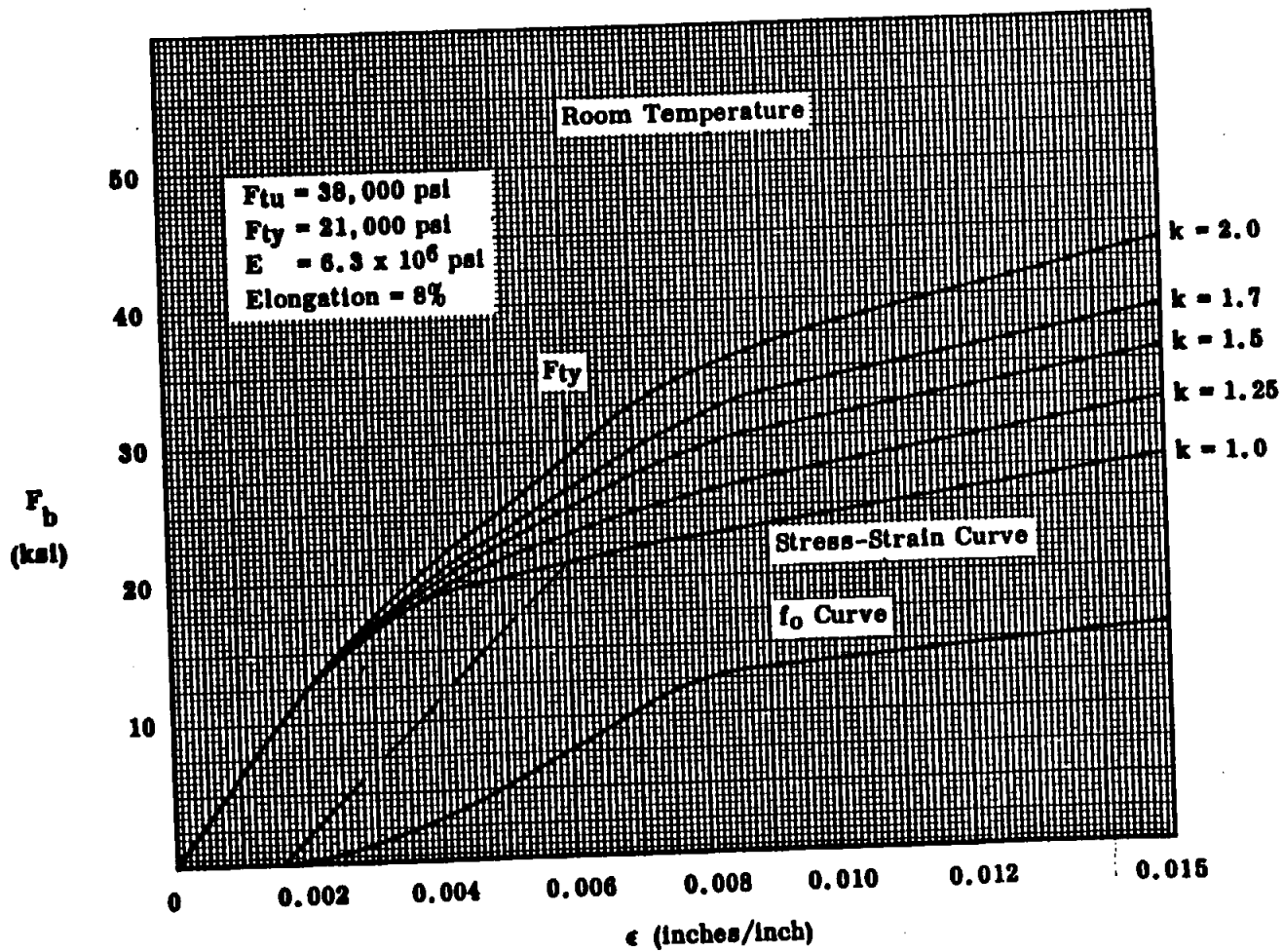
Minimum Plastic Bending Curves
Monel Alloy Cold Rolled, Annealed Sheet



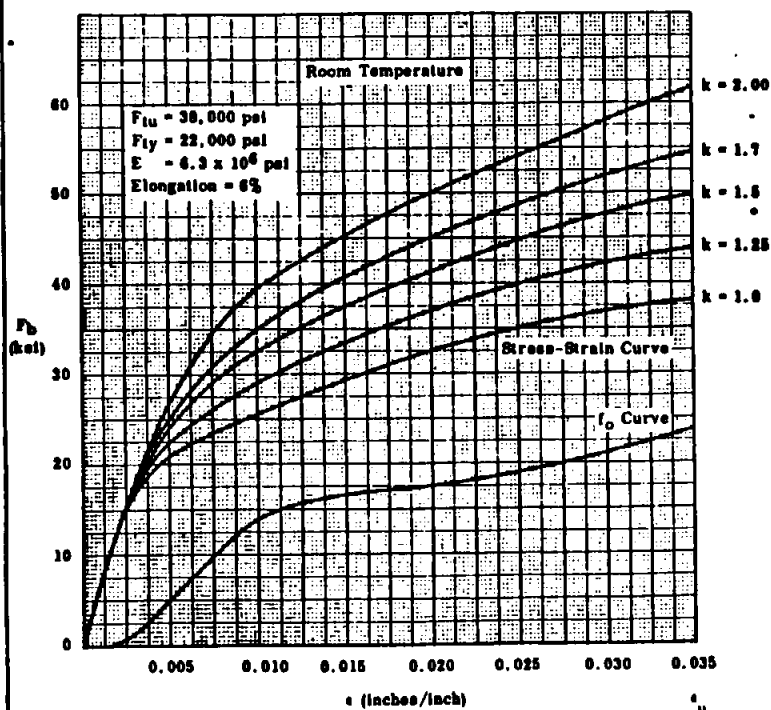
Minimum Plastic Bending Curves
Monel Alloy Cold Rolled, Annealed Sheet



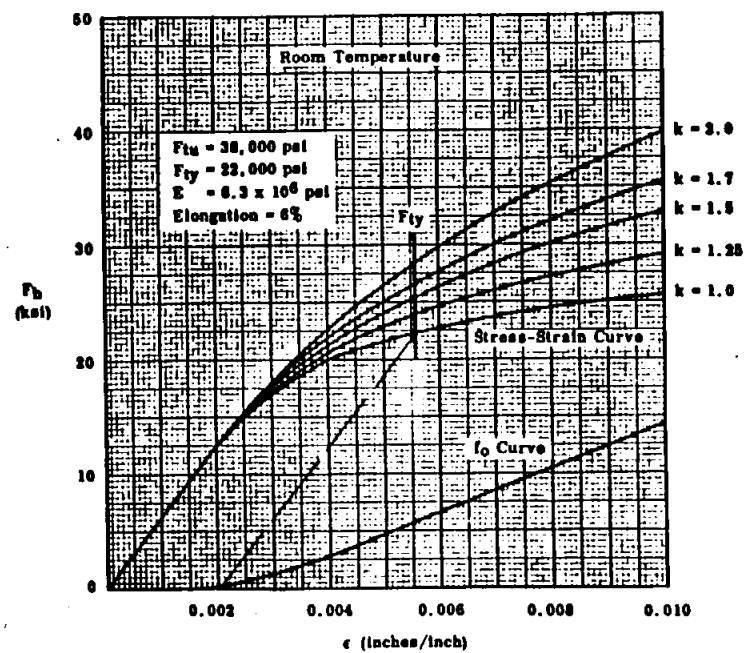
Minimum Plastic Bending Curves
A-Z61A Magnesium Alloy Extrusions (Longitudinal) ≤ 0.249 in.

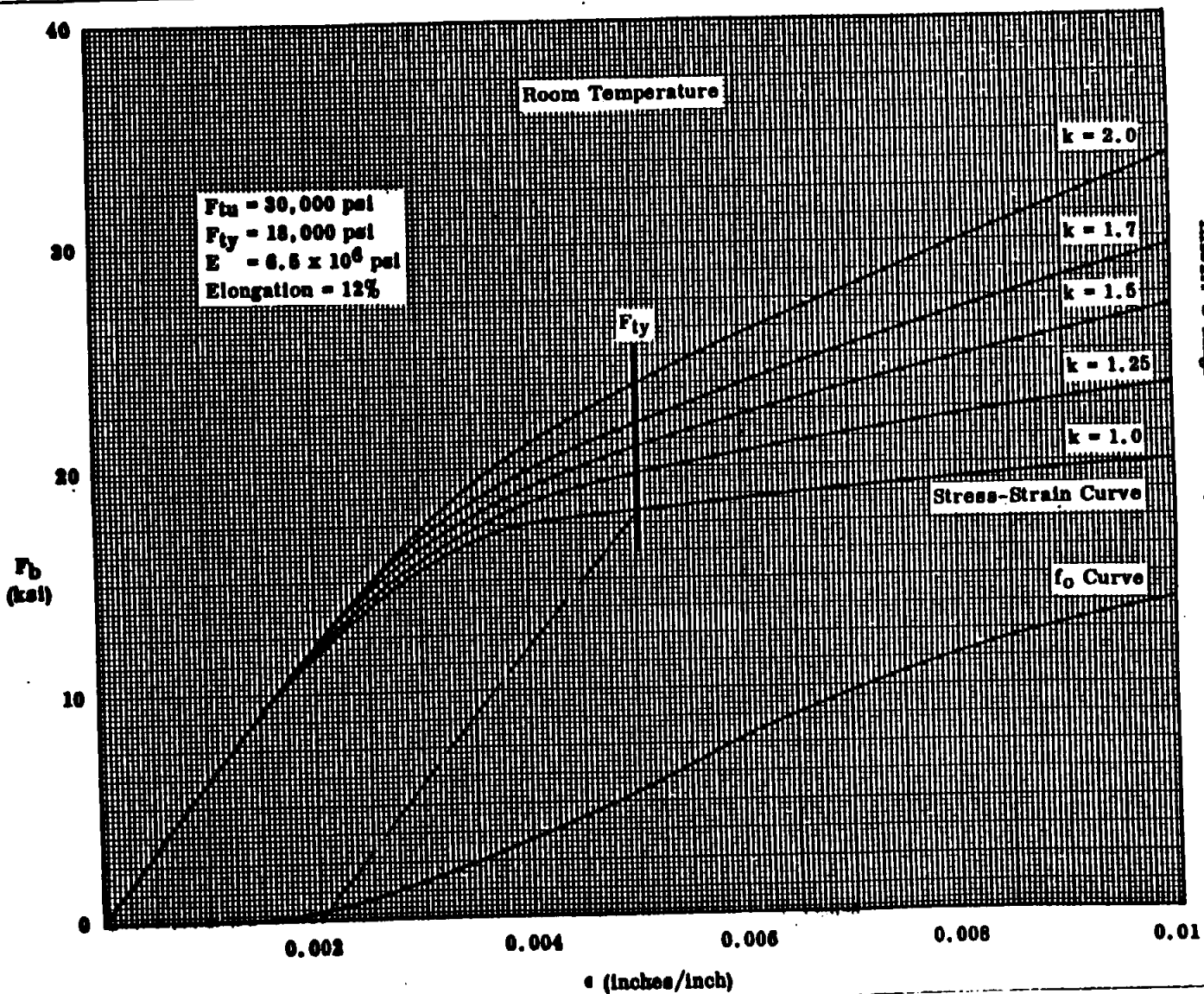


Minimum Plastic Bending Curves
AZ61A Magnesium Alloy Forgings (Longitudinal)

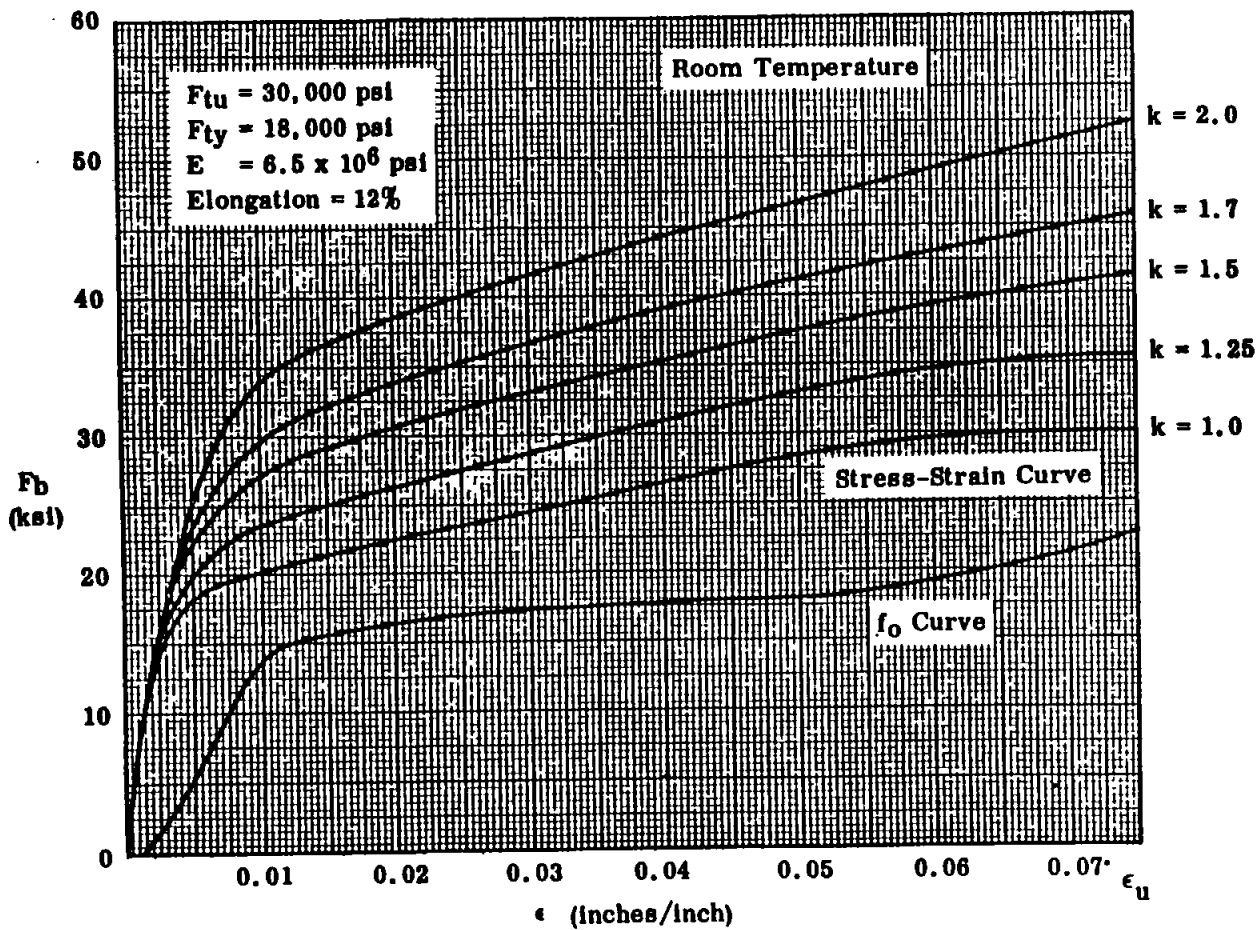


Minimum Plastic Bending Curves
AZ61A Magnesium Alloy Forgings (Longitudinal)

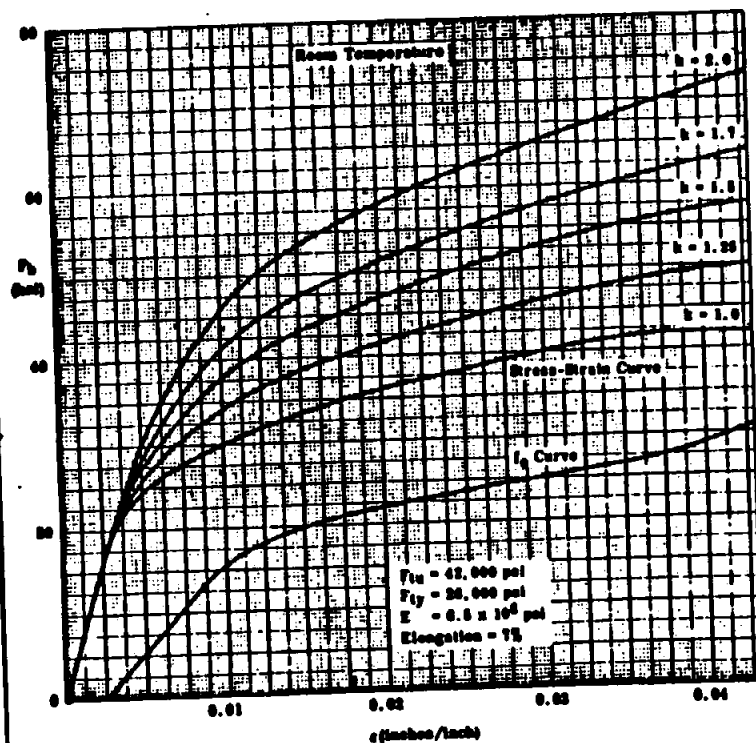




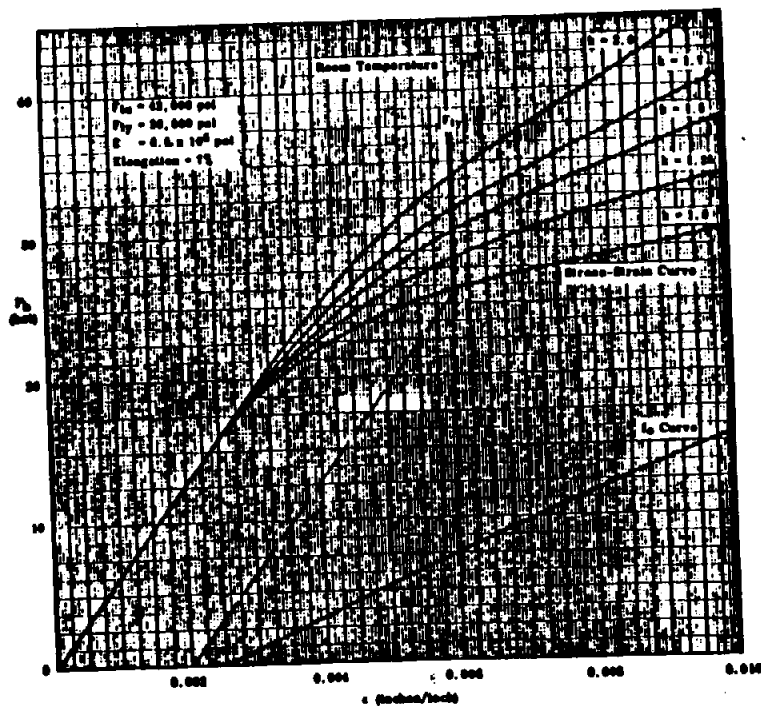
Minimum Plastic Bending Curves
for HK31A-0 Magnesium Alloy Sheet.
Thickness $\geq .016$ and $\leq .250$



Minimum Plastic Bending Curves
ZK60A Magnesium Alloy Forgings (Longitudinal)



Minimum Plastic Bending Curves
ZK60A Magnesium Alloy Forgings (Longitudinal)



STRUCTURAL ANALYSIS MANUAL
GENERAL DYNAMICS/CONVAIR AND SPACE SYSTEMS DIVISION

Data Source, Section 1.3 Reference 2 .

17.30 ELASTIC-PLASTIC ENERGY THEORY* FOR BENDING

17.30.01 GENERAL

The Elastic-Plastic Energy Theory is defined as an extension of the Elastic Energy Theory** into the plastic range of a material. This section will consider only energy due to bending stresses which may be in the elastic or plastic range, or both. Plastic bending curves found in Section 17.7 will be required. Deflections of statically determinate structures due to bending with any or all fiber stresses in the plastic range can be readily determined. Partially or completely plastic statically indeterminate structures can also be solved by procedures similar to those used in the Elastic Energy Theory. Other elastic theories could have been extended as well to include plastic bending effects but the Elastic Energy Theory was chosen due to its simplicity and common usage.

Elastic theories are accurate only if no part of a structure is stressed beyond the proportional limit of a material (no plastic strain). In structures designed to stress levels beyond the proportional limit, the error of an elastic deflection analysis is dependent on the amount of plastic strain involved. In some cases this error may be as much as 100% or more. Therefore when deflection is a limiting factor and plastic strains are involved, an analysis such as the Elastic-Plastic Energy Theory should be used.

- * The Elastic-Plastic Energy Theory was developed for the Structures Manual and is not known to exist in any other publication.
- ** The Elastic Energy Theory is also known as the Theory of Virtual Work.

STRUCTURAL ANALYSIS MANUAL
GENERAL DYNAMICS/CONVAIR AND SPACE SYSTEMS DIVISION

17.30.02 DISCUSSION OF MARGIN OF SAFETY

In calculating the margin of safety at yield or ultimate, deflections must be considered as well as loads and/or stress levels, etc.; e.g., although a positive margin of safety for a structural element may be shown on the basis of loads, excessive deflections may occur. If the deflections are then the most critical design condition, the margin of safety becomes

$$M.S. = \frac{\text{Permissible Load}}{\text{Applied Load}} - 1 \quad (17.30.01)$$

where the Permissible Load is the calculated load corresponding to the maximum permissible deflection. Equation 17.30.12 may be used in obtaining a permissible load level for a maximum permissible deflection by a trial and error process.

17.30.03 ASSUMPTIONS AND CONDITIONS

1. Energy is conserved; i.e., the external work due to a virtual load moving through a real deflection is equal to the internal strain energy developed during that deflection.
2. Plane sections remain plane; i.e., the strain is linearly distributed across any cross-section.
3. Poisson's ratio effects are negligible.
4. The deformations are of a magnitude so small as to not materially affect the geometric relations of various parts of a structure to one another.

STRUCTURAL ANALYSIS MANUAL
GENERAL DYNAMICS/CONVAIR AND SPACE SYSTEMS DIVISION

17.30.04 DEFINITIONS

- dA - cross-sectional area of an infinitesimal volume, dV .
- c - distance from the neutral axis to the extreme fibers of a cross-section.
- δ - real deformation of an infinitesimal volume, dV , in the x-direction.
- Δ - real vertical deflection of a beam at the point of application of a virtual load.
- ϵ_b - total (elastic plus plastic) strain of an infinitesimal volume, dV , in the x-direction.
- $\epsilon_{b_{max}}$ - extreme fiber strain of a cross-section.
- F_v - virtual normal force acting on dA .
- m - virtual bending moment in a beam due to the application of a virtual load.
- W_e - external work equal to a virtual load moving through a real deflection.
- W_i - internal strain energy equal to a summation of internal virtual forces times their real deflections.
- Q - virtual unit load.
- f_{b_v} - virtual bending stress on dA due to m .

17.30.05 DEFLECTIONS OF STATICALLY DETERMINANT BEAMS

Consider the infinitesimal volume dV of Figure 17.30.01(a) and (b)

$$f_{b_v} = \frac{my}{I} \quad (17.30.02)$$

$$\begin{aligned} F_v &= \text{stress} \times \text{area} = f_{b_v} dA \\ &= \frac{my}{I} dA \end{aligned} \quad (17.30.03)$$

$$\delta = \epsilon_b dx \quad (17.30.04)$$

STRUCTURAL ANALYSIS MANUAL
GENERAL DYNAMICS/CONVAIR AND SPACE SYSTEMS DIVISION

Since plane sections remain plane,

$$\epsilon_b = \epsilon_{b_{\max}} \frac{y}{c} \quad (17.30.05)$$

and

$$\delta = \epsilon_{b_{\max}} \frac{y}{c} dx \quad (17.30.06)$$

By definition,

$$W_e = Q\Delta \quad (17.30.07)$$

$$W_i = \sum F_v \delta \quad (17.30.08)$$

Since energy is conserved,

$$W_e = W_i \quad (17.30.09)$$

or

$$Q\Delta = \sum F_v \delta \quad (17.30.10)$$

Substituting Equations 17.30.03 and 17.30.06 into Equation 17.30.10 and since Q is equal to unity,

$$\begin{aligned} \Delta &= \int_A \int_0^L \left(\frac{my}{I} dA \right) \left(\epsilon_{b_{\max}} \frac{y}{c} dx \right) \\ &= \int_A \int_0^L \frac{y^2 dA}{I} \frac{m \epsilon_{b_{\max}}}{c} dx \quad (17.30.11) \end{aligned}$$

STRUCTURAL ANALYSIS MANUAL
GENERAL DYNAMICS/CONVAIR AND SPACE SYSTEMS DIVISION

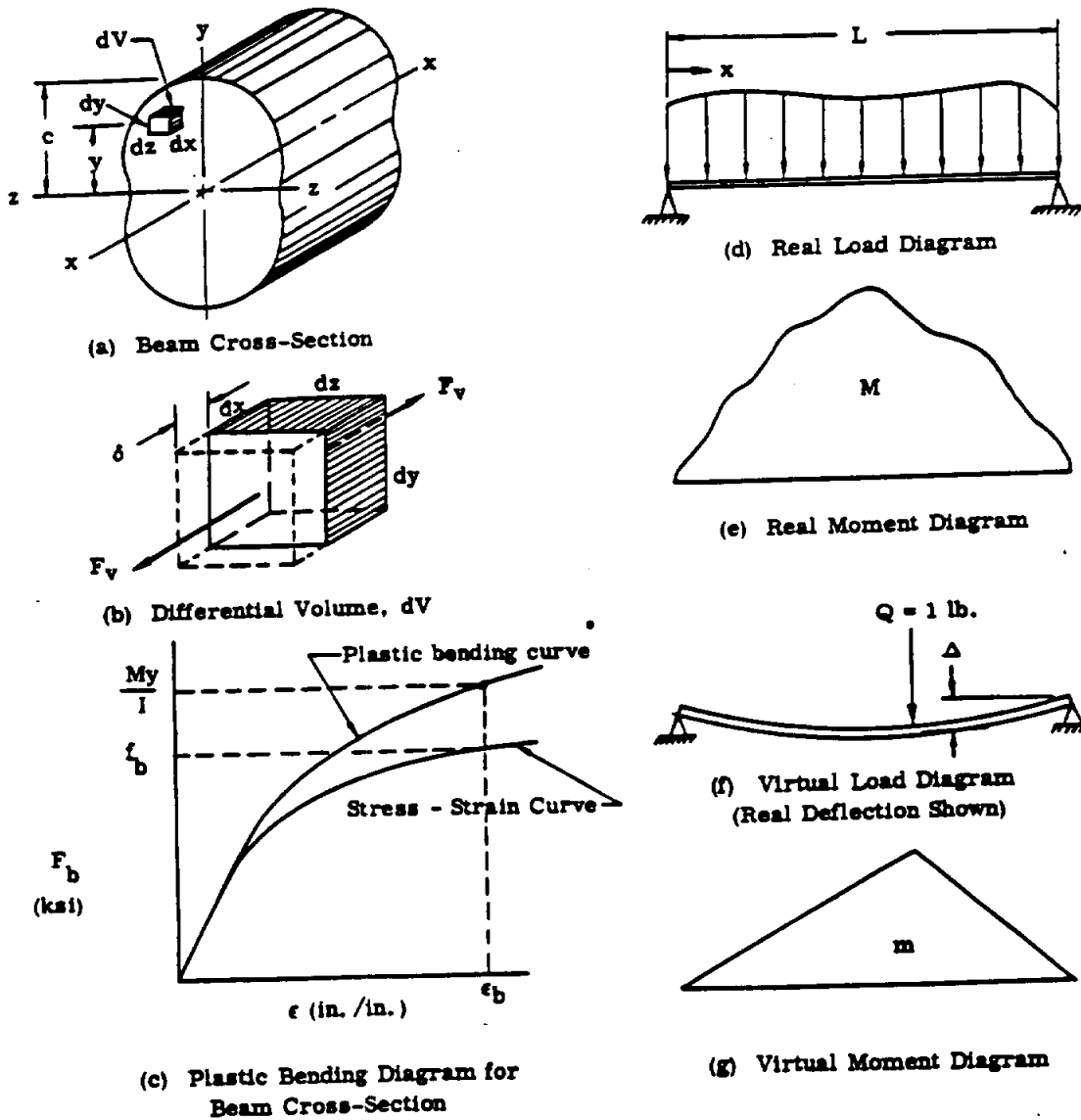
But, by definition, $I = \int_A y^2 dA$,

$$\therefore \Delta = \int_0^L \frac{m \epsilon_{b_{\max}}}{c} dx \quad (17.30.12)$$

Equation 17.30.12 can now be solved graphically to find Δ . $\epsilon_{b_{\max}}$ can be determined from a plastic bending curve for the applicable material as shown in Figure 17.30.01(c). Enter the F_b (modulus of rupture) scale with Mc/I and move horizontally across to the plastic bending curve for the specific cross-section; this intersection locates the corresponding $\epsilon_{b_{\max}}$ on the ϵ (strain) scale. For beams with varying cross-section, c may be a variable.

STRUCTURAL ANALYSIS MANUAL
GENERAL DYNAMICS/CONVAIR AND SPACE SYSTEMS DIVISION

Figure 17.30.01



STRUCTURAL ANALYSIS MANUAL
GENERAL DYNAMICS/CONVAIR AND SPACE SYSTEMS DIVISION

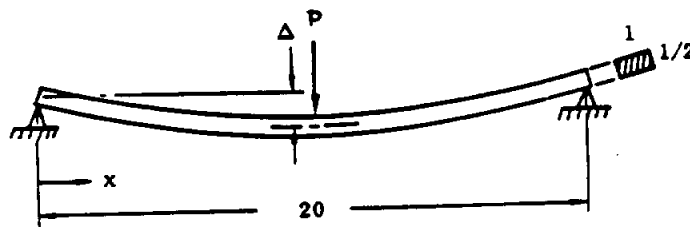
17.30.06 EXAMPLE PROBLEM

A rectangular beam, simply supported at the ends, is subjected to a concentrated vertical load at its center. Find the vertical deflection of the beam at its center.

Material: 2024-T3 Aluminum Alloy Plate

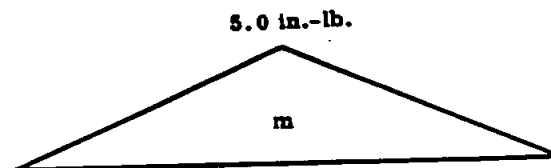
Beam dimensions: $1/2$ in. \times 1 in. \times 20 in.

Load: $P = 400$ lb



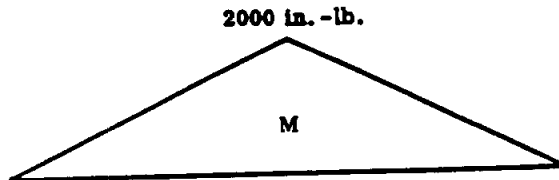
PROCEDURE:

1. Apply a virtual unit load, Q , at the beam center and construct the virtual moment diagram, m .



STRUCTURAL ANALYSIS MANUAL
GENERAL DYNAMICS/CONVAIR AND SPACE SYSTEMS DIVISION

2. Construct the real moment diagram, M .



3. Calculate the real bending stress, F_b , for each value of x by:

$$F_b = \frac{Mc}{I}$$

4. Enter the plastic bending curves in Section 17.7 (at $k=1.5$ for a rectangular cross-section) with each value of F_b from Step 3 and determine $\epsilon_{b_{\max}}$ for each value of x .
5. Multiply the value of m by the corresponding value of $\epsilon_{b_{\max}}$ to obtain a value of $m \epsilon_{b_{\max}}$ for each value of x .
6. Tabulate the results of the previous steps (see Table 17.30.01).
7. Construct a plot of $m \epsilon_{b_{\max}}$ vs. x and determine the area under the curve. This area represents $\int_0^L m \epsilon_{b_{\max}} dx$. (See Figure 17.30.02.)

STRUCTURAL ANALYSIS MANUAL
GENERAL DYNAMICS/CONVAIR AND SPACE SYSTEMS DIVISION

8. Calculate Δ :

$$\Delta = \int_0^L \frac{m \epsilon_{b_{\max}}}{c} dx \quad (\text{Ref eq 17.30.12})$$

$$c = 0.250 \text{ in.}$$

$$\int_0^L m \epsilon_{b_{\max}} dx = 0.165 \quad (\text{by graphical integration})$$

$$\therefore \Delta = \left(\frac{0.165}{0.250} \right) = \underline{\underline{0.661 \text{ in.}}}$$

By an elastic analysis, Δ was found to be 0.6104 in. which is 7.7% in error. Partially plastic fiber stresses existed only over the middle 8 inches in this example. The elastic analysis would be considerably more in error for higher loadings and/or beams in which the plastic stresses exist over greater lengths; e.g., beams of constant moment, etc.

STRUCTURAL ANALYSIS MANUAL
GENERAL DYNAMICS/CONVAIR AND SPACE SYSTEMS DIVISION

EXAMPLE PROBLEM, χ vs. $m\epsilon_{b\max}$ TABLE

Table 17.30.01

P = 400 lb.

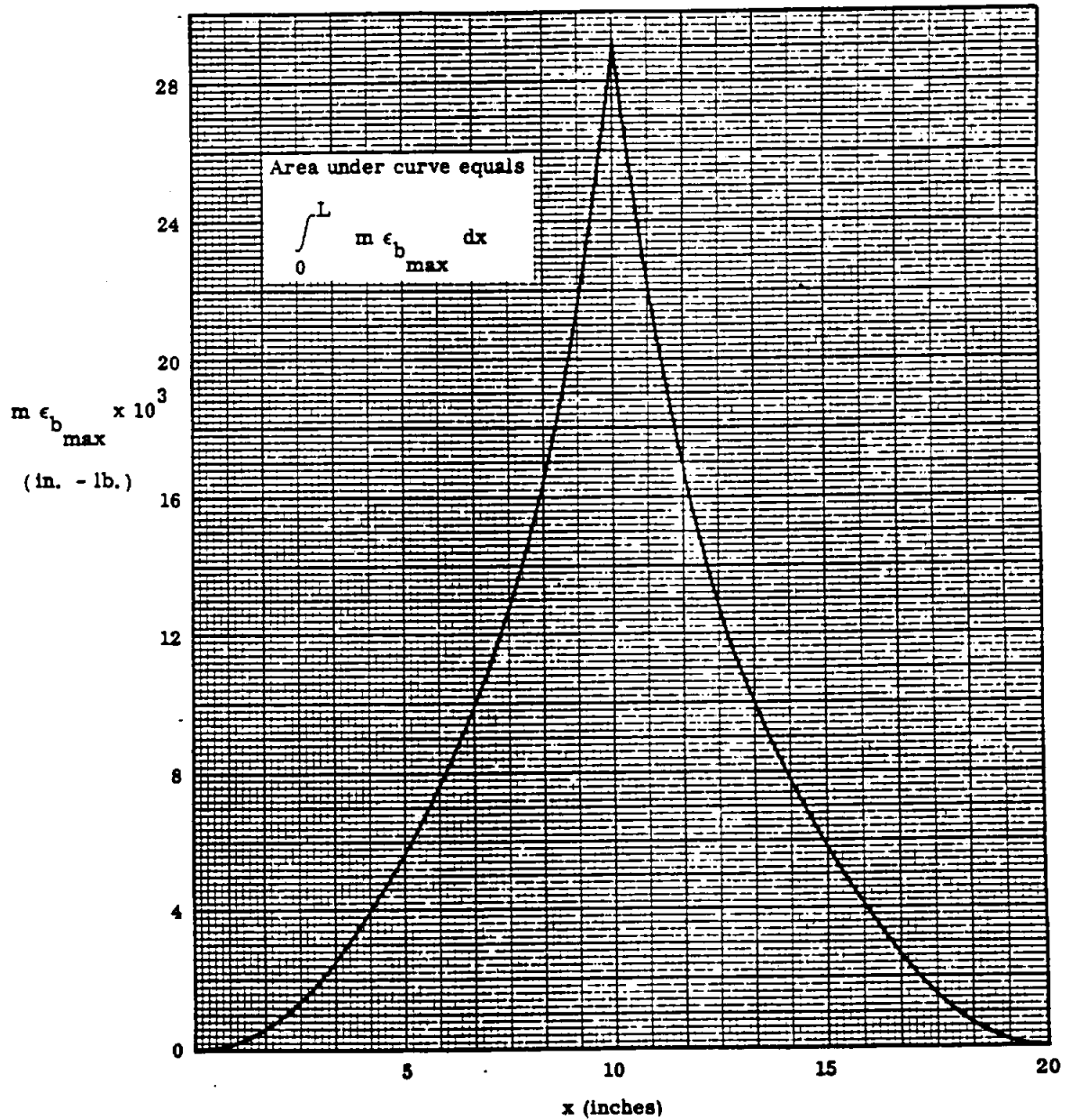
x, in.	m, in. -lb.	M, in. -lb.	Mc/I, ksi	$\epsilon_{b\max}'$ in./in. $\times 10^{-3}$	$m \epsilon_{b\max}'$ in. -lb. $\times 10^{-3}$
0	0	0	0	0	0
1	.5	200	4.8	.4570	.2285
2	1.0	400	9.6	.9140	.9140
3	1.5	600	14.4	1.3710	2.0565
4	2.0	800	19.2	1.8280	3.6560
5	2.5	1000	24.0	2.2850	5.7125
6	3.0	1200	28.8	2.7420	8.2260
7	3.5	1400	33.6	3.14	10.9900
8	4.0	1600	38.4	3.80	15.2000
9	4.5	1800	43.2	4.64	20.8800
10	5.0	2000	48.0	5.83	29.1500
11	4.5	1800	43.2	4.64	20.8800
12	4.0	1600	38.4	3.80	15.2000
13	3.5	1400	33.6	3.14	10.9900
14	3.0	1200	28.8	2.7420	8.2260
15	2.5	1000	24.0	2.2850	5.7125
16	2.0	800	19.2	1.8280	3.656
17	1.5	600	14.4	1.3710	2.0565
18	1.0	400	9.6	.9140	.9140
19	.5	200	4.8	.4570	.2285
20	0	0	0	0	0

36E

STRUCTURAL ANALYSIS MANUAL
GENERAL DYNAMICS/CONVAIR AND SPACE SYSTEMS DIVISION

EXAMPLE PROBLEM, χ vs. $m\epsilon_{b\max}$ PLOT

Figure 17.30.02





STRUCTURAL ANALYSIS MANUAL
GENERAL DYNAMICS/CONVAIR AND SPACE SYSTEMS DIVISION

Data Source, Section 1.3 Reference **6**

SUBJECT: Fatigue Considerations for Parts Subject to Frequent Applications of Near-Limit Loads and Parts Designed by Modulus of Rupture.

INTRODUCTION

Many parts in various components of the airplane are subjected to frequent applications of near-limit loads during the service life of the airplane. The biggest proportion of parts so affected are those on which the loads result from hydraulic pressure, and from other pressure systems such as cabin pressurization. The linkage, attachment lugs and other carry-through parts of the landing gear retracting mechanism, hinges and latches of cabin door and emergency exits are typical examples of parts falling into such a category. Components of some control systems where the operating loads are close to the maximum design loads may also be affected.

It is readily apparent from the examination of any typical S-N curve that the number of load applications that can be sustained when high loads are applied are relatively low. Thus to insure adequate service life it becomes necessary to provide limitations on the degree of exploitation of the maximum static strength of materials, in addition to the normal practice of good design by avoiding or minimizing stress concentrations wherever possible.

Another category of parts requiring special consideration from a fatigue standpoint are those designed by the use of bending modulus of rupture. From the standpoint of fatigue, the critical stresses are those acting at the surface of the part, and by virtue of the fact that the plasticity of a material is exploited in determining the modulus of rupture, the true surface stresses on parts subjected to bending loads, compared to those under axial loading, are relatively higher when operating at the same percentage of ultimate strength. This can be verified by examining any of the curves in

SECTN. 17.0 For example in Figure 14 for steel at a 180 ksi level it can be seen that a member with $k = 1.8$ being loaded to half the allowable moment would be subjected to a true surface stress of 79% of material strength compared with 50% when loaded axially in tension. The difference, of course, is dependent on "section factor" k , being zero for $k = 1$ and varying to a maximum value at $k = 2$. It is therefore obvious that some limitation on the exploitation of modulus of rupture is necessary when the spread between operating loads and design limit loads is not large.

In order to provide adequate strength and insure trouble-free service during the useful life of the airplane, this memo establishes policies for the detail design and analysis of parts falling in the categories discussed above.

This memo is not applicable to the shell components of the airplane since fatigue problems in such structure must be given more detailed consideration.

STRUCTURAL ANALYSIS MANUAL
GENERAL DYNAMICS/CONVAIR AND SPACE SYSTEMS DIVISION

The application of procedures covered by this memo will in many cases result in larger and thereby heavier parts. While the weight penalty in an individual case may be small, the effect may become considerable in the aggregate. Therefore, extreme care and judgement are to be exercised in selecting components to which this memo is to be applied. All components so chosen are to be called to the attention of the Project Structures Engineer for approval with regard to use of this memo.

II. Parts Subject to Frequent Applications of Near-Limit Loads

Parts and systems falling into this category may require a formal fatigue analysis. It is difficult, by the use of the expedient of reduced static allowables, to account for all possible combinations of loading configurations and life requirements. However, if a formal fatigue analysis is not made, the following requirements shall be adhered to.

- A. Bending modulus of rupture shall not be used for parts loaded in bending.
- B. The allowable ultimate tensile stress, bending or axial shall be based on F_{tu} of material, reduced as follows:

<u>Aluminum Alloys</u>	<u>Reduced Allowable</u>
2014, 7075, 7178, 7079	.50 F_{tu}
2024	.60 F_{tu}
<u>Steel</u>	
260 ksi and higher	.50 F_{tu}
180 ksi and lower	.60 F_{tu}

For steel with minimum specified heat treat varying between 180 and 260 ksi, linear interpolation of the reduction factor may be used.

In using SECTION 14.0 for the design of lugs all formulas containing F_{tu} as a parameter shall use the reduced value of F_{tu} for the pertinent material. When doing so, fitting and casting factors, and the minimum margin of safety requirements may be neglected, however, the "provision for bushing" requirement is to be retained and the lug designed with the hole based on bushing diameter rather than pin diameter. This would also be applicable to any other stress memo or source of reference containing formulas having F_{tu} as a parameter.

For the selection of the pin size in connection with lugs or clevis type ends of parts in the category under consideration, the normal shear allowables may be used, however, when checking for pin bending the allowable ultimate (mc/I) stress shall not exceed the F_{tu} (unreduced) of the pin material.

STRUCTURAL ANALYSIS MANUAL
GENERAL DYNAMICS/CONVAIR AND SPACE SYSTEMS DIVISION

III. Parts Designed by Modulus of Rupture

This category is distinct from that covered in Section II above primarily in the degree of difference between operating and design limit loads. While Section II covers the condition where the operating and design limit loads are practically the same, this section applies to a condition where the operating load is an appreciable percentage of the design limit load. Landing gear components are typical examples of parts which have such loads frequently applied, due to landing or taxiing.

In the design of parts subjected to bending where the spread between operating and design limit loads is not large, thus making these parts potentially critical in fatigue, the use of plastic bending allowables shall be limited as follows.

- A. The "section factor" k in SECTION 17.0 used in determining the ultimate bending strength shall be taken as the actual value of k or that obtained from formulas given below, whichever is lower.

$$k = \left(\frac{S}{K_T} \right)^{.63} \quad \text{for steel parts}$$

$$k = \left(\frac{S}{K_T} \right)^{.83} \quad \text{for aluminum parts}$$

where K_T is the estimated stress concentration factor applicable to the section of the part being checked. Values of K_T for some sections and types of "stress raisers" may be found in SECT. 13.0

Where k comes out less than 1 use kF_{tu} as the allowable stress.

- B. The procedure specified under III-A above is applicable to "compact" sections which, under bending loads, fail by rupture. For sections in bending, critical on the compression side where failure is by crippling, the applied tensile stress on the tension side may be low enough to preclude any reduction in allowable loads.
- C. Tubular members require special consideration. At low values of D/t tubes fail by rupture and at larger values of D/t they fail by plastic or elastic buckling. In order to cover the full range of possible variations in D/t , the following procedure is to be used.
1. For tube under consideration determine D/t .
 2. From Figure 1 of SECT. 17.11 determine the actual "section factor" designated by k_a .
 3. From equations in III-A of this memo compute "section factor" designated k_o .

STRUCTURAL ANALYSIS MANUAL
GENERAL DYNAMICS/CONVAIR AND SPACE SYSTEMS DIVISION

III. Parts Designed by Modulus of Rupture - Con't.

C. Con't.

4. If $k_0 < k_a$, determine the allowable bending stress from paragraph 17.10 using k_0 . Compare with F_{bu} from SECT. 17.10 and use the lower value.

If $k_0 \geq k_a$, determine the allowable bending strength from SECT. 17.10

- D. Another category of parts where the modulus of rupture is not to be exploited consists of those parts where the stress distribution is not precisely known or where restraints are present to restrict deformations thereby preventing fulfillment of the basic assumptions of the bending theory. The intersection of an axle and strut in a landing gear is a typical area where such a condition exists. In such cases the allowable stress shall be taken as the F_{tu} of material.

- IV. The procedures outlined herein are to be used for the design and preliminary analysis of selected components. For final analysis write up, the normal analysis methods are to be used, with the resulting higher margins of safety shown. To preclude the possibility of these higher margins being used to salvage parts not conforming to drawing requirements, it is to be indicated that these margins are due to fatigue considerations and are not to be used for salvage.

STRUCTURAL ANALYSIS MANUAL
GENERAL DYNAMICS/CONVAIR AND SPACE SYSTEMS DIVISION

Data Source, Section 1.3 Reference 28

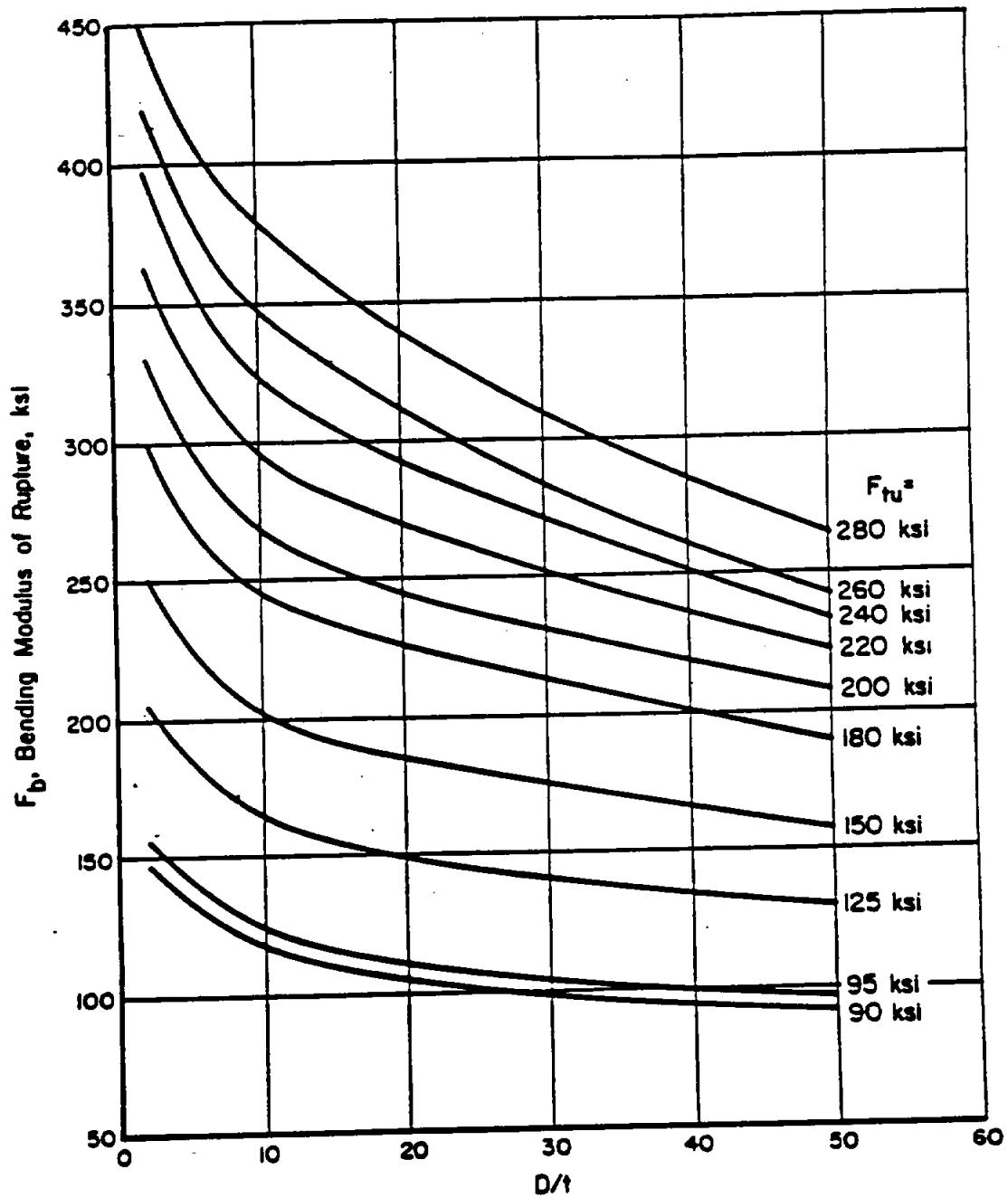
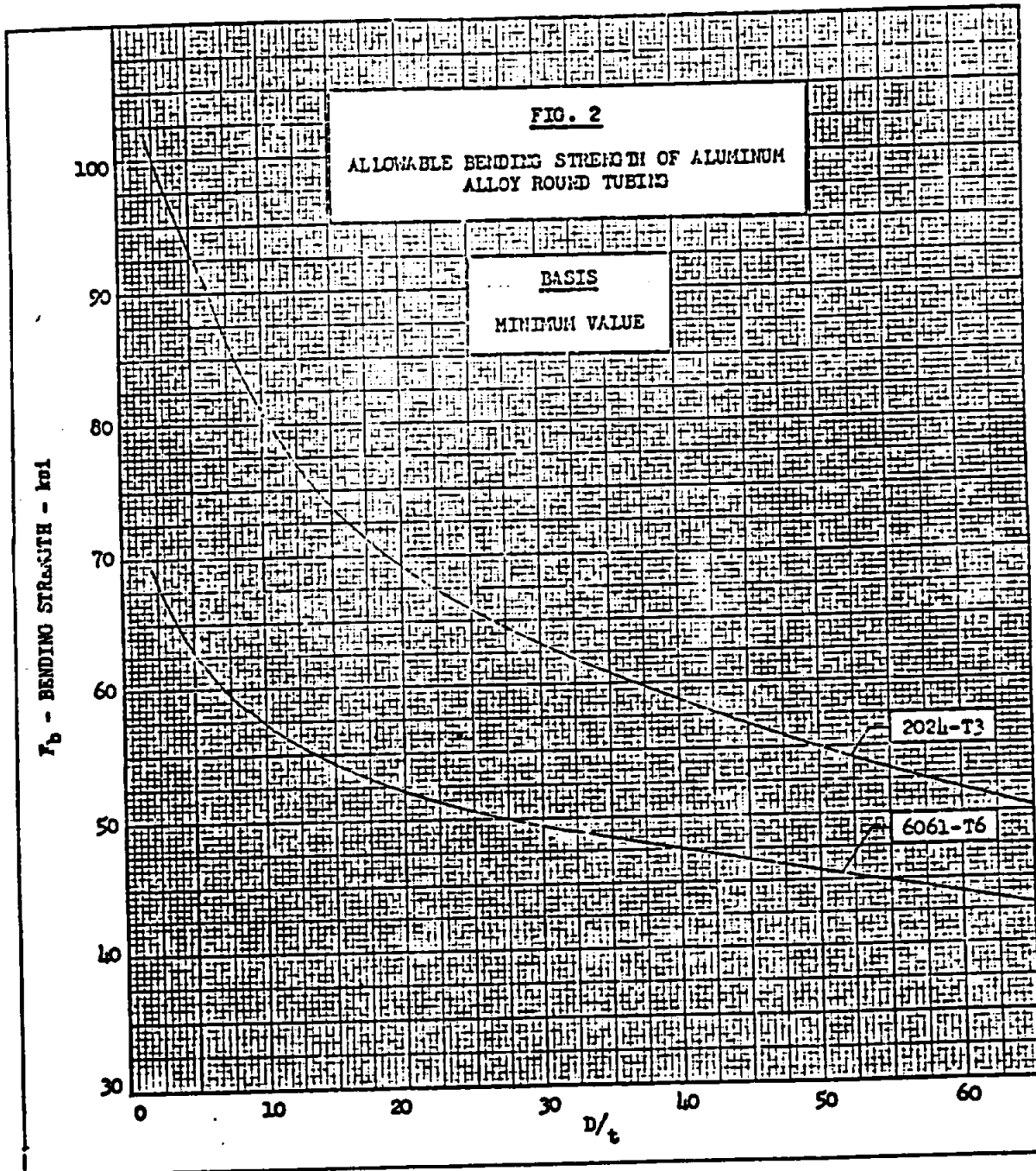


FIGURE 2.8.1.1. *Bending modulus of rupture for round low-alloy-steel tubing.*

2-204

STRUCTURAL ANALYSIS MANUAL **GENERAL DYNAMICS/CONVAIR AND SPACE SYSTEMS DIVISION**

Data Source, Section 1.3 Reference **6**



STRUCTURAL ANALYSIS MANUAL
GENERAL DYNAMICS/CONVAIR AND SPACE SYSTEMS DIVISION

Data Source, Section 1.3 Reference 6

SUBJECT: Shear Stress in Round Tubes

1. Transverse and Longitudinal Shear (With Bending)

The conventional formula for shear stress, $f_s = \frac{SQ}{bI}$, has been extended to the plastic range and may be expressed as:

$$f_{s_{max.}} = R \times \frac{S}{A}$$

where:

- $f_{s_{max.}}$ = the transverse and longitudinal shear stress at the neutral axis of a round tube
- S = the shear load at the section
- A = the cross-sectional area
- R = a factor dependent upon the $\frac{D}{t}$ ratio and the degree of plasticity

The factor, R , may be determined in the following manner:

- a. Calculate $f_b = \frac{Mc}{I}$, the applied bending stress at the section.
- b. From Fig. 1 obtain the section factor, k , for the proper $\frac{D}{t}$ ratio.
- c. From the equations in Table I calculate the C value for the proper k value, f_b , and material. When C is less than or equal to zero all of the material at the section is in the elastic range. When C is equal to one or greater, all of the material at the section is in the plastic range. Intermediate values of C represent the degree of plasticity.
- d. Enter Fig. 1 with the $\frac{D}{t}$ ratio and obtain the R value corresponding to the C value calculated above.

STRUCTURAL ANALYSIS MANUAL
GENERAL DYNAMICS/CONVAIR AND SPACE SYSTEMS DIVISION

When the shear stress is determined in the above manner, the ultimate allowable shear stress for the material shall be used in calculating the margin of safety.

2. Transverse Shear Stress (Without Bending)

When only shear exists, such as in tubular shear bolt-lug connections, the shear stress shall be calculated by means of the formula.

$$f_{s \text{ ave.}} = \frac{S}{A}$$

where:

$f_{s \text{ ave.}}$ = the average shear stress over the section

S = the shear load at the section

A = the cross-sectional area

When shear stress is determined in this manner, the allowable ultimate and yield shear stresses shall be determined from Fig. 2. The yield allowables in Fig. 2 are such as to limit permanent set to 1% of the outside diameter.

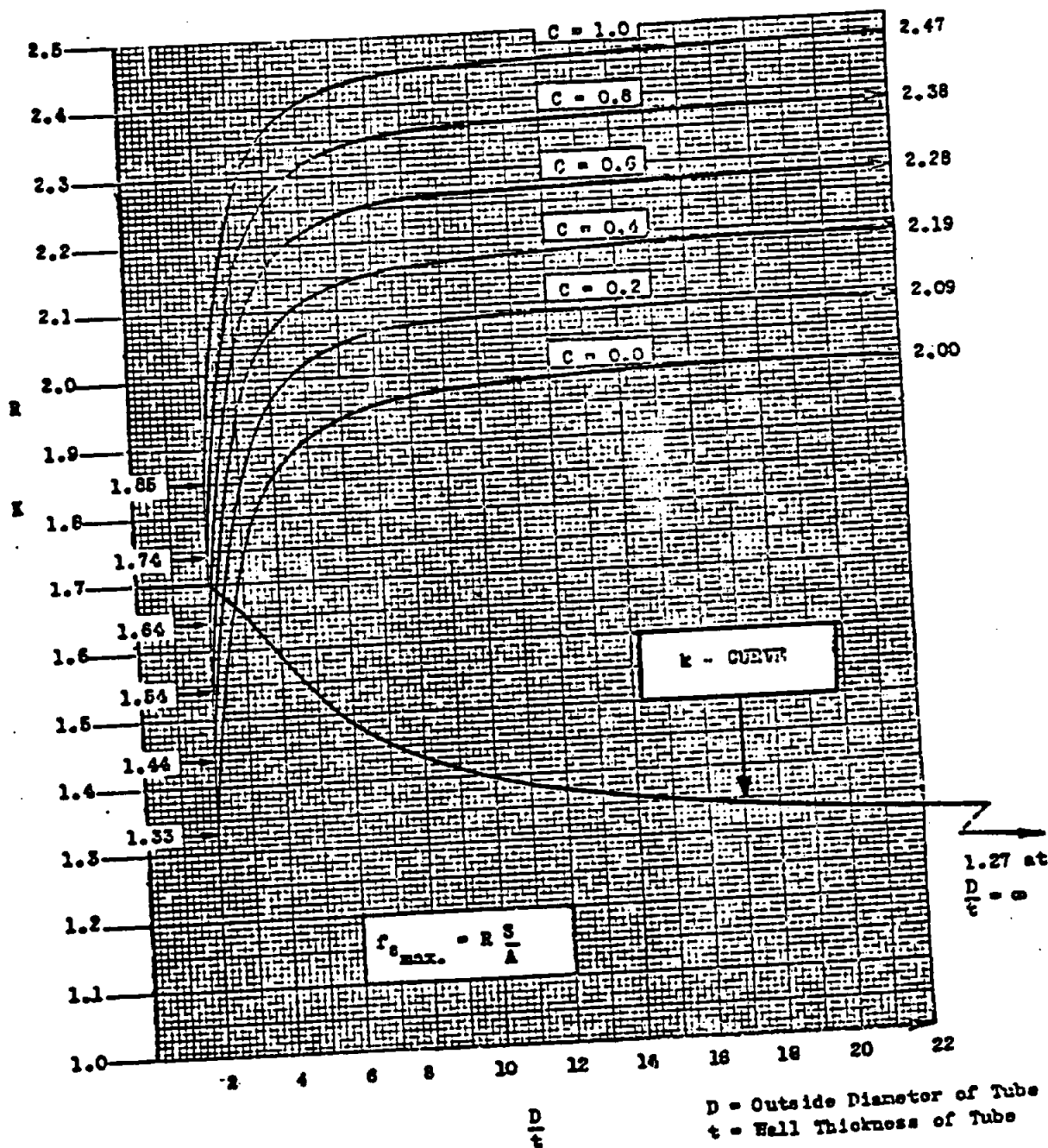
STRUCTURAL ANALYSIS MANUAL
GENERAL DYNAMICS/CONVAIR AND SPACE SYSTEMS DIVISION

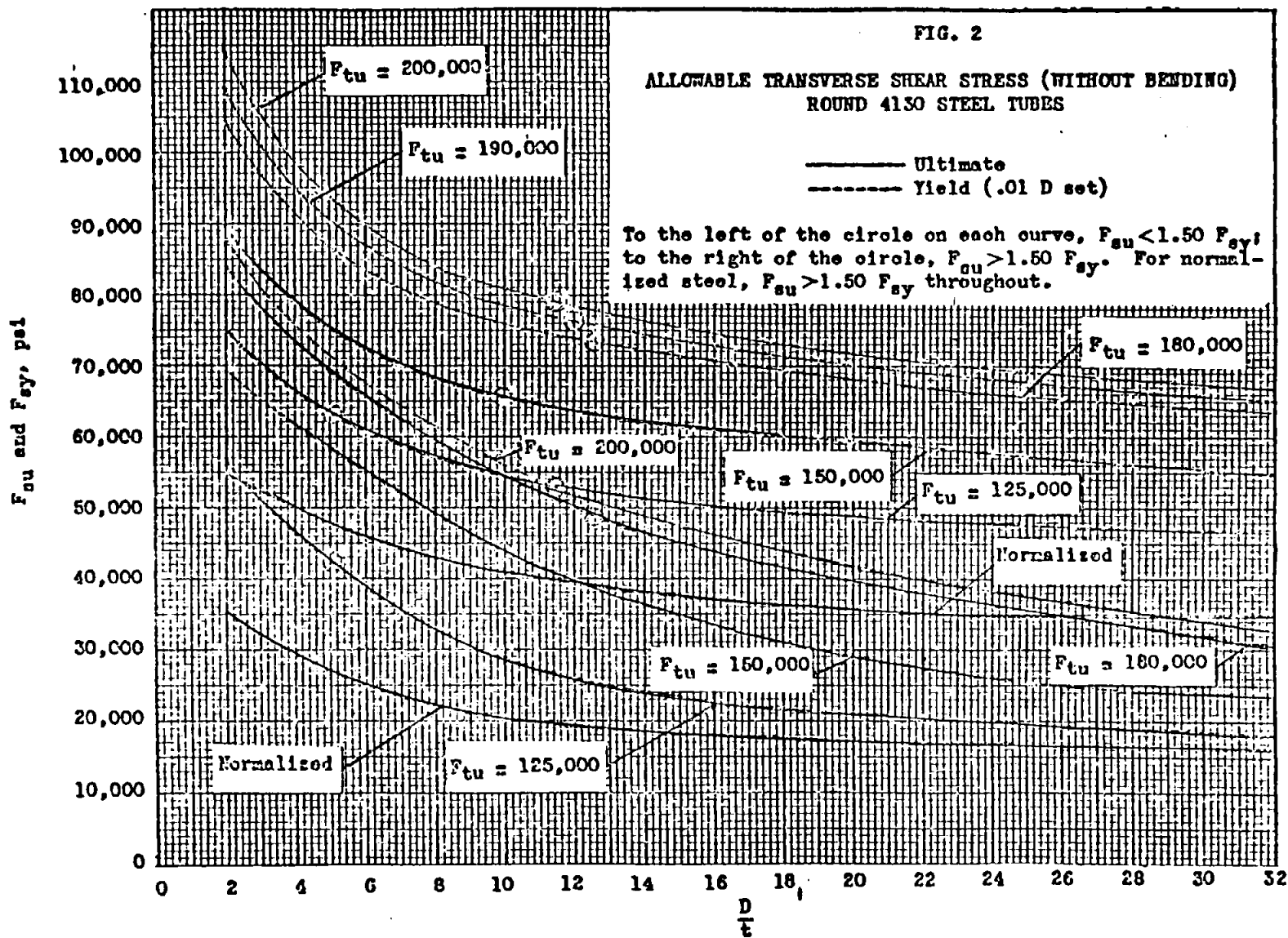
TABLE I
FORMULAE FOR EVALUATION OF "C"

Material and H.T.		$C = \frac{f_b - F_{tp}}{F_b - F_{tp}}$
4130 and 8630	90,000	$\frac{f_b \times 10^{-3} - 50}{82x - 42}$
	95,000	$\frac{f_b \times 10^{-3} - 55}{86x - 46}$
	125,000	$\frac{f_b \times 10^{-3} - 90}{112x - 78}$
	150,000	$\frac{f_b \times 10^{-3} - 115}{146x - 111}$
	180,000	$\frac{f_b \times 10^{-3} - 140}{170x - 130}$
24ST		$\frac{f_b \times 10^{-3} - 30}{58x - 24}$

STRUCTURAL ANALYSIS MANUAL **GENERAL DYNAMICS/CONVAIR AND SPACE SYSTEMS DIVISION**

FIGURE 1
SHEAR STRESS IN ROUND TUBES





STRUCTURAL ANALYSIS MANUAL
GENERAL DYNAMICS/CONVAIR AND SPACE SYSTEMS DIVISION

SECTION 18.0

RINGS, FRAMES & ARCHES

**ANALYSIS METHODS FOR RINGS FRAMES AND ARCHES ARE PRESENTED
IN THIS SECTION.**

		PAGE
18.1	RIGID RINGS	18.1.1
18.2	BENTS & SEMI-CIRCULAR ARCHES	18.2.1
18.3	RIGID AND FLEXIBLE RINGS	18.3.1
18.4	REDUNDANT FRAMES	18.4.1

STRUCTURAL ANALYSIS MANUAL
GENERAL DYNAMICS/CONVAIR AND SPACE SYSTEMS DIVISION

Data Source, Section 1.3 Reference 5

B 6.1.0 Rigid Rings

Sign Convention

Moments which produce tension on the inner fibers are positive.

Transverse forces which act upward to the left of the cut are positive.

Axial forces which produce tension in the frame are positive.



Fig. B 6.1.0-5 Positive Sign Convention

In-Plane Load Cases

Coefficients to obtain slope, deflection, bending moment, shear, and axial force along with equations for these values are given for some of the frequently occurring load cases.

NOMENCLATURE

R	=	RING RADIUS, IN
E	=	RING MATERIAL YOUNG'S MODULUS, PSI
I	=	RING SECTION MOM. OF I, IN ⁴
P	=	APPLIED LOAD, LB.
M ¹	=	APPLIED BENDING MOMENT, IN.-LB.
M	=	RING IN-PLANE BENDING MOMENT, IN.-LB.
Q	=	RING IN-PLANE SHEAR FORCE, LB
N	=	RING IN-PLANE AXIAL LOAD, LB
Δ	=	RING IN-PLANE DEFLECTION, IN
θ	=	RING IN-PLANE SLOPE, RADIANS
φ	=	ANGULAR DISTANCE FROM DATUM, DEGREES

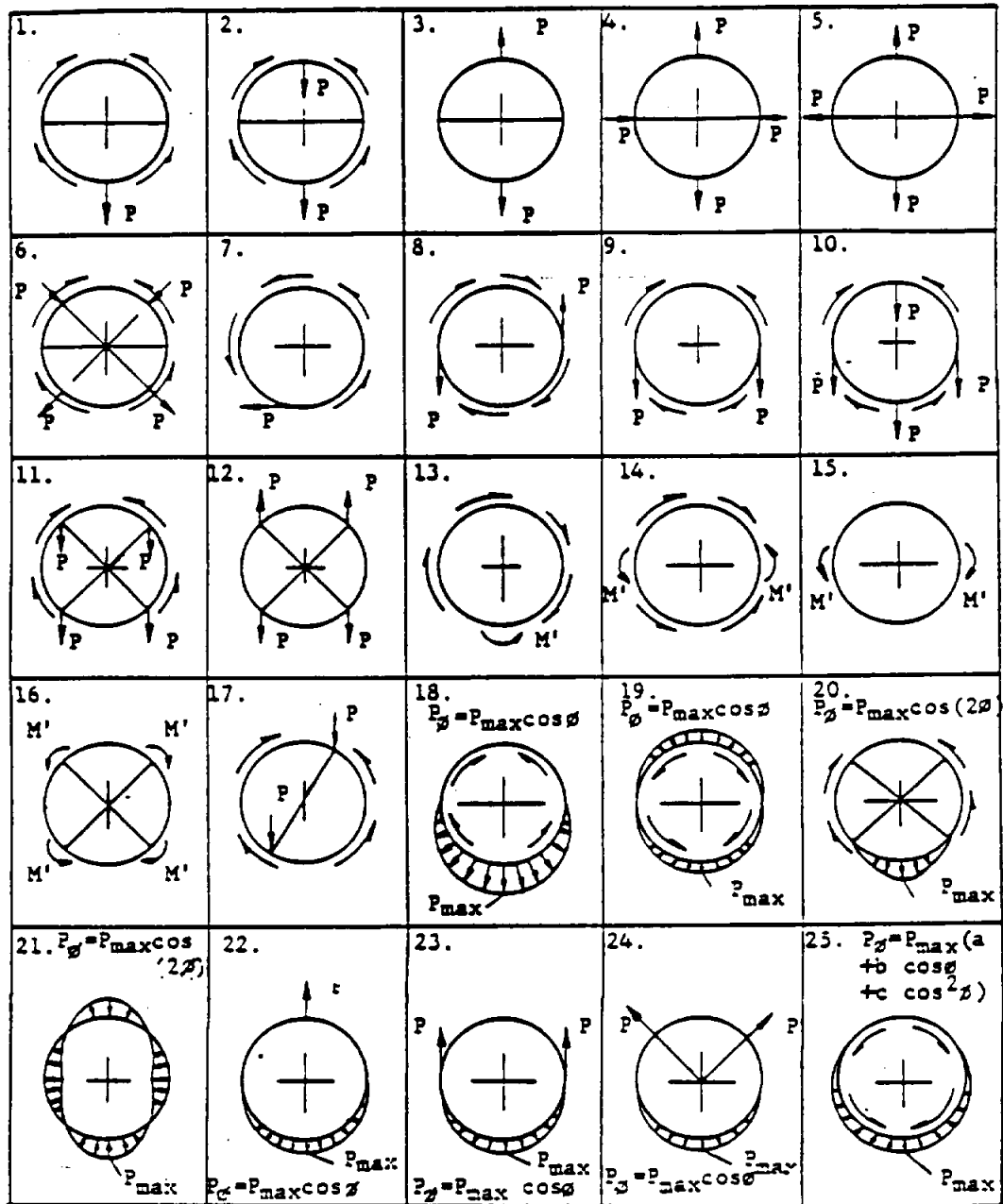
Flexible ring analysis is given in Section 18.3

384

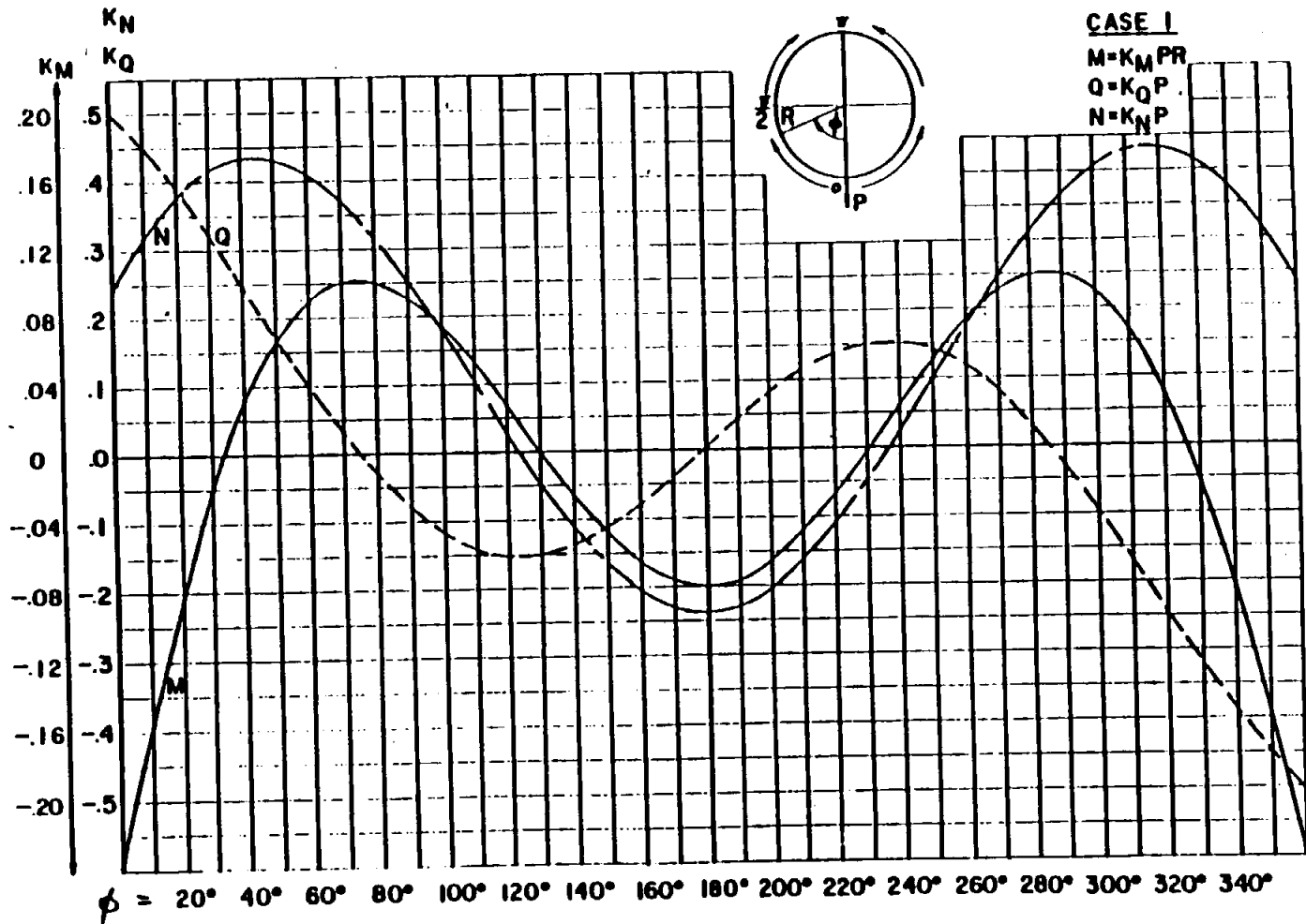
STRUCTURAL ANALYSIS MANUAL
GENERAL DYNAMICS/CONVAIR AND SPACE SYSTEMS DIVISION

B 6.1.1 In-Plane Load Cases (Cont'd)

Index

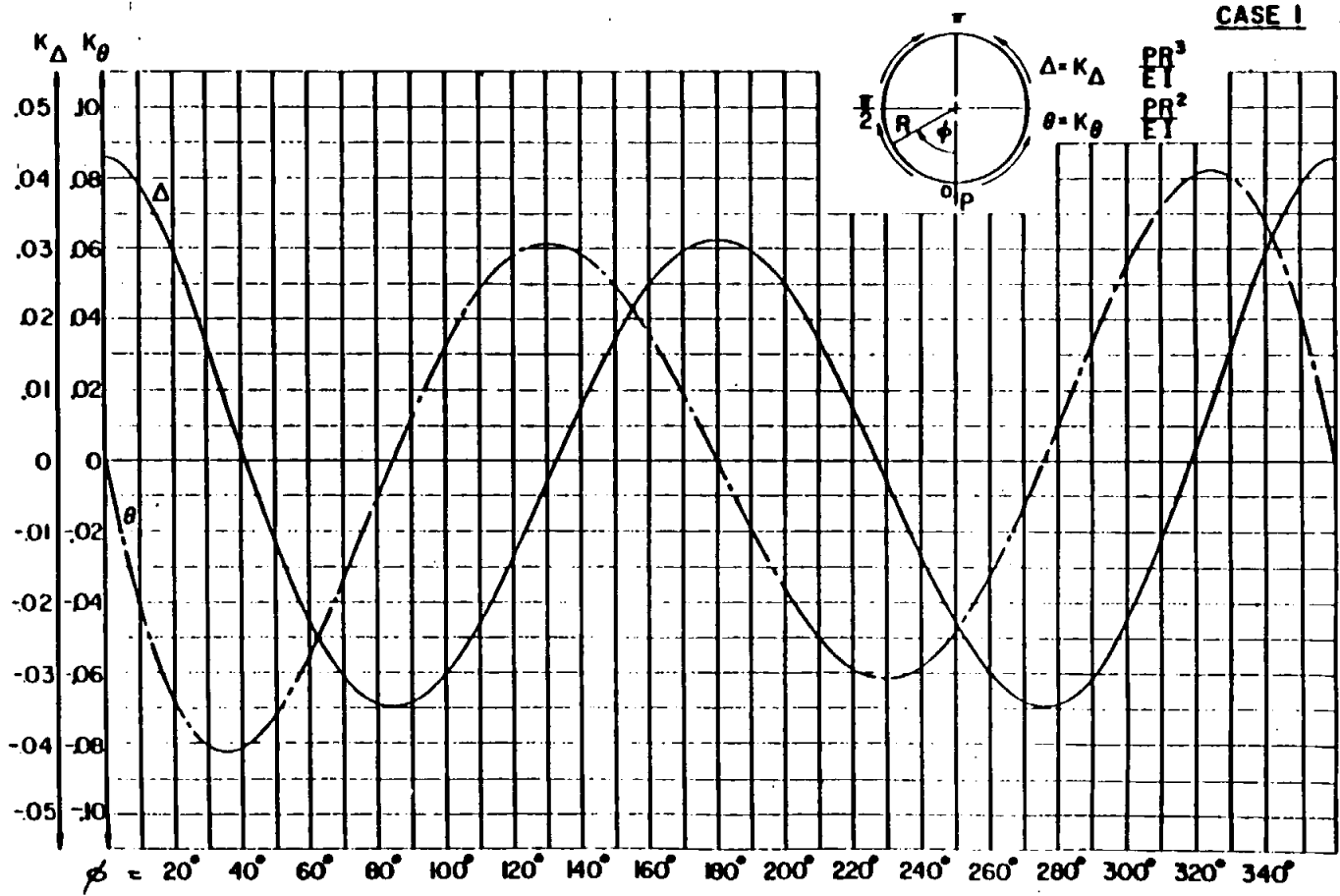


B 6.1.1.1 In-Plane Load Cases (Cont'd)

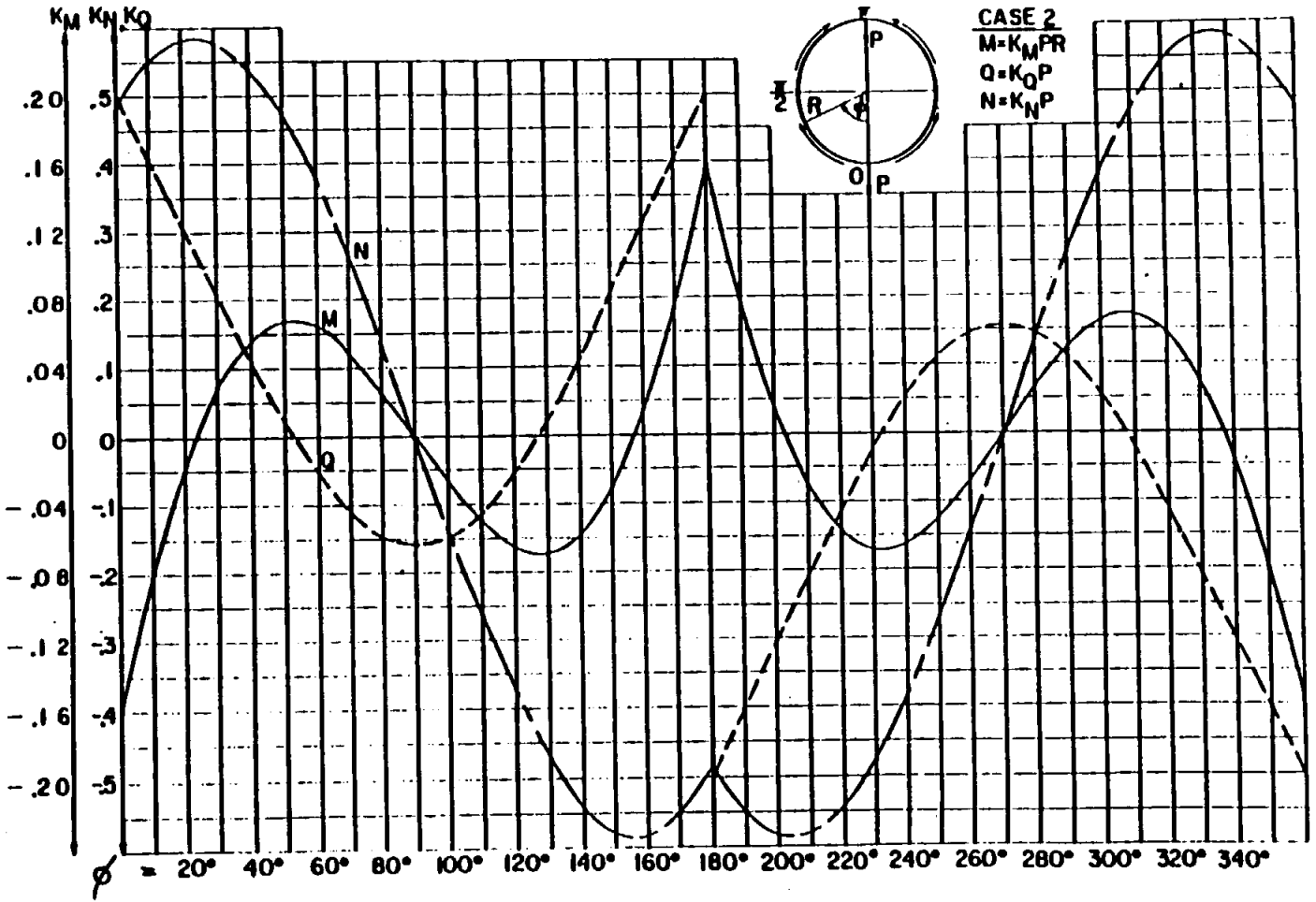


B 6.1.1 In-Plane Load Cases (Cont'd)

CASE I

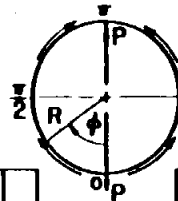


8 6.1.1.1 In-Plane Load Cases (Cont'd)



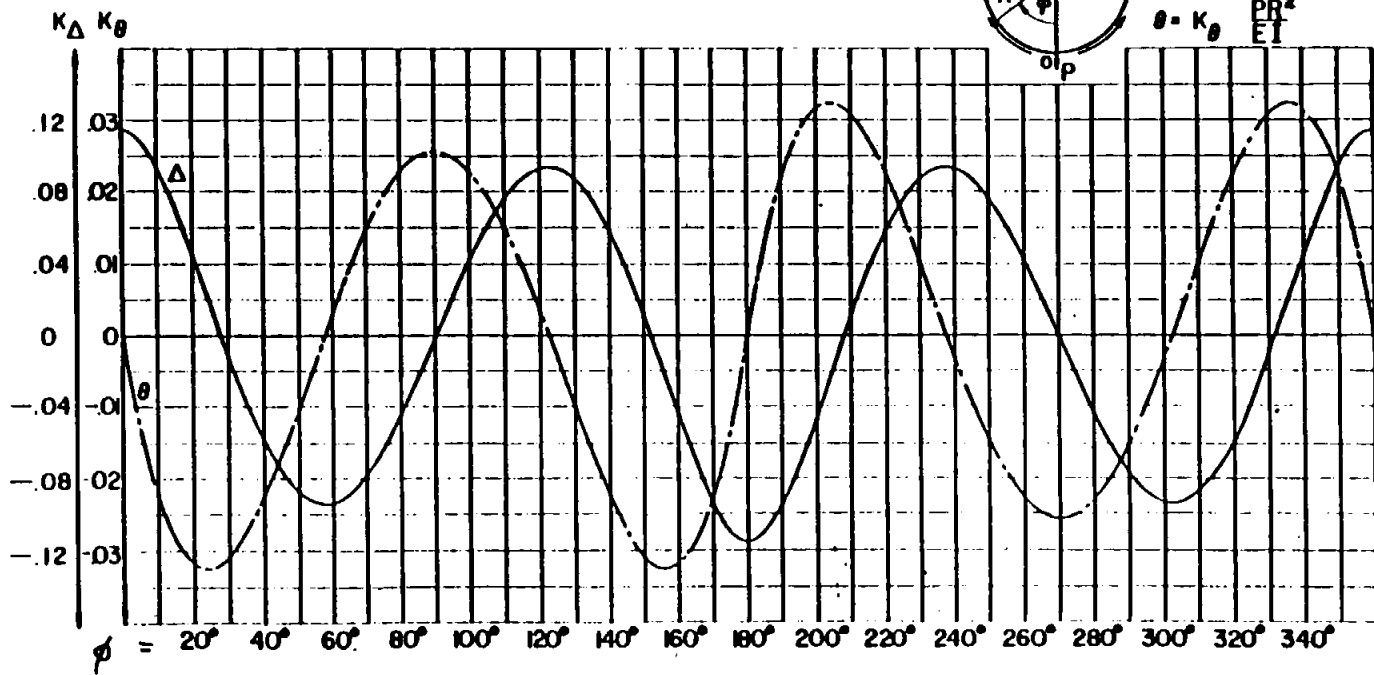
B 6.1.1 In-Plane Load Cases (Cont'd)

CASE 2

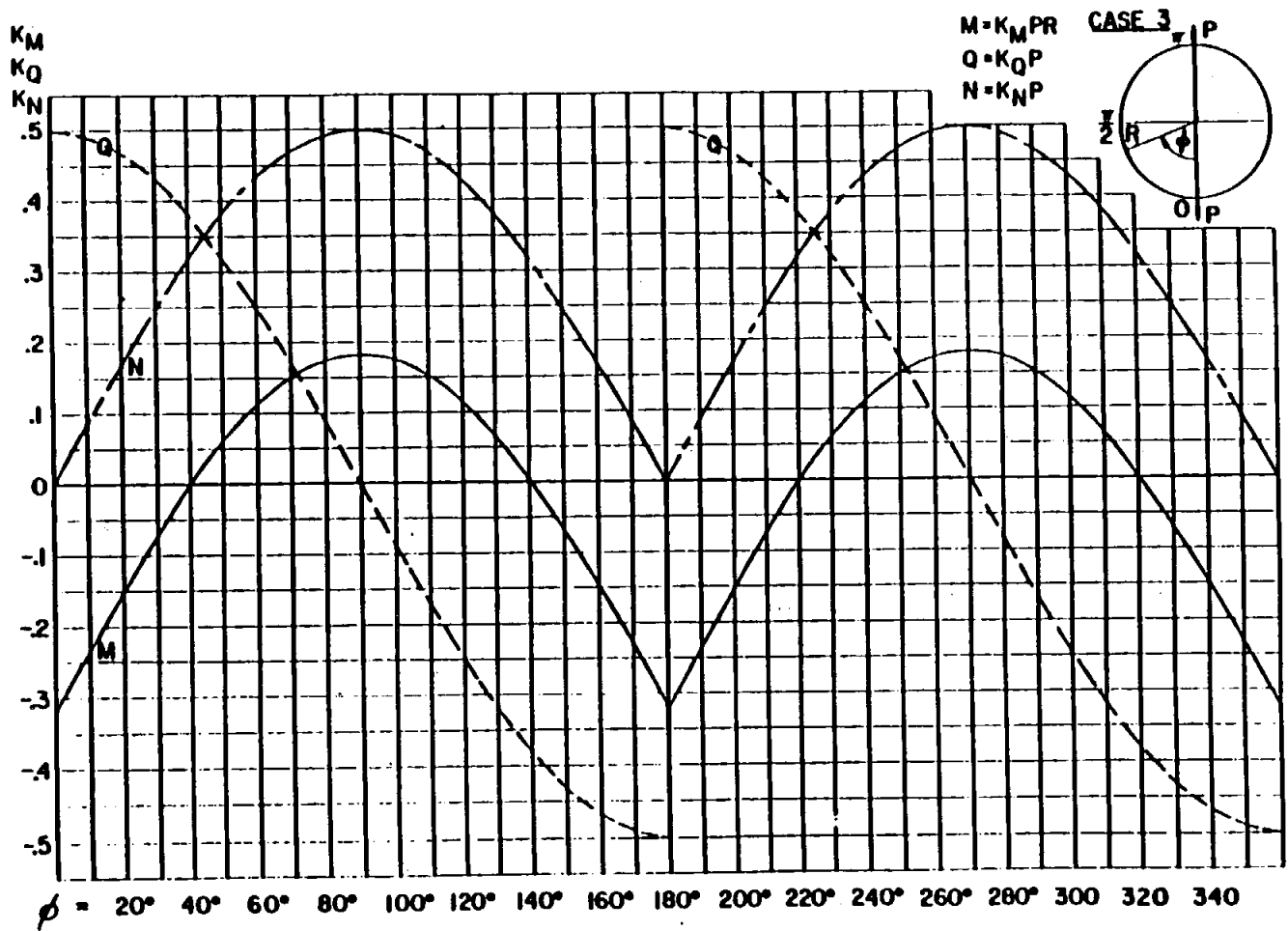


$$\Delta = K_{\Delta} \frac{PR^3}{EI}$$

$$\theta = K_{\theta} \frac{PR^2}{EI}$$



3.6.1.1 In-Plane Load Cases (Cont'd)

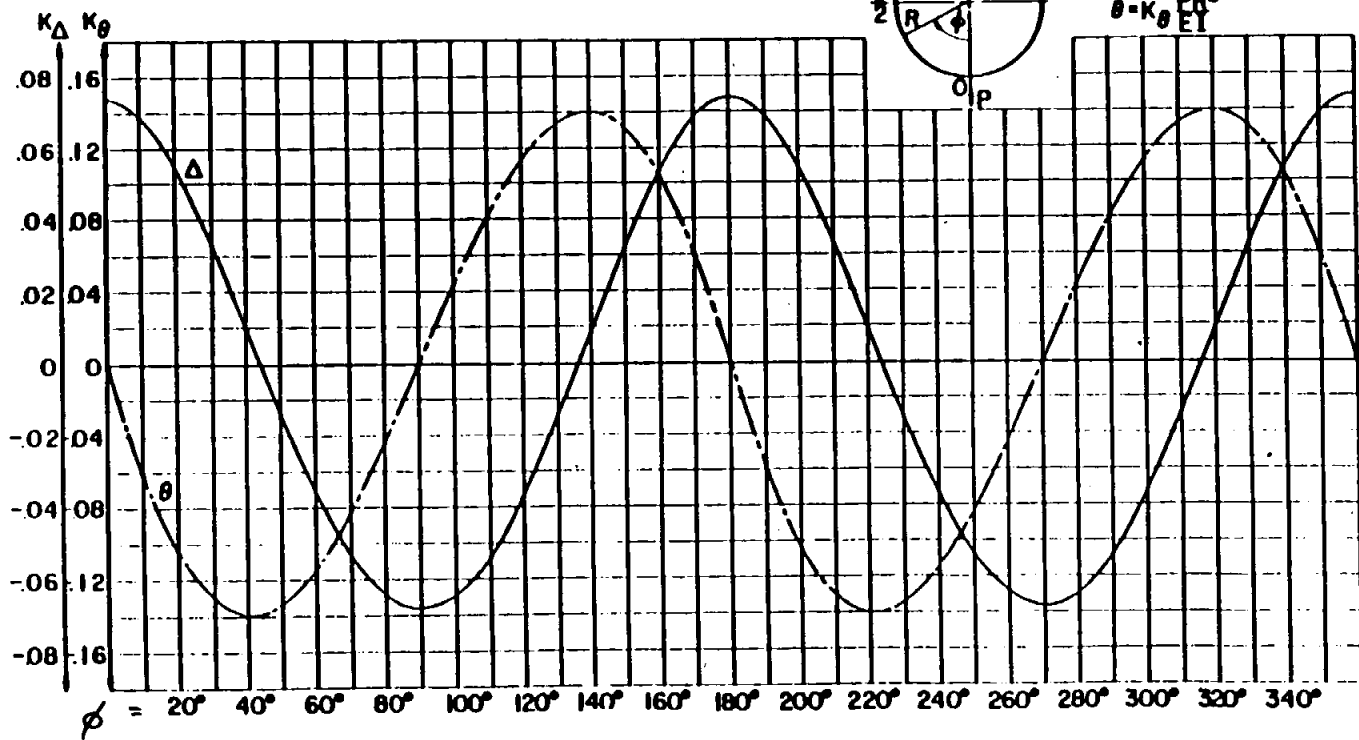
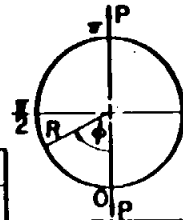


B 6.1.1 In-Plane Load Cases (Cont'd)

CASE 3

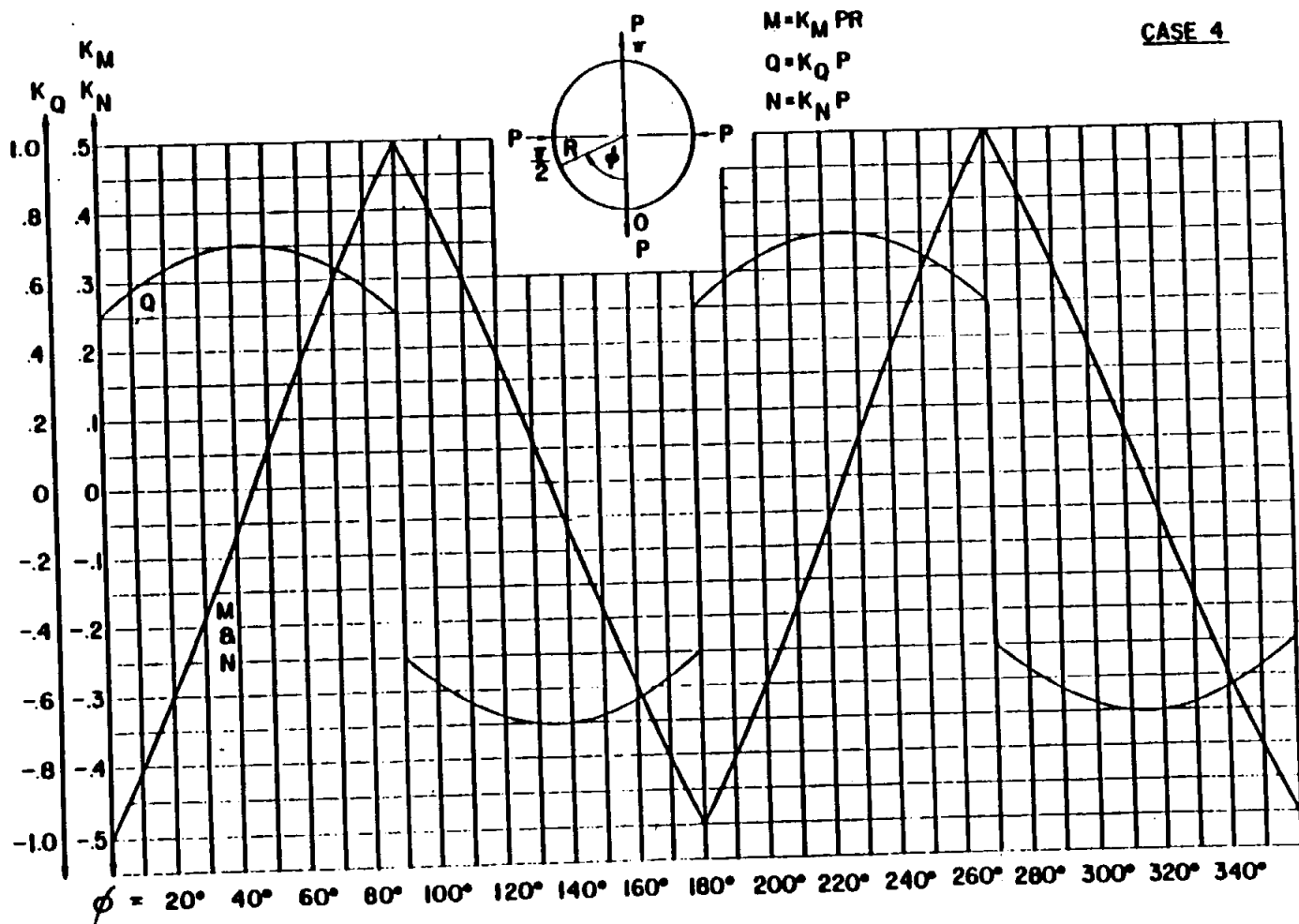
$$\Delta = K_{\Delta} \frac{PR^3}{EI}$$

$$\theta = K_{\theta} \frac{PR^2}{EI}$$

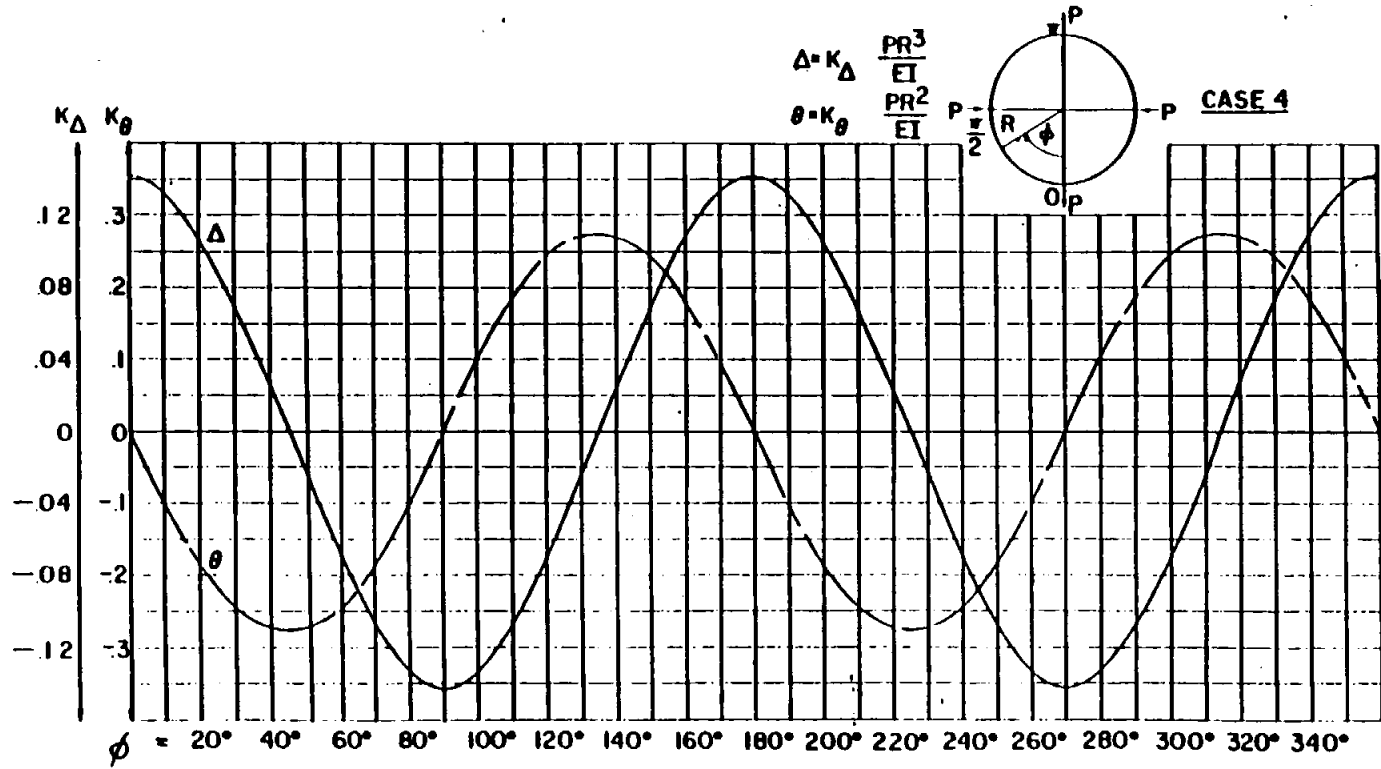


S 6.1.1 In-Plane Load Cases (Cont'd)

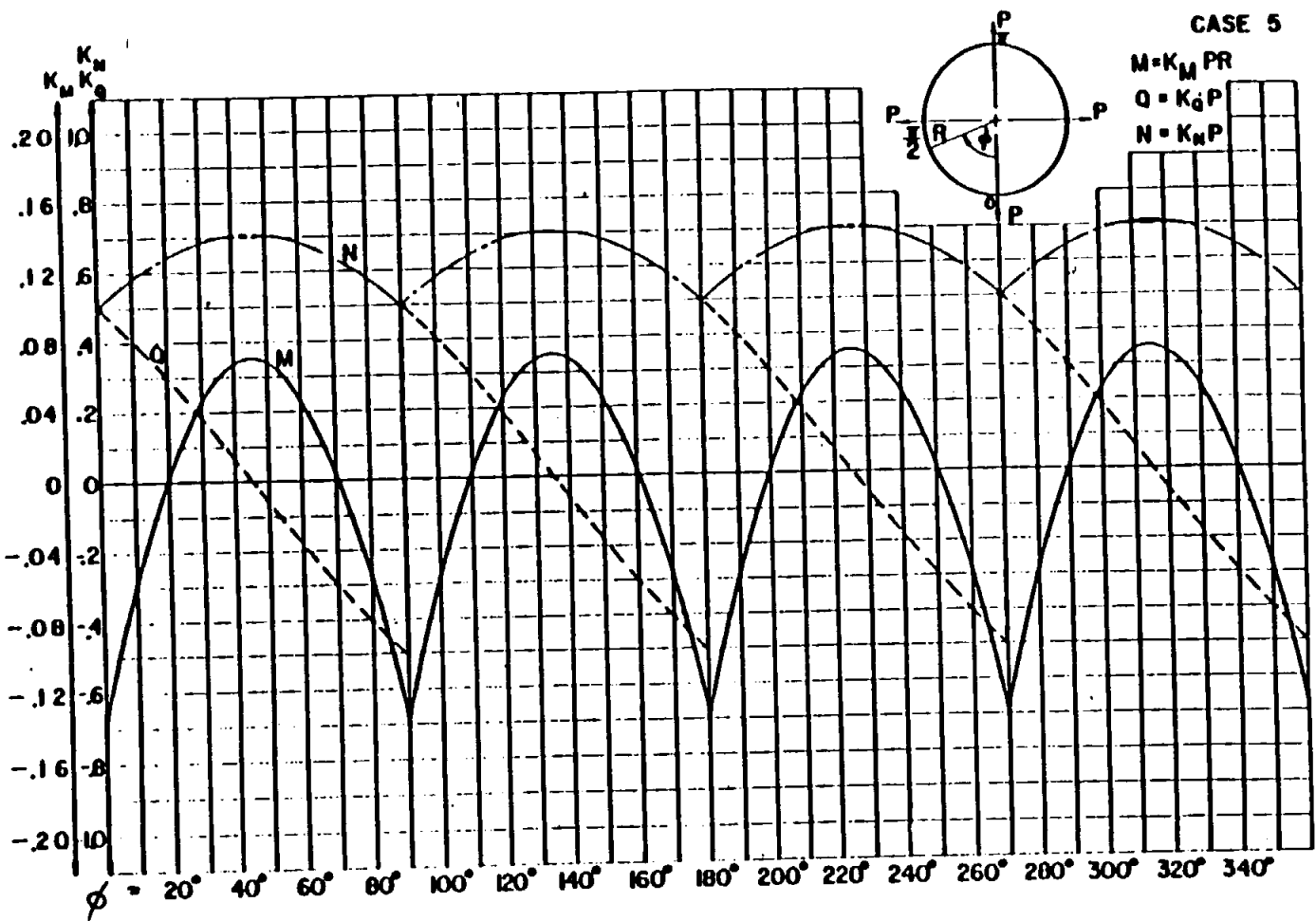
CASE 4



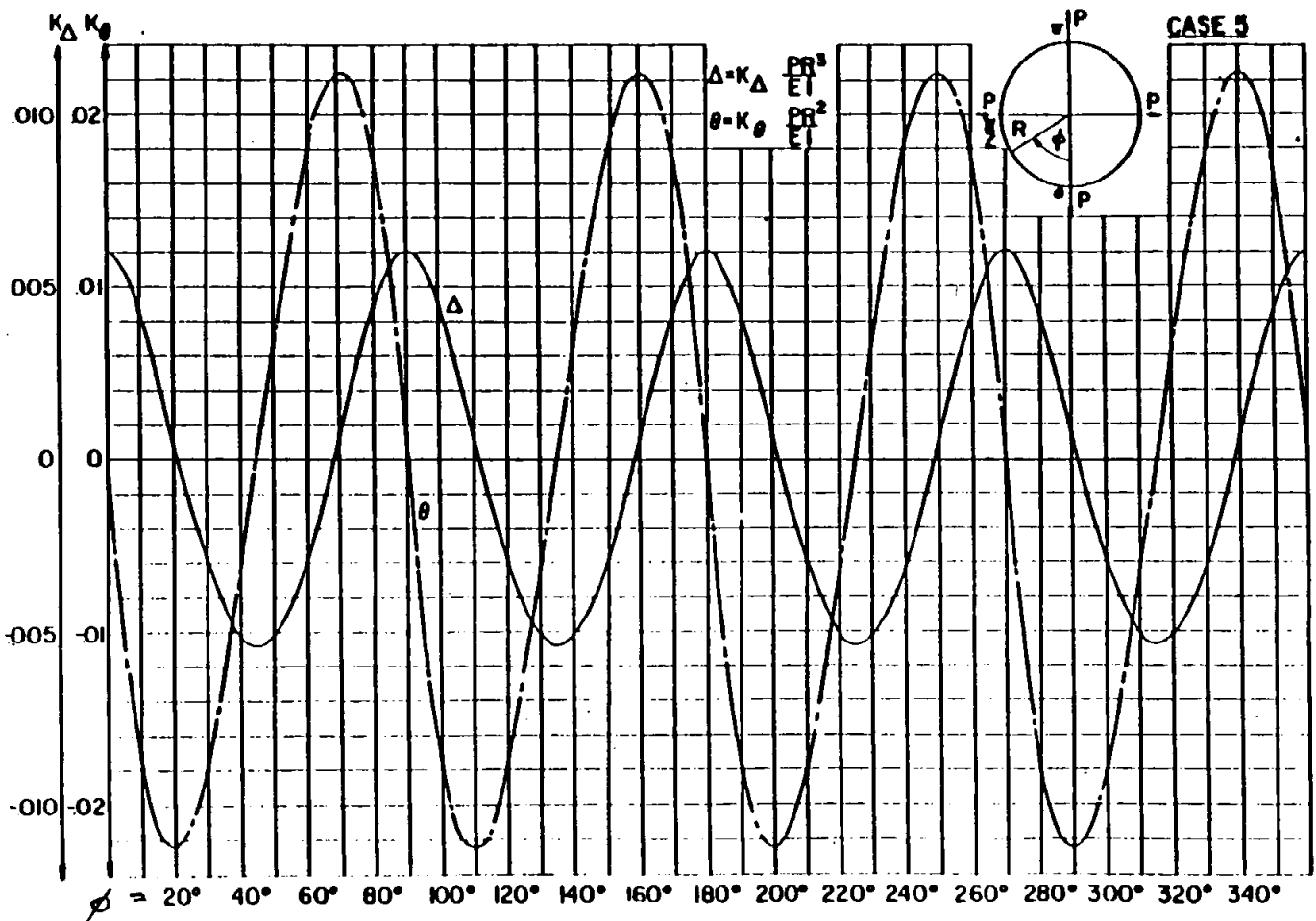
B 6.1.1 In-Plane Load Cases (Cont'd)



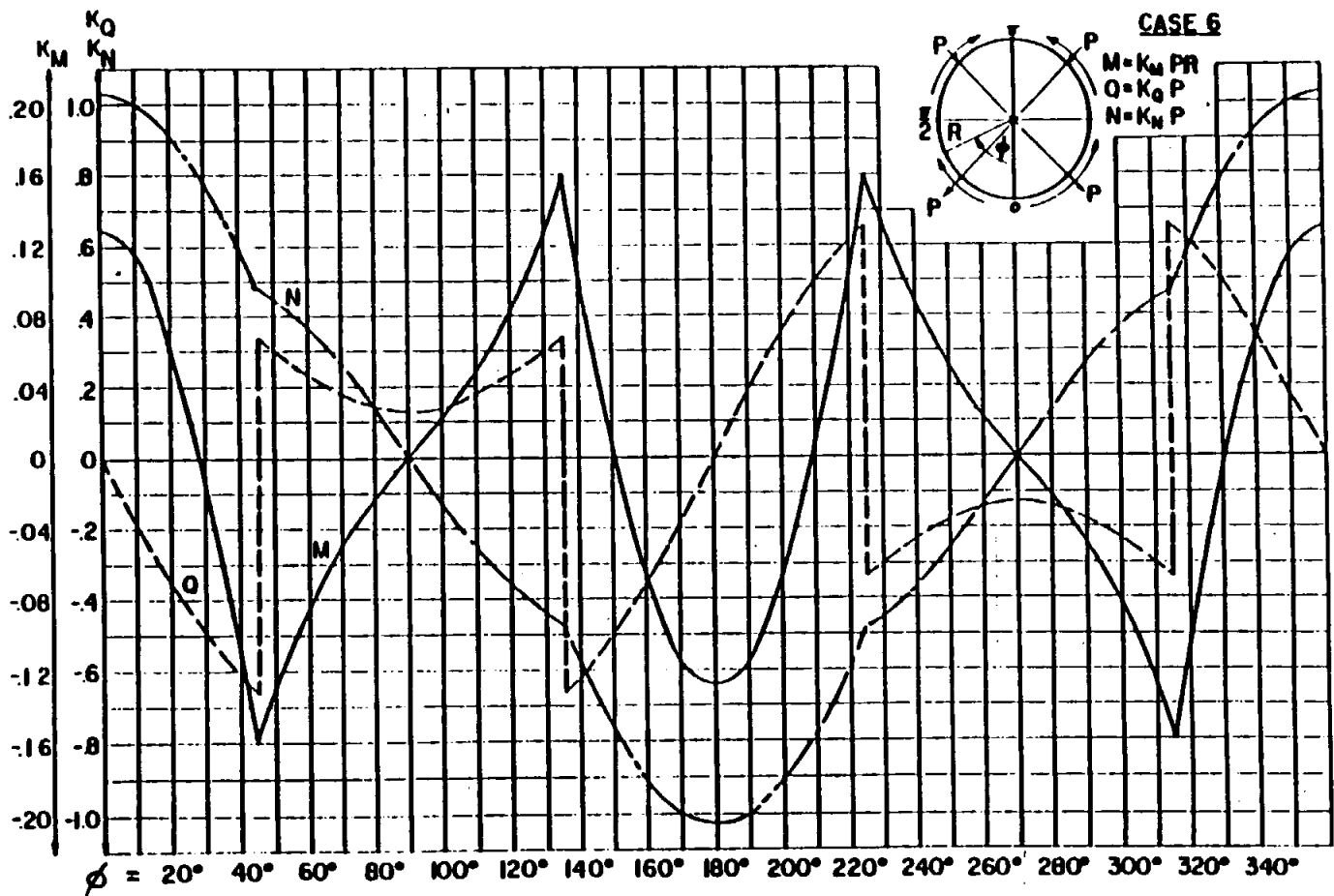
B 6.1.1.1 In-Plane Load Cases (Cont'd)



B 6.1.1.1 In-Plane Load Cases (Cont'd)

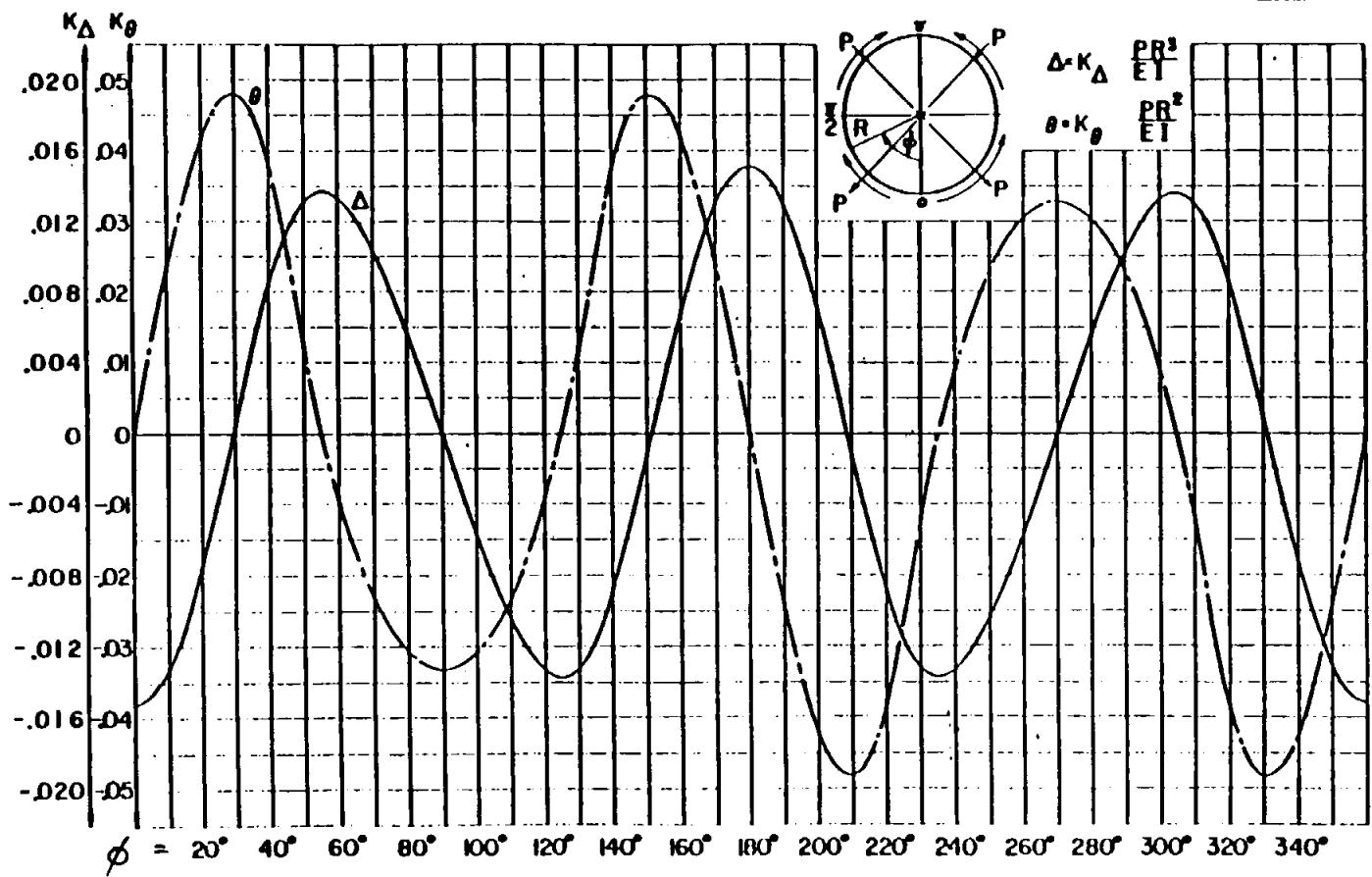


B 6.1.1.1 In-Plane Load Cases (Cont'd)



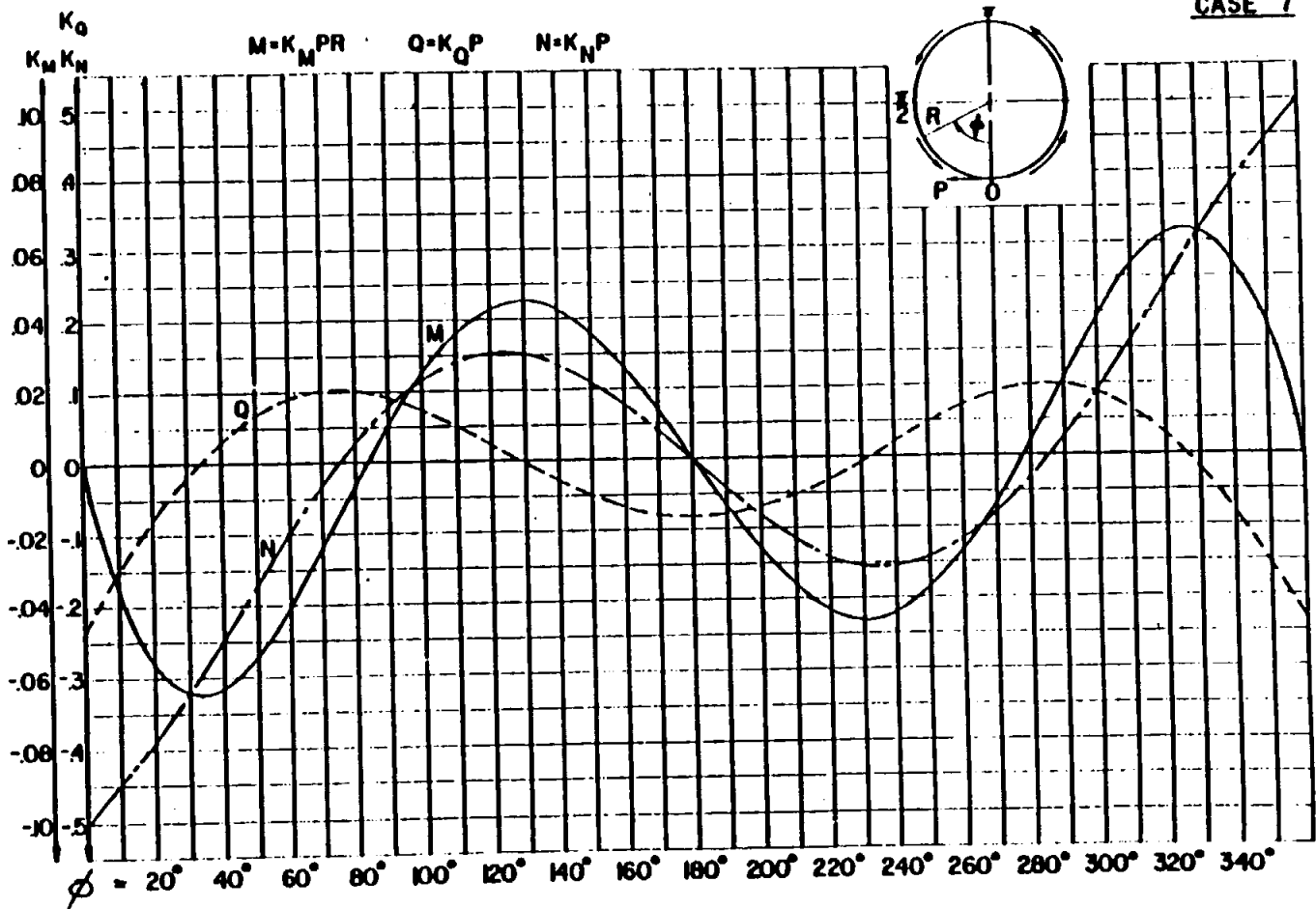
B 6.1.1 In-Plane Load Cases (Cont'd)

CASE 6



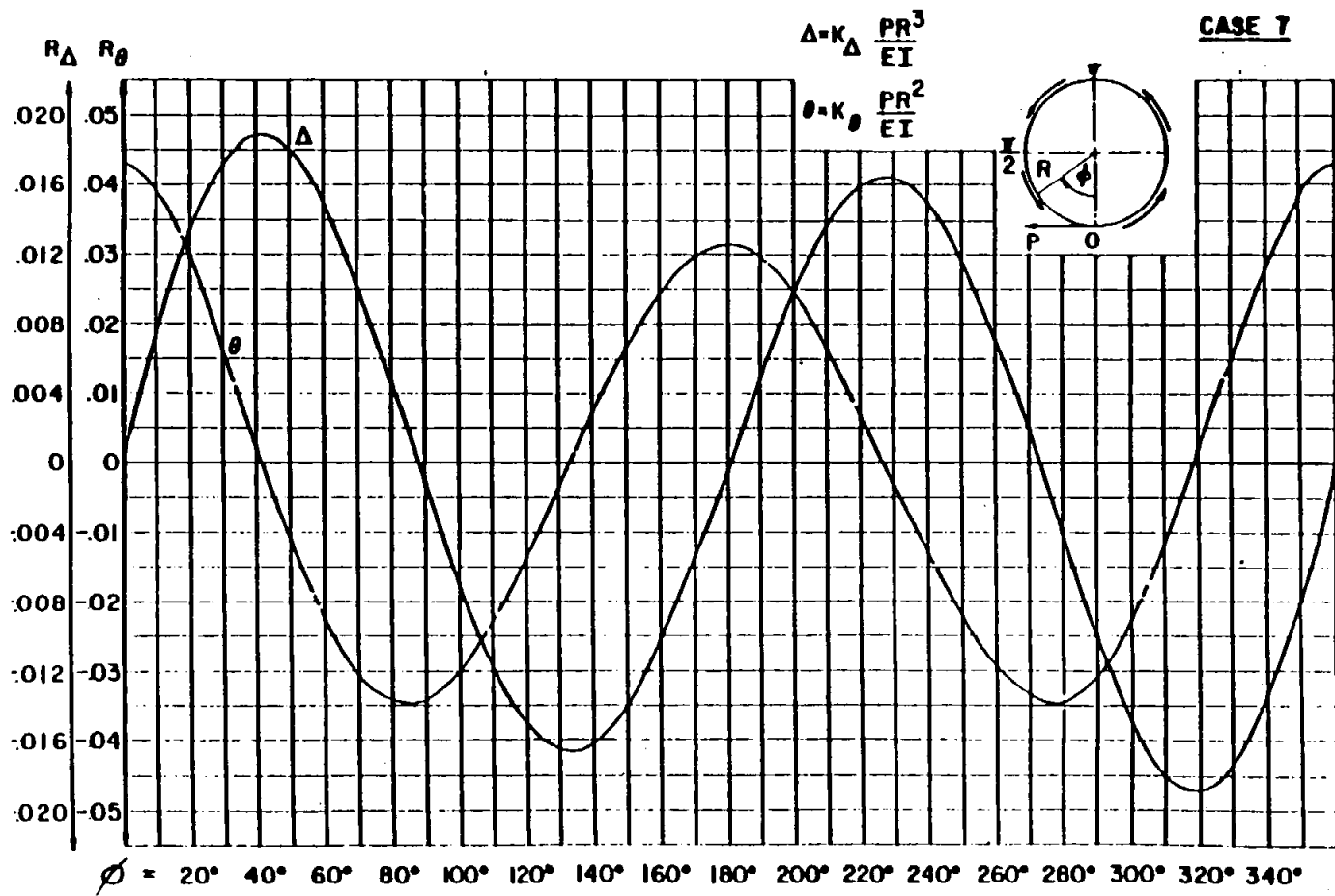
8.6.1.1 In-Plane Load Cases (Cont'd)

CASE 7



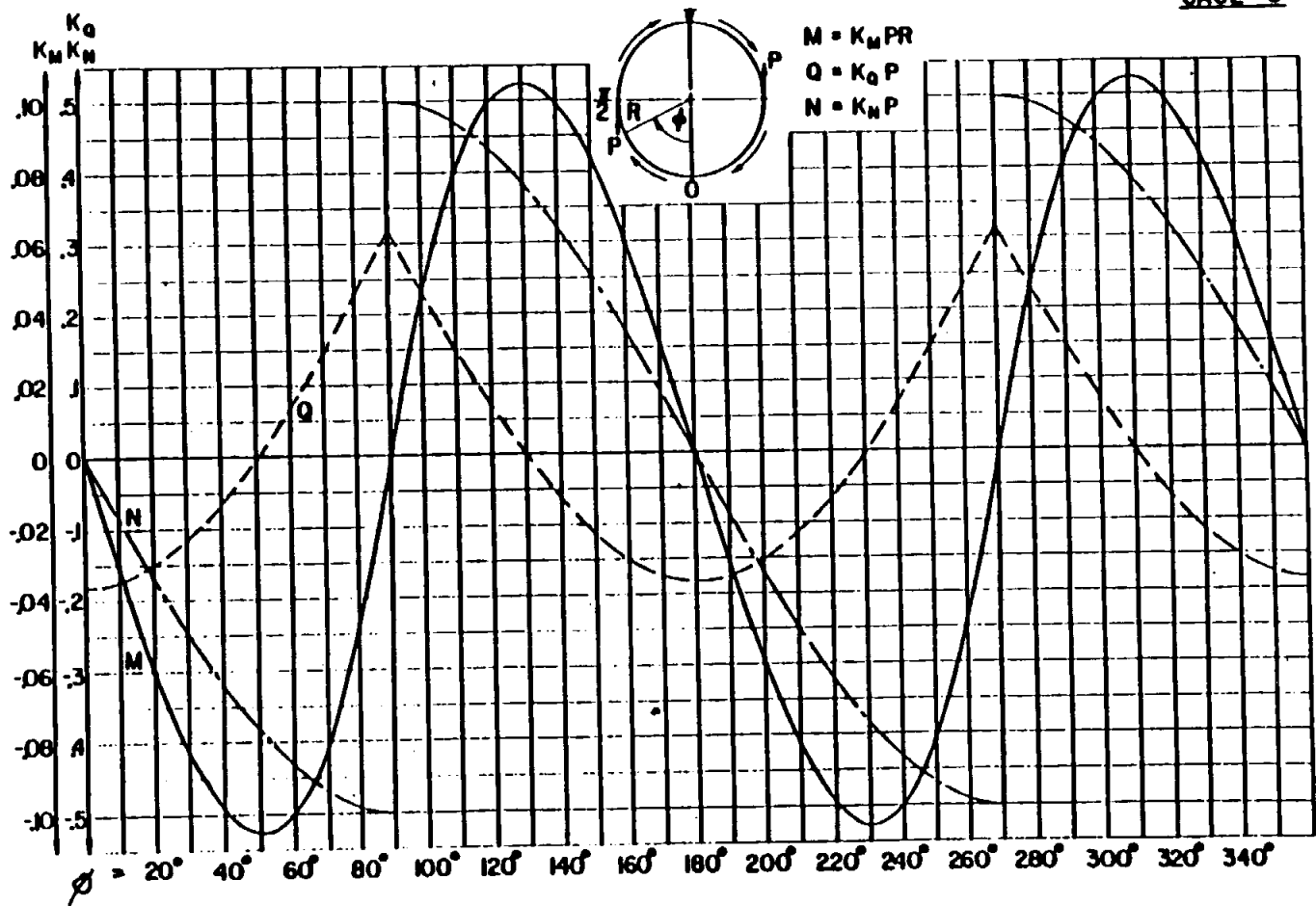
B 6.1.1.1 In-Plane Load Cases (Cont'd)

CASE 7



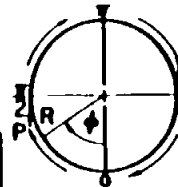
B 6.1.1.1 In-Plane Load Cases (Cont'd)

CASE 8



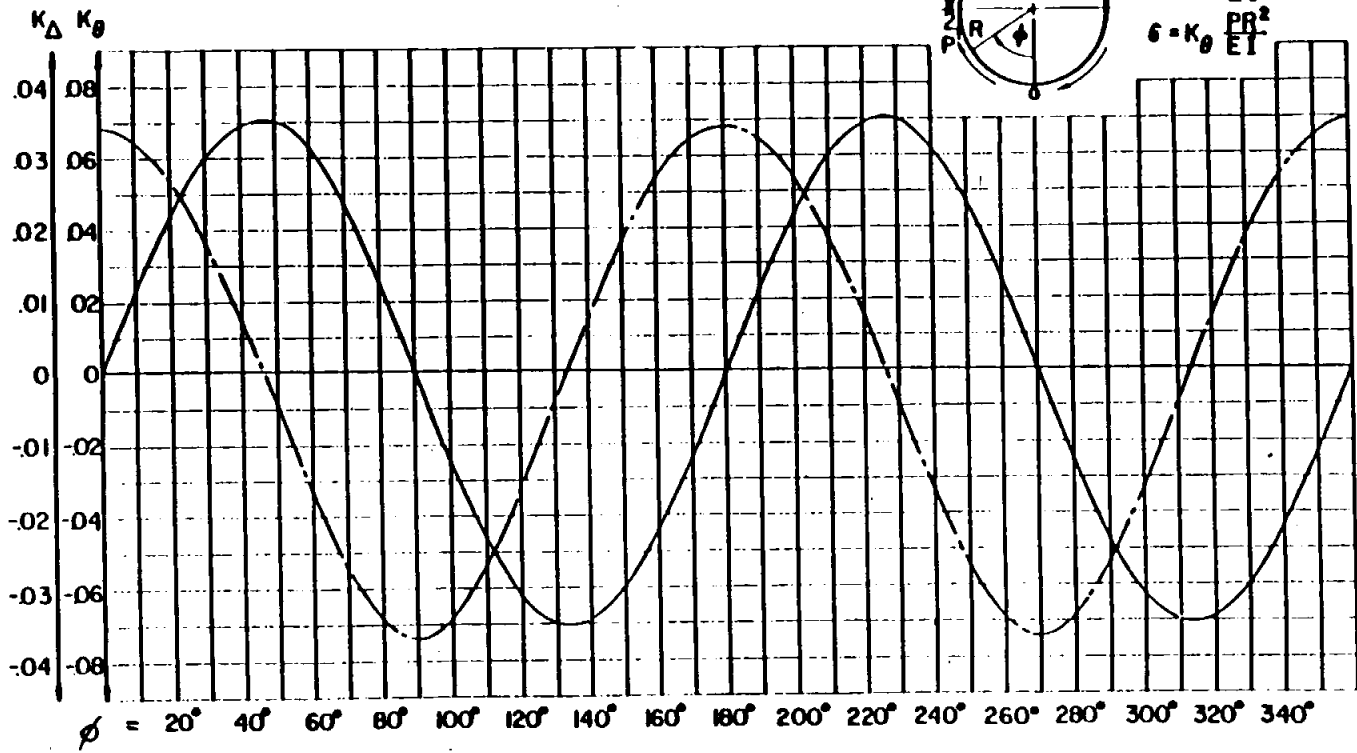
B 6.1.1.1 In-Plane Load Cases (Cont'd)

CASE 6

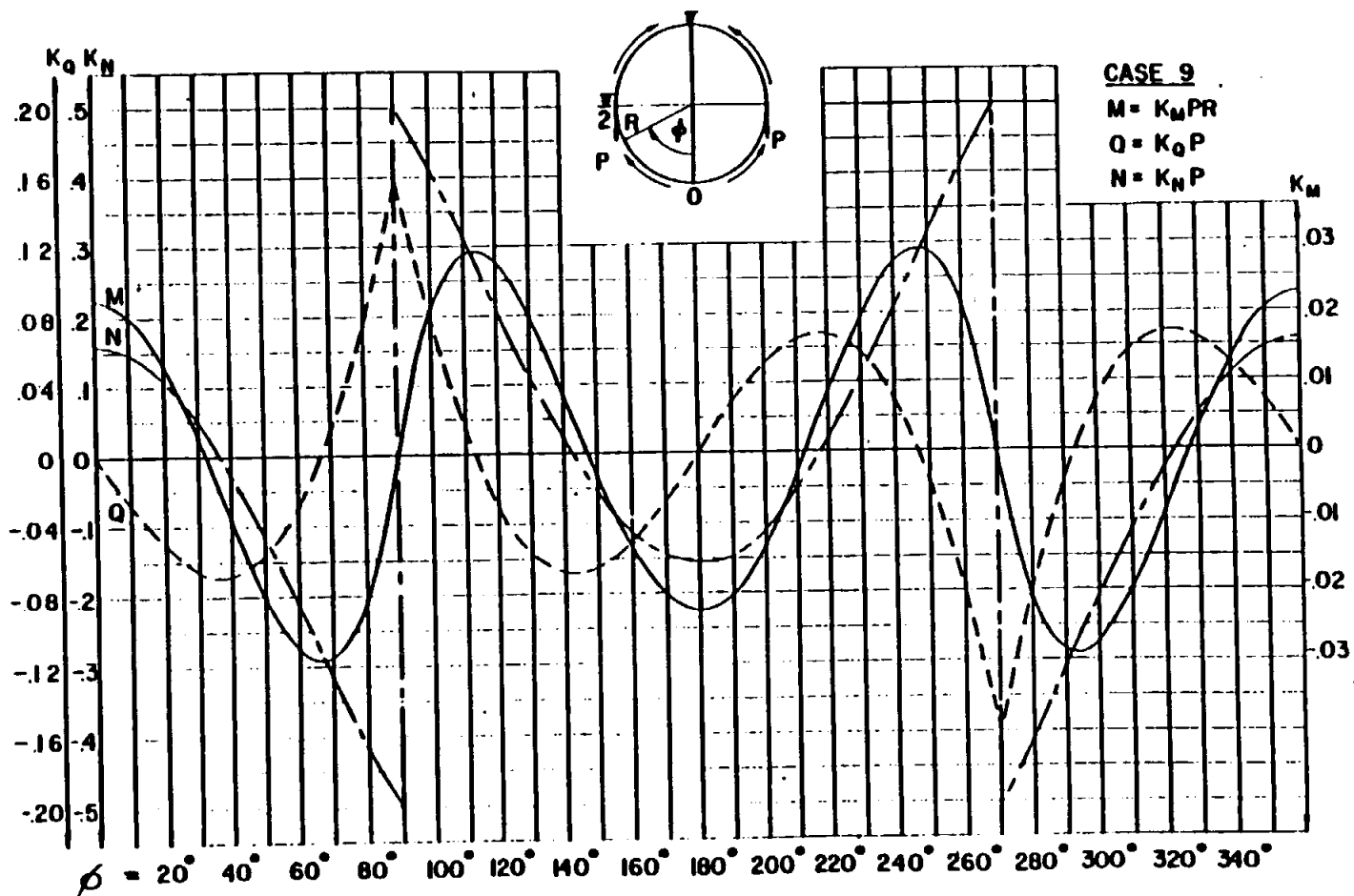


$$\Delta = K_{\Delta} \frac{PR^3}{ET}$$

$$\delta = K_{\delta} \frac{PR^2}{ET}$$

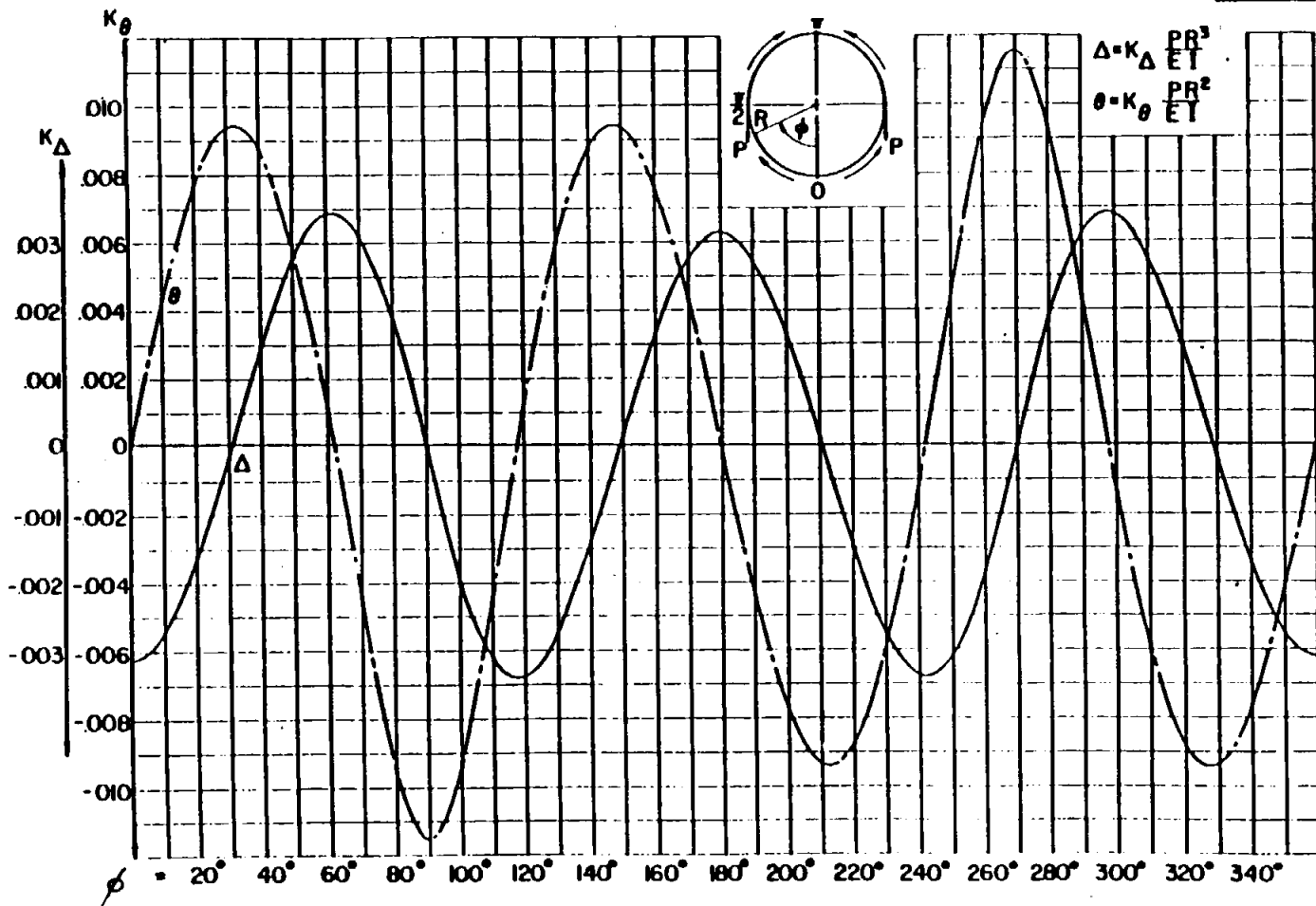


9.6.1.1 In-Plane Load Cases (Cont'd)

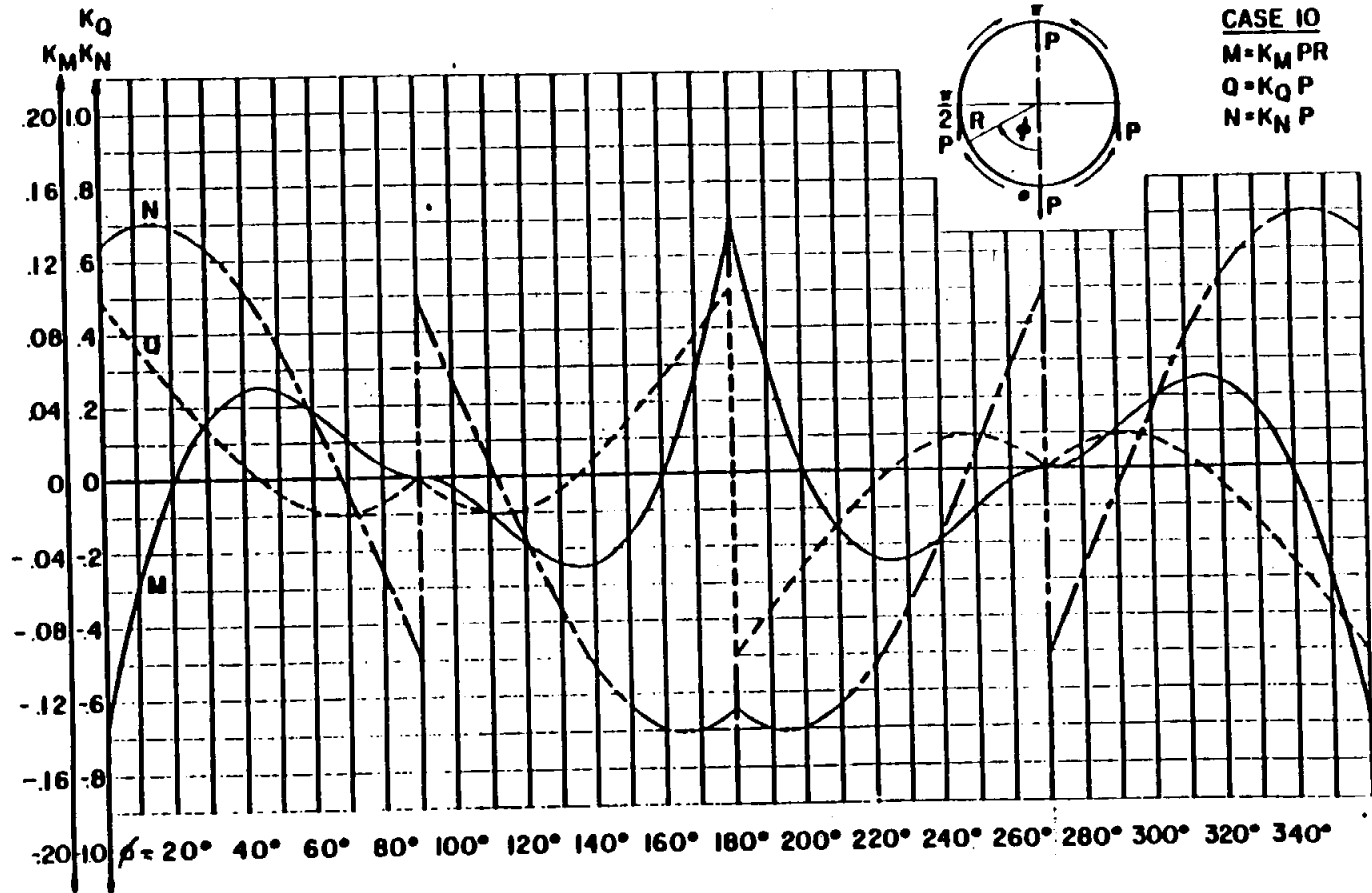


9 6.1.1 In-Plane Load Cases (Cont'd)

CASE 9



B 6.1.1.1 In-Plane Load Cases (Cont'd)

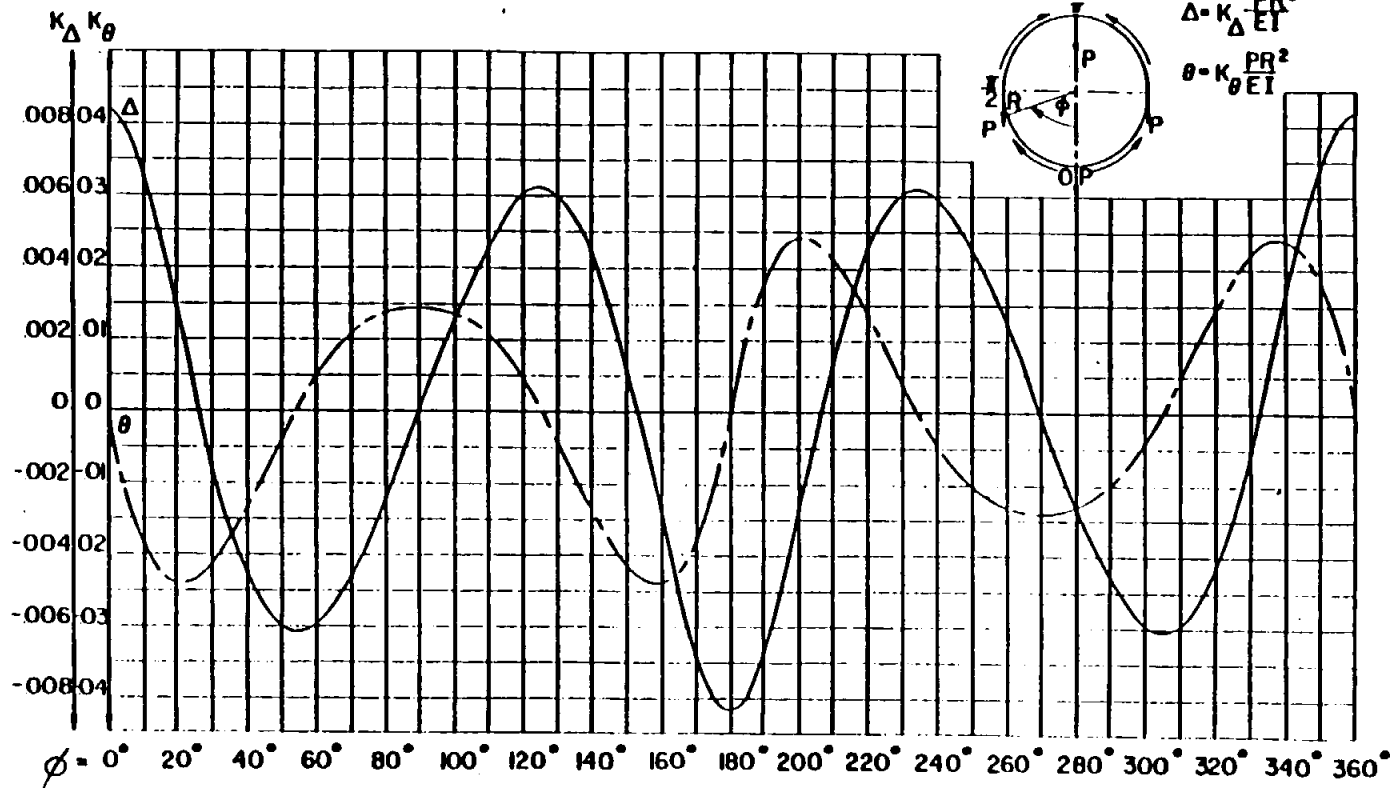
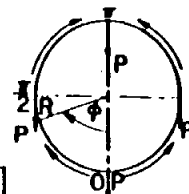


B 6.1.1 In-Plane Load Cases (Cont'd)

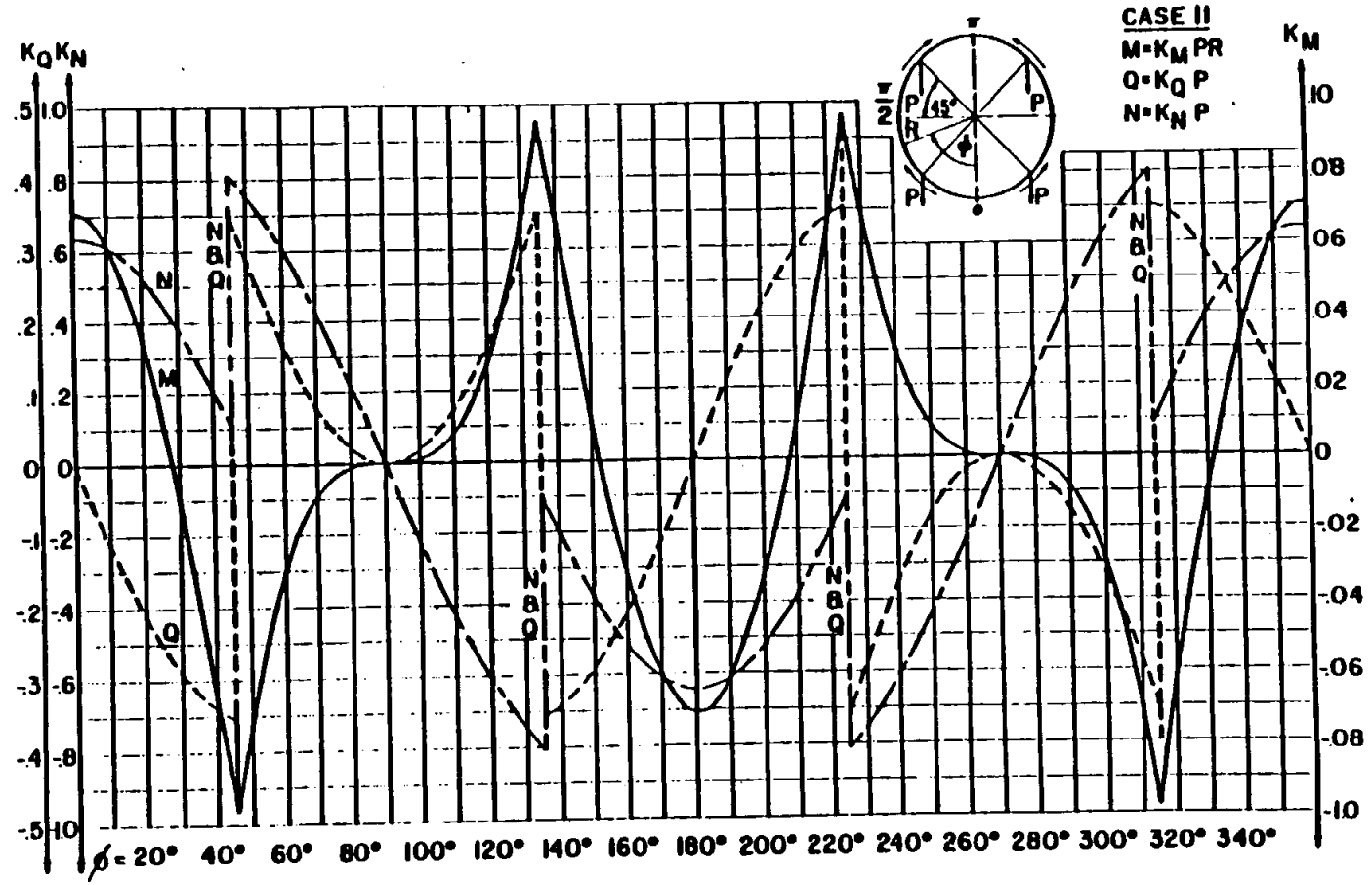
CASE 10

$$\Delta = K_{\Delta} \frac{PR^3}{EI}$$

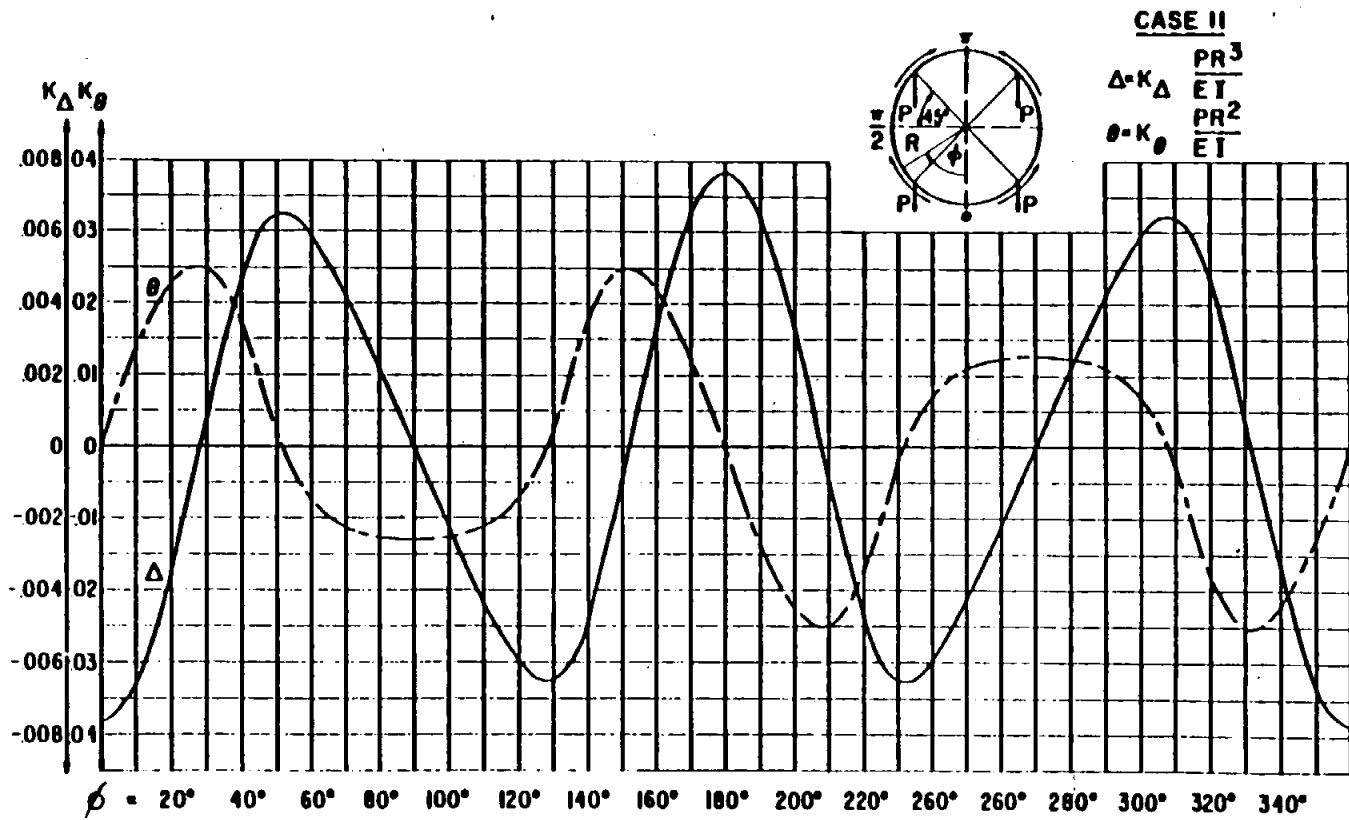
$$\theta = K_{\theta} \frac{PR^2}{EI}$$



B 6.1.1 In-Plane Load Cases (Cont'd)

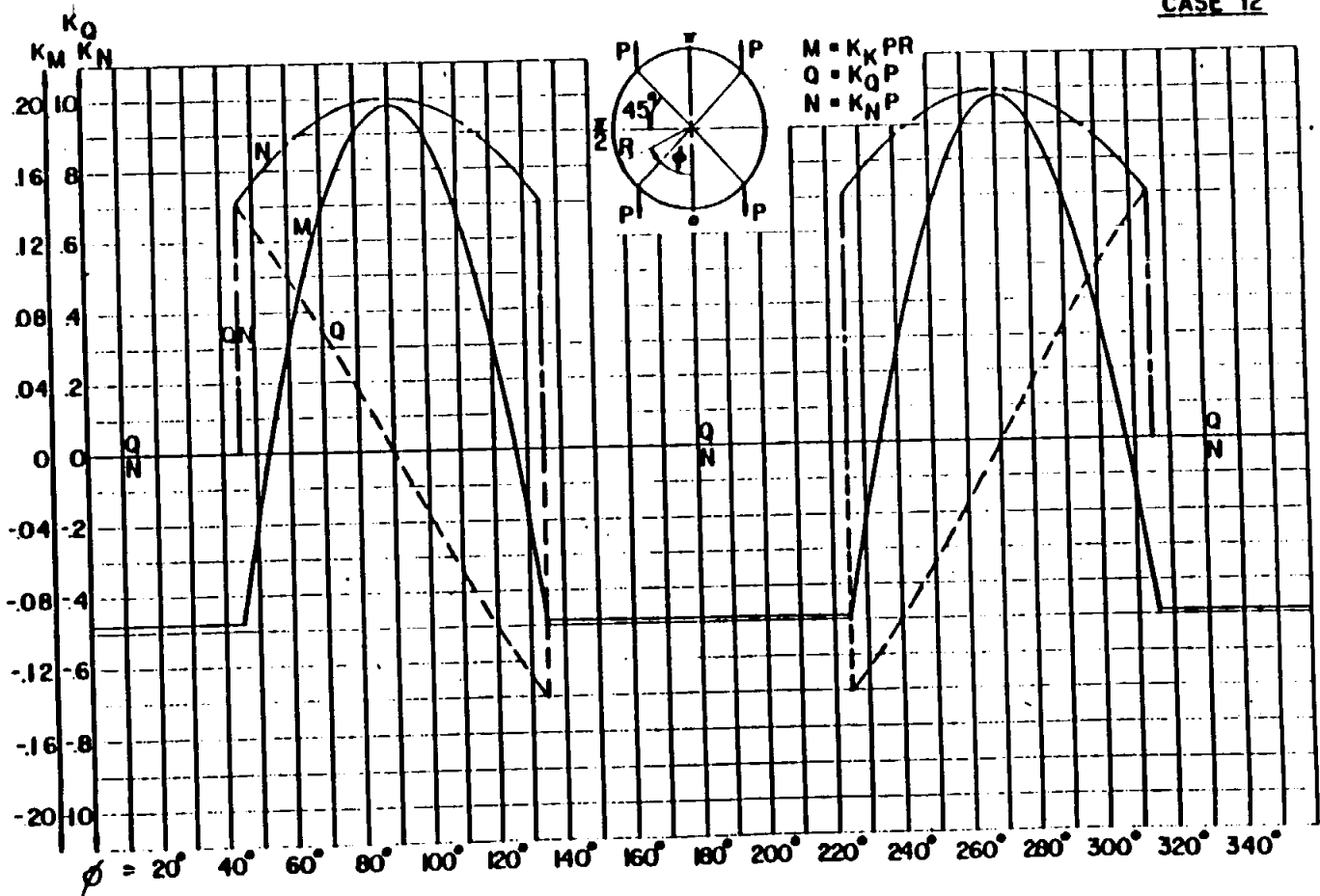


B 6.1.1 In-Plane Load Cases (Cont'd)



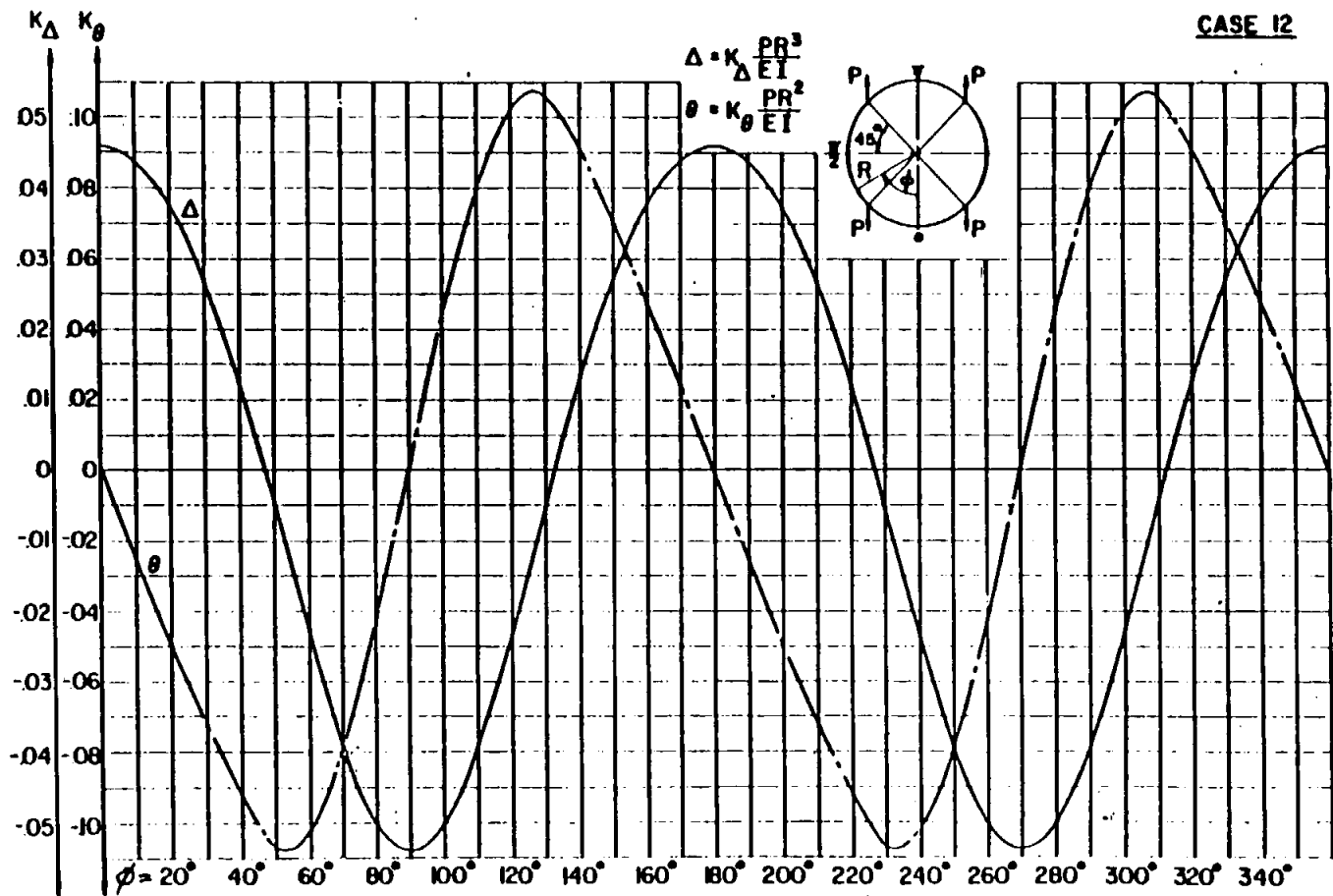
B 6.1.1.1 In-Plane Load Cases (Cont'd)

CASE 12



8 6.1.1.1 In-Plane Load Cases (Cont'd)

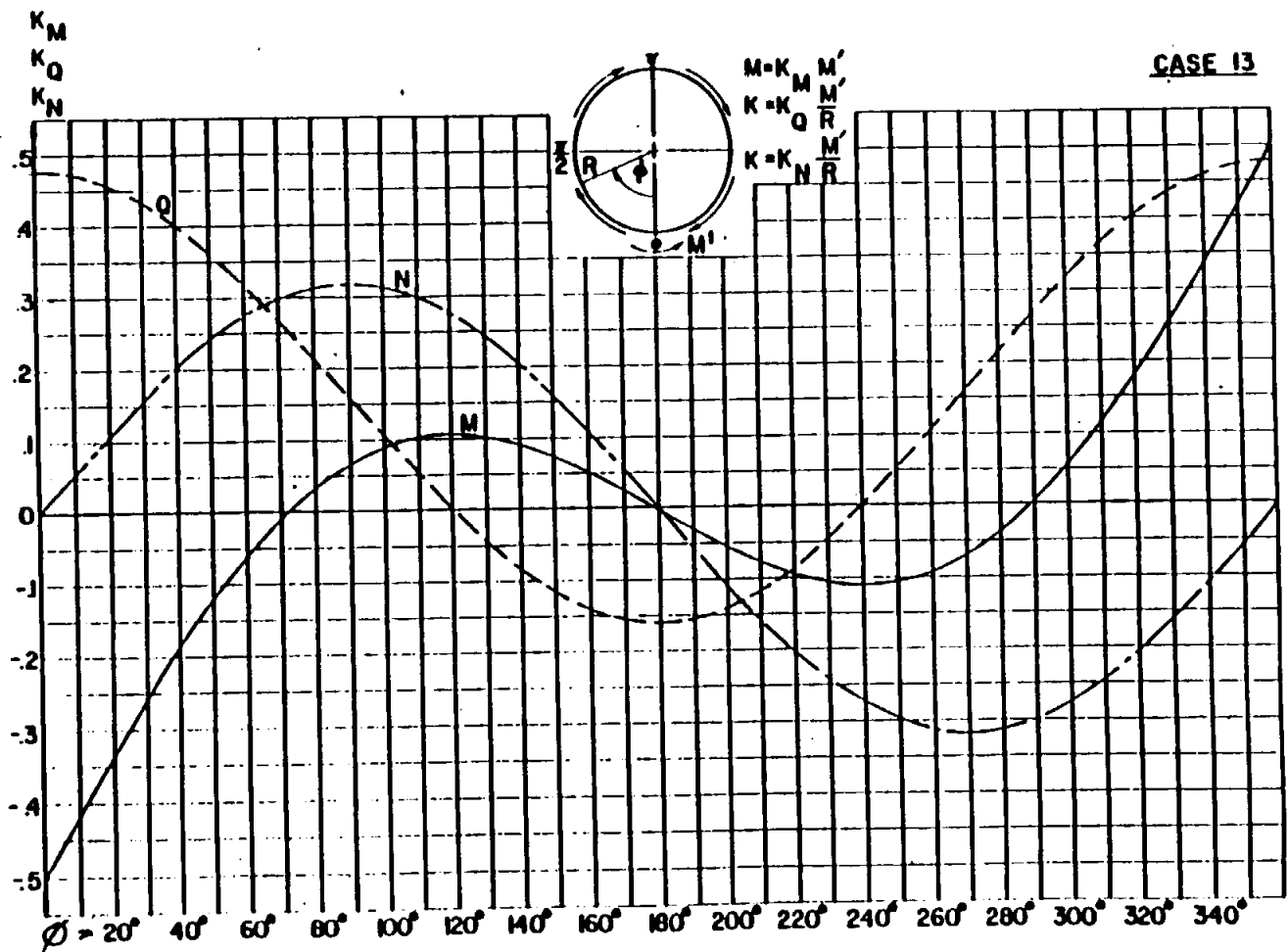
CASE 12



STRUCTURAL ANALYSIS MANUAL
GENERAL DYNAMICS/CONVAIR AND SPACE SYSTEMS DIVISION

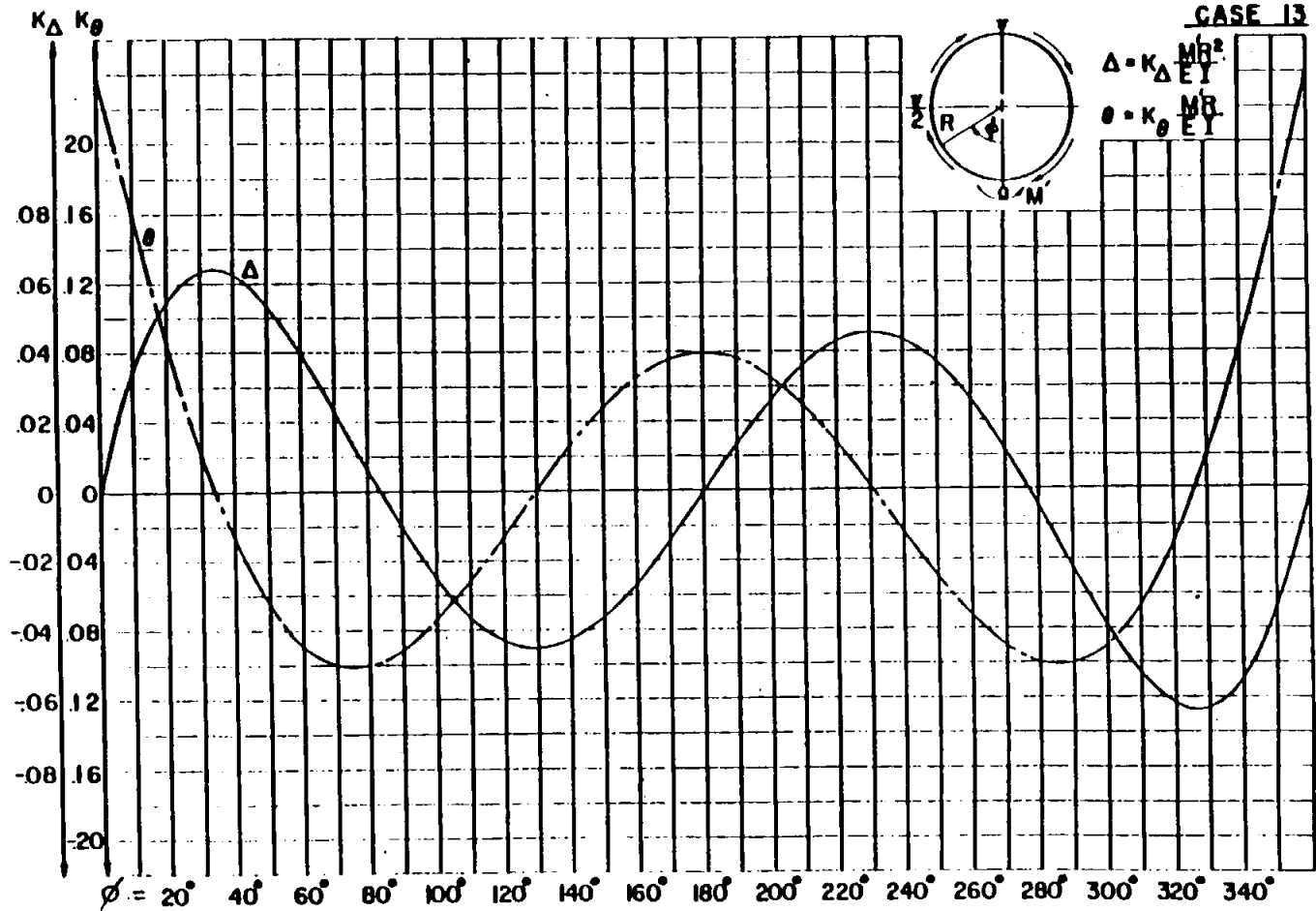
B 6.1.1.1 In-Plane Load Cases (Cont'd)

CASE 13



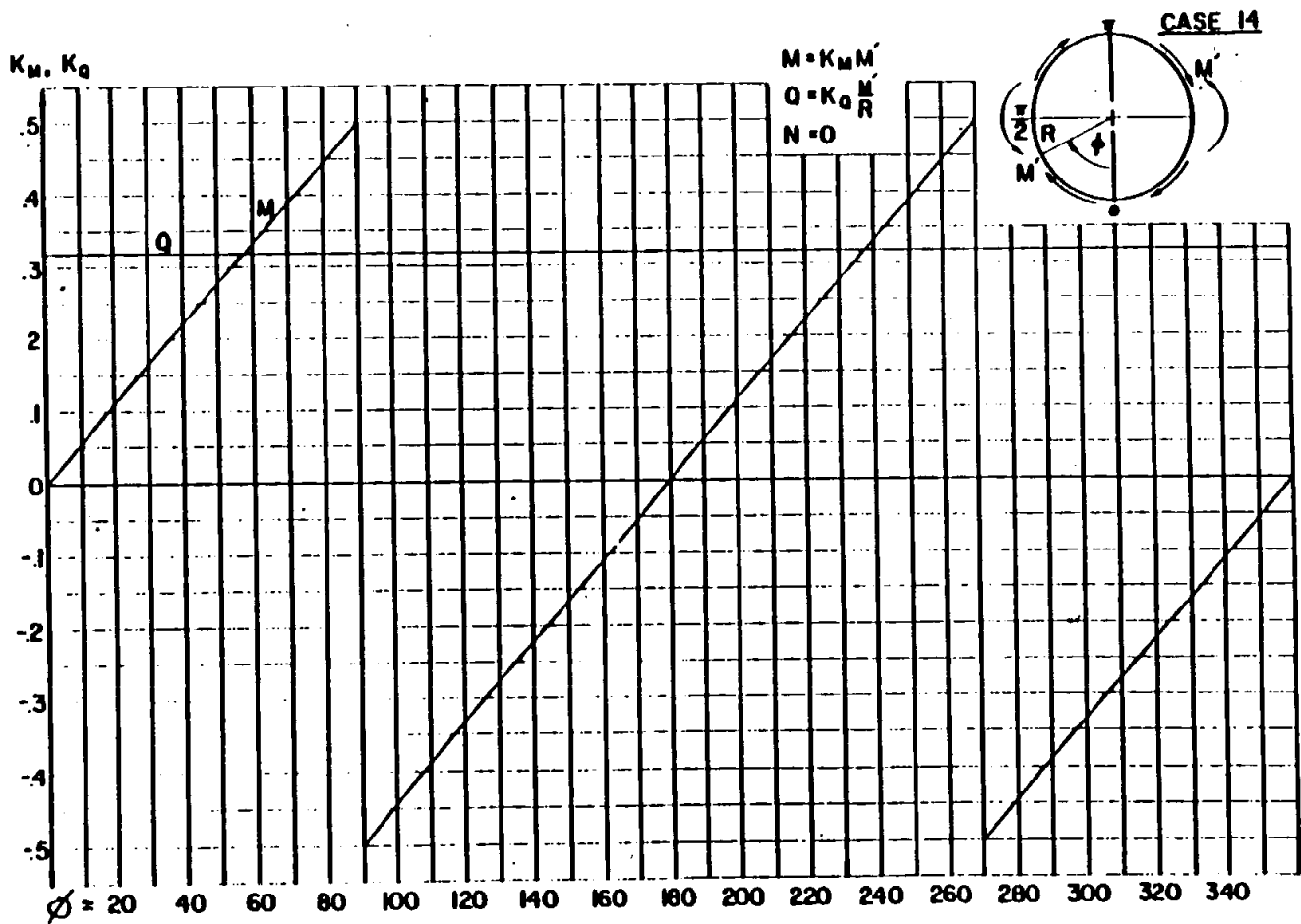
B 6.1.1.1 In-Plane Load Cases (Cont'd)

CASE 13



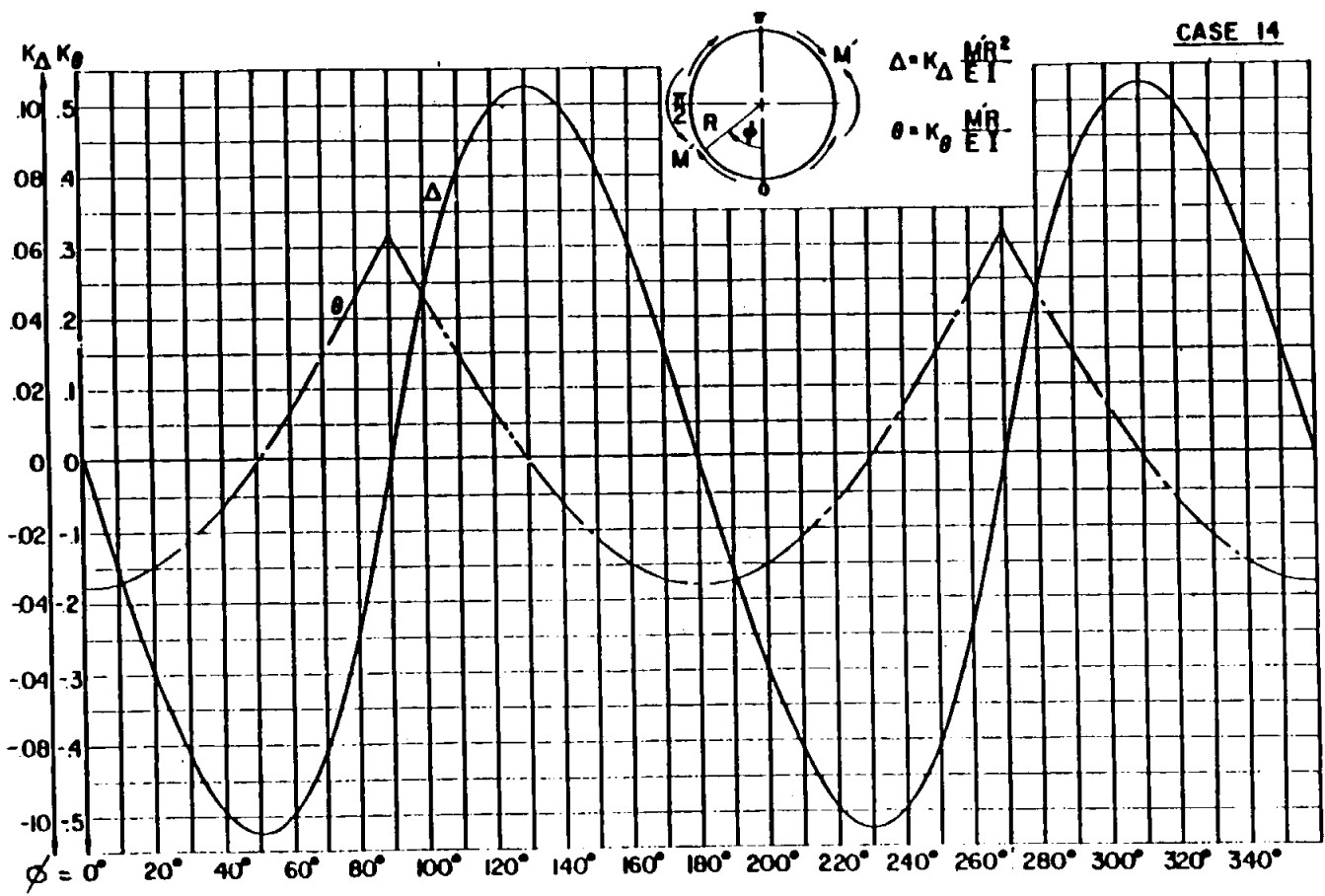
STRUCTURAL ANALYSIS MANUAL
GENERAL DYNAMICS/CONVAIR AND SPACE SYSTEMS DIVISION

B 6.1.1 In-Plane Load Cases (Cont'd)



8.6.1.1 In-Plane Load Cases (Cont'd)

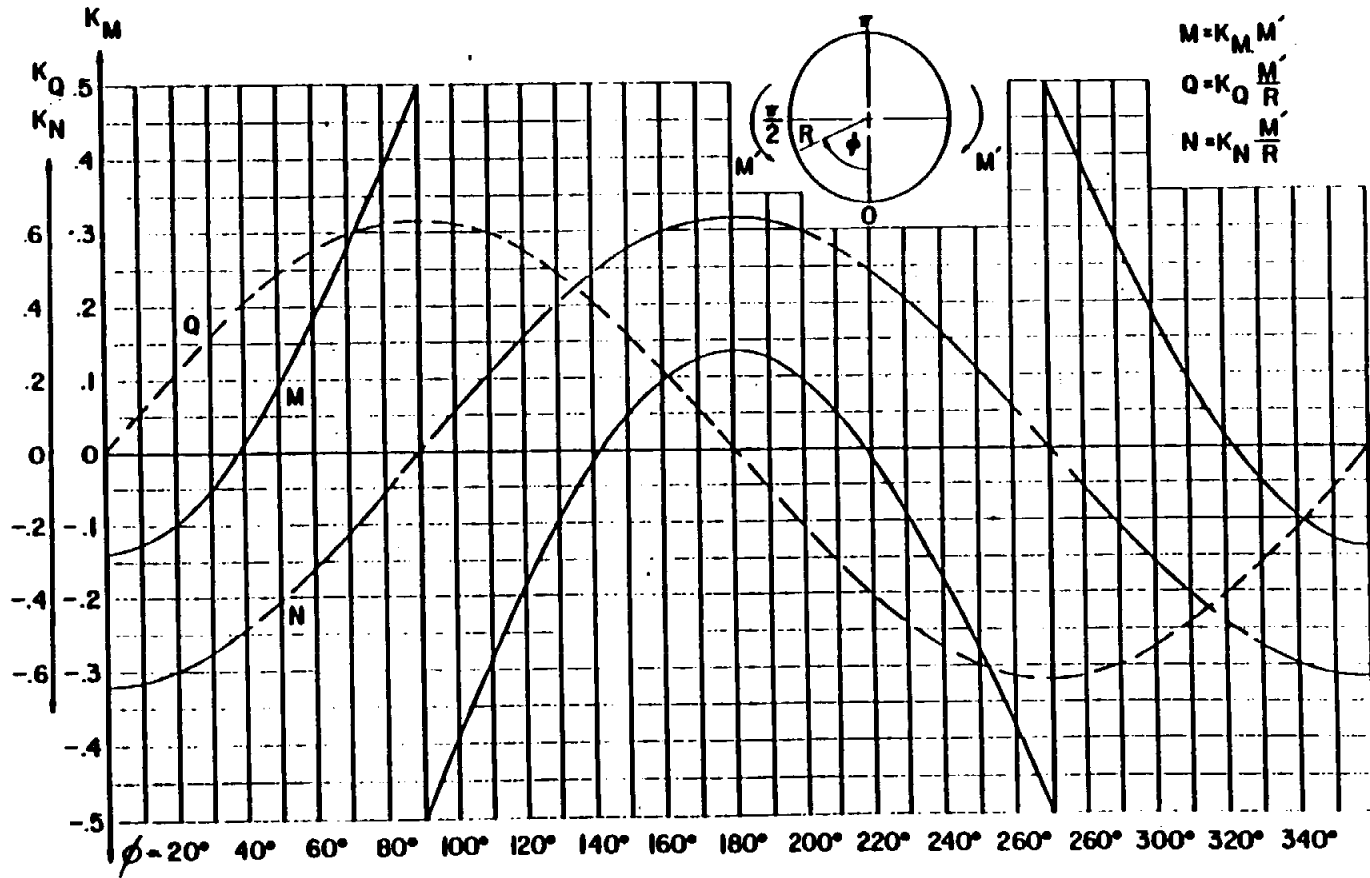
CASE 14



8.6.1.1 In-Plane Load Cases (Cont'd)

CASE 15

$$\begin{aligned} M &= K_M M' \\ Q &= K_Q \frac{M'}{R} \\ N &= K_N \frac{M'}{R} \end{aligned}$$

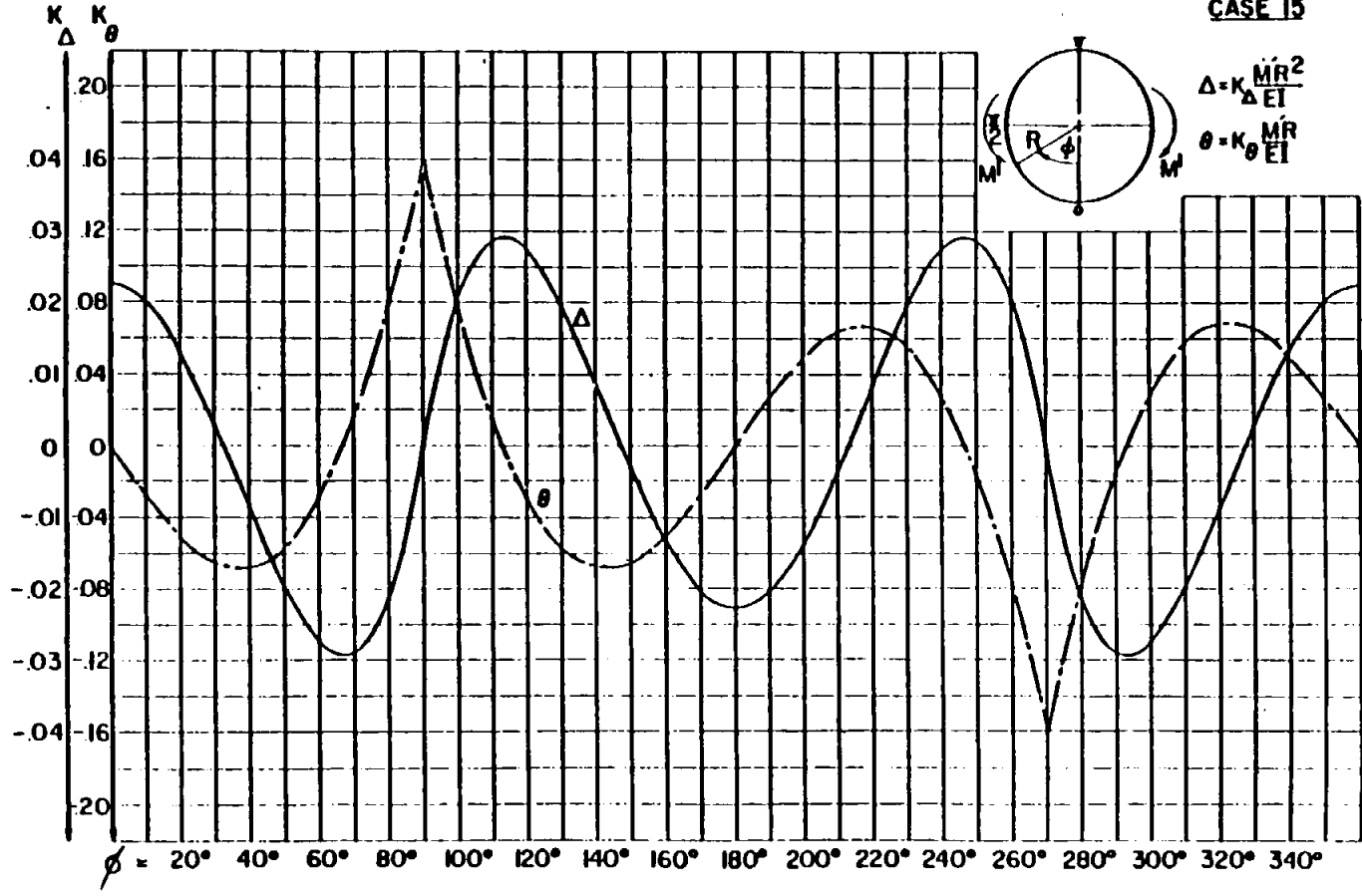
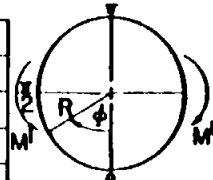


B 6.1.1 In-Plane Load Cases (Cont'd)

CASE 15

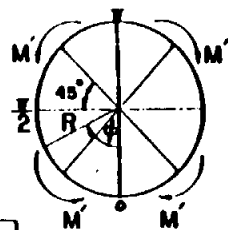
$$\Delta = K_{\Delta} \frac{MR^2}{EI}$$

$$\theta = K_{\theta} \frac{MR}{EI}$$

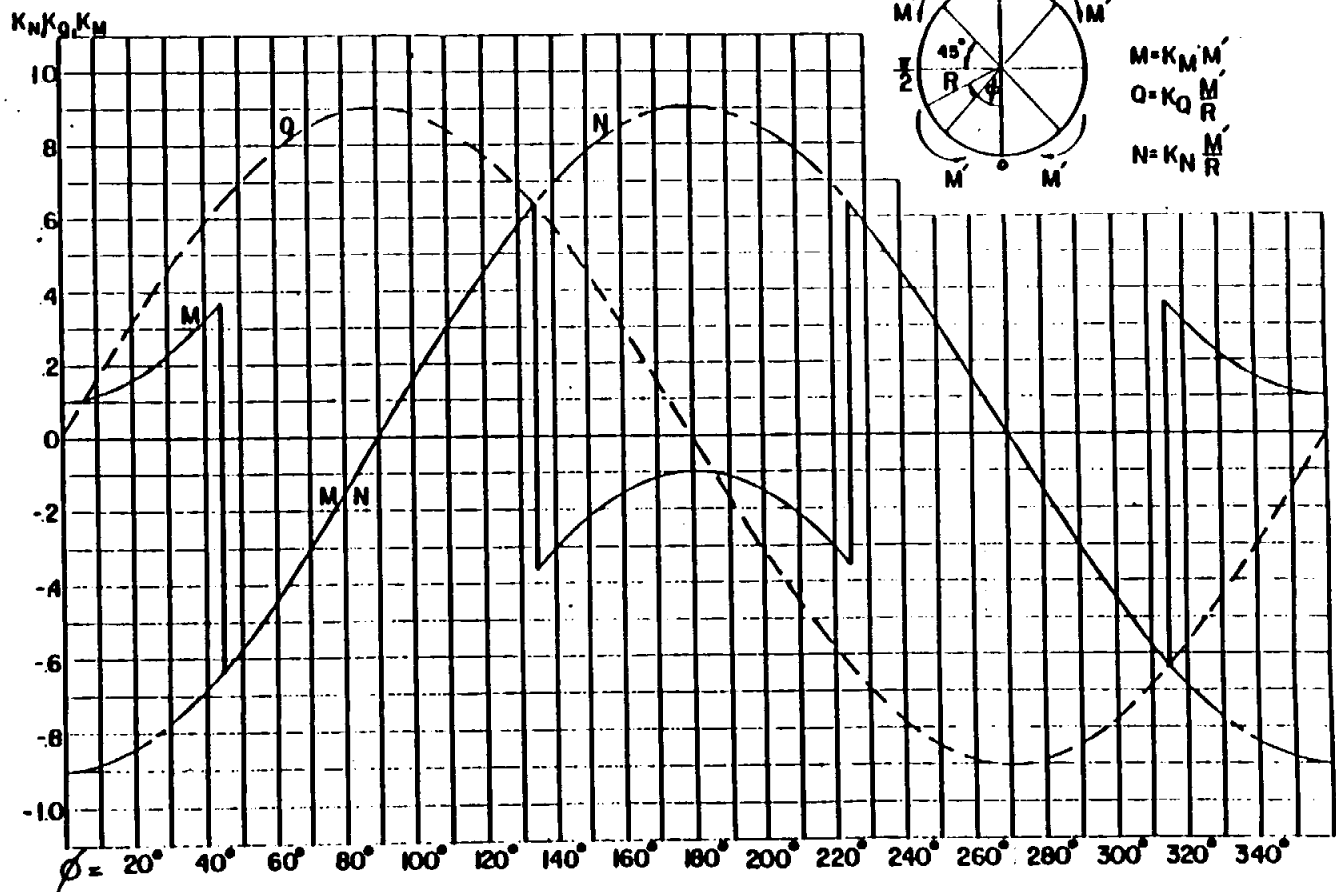


B 6.1.1.1 In-Plane Load Cases (Cont'd)

CASE 16

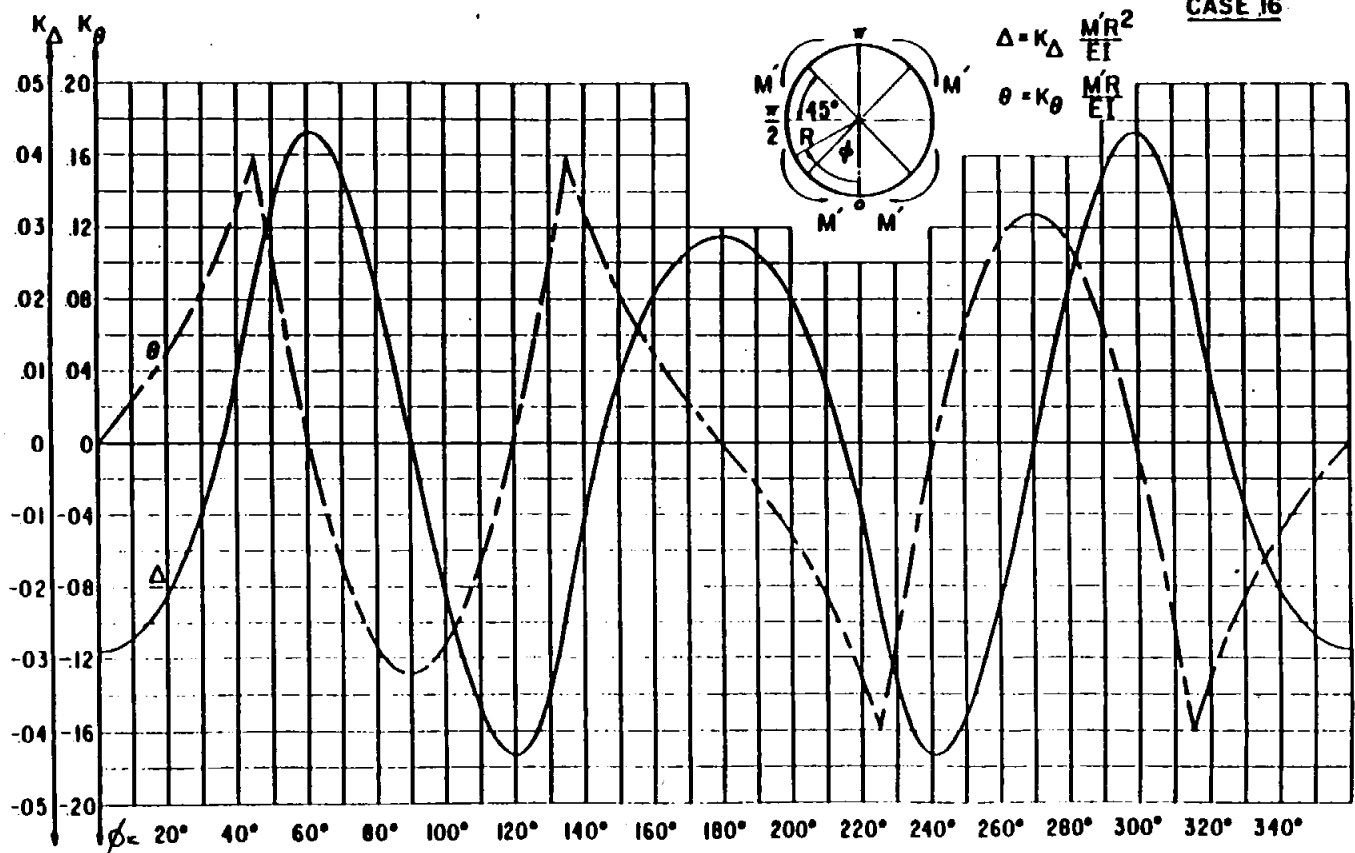


$$\begin{aligned} M &= K_M M' \\ Q &= K_Q M' \\ N &= K_N M' \end{aligned}$$

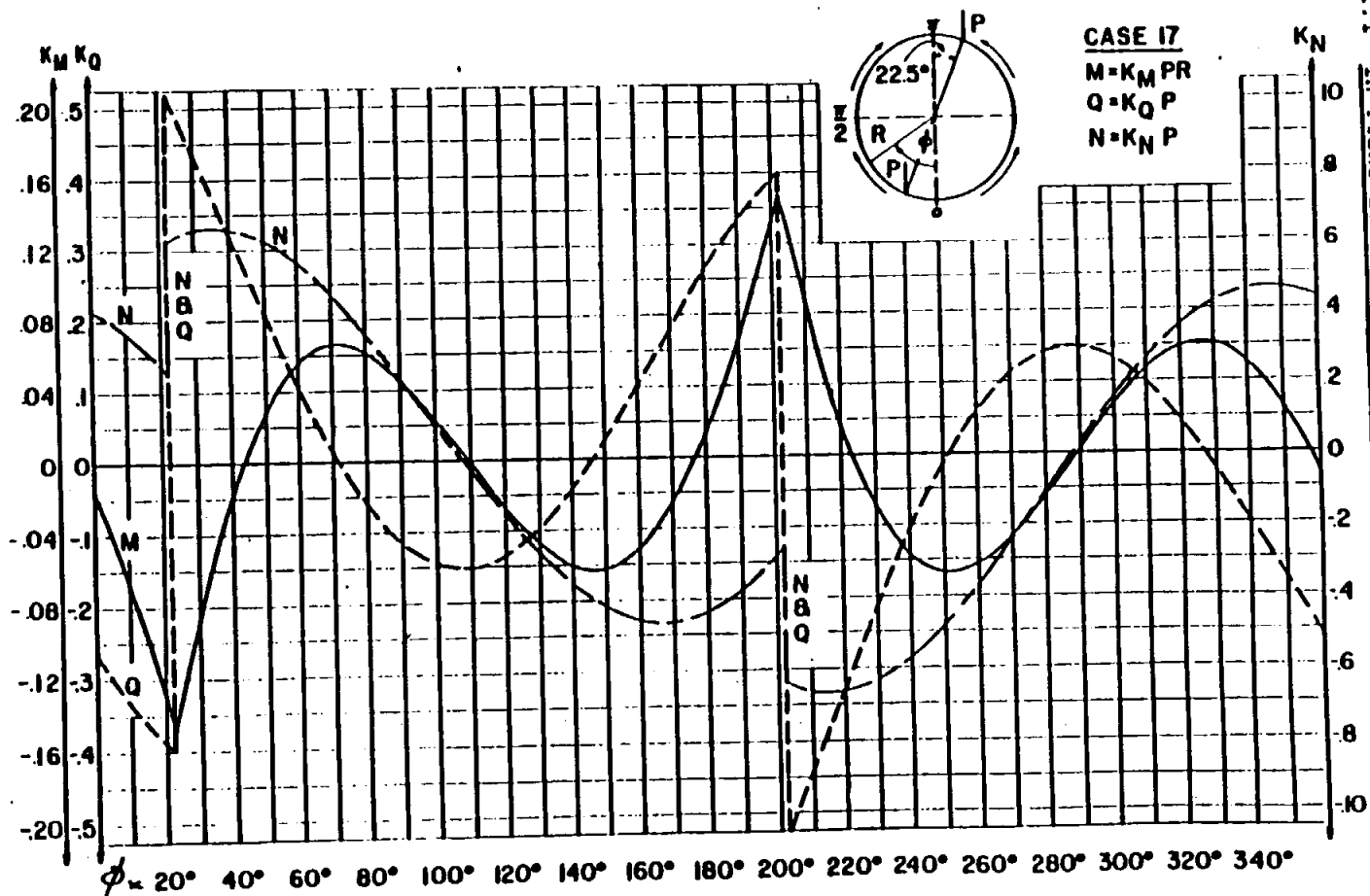


B 6.1.1 In-Plane Load Cases (Cont'd)

CASE 16



B 6.1.1.1 In-Plane Load Cases (Cont'd)

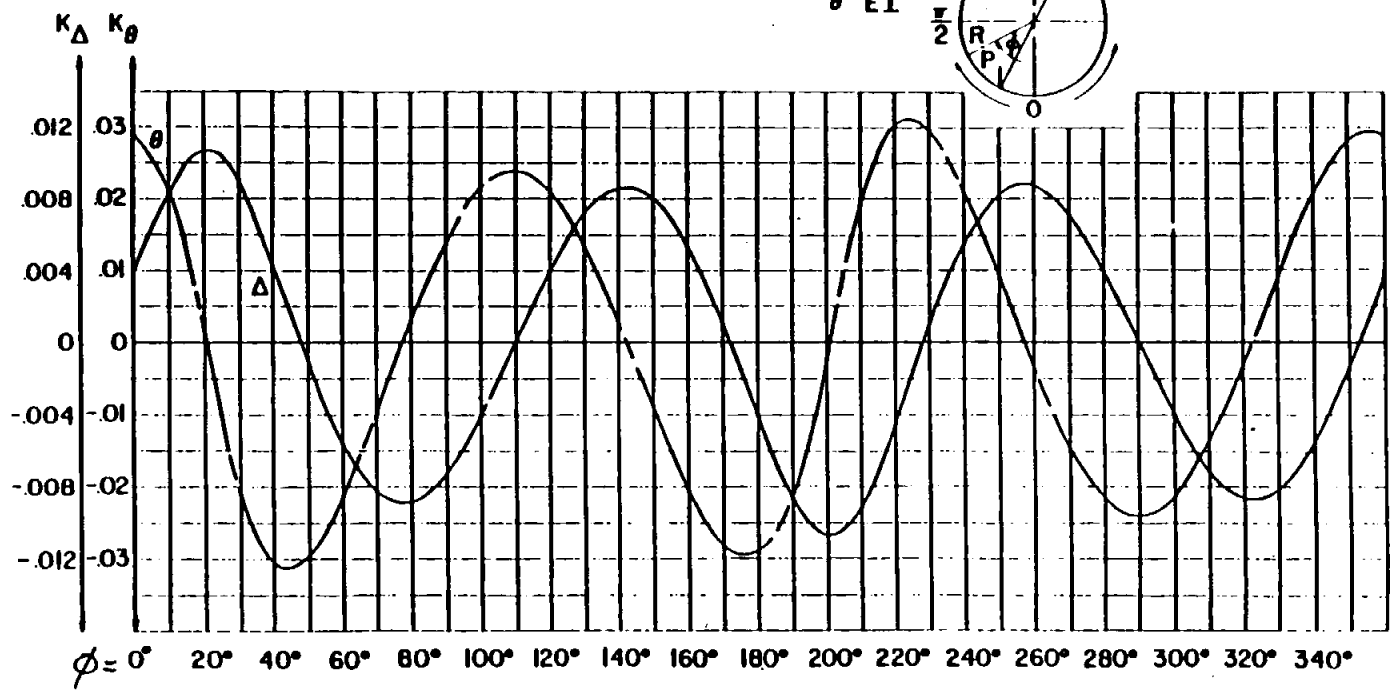
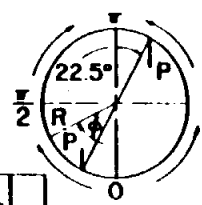


B 6.1.1.1 In-Plane Load Cases (Cont'd)

CASE 17

$$\Delta = K_{\Delta} \frac{PR^3}{EI}$$

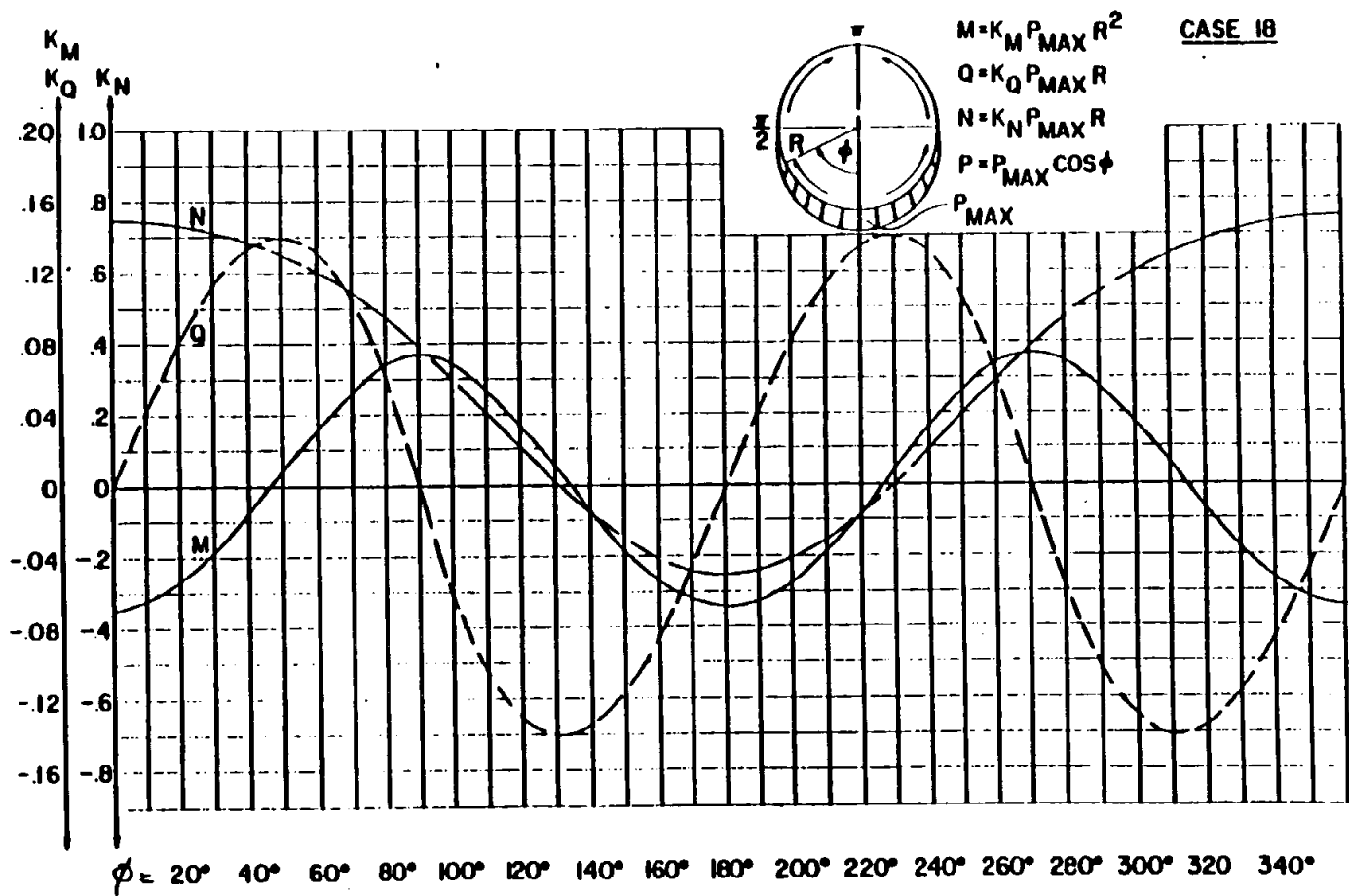
$$\theta = K_{\theta} \frac{PR^2}{EI}$$



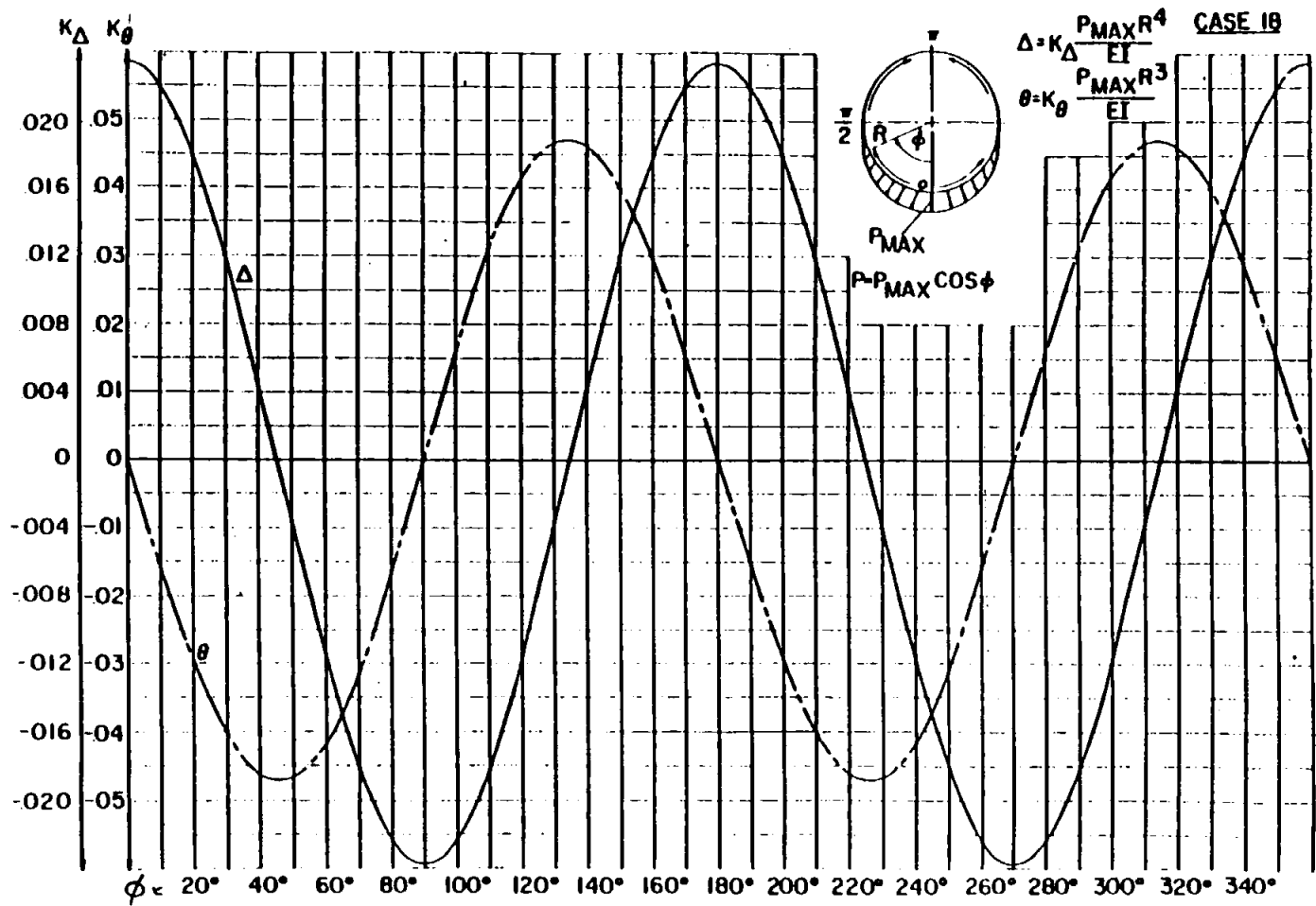
419

8 6.1.1 In-Plane Load Cases (Cont'd)

CASE 18



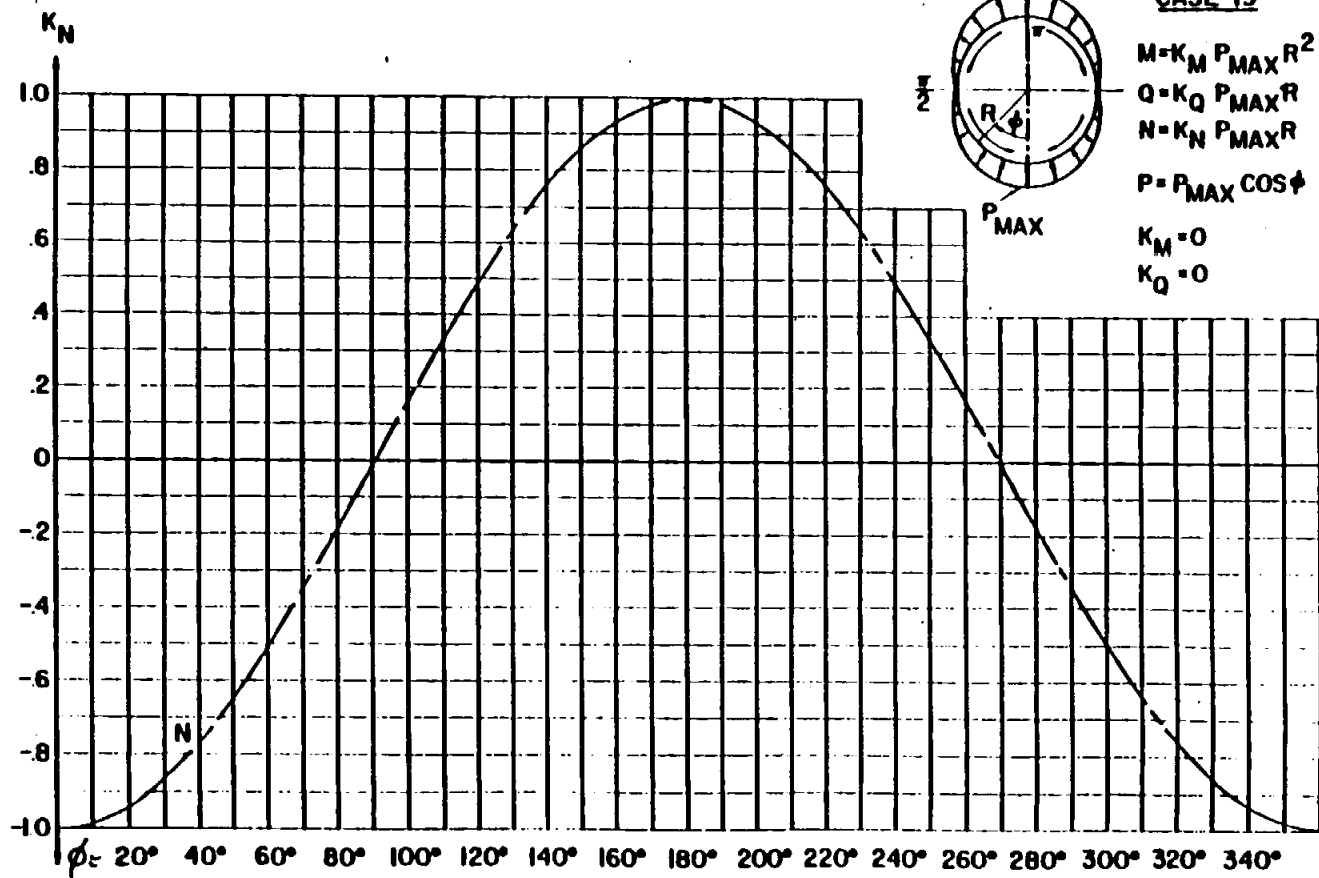
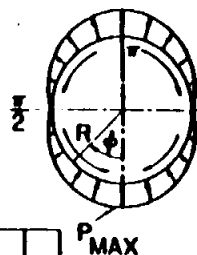
B 6.1.1.1 In-Plane Load Cases (Cont'd)



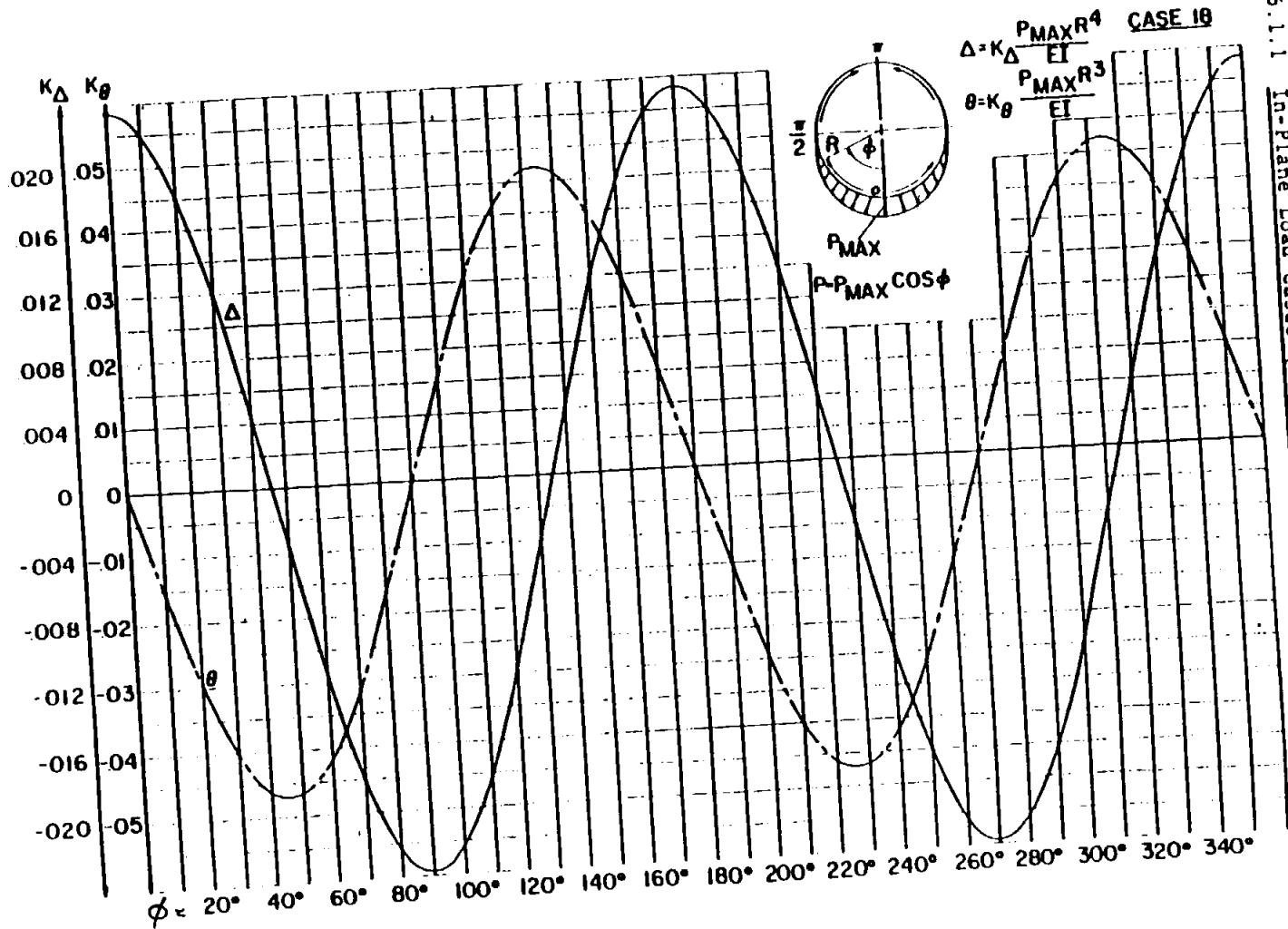
8.6.1.1 In-Plane Load Cases (Cont'd)

CASE 19

$$\begin{aligned} M &= K_M P_{MAX} R^2 \\ Q &= K_Q P_{MAX} R \\ N &= K_N P_{MAX} R \\ P &= P_{MAX} \cos \phi \\ K_M &= 0 \\ K_Q &= 0 \end{aligned}$$



B 6.1.1.1 In-Plane Load Cases (Cont'd)



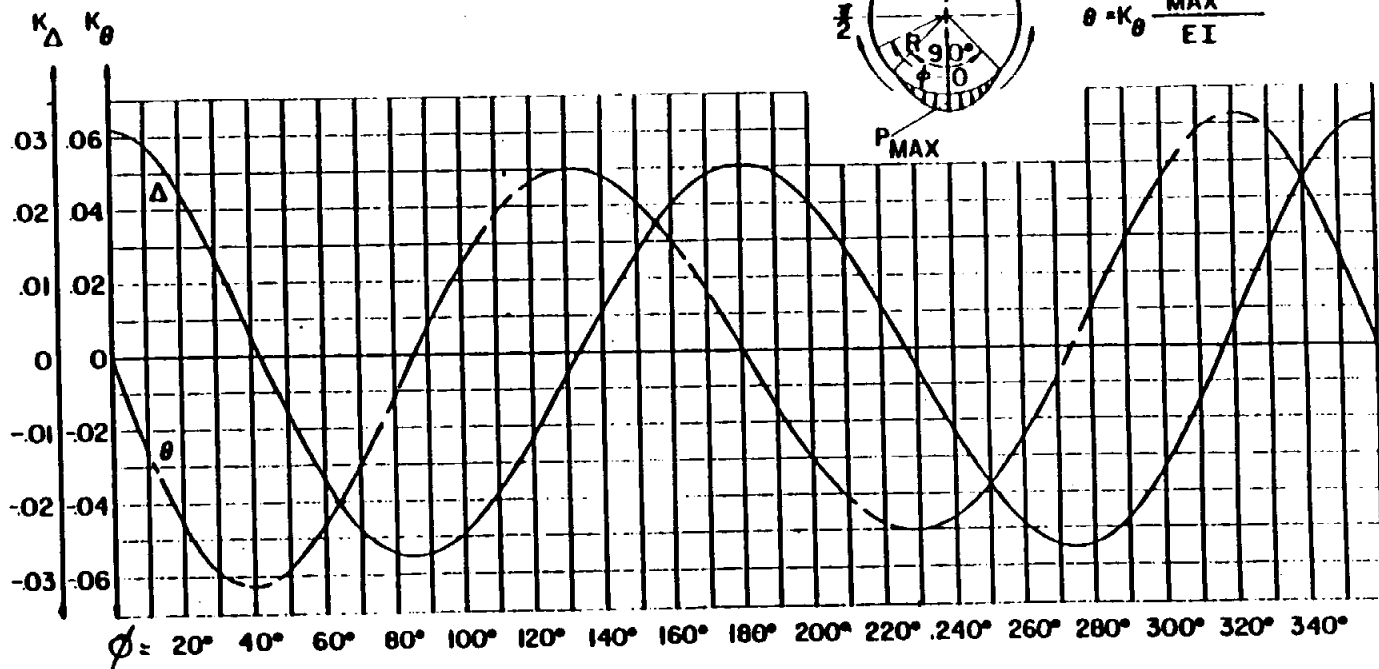
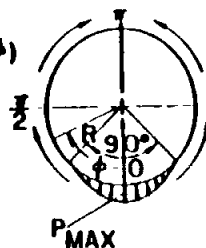
8.6.1.1 In-Plane Load Cases (Cont'd)

CASE 20

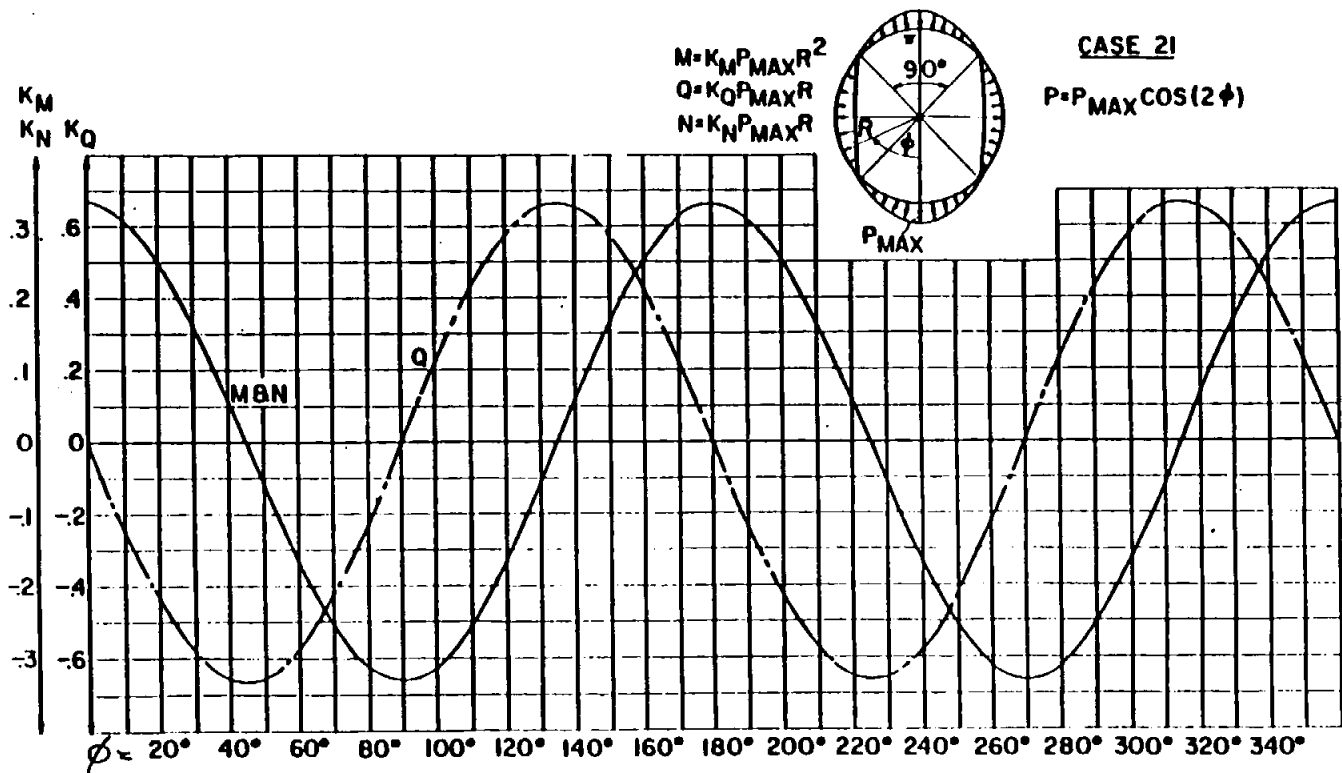
$$\Delta = K_{\Delta} \frac{P_{MAX} R^4}{EI}$$

$$\theta = K_{\theta} \frac{P_{MAX} R^3}{EI}$$

$$P = P_{MAX} \cos(2\phi)$$



B 6.1.1 In-Plane Load Cases (Cont'd)



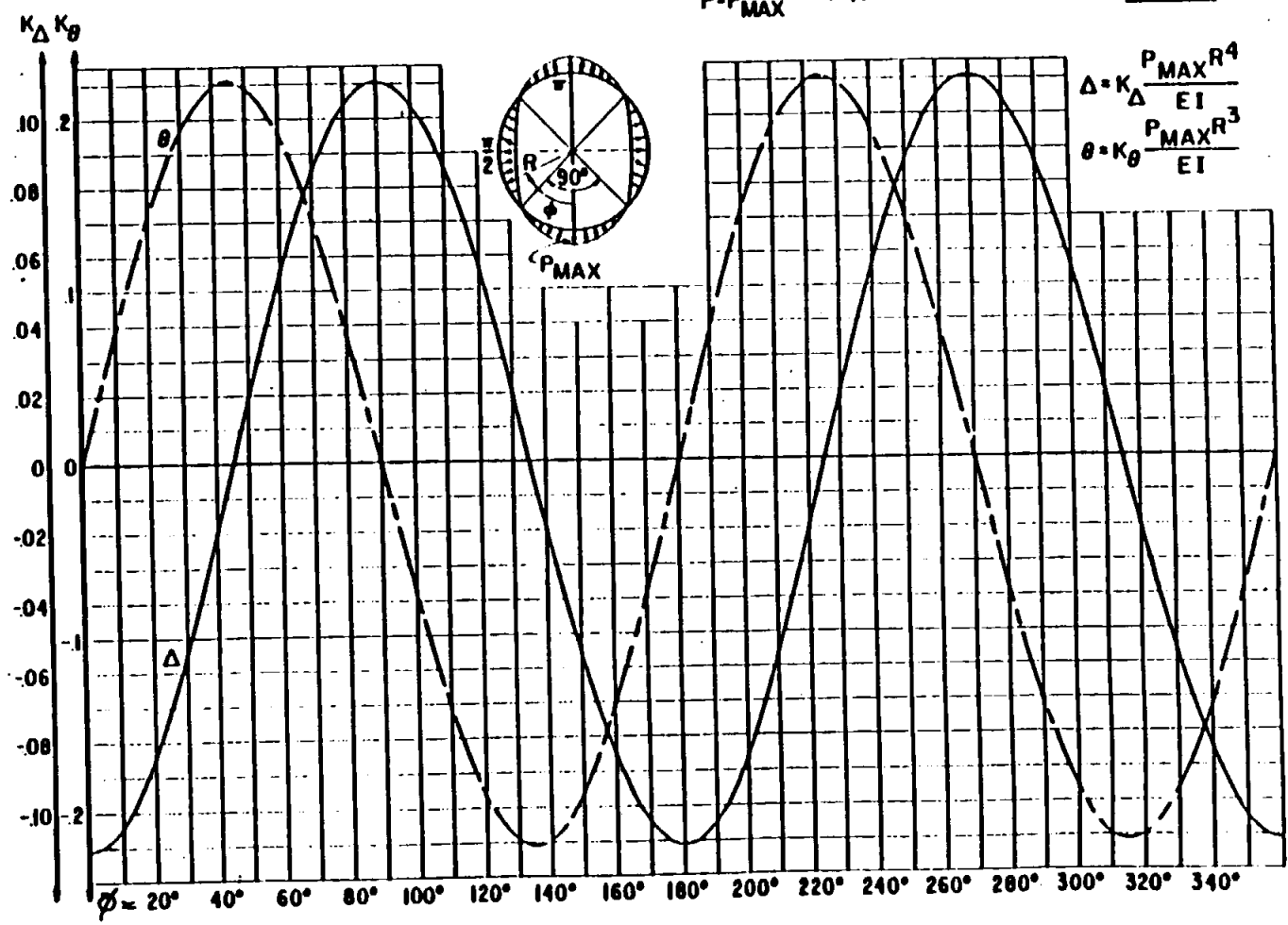
B 6.1.1 In-Plane Load Cases (Cont'd)

CASE 21

$$P = P_{MAX} \cos(2\phi)$$

$$\Delta = K_{\Delta} \frac{P_{MAX} R^4}{EI}$$

$$\theta = K_{\theta} \frac{P_{MAX} R^3}{EI}$$



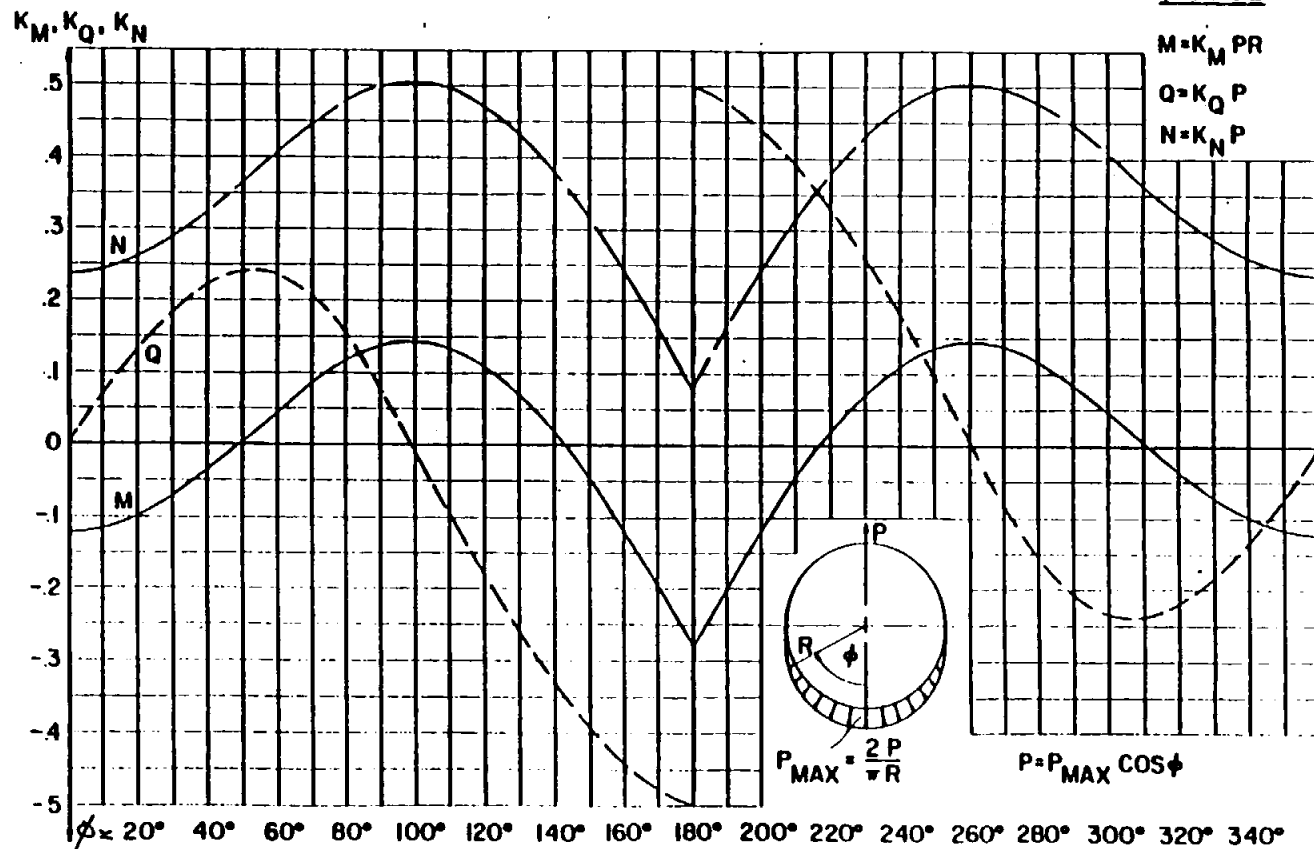
B 6.1.1 In-Plane Load Cases (Cont'd)

CASE 22

$$M = K_M P R$$

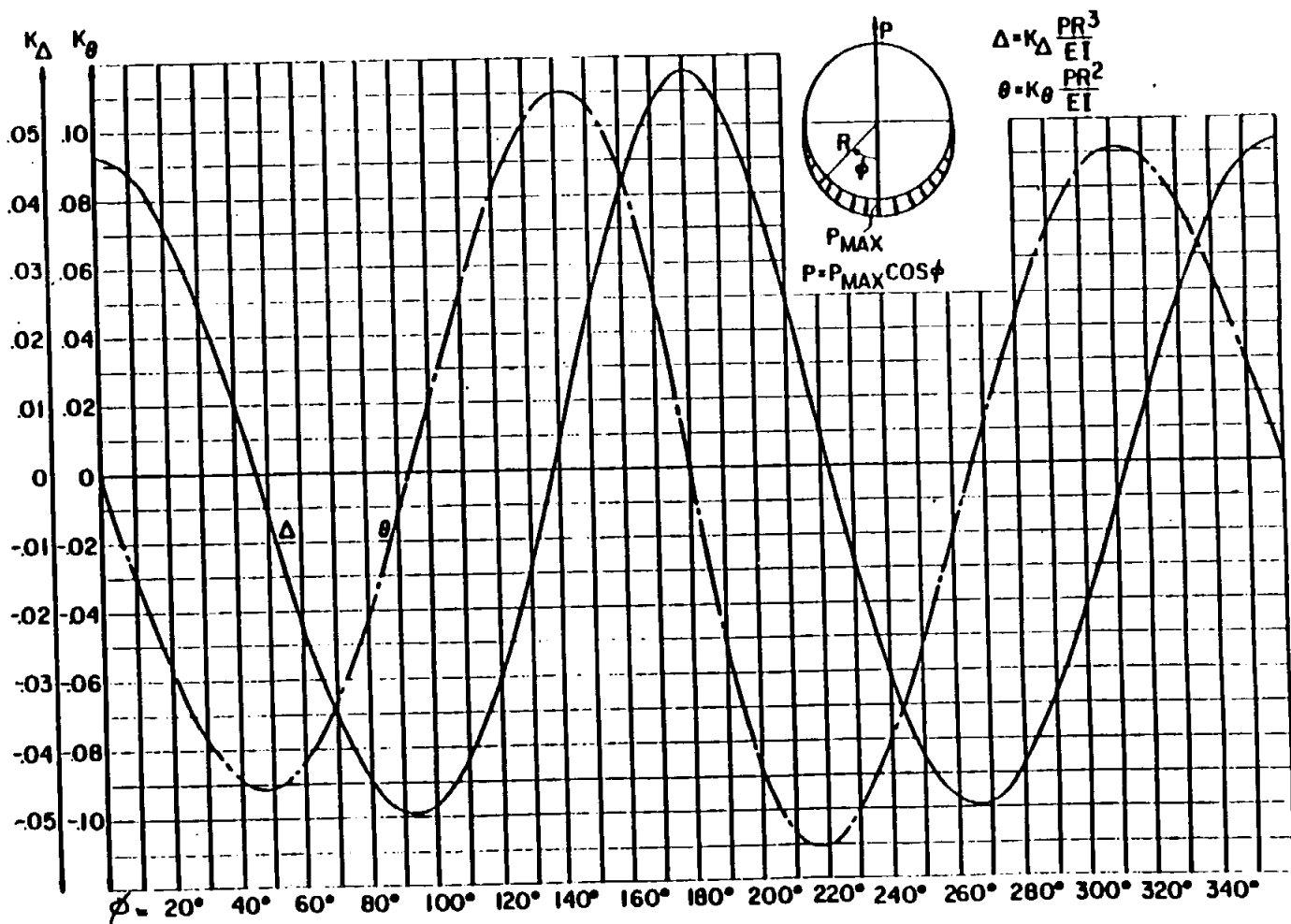
$$Q = K_Q P$$

$$N = K_N P$$



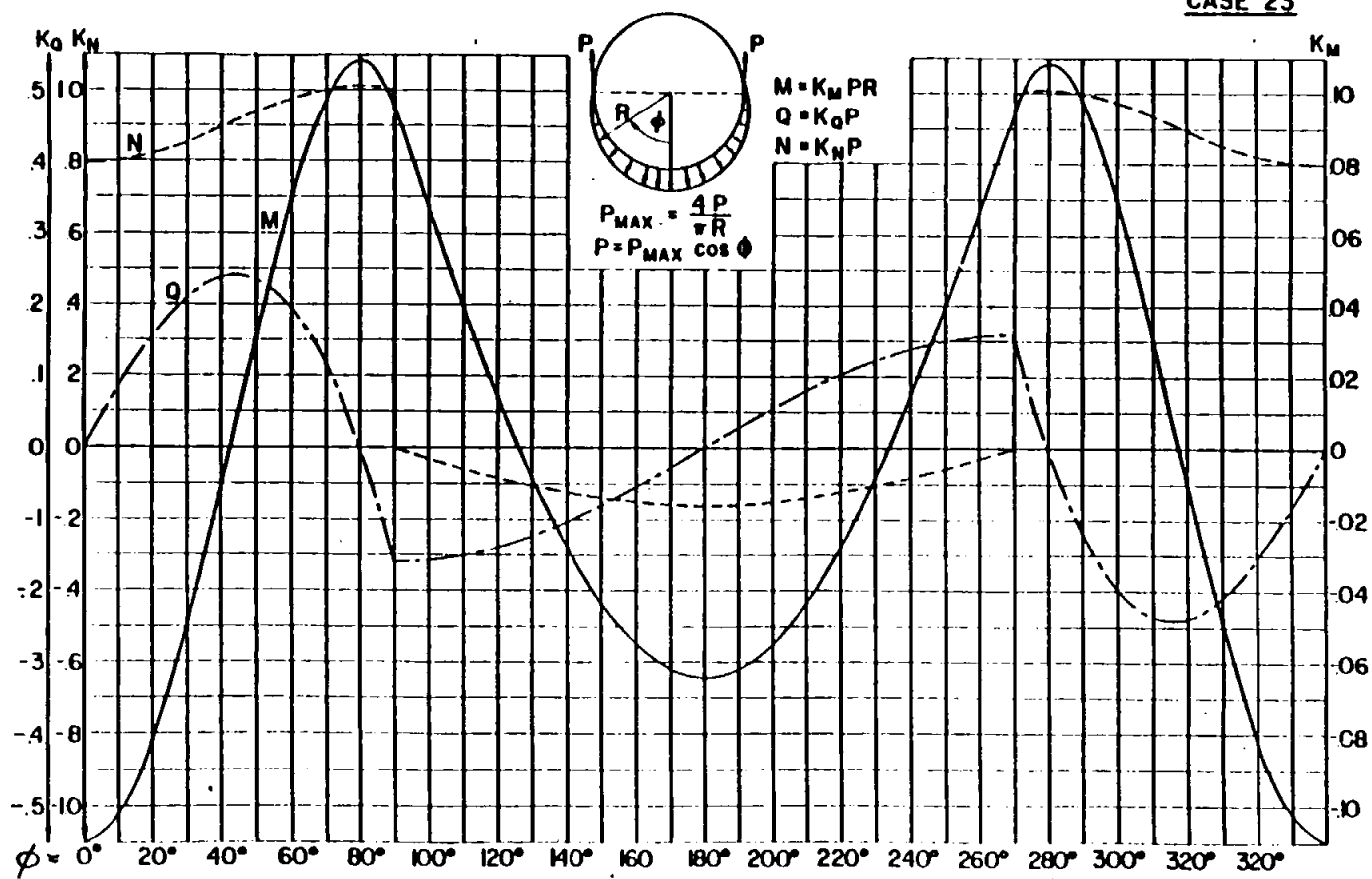
8.6.1.1 In-Plane Load Cases (Cont'd)

CASE 22



B 6.1.1.1 In-Plane Load Cases (Cont'd)

CASE 23





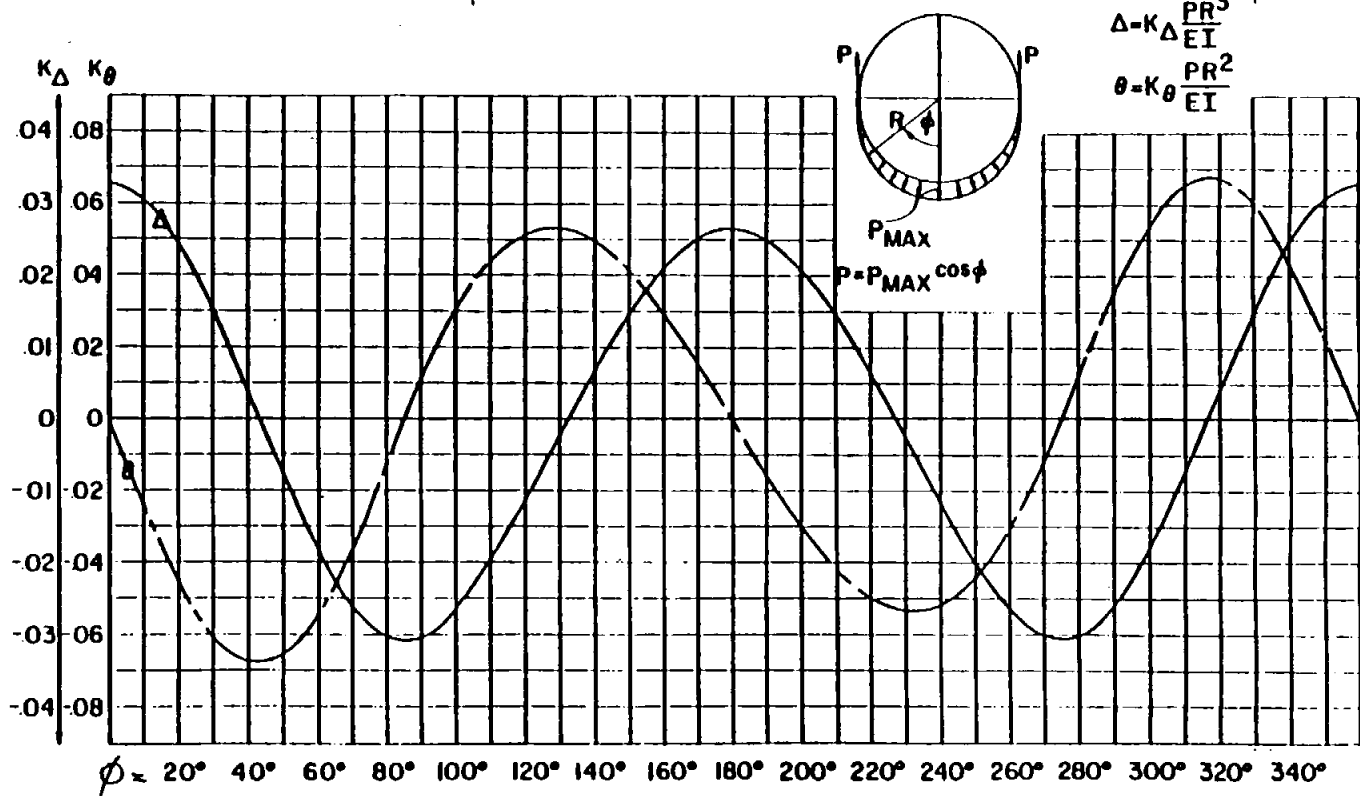
430

B.6.1.1 In-Plane Load Cases (Cont'd)

CASE 23

$$\Delta = K_{\Delta} \frac{PR^3}{EI}$$

$$\theta = K_{\theta} \frac{PR^2}{EI}$$



B 6.1.1 In-Plane Load Cases (Cont'd)

CASE 24

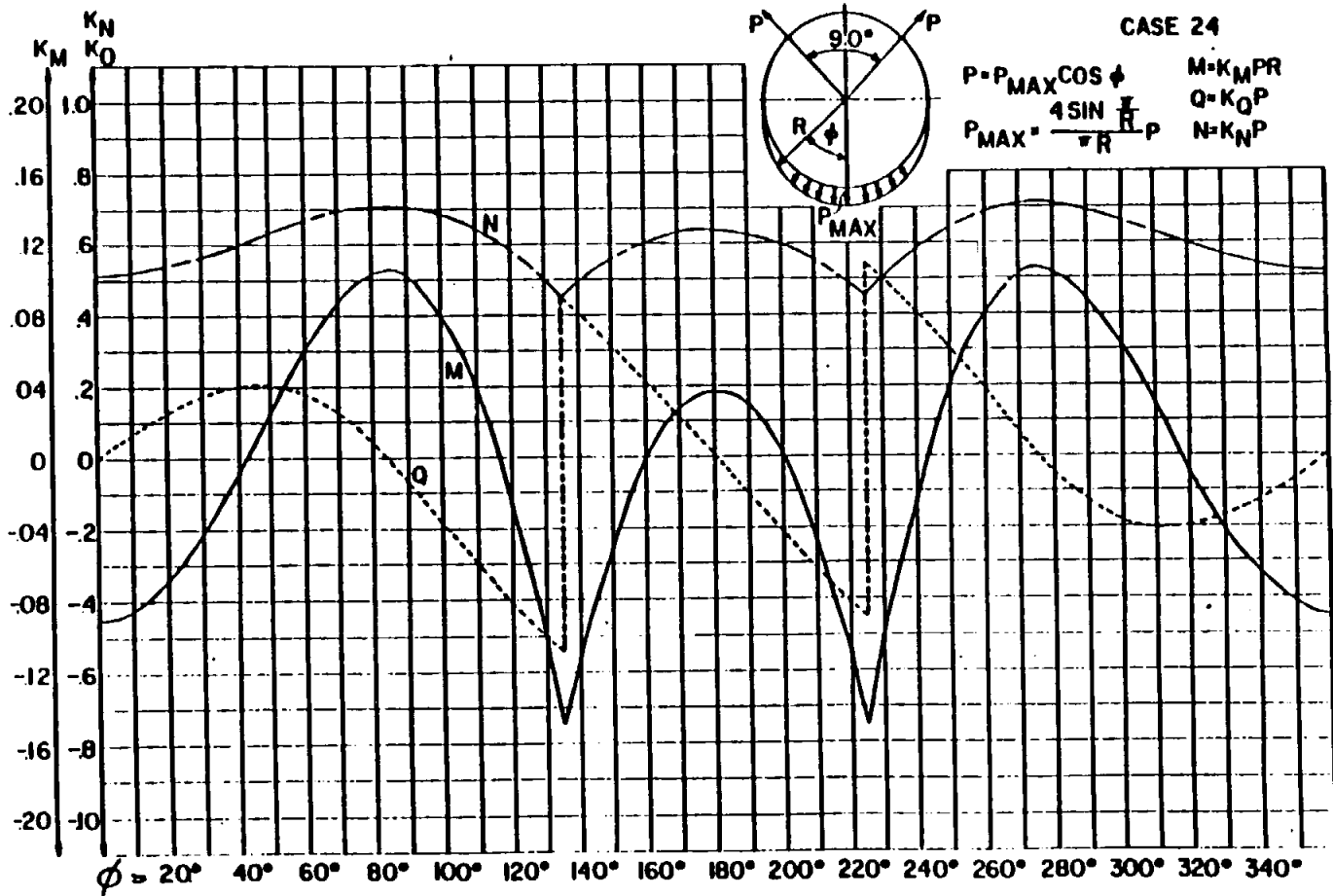
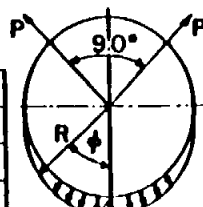
$$P = P_{MAX} \cos \phi$$

$$P_{MAX} = \frac{4 \sin \frac{\pi}{R} P}{\pi R}$$

$$M = K_M P R$$

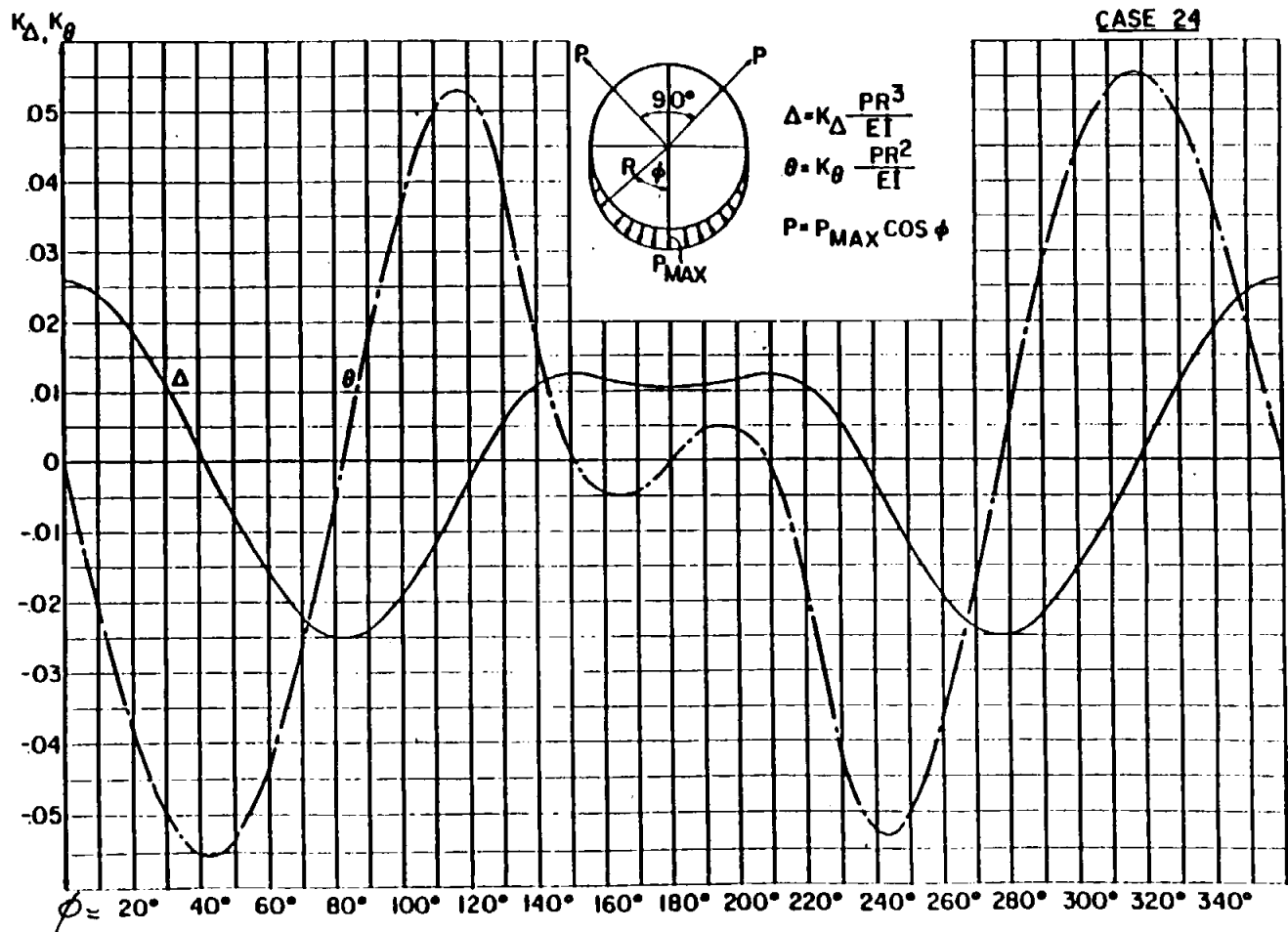
$$Q = K_Q P$$

$$N = K_N P$$



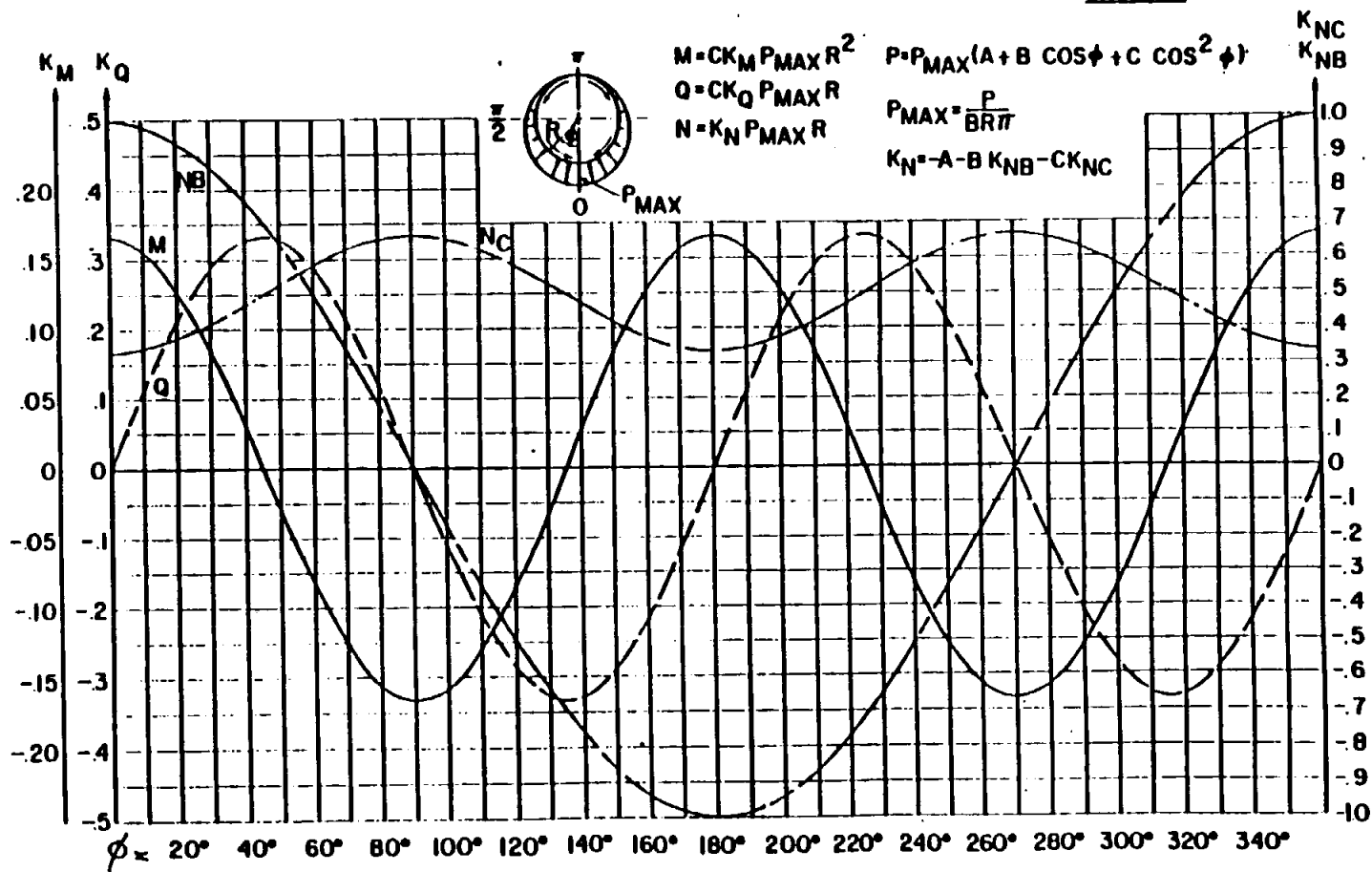
B 6.1.1 In-Plane Load Cases (Cont'd)

CASE 24



B 6.1.1 In-Plane Load Cases (Cont'd)

CASE 25



STRUCTURAL ANALYSIS MANUAL
GENERAL DYNAMICS/CONVAIR AND SPACE SYSTEMS DIVISION

B 6.1.1 In-plane Load Cases (Cont'd)

Deflection curves for the three basic load cases due to shear and normal forces are displayed on the following pages. A shape factor (β) that is to be used with the curves for shear deflection of various cross-sections is tabulated below.

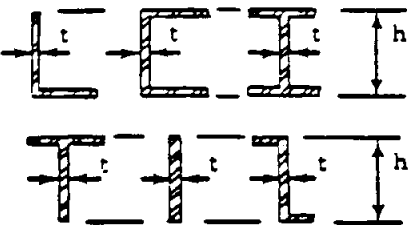
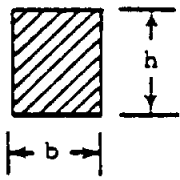
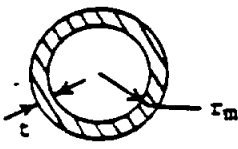
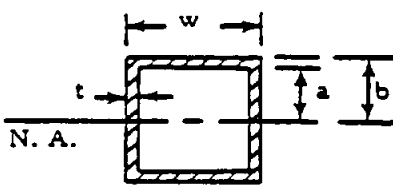
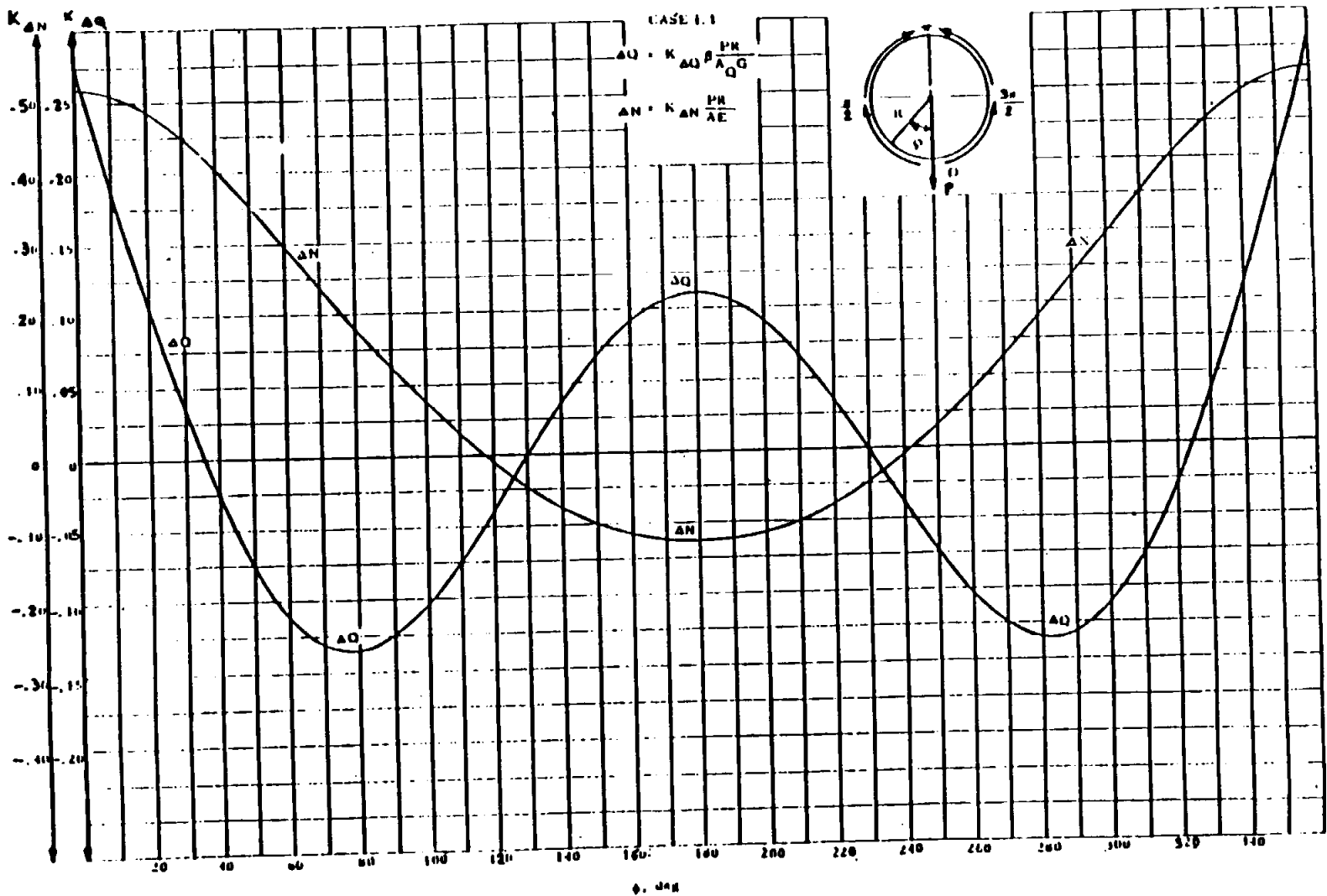
Cross-Section	Shear Area	Shape Factor, β
	Area of Web $A_Q = th$	$\beta = 1.00$
	Entire Area $A_Q = bh$	$\beta = 1.20$ for $b \geq 0.50 h$ $\beta = 1.00$ for $b < 0.50 h$
	Entire Area $A_Q = 2\pi r_m t$	$\beta = 2.00$
 ρ = radius of gyration with respect to the neutral axis	Entire Area $A_Q = (w)^2 - (2a)(w-2t)$	$\beta = \left[1 + \frac{3(b^2 - a^2)}{2b^3} \frac{a}{t} \left(\frac{w}{t} - 1 \right) \right] \left[\frac{4b^2}{10\rho^2} \right]$ <p>If the flanges are of nonuniform thickness, they may be replaced by an "equivalent" section whose flanges have the same width and area as those of the actual section.</p>

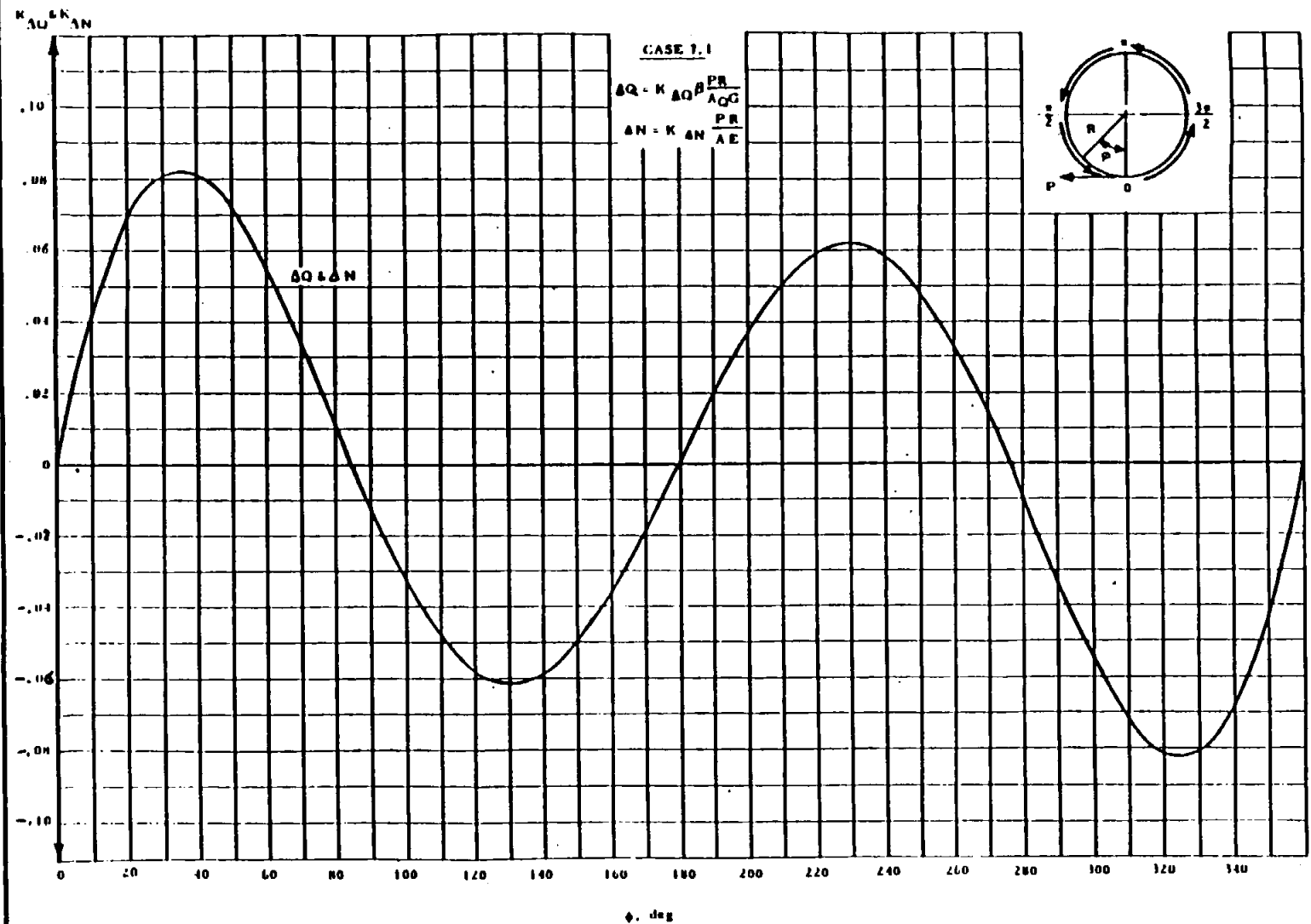
Fig. B6.1.1-1

3-1.1.1 In-Plane Load Cases Cont'd



STRUCTURAL ANALYSIS MANUAL
GENERAL DYNAMICS/CONVAIR AND SPACE SYSTEMS DIVISION

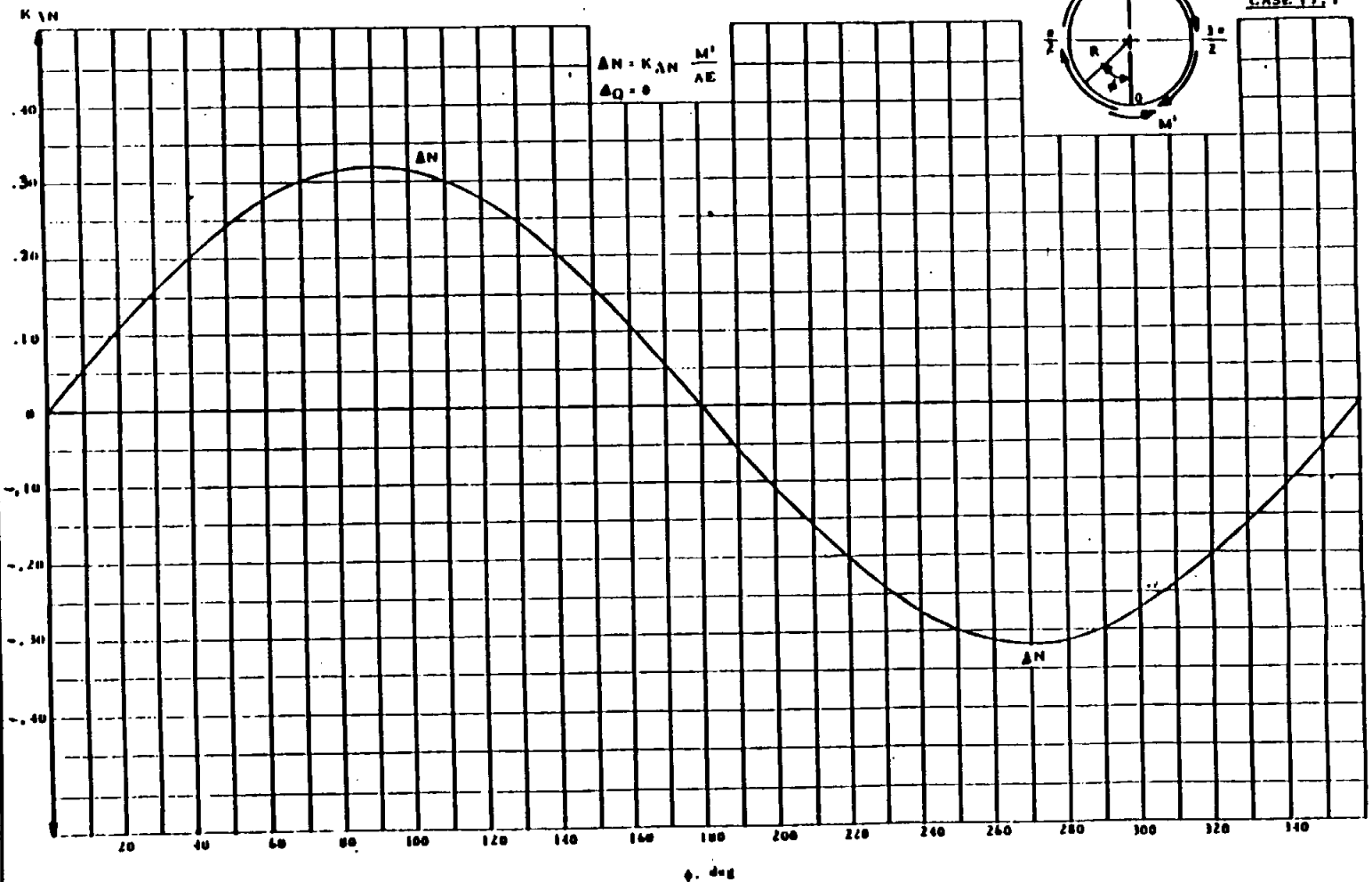
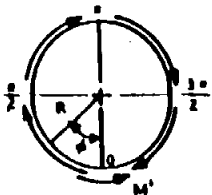
B 6.1.1 In-Plane Load Cases (Cont'd)



GENERAL DYNAMICS/CONVAIR AND SPACE SYSTEMS DIVISION

3.5.1.1 In-Plane Load Cases (Cont'd)

CASE: 11, 1



STRUCTURAL ANALYSIS MANUAL
GENERAL DYNAMICS/CONVAIR AND SPACE SYSTEMS DIVISION

B 6.1.2 Out-of-plane Load Cases

Sign Convention

The following sign convention is given to define the positive directions for out-of-plane loads.

Moments which produce tension on the inner fibers are positive. Torque "T" and lateral shear "V" are positive as shown in Fig. B 6.1.2-1.

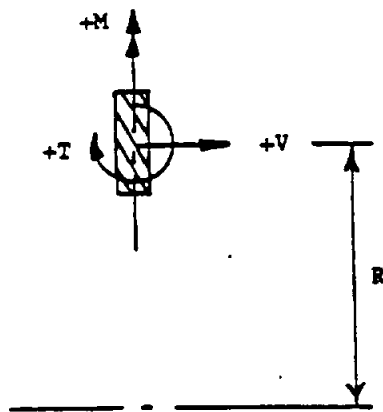
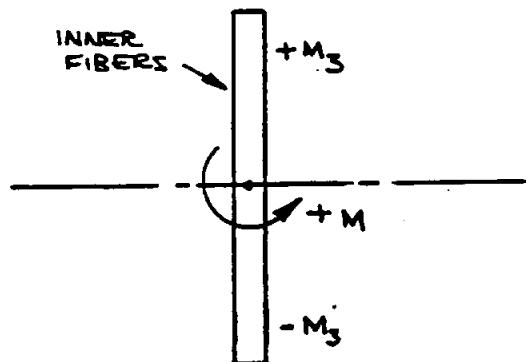


Fig. B 6.1.2-1



STRUCTURAL ANALYSIS MANUAL
GENERAL DYNAMICS/CONVAIR AND SPACE SYSTEMS DIVISION

B 6.1.2 Out-of-Plane Load Cases (Cont'd)

Index

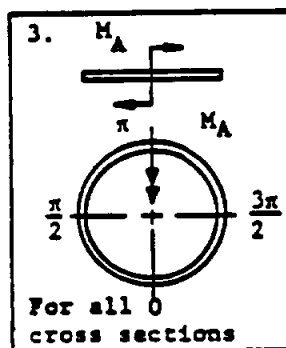
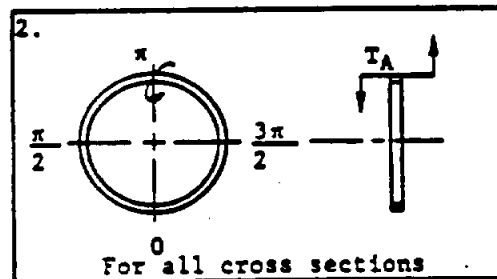
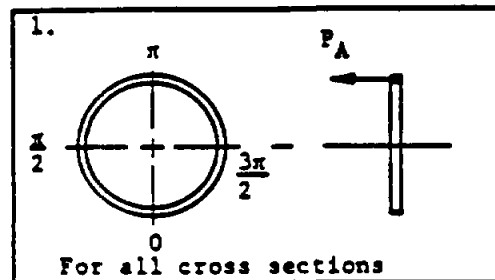
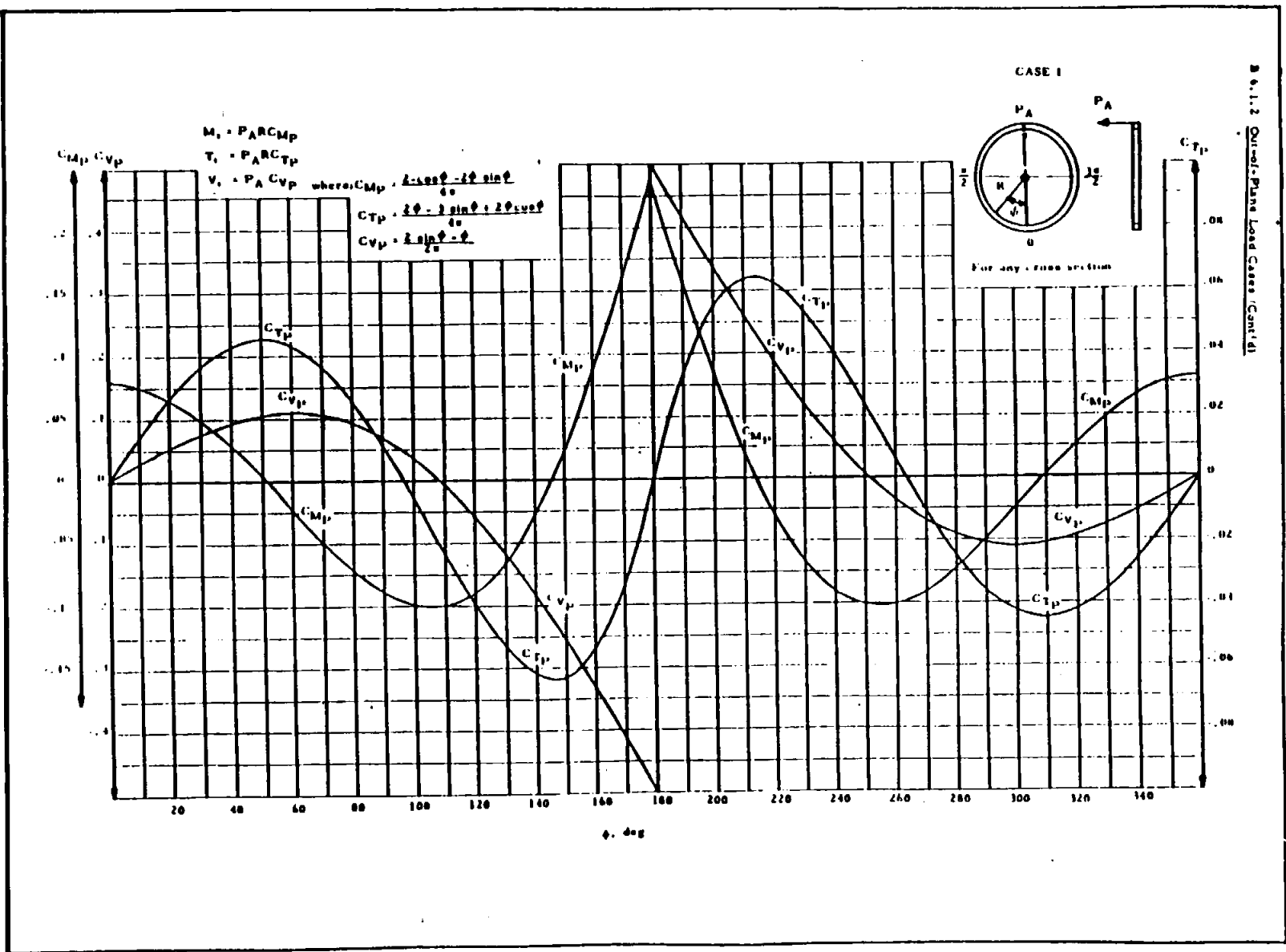


Fig. B 6.1.2-2

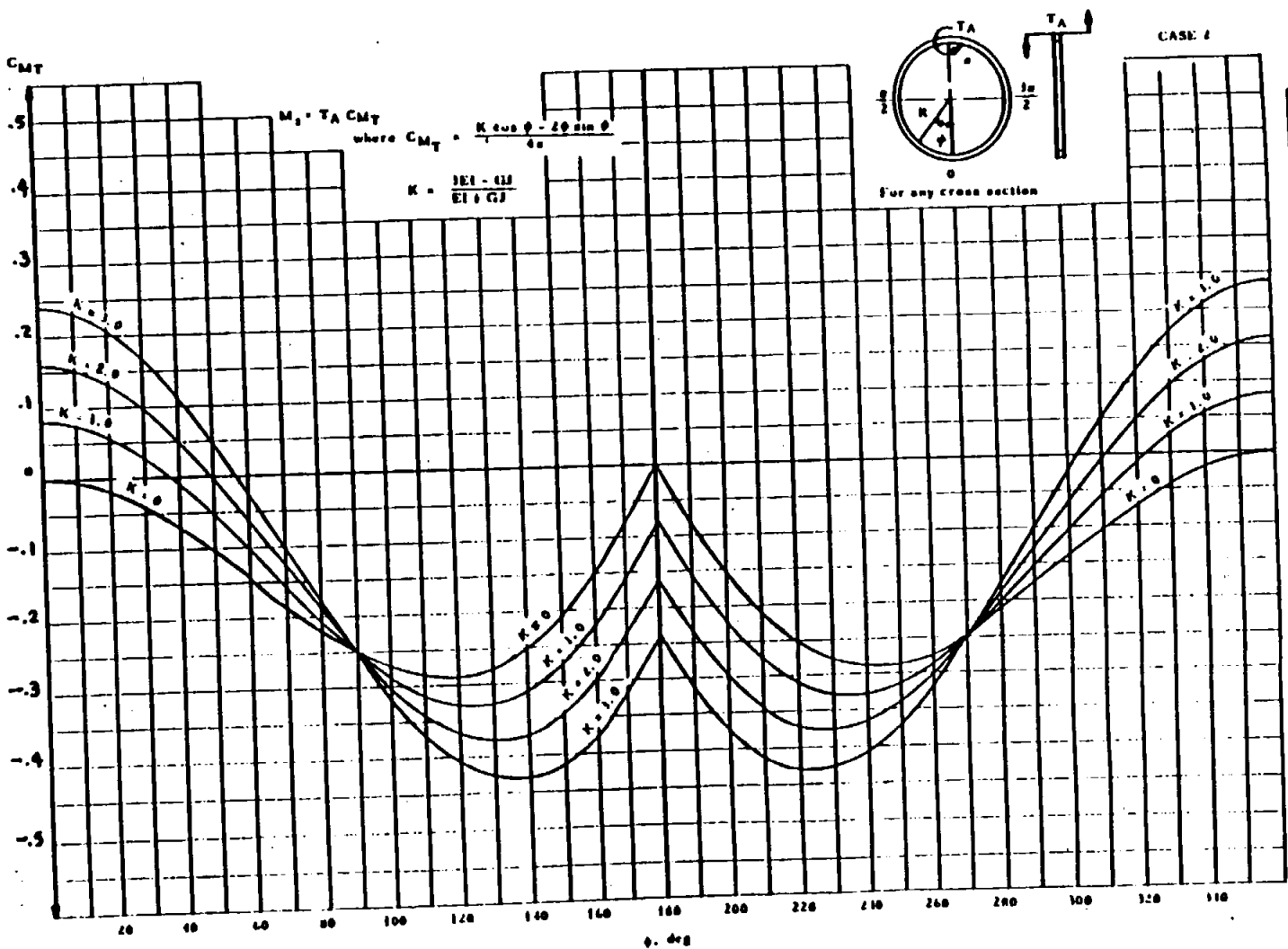
P_A = APPLIED OUT-OF-PLANE AXIAL LOAD, LB.
 T_A = APPLIED OUT-OF-PLANE TORQUE, IN.-LB.
 M_A = APPLIED OUT-OF-PLANE MOMENT, IN.-LB.

M_1 = RESULTANT RING BENDING MOMENT, IN.-LB.
 T_1 = RESULTANT RING TORQUE, IN.-LB.
 V_1 = RESULTANT RING SHEAR, LB.

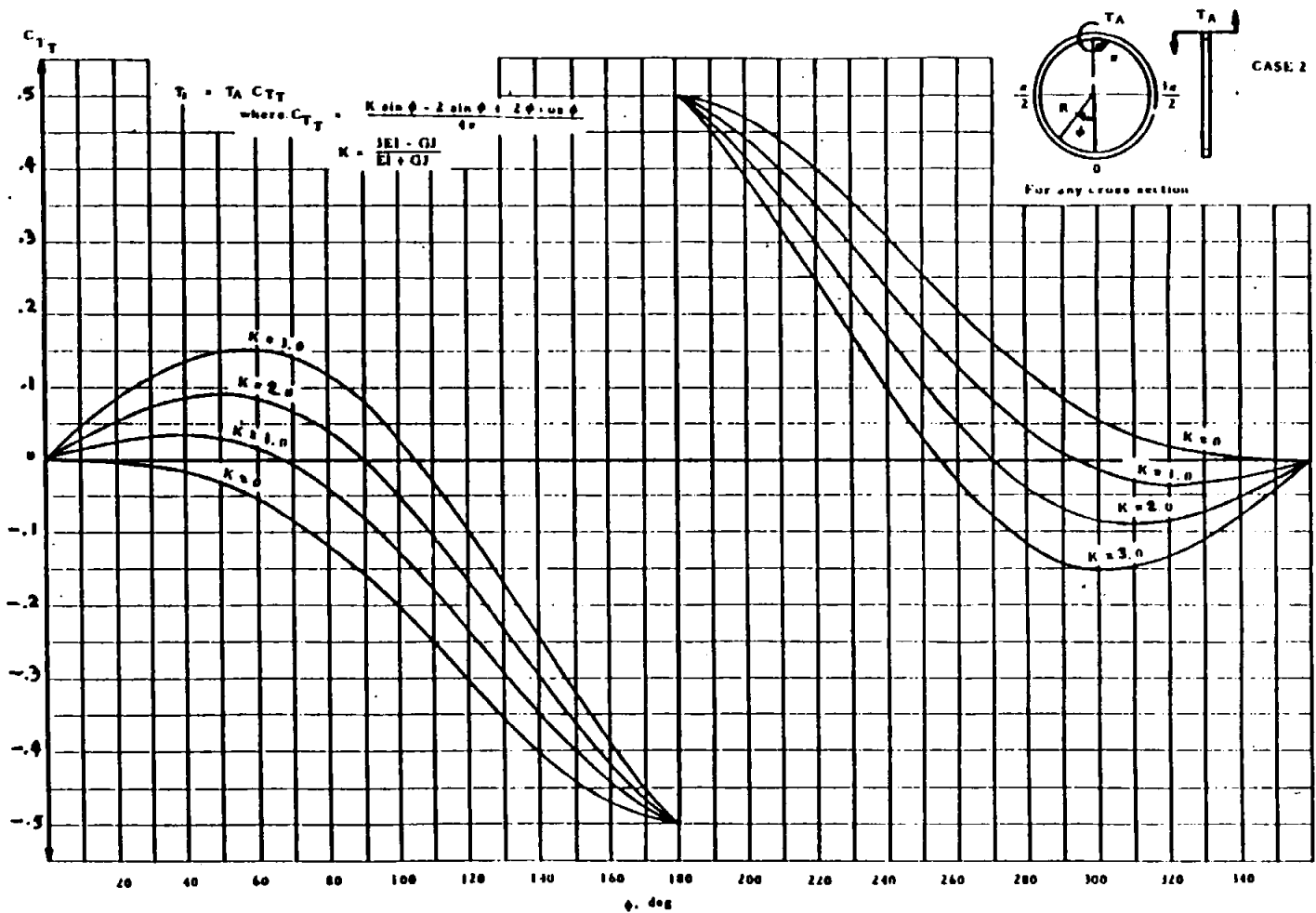
8-6.1.2 Out-of-Plane Load Cases (Cont'd)



B 6.1.2 Out-of-Plane Load Case (Cont'd)

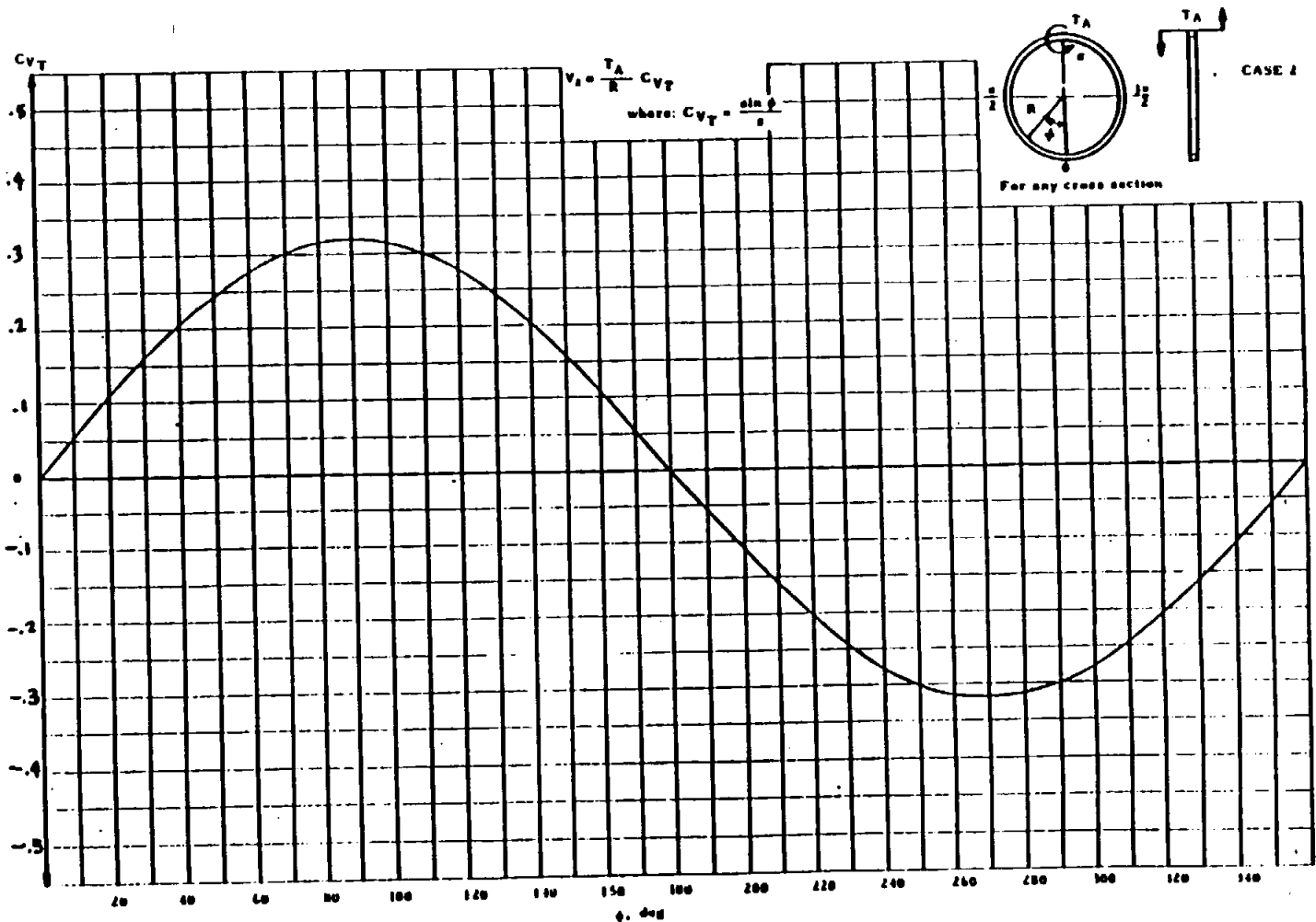


B 6.1.2 Out-of-Plane Load Cases (Cont'd)

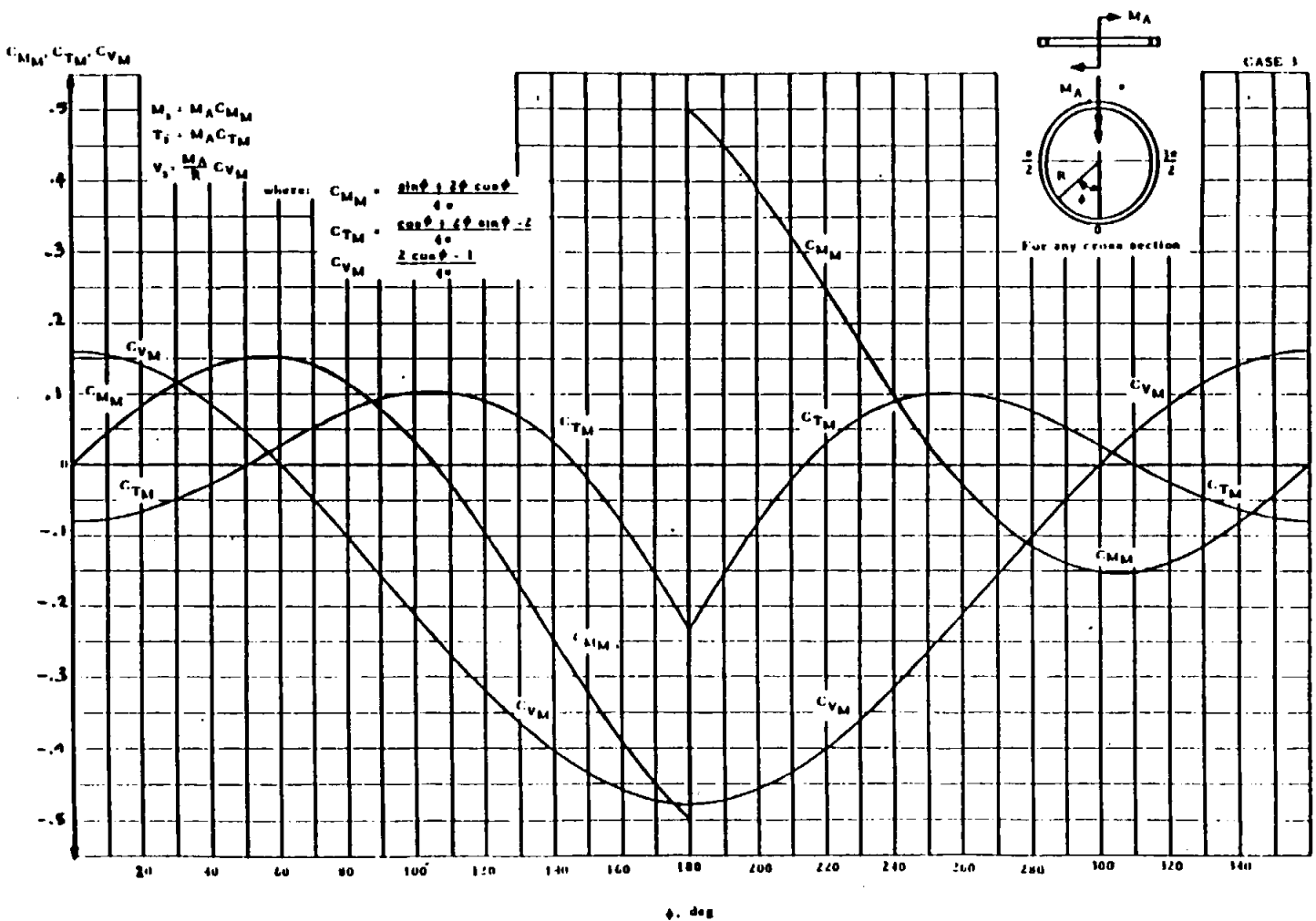


STRUCTURAL ANALYSIS MANUAL GENERAL DYNAMICS/CONVAIR AND SPACE SYSTEMS DIVISION

8.6.1.2 Out-of-Plane Load Cases (Case 4)



B 6.1.2 Out-of-Plane Load Cases (Cont'd)



STRUCTURAL ANALYSIS MANUAL
GENERAL DYNAMICS/CONVAIR AND SPACE SYSTEMS DIVISION

References

1. MacNeal, Richard H., and John A. Bailie, Analysis of Frame-Reinforced Cylindrical Shells, Part I - Basic Theory. NASA TN D-400, 1960.
2. MacNeal, Richard H., and John A. Bailie, Analysis of Frame-Reinforced Cylindrical Shells, Part II - Discontinuities of Circumferential-Bending Stiffness in the Axial Directions. NASA TN D-401, 1960.
3. MacNeal, Richard H., and John A. Bailie, Analysis of Frame-Reinforced Cylindrical Shells, Part III - Applications. NASA TN D-402, 1960.

STRUCTURAL ANALYSIS MANUAL
GENERAL DYNAMICS/CONVAIR AND SPACE SYSTEMS DIVISION

Data Source, Section 1.3 Reference 3

§ 3.1.4 Particular Solution of Bents and Semicircular Arches

In the tables that follow, formulas for computing reactions are given for several load cases. In all cases constraining moments, reaction, and applied loads are positive when acting as shown and

$$K = \frac{I_2 h}{I_1 L} \quad \text{for cases 1 through 18}$$

$$K = \frac{I_1 S_2}{I_2 S_1} \quad \text{for cases 19 through 28}$$

STRUCTURAL ANALYSIS MANUAL
GENERAL DYNAMICS/CONVAIR AND SPACE SYSTEMS DIVISION

3.5.1.4 Particular Solution of Bents and Semicircular Arches (Cont'd)

Table 3.5.1.4-1 Reactions and Constraining Moments in Two Legged Rectangular Bents

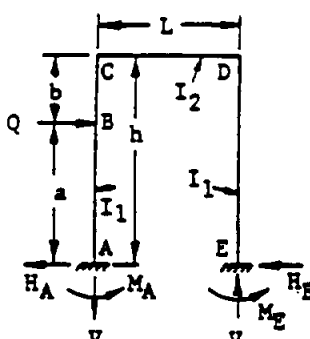
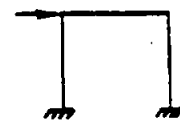
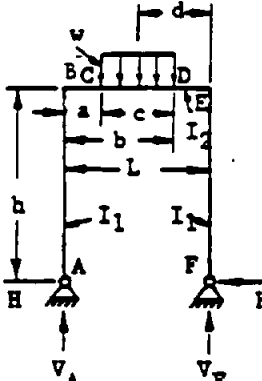
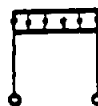
<p>1. VERT. CONCENTRATED LOAD</p>	$V_A = \frac{Qb}{L} \quad V_E = Q - V_A$ $H = \frac{30ab}{2Lh(2K + 3)}$ <p>FOR SPECIAL CASE: $a = b = \frac{L}{2}$</p> $V_A = V_E = \frac{Q}{2}$ $H = \frac{30L}{8h(2K + 3)}$
<p>2. VERT. CONCENTRATED LOAD</p>	$V_A = \frac{Qb}{L} \left[1 + \frac{a(b-a)}{L^2(6K+1)} \right] \quad V_E = Q - V_A$ $H = \frac{30ab}{2Lh(K+2)}$ $M_A = \frac{Qab}{L} \left[\frac{1}{2(K+2)} - \frac{(b-a)}{2L(6K+1)} \right]$ $M_E = \frac{Qab}{L} \left[\frac{1}{2(K+2)} + \frac{(b-a)}{2L(6K+1)} \right]$ <p>FOR SPECIAL CASE: $a = b = \frac{L}{2}$</p> $V_A = V_E = \frac{Q}{2} \quad M_A = M_E = \frac{QL}{8(K+2)}$
<p>3. HORIZ. CONCENTRATED LOAD</p>	$V = \frac{Qa}{L} \quad H_A = Q - H_E$ $H_E = \frac{Qa}{2h} \left[\frac{bK(a+h)}{h^2(2K+3)} + 1 \right]$ <p>FOR SPECIAL CASE: $b = 0, a = h$</p> $V = \frac{Qh}{L}$ $H_E = H_A = \frac{Q}{2}$

44

STRUCTURAL ANALYSIS MANUAL
GENERAL DYNAMICS/CONVAIR AND SPACE SYSTEMS DIVISION

B 5.1.4 Particular Solution of Bents and Semicircular Arches (Cont'd)

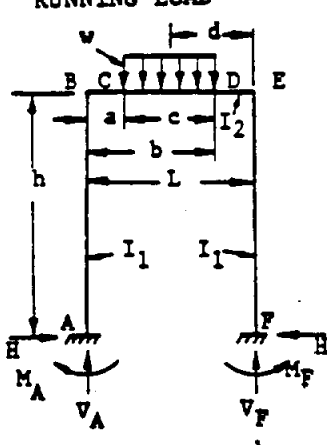
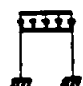
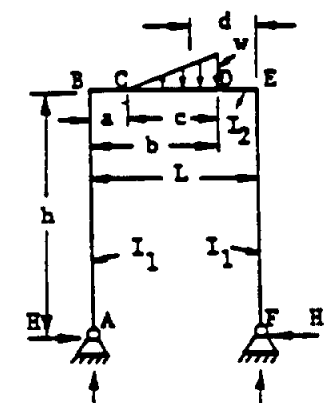
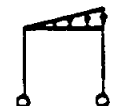
Table B 5.1.4-1 Reactions and Constraining Moments in Two Legged Rectangular Bents (Cont'd)

<p>4. HORIZ. CONCENTRATED LOAD</p> 	$V = \frac{3Qa^2K}{Lh(6K+1)} \quad H_A = Q - H_E$ $H_E = \frac{Qab}{2h^2} \left[\frac{h}{b} - \frac{h+b+K(b-a)}{h(K+2)} \right]$ $M_A = \frac{Qa}{2h} \left[\frac{b(h+b+bK)}{h(K+2)} + h - \frac{3aK}{(6K+1)} \right]$ $M_E = \frac{Qa}{2h} \left[\frac{-b(h+b+bK)}{h(K+2)} + h - \frac{3aK}{(6K+1)} \right]$ <p>FOR SPECIAL CASE: $b = 0, a = h$</p> $V = \frac{3QhK}{L(6K+1)}$ $H_A = H_E = \frac{Q}{2}$ $M_A = M_E = \frac{Qh(3K+1)}{2(6K+1)}$ 
<p>5. VERT. UNIFORM RUNNING LOAD</p>  <p style="text-align: center;">$d = L - \frac{a}{2} - \frac{b}{2}$</p>	$V_A = \frac{wcd}{L}$ $V_F = wc - V_A = \frac{wc}{L} \left(a + \frac{c}{2} \right) = wc \left(1 - \frac{d}{L} \right)$ $H = \frac{3}{2h} \left[\frac{x_1 + x_2}{2K+3} \right] = \frac{3wc}{24Lh(2K+3)} \left[12dL - 12d^2 - c^2 \right]$ <p>where:</p> $x_1 = -\frac{wc}{24L} \left[24\frac{d^3}{L} - 6\frac{bcd^2}{L} + 3\frac{c^2}{L} + 4c^2 - 24d^2 \right]$ $x_2 = \frac{wc}{24L} \left[24\frac{d^3}{L} - 6\frac{bcd^2}{L} + 3\frac{c^3}{L} + 2c^2 - 48d^2 + 24dL \right]$ <p>FOR SPECIAL CASE: $a = 0, c = b = L, d = \frac{L}{2}$</p> $V_A = V_F = \frac{wL}{2}$ $H = \frac{wL^2}{4h(2K+3)}$ 

STRUCTURAL ANALYSIS MANUAL
GENERAL DYNAMICS/CONVAIR AND SPACE SYSTEMS DIVISION

B 5.1.4 Particular Solution of Bents and Semicircular Arches (Cont'd)

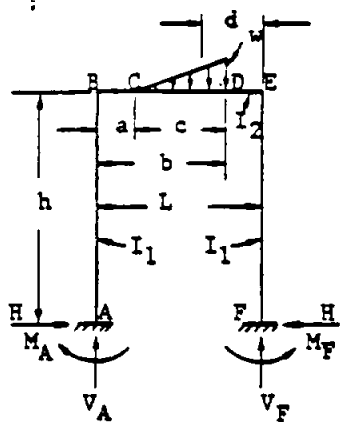
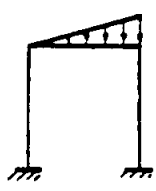
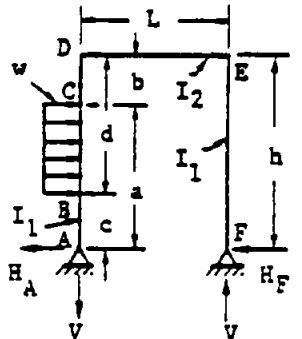
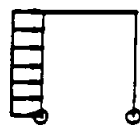
**Table B 5.1.4-1 Reactions and Constraining Moments in
Two Legged Rectangular Bents (Cont'd)**

<p>6. VERT. UNIFORM RUNNING LOAD</p>  <p style="text-align: center;">$d = L - \frac{a}{2} - \frac{b}{2}$</p>	$V_A = \frac{wcd}{L} + \frac{X_1 - X_2}{L(6K + 1)}$ <p style="text-align: center;">X_1 and X_2 are given in case 5</p> $V_F = wc - V_A$ $H = \frac{3(X_1 + X_2)}{2h(K + 2)} \quad M_A = \frac{X_1 + X_2}{2(K + 2)} - \frac{X_1 - X_2}{2(6K + 1)}$ $M_F = \frac{X_1 + X_2}{2(K + 2)} + \frac{X_1 - X_2}{2(6K + 1)}$ <p><u>FOR SPECIAL CASE:</u> $a = 0, c = b = L, d = \frac{L}{2}$</p> $V_A = V_F = \frac{wL}{2}$ $H = \frac{wL^2}{4h(K + 2)} \quad M_A = M_F = \frac{wL^2}{12(K + 2)}$ 
<p>7. VERT. TRIANGULAR RUNNING LOAD</p>  <p style="text-align: center;">$d = L - \frac{a}{3} - \frac{2b}{3}$</p>	$V_A = \frac{wcd}{2L}$ $V_F = \frac{wc}{2} - V_A = \frac{wc}{2L} \left(a + \frac{2c}{3} \right)$ $H = \frac{3}{2h} \left[\frac{X_3 + X_4}{2K + 3} \right] = \frac{3wc}{4Lh(2K + 3)} \left[dL - \frac{c^2}{18} - d^2 \right]$ <p><u>WHERE:</u></p> $X_3 = -\frac{wc}{2L} \left[\frac{d^3}{L} + \frac{c^2}{9} + \frac{51c^3}{810L} + \frac{c^2b}{6L} - d^2 \right]$ $X_4 = \frac{wc}{2L} \left[\frac{d^3}{L} + \frac{c^2}{18} + \frac{51c^3}{810L} - \frac{c^2b}{6L} - 2d^2 + dL \right]$ <p><u>FOR SPECIAL CASE:</u> $a=0, c=b=L, d = \frac{L}{3}$</p> $V = \frac{wL}{6}$ $H = \frac{wL^2}{8h(2K + 3)}$ 

STRUCTURAL ANALYSIS MANUAL
GENERAL DYNAMICS/CONVAIR AND SPACE SYSTEMS DIVISION

B 5.1.4 Particular Solution of Bents and Semicircular Arches (Cont'd)

**Table B 5.1.4-1 Reactions and Constraining Moments in
Two Legged Rectangular Bents (Cont'd)**

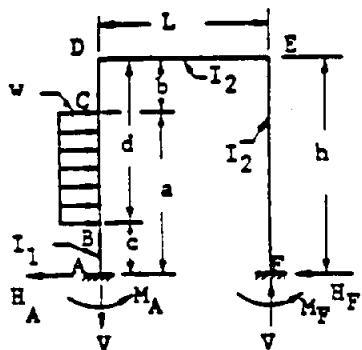
<p>8. VERT. TRIANGULAR RUNNING LOAD</p>  <p style="text-align: center;">$d = L - \frac{a}{3} - \frac{2b}{3}$</p>	$V_A = \frac{wcd}{2L} + \frac{X_3 - X_4}{L(6K + 1)} \quad \begin{matrix} X_3 \text{ and } X_4 \text{ are} \\ \text{given in case 7} \end{matrix}$ $V_F = \frac{wd}{2} - V_A \quad H = \frac{3(X_3 + X_4)}{2h(K + 2)}$ $M_A = \frac{X_3 + X_4}{2(K + 2)} - \frac{X_3 - X_4}{2(6K + 1)}$ $M_F = \frac{X_3 + X_4}{2(K + 2)} + \frac{X_3 - X_4}{2(6K + 1)}$ <p>FOR SPECIAL CASE: $a=0, c=b=L, d = \frac{L}{3}$</p> $V_A = \frac{wL}{6} \left[1 - \frac{1}{10(6K + 1)} \right]$ $V_F = \frac{wL}{3} \left[1 + \frac{1}{20(6K + 1)} \right]$ $H = \frac{wL^2}{8h(K + 2)}$ $M_A = \frac{wL^2}{120} \left[\frac{5}{K + 2} + \frac{1}{6K + 1} \right]$ $M_F = \frac{wL^2}{120} \left[\frac{5}{K + 2} - \frac{1}{6K + 1} \right]$ 
<p>9. HORIZ. UNIFORM RUNNING LOAD</p> 	$V = \frac{w(a^2 - c^2)}{2L} \quad H_A = w(a - c) - H_F$ $H_F = \frac{w(a^2 - c^2)}{4h} + \frac{K}{8h^3(2K + 3)} \left[\frac{w(a^2 - c^2)(2h^2 - a^2 - c^2)}{8h^3(2K + 3)} \right]$ <p>FOR SPECIAL CASE: $c=0, b=0, a=d=h$</p> $V = \frac{wh^2}{2L}$ $H_A = wh - H_F$ $H_F = \frac{wh}{4} \left[1 + \frac{K}{2(2K + 3)} \right]$ 

STRUCTURAL ANALYSIS MANUAL
GENERAL DYNAMICS/CONVAIR AND SPACE SYSTEMS DIVISION

B 5.1.4 Particular Solution of Bents and Semicircular Arches (Cont'd)

**Table B 5.1.4-1 Reactions and Constraining Moments in
Two Legged Rectangular Bents (Cont'd)**

**10. HORIZ. UNIFORM
RUNNING LOAD**



$$V = \frac{w(a^2 - c^2)}{2L} - \frac{M_A}{L} - \frac{M_F}{L}$$

$$H_A = w(a - c) - H_F$$

$$H_F = \frac{w(a^2 - c^2)}{4h} - \frac{X_5}{2h} + \frac{X_6(K - 1)}{2h(K + 2)}$$

WHERE:

$$X_5 = \frac{w}{12h^2} [d^3(4h - 3d) - b^3(4h - 3b)]$$

$$X_6 = \frac{w}{12h^2} [a^3(4h - 3a) - c^3(4h - 3c)]$$

$$M_A = \frac{(3K + 1) \left[\frac{w(a^2 - c^2)}{2} - X_5 \right]}{2(6K + 1)} + \frac{X_6}{2} \left[\frac{1}{K + 2} + \frac{3K}{6K + 1} \right] + X_5$$

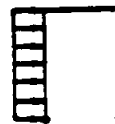
$$M_F = \frac{(3K + 1) \left[\frac{w(a^2 - c^2)}{2} - X_5 \right]}{2(6K + 1)} - \frac{X_6}{2} \left[\frac{1}{K + 2} - \frac{3K}{6K + 1} \right]$$

FOR SPECIAL CASE: $c=0, b=0, a=d=h$:

$$V = \frac{wh^2K}{L(6K + 1)} \quad H_A = wh - H_F$$

$$H_F = \frac{wh(2K + 3)}{8(K + 2)} \quad M_F = \frac{wh^2}{24} \left[\frac{18K + 5}{6K + 1} - \frac{1}{K + 2} \right]$$

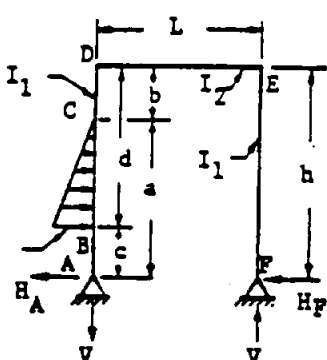

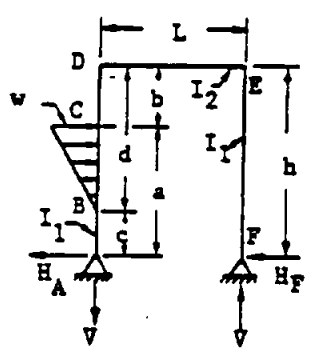
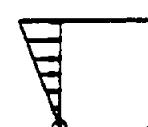
$$M_A = \frac{wh^2}{24} \left[\frac{30K + 7}{6K + 1} + \frac{1}{K + 2} \right]$$



STRUCTURAL ANALYSIS MANUAL
GENERAL DYNAMICS/CONVAIR AND SPACE SYSTEMS DIVISION

B 5.1.4 Particular Solution of Bents and Semicircular Arches (Cont'd)

**Table B 5.1.4-1 Reactions and Constraining Moments in
Two Legged Rectangular Bents (Cont'd)**

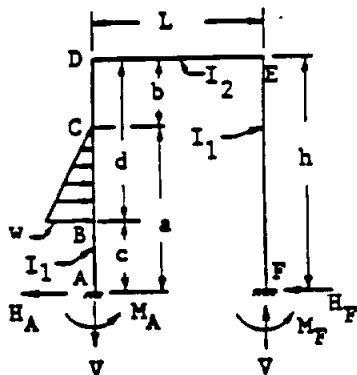
<p>11. HORIZ. TRIANGULAR RUNNING LOAD</p> 	$V = \frac{w}{6L} (a^2 + ac - 2c^2) \quad H_A = \frac{w(a - c)}{2} - H_F$ $H_F = \frac{VL}{2h} + \frac{KX_7}{(2K + 3)h} \quad \text{WHERE:}$ $X_7 = \frac{w}{120h^2(d-b)} \left[3(4d^5 + b^5) - 15h(3d^4 + b^4) + 20h^2(2d^3 + b^3) - 15bd^2(2h-d)^2 \right]$ <p>FOR SPECIAL CASE: $b=c=0, a=d=h$:</p> $V = \frac{wh^2}{6L} \quad H_A = \frac{wh}{2} - H_F$ $H_F = \frac{wh}{12} \left[1 + \frac{7K}{10(2K + 3)} \right]$ 
<p>12. HORIZ. TRIANGULAR RUNNING LOAD</p> 	$V = \frac{w}{6L} (2a + c)(a - c)$ $H_A = \frac{w(a - c)}{2} - H_F \quad H_F = \frac{VL}{2h} + \frac{KX_{10}}{h(2K + 3)}$ <p>WHERE:</p> $X_{10} = \frac{w}{120h^2(a-c)} \left[-30h^2c(a^2 - c^2) + 20h^2(a^3 - c^3) + 15c(a^4 - c^4) - 12(a^5 - c^5) \right]$ <p>FOR SPECIAL CASE: $b=c=0, a=d=h$:</p> $V = \frac{wh^2}{3L}$ $H_A = \frac{wh}{2} - H_F$ $H_F = \frac{wh}{10} \left[\frac{4K + 5}{2K + 3} \right]$ 

STRUCTURAL ANALYSIS MANUAL
GENERAL DYNAMICS/CONVAIR AND SPACE SYSTEMS DIVISION

B 5.1.4 Particular Solution of Bents and Semicircular Arches (Cont'd)

Table B 5.1.4-1 Reactions and Constraining Moments in Two Legged Rectangular Bents (Cont'd)

13. HORIZ. TRIANGULAR RUNNING LOAD



$$V = \frac{w(a^2 + ac - 2c^2)}{6L} - \frac{M_A}{L} - \frac{M_F}{L}$$

$$H_A = \frac{w(a - c)}{2} - H_F$$

$$H_F = \frac{w(a^2 + ac - 2c^2)}{12h} - \frac{X_8}{2h} + \frac{X_9(K-1)}{2h(K+2)}$$

WHERE:

$$X_8 = \frac{w}{60h^2(d-b)} \left[15(h+b)(d^4 - b^4) - 12(d^5 - b^5) - 20bh(d^3 - b^3) \right]$$

$$X_9 = \frac{w}{60h^2(d-b)} \left[10d^2h^2(2d-3b) + 10bh(4d^3 + b^2h - b^3) - d^4(30h+15b) + 12d^5 + 3b^5 \right]$$

$$M_A = \frac{(3K+1) \left[\frac{w(a^2 + ac - 2c^2)}{6} - X_8 \right]}{2(6K+1)}$$

$$+ \frac{X_9}{2} \left[\frac{1}{K+2} + \frac{3K}{6K+1} \right] + X_8$$

$$M_F = \frac{(3K+1) \left[\frac{w(a^2 + ac - 2c^2)}{6} \right] - X_8}{2(6K+1)}$$

$$- \frac{X_8}{2} \left[\frac{1}{K+2} - \frac{3K}{6K+1} \right]$$

FOR SPECIAL CASE: $b=c=0, a=d=h$

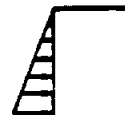
$$V = \frac{wh^2K}{4L(6K+1)}$$

$$H_A = \frac{wh}{2} - H_F$$

$$H_F = \frac{wh(3K+4)}{40(K+2)}$$

$$M_F = \frac{wh^2}{60} \left[\frac{27K+7}{2(6K+1)} - \frac{1}{K+2} \right]$$

$$M_A = \frac{wh^2}{60} \left[\frac{27K+7}{2(6K+1)} + \frac{3K+7}{K+2} \right]$$

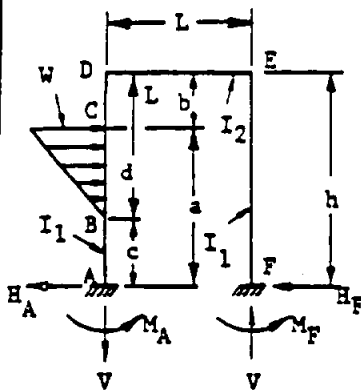


STRUCTURAL ANALYSIS MANUAL
GENERAL DYNAMICS/CONVAIR AND SPACE SYSTEMS DIVISION

B 5.1.4 Particular Solution of Bents and Semicircular Arches (Cont'd)

**Table B 5.1.4-1 Reactions and Constraining Moments in
Two Legged Rectangular Bents (Cont'd)**

**14. HORIZ. TRIANGULAR
RUNNING LOAD**



$$V = \frac{w(2a+c)(a-c)}{6L} - \frac{M_A}{L} - \frac{M_F}{L}$$

$$H_A = \frac{w(a-c)}{2} - H_F$$

$$H_F = \frac{w(2a^2-ac-c^2)}{12h} - \frac{X_{11}}{2h} + \frac{X_{12}(K-1)}{2h(K+2)}$$

where:

$$X_{11} = \frac{w}{60h^2(d-b)} \left[5hd^4 - 3d^5 - 20hdb^3 - 12b^4(d+h) \right]$$

$$X_{12} = \frac{w}{60h^2(a-c)} \left[15(h+c)(a^4-c^4) - 12(a^5-c^5) - 20ch(a^3-c^3) \right]$$

$$M_A = \frac{[3K+1] \left[\frac{w(2a^2-ac-c^2)}{6} - X_{11} \right]}{2(6K+1)}$$

$$+ \frac{X_{12}}{2} \left[\frac{1}{K+2} + \frac{3K}{6K+1} \right] + X_{11}$$

$$M_F = \frac{[3K+1] \left[\frac{w(2a^2-ac-c^2)}{6} - X_{11} \right]}{2(6K+1)} - \frac{X_{22}}{2}$$

$$\left[\frac{1}{K+2} - \frac{3K}{6K+1} \right]$$

FOR SPECIAL CASE: $b=c=0, a=d=h$

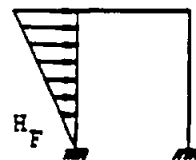
$$V = \frac{3Kwh^2}{4L(6K+1)}$$

$$H_A = \frac{wh}{2} - H_F$$

$$H_F = \frac{wh(7K+11)}{40(K+2)}$$

$$M_A = \frac{wh^2}{120} \left[\frac{87K+22}{6K+1} + \frac{3}{K+2} \right]$$

$$M_F = \frac{wh^2}{40} \left[\frac{21K+6}{6K+1} - \frac{1}{K+2} \right]$$

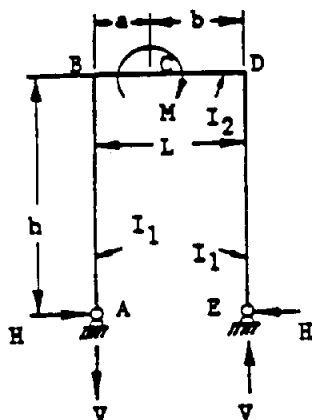


STRUCTURAL ANALYSIS MANUAL
GENERAL DYNAMICS/CONVAIR AND SPACE SYSTEMS DIVISION

B 5.1.4 Particular Solution of Bents and Semicircular Arches (Cont'd)

Table B 5.1.4-1 Reactions and Constraining Moments in Two Legged Rectangular Bents (Cont'd)

15. MOMENT ON HORIZ. SPAN



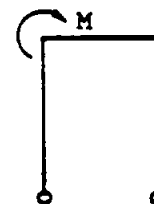
$$V = \frac{M}{L}$$

$$H = \frac{3(b - L/2)M}{Lh(2K + 3)}$$

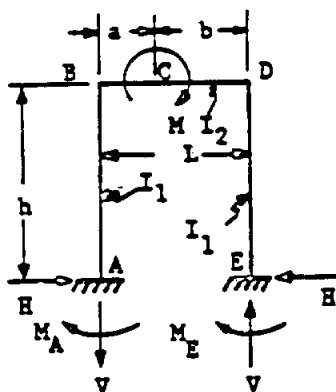
FOR SPECIAL CASE: $a=0, b=L$

$$V = \frac{M}{L}$$

$$H = \frac{3M}{2h(2K + 3)}$$



16. MOMENT ON HORIZ. SPAN



$$V = \frac{6(ab + L^2K)M}{L^3(6K + 1)}$$

$$H = \frac{3(b - a)M}{2Lh(K + 2)}$$

$$M_A = M \left[\frac{6ab(K+2) - L[a(7K+3) - b(5K-1)]}{2L^2(K+2)(6K+1)} \right]$$

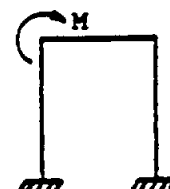
$$M_E = VL - M - M_A$$

FOR SPECIAL CASE: $a=0, b=L$

$$V = \frac{6KM}{L(1 + 6K)}$$

$$H = \frac{3M}{2h(K + 2)}$$

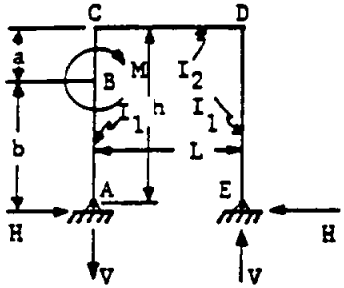
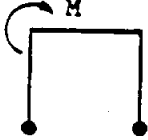
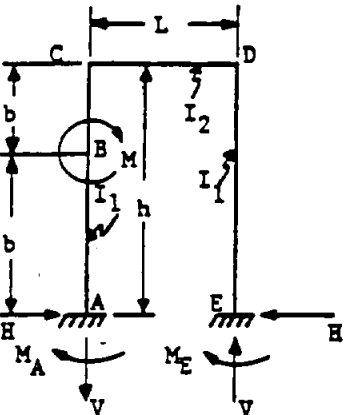
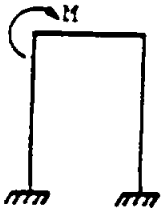
$$M_A = \frac{(5K - 1)M}{2(K + 2)(6K + 1)}$$



STRUCTURAL ANALYSIS MANUAL
GENERAL DYNAMICS/CONVAIR AND SPACE SYSTEMS DIVISION

B 5.1.4 Particular Solution of Bents and Semicircular Arches (Cont'd)

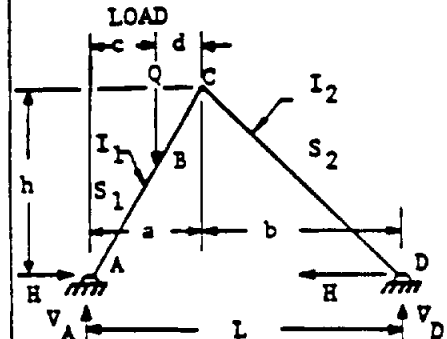
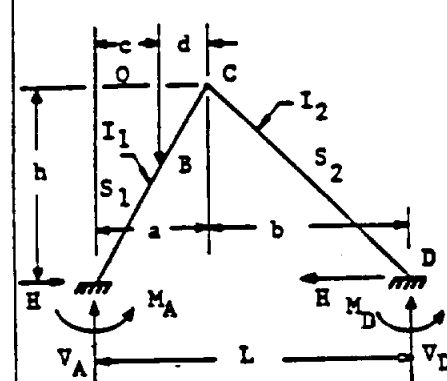
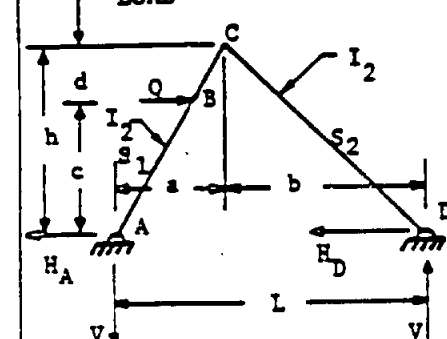
**Table B 5.1.4-1 Reactions and Constraining Moments in
Two Legged Rectangular Bents (Cont'd)**

<p>17. MOMENT ON SIDE SPAN</p> 	$V = \frac{M}{L} \quad H = \frac{3 [K(2ab+a^2) + h^2] M}{2h^3(2K+3)}$ <p><u>FOR SPECIAL CASE:</u> $a=0, b=h$</p> $V = \frac{M}{L} \quad H = \frac{3M}{2h(2K+3)}$ 
<p>18. MOMENT ON SIDE SPAN</p> 	$V = \frac{6bKM}{hL(6K+1)} \quad H = \frac{3bM [2a(K+1) + b]}{2h^3(K+2)}$ $M_A = \frac{-M}{2h^2(K+2)(6K+1)} [4a^2+2ab+b^2+K(26a^2-5b^2) + 6aK^2(2a-b)]$ $M_E = VL - M - M_A$ <p><u>FOR SPECIAL CASE:</u> $a=0; b=h$</p> $V = \frac{6KM}{L(6K+1)} \quad H = \frac{3M}{2h(K+2)}$ $M_A = \frac{M(5K-1)}{2(K+2)(6K+1)}$ 

STRUCTURAL ANALYSIS MANUAL
GENERAL DYNAMICS/CONVAIR AND SPACE SYSTEMS DIVISION

B 5.1.4 Particular Solution of Bents and Semicircular Arches (Cont'd)

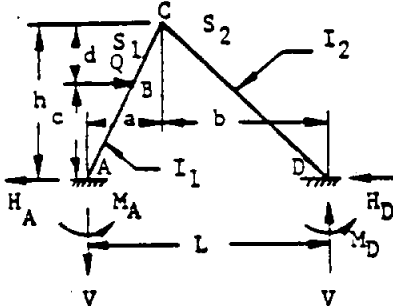
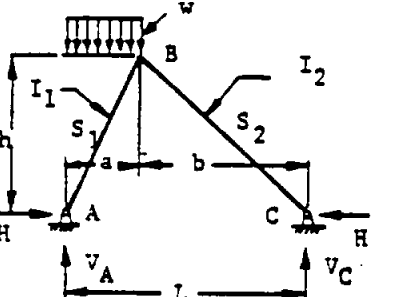
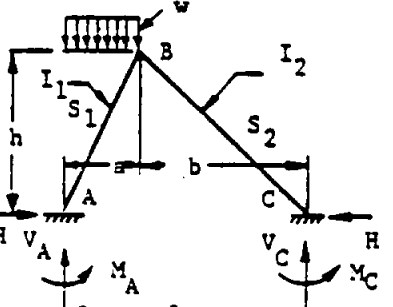
Table B 5.1.4-2 Reactions and Constraining Moments in Triangular Bents (Cont'd)

<p>19. VERT. CONCENTRATED LOAD</p> 	$V_A = Q - V_D$ $V_D = \frac{Qc}{L}$ $H = \frac{Qc}{h} \left[\frac{b}{L} + \frac{d(a+c)}{2a^2(K+1)} \right]$
<p>20. VERT. CONCENTRATED LOAD</p> 	$V_A = Q - V_D$ $V_D = \frac{Qc}{L} \left[1 - \frac{d(a+d)}{2a^2} \right]$ $H = \frac{Qcb}{Lh} + \frac{Qcd}{6La^2h(K+1)} \left[-b(3K+4) - 2L \left[\frac{(a+d)}{L} \right] + 2(2L+b)(a+c) + 3ac \right]$ $M_A = \frac{Qcd}{6a^2(K+1)} \left[(a+d)(3K+4) - 2(a+c) \right]$ $M_D = \frac{Qc^2d}{2a^2(K+1)}$
<p>21. HORIZ. CONCENTRATED LOAD</p> 	$V = \frac{Qc}{L}$ $H_A = Q - H_D$ $H_D = \frac{Qc}{h} \left[\frac{b}{L} + \frac{d(h+c)}{2h^2(K+1)} \right]$

STRUCTURAL ANALYSIS MANUAL
GENERAL DYNAMICS/CONVAIR AND SPACE SYSTEMS DIVISION

B 5.1.4 Particular Solution of Bents and Semicircular Arches (Cont'd)

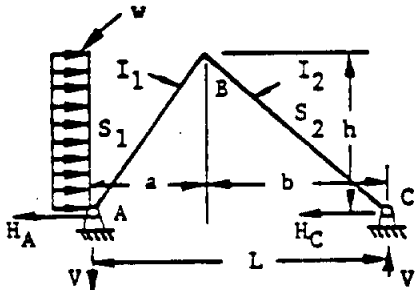
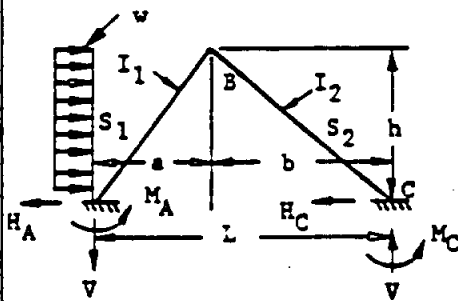
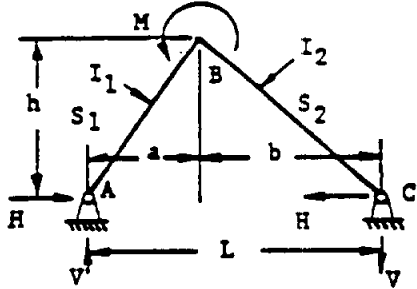
Table B 5.1.4-2 Reactions and Constraining Moments in Triangular Bents (Cont'd)

<p>22. HORIZ. CONCENTRATED LOAD</p> 	$V = \frac{Qc}{L} \left[1 - \frac{d(h+d)}{2h^2} \right]; \quad H_A = Q - H_D$ $H_D = \frac{Qc}{Lh} \left\{ b + \frac{d}{6h^2(K+1)} \left[(h+d)(-b[3K+4] - 2L) + 2(2L+b)(h+e) + 3ac \right] \right\}$ $M_A = \frac{Qcd}{6h^2(K+1)} \left[(h+d)(3K+4) - 2(h+c) \right]$ $M_D = \frac{Qcd}{6h^2(K+1)} (h + 2c + d)$
<p>23. VERTICAL UNIFORM RUNNING LOAD</p> 	$V_A = wa \left[1 - \frac{a}{2L} \right]$ $V_C = \frac{wa^2}{2L}$ $H = \frac{wa^2}{8h} \left[\frac{4b}{L} + \frac{1}{1+K} \right]$
<p>24. VERTICAL UNIFORM RUNNING LOAD</p> 	$V_A = wa \left[1 - \frac{3a}{8L} \right] ; \quad V_C = \frac{3wa^2}{8L}$ $H = \frac{wa^2}{24Lh(K+1)} \left[b(10 + 9K) + 2L + a \right]$ $M_A = \frac{wa^2(3K+2)}{24(K+1)}$ $M_C = \frac{wa^2}{24(K+1)}$

STRUCTURAL ANALYSIS MANUAL
GENERAL DYNAMICS/CONVAIR AND SPACE SYSTEMS DIVISION

B 5.1.4 Particular Solution of Bents and Semicircular Arches (Cont'd)

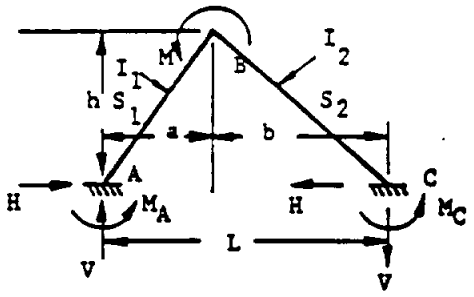
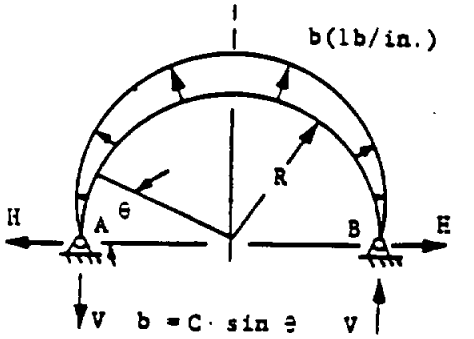
Table B 5.1.4-2 Reactions and Constraining Moments in Triangular Bents (Cont'd)

<p>25. HORIZ. UNIFORM RUNNING LOAD</p> 	$V = \frac{wh^2}{2L}$ $H_A = wh - H_C$ $H_C = \frac{wh}{8} \left[\frac{4b}{L} + \frac{1}{K+1} \right]$
<p>26. HORIZ. UNIFORM RUNNING LOAD</p> 	$V = \frac{3wh^2}{8L}$ $M_A = wh - M_C$ $M_C = \frac{wh}{8L(K+1)} [b(3K+4) + a]$ $M_A = \frac{wh^2(3K+2)}{24(K+1)} \quad M_C = \frac{wh^2}{24(K+1)}$
<p>27. APPLIED MOMENT AT APEX</p> 	$V = \frac{M}{L}$ $H = \frac{M}{hL} \left[\frac{a - bK}{K+1} \right]$

STRUCTURAL ANALYSIS MANUAL
GENERAL DYNAMICS/CONVAIR AND SPACE SYSTEMS DIVISION

B 5.1.4 Particular Solution of Bents and Semicircular Arches (Cont'd)

**Table B 5.1.4-3 Reactions and Constraining Moments in
 Triangular Bents and Semicircular Frames
 or Arches (Cont'd)**

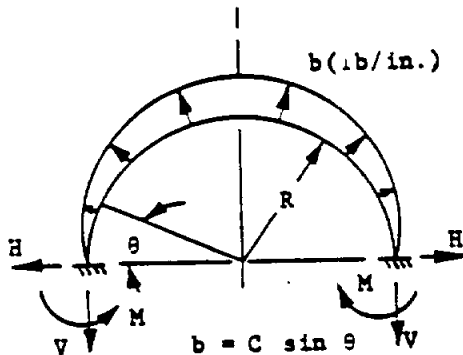
<p>28. APPLIED MOMENT AT APEX</p> 	$V = \frac{3M}{2L}$ $H = \frac{3M(a - bK)}{2hL(K + 1)}$ $M_A = \frac{KM}{2(K + 1)}$ $M_C = \frac{M}{2(K + 1)}$
<p>29. SINUSOIDAL NORMAL PRESSURE</p> 	$V = \frac{C\pi R}{4}$ $H = \frac{CR}{4}$ $M_\theta = \frac{CR^2}{4} \left[(\pi - 2\theta) \cos \theta - \pi + 3 \sin \theta \right]$ <p>(Positive moment acts clockwise on section ahead.)</p>

STRUCTURAL ANALYSIS MANUAL
GENERAL DYNAMICS/CONVAIR AND SPACE SYSTEMS DIVISION

B 5.1.4 Particular Solution of Bents and Semicircular Arches (Cont'd)

**Table B 5.1.4 Reactions and Constraining Moments in
Semicircular Frames or Arches (Cont'd)**

**30. SINUSOIDAL
NORMAL PRESSURE**



$$V = \frac{C\pi R}{4}$$

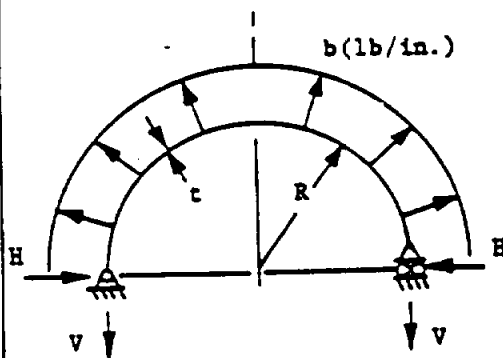
$$H = \frac{CR}{4} \left[\frac{3\pi^2 - 32}{8 - \pi^2} \right] = .31974CR$$

$$M = \frac{CR^2}{4} \left[\frac{\pi^3 - 10\pi}{8 - \pi^2} \right] = .05478CR^2$$

$$M_\theta = CR^2 \left[.81974 \sin \theta - .84018 + \frac{\cos \theta}{2} \left(\frac{\pi}{2} - \theta \right) \right]$$

(Positive moment acts clockwise on section ahead.)

**31. UNIFORM NORMAL
PRESSURE**



$M = 0$ at all points since pin points permit a uniform hoop tension. T , where:

$$T = V = bR$$

$$H = 0$$

STRUCTURAL ANALYSIS MANUAL
GENERAL DYNAMICS/CONVAIR AND SPACE SYSTEMS DIVISION

B5.0.0 FRAMES

References

1. Timoshenko, S., Theory of Structures, McGraw-Hill Book Company, Inc., New York, 1945.
2. Sutherland, H. and Bowman, H. L., Structural Theory, Fourth Edition, John Wiley & Sons, Inc., New York, 1954.
3. Wilbur, J. B. and Norris, C. H., Elementary Structural Analysis, First Edition, McGraw-Hill Book Co., Inc., New York, 1948.
4. Grinter, L. E., Theory of Modern Steel Structures, Vol. II, The Macmillan Co., New York, 1949.
5. Perry, D. J., Aircraft Structures, McGraw-Hill Book Co., Inc., New York, 1950.
6. Argyris, J. H., Dunne, P. C., Tye, W., et al., Structural Principles and Data, Fourth Edition, The New Era Publishing Co., Ltd., London, No date.
7. Roarke, R. J., Formulas for Stress and Strain, p 1120, Third Edition, McGraw-Hill Book Co., Inc., New York, 1954.

STRUCTURAL ANALYSIS MANUAL

GENERAL DYNAMICS/CONVAIR AND SPACE SYSTEMS DIVISION

Data Source, Section 1.3 Reference 1

Circular Rings

Rigid and Flexible Rings

The equations in Table 4.3.2.1 can be used for both rigid frames and flexible frames. For a flexible frame, calculate the relative stiffness factor, $d = \frac{GtR^4}{EI}$ or $d = \frac{KR^3}{EI}$ where $K = \frac{RtG}{L}$;

$$L = L_0 \left[1 + \frac{Gt L_0^2}{Et'R^2} \right]$$

where:

- t = average skin thickness
- G = modulus of elasticity in shear (skin)
- R = mean radius between skin and ring neutral axis
- E = modulus of elasticity in tension and compression (frame)
- I = moment of inertia of frame
- L_0 = distance of frame to rigid base (for example: distance to a wing spar) " L_0 " should not be less than " $R/2$ " or greater than " $2R$."
- t' = thickness of a fictitious "stringer skin" with a cross sectional area equal to the sum of the stringer areas and the part of the skin area that is effective in resisting longitudinal stresses.

When a ring is assumed infinitely rigid, the relative stiffness factor, "d," is zero. Curves of various values of "d" are plotted in Figures 4.3.2.2 through 4.3.2.31. From these figures, the appropriate coefficient "C" can be determined for use with the equations in Table 4.3.2.1.

When a ring is assumed infinitely rigid, the shear flow distributions, $\frac{VQ}{I}$ and $\frac{T}{2A}$, are assumed as shown in Fig. 4.3.2-1a. If the ring is assumed finitely flexible, the shear flow changes from a sine wave to a pattern shown in Fig. 4.3.2-1b.

The curves as shown in Fig. 4.3.2.2 through 4.3.2.31 have been derived for the ideal case of a continuous circular shell-supported frame of constant EI with any system of applied loads in the plane of the frame.

Rings which vary considerably from the ideal case may be handled with reasonable accuracy by approximating "equivalent ideal conditions."

The results of any system of loading may be obtained by breaking the system down into a series of individual radial, tangential, and moment components and superimposing the individual results.

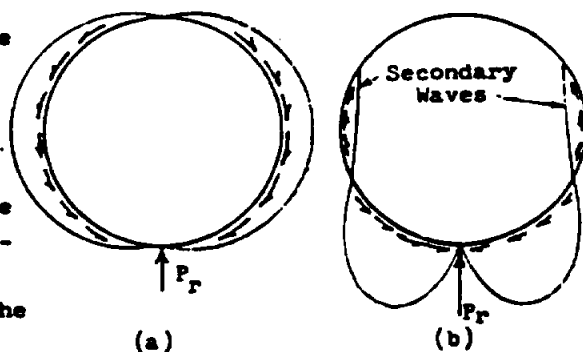


Fig. 4.3.2-1

STRUCTURAL ANALYSIS MANUAL
GENERAL DYNAMICS/CONVAIR AND SPACE SYSTEMS DIVISION

Approximation Method When "t," "R," or "I" Does Not Remain Constant

The relative importance of the skin thickness at any point is proportional to the intensity of the shear flow acting on the ring at that point. The skin thickness need be considered over the first primary wave of shear flow (load to shear reversal as noted on plots). A trial, using an assumed thickness, may be necessary to locate approximately the first primary shear flow wave. Then the average effective skin thickness may be obtained as follows:

- (1) Obtain the actual weighted average of skin thickness over approximately the first primary wave of shear flow for both the fore and aft sides of the ring.
- (2) If " L_0 " is less than the radius of the shell, the effective thickness on that side of the ring should be increased by the ratio R/L_0 .
- (3) Then "t" is the average thickness of the skins on each side of the frame.

The ring radius, "R," and the moment of inertia, "I," need to be constant or slightly varying only from the loading point around through the region of appreciable bending moment. If "R" and "I" vary slightly in this region, use average values of "R" and "I." If "R" varies considerably, overlapping assumptions may be applied. If "I" varies considerably, an approximate equivalent moment of inertia may be used as follows:

$$I' = \frac{\text{length of arc}}{\sum (ds/I)}$$

where the length of the arc and $\sum (ds/I)$ are continued over only the region of appreciable bending moment. For a case of varying curvature the approximate point on the actual ring for which the coefficients apply may be obtained by laying out around the ring a distance of $R\theta \frac{\pi}{180^\circ}$ inches, where "R" is the assumed radius and θ is measured in degrees from the loading to any point on the assumed equivalent circle.

Where one adjacent ring of approximately the same flexural proportions is similarly loaded, use $d = \frac{1}{2} \frac{GtR^4}{EIL}$;

where both adjacent rings are similarly loaded, use $(d = \frac{1}{4} \frac{GtR^4}{EIL})$.

Procedure

1. Select the appropriate equation from Table 4.3.2.1
2. Calculate the relative stiffness factor, d.
3. For any particular type loading, obtain the appropriate "C" value from one of the curves in Figures 4.3.2.2 thru 4.3.2.31.
4. Substitute the "C" value into the equation selected in step 1.

STRUCTURAL ANALYSIS MANUAL
GENERAL DYNAMICS/CONVAIR AND SPACE SYSTEMS DIVISION

Summary of Assumptions

When using the foregoing equations and the curves in Figures 4.3.2.2 through 4.3.2.31, it should be noted that the mathematical derivations were based on the following assumptions:

1. The frame is of constant initial curvature and constant flexural rigidity.
2. The supporting skin is of constant thickness and continuously attached to the frame.
3. The skin shear flow is proportional to the tangential deflection of the ring with respect to "rigid structure."
4. The frame complies with the assumptions for the flexure theory of curved beams with uniform rectangular cross sections.
5. All loading is in the plane of the frame.
6. The distortion of the frame, under loading, alters the skin shear-flow distribution but does not alter the geometry of the frame.
7. The skin shear flow acts along the elastic axis of the frame.
8. The frame undergoes no axial deformations.
9. The structure is loaded within the elastic limit.

NOTE: $M_{+0} = \dots = M_{-0}$ denotes graph is symmetrical and the moment has the same sign whichever way "0" is taken.

REFERENCES

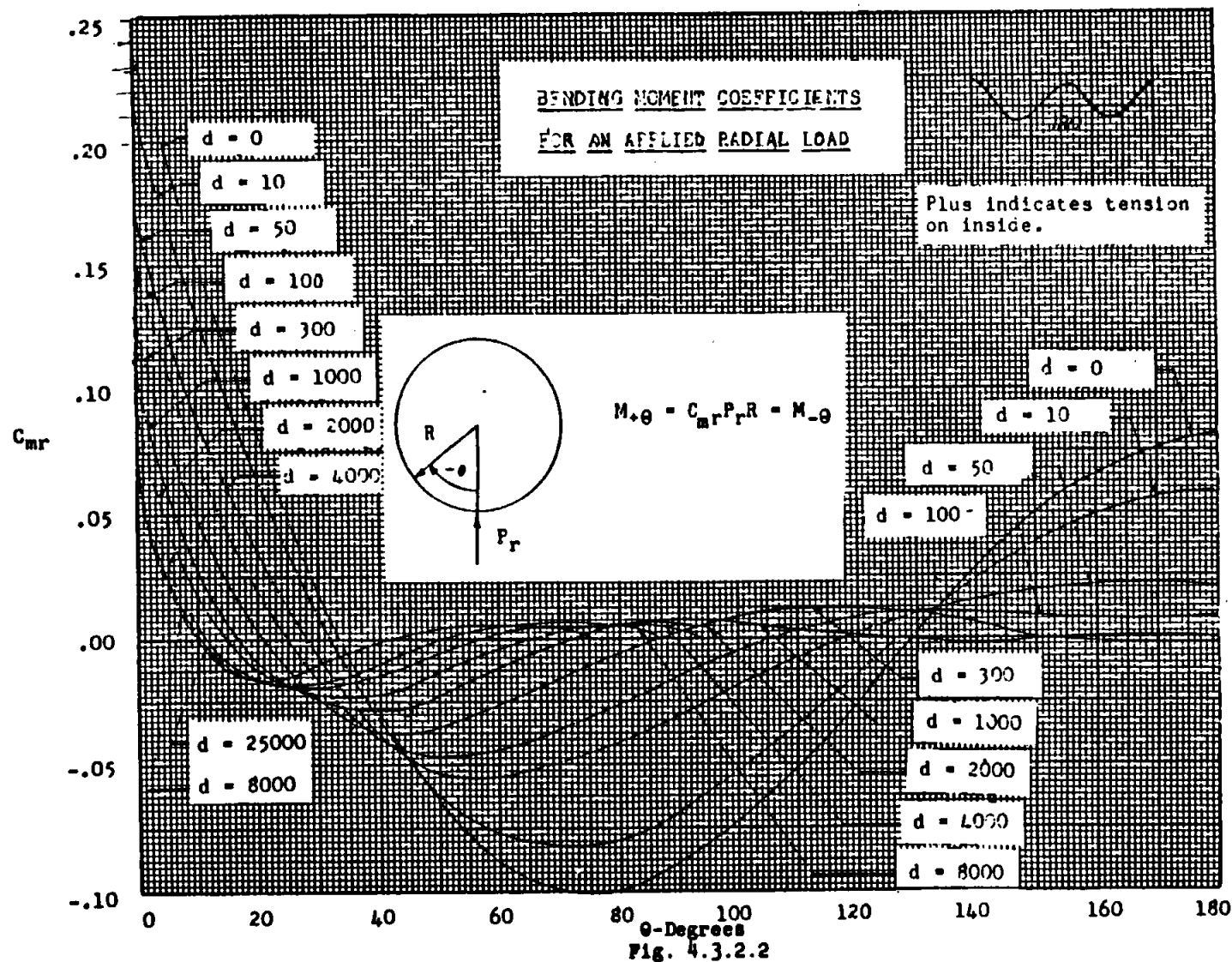
Wignet, J. E., Combs, R. and Ensrud, A. F., N.A.C.A. 929, Analysis of Circular Shell-Supported Frames, Washington, 1944

Additional rigid ring loading conditions are given in Section 18.1

TABLE 4.3.2.1
FORMULAS FOR DIFFERENT
LOADING CONDITIONS

	Radial Load	Tangential Load	Moment Load	Applied Rotation	Applied Horizontal Displacement
Bending Moment	$m = C_{mr} P_r R$	$m = C_{mt} P_t R$	$m = C_{mm} M$	$m = C_{m\delta} \delta \delta \delta \frac{EI}{R}$	$M = C_{m\delta} x \delta x \frac{EI}{R^2}$
Shearing Force	$S = C_{sr} P_r$	$S = C_{st} P_t$	$S = C_{sm} \frac{M}{R}$	$S = C_{s\delta} \delta \delta \delta \frac{EI}{R^3}$	
Axial Force	$F = C_{ar} P_r$	$F = C_{at} P_t$	$F = C_{am} \frac{M}{R}$	$F = C_{a\delta} \delta \delta \delta \frac{EI}{R^3}$	
Shear Flow	$q = C_{qr} \frac{P_r}{R}$ (lb/in.)	$q = C_{qt} \frac{P_t}{R}$ (lb/in.)	$q = C_{qm} \frac{M}{R^2}$ (lb/in.)	$q = C_{q\delta} \delta \delta \delta \frac{EI}{R^3}$	
Tangential Deflection	$\Delta T = \frac{R}{K} q = -C_{\Delta T_r} \frac{P_r}{K}$	$\Delta T = \frac{R}{K} q = -C_{\Delta T_t} \frac{P_t}{K}$	$\Delta T = \frac{R}{K} q = -C_{\Delta T_m} \frac{M}{KR}$	$\Delta T = -C_{\Delta T\delta} \delta \delta \delta \frac{R}{d}$	
Radial Deflection	$\Delta R = \frac{R}{K} \frac{dq}{d\theta} = C_{\Delta R_r} \frac{P_r}{K}$	$\Delta R = -\frac{R}{K} \frac{dq}{d\theta} = C_{\Delta R_t} \frac{P_t}{K}$	$\Delta R = -\frac{R}{K} \frac{dq}{d\theta} = C_{\Delta R_m} \frac{M}{KR}$	$\Delta R = C_{\Delta R\delta} \delta \delta \delta \frac{R}{d}$	
Sectional Rotation	$\Delta \theta = -\frac{1}{K} \left(q + \frac{d^2 q}{d\theta^2} \right)$ $= C_{\Delta \theta_r} \frac{P_r}{KR}$	$\Delta \theta = -\frac{1}{K} \left(q + \frac{d^2 q}{d\theta^2} \right)$ $= C_{\Delta \theta_t} \frac{P_t}{KR}$	$\Delta \theta = -\frac{1}{K} \left(q + \frac{d^2 q}{d\theta^2} \right)$ $= C_{\Delta \theta_m} \frac{M}{KR^2}$	$\Delta \theta = C_{\Delta \theta\delta} \delta \delta \delta \left(\frac{1}{d} \right)$	

* m represents internal resisting moment
M represents external applied moment



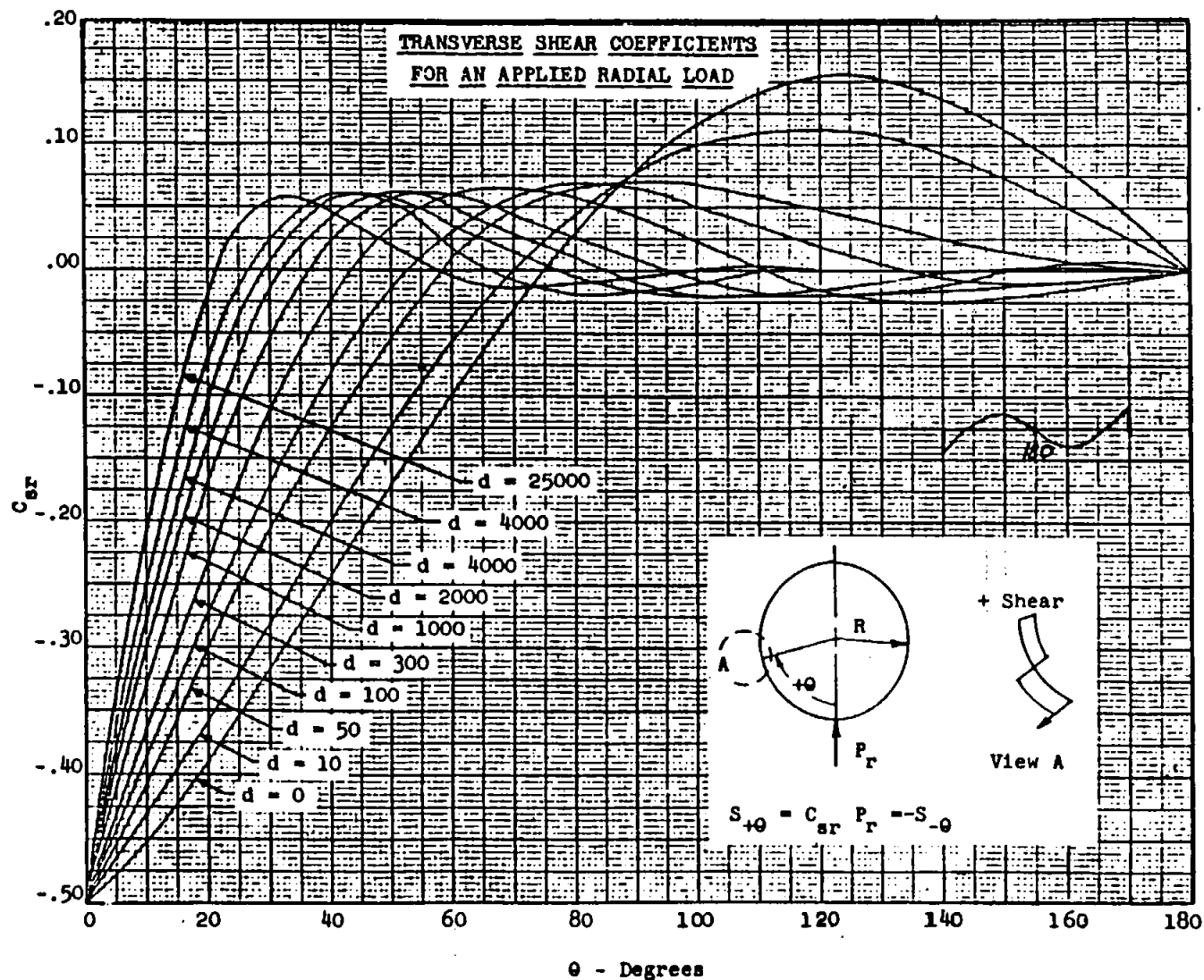
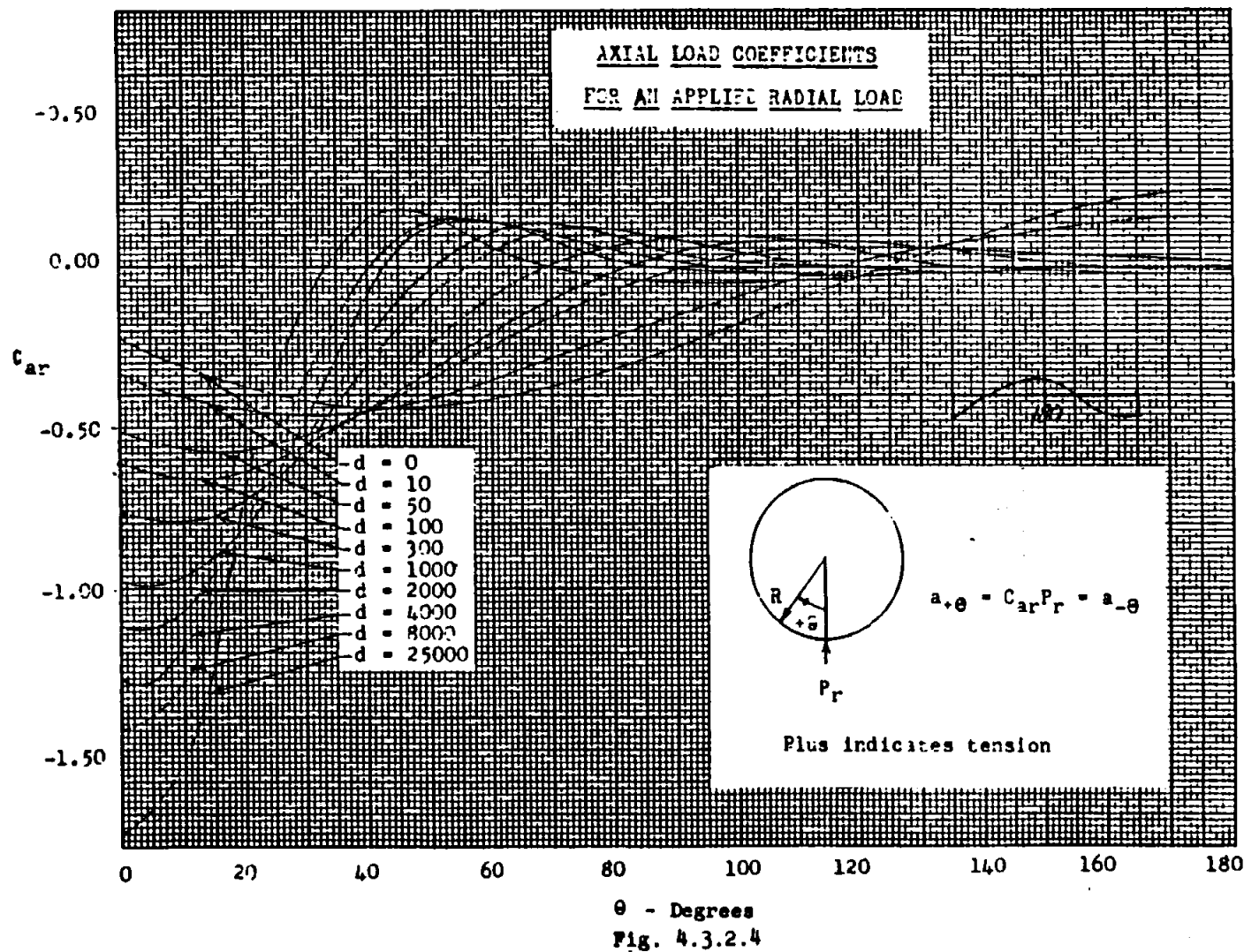
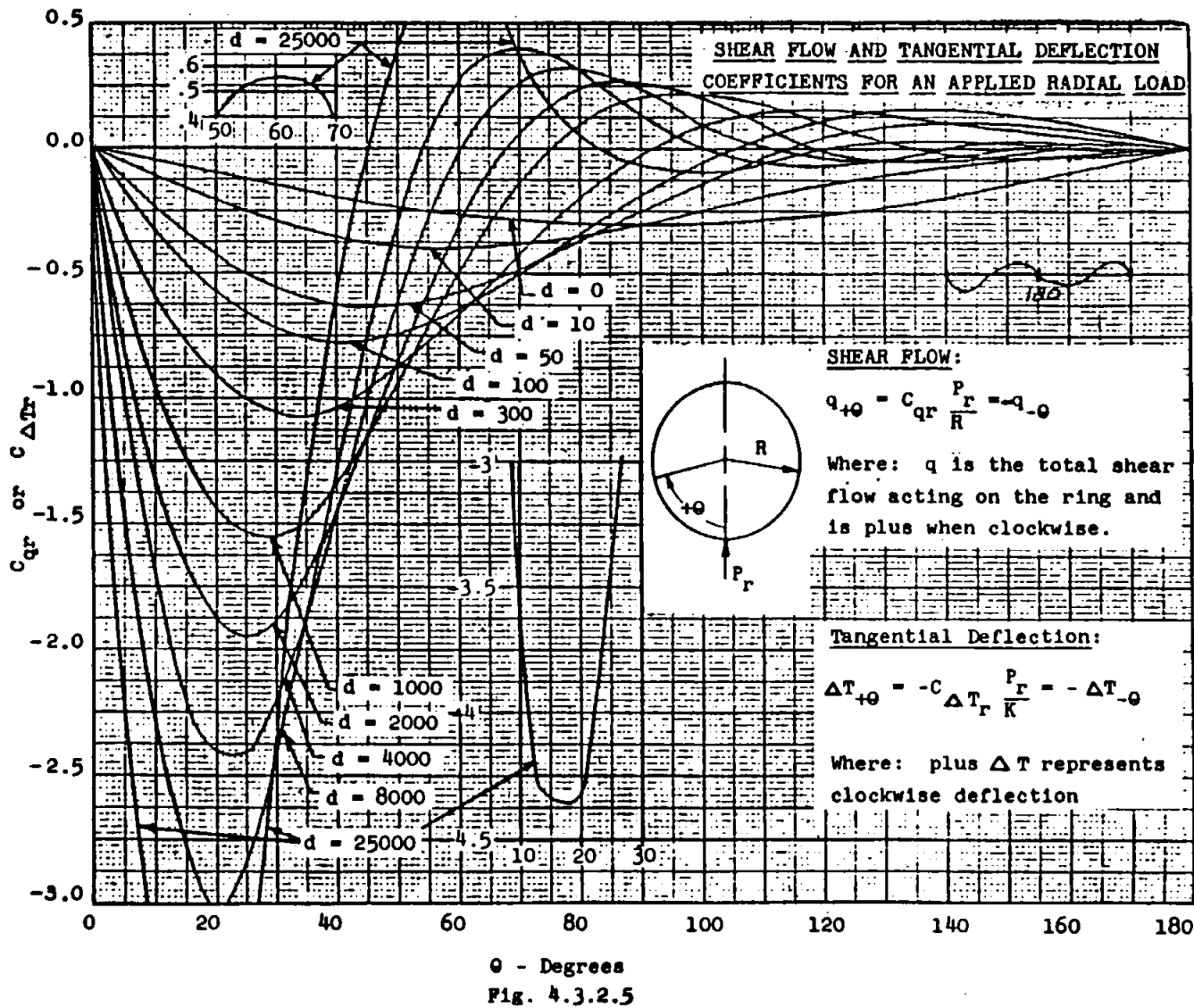


FIG. 4.3.2.1

469





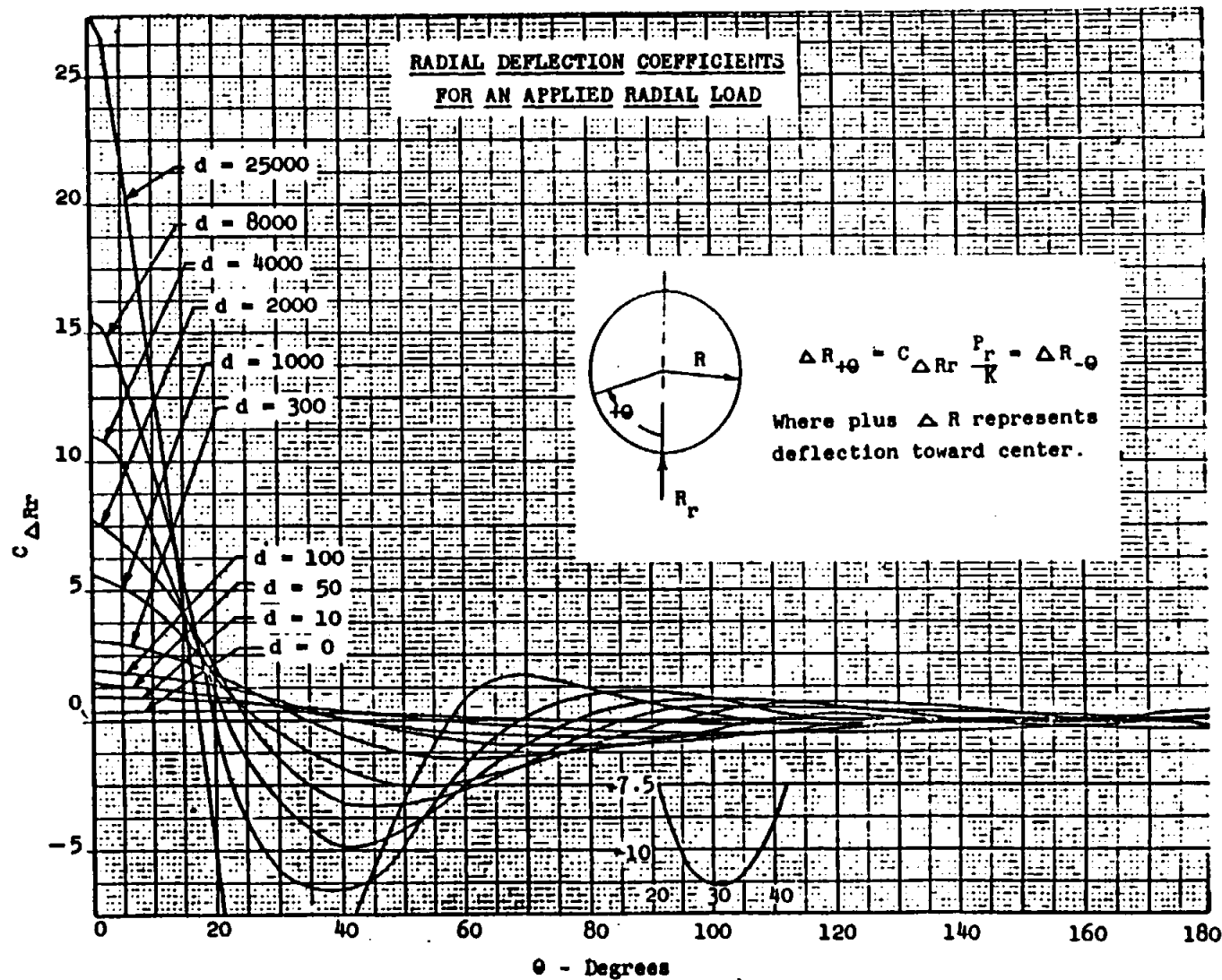
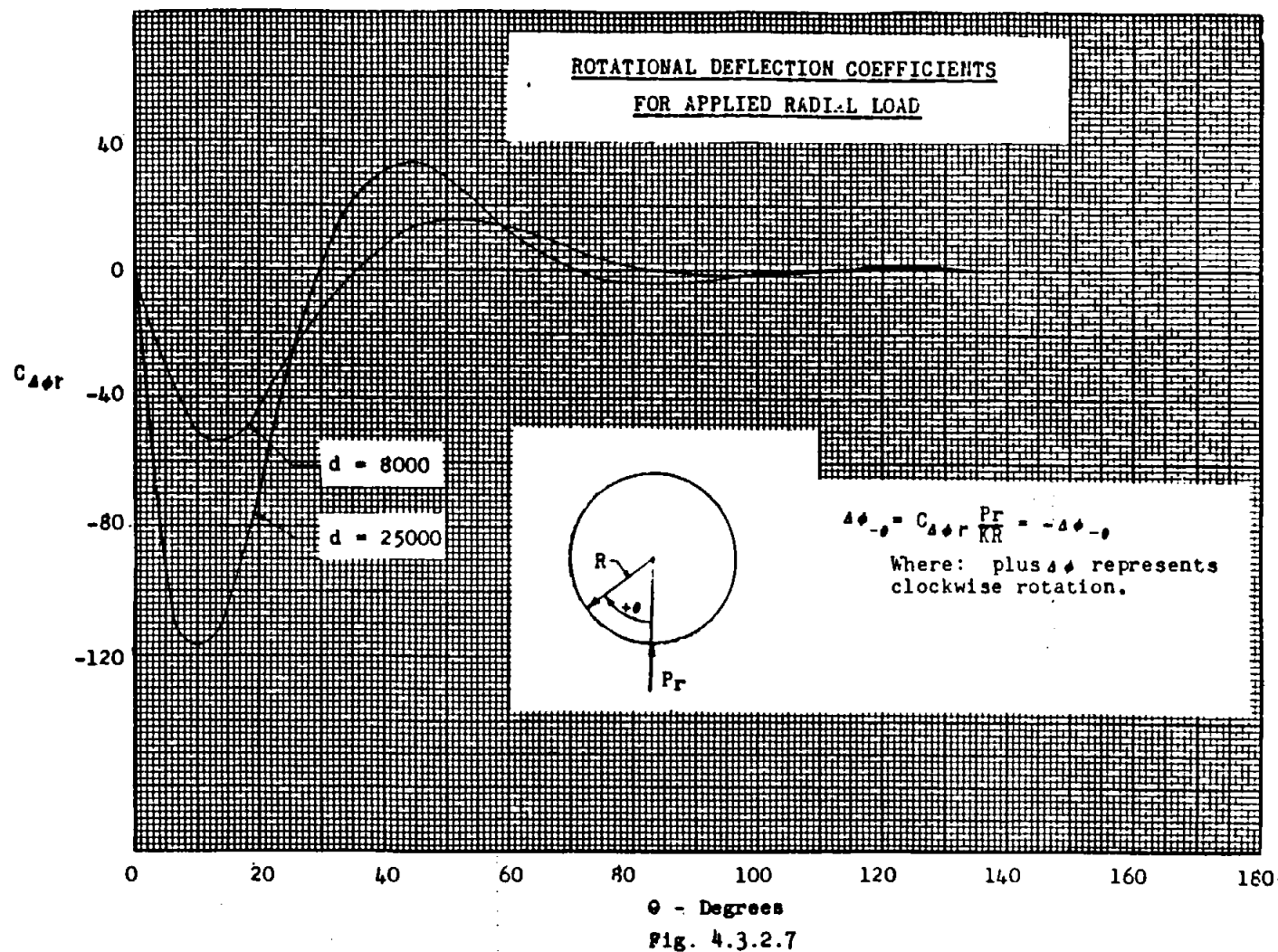


Fig. 4.3.2.6



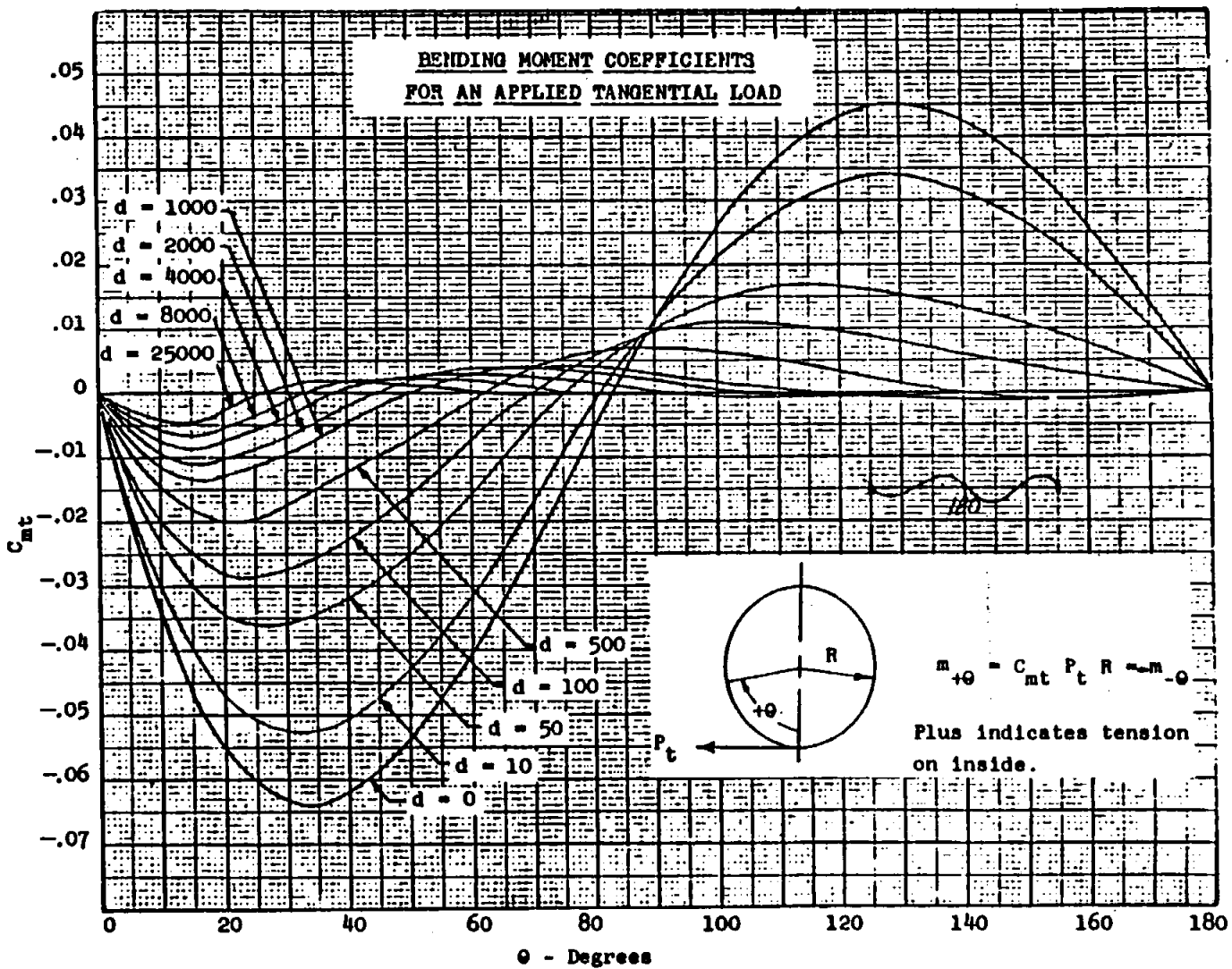


Fig. 4.3.2.8

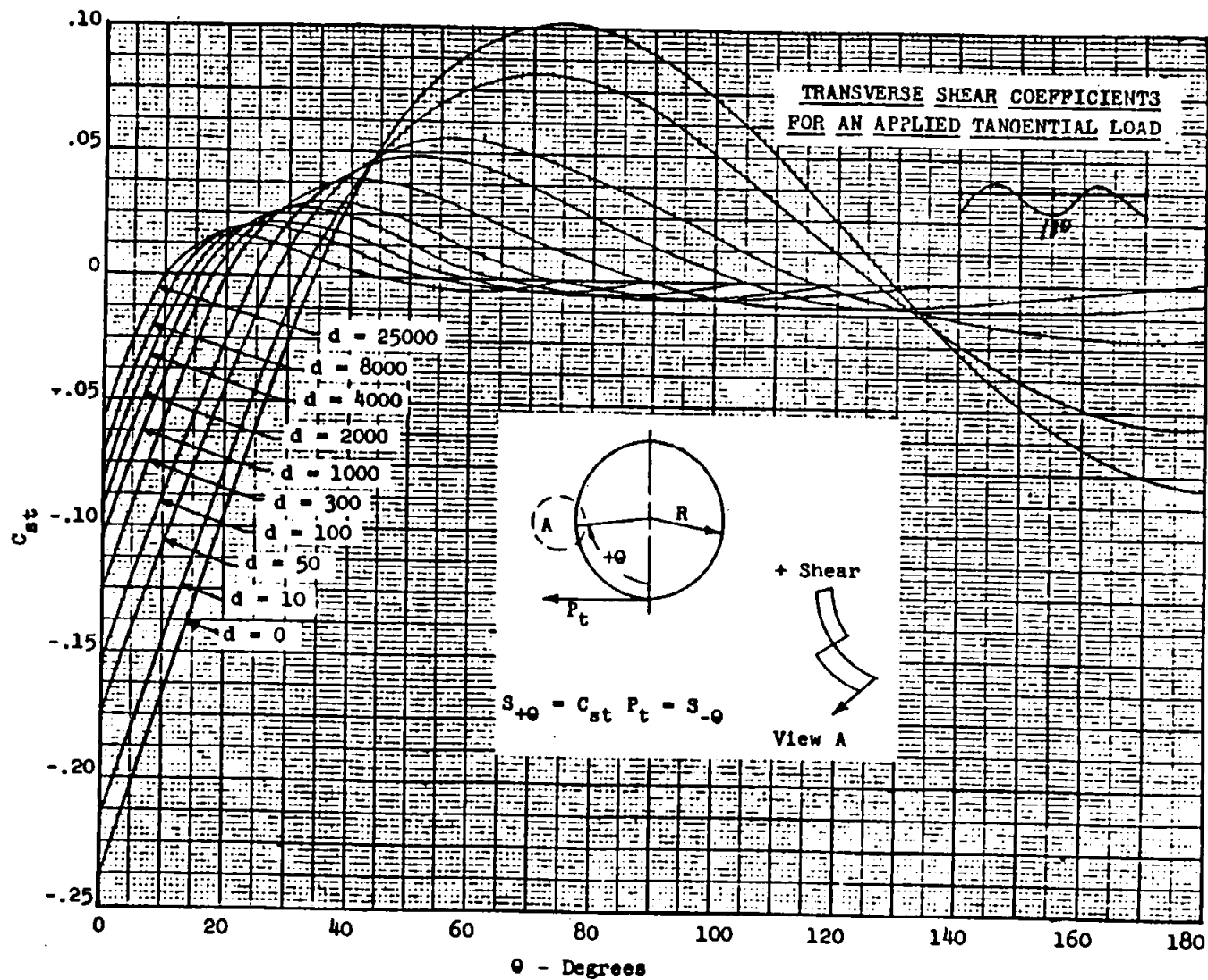
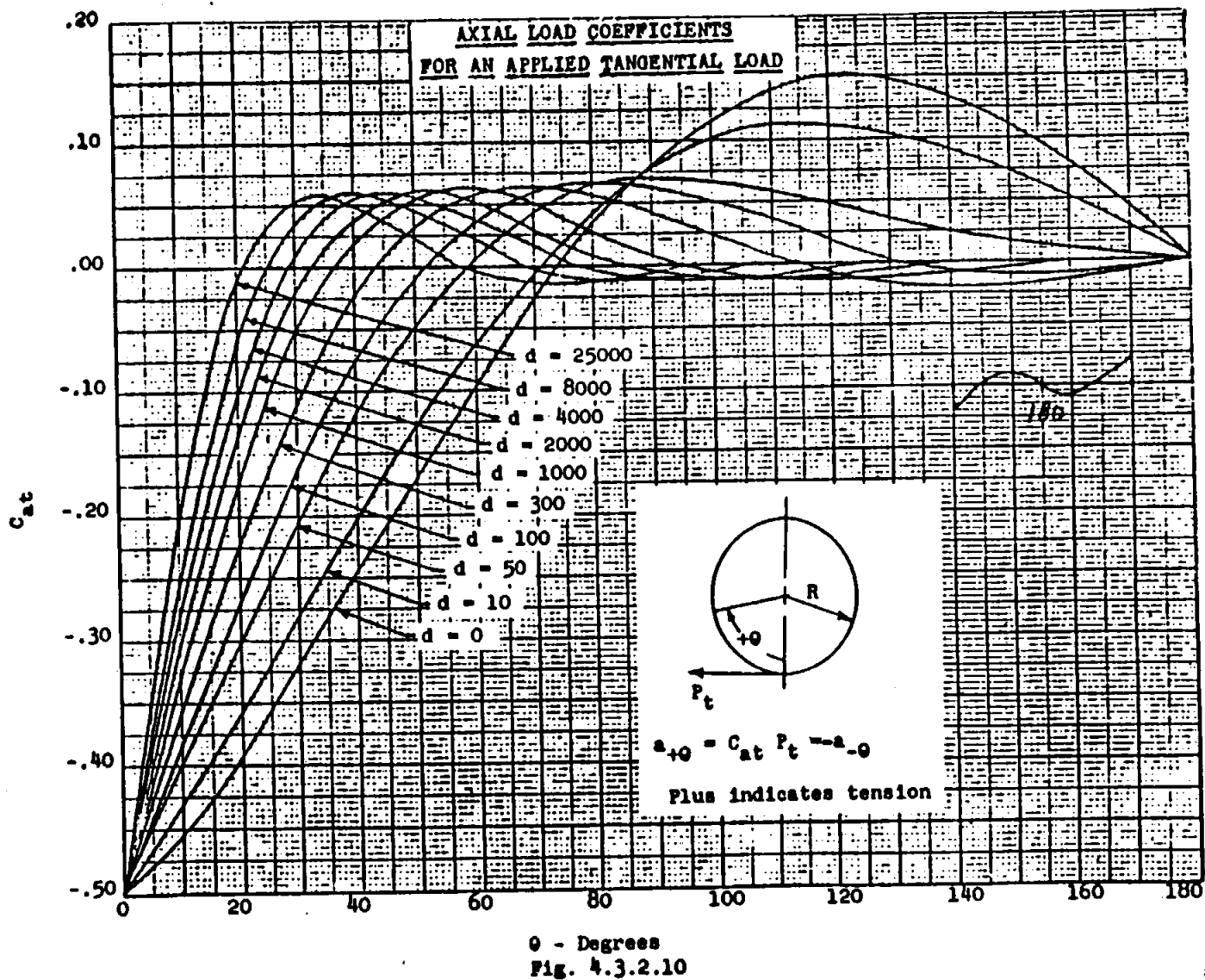


Fig. 4.3.2.9



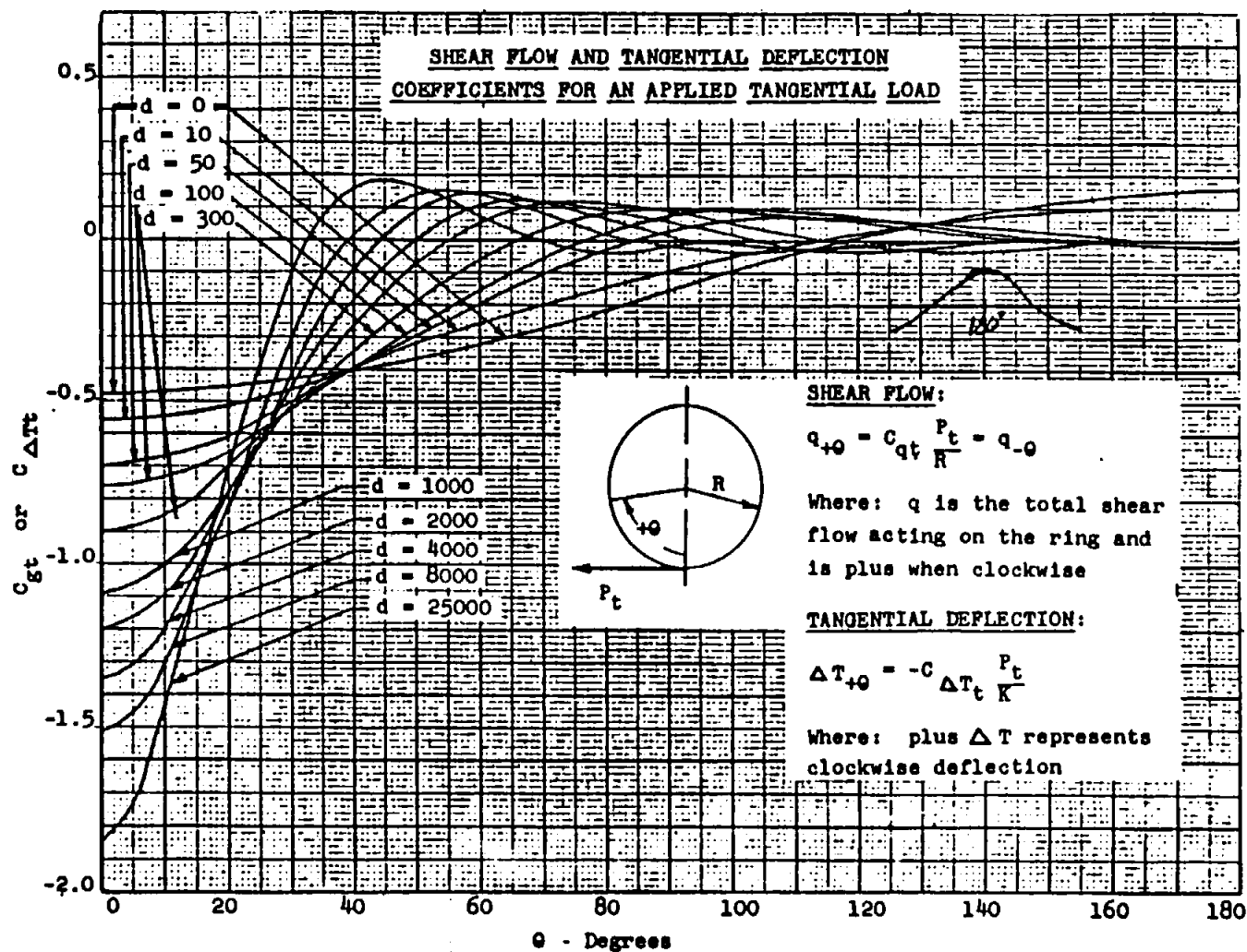
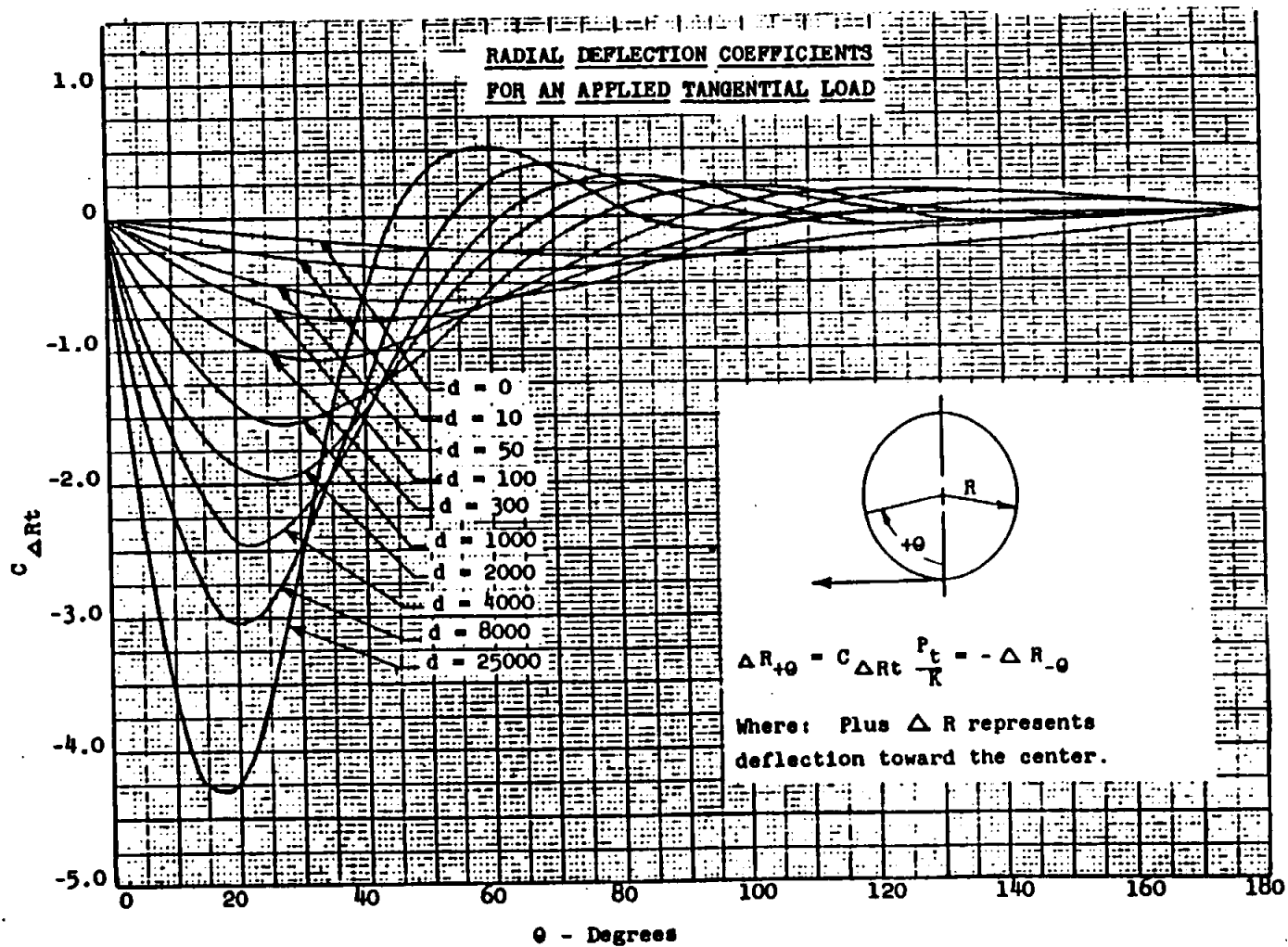


Fig. 4.3.2.11



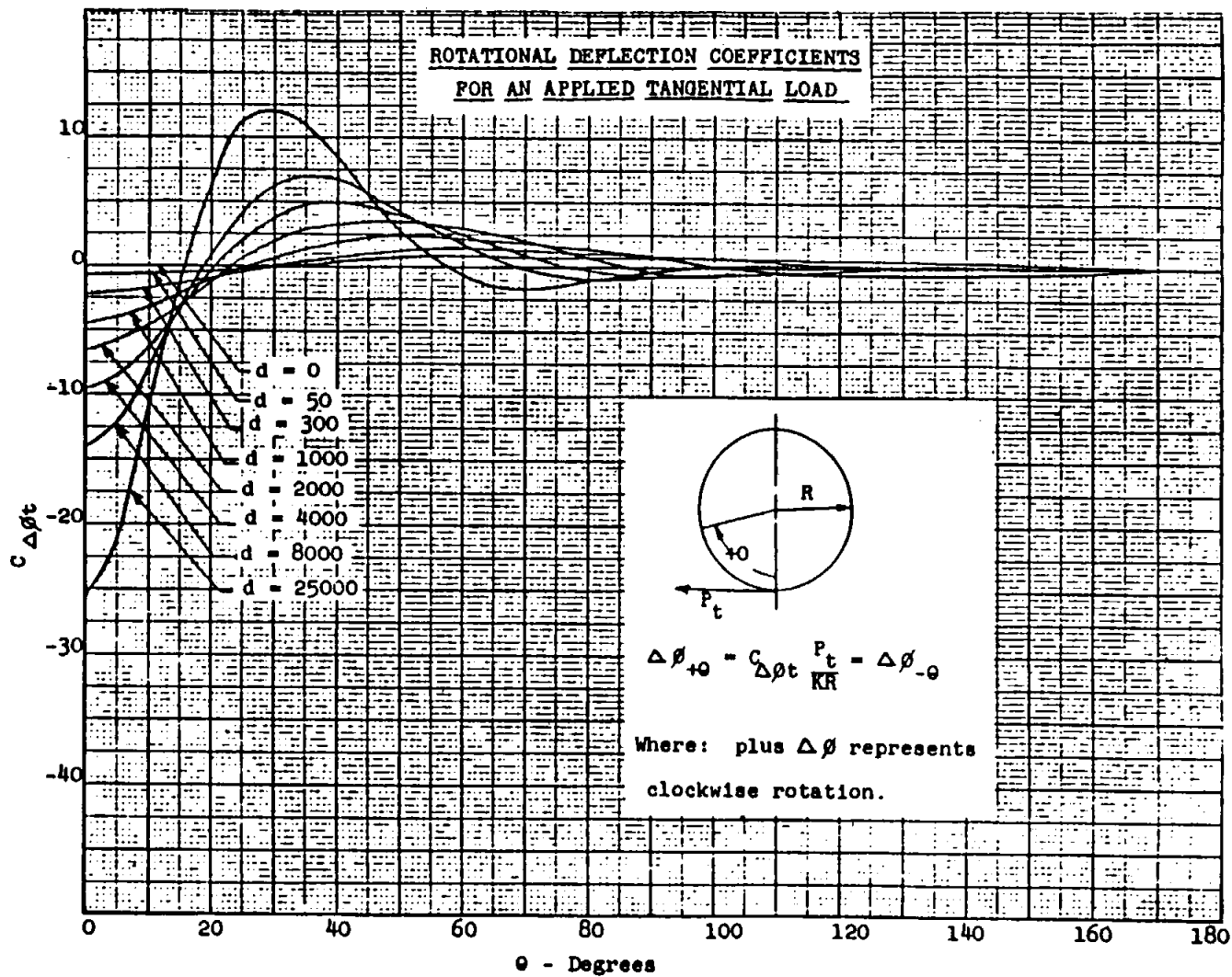
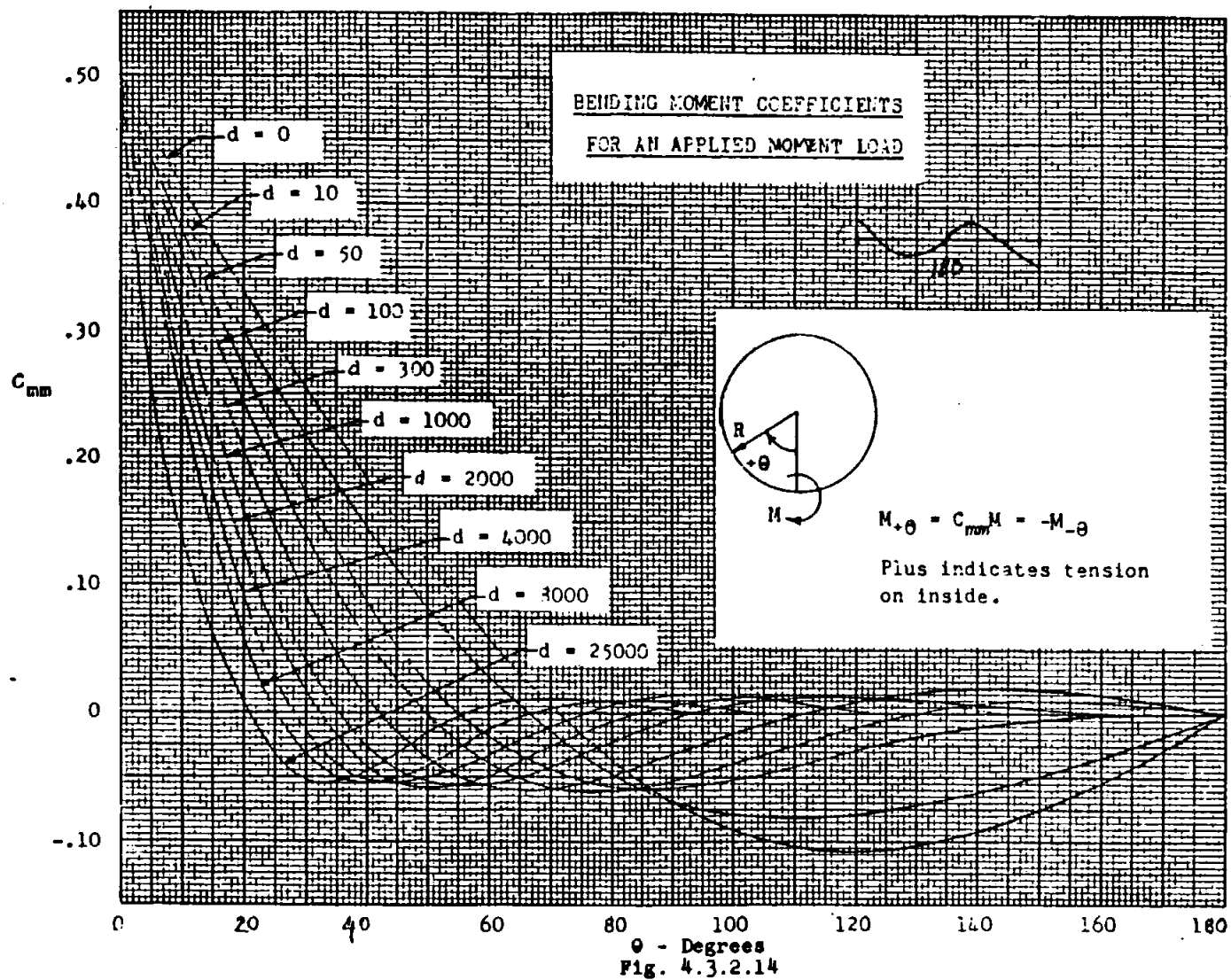


Fig. 4.3.2.13



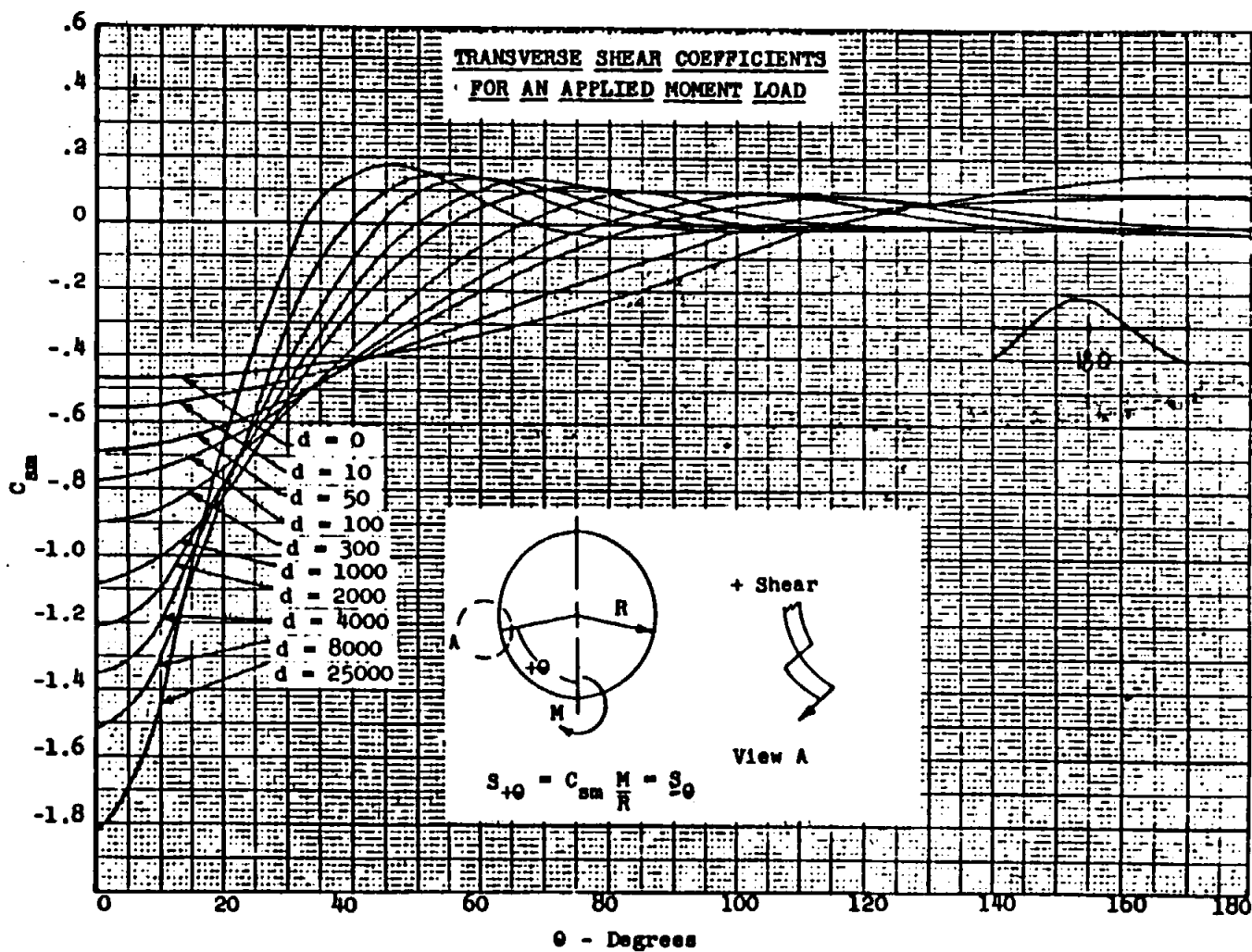


Fig. 4.3.2.15

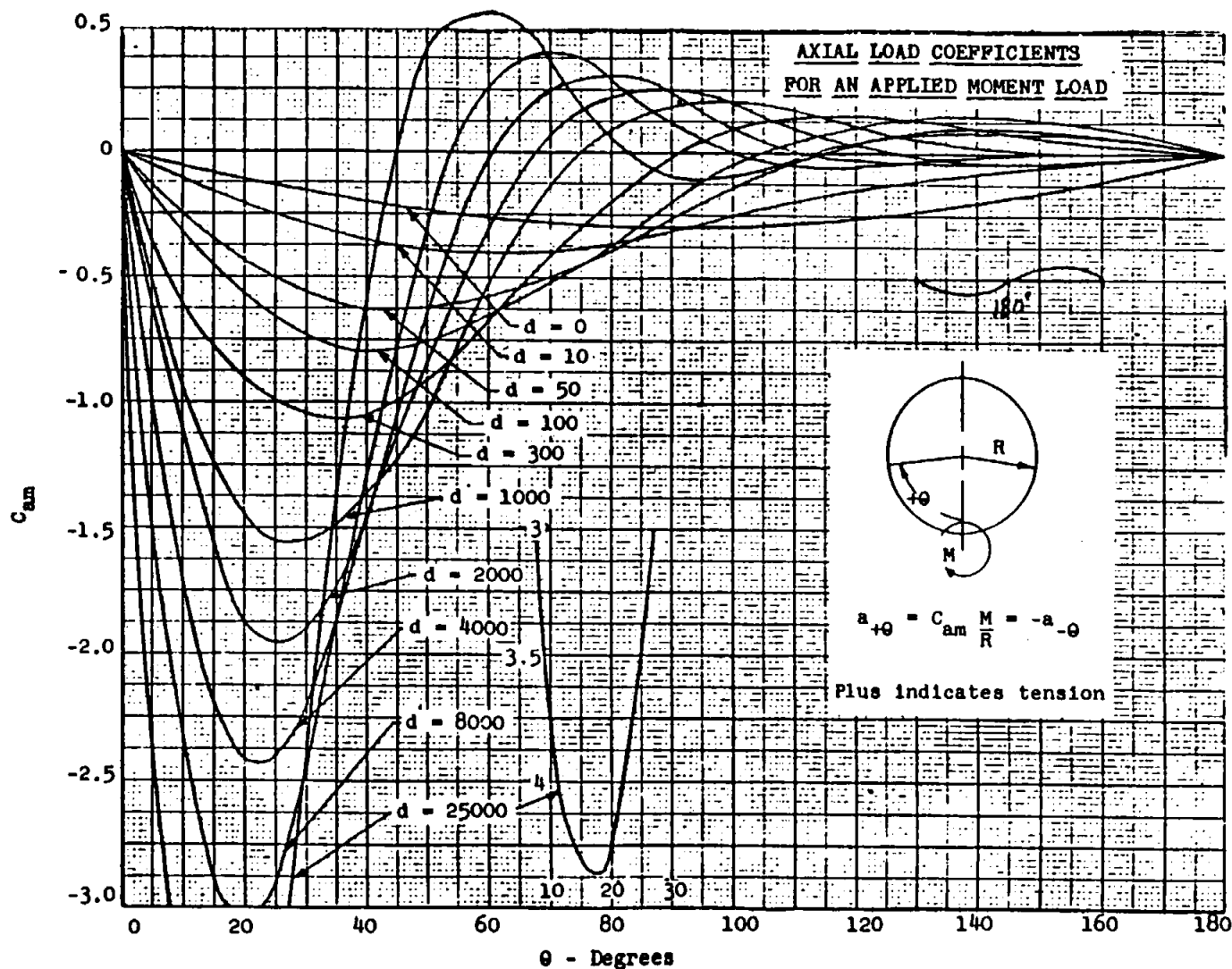
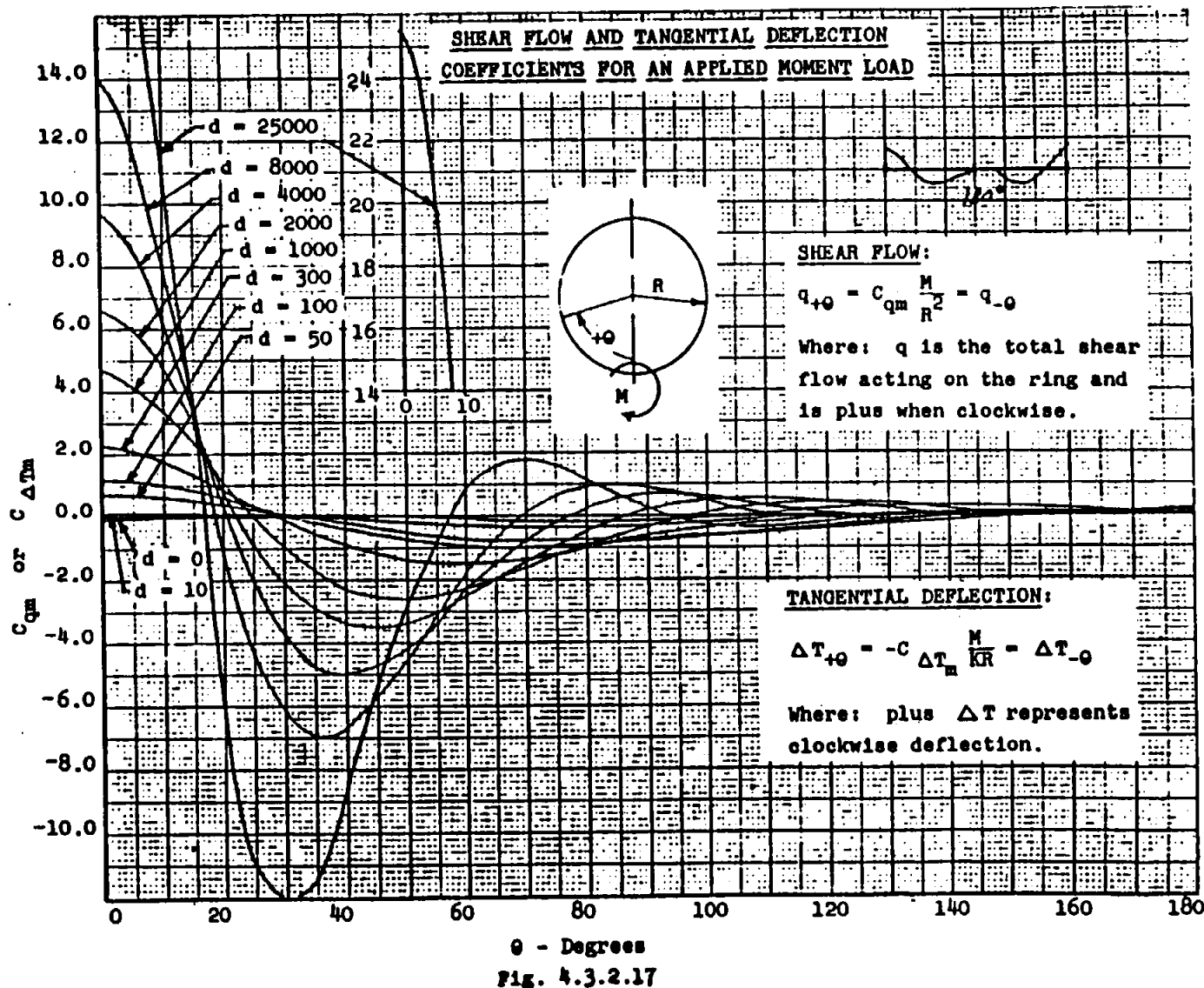


Fig. 4.3.2.16



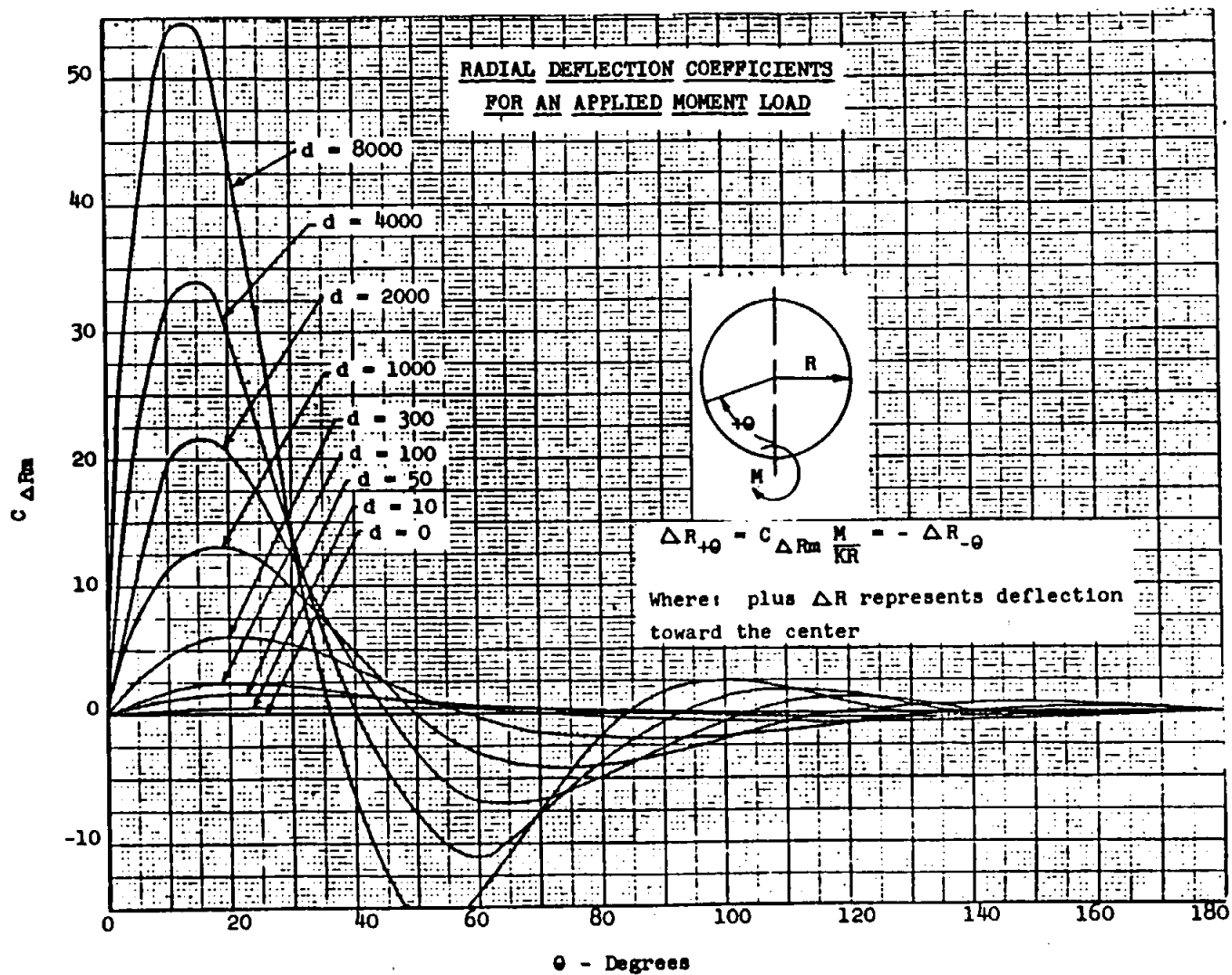


Fig. 4.3.2.18

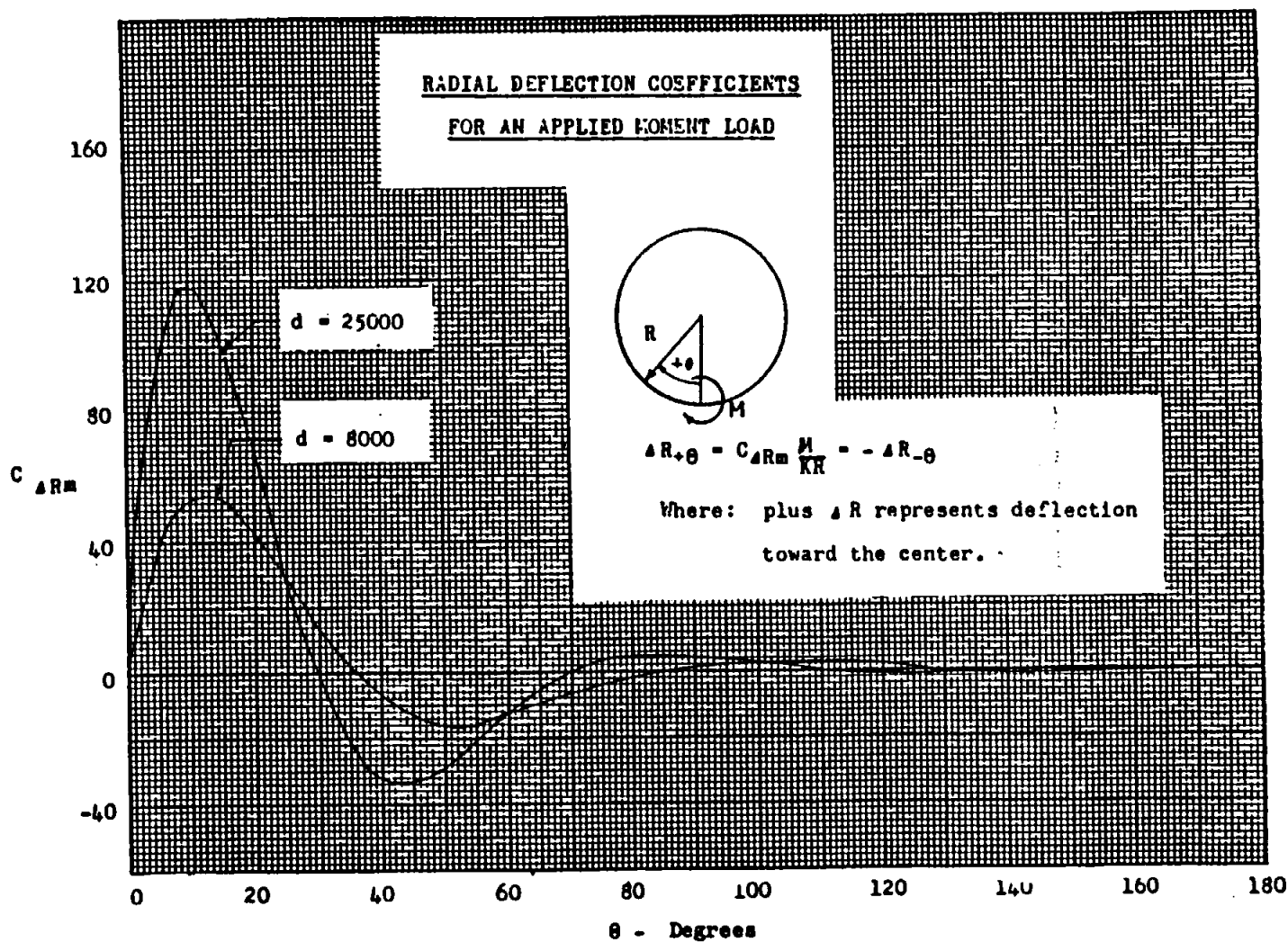
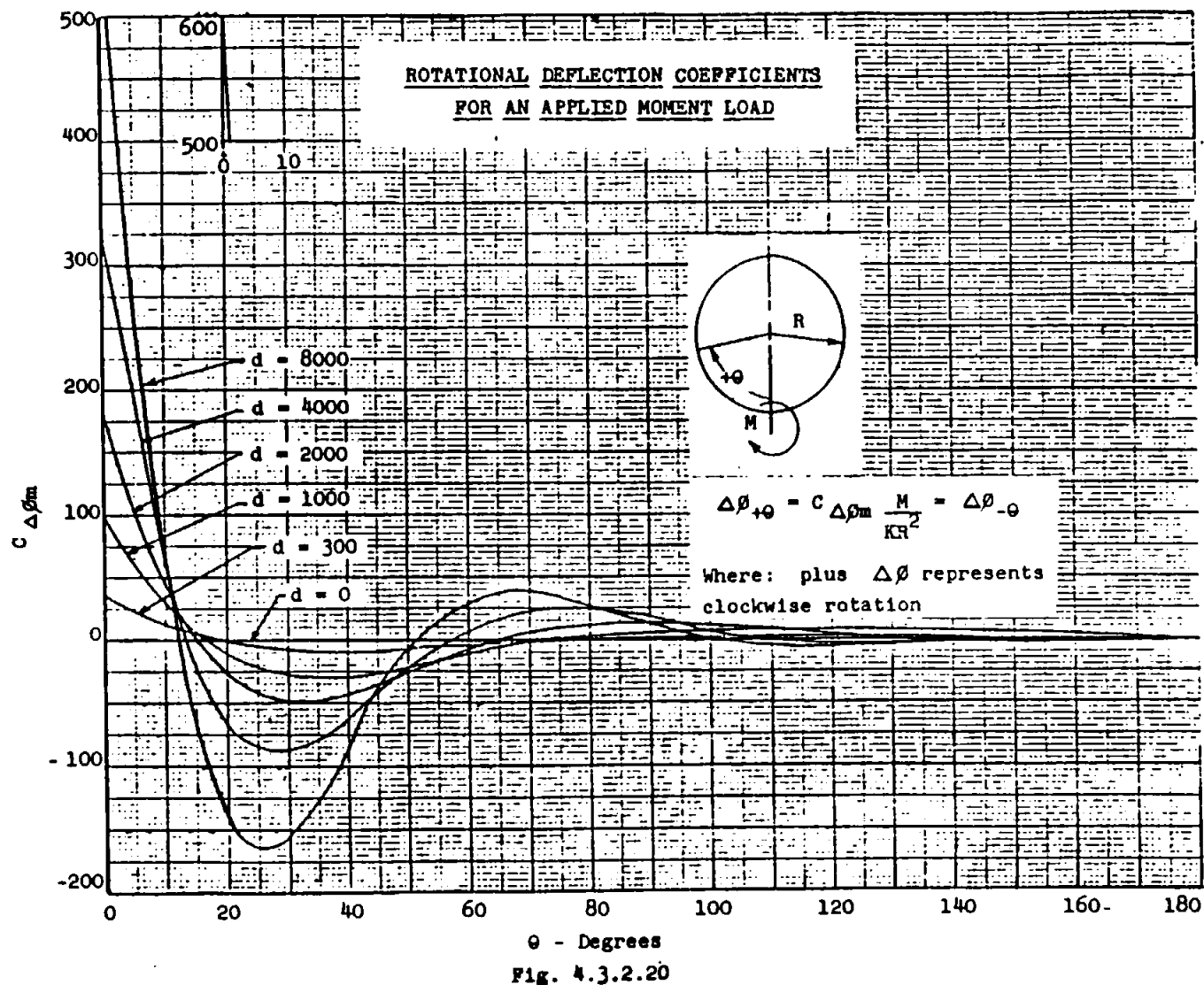
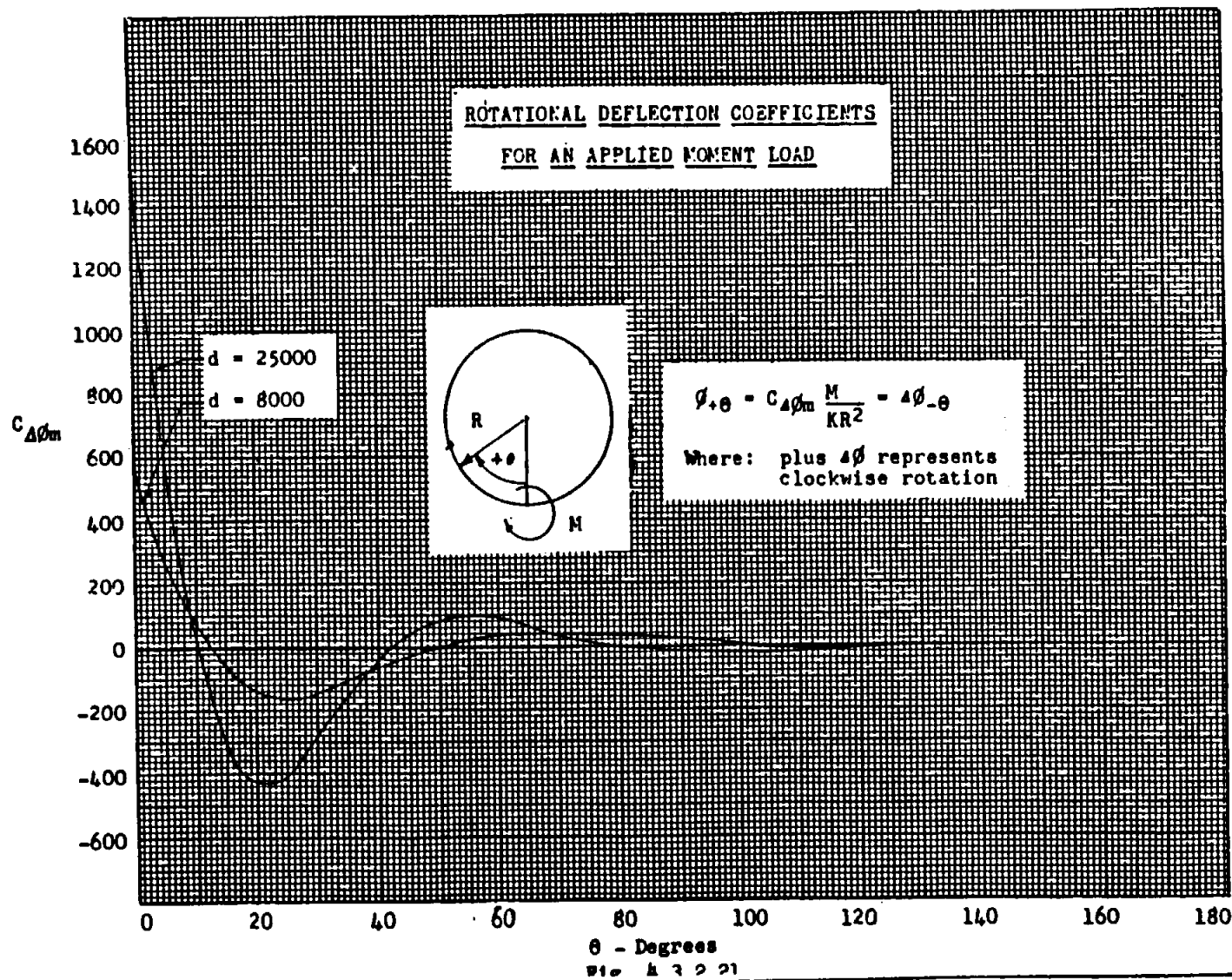
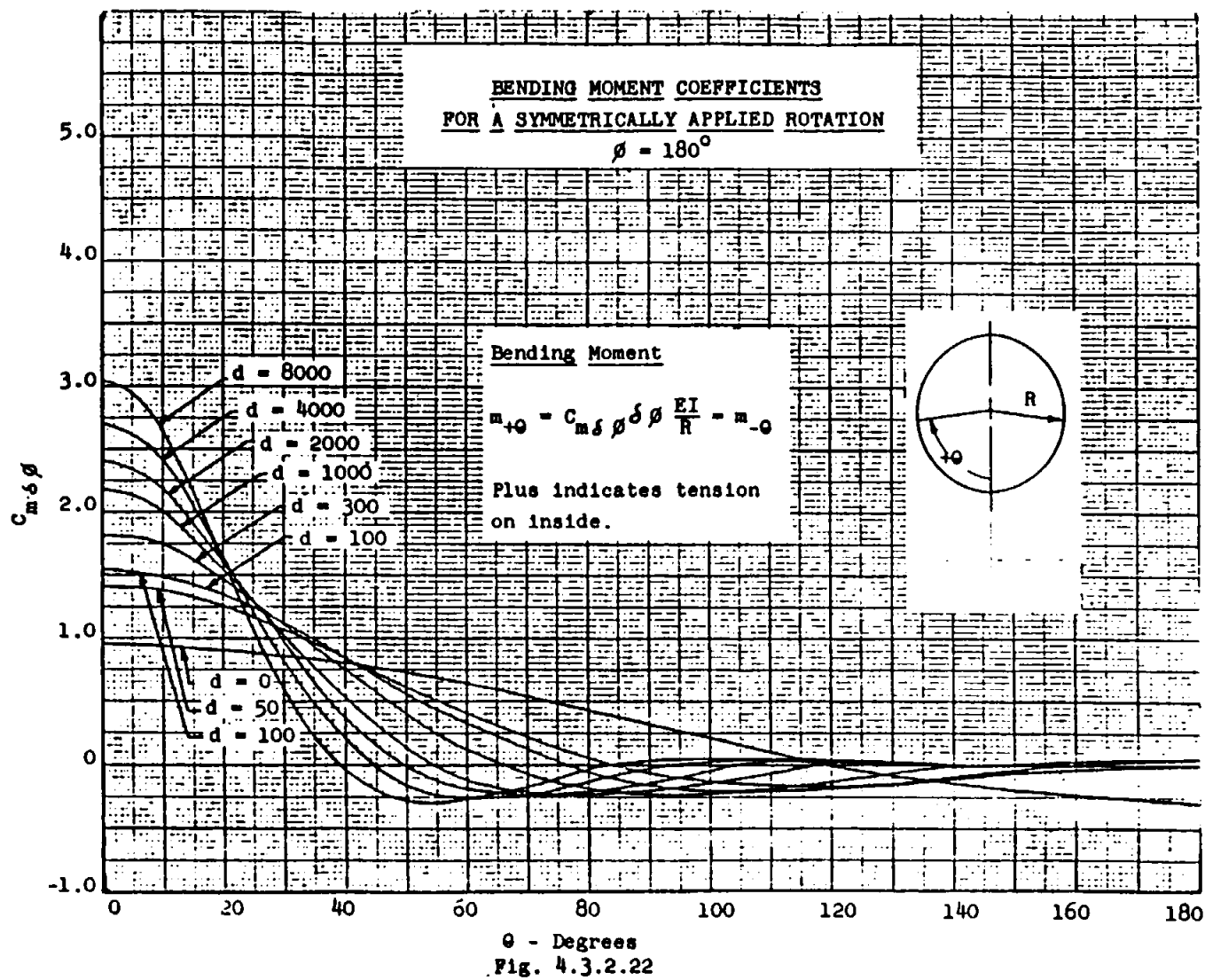
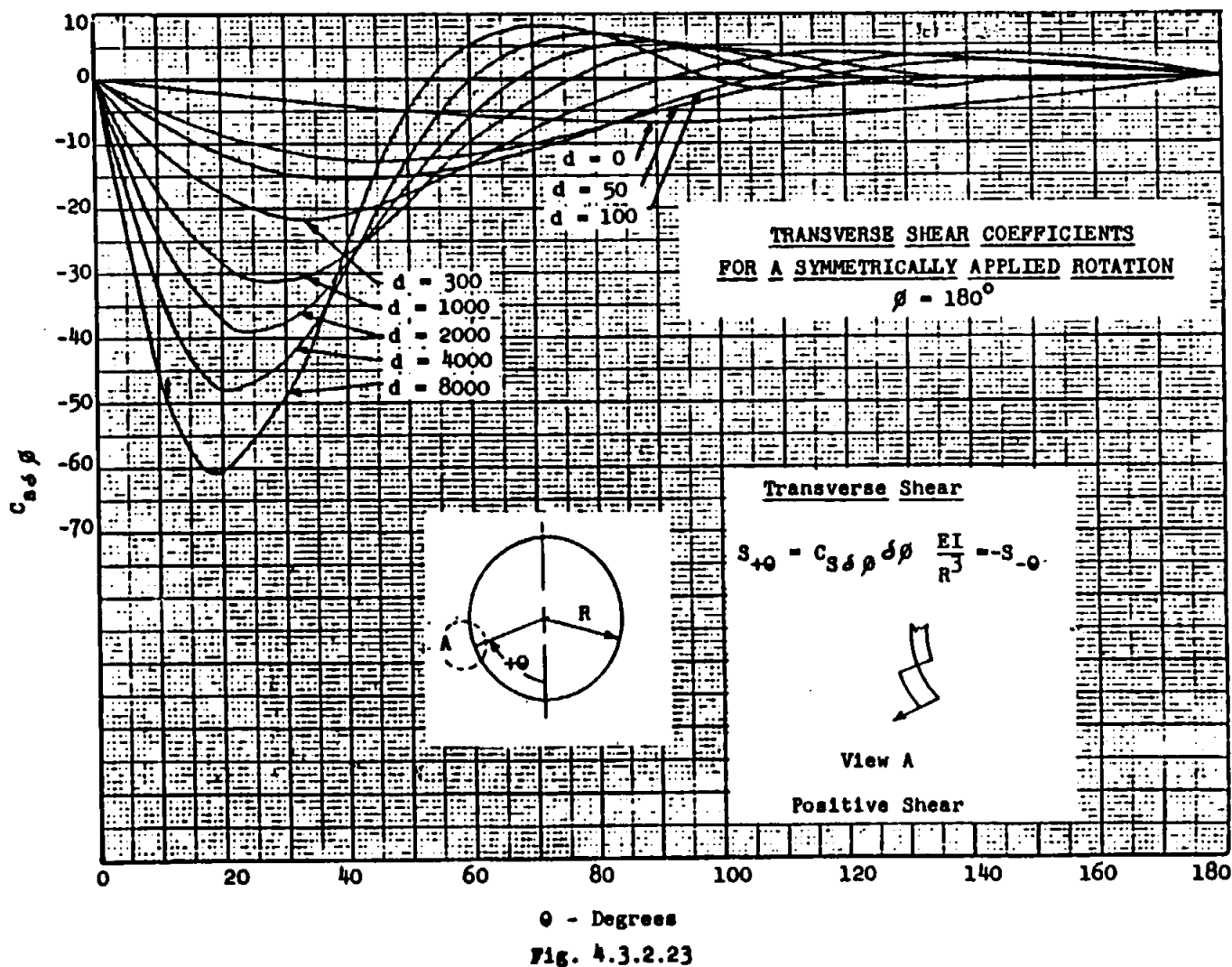


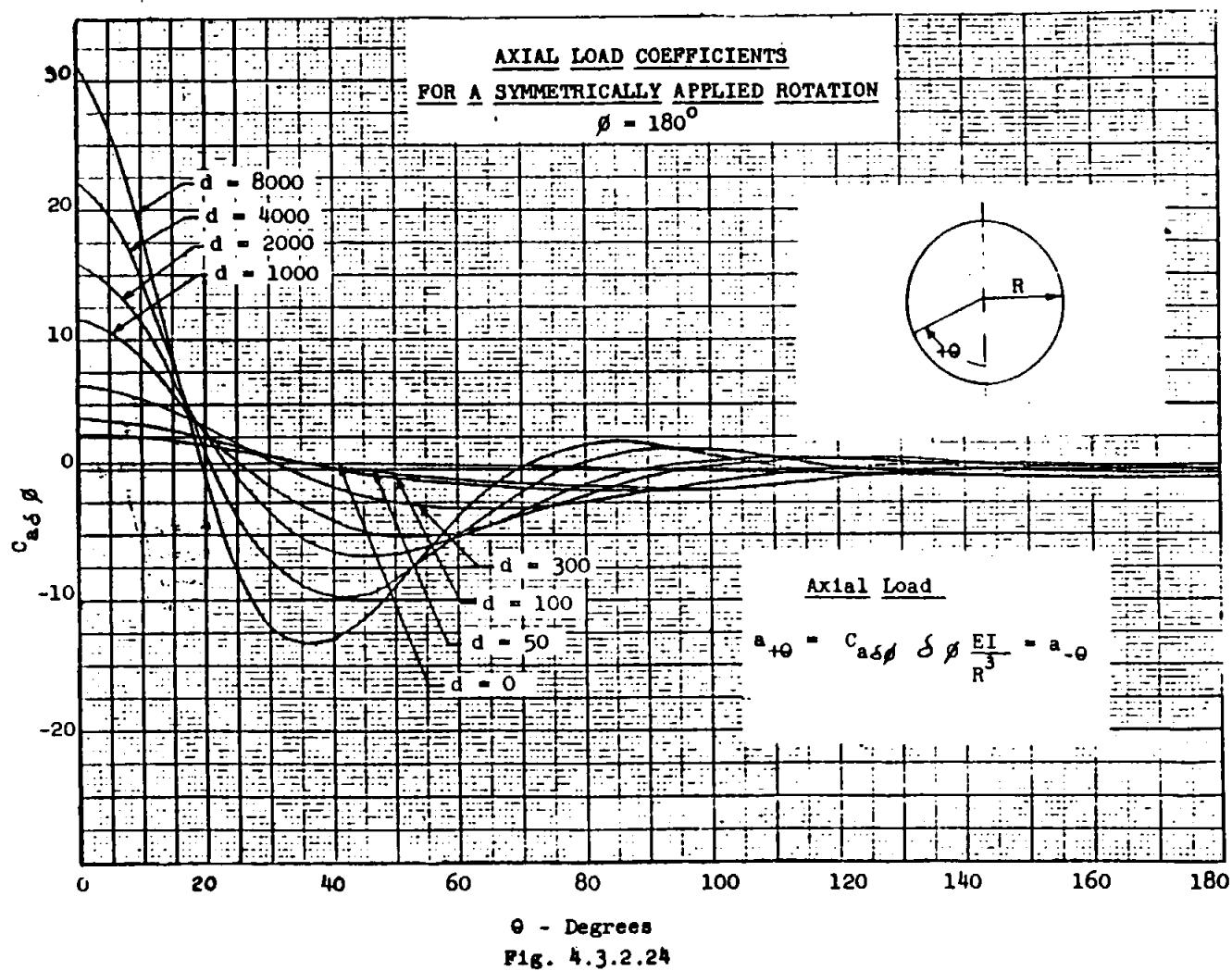
Fig. 4.3.2.19

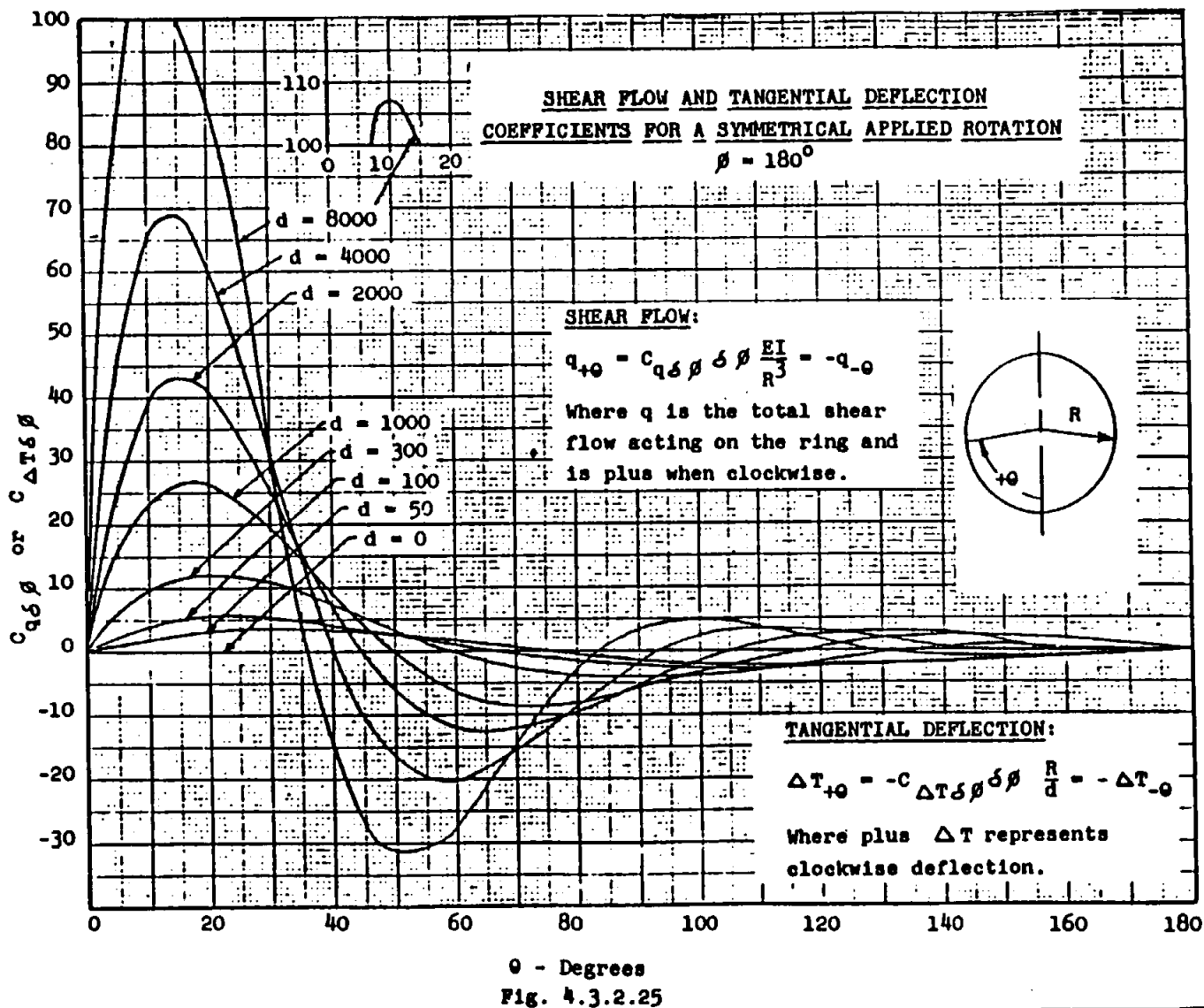












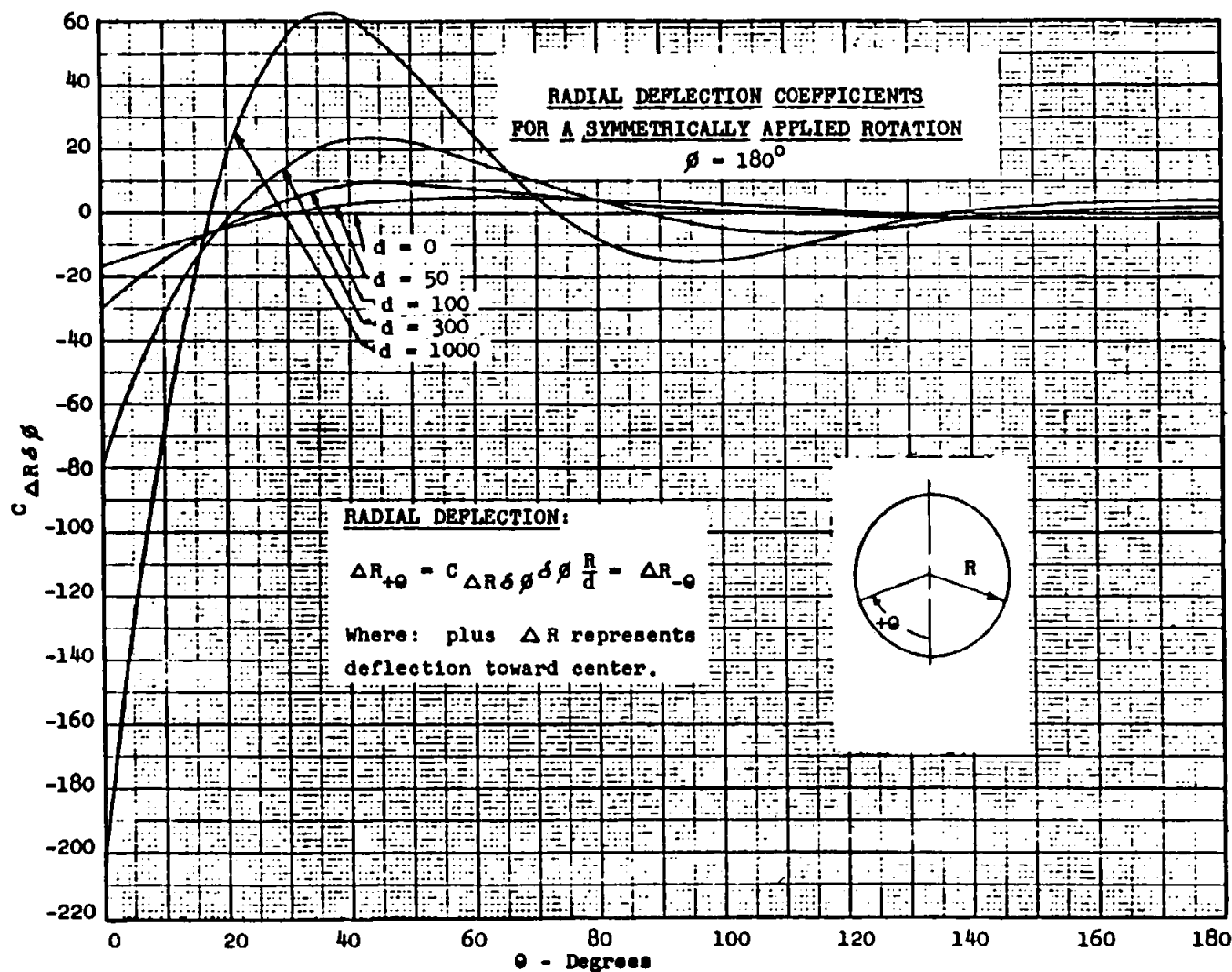
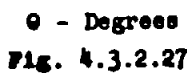


Fig. 4.3.2.26



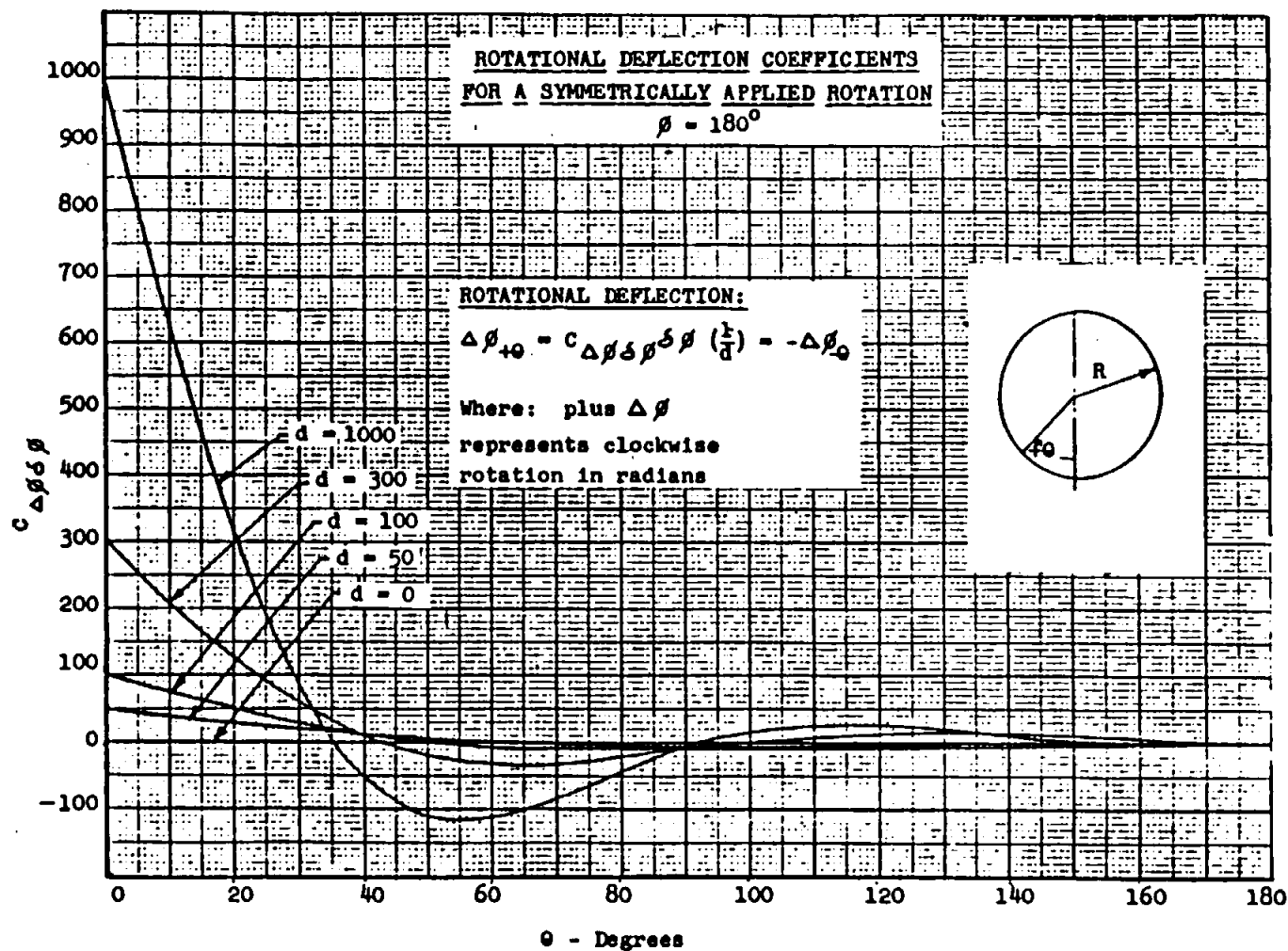


Fig. 4.3.2.28

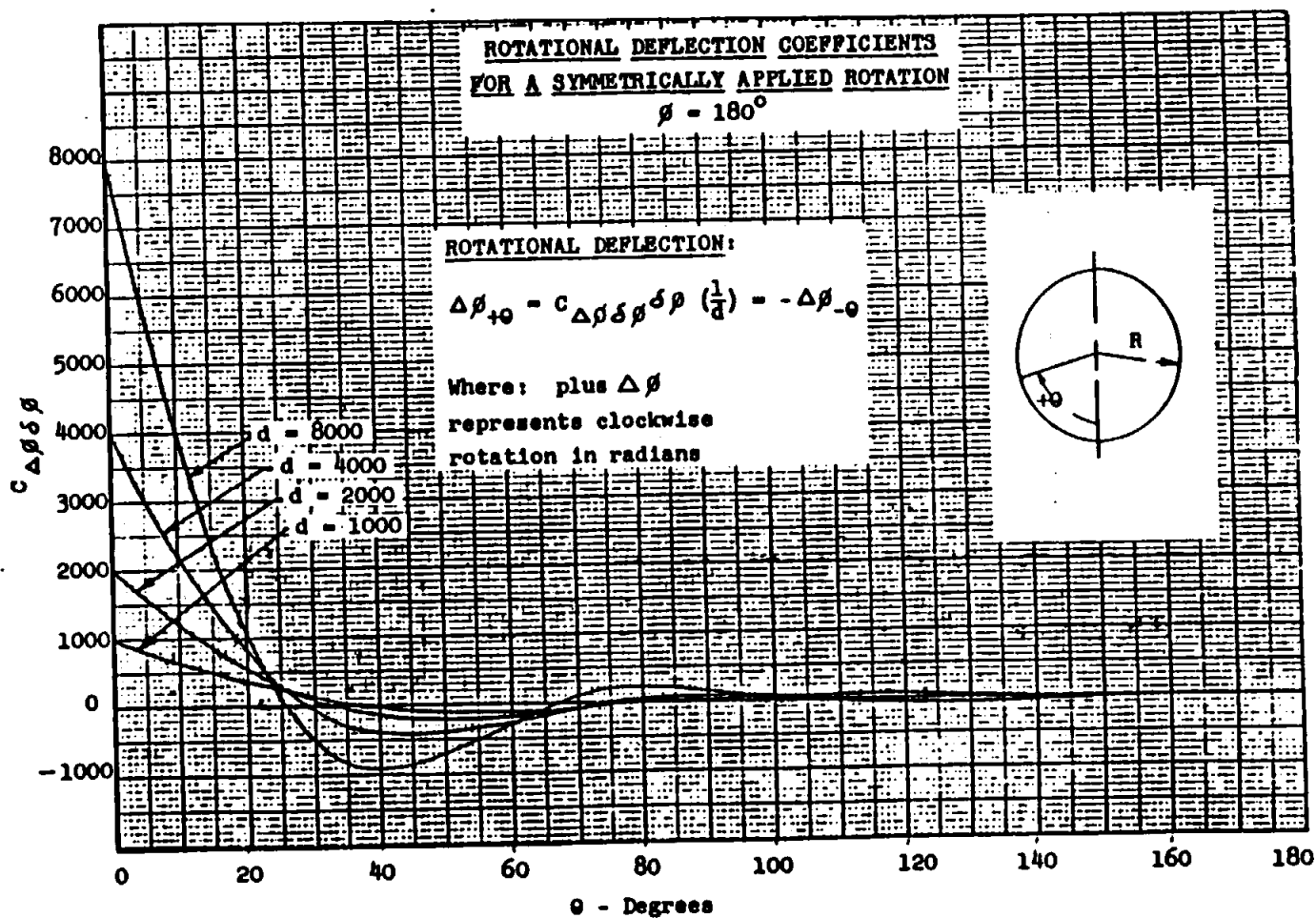
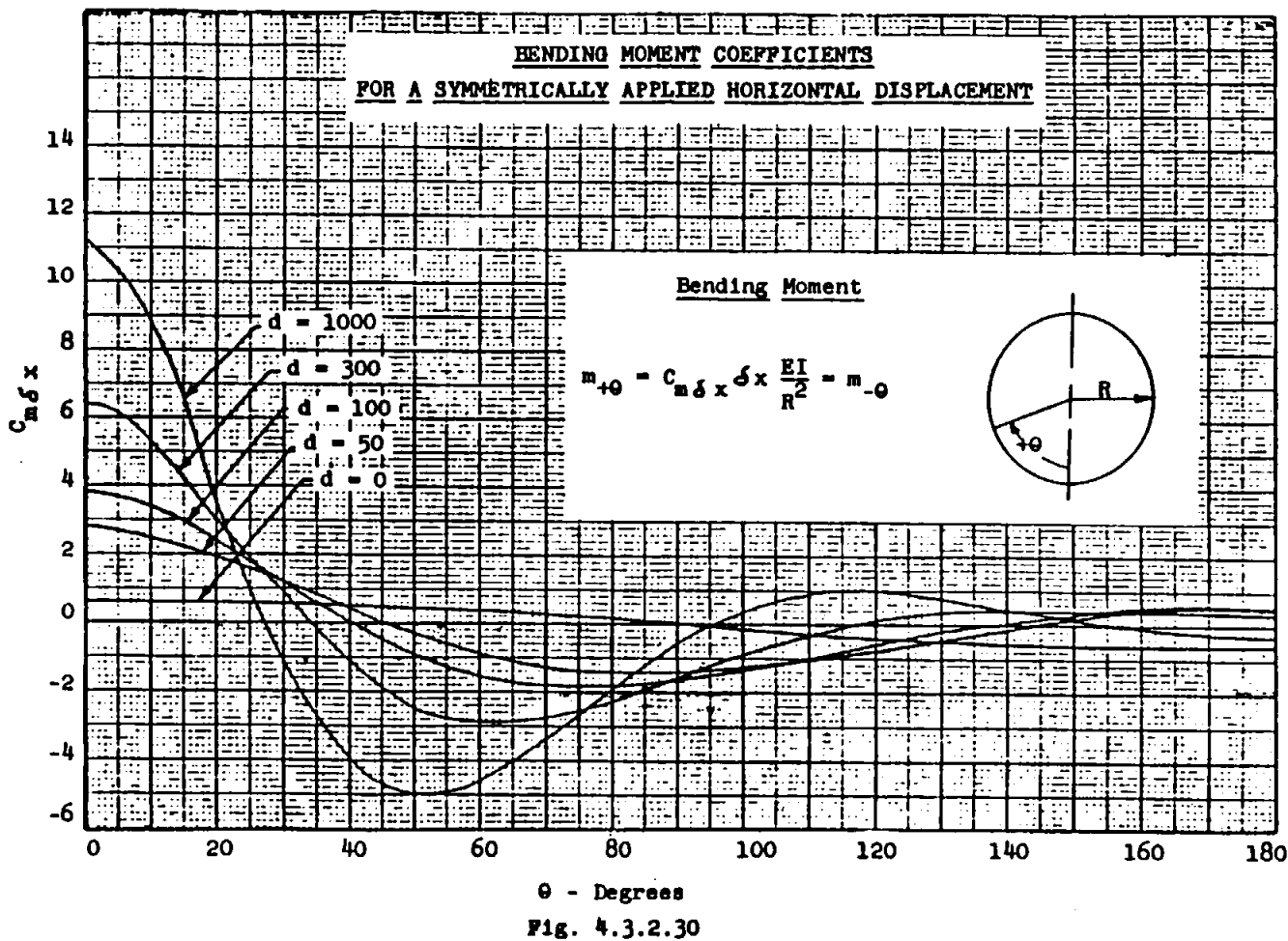
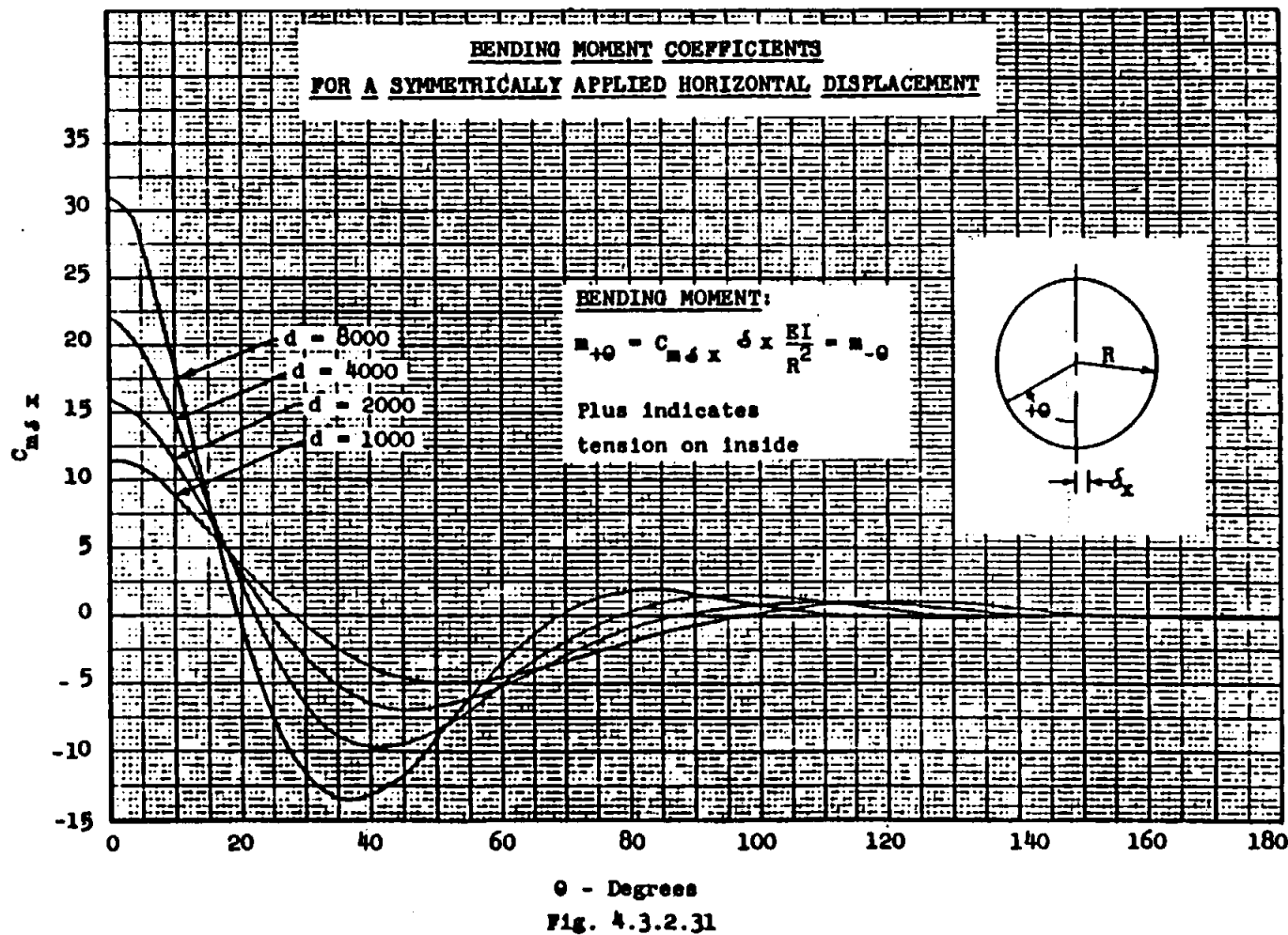


Fig. 4.3.2.29





STRUCTURAL ANALYSIS MANUAL
GENERAL DYNAMICS/CONVAIR AND SPACE SYSTEMS DIVISION

REFERENCES

BEAMS

- 4.1.0 Peery, D. J., Ph.D., Aircraft Structures, McGraw-Hill, 1950
- 4.2.0 Grinter, T. E., Ph.D., C.E., Theory of Modern Steel Structures,
The Macmillan Company, 1956.
- Peery, D. J., Ph.D., Aircraft Structures, McGraw-Hill, 1950
- Bruhn, E. F., Analysis and Design of Aircraft Structures,
Tri-State Offset Company, 1958.
- 4.3.0 N.A.C.A. 929
- 4.6.0 Peery, D. J., Ph.D., Aircraft Structures, McGraw-Hill, 1950
- 4.7.0 N.A.C.A. TN 2661
N.A.C.A. TN 2662

STRUCTURAL ANALYSIS MANUAL
GENERAL DYNAMICS/CONVAIR AND SPACE SYSTEMS DIVISION

Data Source, Section 1.3 Reference 6

REDUNDANT FRAMES

SUBJECT: Structural Deformations by Method of Pictorial Integration

Introduction

This memo presents several tables which facilitate the determination of deformations of structural members due to bending moments. These values may be used to advantage in the analysis of simple redundant structures.

A. OUTLINE OF METHOD - DEFORMATIONS

In order to find any deformation in a structure due to any external loading, proceed as follows:

1. Draw the moment diagram due to the actual loading. Denote these moments by M_0 .
2. Remove the actual loading. Apply a fictitious load equal to unity at the point where the deformation is to be found. This unit load must be of such a type and applied in such a manner that (load) \times (deformation) = work; for example, if the deformation to be found is a rotation, the unit load must then be a moment. Draw the moment diagram for this unit load. Denote these moments by M_a .
3. Compute deformation from the formula

$$\delta_{0a} = \frac{1}{EI} \int M_0 M_a ds = \frac{1}{EI} \overline{\delta_{0a}}$$

where $\overline{\delta_{0a}}$ is given in Table II for various combinations of moment diagrams M_0 and M_a .

STRUCTURAL ANALYSIS MANUAL
GENERAL DYNAMICS/CONVAIR AND SPACE SYSTEMS DIVISION

OUTLINE OF METHOD - DEFORMATIONS (Cont'd)

Table II will be found inapplicable to curved members.

B. OUTLINE OF METHOD - ANALYSIS OF REDUNDANT STRUCTURES

In order to determine the redundant forces and moments in a structure for which it may be assumed that only bending-moment deformations affect the magnitudes of the redundants, proceed as follows:

1. Cut the structure at convenient points to make it statically determinate. Denote the redundant forces or moments by X_a , X_b , etc.
2. Draw the moment diagrams for $X_a = 1$, $X_b = 1$, etc., acting on the statically determinate structure. Designate these moments M_a , M_b , etc.
3. Draw the moment diagram M_0 for the actual applied loads acting on the statically determinate structure. (Use same sign convention as in Step 2.)
4. Evaluate the various δ 's which will be needed in Step 5, by means of Tables I and II.
5. Determine X_a , X_b , etc., by substituting in the following formulas:

One degree redundancy: $X_a = -\frac{\delta_{0a}}{\delta_{aa}}$

Two degree redundancy: $X_a = -\frac{\delta_{0a}\delta_{bb} - \delta_{ob}\delta_{ab}}{\delta_{aa}\delta_{bb} - (\delta_{ab})^2}$

$X_b = -\frac{\delta_{ob}\delta_{aa} - \delta_{0a}\delta_{ab}}{\delta_{aa}\delta_{bb} - (\delta_{ab})^2}$

Three degree redundancy: $X_a\delta_{aa} + X_b\delta_{ba} + X_c\delta_{ca} + \delta_{0a} = 0$

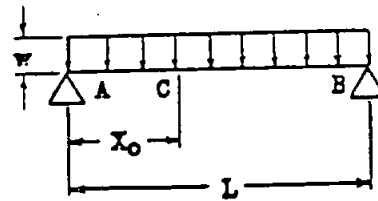
$X_b\delta_{ab} + X_b\delta_{bb} + X_c\delta_{cb} + \delta_{0b} = 0$

$X_c\delta_{ac} + X_b\delta_{bc} + X_c\delta_{cc} + \delta_{0c} = 0$

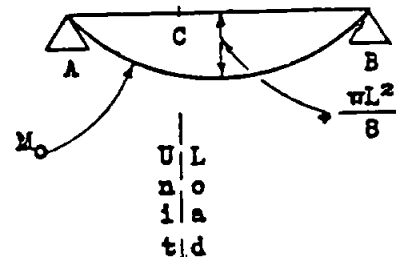
STRUCTURAL ANALYSIS MANUAL
GENERAL DYNAMICS/CONVAIR AND SPACE SYSTEMS DIVISION

C. EXAMPLE:

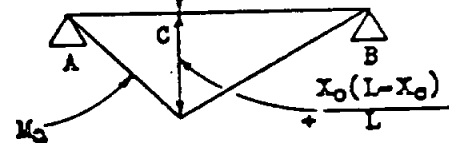
Determine the deflection at any point C in a simply supported beam with uniform load.



First draw the bending moment diagram M_0 for the actual loading:



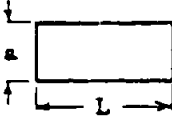
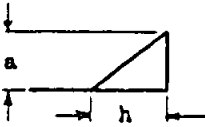
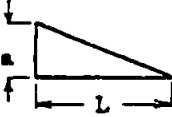
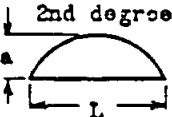
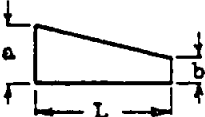
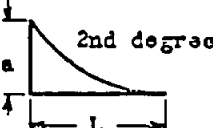
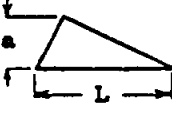
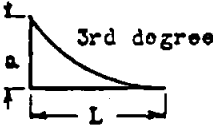
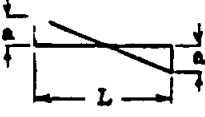
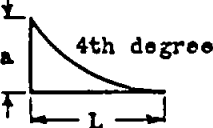
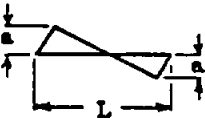
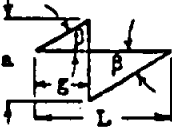
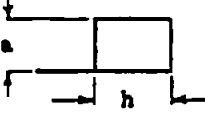
Next apply a fictitious unit load at C and draw the resulting moment diagram M_a :



Then obtain the formula for $\bar{\delta}_{oa}$ from Table II, Case 4(j), and compute δ_{oa} :

$$\begin{aligned}\delta_{oa} &= \frac{1}{EI} \bar{\delta}_{oa} = \frac{1}{EI} \frac{L a c}{3} \left[1 + \frac{gh}{L^2} \right] \\ &= \frac{1}{EI} \frac{(L) \left[\frac{X_0(L - X_0)}{L} \right] \frac{wL^2}{8}}{3} \left[1 + \frac{X_0(L - X_0)}{L^2} \right] \\ &= \frac{wL^4}{24 EI} \frac{X_0}{L} \left[1 - 2 \frac{X_0^2}{L^2} + \frac{X_0^3}{L^3} \right]\end{aligned}$$

STRUCTURAL ANALYSIS MANUAL
GENERAL DYNAMICS/CONVAIR AND SPACE SYSTEMS DIVISION

<p style="text-align: center;">TABLE I - VALUES OF $\bar{\delta}_{mm}$</p> <p style="text-align: center;">$\bar{\delta}_{mm}$ is defined as $\int_0^L M_m^2 ds$ for any moment diagram M_m</p>					
Case	M_m	$\bar{\delta}_{mm}$	Case	M_m	$\bar{\delta}_{mm}$
1		La^2	9		$\frac{La^2}{3} \frac{h}{L}$
2		$\frac{La^2}{3}$	10		$\frac{8La^2}{15}$
3		$\frac{L(a^2 + b^2 + ab)}{3}$	11		$\frac{La^2}{5}$
4		$\frac{La^2}{3}$	12		$\frac{La^2}{7}$
5		$\frac{La^2}{3}$	13		$\frac{La^2}{9}$
6		$\frac{La^2}{3}$			
7		$\frac{La^2}{3} (1 - 3 \frac{\xi}{L} + 3 \frac{\xi^2}{L^2})$			
8		$La^2 \frac{h}{L}$			

STRUCTURAL ANALYSIS MANUAL
GENERAL DYNAMICS/CONVAIR AND SPACE SYSTEMS DIVISION

TABLE II - VALUES OF δ_{mn} δ_{mn} is defined as $\int_0^L M_m M_n ds$ for any two moment diagrams M_m and M_n					
Case	M_m	δ_{mn} or $\bar{\delta}_{mn}$	Case	M_n	δ_{mn} or $\bar{\delta}_{mn}$
1(a)		Lac	1(i)		$\frac{Lac}{2} \frac{f}{L}$
1(b)		$\frac{Lac}{2}$	1(j)		$\frac{Lac}{2} \left[\frac{R}{c} \left(\frac{S}{L} - 1 \right) + 1 \right]$
1(c)		$\frac{Lac(a+b)}{2}$	1(k)		$\frac{2}{3} \frac{Lac}{L}$
1(d)		$\frac{Lac}{2}$	1(l)		$\frac{Lac}{3}$
1(e)		0	1(m)		$\frac{Lac}{4}$
1(f)		0	1(n)		$\frac{Lac}{5}$
1(g)		$-\frac{Lac}{2} \left[1 - 2 \frac{e}{L} \right]$			
1(h)		$Lac \frac{f}{L}$			

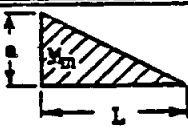



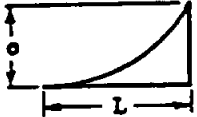
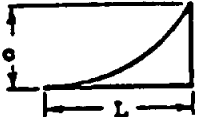
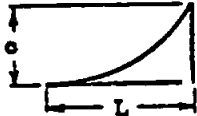
STRUCTURAL ANALYSIS MANUAL
GENERAL DYNAMICS/CONVAIR AND SPACE SYSTEMS DIVISION

TABLE II (continued)

$\bar{\delta}_{mn}$ is defined as $\int_0^L M_m M_n ds$ for any two moment diagrams M_m and M_n

Case	M_n	$\bar{\delta}_{mn}$ or $\bar{\delta}_{nm}$	Case	M_n	$\bar{\delta}_{mn}$ or $\bar{\delta}_{nm}$
2(a)		$\frac{Lac}{3}$	2(i)		$\frac{Lac}{2} \frac{f^2}{L^2}$
2(b)		$\frac{Lac}{6}$	2(j)		$\frac{Lac}{2} \left[1 - \frac{f^2}{L^2} \right]$
2(c)		$\frac{Lc(2c+d)}{6}$	2(k)		$\frac{Lac}{6} \frac{f^2}{L^2}$
2(d)		$\frac{Lac}{4}$	2(l)		$\frac{Lac}{6} \frac{c}{L} \left[3 - \frac{c}{L} \right]$
2(e)		$\frac{Lac}{6} \left[1 + \frac{f}{L} \right]$	2(m)		$\frac{Lac}{3}$
2(f)		$\frac{Lac}{6}$	2(n)		$\frac{Lac}{4}$
2(g)		$\frac{Lac}{6} \left[1 - \frac{c}{L} \right]$	2(o)		$\frac{Lac}{5}$
2(h)		$\frac{Lac}{6} \left[1 - 3 \frac{f^2}{L^2} \right]$	2(p)		$\frac{Lac}{6}$

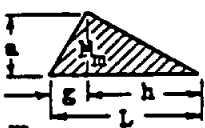
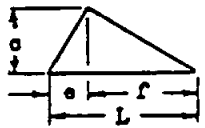
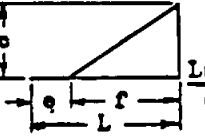
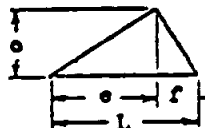
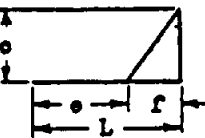
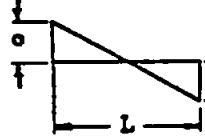
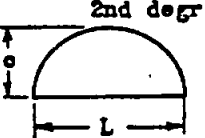
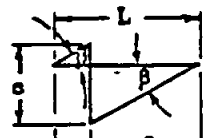
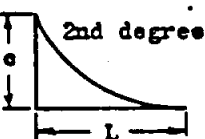
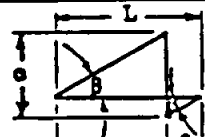
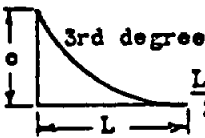
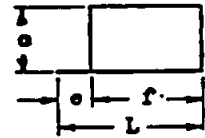
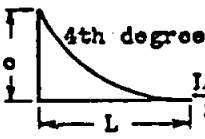
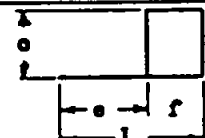
STRUCTURAL ANALYSIS MANUAL
GENERAL DYNAMICS/CONVAIR AND SPACE SYSTEMS DIVISION

TABLE II (continued)			
$\bar{\delta}_{mn}$ is defined as $\int_0^L M_m M_n dx$ for any two moment diagrams M_m and M_n			
Case	M_n	$\bar{\delta}_{mn}$ or $\bar{\delta}_{nm}$	
			
2(q)		$\frac{Lac}{12}$	
2(r)		$\frac{Lac}{20}$	
2(s)		$\frac{Lac}{30}$	

STRUCTURAL ANALYSIS MANUAL
GENERAL DYNAMICS/CONVAIR AND SPACE SYSTEMS DIVISION

TABLE I: (Continued)					
$\bar{\delta}_{mn}$ is defined as $\int_0^L v_m M_n ds$ for any two moment diagrams M_m and M_n					
Case	v_m	$\bar{\delta}_{mn}$ or $\bar{\delta}_{nm}$	Case	v_n	$\bar{\delta}_{mn}$ or $\bar{\delta}_{nm}$
3(a)		$\frac{L(2ao + 2bd + ad + bc)}{6}$	3(i)		$\frac{Lo(a + b)}{3}$ 2nd degree
3(b)		$\frac{Lc(a + b)}{4}$	3(j)		$\frac{Lo}{12} (3a + b)$
3(c)		$\frac{Lc}{6} \left[(a + b) + a \frac{f}{L} + b \frac{o}{L} \right]$	3(k)		$\frac{Lc}{20} (4a + b)$
3(d)		$\frac{Lo(a - b)}{6}$	3(l)		$\frac{Lo}{30} (5a + b)$
3(e)		$\frac{L(a - b)o}{6} \left(1 - \frac{o}{L} \right)$			
3(f)		$\frac{Lo}{6} \left[a \left(1 - \frac{f^2}{L^2} \right) - b \left(1 - \frac{o^2}{L^2} \right) \right]$			
3(g)		$\frac{Lo}{2} \left[(a - b) \frac{f^2}{L^2} + 2b \frac{f}{L} \right]$			
3(h)		$\frac{Lc}{6} \left[a \frac{f^2}{L^2} + b \frac{f}{L} \left(3 - \frac{f}{L} \right) \right]$			

STRUCTURAL ANALYSIS MANUAL
GENERAL DYNAMICS/CONVAIR AND SPACE SYSTEMS DIVISION

TABLE II (Continued)					
$\bar{\delta}_{mn}$ is defined as $\int_0^L M_m M_n ds$ for any two moment diagrams M_m and M_n					
					
Case	M_m	$\bar{\delta}_{mn}$ or $\bar{\delta}_{nn}$	Case	M_n	$\bar{\delta}_{mn}$ or $\bar{\delta}_{nn}$
4(a)		When $e = g$ $\frac{Lac}{3}$	4(h)		When $e \leq g$ $\frac{Lac}{6} \left[1 + \frac{g}{L} - \frac{e}{f} - \frac{eh}{fL} + \frac{e^2}{fgL} \right]$
4(b)		When $e \geq g$ $\frac{Lac}{6} \frac{(L^2 - g^2 - f^2)}{hg}$	4(i)		When $e \geq g$ $\frac{Lac}{6} \frac{f^2}{hL}$
4(c)		$\frac{Lac}{6} \left[\frac{h}{L} - \frac{f}{L} \right]$	4(j)		2nd degree $\frac{Lac}{3} \left[1 + \frac{gh}{L^2} \right]$
4(d)		When $e \leq g$ $\frac{Lac}{6} \left[\frac{3e^2}{gL} - 1 - \frac{h}{L} \right]$	4(k)		2nd degree $\frac{Lac}{12} \left[1 + \frac{h}{L} + \frac{h^2}{L^2} \right]$
4(e)		When $e \geq g$ $\frac{Lac}{6} \left[1 - \frac{3e^2}{hL} + \frac{f}{L} \right]$	4(l)		3rd degree $\frac{Lac}{20} \left[1 + \frac{h}{L} + \frac{h^2}{L^2} + \frac{h^3}{L^3} \right]$
4(f)		When $e \leq g$ $\frac{Lac}{2} \left[1 - \frac{e^2}{gL} \right]$	4(m)		4th degree $\frac{Lac}{30} \left[1 + \frac{h}{L} + \frac{h^2}{L^2} + \frac{h^3}{L^3} + \frac{h^4}{L^4} \right]$
4(g)		When $e \geq g$ $\frac{Lac}{2} \frac{f^2}{hL}$			

STRUCTURAL ANALYSIS
GENERAL DYNAMICS/CONVAIR AND SPACE SYSTEMS DIVISION

SECTION 19.0

THERMAL EFFECTS

Thermal stress analysis methods, for various common structural elements, are presented in this section.

	<u>PAGE</u>
19.1 GENERAL.....	19.1.1
19.2 BEAMS AND COLUMNS.....	19.2.1
19.3 FLAT PLATES.....	19.3.1
19.4 BOX BEAMS.....	19.4.1
19.5 BOLTED JOINTS.....	19.5.1
19.6 THERMAL BUCKLING.....	19.6.1
19.7 THERMAL STRUCTURAL ANALYSIS WITH MSC/NASTRAN.....	19.7.1

STRUCTURAL ANALYSIS MANUAL

GENERAL DYNAMICS/CONVAIR AND SPACE SYSTEMS DIVISION

Data Source, Section 1.3 Reference |

11.0.0

THERMAL STRESS ANALYSIS

11.1.0

General Discussion

Thermal stresses may result from conditions such as:

- a. Unequal heating causing a non-linear, non-uniform temperature distribution within a beam or plate (if there are no external restraints, the stresses will be self-balancing),
- b. Unsymmetrical heating through the thickness of the plate or beam producing bending moments with, or without, external restraints (a linear temperature distribution through the thickness with no external restraints produces no thermal stresses in a homogeneous material).
- c. Heating of a plate or beam attached to a cooler sub-structure,
- d. "Soak" heating or cooling of the entire structure when the components have different coefficients of thermal expansion.

Thermal stresses can be added linearly to load stresses if the total stress is below the proportional limit of the material (above the proportional limit, the sum of the thermal and mechanical stresses can be obtained using a strain analysis).

11.2.0

Methods for Determining Thermal Stresses in Stable Structures.

General

The following three equations will give the total strains in the x, y, and z directions.

$$\epsilon_x = \frac{1}{E} [\sigma_x - \mu(\sigma_y + \sigma_z)] + \alpha(T - T_0) \quad (1)$$

$$\epsilon_y = \frac{1}{E} [\sigma_y - \mu(\sigma_z + \sigma_x)] + \alpha(T - T_0) \quad (2)$$

$$\epsilon_z = \frac{1}{E} [\sigma_z - \mu(\sigma_x + \sigma_y)] + \alpha(T - T_0) \quad (3)$$

Where: α is the coefficient of thermal expansion and " T_0 " is the reference temperature corresponding to zero thermal stress.
" T " is the temperature at the point (x, y, z).

The equations for stress in the x, y, and z directions are:

$$\sigma_x = \frac{E\mu}{(1+\mu)(1-2\mu)} (\epsilon_x + \epsilon_y + \epsilon_z) + \frac{E}{(1+\mu)} \epsilon_x - \frac{\alpha E(T - T_0)}{1-2\mu} \quad (4)$$

$$\sigma_y = \frac{E\mu}{(1+\mu)(1-2\mu)} (\epsilon_x + \epsilon_y + \epsilon_z) + \frac{E}{(1+\mu)} \epsilon_y - \frac{\alpha E(T - T_0)}{1-2\mu} \quad (5)$$

$$\sigma_z = \frac{E\mu}{(1+\mu)(1-2\mu)} (\epsilon_x + \epsilon_y + \epsilon_z) + \frac{E}{(1+\mu)} \epsilon_z - \frac{\alpha E(T - T_0)}{1-2\mu} \quad (6)$$

STRUCTURAL ANALYSIS MANUAL
GENERAL DYNAMICS/CONVAIR AND SPACE SYSTEMS DIVISION
 Data Source, Section 1.3 Reference |

In the plane stress case ($\sigma_z = 0$), these equations become

$$\sigma_x = \frac{E}{1-\mu^2} (\epsilon_x + \mu\epsilon_y) - \frac{E\alpha(T-T_0)}{1-\mu} \quad (7)$$

$$\sigma_y = \frac{E}{1-\mu^2} (\epsilon_y + \mu\epsilon_x) - \frac{E\alpha(T-T_0)}{1-\mu} \quad (8)$$

For uniaxial conditions ($\sigma_y = 0$, $\sigma_z = 0$)

$$\sigma_x = E \epsilon_x - E\alpha(T-T_0) = E [\epsilon_x - \alpha(T-T_0)] \quad (9)$$

11.2.1

Beams and Columns

A. Uniform Heating

Typical applications of the thermal stress equations involving uniaxial stresses are:

1. Full Restraint of a Uniformly Heated Bar (Stable Structure)

- (a) Prismatic bar restrained against expanding in lengthwise direction.

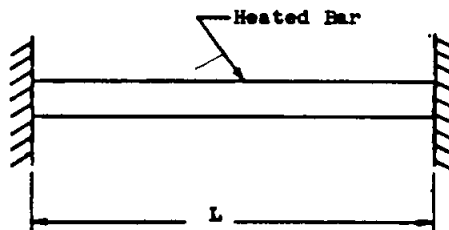


Fig. 11.2.1-1

$$P = -AE\alpha(T-T_0)$$

$$\sigma = -E\alpha(T-T_0) \text{ Minus sign indicates compressive stress.}$$

- (b) Restrained prismatic bar having a gap, heated uniformly

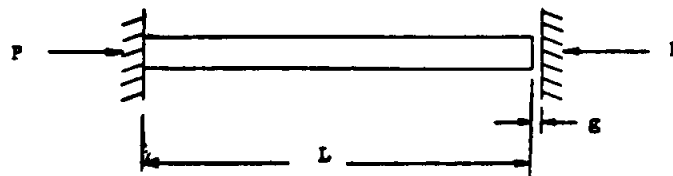


Fig. 11.2.1-2

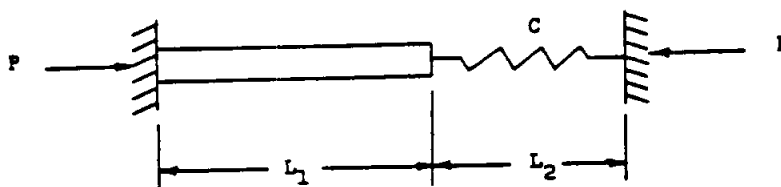
STRUCTURAL ANALYSIS MANUAL
GENERAL DYNAMICS/CONVAIR AND SPACE SYSTEMS DIVISION

$$\text{If } \epsilon/L \geq \alpha(T-T_0), \quad P = 0$$

$$\text{If } \epsilon/L < \alpha(T-T_0), \quad P = -E\alpha\epsilon(T-T_0) + \frac{EA\epsilon}{L}$$

$$\sigma = -E\alpha(T-T_0) + \frac{E\epsilon}{L}$$

2. Partial Restraint of a Uniformly Heated or Cooled Prismatic Bar



Partially Restrained Rod and Spring

Fig. 11.2.1-3

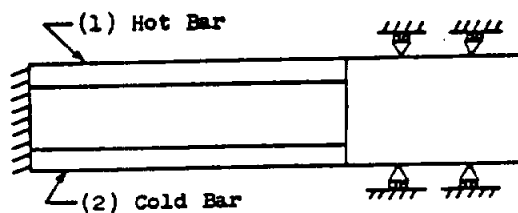
C = Spring constant for " L_2 " at its final temperature " T ."

$$P = - \frac{\alpha_1 L_1 (T-T_0)_1 + \alpha_2 L_2 (T-T_0)_2}{1/C + L_1/A_1 E_1} \quad (1)$$

Note: The spring may represent an elastic structure where " C " is its spring constant at final temperature.

3. Two Bars at Different Temperatures

Two bars are attached such that the cold bar restrains the expansion of the hot bar. The bars are assumed to remain straight, no bending.



(End supports prevent angular rotation only)

Fig. 11.2.1-4

STRUCTURAL ANALYSIS MANUAL
GENERAL DYNAMICS/CONVAIR AND SPACE SYSTEMS DIVISION

$$\sigma_1 = -E_1 \alpha_1 (T_1 - T_0) c_1$$

$$\sigma_2 = \frac{-A_1}{A_2} \sigma_1$$

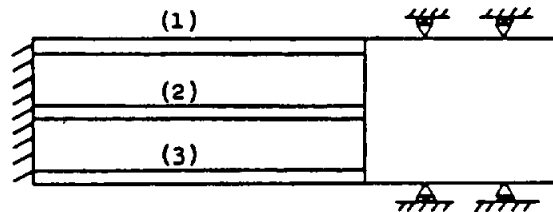
where

$$c_1 = \left[\frac{E_2 A_2}{E_1 A_1 + E_2 A_2} \right] \left[1 - \frac{\alpha_2 (T_2 - T_0)}{\alpha_1 (T_1 - T_0)} \right] \quad (2)$$

and the subscripts correspond to the respective members.

4. Three Bars at Different Temperatures

If three bars are heated and each at a different temperature, the stress would be: (Bars are assumed to remain straight).



(End supports prevent angular rotation only)

Fig. 11.2.1-5

$$\sigma_1 = -E_1 \alpha_1 (T_1 - T_0) c_1 \quad (3)$$

$$\sigma_2 = -E_2 \alpha_2 (T_2 - T_0) c_2 \quad (4)$$

$$\sigma_3 = -\frac{1}{A_3} (\sigma_1 A_1 + \sigma_2 A_2) \quad (5)$$

where:

$$c_1 = \left[\frac{A_2 E_2 + A_3 E_3}{A_1 E_1 + A_2 E_2 + A_3 E_3} \right] \left[1 - \frac{A_2 \alpha_2 E_2 (T_2 - T_0) + A_3 \alpha_3 E_3 (T_3 - T_0)}{\alpha_1 (T_1 - T_0) (A_2 E_2 + A_3 E_3)} \right]$$

$$c_2 = \left[\frac{A_1 E_1 + A_3 E_3}{A_1 E_1 + A_2 E_2 + A_3 E_3} \right] \left[1 - \frac{A_1 \alpha_1 E_1 (T_1 - T_0) + A_3 \alpha_3 E_3 (T_3 - T_0)}{\alpha_2 (T_2 - T_0) (A_1 E_1 + A_3 E_3)} \right]$$

STRUCTURAL ANALYSIS MANUAL

GENERAL DYNAMICS/CONVAIR AND SPACE SYSTEMS DIVISION

General Equation

The general equation to be used for any number of bars (no bending) is:

$$\sigma_1 = E_1 \left[\frac{\sum_{i=1}^n E_i A_i \alpha_i (T_i - T_o)}{\sum_{i=1}^n E_i A_i} + \frac{P}{\sum_{i=1}^n A_i E_i} - \alpha_1 (T_i - T_o) \right] \quad (6)$$

where subscript "i" refers to the bar in question, and "P" is the externally applied axial load.

B. Beams With Varying Temperature

The following equations are to be used for thermal stresses when the temperature varies through the depth of the beam.

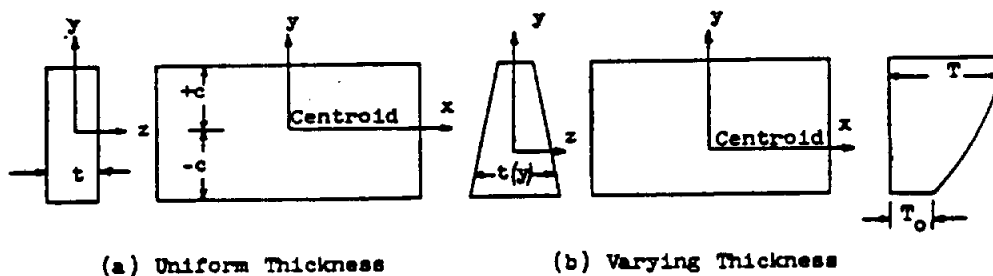


Fig. 11.2.1-6

a. Uniform Thickness

$$\sigma_x = -\alpha E (T - T_o) + \frac{1}{2c} \int_{-c}^{+c} \alpha E (T - T_o) dy \quad (7)$$

$$+ \frac{3y}{2c^3} \int_{-c}^{+c} \alpha E (T - T_o) y dy$$

Note:

- (1) If the beam is restrained from expanding and bending, drop the last two terms,
- (2) If the beam is restrained from expansion but is free to bend, drop the middle term.
- (3) If the beam is restrained in bending only, drop the last term.

b. Varying Thickness

If the beam has a varying width through its depth and is symmetrical about its vertical centerline, the above equation has the following form:

STRUCTURAL ANALYSIS MANUAL
GENERAL DYNAMICS/CONVAIR AND SPACE SYSTEMS DIVISION

$$\begin{aligned} \sigma_x = & -\alpha E(T-T_0) + \frac{1}{A} \int_A \alpha E(T-T_0)t \, dy \\ & + \frac{y}{I_z} \int_A \alpha E(T-T_0)yt \, dy \end{aligned} \quad (8)$$

Where " I_z " is moment of inertia about the centroidal axis,
 and " t " is a function of " y " as shown in Fig. 11.2.1-6(b).

C. Prismatic Bars With Linear Temperature Gradient
Between the Two Faces

The following cases are typical for bars subjected to a linear temperature change between the faces:

Case 1

Restrained rectangular bar, both faces at uniform temperature.

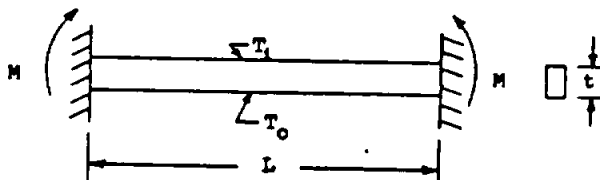


Fig. 11.2.1-7

$$M = \frac{EI\alpha(T_1-T_0)}{t} \quad (9)$$

$$\sigma_{b_{max}} = \pm \frac{E\alpha(T_1-T_0)}{2} \quad (10)$$

Case 2

Pin-ended rectangular cross section column with end load, "P".
 Both faces at uniform temperature.

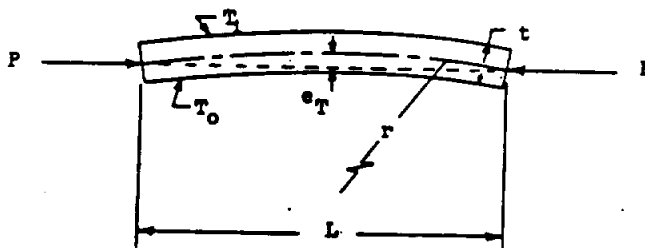


Fig. 11.2.1-8

STRUCTURAL ANALYSIS MANUAL

GENERAL DYNAMICS/CONVAIR AND SPACE SYSTEMS DIVISION

This becomes a beam-column as a result of " e_T ", the eccentricity due to temperature.

$$e_T \approx \frac{\alpha(T_1 - T_0)L^2}{8t} \quad (11)$$

$$P' = \frac{\pi^2 EI}{L^2} \quad (\text{Euler's eq.}) \quad (12)$$

$$e_{\text{final}} = \frac{e_T \pm e_1}{1 - \frac{P}{P'}} \quad (13)$$

(e_1 - any initial eccentricity that either adds to or subtracts from e_T)

$$M_{\text{max}} = P(e_{\text{final}}) \quad (14)$$

- D. General Equation for Determining Stresses in A Member Subjected to External Forces, Moments, and With a Temperature Variation in the "y" and "z" Directions

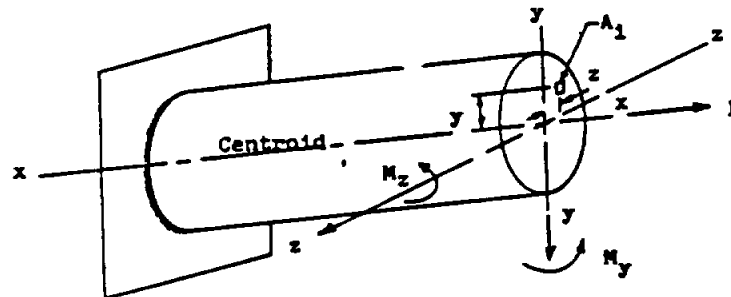


Fig. 11.2.1-11

$$\begin{aligned} \sigma_1 = E_1 \left[y_1 \left(\frac{M_z + \sum_{i=1}^n y_i E_i A_i \alpha_i (T_1 - T_0)}{\sum_{i=1}^n y_i^2 E_i A_i} \right) \right. \\ + z_1 \left(\frac{M_y + \sum_{i=1}^n z_i E_i A_i \alpha_i (T_1 - T_0)}{\sum_{i=1}^n z_i^2 E_i A_i} \right) \\ \left. + \left(\frac{P + \sum_{i=1}^n E_i A_i \alpha_i (T_1 - T_0)}{\sum_{i=1}^n E_i A_i} \right) \right] - E_1 \alpha_1 (T_1 - T_0) \quad (15) \end{aligned}$$

Where:

M_z - Moment about the z-axis

M_y - Moment about the y-axis

NOTE:

[This solution applies to a prismatic beam with constant cross section.]

STRUCTURAL ANALYSIS MANUAL

GENERAL DYNAMICS/CONVAIR AND SPACE SYSTEMS DIVISION

Data Source, Section 1.3 Reference 1

1 refers to the 1th element ; A_1 is the area of the 1th element
 y & z are assumed as the principal axes

$(T_1 - T_0)$ is a function of y and z , and is independent
of the x -direction.

If no bending in the x - z plane is assumed, the quantity in the
second parenthesis of equation (15) will be eliminated.

11.2.2 Flat Plates (Non-Uniform Temperature)

The following equation is the general expression for flat plates with
the temperature varying through the depth only (independent of the lengthwise
directions). (Ref. 11.2.2-1.)

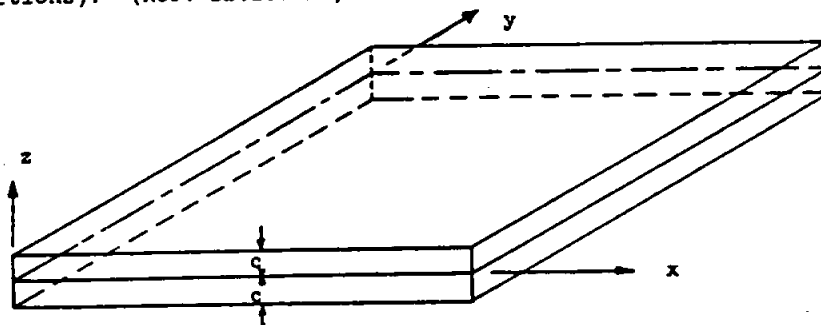


Fig. 11.2.2-1

$$\sigma_x = \sigma_y = -\frac{\alpha E(T - T_0)}{(1 - \mu)} + \frac{1}{2c(1 - \mu)} \int_{-c}^c \alpha E(T - T_0) dz \quad (1)$$

$$+ \frac{3z}{2c^3(1 - \mu)} \int_{-c}^c \alpha E(T - T_0) z dz$$

Note: This equation is not valid near the edges
of the plate.

1. Flat Plate of Any Shape, Rotationally Restrained at the Edges,
With Linear Temperature Gradient Between Two Faces, Both
at Uniform Temperature

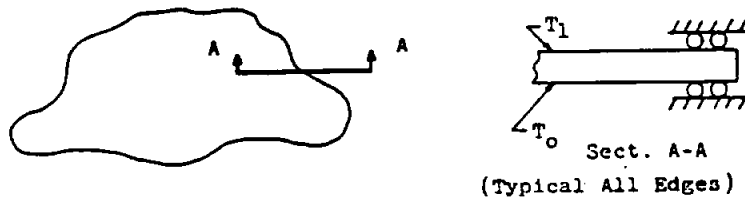


Fig. 11.2.2-2

STRUCTURAL ANALYSIS MANUAL
GENERAL DYNAMICS/CONVAIR AND SPACE SYSTEMS DIVISION

$$\sigma_{\max} = \pm \frac{E\alpha(T_1 - T_0)}{2(1-\nu)} \quad (2)$$

Square Plate Rotationally Restrained at the Edges, With Linear Temperature Gradient Between Two Faces, Both at Uniform Temperature

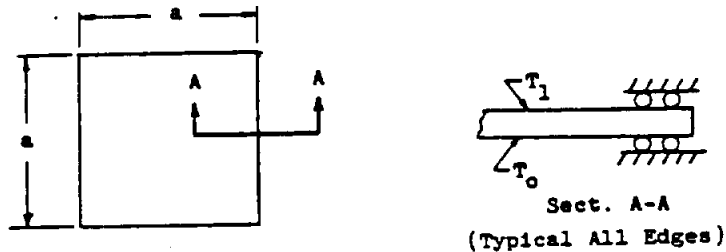


Fig. 11.2.2-3

Near the edges:

$$\sigma_{b_{\max}} = \frac{E\alpha}{2} (T_1 - T_0) \quad (3)$$

Away from the edges:

$$\sigma_{b_{\max}} = \frac{E\alpha(T_1 - T_0)}{2(1-\nu)} \quad (4)$$

11.2.3

Flat Plates (Uniform Heating)

The following thermal stress equations involving biaxial stresses are given with the assumptions that there is uniform heating, no bending, and that the edges remain straight and parallel.

1. Uniformly Heated or Cooled Rectangular Plate Restrained in the x and y Directions Only

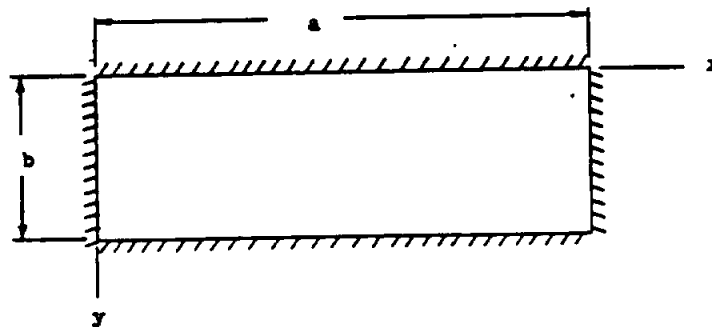


Fig. 11.2.3-1

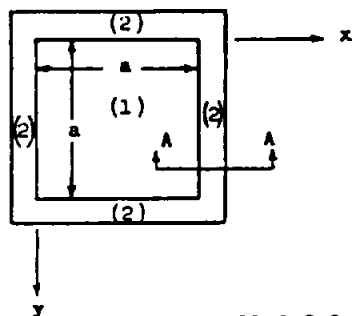
$$\sigma_x = \sigma_y = - \frac{E\alpha}{(1-\nu)} (T - T_0) \quad (1)$$

STRUCTURAL ANALYSIS MANUAL

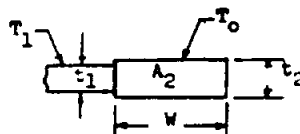
GENERAL DYNAMICS/CONVAIR AND SPACE SYSTEMS DIVISION

2. Partial Restraint of a Uniformly Heated or Cooled Square Plate

The restraint is equal in the "x" and "y" direction.



Note: Frame assumes no bending but will expand axially.



View A-A
(Typical All Edges)

Fig. 11.2.3-2

This is an approximate solution only.

$$\sigma_{x_1} = \sigma_{y_1} = \frac{-E_1 \alpha_1 (T_1 - T_0) K}{1 - \mu} \quad (2)$$

$$\sigma_2 = -\frac{A_1}{A_2} \sigma_{x_1} = -\frac{A_1}{A_2} \sigma_{y_1} \quad (3)$$

where:

$$A_1 = at_1$$

$$A_2 = 2wt_2$$

Subscripts (1) and (2) refer to the plate and edge member, respectively.

$$K = \frac{1 - \frac{\alpha_2 (T_2 - T_0)}{\alpha_1 (T_1 - T_0)}}{1 + \frac{E_1 A_1}{(1 - \mu)(E_2 A_2)}}$$

3. Partial Restraint of a Uniformly Heated Rectangular Plate

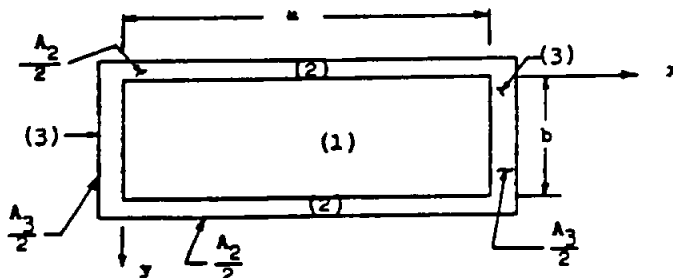


Fig. 11.2.3-3

STRUCTURAL ANALYSIS MANUAL
GENERAL DYNAMICS/CONVAIR AND SPACE SYSTEMS DIVISION

Data Source, Section 1.3 Reference)

$$\sigma_{x_1} = \frac{E_1}{1-\mu^2} \left[\epsilon_x + \mu \epsilon_y - (1+\mu)\alpha_1 (T_1 - T_0) \right] \quad (4)$$

$$\sigma_{y_1} = \frac{E_1}{1-\mu^2} \left[\epsilon_y + \mu \epsilon_x - (1+\mu)\alpha_1 (T_1 - T_0) \right] \quad (5)$$

$$\sigma_2 = E_2 \left[\epsilon_x - \alpha_2 (T_2 - T_0) \right] \quad (6)$$

$$\sigma_3 = E_3 \left[\epsilon_y - \alpha_3 (T_3 - T_0) \right] \quad (7)$$

Using the following equilibrium conditions:

$$\Sigma F_x = \sigma_{x_1} A_{x_1} + \sigma_2 A_2 = 0$$

$A_{x_1} = bt$, $A_2 =$ area of both (2) members and t is the thickness of member 1

$$\Sigma F_y = \sigma_{y_1} A_{y_1} + \sigma_3 A_3 = 0$$

$A_{y_1} = at$, $A_3 =$ area of both (3) members

The above equations can be solved for the two unknowns, " ϵ_x " and " ϵ_y ."

Upon determining " ϵ_x " and " ϵ_y ," the stress in the plate and the edge members can be obtained by substituting back in equations (4), (5), (6), and (7).

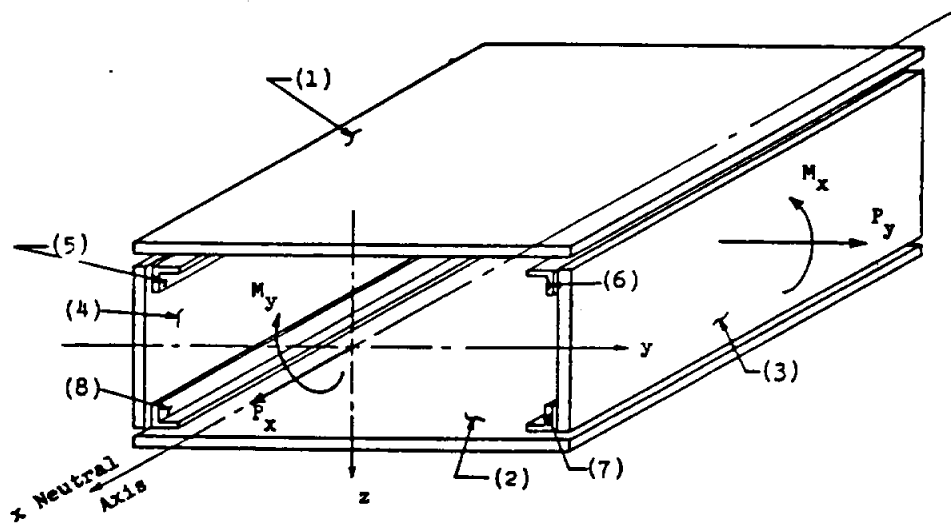
Note: These equations are approximate.

11.2.4.

Box Beams

The following equations can be used for approximately determining the thermal stresses of composite structures (box beams). Bending of the box-beam about the "x" and "y" axis is considered and it is assumed that bending stresses in the components of the box beam are negligible.

STRUCTURAL ANALYSIS MANUAL
GENERAL DYNAMICS/CONVAIR AND SPACE SYSTEMS DIVISION



Typical Composite (or Box-Beam)
Structure

Fig. 11.2.4-1

$$\sigma_{x_1} = \frac{E_1}{(1-\mu^2)} \left[\epsilon_x + \mu \left(\epsilon_y + \frac{1}{\rho_y} z_1 \right) + \frac{1}{\rho_x} z_1 - (1+\mu) \alpha_1 (T_1 - T_0) \right] \quad (1)$$

where 1 refers to
the skin component

$$\sigma_{y_1} = \frac{E_1}{(1-\mu^2)} \left[\epsilon_y + \mu \left(\epsilon_x + \frac{1}{\rho_x} z_1 \right) + \frac{1}{\rho_y} z_1 - (1+\mu) \alpha_1 (T_1 - T_0) \right] \quad (2)$$

$$\sigma_{x_n} = E_n \left[\epsilon_x + \frac{1}{\rho_x} z_n - \alpha_n (T_n - T_0) \right] \quad (3)$$

where n refers to
the edge members

$$\sigma_{y_n} = E_n \left[\epsilon_y + \frac{1}{\rho_y} z_n - \alpha_n (T_n - T_0) \right] \quad (4)$$

where:

z_1 - Distance from neutral plane to centroid of 1th or nth component.

STRUCTURAL ANALYSIS MANUAL

GENERAL DYNAMICS/CONVAIR AND SPACE SYSTEMS DIVISION

i refers to the i^{th} component

ϵ_x and ϵ_y = Strains at the centroid of the structure.

$\frac{1}{R_x}$ and $\frac{1}{R_y}$ = Curvature in x-z and y-z plane, respectively.

The curvatures, $\frac{1}{R_x}$ and $\frac{1}{R_y}$ will be assumed to be the same for all components of the structure.

The equilibrium equations for Figure 11.2.4-1 are:

$$\sum F_x = \sum_{i=1}^n \sigma_{x_i} A_i - P_x = 0 \quad (5)$$

$$\sum F_y = \sum_{i=1}^n \sigma_{y_i} A_i - P_y = 0 \quad (6)$$

$$\sum (M)_{(x-z)} = \sum_{i=1}^n \sigma_{x_i} A_i z_i - M_y = 0 \quad (x-z \text{ plane}) \quad (7)$$

$$\sum (M)_{(y-z)} = \sum_{i=1}^n \sigma_{y_i} A_i z_i - M_x = 0 \quad (y-z \text{ plane}) \quad (8)$$

where:

Webs and attachment angles in the "y" direction are not shown for the sake of clarity.

- (1) and (2) - Outer Skins
- (3) and (4) - Webs
- (5) thru (8) - Attachment Angles

"z" is the distance from the neutral plane of the box beam to the neutral axis of the individual component.

P_x = External load in "x" direction (+) if tensile

P_y = External load in "y" direction

M_y = Externally applied moment about y-axis

M_x = Externally applied moment about x-axis

((+) as shown in Figure 11.2.4-1.)

Procedure

1. By substituting the stress expressions (1), (2), (3) and (4) into the four equilibrium equations, and performing the indicated summation or integration, four equations are obtained which contain the unknown strains and curvatures ϵ_x , ϵ_y , $\frac{1}{R_x}$, and $\frac{1}{R_y}$.
2. The numerical values of these unknowns are obtained by the simultaneous solution of the four equations.

STRUCTURAL ANALYSIS MANUAL

GENERAL DYNAMICS/CONVAIR AND SPACE SYSTEMS DIVISION

Data Source, Section 1.3 Reference /

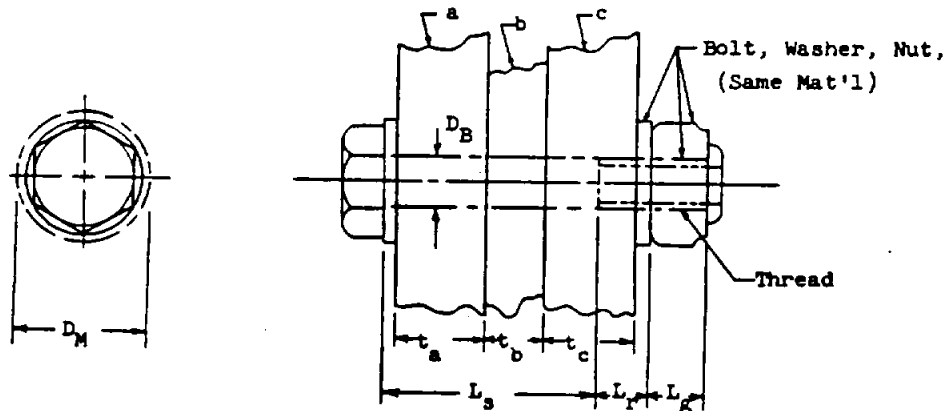
3. Finally, the strains and curvatures thus obtained are substituted into equations (1), (2), (3), and (4) to provide the stress distribution.

11.2.5

Bolted and Riveted Joints

A. Bolt Pre-Load Due to Temperature

Bolts and other threaded fasteners, clamping one or more thicknesses of materials together and exposed to temperature change after installation, are subjected to thermal loads which either add to or subtract from installation pre-loads.



Bolt Assembly Exposed to Temperature After Installation
Fig. 11.2.5-1

- T - Final temperature of the entire assembly.
 T_0 - Initial temperature of the entire assembly before heating.
 D_M - Effective diameter of material exerting thermal load on bolt; assumed equal to twice D_B
 D_B - Bolt diameter
 t_M - Total material thickness ($t_a + t_b + t_c$)
 A_M - Cross-sectional area of resisting material based on D_M

$$A_M = \frac{\pi}{4}(D_M^2 - D_B^2) = \frac{3}{4} \pi D_B^2$$

- L_B - Effective length of bolt under load ($L_s + L_r + \frac{L_g}{2}$)
 L_s - Length of non-threaded shank of bolt
 L_r - Length of threaded length of bolt not engaged by the nut
 L_g - Length of threaded length of bolt engaged by the nut
 A_s - Cross-sectional area of shank of bolt
 A_r - Cross-sectional area of root dia. of bolt
 P_T - Thermal load; (plus (+) is tension in the bolt; minus (-) would unload a pre-loaded bolt)
 e_B - Deformation of the bolt over length, L_B

STRUCTURAL ANALYSIS MANUAL
GENERAL DYNAMICS/CONVAIR AND SPACE SYSTEMS DIVISION

e_M - Deformation of the material over length, t_M
 g - Gap (inches)

Assume washer deformation to be negligible.

$$e_P = \alpha_B L_B (T - T_0) + \frac{P}{E_B} \left(\frac{t_s}{A_s} + \frac{t_r}{A_r} + \frac{t_g}{2A_r} \right) \quad (1)$$

$$e_M = (T - T_0) (\alpha_a t_a + \alpha_b t_b + \alpha_c t_c) - P \left(\frac{t_a}{A_a E_a} + \frac{t_b}{A_b E_b} + \frac{t_c}{A_c E_c} \right) \quad (2)$$

$$e_B = e_M \quad (3)$$

$$P_T = \frac{(T - T_0) (\alpha_a t_a + \alpha_b t_b + \alpha_c t_c - \alpha_B L_B)}{\frac{1}{E_B} \left(\frac{t_s}{A_s} + \frac{t_r}{A_r} + \frac{t_g}{2A_r} \right) + \left(\frac{t_a}{A_a E_a} + \frac{t_b}{A_b E_b} + \frac{t_c}{A_c E_c} \right)} \quad (4)$$

For a, b, and c being of the same material, the equation reduces to:

$$P_T = \frac{(T - T_0) (\alpha_M t_M - \alpha_B L_B)}{\frac{1}{E_B} \left(\frac{t_s}{A_s} + \frac{t_r}{A_r} + \frac{t_g}{2A_r} \right) + \frac{t_M}{A_M E_M}} \quad (5)$$

(Tension in bolt if $T > T_0$ and $\alpha_M > \alpha_b$)

If a gap exists and the nut is finger-tight, i.e., no pre-load, equation (4) becomes:

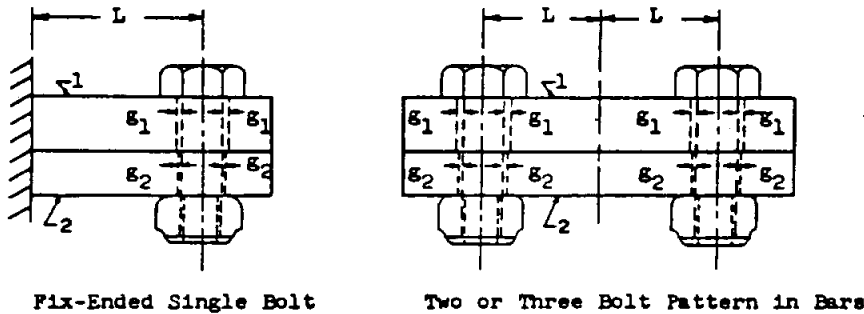
$$P_T = \frac{-g + (T - T_0) (\alpha_a t_a + \alpha_b t_b + \alpha_c t_c - \alpha_B L_B)}{\frac{1}{E_B} \left(\frac{t_s}{A_s} + \frac{t_r}{A_r} + \frac{t_g}{2A_r} \right) + \left(\frac{t_a}{A_a E_a} + \frac{t_b}{A_b E_b} + \frac{t_c}{A_c E_c} \right)} \quad (6)$$

and equation (5) becomes

$$P_T = \frac{-g + (T - T_0) (\alpha_M t_M - \alpha_B L_B)}{\frac{1}{E_B} \left(\frac{t_s}{A_s} + \frac{t_r}{A_r} + \frac{t_g}{2A_r} \right) + \frac{t_M}{A_M E_M}} \quad (7)$$

STRUCTURAL ANALYSIS MANUAL
GENERAL DYNAMICS/CONVAIR AND SPACE SYSTEMS DIVISION

- B. Dissimilar Materials Subjected to a Uniform Temperature Change From the Same Initial Temperature, T_0 , to a Final Temperature, T_1 and T_2 .



Two* Bars; All Bolts Assumed Concentric in Holes

Fig. 11.2.5-2

For cooling and $|\alpha_1 (T_1 - T_0)| < |\alpha_2 (T_2 - T_0)|$

For heating and $|\alpha_1 (T_1 - T_0)| > |\alpha_2 (T_2 - T_0)|$

For heating of bar 1 or cooling of bar 2, or both;

$$P = \frac{\alpha_1 (T_1 - T_0) - \alpha_2 (T_2 - T_0) - \frac{\epsilon_1 + \epsilon_2}{L}}{\frac{1}{A_1 E_1} + \frac{1}{A_2 E_2}} \quad (8)$$

(The force "P" will be compressive in 1 and tensile in 2.)

For cooling and $|\alpha_1 (T_1 - T_0)| > |\alpha_2 (T_2 - T_0)|$

For heating and $|\alpha_1 (T_1 - T_0)| < |\alpha_2 (T_2 - T_0)|$

For heating of bar 2 or cooling of bar 1, or both;

$$P = \frac{\alpha_2 (T_2 - T_0) - \alpha_1 (T_1 - T_0) - \frac{\epsilon_1 + \epsilon_2}{L}}{\frac{1}{A_1 E_1} + \frac{1}{A_2 E_2} + 1} \quad (9)$$

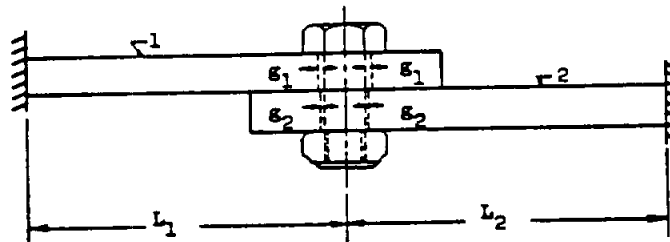
*Hole elongations neglected

STRUCTURAL ANALYSIS MANUAL
GENERAL DYNAMICS/CONVAIR AND SPACE SYSTEMS DIVISION

(The force "P" will be compressive in 2 and tensile in 1)
 For riveted joints ϵ_1 and ϵ_2 are set equal to zero.

$$P_{\text{rivet}} = \pm \frac{\alpha_1(T_1 - T_0) - \alpha_2(T_2 - T_0)}{\frac{1}{A_1 E_1} + \frac{1}{A_2 E_2}} \quad (10)$$

- C. Two Fastened Bars With Fixed Ends Subjected to a Uniform Temperature Change From the Same Initial Temperature, T_0 , to a Final Temperature, T_1 and T_2 .



Two* Bars With Opposite Ends Fixed

Fig. 11.2.5-3

- (a) Bar 1 and Bar 2 Heated;

$$P = - \frac{\alpha_1 L_1 (T_1 - T_0) - \alpha_2 L_2 (T_2 - T_0) + \epsilon_1 + \epsilon_2}{\frac{L_1}{A_1 E_1} + \frac{L_2}{A_2 E_2}} \quad (11)$$

(Both bars in compression)

- (b) Both Bars Cooled;

$$P = - \frac{\alpha_1 L_1 (T_1 - T_0) - \alpha_2 L_2 (T_2 - T_0) - \epsilon_1 - \epsilon_2}{\frac{L_1}{A_1 E_1} + \frac{L_2}{A_2 E_2}} \quad (12)$$

(Both bars in tension)

For riveted joints ϵ_1 and ϵ_2 are set equal to zero

$$P_{\text{rivet}} = \pm \frac{\alpha_1 L_1 (T_1 - T_0) + \alpha_2 L_2 (T_2 - T_0)}{\frac{L_1}{A_1 E_1} + \frac{L_2}{A_2 E_2}}$$

(Compressive if both heated,
 Tensile if both cooled.)

* Hole Elongations Neglected

STRUCTURAL ANALYSIS MANUAL

GENERAL DYNAMICS/CONVAIR AND SPACE SYSTEMS DIVISION

Data Source, Section 1.3 Reference /

11.3.0

Thermal Buckling of Columns and Plates

Buckling is assumed to occur in the elastic range in this section.

11.3.1

Column Buckling

A. Column Buckling Due to Temperature Differential Only

The following general equation can be used to determine the temperature differential which would initiate column buckling.

$$\left[\alpha(T-T_0) \right]_{cr} = \frac{c \pi^2 I_{min}}{AL^2 c_1} = \frac{c \pi^2 k^2}{L^2 c_1} \quad (1)$$

where

$T-T_0$ = Increase in temperature of column

c = Column fixity coefficient

$$c_1 = \frac{C}{C + \frac{AE}{L}} \quad (\text{Also see Eq. 11.2.1(2)}) \quad (2)$$

C = Longitudinal stiffness of the restraining structure (lb/in.)

$\frac{AE}{L}$ = Longitudinal stiffness of the column (lb/in.)

B. Simple Beam Initially Crooked, Deflected, or Both, With Complete Axial End Restraint, Subjected to Installation Pre-Load, P_1 , and Uniform Temperature Change

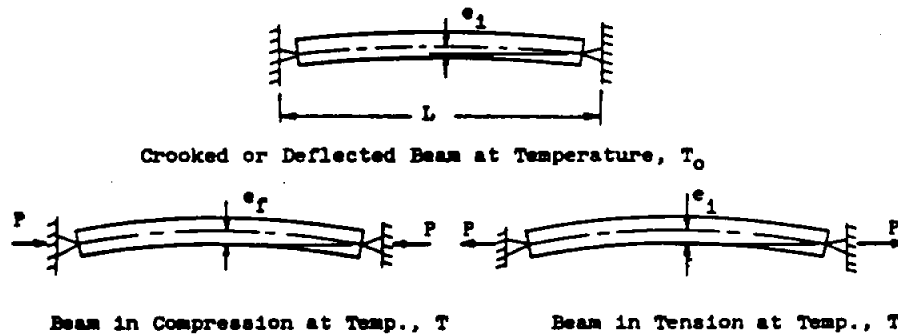


Fig. 11.3.1-1

$$P = P_1 + P_{thermal}$$

$$P = P_1 - E\alpha A(T-T_0)$$

$$\left[\begin{array}{l} + P_1 \text{ is tension} \\ - P_1 \text{ is compression} \end{array} \right]$$

STRUCTURAL ANALYSIS MANUAL
GENERAL DYNAMICS/CONVAIR AND SPACE SYSTEMS DIVISION

Beam in compression:

$$P' = \frac{\pi^2 EI}{L^2} \quad (3)$$

$$e_r = \frac{e_1}{1 - P/P'} \quad (4)$$

$$M_{\max} = P(e_r) \quad (5)$$

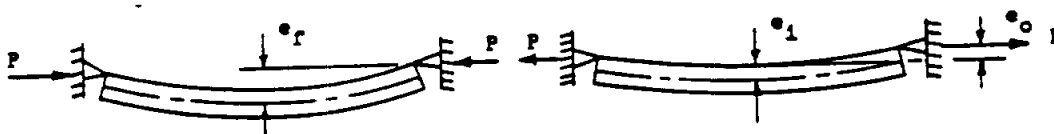
Beam in tension:

$$M_{\max} = P(e_1) \quad \left[\begin{array}{l} \text{Assuming tension insufficient to} \\ \text{significantly straighten beam} \end{array} \right] \quad (6)$$

C. Simple Beams (Axial End Restraint Eccentric to the Elastic Axis)
Subjected to Installation Pre-Load, P_1 , and a Uniform Temperature
Change



Crooked or Deflected Beam at Temperature, T_0



Beam in Compression at Temp., T

Beam in Tension at Temp., T

Fig. 11.3.1-2

$$P = P_1 + P_{\text{thermal}}$$

$$= P_1 - E\alpha A(T - T_0)$$

$$\left[\begin{array}{l} + P_1 \text{ is Tension} \\ - P_1 \text{ is Compression} \end{array} \right]$$

Beam in compression:

$$P' = \frac{\pi^2 EI}{L^2}$$

$$e_r = \frac{e_0}{\cos\left(\frac{\pi}{2}\sqrt{P/P'}\right)} + \frac{e_1}{1 - P/P'}$$

$$M_{\max} = P(e_r) \quad (7)$$

STRUCTURAL ANALYSIS MANUAL

GENERAL DYNAMICS/CONVAIR AND SPACE SYSTEMS DIVISION

Beam in tension:

$$M_{\max} = P(e_0 + e_1) \quad (8)$$

Assuming tension insufficient
to significantly straighten
beam

11.3.2

Flat Plates (Uniformly Heated From T_0 to T_1)

The following method can be used to determine the temperature differential causing plate buckling:

(This analysis applies to loading by thermal forces, only)

Condition 1: Plate is fully restrained from thermal expansion in the "x" direction only

$$(T_1 - T_0)_{cr} = \frac{K\pi^2}{12(1-\mu)\alpha} \left(\frac{t}{b}\right)^2 \quad (1)$$

Values of "K" can be obtained for panels with various edge conditions from PG. 6.1.7 TO PG 6.1.12

Condition 2: Plate is fully restrained from thermal expansion in both the "x" and "y" directions.

(a) All edges simply supported:

$$(T_1 - T_0)_{cr} = \frac{\pi^2}{12(1-\mu^2)} \left(\frac{t}{b}\right)^2 \left[\frac{(1-\mu)}{\alpha} \left(1 + \frac{b^2}{a^2}\right) \right] \quad (2)$$

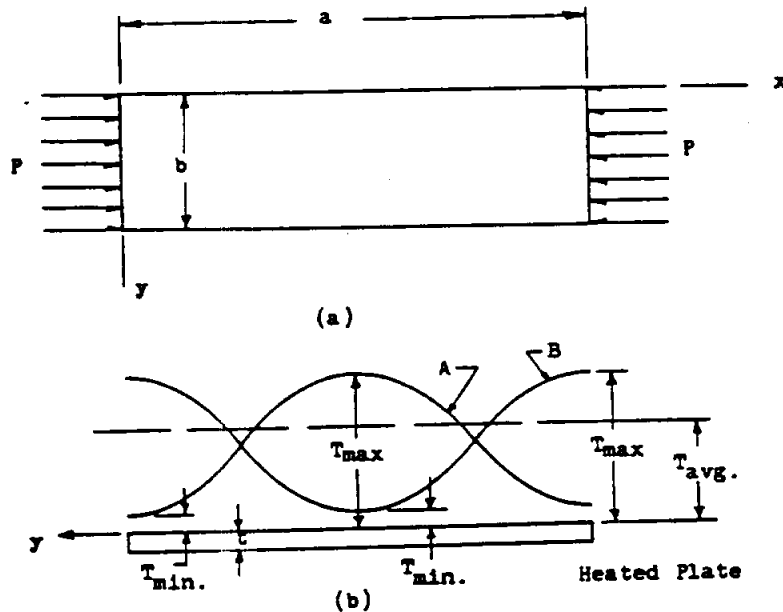
(b) All edges clamped:

The following equation can be used if the plate does not differ much from a square plate.

$$(T_1 - T_0)_{cr} = \frac{\pi^2}{12(1-\mu^2)} \left(\frac{t}{b}\right)^2 \frac{4(1-\mu)}{\alpha \left(1 + \frac{a^2}{b^2}\right)} \left(\frac{3b^2}{a^2} + \frac{3a^2}{b^2} + 2\right) \quad (3)$$

Condition 3: Buckling of simply supported rectangular plates when the temperature varies in the "y" direction and is constant in the "x" direction.

STRUCTURAL ANALYSIS MANUAL
GENERAL DYNAMICS/CONVAIR AND SPACE SYSTEMS DIVISION



Flat Plate With Temperature Varying in "y"
 Direction Constant in "x" Direction

Fig. 11.3.2-1

(1) Assumptions:

- (a) The plate is fully restrained in "x" direction and allowed to expand in the "y" direction,
- (b) All edges remain straight and parallel,
- (c) No variation in heating through the plate's thickness.
- (d) Adjacent panels do not affect the stability of panel to be analyzed, and
- (e) Temperature distribution in the panel can be expressed approximately as a cosine curve.
 (See Fig. 11.3.2-1(b).)

(2) Equation for calculating critical temperature differential:

$$(T_{av.} - T_o)_{cr} = \beta \left[\frac{\pi^2 t^2}{3(1-\mu^2)b^2\alpha} + \frac{P}{bt\alpha E} \right] \quad (4)$$

where: P is total load on the plate, pounds

T_o is the temperature of the structure, °F.

(3) Procedure:

- (a) Determine the average temperature in panel (T_{av}) from the temperature distribution curve,

STRUCTURAL ANALYSIS MANUAL
GENERAL DYNAMICS/CONVAIR AND SPACE SYSTEMS DIVISION

- (b) Determine the constant " γ " from the following equations:

$$\gamma = \pm \frac{(T_{av} - T_{min})}{T_{av}} \quad (5a)$$

or

$$\gamma = \pm \frac{(T_{max} - T_{av})}{T_{av}} \quad (5b)$$

Use the value of " γ " which produces the smallest value of " β ".

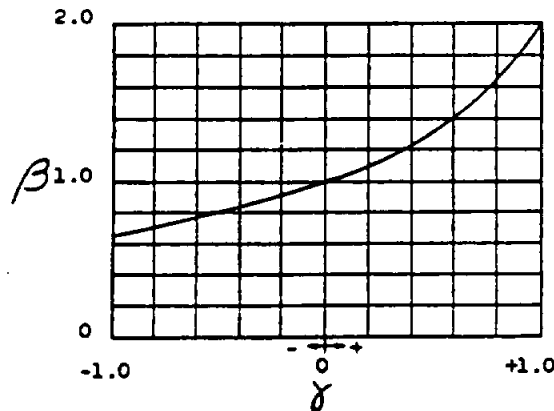
- (c) From the curve in Fig. 11.3.2-2, determine " β ".
- (d) Solve for $(T_{av} - T_o)$ using equation (4).
 ("P" is negative if it is a compression load)
- (e) $(T_{av} - T_o)_{actual}$ must be less than the value calculated in (d) if the plate is not to buckle.
- (4) Observations:
- (a) If the bracket in equation (4) is ≤ 0 , the panel will not sustain any thermal stress in the "x" direction.
- (b) The value of "E" and " α " should be evaluated at the highest panel temperature.

The average temperature distribution, T_{av} , may be determined graphically by using the temperature distribution curves "A" and "B" from Figure 11.3.2-1b.

The sign " γ " can be determined as follows:

If the peak temperature appears in the center of the panel (such as curve "A", Figure 11.3.2-1b), " γ " should be taken as minus.

If the valley of the curve appears in the center (such as curve "B"), " γ " should be taken as positive.



Critical Values of β

Fig. 11.3.2-2

STRUCTURAL ANALYSIS MANUAL

GENERAL DYNAMICS/CONVAIR AND SPACE SYSTEMS DIVISION

11.3.3

Inter-Rivet Thermal Buckling

The following equations assume that only a thermal load is acting.

- (1) Critical thermal strain for elastic buckling between rivets:

$$[\alpha(T-T_0)]_{cr} = \frac{\pi^2 t^2}{3L^2} \quad (1)$$

where:

t = skin thickness

L = Length of skin between rivet centerlines

Equation 2 will give the approximate critical thermal strain when the bending stress (induced by the thermal load) equals the yield stress of the material at the given temperature.

$$[\alpha(T-T_0)]_{cr} = \frac{\pi^2 t^2}{3L^2} + \frac{L^2}{4\pi^2 E t^2} \left[F_{cy} - \frac{\pi^2 E}{3} \left(\frac{t}{L} \right)^2 \right]^2 \quad (2)$$

Procedure:

- (a) From an appropriate high temperature stress-strain curve, obtain the 0.2% yield stress, and the elastic modulus.
- (b) Substitute this F_{cy} into the formula and determine

$$[\alpha(T-T_0)]_{cr}$$

- (c) If " T " is in excess of the assumed temperature used originally to select a stress-strain curve, the process should be repeated using a new F_{cy} and modulus, E , at the higher temperature.

11.4.0

Thermal Deflections of Structural Components

1. Simply supported beams with temperatures varying through the depth only

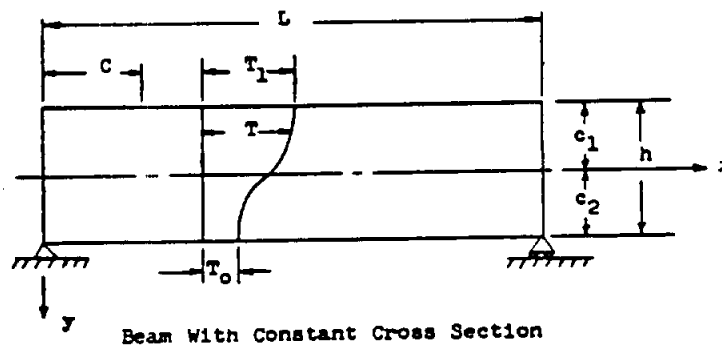


Fig. 11.4.0-1

STRUCTURAL ANALYSIS MANUAL

GENERAL DYNAMICS/CONVAIR AND SPACE SYSTEMS DIVISION

Deflection of the beam at any point "C" :

$$\delta_c = \frac{LC-C^2}{2I_z} \int_{y=-C_1}^{y=C_2} \alpha y T b dy \quad (1)$$

b = the width (May be a function of "y" and assumed to be symmetric about the vertical centerline.)

If " α " is assumed constant and the temperature varies linearly through the depth of the beam, then:

$$\delta_c = \frac{\alpha (T_1 - T_0) (LC - C^2)}{2h} \quad (2)$$

For " δ " at the center of the beam ($C = L/2$):

$$\delta = \frac{\alpha (T_1 - T_0) L^2}{8h} \quad (3)$$

The general equation for δ_c along the length "L", can be written in summation form to facilitate a numerical integration: (See Figure 11.4.0-2)

$$\delta_c = \sum_{i=1}^{i=k} \left(\frac{L-C}{L} \right) x_i \left[\int_A \frac{\alpha_1}{I_1} (T_1 - T_0) y dA \right]_1 \Delta x_i + \quad (4)$$

$$\sum_{i=k+1}^{i=n} \frac{C}{L} (L-x_i) \left[\int_A \frac{\alpha_1}{I_1} (T_1 - T_0) y dA \right]_1 \Delta x_i$$

Note: The symbol \int_A represents the integral over a cross sectional area.

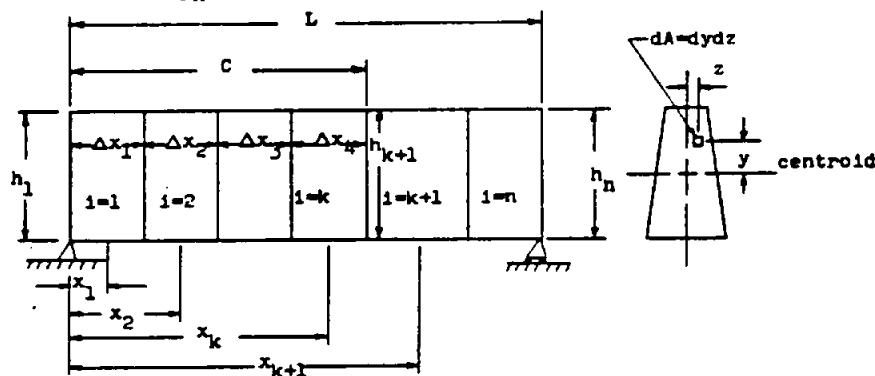


Fig. 11.4.0-2

STRUCTURAL ANALYSIS MANUAL
GENERAL DYNAMICS/CONVAIR AND SPACE SYSTEMS DIVISION

2. Cantilever beams with temperatures varying through the depth

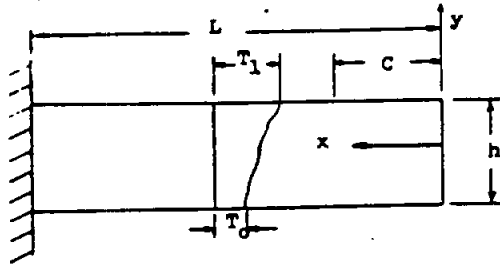


Fig. 11.4.0-3

The deflection at "C" is :

$$\delta_c = - \int_{x=c}^L \frac{(x-c)}{EI_z} \left[\int_A E\alpha y T dA \right] dx \quad (5-a)$$

If E and I_z are constant, the expression becomes:

$$\delta_c = - \frac{(L-c)^2}{2EI} \int_A E\alpha y T dA \quad (5-b)$$

If E, I_z , and α are constant, and the temperature varies linearly through the depth, then:

$$\delta_c = - \frac{(L-c)^2 \alpha (T_1 - T_0)}{2h} \quad (5-c)$$

The deflection at the end of the beam ($c=0$) is:

$$\delta_0 = - \frac{\alpha (T_1 - T_0) L^2}{2h} \quad (6)$$

If α , I, and $(T-T_0)$ are functions of "x", it may be advisable to use a numerical approximation to find the deflection at the end of the beam.

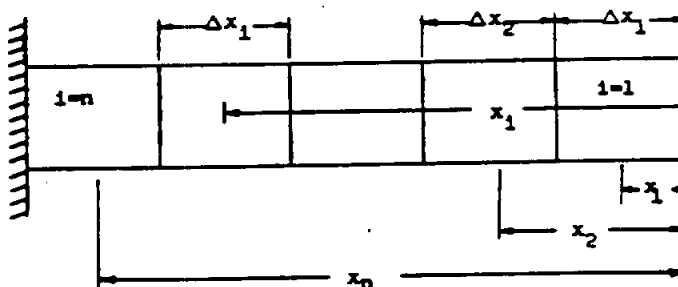


Fig. 11.4.0-4

STRUCTURAL ANALYSIS MANUAL
GENERAL DYNAMICS/CONVAIR AND SPACE SYSTEMS DIVISION

$$\delta_o = - \sum_{i=1}^{i=n} \frac{x_1}{EI_z} \left[\int_A E\alpha_y T dA \right]_1 \Delta x_1 \quad (7-a)$$

or,

$$\delta_o = - \sum_{i=1}^{i=n} \frac{x_1}{EI_z} \left[\sum_A (E\alpha)_1 y_1 T_1 A_1 \right]_1 \Delta x_1 \quad (7-b)$$

where "y" or "y₁" is measured from the centroid of the cross section.

3. Simply-supported flat plate with temperature varying through the plate's thickness

The following equation gives the approximate deflection in the center of a simply-supported plate.

$$\delta_{\max} = \frac{\left[\int_{-t/2}^{t/2} \alpha T_y dy \right] a^2}{8I} \quad (8)$$

where:

$$I = \frac{h^3(1-\mu)}{12(1-\mu^2)}$$

t = plate thickness

a = length of plate edge

If $T = \frac{T_1+T_2}{2} + \left(\frac{T_1-T_2}{t} \right) y$ (linear through the plate's thickness)

then

$$\delta_{\max} = \frac{a^2 \alpha (T_1 - T_2) (1-\mu)}{8t} \quad (9)$$

where:

T₁ = Temperature of upper surface

T₂ = Temperature of lower surface

STRUCTURAL ANALYSIS MANUAL

GENERAL DYNAMICS/CONVAIR AND SPACE SYSTEMS DIVISION

11.5.0

Plastic Strain Analysis

11.5.1

Strains Due to Thermal Stresses Only

Maximum thermal stresses calculated by the use of elastic equations must be within the elastic range of the material at the final temperature "T." This may be determined by the use of stress-strain curves.

Thermal stresses may be evaluated in the plastic range for constant stable cross sections, excepting springs, by the following:

1. Evaluate the erroneous elastic thermal stress, σ , by the elastic equations.
2. Calculate the actual thermal strain by $\epsilon = \sigma/E$.
3. Locate this thermal strain on the appropriate stress-strain curve at the final temperature "T" and read the actual thermal stress.

11.5.2

Strain Analysis of a Beam Subjected to Thermal Stresses and External Loads

The following assumptions are made:

1. The temperature varies in the "y" (depthwise) direction only.
2. The stresses are uniaxial.
3. Plane cross sections remain plane after bending.
4. Stress-strain curves are available for the material and temperatures of the beam.
5. The beam is prismatic and is symmetric about the "xy" plane.

The beam is considered to be made up of longitudinal strips at various distances, "y₁", from the neutral axis of the beam.

The strain corresponding to the stress in the 1th strip is:

$$\epsilon_{m1} = \epsilon_0 + \frac{1}{\rho} y_1 - (\alpha \Delta T)_1 \quad (1)$$

where:

ϵ_0 = the strain in the "x" direction at the neutral axis

$\frac{1}{\rho}$ = the bending curvature in the "xy" plane

$(\alpha \Delta T)_1$ = thermal strain of the 1th strip at distance "y₁" from the neutral axis.

Equations (2) and (3) and the following discussion outlines a method for determining the unknowns, ϵ_0 and $\frac{1}{\rho}$.

The summation of forces,

$$P_E - \sum_{i=1}^n \sigma_i A_i = 0 \quad (2)$$

STRUCTURAL ANALYSIS MANUAL
GENERAL DYNAMICS/CONVAIR AND SPACE SYSTEMS DIVISION

and the summation of moments,

$$M_E - \sum_{i=1}^n \sigma_i y_i A_i = 0 \quad (3)$$

where:

A_i = cross sectional area of the i^{th} strip

P_E = the externally applied axial load.
(Tensile load is positive)

M_E = the externally applied end moment.
(A positive end moment will cause a
tensile stress in the " $y > 0$ " portion
of the beam cross section.)

If the stresses in all the strips are within the proportional limit, then the conventional method of section 11.2.1 is used to solve for the stresses in the various strips.

If the proportional limit is exceeded, a trial and error strain analysis is used as follows:

Trial values of both ϵ_o and $1/\rho$ are substituted into equation (1) to provide a value of strain for each strip. The stresses " σ_i " corresponding to the strains " ϵ_{mi} " are taken from stress-strain curves for the material at the various temperatures involved.

These stresses are then substituted into Eq. (2) and Eq. (3). If the proper values of ϵ_o and $1/\rho$ have been assumed, then Eq. (2) and Eq. (3) are satisfied, otherwise new values of ϵ_o and/or $1/\rho$ must be tried until the proper values are obtained.

STRUCTURAL ANALYSIS MANUAL
GENERAL DYNAMICS/CONVAIR AND SPACE SYSTEMS DIVISION

REFERENCES

- 11.0.0** THERMAL STRESS ANALYSIS
- 11.1.0** Convair Astronautics, Structures Manual, Thermal Effects,
Section 19.00, 1959
- 11.2.0** Timoshenko, S. P., and Goodier, J. N., Theory of Elasticity, 1951;
Gatewood, B. E., Thermal Stresses, 1957
- 11.2.1** Gatewood, B. E., Thermal Stresses, 1957
Convair Astronautics Structures Manual, Thermal Effects,
Section 19.00, 1959
Timoshenko, S. P., Theory of Elastic Stability, 1936
Hotchkiss, H. H., Thermal Stress Lecture Notes, Convair-Port Worth,
Advanced Structural Analysis Course, 1959
- 11.2.2** Timoshenko, S. P., Theory of Plates and Shells, 1940
- 11.2.3** Gatewood, B. E., Thermal Stresses, 1957
Hotchkiss, H. H., Thermal Stress Lecture Notes, Convair-Port Worth,
Advanced Structural Analysis Course, 1959
- 11.2.4** Schoeller, W. C., SRG-TN-7, Thermal Stresses in Aircraft Structures
Due to Aerodynamic Heating, 1959
- 11.2.5** Convair Astronautics, Structures Manual, Thermal Effects,
Section 19.00, 1959
- 11.3.1** Timoshenko, S. P., Theory of Elastic Stability, 1936
Convair Astronautics Structures Manual, Thermal Effects,
Section 19.00, 1959
- 11.3.2** Hoff, N. J., Thermal Buckling of Supersonic Wing Panels,
Journal of Aeronautical Sciences, 1956
Timoshenko, S. P., Theory of Elastic Stability, 1936
- 11.3.3** Hotchkiss, H. H. Thermal Stress Lecture Notes, Convair-Port Worth,
Advanced Structural Analysis Course, 1959
- 11.4.0** Hotchkiss, H. H., SRG-34, Methods of Thermal Stress Calculation, 1959
Gatewood, B. E., Thermal Stresses, 1957
Goodier, J. N., Thermal Stress and Deformation, Journal of Applied
Mechanics, 1957
Boley, B. A., The Calculation of Thermoelastic Beam Deflections
by the Principle of Virtual Work, Journal of Aeronautical Sciences, 1957
Goodman, S., and Russell, S. B., Transient Temperature and Stress
Distributions in Beams, National Bureau of Standards Report 3630, 1954
- 11.5.0** Convair Astronautics, Structures Manual, Thermal Effects,
Section 19.00, 1959
Hotchkiss, H. H., Thermal Stress Lecture Notes, Convair-Port Worth,
Advanced Structural Analysis Course, 1959

STRUCTURAL ANALYSIS MANUAL

GENERAL DYNAMICS/CONVAIR AND SPACE SYSTEMS DIVISION

SYNOPSIS

Thermal Structural Analysis with MSC/NASTRAN

Complex thermally loaded structures can be analyzed using MSC/NASTRAN. The capabilities include linear elastic analyses for stresses and deflections as well as extended capabilities for the analyses of structures containing material and geometric nonlinearities.

Location of Thermal Stress Analysis Information in MSC Documents

Table 1 on page 1.3-28 of Volume I of the User's Manual lists the thermal loading capabilities of the various elements. This table also shows which elements ~~also~~ have material and geometric nonlinear capabilities.

Section 1.5.1, page 1.5-3 of Volume I of the User's Manual describes the method of applying thermal loads to the model.

Section 1.5.4, page 1.5-8 of Volume I of the User's Manual describes how loads are handled in Super-element analyses.

The TEMPERATURE case control card which selects thermal effects is described on page 2.3-98 of Volume I of the User's Manual.

The bulk data cards that define temperature dependent material properties begin with MATT and are described beginning on page 2.4-202 of Volume I of the User's Manual.

The bulk data cards that define temperatures start with the TEMP and are described beginning on page 2.4-347 of Volume I of the User's Manual.

The Demonstration Problem Manual contains two problems that show the use of NASTRAN for thermal-structural analysis. The first problem is number D2434 and the second is number D2401N. (Unfortunately, page numbers are meaningless in this manual.) D2401N shows how to use thermal loads in SUBCOM's.

The Verification Problem Manual has an example of a structure with thermal loads on page 3.2403-1.

Sections 2.6.4, 2.6.5, and 2.6.7 of the Handbook for Linear Analysis contain guidance in thermal structural analysis.



STRUCTURAL ANALYSIS MANUAL
GENERAL DYNAMICS/CONVAIR AND SPACE SYSTEMS DIVISION

SECTION 20.0

STATISTICAL ANALYSIS

BASIC STRUCTURAL ANALYSIS TECHNIQUES ARE PRESENTED IN THIS SECTION.

	PAGE
20.1 INTRODUCTION	20.1.1
20.2 DEFINITIONS	20.2.1
20.3 DISCUSSION	20.3.1
20.4 SAMPLE PROBLEMS	20.4.1
20.5 TABLES OF STATICAL VALUES	20.5.1

STRUCTURAL ANALYSIS MANUAL
GENERAL DYNAMICS/CONVAIR AND SPACE SYSTEMS DIVISION

Data Source, Section 1.3 Reference 47

SUBJECT: Sigma, Sample Standard Deviation, and Probability Levels

1.0 INTRODUCTION

This memorandum presents definitions and applications of some important statistical terms. Graphs are presented by which rapid selection of optimum sample sizes and estimates of tolerance factors may be made. Sample problems are included showing some typical applications.

2.0 DEFINITIONS

Population	The group of all possible observations of values from which a random sample may be selected.
Normal Population	A population whose frequency distribution function is the Normal or Gaussian distribution function (see Ref. 1).
X_i	i^{th} value in sample of population.
N	Sample size; number of specimens in sample.
μ	Population Mean; mean value for an entire population.
\bar{X}	Sample Mean; mean value for a sample of size N from an entire population

$$\bar{X} = \frac{1}{N} \sum_{i=1}^N X_i$$

σ Standard Deviation of entire population; a measure of dispersion; the root-mean-square of the deviations from the arithmetic mean of the population:

$$\sigma = \sqrt{\frac{\sum_{i=1}^N (X_i - \bar{X})^2}{N}}$$

STRUCTURAL ANALYSIS MANUAL
GENERAL DYNAMICS/CONVAIR AND SPACE SYSTEMS DIVISION

Data Source, CONVAIR (ASTRONAUTICS) DIVISION
GENERAL DYNAMICS CORPORATION

STRUCTURES TECHNICAL MEMORANDUM NO. 8

SUBJECT: Sigma, Sample Standard Deviation and Probability Levels

2.0 DEFINITIONS (Cont'd.)

- Sample Standard Deviation; a measure of dispersion; a special form of average deviation from the arithmetic mean of the sample; square root of the sample variance:

$$s = \sqrt{\frac{\sum_{i=1}^N (X_i - \bar{X})^2}{N - 1}}$$

- σ^2 Variance of entire population.

- s^2 Sample Variance; the best unbiased estimate of σ^2 :

$$s^2 = \frac{\sum_{i=1}^N (X_i - \bar{X})^2}{N - 1} = \frac{N \sum_{i=1}^N (X_i)^2 - (\sum_{i=1}^N X_i)^2}{N(N - 1)}$$

- k Tolerance Factor; a function of probability and confidence levels, sample size, distribution function, and whether single or two-tailed. Refer to Figures 4 through 7 for tolerance factors for the Normal Distribution with 95% confidence.

- "A" value That level which would be exceeded by at least 90% of the entire population with 95% confidence; i.e., the confidence is 95% that at least 90% of the entire population would exceed the "A" value; determined by $\bar{X} - ks$.

- "B" value That level which would be exceeded by at least 90% of the entire population with 95% confidence; i.e., the confidence is 95% that at least 90% of the entire population would exceed the "B" value; determined by $\bar{X} - ks$.

STRUCTURAL ANALYSIS MANUAL
GENERAL DYNAMICS/CONVAIR AND SPACE SYSTEMS DIVISION

Data Source, CONVAIR (ASTRONAUTICS) DIVISION
GENERAL DYNAMICS CORPORATION

STRUCTURES TECHNICAL MEMORANDUM NO. 8

SUBJECT: Signa, Sample Standard Deviation, and Probability Levels

3.0 DISCUSSION

Statistics and probability offer the engineer powerful tools to evaluate the variations in design parameters. Because statistical methods are techniques used to obtain, analyze, and present numerical data, their application to engineering problems is becoming increasingly frequent. Means of predicting rare occurrences or determining attributes of entire populations from the data of small randomly selected samples are of particular importance to Structures and Design Engineers.

Most manufactured articles are designed to function and to maintain their structural integrity while exposed to adverse environmental conditions. Design levels of load, strength, temperature, and other environment must be more severe than the expected average; e.g., one half of the production of manufactured articles designed to average levels would fail. Cost and importance of mission success require that the design of aerospace vehicles be at high levels of structural reliability. The use of statistics to establish design allowables, design loads, and to determine the probability of failure will aid in producing structures of more optimum design with predictable structural reliability.

Considerable confusion exists concerning the use of statistical terms such as σ , the standard deviation of an entire population and s , a sample standard deviation. In order to determine design probability levels, the practice of adding or subtracting $3s$ from a mean expected value has been used and the resulting value referred to as a " 3σ " value. It has sometimes been assumed that these procedures always result in 99.8% probability levels; however, this is not true since the sample size must be considered. For example, in loads determination when only a small random sample of data is available for single-tailed problems (defined later), the maximum expected load calculated by using the mean plus $3s$ will result in less than 99.8% probability. For the limiting case of an infinite sample size, $s = \sigma$ and a " 3σ " value would result in a 99.865% probability level.

For surface-to-surface missiles, Ref. 4 recommends¹ a 99.8% probability level for the determination of limit gust loads; i.e., the limit loads will not be exceeded more than two times in 1000. For single-tail determination of limit gust loads from a normal population, $\bar{X} + ks$ must be used where $6.2 > k > 2.9$ for $6 < N < \infty$ and k depends on the sample size of N , as can be seen in Figure 4. For more accurate determination of k , see Ref. 1.

¹The probability of exceedance for limit incremental gust response (load factor, bending moment, etc.), as stated in Ref. 4, shall be not greater than 0.002 for surface-to-surface missiles, 0.01 for surface-to-air missiles, and 0.02 for air launched missiles. For a particular vehicle, the structural design criteria for that vehicle specifies the applicable probability levels.

STRUCTURAL ANALYSIS MANUAL
GENERAL DYNAMICS/CONVAIR AND SPACE SYSTEMS DIVISION

SUBJECT: Sigma, Sample Standard Deviation, and Probability Levels

3.0 DISCUSSION (cont'd)

Table 1 shows probability levels for 1σ , 2σ , and 3σ values for single-tailed and two-tailed distribution problems. Single-tailed problems generally involve establishing, to some confidence level, a value above (or below) which a proportion (probability level) of the population would fall. Two-tailed problems generally involve establishing, to some confidence level, a range within which a proportion (probability level) of the population would fall. Refer to Figures 2 and 3.

TABLE 1

TYPE	RANGE	PROBABILITY THAT RANDOMLY SELECTED X_1 IS IN RANGE
Single-Tailed Problems	$-\infty$ to $\mu + \sigma$	84.13%
	$\mu - \sigma$ to $+\infty$	84.13%
	$-\infty$ to $\mu + 2\sigma$	97.73%
	$\mu - 2\sigma$ to $+\infty$	97.73%
Two-Tailed Problems	$-\infty$ to $\mu + 3\sigma$	99.865%
	$\mu - 3\sigma$ to $+\infty$	99.865%
	$\mu - \sigma$ to $\mu + \sigma$	68.26%
	$\mu - 2\sigma$ to $\mu + 2\sigma$	95.45%
	$\mu - 3\sigma$ to $\mu + 3\sigma$	99.73%

Notice that Table 1 is applicable only if the true population mean μ and standard deviation σ are known. If it is desired to obtain the same probability levels when only estimates (\bar{X} and s) of the true population mean and standard deviation are known, the range has to be increased by changing the tolerance factor k (k is a function of the sample size used to obtain \bar{X} and s as can be seen in Figures 5 and 7).

One of the most common and basic statistical analysis procedures is that of analyzing a sample of random data from an entire population to determine to some confidence level an expected limiting value (or range of values) corresponding to an acceptable probability level.

STRUCTURAL ANALYSIS MANUAL
GENERAL DYNAMICS/CONVAIR AND SPACE SYSTEMS DIVISION

SUBJECT: Sigma, Sample Standard Deviation, and Probability Levels

3.0 DISCUSSION (cont'd)

An example of particular interest to Structures personnel is that of determining an allowable strength from element tests of randomly selected specimens. Figure 1 shows a histogram of data which appear to be approximately normally distributed². Figure 2 shows the estimated normal distribution for the entire population from which the random sample was selected. \bar{X} and s may be computed from the data as shown in DEFINITIONS. It is generally desired to obtain "A" and/or "B" values (Ref. DEFINITIONS). In these cases, the one-sided tolerance factor k may be determined from a table as in Ref. 1 or from Figures 4 and 5 of this memorandum.

Convair-Astronautics Digital Computer Program Nos. 1944^{3,4} and 2104⁴ should be used for analyses to determine "A" (and "B") values from the data of random samples using one-sided tolerance factors; e.g., to be 95% confident that 99% (or 90%) of the data from the entire population will exceed the resulting "A" (or "B") values of $\bar{X} - ks$. Digital Computer Program No. 1944 may be used only for normal distributions; however, Program No. 2104 analyzes input data as normal, log-normal, square root-normal, and reciprocal-normal and prints out the "A" and "B" values for each distribution function. For further information on input and output from Programs 1944 and 2104, see Ref. 7.

For small sample sizes and/or for rapid estimates, Figures 4 and 5 may be used for the above type of calculations for the normal distribution; i.e., for single-tailed distribution problems where an upper or lower limit is to be established to 90% or 99% probability with 95% confidence.

Figures 6 and 7 are presented for two-tailed problems; e.g., the values $\bar{X} \pm ks$ are to be established to the 90% or 99% probability level with 95% confidence so that any value X_1 randomly selected from the population is such that

$$\bar{X} - ks < X_1 < \bar{X} + ks.$$

An additional application of Figures 4 and 5 would be their use as a method to aid in the selection of the optimum number of specimens for a test program where testing costs, vehicle weight savings, time, etc. must be considered. In general, Figures 4 and 5 present, for various probability levels, the relationship between sample size and tolerance factors. Figures 6 and 7 may be used to observe, for various sample sizes, the effect of tolerance factors on probability.

²A discussion of the Normal Distribution is presented in Ref. 1

³Ref. 6

⁴Ref. 7

STRUCTURAL ANALYSIS MANUAL
GENERAL DYNAMICS/CONVAIR AND SPACE SYSTEMS DIVISION

Data Source, CONVAIR (ASTRONAUTICS) DIVISION
GENERAL DYNAMICS CORPORATION

STRUCTURES TECHNICAL MEMORANDUM NO. 8

SUBJECT: Sigma, Sample Standard Deviation, and Probability Levels

4.0 SAMPLE PROBLEMS

4.1 Problem:

A randomly selected sample of 10 specimens (from various lots) of a particular material and condition were tested to failure and ultimate strengths recorded. Find the "A Value" of ultimate strength for the material and condition using these test results and assuming the population to be normal.

Solution Procedure:

Evaluate the sample mean \bar{X} and the sample standard deviation s as shown in Paragraph 2.0, DEFINITIONS. Enter Figure 4 for $N = 10$ and read $k = 3.98$ for 99% probability. Therefore, the "A Value" would be found from $\bar{X} - 3.98s$.

Comments:

The result is the best statistical estimate of the ultimate strength of this material and condition at 99% probability and 95% confidence levels, based on 10 randomly selected specimens. Notice that if 20 specimens had been tested the "A Value" would have been $\bar{X} - 3.28s$ (from Figure 4) and also that s for 20 samples would likely be smaller than s for 10 samples.

Figure 4 was used for the "A Value" because single-tailed tolerance factors were applicable; i.e., a single-tailed distribution as shown in Figure 2 was applicable since it was desired to establish a value, at 95% confidence, which would be exceeded by 99% of the population. Convair-Astronautics Digital Computer Programs Nos. 1944 or 2104 should be used for problems of this type when large samples are involved.

4.2 Problem:

A randomly selected sample of N specimens of sheet from various lots of steel purchased to a particular specification and as a particular nominal gage thickness was accurately measured and the individual thicknesses recorded. Based on this sample and the assumption that the population is normal, it is desired to determine 99% probability values for the expected extremes of thickness with 95% confidence for other sheets of the same nominal thickness and purchased to the same specification.

Solution:

Evaluate the sample mean \bar{X} and the sample standard deviation s as shown in Paragraph 2.0, DEFINITIONS. Enter Figure 6 with the sample size N and read from the 99% curve the value of k for $\bar{X} \pm ks$. The values of $\bar{X} \pm ks$ are the desired solution.

STRUCTURAL ANALYSIS MANUAL
GENERAL DYNAMICS/CONVAIR AND SPACE SYSTEMS DIVISION

SUBJECT: Sigma, Sample Standard Deviation, and Probability Levels

4.0 SAMPLE PROBLEMS (Cont'd)

4.2 Comments:

The solution represents the extreme values of the desired range; i.e., there is 95% confidence that at least 99% of measured values would lie within this range for material purchased as the same gage and to the same specification. This solution is an example of a two-tail problem as in Figure 3 and uses two-tailed tolerance factors as shown in Figure 5.

4.3 Problem:

A random sample of 6 specimens were selected from a normal population. What would be the probability level at 95% confidence for a "3s" value if single-tailed tolerance limits are applicable?

Solution:

Referring to Figure 5, for $N = 6$ and $\bar{X} + 3s$ or $\bar{X} - 3s$, the probability is 90%.

Discussion:

The result indicates that the 3s value (often erroneously referred to as a "3σ" value) for a sample size of 6 corresponds closely to the "B" value. Notice from Figure 5 that for $N = 6$, a 5.1s value would be required to establish an "A" value.

STRUCTURAL ANALYSIS MANUAL
GENERAL DYNAMICS/CONVAIR AND SPACE SYSTEMS DIVISION

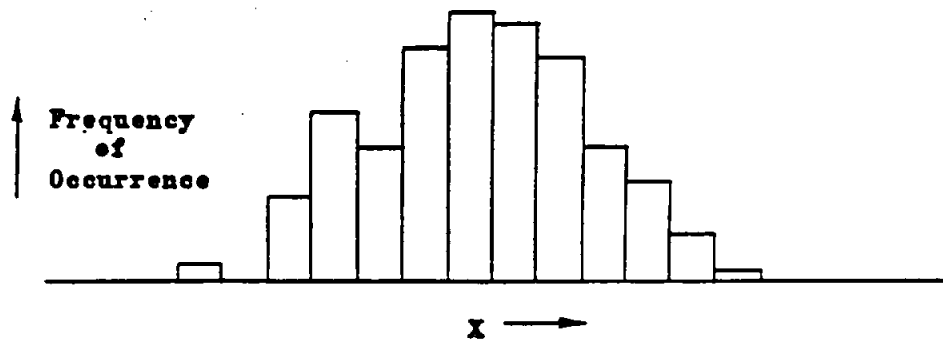


Figure 1: Histogram of Randomly Selected Sample Data

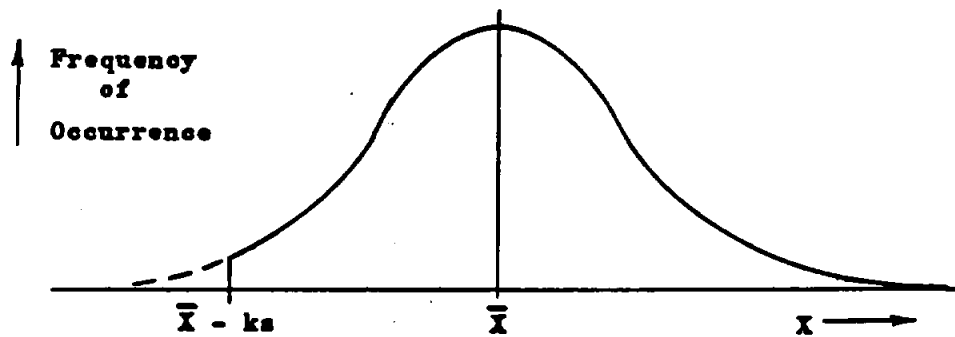


Figure 2: Estimated Normal Distribution for Population (Single-Tailed)

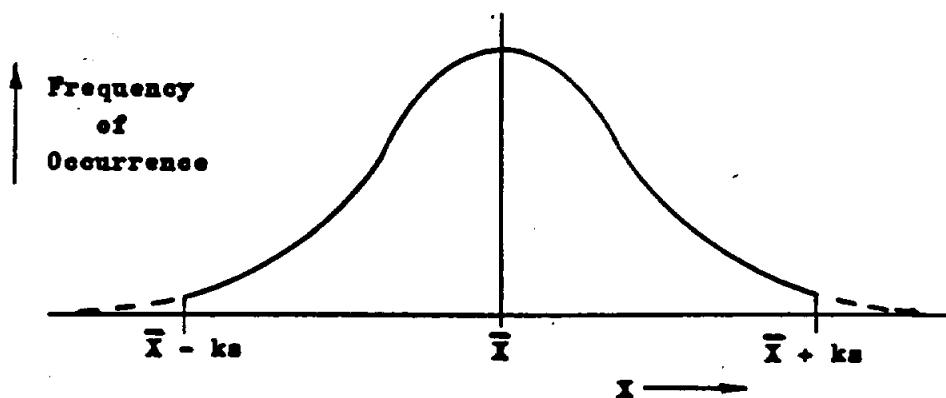
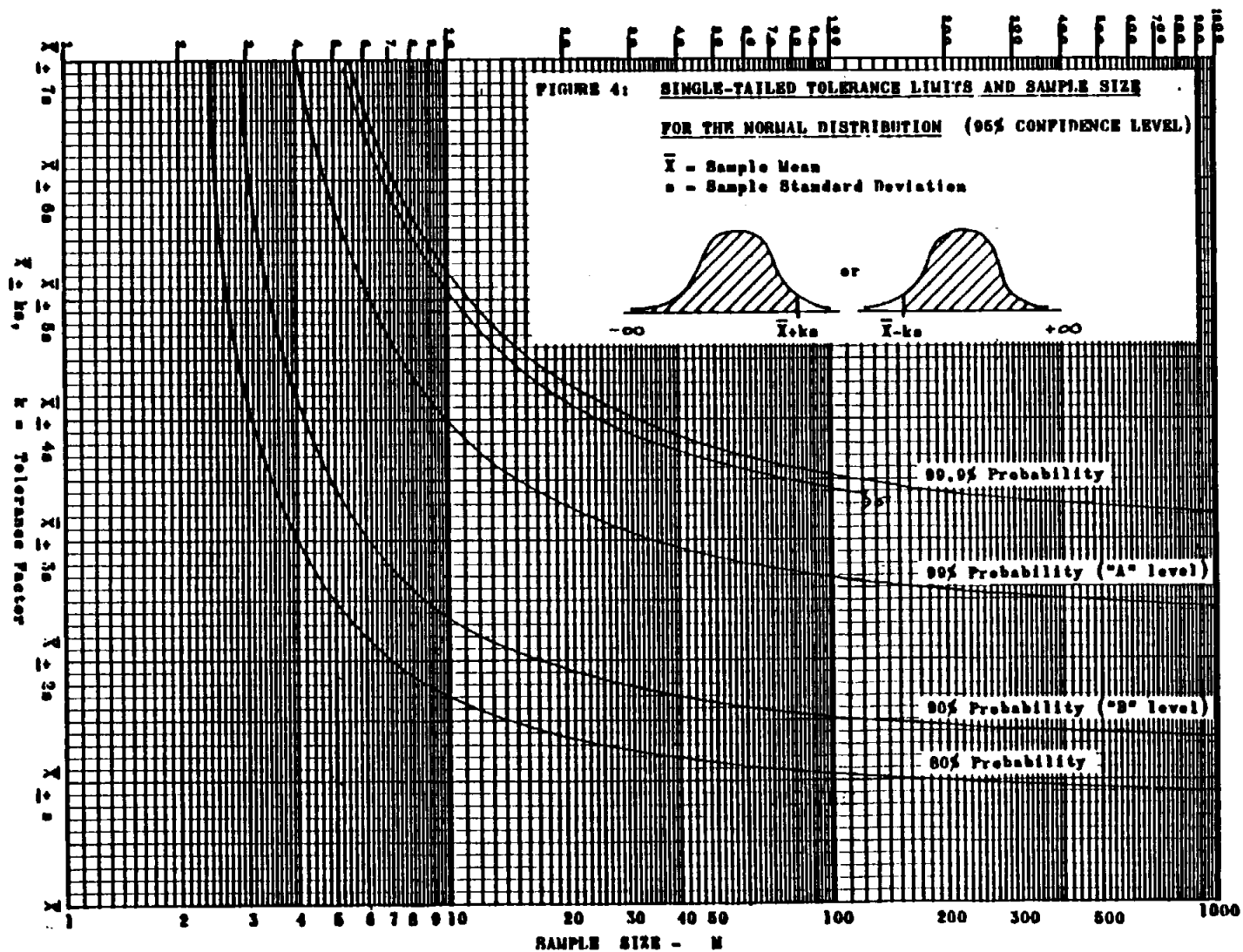
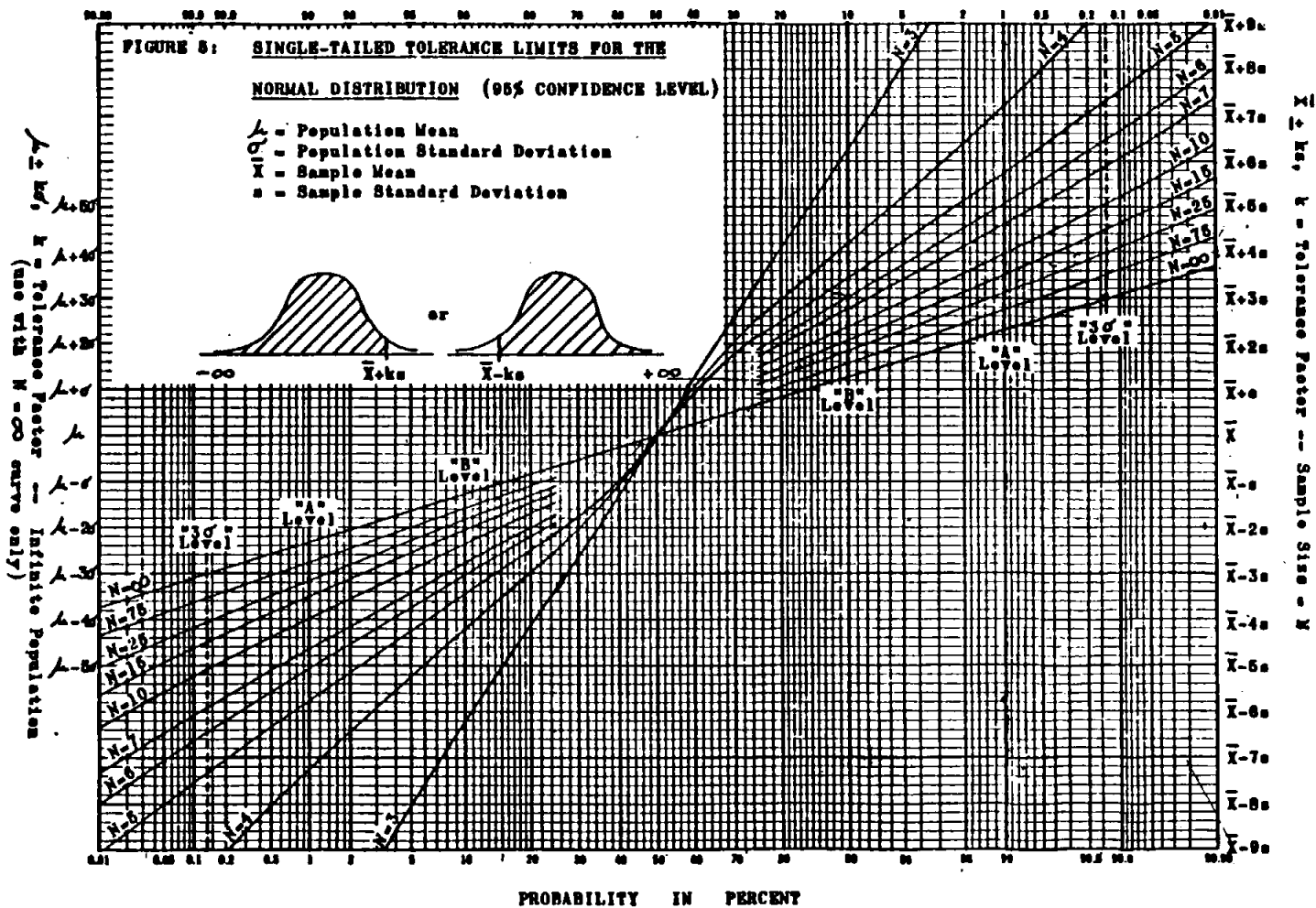
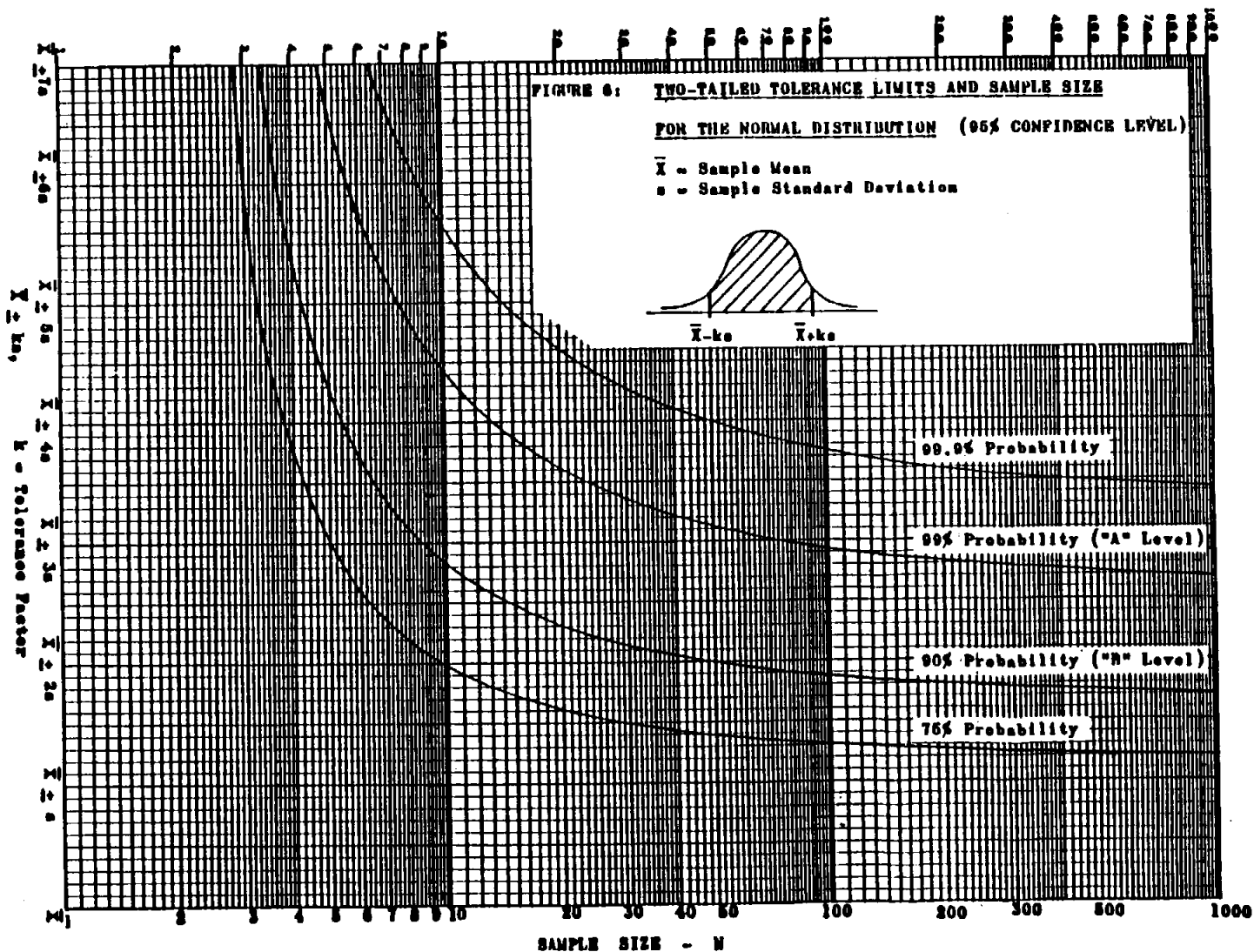
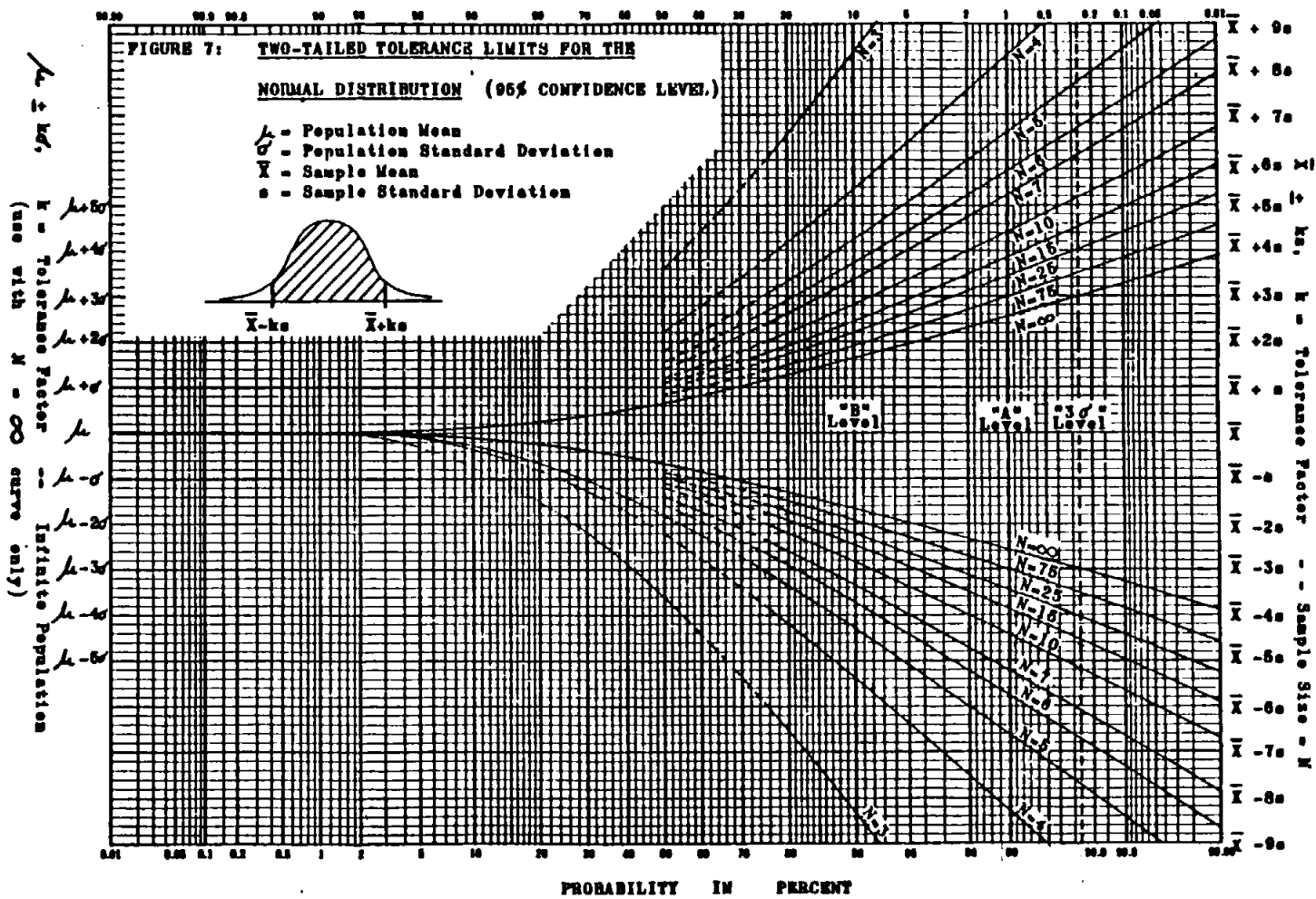


Figure 3: Estimated Normal Distribution for Population (Two-Tailed)









STRUCTURAL ANALYSIS MANUAL
GENERAL DYNAMICS/CONVAIR AND SPACE SYSTEMS DIVISION

SUBJECT: Sigmas, Sample Standard Deviation, and Probability Levels

REFERENCES

1. Schumacher, J. G., "Statistical Determination of Strength Properties," Convair-Astronautics Report AZS-27-274, 11 November 1958, revised 29 December 1959, 37p.
2. Arkin, H., and Colton, R. R., "Tables for Statisticians," Barnes and Noble, Inc., N.Y., 1950, 152p.
3. Schumacher, J. G., and McClure, E. E., "Survey of Structural Safety," Convair-Astronautics Report AZS-009, 4 September 1959, 37p.
4. MIL-M-8856, "Military Specification -- Missiles, Guided: Strength and Rigidity Requirements," 22 June 1959, 9p.
5. Bowker, Albert H., "Tolerance Limits for Normal Distributions," Techniques of Statistical Analysis, edited by Eisenhart, Hastay, and Wallis, McGraw-Hill, N.Y., 1947, Chapter 2.
6. McClure, E. E., "Digital Computer Programs and Subroutines with Structural Applications," Convair-Astronautics Structures Technical Memorandum No. 7, 20 February 1960, 17p.
7. Dittos, F. A., "Statistical Determination of Strength Properties by Digital Computer (Program Nos. 1944 and 2104)," Convair-Astronautics Report AZS-011, (in work).

STRUCTURAL ANALYSIS MANUAL
GENERAL DYNAMICS/CONVAIR AND SPACE SYSTEMS DIVISION

SECTION 20.5

TABLES OF STATISTICAL VALUES

REFERENCE

MIL-HDBK-5C, SECTION 9.6.4 "MILITARY STANDARDIZATION
HANDBOOK METALLIC MATERIALS AND ELEMENTS FOR AEROSPACE
VEHICLE STRUCTURES." 15 SEPTEMBER 1976



STRUCTURAL ANALYSIS MANUAL
GENERAL DYNAMICS/CONVAIR AND SPACE SYSTEMS DIVISION

SECTION 21.0

MECHANISMS

ANALYSIS METHODS FOR SOME COMMONLY USED MECHANISMS
ARE PRESENTED IN THIS SECTION.

	PAGE
21.1 BEARINGS	21.1.1
21.2 GEARS	21.2.1
21.3 ACTUATORS	21.3.1

STRUCTURAL ANALYSIS MANUAL
GENERAL DYNAMICS/CONVAIR AND SPACE SYSTEMS DIVISION

Data Source, Section 1.3 Reference 6

SUBJECT: Anti-Friction Bearing Design Data

- REFERENCES:
1. Military Specification MIL-B-7949
 2. Military Specification MIL-B-6038
 3. Handbook of Instructions for Aircraft Designers, AFDCM 80-1
 4. Pafnir Engineering Data Sheets
 5. Shafer Aircraft Roller Bearing Catalog No. 59120

INTRODUCTION :

The minimum design requirement for bearings is that static design yield load shall not exceed the yield load rating of the bearing, where

$$\text{Design Yield Load} = \begin{matrix} 1.00 \text{ limit load (AF and FAA)} \\ 1.15 \text{ limit load (Navy)} \end{matrix}$$

For an ultimate factor of safety of 1.5 or less the ultimate load is not critical.

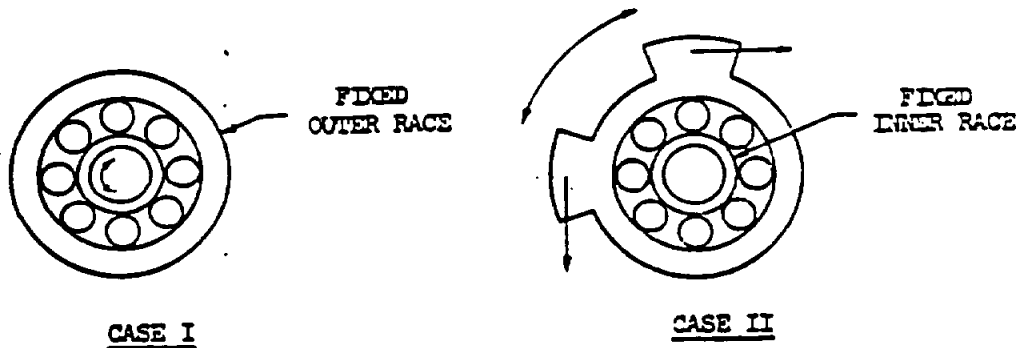
I. BALL BEARINGS

A. General

Radial and thrust yield load ratings, and yield moment ratings for AN ball bearings are given in Table I, for extra wide, double row, ball bearings in Table II, and for torque tube type ball bearings the ratings are given in Table III.

Tables I, II, and III also give the radial ratings of the bearings for an average life of 10,000 complete cycles of 90° oscillation. Two cases of load application are covered, namely

- Case I - Load fixed with respect to the outer race.
Case II - Load fixed with respect to the inner race.



STRUCTURAL ANALYSIS MANUAL
GENERAL DYNAMICS/CONVAIR AND SPACE SYSTEMS DIVISION

BALL BEARINGS (Contd.)

B. Bearing Selection

1. Static Considerations

For most applications it is sufficient to select the bearing on the basis of static allowables using the design yield load as a criterion.

For example, a bearing on a Navy airplane is required to support a limit radial load of 3000#

$$\text{Yield Load} = 1.15 \times 3000 = 3450\#$$

From Table I, either AN200 KP5 or AN201 KP8A would be satisfactory.

2. Life Considerations

In certain cases where there are frequent applications of significant loads and the bearing is subjected to oscillations, it is advisable to select the bearing on the basis of life as well as static considerations. It should be noted the life allowables given below are based on 90° oscillations and are conservative for oscillations of a smaller magnitude.

- a. If a single radial load is selected as the basis for determining life, the average number of allowable cycles is determined from Figure 1, where

$$\text{Life Factor} = \frac{\text{Applied Cyclic Load}}{10,000 \text{ Cycle Load Rating from Tables}}$$

The applied cyclic load should never be higher than limit load.

Taking for example the conditions used in the static analysis with an additional requirement that the bearing be capable of 400,000 cycles under 50% of radial limit load with the load fixed with respect to the outer race. This makes Case I load rating applicable. (per I-A).

Checking the AN201 KP8A bearing which meets the static requirement:

$$50\% \text{ of Limit Load} = .5 \times 3000 = 1500\#$$

$$\text{Life Factor} = \frac{1500}{2670} = .5225$$

From Figure 1, Life = 100,000 cycles

Thus this bearing which meets the static requirement is not satisfactory from the life standpoint.

Checking the AN200 KP5 bearing which also has been shown to meet the static requirement:

$$\text{Life Factor} = \frac{1500}{4900} = .306$$

From Figure 1, Life = 700,000 cycles

Thus this bearing is satisfactory from the standpoint of both the static and life considerations.

STRUCTURAL ANALYSIS MANUAL
GENERAL DYNAMICS/CONVAIR AND SPACE SYSTEMS DIVISION

I. BALL BEARINGS (Contd.)

B. Bearing Selection (Contd.)

2. Life Considerations (Contd.)

- b. In cases where a single load level will not suffice for estimating service conditions, some load spectrum must be determined. From this load spectrum it is possible to determine an equivalent load to be used in selecting a bearing to satisfy design requirements. The equivalent load may be obtained from the following relation:

$$P_e = \left[\sum K_i (P_i)^{3.6} \right]^{\frac{1}{3.6}}$$

P_e = Equivalent load, pounds

P_i = Applied load, pounds

K_i = Proportion of cycles that P_i is applied

The following example illustrates the method of bearing analysis and selection for a given spectrum loading.

A bearing on a Navy airplane is required to support radial limit load of 2000# and withstand 60,000 cycles of oscillations with the following spectrum: 400# for 70% of cycles, 1000# for 25% of cycles, and 1800# for 5% of cycles with the loads fixed with respect to the inner race. This makes Case II applicable.

$$\text{Yield Load} = 1.15 \times 2000 = 2300\#$$

Thus AN201 KP6A bearing with a design yield allowable of 2500 is satisfactory statically.

$$P_e = \left[.70(400)^{3.6} + .25(1000)^{3.6} + .05(1800)^{3.6} \right]^{\frac{1}{3.6}} = 902\#$$

$$\text{Life Factor} = \frac{902}{1710} = .528$$

From Figure 1, Life = 100,000 cycles

This makes the AN201 KP6A bearing satisfactory.

$$M.S. = \frac{2500}{2300} - 1.0 = +.09$$

STRUCTURAL ANALYSIS MANUAL
GENERAL DYNAMICS/CONVAIR AND SPACE SYSTEMS DIVISION

BALL BEARINGS (Contd.)

C. Combined Loadings - Static

When ball bearings are subjected to any combination of radial, thrust, and moment loads the margin of safety shall be determined from the following formula:

$$M.S. = \frac{1}{\frac{P_R}{P_R} + \frac{P_a}{P_a} + \frac{M}{M}} - 1 \quad \text{where}$$

P_R, P_a, M = the applied design yield radial, thrust and moment loads respectively.

P_R, P_a, M = the static design yield radial, thrust and moment allowables respectively.

II. NEEDLE AND ROLLER BEARINGS

Static design yield radial allowables for NAS 505 needle bearings are given in Table IV. Static design yield radial and thrust allowables and radial load ratings for an average life of 10,000 complete 90° cycles for self-aligning roller bearings are given in Table V.

For needle bearings and roller bearings not listed in Tables IV or V, the allowable loads specified by a reliable manufacturer will be acceptable.

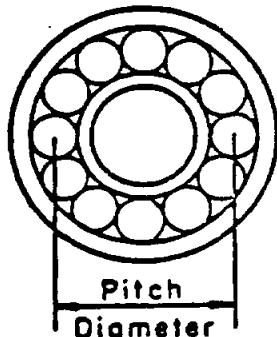
The considerations governing the selection of ball bearings, as discussed in Section I-B of this memo, are equally applicable to the selection of needle and roller bearings.

Needle bearings, in general, cannot transmit thrust or moment loads.

Roller bearings, unless of a special type, cannot transmit thrust but are capable of transmitting moment loads. A conservative method of analysis for a roller bearing transmitting moment is as follows.

STRUCTURAL ANALYSIS MANUAL
GENERAL DYNAMICS/CONVAIR AND SPACE SYSTEMS DIVISION

II. NEEDLE AND ROLLER BEARINGS (Contd.)



$$\text{Bearing Stress} = \frac{P_r}{A} + \frac{MY}{I}$$

Where:

P_r = Design yield radial load

m = Design yield moment

A = Pitch Diameter x Roller Length

$$\text{Pitch Diameter} = \frac{\text{Bore} + \text{O.D.}}{2}$$

y = 1/2 of roller length

I = 1/12 of Pitch Diameter x (Roller Length)

$$\text{Allowable bearing stress} = \frac{\text{Design Yield Radial Allowable}}{\text{Pitch Diameter x Roller Length}}$$

III. BEARINGS USED AS ROLLERS ON TRACKS AND CAM FOLLOWERS

When a bearing is used as a roller on a track, high localized stresses occur in the outer race due to the bending imposed on this race. The bending will overload the balls, needles, or rollers adjacent to the point of contact and relieve those further away. As a result the load that a bearing can maintain under this type of loading is considerably less than its static design yield radial allowable load.

The following allowable yield loads shall be used for bearings being used as rollers:

- A. Bearings listed in Tables I, II, and III - Generally not recommended for this application - 5.5% of the design yield radial allowable specified in Tables.
- B. Bearing specially designed with thickened outer races - allowable given in Table VI.
- C. Cam follower, needle bearing - allowables given in Table VII.

For the allowable loads of tracks see p 21.1.11

STRUCTURAL ANALYSIS MANUAL
GENERAL DYNAMICS/CONVAIR AND SPACE SYSTEMS DIVISION

TABLE I
"AN" BALL BEARINGS

Part Number	Static Design Yield Allowables			Radial Load Rating - lbs. For Average Life of 10,000 Complete 90° Cycles	
	Radial lbs.	Thrust lbs.	Moment in.-lbs.	Case I	Case II
AN 200 K3L	1560	700	58	1520	1260
KP3	1880	900	89	1700	1450
KPL	2680	1200	136	2410	2030
KP5	5620	2500	370	4900	3970
KP6	7910	3500	644	6540	5410
KP8	11800	5200	1170	9320	7700
KPL0	14100	6200	1520	11000	9060
AN 200 KS3L	550	100	Not Applicable	550	480
KS3	900	200		900	770
KSL	1410	300		1410	1200
KS5	2190	300		2190	1890
KS6	2980	400		2980	2580
KS8	3670	500		3670	3290
KSL0	5320	600		4980	4360
AN 201 KF3A	1560	700	50	1500	1250
KPLA	1880	900	89	1690	1450
KP5A	2190	1000	114	1820	1600
KP6A	2500	1100	143	1920	1710
KP8A	3910	1700	277	2870	2550
KPL0A	6700	3000	598	4980	4360
KP12A	8790	3900	945	5980	5320
KP16A	11900	5200	1600	7070	6100
KP20A	13800	6100	2170	7400	6810
AN 202 KP21B	9840	4400	1480	4590	4290
KP23B	10500	4700	1700	4650	4360
KP25B	11300	5000	1930	4680	4420
KP29B	12700	5600	2420	4760	4530
KP33B	14400	6400	3150	4820	4630
KP37B	15800	7000	3780	4880	4690
KPL7B	24700	10900	6880	6600	6390
KPL9B	27500	12100	8520	8150	7840
AN 206 DSP3	1420	200	Not Applicable	1420	1220
DSP4	1780	300		1780	1600
DSP5	3740	600		3740	3300
DSP6	5100	800		4980	4370
DSP8	7120	1000		6340	5570
DSP10	9000	1300		7780	6860

STRUCTURAL ANALYSIS MANUAL

GENERAL DYNAMICS/CONVAIR AND SPACE SYSTEMS DIVISION

TABLE I (Contd.)

"AN" BALL BEARINGS

Part Number	Static Design Yield Allowables			Radial Load Rating - lbs. For Average Life of 10,000 Complete 90° Cycles	
	Radial lbs.	Thrust lbs.	Moment in.-lbs.	Case I	Case II
AN 207 DPF3	2950(1)	1700	38	2950	2830
DPF4	5370(2)	1800	91	3550	3020
DPF5	11000(1)	4000	56	7360	6250
DPF6	15760(1)	5300	278	9690	8120
DPF8	23600(2)	7800	590	14100	11600
DPF10	28400	9400	1600	15300	13100
AN 218 P4	2770	700	414	2090	1800
P5	3280	900	551	2440	2090

1. Bolts of 180,000 psi tensile strength are required to develop the radial load shown.
2. Bolts of 160,000 psi tensile strength are required to develop the radial load shown.

TABLE II

EXTRA WIDE, DOUBLE ROW. BALL BEARINGS

Part Number (Pafnir)	Static Design Yield Allowables			Radial Load Ratings - lbs. For Average Life of 10,000 Complete 90° Cycles	
	Radial lbs.	Thrust lbs.	Moment in.-lbs.	Case I	Case II
DW4K2	1400	500	129	1050	960
DW4K	2770	900	392	2070	1850
DW5	5140	1600	882	2600	2320
DW6	8440	2600	2010	4220	3740
DW8	15520	4700	4860	7610	6520

TABLE III

TORQUE TUBE TYPE BALL BEARINGS

Part Number (Pafnir)	Static Design Yield Allowables			Radial Load Rating - lbs. For Average Life of 10,000 Complete 90° Cycles	
	Radial lbs.	Thrust lbs.	Moment in.-lbs.	Case I	Case II
B538DD	3280	1500	255	1990	1820
B539DD	3750	1700	329	2050	1900
B540DD	4220	1900	414	2110	1970
B541DD	5000	2200	567	2170	2020
B542DD	5950	2700	825	2220	2130
B543DD	6880	3200	1130	2260	2180
B544DD	7980	3600	1470	2300	2220
B545DD	9220	4000	1890	2340	2260
B546DD	10150	4400	2290	2360	2280
KP16BS	8035	1600	Not Applicable	4260	3960
KP21BS	9840	2000		4590	4290
KP23BS	10500	2200		4650	4360
KP25BS	11300	2300		4680	4420
KP29BS	12700	2600		4760	4530
KP33BS	14400	2900		4820	4630
KP37BS	15300	3200		4880	4690
KP47BS	24700	5000		6600	6390
KP49BS	27500	5500		8150	7840

STRUCTURAL ANALYSIS MANUAL
GENERAL DYNAMICS/CONVAIR AND SPACE SYSTEMS DIVISION

TABLE IV

NAS 505 NEEDLE BEARINGS
STATIC DESIGN YIELD ALLOWABLES

Part Number	Radial lbs.	Part Number	Radial lbs.	Part Number	Radial lbs.
NAS 505-3	2700	NAS 505-12	35800	NAS 505-10	104100
-4	4300	-14	45800	-14	113500
-5	6100	-16	50900	-18	123000
-6	9500	-20	56800	-52	132500
-7	12000	-24	66300	-56	145100
-8	17400	-28	75700	-60	154500
-9	22500	-32	85200	-64	164000
-10	28300	-36	94600		

TABLE V

SELF-ALIGNING ROLLER BEARINGS

	Part Number	Static Design Yield Allowables		Radial Load Rating - lbs. For Average Life of 10,000 Complete 90° Cycles
		Radial lbs.	Thrust lbs.	Case I & Case II
Fafnir	GDSRP4	3025	908	2500
	GDSRP5	7350	2200	6000
	GDSRP6	9600	2880	8000
	GDSRP8	12500	3750	10100
	GDSRP10	17700	5310	14800
	GDSRP12	26900	8070	22000
Shafer	ER-4	3140	1660	2600
	ER-5	7350	4300	6100
	ER-6	10100	5800	8500
	ER-8	12800	6400	10900
	ER-10	18600	9300	15500
	ER-12	28800	16700	25000

STRUCTURAL ANALYSIS MANUAL
GENERAL DYNAMICS/CONVAIR AND SPACE SYSTEMS DIVISION

TABLE VI

DESIGN YIELD ALLOWABLES OF BEARINGS USED AS TRACK ROLLERS

Part No.	Radial	Part No. (FAFNR)	Radial lbs.
NAS 502 - 3	900	K3L2	200
- 4	1430	K3L3	200
- 6	2700	KP3AR11-2	300
- 8	4300	K3LPL8	200
- 10	6400	KP4RL6	400
- 12	10700	KP4RL6-2	500
- 14	13700	D7R6-2	1000
NAS 503 - 6	5370	D7R6-3	2000
- 8	9370	K8ARL	500
- 10	15000	DP8A3	1000
- 12	21400	DP8AL	1800
- 14	28900		

TABLE VII

DESIGN YIELD ALLOWABLES FOR CAM FOLLOWERS

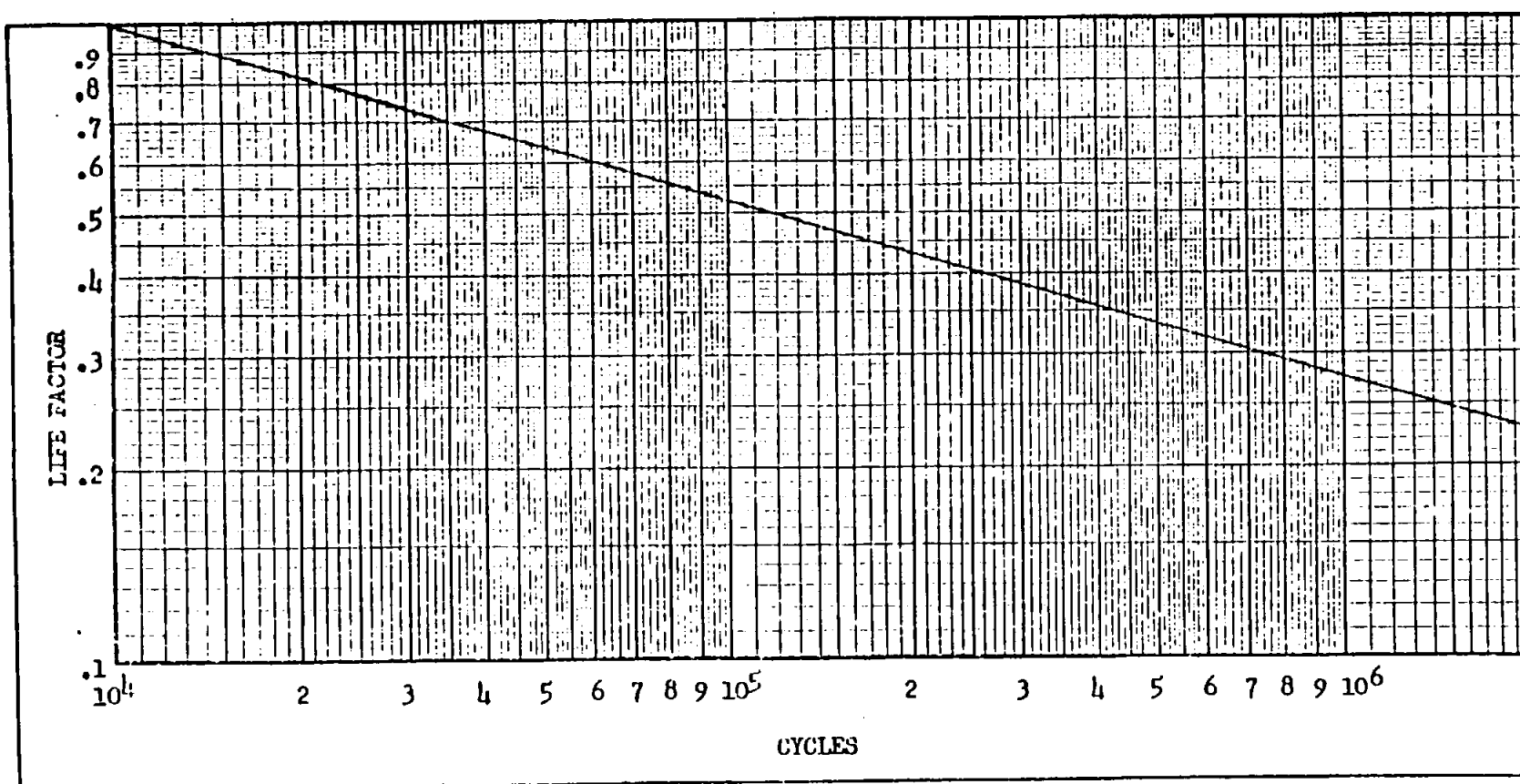
Part No.	Radial
NAS 562 - 3	395
- 4	470
- 5	630
- 6	1275
- 7	1840
- 8	2740

NOTES FOR TABLES VI AND VII

1. Ratings for NAS502 and NAS503 Bearings in Table VI and for NAS562 Cam Followers in Table VII are based on an average life of 100,000 revolutions.
2. For track allowable loads see p. 21.1.11

FIGURE 1

AVERAGE LIFE - COMPLETE 90° OSCILLATORY CYCLES



STRUCTURAL ANALYSIS MANUAL
GENERAL DYNAMICS/CONVAIR AND SPACE SYSTEMS DIVISION

Data Source, Section 1.3 Reference 6

SUBJECT: Allowable Bearing Load - Roller on Track

Introduction

The problem of analyzing the strength of a roller on a track can be resolved into two parts: (1) the surface strength of the track, and (2) the strength of the roller. In par. (1) of this memo are contained formulae for calculating the surface strength of the track. These allowable loads will produce a slight amount of brinelling of the surface of the track. As the roller goes over the track, however, the surface work-hardens and the amount of brinelling diminishes.

1. Allowable Load on Track

The allowable yield load for a steel roller on a steel track is given by the equation

$$P_{ST} = 0.77 \times 10^{-6} (F_{tu})^2 WR$$

and for a steel roller on an aluminum track by the equation

$$P_{AL} = 1.43 \times 10^{-6} (F_{tu})^2 WR$$

Where:

F_{tu} = Ultimate tensile strength of track material (psi)

W = Projected width of roller in contact with track (inches)

R = Radius of roller (inches)

The ultimate allowable is obtained from the above by multiplying by 1.5

2. Allowable Load on Roller

In the cases where the roller is a bearing, the allowable load may be obtained from p 21.1.1 - 21.1.10

STRUCTURAL ANALYSIS MANUAL
GENERAL DYNAMICS/CONVAIR AND SPACE SYSTEMS DIVISION

Data Source, Section 1.3 Reference 2

STRENGTH OF GEARS

SPUR GEARS

Lewis' equation (allowable tooth load):

$$F_a = \frac{S_b Y}{P_d}$$

Where F_a = allowable tooth load in lbs.

s = allowable stress in psi.

b = tooth width in inches

Y = Lewis Factor (see table page 21.2.5)

P_d = Diametral pitch in inches⁻¹

= $\frac{\text{number of teeth in gear}}{\text{pitch diameter}}$

Gear Tooth Load (P_t)

$$P_t = \frac{T}{\frac{PD}{2}} = \frac{2T}{PD}$$

Where PD = pitch diameter of gear in inches

T = torque transmitted by gear in inch-pounds

The Lewis equation for computing an allowable gear tooth load is intended to cover gears under continuous operation and is conservative for the following reasons:

- 1) It assumes only one gear tooth is transmitting the gear load.
- 2) It assumes an arbitrary point at which the gear tooth load is applied - this point is conservative for a tooth in full mesh.
- 3) The method uses low allowable stresses (approx. 1/3 of the material ultimate stress).

Consequently gears designed by the Lewis formula and static tested have been known to take up to approximately 28 times the calculated load before tooth failure occurs. (Vultee Report 275 test #39).

It is evident that Lewis Equation should be modified to cover air frame gears, the majority of which are under intermittent operation, low pitch line velocities, and very seldom operate at limit load.

STRUCTURAL ANALYSIS MANUAL
GENERAL DYNAMICS/CONVAIR AND SPACE SYSTEMS DIVISION

STRENGTH OF GEARS - (Continued)

SPUR GEARS (Cont.)

The Lewis Equation is modified in the following manner to make it more applicable for air frame spur gears:

$$F_a = \frac{K S b Y}{P_d}$$

$K = 3^*$ for Vital gears of intermittent operation at low pitch line velocities

$S =$ Ultimate Tension stress of gear material (p.s.i.)

$b =$ tooth width (inches)

$Y =$ Lewis factor (page 21.2.5)

$P_d =$ Diametral pitch

Vital gears are defined as those whose failure would immediately prevent the safe flight or landing of the airplane.

* See page (21.2.3) for discussion of these factors.

BEVEL GEARS

The Lewis Equation for bevel gears $F_a = \frac{S_o Y b}{P_d} \times (1 - \frac{b}{L})$ is modified in the same manner as the equation for spur gears

$$F_a = \frac{K S b Y}{P_d} (1 - \frac{b}{L})$$

Where $K = 3^*$ for vital gears of intermittent operation at low pitch line velocities.

$K = 5^*$ for non-vital gears of intermittent operation at low pitch line velocities.

$S =$ Ultimate tension stress of gear material p.s.i.

STRUCTURAL ANALYSIS MANUAL
GENERAL DYNAMICS/CONVAIR AND SPACE SYSTEMS DIVISION

STRENGTH OF GEARS - (Continued)

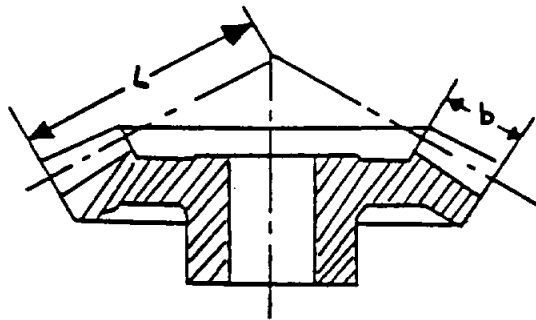
BEVEL GEARS (CONT.)

b = Tooth width (Inches)

Y = Lewis factor (Table pg. 21.2.5)

P_d = Diametral Pitch

L = Length of pitch cone element



Vital gears are those whose failure would immediately prevent the safe flight or landing of the airplane.

* See page (21.2.4) for discussion on these factors.

WORM GEARS

The teeth of a worm gear are weaker than the threads on the worm and should be checked by the Lewis equation for Spur Gears (21.2.1) However, more teeth are probably in contact in the worm gears than in spur gears, which makes this method conservative for checking worm gears. Allowance may be made for this conservativeness by distributing the load over the number of teeth in contact. The number of teeth in contact can be found by dividing the angle of action of the gear by the pitch angle.

SUMMARY

The following precautions should be taken when using the factors ($K = 3$ and $K = 5$) to determine gear teeth size.

STRUCTURAL ANALYSIS MANUAL
GENERAL DYNAMICS/CONVAIR AND SPACE SYSTEMS DIVISION

STRENGTH OF GEARS - Continued)

SUMMARY (Cont.)

- 1) The gear should be one which operates intermittently and at low speeds, preferably a gear which does not operate at its full limit load the majority of the time such as tab system gears, landing gear retracting gears, etc.
- 2) The gear shafts should be supported by rather rigid supports - flexible supports may cause the gear teeth faces to be loaded eccentrically thus leading to possible gear tooth failure.
- 3) A reasonably rigid gear shaft should be used - gear shaft deflection induces improper meshing of gear teeth
- 4) Close installation tolerances are important for proper operation and long gear life.

Gears under heavy continuous loads require the addition of wear and velocity factors to the Lewis Equation. No attempt is made here to cover the design of these gears as it is felt that they represent a small percentage of air frame gears. A expert should be consulted for the design of this type of gear.

STRUCTURAL ANALYSIS MANUAL
GENERAL DYNAMICS/CONVAIR AND SPACE SYSTEMS DIVISION

VALUES OF Y IN LEWIS' FORMULA											
Number of Teeth	Full Depth 14 1/2 and Cycloidal	Full Depth 20°	Stub Teeth 20°	Follows Stub Teeth, 20							
				$\frac{4}{5}$	$\frac{5}{7}$	$\frac{6}{8}$	$\frac{7}{9}$	$\frac{8}{10}$	$\frac{9}{11}$	$\frac{10}{12}$	$\frac{12}{14}$
10	0.178	0.201	0.261								
11	0.192	0.226	0.289								
12	0.21	0.245	0.311	0.302	0.348	0.32	0.314	0.302	0.314	0.292	0.289
13	0.223	0.264	0.324	0.318	0.361	0.336	0.332	0.317	0.327	0.308	0.302
14	0.235	0.276	0.339	0.33	0.374	0.352	0.348	0.332	0.339	0.32	0.314
15	0.245	0.289	0.349	0.339	0.386	0.364	0.361	0.346	0.348	0.33	0.324
16	0.255	0.295	0.36	0.348	0.396	0.374	0.37	0.355	0.354	0.34	0.333
17	0.264	0.302	0.368	0.358	0.485	0.383	0.38	0.364	0.366	0.349	0.342
18	0.27	0.308	0.377	0.368	0.411	0.39	0.39	0.374	0.374	0.358	0.349
19	0.277	0.314	0.386	0.374	0.414	0.398	0.398	0.383	0.38	0.364	0.355
20	0.283	0.32	0.393	0.38	0.425	0.405	0.405	0.39	0.386	0.371	0.361
21	0.289	0.326	0.399	0.386	0.431	0.411	0.411	0.396	0.392	0.377	0.366
22	0.292	0.33	0.404	0.391	0.436	0.417	0.417	0.402	0.397	0.382	0.371
23	0.296	0.333	0.408	0.396	0.441	0.422	0.422	0.407	0.402	0.387	0.377
24	0.302	0.337	0.411	0.401	0.446	0.427	0.427	0.411	0.405	0.392	0.381
25	0.305	0.34	0.416	0.405	0.449	0.432	0.432	0.417	0.409	0.396	0.386
26	0.308	0.344	0.421	0.409	0.455	0.436	0.436	0.421	0.413	0.401	0.389
28	0.314	0.352	0.43	0.417	0.461	0.443	0.444	0.427	0.421	0.409	0.396
30	0.318	0.358	0.437	0.425	0.468	0.449	0.452	0.433	0.438	0.415	0.402
35	0.327	0.373	0.449	0.436	0.48	0.463	0.465	0.449	0.458	0.427	0.415
40	0.336	0.389	0.459	0.446	0.49	0.475	0.474	0.458	0.446	0.44	0.425
45	0.34	0.399	0.468	0.455	0.5	0.484	0.484	0.464	0.455	0.446	0.433
50	0.346	0.408	0.474	0.461	0.506	0.49	0.49	0.471	0.461	0.452	0.439
60	0.355	0.421	0.484	0.471	0.515	0.5	0.5	0.483	0.471	0.465	0.449
70	0.36	0.429	0.493	0.48	0.521	0.506	0.506	0.49	0.477	0.471	0.465
80	0.363	0.436	0.499	0.488	0.528	0.512	0.512	0.496	0.483	0.477	0.461
90	0.366	0.442	0.503	0.492	0.532	0.517	0.516	0.499	0.487	0.481	0.466
100	0.368	0.446	0.506	0.496	0.536	0.521	0.521	0.503	0.49	0.484	0.471
150	0.375	0.468	0.518	0.509	0.546	0.534	0.531	0.515	0.503	0.496	0.484
200	0.378	0.453	0.524	0.515	0.553	0.54	0.536	0.521	0.509	0.503	0.49
Rack	0.39	0.484	0.55	0.543	0.578	0.562	0.553	0.54	0.534	0.528	0.521

* Fractional designation for the pitch of the gear. The numerator of this designation is the actual pitch of the gear, whereas the denominator indicates the pitch of the cutter used in cutting the teeth and this determines their depth.

STRUCTURAL ANALYSIS MANUAL **GENERAL DYNAMICS/CONVAIR AND SPACE SYSTEMS DIVISION**

Data Source, Section 1.3 Reference 4

ACTUATORS

31.3 FRICTION EFFECTS OF SLIDING PARTS IN ACTUATORS

A friction force will oppose the movement of one surface relative to the surface with which it is in contact.

This force is exerted tangentially to the surfaces and opposite to the direction of motion. The effects of friction, including the flexibility effects of the mechanism, are graphically illustrated in Fig. 31.3-1.

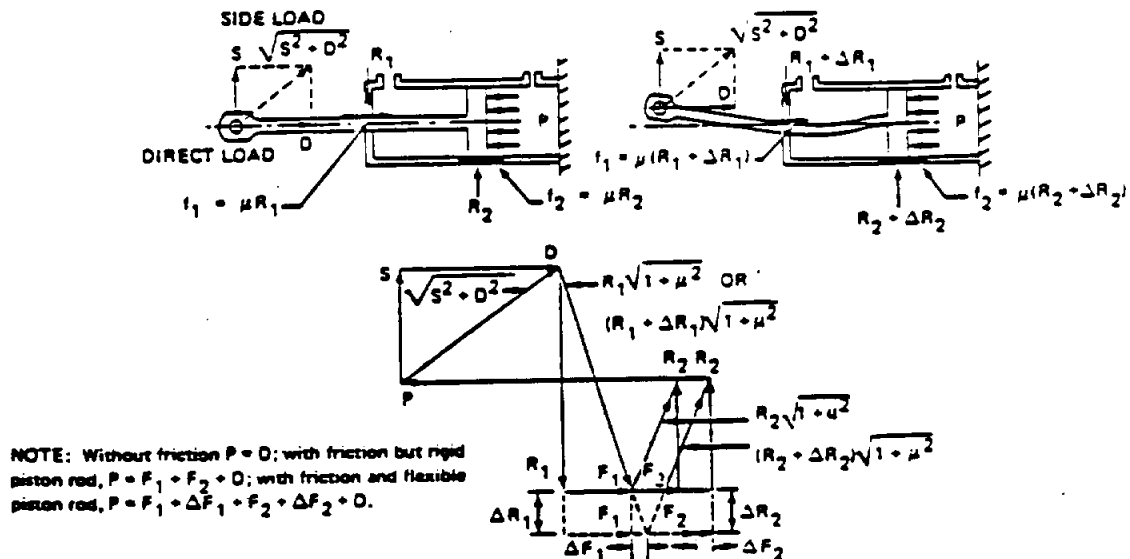


FIGURE 31.3-1

STRUCTURAL ANALYSIS MANUAL

GENERAL DYNAMICS/CONVAIR AND SPACE SYSTEMS DIVISION

31.3 FRICTION EFFECTS OF SLIDING PARTS IN ACTUATOR (Continued)

It is seen in Fig. 31.3-1 that an increase in the magnitudes of the reactions R_1 and R_2 (either due to a further extension of the piston), an increase in the side load, or further deflection of the piston, or all three, will cause an increase in friction forces F_1 and F_2 . This requires an increase in actuator force P to balance the piston external loads. It is possible that the force required to overcome the friction may be greater than that required to move primary load D .

31.4 STRENGTH ANALYSIS OF HYDRAULIC OR PNEUMATIC ACTUATORS

In general, hydraulic or pneumatic actuators are strength checked for the following criteria:

- As a pressure vessel
- As a column

Also, dimensional tolerances are checked for any deleterious effects on actuator performance.

31.4.1 Pressure Vessel Analysis

Design pressures for actuators are defined in MIL-H-5440D and MIL-P-5518C. These pressures, unless specifically defined otherwise, are defined as a percentage of nominal system pressure. (See Fig. 31.4-1.)

ACTUATOR DESIGN PRESSURE

Pressure	Nominal System Pressure (%)		Example: Hydraulic (3,000 psi)
	HYDRAULIC	PNEUMATIC	
Operating	100	100	3,000
Proof	150	200	4,500
Burst	250	400	7,500

FIGURE 31.4-1

The actuator cylindrical body is subject to hoop and axial tension due to internal pressure. An expression for determining cylinder-wall minimum thickness for maximum tension is:

$$t_c = \frac{Pd}{2F_{tu}}$$

where:

P = burst pressure
 d = inside diameter of the cylinder

Stress concentrations should be carefully considered and stress levels kept at a low enough level to meet fatigue requirements. Just as the actuator cylinder body is subject to an internal pressure, the actuator piston rod is subject to an external pressure. An expression for determining hollow-piston-rod wall thickness is:

$$t_p = D \sqrt{\frac{3(P\mu - \mu^2)}{2E}}$$

where:

P = burst pressure
 D = piston rod outside diameter
 μ = Poisson's ratio (0.3 for metals)

31.4.2 Stepped Column Analysis

To allow for tolerance slop, an actuator assembly in its fully extended position, being initially bowed, should be strength checked as a stepped beam column. The bending moment at any point along the column is equal to the compression load multiplied by the displacement of this point from the load line. Also, if the end joints of the actuator utilize bushings or spherical bearings, then friction moments opposing motion should be added to the bending moment previously mentioned when relative motion occurs. Bending-moment transmission occurs between piston and cylinder overlap; consequently, if the resulting bearing loads are high, galling, binding, and excessive wear may occur.

Reference Δ presents the following method of analysis.

31.4.2.1 Stability Analysis

Figure 31.4.2.1-1 shows the extended actuator.

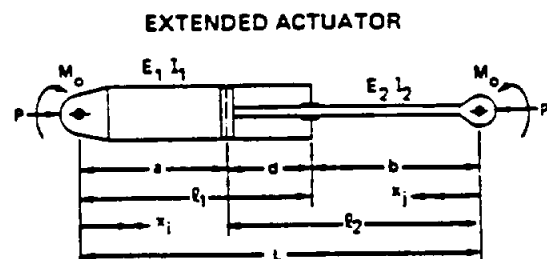


FIGURE 31.4.2.1-1

Δ Author unknown. "Stepped Column Analysis," Bendix Report No. 1640, Indiana, May 1961

STRUCTURAL ANALYSIS MANUAL

GENERAL DYNAMICS/CONVAIR AND SPACE SYSTEMS DIVISION

31.4.2.1 STABILITY ANALYSIS (Continued)

To determine critical buckling load P_{cr} , it is first necessary to evaluate buckling and stiffness-ratio parameters λ and β from Figs. 31.4.2.1-2 and 31.4.2.1-3, where:

$$\lambda^2 = \frac{P_{cr} L^2}{\pi^2 E_2 I_2} \quad \text{and} \quad \beta = \sqrt{\frac{E_2 I_2}{E_1 I_1}}$$

Hence:

$$P_{cr} = \frac{\lambda^2 \pi^2 E_2 I_2}{L^2}$$

Critical buckling stress $F_{cr} = P_{cr}/A_2$. If the stress exceeds the proportional limit of the material, then stiffness-ratio parameter β is calculated using the tangent modulus. This requires a trial-and-error approach, because the value of E must be assumed initially and be compatible with the resulting stress.

31.4.2.2 Column Deflections

If rotation occurs during operation, then end frictions moments M_0 are introduced.

$$M_0 = \mu P \frac{D}{2}$$

where:

μ = coefficient of friction

P = maximum operating load at the particular piston position times 1.5

D = pin diameter

Column deflections due to end moment M for various actuator configurations are given below:

$$Y_1 = Mx_1 \left\{ \frac{b}{L} \left[\frac{a^2}{3E_1 I_1 L} + \frac{b+d}{E_2 I_2} \left(\frac{1}{2} - \frac{d}{6(b+d)} \right) - \frac{b}{3L} \right] + \frac{a(a+2d)}{6E_1 I_1 L} \right\} - \frac{Mx_1^3}{6E_1 I_1 L}$$

for $0 \leq x_1 \leq a$ (measured from cylinder end of column).

$$Y_1 = Mx_1 \left\{ \frac{a}{L} \left[\frac{a(a-d)}{3E_1 I_1 L} + \frac{b}{E_2 I_2} \left(\frac{1}{2} - \frac{b}{6(b+d)} - \frac{b}{3L} \right) + \frac{d^2/3 + bd - b^2/2 - b/L (d^2/3 + bd/2 + b^2/6)}{E_2 I_2 (b-d)} \right] - \frac{Mx_1^2}{6E_2 I_2} \left(3 - \frac{x_1}{L} \right) \right\}$$

for $0 \leq x_1 \leq b$

$$Y_1 = Mx_1 \left\{ \frac{a}{L} \left[\frac{a(a-d)}{3E_1 I_1 L} - \frac{b}{E_2 I_2} \left(\frac{1}{2} - \frac{b}{6(b+d)} - \frac{b}{3L} \right) + \frac{d^2/3 + bd - b^2/2 - b/L (d^2/3 + bd/2 + b^2/6)}{E_2 I_2 (b-d)} \right] - \frac{Mx_1^2}{6E_2 I_2} \left(3 - \frac{x_1}{L} \right) + \frac{M}{E_2 I_2} \left[\frac{a(x_1 - b)^3}{6Ld} \right] \right\}$$

for $b \leq x_1 \leq (b+d)$.

Deflections caused by initial imperfections, such as misalignment and tolerance slip, should be added to those deflections caused by the end friction moment.

Initial slop deflections, δ_0 , may be obtained from the following expression (Fig. 31.4.2.2-1):

$$\delta_0 = l_1 \times \theta_0 \text{ (approximately)}$$

where:

l_1 = length of cylinder

θ_0 = initial slop angle

SLOP DEFLECTION

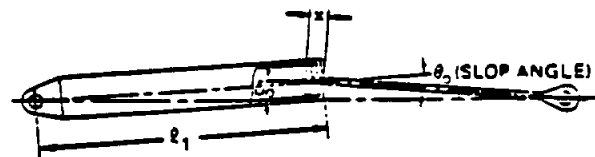


FIGURE 31.4.2.2-1

STRUCTURAL ANALYSIS MANUAL
GENERAL DYNAMICS/CONVAIR AND SPACE SYSTEMS DIVISION

31.4.2.2 COLUMN DEFLECTIONS
(Continued)

$$\theta_o = \frac{D_c - D_p + D_b - D_r}{2X}$$

where:

- D_c = maximum tolerance of inner diameter of cylinder
- D_p = minimum tolerance of outer diameter of piston
- D_b = maximum tolerance of inner diameter of cylinder cap
- D_r = minimum tolerance of outer diameter of piston rod
- X = total length of piston cylinder overlap

The sum of these two deflections (slop and end moment) should then be multiplied by magnification factor K (given below) to obtain the final deflection curve:

$$K = \frac{1}{1 - \frac{P}{P_{cr}}}$$

Bending moment M_X at any point along the column is given by the following expression:

$$M_X = P\delta + M_o$$

where M_o is the end friction moment.

31.4.2.3 Margin of Safety

To determine whether a fluid column will fail under the combined action of the applied compressive load, end moment, and moment due to eccentricities, the following two margins of safety must be obtained.

Piston rod:

$$MS = \frac{1}{R_c + R_b} - 1$$

where:

- $R_c = P/P_{cr}$
- $R_b = f_b/F_b$
- f_b = bending stress including beam column effect
- F_b = bending modulus of rupture

Cylinder:

$$MS = \frac{1}{\sqrt{R_b^2 + R_{ht}^2} + R_b R_{ht}} - 1$$

where:

- $R_b = f_{bu}/F_{by}$
- $R_{ht} = f_{htu}/F_{ty}$
- F_{ty} = tensile yield stress
- f_{htu} = applied ultimate hoop tension stress
- F_{by} = bending modulus of yield
- f_{bu} = applied ultimate bending stress including beam column effect

STRUCTURAL ANALYSIS MANUAL
GENERAL DYNAMICS/CONVAIR AND SPACE SYSTEMS DIVISION

31.4.2-1 STABILITY ANALYSIS (Continued)

BUCKLING AND STIFFNESS-RATIO PARAMETERS λ AND β

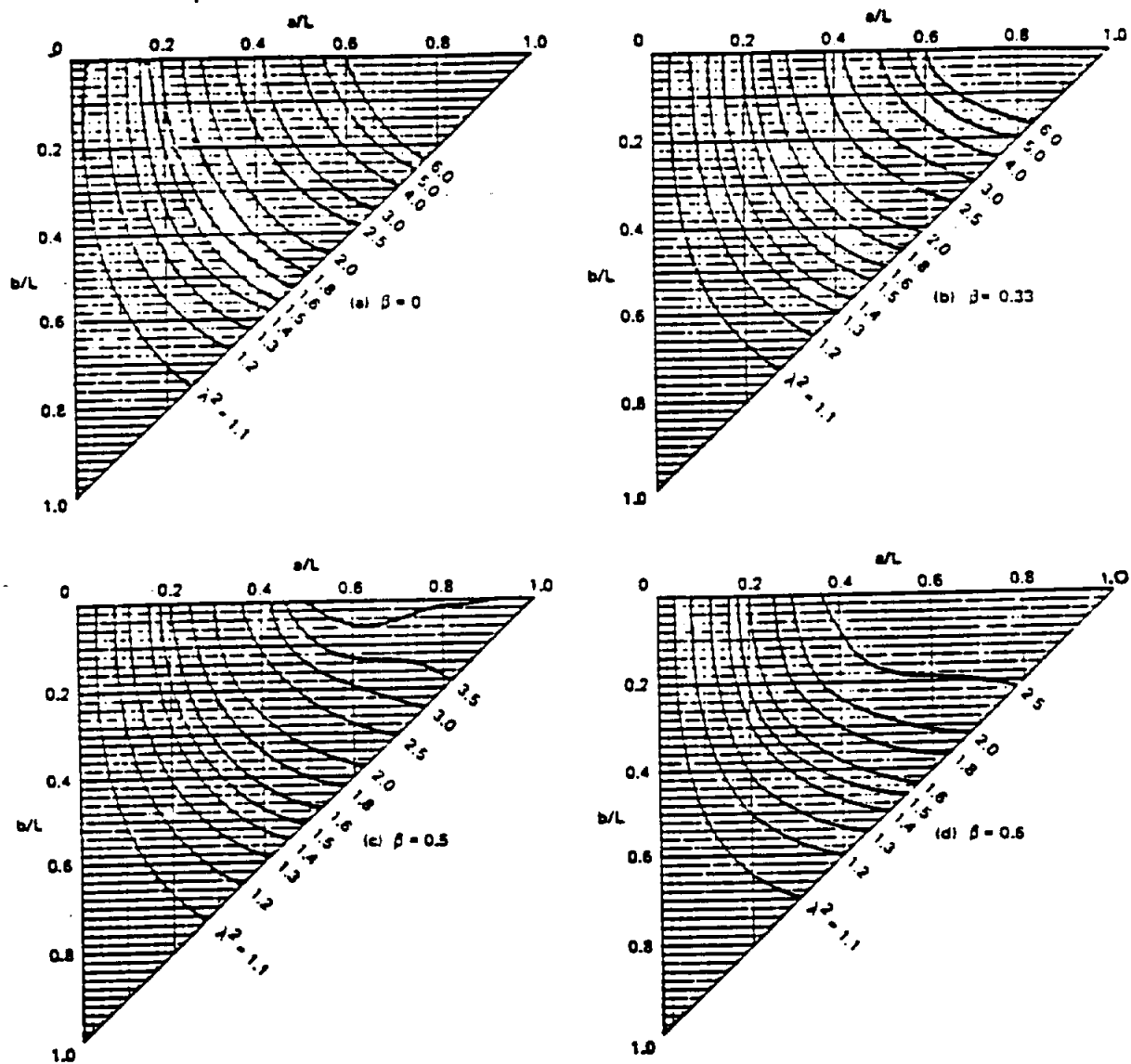


FIGURE 31.4.2-2

STRUCTURAL ANALYSIS MANUAL
GENERAL DYNAMICS/CONVAIR AND SPACE SYSTEMS DIVISION

11.4.2-1 STABILITY ANALYSIS (Concluded)

BUCKLING AND STIFFNESS-RATIO PARAMETERS λ AND β (CONCLUDED)

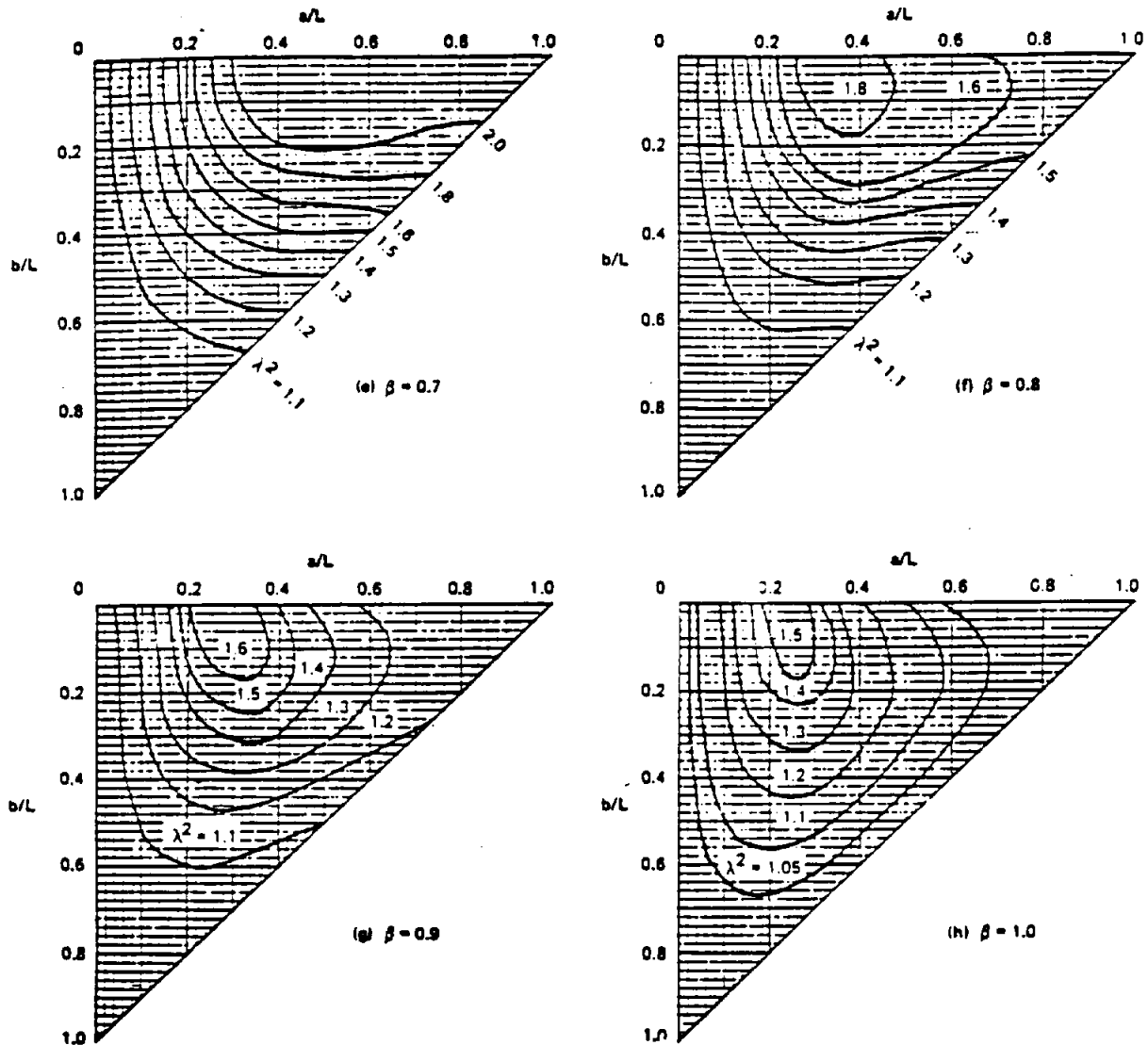


FIGURE 3] 4.2.1-2 (CONCLUDED)

STRUCTURAL ANALYSIS MANUAL
GENERAL DYNAMICS/CONVAIR AND SPACE SYSTEMS DIVISION

SECTION 22.0

COMPOSITE MATERIALS

Basic analytical methods of analysis and material strength allowables for composite material structures are contained in this section.

	<u>PAGE</u>
22.1 FIBERGLASS LAMINATES, POLYESTER RESINS	22.1.1
22.2 FIBERGLASS LAMINATES, PHENOLIC OR EPOXY RESIN	22.2.1
22.3 KEVLAR EPOXY DESIGN ALLOWABLES	22.3.1

STRUCTURAL ANALYSIS MANUAL
GENERAL DYNAMICS/CONVAIR AND SPACE SYSTEMS DIVISION

Data Source, Section 1.3 Reference 6

SUBJECT: Fiberglass Laminates POLYESTER RESINS

- REFERENCES: 1. ANC-17 (June, 1955), Part I OR MIL-HDBK-17A.
 2. U.S. Forest Products Laboratory Report 1803-B
 3. U.S. Forest Products Laboratory Report 1824-A
 4. U.S. Forest Products Laboratory Report 1853

INTRODUCTION

This memo contains general information about glass fabric laminates bonded with polyester resins and the allowables to be used in the design.

An additional factor of safety of 1.33 shall be used in the design of structural parts made from laminated plastics.

In application, this factor is to be used in computing margins of safety as follows:

$$M. S. = \frac{\text{Allowable Stress}}{\text{Applied Ultimate Stress} \times 1.33} \quad -1$$

This additional factor is required because of the observed discrepancy between allowable strength based on minimum specification values for wet laminates and the observed strengths of production parts.

The 1.33 factor is not required provided that design strengths are substantiated by strength tests of tag-end coupons, and by destructive testing of important parts throughout the full course of production. Provision for this substantiation should exist on drawings, in process specifications and quality control testing directives, or other documentation which must be kept in force throughout production. Structures division office approval shall be obtained prior to omission of the 1.33 factor so that the required substantiating tests may be included in the pertinent part specifications.

STRUCTURAL ANALYSIS MANUAL
GENERAL DYNAMICS/CONVAIR AND SPACE SYSTEMS DIVISION

Much of the information included herein was extracted from reference (1) and was modified where deemed helpful for clarity and/or ease of application in design and analysis.

General

A. Plastic laminates, as covered herein, consist of bi-directional, uni-directional and non-woven glass mat fabrics.

1. A bi-directional, or satin weave fabric is woven in such a way that each warp and fill yarn goes under one yarn and over the next seven yarns. The approved bi-directional materials are fabric numbers 120, 181, 182, 183, 1581, 7781, and 7581.
2. A uni-directional fabric is made with strong warp yarns and relatively few weaker fill yarns to give maximum strength in the warp direction. Uni-directional fabric number is 143.
3. Non-woven mat consists of chopped glass fiber strands, usually 1/2" to 2" long, laid down in a random pattern.
4. For 181 cloth, nominal thickness of 0.0093 in/ply and minimum thickness of 0.0085 in/ply are recommended.
5. When the ply orientation is not called out on the drawing, the lower of 0°, 90°, or 45° orientation should be used for analysis.
 - ie. For 181 cloth, use 45° strength for tension and compression. Use 90° strength for in-plane shear.Also, use this criteria for modulus in buckling calculations.
6. Specification values are usually higher than design. Many specifications list minimum average values, rather than 'A' values. Care should be exercised in determining appropriate design values. Determination of allowables is the responsibility of the Structural Analysis Group. Inadequate testing can lead to incorrect strength determination.
7. Poor interlaminar strength is a characteristic of laminated plastics. Analysis of angles and bend radii requires special attention. Guidelines are outlined in the following references:

883-O-86-115, Analysis of Laminated Angles for Interlaminar Tension Stress.
R. E. Carlson, 6 December 1986.

883-O-87-040, Compression and Short Beam Shear Allowables of Glass/Epoxy and Aramid/Epoxy for Titan/Centaur. R. E. Carlson, 20 May 1987.

883-O-86-116, Stress Approval of Glass/Epoxy and Aramid/Epoxy Composites for Titan/Centaur. R. E. Carlson, 9 December 1986.

STRUCTURAL ANALYSIS MANUAL
GENERAL DYNAMICS/CONVAIR AND SPACE SYSTEMS DIVISION

I. General (cont'd)

- B. The engineering part drawing shall specify the type of fabric (depending on the electrical and structural requirements of the part), the grade of fabric (depending on flammability requirements of the part) and the class of fabric (depending on the maximum operating temperature to which the part will be subjected).
- C. The nomenclature used in this stress memo is as defined in M-H-S with the following additions:
- a - Under compression loading, length of unloaded side of panel, and the length of either side for shear loads (Paragraph II:G:2).
 - b - Under compression loading, length of loaded side of panel, and the length of either side for shear loads (Paragraph II:G:2); subscript denoting "bonding".
 - E_b - Modulus of elasticity in bending.
 - F_{ocr} - Critical compressive stress for buckling of rectangular panels.
 - K - Buckling constant; with subscript "s" denoting "shear", and subscript "c" denoting "compression".
 - ϕ - Angle between the direction of load and the warp direction of fabric, except for bending properties the angle between the direction of bending stress and the warp direction of the laminate.

II. Basic Mechanical Properties at Room Temperature

A. Tension, Compression, Flexure and Shear Properties

Fabrics, woven as described above, have different strength properties in the range between parallel and normal to the warp direction. Design allowables at room temperature for the various fabrics at loading angles of 0°, 45° and 90° to the warp direction are given in Table I. Allowables for non-woven mat fabric are also included.

In order to satisfy particular requirements for a given application, mechanical properties can be tailored by cross-laminating, or by ply orientation in such a manner as to give nearly equal strength in all directions of loading. Figures 1 through 12 show variation in properties at angles of loading relative to the warp direction of the face ply.

For shear loading, the panel must be orientated to show the relationship between shear flow direction and base line as shown by the sketch on Figures 6 thru 9 and angle of loading, ϕ , is measured from the base line to the direction of warp in a counter-clockwise direction.

The figures mentioned above give allowables for laminates with the specified numbers (and/or multiples of those numbers) of plies. In actual practice, the outer plies of a laminate are oriented in such a way that their warp directions are parallel. Therefore, properties slightly higher than those shown in Figures 1 through 12 may be attained, the effect of the one additional face

STRUCTURAL ANALYSIS MANUAL
GENERAL DYNAMICS/CONVAIR AND SPACE SYSTEMS DIVISION

II. Basic Mechanical Properties at Room Temperature (cont'd)

A. Tension, Compression, Flexure and Shear Properties (cont'd)

ply decreasing as the number of plies increases. Since the effect of the additional parallel-oriented ply has been disregarded in the given allowables, it shall also be conservatively disregarded in design.

The design allowables of Table I and Figures 1 through 12 are for laminates .125 thick and over. For laminate thicknesses less than .125, correction on all properties shall be made in accordance with the "multiplying factors" shown in Figure 13.

In the fabrication of a multi-ply laminate, especially in the case of a large part, it may be necessary to use more than one sheet of fabric in a ply. In such an instance, the sheets will be laid up with an overlap as designated in the applicable process specification. The effect of overlapping the fabric will be to reduce the tensile strength of the laminate, in the region of the overlap, in direct proportion of the number of spliced plies relative to the total number of plies in a section where all plies are continuous. None of the other properties, except tensile strength, will be affected by the overlapped ply.

B. Bearing Properties

Ultimate bearing stresses of a parallel-laminated bi-directional fabric loaded at 0° , 45° and 90° to the warp direction are given in Figures 14, 15 and 16, respectively, as a function of the edge distance ratio (a/D), fastener spacing (or lug width) ratio (W/D), and the fastener diameter to thickness ratio (D/t). Comparable curves for a cross-laminated uni-directional fabric are given in Figures 17 and 18, and for mat fabric in Figure 19.

The data are presented for a range of D/t ratios from 1 to 4. Extrapolation beyond this range is not recommended. For applications beyond the given limits, bearing strength shall be determined by test on representative specimens of the desired configuration.

For a specific edge distance ratio (a/D) and a given fastener diameter to laminate thickness ratio (D/t), the ultimate bearing stress is read as the ordinate of the curve. However, to develop this bearing stress, a corresponding (or longer) fastener spacing to fastener diameter ratio (W/D) must be maintained to prevent tension failure at the net section. Conversely, for a specific W/D ratio, a corresponding a/D ratio can be obtained from the curve.

For applications using bi-directional fabrics laminated at various angles to the face ply, or uni-directional fabrics with plies oriented at angles other than 90° to each other, bearing strength shall be determined by test on representative specimens of the desired configuration.

C. Tension Efficiency

Tension efficiency for parallel-laminated bi-directional fabrics, cross-laminated uni-directional fabric and mat fabric can be determined from

STRUCTURAL ANALYSIS MANUAL
GENERAL DYNAMICS/CONVAIR AND SPACE SYSTEMS DIVISION

II. Basic Mechanical Properties at Room Temperature (cont'd)

C. Tension Efficiency (cont'd)

the curves of Figures 14 thru 19. For any fastener spacing (N/D) within the range of the non-horizontal portion of each curve, a corresponding allowable bearing stress, F_{bru} , can be obtained. The tensile stress on the net section of the laminate can then be computed as $F_{bru}/(N/D-1)$; and tension efficiency can be calculated by dividing the tensile stress on the net section by the allowable tensile strength of the laminate. This data is applicable to single-row attachments only. The effect of multiple-row attachments must be substantiated by test.

D. Fatigue Strength

Presented in Figures 20 and 21 are curves showing the effects of various mean stresses on the fatigue strength of unnotched and notched specimens, respectively, of parallel-laminated bi-directional fabric loaded at 0° to the warp direction.

Shown in Figure 22 is the effect of load, applied at 0° and 45° to the warp direction on the fatigue strength of a parallel-laminated bi-directional fabric tested axially at zero mean stress ($R = -1$). The fatigue strength of notched specimens is 20% and 15% lower than that of unnotched specimens at the low and high cyclic ranges, respectively, when the laminate is loaded at 0° to the warp direction. Notching has little effect on fatigue strength of the laminate when load is applied at 45° to the warp direction.

The fatigue strength of a laminate loaded through a pin is the same as that indicated for a notched specimen loaded axially in tension as shown in Figures 21 and 22.

E. Creep

At room temperature, creep parallel and perpendicular to the warp direction of parallel- and cross-laminates is insignificant. With initial deformation on the order of 1 to 1-1/4%, the additional deformation due to creep is negligible. Creep may not be negligible for configurations other than parallel- and cross-laminated or for loading at angles intermediate between parallel and perpendicular to the warp direction. There is no available test data to indicate the behavior of these latter laminate configurations at the intermediate loading angles.

F. Stress-Rupture

Tensile and compressive stress-rupture characteristics of a parallel-laminated bi-directional fabric are presented in Figure 23. These curves show that the failing stress is lowered with increased time under load and that the notched rupture stress is about 80% of the unnotched strength for any given period of loading.

G. Buckling Stress - Compression and Shear

The buckling stress in compression and shear for Type I, II and III parallel-laminated fabrics loaded parallel or perpendicular to the warp direction, can

STRUCTURAL ANALYSIS MANUAL
GENERAL DYNAMICS/CONVAIR AND SPACE SYSTEMS DIVISION

II. Basic Mechanical Properties at Room Temperature (cont'd)

G. Buckling Stress - Compression and Shear (cont'd)

be determined from the curves of Figures 25 and 27, respectively. Figures 24 and 26 give curves for the buckling constants, $\sqrt{K_c}$ and $\sqrt{K_s}$, respectively, for various edge conditions along with multiplying factors to account for laminate thickness.

1. Compression Buckling Stress

To obtain the compression buckling stress, enter Figure 25 with an effective $(b/t)_e = \frac{b/t}{\sqrt{K_c}}$ and read the stress, F_{ocr} , as the ordinate for the applicable material. The value obtained is for a laminate thickness equal to or greater than .125.

For laminate thickness less than .125, a double correction is necessary. Multiply the $\sqrt{K_c}$ obtained by the factor applicable to the thickness as obtained from the upper curve of Figure 24.

Enter Figure 25 with an effective $(b/t)_e = \frac{b/t}{\sqrt{K_c}}$ and obtain a value of stress which is then corrected for thickness using the flexure modulus factor from Figure 13.

2. Shear Buckling Stress

To obtain the shear buckling stress proceed as follows:

- a. Designate the side of the panel parallel to the warp direction as "b" and compute b/a. With this value of b/a, enter Figure 26 and read a value for $\sqrt{K_s}$ from the curve labeled "CASE A" for the applicable edge condition and material.

In the event the value of b/a exceeds the range of "CASE A" curve, proceed as indicated in paragraph b. below.

- b. Designate the side of the panel perpendicular to the warp direction as "b" and compute b/a. With this value of b/a, enter Figure 26 and read a value for $\sqrt{K_s}$ from the curve labeled "CASE B" for the applicable edge condition and material.

- c. Enter Figure 27 with an effective $(b/t)_e = \frac{b/t}{\sqrt{K_s}}$ and read the shear buckling stress from the curve ("CASE A" or "CASE B") that is consistent with the case used to obtain $\sqrt{K_s}$. For bi-directional fabrics a common curve is used for both "CASE A" and "CASE B". The shear buckling stress obtained is for a laminate thickness equal to or greater than .125.

For laminate thickness less than .125 a double correction is necessary. Multiply the $\sqrt{K_s}$ obtained by the factor applicable to the thickness as obtained from the upper curve of Figure 26. Enter

Figure 27 with an effective $(b/t)_e = \frac{b/t}{\sqrt{K_s}}$ and obtain a value of stress which is then corrected for thickness using the flexure modulus factor from Figure 13.

STRUCTURAL ANALYSIS MANUAL
GENERAL DYNAMICS/CONVAIR AND SPACE SYSTEMS DIVISION

II. Basic Mechanical Properties at Room Temperature (cont'd)

H. Column and Crippling Allowables

Figure 28 gives the column allowables for Type I, II and III parallel-laminated, bi-directional and uni-directional fabrics for laminate thickness equal to or greater than .125. For laminate thickness less than .125, the allowable column stress for a specified L'/ρ ratio equals the applicable value as obtained from Figure 28 multiplied by the compressive modulus factor obtained from Figure 13.

Crippling allowables for Type I, II and III parallel-laminated bi-directional and uni-directional fabrics are given in Figure 29 for laminate thickness equal to or greater than .125. For laminate thickness less than .125, the allowable crippling stress for a specific b/t ratio equals the applicable stress as obtained from Figure 29 multiplied by the compressive strength factor as obtained from Figure 13.

III. Basic Mechanical Properties at Other Than Room Temperature

A. Properties at Low Temperatures

Mechanical properties of glass fabric laminates tend to increase with decreasing temperature down to -300°F. In view of this behavior, basic mechanical properties at room temperature will be conservatively used for the design of parts operating at reduced temperatures.

B. Properties at Elevated Temperatures

Tensile and compressive strengths of glass fabric laminates operating at temperatures of 250°F are reduced on the order of 30% and 40%, respectively. Since the magnitude of reduction in strength is dependent to a large extent on the technique used in bonding the laminate, elevated temperature properties shall be obtained by test.

IV. Basic Mechanical Properties at Various Lay-Ups

The design allowables given in Table I are for parallel laminates in any number of plies. The strength of a laminate, however, can be tailored to give nearly equal values in all directions by stacking the plies at optimum angles to the warp direction of the fabric in the face ply.

A. Tensile, Compressive and Shear Strengths

Tensile, compressive and shear design allowable strengths of bi-directional and uni-directional fabrics, laminated in several lay-ups and loaded at various angles to the warp direction of the face ply are given in Figures 1 thru 9. Strengths of other lay-ups may be taken as the average of the properties of the component layers, weighted according to the area they occupy. That is,

$$F = \frac{1}{A} \sum_{i=1}^{i=n} F_i A_i$$

- F = property of the laminate
- F_i = strength property of the i th ply as obtained from Figures 1 thru 9.
- A_i = cross-sectional area of i th ply
- A = cross-sectional area of the laminate

STRUCTURAL ANALYSIS MANUAL
GENERAL DYNAMICS/CONVAIR AND SPACE SYSTEMS DIVISION

IV. Basic Mechanical Properties at Various Lay-Ups (cont'd)

B. Flexural Strength

Design allowable flexural strengths of parallel-laminated bi-directional and uni-directional fabrics at various angles of loading are given in Figure 10. Flexural strengths of other lay-ups may be taken as the average of the properties of the component layers, weighted according to the proportion they contribute to the moment of inertia of the laminate cross-section. That is,

$$F_b = \frac{1}{I} \sum_{i=1}^{i=N} F_i I_i$$

where: F_b = the bending strength of the laminate
 F_i = the bending strength of i^{th} ply as obtained from Fig. 10
 I_i = moment of inertia of i^{th} ply about laminate neutral axis
 I = moment of inertia of the laminate

C. Compressive Modulus of Elasticity

Compressive modulus of elasticity design allowables for bi-directional and uni-directional fabrics, laminated in several lay-ups and loaded at various angles to the warp direction of the face ply are given in Figures 11 and 12. The modulus of elasticity of other lay-ups may be taken as the average of the component layers of material in the laminate, weighted according to the area they occupy. That is,

$$E_o = \frac{1}{A} \sum_{i=1}^{i=N} E_i A_i$$

where: E_o = the modulus of elasticity of the laminate
 E_i = the modulus of elasticity of the i^{th} ply as obtained from Figures 11 or 12
 A_i = cross-sectional area of the i^{th} ply
 A = cross-sectional area of the laminate

TABLE I - DESIGN MECHANICAL PROPERTIES FOR PARALLEL LAMINATES OF GLASS FABRIC AND MAT¹
(in KIPS per square inch)

Fabric	Structural - Type I, II, III							Semi-Structural - Type IV and IV-A ⁶							Non-Structural - Type V	
	Bi-directional ³			Uni-directional ⁴			Mat	Bi-directional ³			Uni-directional ⁴			Mat	All except Mat	Mat
Angle of ² Loading - Deg.	0	45	90	0	45	90		0	45	90	0	45	90		0	
F_{tu}	38.0	16.3	35.1	76.0	11.7	8.95	18.0	33.0	14.2	30.5	60.0	9.38	7.2	13.0	20.0	4.5
F_{cu}	29.0	15.9	23.5	45.0	14.1	19.0	18.0	20.0	13.5	16.2	30.0	11.0	12.7	13.0	15.0	9.0
F_{bu}	40.0	18.3	35.7	78.0	13.6	15.1	19.2	30.0	14.1	26.8	60.0	10.4	9.7	16.0	15.0	12.0
F_{su}	8.34	⁵ --	8.34	7.44	⁵ --	7.44	9.2	7.28	⁵ --	7.28	5.93	⁵ --	5.93	7.6	4.4	2.6
E	2040	1480	1820	6390	920	420	1110	1800	1300	1600	4550	1250	355	1050	--	--
E_a	2730	1630	2590	4910	1530	1510	1300	2400	1440	2280	4150	1290	1275	1230	--	--
E_b	2500	--	2350	4500	--	1360	1090	2200	--	2070	3800	--	1150	1030	1500	--
G	550			550			580	465			465			550	--	--
μ	.16			.16			.16	.16			.16			.16	.16	.16

NOTES:

- Based on wet strength properties of ANC-17, for laminate thickness .125 and over.
- Angle between direction of load and direction of warp, except for bending modulus, which is the angle between the direction of bending stress and the warp direction of the laminate.
- Bi-directional material made from 120, 181, 182 or 183 fabric.
- Uni-directional material made from 143 fabric.
- Refer to applicable Figures 6 thru 9 for shear strength, depending on direction of shear flow.
- For Grade C, Class 4 laminates the F_{cu} values for all of the Type IV and IV-A material are reduced by 5 kips.

STRUCTURAL ANALYSIS MANUAL
GENERAL DYNAMICS/CONVAIR AND SPACE SYSTEMS DIVISION

FIGURE INDEX

<u>FIGURE</u>	<u>SUBJECT</u>
1	Tensile Strength - Bi-Directional Fabrics, Types I, II, III, IV, IV-A
2	" " - Uni-Directional " , " " " " " "
3	Compressive " - Bi-Directional " , " " " " " "
4	" " - Uni-Directional " , Types I, II, III
5	" " - " " " , Types IV, IV-A
6	Shear " - Bi-Directional " , Types I, II, III
7	" " - " " " , Types IV, IV-A
8	" " - Uni-Directional " , Types I, II, III
9	" " - " " " , Types IV, IV-A
10	Bending Modulus of Rupture - Bi-Directional and Uni-Directional Fabrics, Types I, II, III, IV, IV-A
11	Compressive Modulus of Elasticity - Bi-Directional Fabrics, Types I, II, III, IV, IV-A
12	Compressive Modulus of Elasticity - Uni-Directional Fabrics, Types I, II, III, IV, IV-A
13	Multiplying Factors for Ultimate Strengths and Moduli of Elasticity
14	Bearing Strength - Parallel-Laminated Bi-Directional Fabric, $\phi = 0^\circ$
15	" " - " " " " " , $\phi = 45^\circ$
16	" " - " " " " " , $\phi = 90^\circ$
17	" " - Cross-Laminated Uni-Directional Fabric, $\phi = 0^\circ \text{ \& } 90^\circ$
18	" " - " " " " " , $\phi = 45^\circ$
19	" " - Bonded Mat Laminate
20	Axial Fatigue Strength - Unnotched Parallel-Laminated, Bi-Directional Fabric
21	" " " - Notched " " , " " "
22	S-N Curves - Notched and Unnotched, Parallel-Laminated, Bi-Directional Fabric
23	Tensile & Compressive Stress-Rupture - Parallel-Laminated, Bi- " "
24	Compressive Buckling Constant - Parallel-Laminated, Bi-Directional and Uni-Directional Fabrics, Types I, II, III, $\phi = 0^\circ \text{ \& } 90^\circ$
25	Compressive Buckling Stress - Parallel-Laminated, Bi-Directional and Uni-Directional Fabrics, Types I, II, III, $\phi = 0^\circ \text{ \& } 90^\circ$
26	Shear Buckling Constant - Parallel-Laminated, Bi-Directional and Uni-Directional Fabrics, Types I, II, III
27	Shear Buckling Stress - Parallel-Laminated, Bi-Directional and Uni-Directional Fabrics, Types I, II, III
28	Column Stresses - Parallel-Laminated Fabrics, Types I, II, III
29	Crippling Stresses (per S.M. 110) - Parallel-Laminated Fabrics, Types I, II, III

STRUCTURAL ANALYSIS MANUAL

GENERAL DYNAMICS/CONVAIR AND SPACE SYSTEMS DIVISION

FIGURE 1

TENSILE STRENGTH OF BI-DIRECTIONAL FABRICS
FOR VARIOUS ANGLES OF LOADING AT SEVERAL LAY-UPS
TYPES I, II & III
(FOR TYPES IV & IV-A, MULTIPLY VALUES BY .868)

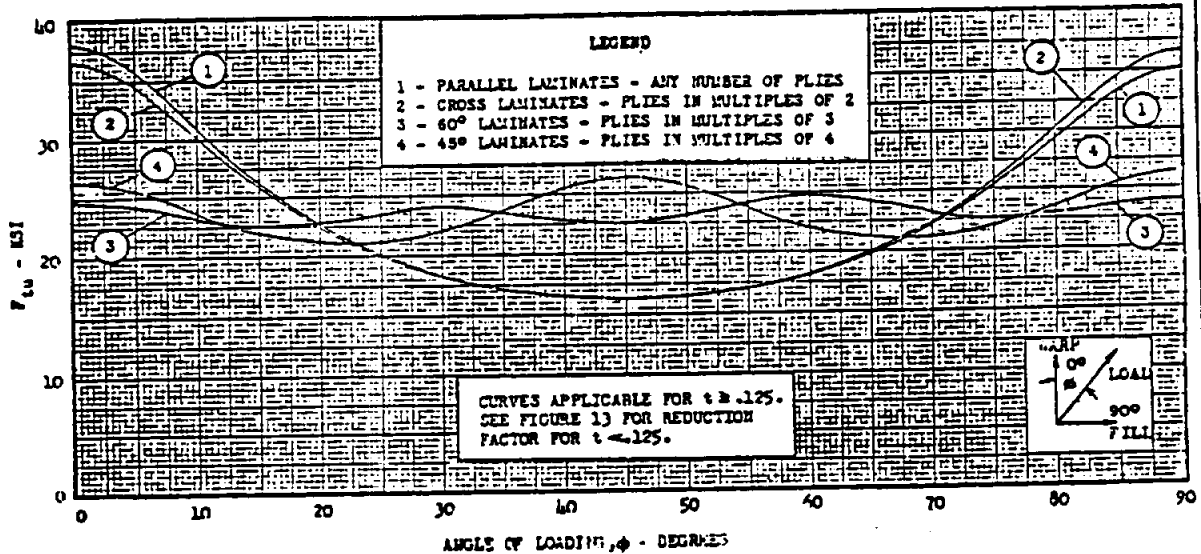
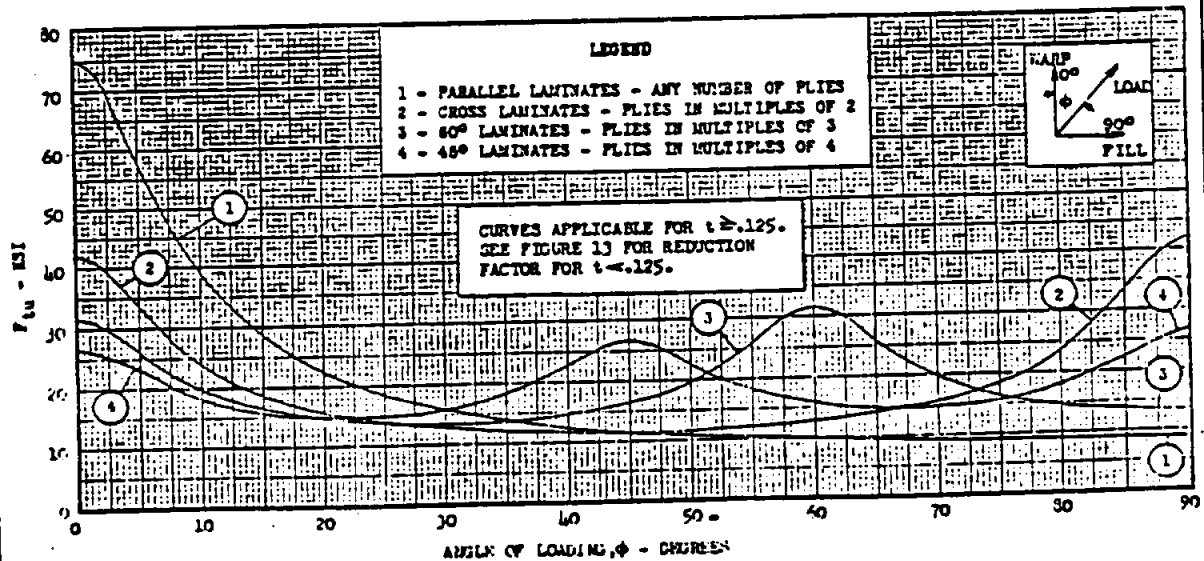


FIGURE 2

TENSILE STRENGTH OF UNI-DIRECTIONAL FABRICS
FOR VARIOUS ANGLES OF LOADING AT SEVERAL LAY-UPS
TYPES I, II & III
(FOR TYPES IV & IV-A, MULTIPLY VALUES BY .80)



STRUCTURAL ANALYSIS MANUAL **GENERAL DYNAMICS/CONVAIR AND SPACE SYSTEMS DIVISION**

FIGURE 3

COMPRESSIVE STRENGTH OF BI-DIRECTIONAL FABRICS
 FOR VARIOUS ANGLES OF LOADING AT SEVERAL LAY-UPS
 TYPES I, II, III, IV & IV-A

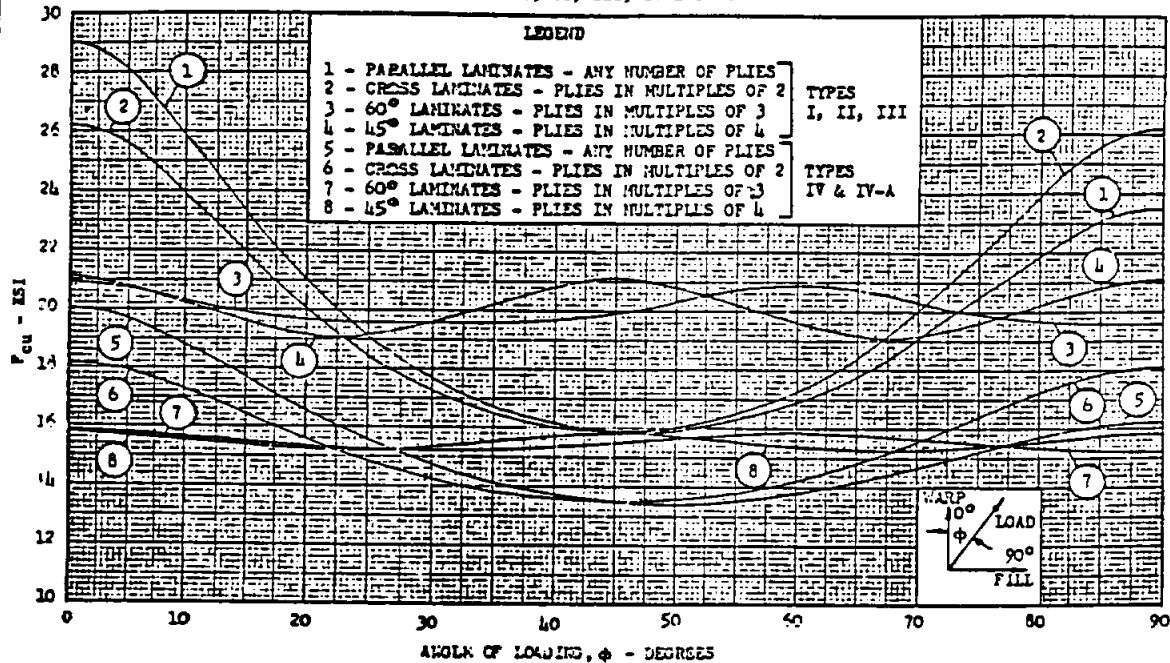
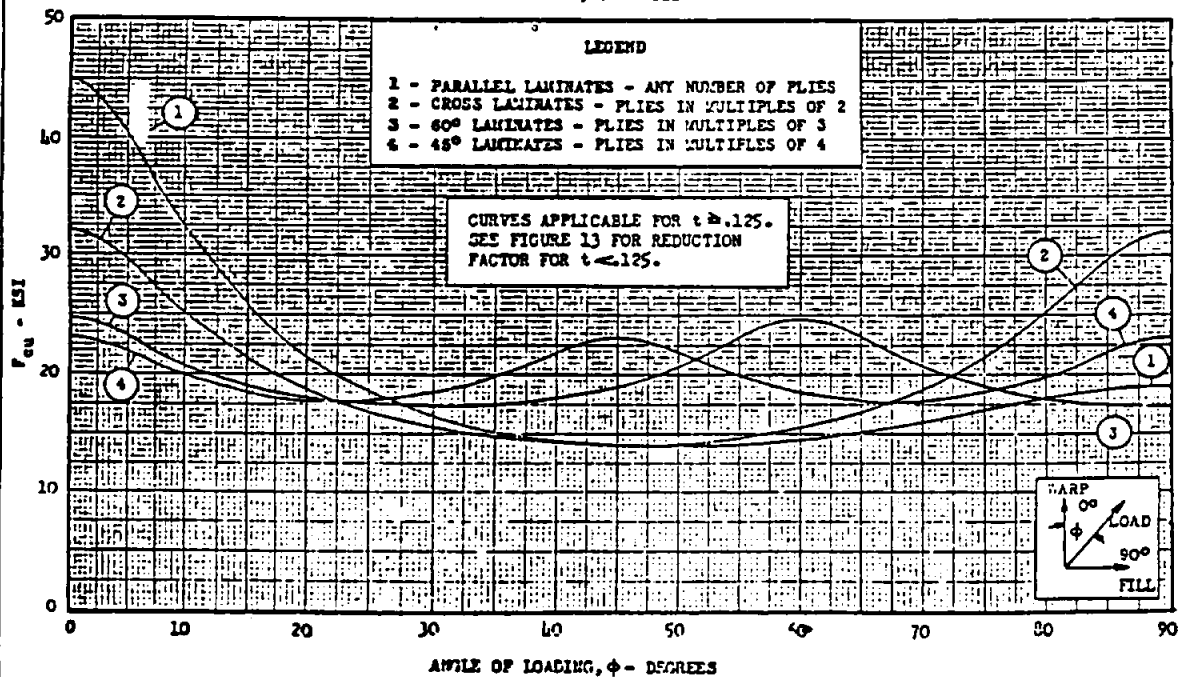


FIGURE 4

COMPRESSIVE STRENGTH OF UNI-DIRECTIONAL FABRICS
 FOR VARIOUS ANGLES OF LOADING AT SEVERAL LAY-UPS
 TYPES I, II & III



STRUCTURAL ANALYSIS MANUAL

GENERAL DYNAMICS/CONVAIR AND SPACE SYSTEMS DIVISION

FIGURE 5

COMPRESSIVE STRENGTH OF UNI-DIRECTIONAL FABRIC
FOR VARIOUS ANGLES OF LOADING AT SEVERAL LAY-UPS
TYPES IV & IV-A

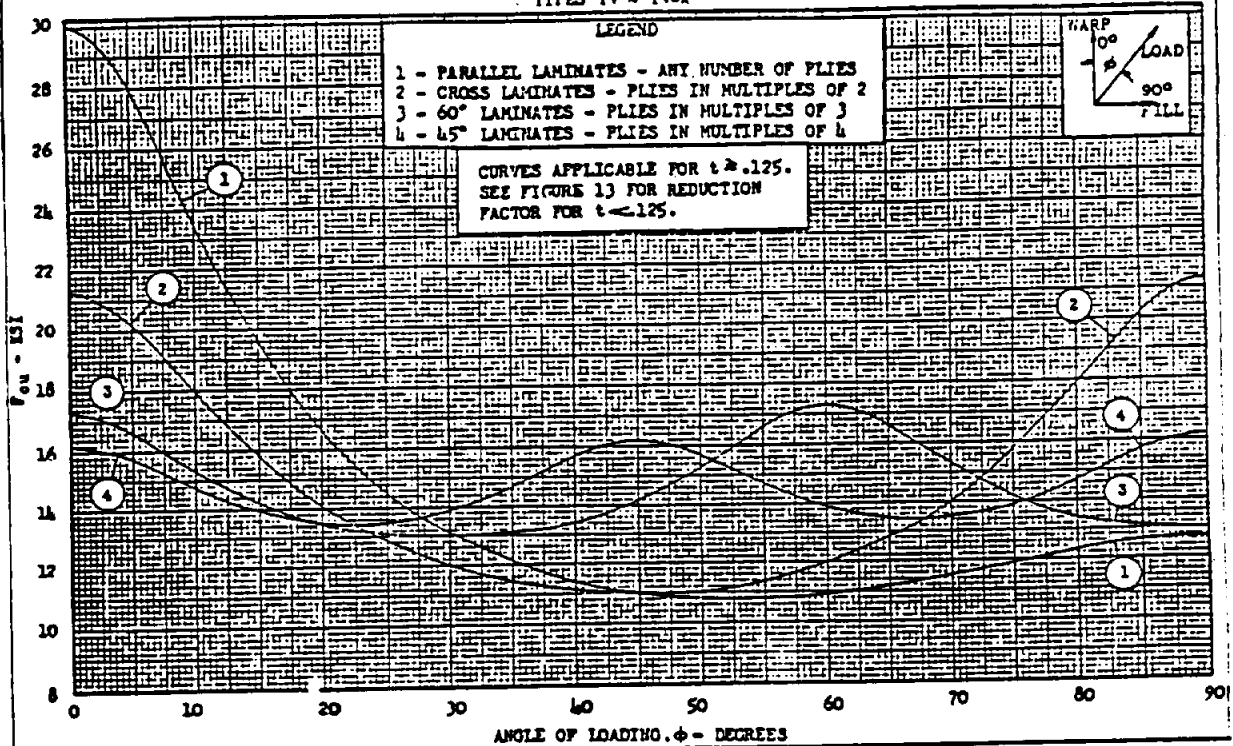
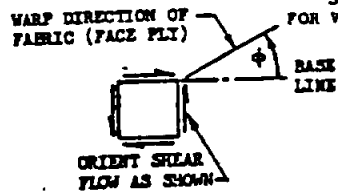


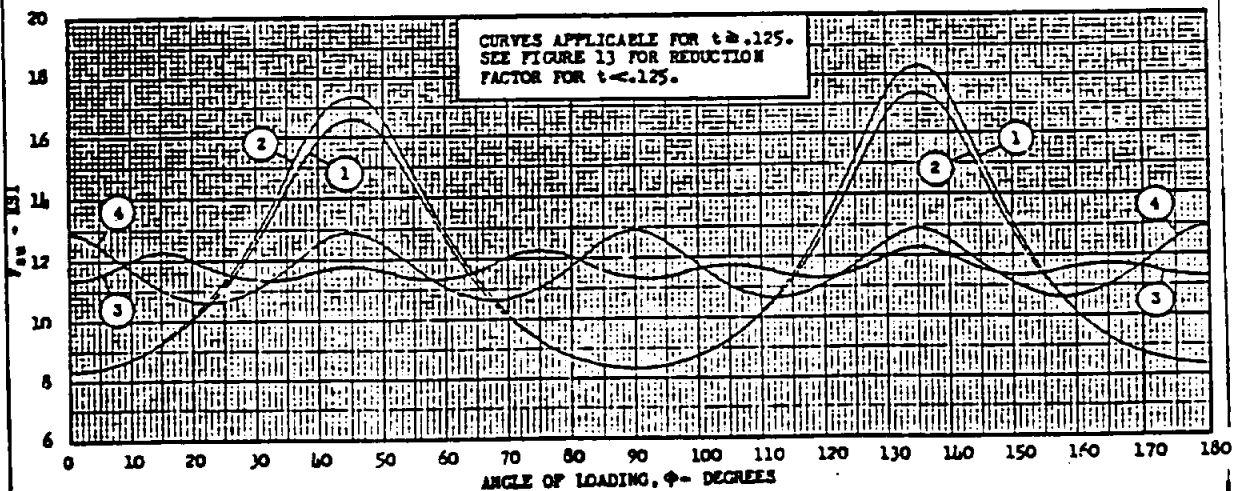
FIGURE 6

SHEAR STRENGTH OF BI-DIRECTIONAL FABRICS
FOR VARIOUS ANGLES OF LOADING AT SEVERAL LAY-UPS
TYPES I, II & III



LEGEND

- 1 - PARALLEL LAMINATES - ANY NUMBER OF PLYS
2 - CROSS LAMINATES - PLYS IN MULTIPLES OF 2
3 - 60° LAMINATES - PLYS IN MULTIPLES OF 3
4 - 45° LAMINATES - PLYS IN MULTIPLES OF 4



STRUCTURAL ANALYSIS MANUAL

GENERAL DYNAMICS/CONVAIR AND SPACE SYSTEMS DIVISION

FIGURE 7
SHEAR STRENGTH OF BI-DIRECTIONAL FABRICS
FOR VARIOUS ANGLES OF LOADING AT SEVERAL LAY-UPS
TYPES IV & IV-A

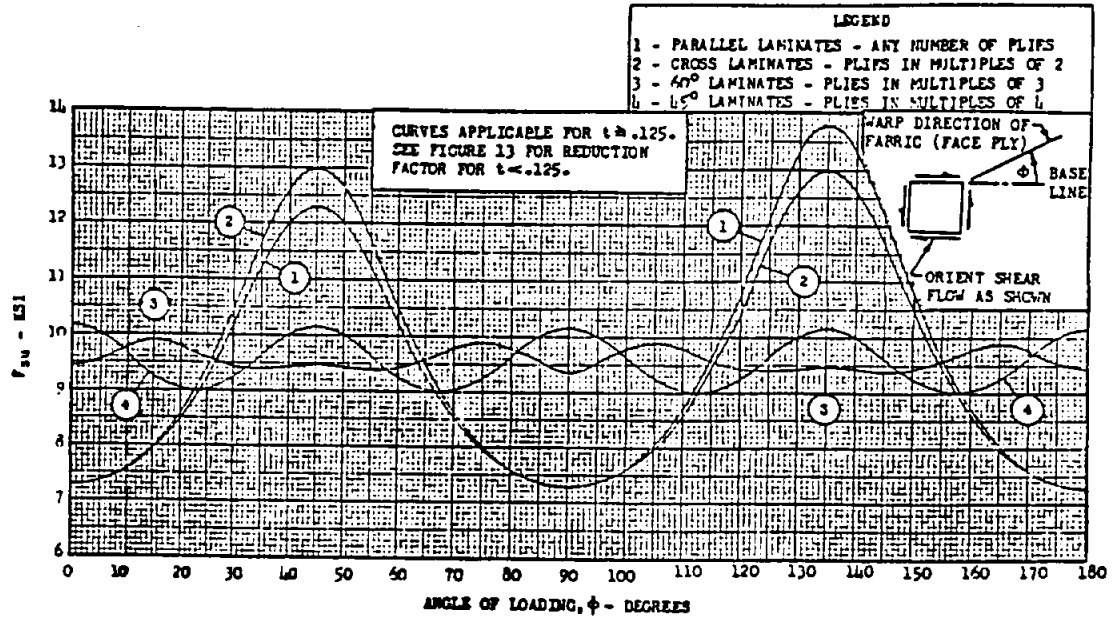
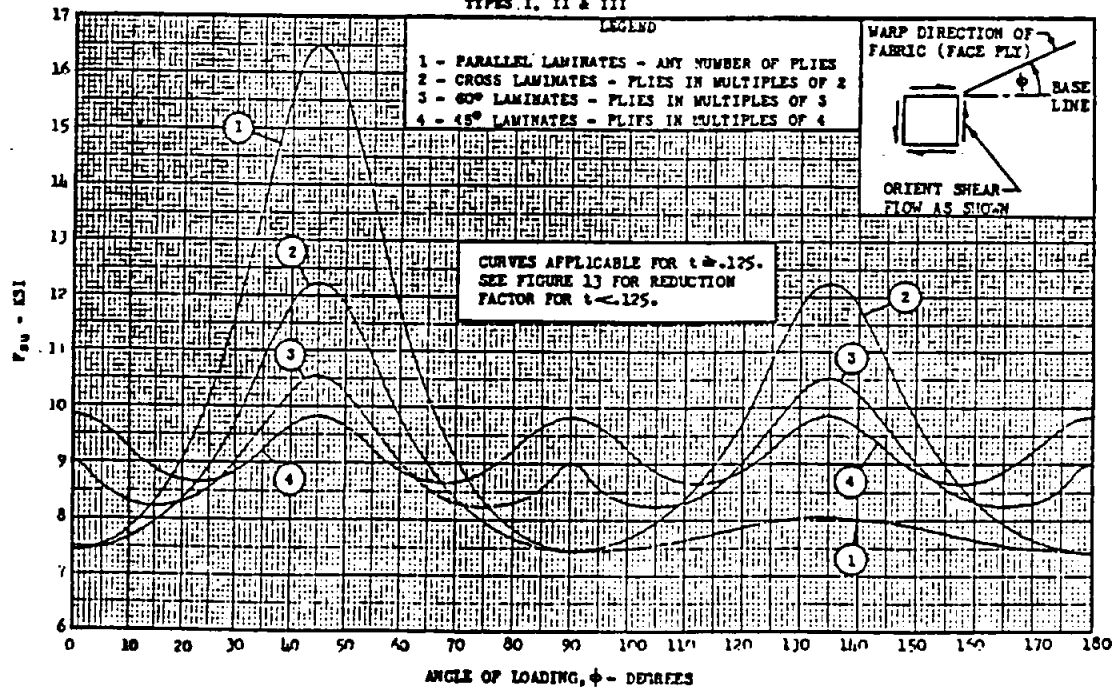


FIGURE 8
SHEAR STRENGTH OF UNI-DIRECTIONAL FABRICS
FOR VARIOUS ANGLES OF LOADING AT SEVERAL LAY-UPS
TYPES I, II & III



STRUCTURAL ANALYSIS MANUAL

GENERAL DYNAMICS/CONVAIR AND SPACE SYSTEMS DIVISION

FIGURE 9
SHEAR STRENGTH OF UNI-DIRECTIONAL FABRICS
FOR VARIOUS ANGLES OF LOADING AT SEVERAL LAY-UPS
TYPES IV & IV-A

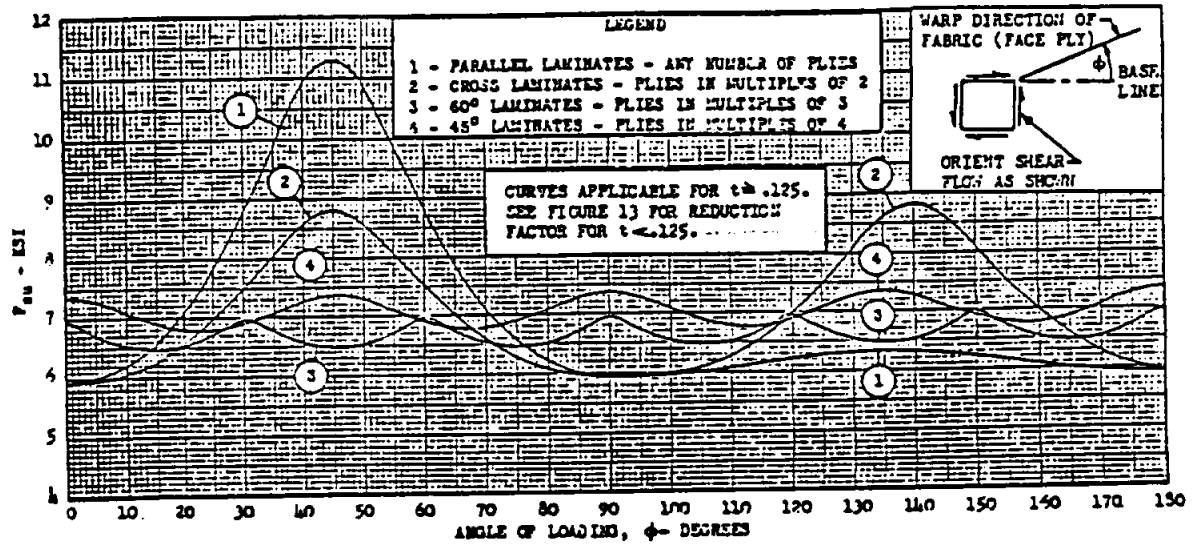
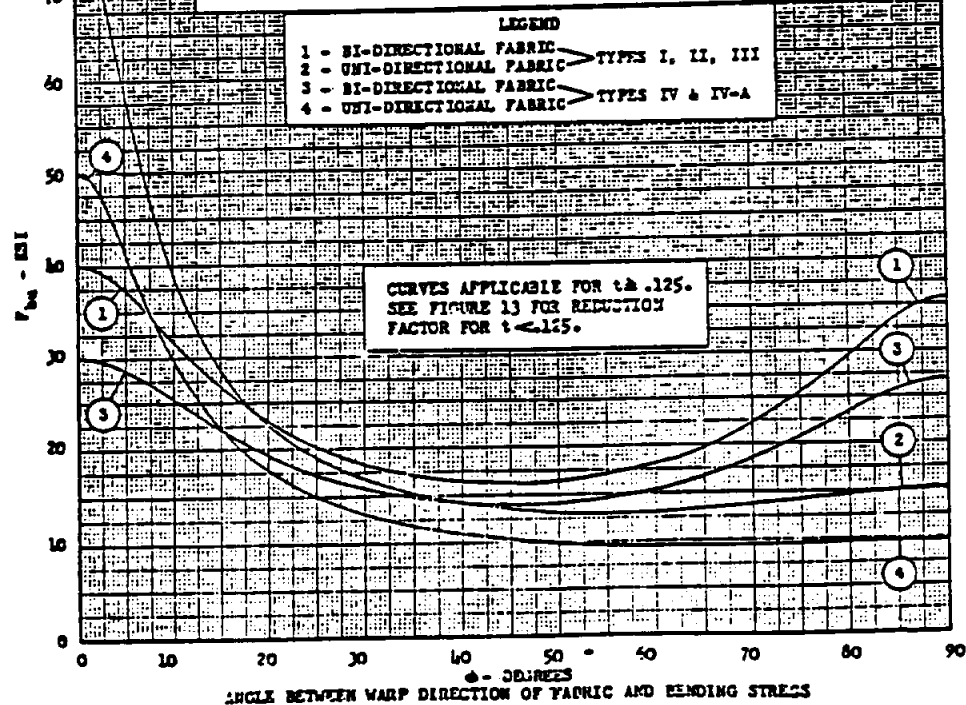


FIGURE 10
BENDING MODULUS OF RUPTURE
OF PARALLEL LAMINATED UNI-DIRECTIONAL AND BI-DIRECTIONAL FABRICS
AS A FUNCTION OF WARP ORIENTATION TO BENDING STRESS



STRUCTURAL ANALYSIS MANUAL

GENERAL DYNAMICS/CONVAIR AND SPACE SYSTEMS DIVISION

FIGURE 11

COMPRESSIVE MODULUS OF ELASTICITY OF BI-DIRECTIONAL FABRICS
FOR VARIOUS ANGLES OF LOADING AT SEVERAL LAY-UPS
TYPES I, II & III

(FOR TYPES IV & IV-A, MULTIPLY VALUES BY .88)

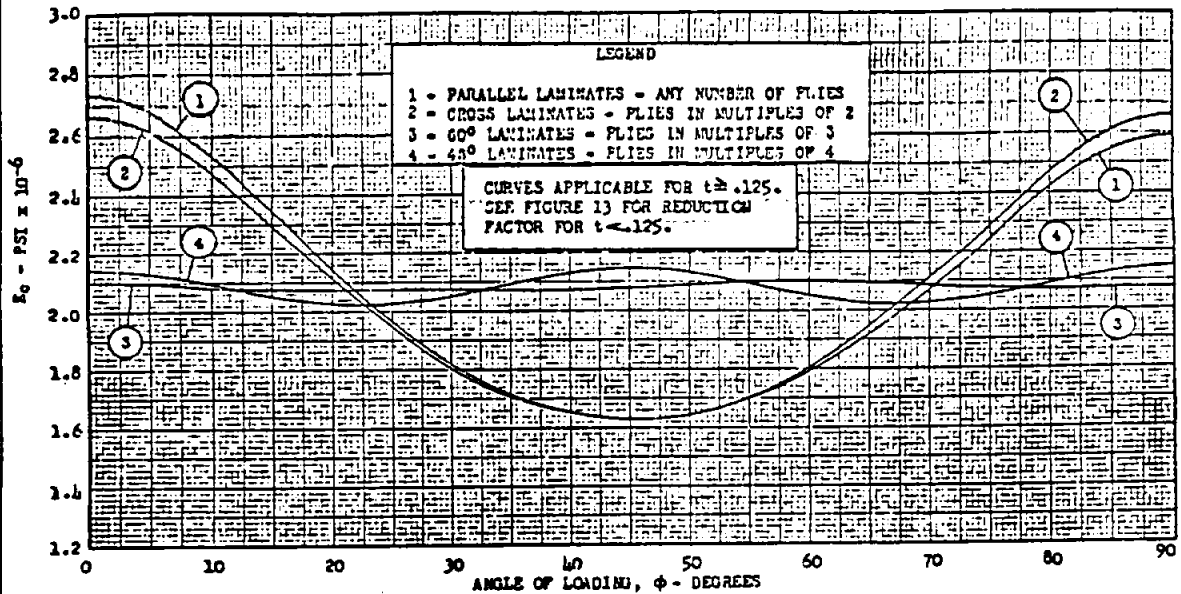
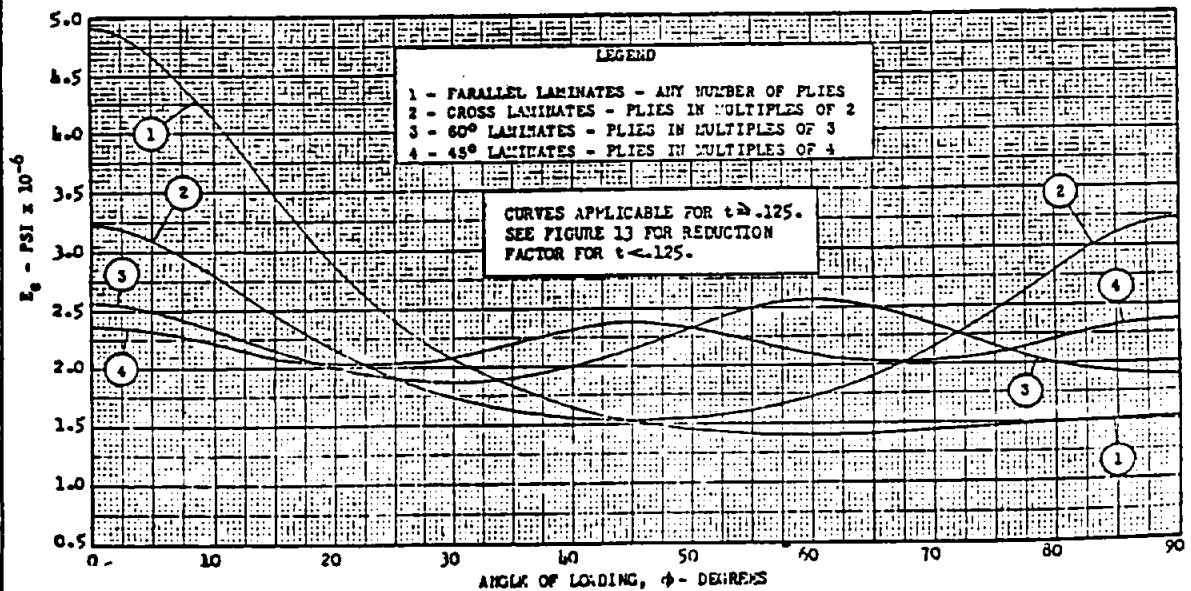


FIGURE 12

COMPRESSIVE MODULUS OF ELASTICITY OF UNI-DIRECTIONAL FABRIC
FOR VARIOUS ANGLES OF LOADING AT SEVERAL LAY-UPS
TYPES I, II & III

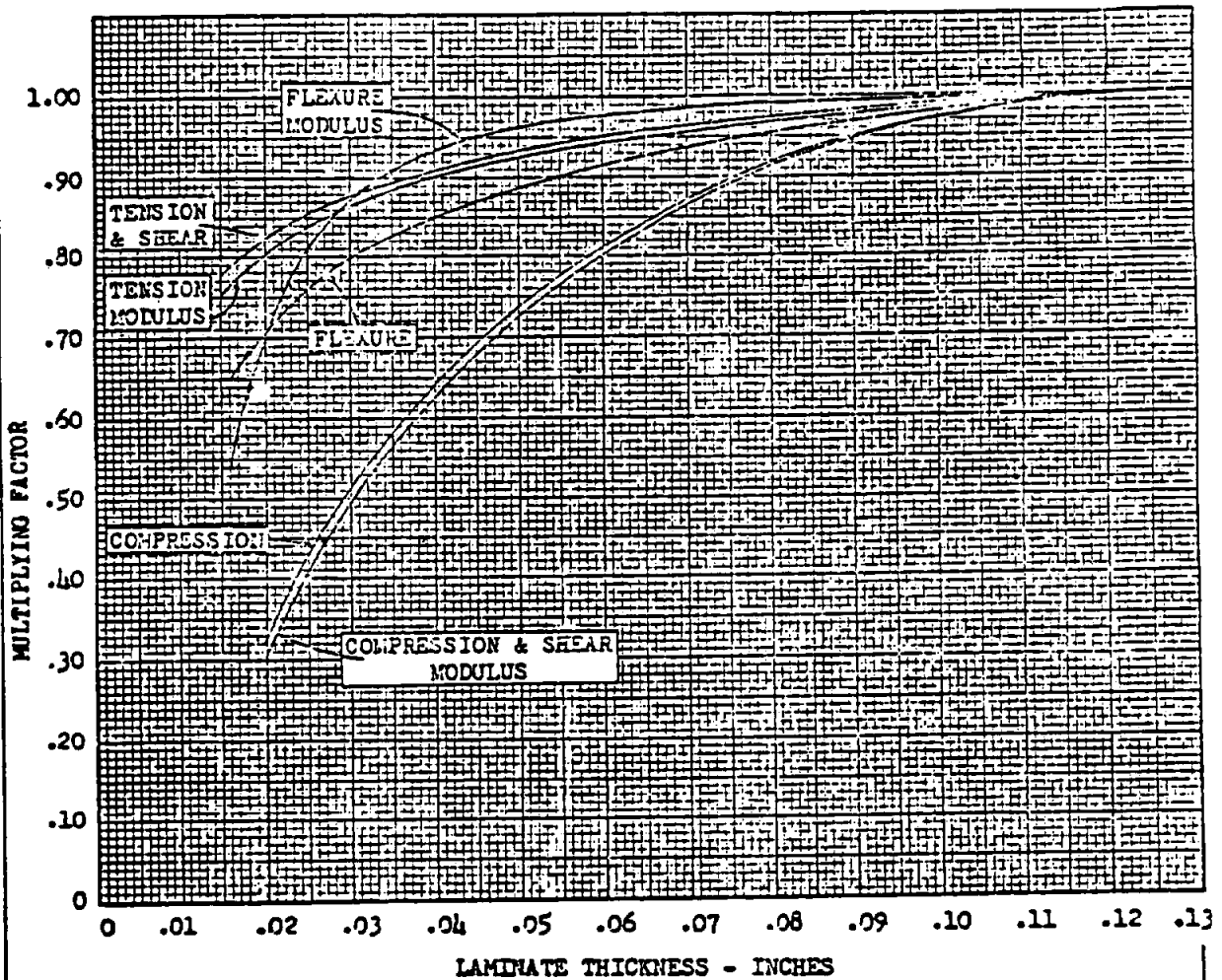
(FOR TYPES IV & IV-A, MULTIPLY VALUES BY .844)



STRUCTURAL ANALYSIS MANUAL
GENERAL DYNAMICS/CONVAIR AND SPACE SYSTEMS DIVISION

FIGURE 13

MULTIPLYING FACTORS FOR ULTIMATE STRENGTHS
AND MODULI OF ELASTICITY OF GLASS-FABRIC LAMINATES
AT VARIOUS THICKNESSES



STRUCTURAL ANALYSIS MANUAL **GENERAL DYNAMICS/CONVAIR AND SPACE SYSTEMS DIVISION**

FIGURE 14
 BEARING STRENGTH OF PARALLEL-LAMINATED BI-DIRECTIONAL FABRIC
 LOADING PARALLEL TO WARP DIRECTION

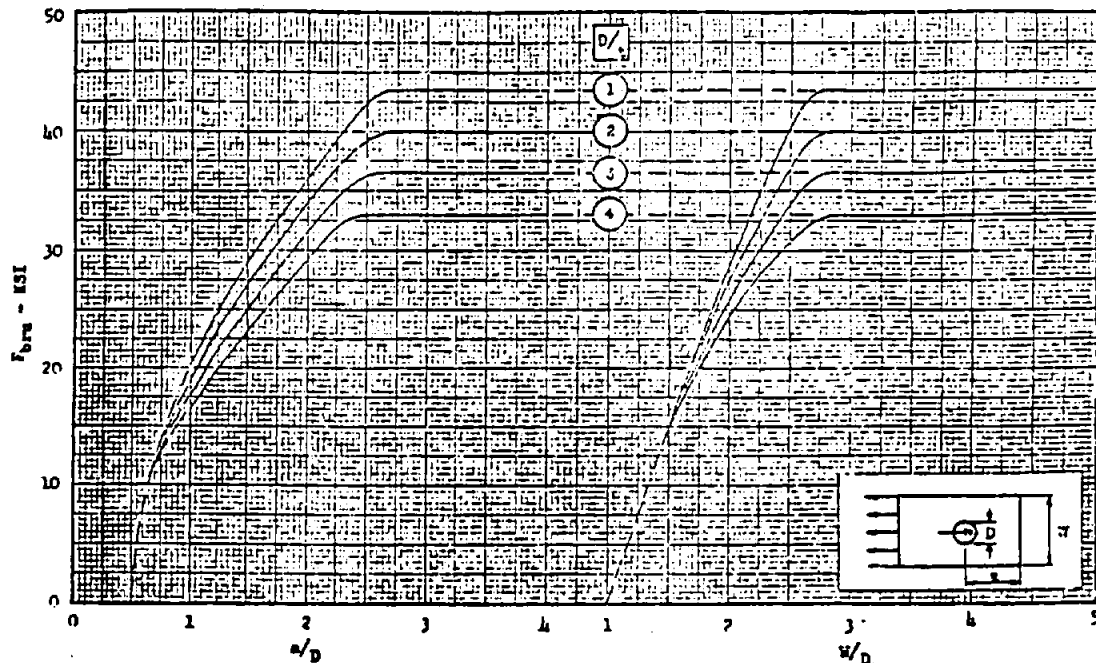
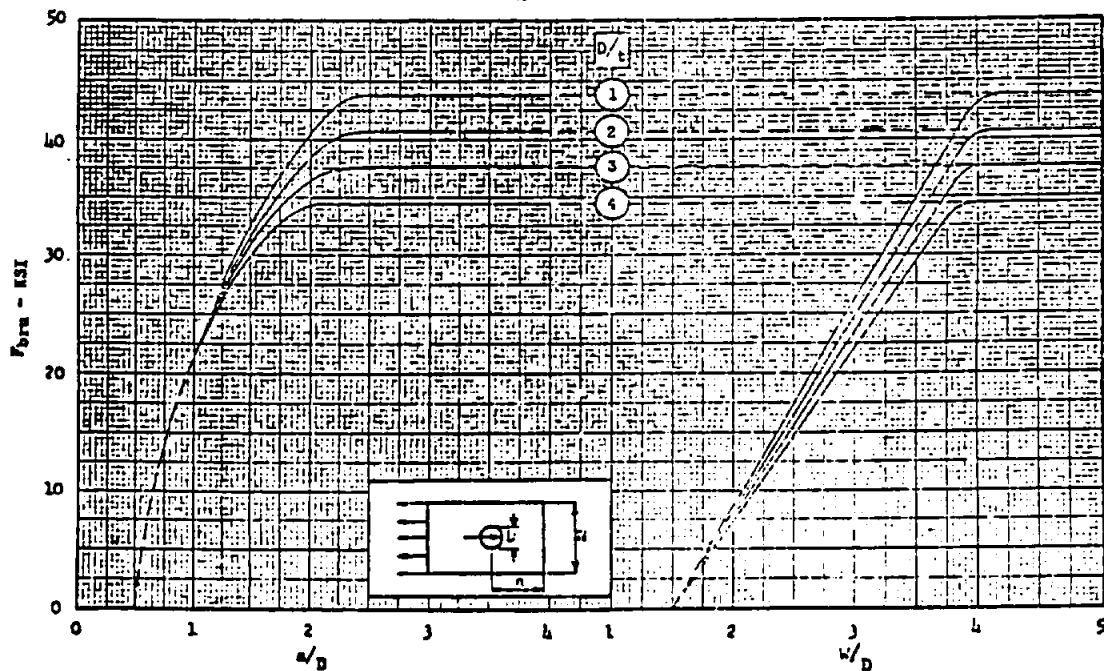


FIGURE 15
 BEARING STRENGTH OF PARALLEL-LAMINATED BI-DIRECTIONAL FABRIC
 LOADING 45° TO WARP DIRECTION



STRUCTURAL ANALYSIS MANUAL **GENERAL DYNAMICS/CONVAIR AND SPACE SYSTEMS DIVISION**

FIGURE 16

BEARING STRENGTH OF PARALLEL-LAMINATED BI-DIRECTIONAL FABRIC
 LOADING PERPENDICULAR TO WARP DIRECTION

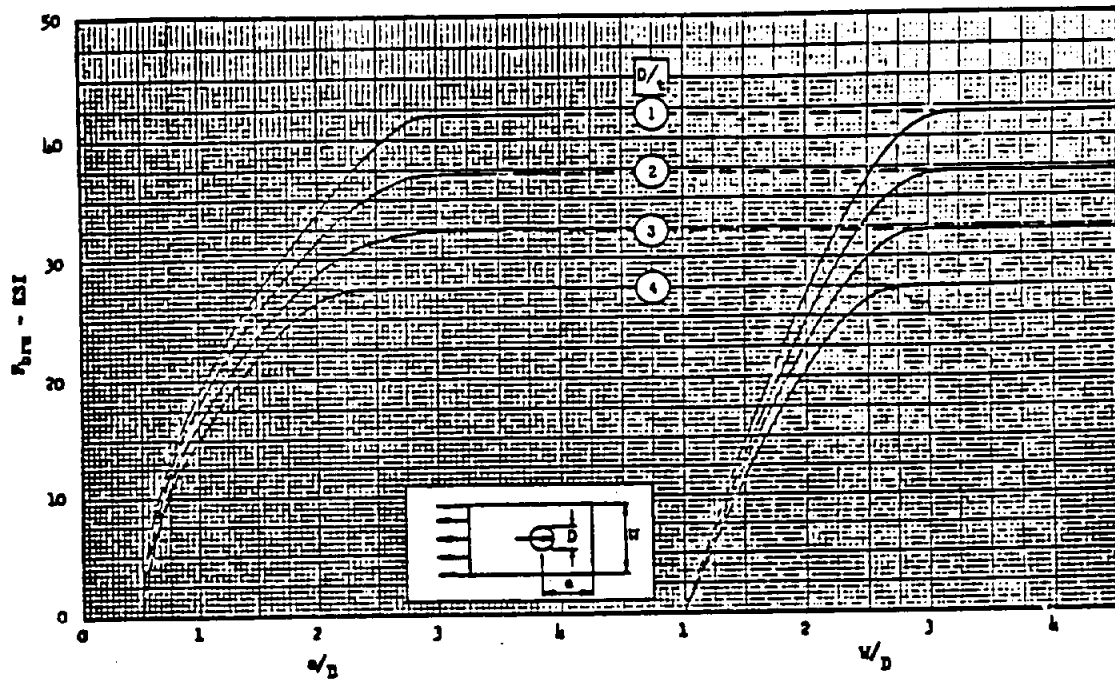
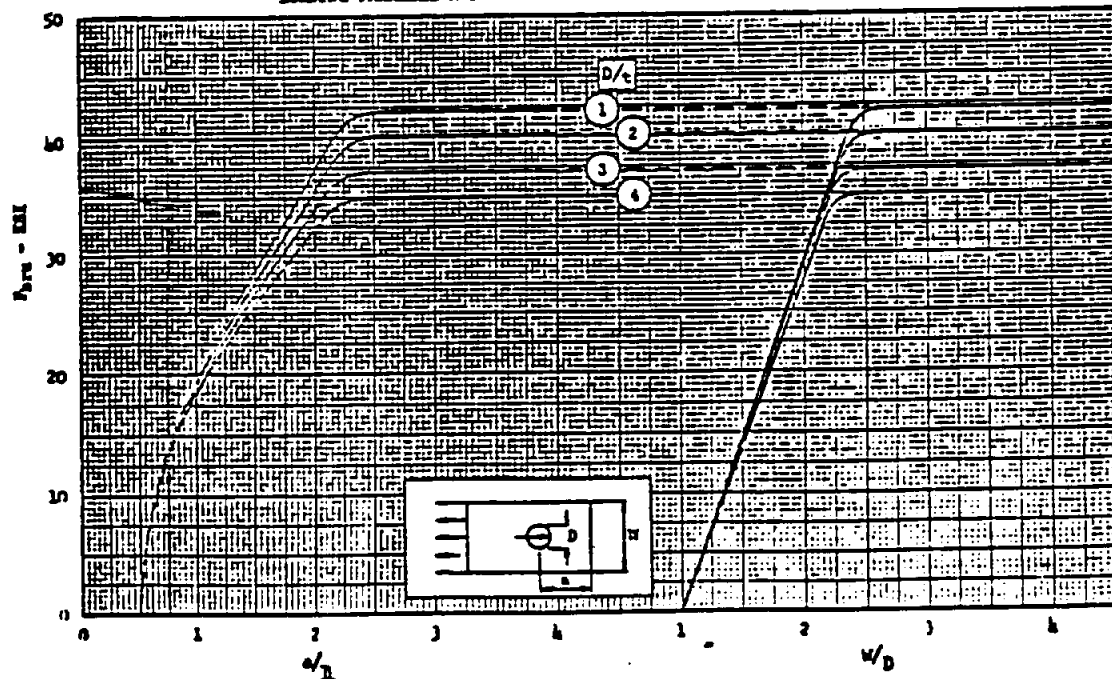


FIGURE 17

BEARING STRENGTH OF CROSS-LAMINATED UNI-DIRECTIONAL FABRIC
 LOADING PARALLEL AND PERPENDICULAR TO WARP DIRECTION



STRUCTURAL ANALYSIS MANUAL
GENERAL DYNAMICS/CONVAIR AND SPACE SYSTEMS DIVISION

FIGURE 18

BEARING STRENGTH OF CROSS-LAMINATED UNI-DIRECTIONAL FABRIC

LOADING 45° TO WARP DIRECTION

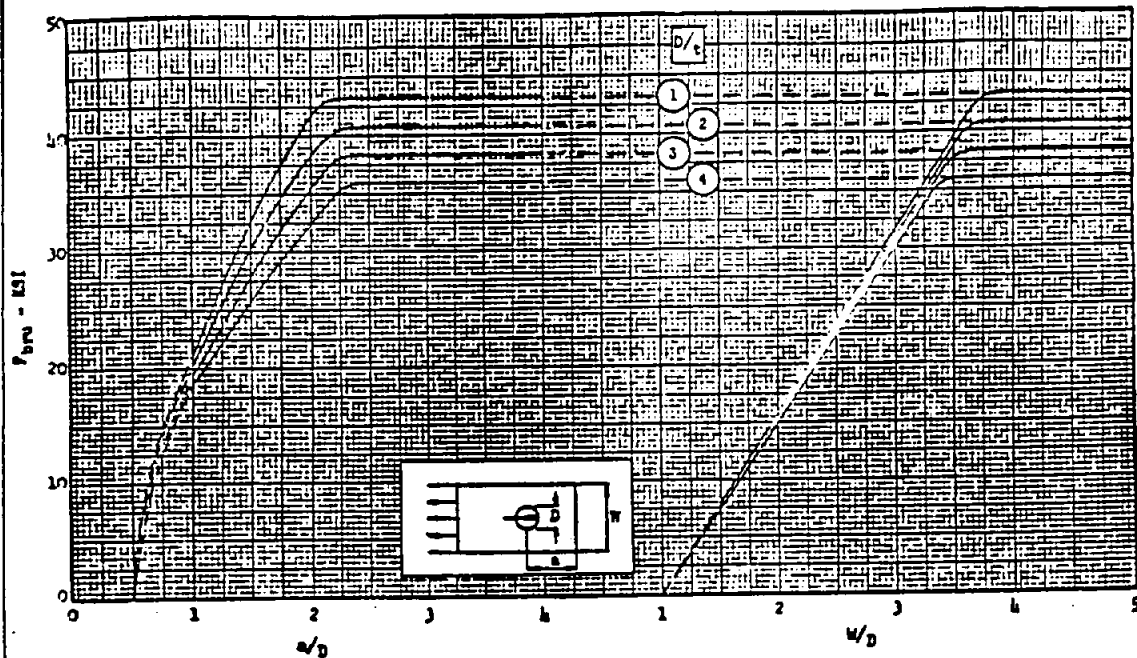
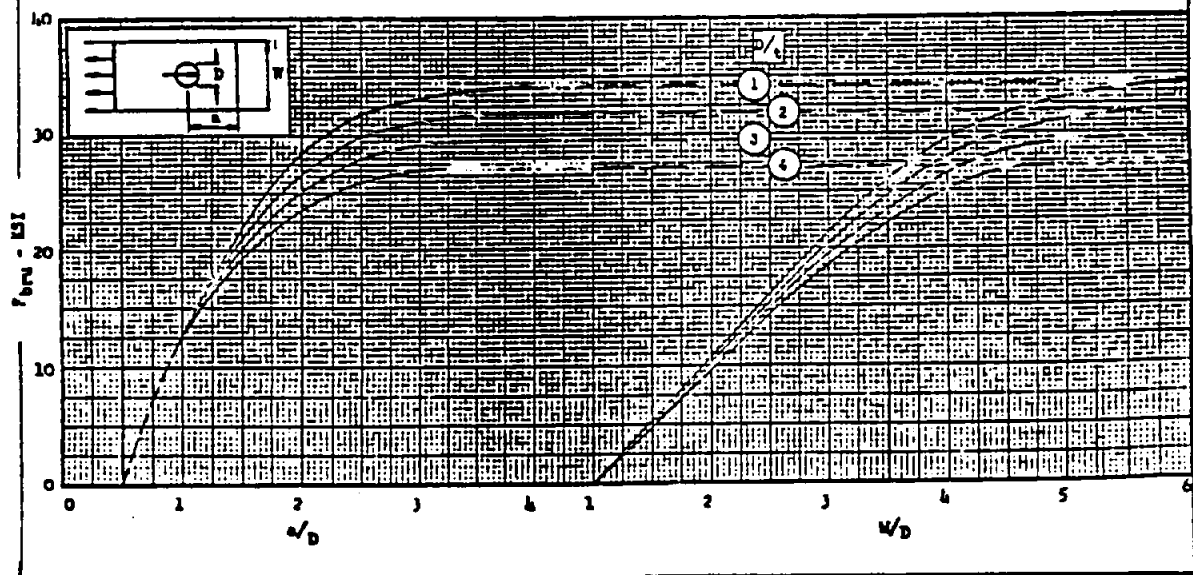
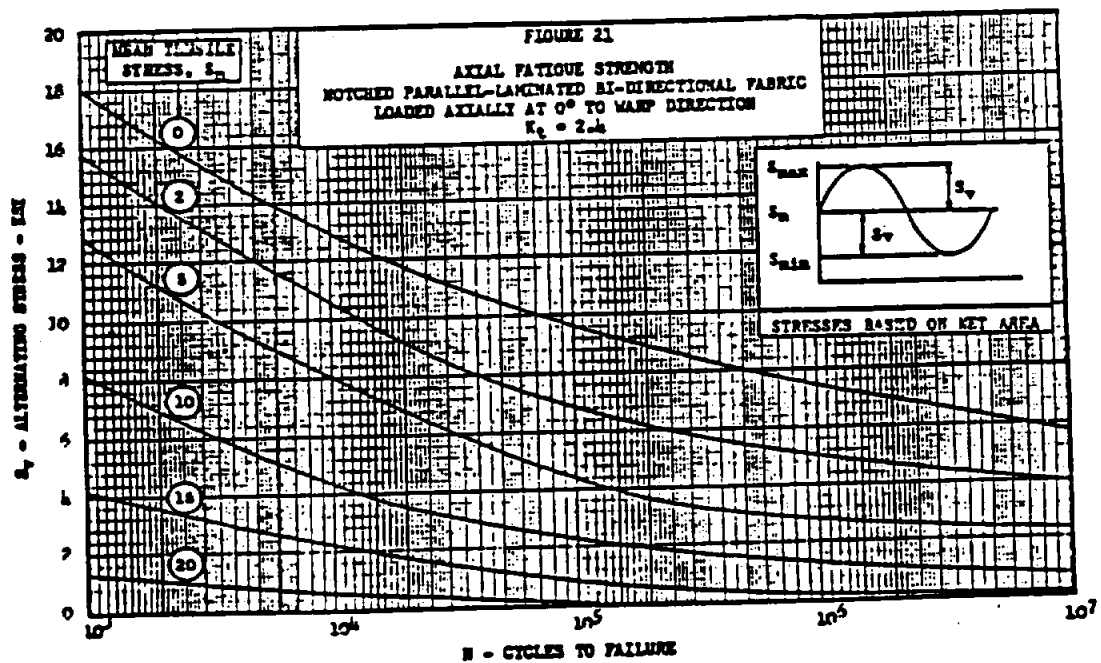
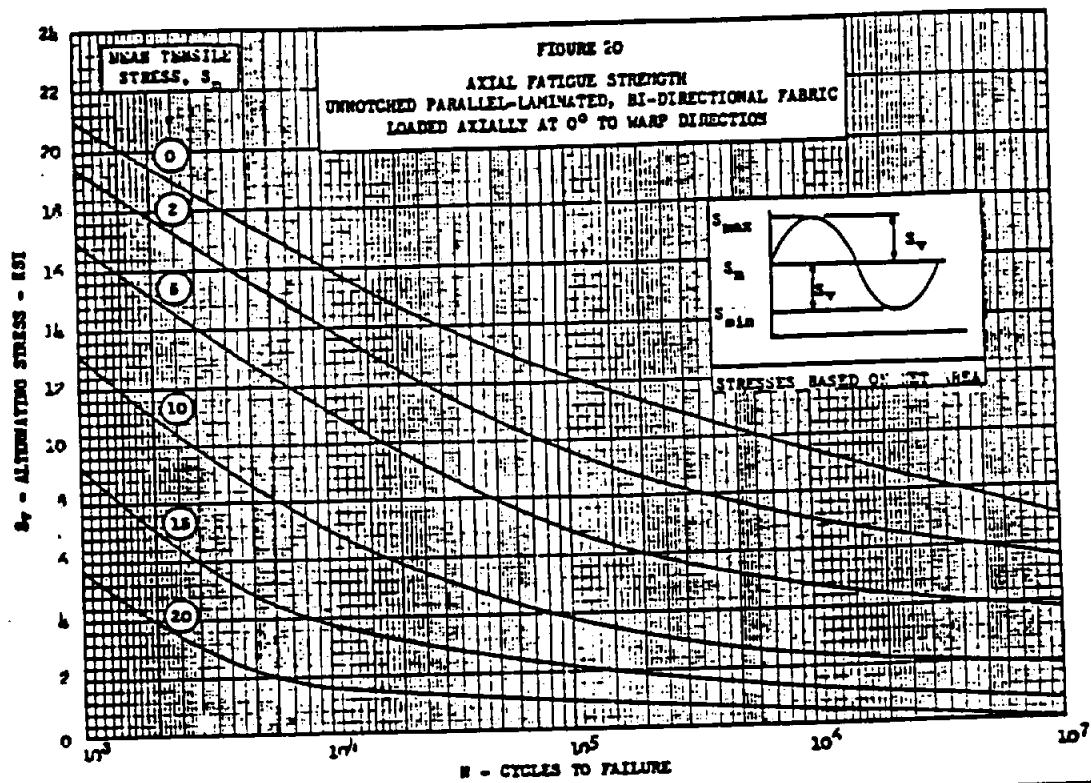


FIGURE 19

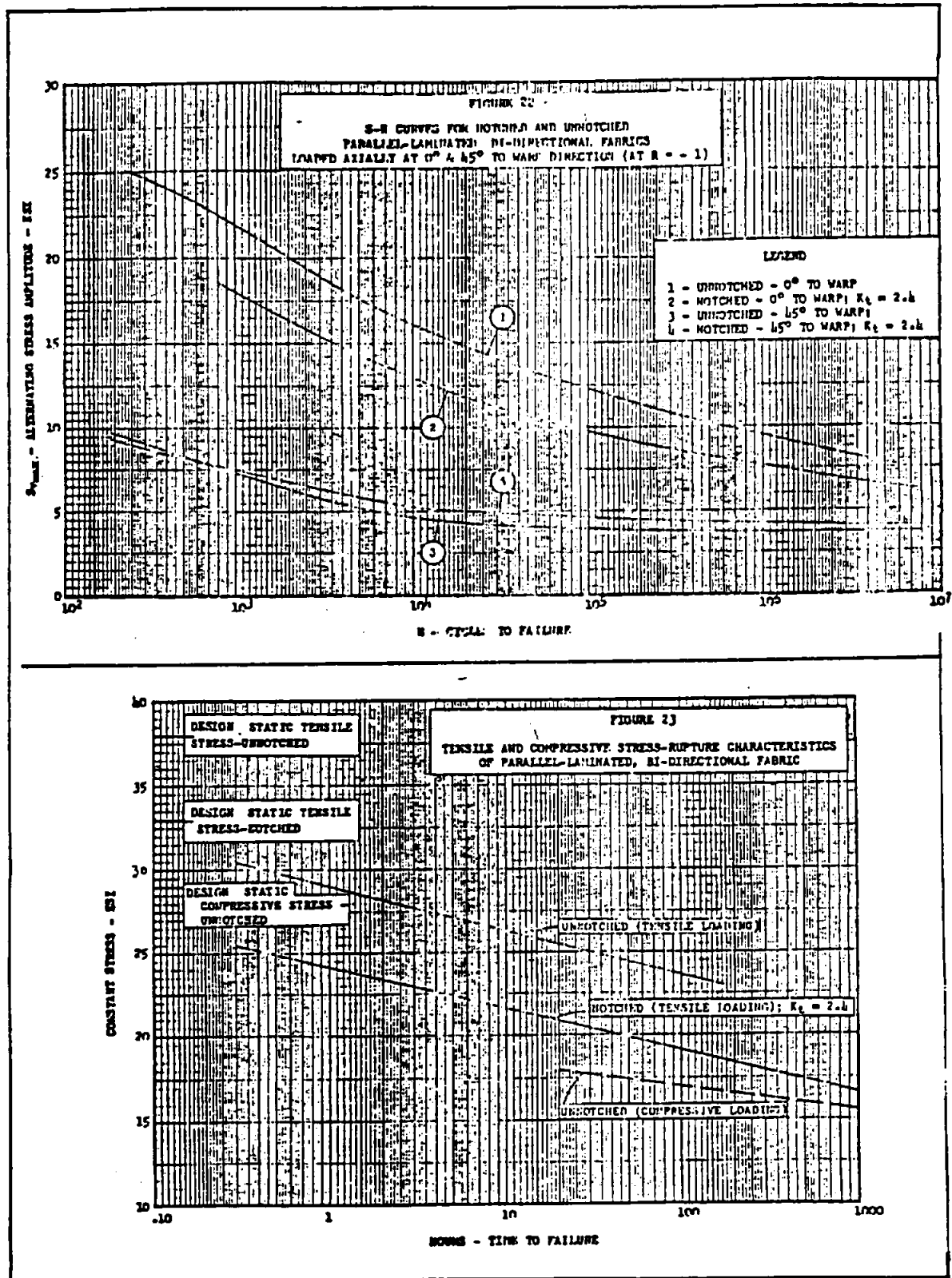
BEARING STRENGTH OF BONDED MAT LAMINATE



STRUCTURAL ANALYSIS MANUAL **GENERAL DYNAMICS/CONVAIR AND SPACE SYSTEMS DIVISION**

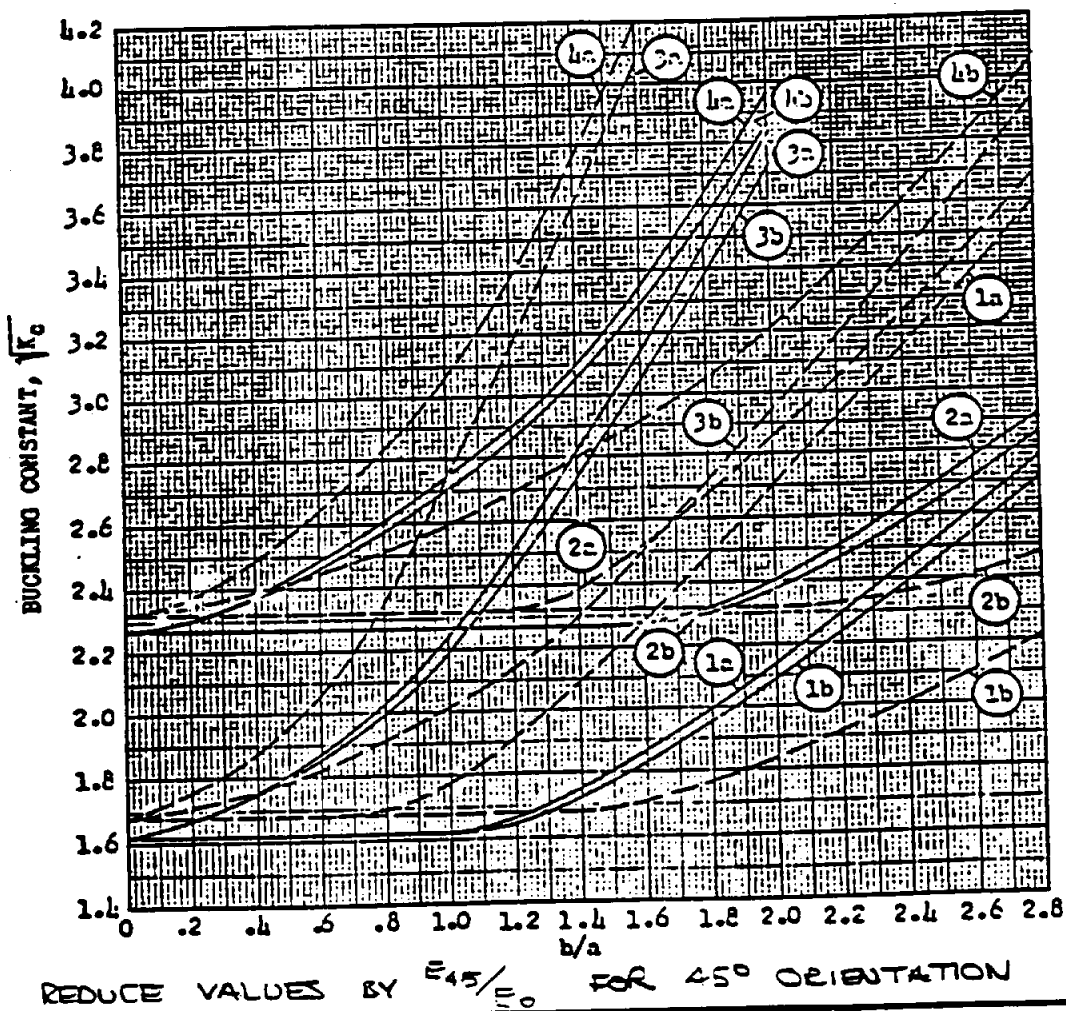
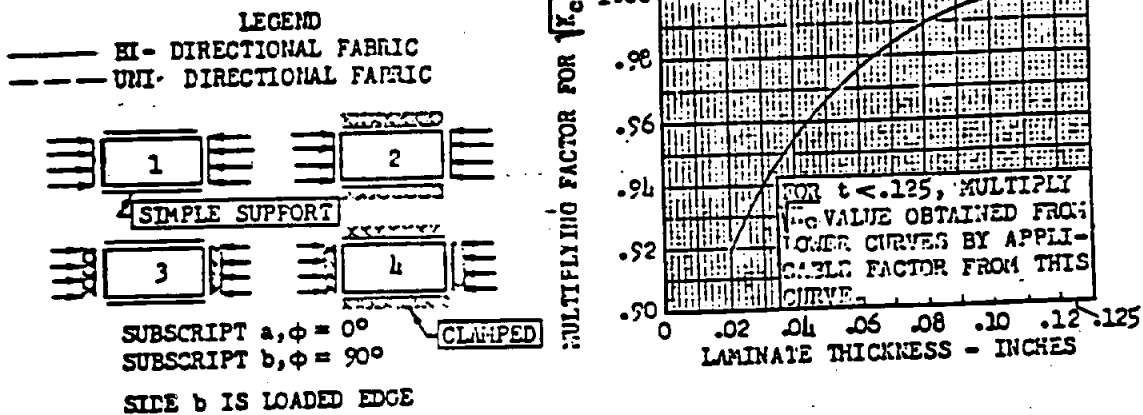


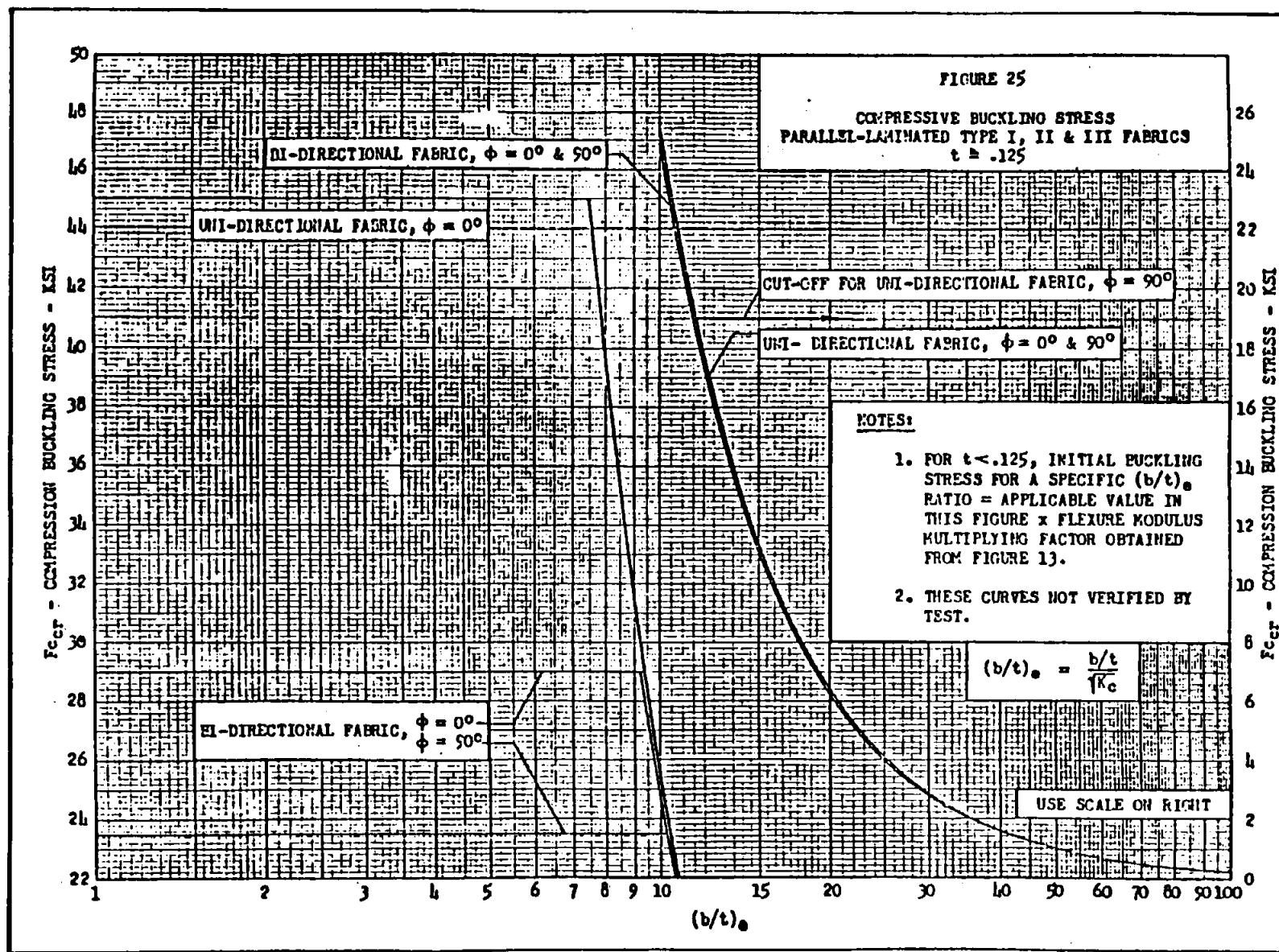
STRUCTURAL ANALYSIS MANUAL
GENERAL DYNAMICS/CONVAIR AND SPACE SYSTEMS DIVISION



STRUCTURAL ANALYSIS MANUAL **GENERAL DYNAMICS/CONVAIR AND SPACE SYSTEMS DIVISION**

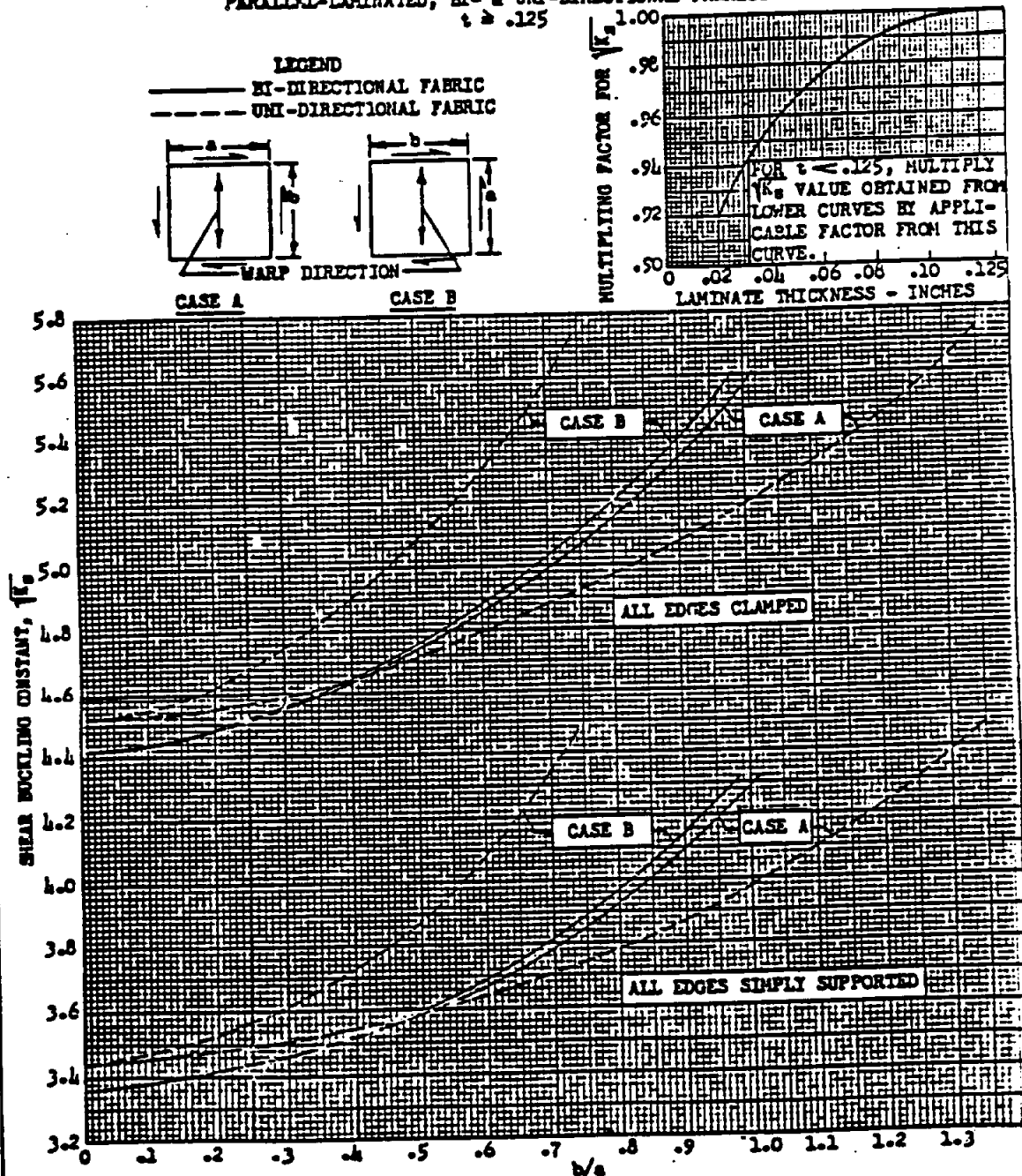
FIGURE 24
COMPRESSIVE BUCKLING CONSTANT
PARALLEL-LAMINATED, BI- & UNI-DIRECTIONAL FABRICS
 $\phi = 0^\circ \text{ \& \; } 90^\circ \quad t \geq .125$

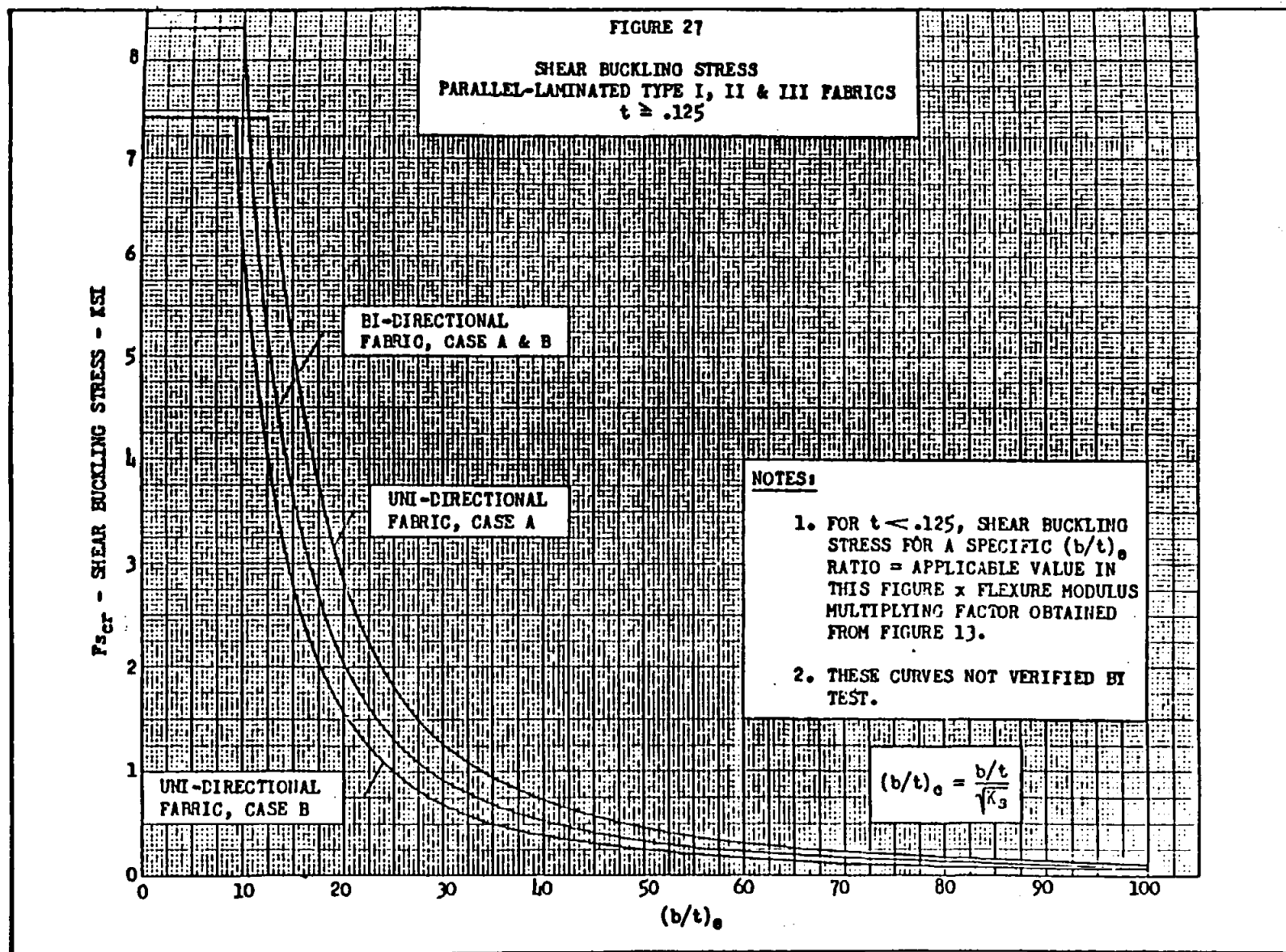


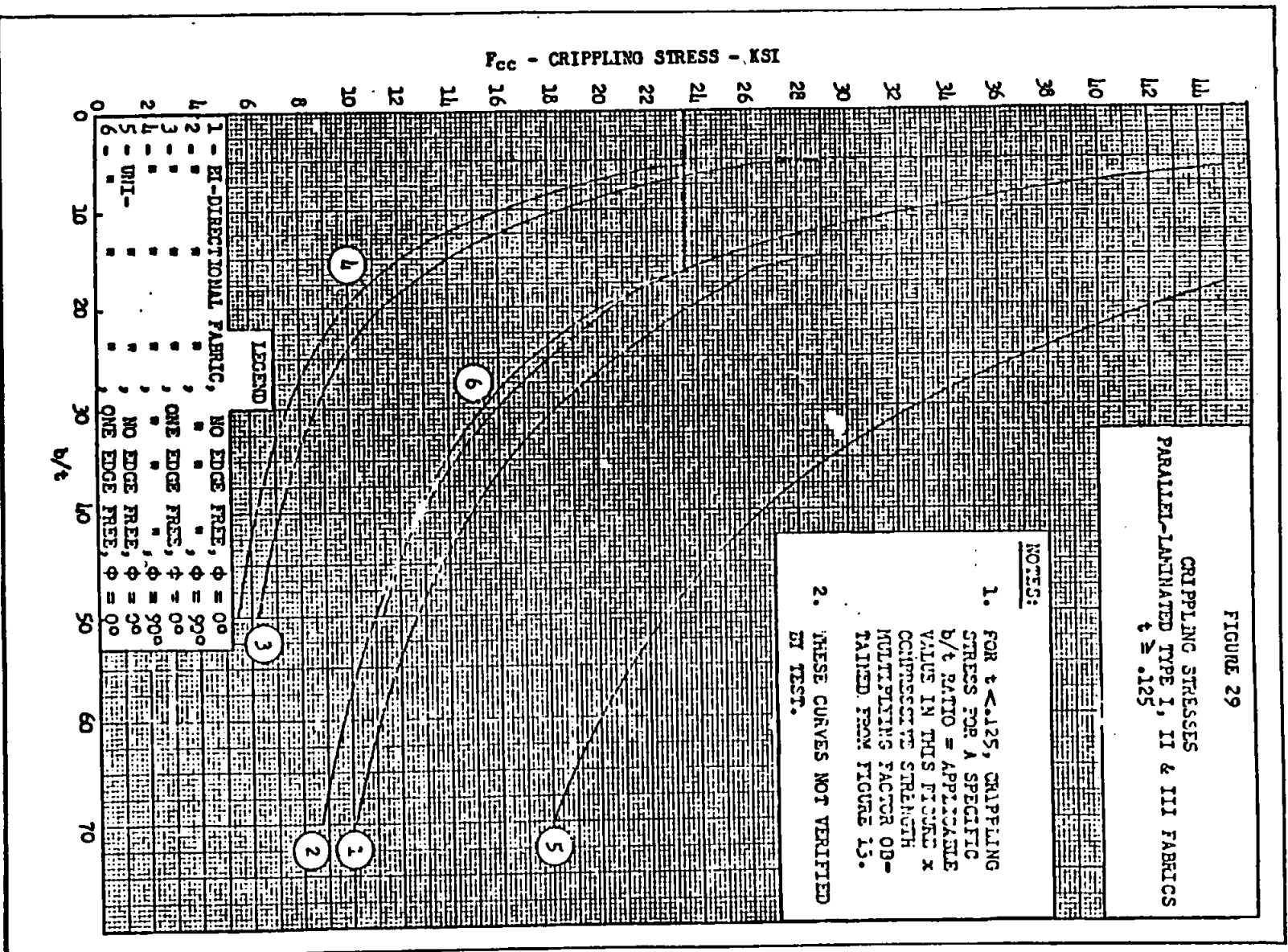


STRUCTURAL ANALYSIS MANUAL **GENERAL DYNAMICS/CONVAIR AND SPACE SYSTEMS DIVISION**

FIGURE 26
SHEAR BUCKLING CONSTANT
PARALLEL-LAMINATED, BI- & UNI-DIRECTIONAL FABRICS
 $t \geq .125$







STRUCTURAL ANALYSIS MANUAL
GENERAL DYNAMICS/CONVAIR AND SPACE SYSTEMS DIVISION

Data Source, Section 1.3 Reference 30

NONMETALLIC MATERIALS
PHENOLIC OR EPOXY RESIN

5.1 GENERAL

Nonmetallic structural elements used in Centaur are composite systems of glass reinforced plastic (GRP). Various composite systems are used for solid laminates and honeycomb sandwich plates. The mechanical properties of GRP systems vary considerably with the specific materials used and the fabrication techniques employed. General design criteria and related information are included in Reference 44. Minimum strength requirements, for specific GRP solid laminate systems used in Centaur structures, have been developed and are included in their respective purchase specifications.

5.2 MATERIALS AND MECHANICAL PROPERTIES

Materials used in Centaur GRP systems are:

- a. Bi-directional glass cloth (wet lay-up or preimpregnated with resin);
- b. Phenolic (MIL-R-9299) or epoxy (high temperature resistant, thermosetting) resins of a low pressure laminating type;
- c. Dry film structural adhesive (epoxy-phenolic) for use in sandwich structure;
- d. Glass fabric phenolic honeycomb core material.

Physical and mechanical properties taken from Reference 44 and specific purchase specifications are presented in Tables 5.1 through 5.5.

5.2.1 VARIANCE OF BASIC MECHANICAL PROPERTIES WITH THICKNESS. The data in Tables 5-1 through 5-4 are presented for laminate thicknesses of about 1/8 to 1/4 inch. Test data has demonstrated substantial reductions in tensile, compressive and flexural strength for thin laminates, particularly those less than about 1/32 inch. Thickness reduction factors are contained in Figure 5-1.

5.2.2 BOLT BEARING ALLOWABLES. Bolt bearing allowables for GRP laminates, taken from Reference 48 are presented in Figures 5-2 through 5-5. Figure 5-2 presents maximum allowable bolt bearing as a function of bolt diameter and laminate thickness. Figures 5-3, 5-4, and 5-5 are reduction factors for skin thickness, edge distance, or bolt spacing and temperature, respectively.

TABLE 5-1. MECHANICAL PROPERTIES - PARALLEL LAMINATES OF GLASS FABRIC -
PHENOLIC RESIN (ROOM TEMPERATURE)

	Laminate	Angle of Loading (deg)	Modulus of Elasticity $\times 10^6$ (PSI)	Ultimate Strength (PSI)
F_{tu}	120 FABRIC	0	2.56	38,000
		90	2.41	35,700
		45	1.76	17,900
	181 FABRIC	0	2.34	38,000
		90	2.15	35,100
		45	1.57	17,800
F_{cu}	120 FABRIC	0	2.73	30,000
		90	2.71	26,100
	181 FABRIC	0	2.94	30,000
		90	2.82	31,600
F_b	120 FABRIC	0	2.50	45,000
		90	2.43	35,700
	181 FABRIC	0	2.50	45,000
		90	2.35	40,900
EDGEWISE SHEAR	120 FABRIC	0 & 90	0.64	9,230
	181 FABRIC	0 & 90	0.57	9,180

(DATA FROM REFERENCE 44)

TABLE 5-2. MECHANICAL PROPERTIES - PARALLEL LAMINATES OF GLASS FABRIC - EPOXY RESIN (ROOM TEMPERATURE)

	Laminate	Angle of Loading (deg)	Modulus of Elasticity $\times 10^6$ (PSI)	Ultimate Strength (PSI)
F_{tu}	120 FABRIC	0	2.2	45,000
		90	2.1	43,700
		45	1.6	22,800
	181 FABRIC	0	2.88	45,000
		90	2.66	42,400
		45	2.20	26,600
F_{cu}	120 FABRIC	0	3.25	45,000
		90	2.85	43,600
	181 FABRIC	0	3.28	45,000
		90	3.14	38,200
F_b	120 FABRIC	0	3.20	65,000
		90	3.10	62,400
	181 FABRIC	0	3.20	65,000
		90	3.04	57,000
EDGEWISE SHEAR	120 FABRIC	0 & 90	0.580	11,800
	181 FABRIC	0 & 90	0.810	14,000

(DATA FROM REFERENCE 44)

TABLE 5-3. LONGITUDINAL MECHANICAL PROPERTIES OF GLASS-REINFORCED PLASTIC-EPOXY RESIN

Material		Epoxy Wet Lay-Up (2)			Epoxy Preimpregnated (3)			
		Class I		Class I	Class I and II		Class I and II	Class II
Name of Test	Fabric Style	Room Temp.		300°F	Room Temp.		300°F	500°F
		Dry	Wet (6)		Dry	Wet (6)		
ULTIMATE FLEXURAL STRENGTH KSI (4)	120	65	58	42	50	45	42	20
	181	65	58	42	50	45	42	20
	183	65	58	42	50	45	42	20
	143	117	104	76	90	80	76	32
FLEXURAL MODULUS OF ELASTICITY $\times 10^6$ PSI (5)	120	2.9	2.4	2.2	2.4	2.4	2.4	2.0
	181	2.9	2.4	2.2	2.4	2.4	2.4	2.0
	183	2.9	2.4	2.2	2.4	2.4	2.4	2.0
	143	5.0	4.1	3.8	4.1	4.1	3.6	3.1
ULTIMATE TENSILE STRENGTH KSI (4)	120	47	45	30	40	36	33	26
	181	47	45	30	40	36	33	26
	183	47	45	30	40	36	33	26
	143	91	87	58	77	68	58	50
ULTIMATE COMPRESSIVE STRENGTH (EDGEWISE) KSI (4)	120	48	45	25	35	32	25	14
	181	48	45	25	35	32	25	14
	183	48	45	25	35	32	25	14
	143	70	66	37	52	44	37	20

NOTES:

- (1) ALL PROPERTIES LISTED ARE FOR PARALLEL LAMINATED PANELS TESTED IN THE DIRECTION OF THE WARP.
- (2) LAMINATES MADE FROM EPOXY RESIN AND GLASS FABRIC (NOT PREIMPREGNATED).
- (3) LAMINATES MADE FROM EPOXY RESIN PREIMPREGNATED GLASS FABRIC.
- (4) KSI = THOUSANDS OF POUNDS PER SQUARE INCH.
- (5) PSI = POUNDS PER SQUARE INCH.
- (6) THE WET TEST, WHERE THE MATERIAL IS SUBJECT TO TWO HOURS IN BOILING WATER, SIMULATES SEVERAL YEARS OF WEATHERING EXPOSURE DAMAGE TO THE SUN AND RAIN.

(FROM GD/A 0-73009 SPECIFICATION FOR EPOXY LAMINATING MATERIALS FOR USE IN GLASS REINFORCED PLASTIC AND SANDWICH CONSTRUCTION).

STRUCTURAL ANALYSIS MANUAL
GENERAL DYNAMICS/CONVAIR AND SPACE SYSTEMS DIVISION

TABLE 3-4. LONGITUDINAL MECHANICAL PROPERTIES OF GLASS REINFORCED
 PLASTIC - PHENOLIC RESIN PREIMPREGNATED

Name of Test	Test Conditions			
	Fabric Style No.	Dry	Wet	500°
ULTIMATE FLEXURAL STRENGTH (FLATWISE) (2) KSI	120	50	45	40
	143	90	81	72
	181	50	45	40
	183	45	40	38
FLEXURAL MODULUS OF ELASTICITY PSI (3) x 10 ⁶	120	2.9	2.5	2.4
	143	5.2	4.3	4.3
	181	3.0	2.5	2.5
	183	2.9	2.5	2.4
ULTIMATE COMPRESSIVE STRENGTH (EDGEWISE) KSI(3)	120	33	30	28
	143	51	44	38
	181	35	30	26
	183	30	27	23
ULTIMATE TENSILE STRENGTH KSI(2)	120	40	38	30
	143	77	73	58
	181	40	38	30
	183	43	40	32

(1) ALL PROPERTIES LISTED ARE FOR PARALLEL LAMINATED PANELS,
 TESTED IN DIRECTION OF THE WARP.

(2) KSI = THOUSANDS OF POUNDS PER SQUARE INCH.

(3) PSI = POUNDS PER SQUARE INCH.

(FROM GD/A 0-73003 SPECIFICATION FOR GLASS FABRICS, PHENOLIC PRESSURE
 PREIMPREGNATED - LOW PRESSURE LAMINATING)

TABLE 5-5. GLASS FABRIC HONEYCOMB CORE MATERIAL - PHYSICAL AND MECHANICAL PROPERTIES

Resin Nomenclature	Cell Nomenclature	Density Range Lbs/cu ft	Bare Flatwise Compressive Strength Psi (Minimum)		Beam Shear Strength Psi (Minimum)			
			75 ± 10° F	500 ± 5° F	L-Direction		W-Direction	
					75 ± 10° F	500 ± 5° F	75 ± 10° F	500 ± 5° F
HRP (Heat Resistant Phenolic)	Hexagonal 3/16	4.0 min. 4.6 max.	345	180	160	105	80	55
HRP (Heat Resistant Phenolic)	Hexagonal 3/16	5.5 min. 6.4 max.	700	365	330	220	170	110
HRP (Heat Resistant Phenolic)	Hexagonal 3/16	7.6 min. 8.8 max.	1120	580	560	370	300	200
HRP (Heat Resistant Phenolic)	Over-Expanded 1/4	4.1 min. 4.7 max.	325	170	100	66	115	75
HRP (Heat Resistant Phenolic)	Over-Expanded 1/4	5.7 min. 6.6 max.	695	360	210	140	225	150
HRP (Heat Resistant Phenolic)	Over-Expanded 1/4	6.5 min. 8.0 max.	625	325	290	190	290	190
HRP (Heat Resistant Phenolic)	Over-Expanded 1/4	7.8 min. 9.0 max.	1170	610	360	240	360	240

TABLE 5-5. GLASS FABRIC HONEYCOMB CORE MATERIAL - PHYSICAL AND MECHANICAL PROPERTIES (Continued)

Resin Nomenclature	Cell Nomenclature	Density Range Lbs/cu ft	Bare Flatwise Compressive Strength Psi (Minimum)		Beam Shear Strength Psi (Minimum)			
			75 ± 10° F	500 ± 5° F	L-Direction		W-Direction	
					75 ± 10° F	500 ± 5° F	75 ± 10° F	500 ± 5° F
HRP (Heat Resistant Phenolic)	Over-Expanded 3/8	3.0 min. 3.6 max.	250	130	130	85	130	85
HRP (Heat Resistant Phenolic)	Over-Expanded 3/8	5.0 min. 6.0 max.	675	350	230	150	230	150

- NOTES: (1) The 500° F Bare Compressive Strength values are based on 52% of the room temperature values.
 (2) The 500° F Beam Shear Strength values are based on 66% of the room temperature values.
 (3) L-Direction is the longitudinal core ribbon direction.
 (4) W-Direction is the transverse core ribbon direction.

(From GD/A 0-73017 - Specification for Core Material, Glass Fabric, Phenolic)

STRUCTURAL ANALYSIS MANUAL **GENERAL DYNAMICS/CONVAIR AND SPACE SYSTEMS DIVISION**

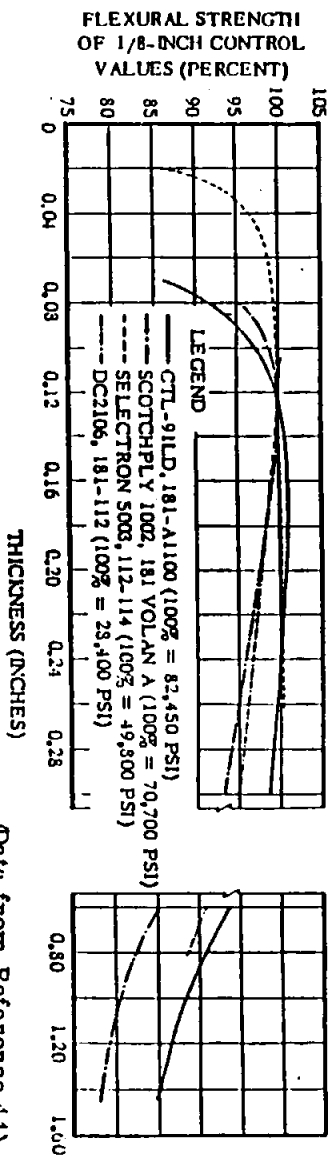
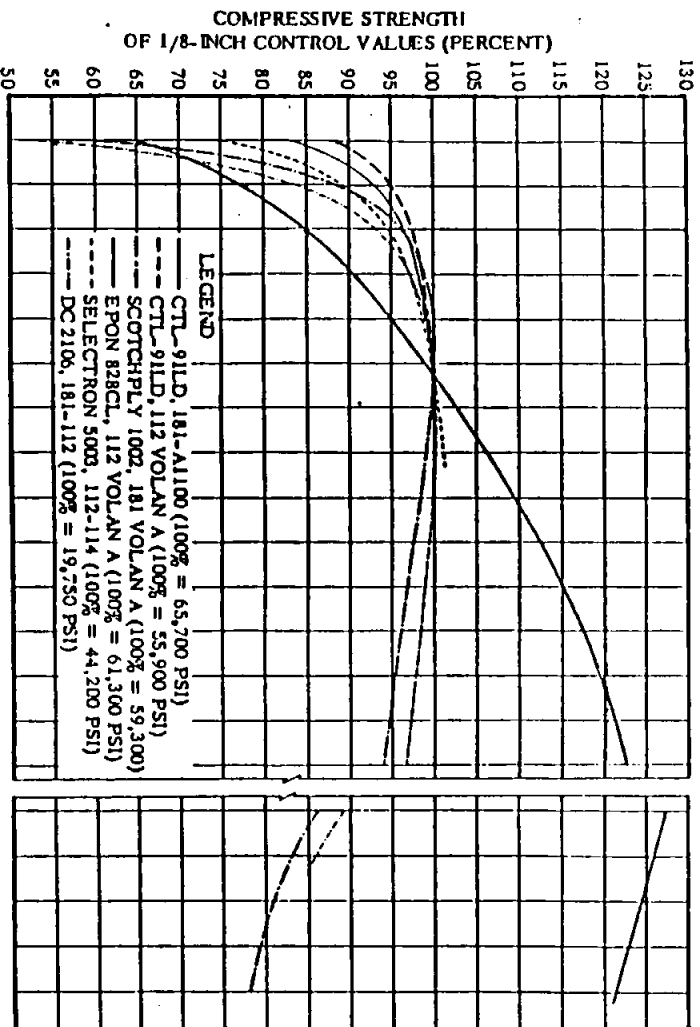
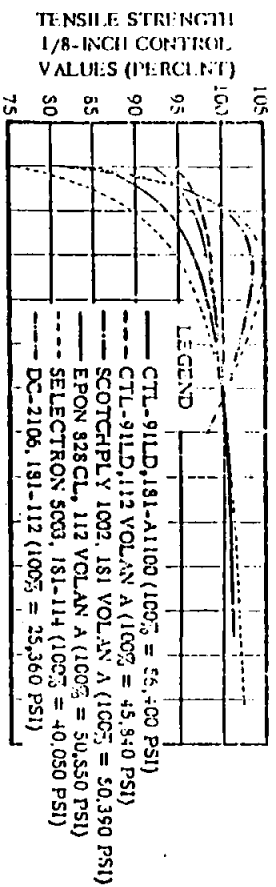


Figure 5-1. Effect of Thickness on the Tensile, Compressive, and Flexural Strengths of Various Reinforced Plastic Laminates. Expressed as Percent of the 1/8-inch-thick Control Values

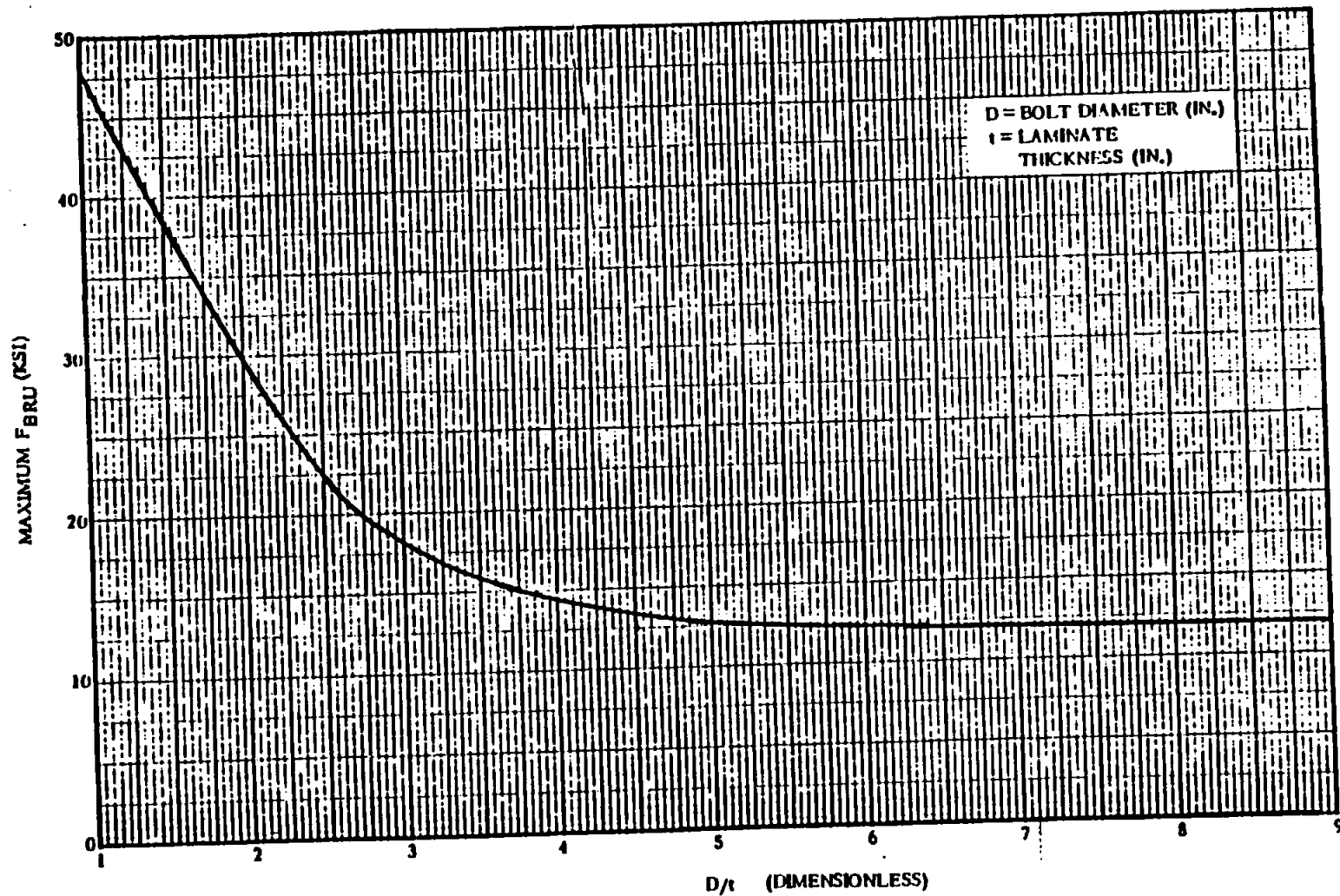


Figure 5-2. Maximum Allowable Bolt Bearing Stress Vs D/t
(Solid Laminate Phenolic 181 & 120 Glass Cloth)

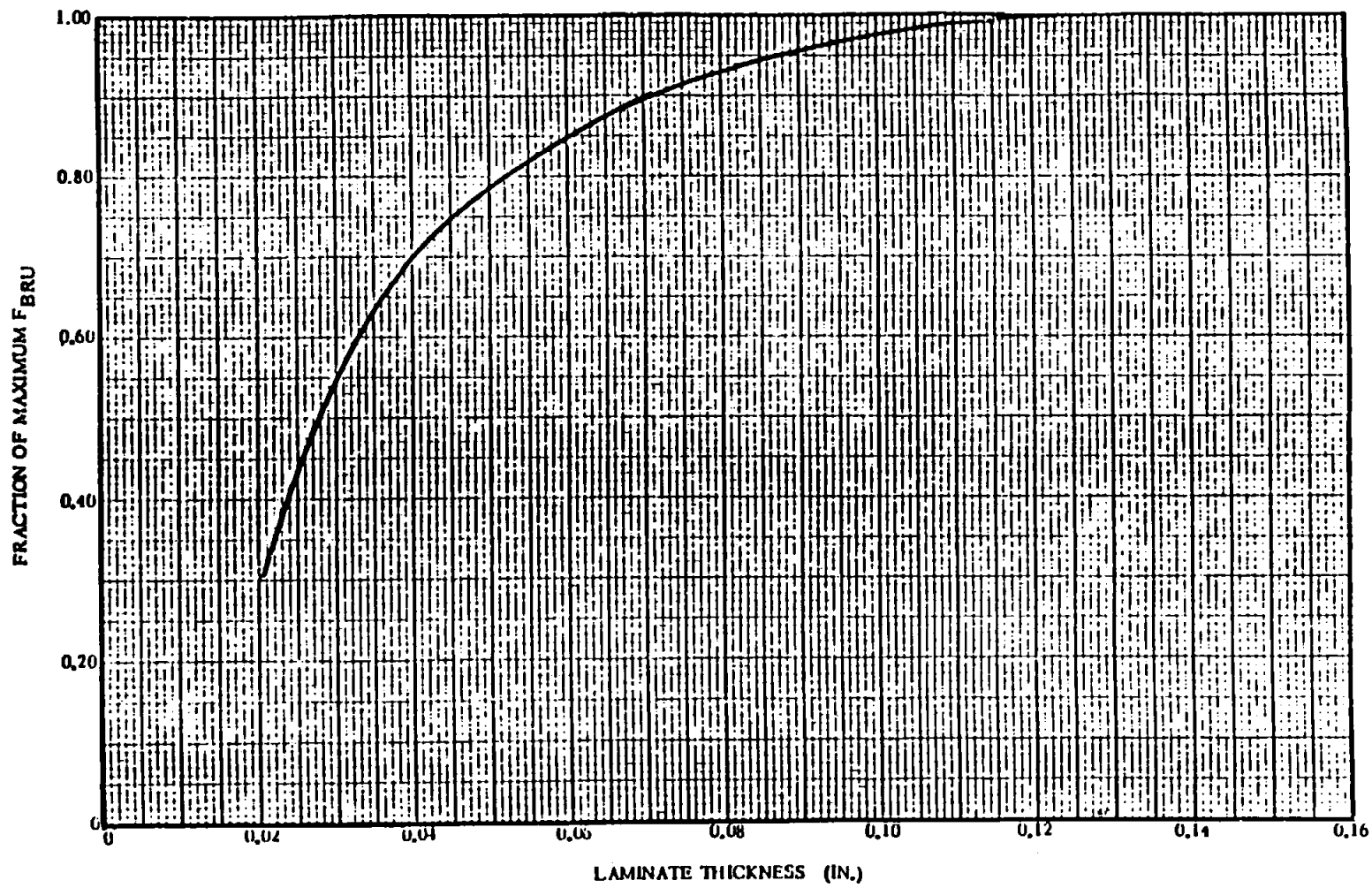


Figure 5-3. Fraction of Allowable Bolt Bearing Stress Permissible Vs Laminate Thickness
(Solid Laminate Phenolic 181 & 120 Glass Cloth)

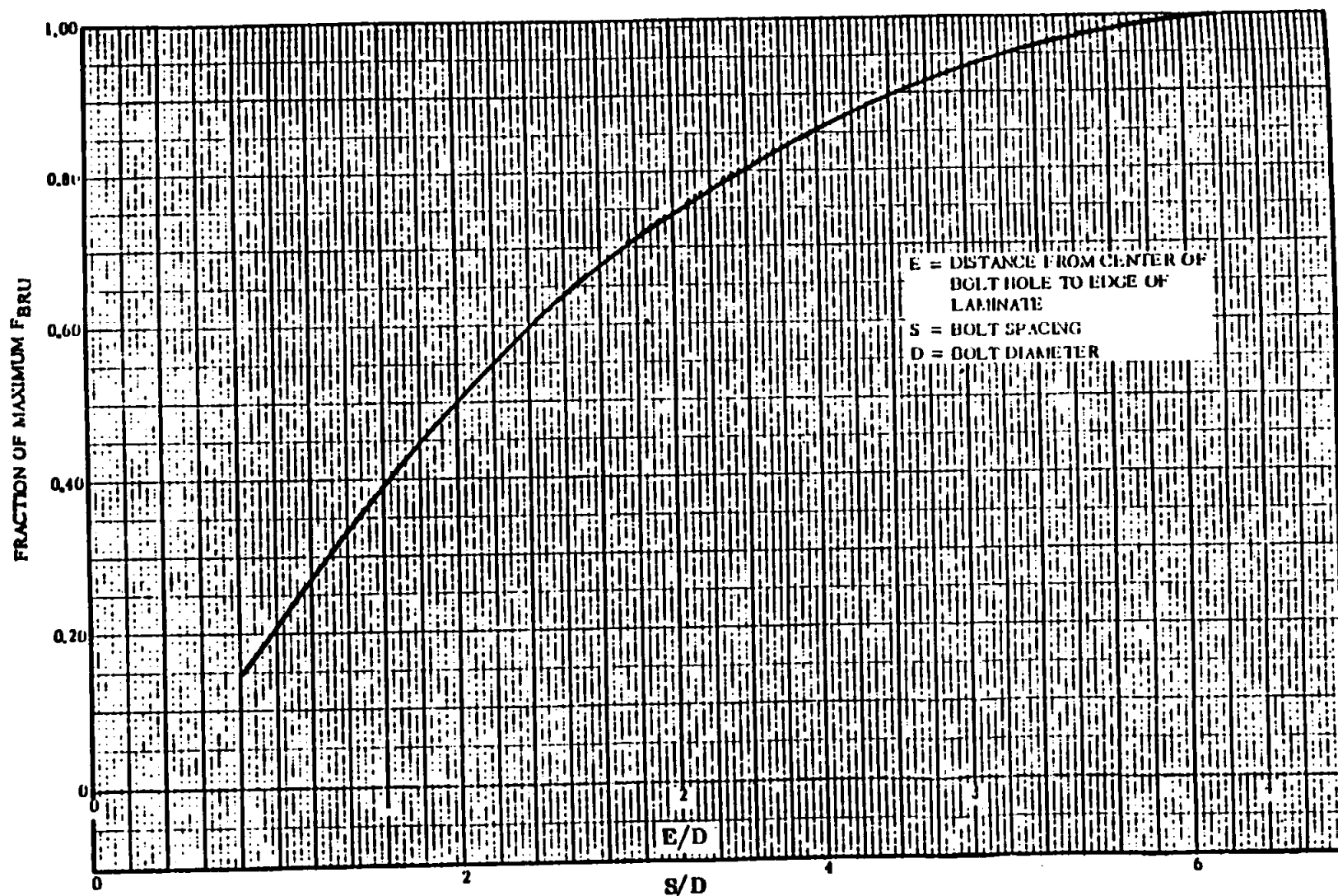


Figure 5-4. Fraction of Allowable Bolt Bearing Stress Permissible Vs S/D and E/D Ratios
(Solid Laminate Phenolic 181 & 120 Glass Cloth)

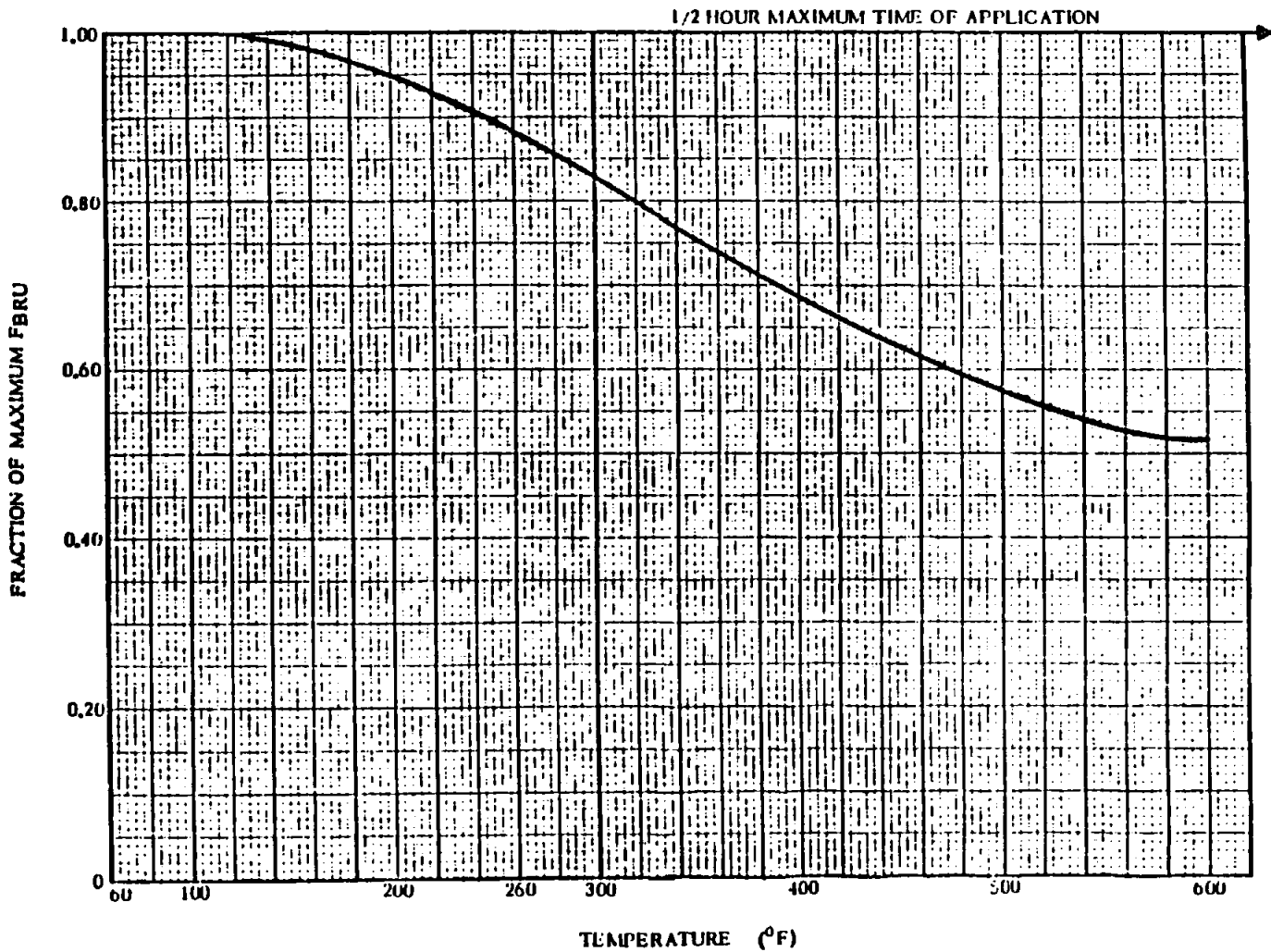


Figure 5-5. Fraction of Allowable Bolt Bearing Stress Permissible Vs Temperature of Application
(Solid Laminate Phenolic 181 & 120 Glass Cloth)

STRUCTURAL ANALYSIS MANUAL
GENERAL DYNAMICS/CONVAIR AND SPACE SYSTEMS DIVISION

REFERENCES

1. Strength of Metal Aircraft Elements; MIL-HDBK-5; Armed Forces Supply Center, Washington 25, D. C.; March 1961.
2. Structures Memoranda; GD Convair.
3. Specification for Steel, Corrosion Resistant Sheet and Plate Type 301-1/4 Hard; GD/A 0-71013; 30 June 1961.
4. Specification for Steel, Corrosion Resistant Sheet and Strip Type 301-1/2 Hard; GD/A 0-71012 Rev. A; 5 April 1961.
5. Specification for Steel, Corrosion Resistant, Sheet and Coil Stock, Type 301-3/4 Hard; GD/A 0-71005 Rev. E; 26 May 1958.
6. Specification for Steel, Corrosion Resistant, Sheet and Coil Stock, Type 301 Extra Hard 200,000 Psi Ultimate; GD/A 0-71004 Rev. D; 25 April 1958.
7. Specification for Steel, Corrosion Resistant, Sheet and Coil Type 301 Extra Hard 200,000 Psi Ultimate; GD/A 0-71022 Rev. A; 5 April 1962.
8. Environmental Tests for Hydrogen Tank Skins; GD/A 0-71016 Rev. B.
9. CRES301 Stainless Steel Sheet, Poisson's Ratio at -320° F and +600° F; GD/A 7E1264.
10. CRES Type 301 and 321 Stainless Steel Sheet - Poisson's Ratio at Ambient Temperature; GD/A 7E1263; 5 June 1959.
11. Specification for Nickel Base Alloy 718, Age Hardenable, Bars and Forgings; GD/A 0-71037; 6 August 1964.
12. Specification for Nickel Base Alloy 718, Age Hardenable, Sheet, Strip and Plate; GD/A 0-71038; 16 August 1964.
13. Process for Welding, Metal Arc and Gas-Steels and Corrosion and Heat Resistant Alloys; MIL-W-8611A; 24 July 1957.
14. Welding, Resistance: Aluminum, Magnesium, Non-Hardening Steels or Alloys, Nickel Alloys, Heat-Resisting Alloys, and Titanium Alloys. Spot and Seam; MIL-W-6858B; 2 November 1960.
15. Quality Acceptance Standards for Fusion Welds of Centaur Components; GD/A 0-77008; 14 December 1962.
16. Properties of 321 Stainless Steel Joints at Room Temperature and -423° F; GD/A 55E154; 25 September 1961.
17. Military Specifications: Process for Welding of Aluminum Alloys; MIL-W-8604; 5 June 1953.
18. The Effects of Nickel Foil on the Strength of Resistance Welds in Type 301 Stainless Steel at Room and Cryogenic Temperatures; GD/A AR-592-1-412; 12 April 1963.
19. Effects of Temper on Shear and Cross-Tension Strength of Type 301; GD/A MRC-M-1522, 17 February 1964.

STRUCTURAL ANALYSIS MANUAL
GENERAL DYNAMICS/CONVAIR AND SPACE SYSTEMS DIVISION

20. Aerospace Structural Metals Handbook, Volume I, Ferrous Alloys; Syracuse University Press; March 1964.
21. Aerospace Structural Metals Handbook, Volume II, Non-Ferrous Alloys; Syracuse University Press; March 1964.
22. Cryogenic Materials Data Handbook; Air Force Materials Laboratory, AF 32 (657)-9161; July 1965.
23. GD/C Heli Arc Spotweld Qualification/Certification; Approved by Engineering and Process Control; 9 May 1965.
24. Welding, Spot, Inert-Gas Shielded Arc; MIL-W-27664; 10 October 1962.
25. Shear and Tension Strength of Tig Spot Welds in a Six-Layer Stainless Steel Buildup that Simulates Centaur Yaw and Helium Bracket Attachment Points; GD/C ZZL-65-031; 21 October 1965.
26. Butt Weld and Seam Weld Yielding for 0.026-301 Half-Hard Stainless Steel; GD/C MGR-M-139; 2 November 1964.
27. Centaur Tank Corrosion Tests and X-rays; GD/C-BNZ65-032; 1 August 1965.
28. Shear and Cross Tension Properties of 321/301 Stainless Steel Seam Welds; GD/C MGR-M-549; 4 November 1965.
29. Seam Weld Tests on 301 (1/2 Hard) Stainless Steel (2 Doublers); GD/C MGR-M-174; 17 November 1964.
30. The Effects of Nickel Foil on the Strength of Resistance Spot Welds in Multiple Sheet Pile-Up of Types 301 and 321 Stainless Steel at Room and Cryogenic Temperatures; GD/C ZZL-64-011; 1 July 1964.
31. Shear and Cross Tension Values of Resistance Spot Welded Skins at M. S. 412.72; GD/C MGR-M-406; 21 May 1965.
32. Stress Concentration Design Factors; Peterson, R. E.; John Wiley & Sons, Inc.
33. Specification for Dynamic Etching of Corrosion Resistance Steel; GD/C 0-75091 Rev. B; 11 April 1963.
34. The Effects of Chemical Milling and Chemically Milled Steps on the Mechanical Properties of Type 301 EH & Type 310 EH Stainless Steels at Room & Liquid Hydrogen Temperatures; GD/C AR-592-1-473; 3 July 1963.
35. Additional Information Pertaining to the Effects of Chemical Milling on the Mechanical Properties of Cold Rolled Stainless Steel; GD/C ZZL-64-018; 16 April 1964.
36. Final Stress Analysis Centaur Vehicle AC-6 - AC-15; GD/C-BTD65-023; 15 May 1965.
37. Structures Manual; Volume I & II; GD Convair.
38. Smooth & Sharp-Notch Tensile Properties of Cold-Reduced 301 and 304L Stainless Steel Sheet at 75° F, -320° F and -423° F; NASA TND-592, Hanson, M. P.; February 1961.
39. Mechanical Properties of High Strength 301 Stainless Steel Sheet at 70° F, -320° F, -423° F in the Base Metal & Welded Joint Configuration; ASTM STP No. 287; 1960.
40. Quality Verification Laboratory Test Report; GD/C Data Reports; 1961-1965.

STRUCTURAL ANALYSIS MANUAL
GENERAL DYNAMICS/CONVAIR AND SPACE SYSTEMS DIVISION

41. The Effects of Cryogenic Temperature on the Mechanical Properties of High Strength Sheet Alloys (cold worked Austenitic Stainless Steels): GD/A ERR-AN-003; 16 May 1960.
42. Physical and Mechanical Properties of Pressure Vessel Materials for Application in a Cryogenic Environment: GD/A ASD-TDR-62-258; March 1962.
43. Selection of Materials for Cryogenic Applications in Missiles & Aerospace Vehicles: GD/A MRG-132-1; February 1960.
44. MIL-HDBK 17- Plastics for Flight Vehicles.
45. Static and Fatigue Strength of CRES01 (GD/A 0-71004 & 0-71022) Stainless Steel at Room Temperature and -320°F; GDA7E2378; 7 October 1959.
46. GD/FW Report E. M. No. 24. 155- Glass Reinforced Plastic Parts - Material Selection, Design Information, and Drawing Procedure; 29 September 1959.
47. GD/FW Report FMS-0013 (C). Core Material-Glass Fabric Reinforced Plastic Honeycomb, Intermediate Temperature Resistant; 15 May 1961.
48. GD/FW Report E. M. No. 24. 294 - Bolt Bearing Design Allowables for FMS-0031 Class III and VI 120 and 181 Glass Fabric Reinforced Plastic Laminate; 8 October 1959.
49. GD/Fort Worth Report MR-SS-012, Centaur Lightweight Insulation Panel Structural Allowables Report; 12 February 1964.
50. GD/FW Structures Manual - Volume I.
51. WADD TR 60-123 "Cylindrical Sandwich Construction Design", Section II; February 1960.
52. NACA TN3783 Handbook of Structural Stability Part III - Buckling of Curved Plates and Shells.

STRUCTURAL ANALYSIS MANUAL
GENERAL DYNAMICS/CONVAIR AND SPACE SYSTEMS DIVISION

Data Source, Section 1.3 Reference 4/

Subject: Allowables for 0-06166-2 Aramid/Epoxy

- References:**
1. 0-06166, Material specification for fabric, Aramid, epoxy impregnated, non-flammable.
 2. 0-73829, Process specification for fabric, laminate, Aramid, epoxy impregnated, fabrication of.
 3. Proposed chapter 5, Kevlar-epoxy materials, proposed chapter for revised MIL-HDBK-17, 1 June 84, Army Materials and Mechanics Research Center.
 4. General Dynamics Quality Verification Test Report (QVTR) Data.
 5. Kevlar 49 data manual, Dupont, 1986 and 1974.
 6. Advanced Composites Design Guide, 4.1.1/5.91.AF5, July 1983.
 7. Design Allowables for Centaur Structural Materials, GDC-BTD65-168, 1 February 1966.

PROBLEM: Aramid/epoxy (Kevlar/epoxy) allowables are needed for use in structural analysis of the Titan/Centaur.

RECOMMENDATION: Use the allowables data contained in this memo for structural analysis of Titan/Centaur aramid/epoxy components made from 0-06166-2. For components made from 0-06166-1 use 90% of the values contained herein.

DISCUSSION: This memo establishes structural allowables for aramid/epoxy fabric laminate per references 1 and 2 for the Titan/Centaur program. A word of caution to the analyst is appropriate. Aramid (Kevlar) is a high tensile strength fiber, has an excellent ratio of tensile strength to density, and has a linear tensile stress-strain curve. Compressive properties of aramid/epoxy are significantly different including a much lower compressive strength, a non-linear compressive stress-strain

STRUCTURAL ANALYSIS MANUAL
GENERAL DYNAMICS/CONVAIR AND SPACE SYSTEMS DIVISION

DISCUSSION: (cont'd)

curve, a compressive yield stress and a relatively low compressive strength to density ratio. Compressive properties are also reduced by moisture absorption from the atmosphere. Flexure properties are a combination of tensile properties on one side of the neutral axis and compression properties on the other side. Flexure also has a non-linear stress-strain curve and a yield stress. For flexure and compression applications fiberglass/epoxy, Reference 7, should also be evaluated before making a final material selection. Material properties and structural allowables are summarized in Table 1 and Figures 1 through 5. These allowables are based on test data. Where specific test data is not available allowables are obtained by reducing typical data from References 5 and 6 and these allowables are necessarily conservative. For design use the "wet" values as it is impossible to prevent moisture absorption over a period of time. For test coupon acceptance use specification minimum values. For optimal properties the warp (0°) direction should be specified on the engineering drawing. No attempt was made to establish elevated temperature allowables, but one should expect severe degradation of compressive strength for hot, wet conditions.

Drawing notes shall include requirements for test specimens on all structural parts made from 0-06166-1 or -2 material. Both flexure and short beam shear (SBS) tests shall be called for per reference 2 to insure product quality. Reference 2 requires revision to add SBS tests (ASTM D 2344) and until it is revised the SBS tests shall be called out in the drawing notes as follows:

Test five (5) longitudinal short beam shear specimens per ASTM D 2344. Minimum average acceptance value 4.5 ksi.

Tensile properties are based on Reference 3 and confirmed by References 4, 5 and 6. Adjustment is made to account for the acceptance values of Reference 1.

Compression properties are based on Reference 3 and confirmed by References 5 and 6. No compressive data was available from Reference 4. It is apparent that the compression strength acceptance value of Reference 1 should be increased from 15ksi to 24ksi. I plan to submit an ECR to the spec for this change. Until the ECR is approved use $F_{cu_A} = 12 \text{ ksi}$.

Flexure properties are based on Reference 4 and confirmed by Reference 5. No flexure data was contained in Reference 3. Adjustment is made to account for the acceptance values of References 1 and 2. Flexure data is only for rectangular sections.

STRUCTURAL ANALYSIS MANUAL
GENERAL DYNAMICS/CONVAIR AND SPACE SYSTEMS DIVISION

DISCUSSION(cont'd)

In plane shear, interlaminar shear, bearing and coefficient of thermal expansion are based on Reference 5 and adjusted using engineering judgement to obtain allowables. These allowables are designated as estimated A (Est. A) values in Table 1.

Effects of temperature on mechanical properties may be found in References 5 and 6.

An expanded testing program most likely would result in increased allowables in some cases, but time and budget do not permit such a program at this time.

STRUCTURAL ANALYSIS MANUAL
GENERAL DYNAMICS/CONVAIR AND SPACE SYSTEMS DIVISION

TABLE 1 0-06166-2 ARAMID/EPOXY DESIGN PROPERTIES

<u>TENSION</u>		BASIS	DRY	WET	COMMENTS
FTU _{0,90}	(ksi)	A	51	51	
ET _{0,90}	(msi)	Typical	4.5	4.0	Fig. 1
FTU ₄₅	(ksi)	A	20	20	
ET ₄₅	(msi)	Typical	1.1	1.0	Fig. 2
<u>COMPRESSION</u>					
FCU _{0,90}	(ksi)	A	21 *	19 *	
FCY _{0,90}	(ksi)	A	10	9	
EC _{0,90}	(msi)	Typical	4.5	4.0	Fig. 1
FCU ₄₅	(ksi)	A	15 *	13 *	
FCY ₄₅	(ksi)	A	5	4.5	
EC ₄₅	(msi)	Typical	1.0	0.9	Fig. 2
<u>FLEXURE</u> (Rectangular Cross-Sections Only)					
FFU _{0,90}	(ksi)	A	49	44	
FFY _{0,90}	(ksi)	A	24	21	
EF _{0,90}	(msi)	Typical	4.0	3.3	Fig. 3
FFU ₄₅	(ksi)	A	19	17	
FFY ₄₅	(ksi)	A	10	9	
EF ₄₅	(msi)	Typical	1.0	0.9	
<u>IN PLANE SHEAR</u>					
FSU _{0,90}	(ksi)	Est. A.	10	9	
G _{0,90}	(msi)	Typical	0.3	0.3	Fig. 4
FSU ₄₅	(ksi)	Est. A	21	19	
G ₄₅	(msi)	Typical	3.0	3.0	Fig. 4

* Until 0-06166 is changed to reflect the increased compressive strength use Fcu₀ = 12 ksi dry, 11 ksi wet, Fcu₄₅ = 8ksi dry, 7ksi wet

STRUCTURAL ANALYSIS MANUAL
GENERAL DYNAMICS/CONVAIR AND SPACE SYSTEMS DIVISION

TABLE 1 0-06166-2 ARAMID/EPOXY DESIGN PROPERTIES (CONT'D)

<u>INTERLAMINAR SHEAR</u> (Short Beam Shear)	BASIS	DRY	WET	COMMENTS
F _{SBS} (ksi)	Est. A	4.5	3.5	

BEARING

Use linear interpolation, see Fig. 5

Do not exceed $D/t = 2.0$ without testing

Maintain $\frac{e}{D} \geq 3.0$ and $\frac{s}{D} \geq 4.0$
 $D/t = 0.81$

F _{BRU0} (4%)(ksi)	Est. A	23	20	Fig. 5
-----------------------------	--------	----	----	--------

F _{BRY0} (ksi)	Est. A	14	12	
-------------------------	--------	----	----	--

$D/t = 1.62$

F _{BRU0} (4%)(ksi)	Est. A	17	15	Fig. 5
-----------------------------	--------	----	----	--------

F _{BRY0} (ksi)	Est. A	9	8	
-------------------------	--------	---	---	--

COEFF. THERMAL EXPANSION

$\alpha_{0,90}$ ($\mu\text{E}/\text{F}$)	0 to 2.2	--
--	----------	----

resin ($\mu\text{E}/\text{F}$)	50 to 65	--
----------------------------------	----------	----

DENSITY

ρ (lb/in ³)	0.049	0.050
------------------------------	-------	-------

THICKNESS

0-06166-1 (inches/ply)	0.004
------------------------	-------

0-06166-2 (inches/ply)	0.009
------------------------	-------

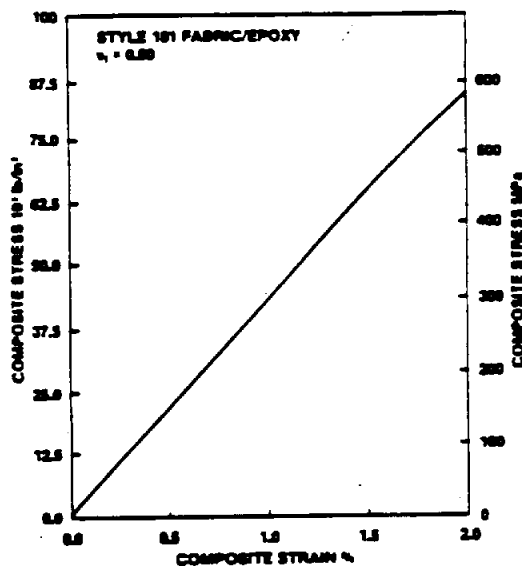
STRUCTURAL ANALYSIS MANUAL
GENERAL DYNAMICS/CONVAIR AND SPACE SYSTEMS DIVISION

KEVLAR

MAY 1986

Typical Fabric Composite Stress-Strain Response At Room Temperature
Du Pont Fabric Style 181¹ Of KEVLAR[®] 49 Reinforced Epoxy (WARP DIRECTION)

TENSION



COMPRESSION

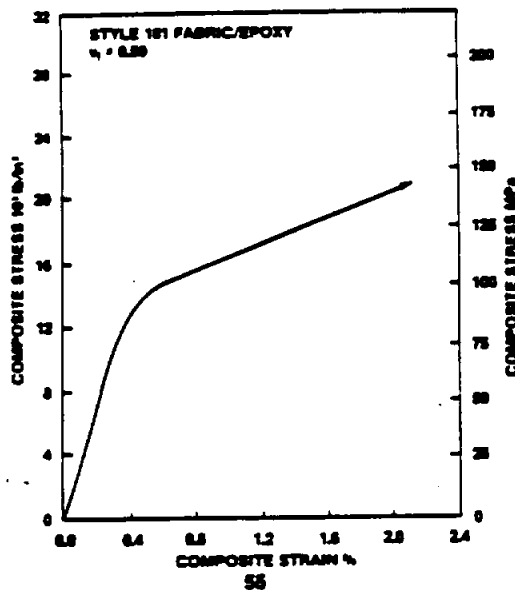


FIGURE 1

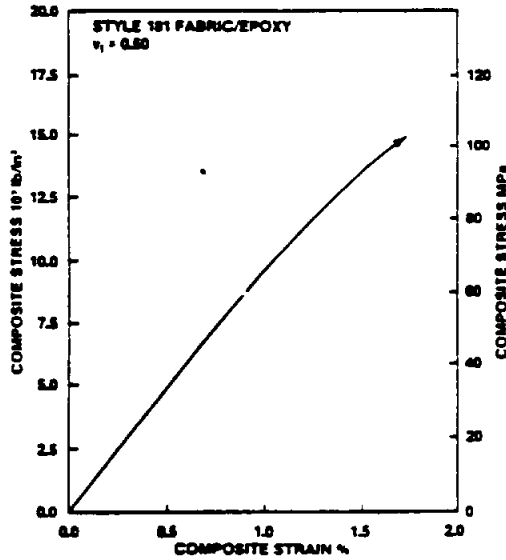
630

KEVLAR

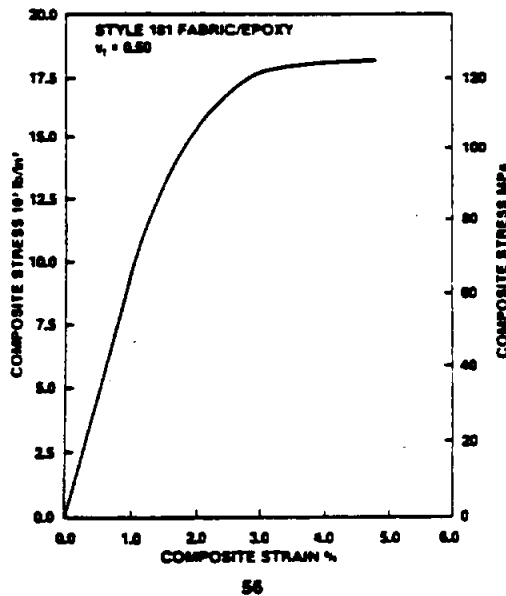
MAY 1986

Typical Fabric Composite Stress-Strain Response At Room Temperature
Du Pont Fabric Style 181¹ Of KEVLAR[®] 49 Reinforced Epoxy (Bias Direction (45°))

TENSION



COMPRESSION



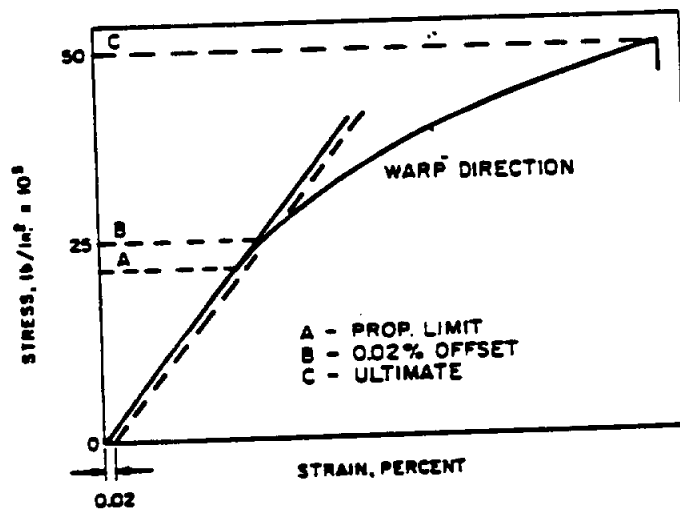
See Section 1 for Fabric Construction

56

FIGURE 2

STRUCTURAL ANALYSIS MANUAL
GENERAL DYNAMICS/CONVAIR AND SPACE SYSTEMS DIVISION

FABRIC COMPOSITE OF STYLE 181 "KEVLAR" 49
FLEXURAL STRESS-STRAIN CURVE



AMERICAN CYANAMID BP-907 EPOXY
AUTOCLAVE MOLDED
50 VOLUME PERCENT FABRIC

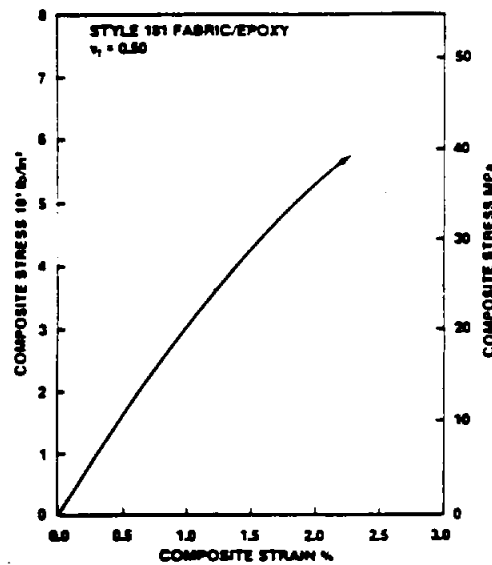
FIGURE 3

KEVLAR

MAY 1986

Typical Fabric Composite Shear Stress-Strain Response At Room Temperature
Du Pont Fabric Style 181¹ Of KEVLAR[®] 49 Reinforced Epoxy

WARP DIRECTION



BIAS DIRECTION (45°)

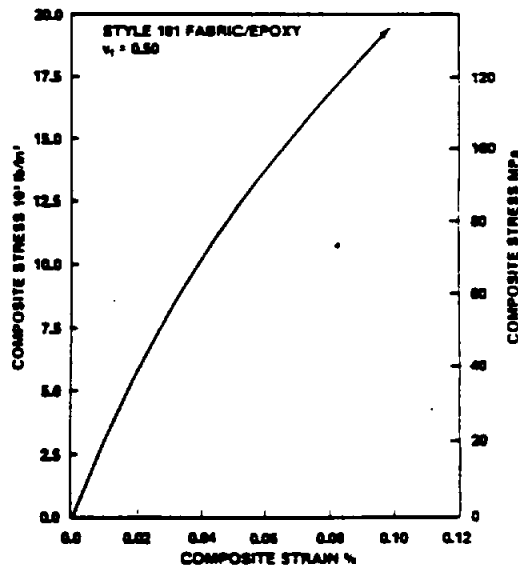


FIGURE 4

STRUCTURAL ANALYSIS MANUAL
GENERAL DYNAMICS/CONVAIR AND SPACE SYSTEMS DIVISION

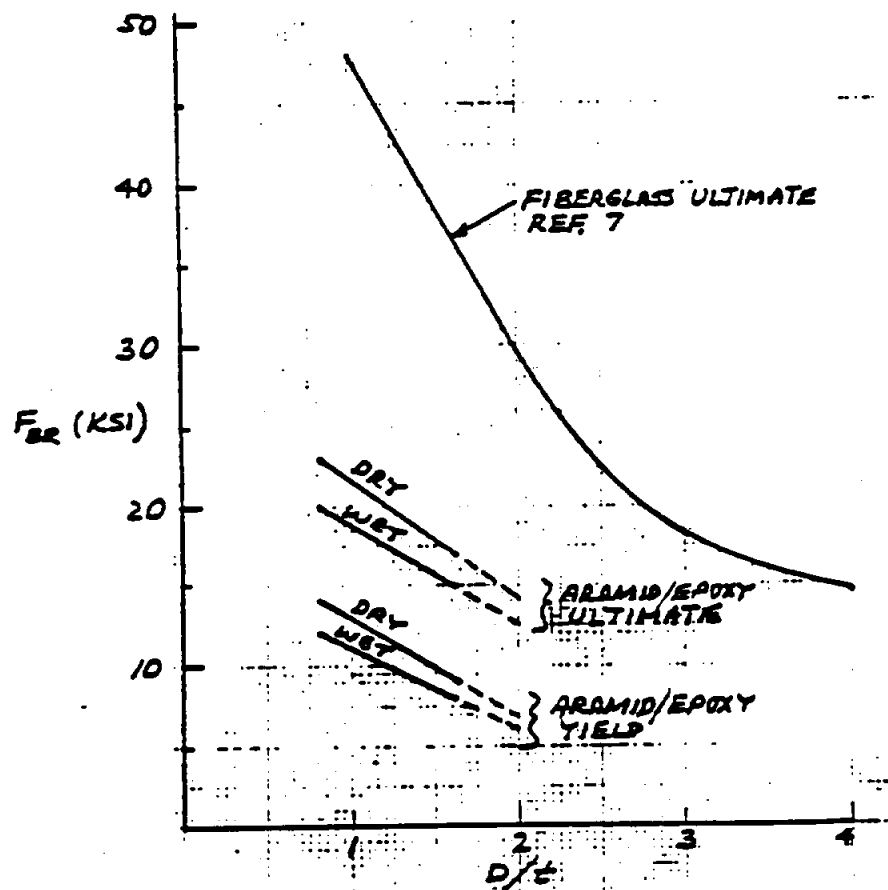


FIGURE 5

STRUCTURAL ANALYSIS MANUAL
GENERAL DYNAMICS/CONVAIR AND SPACE SYSTEMS DIVISION

SECTION 23.0

FRACTURE MECHANICS THEORY AND METHODS OF APPLICATION ARE CONTAINED
IN THIS SECTION

	PAGE
23.1 GENERAL	23.1.1
23.2 STRESS-INTENSITY FACTORS	23.2.1
23.3 FLAW GROWTH	23.3.1
23.4 APPLICATION OF TECHNOLOGY	23.4.1
23.5 DAMAGE TOLERANCE	23.5.1

STRUCTURAL ANALYSIS MANUAL
GENERAL DYNAMICS/CONVAIR AND SPACE SYSTEMS DIVISION

Data Source, Section 1.3 Reference 5

TABLE OF CONTENTS

	Page
E2 FRACTURE MECHANICS	23. 1. 1
2.1 GENERAL	23. 1. 1
2.1.1 Comparison of Fatigue and Fracture Mechanics	23. 1. 2
2.2 STRESS-INTENSITY FACTORS	23. 2. 1
2.2.1 Plane Strain	23. 2. 2
2.2.1.1 Correction for Deep Surface Flaws	23. 2. 6
2.2.2 Plane Stress	23. 2. 12
2.2.2.1 Through-the-Thickness Cracks	23. 2. 16
2.2.3 Experimental Determination	23. 2. 17
2.3 FLAW GROWTH	23. 3. 1
2.3.1 Sustained Load Flaw Growth	23. 3. 1
2.3.1.1 Environmental Effects	23. 3. 2
2.3.2 Cyclic Load Flaw Growth	23. 3. 3
2.3.2.1 Theories	23. 3. 3
I. Paris	23. 3. 5
II. Foreman	23. 3. 7
III. Tiffany	23. 3. 10
2.3.2.2 Crack Growth Retardation	23. 3. 10
I. Wheeler's Retardation Parameter	23. 3. 10
II. The Significance of Fatigue Crack Closure	23. 3. 13
2.3.2.3 Transition from Partial-Thickness Cracks to Through-Thickness Cracks	23. 3. 17
2.3.3 Combined Cyclic and Sustained Flaw Growth	23. 3. 17
2.4 APPLICATION OF FRACTURE MECHANICS TECHNOLOGY	23. 4. 1
2.4.1 Selection of Materials	23. 4. 1
2.4.1.1 Static Loading	23. 4. 4
I. Example Problem A	23. 4. 5
2.4.1.2 Cyclic or Sustained Loading	23. 4. 9
I. Example Problem A	23. 4. 9
II. Example Problem B	23. 4. 17

STRUCTURAL ANALYSIS MANUAL
GENERAL DYNAMICS/CONVAIR AND SPACE SYSTEMS DIVISION

TABLE OF CONTENTS (Concluded)

	Page
2.4.2 Predicting Critical Flaw Sizes	23. 4.19
2.4.2.1 Surface Cracks	23. 4.20
I. Example Problem A	23. 4.21
II. Example Problem B	23. 4.22
2.4.2.2 Embedded Flaws	23. 4.24
2.4.2.3 Through-the-Thickness Cracks	23. 4.26
I. Example Problem A	23. 4.26
2.4.3 Structure Design	23. 4.29
2.4.3.1 Service Life Requirements and Predictions	23. 4.29
I. Example Problem A (Thick-Walled Vessel)	23. 4.36
II. Example Problem B (Thin-Walled Vessel)	23. 4.40
2.4.3.2 Allowable Initial Flaw Size	23. 4.47
I. Example Problem A	23. 4.48
2.4.3.3 Nondestructive Inspection Acceptance Limits	23. 4.49
2.4.3.4 Proof-Test Factor Selection	23. 4.54
I. Example Problem A	23. 4.57
REFERENCES	23. 4.60

STRUCTURAL ANALYSIS MANUAL
GENERAL DYNAMICS/CONVAIR AND SPACE SYSTEMS DIVISION

Data Source, Section 1.3 Reference 5

E2 FRACTURE MECHANICS.

2.1 GENERAL.

Structures subjected to constant loads at moderate temperatures have been designed primarily on the basis of the yield strength and/or ultimate strength of the material. Many of these structures have failed prematurely at stresses below the yield strength, with disastrous consequences. These brittle failures have occurred in such diverse structures as storage tanks, suspension bridges, aircraft landing gears, and rocket motor cases. An examination of such failures indicated one predominant feature: A small defect or flaw was usually found at the failure origin.

Therefore, the key to brittle fracture control lies in understanding both the weakening effects of flaws and cracks in metals and those factors that influence this effect. To be useful in an engineering sense, this understanding must be translated into the types of tests and structural mechanics familiar to the metal producer and designer. The body of knowledge concerning this type of failure has become known as fracture mechanics.

Basic to fracture mechanics is the understanding of the state of stress near the tip of a sharp crack and the relationship between gross stress and flaw geometry. These concepts are discussed in subsection 2.2, Stress-Intensity Factors.

Flaw growth or crack propagation under cyclic loads is a basic problem which is handled best by fracture mechanics concepts. A thorough discussion of flaw growth is given in subsection 2.3.

Finally, subsection 2.4, Application of Fracture Mechanics Technology, relates stress-intensity factors and flaw growth to the engineering design and analysis of structures. Particular attention is given to pressure-vessel design because of its importance in the aerospace industry.

STRUCTURAL ANALYSIS MANUAL
GENERAL DYNAMICS/CONVAIR AND SPACE SYSTEMS DIVISION

2.1.1 Comparison of Fatigue and Fracture Mechanics.

Similarities and dissimilarities between fatigue and fracture mechanics are summarized in Table E2-1. Both fatigue and fracture mechanics depend primarily on results of laboratory tests; however, the fracture mechanics concept makes it possible to handle fracture considerations in a quantitative manner and has shown greater applicability to fatigue crack propagation.

STRUCTURAL ANALYSIS MANUAL
GENERAL DYNAMICS/CONVAIR AND SPACE SYSTEMS DIVISION

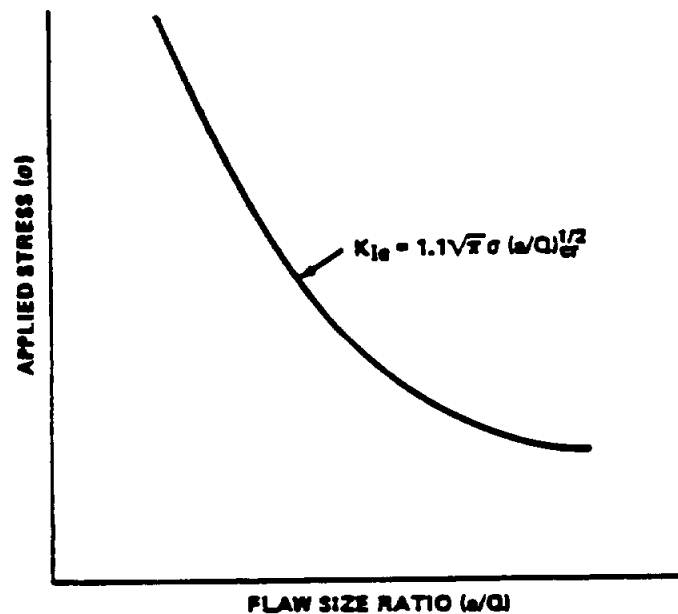


FIGURE E2-6. APPLIED STRESS VERSUS CRITICAL FLAW SIZE RATIO

Experimental data obtained on several materials with varying flaw sizes and shapes appear to provide a fair degree of substantiation of the Kobayashi magnification factor; however, more experimental investigations are being performed. Typical curves for M_k for two different materials are shown in Figs. E2-7 and E2-8.

2.2.2 Plane Stress.

An important consideration in fracture mechanics is the "state of stress," or simply the directions and magnitudes of the applied stresses and strains. In general, the state of stress in a body is three-dimensional, that is, stresses and strains exist in all three principal directions.

For thin sheet specimens subjected to in-plane external loads which do not vary through the thickness, a condition of plane stress is thought to prevail. As such, strain in the thickness direction is virtually unsuppressed and considerable plastic flow attends the cracking process.

STRUCTURAL ANALYSIS MANUAL
GENERAL DYNAMICS/CONVAIR AND SPACE SYSTEMS DIVISION

Data Source, Section 1.3 Reference 5

2.2 STRESS-INTENSITY FACTORS.

To understand how fracture mechanics is used in design, it is helpful first to learn some of the theory on which it is based.

The precise goal of fracture mechanics can be stated concisely: It attempts to provide a quantitative measure of resistance to unstable crack propagation. This measure must be independent of the size and shape of the crack, the geometry of the part containing the crack, and the manner in which external loads are applied to the part.

The search for a quantitative value focuses on the conditions in the vicinity of the crack tip where fracture takes place.

The stress fields near crack tips can be divided into three basic types, each associated with a local mode of deformation, as shown in Fig. E2-1. The opening mode, I, is associated with a local displacement in which the crack surfaces move directly apart. The edge-sliding mode, II, is characterized by displacements in which the crack surfaces slide over one another. In mode III, tearing, the crack surfaces slide with respect to one another parallel to the leading edge. Mode I is the most critical mode and is the only one to be discussed in this section. For information on modes II and III, see Ref. 1.

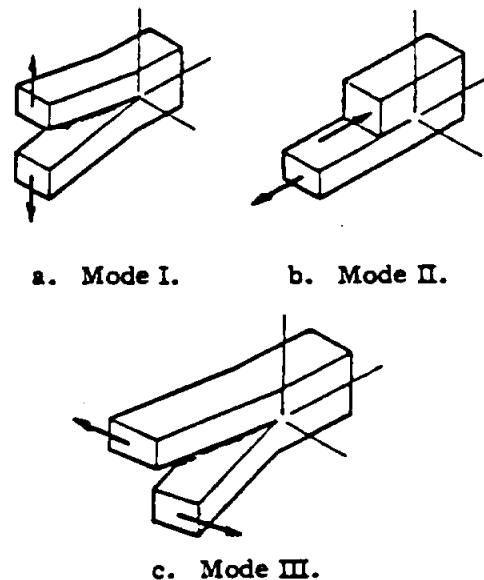
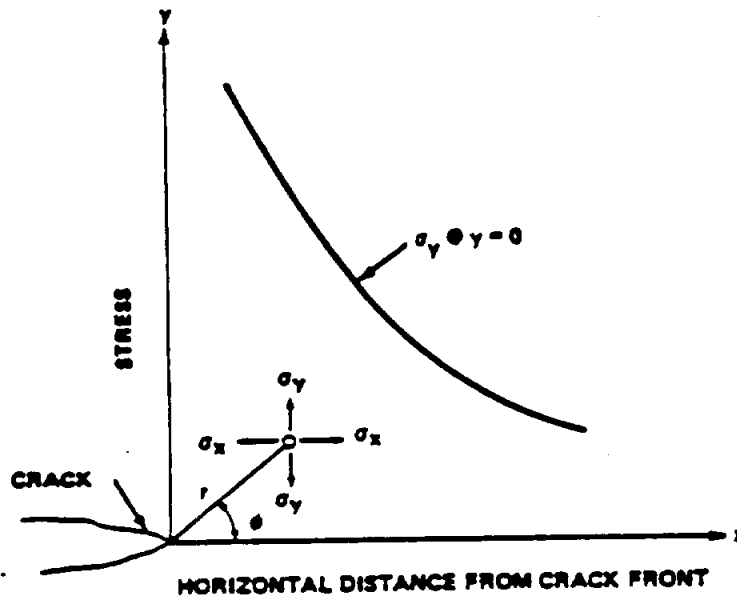


FIGURE E2-1. THREE DISPLACEMENT MODES FOR CRACK SURFACES

STRUCTURAL ANALYSIS MANUAL
GENERAL DYNAMICS/CONVAIR AND SPACE SYSTEMS DIVISION

2.2.1 Plane Strain.

The stress conditions, or plane-strain elastic stress field, at the crack tip for mode I are defined by the expressions shown in Fig. E2-2 (Ref. 2). These equations give the components of stress (σ = normal stress, τ = shear stress) in terms of the polar coordinates r and ϕ for opening-mode (perpendicular) crack surface displacements. Only the first term of each equation



$$\sigma_y = \frac{K_I}{(2\pi r)^{1/2}} \cos \frac{\phi}{2} \left(1 + \sin \frac{\phi}{2} \sin \frac{3\phi}{2} \right) \dots$$

$$\sigma_x = \frac{K_I}{(2\pi r)^{1/2}} \cos \frac{\phi}{2} \left(1 - \sin \frac{\phi}{2} \sin \frac{3\phi}{2} \right) \dots$$

$$\tau_{xy} = \frac{K_I}{(2\pi r)^{1/2}} \cos \frac{\phi}{2} \sin \frac{\phi}{2} \cos \frac{3\phi}{2} \dots$$

FIGURE E2-2. RELATIONSHIP BETWEEN STRESS-INTENSITY FACTOR, K_I , AND STRESS COMPONENTS IN THE VICINITY OF A CRACK

STRUCTURAL ANALYSIS MANUAL
GENERAL DYNAMICS/CONVAIR AND SPACE SYSTEMS DIVISION

is shown. The complete equations are power series in r/a (crack tip radius/crack half-length). For practical purposes, all terms beyond the first are negligible.

All the three stress components are proportional to a scalar quantity that has been designated the stress-intensity factor, K_I . This factor is independent of r and ϕ and therefore gives a single description of the stress intensity at any point near the crack tip. It is a purely numerical quantity which, if known, provides complete knowledge of the stress field at the crack tip.

The basic assumption in fracture mechanics is that an unstable fracture occurs when K_I reaches a critical value designated K_{Ic} , commonly called fracture toughness. It is important to appreciate the difference between K_I and K_{Ic} . The stress-intensity factor K is simply a coefficient in an equation describing the elastic stresses in the vicinity of a crack tip. Fracture toughness K_{Ic} is a particular value of K_I corresponding to unstable propagation of the crack. This value is a material property and reflects a material's ability to withstand a given stress at a crack tip. The difference between K_I and K_{Ic} is analogous to the difference between stress and strength for a body free of discontinuities.

Irwin (Ref. 3) used the expressions shown in Fig. E2-2 with the Green and Sneddon analysis (Ref. 4) to show that the expression for the stress intensity around the crack periphery for the embedded elliptical flaw (Fig. E2-3) is

$$K_I = \frac{\sqrt{\pi}}{\phi} \sigma \sqrt{2} \left\{ \frac{1}{c^2} [a^2 \cos^2 \phi + c^2 \sin^2 \phi] \right\}^{1/4},$$

STRUCTURAL ANALYSIS MANUAL
GENERAL DYNAMICS/CONVAIR AND SPACE SYSTEMS DIVISION

where σ is the uniform stress perpendicular to the crack. The parametric equations of the flaw periphery are $x = c \cos \phi$ and $y = a \sin \phi$, where c is the semimajor axis of the ellipse, a is the semiminor axis of the ellipse, and ϕ is the complete elliptical integral of the second kind corresponding to the modulus $k = [(c^2 - a^2)/c^2]^{1/2}$; i.e.,

$$\phi = \int_0^{\pi/2} \left[1 - \left(\frac{c^2 - a^2}{c^2} \right) \sin^2 \phi \right]^{1/2} d\phi$$

or $\phi = 1 + 4.593 (a/2c)^{1.65}$. Values of ϕ can be obtained for various values of $a/2c$ from the graph shown in Fig. E2-4.

In seeking an expression for the stress intensity for a semielliptical surface flaw in a finite-thickness plate, Irwin assumed that

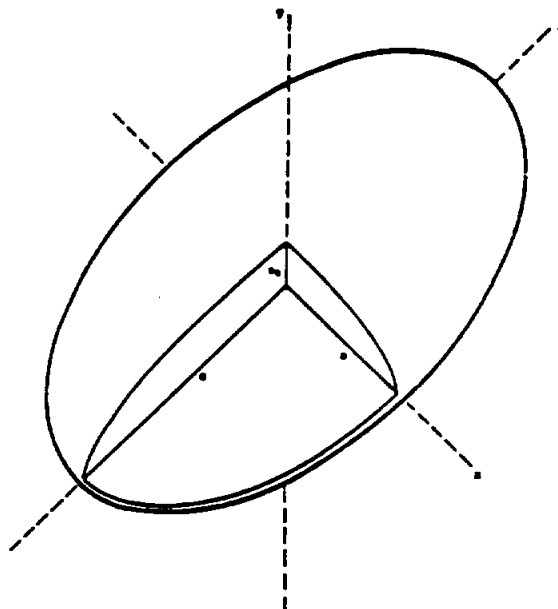
$$K_I = \alpha \frac{\sqrt{\pi}}{\phi} \sigma \sqrt{a\gamma} \left\{ \frac{1}{c^2} [a^2 \cos^2 \phi + c^2 \sin^2 \phi] \right\}^{1/4},$$

where α is a correction factor to account for the effect on stress intensity of the stress-free surface from which the flaw emanates, and γ is a correction factor to account for the effect on stress intensity of the plastic yielding around the flaw periphery.

Values of α and γ were estimated by Irwin and considered valid for surface flaws with a/c ratios less than one and flaw depths not exceeding 50 percent of the plate thickness. The resulting expression for the stress intensity was

$$K_I = 1.1 \sqrt{\pi} \sigma (a/Q)^{1/2} \left\{ \frac{1}{c^2} [a^2 \cos^2 \phi + c^2 \sin^2 \phi] \right\}^{1/4},$$

STRUCTURAL ANALYSIS MANUAL
GENERAL DYNAMICS/CONVAIR AND SPACE SYSTEMS DIVISION



**FIGURE E2-3. EMBEDDED ELLIPTICAL-SHAPED CRACK UNDER
 UNIFORM TENSILE STRESS IN y-DIRECTION**

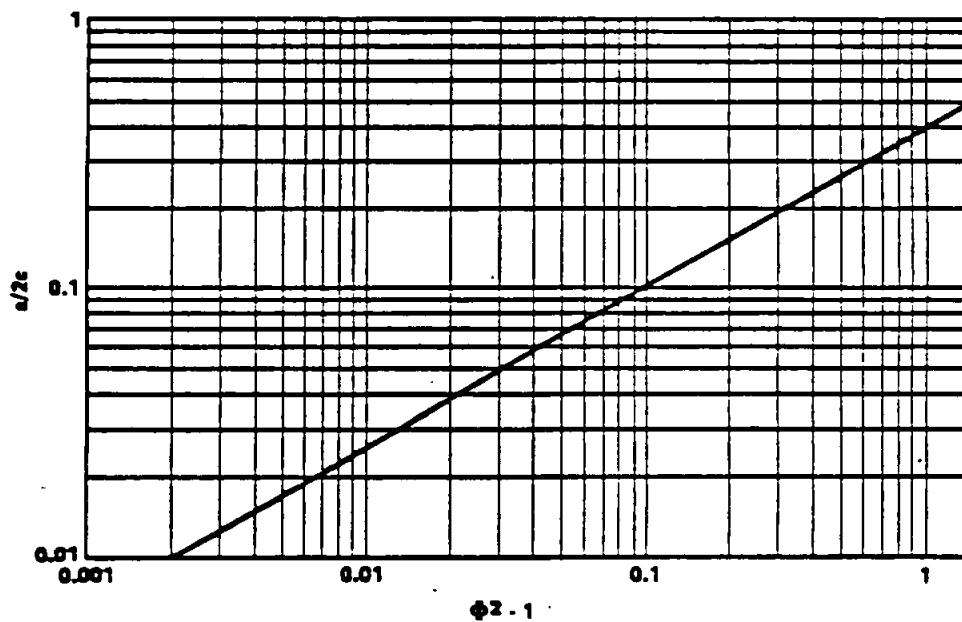


FIGURE E2-4. SHAPE FACTOR VALUES

STRUCTURAL ANALYSIS MANUAL
GENERAL DYNAMICS/CONVAIR AND SPACE SYSTEMS DIVISION

where $Q = \phi^2 - 0.212 (\sigma / \sigma_{ys})^2$, and σ_{ys} is the uniaxial yield strength of the material. Figure E2-5 shows the relationship between Q and the flaw depth-to-width ratio.

The maximum value of K_I occurs at the end of the semiminor axis of the ellipse and has a value of

$$K_I = 1.1 \sqrt{\pi} \sigma (a/Q)^{1/2} .$$

At some value of σ the flaw size becomes unstable and propagates rapidly. The value of K_I computed at the inception of this instability is called the critical value of K_I and is designated K_{Ic} . Thus, K_{Ic} is the stress intensity necessary to cause fracture under plane-strain conditions and is commonly called the plane-strain fracture toughness. Thus,

$$K_{Ic} = 1.1 \sqrt{\pi} \sigma (a/Q_{cr})^{1/2} .$$

Figure E2-6 is a graphical representation of this equation. Some typical values of K_{Ic} for space shuttle materials are shown in Table E2-2.

Stress-Intensity factors for other shapes of cracks, different loading conditions, and crack location are given in Table E2-3. (SEE REFS. 27, 28, 29)

2.2.1.1 Correction for Deep Surface Flaws.

For surface flaws that are deep with respect to plate thickness, that is, when the crack approaches the opposite surface, Irwin's equation has been modified by Kobayashi (Ref. 5) as follows:

$$K_I = 1.1 M_k \sqrt{\pi} \sigma (a/Q)^{1/2} ,$$

where M_k is the magnification factor for deep flaw effects.

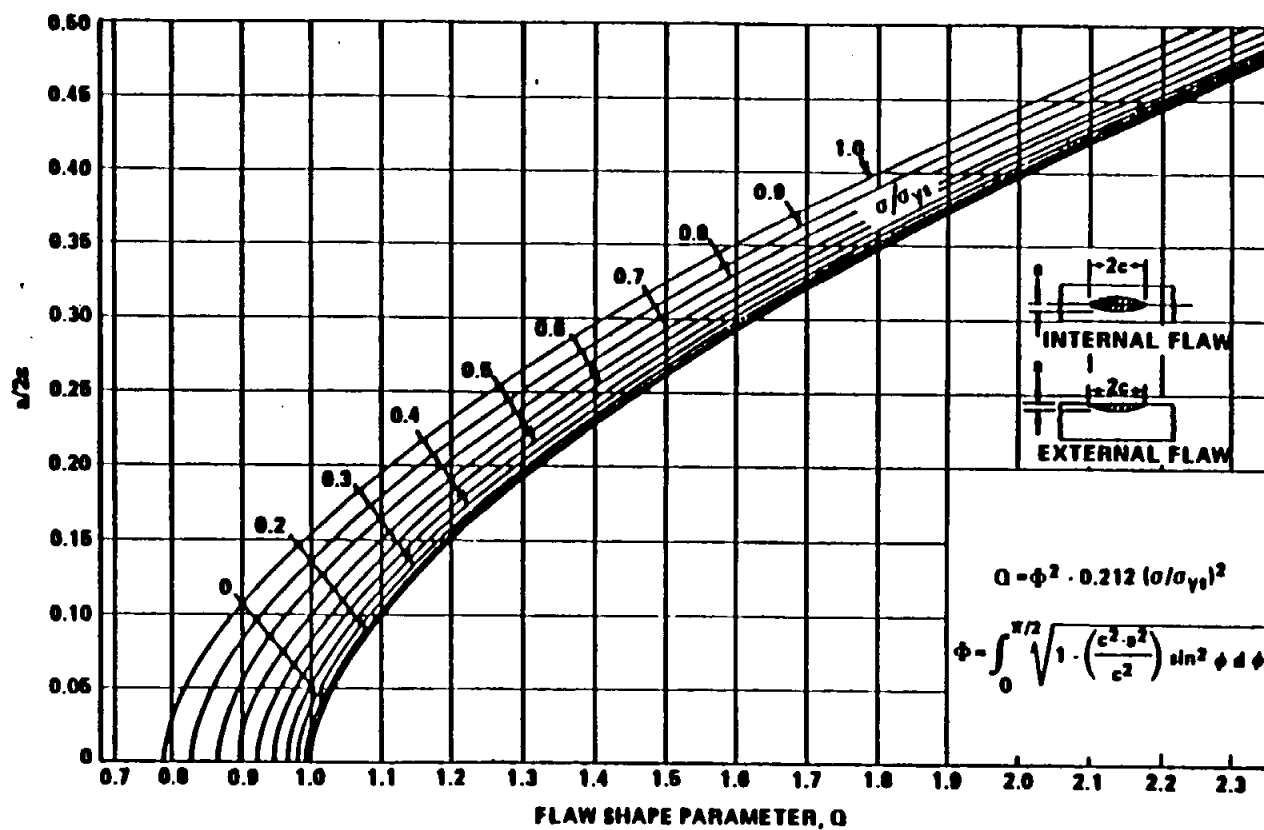


FIGURE E2-5. SHAPE PARAMETER CURVES FOR SURFACE AND INTERNAL FLAWS

STRUCTURAL ANALYSIS MANUAL
GENERAL DYNAMICS/CONVAIR AND SPACE SYSTEMS DIVISION

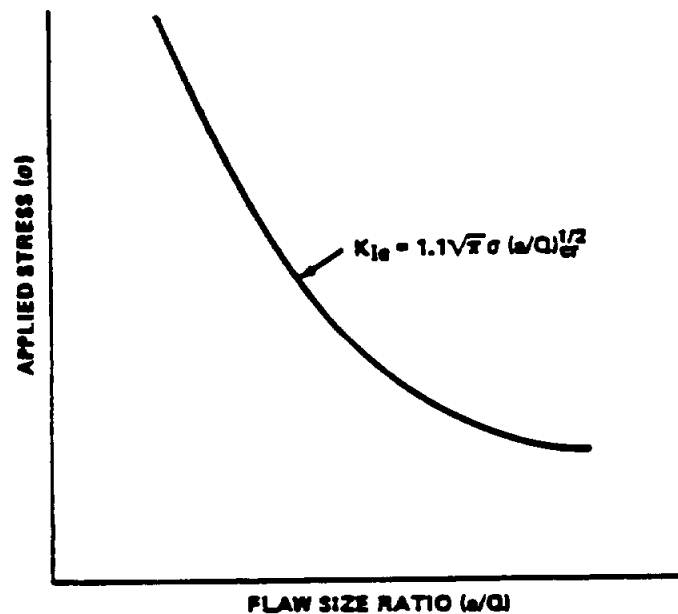


FIGURE E2-6. APPLIED STRESS VERSUS CRITICAL FLAW SIZE RATIO

Experimental data obtained on several materials with varying flaw sizes and shapes appear to provide a fair degree of substantiation of the Kobayashi magnification factor; however, more experimental investigations are being performed. Typical curves for M_k for two different materials are shown in Figs. E2-7 and E2-8.

2.2.2 Plane Stress.

An important consideration in fracture mechanics is the "state of stress," or simply the directions and magnitudes of the applied stresses and strains. In general, the state of stress in a body is three-dimensional, that is, stresses and strains exist in all three principal directions.

For thin sheet specimens subjected to in-plane external loads which do not vary through the thickness, a condition of plane stress is thought to prevail. As such, strain in the thickness direction is virtually unsuppressed and considerable plastic flow attends the cracking process.


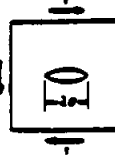
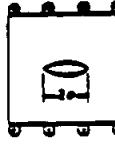
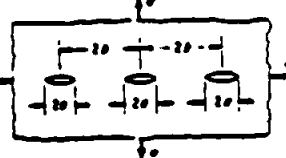
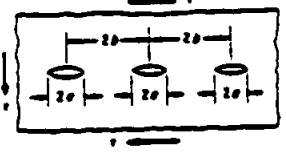
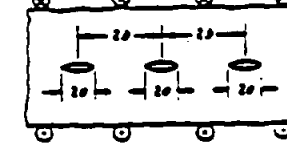
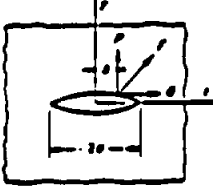
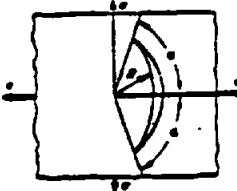
STRUCTURAL ANALYSIS MANUAL
GENERAL DYNAMICS/CONVAIR AND SPACE SYSTEMS DIVISION

**Table E2-2. Properties of Typical Materials Considered
for Use on Space Shuttle**

Alloy	F_{tu} (ksi)	F_{ty} (ksi)	K_{Ic} (ksi - in. ^{1/2})
4340 (High Strength)	260	217	52
4340 (Low Strength)	180	158	100
D6AC (High Strength)	275	231	61
D6AC (Low Strength)	218	203	112
18 Ni (250)	263	253	76
18 Ni (200)	206	198	100
12 Ni	190	180	226
9 Ni - 4 Cr	190	180	160
HY - 150	150	140	250
T - 1	115	100	180
2014-T6	66	60	23
2024-T4	62	47	28
2219-T87	63	51	27
6061-T6	42	36	31
7075-T6	76	69	26
6Al-4V (STA)	169	158	51
5Al-2.5 Sn	125	118	120

STRUCTURAL ANALYSIS MANUAL
GENERAL DYNAMICS/CONVAIR AND SPACE SYSTEMS DIVISION

Table E2-3. Stress-Intensity Factors

 <p>Case 1 Infinite cracked sheet with uniform normal stress at infinity</p> $K_I = \sigma \sqrt{\pi a}$ $K_{II} = K_{III} = 0$	 <p>Case 2 Infinite cracked sheet with uniform in-plane shear at infinity</p> $K_{II} = \tau \sqrt{\pi a}$ $K_I = K_{III} = 0$	 <p>Case 3 Infinite sheet with internal crack subject to out-of-plane shear at infinity</p> $K_{III} = \tau \sqrt{\pi a}$ $K_I = K_{II} = 0$
 <p>Case 4 Periodic array of cracks along a line in a sheet, uniform stress at infinity</p> $K_I = \sigma \sqrt{\pi a} \left(\frac{2b}{\pi a} \tan \frac{\pi a}{2b} \right)^{1/2}$ $K_{II} = K_{III} = 0$	 <p>Case 5 Periodic array of cracks along a line in a sheet, uniform in-plane shear stress at infinity</p> $K_{II} = \tau \sqrt{\pi a} \left(\frac{2b}{\pi a} \tan \frac{\pi a}{2b} \right)^{1/2}$ $K_I = K_{III} = 0$	 <p>Case 6 Periodic array of cracks along a line in a sheet, uniform out-of-plane shear at infinity</p> $K_{III} = \tau \sqrt{\pi a} \left(\frac{2b}{\pi a} \tan \frac{\pi a}{2b} \right)^{1/2}$ $K_I = K_{II} = 0$
<p>Case 7 Concentrated force on the surface of a crack in an infinite sheet</p>  $K_I = \frac{P}{2\sqrt{\pi a}} \left(\frac{a+b}{a-b} \right)^{1/2} + \frac{Q}{2\sqrt{\pi a}} \left(\frac{a-1}{a+1} \right)$ $K_{II} = \frac{-P}{2\sqrt{\pi a}} \left(\frac{a-1}{a+1} \right) + \frac{Q}{2\sqrt{\pi a}} \left(\frac{a+b}{a-b} \right)^{1/2}$ <p>$a = 3.4 \pi$ (for plane stress)</p>		<p>Case 8 Curved crack in equal biaxial stress field</p>  $K_I = \frac{\sigma \sqrt{R}}{\left(1 + \sin^2 \frac{\alpha}{2}\right)} \left(\frac{\sin \alpha (1 + \cos \alpha)}{2} \right)^{1/2}$ $K_{II} = \frac{\sigma \sqrt{R}}{\left(1 + \sin^2 \frac{\alpha}{2}\right)} \left(\frac{\sin \alpha (1 - \cos \alpha)}{2} \right)^{1/2}$

STRUCTURAL ANALYSIS MANUAL
GENERAL DYNAMICS/CONVAIR AND SPACE SYSTEMS DIVISION

Table E2-3. (Continued)

Case 9
Inclined crack in uniform tension in infinite sheet

$$K_I = \sigma \sin^2 \beta \sqrt{\pi a}$$

$$K_{II} = \sigma \sin \beta \cos \beta \sqrt{\pi a}$$

Case 10

Crack in infinite sheet subject to arbitrary force and couple at a remote point

At right end

$$K = \frac{1}{2\sqrt{\pi a} (1 + \alpha)} \left\{ (P + iQ) \left[\frac{a + z_0}{\sqrt{z_0^2 - a^2}} - \frac{\alpha(a + z_0)}{(z_0^2 - a^2)^{3/2}} - 1 + \alpha \right] + \frac{a(P - iQ)(z_0 - z_0) + \alpha(1 + \alpha)M}{(z_0 - a)(z_0^2 - a^2)^{3/2}} \right\}$$

$\alpha = (3 - \nu)/(1 + \nu)$ for plane stress $\alpha = 3 - 4\nu$ for plane strain
 $z_0 = x_0 + iy_0$ $\bar{z}_0 = x_0 - iy_0$

Case 12
Edge crack in a semi-infinite body subjected to shear

$$K_I = K_{II} = 0$$

$$K_{III} = \tau \sqrt{\pi a}$$

Case 13
Central crack in strip subject to tension (finite width)

$$K_I = \sigma \sqrt{\pi a} f(\lambda)$$

$$\lambda = a/b$$

λ	$f(\lambda)$
0.074	1.00
0.207	1.03
0.275	1.05
0.337	1.09
0.410	1.13
0.466	1.18
0.535	1.25
0.592	1.33

L/r	One Crack — RL/r		Two Crack — RL/r	
	Uniaxial Stress	Biaxial Stress	Uniaxial Stress	Biaxial Stress
0	3.39	2.26	3.39	2.26
0.1	2.73	1.98	2.73	1.98
0.2	2.30	1.82	2.41	1.83
0.3	2.04	1.67	2.15	1.70
0.4	1.86	1.58	1.96	1.61
0.5	1.73	1.49	1.83	1.57
0.6	1.64	1.42	1.71	1.52
0.8	1.47	1.32	1.58	1.43
1.0	1.37	1.22	1.45	1.38
1.5	1.18	1.06	1.29	1.26
2.0	1.06	1.01	1.21	1.20
3.0	0.94	0.93	1.14	1.13
5.0	0.81	0.81	1.07	1.06
10.0	0.75	0.75	1.03	1.03
∞	0.707	0.707	1.00	1.00

Case 11

Cracks from hole in infinite sheet

$$K_I = \sigma \sqrt{Lr} f\left(\frac{L}{r}\right)$$

$$K_{II} = 0$$

Case 14

Notched beam in bending

$$K_I = \frac{6M}{(h - a)^{3/2}} g(a/h)$$

$$K_{II} = K_{III} = 0$$

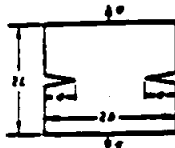
a/h	g(a/h)
0.05	0.36
0.1	0.49
0.2	0.60
0.3	0.66
0.4	0.69
0.5	0.72
0.6	0.73
> 0.6	0.73

STRUCTURAL ANALYSIS MANUAL
GENERAL DYNAMICS/CONVAIR AND SPACE SYSTEMS DIVISION

Table E2-3. (Concluded)

a/b	R/b $L/b = 1$	R/b $L/b = 3$	R/b $L/b = \infty$
0.1	1.13	1.12	1.12
0.2	1.13	1.11	1.12
0.3	1.14	1.09	1.13
0.4	1.16	1.06	1.14
0.5	1.16	1.03	1.15
0.6	1.18	1.01	1.15
0.7	1.03	1.00	1.16
0.8	1.01	1.00	1.17
0.9	1.00	1.00	1.19

Case 15
Double-edge notch



$$K_I = \sigma \sqrt{\pi} \left(\frac{2L}{\pi} \ln \frac{2L}{b} \right)^{1/2} R/b$$

$$K_{II} = K_{III} = 0$$

for $L = \infty$:

$$K_I = \sigma \sqrt{\pi} \left[\frac{2L}{\pi} \left(\ln \frac{2L}{b} + 0.1 \ln \frac{2L}{b} \right) \right]^{1/2}$$

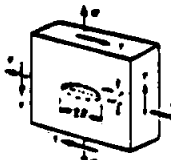
Case 16
Semi-elliptical surface crack in plate subject to general stresses

$$K_I = \left[1 + 0.12 \left(1 - \frac{a}{b} \right) \right] \frac{\sigma \sqrt{\pi}}{\phi_0} \left(\frac{2L}{\pi} \ln \frac{2L}{b} \right)^{1/2}$$

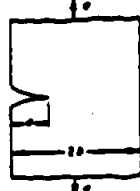
$$K_{II} = 0$$

$$K_{III} = \frac{\sigma \sqrt{\pi}}{\phi_0} \left(\frac{2L}{\pi} \ln \frac{2L}{b} \right)^{1/2}$$

where ϕ_0 is given by

$$\phi_0 = \int_0^{\pi/2} \left[1 - \left(\frac{b^2 - a^2}{b^2} \right) \sin^2 \theta \right]^{1/2} d\theta$$


Case 18
Single-edge notch




$$K_I = \sigma \sqrt{\pi} R/b$$

$$K_{II} = K_{III} = 0$$

a/b	R/b	R/b
0.1	1.13	1.14
0.2	1.13	1.19
0.3	1.09	1.29
0.4	1.06	1.37
0.5	1.03	1.50
0.6	1.01	1.66
0.7	1.00	1.87
0.8	1.00	2.12
0.9	1.00	2.44
1.0	1.00	2.87

Case 19
Round bar in tension with circumferential crack

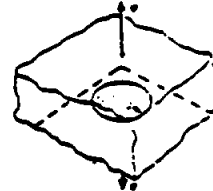


$$K_I = \sigma \sqrt{\pi} \sqrt{D} f(D/D)$$

$$K_{II} = K_{III} = 0$$

a/D	R/D	a/D	R/D
0	0	0.70	0.240
0.1	0.111	0.75	0.237
0.2	0.153	0.80	0.231
0.3	0.185	0.85	0.225
0.4	0.209	0.90	0.219
0.5	0.227	0.95	0.192
0.6	0.238	0.97	0.170
0.65	0.240	1.00	0

Case 20
Circular crack in an infinite body subject to uniform tension



$$K_I = 3\sigma \sqrt{\frac{a}{r}}$$

$$K_{II} = K_{III} = 0$$

Case 17
Two equal corner cracks in an infinite sheet subject to uniform tension

At the near ends

$$K_I = \sigma \sqrt{\pi} \frac{b^2 \frac{E(a)}{K(a)} - a^2}{(b^2 - a^2)^{3/2}}$$

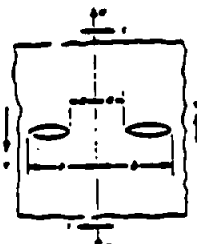
$$K_{II} = \sigma \sqrt{\pi} \frac{b^2 \frac{E(a)}{K(a)} - a^2}{(b^2 - a^2)^{3/2}}$$

At the far ends

$$K_I = \sigma \sqrt{\pi} \left(\frac{1}{a} - \frac{E(a)}{\mu K(a)} \right)$$

$$K_{II} = \sigma \sqrt{\pi} \left(\frac{1}{a} - \frac{E(a)}{\mu K(a)} \right)$$

where $\mu = \left[1 - \left(\frac{a^2}{b^2} \right) \right]^{1/2}$




E and K are the complete elliptic integrals $E(a)$ and $K(a)$ of the first and second kinds respectively

Case 21
Elliptical crack in infinite body subject to uniform tension

For point on crack edge determined by angle β

$$K_I = \frac{\sigma \sqrt{\pi}}{\phi_0} \left(\sin^2 \beta + \frac{a^2}{b^2} \cos^2 \beta \right)^{1/2}$$

$$K_{II} = K_{III} = 0$$

$$\phi_0 = \int_0^{\pi/2} \left[1 - \left(\frac{b^2 - a^2}{b^2} \right) \sin^2 \theta \right]^{1/2} d\theta$$


STRUCTURAL ANALYSIS MANUAL
GENERAL DYNAMICS/CONVAIR AND SPACE SYSTEMS DIVISION

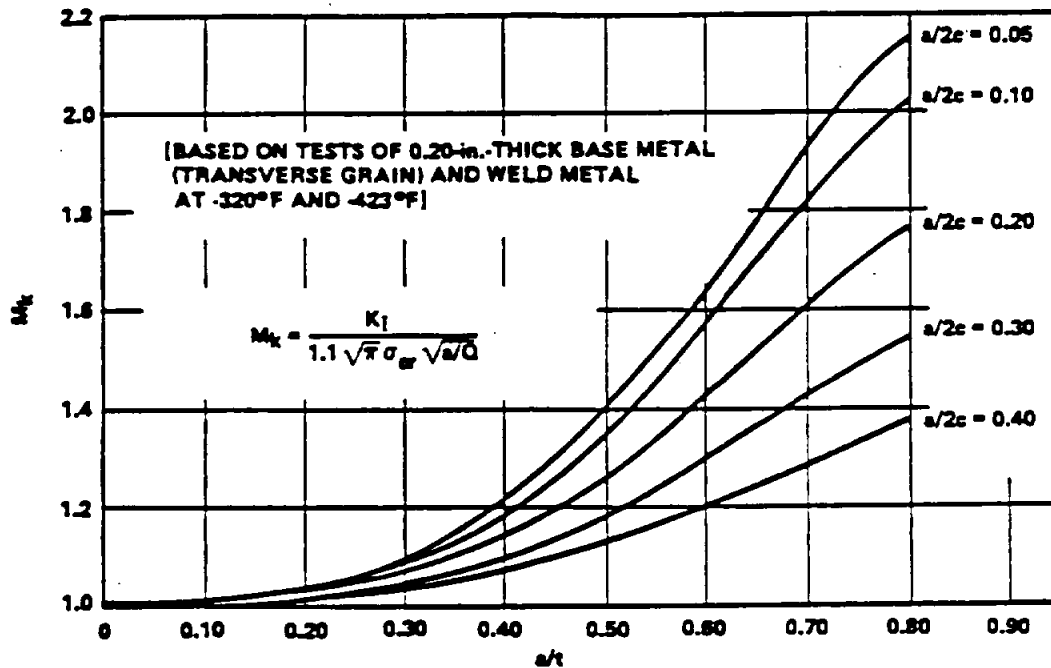


FIGURE E2-7. M_k CURVES FOR 5Al-2.5Sn (ELI) TITANIUM ALLOY

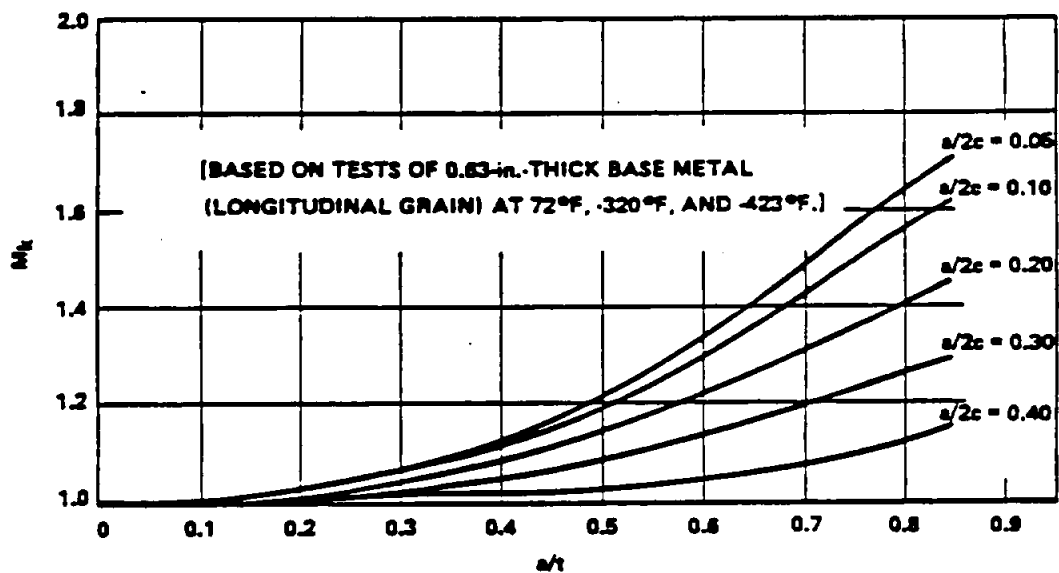


FIGURE E2-8. M_k CURVES FOR 2219-T87 ALUMINUM ALLOY

STRUCTURAL ANALYSIS MANUAL
GENERAL DYNAMICS/CONVAIR AND SPACE SYSTEMS DIVISION

For thick specimens, strain in the thickness direction is suppressed considerably by the very thickness of the material and noticeably less plastic flow is associated with the cracking process.

A laboratory plate specimen is seldom completely in either plane stress or plane strain but rather in some proportion of both. At the free surfaces of the plate there are no transverse stresses to restrain plastic flow (a condition of plane stress). In contrast, at mid-thickness, plane-strain conditions prevail and much less plastic flow occurs. A schematic representation of the crack-tip plastic zone in a plate specimen is shown in Fig. E2-9.

The size of the plane stress plastic zone is thought to be related to the amount of shear tip left at the fracture surface. Thus, the appearance of the fracture will vary according to the proportions of plane stress and plane strain conditions through the thickness of the plate.

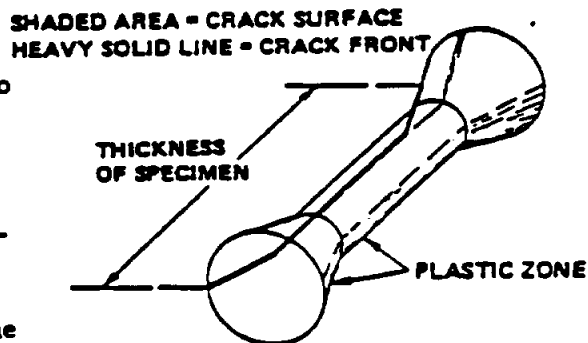


FIGURE E2-9. REPRESENTATION
OF PLASTICALLY DEFORMED
REGION AT A CRACK FRONT

The influence of stress state (and associated plasticity) on the fracture toughness is illustrated in Fig.

E2-10, which shows the effect of plate thickness on the toughness and fracture appearance. This figure shows that the larger thicknesses are characterized by low values of toughness. This corresponds to a completely square (brittle-appearing) fracture appearance.

STRUCTURAL ANALYSIS MANUAL
GENERAL DYNAMICS/CONVAIR AND SPACE SYSTEMS DIVISION

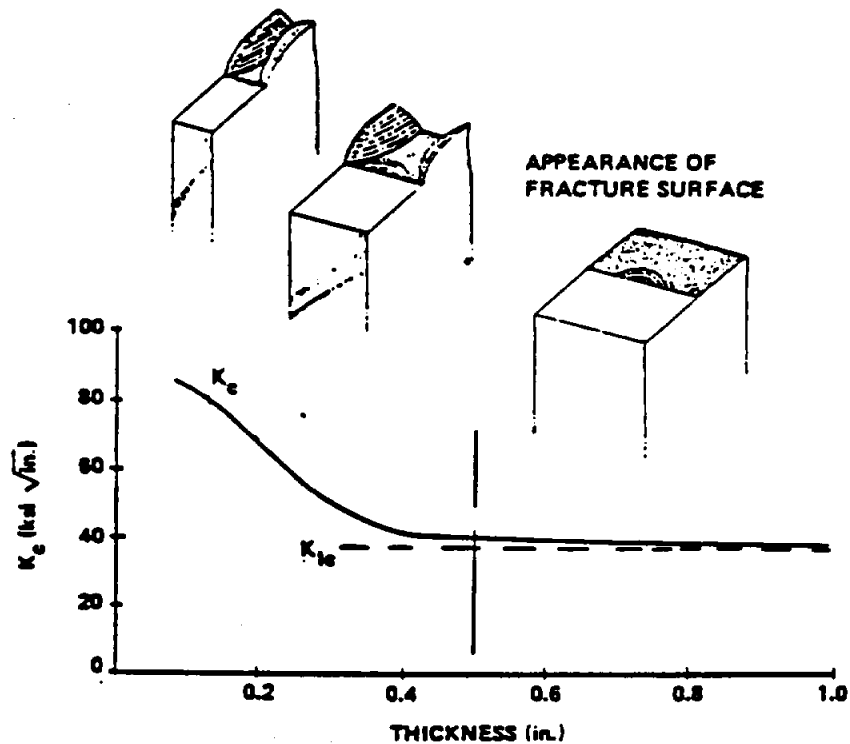


FIGURE E2-10. EFFECT OF PLATE THICKNESS ON FRACTURE TOUGHNESS AND PHYSICAL APPEARANCE OF THE FRACTURE

A reduction in plate thickness decreases the degree of plastic constraint at the advancing crack tip. This enlarges the local plastic zone and consequently raises the fracture toughness. The development of a larger plastic zone, in turn, relaxes the stress in the thickness direction, which further decreases constraint. The process is self-accelerating and the fracture toughness increases rapidly in a narrow range of thickness variation, as shown in Fig. E2-10.

In the aerospace industry thicknesses of structures are usually thin enough to fall in the region of plane stress behavior and as a result more testing in this area is being done. However, a determination of plane stress

STRUCTURAL ANALYSIS MANUAL
GENERAL DYNAMICS/CONVAIR AND SPACE SYSTEMS DIVISION

intensity factors is far more complicated than was first supposed and considerable research is needed. It is very hard to determine when unstable crack propagation occurs because the unstable condition is approached very gradually as crack length increases.

At present there is no direct method for translating laboratory data for the mixed mode fracture condition to useful numbers for designing practical hardware.

2.2.2.1 Through-the-Thickness Cracks.

In thin-walled structures, cracks may grow through the thickness before catastrophic failure occurs or a through-the-thickness crack may exist before any load is applied. The basic plane stress equation for through-thickness cracks corrected for plastic zone in an infinitely wide plate is

$$K_c^2 = \sigma^2 \left(\pi \frac{l_c}{2} + \frac{1}{2} \frac{K_c^2}{\sigma_y^2} \right) ,$$

where l_c is the length of the through-thickness crack at failure (in.), σ is the stress normal to the plane of the crack at failure (ksi), σ_y is the yield strength (ksi), and K_c is the critical plane-stress stress intensity (ksi $\sqrt{\text{in.}}$).

The critical plane stress intensity for a finite-width panel containing a through-thickness crack is

$$K_c = \sigma \left\{ w \tan \left[\frac{\pi}{2w} \left(l_c + \frac{K_c^2}{\pi \sigma_y^2} \right) \right] \right\}^{1/2} ,$$

where w is the width of the panel (in.).

STRUCTURAL ANALYSIS MANUAL
GENERAL DYNAMICS/CONVAIR AND SPACE SYSTEMS DIVISION

2.2.3 Experimental Determination.

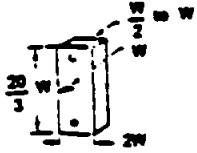
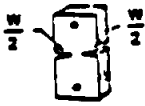

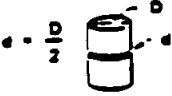


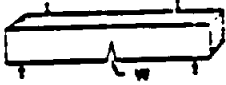
Among the most important recent progress in fracture mechanics is the improved understanding of how the behavior of test specimens relates to the design of structural components. Numerous tests have been performed on a variety of specimen types, some of which are shown in Table E2-4. The tests were designed to determine the specimen types, procedures, and data analysis which result in K_{Ic} determinations that are independent of crack and specimen geometry and manner of external loading.

At present no fracture mechanics test is universally used to determine K_{Ic} values because no one test gives valid data for all materials; each of the tests has its limitations. For instance, ASTM committee No. E-24 has been working for several years to bring out a standard (E399-70T is proposed), but this test may not be valid for low-strength, high-toughness materials.

Table E2-4 describes some types of fracture specimens, the data obtained, and their uses and limitations. For detailed information on these and other specimens, how to set up and conduct the tests, what data to obtain, and how to analyze data, see Refs. 1, 6, and 7.

STRUCTURAL ANALYSIS MANUAL
GENERAL DYNAMICS/CONVAIR AND SPACE SYSTEMS DIVISION

Table E2-4. Seven Common Types of Fracture Specimens

Specimen	Loading	Data Obtained	Uses/Limitations
 Single-Edge Crack	Uniaxial tension, induced bending	Breaking stresses, K_{Ic}	
 Double-Edge Crack	Uniaxial tension	Breaking stresses, K_{Ic}	Cracks must be equal in size
 Central Through-Crack	Uniaxial tension (static or cyclic)	Breaking stresses, K_{Ic} , flaw growth rates, K_{Ic} , I_o , I_c	Simulates penetration flaw in hardware. K_{Ic} is width dependent.
 Round Bar Notched	Uniaxial tension (cyclic or static) or rotating flexure fatigue	Breaking stresses, K_{Ic}	Simulates bolts and shafts. Difficult to form concentric precrack.
 Crackline-Loaded Wedge Opening, or Compact Tension	Tension with induced bending	K_{Ic} , K_{II}	Compact
 Partial-Thickness Crack	Uniaxial tension (static or cyclic)	Breaking stresses, flaw sizes, apparent K_{Ic}	Simulates natural flaws in hardware. Difficult to analyze. May not provide valid K_{Ic} values.
 ASTM Cracked Slow Bend	Three-point loading	K_{Ic}	Only standardized test for K_{Ic} . Not applicable to most thin and tough materials.

STRUCTURAL ANALYSIS MANUAL
GENERAL DYNAMICS/CONVAIR AND SPACE SYSTEMS DIVISION

Data Source, Section 1.3 Reference 5

2.3 FLAW GROWTH.

2.3.1 Sustained Load Flaw Growth.

One of the most serious structural problems that can arise in the aerospace industry is the delayed time failure of pressure vessels caused by sustained pressurization. In some cases, through-the-thickness cracks have formed and the vessels leaked under sustained loading. In other cases, small surface cracks or embedded flaws grew to critical sizes before growing through the thickness of the shell. When this happens, complete catastrophic fracture ensues. To predict such failures one must know the conditions under which subcritical flaw growth can occur, as well as either the actual initial flaw size or the maximum possible initial flaw size in the vessel when it is placed into service.

When the sustained stress flaw growth is environmentally induced, it is often termed stress corrosion.

The surface-flawed or "part-through" type of cracked specimen has probably found the widest use in evaluating sustained stress flaw growth in both "thick- and thin-walled" aerospace pressure vessels. With this specimen, the initial flaw closely simulates the type of flaws often encountered in service and it can be oriented to suit the flaw growth characteristics desired.

A procedure for laboratory evaluation of sustained stress flaw growth using surface flawed specimens is schematically illustrated in Fig. E2-11. The K_{Ic} for the material is first established from static (pull) tests. Then, using a batch of flawed specimens, each flawed specimen is loaded with different initial loads (various fractions of K_{Ic}) and the time required for failure observed, e.g., specimens 1 and 2, illustrated in Fig. E2-11. If failure does not occur in a reasonable time (e.g., specimens 3 and 4), it is still possible to obtain crack growth information by "marking" the crack front (applying some low-stress fatigue cycles) and pulling the specimen apart.

STRUCTURAL ANALYSIS MANUAL
GENERAL DYNAMICS/CONVAIR AND SPACE SYSTEMS DIVISION

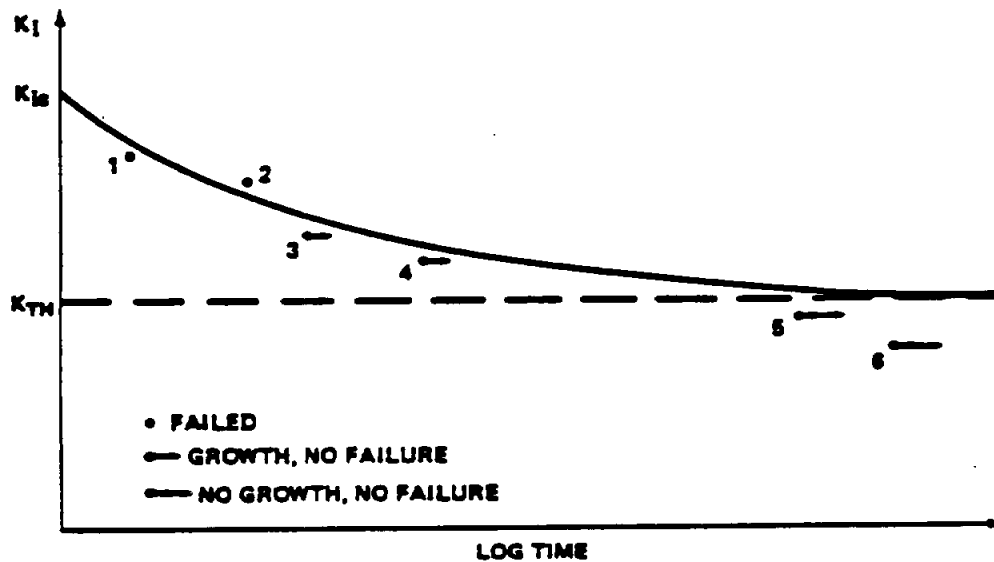


FIGURE E2-11. SCHEMATIC ILLUSTRATION OF A PROCEDURE
FOR LABORATORY EVALUATION OF SUSTAINED STRESS FLOW
GROWTH USING SURFACE FLAWED SPECIMENS

A point is finally reached at which neither failure nor flow growth occurs. The highest level of K for which this condition occurs is called the threshold stress intensity, K_{TH} ; or K_{Isc} if due to stress corrosion cracking.

2.3.1.1 Environmental Effects.

The discovery of a unique K_{TH} can be 80 percent of K_{Ic} or higher in relatively inert environments; hostile media can reduce the value to less than half of K_{Ic} .

Considerable evidence indicates that sustained load flow growth is most severe under conditions of plane strain with K_{TH} values determined from through-the-thickness cracked specimen tests increasing with a decrease in specimen thickness.

STRUCTURAL ANALYSIS MANUAL
GENERAL DYNAMICS/CONVAIR AND SPACE SYSTEMS DIVISION

Studies of flaw growth and stress intensity in aggressive environments indicate a monotonic relation between increasing stress intensity and growth rate and design correlations have been determined for the critically important materials, titanium, and high-strength steels. In these tests for K_{TH} , a wide scatter, abnormally short times to failure, and very marked dependence on environmental characteristics (media and temperature) are encountered.

During the past few years a considerable amount of sustained load flaw growth data has been obtained on a number of different material-environment combinations. A summary of some K_{TH} information is given in Table E2-5.

2.3.2 Cyclic Load Flaw Growth.

Understanding crack propagation under cyclic loads is a basic requirement for the application of fracture mechanics to the design of structures for service life. Subcritical flaw-growth characteristics for various materials are generally determined through the laboratory testing of flawed specimens. These empirical data are then correlated to various crack-propagation theories which have been proposed. The following is a discussion of some of the more prominent theories.

2.3.2.1 Theories.

A number of studies dealing with fatigue crack propagation have shown that the stress intensity factor K is the most important variable affecting fatigue crack growth rates. The availability of a master curve for a particular material relating fatigue crack-growth rate and range of stress-intensity factor would enable a designer to predict growth rates for any cracked body configuration.

Numerous "laws" of fatigue crack growth have been published during the last 10 years. Basically, all the various equations that have been obtained are simply the attempt of an individual investigator to obtain a curve that will

STRUCTURAL ANALYSIS MANUAL
GENERAL DYNAMICS/CONVAIR AND SPACE SYSTEMS DIVISION

Table E2-5. Typical Threshold Stress-Intensity Data for Various Material-Environment Combinations

Material	Temp. (°F)	σ_{ys} (ksi)	Typ. K_{IS} (ksi $\sqrt{\text{in.}}$)	Fluid Environment	K_{TH}^a / K_{IC}
6Al-4V Titanium Forging - STA	R.T.	160	44	Methanol	0.24
	R.T.	160	44	From M. F.	0.34
	R.T.	160	44	N ₂ O ₄ (0.30% NO)	0.74
	R.T.	160	44	N ₂ O ₄ (0.60% NO)	0.83
	R.T.	160	44	H ₂ O (distilled) + Na ₂ CrO ₄	0.82
	R.T.	160	44	H ₂ O (distilled)	0.86
	R.T.	160	44	Helium, Air, or COX	0.90
	R.T.	160	44	Aerospace 30	0.82
	R.T.	160	44	From T. F.	0.80
	90	160	44	N ₂ O ₄ (0.30% NO)	0.71
	90	160	44	N ₂ O ₄ (0.60% NO)	0.73
	100	160	44	Monomethylhydrazine	0.73
	110	160	44	Aerospace 30	0.73
6Al-4V Titanium Weldments (Heat-Affected Zones)	R.T.	126	39	Methanol	0.24
	R.T.	126	39	From M. F.	0.40
	R.T.	126	39	H ₂ O (Distilled)	0.86
	R.T.	126	39	H ₂ O (Distilled) + Na ₂ CrO ₄	0.82
5Al-2.5 Sn (FLI) Titanium Plate	-320	180	64	LN ₂ ($\sigma < \text{Prop. Limit}$)	<0.80
	-420	180	64	LN ₂ ($\sigma < \text{Prop. Limit}$)	0.82
	-423	210	32	LH ₂	<0.80
2219-T8T Aluminum Plate	R.T.	54	36	Air	0.80 ¹
	-320	66	41	LN ₂	0.82 ¹
	-423	72	44	LH ₂	<0.80 ¹
4330 Steel	R.T.	295	90	Water	0.24
4340 Steel	R.T.	>290	840	Salt water	<0.20
GTA Welds					
18 Ni (200) Steel	R.T.	200	130	Salt-water Spray	<0.70
18 Ni (250) Steel	R.T.	235	73	Salt-water Spray	<0.70
12 Ni-3 Cr-3 Mo Steel	R.T.	170	153	Salt-water Spray	<0.70
9 Ni-4 Co-2.8C Steel	R.T.	170	120	Salt-water Spray	<0.70
5 Ni-Cr-Mo Steel	R.T.	140	>200	Salt-water Spray	<0.70
Inconel 718	R.T.	165	>120	Gaseous Hydrogen at 5000 psig	0.25
2219-T8S1 Aluminum Plate	R.T.	50		N ₂ O ₄	0.70
2021-T8S1 Aluminum Plate	R.T.	65	30.3	N ₂ O ₄	0.33

a. No failure K_{TH} ; some growth observed at lower values.

STRUCTURAL ANALYSIS MANUAL
GENERAL DYNAMICS/CONVAIR AND SPACE SYSTEMS DIVISION

best fit his data. Some have used curve-fitting techniques to obtain a high-order polynomial to fit the data, others have used a statistics approach, and still others have divided the data into regions and constructed straight lines with different slopes in each region.

The choice between equations may be that of simplicity of equation versus accuracy of flaw-growth prediction given from the equation over the range of interest. For example, an equation may be very simple and give good results over a limited range of data, but out of this range the equation may be quite inaccurate.

I. Paris.

Paris and Erdogan (Ref. 8), for example, argued that the growth rate should be a function of the stress-intensity factor K on the grounds that this factor defines the elastic stress field around the crack tip. They found that a large body of data could be fitted by an expression of the form

$$\frac{da}{dN} = c (\Delta K)^n ,$$

where c is a material constant, ΔK is the range of stress-intensity factor, and n is an exponent having a typical value of four for steel.

An example of Paris's equation for a typical steel is shown in Fig. E2-12. On a log-log plot, the equation becomes a straight line. The slope of the line is four, which is the value of n . The constant $c = 5.6 \times 10^{-24}$ is obtained by substitution of data into the Paris equation and solving for c . Separate values of the coefficients c and n must be computed for each value of R (load ratio) because Paris's equation does not have R as a function.

STRUCTURAL ANALYSIS MANUAL
GENERAL DYNAMICS/CONVAIR AND SPACE SYSTEMS DIVISION

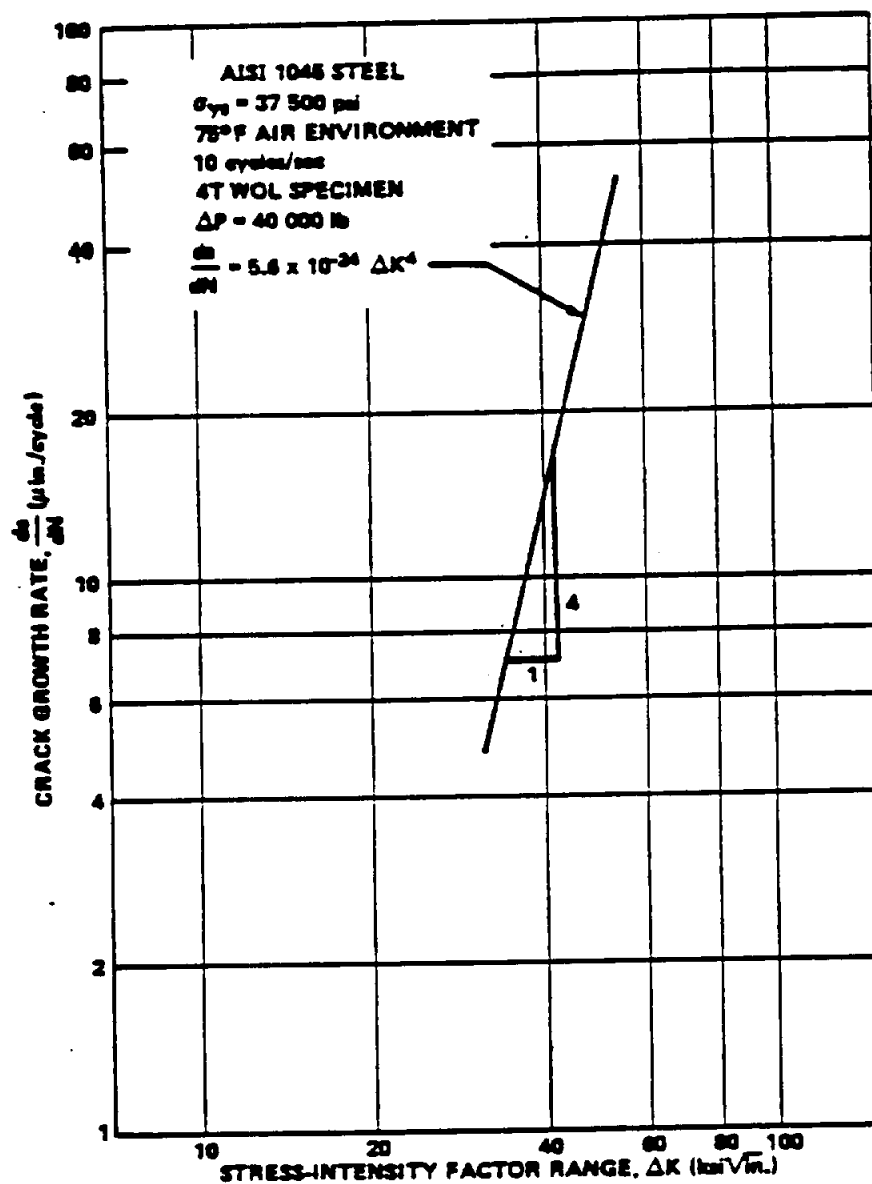


FIGURE E2-12. FATIGUE CRACK GROWTH RATE VERSUS STRESS-INTENSITY FACTOR RANGE FOR AISI 1045 STEEL

STRUCTURAL ANALYSIS MANUAL
GENERAL DYNAMICS/CONVAIR AND SPACE SYSTEMS DIVISION

II. Foreman.

The Paris fourth-power crack growth rate equation was modified by Foreman et al. (Ref. 9) to account for the observed behavior that crack growth rates tend to increase rapidly toward an apparent instability as the maximum applied stress intensity approaches the fracture toughness of the material. Foreman also modified the Paris law to account for the observed behavior and to explicitly express the effect of load ratio, $R = K_{\min}/K_{\max}$. The Foreman expression for plane-stress conditions is

$$\frac{da}{dN} = \frac{c (\Delta K)^n}{(1 - R) K_c - \Delta K} ,$$

where c and n are constants dependent on material and test conditions.

$$\Delta K = (K_{\max} - K_{\min}) \text{ during a load cycle.}$$

K_c = plane stress fracture toughness of the material.

A comparison of Paris's and Foreman's equations was made by Hudson in Ref. 10 for 2024-T3 and 7075-T6 aluminum. It was found that the 7075-T6 data fell into an S shape or reflex type of curvature. A reflex curvature is also obtained from Foreman's equation; it is induced by ΔK approaching $(1 - R) K_c$ in the denominator. This intrinsic shape is the primary reason for the excellent fit of the data by using Foreman's equation. Paris's equation does not provide for this reflex curvature; consequently, the equation cannot fit the data at high or low growth rates as well as Foreman's equations.

The constant n in Foreman's equation is the slope of the curve in the straight-line midrange and c is determined from the substitution of data

STRUCTURAL ANALYSIS MANUAL
GENERAL DYNAMICS/CONVAIR AND SPACE SYSTEMS DIVISION

value into the equation. It should be noted that n and c will change, depending on the type of plot used. Generally, a log-log plot of ΔK in $\text{psi } \sqrt{\text{in.}}$ and da/dN in microinches/inch is used.

Foreman's equation for 2219-T87 is shown in Fig. E2-13 and some typical values of c and n for other common materials are given in Table E2-6.

Table E2-6. Crack Propagation Coefficients for Foreman's Equation

$\frac{da}{dN} = \frac{c (\Delta K)^n}{(1 - R) K_c - \Delta K}$ <p>da/dN in./cycle</p> <p>ΔK and K_c $\text{psi } \sqrt{\text{in.}}$</p>				
Material	Temp. (°F)	c	n	K_{Ic} $\text{psi } \sqrt{\text{in.}}$
2219-T87	R. T.	1.4×10^{-11}	2.5	33,000
	300	1.5×10^{-11}	2.47	31,600
	-320	9.0×10^{-13}	2.7	36,200
TI-8Al-4V	R. T.	7.8×10^{-14}	3.0	81,000
2024-T3	R. T.	3.22×10^{-14}	3.38	
7075-T6	R. T.	2.13×10^{-13}	3.21	
517A (TI)				

The solution of the Foreman equation can be formulated as an initial-value problem and can be solved by direct numerical integration using the Runge-Kutta method. For most practical problems, an initial crack size is

666

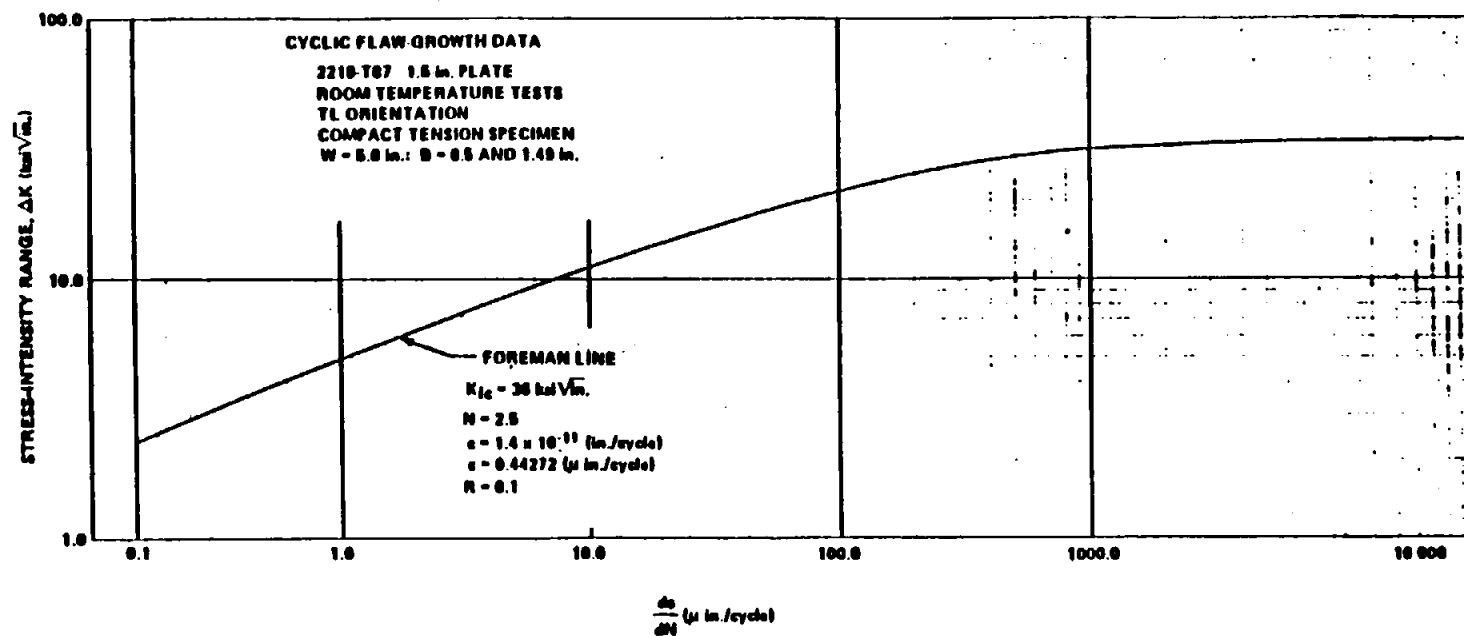


FIGURE E2-13. CRACK GROWTH VERSUS STRESS-INTENSITY FACTOR RANGE FOR 2219-T87

STRUCTURAL ANALYSIS MANUAL
GENERAL DYNAMICS/CONVAIR AND SPACE SYSTEMS DIVISION

known at an initial value of N , such as $N = 0$. The problem is to determine the crack length (or additionally the stress-intensity factor) after a given number of cycles.

III. Tiffany.

An alternate approach to plane-strain flaw-growth rates has been presented by Tiffany (Ref. 11). Tiffany noted that the cyclic lives of specimens were primarily a function of the ratio of maximum initial stress intensity applied to the flaw during the first loading cycle (K_{II}) to the plane-strain fracture toughness of the material (K_{Ic}). Accordingly, cyclic life data were plotted on K_{II}/K_{Ic} versus cycles-to-failure graphs, where it was observed that data for particular test conditions and material-environment combinations could be reasonably represented by a unique curve. Flaw-growth rates were computed using the slopes of the cyclic life curves. Because the analysis required knowledge of only the initial and final conditions for each test, the Tiffany method was called an end-point analysis. The use of K_{II}/K_{Ic} versus cycles-to-failure curves for practical design problems is common in the aerospace industry (Ref. 12). Figure E2-14 shows a K_{II}/K_{Ic} versus cycles-to-failure curve for 2219-T87 at room temperature.

2.3.2.2 Crack Growth Retardation.

I. Wheeler's Retardation Parameter.

The retardation of crack growth is a phenomenon which occurs because of varying load levels. Retardation has been shown to occur particularly after a high level of load followed by a lower level of load.

Many papers have discussed crack growth retardation to some extent but a computational technique has not been presented which is sufficiently simple and accurate to gain widespread use (Ref. 13).

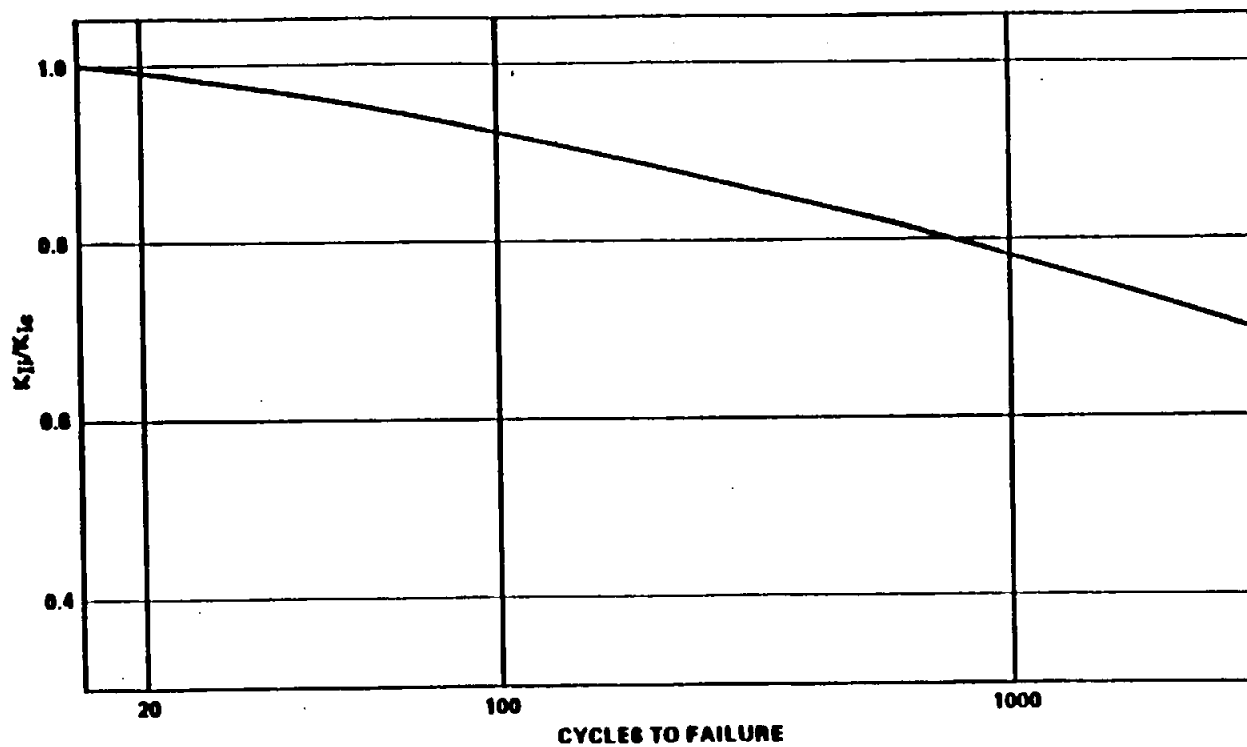


FIGURE E2-14. CYCLIC GROWTH RATE DATA FOR 2219-T87 AT ROOM TEMPERATURE

STRUCTURAL ANALYSIS MANUAL
GENERAL DYNAMICS/CONVAIR AND SPACE SYSTEMS DIVISION

Wheeler (Ref. 13) suggests that more accurate crack growth predictions can be made by introducing a retardation parameter in the crack growth equation, which serves to delay the crack growth after a high load application. His equation for crack length is

$$a_r = a_o + \sum_{i=1}^r C_{pi} f(\Delta K_i) ,$$

where a_r is the crack length after r load applications, a_o is the initial crack length, C_{pi} is the retardation parameter at i^{th} load, and ΔK_i is the change in the stress-intensity factor at i^{th} load. The retardation parameter is taken in the following form:

$$C_p = \left(\frac{R_y}{a_p - a} \right)^m , \quad a + R_y < a_p ,$$

$$C_p = 1 , \quad \text{and} \quad a + R_y \geq a_p$$

where R_y is the extent of the current yield zone, $a_p - a$ is the distance from crack tip to elastic-plastic interface (Fig. E2-15), and m is the shaping exponent dependent upon material and test data.

This parameter has been used successfully to predict the growth of cracks in specimens subjected to six different spectra, having three different physical configurations, and made of two materials (Ref. 13). It is believed that this approach represents a useful improvement on the idea of linear cumulative crack growth, which can be used with confidence in design and analysis.

STRUCTURAL ANALYSIS MANUAL
GENERAL DYNAMICS/CONVAIR AND SPACE SYSTEMS DIVISION

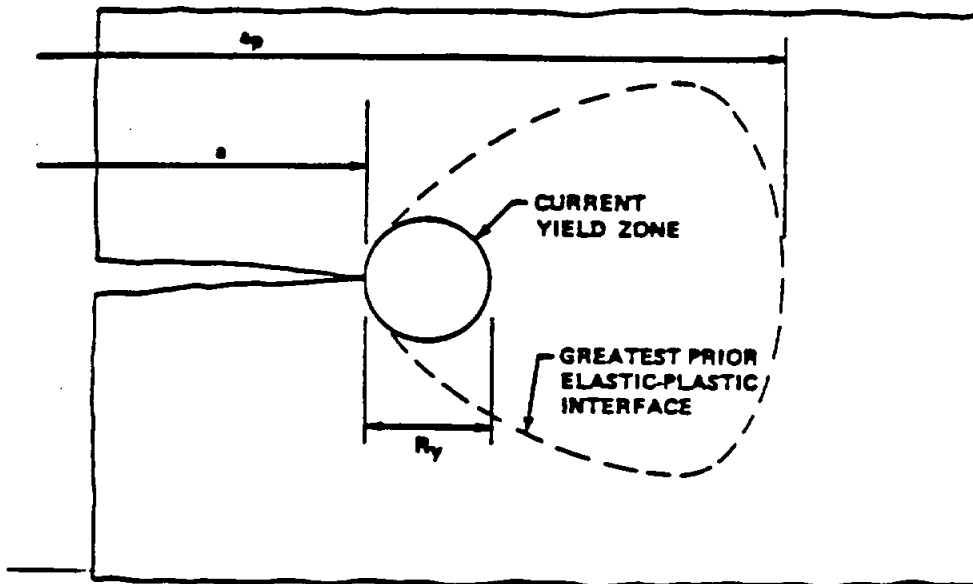


FIGURE E2-15. CRACK TIP YIELD ZONES

The computational scheme for incorporating this retardation parameter in crack growth predictions requires that the crack be grown one load application at a time. This amounts to a piecewise linearization of a highly nonlinear process. The use of a high-speed digital computer is obviously required to perform any realistic analysis. This technique has been incorporated into the computer program CRACKS.

II. The Significance of Fatigue Crack Closure.

Recent work by Elber (Refs. 14 and 15) has shown that fatigue cracks in sheets of aluminum alloy close before all tensile load is removed. Significant compressive stresses are transmitted across the crack at zero load. In previous work, usually the assumption has been made implicitly that a crack is closed under compressive loads and open under tensile loads. The determination of the crack closure stress must, therefore, be a necessary step in the stress analysis of a cracked structure.

STRUCTURAL ANALYSIS MANUAL
GENERAL DYNAMICS/CONVAIR AND SPACE SYSTEMS DIVISION

Elber (Ref. 15) obtains an empirical relation for the crack opening stress level and uses it as a basis for a crack propagation equation. The analysis of qualitative experiments on variable amplitude loading shows that the crack closure phenomenon could account for acceleration and retardation effects in crack propagation.

Crack closure stress can be explained by the existence of a zone of material behind the crack tip having residual tensile strains. In Fig. E2-16 a fatigue crack produced under constant amplitude loading is shown at three crack lengths. Figure E2-16a shows the crack tip surrounded by a plastic zone as it is represented normally. Figure E2-16b shows the crack at a greater crack length surrounded by a larger plastic zone because the stress intensity is higher. The plastic zone of Figure E2-16a has been retained to show that the material had been subjected previously to plastic deformations. Figure E2-16c represents the crack surrounded by the envelope of all zones which during crack growth had been subjected to plastic deformations. During a single cycle of crack growth, residual tensile deformations are left in the material behind the moving crack front, as only elastic recovery occurs after separation of the surfaces.

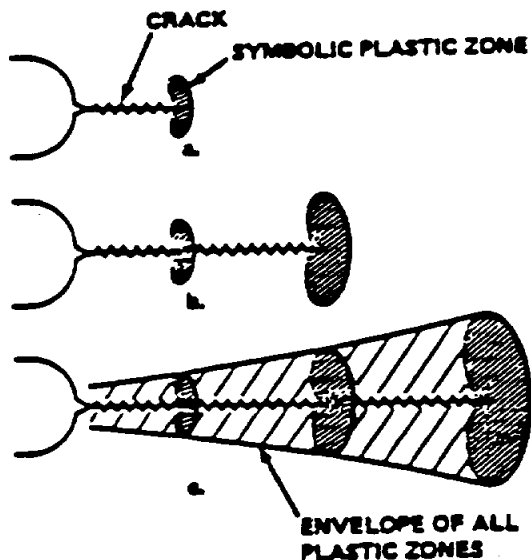


FIGURE E2-16. DEVELOPMENT OF
A PLASTIC ZONE AROUND A
FATIGUE CRACK

STRUCTURAL ANALYSIS MANUAL
GENERAL DYNAMICS/CONVAIR AND SPACE SYSTEMS DIVISION

Crack propagation can occur only during that portion of the loading cycle in which the crack is fully open at the crack tip; therefore, in attempting to analytically predict crack propagation rates, it seems reasonable that the crack opening stress level should be used as a reference stress level from which an effective stress range could be obtained. The effective stress range is defined there as

$$\Delta S_{\text{eff}} = S_{\text{max}} - S_{\text{op}} ,$$

where S_{op} is the crack opening stress.

An effective stress range ratio is then defined as

$$U = \frac{(S_{\text{max}} - S_{\text{op}})}{(S_{\text{max}} - S_{\text{min}})} = \frac{\Delta S_{\text{eff}}}{\Delta S} .$$

Constant amplitude loading tests were conducted to establish the relationship between U and three variables which were anticipated to have a significant effect on U , namely, stress-intensity range, crack length, and stress ratio.

For the given range of testing conditions, only the stress ratio R is a significant variable. The relation between U and R is linear and can be expressed as

$$U = 0.5 + 0.4 R \text{ where } -0.1 < R < 0.7$$

for 2024-T3 aluminum alloy.

STRUCTURAL ANALYSIS MANUAL
GENERAL DYNAMICS/CONVAIR AND SPACE SYSTEMS DIVISION

One of the most important problems in aircraft structures is the inability to predict accurately the rate of fatigue crack propagation under variable amplitude loading. In attempts to calculate these crack rates on the basis of constant amplitude data, interaction effects are usually ignored, leading to errors of significant magnitude.

Crack closure may be a significant factor in causing these interaction effects. This can be shown by the following example. Assume that a crack in 2024-T3 aluminum is propagating under the conditions $R = 0$ and $K_{\max} = 20 \text{ MN/m}^{3/2}$. Under these conditions the crack opening level is at $K_{\text{op}} = 10 \text{ MN/m}^{3/2}$. If the stress-intensity range suddenly is halved, the new conditions are $K_{\max} = 10 \text{ MN/m}^{3/2}$ and $R = 0$. The crack opening level, however, is still at $K_{\text{op}} = 10 \text{ MN/m}^{3/2}$, equal to the new peak stress intensity, so the crack does not open. Therefore, the crack does not propagate until the crack opening level changes. The behavior of the crack opening stress level under variable amplitude loading must therefore be investigated.

It has been observed that a crack will continue to grow for some time after a high load application followed by loads of smaller magnitude. This has been termed delayed retardation. Such retardation of crack growth after a single high load can be explained by examining the behavior of the large plastic zone left by the high-load cycle ahead of the crack tip. The elastic material surrounding this plastic zone acts like a clamp on this zone, causing the compressive residual stresses. As long as this plastic zone is ahead of the crack tip, this clamping action does not influence the crack opening. As the crack propagates into the plastic zone, the clamping action will act on the new fracture surfaces. This clamping action, which builds up as the crack propagates into the plastic zone, requires a larger, externally applied stress to open the crack; hence, the crack will propagate at a decreasing rate into this zone and may come to a standstill.

STRUCTURAL ANALYSIS MANUAL
GENERAL DYNAMICS/CONVAIR AND SPACE SYSTEMS DIVISION

2.3.2.3 Transition from Partial-Thickness Cracks to Through-Thickness Cracks.

It was shown in Section 2.2 that the stress intensity was different for partial-thickness cracks and for through-the-thickness cracks. Also, for through-the-thickness cracks, corrections must be made for a finite plate within the stress intensity equation (Table E2-3, Case 13).

Often in crack propagation problems a crack will initially be a partial-thickness crack and will grow until it extends through the thickness. When this occurs, corrections in the stress-intensity expression must be made.

The transition from a surface flaw to a through crack is chosen to be the point when the plastic zone reaches the back face of the material. The value of a (crack length) for which this occurs is given as

$$a_t = t - \frac{1}{2\pi} \left(\frac{K_{\max}}{\sigma_{ys}} \right)^2$$

2.3.3 Combined Cyclic and Sustained Flaw Growth.

Tiffany and Masters (Ref 1) hypothesized that below the sustained stress threshold stress-intensity value (K_{TH}), cyclic speed (or hold time at maximum load) probably would not affect the cyclic flaw growth rate, but above K_{TH} it could have a large effect. In other words, the minimum cyclic life was limited to the number of cycles required to increase the initial stress intensity K_{II} to the K_{TH} value, and above the K_{TH} level, failure could occur in one additional cycle if the hold time were sufficiently long.

To date there is only a limited amount of experimental data to substantiate this prediction. However, the data do tend to support the original Tiffany-Masters hypothesis of no significant effect of cyclic speed on flaw growth rates below the sustained stress threshold stress intensity.

STRUCTURAL ANALYSIS MANUAL
GENERAL DYNAMICS/CONVAIR AND SPACE SYSTEMS DIVISION

Data Source, Section 1.3 Reference 5

2.4 APPLICATION OF FRACTURE MECHANICS TECHNOLOGY.

2.4.1 Selection of Materials.

In the material selection and design of a tension-loaded structure, such as a pressure vessel, the following questions must be considered:

1. What are the critical flaw sizes (sizes which cause failure) in the different parts of the structure at expected operational stress levels?
2. What are the maximum initial flaw sizes likely to exist in the structure before service?
3. Will these initial flaws grow to critical size and cause failure during the expected service life of the structure?

The answers to these questions depend heavily upon the inherent fracture toughness and subcritical flaw-growth characteristics of the structural material. Fracture toughness data derived from test specimens are used in fracture mechanics analysis to predict critical flaw sizes, evaluate subcritical flaw growth, and estimate structural life. They can also be used to determine the maximum possible initial flaw size in a structure after a proof load.

As previously mentioned (Section 2.2), the types of flaws encountered in fabricated structures can be categorized as surface flaws, embedded flaws, and through-the-thickness cracks. For surface and embedded flaws, the degree of constraint at the crack leading edge is high, and plane-strain conditions generally prevail. The initial flaws may or may not reach critical size before growing through the thickness, depending upon the plane-strain fracture toughness (K_{Ic}) value, the applied stress levels, and the material thickness. If the calculated critical flaw size is small with respect to the wall thickness, the formation of a through-the-thickness crack before fracture is not likely.

STRUCTURAL ANALYSIS MANUAL
GENERAL DYNAMICS/CONVAIR AND SPACE SYSTEMS DIVISION

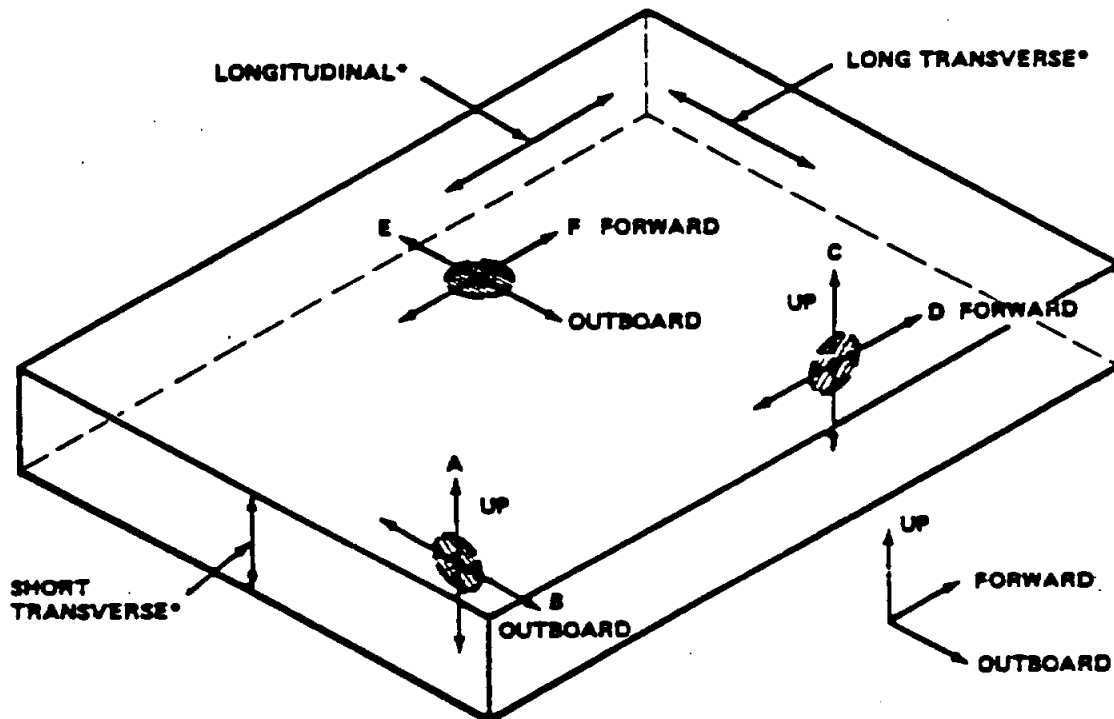
For through-the-thickness cracks, the mode of fracture for a given material, stress level, and test temperature depends upon the material thickness. If the material is relatively thin, plane-stress conditions generally predominate. With increasing thickness, the fracture appearance changes from that of full shear to an essentially flat or plane-strain fracture. Thus, for thin sections containing through-the-thickness cracks, the plane-stress fracture toughness (K_{Ic}) values are important, and as the thickness is increased the plane-strain (K_{Ic}) values should be used. The theory of this has been discussed in detail (Section 2.2.2).

The common types of fracture specimens and their requirements have also been discussed (Section 2.2.3). It is appropriate to point out the significance of end-hardware application and material anisotropy on specimen selection and to show fracture-toughness correlations among several of the more common specimens.

Just as conventional mechanical properties generally vary to some degree among various forms and grain directions in a given basic alloy, it has been found from fracture tests performed thus far on various materials that fracture toughness values also vary. In a rolled plate or forging, six directions of flaw propagation are possible, and plane-strain toughness (K_{Ic}) values may differ in each of these directions (Fig. E2-17). The need to determine the K_{Ic} values in each of these directions depends on the direction of the applied stresses in the hardware.

Considering the banding and delamination problems in some thick plates, it appears that the K_{Ic} values can be different between the A and B directions and, likewise, the C and D directions. This has actually been found to be the case from investigation (Ref. 16) and tends to explain the differences in K_{Ic} values obtained using surface-flawed and round-notched-bar or single-edge-notched fracture specimens. The surface-flawed specimen

STRUCTURAL ANALYSIS MANUAL
GENERAL DYNAMICS/CONVAIR AND SPACE SYSTEMS DIVISION



A - F: DIRECTIONS OF FLAW PROPAGATION
*GRAIN DIRECTION

FIGURE E2-17. STRESS FIELD, GRAIN DIRECTIONS, AND
POSSIBLE DIRECTIONS OF FLAW PROPAGATION

is normally used to measure toughness in either the A or C directions, and the single-edge-notched or center-cracked (pop-in) specimens measure toughness in the B or D directions. The round notched bar (removed so that its longitudinal axis is parallel to the plate surface) measures the lower of either the A or B directions or the lower of either the C or D directions. For material where there are no pronounced directional effects, the same toughness should be obtained regardless of which specimen is used. In the short transverse direction of materials, there appears to be no reason for a significant difference in K_{Ic} values between the E and F directions, although there is no apparent experimental substantiation of this.

STRUCTURAL ANALYSIS MANUAL
GENERAL DYNAMICS/CONVAIR AND SPACE SYSTEMS DIVISION

For weldments, it is known that there can be differences in fracture toughness between the weld centerline and the heat-affected zone. In addition, it is considered probable that fracture toughness as well as subcritical flaw growth characteristics vary within the heat-affected zone so that for the establishment of realistic allowable flaw sizes, the minimum K_{Ic} values must be determined.

The foregoing discussion makes clear the necessity for insuring the use of comparable valid fracture toughness and subcritical flaw growth data when they are available, or the selection of proper specimen types to obtain the desired directional data, in comparing materials for selection. While round-notched-bar specimens might be considered desirable because they automatically obtain the lower toughness values in either the A or B directions or the lower in either the C or D directions, it may not always be possible to use the specimen type because of material thickness limitations (i. e., the required specimen diameter for valid K_{Ic} exceeds the hardware wall thickness). In such a case, the single-edge-notched specimen might be used for toughness in the B and D directions and the surface-flawed specimen in the A and C directions.

In summary, it presently appears that there is no single "best fracture specimen" to use in all situations where toughness data are needed for material comparisons and selection, nor is such required. Of primary importance is that the selected specimen toughness data for different materials provide a valid comparison for selection and be representative of toughness and flaw growth characteristics of the material as used in the hardware application.

2.4.1.1 Static Loading.

An evaluation of the resistance of materials to catastrophic brittle fracture requires the following basic material properties:

STRUCTURAL ANALYSIS MANUAL
GENERAL DYNAMICS/CONVAIR AND SPACE SYSTEMS DIVISION

1. Plane-strain fracture toughness, K_{Ic}
2. Conventional tensile yield strength, σ_{ys}

An evaluation of materials based on the data accumulated from test specimens can be illustrated best by using a hypothetical example.

I. Example Problem A.

Three materials — a steel, a titanium, and an aluminum alloy — are initially selected as potential candidate materials for minimum weight design. The yield strength of each is chosen to attain nearly equivalent strength/weight ratios. The yield strengths and K_{Ic} values obtained from the tested specimens and design requirement are shown in the following table.

Alloy	Density (lb/in. ³)	σ_{ys} (ksi)	$\sigma_{ys}/\text{Density}$ $\times 1000$ (in.)	K_{Ic} (ksi $\sqrt{\text{in.}}$)	Applied Stress $1/2 \sigma_{ys}$ (ksi)
Steel	0.284	250	880	100	125
Aluminum	0.098	85	870	30	42.5
Titanium	0.163	140	860	80	70

Assume that

1. The defect is a semielliptical surface flaw with $a/2c = 0.2$.
2. The defect is located in a thick plate loaded in tension.

To decide which material provides the most fracture resistance is to establish which material requires the largest critical flaw size for catastrophic fracture.

For "thick walled" structures critical flaw sizes can be determined from the following equation:

STRUCTURAL ANALYSIS MANUAL
GENERAL DYNAMICS/CONVAIR AND SPACE SYSTEMS DIVISION

$$(a/Q)_{cr} = \frac{1}{1.21\pi} \left(\frac{K_{Ic}}{\sigma} \right)^2$$

or

$$a_{cr} = \frac{Q}{1.21\pi} \left(\frac{K_{Ic}}{\sigma} \right)^2$$

where the shape factor parameter can be obtained from Fig. E2-5. For this comparison, $Q = 1.26$.

The results are shown in the following table.

Alloy	Depth, a_{cr} (in.)	Length, $2c$ (in.)
Steel	0.212	1.06
Aluminum	0.165	0.83
Titanium	0.432	2.16

Conclusion.

The titanium alloy is most fracture resistant in terms of requiring the largest critical flaw size defect, a_{cr} , for catastrophic fracture.

This conclusion could have been reached by considering the K_{Ic}/σ_{ys} ratios for the various materials shown in the following table.

Alloy	K_{Ic}/σ_{ys} ($\sqrt{\text{in.}}$)
Steel	0.400
Aluminum	0.353
Titanium	0.572

STRUCTURAL ANALYSIS MANUAL
GENERAL DYNAMICS/CONVAIR AND SPACE SYSTEMS DIVISION

The titanium, having the highest K_{Ic}/σ_{ys} ratio, could be expected to be the toughest material for the given application.

Tiffany and Masters (Ref. 17) showed that for screening several materials, K_{Ic} data are often plotted as shown in Fig. E2-18a. Recognizing that the operating stress levels are generally controlled to a fixed percentage of the unflawed tensile strength by the design safety factor, the data shown in Fig. E2-18a might be more appropriately plotted as shown in Fig. E2-18b. The ordinate is directly proportional to the critical flaw size, thus placing the influence of varying materials strength in better perspective. From Fig. E2-18b the three materials can be compared upon the basis of equal critical flaw size. For example, structures designed from a 200-ksi steel, a 135-ksi titanium, and a 70-ksi aluminum would all have approximately the same critical flaw size. Considering the effect of weight, one might wish to make the comparison shown in Fig. E2-18c. This shows that titanium provides a somewhat lighter tank on the basis of equal flaw size.

Based on considerations of the practical capability of available nondestructive inspection (NDI) techniques, the resistance to catastrophic fracture could also be evaluated by calculating the maximum allowable applied stress for equivalent defects in each material.

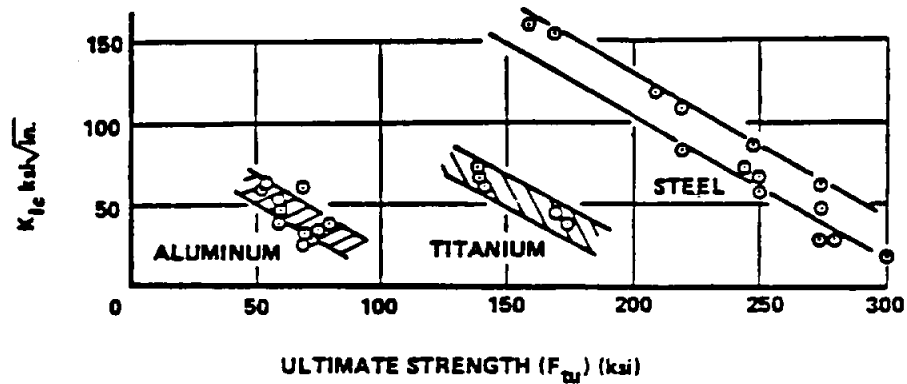
Reevaluate the preceding example, assuming that the minimum detectable flaw is 0.15 in. deep by 0.75 in. long.

Rearranging the basic equation results in

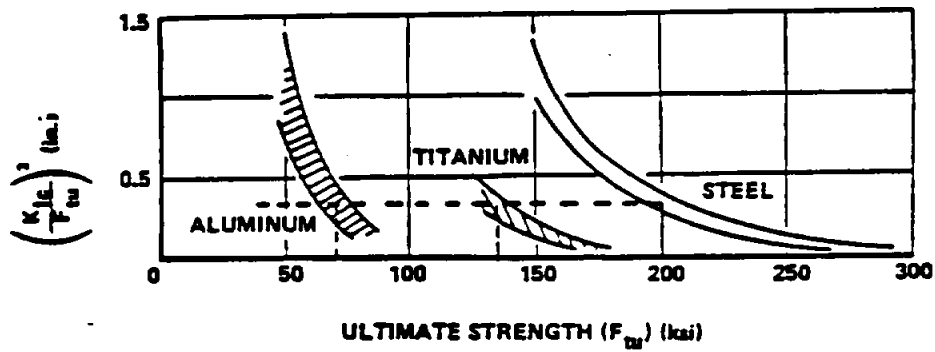
$$\sigma^2 = \frac{K_{Ic}^2 (Q)}{1.21\pi (a)}$$

The resulting critical fracture stresses and other pertinent information are summarized in the following table.

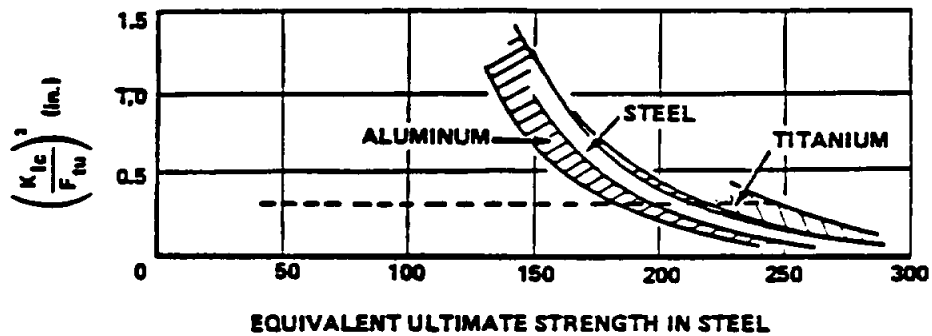
STRUCTURAL ANALYSIS MANUAL
GENERAL DYNAMICS/CONVAIR AND SPACE SYSTEMS DIVISION



a.



b.



c.

FIGURE E2-18. MATERIAL COMPARISONS (BASE METAL, ROOM-TEMPERATURE TRENDS)

STRUCTURAL ANALYSIS MANUAL
GENERAL DYNAMICS/CONVAIR AND SPACE SYSTEMS DIVISION

Alloy	σ_{ys} (ksi)	Design Stress $0.5 \sigma_{ys}$ (ksi)	Fracture Stress σ (ksi)	Safety Factor $\sigma / 0.5 \sigma_{ys}$
Steel	250	125	144	1.15
Aluminum	85	42.5	43	1.01
Titanium	140	70	112	1.60

From the above data it is apparent that the titanium provided the greatest safety factor and resistance to fracture.

2.4.1.2 Cyclic or Sustained Loading.

An evaluation of the resistance of materials to fracture requires the consideration of the crack growth rate characteristics in addition to other material properties.

Some examples of data obtained from tests are shown in Figs. E2-19 and E2-20 (Ref. 18). The realistic and practical approach for comparing materials is to evaluate their crack growth characteristics under a given application condition. Let us consider the following hypothetical example.

I. Example Problem A.

1. Materials to be considered are the steel and aluminum alloys for which the data are given in Figs. E2-19 and E2-20.
2. The component of interest is a thick plate cyclic loaded in tension under stresses that vary from zero to maximum tension during each cycle.
3. The design fixes σ_{max} as one-half the yield strength for each material: 88 ksi for steel and 32 ksi for aluminum.
4. The worst possible type of flaw that is envisioned is a semi-elliptical surface flaw with $a/2c = 0.20$.

STRUCTURAL ANALYSIS MANUAL
GENERAL DYNAMICS/CONVAIR AND SPACE SYSTEMS DIVISION

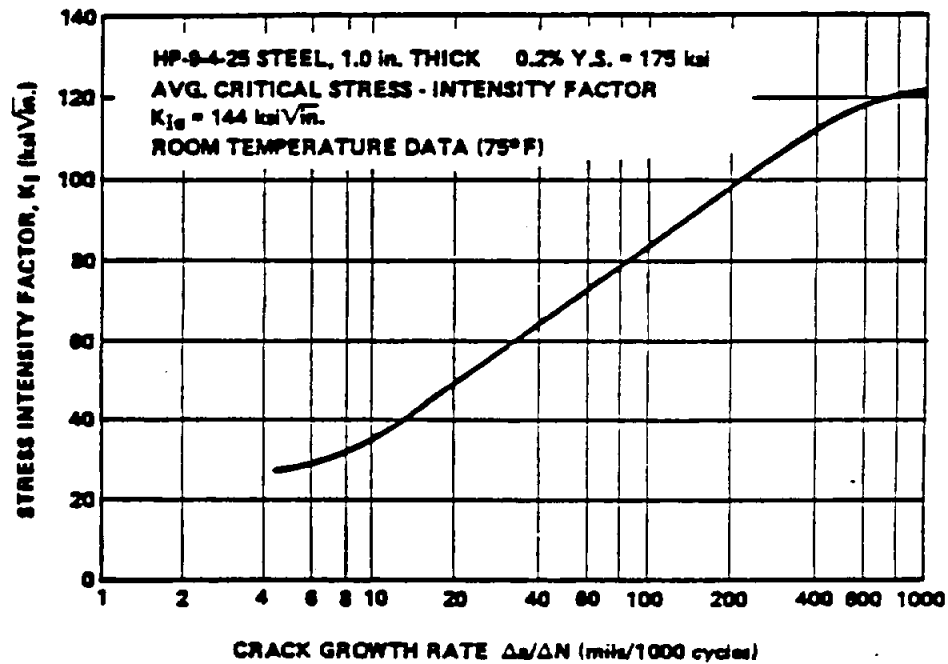


FIGURE E2-19. CRACK GROWTH RATE FOR HP-9-4-25 STEEL

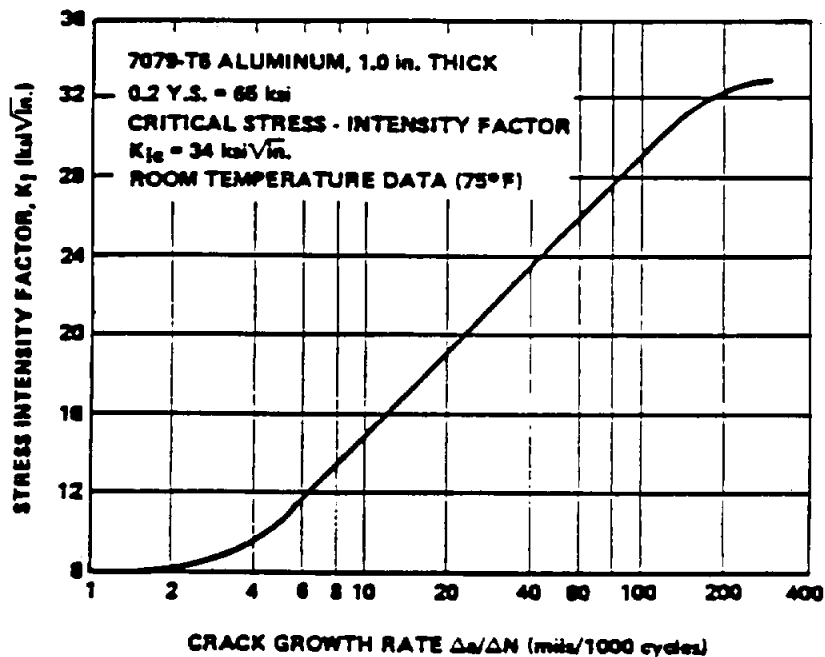


FIGURE E2-20. CRACK GROWTH RATE FOR 7079-T6 ALUMINUM

STRUCTURAL ANALYSIS MANUAL
GENERAL DYNAMICS/CONVAIR AND SPACE SYSTEMS DIVISION

5. The minimum size flaw that could be detected by the NDI technique is 0.15 in. deep by 0.72 in. long. Therefore, each material is assumed to contain this flaw.

Under these circumstances, which material has the longest life?

Solution.

Step 1. The first step is to compute the value of the initial stress intensity, K_{II} , for each material for the prevailing conditions of defect size and stress. The appropriate expression for K_{II} for the stipulated defect and component geometry is

$$K_{II}^2 = \frac{1.21 \pi a \sigma^2}{Q}$$

where

a = crack = 0.15 in. = specified,

σ = applied stress (maximum during cycle) = $1/2 \sigma_{ys}$ each material,

steel = 88 ksi, aluminum = 32 ksi,

σ_{ys} = yield strength, steel = 175 ksi, aluminum = 65 ksi,

and

Q = 1.26 for specified flaw geometry.

The calculations reveal the following:

$$K_{II}^2 = \frac{1.21 \pi (0.15) (88\ 000)^2}{1.26}$$

STRUCTURAL ANALYSIS MANUAL
GENERAL DYNAMICS/CONVAIR AND SPACE SYSTEMS DIVISION

and

$$K_{II} = 59\,000 \text{ psi} \sqrt{\text{in.}}$$

for steel, and

$$K_{II}^2 = \frac{1.21 \pi (0.15) (32\,000)^2}{1.26}$$

and

$$K_{II} = 21\,500 \text{ psi} \sqrt{\text{in.}}$$

for aluminum.

The crack growth rates for the two materials at the beginning of life can now be determined from Figs. E2-19 and E2-20 using their respective K_I values for the imposed conditions. The results are shown in the following table.

Alloy	K_I (psi $\sqrt{\text{in.}}$)	Crack Growth Rates (mils/cycle)
Steel	59 000	0.035
Aluminum	21 500	0.030

However, a knowledge of the crack growth rates at the beginning of life is not sufficient to determine the respective life expectancy of each material. One must consider the change in K_I and the associated change in crack growth rates for each material as the crack grows during service as well as the threshold stress intensity, K_{TH} .

STRUCTURAL ANALYSIS MANUAL
GENERAL DYNAMICS/CONVAIR AND SPACE SYSTEMS DIVISION

Step 2. The growth rate data illustrated in the form shown in Figs. E2-21 and E2-22 (Ref. 18) provide a convenient method for evaluating the life expectancy without becoming intimately involved with changes in K_I and growth rates. Figures E2-21 and E2-22 are constructed from the same basic test data as were used to construct Figs. E2-19 and E2-20. To utilize Figs. E2-21 and E2-22 it is necessary to know the ratio of K_{II} to K_{Ic} . The previous calculations in Step 1 showed that K_I is 59 ksi $\sqrt{\text{in.}}$ for steel and 21.5 ksi $\sqrt{\text{in.}}$ for aluminum. Since the K_{Ic} values for each material were known from static toughness tests, the K_{II}/K_{Ic} ratios are readily determined:

$$\frac{K_{II}}{K_{Ic}} = \frac{59\ 000}{144\ 000} = 0.41$$

for steel, and

$$\frac{K_{II}}{K_{Ic}} = \frac{21\ 500}{34\ 000} = 0.63$$

for aluminum.

The cyclic life corresponding to these K_{II}/K_{Ic} values may be determined directly from Figs. E2-21 and E2-22 — steel, 1800 cycles, and aluminum, 4000 cycles, if the time at maximum stress is short during each cycle.

Thus, for this specific example where both materials contained the same given size and type of defect and both were stressed to one-half their yield strengths, the aluminum has the greatest life expectancy.

It should be emphasized that the result of this example cannot be used to generalize the relative behavior of the two materials. For other conditions of initial defect sizes and/or applied stresses, it is possible that the steel

STRUCTURAL ANALYSIS MANUAL
GENERAL DYNAMICS/CONVAIR AND SPACE SYSTEMS DIVISION

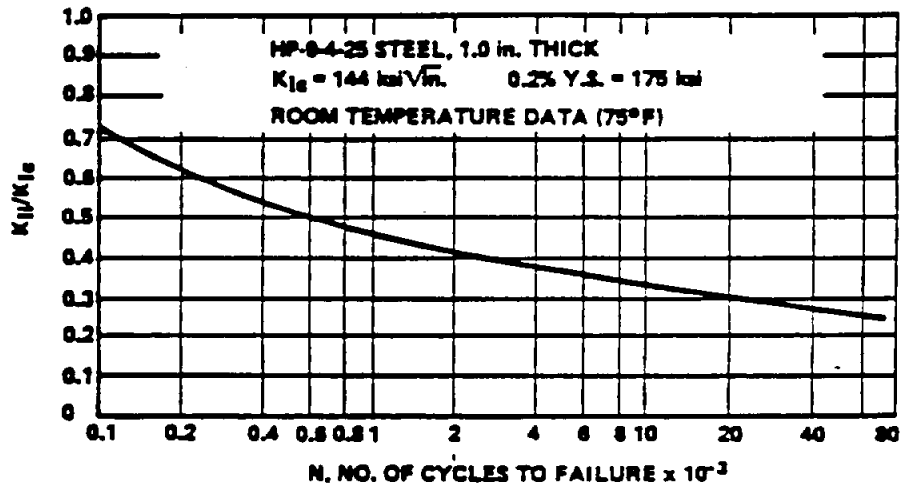


FIGURE E2-21. COMBINED CYCLIC FLAW GROWTH DATA FOR
 HP-9-4-25 STEEL PLATE

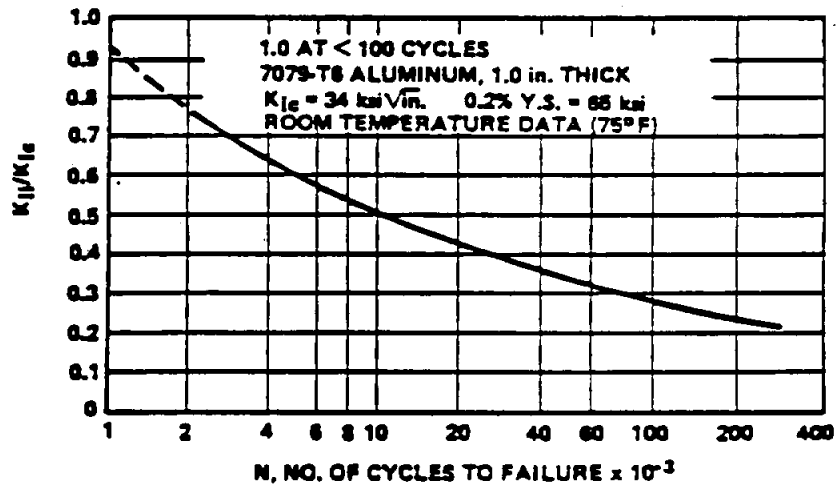


FIGURE E2-22. COMBINED CYCLIC FLAW GROWTH DATA FOR
 7079-T6 ALUMINUM PLATE

STRUCTURAL ANALYSIS MANUAL
GENERAL DYNAMICS/CONVAIR AND SPACE SYSTEMS DIVISION

could have the greater life expectancy. This is demonstrated in the following table, which shows the life expectancy of the two materials for a wide range of initial defect sizes and for a constant applied stress of $\sigma_{ys}/2$.

Initial Defect Depth a_i (in.)	Initial Stress-Intensity Factor K_{II} (ksi $\sqrt{\text{in.}}$)		$\frac{K_{II}}{K_{Ic}}$		Cycles to Failure N (Life Expectancy)	
	Steel	Aluminum	Steel	Aluminum	Steel	Aluminum
0.05	19.6	7.2	0.136	0.210	$>>300 \times 10^3$	300×10^3
0.07	27.5	10.1	0.191	0.297	$>100 \times 10^3$	100×10^3
0.10	39.4	14.3	0.274	0.420	30×10^3	21×10^3
0.15	59.0	21.5	0.410	0.632	1.8×10^3	4×10^3
0.20	78.8	28.7	0.540	0.845	0.37×10^3	1.5×10^3
0.25	98.4	35.9	0.683	>1.0	0.25×10^3	---

From the table it is seen that when the initial defect depth is 0.15 in. or larger, the aluminum will have the longer life N. However, when the initial defect depth is 0.10 in. or smaller, the steel will have the greater life expectancy. Although the steel has the larger absolute value of fracture toughness, K_{Ic} , and therefore has the largest critical crack size for catastrophic failure, it also has a greater crack growth rate for a given change in K as seen from the differences in slope of the growth rate curves shown in Figs. E2-23 and E2-24 (Ref. 18). Therefore, it is possible to have a "crossover" situation between the life expectancies of steel and aluminum, as noted in the table.

Again, the life expectancies in preceding table reflect short time at maximum cyclic stress. If the time at maximum stress is long, the portion of time that the stress-intensity level is above the threshold stress intensities

STRUCTURAL ANALYSIS MANUAL
GENERAL DYNAMICS/CONVAIR AND SPACE SYSTEMS DIVISION

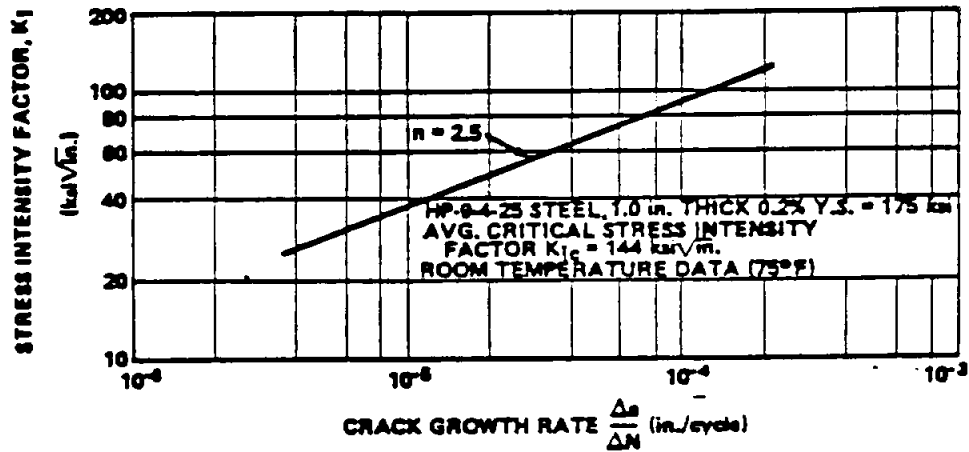


FIGURE E2-23. CRACK GROWTH RATE AS A FUNCTION OF STRESS INTENSITY FOR HP-9-4-25 STEEL

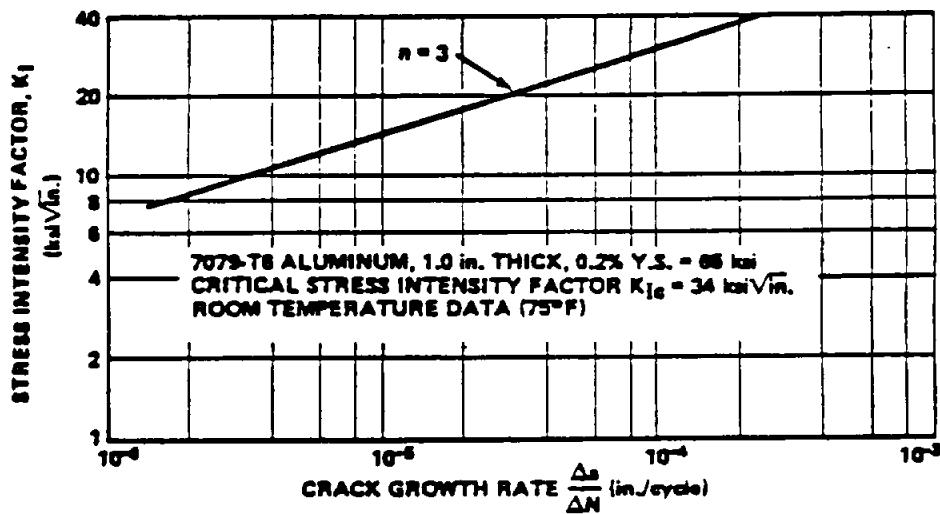


FIGURE E2-24. CRACK GROWTH RATE AS A FUNCTION OF STRESS INTENSITY FOR 7079-T6 ALUMINUM

STRUCTURAL ANALYSIS MANUAL
GENERAL DYNAMICS/CONVAIR AND SPACE SYSTEMS DIVISION

for the steel and aluminum would cause reductions in the cyclic lives for the different initial defect sizes.

The materials could also be compared in another manner by using the data provided in Figs. E2-21 and E2-22 to answer the question of which material could tolerate the largest initial defect (of a given type) that would not grow to a critical size during some given minimum lifetime for the component.

II. Example Problem B.

Known Information:

Plate cyclic loaded (sinusoidal) in tension.

Required life — 50 000 cycles.

Applied stress (maximum stress during cycle) one-half yield strength:

steel = 88 000 psi.

aluminum = 32 000 psi.

Type of defect — semielliptical surface flaw with $a/c = 0.4$.

Fracture toughness, K_{Ic} :

steel = 144 000 psi $\sqrt{\text{in.}}$

aluminum = 34 000 psi $\sqrt{\text{in.}}$

Unknown Information: Which material can tolerate the largest initial defect?

Solution.

Step 1. From Figs. E2-21 and E2-22, find the K_{II}/K_{Ic} ratio corresponding to the desired life of 50 000 cycles:

$$\frac{K_{II}}{K_{Ic}} \text{ at } 50\,000 \text{ cycles} = 0.25$$

STRUCTURAL ANALYSIS MANUAL
GENERAL DYNAMICS/CONVAIR AND SPACE SYSTEMS DIVISION

for steel; and

$$\frac{K_{II}}{K_{Ic}} \text{ at } 50\,000 \text{ cycles} = 0.34$$

for aluminum.

Step 2. Knowing the K_{Ic} and K_{II}/K_{Ic} ratio corresponding to 50 000 cycles, solve for K_{II} :

$$K_{II} = 0.25 K_{Ic} = 0.25 (144\,000 \text{ psi} \sqrt{\text{in.}}) = 36\,000 \text{ psi} \sqrt{\text{in.}}$$

for steel, and

$$K_{II} = 0.34 K_{Ic} = 0.34 (34\,000 \text{ psi} \sqrt{\text{in.}}) = 11\,500 \text{ psi} \sqrt{\text{in.}}$$

for aluminum.

Step 3. Since K_{II} depends upon stress and defect size, it is now possible to solve for defect size knowing stress. For semielliptical surface defects with $a/c = 0.4$, the following expression is appropriate:

$$a_i = \frac{K_{II}^2(Q)}{1.21 \pi \sigma^2} ;$$

for steel,

$$a_i = \frac{(36\,000)^2 (1.26)}{1.21 \pi (88\,000)^2}$$

STRUCTURAL ANALYSIS MANUAL
GENERAL DYNAMICS/CONVAIR AND SPACE SYSTEMS DIVISION

and

$$a_i = 0.056 \text{ in.}$$

when the defect is 0.056 in. deep by 0.28 in. long; for aluminum,

$$a_i = \frac{(11\,500)^2 (1.26)}{1.21 \pi (32\,000)^2}$$

and

$$a_i = 0.043 \text{ in.}$$

when the defect is 0.043 in. deep by 0.215 in. long.

Thus, it is apparent that for the condition imposed, the steel could tolerate a slightly larger initial defect than could the aluminum. Since the difference in the maximum allowable initial defect size is not great, the ultimate choice of a material for this situation may depend more heavily on other comparative factors, i.e., the applicability and capability of NDI techniques, the type and size of insidious defects as related to the maximum allowable initial defect size, availability, ease of fabrication, costs, etc.

2.4.2 Predicting Critical Flaw Sizes.

As mentioned in Section 2.2.3, plane-strain stress intensity (K_{Ic}) values can be obtained from several types of specimens. With valid data for a given material form, heat treatment, test temperature, and environment, critical flaw sizes can be calculated for given hardware operating stresses. The engineering usefulness of the basic stress-intensity concept in the prediction of critical flaw sizes and the use of a/Q to describe flaw size has

STRUCTURAL ANALYSIS MANUAL
GENERAL DYNAMICS/CONVAIR AND SPACE SYSTEMS DIVISION

been supported by a number of hardware correlations, some of which are shown in Refs. 17 and 19. Comparisons between measured critical flaw sizes on test hardware and predicted critical flaw sizes based on test specimen plane-strain toughness data have shown good correlation.

From the equation shown in Fig. E2-6, it is apparent that critical flaw size is equally as dependent on applied stress as on the material fracture toughness. The following sections show approaches for calculating critical flaw sizes for the three basic types of initial flaws (surface, embedded, or through-the-thickness) based on the appropriate fracture toughness values measured from valid specimen tests.

2.4.2.1 Surface Cracks.

Calculations for surface flaws can be carried out by rearranging the stress-intensity equation developed by Irwin (Section 2.2.1),

$$(a/Q)_{cr} = \frac{1}{1.21\pi} \left(\frac{K_{Ic}}{\sigma} \right)^2$$

for a "thick-walled" structure (i.e., flaw depth less than half of the material thickness) where K_{Ic} is the plane-strain fracture toughness obtained from fracture toughness specimen tests, σ is the applied stress in structure normal to the plane of flaw, a_{cr} is the critical flaw depth, Q is the flaw shape parameter (obtained from Fig. E2-5), and $(a/Q)_{cr}$ is critical flaw size.

Since the flaw size is an unknown quantity, it is necessary to assume a flaw aspect ratio, $a/2c$, to determine Q . Using the preceding equation, the critical flaw depth, a_{cr} , can be determined for a specific value of σ and K_{Ic} .

STRUCTURAL ANALYSIS MANUAL
GENERAL DYNAMICS/CONVAIR AND SPACE SYSTEMS DIVISION

I. Example Problem A.

Aluminum alloy 2219-T87 is selected as the material for use in a 20-in.-diam spherical gas bottle. The bottle is to operate at 4000 psig and be stored in a liquid-nitrogen propellant tank.

What is the critical flaw size?

A. Assumptions.

1. The defect is a semielliptical surface flaw with $a/2c = 0.2$.
2. The operating stress is $\sigma = 80$ percent (yield strength of the material).

B. Solution.

The yield strength and K_{Ic} values obtained from the tested specimens are as follows:

$$\sigma_{ys} = 60 \text{ ksi}$$

and

$$K_{Ic} = 37 \text{ ksi} \sqrt{\text{in.}}$$

The operating stress is

$$\sigma = 0.80 (\sigma_{ys}) = 0.80 (60) = 48 \text{ ksi}$$

The wall thickness required is

$$t_{\text{req}} = \frac{PR}{2\sigma} = \frac{(4000)(10)}{(2)(48\,000)} = 0.417 \text{ in.}$$

STRUCTURAL ANALYSIS MANUAL
GENERAL DYNAMICS/CONVAIR AND SPACE SYSTEMS DIVISION

For thick-walled structures,

$$a_{cr} = \frac{Q}{1.21 \pi} \left(\frac{K_{Ic}}{\sigma} \right)^2,$$

where the shape parameter Q can be found from Fig. E2-5. For this problem $Q = 1.18$; then

$$a_{cr} = \frac{1.18}{1.21 (\pi)} \left(\frac{37}{48} \right)^2 = 0.184 \text{ in.}$$

and

$$2c = a/0.20 = 0.184/0.2 = 0.92 \text{ in.}$$

For surface flaws that are deep with respect to material thickness, the flaw magnification factor, M_k , can be applied to give a more accurate critical flaw size,

$$(a/Q)_{cr} = \frac{1}{1.21 \pi} \left(\frac{K_{Ic}}{M_k \sigma} \right)^2,$$

for thin-walled structures.

II. Example Problem B.

Use the same design that was shown in Example Problem A except that the spherical diameter of the bottle is 15 in. The wall thickness required is

$$t_{req} = \frac{PR}{2\sigma} = \frac{4000 (7.5)}{2 (48\,000)} = 0.313 \text{ in.}$$

STRUCTURAL ANALYSIS MANUAL
GENERAL DYNAMICS/CONVAIR AND SPACE SYSTEMS DIVISION

For thin-walled structures,

$$a_{cr} = \frac{Q}{1.21 \pi} \left(\frac{K_{Ic}}{M_k \sigma} \right)^2$$

Flaw magnification factors, M_k , for the 2219-T87 aluminum are available from Fig. E2-8. Since the critical flaw depth, a_{cr} , is unknown, a "trial-and-error" iterative solution is necessary to determine the magnification factor corresponding to the critical flaw depth.

Without a magnification factor, $a_{cr} = 0.184$ in. (Example Problem A).

For $a/t = 0.184/0.313 = 0.59$, $M_k = 1.21$,

$$a_{cr} = \frac{1.18}{1.21 \pi} \left[\frac{37}{1.21 (48)} \right]^2 = 0.126 \text{ in.} < 0.184 \text{ in.}$$

Take an average $a = \frac{0.184 + 0.126}{2} = 0.155$ in.

For $a/t = 0.155/0.313 = 0.50$, $M_k = 1.15$,

$$a_{cr} = \frac{1.18}{1.21 \pi} \left[\frac{37}{1.15 (48)} \right]^2 = 0.139 \text{ in.} < 0.155 \text{ in.}$$

Take an average $a = \frac{0.155 + 0.139}{2} = 0.147$ in.

For $a/t = 0.147/0.313 = 0.47$, $M_k = 1.13$,

$$a_{cr} = \frac{1.18}{1.21 \pi} \left[\frac{37}{1.13 (48)} \right]^2 = 0.144 \approx 0.147 \text{ in.}$$

Further reiteration will provide more accuracy if desired.

STRUCTURAL ANALYSIS MANUAL
GENERAL DYNAMICS/CONVAIR AND SPACE SYSTEMS DIVISION

If adequate flaw magnification values are not available for a particular material, a reasonable estimate for M_k is the approximate Kobayashi solution shown in Fig. E2-25. However, it should be understood that its use can result in somewhat conservative answers for more ductile materials and perhaps unconservative answers for more brittle materials.

2.4.2.2 Embedded Flaws.

The calculations for embedded flaws in thick-walled structures will be the same as for surface flaws except that a_{cr} is the one-half critical flaw depth of the embedded flaw, and the correction factor of 1.21 for the effect on stress intensity of the stress-free surface (Section 2.2.1) is eliminated. Thus the equation for one-half critical internal flaw size is

$$(a/Q)_{cr} = \left(\frac{1}{\pi} \frac{K_{Ic}}{\sigma} \right)^2$$

Although flaw magnification effects have been studied for deep surface flaws, apparently no similar research has been done for internal flaws with large flaw-depth-to-material-thickness ratios. The fact that internal flaws are hidden, making their size difficult if not impossible to accurately determine, presents a problem in the study of internal flaw magnification effects. The assumption might be made that the same flaw magnification factors, M_k , used for deep surface flaws might be applied to the equation for critical embedded flaw sizes. However, there is no evidence of how conservative or unconservative this assumption is.

On the other hand, to account for the lack of knowledge about flaw geometry and orientation, it can be conservatively assumed that flaws are surface (or barely subsurface) flaws and that they are long in relation to depth ($Q \approx 1.0$).

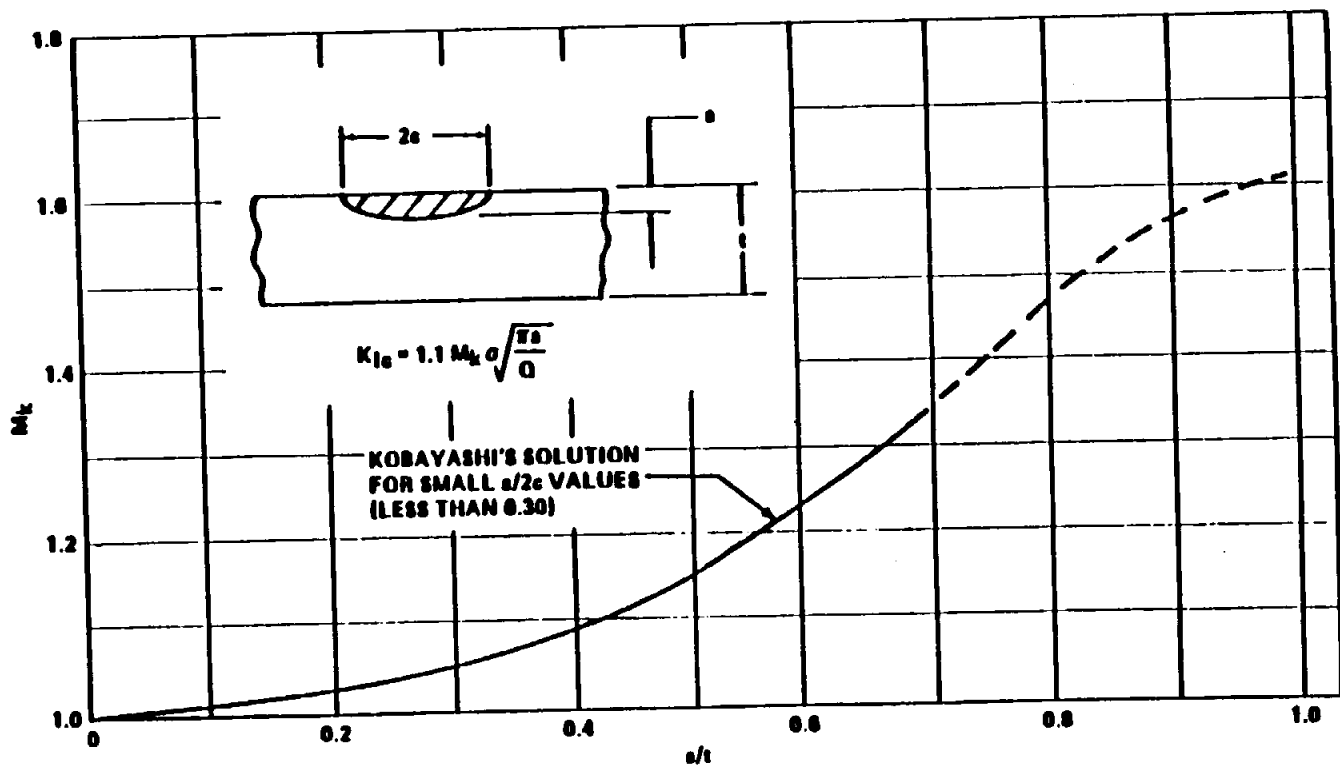


FIGURE E2-25. STRESS-INTENSITY MAGNIFICATION FACTORS FOR DEEP SURFACE FLAWS

STRUCTURAL ANALYSIS MANUAL
GENERAL DYNAMICS/CONVAIR AND SPACE SYSTEMS DIVISION

2.4.2.3 Through-the-Thickness Cracks.

To calculate through-the-thickness critical crack length, the basic plane stress equation for through-the-thickness cracks in an infinitely wide plate (Section 2.2.2.1) can be rearranged to give

$$l_{cr}/2 = \frac{1}{\pi} \left(\frac{K_c}{\sigma} \right)^2 - \frac{1}{2\pi} \left(\frac{K_c}{\sigma_{ys}} \right)^2 ,$$

where K_c is the plane stress fracture toughness obtained from an edge-notched or center-cracked specimen, σ is the applied stress in the structure normal to the plane of the crack, σ_{ys} is the tensile yield strength of the material, and l_{cr} is the critical crack length.

I. Example Problem A.

Aluminum alloy 2219-T87 is selected as the material for use in a 15-in. diameter compressed air cylinder. The cylinder is to operate at 1000 psig in ambient room atmosphere.

What is the critical flaw size?

A. Assumptions.

1. The defect is a semielliptical surface flaw with $a/2c = 0.2$.
2. The operating stress is $\sigma = 80$ percent of material yield strength.

B. Solution.

The yield strength and K_{Ic} values obtained from test specimens are as follows:

$$\sigma_{ys} = 50 \text{ ksi}$$

STRUCTURAL ANALYSIS MANUAL
GENERAL DYNAMICS/CONVAIR AND SPACE SYSTEMS DIVISION

and

$$K_{Ic} = 32 \text{ ksi } \sqrt{\text{in.}}$$

An estimate of K_c versus material thickness based on 2219-T87 test specimens is shown in Fig. E2-26 (Refs. 20 and 21).

The operating stress is

$$\sigma = 0.80 (\sigma_{ys}) = 0.80 (50) = 40 \text{ ksi}$$

The wall thickness required is

$$t_{\text{req}} = \frac{PR}{\sigma} = \frac{1000 (7.5)}{40\,000} = 0.188 \text{ in.}$$

For thick-walled structures,

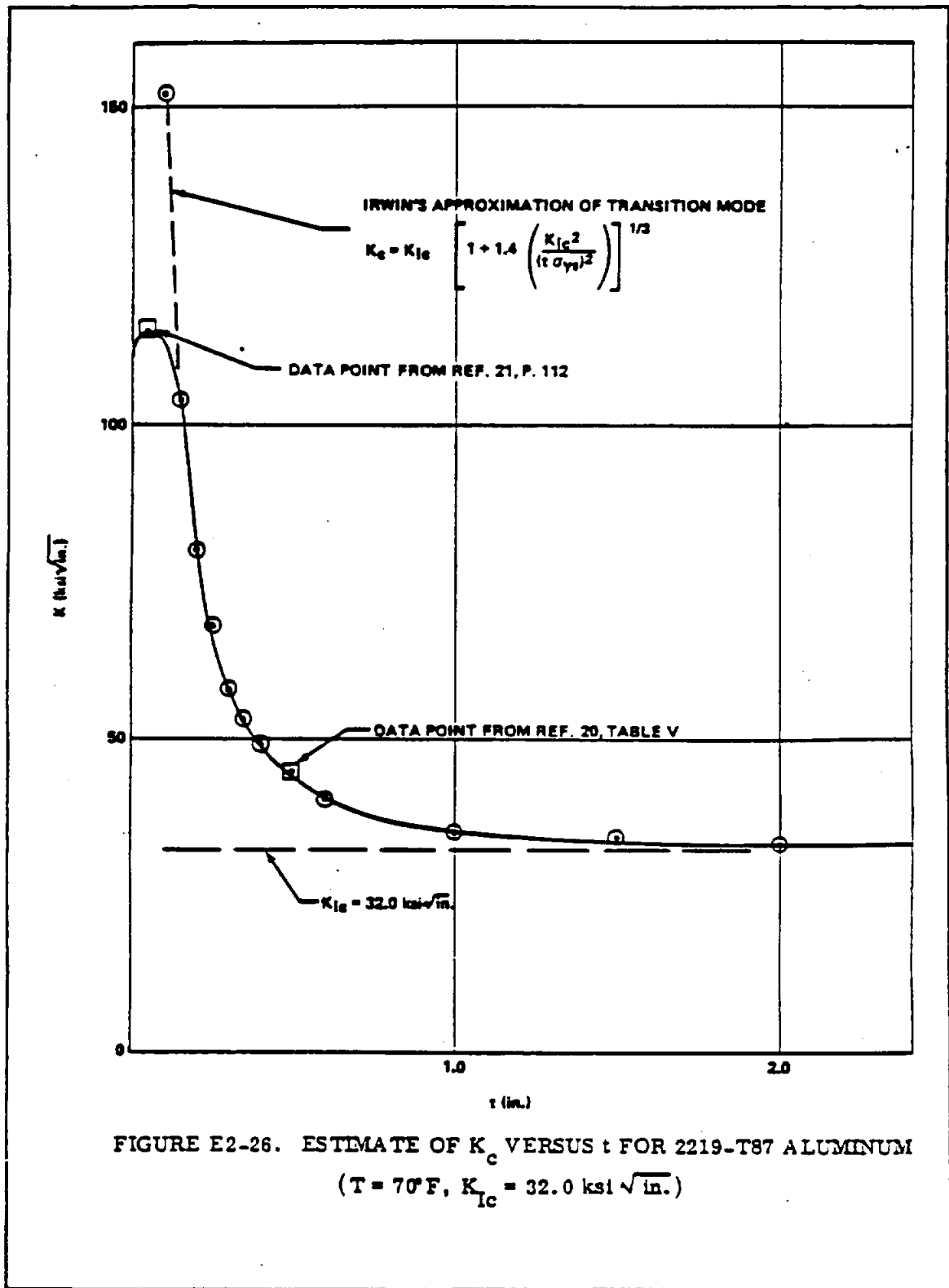
$$a_{\text{cr}} = \frac{Q}{1.21 \pi} \left(\frac{K_{Ic}}{\sigma} \right)^2$$

From Fig. E2-5, $Q = 1.18$; then

$$a_{\text{cr}} = \frac{1.18}{1.21 \pi} \left(\frac{32}{40} \right)^2 = 0.199 > 0.188 \text{ in.}$$

Therefore, the critical flaw is apparently a through-the-thickness crack and the tank will leak before failure. The critical crack length of failure is predicted to be

STRUCTURAL ANALYSIS MANUAL
GENERAL DYNAMICS/CONVAIR AND SPACE SYSTEMS DIVISION



STRUCTURAL ANALYSIS MANUAL
GENERAL DYNAMICS/CONVAIR AND SPACE SYSTEMS DIVISION

$$l_{cr} = \frac{2}{\pi} \left(\frac{K_c}{\sigma} \right)^2 - \frac{1}{\pi} \left(\frac{K_c}{\sigma_{ys}} \right)^2$$

The plane-stress fracture toughness value, K_c , from Fig. E2-26, is 84 ksi $\sqrt{\text{in.}}$.

$$l_{cr} = \frac{2}{\pi} \left(\frac{84}{40} \right)^2 - \frac{1}{\pi} \left(\frac{84}{50} \right)^2 = 2.81 - 0.91 = 1.90 \text{ in.}$$

2.4.3 Structure Design.

2.4.3.1 Service Life Requirements and Predictions.

With pressure cycles and time at stress, an initial flaw or defect in a structure will grow in size until it attains the critical size at the applied operating stress level, and failure will result. The flaw-growth potential (in inches) is equal to the critical size minus the initial size. The life of the structure directly depends upon this flaw-growth potential and the subcritical flaw-growth characteristics of the material.

The determination of the initial flaw sizes generally relies upon the use of NDI procedures; however, the conventional proof test can be considered to be one of the most positive inspection procedures available. A successful proof test actually defines the maximum possible initial flaw size that exists in the vessel. This results from the functional relationship between stress level and flaw size as defined by the critical stress intensity (K_{Ic}) and illustrated in Fig. E2-6.

Probably the most predominant types of subcritical flaw growth are fatigue growth resulting from cyclic stress and environmentally induced sustained stress growth. Also, growth may occur even in the absence of severe environmental effects if the initial flaw size approaches the critical flaw size.

STRUCTURAL ANALYSIS MANUAL
GENERAL DYNAMICS/CONVAIR AND SPACE SYSTEMS DIVISION

The technique used for predicting the subcritical cyclic or sustained stress flaw growth makes use of fracture specimen testing and the stress-intensity concept.

It has been shown (Refs. 6 and 17) that the time or cycles to failure at a given maximum applied gross stress level depends on the magnitude of the initial stress intensity at the flaw tip, K_{II} , compared with the critical stress intensity, K_{Ic} [that is, cycles or time to failure = $f(K_{II}/K_{Ic})$]. Also, it is seen that the ratio of initial flaw size to critical flaw size is related to the stress-intensity ratio as follows:

$$\left(\frac{K_{II}}{K_{Ic}}\right)^2 = \frac{\frac{a_i}{Q_i}}{\frac{a_{cr}}{Q_{cr}}}$$

Thus, if cyclic or sustained stress fracture specimens are used to obtain experimentally the K_{II}/K_{Ic} versus cycles or time curves for a material, the cycles or time required for any given initial flaw to grow to critical size can be predicted. Conversely, if the required life of the structure is known in terms of stress cycles or time at stress, the maximum allowable initial flaw size can be determined.

The cyclic flaw-growth data are plotted in terms of stress-intensity ratio, K_{II}/K_{Ic} , versus log of cycles, as shown schematically in Fig. E2-27a. By squaring the ordinate value, the plot of the ratio of initial flaw size to critical flaw size versus the log of cycles (Fig. E2-27b) can be obtained. It should also be recognized that flaw size can be determined after any incremental number of cycles. For example, if the initial flaw-size ratio was 0.40, the flaw would have grown in A cycles, increasing the ratio to 0.6; in B cycles, it would have grown to 0.8, etc.

STRUCTURAL ANALYSIS MANUAL
GENERAL DYNAMICS/CONVAIR AND SPACE SYSTEMS DIVISION

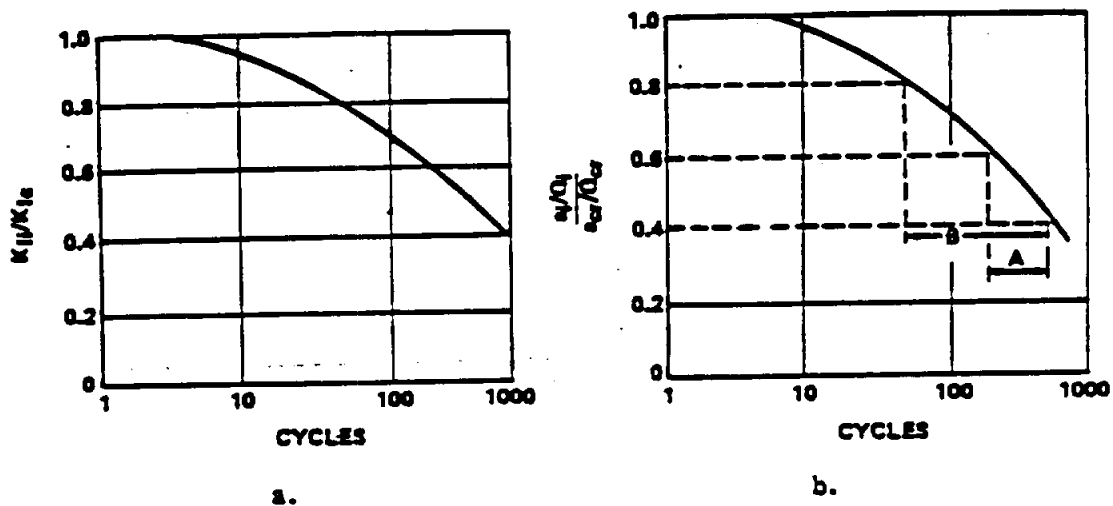


FIGURE E2-27. SCHEMATIC REPRESENTATION OF CYCLIC
 FLAW GROWTH

Cyclic flaw-growth data have been obtained on a number of materials used in the aerospace industry. Some such data are shown in Figs. E2-28 and E2-29.

The application of fracture-specimen testing to define the effects of sustained load on flaw growth is essentially the same as used in defining cyclic flaw growth. A constant load is applied to a flawed specimen such that the initial stress intensity is less than the critical value and the time to failure is recorded. The K_{II}/K_{Ic} values are computed and the K_{II}/K_{Ic} ratio is plotted versus log of time to failure.

Plots of K_{II}/K_{Ic} versus log of time for most materials indicate the existence of a threshold stress-intensity level below which sustained stress growth does not occur. Figure E2-30 shows data for 17-7 PH steel tested in both dry and wet environments, and Fig. E2-31 shows surface-flawed specimen data for 2219-T87 aluminum tested in liquid nitrogen. In neither case does it seem that the environment played an important role in the sustained stress growth. In both cases the apparent threshold stress-intensity levels are quite high.

STRUCTURAL ANALYSIS MANUAL
GENERAL DYNAMICS/CONVAIR AND SPACE SYSTEMS DIVISION

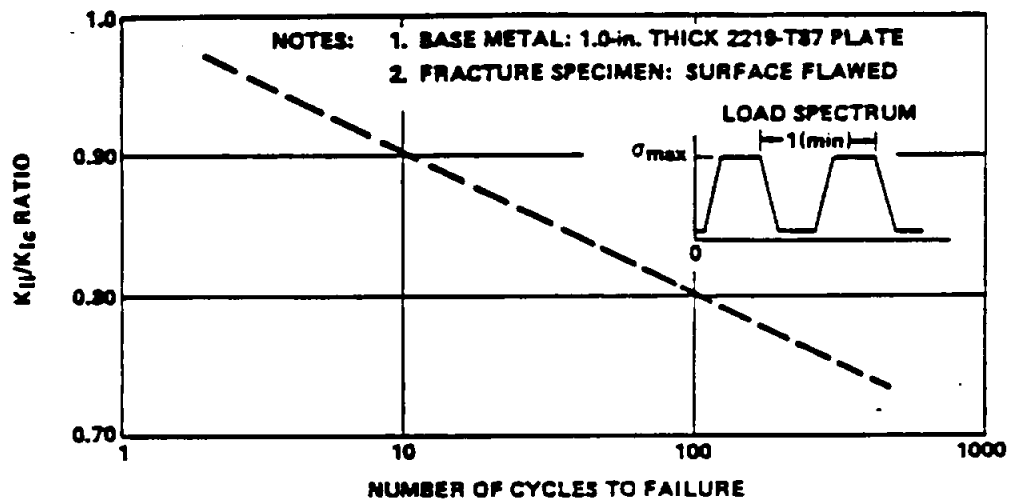


FIGURE E2-28. BASE METAL CYCLIC FLAW-GROWTH DATA
 (-320 °F, LONGITUDINAL GRAIN)

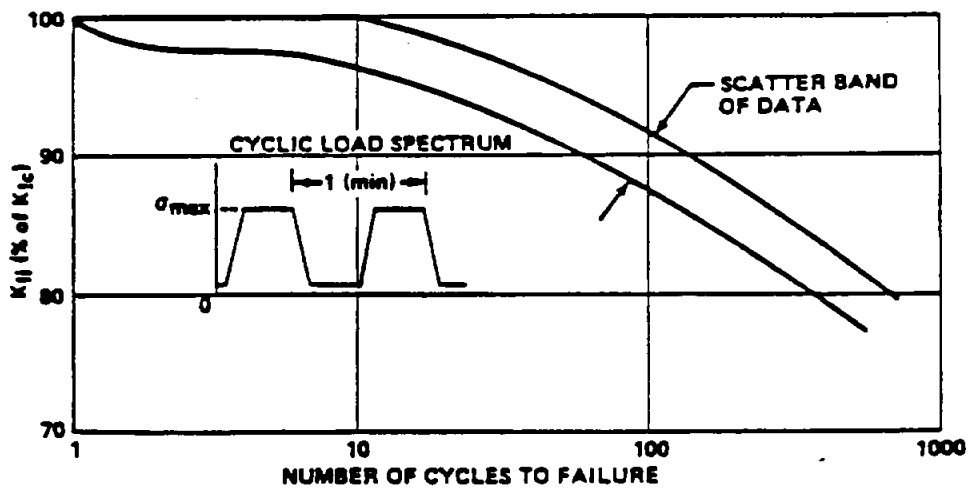
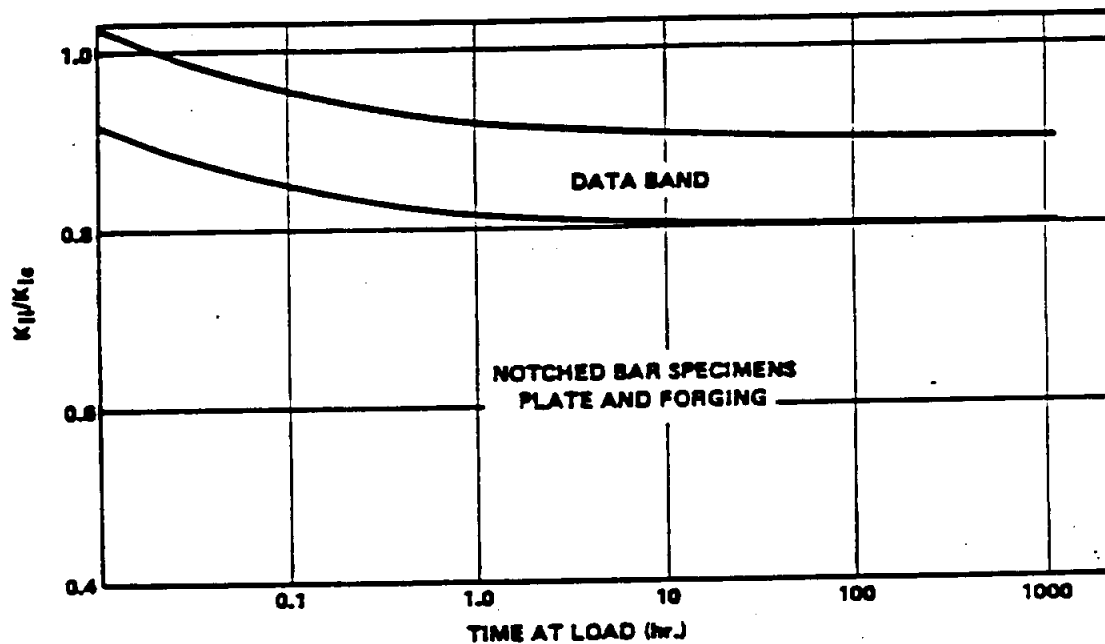


FIGURE E2-29. CYCLIC FLAW-GROWTH DATA OF 6Al-4V
 TITANIUM PLATE TESTED AT -320 °F

STRUCTURAL ANALYSIS MANUAL
GENERAL DYNAMICS/CONVAIR AND SPACE SYSTEMS DIVISION



**FIGURE E2-30. SUSTAINED STRESS FLAW-GROWTH DATA FOR
 ROOM-TEMPERATURE TESTS OF 17-7 PH STEEL**

Let us now consider the significance of sustained stress flaw growth and specifically the threshold stress-intensity concept on the estimated total cyclic life of a tension-loaded structure containing an initial crack or crack-like flaw. To illustrate this, the schematic representation of the K-N curve is reconstructed in Fig. E2-32, but superimposed on this curve is a horizontal line at $K_{II}/K_{Ic} = 0.80$. This is assumed to be the threshold stress intensity. Now consider the situation where the initial flaw size and applied cyclic stress result in an initial stress intensity equal to 50 percent of the critical value. From the curve, it is seen that it would take a total of A cycles to grow this initial flaw to critical size and cause failure. However in B cycles, the initial flaw would have increased in size enough to cause the stress intensity to reach the threshold value of $K_{II}/K_{Ic} = 0.80$. With additional cycles the

STRUCTURAL ANALYSIS MANUAL
GENERAL DYNAMICS/CONVAIR AND SPACE SYSTEMS DIVISION

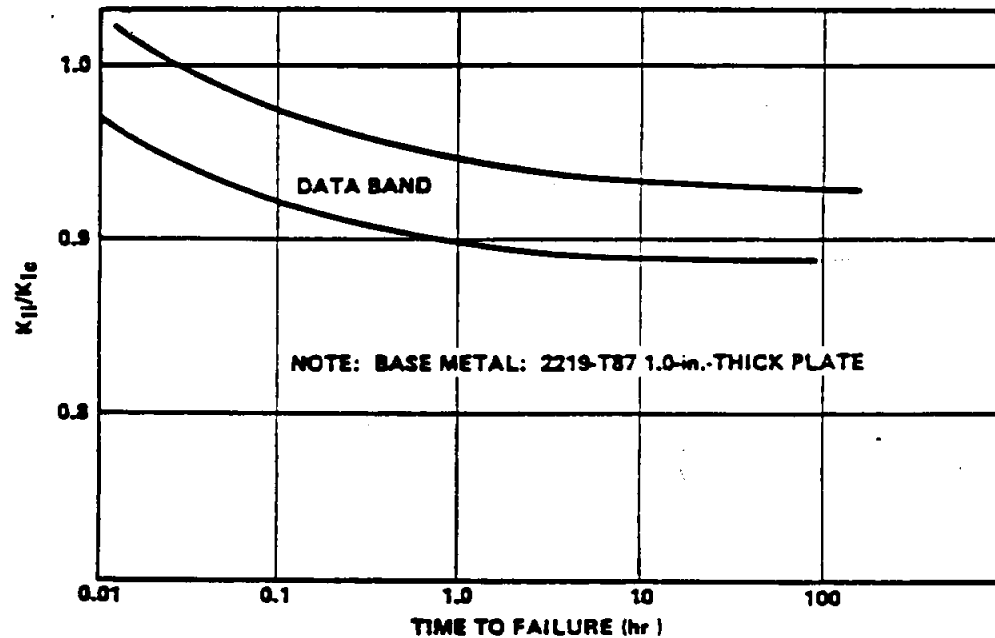


FIGURE E2-31. SUSTAINED STRESS FLAW-GROWTH DATA FOR
 2219-T87 ALUMINUM AT -320 °F

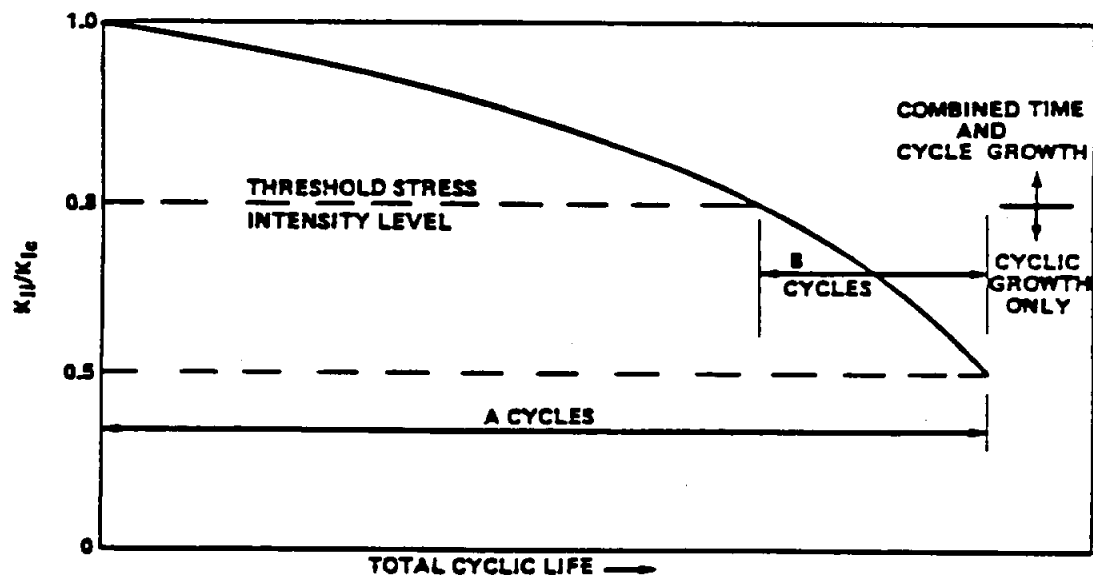


FIGURE E2-32. COMBINED CYCLIC AND SUSTAINED STRESS FLAW
 GROWTH SCHEMATIC INTERPRETATION

STRUCTURAL ANALYSIS MANUAL
GENERAL DYNAMICS/CONVAIR AND SPACE SYSTEMS DIVISION

stress intensity would further increase and, if the stress were sustained sufficiently long, it appears possible that failure could occur on the $(B + 1)$ cycle.

If, on the other hand, the cycles were applied with little time at maximum cyclic stress, it appears that the total of A cycles could be realized. It is hypothesized that below the threshold K -value, the time at sustained stress has little or no effect on cyclic life. Above the threshold value there will be an interaction such that failure could occur anywhere within the range of $(B + 1)$ to A cycles, depending on the time the maximum stress is held during each cycle. The development of the exact time-cycle interaction curves above the threshold value would be a complex and expensive task and, as applied to most tankage structure, may not be of great importance. It appears more rational to determine the basic cyclic data and the threshold-intensity values and then verify (through prolonged-time specimen cyclic tests) that time at load is not of major significance below the threshold value. In the application of the data to fatigue-life estimation, the maximum allowable stress intensity would be limited to the threshold value as determined for the material in question and for the applicable service environment. If the threshold is very low, steps should be taken to protect the material from the environment.

The operational cyclic life of pressure vessels can be determined if the following data are available:

1. Proof-test factor α .
2. Maximum design operating stress σ_{op} .
3. Fracture toughness K_{Ic} .
4. Experimental cyclic and sustained stress flaw growth for the vessel material.

STRUCTURAL ANALYSIS MANUAL
GENERAL DYNAMICS/CONVAIR AND SPACE SYSTEMS DIVISION

If the cycles to be applied to the vessel have short hold time at the maximum stress σ_{op} , the stress intensity at σ_{op} can be allowed to reach the critical value K_{Ic} and therefore the allowable flaw growth potential is $a_{cr} - a_i$. For long hold times at the maximum stress, the stress intensity could not be allowed to exceed the sustained stress threshold value K_{TH} and the allowable flaw growth potential is $a_{th} - a_i$. Typical threshold stress-intensity data can be obtained from Refs. 12 and 22.

I. Example Problem A (Thick-Walled Vessel).

Cyclic life prediction can be made by utilizing the proof-test factor and the relationships between K_{II}/K_{Ic} and cycles to failure for various values of R (ratio of minimum to maximum stress during a cycle) for the material-environment combination.

The procedure for assessing the structural integrity of the thick-walled vessels follows. In the first analysis for the assessment of the structural integrity of the thick-walled vessel, it is always assumed that all the pressure cycles are applied at $R = 0$. Since the analysis based on $R = 0$ will always show the remaining cyclic life less than that based on the analysis of $R \neq 0$ (actual R ratios), the prediction of cyclic life based on the analysis of $R = 0$ is invariably conservative. If the pressure vessel is shown unsatisfactory for the flight based on $R = 0$, then the prediction analysis for the remaining cyclic life is conducted based on the actual R values at which the cycles are applied. An excellent illustrative example abstracted from Ref. 12 is given as follows.

Suppose that a thick-walled 6Al-4V (STA) titanium helium tank is successfully proof tested at a proof-test factor of 1.50 times the maximum design operating stress. Suppose that the proof-tested tank is subjected to the following pressure cycles before the flight, as shown in Fig. E2-33:

STRUCTURAL ANALYSIS MANUAL
GENERAL DYNAMICS/CONVAIR AND SPACE SYSTEMS DIVISION

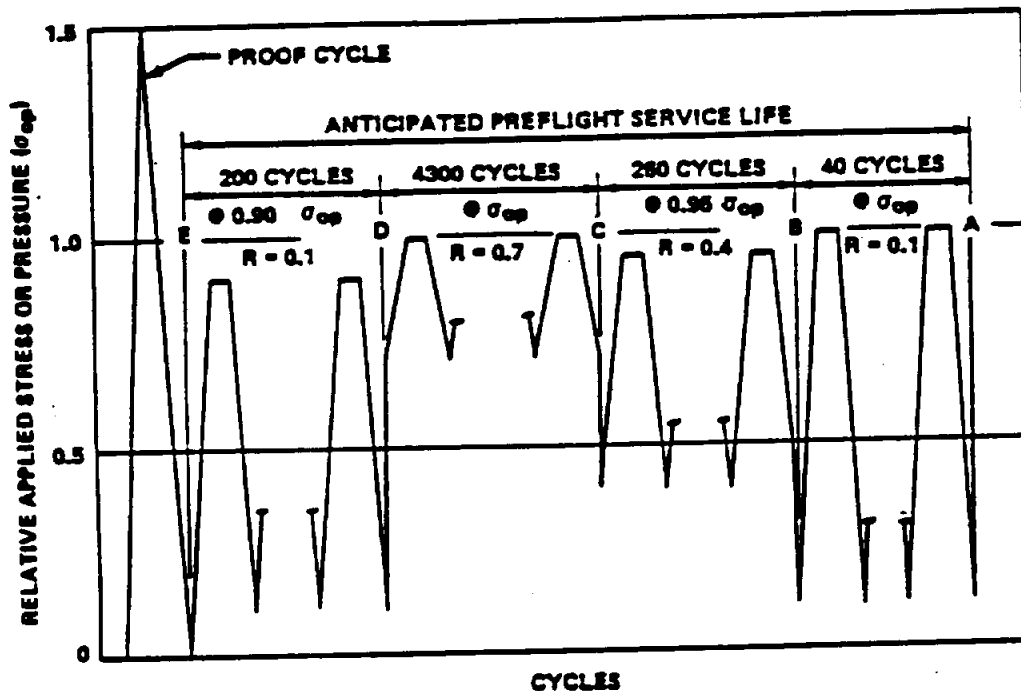


FIGURE E2-33. CYCLIC HISTORY OF A THICK-WALLED VESSEL
(EXAMPLE PROBLEM A)

1. 200 loading cycles with the maximum stress as 90 percent of σ_{op} and $R = 0.1$.
2. 4300 loading cycles with the maximum stress as σ_{op} and $R = 0.7$.
3. 260 loading cycles with the maximum stress as 95 percent of σ_{op} and $R = 0.4$.
4. 40 loading cycles with the maximum stress as σ_{op} and $R = 0.1$.

The cyclic life curves for 6Al-4V (STA) titanium for the environment of room-temperature air are reproduced for $R = 0.0$, $R = 0.1$, $R = 0.4$, and $R = 0.7$ in Fig. E2-34. The difference between the plots of cyclic life against K_{II}/K_{Ic} for $R = 0$ and $R = 0.1$ is negligible for this material-environment

NOTE. $R = \frac{K_{MIN.}}{K_{MAX.}}$

712

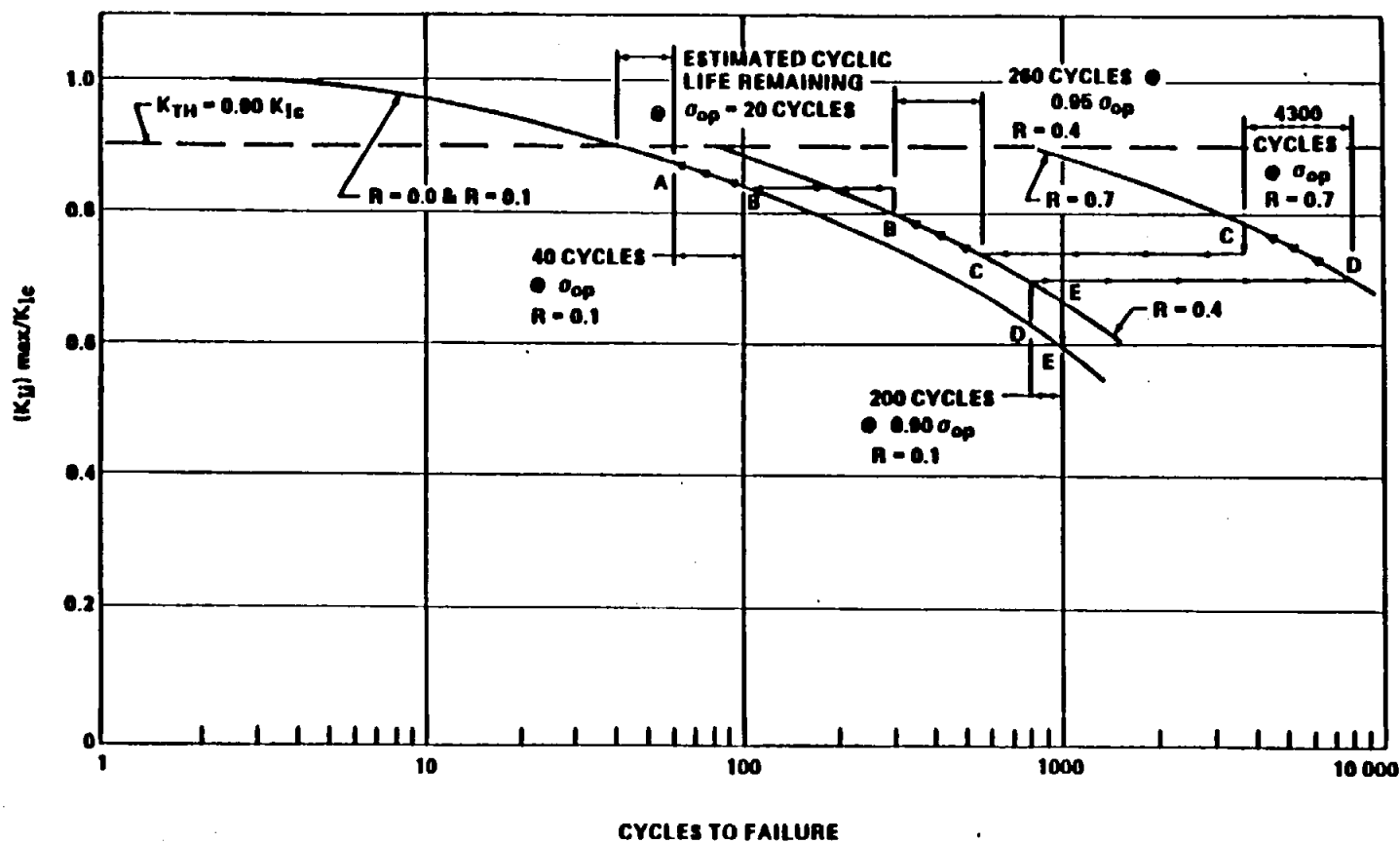


FIGURE E2-34. PREDICTION OF CYCLIC LIFE OF A THICK-WALLED VESSEL
(EXAMPLE PROBLEM A)

STRUCTURAL ANALYSIS MANUAL
GENERAL DYNAMICS/CONVAIR AND SPACE SYSTEMS DIVISION

combination, and hence both are shown by the same plot in Fig. E2-34. The threshold stress-intensity level for the material in the environment of room-temperature air is 90 percent of K_{Ic} .

The maximum possible K_{II}/K_{Ic} ratio that could exist in the vessel after the proof test at σ_{op} is $1/\alpha = 0.667$. It can be seen from the $R = 0$ plot in Fig. E2-34 that the maximum cycles to failure are about 600 at σ_{op} if the hold times at maximum stress are small. If the analysis is based on $R = 0$ instead of actual R , the pressure-cycle history shows that the vessel is critical. In the following, the assessment of the vessel is made based on the appropriate values of R .

At the beginning of 200 loading cycles with the maximum stress as $0.90 \sigma_{op}$, the maximum K_{II}/K_{Ic} is given by $0.90 \times 0.667 = 0.60$. This point is indicated by E on $R = 0.1$ curve. The 200 loading cycles of $0.90 \sigma_{op}$ and $R = 0.1$ change the K_{II}/K_{Ic} ratio from Point E to Point D on the plot of $R = 0.1$. The K_{II}/K_{Ic} ratio at the end of 200 loading cycles of $R = 0.1$ is 0.63.

The stress is increased by 10 percent at the end of 200 cycles. Hence, the K_{II}/K_{Ic} ratio at the beginning of 4300 cycles at σ_{op} and $R = 0.7$ is $(1.0/0.9) \times 0.63 = 0.70$. This is shown by Point D on the plot of $R = 0.7$. The 4300 loading cycles at σ_{op} and $R = 0.7$ change the K_{II}/K_{Ic} ratio from Point D to Point C on the plot of $R = 0.7$, where its value is 0.78.

The stress is decreased by 5 percent at the end of 4300 cycles. Hence the K_{II}/K_{Ic} ratio at the beginning of 260 cycles at $0.95 \sigma_{op}$ is $(0.95/1.0) \times 0.78 = 0.74$, which is shown by Point C on the $R = 0.4$ plot. The 260 cycles at $0.95 \sigma_{op}$ and $R = 0.4$ change the K_{II}/K_{Ic} ratio from Point C to Point B on the $R = 0.4$ plot, where its value is 0.80.

STRUCTURAL ANALYSIS MANUAL
GENERAL DYNAMICS/CONVAIR AND SPACE SYSTEMS DIVISION

The stress is increased by 5 percent at the end of 260 cycles. Hence, the K_{II}/K_{Ic} ratio at the beginning of 40 cycles at σ_{op} is $(1.0/0.95) \times 0.80 = 0.84$, which is illustrated by Point B on the $R = 0.1$ plot. The 40 cycles at σ_{op} and $R = 0.1$ increase the K_{II}/K_{Ic} ratio from 0.84 to 0.875, which is shown by Point A in Fig. E2-34.

Since the stress intensity at the end of 40 cycles at σ_{op} is less than the threshold stress intensity, the vessel is considered to be safe for the flight. It will take 20 loading cycles at σ_{op} and $R = 0.1$ to increase K_{II}/K_{Ic} from 0.875 to 0.90. Thus, the estimated minimum cyclic life remaining for the vessel is 20 cycles.

II. Example Problem B (Thin-Walled Vessel).

In thin-walled vessels the flaw depth becomes deep with respect to the wall thickness prior to reaching the critical size. Therefore, Kobayashi's magnification factor for deep surface flaws M_k must be considered. In thin-walled vessels it is assumed that the flaws are long with respect to their depth and, consequently, Q is assumed to be equal to unity in the Kobayashi equation.

To determine the cyclic life of a thin-walled vessel, the following relations are required (Ref. 22).

1. Proof-test factor, σ_{op} , K_{Ic} , and K_{TH} .
2. The σ versus a curve, similar to Fig. E2-35, to determine the flaw size, a_i , a_{cr} , and a_{Th} . The curve is obtained from the following equation:

$$\sigma = \frac{K_I}{(1.1 M_k \sqrt{\pi a})}$$

STRUCTURAL ANALYSIS MANUAL
GENERAL DYNAMICS/CONVAIR AND SPACE SYSTEMS DIVISION

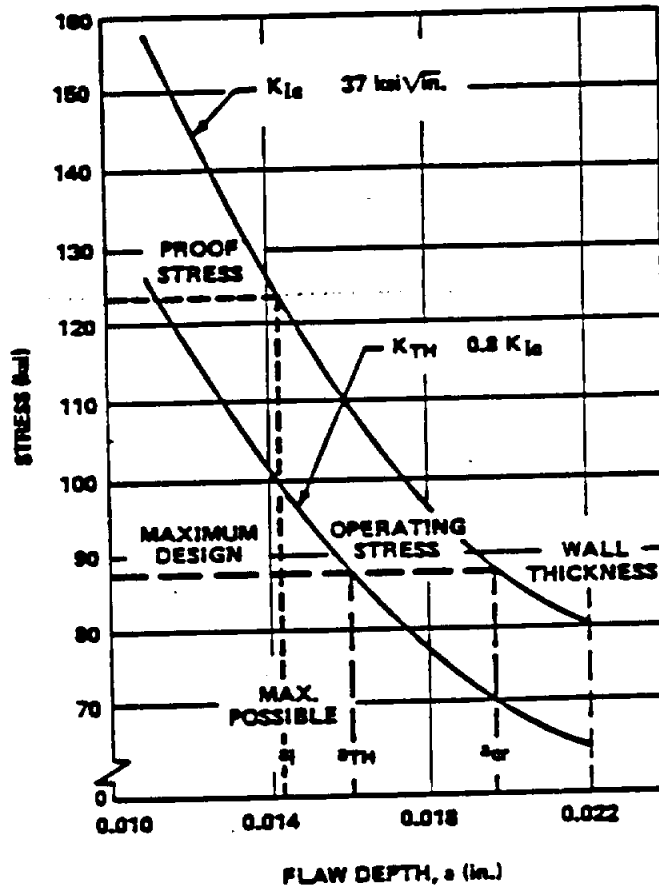


FIGURE E2-35. DETERMINATION OF INITIAL AND CRITICAL FLAW SIZES

3. The K_{II}/K_{Ic} versus flaw growth rate da/dN to determine the flaw growth rate at any stress level. The flaw growth rates can be obtained by differentiating the K_{II}/K_{Ic} versus cycles to failure curve, similar to that of Fig. E2-36 (Ref. 22). This curve is obtained from the specimens where a_{cr}/t is less than half. For an assumed maximum cyclic stress level, say σ_1 , the given K_{II}/K_{Ic} versus N curve can be converted to an a/Q versus N curve by the equation

$$a/Q = \frac{1}{1.21 \pi} \left(\frac{K_{II}}{\sigma_1} \right)^2$$

STRUCTURAL ANALYSIS MANUAL
GENERAL DYNAMICS/CONVAIR AND SPACE SYSTEMS DIVISION

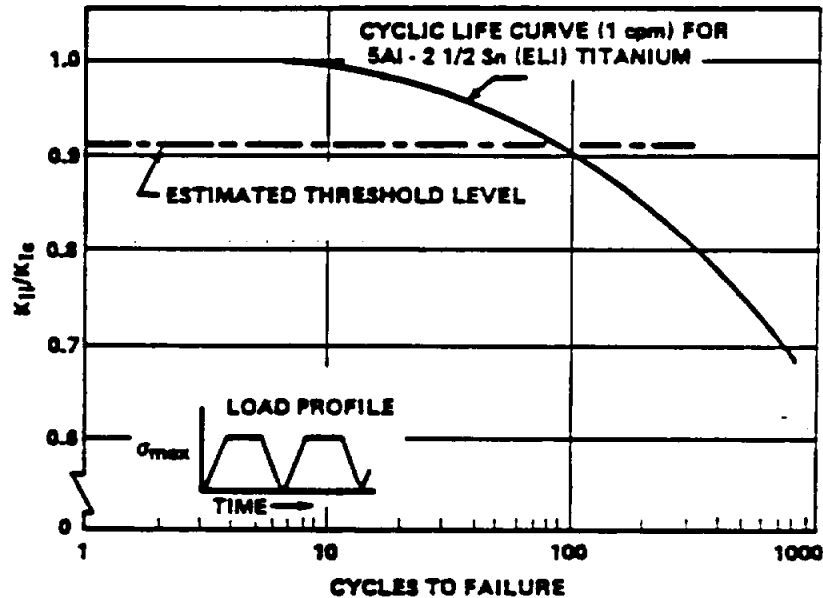


FIGURE E2-36. COMBINED SUSTAINED AND CYCLIC STRESS
 LIFE DATA [5 Al - 2 1/2 Sn (ELI) TITANIUM
 AT -320 °F]

The slope of the a/Q versus N curve gives the plot for the flaw growth rate $d(a/Q)/dN$ versus K_{II}/K_{Ic} for the stress level σ_1 . From the preceding equation for a given K_{II} , a/Q at the stress level σ_2 is related with a/Q at σ_1 as

$$(a/Q)_{\sigma_2} = \left(\frac{\sigma_1}{\sigma_2}\right)^2 \left(\frac{a}{Q}\right)_{\sigma_1}$$

From this equation it can be concluded that the flaw growth rate at any stress level σ_2 is related to the growth rate at σ_1 as follows:

$$[d(a/Q)/dN]_{\sigma_2} = (\sigma_1/\sigma_2)^2 [d(a/Q)/dN]_{\sigma_1}$$

STRUCTURAL ANALYSIS MANUAL
GENERAL DYNAMICS/CONVAIR AND SPACE SYSTEMS DIVISION

The prediction of the remaining cycle life and the structural integrity of the thin-walled vessel is demonstrated by an illustrative example abstracted from Ref. 22 and is given as follows.

Suppose that a thin-walled 6Al-4V titanium (STA) propellant tank containing N_2O_4 at room temperature is successfully proof tested with water at room temperature to a proof-test factor of 1.41 times the maximum design operating stress, σ_{op} . Suppose that the proof-tested tank is subjected to the following pressure cycles before the flight:

1. Twenty loading cycles with the maximum stress as 90 percent of σ_{op} .
2. Twelve loading cycles with the maximum stress as 95 percent of σ_{op} .
3. Five loading cycles with the maximum stress as σ_{op} .

It is desired to assess the structural integrity of the pressure vessel from the fracture mechanics standpoint and estimate the minimum cyclic life remaining for the vessel at σ_{op} . This example is treated with specific numbers since the stress-intensity factor has to be corrected for the a/t ratio according to Fig. E2-25. The thickness of the tank is 0.022 in. The maximum design operating stress, σ_{op} , is 87.5 ksi. The material of this gage under the above-mentioned environmental conditions has the minimum fracture toughness of 37 ksi $\sqrt{\text{in.}}$ and the threshold stress intensity of 80 percent of K_{Ic} .

The σ versus a plots are given for K_{Ic} and $K_{TH} = 0.80 K_{Ic}$ in Fig. E2-35. Since the proof stress is $1.41 \times \sigma_{op} = 123.6$ ksi, it is clear from Fig. E2-35 that the maximum possible a_i that could exist is 0.0143 in. Here it is assumed that the depressurization from the proof pressure is

STRUCTURAL ANALYSIS MANUAL
GENERAL DYNAMICS/CONVAIR AND SPACE SYSTEMS DIVISION

rapid enough so that no significant flaw growth occurs during the depressurization. Also, as shown in Fig. E2-35, for the stress level of σ_{op} , a_{cr} is 0.0196 in. and a_{TH} is 0.0160 in.

The plot of the K_{II}/K_{Ic} versus flaw growth rate for 6AL-4V titanium at room temperature is reproduced in Fig. E2-37 for $\sigma = 100$ ksi. The 99-percent confidence level flaw growth rate curve is obtained from the cyclic data of $R = 0.0$; it is assumed in this example that all the cycles are applied at $R = 0.0$.

Taking into account the effect of stress level on the flaw growth rates, the rates are arithmetically integrated from $a_i = 0.0143$ in. to $a_{cr} = 0.0196$ in. according to Fig. E2-38 to calculate the cycles to failure for the stress level of σ_{op} . The plot of flaw depth against cycles to failure for the stress level of σ_{op} is shown in Fig. E2-39.

When the maximum cyclic stress is $0.95 \sigma_{op}$, a_i is still 0.0143 in. but a_{cr} is 0.0208 in. and $a_{TH} = 0.0167$ in. from Fig. E2-35. Based on the stress level of $0.95 \sigma_{op}$, the flaw growth rates are integrated from $a_i = 0.0143$ in. to $a_{cr} = 0.208$ in. to calculate the cycles to failure. A similar procedure is followed to obtain the relation of flaw depth against cycles to failure for the stress level of $0.90 \sigma_{op}$. These plots are shown in Fig. E2-39.

At the end of the proof cycle and the beginning of the first cycle at the maximum cyclic stress of $0.90 \sigma_{op}$, the maximum possible flaw depth is 0.0143 in. This is shown by Point D in Fig. E2-39. The 20 loading cycles with the maximum stress as $0.90 \sigma_{op}$ change a from Point D to Point C on the plot of $0.90 \sigma_{op}$ (Fig. E2-39).

STRUCTURAL ANALYSIS MANUAL
GENERAL DYNAMICS/CONVAIR AND SPACE SYSTEMS DIVISION

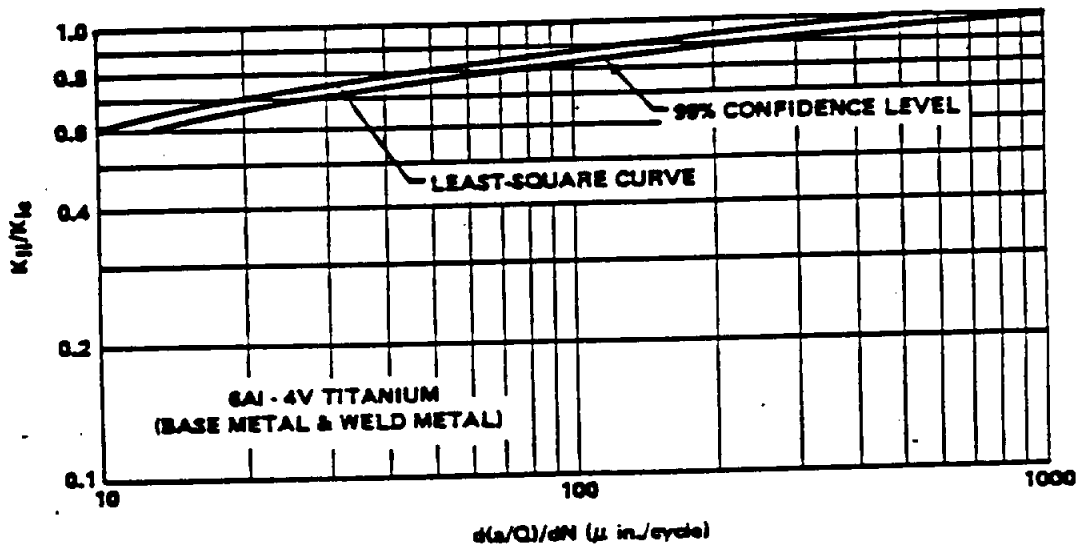
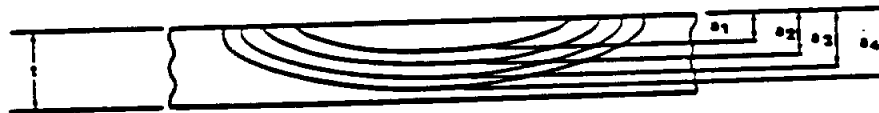


FIGURE E2-37. CYCLIC FLOW-GROWTH RATES
(FOR $\sigma_{max} = 100$ ksi)



a	Δa	a/t	M_K^a	K^b	MEAN K	MEAN ^c da/dN	ΔN	N
a_1		a_1/t	M_{K1}	K_1	$\frac{K_1 + K_2}{2}$	$da_{1,2}/dN$	ΔN_1	ΔN_1
a_2	$a_2 - a_1$	a_2/t	M_{K2}	K_2	$\frac{K_2 + K_3}{2}$	$da_{2,3}/dN$	ΔN_2	$\Delta N_1 +$
a_3	$a_3 - a_2$							ΔN_2
								$\Delta N_1 +$
								$\Delta N_2 +$
								ΔN_3

- a. Obtain from Kobayashi's solution of M_K vs a/t
b. $K = 1.1 \sqrt{\pi} \sigma(a)/1/2 M_K$
c. Obtain from base K vs da/dN curve.

FIGURE E2-38. ARITHMETIC INTEGRATION OF FLOW-GROWTH-RATE
DATA (DEEP FLAWS IN THIN-WALLED VESSELS)

720

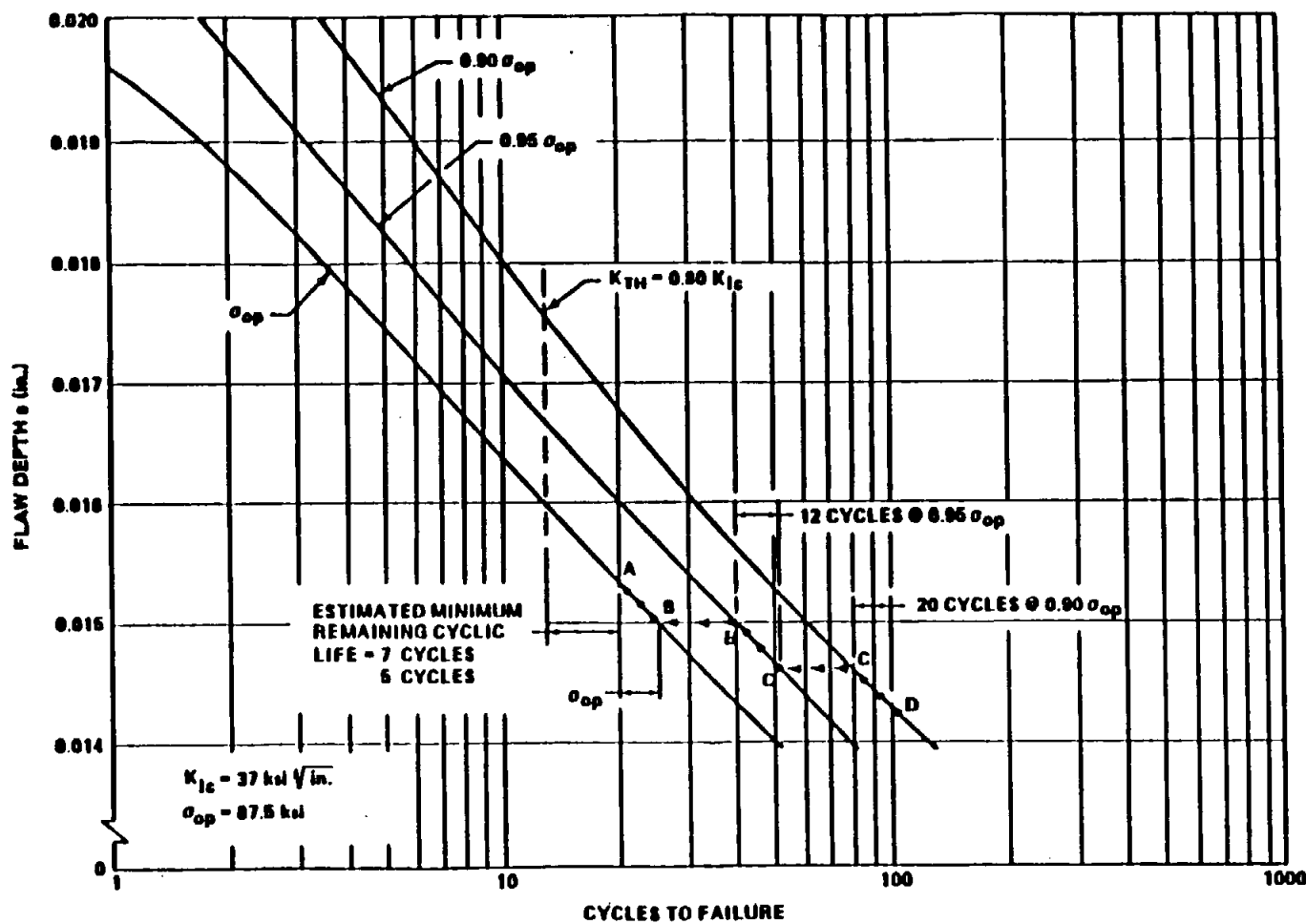


FIGURE E2-39. PREDICTION OF CYCLIC LIFE OF A THIN-WALLED VESSEL
(ILLUSTRATIVE EXAMPLE)

STRUCTURAL ANALYSIS MANUAL
GENERAL DYNAMICS/CONVAIR AND SPACE SYSTEMS DIVISION

The tank-wall stress is increased by 5 percent at the end of 20 loading cycles with the maximum stress as $0.90 \sigma_{op}$. The flaw size remains the same during the stress increase. This is shown by Point C on the plot of $0.95 \sigma_{op}$ in Fig. E2-39.

The 12 loading cycles with the maximum stress as $0.95 \sigma_{op}$ change a from Point C to Point B on the plot of $0.95 \sigma_{op}$ in Fig. E2-39.

At the end of 12 loading cycles with the maximum stress as $0.95 \sigma_{op}$, the stress is increased by 5 percent. This is shown by Point B on the plot of σ_{op} in Fig. E2-39.

The five loading cycles with the maximum stress as σ_{op} change a from Point B to Point A on the plot of σ_{op} in Fig. E2-39. The flaw depth at A is 0.01534 in. This is smaller than a_{TH} , which is 0.0160 in. Hence the vessel is considered to be safe for the flight. Also from Fig. E2-39, it will take seven cycles at σ_{op} to increase the flaw depth from 0.01534 in. to 0.0160 in. Hence, the minimum estimated cyclic life remaining for the vessel is seven cycles.

2.4.3.2 Allowable Initial Flaw Size.

Allowable initial flaw sizes in a designed structure depend on the service life requirements for the structure and fracture toughness properties of the material selected. The prevention of failure requires that either the actual initial flaw sizes or the maximum possible initial flaw size be known. Nondestructive inspection provides the only means of determining actual initial flaw sizes. A successful proof test specifies the maximum possible initial flaw size which can exist after the proof test and, in turn, provides the maximum possible initial to critical stress-intensity ratio, K_{II}/K_{Ic} . To determine the maximum allowable initial flaw size, the initial to critical stress-intensity ratio, based on the service life requirements, must be determined.

STRUCTURAL ANALYSIS MANUAL
GENERAL DYNAMICS/CONVAIR AND SPACE SYSTEMS DIVISION

The calculation of allowable initial flaw size is demonstrated by the following example.

I. Example Problem A.

A cyclic loaded pressure vessel of aluminum alloy must meet the following design conditions:

1. Required minimum life, 40 000 cycles.
2. Maximum stress in a cycle $1/2 \sigma_{ys} = 35\ 000$ psi.
3. K_{Ic} of weld metal = $15\ 000$ psi $\sqrt{\text{in.}}$
4. Semielliptical surface defect (length $4 \times$ depth).

What is the allowable initial flaw size which will grow to a critical size in 40 000 cycles?

Solution.

From Fig. E2-40 (Ref. 18), the K_{II}/K_{Ic} ratio corresponding to 40 000 cycles of life is 0.36. The initial stress intensity can now be determined:

$$K_{II}/K_{Ic} = 0.36 = \frac{K_{II}}{15\ 000}$$

and

$$K_{II} = 0.36 (15\ 000) = 5400 \text{ psi } \sqrt{\text{in.}}$$

Knowing the design stress of 35 000 and the expression of the type of defect, it is now possible to find the defect size corresponding to a K_{II} of 5400 psi $\sqrt{\text{in.}}$:

STRUCTURAL ANALYSIS MANUAL
GENERAL DYNAMICS/CONVAIR AND SPACE SYSTEMS DIVISION

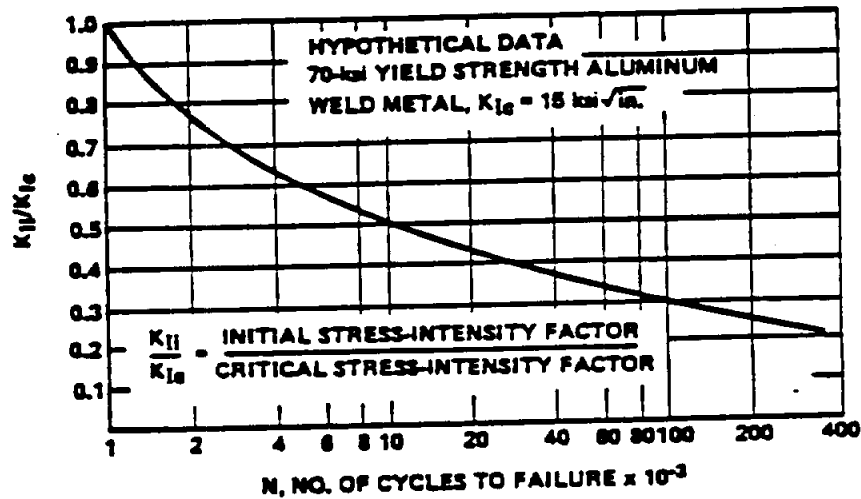


FIGURE E2-40. CYCLIC FLAW-GROWTH DATA FOR ALUMINUM ALLOY

$$a_1 = \frac{K_{II}^2 Q}{1.21 \pi \sigma^2} = \frac{(5400)^2 (1.4)}{1.21 \pi (35\,000)^2} = 0.0088 \text{ in.}$$

The value of $Q = 1.4$ is taken from Fig. E2-5 for $a/2c = 1/4 = 0.25$ and $\sigma/\sigma_{ys} = 1/2 = 0.50$.

$$2c_1 = 4a_1 = 4(0.0088) = 0.0352 \text{ in.}$$

Therefore, the size of an initial flaw which will just grow to a critical size in 40 000 cycles is 0.0088 in. deep by 0.0352 in. long.

2.4.3.3 Nondestructive Inspection Acceptance Limits.

The NDI requirements for any given structure are a function of the allowable flaw sizes. They are limited by any economic or schedule implications associated with a proof-test failure and by the reliability of the

STRUCTURAL ANALYSIS MANUAL
GENERAL DYNAMICS/CONVAIR AND SPACE SYSTEMS DIVISION

inspection techniques for detecting initial flaws. Allowances should be made for any lack of specific knowledge of flaw geometry and orientation. When there is a lack of flaw definition, the worst possible flaw geometry and orientation might be assumed.

Also, in arriving at acceptance limits, the allowable spacing for internal or surface flaws (that is, aligned flaws in weldments) must be considered. An approximate analytical solution for the interaction of elliptically shaped coplanar flaws has been obtained by Kobayashi and Hall (Ref. 23). The results are shown in Fig. E2-41 along with experimental results on several Ladish D6AC steel specimens containing two coplanar semielliptical surface flaws. The curves are plotted in terms of stress-intensity magnification ratio (K_1/K_2) versus flaw spacing ratio (d/a). Probably the most significant point is that there is very little interaction between coplanar flaws unless they are surprisingly close together.

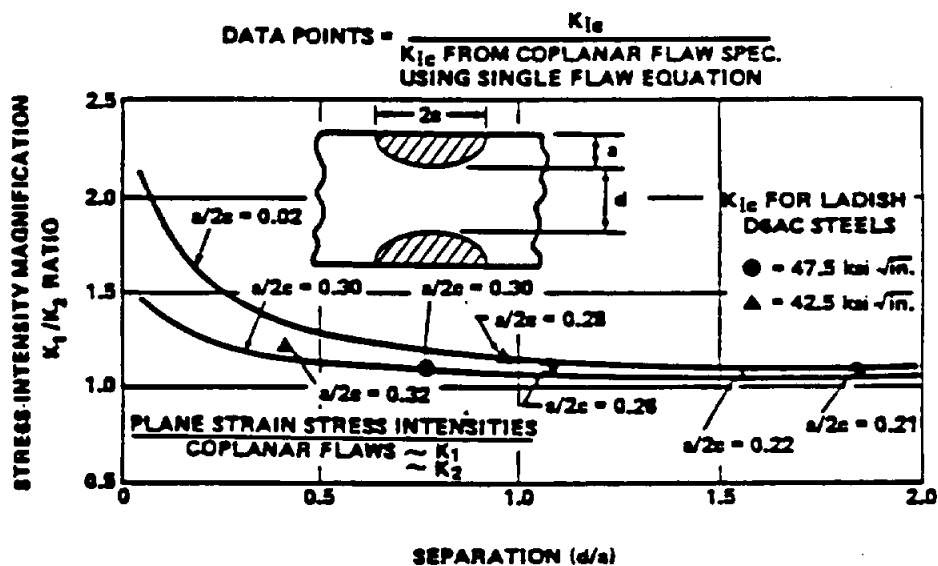


FIGURE E2-41. STRESS-INTENSITY MAGNIFICATION FOR TWO
 COPLANAR ELLIPTICAL FLAWS

STRUCTURAL ANALYSIS MANUAL
GENERAL DYNAMICS/CONVAIR AND SPACE SYSTEMS DIVISION

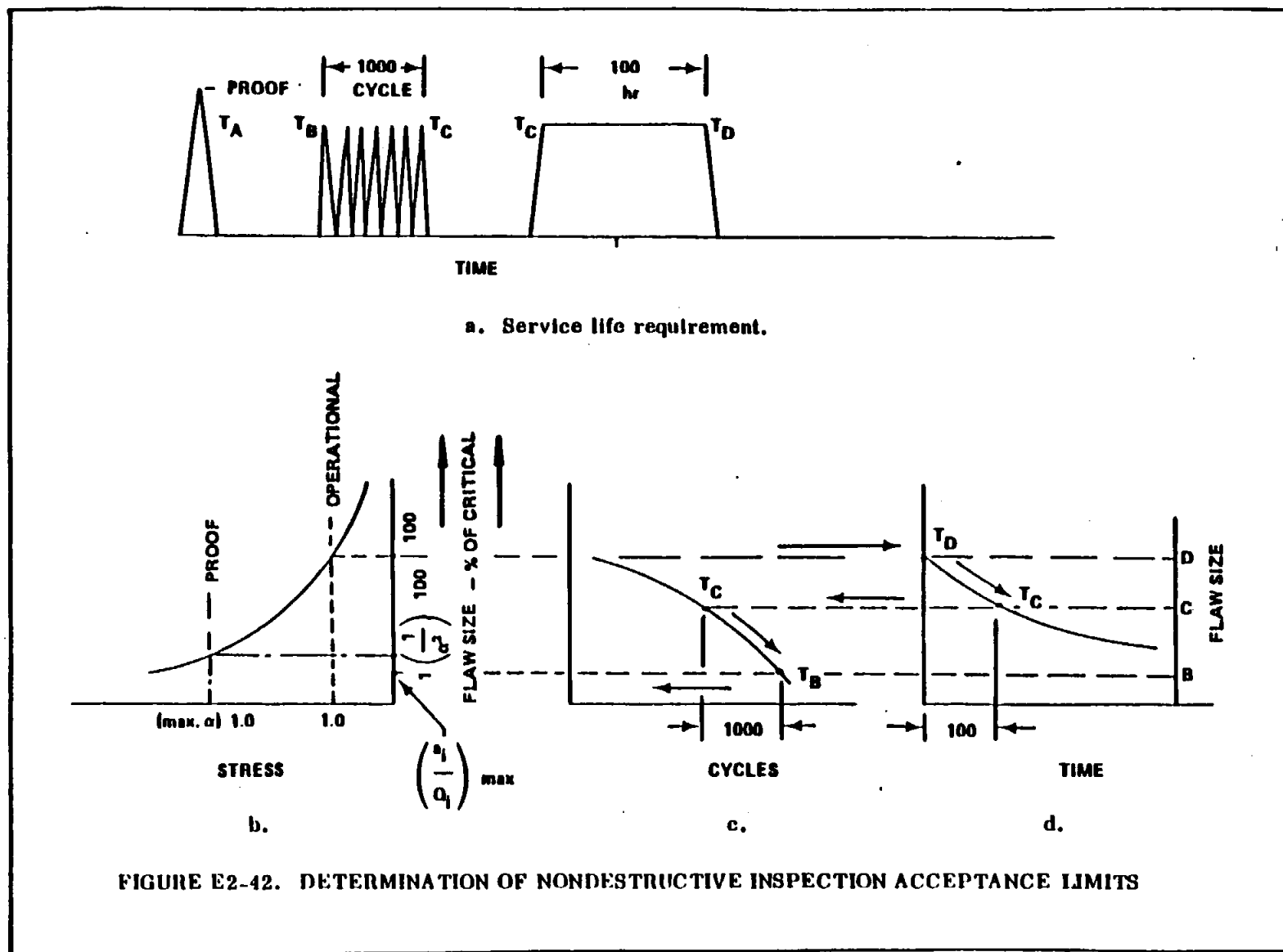
The establishment of NDI acceptance limits when service life requirements are known might best be shown by an illustrative example involving a hypothetical pressure vessel that is expected to encounter a rather complex loading history.

Figure E2-42a shows the assumed service life requirement consisting of one proof-test cycle (at a stress level of α times the operating stress) followed by 1000 cycles and then 100 hr, both at a constant operating stress level of ($\sigma = 1.0$). To define the minimum inspection standards required prior to service, it is necessary to determine the critical flaw size, $(a/Q)_{cr}$, at the end of service (Section 2.4.2) and work backwards, evaluating all portions of the loading profile that can cause flaw growth.

Figure E2-42b represents a dimensionless relationship of stress-to-flaw size as shown previously (Fig. E2-6). The ordinate now is plotted in terms of percentage of critical flaw size at operating stress. Figures E2-42c and d are schematic representations of the cyclic load flaw growth and sustained load flaw growth, respectively.

The approach is as follows:

1. The critical flaw size at operating stress is represented as 100 percent of critical and is the maximum allowed at time T_D (at the end of the service life).
2. Maximum allowed flaw size at time T_C is shown by Point C and represents the maximum allowable flaw size at the start of the 100-hr sustained stress period.
3. The effect of cyclic loading is shown in Fig. E2-42c by moving 1000 cycles from T_C to T_B . Point B then represents the maximum allowable size at time T_B or at the start of the 1000-cycle period. This size is the maximum allowable size before the vessel is placed in service.



STRUCTURAL ANALYSIS MANUAL
GENERAL DYNAMICS/CONVAIR AND SPACE SYSTEMS DIVISION

4. It can be shown that the previous one-cycle proof test generally has a negligible effect on flaw growth compared with the chosen service life.

Note in this schematic illustration that the maximum allowable flaw size is less than that which could have been present during a successful proof test, and thus the proof test could not guarantee successful fulfillment of the service life requirement. As a result, NDI must be capable of detecting flaws as small as $(a_i/Q_i)_{\max}$.

If it is determined that inspection technique limitations preclude the assurance of service life reliability, then either the proof-test factor must be increased to assure that $(a_i/Q_i)_{\max}$ is the largest possible existing flaw size at the beginning of service life, or conservative assumptions might be made about flaw geometry and orientation to account for the inability to detect small flaw depths. For example, the length (L) of an indication seen in X-ray inspection could be assumed to be the minor axis of an elliptical flaw where the major axis is large with respect to the minor axis (i.e., $L = 2a$, $Q \approx 1.0$). Consequently, the critical flaw size must be larger (and the operating stress lower) in order to meet the service life requirements. In other words, both $(a_i/Q_i)_{\max}$ and $(a/Q)_{\text{cr}}$ move higher up the ordinate of Fig. E2-42b.

It should be noted that in terms of "percentage of critical," flaw size is independent of actual stress and toughness values. Obviously, the determination of finite maximum allowable flaw sizes (or smallest flaw size for NDI detection) requires a detailed knowledge of applied stresses in the various tank locations and of the fracture toughness of the materials used. This has been illustrated by the Example Problem A in Section 2.4.3.2 in which the allowable initial flaw size in an aluminum alloy pressure vessel is calculated based on a required service life. In the case where NDI acceptance limits are being considered, the calculated initial flaw depth and length are the minimum dimensions which NDI must be capable of detecting.

STRUCTURAL ANALYSIS MANUAL
GENERAL DYNAMICS/CONVAIR AND SPACE SYSTEMS DIVISION

2.4.3.4 Proof-Test Factor Selection.

It has been previously noted that a successful proof test determines the maximum possible flaw size which can exist after the proof test and prior to the beginning of service. The proof test is the most powerful inspection test presently available and offers the most reliable method for guaranteed service life.

Figure E2-43 shows a schematic theoretical relationship between the critical flaw size, $(a/Q)_{cr}$, and the corresponding fracture stress, as previously illustrated in Fig. E2-6, along with a similar relationship between initial flaw size $(a/Q)_i$ and stress level. The relationships hold true for applied stresses below the yield strength of the material. For stresses above

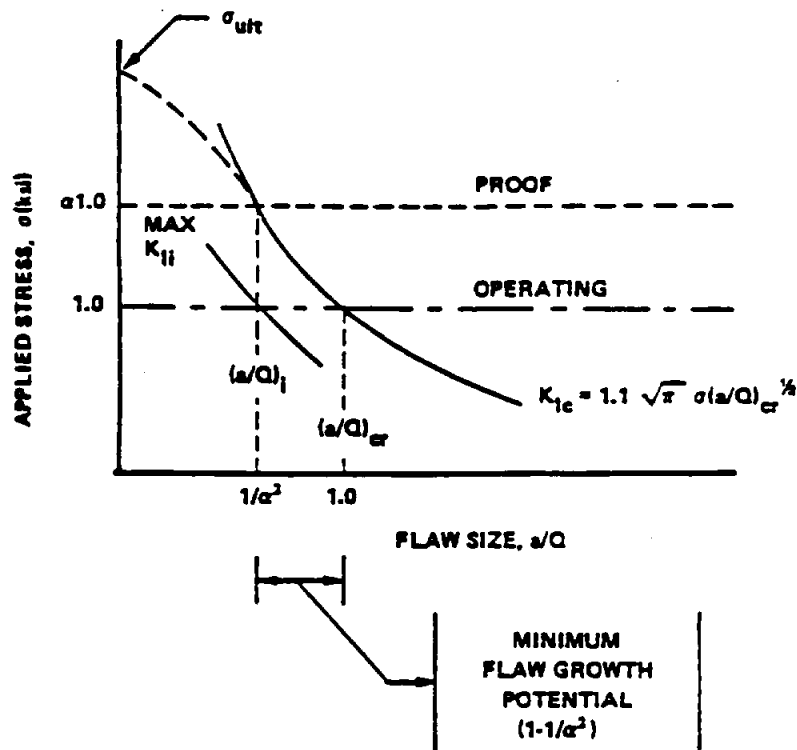


FIGURE E2-43. TYPICAL MATERIAL STRESS-INTENSITY
 RELATIONSHIP

STRUCTURAL ANALYSIS MANUAL
GENERAL DYNAMICS/CONVAIR AND SPACE SYSTEMS DIVISION

the yield value the relationships follow some experimentally determined curve up to the ultimate strength, σ_{ult} . If proof pressure is α times the operating pressure, the critical flaw size is

$$(a/Q)_{cr_{proof}} = \max (a/Q)_{i_{oper}} = \frac{1}{1.21 \pi} \left(\frac{K_{Ic}}{\alpha \sigma_{oper}} \right)^2$$

and

$$(a/Q)_{cr_{oper}} = \frac{1}{1.21 \pi} \left(\frac{K_{Ic}}{\sigma_{oper}} \right)^2$$

Thus the proof-test factor, α , is a function of the maximum initial flaw size and critical flaw size for the operating pressure level

$$\frac{(a/Q)_{i_{oper}}}{(a/Q)_{cr_{oper}}} = \frac{1}{\alpha^2}$$

Since subcritical flaw growth is a function of the initial stress intensity as compared with the critical value, the proof-test factor can be related as

$$\frac{\max K_{II}}{K_{Ic}} = \frac{1.1 \sqrt{\pi} \sigma_{oper} (a/Q)_{i_{oper}}^{1/2}}{1.1 \sqrt{\pi} \alpha \sigma_{oper} (a/Q)_{i_{oper}}^{1/2}} = \frac{1}{\alpha}$$

where K_{II} is the initial stress intensity at the operating stress level and temperature, and K_{Ic} is the fracture toughness value at proof test

STRUCTURAL ANALYSIS MANUAL
GENERAL DYNAMICS/CONVAIR AND SPACE SYSTEMS DIVISION

temperature. It should be noted that lower proof test factors (and therefore lower proof stresses) can be employed if the proof test is performed at a temperature where the material has a lower K_{Ic} than at operating temperature and, consequently, greater susceptibility to flaws. In this way the risk of proof-test failure is minimized insofar as practical.

The maximum K_{Ic} at proof temperature should be employed in the equation rather than the minimum or average K_{Ic} because it results in the selection of a higher proof factor, a conservative event. Figure E2-44 illustrates the difference between the use of maximum and minimum K_{Ic} at proof temperature. For a given maximum initial flaw size, $(a/Q)_i$ (max), the proof stress required by K_{Ic} (min.) is less than that required by K_{Ic} (max.). In fact, if K_{Ic} (min.) were used and a component fabricated from material characteristic of K_{Ic} (max.) and containing a flaw slightly longer than $(a/Q)_i$ (max) were proof tested at the lower level, the component would pass

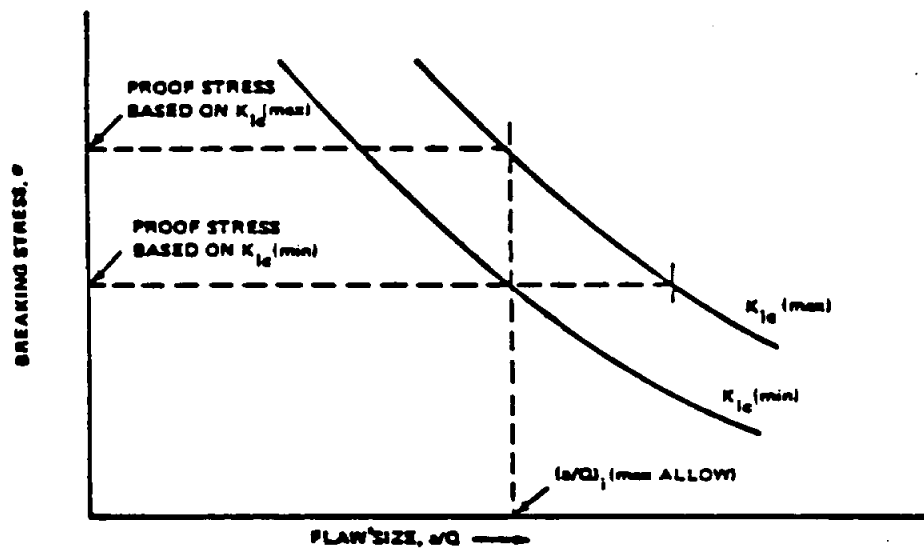


FIGURE E2-44. DETERMINATION OF PROOF STRESS BY MAXIMUM AND MINIMUM VALUES OF K_{Ic}

STRUCTURAL ANALYSIS MANUAL
GENERAL DYNAMICS/CONVAIR AND SPACE SYSTEMS DIVISION

the proof test successfully but probably would fail in service. The use of $K_{Ic} \text{ (max)}_p$ in the proof-factor equation precludes this.

It has been shown by analysis that regardless of the structural wall thickness, the required minimum proof-test factor α is always $1 \div$ allowable K_{II}/K_{Ic} . However, the value of the proof test in providing assurance against service failure changes with decreasing wall thickness and/or increasing fracture toughness, K_{Ic} , the same as occurs with the predicted pressure vessel failure mode. This is discussed in more detail in Ref. 22 and illustrated in Fig. E2-45.

Having experimentally obtained the cyclic and sustained flaw growth for a material under consideration, the necessary proof-test factor can be determined to assure that the structure will meet the service life requirements. Proof-factor determination can be applied to at least two general problem areas in the design of structural components:

1. Evaluation and modification of proof-test conditions for current components for which operating stress and mission are already fixed.
2. Preliminary design of components intended for known missions, including selection of material, maximum operating stress, minimum proof stress, and proof temperature.

The following sample problem illustrates the proper selection of a proof-test factor for a hypothetical pressure vessel design.

I. Example Problem A.

Suppose that a thick-walled liquid nitrogen 5Al-2.5Sn (ELI) titanium pressure vessel must meet a service life requirement of 600 pressure cycles where the pressure is sustained for a prolonged period during each cycle. The vessel has already been successfully proof tested with LN_2 to a proof factor

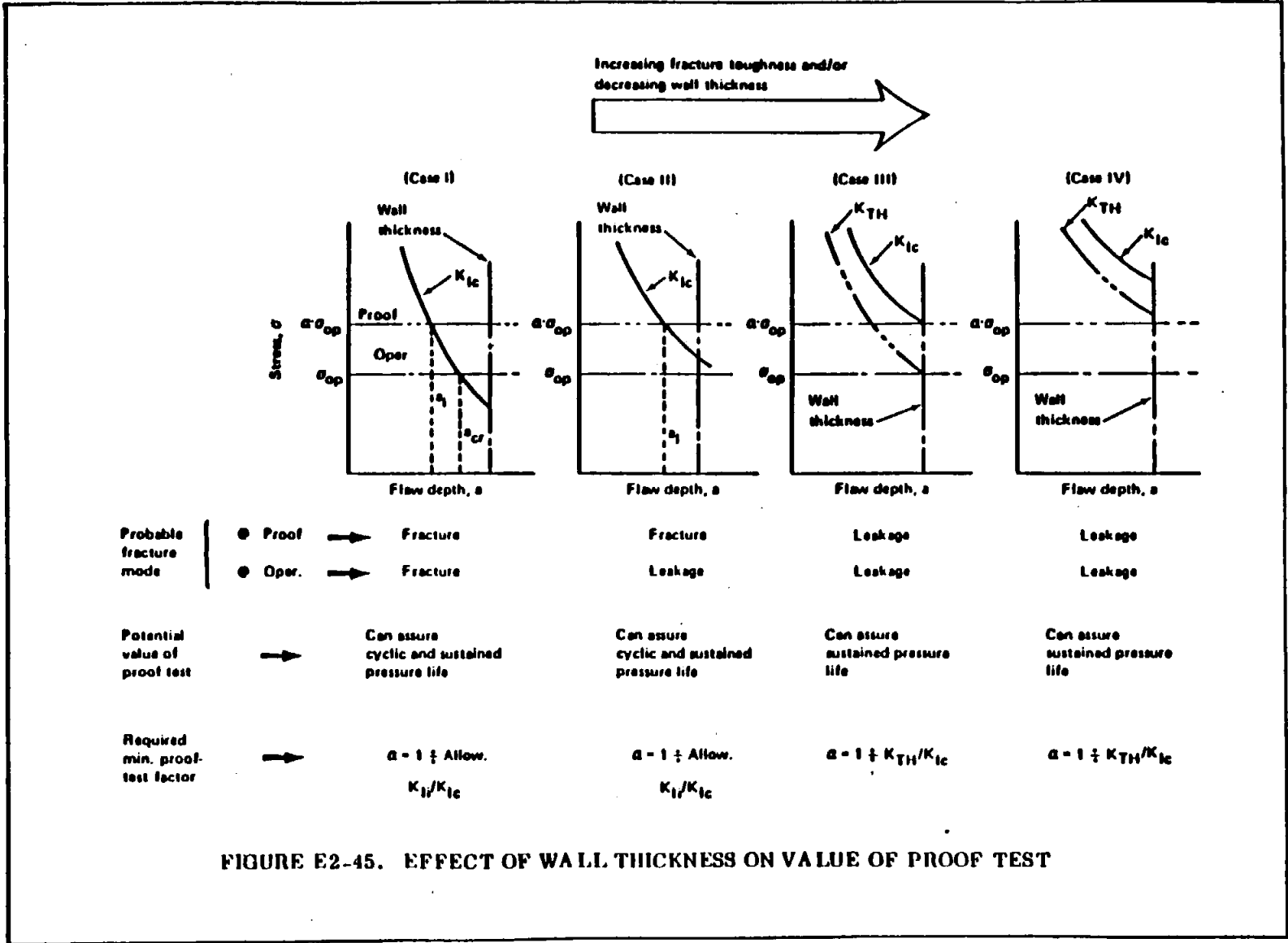


FIGURE E2-45. EFFECT OF WALL THICKNESS ON VALUE OF PROOF TEST

STRUCTURAL ANALYSIS MANUAL
GENERAL DYNAMICS/CONVAIR AND SPACE SYSTEMS DIVISION

$\alpha = 1.25$. Will this proof factor assure that no failure occurs during the service life and if not, what proof factor is required?

The cyclic life curve for 5Al-2.5Sn (ELI) titanium is reproduced in Fig. E2-36. The estimated threshold stress-intensity value for sustained-stress flaw growth (K_{TH}/K_{Ic}) is approximately 0.92.

For long hold time, $\max. K_{II}/K_{Ic} = 1/\alpha = 1/1.25 = 0.80$. From Fig. E2-36 for $K_{II}/K_{Ic} = 0.80$, $N = 300$ cycles. For $K_{TH}/K_{Ic} = 0.92$, $N = 100$ cycles.

In 300 cycles minus 100 cycles, or 200 cycles, the stress intensity would have reached the estimated threshold value for sustained-stress flaw growth. Thus the predicted minimum life would be only 200 cycles and the proof factor of 1.25 will not assure a service life of 600 cycles.

For 100 cycles plus 600 cycles, or 700 cycles,

$$K_{II}/K_{Ic} = 0.70 = \frac{1}{\alpha}$$

and

$$\alpha = \frac{1}{0.70} = 1.43$$

Thus, the 600-cycle service life requires a proof-test factor of 1.43 times the operating pressure.

STRUCTURAL ANALYSIS MANUAL
GENERAL DYNAMICS/CONVAIR AND SPACE SYSTEMS DIVISION

REFERENCES

1. Fracture Toughness Testing and its Applications. ASTM Special Technical Publication No. 381, American Society for Testing and Materials, April 1965.
2. Irwin, G. R.: Fracture and Fracture Mechanics Report No. 202, T&AM Department of Theoretical and Applied Mechanics, University of Illinois, October 1961.
3. Irwin, G. R.: Crack Extension Force for a Part-Through Crack in a Plate. Journal of Applied Mechanics, Vol. 84 E, No. 4, December 1962.
4. Green, A. E.; and Sneddon, I. N.: The Distribution of Stress in the Neighborhood of a Flat Elliptical Crack in an Elastic Solid. Proceedings of the Cambridge Philosophical Society, Vol. 46, 1959.
5. Kobayashi, A. S.: On the Magnification Factors of Deep Surface Flaws. Structural Development Research Memorandum No. 16, The Boeing Co., December 1965.
6. Plane Strain Crack Toughness Testing. ASTM Special Technical Publication No. 410, American Society for Testing and Materials, December 1967.
7. Review of Developments in Plane Strain Fracture Toughness Testing. ASTM Special Technical Publication No. 463, American Society for Testing and Materials, September 1970.
8. Paris, P. C.; and Erdogan, F.: A Critical Analysis of Crack Propagation Laws. Journal of Basic Engineering, Transactions of the ASME, Series D, Vol. 85, 1963.
9. Foreman, R. G.; Kearney, V. E.; and Engle, R. M.: Numerical Analysis of Crack Propagation in Cyclic-Loaded Structures. Journal of Basic Engineering, Transactions of the ASME, September 1967.
10. Hudson, M. C.: Effect of Stress Ratio on Fatigue-Crack Growth in 7075-T6 and 2024-T3 Aluminum-Alloy Specimens. NASA TN D-5390, August 1969.

STRUCTURAL ANALYSIS MANUAL
GENERAL DYNAMICS/CONVAIR AND SPACE SYSTEMS DIVISION

REFERENCES (Continued)

11. Tiffany, C. F.; Lorenz, P. M.; and Hall, L. R.: Investigation of Plane-Strain Flaw Growth in Thick-Walled Tanks. NASA CR-54837, 1966.
12. Fracture Control of Metallic Pressure Vessels. NASA SP-8040, May 1970.
13. Wheeler, O. E.: Spectrum Loading and Crack Growth. Transactions of the ASME, Journal of Basic Engineering, March 1972.
14. Elber, W.: Fatigue Crack Closure Under Cyclic Tension. Engineering Fracture Mechanics, Vol. II, No. 1, Pergamon Press, July-1970.
15. Elber, Wolf: The Significance of Fatigue Crack Closure. Damage Tolerance in Aircraft Structures, ASTM Special Technical Publications 486, American Society for Testing and Materials, 1971, pp. 230-242.
16. Pellissier, G. E.: Some Microstructural Aspects of Maraging Steel in Relation to Strength and Toughness. Technical Documentary Report RTD-TDR-63-4048. Air Force Materials Laboratory, Wright-Patterson Air Force Base, Ohio, November 1963.
17. Tiffany, C. F.; and Masters, J. N.: Applied Fracture Mechanics. ASTM Special Technical Publication No. 381, American Society for Testing and Materials, April 1965.
18. Wessel, E. T., et al. Engineering Methods for the Design and Selection of Materials Against Fracture. AD 801005, June 1966.
19. Progress in the Measurement of Fracture Toughness and the Application of Fracture Mechanics to Engineering Problems. American Society for Testing and Materials Special Committee on Fracture Testing of High-Strength Metallic Materials, Materials Research and Standards, Vol. 4, No. 3, March 1964, p. 107.
20. Pyle, R.; Schillinger, D. E.; and Carman, C. M.: Plane Strain Fracture Toughness and Mechanical Properties of 2219-T87 Aluminum and 5AL-2.5Sn(ELI) Titanium Alloy Weldments and One Inch Thick 3AL-2.5Sn(ELI) Titanium Alloy Plate. NASA CR-72154, Department of the Army, Frankfort Arsenal, September 1968.

STRUCTURAL ANALYSIS MANUAL
GENERAL DYNAMICS/CONVAIR AND SPACE SYSTEMS DIVISION

REFERENCES

21. Wilhem, D. P.: Fracture Mechanics Guidelines for Aircraft Structural Applications. AFFDL-TR-69-111, Northrop Corp., February 1970.
22. Shah, R. C.: Fracture Mechanics Assessment of Apollo Launch Vehicle and Spacecraft Pressure Vessels. Vol. 1, Report D2-114248-1, The Boeing Co., November 1968.
23. Kobayashi, A. S.; and Hall, L. R.: On the Correction of Stress Intensity Factors for Two Embedded Cracks. Structural Development Research Memorandum No. 9, The Boeing Co., 1963.
24. Advanced Crack Propagation Predictive Analysis Computer Program: "FLAGRO IV", T. Hu, Rockwell International, SOD 79-0280, September 1979.
25. Fatigue Crack Growth Computer Program: "NASA/FLAGRO", JSC-22267, 1981.
26. Damage Tolerance Material Properties for Shuttle/Centaur Vehicle and CISS Structure, GDSS-SSC-86-019, July 1986.
27. The Stress Analysis of Cracks Handbook, H. Tada, P. C. Paris and G. R. Irwin, Del Research Corporation, Hellertown, Pennsylvania, 1973.
28. Handbook of Stress-Intensity Factors, G. C. Sih, Institute of Fracture and Solid Mechanics, Lehigh University, Bethlehem, Pennsylvania, 1973.
29. Compendium of Stress Intensity Factors, D. P. Rooke and D. J. Cartwright, Her Majesty's Stationery Office, London, 1976.
30. "Investigations of Deep Flaws in Thin-Walled Tanks", N. J. Masters, W. P. Haese and R. W. Finger, NASA CR-72606, December 1969.
31. Fracture Control Method for Composite Tanks with Load Sharing Liners, W. D. Bixler, NASA CR-134750, D180-18850-1, July 1975.
32. "Sustained Load Crack Growth Design Data for Ti-6Al-4V Titanium Alloy Tanks containing Hydrazine", J. C. Lewis and J. T. Kenny, AIAA Paper No. 76-769, July 1976.
33. Forman, R. G., NASA TND-7952, "Environmental Crack-Growth Behavior of High Strength Pressure Vessel Alloys", Lyndon B. Johnson Space Center, Houston, Texas, April 1975.

STRUCTURAL ANALYSIS MANUAL
GENERAL DYNAMICS/CONVAIR AND SPACE SYSTEMS DIVISION

34. Cotter, K. H., "Leak-Before-Burst Criteria applied to Cryoformed Pressurant Tanks", AIAA-86-1503, AIAA/ASME/SAE/ASEE 22nd Joint Propulsion Conference, Huntsville, Alabama, June 16-18, 1986.
35. MIL-STD-1522A (USAF), Standard General Requirements for Safe Design and Operation of Pressurized Missile and Space Systems, 28 May 1984.
36. 65-00223, Fracture Control Plan, Shuttle/Centaur, 9 April 1986.
37. NASA Handbook NHB1700.7A, Fracture Control Requirements for Payloads using the Space Transportation System (STS).

STRUCTURAL ANALYSIS MANUAL
GENERAL DYNAMICS/CONVAIR AND SPACE SYSTEMS DIVISION

DAMAGE TOLERANCE

MATERIAL DATA

The most comprehensive compilation of material fracture toughness data is the "Damage Tolerance Design Handbook", MCIC-HB-01. This four volume set published by the Metals and Ceramic Information Center of the Batelle Columbus Laboratories.

Other sources of material fracture data are MIL-HDBK-5D and "Fracture Mechanics Evaluation of B-1 Materials", AFML-TR-76-137. and Ref. 26.

COMPUTER PROGRAMS

Two programs are currently available at Convair for fracture analysis. Both run on the Cyber.

(REF. 24)

FLAGRO IV was written by Rockwell and was used extensively on the Space Shuttle program. This is a Fortran IV program and input parameters are read from a formatted data file. The user specifies the problem geometry by selecting one of 14 flaw types and the corresponding parameters such as thickness, width, hole size, edge distance and crack size. Material data can be either input manually or taken from the program's library of information on common materials. Non uniform stress distributions are handled by variable correction factors. Any loading spectrum can be applied but duration of load is not accounted for. The user can opt to take advantage of retardation when high load cycles are followed by low load cycles. Three types of growth rate equations (Colli Priest, Paris, and direct interpolation from data) are available in the program. The software library accession number is P5953 for FLAGRO IV.

(REF. 25)

NASA /FLAGRO was produced by NASA's LBJ Space Center in 1987. It has much more capability than FLAGRO IV. The Material Data Library is extensive, the user has 25 flaw geometry types to choose from, and bending moments as well as axial stresses can be applied. The program is interactive and menu driven with graphics capability.

STRUCTURAL ANALYSIS MANUAL
GENERAL DYNAMICS/CONVAIR AND SPACE SYSTEMS DIVISION

DAMAGE TOLERANCE

DAMAGE TOLERANCE REQUIREMENTS

In order to comply with current military, FAA, and NASA requirements, materials selected for critical structural applications must have adequate fracture toughness to tolerate, without failure under design loads, flaws caused by manufacture and cracks grown during service.

In the case of the Air Force the governing document usually referred to in the procurement contract is MIL-A-83444 "Airplane Damage Tolerance Requirements." That document specifies the following:

- 1) Initial flaw size assumptions. The size of the flaw assumed to be initially existing in the material is defined as a function of structure geometry, method of manufacture and reliability of inspection technique.
- 2) Initial and in-service inspection requirements.
- 3) Residual strength requirements. Residual strength analysis is conducted to determine the capability of a structure containing damage to withstand a single load without catastrophic failure.

Multiple load path designs with crack arrest features can be qualified under MIL-A-83444 either as slow crack growth structure or as fail safe structure. Single load path designs must be qualified as slow crack growth structure.

A companion document to MIL-A-83444 is the "USAF Damage Tolerant Design Handbook". It gives a summary of 83444 as well as explaining the rationale behind it.

The handbook also provides an in depth review of the analytical methods for determining residual strength as well as estimating the rate of crack growth as a function of time, cyclic load and sustained load. It gives examples indicating the limitations of methods and use of material data.

SEE ALSO REFS. 35 & 36.

STRUCTURAL ANALYSIS MANUAL
GENERAL DYNAMICS/CONVAIR AND SPACE SYSTEMS DIVISION

SECTION 24.0

COMPUTERIZED METHODS

A LISTING OF THE COMMONLY USED COMPUTER CODES WILL BE INCLUDED
IN THIS SECTION WHEN AVAILABLE.

STRUCTURAL ANALYSIS MANUAL
GENERAL DYNAMICS/CONVAIR AND SPACE SYSTEMS DIVISION

SECTION 24.1

COMPUTERIZED METHODS, NON-LINEAR ANALYSIS

A LISTING OF NON-LINEAR COMPUTERIZED METHODS WILL BE INCLUDED
IN THIS SECTION WHEN AVAILABLE.

STRUCTURAL ANALYSIS MANUAL
GENERAL DYNAMICS/CONVAIR AND SPACE SYSTEMS DIVISION

SECTION 25.0

OPTIMIZATION DESIGN

OPTIMIZATION DESIGN METHODS WILL BE INCLUDED IN THIS SECTION
WHEN AVAILABLE.



74A

STRUCTURAL ANALYSIS MANUAL
GENERAL DYNAMICS/CONVAIR AND SPACE SYSTEMS DIVISION

SECTION 26.0

MISCELLANEOUS TABLES AND CHARTS

Miscellaneous data contained in this section includes:

	PAGE
TEMPERATURE CONVERSION	26.1.1
SI UNITS AND PREFIXES	26.1.1
METRIC CONVERSION FACTORS	26.2.1
HARDNESS CONVERSION	26.3.1
STANDARD ATMOSPHERE	26.4.1
TEMPERATURE VS. ALTITUDE	26.5.1
COEFFICIENTS OF STATIC AND SLIDING FRICTION	26.6.1

STRUCTURAL ANALYSIS MANUAL

GENERAL DYNAMICS/CONVAIR AND SPACE SYSTEMS DIVISION

Data Source, Section 1.3 Reference 1

CONVERSION FACTORS

Table 5 shows conversion factors for most technical units. Equations for converting from one unit of temperature to the other are shown below:

$$\begin{aligned}\text{°R} &= 1.8(\text{°K} - 273.16) + 491.69 \\ \text{°R} &= 1.8\text{°C} + 491.69 \\ \text{°R} &= \text{°F} + 459.69\end{aligned}$$

$$\begin{aligned}\text{°K} &= 5/9(\text{°R} - 491.69) + 273.16 \\ \text{°K} &= 5/9(\text{°F} - 32) + 273.16 \\ \text{°K} &= \text{°C} + 273.16\end{aligned}$$

$$\begin{aligned}\text{°C} &= 5/9(\text{°R} - 491.69) \\ \text{°C} &= 5/9(\text{°F} - 32) \\ \text{°C} &= \text{°K} - 273.16\end{aligned}$$

$$\begin{aligned}\text{°F} &= 1.8(\text{°K} - 273.16) + 32 \\ \text{°F} &= 1.8\text{°C} + 32 \\ \text{°F} &= \text{°R} - 459.69\end{aligned}$$

TABLE 1 Derived SI Units with Special Names

Quantity	Unit	Sym- bol	Formula
frequency (of a periodic phenomenon)	hertz	Hz	1/s
force	newton	N	kg · m/s ²
pressure, stress	pascal	Pa	N/m ²
energy, work, quantity of heat	joule	J	N · m
power, radiant flux	watt	W	J/s
quantity of electricity, electric charge	coulomb	C	A · s
electric potential, potential difference, electromotive force	volt	V	W/A
electric capacitance	farad	F	C/V
electric resistance	ohm	Ω	V/A
electric conductance	siemens	S	A/V
magnetic flux	weber	Wb	V · s
magnetic flux density	tesla	T	Wb/m ²
inductance	henry	H	Wb/A
Celsius temperature	degree Celsius	°C	K
luminous flux	lumen	lm	cd · sr
illuminance	lux	lx	lm/m ²
activity (of a radionuclide)	becquerel	Bq	1/s
absorbed dose	gray	Gy	J/kg
dose equivalent	sievert	Sv	J/kg

TABLE 2 Base SI Units

Quantity	Unit	Symbol
length	metre	m
mass	kilogram	kg
time	second	s
electric current	ampere	A
thermodynamic temperature	kelvin	K
amount of substance	mole	mol
luminous intensity	candela	cd

STRUCTURAL ANALYSIS MANUAL

GENERAL DYNAMICS/CONVAIR AND SPACE SYSTEMS DIVISION

TABLE 3 Some Common Derived Units of SI

Quantity	Unit	Symbol
absorbed dose rate	gray per second	Gy/s
acceleration	metre per second squared	m/s ²
angular acceleration	radian per second squared	rad/s ²
angular velocity	radian per second	rad/s
area	square metre	m ²
concentration (of amount of substance)	mole per cubic metre	mol/m ³
current density	ampere per square metre	A/m ²
density, mass	kilogram per cubic metre	kg/m ³
electric charge density	coulomb per cubic metre	C/m ³
electric field strength	volt per metre	V/m
electric flux density	coulomb per square metre	C/m ²
energy density	joule per cubic metre	J/m ³
entropy	joule per kelvin	J/K
exposure (X and gamma rays)	coulomb per kilogram	C/kg
heat capacity	joule per kelvin	J/K
heat flux density		
irradiance	watt per square metre	W/m ²
luminance	candela per square metre	cd/m ²
magnetic field strength	ampere per metre	A/m
molar energy	joule per mole	J/mol
molar entropy	joule per mole kelvin	J/(mol·K)
molar heat capacity	joule per mole kelvin	J/(mol·K)
moment of force	newton metre	N·m
permeability (magnetic)	henry per metre	H/m
permittivity	farad per metre	F/m
power density	watt per square metre	W/m ²
radiance	watt per square metre steradian	W/(m ² ·sr)
radiant intensity	watt per steradian	W/sr
specific heat capacity	joule per kilogram kelvin	J/(kg·K)
specific energy	joule per kilogram	J/kg
specific entropy	joule per kilogram kelvin	J/(kg·K)
specific volume	cubic metre per kilogram	m ³ /kg
surface tension	newton per metre	N/m
thermal conductivity	watt per metre kelvin	W/(m·K)
velocity	metre per second	m/s
viscosity, dynamic	pascal second	Pa·s
viscosity, kinematic	square metre per second	m ² /s
volume	cubic metre	m ³
wave number	1 per metre	1/m

TABLE 4 SI Prefixes

Multiplication Factor	Prefix	Symbol
1 000 000 000 000 000 000 = 10 ¹⁸	exa	E
1 000 000 000 000 000 = 10 ¹⁵	peta	P
1 000 000 000 000 = 10 ¹²	tera	T
1 000 000 000 = 10 ⁹	giga	G
1 000 000 = 10 ⁶	mega	M
1 000 = 10 ³	kilo	k
100 = 10 ²	hecto	h
10 = 10 ¹	deka	da
0.1 = 10 ⁻¹	deci	d
0.01 = 10 ⁻²	centi	c
0.001 = 10 ⁻³	milli	m
0.000 001 = 10 ⁻⁶	micro	μ
0.000 000 001 = 10 ⁻⁹	nano	n
0.000 000 000 001 = 10 ⁻¹²	pico	p
0.000 000 000 000 001 = 10 ⁻¹⁵	femto	f
0.000 000 000 000 000 001 = 10 ⁻¹⁸	atto	a

STRUCTURAL ANALYSIS MANUAL
GENERAL DYNAMICS/CONVAIR AND SPACE SYSTEMS DIVISION

TO CONVERT	INTO	MULTIPLY BY
acres	sq. feet	43,560.0
acres	sq. meters	4,047.0
atmospheres	kgs/sq. cm	1.0333
atmospheres	pounds/sq. in.	14.70
atmospheres	newton/sq. meter	1.013×10^5
Btu	foot-lbs	778.3
Btu	joules	1,054.8
Btu	kilowatt-hrs	2.928×10^{-4}
centimeters	feet	3.281×10^{-2}
centimeters	inches	0.3937
centimeters	meters	0.01
centimeter-grams	cm-dynes	980.7
centimeter-grams	meter-kgs	10^{-5}
centimeter-grams	pound-feet	7.233×10^{-5}
centimeters/sec	feet/min	1.1969
centimeters/sec	feet/sec	0.03281
centimeters/sec	kilometers/hr	0.036
centimeters/sec	knots	0.1943
centimeters/sec	meters/min	0.6
centimeters/sec	miles/hr	0.02237
centimeters/sec/sec	feet/sec/sec	0.03281
centimeters/sec/sec	kms/hr/sec	0.036
centimeters/sec/sec	meters/sec/sec	0.01
centimeters/sec/sec	miles/hr/sec	0.02237
coulombs	faradays	1.036×10^{-5}
coulombs/sq.in	coulombs/sq. meter	1,550.
cubic centimeters	cu. inches	0.06102
cubic centimeters	liters	0.001
cubic feet	cu. meters	0.02832
cubic feet	gallons (U.S. liq.)	7.48052
cubic feet	liters	28.32
cubic inches	cu. meters	16,387.06
cubic inches	liters	0.01639
cubic inches	quarts (U.S. liq.)	0.01732
cubic meters	cu. feet	35.31
cubic meters	cu. inches	61,023.0
cubic meters	cu. yards	1.308
cubic meters	gallons (U.S. liq.)	264.2
cubic meters	liters	1,000.0
degrees (angle)	radians	0.01745
degrees/sec	revolutions/min	0.1667
drams (U.S., fluid or apoth.)	cubic cm.	3.6967
drams	grams	1.7718
drams	grains	27.3437
drams	ounces	0.0625

TABLE 5. CONVERSION FACTORS

STRUCTURAL ANALYSIS MANUAL
GENERAL DYNAMICS/CONVAIR AND SPACE SYSTEMS DIVISION

TO CONVERT	INTO	MULTIPLY BY
feet	meters	0.3048
feet of water	atmospheres	0.02950
feet of water	in. of mercury	0.8826
feet of water	kgs/sq/meter	304.8
feet of water	pounds/sq. ft	62.43
feet of water	pounds/sq. in.	0.4335
feet/min	cms/sec	0.5080
feet/min	kms/hr	0.01829
feet/min	miles/hr	0.01136
feet/sec	cms/sec	30.48
feet/sec	kms/hr	1.097
feet/sec	knots	0.5921
feet/sec	miles/hr	0.6818
foot-pounds	Btu	1.286×10^{-3}
foot-pounds	gram-calories	0.3238
foot-pounds	joules	1.356
foot-pounds	kg-calories	3.24×10^{-4}
foot-pounds	kg-meters	0.1383
foot-pounds	kilowatt-hrs	3.766×10^{-7}
foot-pounds	newton-meters	1.356
foot-pounds/min	horsepower	3.030×10^{-5}
foot-pounds/sec	Btu/hr	4.6263
foot-pounds/sec	horsepower	1.818×10^{-3}
foot-pounds/sec	kilowatts	1.356×10^{-3}
gallons	cu. cms.	3,785.0
gallons	cu. feet	0.1337
gallons	cu. inches	231.0
gallons	liters	3.785
gallons (liq. Br. Imp.)	gallons (U.S. liq.)	1.20095
gallons (U.S.)	gallons (Imp.)	0.83267
gallons of water	pounds of water	8.3453
gallons/min	cu. ft/sec	2.228×10^{-3}
gallons/min	liters/sec	0.06308
grains (troy)	grains (avdp)	1.0
grains (troy)	grams	0.06480
grams	dynes	980.7
grams	grains	15.43
grams	joules/meter (newtons)	9.807×10^{-3}
grams	ounces (avdp)	0.03527
grams	ounces (troy)	0.03215
grams	poundals	0.07093
grams/cu. cm.	pounds/cu. ft.	62.43
grams/cu. cm.	pounds/cu. in.	0.03613
grams/liter	grains/gal	58.417
grams/liter	pounds/1,000 gal	8.345
grams/liter	pounds/cu. ft.	0.062427
grams/sq. cm.	pounds/sq. ft.	2.0481

TABLE 5 CONVERSION FACTORS

STRUCTURAL ANALYSIS MANUAL
GENERAL DYNAMICS/CONVAIR AND SPACE SYSTEMS DIVISION

TO CONVERT	INTO	MULTIPLY BY
horsepower	Btu/min	42.44
horsepower	foot-lbs/min	33,000.
horsepower	foot-lbs/sec	550.0
horsepower (550 ft lb/sec)	horsepower(metric)(342.5 ft lb/sec)	1.014
horsepower	kilowatts	0.7457
horsepower	watts	745.7
horsepower-hrs	Btu	2,547.
horsepower-hrs	foot-lbs	1.98×10^4
inches	centimeters	2.540
inches of mercury	atmospheres	0.03342
inches of mercury	feet of water	1.133
inches of mercury	kgs/sq. meter	345.3
inches of mercury	pounds/sq. ft.	70.73
inches of mercury	pounds/sq. in.	0.4912
inches of water (at 4°C)	inches of mercury	0.07355
inches of water (at 4°C)	pounds/sq. ft.	5.204
inch-pounds	newton-meters	0.11298
joules	kg-meters	0.1020
joules/cm	poundals	723.3
joules/cm	pounds	22.48
kilograms	poundals	70.93
kilograms	pounds	2.205
kilograms/cu. meter	pounds/cu. ft.	0.06243
kilograms/meter	pounds/ft.	0.6720
kilograms/sq. cm.	atmospheres	0.9678
kilograms/sq. cm.	pounds/sq. in.	14.22
kilogram-calories	Btu	3.968
kilogram-calories	foot-pounds	3,088.
kilogram-calories	kg-meters	426.9
kilogram meters	foot-pounds	7.233
kilometers	feet	3,281.
kilometers	miles	0.6214
kilometers/hr	cms/sec	27.78
kilometers/hr	feet/min	54.68
kilometers/hr	feet/sec	0.9113
kilometers/hr	knots	0.5396
kilometers/hr	meters/min	16.67
kilowatts	Btu/min	56.92
kilowatts	foot-lbs/sec	737.6
kilowatts	horsepower	1.341
kilowatt-hrs	Btu	3,413.
kip	kilonewton	4.4482
kip/sq. in.	megapascals	6.8948
knots	kilometers/hr	1.8532
knots	nautical miles/hr	1.0
knots	statute miles/hr	1.151
knots	feet/sec	1.689
knots	meters/sec	0.5148

TABLE 5 CONVERSION FACTORS

STRUCTURAL ANALYSIS MANUAL
GENERAL DYNAMICS/CONVAIR AND SPACE SYSTEMS DIVISION

TO CONVERT	INTO	MULTIPLY BY
liters	cu. cm.	1,000.0
liters	cu. feet	0.03531
liters	cu. inches	61.02
liters	quarts (U.S. liq.)	1.057
Megapascal	pounds/sq. in.	145.039
Megapascal	newton/sq. mm	1.0
meters	feet	3.281
meters	inches	39.37
meters/min	cms/sec	1.667
meters/min	feet/sec	0.05468
meters/min	knots	0.03238
meters/min	miles/hr	0.03728
meters/sec	feet/min	196.8
meters/sec	kilometers/hr	3.6
meters/sec	miles/hr	2.237
meters/sec	miles/min	0.03728
meter-kilograms	pound-feet	7.233
miles (naut.)	feet	6,080.27
miles (naut.)	kilometers	1.853
miles (naut.)	miles (statute)	1.1516
miles (statute)	feet	5,280
miles (statute)	kilometers	1.609
miles (statute)	miles (naut.)	0.8684
miles/hr	feet/sec	1.467
miles/hr	knots	0.8684
miles/hr	meters/sec	0.4470
millimeters	inches	0.03937
mils	inches	0.001
Newton	pounds	0.22481
Newton	Dynes	1×10^5
Newton-meter	inch-pound	8.8507
Newton/sq. mm	Megapascal	1.0
ounces	grains	437.5
ounces	grams	28.3495
ounces	ounces (troy)	0.9115
poundals	grams	14.10
poundals	pounds	0.03108
pounds	grams	453.5924
pounds	kilograms	0.4536
pounds	newtons	4.4482
pounds	ounces	16.0
pounds	ounces (troy)	14.5833
pounds	poundals	32.17
pounds	pounds (troy)	1.21528
pounds of water	cu. feet	0.01602
pounds of water	gallons	0.1198
pound-feet	cm-grams	13,825.
pound-feet	meter-kgs	0.1383
pounds/cu. ft.	kgs/cu. meter	16.02

TABLE 5 CONVERSION FACTORS

STRUCTURAL ANALYSIS MANUAL
GENERAL DYNAMICS/CONVAIR AND SPACE SYSTEMS DIVISION

TO CONVERT	INTO	MULTIPLY BY
pounds/cu. in.	kgs/cu. meter	2.768×10^4
pounds/ft	kgs/meter	1.488
pounds/in.	gms/cm	178.6
pounds/sq.in.	atmospheres	0.06804
pounds/sq.in.	feet of water	2.307
pounds/sq.in.	inches of mercury	2.036
pounds/sq.in.	kgs/sq. meter	703.1
pounds/sq.in.	megapascals	6.8948×10^{-3}
quadrants (angle)	degrees	90.0
quadrants (angle)	radians	1.571
radians	degrees	57.30
radians	quadrants	0.6366
radians/sec.	revolutions/min	9.549
radians/sec.	revolutions/sec	0.1592
revolutions	radians	6.283
revolutions/min	degrees/sec	6.0
revolutions/min	radians/sec	0.1047
slug	kilogram	14.5939
slug	pounds	32.17
square centimeters	sq. inches	0.1550
square feet	sq. meters	0.09290
square inches	sq. cms.	6.452
square kilometers	sq. miles	0.3861
square meters	sq. feet	10.76
square millimeters	sq. inches	1.550×10^{-3}
temperature ($^{\circ}\text{C}$) + 273	absolute temperature ($^{\circ}\text{C}$)	1.0
temperature ($^{\circ}\text{C}$) + 17.78	temperature ($^{\circ}\text{F}$)	1.8
temperature ($^{\circ}\text{F}$) + 460	absolute temperature ($^{\circ}\text{F}$)	1.0
temperature ($^{\circ}\text{F}$) - 32	temperature ($^{\circ}\text{C}$)	5/9
tons (long)	kilograms	1,016.
tons (long)	pounds	2,240.
tons (long)	tons (short)	1.120
tons (metric)	kilograms	1,000.
tons (metric)	pounds	2,205.
tons (short)	pounds	2,000.
tons (short)	pounds (troy)	2,430.56
watts	Btu/hr	3.4192

TABLE 5 CONVERSION FACTORS

STRUCTURAL ANALYSIS MANUAL
GENERAL DYNAMICS/CONVAIR AND SPACE SYSTEMS DIVISION

Data Source, Section 1.3 Reference 3

Tensile Strength	Vickers- Firth Diamond	Brinell 3000 kg 10mm Stl Ball	Rockwell		
			A Scale	B Scale	C Scale
ksi	Hardness Number	Hardness Number	60 kg 120 deg Diamond Cone	100 kg 1/16 in. Dia Stl Ball	150 kg 120 deg Diamond Cone
50	104	92	—	58	—
52	108	96	—	61	—
54	112	100	—	64	—
56	116	104	—	66	—
58	120	108	—	68	—
60	125	113	—	70	—
62	129	117	—	72	—
64	135	122	—	74	—
66	139	127	—	76	—
68	143	131	—	77.5	—
70	149	136	—	79	—
72	153	140	—	80.5	—
74	157	145	—	82	—
76	162	150	—	83	—
78	167	154	51	84.5	—
80	171	158	52	85.5	—
82	177	162	53	87	—

HARDNESS CONVERSION TABLE 6

STRUCTURAL ANALYSIS MANUAL
GENERAL DYNAMICS/CONVAIR AND SPACE SYSTEMS DIVISION

Tensile Strength	Vickers- Firth Diamond	Brinell 3000 kg 10mm Stl Ball	Rockwell		
			A Scale	B Scale	C Scale
ksi	Hardness Number	Hardness Number	60 kg 120 deg Diamond Cone	100 kg 1/16 in. Dia Stl Ball	150 kg 120 deg Diamond Cone
83	179	165	53.5	87.5	—
85	186	171	54	89	—
87	189	174	55	90	—
89	196	180	56	91	—
91	203	186	56.5	92.5	—
93	207	190	57	93.5	—
95	211	193	57	94	—
97	215	197	57.5	95	—
99	219	201	57.5	95.5	—
102	227	210	59	97	—
104	235	220	60	98	19
107	240	225	60.5	99	20
110	245	230	61	99.5	21
112	250	235	61.5	100	22
115	255	241	62	101	23
118	261	247	62.5	101.5	24
120	267	253	63	102	25

HARDNESS CONVERSION TABLE C

STRUCTURAL ANALYSIS MANUAL
GENERAL DYNAMICS/CONVAIR AND SPACE SYSTEMS DIVISION

Tensile Strength	Vickers- Firth Diamond	Brinell 3000 kg 10mm Stl Ball	Rockwell		
			A Scale	B Scale	C Scale
kai	Hardness Number	Hardness Number	60 kg 120 deg Diamond Cone	100 kg 1/16 in. Dia Stl Ball	150 kg 120 deg Diamond Cone
123	274	259	63.5	103	26
126	281	265	64	—	27
129	288	272	64.5	—	28
132	296	279	65	—	29
135	304	286	65.5	—	30
139	312	294	66	—	31
142	321	301	66.5	—	32
147	330	309	67	—	33
150	339	318	67.5	—	34
155	348	327	68	—	35
160	357	337	68.5	—	36
165	367	347	69	—	37
170	376	357	69.5	—	38
176	386	367	70	—	39
181	396	377	70.5	—	40
188	406	387	71	—	41
194	417	398	71.5	—	42

HARDNESS CONVERSION TABLE 6

STRUCTURAL ANALYSIS MANUAL
GENERAL DYNAMICS/CONVAIR AND SPACE SYSTEMS DIVISION

Tensile Strength	Vickers- Pirch Diamond	Brinell 3000 kg 10mm Stl Ball	Rockwell		
			A Scale	B Scale	C Scale
			60 kg 120 deg Diamond Cone	100 kg 1/16 in. Dia Stl Ball	150 kg 120 deg. Diamond Cone
ksi	Hardness Number	Hardness Number			
201	428	408	72	—	43
208	440	419	72.5	—	44
215	452	430	73	—	45
221	463	442	73.5	—	46
231	479	453	74	—	47
237	493	464	75	—	48
246	508	476	75.5	—	49
256	523	488	76	—	50
264	539	500	76.5	—	51
273	556	512	77	—	52
283	573	524	77.5	—	53
294	592	536	78	—	54
304	611	548	78.5	—	55

HARDNESS CONVERSION TABLE 6

STRUCTURAL ANALYSIS MANUAL

GENERAL DYNAMICS/CONVAIR AND SPACE SYSTEMS DIVISION

Data Source, Section 1.3 Reference 1

TABLE . 7

STANDARD ATMOSPHERE TABLE

Alt ft	Temp. °F °C	Press. in. Hg lb/ft ²	ρ lb/ft ³	$\sqrt{\frac{\rho}{\rho_0}}$	$\frac{P}{P_0}$	$\frac{T}{T_0}$	$\sqrt{\frac{T}{T_0}}$	$\frac{P}{P_0} \sqrt{\frac{T}{T_0}}$	$\frac{a}{a_0}$	Alt ft
0	59.0	30.0	0.002378	1.000	1.000	1.000	1.000	1.000	1.000	0
1000	53.4	28.9	0.002308	0.980	0.980	0.999	0.999	0.999	0.999	1000
2000	47.8	27.8	0.002238	0.960	0.960	0.998	0.998	0.998	0.998	2000
3000	42.2	26.7	0.002168	0.940	0.940	0.997	0.997	0.997	0.997	3000
4000	36.6	25.6	0.002098	0.920	0.920	0.996	0.996	0.996	0.996	4000
5000	31.0	24.5	0.002028	0.900	0.900	0.995	0.995	0.995	0.995	5000
6000	25.4	23.4	0.001958	0.880	0.880	0.994	0.994	0.994	0.994	6000
7000	19.8	22.3	0.001888	0.860	0.860	0.993	0.993	0.993	0.993	7000
8000	14.2	21.2	0.001818	0.840	0.840	0.992	0.992	0.992	0.992	8000
9000	8.6	20.1	0.001748	0.820	0.820	0.991	0.991	0.991	0.991	9000
10000	3.0	19.0	0.001678	0.800	0.800	0.990	0.990	0.990	0.990	10000
11000	-2.6	17.9	0.001608	0.780	0.780	0.989	0.989	0.989	0.989	11000
12000	-8.2	16.8	0.001538	0.760	0.760	0.988	0.988	0.988	0.988	12000
13000	-13.8	15.7	0.001468	0.740	0.740	0.987	0.987	0.987	0.987	13000
14000	-19.4	14.6	0.001398	0.720	0.720	0.986	0.986	0.986	0.986	14000
15000	-25.0	13.5	0.001328	0.700	0.700	0.985	0.985	0.985	0.985	15000
16000	-30.6	12.4	0.001258	0.680	0.680	0.984	0.984	0.984	0.984	16000
17000	-36.2	11.3	0.001188	0.660	0.660	0.983	0.983	0.983	0.983	17000
18000	-41.8	10.2	0.001118	0.640	0.640	0.982	0.982	0.982	0.982	18000
19000	-47.4	9.1	0.001048	0.620	0.620	0.981	0.981	0.981	0.981	19000
20000	-53.0	8.0	0.000978	0.600	0.600	0.980	0.980	0.980	0.980	20000
21000	-58.6	6.9	0.000908	0.580	0.580	0.979	0.979	0.979	0.979	21000
22000	-64.2	5.8	0.000838	0.560	0.560	0.978	0.978	0.978	0.978	22000
23000	-69.8	4.7	0.000768	0.540	0.540	0.977	0.977	0.977	0.977	23000
24000	-75.4	3.6	0.000698	0.520	0.520	0.976	0.976	0.976	0.976	24000
25000	-81.0	2.5	0.000628	0.500	0.500	0.975	0.975	0.975	0.975	25000
26000	-86.6	1.4	0.000558	0.480	0.480	0.974	0.974	0.974	0.974	26000
27000	-92.2	0.3	0.000488	0.460	0.460	0.973	0.973	0.973	0.973	27000
28000	-97.8	0.2	0.000418	0.440	0.440	0.972	0.972	0.972	0.972	28000
29000	-103.4	0.1	0.000348	0.420	0.420	0.971	0.971	0.971	0.971	29000
30000	-109.0	0.0	0.000278	0.400	0.400	0.970	0.970	0.970	0.970	30000
31000	-114.6	0.0	0.000208	0.380	0.380	0.969	0.969	0.969	0.969	31000
32000	-120.2	0.0	0.000138	0.360	0.360	0.968	0.968	0.968	0.968	32000
33000	-125.8	0.0	0.000068	0.340	0.340	0.967	0.967	0.967	0.967	33000
34000	-131.4	0.0	0.000000	0.320	0.320	0.966	0.966	0.966	0.966	34000
35000	-137.0	0.0	0.000000	0.300	0.300	0.965	0.965	0.965	0.965	35000
36000	-142.6	0.0	0.000000	0.280	0.280	0.964	0.964	0.964	0.964	36000
37000	-148.2	0.0	0.000000	0.260	0.260	0.963	0.963	0.963	0.963	37000
38000	-153.8	0.0	0.000000	0.240	0.240	0.962	0.962	0.962	0.962	38000
39000	-159.4	0.0	0.000000	0.220	0.220	0.961	0.961	0.961	0.961	39000
40000	-165.0	0.0	0.000000	0.200	0.200	0.960	0.960	0.960	0.960	40000
41000	-170.6	0.0	0.000000	0.180	0.180	0.959	0.959	0.959	0.959	41000
42000	-176.2	0.0	0.000000	0.160	0.160	0.958	0.958	0.958	0.958	42000
43000	-181.8	0.0	0.000000	0.140	0.140	0.957	0.957	0.957	0.957	43000
44000	-187.4	0.0	0.000000	0.120	0.120	0.956	0.956	0.956	0.956	44000
45000	-193.0	0.0	0.000000	0.100	0.100	0.955	0.955	0.955	0.955	45000
46000	-198.6	0.0	0.000000	0.080	0.080	0.954	0.954	0.954	0.954	46000
47000	-204.2	0.0	0.000000	0.060	0.060	0.953	0.953	0.953	0.953	47000
48000	-209.8	0.0	0.000000	0.040	0.040	0.952	0.952	0.952	0.952	48000
49000	-215.4	0.0	0.000000	0.020	0.020	0.951	0.951	0.951	0.951	49000
50000	-221.0	0.0	0.000000	0.000	0.000	0.950	0.950	0.950	0.950	50000
51000	-226.6	0.0	0.000000	0.000	0.000	0.949	0.949	0.949	0.949	51000
52000	-232.2	0.0	0.000000	0.000	0.000	0.948	0.948	0.948	0.948	52000
53000	-237.8	0.0	0.000000	0.000	0.000	0.947	0.947	0.947	0.947	53000
54000	-243.4	0.0	0.000000	0.000	0.000	0.946	0.946	0.946	0.946	54000
55000	-249.0	0.0	0.000000	0.000	0.000	0.945	0.945	0.945	0.945	55000
56000	-254.6	0.0	0.000000	0.000	0.000	0.944	0.944	0.944	0.944	56000
57000	-260.2	0.0	0.000000	0.000	0.000	0.943	0.943	0.943	0.943	57000
58000	-265.8	0.0	0.000000	0.000	0.000	0.942	0.942	0.942	0.942	58000
59000	-271.4	0.0	0.000000	0.000	0.000	0.941	0.941	0.941	0.941	59000
60000	-277.0	0.0	0.000000	0.000	0.000	0.940	0.940	0.940	0.940	60000
61000	-282.6	0.0	0.000000	0.000	0.000	0.939	0.939	0.939	0.939	61000
62000	-288.2	0.0	0.000000	0.000	0.000	0.938	0.938	0.938	0.938	62000
63000	-293.8	0.0	0.000000	0.000	0.000	0.937	0.937	0.937	0.937	63000
64000	-299.4	0.0	0.000000	0.000	0.000	0.936	0.936	0.936	0.936	64000
65000	-305.0	0.0	0.000000	0.000	0.000	0.935	0.935	0.935	0.935	65000
66000	-310.6	0.0	0.000000	0.000	0.000	0.934	0.934	0.934	0.934	66000
67000	-316.2	0.0	0.000000	0.000	0.000	0.933	0.933	0.933	0.933	67000
68000	-321.8	0.0	0.000000	0.000	0.000	0.932	0.932	0.932	0.932	68000
69000	-327.4	0.0	0.000000	0.000	0.000	0.931	0.931	0.931	0.931	69000
70000	-333.0	0.0	0.000000	0.000	0.000	0.930	0.930	0.930	0.930	70000
71000	-338.6	0.0	0.000000	0.000	0.000	0.929	0.929	0.929	0.929	71000
72000	-344.2	0.0	0.000000	0.000	0.000	0.928	0.928	0.928	0.928	72000
73000	-349.8	0.0	0.000000	0.000	0.000	0.927	0.927	0.927	0.927	73000
74000	-355.4	0.0	0.000000	0.000	0.000	0.926	0.926	0.926	0.926	74000
75000	-361.0	0.0	0.000000	0.000	0.000	0.925	0.925	0.925	0.925	75000
76000	-366.6	0.0	0.000000	0.000	0.000	0.924	0.924	0.924	0.924	76000
77000	-372.2	0.0	0.000000	0.000	0.000	0.923	0.923	0.923	0.923	77000
78000	-377.8	0.0	0.000000	0.000	0.000	0.922	0.922	0.922	0.922	78000
79000	-383.4	0.0	0.000000	0.000	0.000	0.921	0.921	0.921	0.921	79000
80000	-389.0	0.0	0.000000	0.000	0.000	0.920	0.920	0.920	0.920	80000
81000	-394.6	0.0	0.000000	0.000	0.000	0.919	0.919	0.919	0.919	81000
82000	-400.2	0.0	0.000000	0.000	0.000	0.918	0.918	0.918	0.918	82000
83000	-405.8	0.0	0.000000	0.000	0.000	0.917	0.917	0.917	0.917	83000
84000	-411.4	0.0	0.000000	0.000	0.000	0.916	0.916	0.916	0.916	84000
85000	-417.0	0.0	0.000000	0.000	0.000	0.915	0.915	0.915	0.915	85000
86000	-422.6	0.0	0.000000	0.000	0.000	0.914	0.914	0.914	0.914	86000
87000	-428.2	0.0	0.000000	0.000	0.000	0.913	0.913	0.913	0.913	87000
88000	-433.8	0.0	0.000000	0.000	0.000	0.912	0.912	0.912	0.912	88000
89000	-439.4	0.0	0.000000	0.000	0.000	0.911	0.911	0.911	0.911	89000
90000	-445.0	0.0	0.000000	0.000	0.000	0.910	0.910	0.910	0.910	90000
91000	-450.6	0.0	0.000000	0.000	0.000	0.909	0.909	0.909	0.909	91000
92000	-456.2	0.0	0.000000	0.000	0.000	0.908	0.908	0.908	0.908	92000
93000	-461.8	0.0	0.000000	0.000	0.000	0.907	0.907	0.907	0.907	93000
94000	-467.4	0.0	0.000000	0.000	0.000	0.906	0.906	0.906	0.906	94000
95000	-473.0	0.0	0.000000	0.000	0.000	0.905	0.905	0.905	0.905	95000
96000	-478.6	0.0	0.000000	0.000	0.000	0.904	0.904	0.904	0.904	96000
97000	-484.2	0.0	0.000000	0.000	0.000	0.903	0.903	0.903	0.903	97000
98000	-489.8	0.0	0.000000	0.000	0.000	0.902	0.902	0.902	0.902	98000
99000	-495.4	0.0	0.000000	0.000	0.000	0.901	0.901	0.901	0.901	99000
100000	-501.0	0.0	0.000000	0.000	0.000	0.900	0.900	0.900	0.900	100000

Data Source, Section 1.3 Reference 1

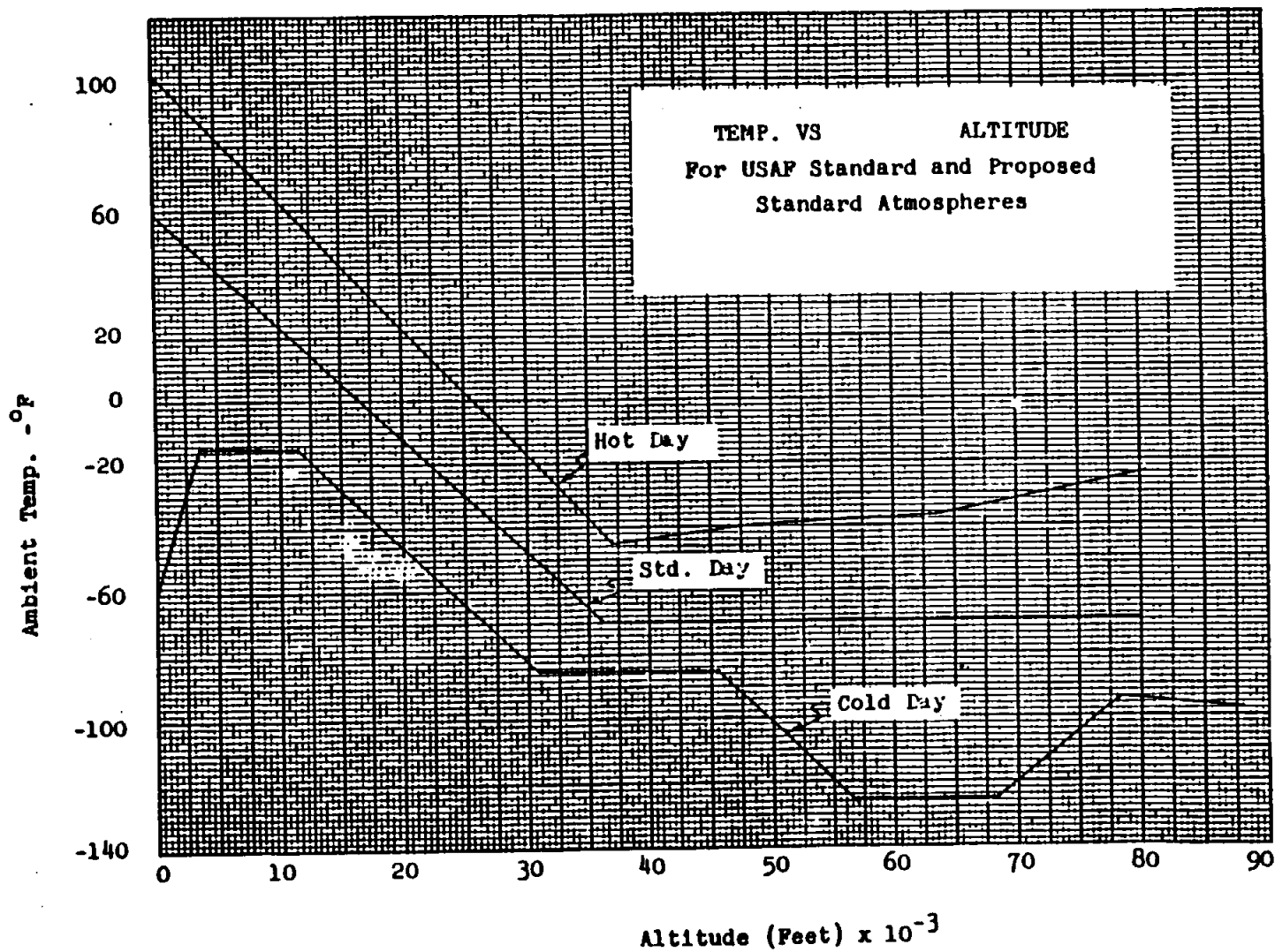


Fig. 1.

STRUCTURAL ANALYSIS MANUAL

GENERAL DYNAMICS/CONVAIR AND SPACE SYSTEMS DIVISION

Table 8. Coefficients of Static and Sliding Friction
(Reference letters indicate the lubricant used; numbers in parentheses give the sources. See footnote)

Materials	Static		Sliding	
	Dry	Greasy	Dry	Greasy
Hard steel on hard steel.....	0.78 (1)	0.11 (1, a) 0.23 (1, b) 0.15 (1, c) 0.11 (1, d) 0.0075 (18, p) 0.0032 (18, A)	0.42 (2)	0.029 (5, A) 0.081 (5, c) 0.080 (5, d) 0.058 (5, j) 0.084 (5, d) 0.105 (5, k) 0.096 (5, l) 0.108 (5, m) 0.12 (5, n)
Mild steel on mild steel.....	0.74 (19)		0.57 (3)	0.09 (3, a) 0.19 (3, u)
Hard steel on graphite.....	0.21 (1)	0.09 (1, a)		
Hard steel on babbitt (ASTM No. 1).....	0.70 (11)	0.23 (1, b) 0.15 (1, c) 0.08 (1, d) 0.085 (1, e)	0.33 (6)	0.16 (1, b) 0.06 (1, c) 0.11 (1, d)
Hard steel on babbitt (ASTM No. 8).....	0.42 (11)	0.17 (1, b) 0.11 (1, c) 0.09 (1, d) 0.08 (1, e)	0.35 (11)	0.14 (1, b) 0.065 (1, c) 0.07 (1, d) 0.08 (11, A)
Hard steel on babbitt (ASTM No. 10).....		0.25 (1, b) 0.12 (1, c) 0.10 (1, d) 0.11 (1, e)		0.13 (1, b) 0.06 (1, c) 0.055 (1, d)
Mild steel on cadmium silver.....				0.097 (2, f)
Mild steel on phosphor bronze.....			0.34 (3)	0.173 (2, f)
Mild steel on copper lead.....				0.145 (2, f)
Mild steel on cast iron.....		0.183 (15, c)	0.23 (6)	0.133 (2, f)
Mild steel on lead.....	0.95 (11)	0.5 (1, f)	0.95 (11)	0.5 (11, f)
Nickel on mild steel.....			0.64 (3)	0.178 (3, z)
Aluminum on mild steel.....	0.61 (8)		0.47 (3)	
Magnesium on mild steel.....			0.42 (3)	
Magnesium on magnesium.....	0.6 (22)	0.08 (22, v)		
Teflon on Teflon.....	0.04 (22)			0.04 (22, f)
Teflon on steel.....	0.04 (22)			0.04 (22, f)
Tungsten carbide on tungsten carbide.....	0.2 (22)	0.12 (22, a)		
Tungsten carbide on steel.....	0.5 (22)	0.08 (22, a)		
Tungsten carbide on copper.....	0.35 (23)			
Tungsten carbide on iron.....	0.8 (23)			
Bonded carbide on copper.....	0.35 (23)			
Bonded carbide on iron.....	0.8 (23)			
Cadmium on mild steel.....			0.46 (3)	
Copper on mild steel.....	0.53 (8)		0.36 (3)	0.18 (17, a)
Nickel on mild steel.....	1.10 (16)		0.53 (3)	0.12 (3, w)
Brass on mild steel.....	0.51 (8)		0.44 (6)	
Brass on cast iron.....			0.30 (6)	
Zinc on cast iron.....	0.85 (16)		0.21 (7)	
Magnesium on cast iron.....			0.25 (7)	
Copper on cast iron.....	1.05 (16)		0.29 (7)	
Tin on cast iron.....			0.32 (7)	
Lead on cast iron.....			0.43 (7)	
Aluminum on aluminum.....	1.05 (16)		1.4 (3)	
Glass on glass.....	0.94 (8)	0.01 (10, p) 0.005 (10, q)	0.40 (3)	0.09 (3, a) 0.116 (3, v)
Carbon on glass.....			0.18 (3)	
Garnet on mild steel.....			0.39 (3)	
Glass on nickel.....	0.78 (8)		0.56 (3)	
Copper on glass.....	0.68 (8)		0.53 (3)	
Cast iron on cast iron.....	1.10 (16)		0.15 (9)	0.070 (9, d) 0.064 (9, n) 0.077 (9, n) 0.164 (9, r) 0.067 (9, s) 0.072 (9, s)
Bronze on cast iron.....			0.22 (9)	
Oak on oak (parallel to grain).....	0.62 (9)		0.48 (9)	
Oak on oak (perpendicular).....	0.54 (9)		0.32 (9)	
Leather on oak (parallel).....	0.61 (9)		0.52 (9)	
Leather on cast iron.....			0.49 (9)	0.075 (9, n)
Laminated plastic on steel.....			0.56 (9)	0.36 (9, i)
Fluted rubber bearing on steel.....			0.35 (12)	0.15 (9, n) 0.05 (12, i) 0.05 (13, i)

(1) Campbell, *Trans. ASME*, 1939; (2) Clarke, Lincoln, and Stierrett, *Proc. A.P.I.*, 1935; (3) Beare and Bowden, *Phil. Trans. Roy. Soc.*, 1935; (4) Dokos, *Trans. ASME*, 1946; (5) Boyd and Robertson, *Trans. ASME*, 1945; (6) Sachs, *Zell. f. angew. Math. und Mech.*, 1924; (7) Honda and Yamaoka, *Jour. I. of M.*, 1925; (8) Tomlinson, *Phil. Mag.*, 1929; (9) Morin, *Acad. Roy. des Sciences*, 1838; (10) Claypoole, *Trans. ASME*, 1943; (11) Tabor, *Jour. Applied Phys.*, 1945; (12) Eyring, *General Discussion on Lubrication, ASME*, 1937; (13) Brazer and Holland-Bowyer, *General Discussion on Lubrication, ASME*, 1937; (14) Burwell, *Jour. S.A.E.*, 1942; (15) Stanton, "Friction," Longmans; (16) Ernst and Marchant, *Conference on Friction and Surface Finish, M.I.T.*, 1940; (17) Gongwer, *Conference on Friction and Surface Finish, M.I.T.*, 1940; (18) Hardy and Bircumshaw, *Proc. Roy. Soc.*, 1925; (19) Hardy and Hardy, *Phil. Mag.*, 1919; (20) Bowden and Young, *Proc. Roy. Soc.*, 1951; (21) Hardy and Doubleday, *Proc. Roy. Soc.*, 1923; (22) Bowden and Tabor, "The Friction and Lubrication of Solids," Oxford; (23) Shooter, *Research*, 4, 1951.

(a) Oleic acid; (b) Atlantic spindle oil (light mineral); (c) castor oil; (d) lard oil; (e) Atlantic spindle oil plus 2 percent oleic acid; (f) medium mineral oil; (g) medium mineral oil plus 1 percent graphite; (h) turbine oil plus 1 percent oleic acid; (i) grease (zinc oxide base); (j) graphite; (k) turbine oil plus 1 percent graphite; (l) turbine oil plus 1 percent stearic acid; (m) turbine oil (medium mineral); (n) olive oil; (p) palmitic acid; (q) ricinoleic acid; (r) dry soap; (s) lard; (t) water; (u) rape oil; (v) 3-in-1 oil; (w) octyl alcohol; (x) triolein; (y) 1 percent lauric acid in paraffin oil.



760

STRUCTURAL ANALYSIS MANUAL
GENERAL DYNAMICS/CONVAIR AND SPACE SYSTEMS DIVISION

SECTION 27.0

REPORT FORMAT

GUIDELINES FOR STRESS ANALYSIS REPORT STANDARDS ARE CONTAINED
IN ZS-7-002 REV. A. 8-14-63.

A COPY OF THIS REPORT IS SHOWN ON THE PAGES FOLLOWING.

STRUCTURAL ANALYSIS MANUAL
GENERAL DYNAMICS/CONVAIR AND SPACE SYSTEMS DIVISION

TITLE

ZS-7-002

STRESS ANALYSIS REPORT STANDARDS

TABLE OF CONTENTS

	<u>PAGE</u>
Table of Contents.....	27.1.1
References.....	27.1.4
Introduction.....	27.1.4
1.0 General Requirements.....	27.1.5
1.1 Preliminary Stress Analysis Reports.....	27.1.5
1.2 Final Stress Analysis Reports.....	27.1.5
1.3 Forms.....	27.1.6
1.4 Headings.....	27.1.6
1.5 Legibility and Reproducibility.....	27.1.6
1.5.1 Final Reports.....	27.1.6
1.5.2 Preliminary Reports.....	27.1.6
1.6 Security.....	27.1.6
2.0 Report Arrangement.....	27.1.7
3.0 Cover.....	27.1.8
4.0 Security Classification Sheet.....	27.1.8
5.0 Title Page.....	27.1.8
5.1 Final Report.....	27.1.8
5.2 Preliminary Report.....	27.1.9
5.3 Arrangement of Title Block.....	27.1.9
5.4 Foreword.....	27.1.9

STRUCTURAL ANALYSIS MANUAL
GENERAL DYNAMICS/CONVAIR AND SPACE SYSTEMS DIVISION

TABLE OF CONTENTS (Cont)

		<u>Page</u>
6.0	Table of Contents.....	27.1.9
7.0	References.....	27.1.10
8.0	Summary.....	27.1.10
9.0	Symbols.....	27.1.11
10.0	Sign Convention.....	27.1.11
11.0	Introduction.....	27.1.11
12.0	Description.....	27.1.12
12.1	Physical Description.....	27.1.12
12.2	Functional Description.....	27.1.12
12.3	Geometry.....	27.1.12
13.0	Section Properties.....	27.1.12
14.0	List of Loading Conditions with Controlling Variables.....	27.1.12
15.0	Summary of Design Criteria.....	27.1.13
16.0	Summary of Method of Analysis, Procedure and Assumptions.....	27.1.13
17.0	Load Analysis.....	27.1.13

STRUCTURAL ANALYSIS MANUAL
GENERAL DYNAMICS/CONVAIR AND SPACE SYSTEMS DIVISION

TABLE OF CONTENTS (Cont)

	<u>Page</u>
18.0 Load Analysis Summary.....	27.1.14
19.0 Stress Analysis.....	27.1.14
19.1 General Requirements.....	27.1.14
19.2 Pertinent Data.....	27.1.14
19.3 Diagrams.....	27.1.15
19.4 Loads.....	27.1.15
19.5 References.....	27.1.15
19.6 Margins of Safety.....	27.1.15
19.7 Calculations.....	27.1.15
19.8 Unorthodox Methods.....	27.1.16
19.9 Special Factors.....	27.1.16
19.10 Allowable Stresses.....	27.1.16
19.11 Non-critical Requirements.....	27.1.16
19.12 New or Revised Stress Analysis.....	27.1.16
Standard Sign Convention and Coordinate Axes.....	27.1.17
Minimum Margins of Safety Summary.....	27.1.22
List of Standard Symbols.....	27.1.23

STRUCTURAL ANALYSIS MANUAL
GENERAL DYNAMICS/CONVAIR AND SPACE SYSTEMS DIVISION

REFERENCES

- | | | |
|----|---------------------------|--|
| 1. | MIL-A-8860
18 May 1960 | Airplane Strength and
Rigidity - General
Specification for |
| 2. | MIL-A-8868
18 May 1960 | Airplane Strength and
Rigidity - Data and Reports |

INTRODUCTION

This specification covers the form, scope, composition and style of all stress analyses to be submitted under terms of the applicable contracts to demonstrate the required structural integrity. It shall apply to both preliminary and final reports as defined herein.

STRUCTURAL ANALYSIS MANUAL
GENERAL DYNAMICS/CONVAIR AND SPACE SYSTEMS DIVISION

1.0 GENERAL REQUIREMENTS:

This specification complies with the intent and applicable scope of Military Specification MIL-A-8868, "Stress Analysis Form and Content." In order to standardize the reports, and to render them of more value to those who use them, certain rules to be followed in the preparation of stress analysis reports are given in the following sections.

1.1 PRELIMINARY STRESS ANALYSIS REPORTS:

Preliminary stress analysis reports contain the calculations performed in analyzing structural components of the contract item prior to Stress Group approval of the drawings, drawing changes, engineering orders, etc., and may include load determination calculations as well as detailed stress analysis. While preliminary reports are not ordinarily submitted to the procuring or licensing agency, as much of the material contained in these reports as possible should be incorporated in the final reports. Preliminary reports serve as reference material for salvage and design change studies. In order to serve their function, these reports must be clear and well defined, although not necessarily as neat as a final report.

1.2 FINAL STRESS ANALYSIS REPORTS:

Final stress analysis reports are compiled for submittal to the procuring or licensing agency as substantiation of the structural adequacy of the design of the contract item and its components. Final reports may serve, also, as reference material for the salvage of defective parts, design changes, or the establishment of operating restrictions. These reports, in addition to following the form outlined below, must meet any further requirements of the procuring agency. Final stress analysis reports shall be given a thorough independent check by the contractor prior to their submission to the procuring agency. The contractor's approval of each report is required, and shall be the signature of the responsible contractor's personnel. The latest stress analysis on each model shall be submitted to the procuring agency to fulfill the stress analysis requirements. If portions of the analysis are under revision, the changes to be made shall be described in an accompanying letter. For each model subsequent to the first experimental model, an Index Report listing all applicable Stress Analysis Reports for that model shall be submitted with the Stress Analysis Reports.

STRUCTURAL ANALYSIS MANUAL
GENERAL DYNAMICS/CONVAIR AND SPACE SYSTEMS DIVISION

2.0 REPORT ARRANGEMENT:

All final and preliminary stress analysis reports shall contain the following items in the order given, as applicable.

SECURITY COVER SHEET

COVER

TITLE PAGE

FOREWORD

TABLE OF CONTENTS

LIST OF REFERENCES

INTRODUCTION

SUMMARY

SYMBOLS

SIGN CONVENTION

PHYSICAL DESCRIPTION

FUNCTIONAL DESCRIPTION

GEOMETRY

SECTION PROPERTIES

LIST OF LOADING CONDITIONS WITH CONTROLLING VARIABLES

SUMMARY OF DESIGN CRITERIA

SUMMARY OF METHOD OF ANALYSIS, PROCEDURE AND ASSUMPTIONS

LOAD ANALYSIS

LOAD ANALYSIS SUMMARY

STRESS ANALYSIS

A discussion of the individual subjects, their content and form, is presented in the following paragraphs.

STRUCTURAL ANALYSIS MANUAL
GENERAL DYNAMICS/CONVAIR AND SPACE SYSTEMS DIVISION

3.0 SECURITY COVER SHEET

For classified reports, a cover sheet is required. This sheet indicates the classification of the report and contains the following note:

"This document contains information affecting the National Defense of the United States within the meaning of the Espionage Laws, Title 18, U.S.C., Section 793 and 794. Its transmission or the revelation of its contents in any manner to an unauthorized person is prohibited by law."

4.0 COVER:

Each basic report shall be enclosed in a standard report cover which provides a cut-out allowing a portion of the title page to be visible when the cover is closed. Although not mandatory, it is recommended that covers be of sufficient light color to permit legible rubber stamping of security and other information thereon. The cover shall be stamped, on the back and front, at the upper and lower edges, as to its classification as defined in Paragraph 1.6.

5.0 TITLE PAGE:

5.1 FINAL REPORT:

The title page of a final report shall contain the following items:

1. Company and Division Name
2. Company Model Designation
3. Procuring Agency Model Designation
4. Report Number
5. Completion Date of Report
6. Title of Report

STRUCTURAL ANALYSIS MANUAL
GENERAL DYNAMICS/CONVAIR AND SPACE SYSTEMS DIVISION

5.1 FINAL REPORT: (CONT.)

7. Contract Number
8. Signature of Person or Persons Preparing the Report
9. Signature of Person or Persons Checking the Report
10. Signature of Structures Group Engineer or his Representative
11. Number of Pages in the Report
12. Number of Diagrams in Report, if Diagrams are Printed by Another Process
13. Record of all Revisions Made After Original Submission of Report to Procuring or Licensing Agency
14. Security Classification of Report

5.2 PRELIMINARY REPORT:

The title page of a preliminary report shall contain all the items listed in Paragraph 5.1, except items numbered 9, 10, 11, 12 and 13.

5.3 ARRANGEMENT OF TITLE BLOCK

The title block is that portion of the title page which is visible through the cut-out of the standard report cover. The title block on all reports shall contain the following information in the order given:

1. Report Number
2. Title of Report
3. Procuring Agency Model Description
4. Contract Number

5.4 FOREWORD

This single page shall summarize what contractual requirements have been satisfied by submittal of the report. (See example on page 27.1.31)

6.0 TABLE OF CONTENTS

The table of contents shall list, in order of their appearance in the report, all major and minor divisions with their appropriate page numbers in such a manner as to form an outline of the report. As a minimum, all items listed in paragraph 2.0, after TABLE OF CONTENTS, shall be included. Major divisions of the stress analysis portion of the report shall be listed.

STRUCTURAL ANALYSIS MANUAL
GENERAL DYNAMICS/CONVAIR AND SPACE SYSTEMS DIVISION

7.0 REFERENCES:

All drawings, report specifications, and other documents which are referred to in the report shall be itemized and numbered in the list of references. Each reference shall subsequently be identified in the report by number to avoid repetition of lengthy titles.

A record of the references used should be kept as the report is being written to obviate the necessity of reviewing the entire report after completion to obtain the references. For additional use of references, see Para. 19.5.

References in the report should be made exactly as in the following examples:

(Ref. p. 35) - denotes a reference to an item on Page 35 of the subject report.

(Ref. No. 4) - denotes a reference to document No. 4 listed in Page of "REFERENCES."

(Ref. GD/A File No. 663-4-63-025) - denotes a reference to an "in-house" memo which has not been incorporated into a referenced document.

8.0 SUMMARY:

The summary describes in concise terms the accomplishments of the report, and in the case of a stress analysis report, contains a tabulation of minimum margins of safety for all components analyzed. This margins of safety summary shall give, in tabular form, the following data for each component. [A sample minimum margin of safety summary sheet is included in this report. (Ref. p. 18).]

1. Part Number
2. Name of Part
3. Material
4. Heat Treatment or Temper
5. Critical Loading Conditions

STRUCTURAL ANALYSIS MANUAL
GENERAL DYNAMICS/CONVAIR AND SPACE SYSTEMS DIVISION

8.0 SUMMARY: (Cont)

6. Type of loading for which the margin of safety is lowest (e.g., tension, compression, etc.).
7. Lowest computed margin of safety. This shall be a total margin, and shall include any special factors which may be required.
8. Special factors included.
9. Report page number on which the minimum margin of safety is computed.

9.0 SYMBOLS:

Whenever possible, the symbols used in a stress analysis report shall conform to those given in "Standard Symbols," listed in this report. All symbols used shall be defined in a list of symbols included in the report. See Para. 23.0 for standard symbols.

10.0 SIGN CONVENTION:

A page showing the sign convention used in the report shall be included. This sign convention shall conform to the convention given in this specification whenever possible. (Ref. Para. 21.0).

11.0 INTRODUCTION:

An introduction shall be included in all stress reports. The introduction shall give the following information:

1. Purpose of the report.
2. Model to which the report is applicable
3. Specification authorizing its preparation
4. The scope of the report, i.e., the extent of the analysis or the area covered by the report, and its limitations.

STRUCTURAL ANALYSIS MANUAL
GENERAL DYNAMICS/CONVAIR AND SPACE SYSTEMS DIVISION

12.0 DESCRIPTION:

A physical and functional description, and a sketch showing the required basic geometry, shall be included in all stress analysis reports. Preliminary reports may combine any or all of these subjects in a single page if this can be done without deleting necessary information.

12.1 PHYSICAL DESCRIPTION:

The physical description shall describe with sketches, drawings and prose, the structure analyzed, its component parts, and its relation to the next assembly and to the entire contract item. This description should leave no question as to the scope of the analysis.

12.2 FUNCTIONAL DESCRIPTION:

The functional description shall describe the method of operation of the structure analyzed, its load points, method of reacting loads, and any limitations on its operation.

12.3 GEOMETRY:

The geometry shall include all critical dimensions, angles, tolerances and their relationship to each other.

13.0 SECTION PROPERTIES:

When section property calculations are extensive they shall be grouped in an organized arrangement and summarized. The sections shall be illustrated in this report. (Ref. Para. 19.3 and Para. 7.0).

14.0 LIST OF LOADING CONDITIONS WITH CONTROLLING VARIABLES:

The list of loading conditions shall include all conditions to which the part is subjected. This list shall include:

1. Condition Number
2. Condition Title
3. Controlling Variables
4. Description of Condition
5. Reference as to source of loads and/or variables.

STRUCTURAL ANALYSIS MANUAL
GENERAL DYNAMICS/CONVAIR AND SPACE SYSTEMS DIVISION

14.0 LIST OF LOADING CONDITIONS WITH CONTROLLING VARIABLES: (Cont)

When all possible loading conditions are not completely covered in the report and it is not obvious that these conditions are not critical, a statement shall be made to the effect that these conditions have been investigated and found to be not critical. Condition numbers and titles shall be consistent with those used in the governing specification and/or design criteria.

15.0 SUMMARY OF DESIGN CRITERIA:

The design criteria summary shall restate all portions of the design criteria, with reference as to the source, which apply to the structure under consideration.

16.0 SUMMARY OF METHOD OF ANALYSIS, PROCEDURE AND ASSUMPTIONS:

This section of the report shall contain a complete statement of the assumptions made regarding loads, their combination, distribution, and method of reaction, and any other assumptions made that are applicable to the analysis. Specific assumptions regarding individual items may be stated in the analysis.

A description of the method of analysis shall be given, together with the reason(s) for its choice if there is a choice of several methods.

The general procedure adopted to carry out the method of analysis shall be described in this section of the report.

17.0 LOAD ANALYSIS:

This section of the report shall contain calculations for the determination of external loads which the structure must sustain as required by the applicable specification and/or design criteria. All basic loads used for calculations shall be referenced as to their source. In cases where the analysis contains conditions in addition to those required by the applicable specification, the origin of the loads or their computation shall be included.

STRUCTURAL ANALYSIS MANUAL
GENERAL DYNAMICS/CONVAIR AND SPACE SYSTEMS DIVISION

17.0 LOAD ANALYSIS: (Cont)

Internal loads shall be computed as needed in the Stress Analysis section of the report. Condition numbers and titles shall be consistent with those used in the "List of Loading Conditions" (Ref. Para. 14.0).

18.0 LOAD ANALYSIS SUMMARY:

This summary shall include all pertinent load information as calculated in the load analysis section of the report. Preferably, this information shall be given in tabular form so that critical conditions and their corresponding loads may be readily obtained. The condition numbers and titles shall be consistent with those used in the "List of Loading Conditions," (Ref. Para. 14.0). The following minimum information shall be given for each condition summarized:

- 1) Condition Number
- 2) Condition Title
- 3) Point at which load is applied.
- 4) Magnitude of load
- 5) Direction of load
- 6) Whether load is yield, limit, ultimate, operating proof or burst.

19.0 STRESS ANALYSIS:

19.1 GENERAL REQUIREMENTS:

Each page shall be titled in sufficient detail to associate that page with a specific load or structural analysis.

19.2 PERTINENT DATA:

The following information shall precede each detail stress analysis:

- 1) Drawing number of part analyzed
- 2) Next assembly number of part analyzed
- 3) Part name
- 4) Material and heat treat information
- 5) Any other information required to describe the part and its material properties
- 6) Each page must be completely identified with heading and subheading.

When computer solutions are used, the basic equations, input, computer program number and a tabulation and/or plot of the computer results shall be included.

STRUCTURAL ANALYSIS MANUAL
GENERAL DYNAMICS/CONVAIR AND SPACE SYSTEMS DIVISION

19.3 DIAGRAMS:

Adequate sketches shall be provided throughout the analysis which will eliminate the necessity of referring to any drawings. The following information shall be given on each sketch:

1. Title
2. Part number of members shown
3. Any information required to locate the sketch on the overall structure.
4. Sections through the structure which are analyzed shall be indicated.

19.4 LOADS:

Loads shall always be identified as yield, limit, ultimate, operating, proof or burst.

19.5 REFERENCES:

Adequate references shall be used throughout the analysis. All data such as section properties, loads, allowable stresses, special factors, dimensions, environmental data, etc., shall be referenced as to their source. Reference notations must be made as shown on Page 6.

19.6 MARGINS OF SAFETY:

Margins of Safety are discussed and shall be calculated as shown in MIL-HDBK-5, "Metallic Materials and Elements for Flight Vehicle Structures." Margins of Safety shall be based on ultimate loads and ultimate allowable stresses or yield loads and yield allowable stresses, whichever produces the lowest margin of safety, unless otherwise specified in applicable specifications. The Margin of Safety shall be set off to the right hand side of the page and underlined twice.

$$M.S. = \frac{\text{allowable load (or allowable stress)}}{\text{design load (or design stress)}} - 1 = \underline{\underline{+x.xx}}$$

19.7 CALCULATIONS:

All steps in the arithmetical work that are necessary for clarity shall be included. Units of all quantities shall be shown.

STRUCTURAL ANALYSIS MANUAL
GENERAL DYNAMICS/CONVAIR AND SPACE SYSTEMS DIVISION

19.8 UNORTHODOX METHODS:

Unorthodox methods of stress analysis shall be substantiated for accuracy and application. The derivation of unusual stress analysis formulae shall be shown.

19.9 SPECIAL FACTORS:

Special factors such as fitting or bearing factors shall not be included until computation of the margin of safety.

19.10 ALLOWABLE STRESSES:

The only approved sources for allowable stresses are the following:

Military (and other Government Agency) Specifications
MIL-HDBK-5, Metallic Materials and Elements for
Flight Vehicle Structures
General Dynamics/Astronautics Specifications
General Dynamics/Astronautics Structures Manual
General Dynamics/Astronautics Structures Technical
Memoranda.

The use of other sources is prohibited. If required allowable stresses are not to be found in the above list of references, the use of other sources must be approved by: the procuring agency's responsible representative or the Chief of Stress. Wherever possible, the allowable strength levels shall be based upon the analysis of representative element tests and reduced to levels comparable to those presented in MIL-HDBK-5.

19.11 NON-CRITICAL REQUIREMENTS:

Items of major structure judged to be not critical on the basis of previous analysis, test, or by comparison with other structure shall be justified by a statement of the reason(s) for not including a detailed analysis.

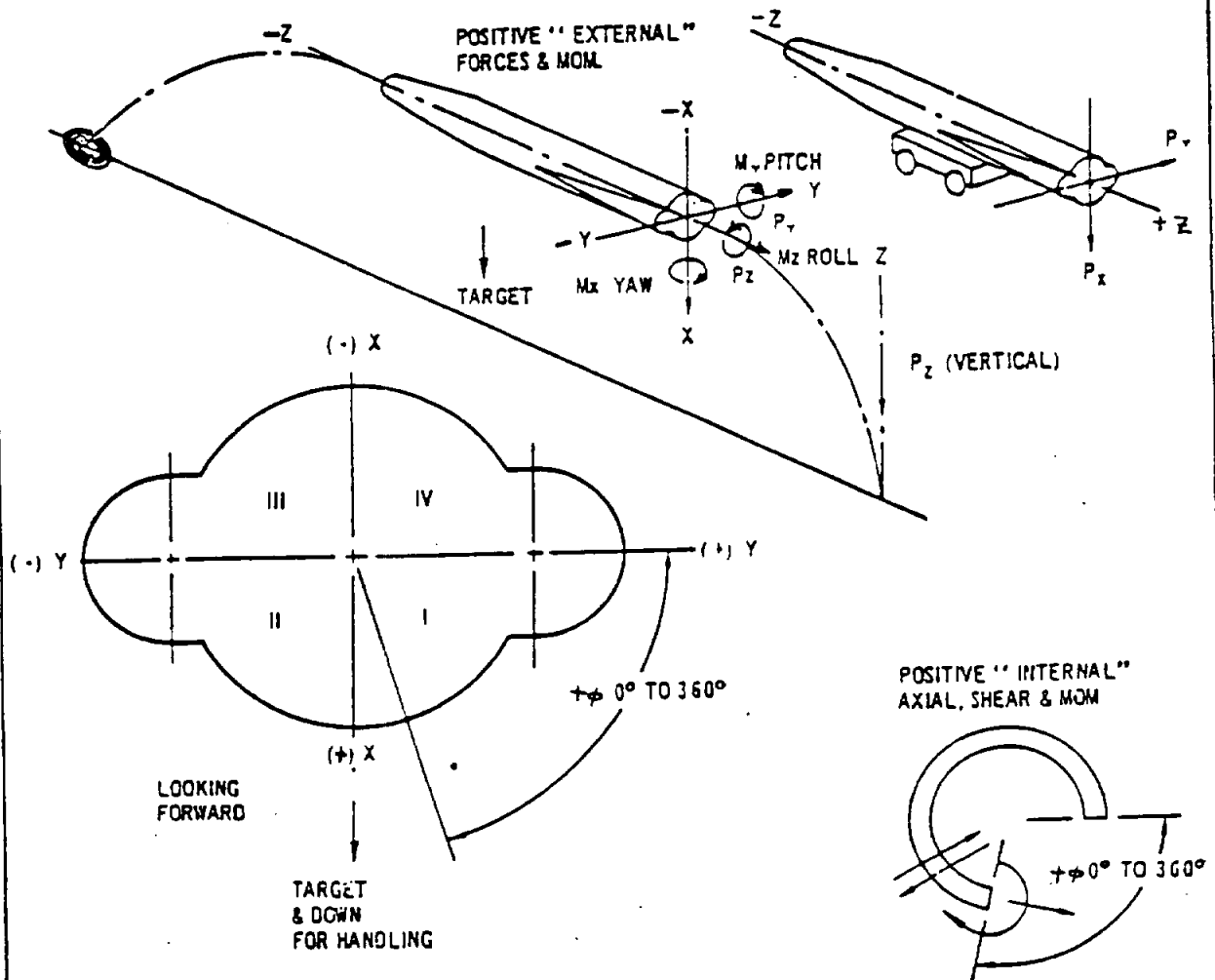
19.12 NEW OR REVISED STRESS ANALYSIS:

New or revised analyses shall be required to cover structural revisions subsequent to the first stress analysis. For all models the structure, at all times, shall be fully justified by the stress analysis. (Revisions to Final Reports must be authorized by the contract).

STRUCTURAL ANALYSIS MANUAL

GENERAL DYNAMICS/CONVAIR AND SPACE SYSTEMS DIVISION

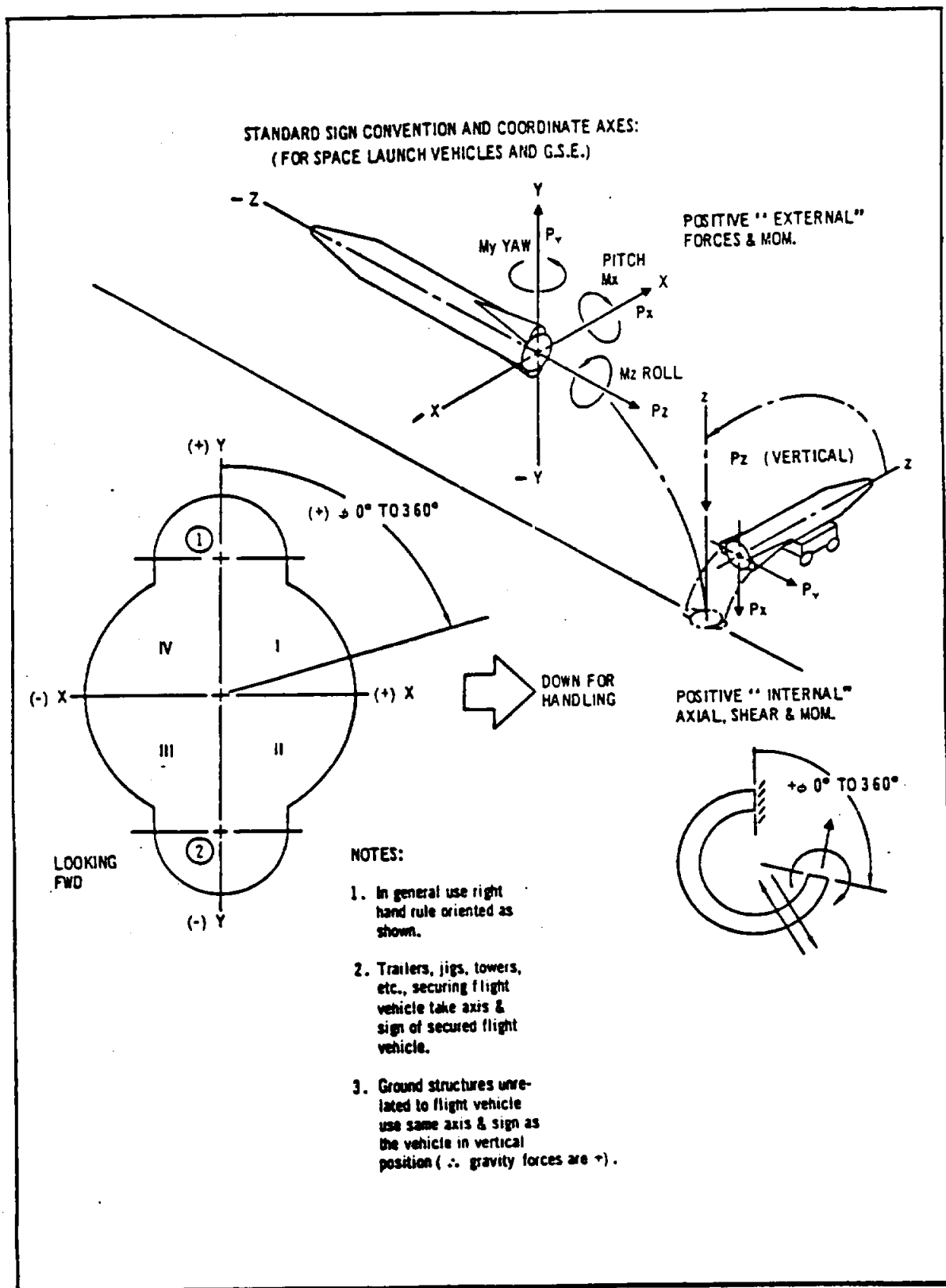
STANDARD SIGN CONVENTION AND COORDINATE AXES (FOR GROUND SUPPORT EQUIPMENT AND FOR D AND E MISSILES EMPLOYING AIG)



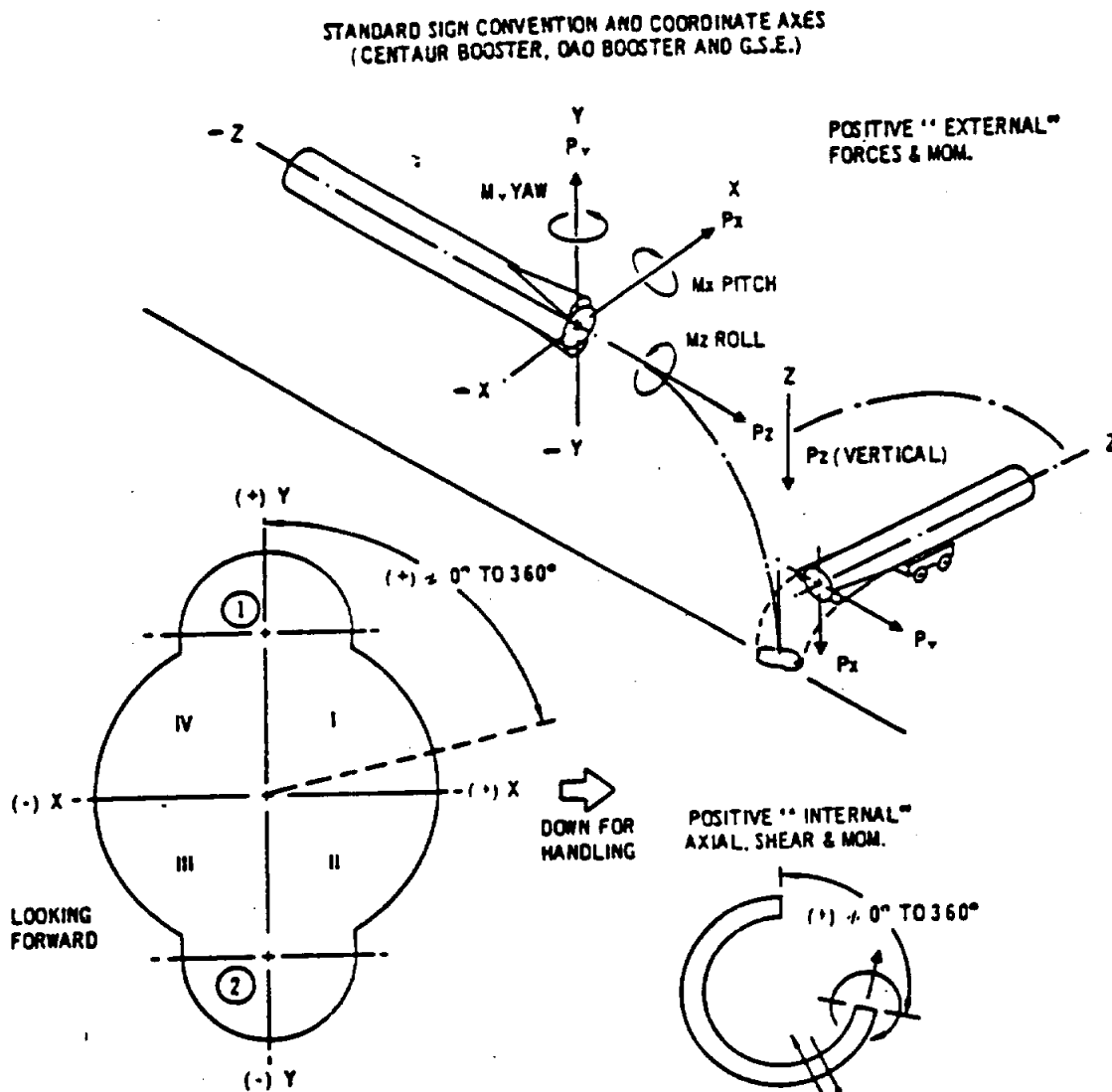
NOTES:

1. In general use right hand rule oriented as shown.
2. Trailers, jigs, towers, etc., securing flight vehicle take axis and sign of secured flight vehicle
3. Ground structures unrelated to flight vehicle use same axis and sign as the vehicle in vehicle position (gravity forces are +).

STRUCTURAL ANALYSIS MANUAL
GENERAL DYNAMICS/CONVAIR AND SPACE SYSTEMS DIVISION



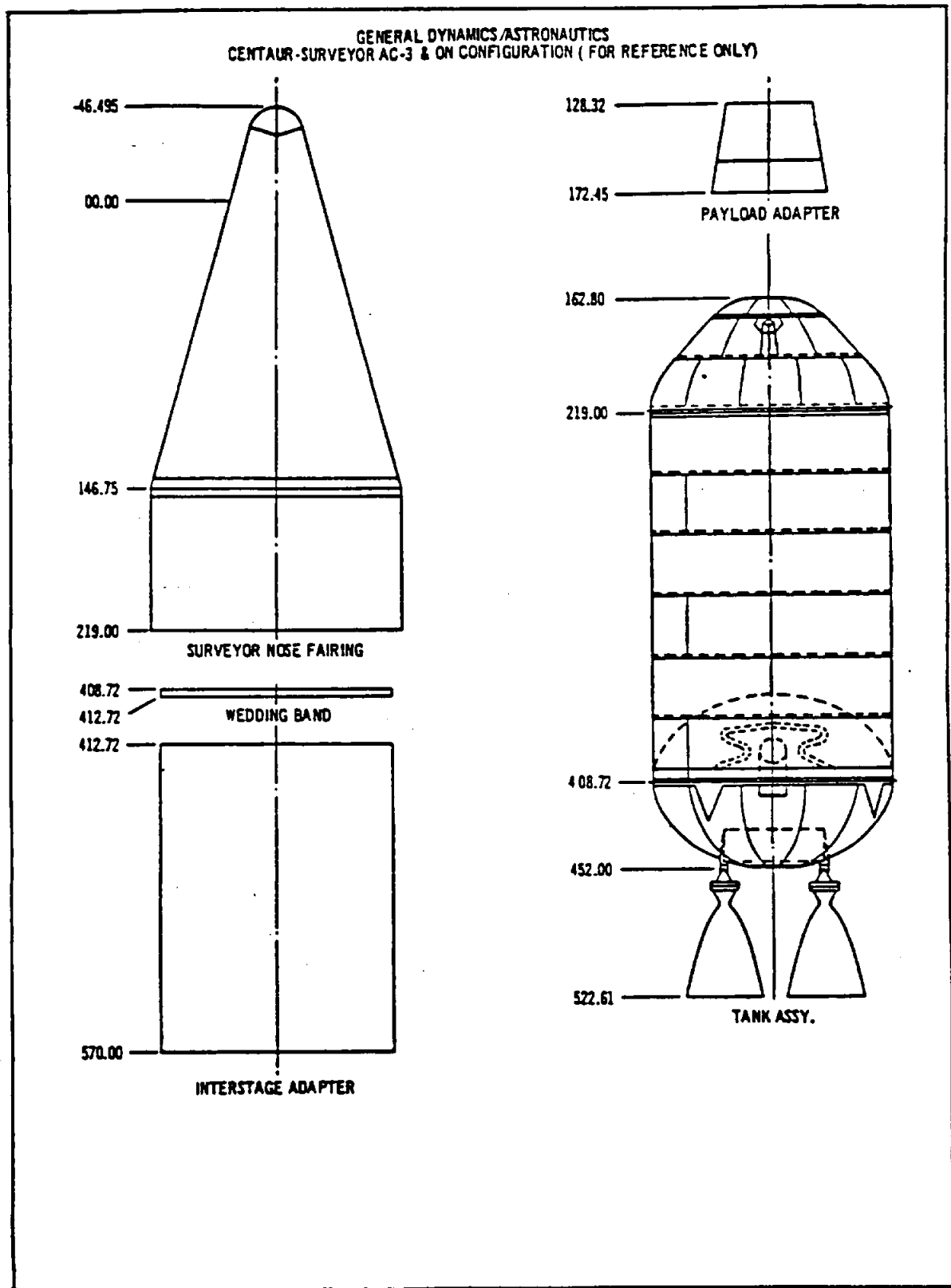
STRUCTURAL ANALYSIS MANUAL
GENERAL DYNAMICS/CONVAIR AND SPACE SYSTEMS DIVISION



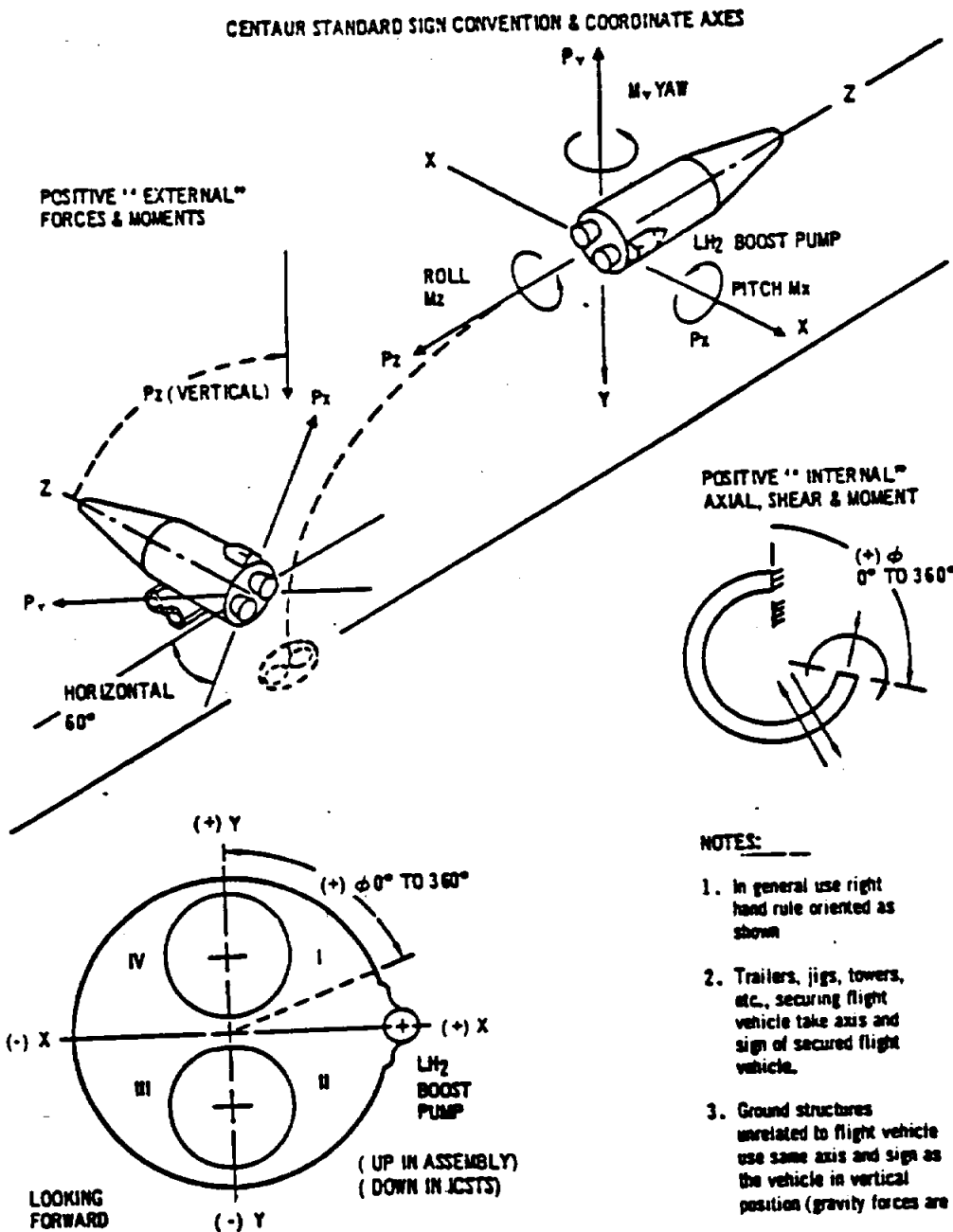
NOTES:

1. In general use right hand rule oriented as shown.
2. Trailers, jigs, towers, etc., securing flight vehicle take axis and sign of secured flight vehicle.
3. Ground structures unrelated to flight vehicle use same axis and sign as the vehicle in vertical position (therefore, gravity forces are +).

STRUCTURAL ANALYSIS MANUAL
GENERAL DYNAMICS/CONVAIR AND SPACE SYSTEMS DIVISION



STRUCTURAL ANALYSIS MANUAL
GENERAL DYNAMICS/CONVAIR AND SPACE SYSTEMS DIVISION



MINIMUM MARGINS OF SAFETY SUMMARY								
PR.	PART NAME	PART NO.	MATERIAL	H.T. KSI	CRITICAL CONDITION	TYPE OF LOADING	M.S.	FACTOR INCLUDED

STRUCTURAL ANALYSIS MANUAL
GENERAL DYNAMICS/CONVAIR AND SPACE SYSTEMS DIVISION

LIST OF STANDARD SYMBOLS

A	Area of cross section, square inches.
a	Subscript "allowable"; long dimension of a plate.
B	Slenderness ratio factor.
b	Width of sections; subscript "bending".
br	Subscript "bearing".
C	Circumference.
C _r	Rivet factor.
c	Fixity coefficient for columns; distance from neutral axis to extreme fiber; subscript "compression".
cr	Subscript "critical".
D	Diameter
d	Depth or height; mathematical operator denoting differential.
E	Modulus of elasticity in tension; average ratio of stress to strain for stress below proportional limit.
e	Elongation; unit deformation or strain; eccentricity; subscript for Euler's formula; subscript "endurance".
E'	Effective modulus of elasticity.
E _c	Modulus of elasticity in compression; average ratio of stress to strain below proportional limit.
E _s	Secant modulus.
E _t	Tangent modulus.
F	Allowable stress; force.
f	Internal (or calculated) stress.

STRUCTURAL ANALYSIS MANUAL
GENERAL DYNAMICS/CONVAIR AND SPACE SYSTEMS DIVISION

LIST OF STANDARD SYMBOLS (Cont)

F_b	Allowable bending stress, modulus of rupture in bending.
f_b	Internal (or calculated) primary bending stress.
f_b'	Internal (or calculated) precise bending stress.
F_{be}	Endurance limit in bending.
f_{br}	Internal (or calculated) bearing stress.
F_{bru}	Ultimate bearing stress.
F_{bry}	Yield bearing stress.
F_c	Allowable compressive stress.
f_c	Internal (or calculated) compressive stress.
F_{cc}	Allowable crushing or crippling stress (upper limit of column stress for local failure).
F_{co}	Column yield stress (upper limit of column stress for primary failure).
F_{cp}	Proportional limit in compression.
F_{cu}	Ultimate compressive stress.
F_{cy}	Compressive yield stress.
F_n	Allowable normal stress.
f_n	Internal (or calculated) normal stress.
F_s	Allowable shearing stress.
f_s	Internal (or calculated) shearing stress.
$F_{s,cr}$	Critical shear stress for buckling of rectangular panels.
F_{se}	Endurance limit in torsion.
F_{sp}	Proportional limit in shear.
F_{st}	Modulus of rupture in torsion.

STRUCTURAL ANALYSIS MANUAL
GENERAL DYNAMICS/CONVAIR AND SPACE SYSTEMS DIVISION

LIST OF STANDARD SYMBOLS (Cont)

F_{su}	Ultimate stress in pure shear. This value represents the average shearing stress over the cross section.
F_t	Allowable tensile stress.
f_t	Internal (or calculated) tensile stress.
F_{tp}	Proportional limit in tension.
F_{tu}	Ultimate tensile stress (from tests of standard specimens).
F_{ty}	Tensile yield stress at which permanent strain equals 0.002 in./in. (from tests of standard specimens).
G	Modulus of rigidity.
g	Acceleration due to gravity.
h	Height or depth; especially the distance between centroids of chords of beams and trusses.
I	Moment of inertia.
i	Slope (due to bending) of neutral plane of a beam, in radians (1 radian = 57.3°).
I_p	Polar moment of inertia.
J	Torsion constant ($=I_p$ for round tubes).
j	Stiffness factor = $\sqrt{EI/P}$
K	A constant, generally empirical; product of inertia, Kip.
ksi	Kips (1,000 pounds) per square inch.
L	Length; subscript "lateral"; lift; subscript "lift".
l	(Not used, to avoid confusion with numeral 1).
M	Applied moment or couple, usually a bending moment.
m	Mass; slope of lift curve.

STRUCTURAL ANALYSIS MANUAL
GENERAL DYNAMICS/CONVAIR AND SPACE SYSTEMS DIVISION

LIST OF STANDARD SYMBOLS (Cont)

M_a	Allowable bending moment.
N	Subscript "normal force".
n	Subscript "normal"; load factor.

(Ground Load Factor Convention)

(With respect to missile longitudinal axis and horizon)

n_L	Longitudinal load factor, positive aft.
n_S	Side load factor, positive to the right, when looking forward.
n_V	Vertical load factor, positive down.

(Flight Load Factor Convention)

n_x	Load factor, positive along the positive X-axis.
n_y	Load factor, positive along the positive Y-axis.
n_z	Load factor, positive along the positive Z-axis.

STRUCTURAL ANALYSIS MANUAL
GENERAL DYNAMICS/CONVAIR AND SPACE SYSTEMS DIVISION

LIST OF STANDARD SYMBOLS (Cont)

O	
o	
P	Applied Load.
p	Subscript "polar"; subscript "proportional limit"; subscript "principal".
P _a	Allowable load.
psi	Pounds per square inch.
Q	Static moment of a cross section.
q	Shear flow; dynamic pressure.
R	Stress ratio = f/T .
r	Radius.
S	Shear force; surface area.
s	Subscript "shear"; subscript "stiffener".
T	Applied torsional moment; torque; thrust.
t	Thickness.
T _a	Allowable torsional moment.
U	Factor of utilization; gust velocity.
u	Subscript "ultimate".
V	Velocity.
v	
W	Weight.
w	Specific weight, lb/cu. in.; distributed transverse loading.
w _e	Effective width of sheet.

STRUCTURAL ANALYSIS MANUAL
GENERAL DYNAMICS/CONVAIR AND SPACE SYSTEMS DIVISION

LIST OF STANDARD SYMBOLS (Cont)

X	
x	Distance along elastic curve of a beam; subscript denoting parallel to or about x-axis.
Y	
y	Deflection (due to bending) of elastic curve of a beam; distance from neutral axis to given fiber; subscript "yield"; subscript denoting parallel to or about y-axis.
Z	Section modulus, I/y .
z	Subscript denoting parallel to or about Z-axis.
Z_p	Polar section modulus = I_p/y (for round tubes).

STRUCTURAL ANALYSIS MANUAL
GENERAL DYNAMICS/CONVAIR AND SPACE SYSTEMS DIVISION

LIST OF STANDARD SYMBOLS (Cont)

A	Alpha	
α		Angle of attack.
B	Beta	
β		Angle of rotation of a normal to the elastic axis.
Γ	Gamma	Dihedral angle.
γ		Shearing strain; ratio of specific heats.
Δ	Delta	Deflection.
δ		Deflection; logarithmic decrement of viscous damping.
E	Epsilon	
ϵ		Normal strain.
Z	Zeta	
ζ		
H	Eta	
η		Efficiency; temperature recovery factor.
Θ	Theta	
θ		Angle of pitch; angle of twist of elastic axis.
		$\dot{\theta}$ Angular displacement of vehicle in pitch.
		$\ddot{\theta}$ Angular velocity of vehicle in pitch.
		$\ddot{\theta}$ Angular acceleration of vehicle in pitch.
I	Iota	
ι		
K	Kappa	
κ		
Λ	Lambda	Sweepback angle.
λ		Wavelength; taper ratio.
M	Mu	
μ		Poisson's ratio; coefficient of viscosity.
N	Nu	
ν		Kinematic viscosity.
Ξ	Xi	
ξ		

STRUCTURAL ANALYSIS MANUAL
GENERAL DYNAMICS/CONVAIR AND SPACE SYSTEMS DIVISION

LIST OF STANDARD SYMBOLS (Cont)

O	Omicron	
o		
Π	Pi	Ratio of circumference to diameter, 3.14159.
π		
P	Rho	Mass density; radius of gyration.
ρ		
Σ	Sigma	Summation.
σ		Normal stress.
T	Tau	Shearing stress.
τ		
Υ	Upsilon	
υ		
Φ	Phi	Angular deflection; angle of roll.
φ		Angular displacement of vehicle in roll.
		Angular velocity of vehicle in roll.
		Angular acceleration of vehicle in roll.
X	Chi	
χ		
Ψ	Psi	Angle of yaw; effective helix angle.
ψ		Angular displacement of vehicle in yaw.
		Angular velocity of vehicle in yaw.
		Angular acceleration of vehicle in yaw.
Ω	Omega	Angular velocity.
ω		Angular velocity; circular frequency.

SUPERSCRIPTS

.	(Dot) (\dot{x}, \dot{y}, \dots)	First derivative with respect to time.
..	(Double dot) ($\ddot{x}, \ddot{y}, \dots$)	Second derivative with respect to time.
'	(Prime) (x', y', \dots)	First derivative with respect to distance; effective or precise value; designation of a second set of axes, or quantities related to such axes.
''	(Double Prime) (x'', y'', \dots)	Second derivative with respect to distance.
-	(Bar) (\bar{x}, \bar{y}, \dots)	Mean value.

STRUCTURAL ANALYSIS MANUAL
GENERAL DYNAMICS/CONVAIR AND SPACE SYSTEMS DIVISION

EXAMPLE OF "FOREWORD"

FOREWORD

This analysis satisfies the requirements to provide a stress analysis in support of the Critical Design Review (CDR), SDRL GD-062.

The stress analysis consists of a compilation of the working stress notes made during the process of the design. Because this report is due to be submitted earlier than the production drawing data pack and because some drawings will not be completed until after CDR, it is not a complete final iteration and hence is not a final stress analysis. The design, the loads calculation, and the stress analysis are an iterative process right up to the time of drawing sign-off. Therefore, this interim stress analysis at this stage of design does not necessarily have all of the final configuration, dimensions, loads or part numbers.

The above described stress analysis completely fulfills the requirement for a stress analysis in support of the CDR. GDSS will, after design release, proceed to complete the documentation of this final iteration, in accordance with normal practice. The final analysis will include final loads, final configuration, part numbers and more exact methods. This is done for the purpose of insuring reliability and making a complete record that can be used for "Material Review Board" decisions and evaluation of future missions. A requirement exists for submitting such final stress analysis to the customer within 90 days after receipt of verification loads cycle (VLC) loads.